EXPERIMENTAL WIND TUNNEL STUDY OF AIRFOILS WITH LARGE FLAP DEFLECTIONS AT LOW REYNOLDS NUMBERS

BY

GREGORY A. WILLIAMSON

THESIS

Submitted in partial fulfillment of the requirements
for the degree of Master of Science in Aerospace Engineering
in the Graduate College of the
University of Illinois at Urbana-Champaign, 2012

Urbana, Illinois

Adviser:

Associate Professor Michael S. Selig

Abstract

Lift, drag, and moment measurements were taken at low Reynolds numbers for four airfoils with trailing edge plain flaps in an attempt to understand the effects of Reynolds number, percent thickness (t/c), percent chord of flap (flap-chord ratio), and flap deflection on airfoil performance. The four airfoils used in this research were the AG40d-02r, AG455ct-02r, W1011, and W1015. The W1011 and W1015 are symmetrical airfoils that were design using PROFOIL specifically for this research. PROFOIL is an inverse airfoil design code that utilizes conformal mapping. The W1011 and W1015 were designed to have similar performance characteristics that favor aerobatic flight. Airfoil performance was predicted computationally using XFOIL during the inverse design of the W1011 and W1015 airfoils. In order to effectively analyze and compare the experimental results, lift and moment increment plots were created. Drag data with large flap deflections ($\delta_f > 20$ deg) was collected to determine the main driving factor for airfoil drag in this regime. Flap deflections ranged from -20 to 65 deg and Reynolds numbers varied from 100,000 to 500,000 depending on the airfoil being tested. The flap sizes tested for this research ranged from 20% to 30% of chord depending on the airfoil being tested.

To my loving Wife for all of her support

Acknowledgments

I would like to express my deepest gratitude to Robert Deters, Gavin Ananda, and Shreyas Narsipur for helping me with my three wind tunnel entries. Their help setting up the LSATs apparatus and collecting data was instrumental in obtaining all of my data. I would also like to thank all of the people who worked on LSATs prior to my arrival to the University of Illinois. Their hard work made it possible for me to gather my data without many problems. The guidance and ideas from my advisor, Dr. Michael Selig, has helped me to accomplish one of long term goals of understanding low Reynolds number airfoils and airfoil design at low Reynolds numbers. For that, I am very grateful. I would also like to thank the following people for their constructive feedback on my thesis document and help with analyzing my data: Giovanni Fiore, Gavin Ananda, Shreyas Narsipur, Agrim Sareen, Adam Ragheb, and Donald Ellison. Their comments helped to improve the quality of my thesis. The excellent wind tunnel models used in this research were crafted by multiple people. The AG40d-02r and AG455ct-02r models were crafted by Mark Drela (hardware fabrication and install, filling, shaping, and polishing), Oleg Golovidov (core preparation and bagging), and Laszlo Horvath (foam core cutting). The E387(C) model was crafted by Jerry Robertson. The W1011 and W1015 models were crafted by Sean Cassidy (hardware installation, core preparation and bagging, filling, shaping, and polishing), Realize,® Inc. (manufactured removable flap parts), and Wagner Machine Company (manufactured flap endplates, model endplates, and aluminum trailing edge). The builders are also acknowledged in the legend of the performance plots found in Section 6.3 and 6.5. Finally, I would like to thank my wife, Renae, for all of her support these past two years. Without her support, I would not have completed my thesis on time.

Table of Contents

List of Tables

List of Figures

Nomenclature

Symbols

c	airfoil chord
C_l	airfoil lift coefficient
C_l/C_d	airfoil lift-to-drag ratio
c_f	flap chord
c_f/c	flap-chord ratio
C_d	airfoil drag coefficient
C_m	airfoil moment coefficient about the quarter chord
P_{atm}	atmospheric pressure
R	ideal gas constant
Re	Reynolds number based on airfoil chord
S	Sutherland temperature (constant)
t	airfoil thickness
T	ambient temperature
T_o	reference temperature
t/c	airfoil thickness ratio
q_∞	freestream dynamic pressure ($= \frac{1}{2}\rho V_\infty^2$)
V_∞	freestream velocity
x_{tr}	x location of boundary layer transition from laminar-to-turbulent flow
α	angle of attack
α^*	design angle of attack for a segment on the airfoil
δ_f	flap deflection
ΔC_l	lift increment
ΔC_m	moment increment about the quarter chord

ΔP_o	total pressure increment
ϕ	arc limit in the circle plane used in inverse airfoil design
ρ	density
μ	dynamic viscosity
μ_o	reference dynamic viscosity at the reference temperature

Abbreviations

CAD	Computer-Aided Design
LSATs	Low-Speed Airfoil Tests
LTPT	Low-Turbulence Pressure Tunnel at NASA Langley Research Center
MAV	Micro Air Vehicle
RC	Radio Controlled
SLA	Stereolithography
UAV	Unmanned Aerial Vehicle
UIUC	University of Illinois at Urbana-Champaign

Chapter 1

Introduction

During the past three decades, the need for unmanned aerial vehicles (UAVs) of all sizes has grown substantially and continues to grow due to their versatility. With a multitude of mission profiles, no one UAV can fulfill every profile. Thus, a diverse range of UAVs exists from the large Northrop Grumman Global Hawk to small micro air vehicles (MAVs) currently under development. A wide variety of UAVs operate in the low Reynolds number regime of 60,000 $\leq Re \leq$ 500,000. In this regime, airfoil aerodynamics play a crucial role in aircraft performance and handling [1].

In the low Reynolds number regime, boundary layer transition from laminar-to-turbulent flow becomes increasingly important. For most low Reynolds number airfoils, this transition takes place naturally through a laminar separation bubble that often results in degraded airfoil performance [2]. The degradation in performance is generally characterized by high drag and nonlinearity in the lift curve [1]. In some cases, airfoils at low Reynolds numbers exhibit hysteresis loops in lift, drag, and moment coefficients that are caused by laminar separation bubbles. Thus, it is important to understand the aerodynamic effects of low Reynolds number flows on airfoil performance to effectively design efficient UAVs.

The use of high-lift devices on aircraft is extremely important. These devices increase payload capacity, shorten takeoff and landing distances, and reduce stall speeds [3]. Numerous studies have been conducted on airfoils at low Reynolds numbers. These studies include systematic studies conducted by Selig, et al. [4–9] as well as Eppler [10], but limited data exists for airfoils with large flap deflections. One study by Ylilammi [11] examined the effects of flap deflections between 0 and 30 deg for two non-symmetrical airfoils. Even though a considerable amount of data can be found on low Reynolds number airfoils, there exists a dearth of experimental data on flapped airfoils in this regime. Besides the study conducted by Ylilammi [11], little work has been performed on highly deflected flapped airfoils at low Reynolds numbers. Therefore, more data is required to better understand the effects of large flap deflections at low Reynolds numbers.

This research has one main objective: study the effects of plain flaps on the performance of low Reynolds number airfoils. Besides the main objective, this research has two secondary objectives: (1) design two low Reynolds number symmetrical airfoils to be used with flaps, (2) fill a current void in experimental data for flapped airfoils at low

Reynolds numbers. To meet these goals, four airfoils (AG40d-02r [12], AG455ct-02r [12], W1011, and W1015) were tested at varying Reynolds numbers and flap deflections. The AG40d-02r had a 25% of chord flap, and the AG455ct-02r had a 30% of chord flap. Both the AG40d-02r and AG455ct-02r flaps were hinged on the lower surface. The W1011 and W1015 each had a 20% and 30% of chord flap and were hinged on the airfoil chordline. The W1011 and W1015 airfoils were designed for this research by the author using PROFOIL [13–15] to be used with flaps by prescribing the transition curve.

In Chapter 2, an overview of low Reynolds number aerodynamics is presented. The laminar separation bubble receives considerable discussion in this chapter because of its important influence on airfoil performance and airfoil design at low Reynolds numbers. Chapter 3 discusses the experimental techniques used to collect the data. Following this in Chapter 4, four sets of data were compared to validate the wind tunnel setup and data taken during this research. A set of data was taken at the beginning of three separate wind tunnel entries. The fourth data set contained benchmark data taken at the Low-Turbulence Pressure Tunnel (LTPT) at NASA Langley Research Center. In Chapter 5, the inverse airfoil design methods used to design the W1011 and W1015 airfoils are discussed. Considerable discussion in this chapter is on the design process used to engineer the W1011 and W1015 airfoils. Chapter 6 presents the experimental data collected and subsequent analyses performed. Within this chapter, the most important information of this document is presented and discussed. Finally, Chapter 7 discusses the conclusions from this research and some final thoughts for future research in this area.

Chapter 2

Review of Low Reynolds Number Airfoils

Low Reynolds number airfoils have been studied extensively since Prandtl defined the boundary layer in 1904. Yet, it is still actively studied by many researchers. The difficulty with low Reynolds number airfoils is its dependence on the laminar boundary layer and transition to turbulent flow. Therefore, a complete understanding of low Reynolds number airfoils begins with the understanding of the laminar boundary layer, laminar separation bubble, and boundary layer transition from laminar-to-turbulent flow. Airfoils operate in the low Reynolds number regime when there exists laminar separation bubbles that produce significant effects on the aerodynamic performance. The Reynolds number range where this occurs varies between airfoils. For this research, the Reynolds number range of 100,000 $\leq Re \leq$ 500,000 was examined because a vast majority of airfoils exhibit adverse effects from laminar separation bubbles within this range. An introduction to the Reynolds number and how it is defined will be covered in the following section.

2.1 Reynolds Number

When analyzing subsonic airfoils, one of the most important variables that should be considered is the Reynolds number. Osborne Reynolds defined the Reynolds number relationship in 1883 during his experiments of pipe flow [16]. The Reynolds number provides a non-dimensional value that characterizes the physical properties of the flow, and it represents the ratio of inertial and viscous forces. Thus, a high Reynolds number flow is dominated by the inertial forces while a lower Reynolds number flow is dominated by the viscous forces. The significance of the Reynolds number is its non-dimensionality. Since a Reynolds number is dimensionless, it can be used to scale objects to fit inside a small wind tunnel. Thus, full scale airplane performance characteristics can be measured with a small wind tunnel provided the Reynolds numbers are the same between the actual airplane and the model. For airfoils, the characteristic length used to define the Reynolds number is the chord length of the airfoil. The Reynolds number is given by

$$Re = \frac{\rho V_\infty c}{\mu} \tag{2.1}$$

where ρ is the density of the fluid, c is the airfoil chord length, V_∞ is the freestream velocity, and μ is the dynamic viscosity. The dynamic viscosity needed to calculate Reynolds number is temperature dependent and can be calculated using the Sutherland viscosity [17] law

$$\frac{\mu}{\mu_0} = \left(\frac{T}{T_0}\right)^{3/2} \left(\frac{T_0 + S}{T + S}\right) \tag{2.2}$$

where T_0 is the reference temperature, μ_0 is the reference dynamic viscosity at the temperature T_0, and S is a constant defined as Sutherland temperature. For the wind tunnel experiments performed in this research, the Sutherland viscosity law was used to determine the test section dynamic viscosity. The temperature-compensated dynamic viscosity was used to calculate the test section Reynolds number discussed in Subsection 3.5.4.

2.2 Laminar Separation Bubble

It is a well-established fact that for an airfoil to achieve low drag at low Reynolds numbers, it is imperative that an airfoil be designed to avoid or at least mitigate laminar separation bubbles [2]. However, in order to design an airfoil to avoid these adverse effects, one must first understand why laminar separation bubbles occur and how they affect airfoil performance. In the following subsection, the phenomenon of the laminar separation bubble is discussed.

2.2.1 The Phenomenon

Laminar separation bubbles have been extensively studied since the early 1900s after Prandtl mathematically defined the boundary layer in 1904. Until that time, scientists and engineers were puzzled by differences between experimental observations and inviscid flow theory. After boundary layer theory was established, researchers starting applying it to many different applications including boundary layer separation at low Reynolds numbers [18]. A laminar separation bubble can be defined as the separation of a laminar boundary layer downstream of the point of minimum pressure, transition in the free shear layer, and reattachment of a turbulent boundary layer downstream from the point of separation [19, 20].

There are three main regions that comprise a laminar separation bubble. These three regions are called: laminar region, turbulent region, and the redeveloping region. A schematic of a laminar separation bubble can be seen in Fig. 2.1.

In the first region, laminar region, the laminar boundary layer separates from the airfoil surface due to strong adverse pressure gradients downstream of the point of minimum pressure [19]. Laminar flow continues in a detached shear layer, but because of the unstable nature of the detached shear layer, it makes a transition to turbulent flow downstream from the point of separation. While in transition, the flow is energized by the entrainment of fluid from

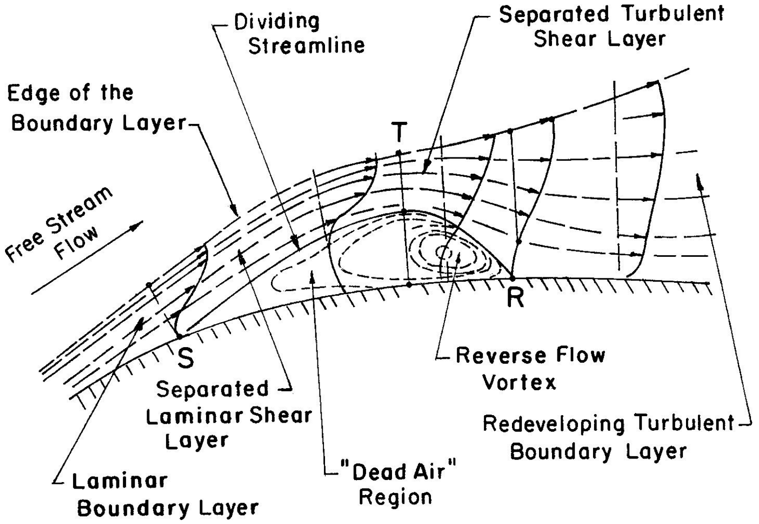

Figure 2.1: Schematic of a laminar separation bubble (taken from Ref. 21).

the freestream that causes the pressure to rise in the bubble [22]. After the flow has been energized sufficiently, it undergoes full transition to a turbulent flow which is where the second region of the laminar separation bubble begins. In this second region, turbulent region, the flow is able to overcome the severe adverse pressure gradient and reattaches to the airfoil surface. After the turbulent flow reattaches to the surface of the airfoil, it enters the third region of the laminar separation bubble structure. In this third region, redeveloping region, the turbulent flow begins to develop a turbulent boundary layer that has a significant increase in skin friction and therefore drag of the airfoil. The turbulent boundary layer is more stable and able to better negotiate severe adverse pressure gradients without separation [23]. Throughout the first two regions of the laminar separation bubble geometry, there is a pocket of reversed or stagnated flow. This portion of the laminar separation bubble causes the streamlines of the flow to be displaced upward. These displaced streamlines lead to adverse effects on airfoil performance, which will be covered in Subsection 2.2.2.

For airfoils, laminar separation bubbles can be classified conceptually as two types: short or long bubble. The structure of the laminar separation bubble described above is the same for both types. The main difference between the two types is the resulting pressure distribution over the airfoil as seen in Fig. 2.2. Short bubbles do not severely affect airfoil performance [23], but long bubbles severely degrade airfoil performance [18], which will be discussed in Subsection 2.2.2. Short bubbles typically occur at the higher ranges of the low Reynolds number regime. Long bubbles typically occur at the mid-to-lower ranges of the low Reynolds number regime.

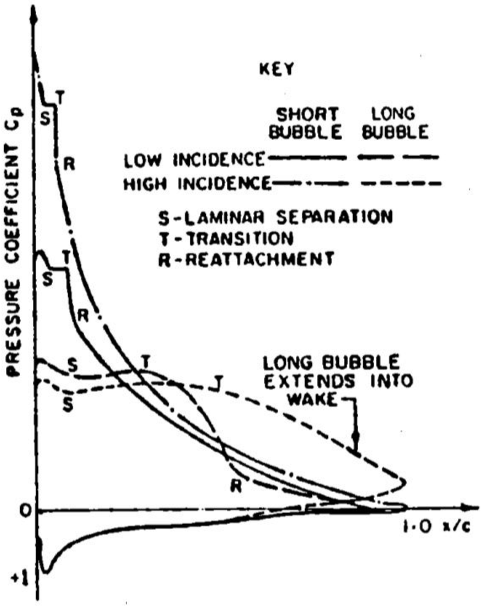

Figure 2.2: Pressure distribution comparing short verse long bubbles (taken from Ref. 24).

2.2.2 Aerodynamic Effects

Laminar separation bubbles will always degrade the performance of an airfoil that has an attached boundary layer from leading to trailing edge [21]. As seen in Fig. 2.3, the pressure distribution over an airfoil has been affected by the presence of a laminar separation bubble. The effects seen in Fig. 2.3 are typical for a short bubble. In Fig. 2.3, the S denotes the separation point, T′ denotes the beginning of transition to turbulent flow, T denotes the point of complete transition to turbulent flow, and R denotes the point of reattachment.

If a laminar separation bubble cannot be avoided, a short bubble is desired because of the minimal effects on the aerodynamic performance [23]. A short bubble minimally affects the aerodynamic performance due to its small size as it mainly acts as a transition-forcing mechanism. The typical short bubble is less than a few percent of the chord in length. With a short bubble, the point of separation can be estimated to occur where the pressure distribution curve begins to “flatten out,” and transition occurs approximately where it begins to decrease again [18]. The point of reattachment can be estimated to occur where the pressure equals the value of a turbulent boundary layer over the airfoil without a laminar separation bubble [22] as seen in Fig. 2.3. With short bubbles, the performance can be estimated by assuming a turbulent boundary layer from the leading edge without separation making their effects on airfoil performance easy to analytically determine. This estimation can be made because the surface pressure distribution with a short bubble approaches that of an attached turbulent boundary layer. As seen in Fig. 2.3, a short bubble reduces the minimum pressure peak attenuating the leading edge suction. The reduction in leading edge suction

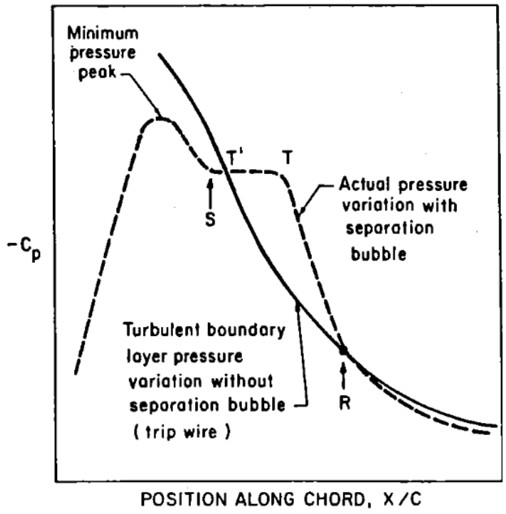

Figure 2.3: Typical pressure distribution with and without a laminar separation bubble (taken from Ref. 19).

will degrade the performance of the airfoil. As angle of attack increases, the bubble moves toward the leading edge (stagnation point) and becomes shorter in length. At some point, the flow becomes completely turbulent at the leading edge and the bubble is bypassed. As the angle of attack is increased even more, the airfoil will eventually stall.

Unlike a short bubble, a long bubble can occupy upward of 15 to 40% of the airfoil surface [21], which negatively affects the pressure distribution over the airfoil as seen in Fig. 2.2. The shape of the pressure distribution for a long bubble follows similar trends as the short bubble, but the actual shape will vary dramatically from the short bubble case. The difference in the pressure distribution curve is due to the large portion of separated flow over the surface of the airfoil. As shown in Fig. 2.2, the minimum pressure peak is reduced compared with the short bubble. The attenuation of the leading edge suction is due to bubble bursting. Bubble bursting is when the minimum pressure peak is reduced to lessen the pressure gradient over the pressure recovery region. The minimum pressure peak is reduced because not enough entrainment of fluid and turbulent mixing caused a great enough pressure rise to form a short bubble [19]. The effects just described severely degrade the performance of airfoils that exhibit a long bubble. The structure of the long bubble is similar to the short bubble, but it is difficult to predict the point of separation and increasingly difficult to predict the point of reattachment. Equations exist to analytically approximate the length of a short bubble [18, 22], but there are no such equations for a long bubble.

The adverse effects of laminar separation bubbles can be seen in Fig. 2.4. Figure 2.4 shows a drag polar of the Eppler E374 airfoil at a Reynolds number of 100,000 with a laminar separation bubble along with a tripped boundary layer (fully turbulent and attached with no laminar separation bubble) for the same airfoil at the same Reynolds number.

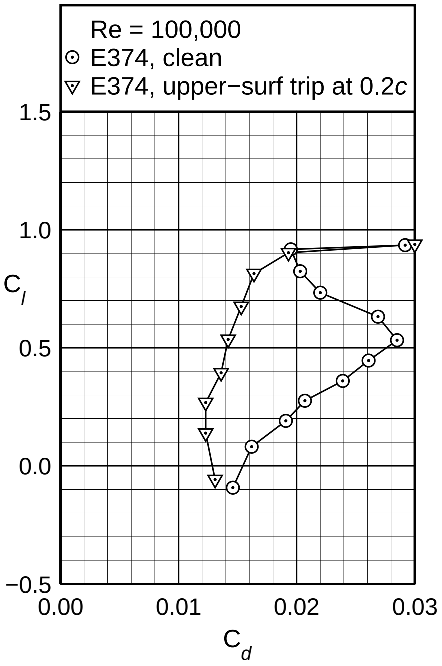

Figure 2.4: Effect of laminar separation bubble and trip on the E374 at Re = 100,000 (taken from Ref. 2).

From Fig. 2.4, it can be seen that the drag due to the laminar separation bubble exceeds that of the tripped boundary layer even though the tripped boundary layer has more skin friction drag because of the turbulent boundary layer. The details of boundary layer trips will be discussed in the Subsection 2.2.3. The rightward bump in the drag polar is caused by the laminar separation bubble. There are two main sources that account for the increase in drag for a laminar separation bubble. The first source is the pressure drag owing to the low pressure of the laminar separation bubble [20]. As the flow separates on the upper surface because of the laminar separation bubble, it creates an area of low pressure that cannot be recovered. This low pressure area creates pressure drag that exceeds the amount for an airfoil with a fully attached flow. The second source is the pressure drag owing to the effective change of the airfoil shape caused by the laminar separation bubble. As previously discussed, laminar separation bubbles displace the streamlines upward due to the separated region. These displaced streamlines cause the effective shape of the airfoil to change, which directly affects the pressure distribution over the airfoil. The resultant effective airfoil shape will more than likely not perform as well as the originally designed airfoil causing an increase in drag. The first source accounts for most of the drag rise attributed to laminar separation bubbles [20].

2.2.3 Means of Mitigation

In trying to cope with laminar separation bubbles, there are four main methods. The four methods are suction and blowing (powered methods), direct airfoil design, usage of a boundary layer trip, and inverse airfoil design. Each method has its pros and cons, which will be explored in the following discussion in the order that they are listed.

Suction and blowing are used to prevent separation by introducing energy into the boundary layer. The concept of suction and blowing to prevent laminar separation has been considered in the past [25], but feasibility of the using this method prevents its wide spread implementation [26].

The direct design method was the first method used for airfoil design. It consists of prescribing the shape of the airfoil first and then analyzing the airfoil for the performance characteristics. The direct design method is considered a “brute force” method by many airfoil designers. When being applied to mitigate the effects of laminar separation bubbles, the direct design method is difficult to use because minute changes to the airfoil shape can dramatically affect the aerodynamic performance of the airfoil. Therefore, the direct design method is not ideally suited for designing airfoils that need to be optimized for specific aerodynamic characteristics or to mitigate the effects of laminar separation bubbles.

A more practical way to mitigate the effects of laminar separation bubbles is to use a boundary layer trip or trip for short. A trip is used to mitigate or eliminate the size of a laminar separation bubble [2]. Trips are normally used on already existing airfoils that have a large separation bubble that adversely affect airfoil performance. A trip works by creating an inflection point in the boundary layer [27]. The inflection point creates instabilities that lead to boundary layer transition from laminar-to-turbulent flow. After the trip, the flow transitions to a turbulent flow that attaches back to the surface of the airfoil as a turbulent boundary layer which has more energy to overcome the adverse pressure gradient and is less susceptible to separating from the surface of the airfoil [23]. The turbulent boundary layer reduces the pressure drag caused by the low pressure region of the laminar separation bubble, but it also increases the skin friction drag owing to the increase in shear stress of the turbulent boundary layer. In addition, a trip adds device drag from the physical height of the trip [2]. In order to utilize the full benefit of the trip, it should be place at the beginning of the laminar separation bubble [28]. This placement is done to minimize the increase in drag due to the turbulent boundary layer while still mitigating the effects of the laminar separation bubble.

One major disadvantage of trips is that a “one trip fits all” statement does not hold true. In fact, an optimal trip at one flight condition may be ineffective or detrimental at another [2]. It has been experimentally proven that the optimum position and height of a trip is dependent on airfoil geometry, Reynolds number, and angle of attack [28]. All of these parameters, besides the airfoil geometry, change on a continual basis. This variability makes it increasingly difficult or near impossible to employ a trip effectively on an airfoil for all flight conditions. Optimizing a trip can be extremely difficult and requires intense testing to validate the gained benefits. There are, however, some general rules that should be followed/observed, which are thoroughly presented in Ref. 28. One key conclusion of the work performed in Ref. 2 on designing airfoils with trips was that a properly designed airfoil in a clean configuration would out perform the same airfoil with a trip for Reynolds numbers higher than $\approx$ 200,000. Therefore, the best way to mitigate the effects of laminar separation bubbles is by the proper design of an airfoil.

There are many ways in which airfoils can be designed, but the most effective method is to use an inverse design methodology. Inverse airfoil design uses specific performance parameters to define the airfoil geometry. Thus, the airfoil can be tailored to specific aerodynamic needs. In the early 1990s, Selig [13, 14] drew upon Eppler's work in inverse design of airfoils through conformal mapping and created the inverse design code PROFOIL. PROFOIL differs from the Eppler code by incorporating the ability to control maximum thickness, thickness distribution, and others. More information regarding PROFOIL and the differences between it and the Eppler code can be found in Refs. 13, 14, and 29. An in-depth discussion on inverse design of airfoils using conformal mapping can be found in Chapter 5.

2.3 Past Experimental Data on Low Reynolds Number Airfoils

In the past few decades, the topic of low Reynolds number airfoils has started to obtain more attention due to the ever expanding applications of Unmanned Aerial Vehicles (UAV). The need for experimental data is absolutely necessary to confirm results obtained from computational methods. The issue with experimental data at low Reynolds numbers is the inconsistency in data between two facilities. These inconsistencies were major hurdles in the early days of experimental work in low Reynolds number airfoil testing but have been mostly overcome. Systematic studies performed by Selig, et al. [4–9] as well as Eppler [10] have provided a well-established baseline for low Reynolds number airfoil data. In regard to experimental data of flapped airfoils in this regime, one study by Ylilammi [11] examined the effects of flap deflections between 0 and 30 deg of two airfoils. The two airfoils were the NACA2412 and SD7062. Ylilammi compared the experimental results with XFOIL, FINFLO, and calculation methods presented by Roskam [30]. XFOIL and FINFLO are two different computational tools. The methods presented in Ref. 30 are mainly based on statistical data and provide good estimates for applications above Reynolds numbers of one million.

Even though a considerable amount of data can be found on low Reynolds number airfoils, there exists a dearth of experimental data on flapped airfoils in this regime. Besides the study conducted by Ylilammi [11], little work has been performed on highly deflected flapped airfoils at low Reynolds numbers. As stated before, one goal of this research is to expand the knowledge and experimental data of flapped airfoils at low Reynolds numbers.

Chapter 3

Experimental Techniques

The experimental setup used to collect the data for this research was developed by Selig, et al. [4–9, 31] and needed no modification in order to collect the experimental data. In this chapter, the capabilities of the University of Illinois at Urbana-Champaign (UIUC) low-turbulence subsonic wind tunnel and Low-Speed Airfoil Tests (LSATs) setup are discussed.

3.1 Wind Tunnel Facility

The research for this research was conducted in the UIUC low-turbulence subsonic wind tunnel. An isometric view of the tunnel can be seen in Fig. 3.1. The wind tunnel is an open-return type with an overall length of 60 ft. The contraction ratio from the inlet to the test section has a ratio of 7.5:1. The test section has a rectangular cross section with a nominal width of 4.0 ft and height of 2.8 ft. The length of the test section is nominally 8 ft. A photograph of the test section can be seen in Fig. 3.2. In order to account for the boundary layer growth on the tunnel walls, the overall cross sectional dimensions of the test section increase by approximately 0.5 in. With a 125-hp alternating current electric motor connected to a five-blade fan, test section speeds are variable up to 160 mph. A photograph of the fan can be seen in Fig. 3.3. The LSATs setup used to collect the data for this research had a Reynolds number range from 40,000 to 500,000. With the LSATs setup, a test section velocity of 80 ft/sec (55 mph) resulted in a Reynolds number of 500,000 based on an airfoil chord of 12 in. In Section 3.3, the LSATs setup will be discussed in detail.

Airfoil performance at low Reynolds numbers is highly dependent on the laminar boundary layer and sensitive to small changes in turbulence intensity [18]. Therefore, airfoil performance at low Reynolds numbers is directly related to boundary layer transition from laminar-to-turbulent flow. Thus, with all low Reynolds number wind tunnel tests, sufficiently low levels of turbulence intensity in the wind tunnel is of the utmost importance to ensure the flow does not prematurely transition from a laminar-to-turbulent flow. It is especially important because low turbulence levels better mimic actual flight conditions. Low turbulence levels were obtained in the wind tunnel by using honeycomb and anti-turbulence screens located in the settling chamber of the wind tunnel. The settling chamber is located in the inlet of the wind tunnel. As the air enters the inlet, it passes through the 4-in thick honeycomb. A photograph of the inlet with the honeycomb can be seen in Fig. 3.4. After the honeycomb, the air passes through the four anti-turbulence screens that further reduce the turbulence levels in the wind tunnel. The screens can be partially removed for cleaning. With an empty test section, the turbulence intensity has been experimentally measured to be less than 0.10% [32]. This level of turbulence intensity has been proven to be an acceptable level for low Reynolds number airfoil experiments [31]. Since the LSATs setup requires other equiment to be mounted into the tunnel besides the airfoil, the turbulence intensity will be affected. The effects of the extra equipment on the turbulence intensity will be discussed in more detail in Subsection 3.4.1.

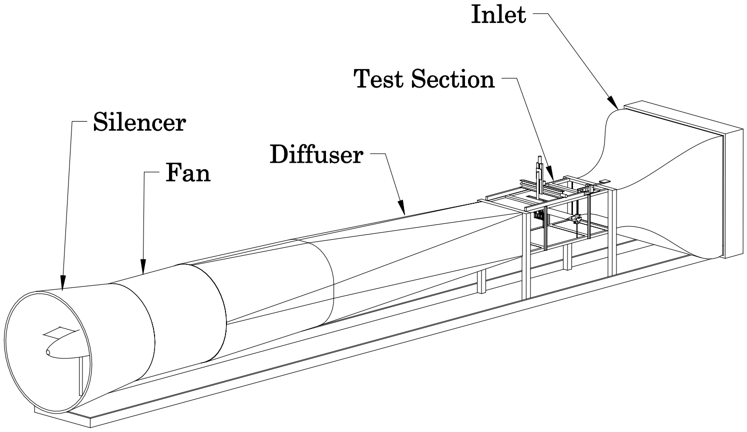

Figure 3.1: Illustration of the UIUC low-speed subsonic wind tunnel (taken from Ref. 33).

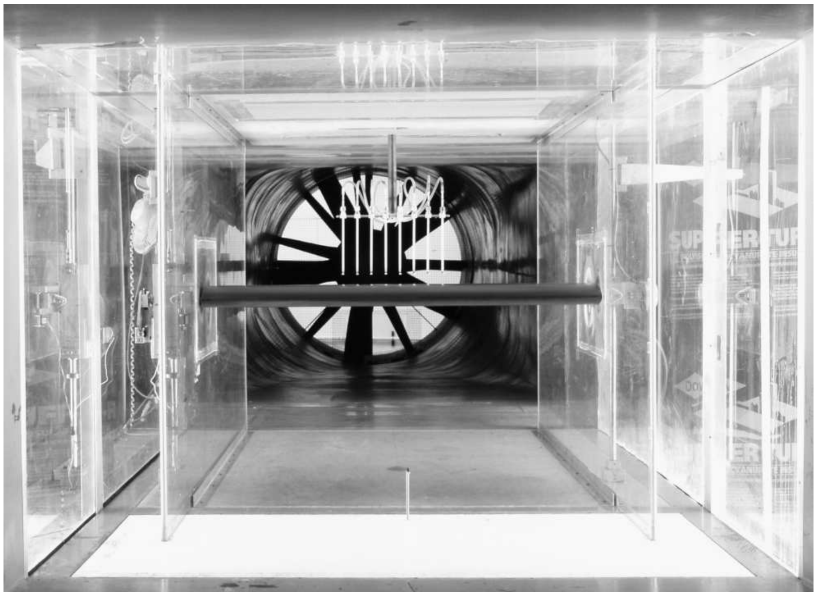

Figure 3.2: Photograph of wind tunnel test section (taken from Ref. 31).

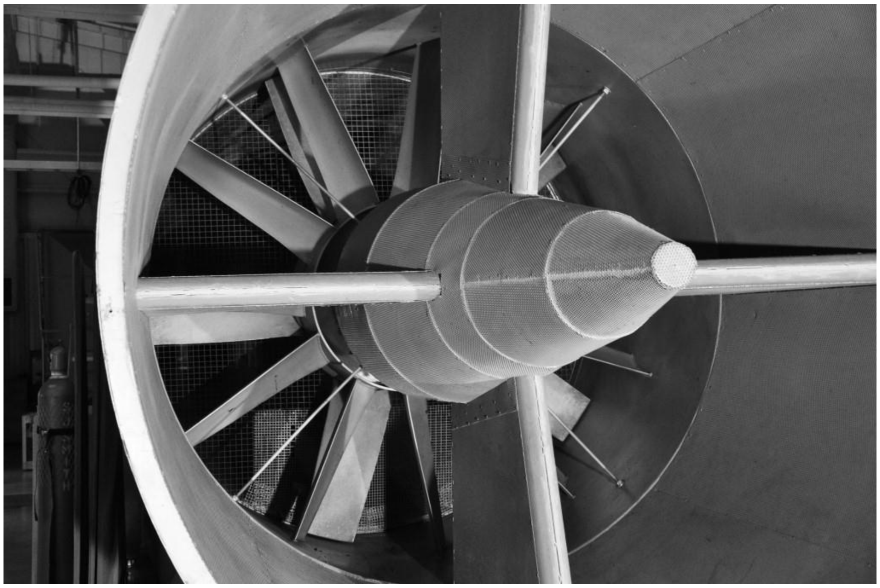

Figure 3.3: Photograph of wind tunnel fan and stators.

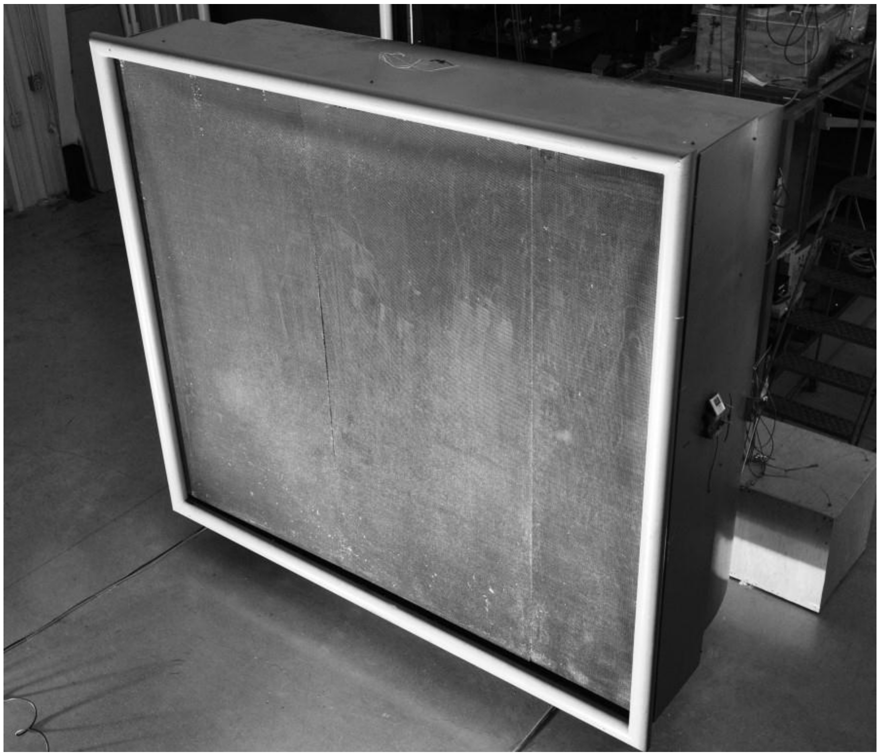

Figure 3.4: Photograph of wind tunnel inlet showing the honeycomb.

3.2 Models

The standard model tested with the LSATs setup has a span of 33 5/8 in and a chord length of 12 in. The mounting holes required to mount the airfoil in the LSATs setup described in Section 3.3 are spaced 5-in apart with the first hole located 2 in from the leading edge. A schematic of the model construction requirements can be found in Refs. 5 and 34.

The four airfoils that were tested for this research can be seen in Fig. 3.5. The first two airfoils plotted in Fig. 3.5 are the AG40d-02r and AG455ct-02r. The AG40d-02r had a 25% of chord flap, and the AG455ct-02r had a 30% of chord flap. Both the AG40d-02r and AG455ct-02r flaps were hinged on the lower surface. The hinge locations are marked by an "×" in Fig. 3.5. The last two airfoils plotted in Fig. 3.5 are the W1011 and W1015. The W1011 and W1015 were designed by the author using PROFOIL and are symmetrical. The W1011 and W1015 were each tested with two different flap sizes. For this research, a 20% and 30% of chord flaps were chosen. The W1011 and W1015 were hinged on the airfoil chord line to maintain symmetry. The hinge locations for the 20% and 30% of chord flaps are marked by an "×" in Fig. 3.5.

The AG455ct-02r airfoil had a preset absolute flap deflection of -2 deg incorporated into the airfoil coordinates. As seen in Fig. 3.6, the chord line was referenced to this configuration. Thus, the angle of attack was also referenced to this configuration. The convention for defining the flap deflections used in Chapter 6 can be seen in Fig. 3.6. The same flap and angle of attack conventions are used for the AG40d-02r airfoil. Since both the AG40d-02r and AG455ct-02r airfoils were designed to be used on RC sailplanes, the flaps were not conventional. The AG455ct-02r airfoil set to an absolute flap deflection of -2 deg had a 2-deg inside corner on the upper surface while the lower surface was flat. For an absolute flap deflection of 0 deg, the lower surface had a 2-deg inside corner while the upper surface was flat [35]. The same holds true for the AG40d-02r airfoil.

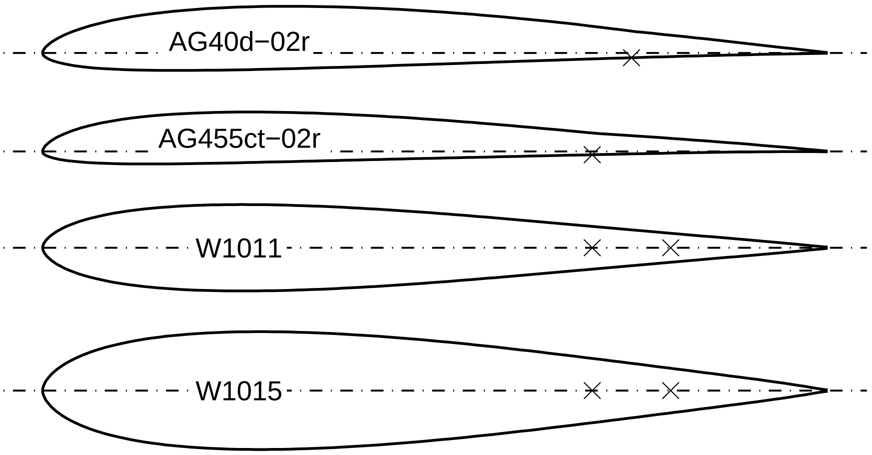

Figure 3.5: Schematic of airfoils tested showing hinge locations.

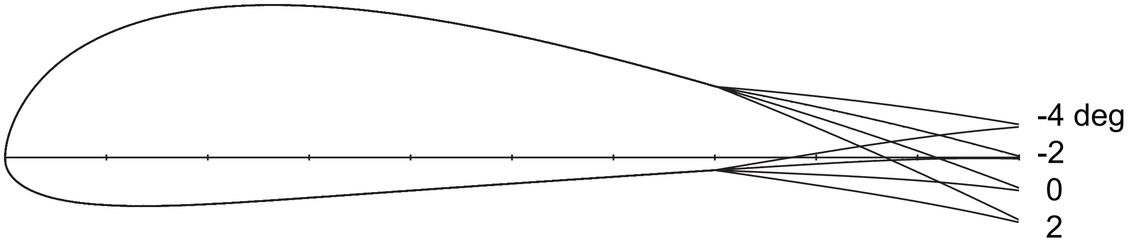

Figure 3.6: AG455ct-02r airfoil with four flap positions −4, −2, 0, +2 deg, shown with the vertical scale exaggerated 3X (taken from personal communications with Drela [35]).

The W1011 and W1015 airfoils employed an interchangeable flap system that allowed any size flap under 30% of chord to be tested on a single front section as seen in Fig. 3.7. As mentioned earlier, two flap sizes (20% and 30% of chord) for each airfoil were chosen for this research. The interchangeable flaps attached to the front portion of the model at the solid vertical line indicated in Fig. 3.7. The interchangeable flap system proved to be advantageous at low Reynolds numbers where airfoil performance is dependent on the laminar boundary layer. With low Reynolds number airfoils, the front 50% to 70% of the airfoil is the most critical due to its effect on boundary layer transition from laminar-to-turbulent flow. The interchangeable flap design allowed this critical portion of the airfoil to stay identical for all flap tests providing a better basis for comparison.

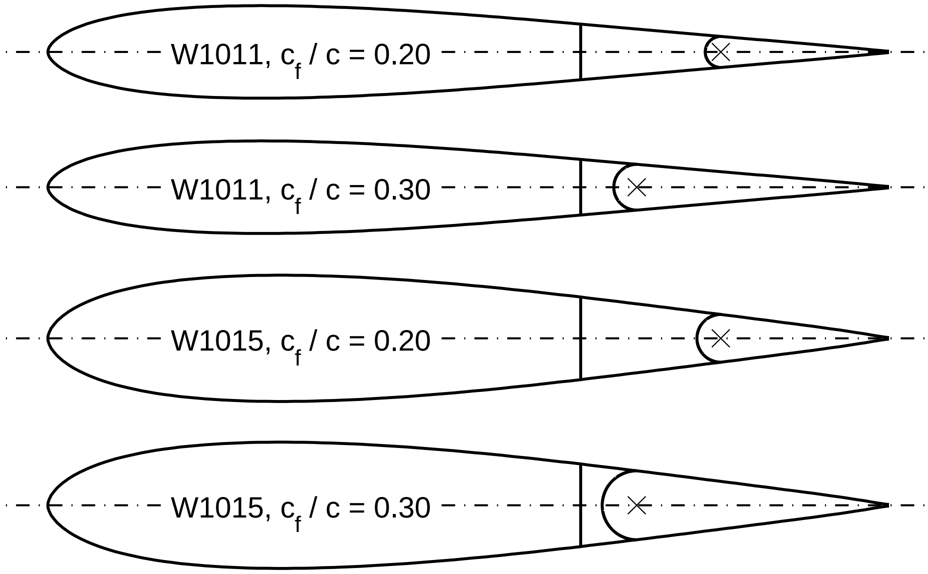

Figure 3.7: Schematic of the W1011 and W1015 airfoils showing the interchangeable flap system with the two selected flap sizes.

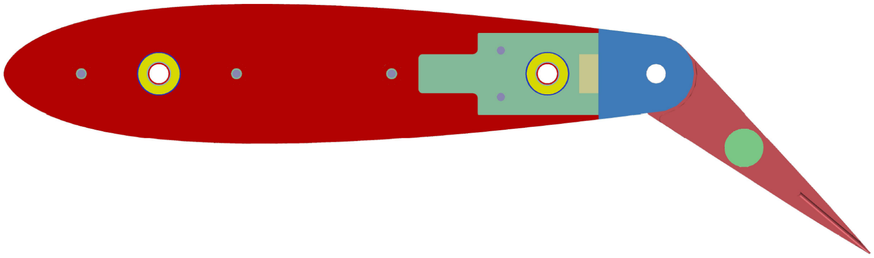

Figure 3.8: Side profile of the CAD model for the 30% of chord flapped W1015 airfoil with $\delta_f = 40$ deg.

The AG40d-02r and AG455ct-02r airfoil models were built by Mark Drela, et al. [9] in the early 2000s. The W1011 and W1015 airfoil models were specifically designed and manufactured for this research. The models were designed by the author using the computer-aided design (CAD) package Pro/ENGINEER Wildfire 4.0. A side profile of the CAD model for the 30% of chord flapped W1015 airfoil with a 40-deg flap can be seen in Fig. 3.8. The front portion of the airfoil models were built by Sean Cassidy and consisted of foam cores wrapped in fiberglass with aluminum end plates to act as sanding guides. The removable flaps and components were manufactured using a stereolithography (SLA) process by Realize,® Inc. of Indianapolis, IN. The material used to manufacture the flaps and supporting components was Accura® Xtreme plastic. The strength and stiffness of the Accura® Xtreme material is average for most SLA plastics. With the Accura® Xtreme material, the flaps and supporting components could be manufactured as one piece eliminating piecewise construction and glue joints. More information regarding the manufacturing capabilities of Realize,® Inc. and material properties of the Accura® Xtreme plastic can be found on the Realize® Inc. website [36].

The interchangeable flap system consisted of two components (“flap attach bracket” and “flap”) each made with the SLA Accura® Xtreme plastic previously described. The “flap attach bracket” connected the “flap” to the front portion of the model. The “flap attach bracket” connected to the front portion of the model via several #6-32 socket cap screws that fastened into an aluminum bar at the rear of the front portion of the model. An exploded view of the CAD model for the 30% of chord flapped W1015 airfoil showing the “flap,” “flap attach bracket,” and front portion of the model separated from each other in Fig. 3.9.

With any experimental test involving airfoils, it is imperative that airfoil models are built with extreme accuracy. Thus, determining the accuracy of the models was extremely important. In order to check the accuracy of each model, a Brown & Sharpe MicroVal® coordinate measuring machine (CMM) was used to digitize each model. The digitizing was accomplished by taking approximately 80 points around the entire airfoil. The spacing between the points was estimated by using the local radius of curvature. A higher density of points was taken near the leading edge due to the small radius of curvature, and a lower density of points was taken in the midsection due to the proportionately large radius of curvature. The accuracy of each model is graphically depicted in Chapter 6 and tabulated in Appendix A.

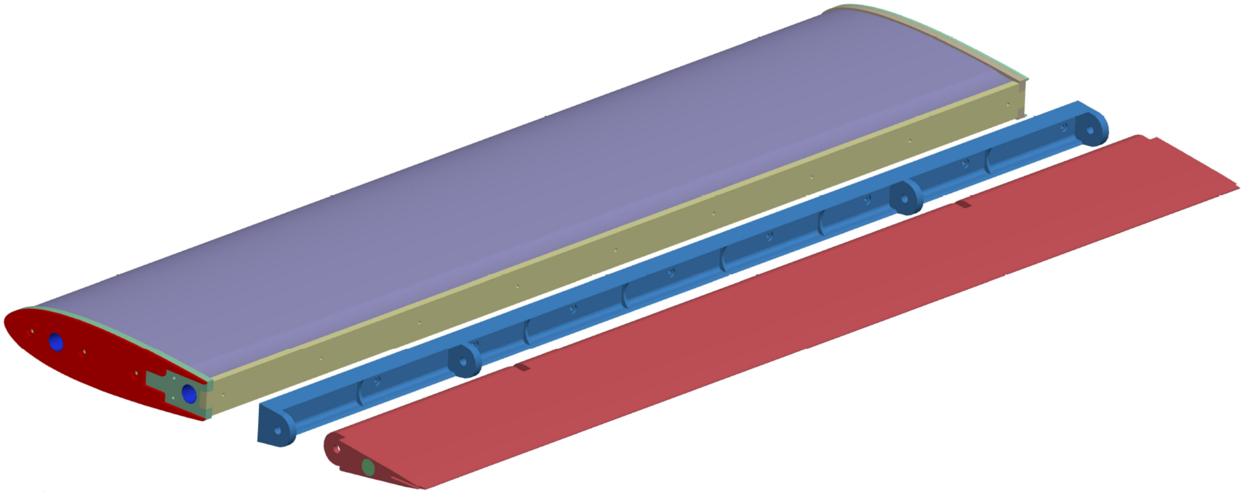

Figure 3.9: Exploded isometric view of the CAD model for the 30% of chord flapped W1015 airfoil.

3.3 Experimental Setup

The LSATs experimental setup, depicted in Fig. 3.10, has several unique features that make it distinct from all the other experimental setups used in the UIUC low-turbulence subsonic wind tunnel. Wind tunnel models are mounted horizontally in the test section between two 3/8-in Plexiglas® splitter plates, which are not shown in Fig. 3.10 for clarity. The splitter plates are 6-ft long and span the height of the tunnel. The purpose of the splitter plates was to isolate the model from the rest of the experimental rigging necessary to obtain lift and moment data. The gap between the model and the splitter plates was nominally 0.05 in. It was extremely important that a gap existed between the model and the splitter plates so that the model was metric to the balance. This gap was checked several times before and during random runs to ensure a gap existed.

On the outer sides of each Plexiglas® splitter plate, a precision stainless steel rod was mounted vertically between the floor and ceiling of the tunnel. The precision rod was firmly mounted to both the ceiling and the floor via two three-degree of freedom mounts. Three degrees of freedom were necessary to allow for proper alignment of the precision rod with respect to one another and the tunnel. Great care was taken to ensure proper alignment of both precision rods. The left-hand side of the model (far side in Fig. 3.10) was free to pivot up and down and rotate (change angle of attack) providing two degrees of freedom. These two degrees of freedom allowed for the proper measurements of lift and moment forces. At this end of the model, the angle of attack was determined using a precision potentiometer. A more detailed explanation of the angle of attack determination can be found in Subsection 3.5.5.

The right-hand side of the model (close side in Fig. 3.10) was connected to the lift carriage which was free to glide up and down the precision rod on linear bearings. The up and down motion of the lift carriage provided one degree

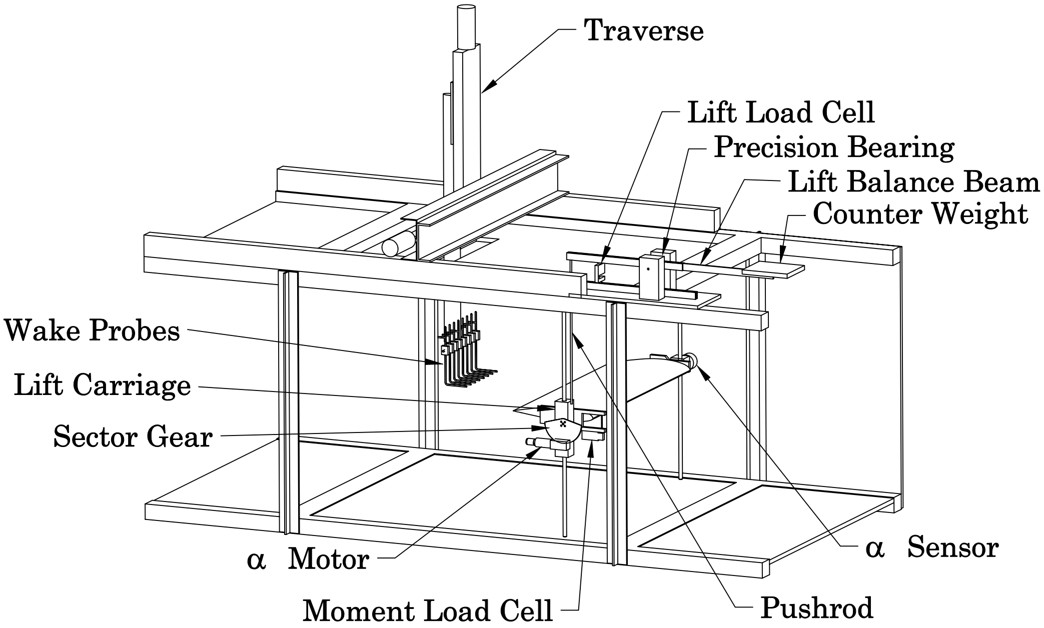

Figure 3.10: Experimental Setup (Plexiglas$^{®}$ splitter plates and traverse enclosure box not shown for clarity) (taken from Ref. 33).

of freedom that allowed for the accurate measurement of the lift force. Linear bearing were employed to remove any stiction issues with the lift carriage that could tamper with the lift force measurement. The lift carriage was connected to the lift balance with a pushrod as seen in Fig. 3.10. The pushrod effectively transferred the lifting load to the lift load cell. A more in-depth discussion about the lift measurement can be found in Subsection 3.5.1. The angle of attack was set by a worm gear that drove a sector gear. The worm was driven by an electric motor controlled by the computer. The computer was able to send the correct signals to the motor because it used the precision potentiometer located on the left-hand side of the model to determine angle of attack measurement. By employing this method, the angle of attack could be set with great accuracy.

The models were connected to the lift carriage and the angle of attack rig via four (two per side) steel pins as shown in Fig. 3.11. The pins pass through ball joint swivel bearings that were firmly mounted to the lift carriage and angle of attack rig. The ball joints allowed the pins to slide in and out (z-direction) and rotate freely in all axes, but they constrained the pins in the x and y directions providing an efficient route for load transfer. The x-axis is aligned with the freestream, and the y-axis is aligned with the lift vector (normal to the freestream). Therefore, the z-axis defines the spanwise direction. The pins passed through slots in the Plexiglas$^{®}$ splitter plates that allow the angle of attack to be varied without hitting the splitter plates ensuring the model stayed metric to the balance. In order to minimize leakage through the slots in the splitter plates, thin plastic wafers were employed. The pins slide into the

Figure 3.11: Photograph of airfoil mounting system.

model mounting holes previously described in Section 3.2. Set screws firmly anchored the model to the steel pins on the lift carriage side only to constrain the model in the z-direction and keep it from contacting the splitter plates. On the angle of attack side (far side in Fig. 3.10), linear bearing inserts were slid into the model mounting holes. These linear bearings unconstrained the model from translating in the z-direction providing another degree of freedom.

Drag measurements were calculated using the momentum deficit method that will be described in Subsection 3.5.3. The momentum deficit method requires pressure measurements of the airfoil wake. In order to obtain the pressure measurements, the wake probes must be movable. A two-axis traverse mounted on top of the wind tunnel seen in Fig. 3.10 was used to move pressure probes. The plenum box that encloses the traverse to prevent leakage into the tunnel is not shown in Fig. 3.10 for clarity. The traverse was manufactured by LinTech® and consists of a vertical and horizontal axis. The traverse was driven by ball lead screws to eliminate slop in the gearing mechanisms. The lead screws were turned with computer controlled stepper motors. Each axis was equipped with a linear encoder to determine the position and send feedback to the steeper motor controller to ensure accurate positioning with virtually no error. The wake probes used to obtain the wake pressure measurements were attached to a 3-ft long boom that extended into the tunnel test section. A more detailed discussion on the drag measurement techniques can be found in Subsection 3.5.3.

3.4 Flow Quality

With any wind tunnel, the ability to produce reliable data is primarily affected by the wind tunnel flow quality [20]. The flow quality of the UIUC low-turbulence subsonic wind tunnel has been studied multiple times and continues to produce high quality flows. In the subsections that follow, a brief overview of the different flow qualities of interest will be discussed. For a comprehensive discussion of the following, refer to Ref. 8. The following discussion should instill confidence in the reader that the wind tunnel exhibits good flow qualities, and that the LSATs test apparatus did not adversely affect the flow quality of the wind tunnel.

3.4.1 Turbulence Intensity

As previously discussed in Section 3.1, the turbulence intensity is of utmost importance when testing at low Reynolds numbers. In Section 3.1, it was stated that the turbulence intensity of the empty test section was less than 0.10%. This value was not representative of the actual turbulence intensity when the LSATs test apparatus was installed because the tunnel test section was no longer empty. The effects of the splitter plates and other LSATs components on the turbulence intensity have been previous documented [8], and the results of their study can be seen in Fig. 3.12.

The effect of the LSATs test apparatus on the turbulence intensity was not constant with respect to Reynolds number. It can be seen from Fig. 3.12 that at Reynolds number of 100,000 the turbulence intensity was relatively unchanged, but there was a significant increase at $Re \geq$ 200,000. By adding a 3-Hz high-pass filter, the turbulence intensity returns to relatively unchanged state. This result suggests the LSATs test apparatus mainly affected the low frequency range by adding velocity fluctuations [8].

3.4.2 Freestream Velocity

A uniform freestream velocity is imperative in obtaining accurate force measurements. The ideal condition is to have a perfectly uniform velocity throughout the entire test section, but obtaining this flow is not practical. Small variations in velocity exist owing to the tunnel walls and the streamline curvature caused by the contraction from the inlet to the test section. Therefore, determining the uniformity of the flow was necessary. The freestream uniformity was previously documented [8], and the results of their study can be seen in Figs. 3.13 and 3.14. Figure 3.13 shows the dynamic pressure variations across the tunnel when the test section was empty. Figure 3.14 shows the dynamic pressure variations across the tunnel with the LSATs test apparatus installed without a model. It should be noted that Figs. 3.13 and 3.14 represents the pressure difference between an upstream probe and a downstream probe. The upstream probe was mounted near the entrance of the splitter plates that was located 1.323 ft upstream of the plane

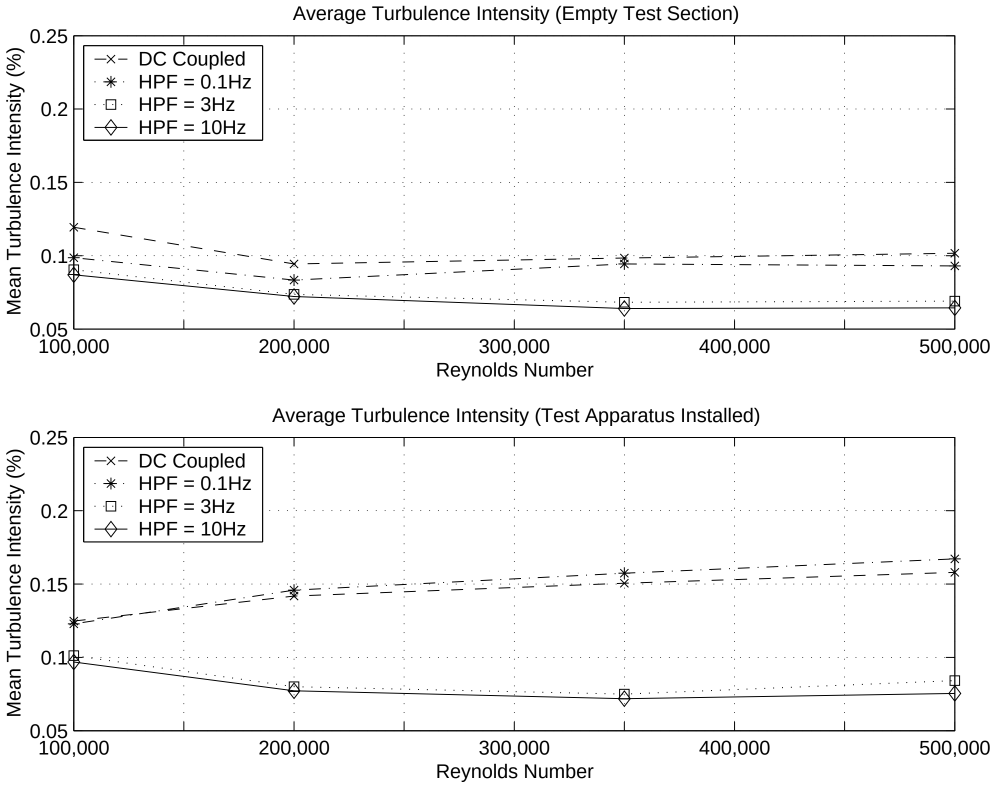

Figure 3.12: Turbulence intensity taken at tunnel center with the LSATs test apparatus installed with no model (taken from Ref. 8).

defined by the model quarter chord location. The downstream probe was traversed within the plane defined by the model quarter chord.

By comparing the two plots, it can be seen that the when the LSATs test apparatus was installed there was an increase in the velocity across the entire surveyed section. This increase in velocity was more than likely due to the blockage of the rigging outside of the splitter plates as well as the boundary layer growth on the splitter plates, which also creates some blockage due to the boundary layer displacement thickness. It is interesting to note that there was a larger discrepancy between cases for lower Reynolds numbers. This discrepancy was more than likely caused by the thicker boundary layer forming over the splitter plates as well as the tunnel walls. The thicker boundary layer would create more blockage and artificially make the test section smaller [8]. The non-uniform freestream velocity effects were taken into account when the data reduction was performed.

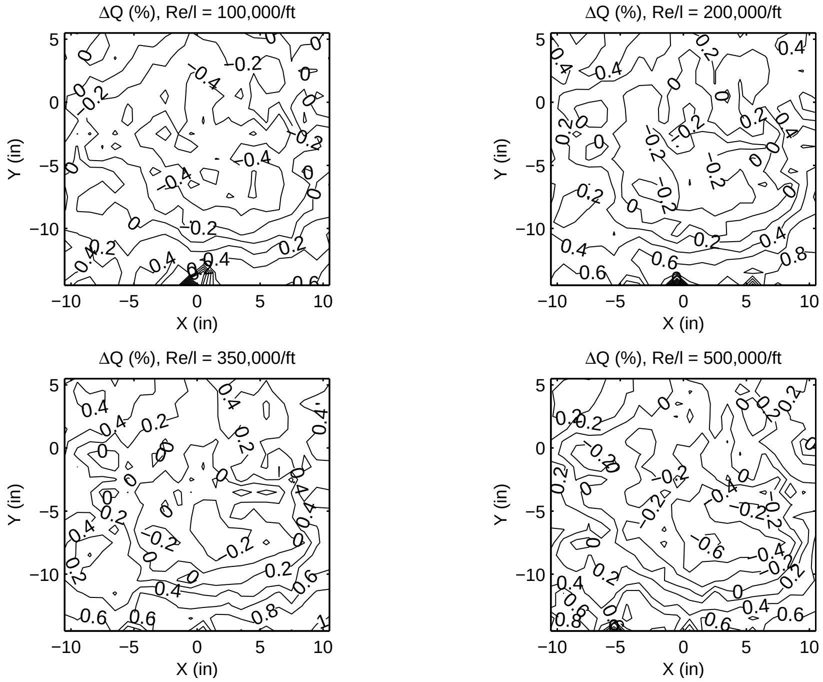

Figure 3.13: Dynamic pressure variations across the test section when empty (taken from Ref. 8).

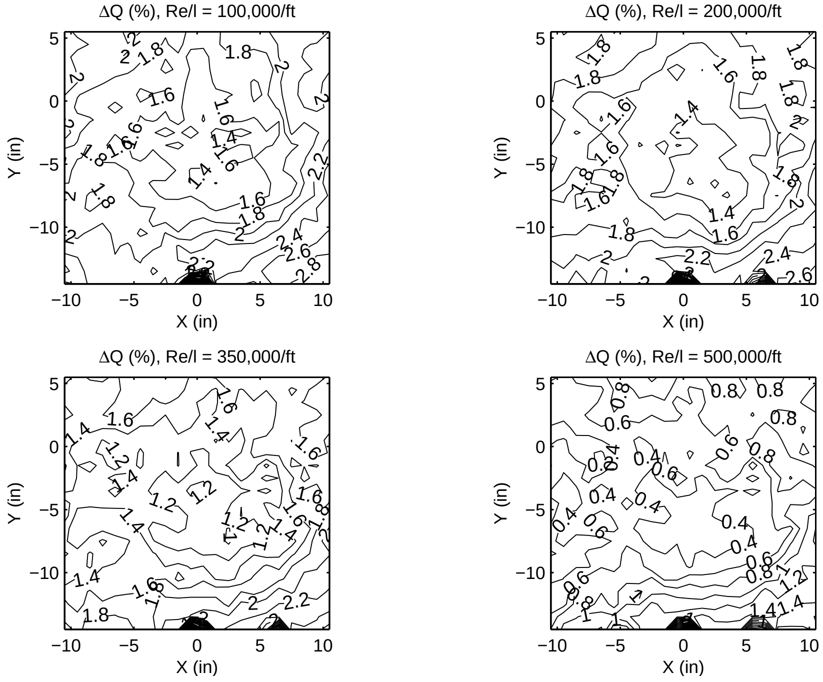

Figure 3.14: Dynamic pressure variations across the test section with LSATs test apparatus installed (taken from Ref. 8).

3.4.3 Freestream Flow Angularity

Just as important as the freestream velocity discussed in Subsection 3.4.2, is the freestream angularity. The freestream angularity is the measure of how parallel the flow is to the axial direction (x-axis). The dilemma with flow angularity does not lie in the employment of pitot static probes because they are insensitive to flows that are ± 12 deg. Instead, flow angularity can induce an artificial angle of attack (α) that would produce skewed performance plots because they are plotted verses α. Therefore, it was important to know the flow angularity within the test section. As with the other flow quality characteristics, the flow angularity has been previous documented [8], and the results of their study can be seen in Fig. 3.15. Figure 3.15 shows the pitch flow angularity across the test section with the LSATs test apparatus installed without a model. The yaw angle was also measured and can be found in Ref. 8. With airfoil testing, the pitch angle is the most important because it directly affects the angle of attack. The flow angularity was determined using a 7-hole probe located 1.5 chord lengths behind the plane defined by the model quarter chord. The chord length was defined in Section 3.2 to be 12 in.

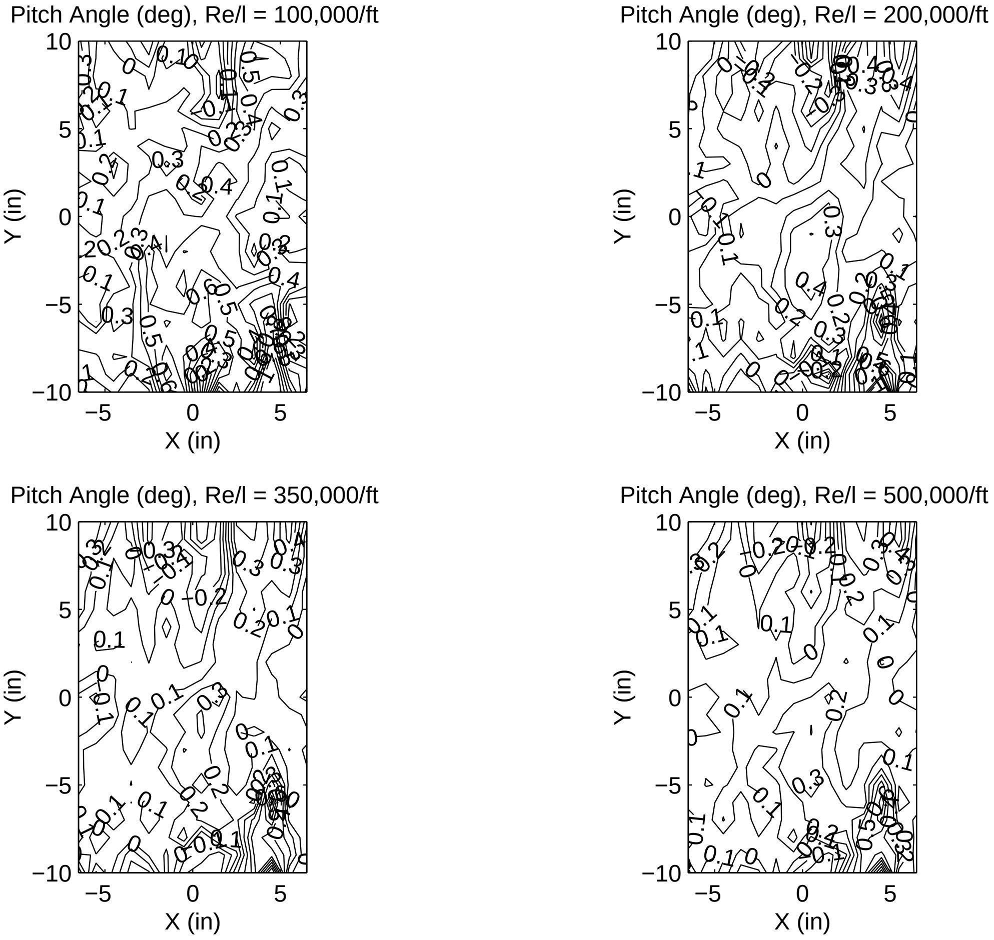

Figure 3.15: Pitch angle variations across the test section with LSATs test apparatus installed (taken from Ref. 8).

It can be seen in Fig. 3.15 that the flow was not perfectly parallel to the axial direction. The minimum pitch angle was obtained at a Reynolds number of 500,000 and grew larger as Reynolds number decreased. At a Reynolds number of 500,000, the pitch angle varied from 0 to 0.2 deg across the region of interest. This range corresponds to a variation of ± 0.1 deg. The maximum preferred flow angularity according to Ref. 37 is ± 0.1 deg.

3.5 Experimental Measurements

In order to obtain the desired non-dimensional aerodynamic coefficients (C_d, C_l, and C_m) and performance plots, the following quantities were measured in the wind tunnel experiments:

- angle of attack (deg)
- lift (lb)
- drag (lb)
- moment (ft-lb)
- freestream velocity (ft/sec)
- density ($slug/ft^3$)
- atmospheric pressure (lb/ft^2)
- temperature (^oR)

In the following subsections, the methods used to obtain these experimental values will be discussed.

3.5.1 Lift Measurement

The lift force is the first of the three critical measurements needed to fully define airfoil performance. To measure the lift force, the LSATs lift beam balance was used. A schematic of the lift beam balance can be seen in Fig. 3.16. The lift beam balance was made up of the following components:

- fulcrum
- load cell
- compression spring
- counterweights

For the pivot point of the fulcrum, two spherical ball bearings were used with one on each side of the fulcrum beam. The bearings were used to reduce friction associated with the fulcrum that could tamper with the lift force

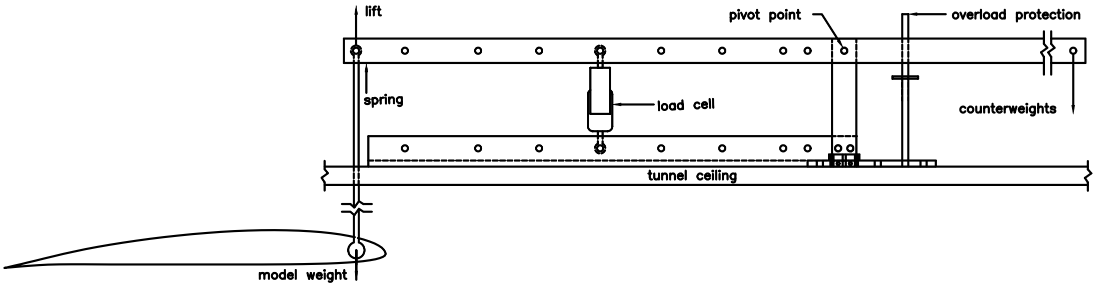

Figure 3.16: LSATs lift beam balance (taken from Ref. 7).

measurement. A strain gage load cell was used to constrain the fulcrum from rotating when a load was applied to it. The lift load was transferred from the lift carriage, described in Section 3.3, to the fulcrum via the pushrod seen in Fig. 3.10. The load cells that were used could only be loaded in tension, which presented a problem. Most airfoils can produced negative lift if the angle of attack is low enough placing a compressive load on the load cell. Thus, counterweights were added to the other side (right side in Fig. 3.16) of the fulcrum to put the load cell in tension when a zero lift force was applied. A compression spring was used near the pushrod attachment point seen in Fig. 3.16 to counteract the weight of the model and to ensure the fulcrum was level when no load was applied. The fulcrum was leveled to ensure the load cell would be loaded entirely in the load cell axial direction with no side force.

The lift force had a strong dependence on Reynolds number. If the Reynolds number was doubled, the lift force would quadruple. The difference in the lift force can vary drastically with the range of Reynolds numbers that can be tested with the LSATs setup discussed in Section 3.1. The lift force also had a dependence on the type of airfoil which was being tested. Some airfoils are designed to attain high lift coefficients while others are designed to attain lower lift coefficients. Therefore, the dependence of the airfoil type was directly related to the range of lift coefficients achieved by an airfoil. In order to have the ability to test such a plethora of airfoils and Reynolds numbers, different loads cells and hole locations for the load cells were used. Depending on the Reynolds number and lift coefficients expected, one of three load cells could be chosen to be place in one of nine hole locations on the lift balance beam. The load cells, manufactured by Interface, Inc., used for these tests had a maximum load capacity of 10, 25, and 50 lb. Each time a new load cell or new hole location was chosen, the load cell was calibrated to ensure proper measurements of the lift force were taken. The lift beam balance has been proven to be repeatable to 0.01% [31].

3.5.2 Pitching Moment Measurement

The pitching moment is the second of the three critical measurements needed to fully define airfoil performance. To measure the pitching moment, the moment balance was used. A cut-away diagram of the moment balance can be

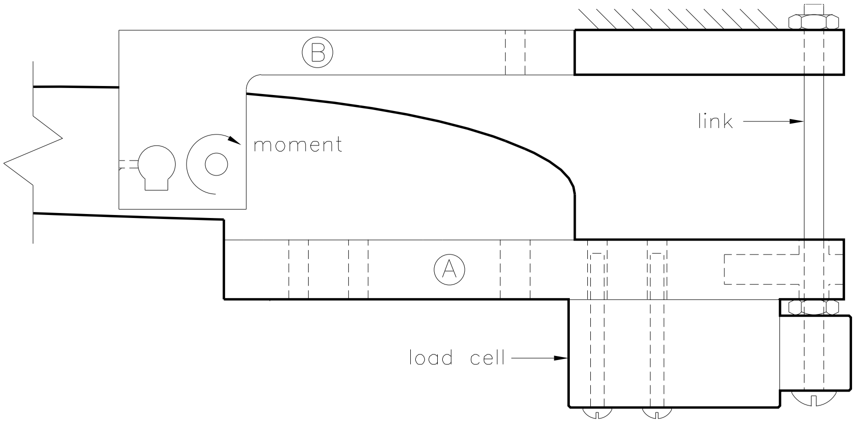

Figure 3.17: LSATs moment balance (taken from Ref. 7).

seen in Fig. 3.17. A 10-lb bidirectional strain gage load cell manufactured by Interface, Inc. was used to measure the force between two parallel members. Member A from Fig. 3.17 is attached to the airfoil and was allowed to freely rotate while member B was firmly attached to the lift carriage. Therefore, any force trying to pitch the airfoil could be captured. There are two locations on member A and B for the load cell to mount allowing for the measurement of vastly varying airfoil pitching moments. The force measured by the load cell was mathematically transferred to the quarter chord location to provide the standard pitching moment coefficient about the quarter chord of the airfoil. In a few cases that involved highly flapped airfoils, the test range was restricted so as not to exceed the pitching moment load cell limits. These few cases mainly occurred for Reynolds numbers around the upper limit of the LSATs setup.

3.5.3 Drag Measurement

The 2-D drag force is the last of the three critical measurements needed to fully define airfoil performance, but it is also the most difficult to accurately measure. The drag force of an airfoil is typically one to two orders of magnitude smaller than the lift force. With loads this small with respect to the lift force, a traditional balance is typically not accurate because of load cell inaccuracies when measuring forces that represent a small percentage of its full scale capacity. When using a balance to capture the drag force, it not only captures 2-D airfoil drag but also other 3-D effects that do not contribute to 2-D airfoil drag. With splitter plates, a balance would capture the 3-D effects owing to the small gaps between the splitter plates and model and the interference drag between the splitter plates and the model. In the case of flapped models, a balance would also capture the drag produced by the flap brackets used to constrain the flap. In order to avoid all of the issues associated with measuring 2-D drag with a balance, the momentum deficit method was used to determine the drag on the airfoils. A schematic of the control volume used for the derivation of the momentum deficit method can be seen in Fig. 3.18. The momentum deficit method was developed by Jones [38], and the final result of the derivation is given by

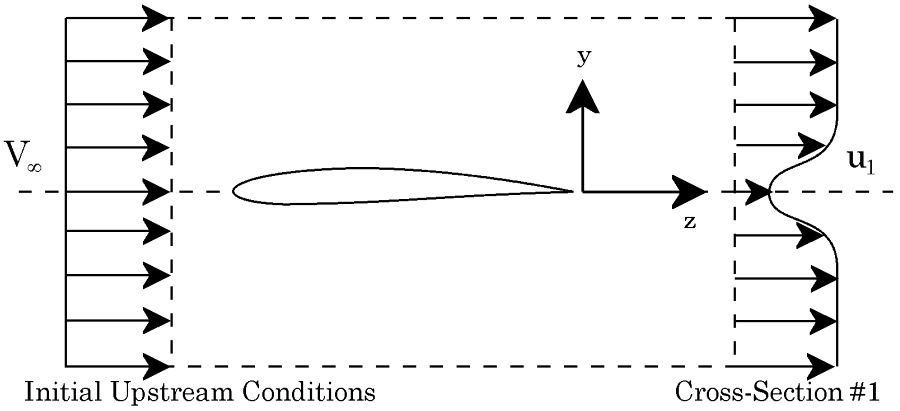

Figure 3.18: Control volume for the 2-D momentum deficit method used to determine the profile drag (taken from Ref. 31).

$$d = \int_{-\infty}^{\infty} \sqrt{q_\infty - \Delta P_0}\left(\sqrt{q_\infty} - \sqrt{q_\infty - \Delta P_0}\right) dy \tag{3.1}$$

The wake measurements were taken approximately 1.25 chord lengths (14.8 in.) behind the trailing edge of the model to ensure the wake had relaxed back to the test section static pressure to satisfy a requirement of Eq. 3.1. This distance proved to be adequate for the wake to relax as seen by the good agreement of the validation data in Chapter 4. The wake required 20 to 130 points nominally space 0.08 in apart to be fully defined depending on the size of the wake. The size of the wake was dependent on flap size, flap deflection angle, angle of attack, and Reynolds number. Only enough angles of attack were taken to define the drag bucket of the airfoil because of the time intensive process of collecting wake data. Wake data collection in stalled region was avoided owing to the size and unsteady effects in the wake caused by separation of the boundary layer from the airfoil surface.

The pressure measurements in the wake were taken using the Baratron® Model 220 differential pressure transducer manufactured by MKS Instruments. As the name implies, the transducer measures the difference in pressure between two inputs. In the case of the wake measurements, the pressure difference was measured between the total pressure ahead of the airfoil and the total pressure in the wake. The transducer had a 1-Torr (1-mm HG or 0.02-psia) full-scale range and a resolution of 0.01% of the full-scale range. The accuracy of the transducer was 0.15% of reading. The transducer was temperature controlled at 45^oC and signal conditioning was performed within the transducer housing. Therefore, the output from the transducer was 0 to 10 V with 10 V being 1 Torr. The transducer was calibrated at the factory and allowed for accurate measurements out of the box so to speak. A complete description of the product can be found on the manufacture's website [39].

Due to the spanwise variation in drag especially apparent at low Reynolds numbers [40], multiple spanwise locations were surveyed and averaged together to provide accurate and consistent drag measurements. The wake rake used to survey the wakes had eight pitot static probes each connected to a Baratron® differential pressure transducers. The probes were equally spaced 1.5 in apart and were positioned to survey the center 10.5 in of the model. The spanwise variations in drag measurements were more pronounced at lower Reynolds numbers ($Re \leq$ 100,000) and seemed to all but disappear at higher Reynolds numbers ($Re \geq$ 200,000). The lower Reynolds numbers may be more susceptible to spanwise variations owing to that fact that the boundary layer at $Re \leq$ 100,000 is more unstable and susceptible to laminar separation bubbles and unsteady effects. The variations may also be caused by measurement inaccuracies. The pressure differentials being measured at $Re \leq$ 100,000 are much smaller than at $Re \geq$ 200,000 leading to difficulties in resolving the small pressure differences. A thorough discussion on spanwise variations of profile drag can be found in Ref. 41.

3.5.4 Freestream Flow Measurement

The performance of low Reynolds number airfoils is highly dependent on the Reynolds number that is being tested. Therefore, it was extremely important to accurately determine the freestream velocity in the test section. A standard approach most tunnels take in determining the freestream velocity is to measure the static pressures at the inlet and test section. The velocity can be determined by applying Bernoulli's principle. Since the LSATs setup used splitter plates and mounts hardware in the tunnel that creates extra blockage, the standard approach did not work. Instead, a pitot static probe located near the entrance of splitter plates was used to determine the freestream velocity. The probe was located 5.2 in above the floor of the tunnel and 15.9 in ahead of the plane defined by the model quarter chord.

The pressure difference between the total and static pressures was measured to determine the freestream velocity. This measurement was taken using a differential pressure transducer with the total and static pressures occupying the two inputs. Depending of the speed at which the tests were run, two different differential pressure transducers were employed. When the tests were below a Reynolds number of 250,000 based on the airfoil chord, a 1-Torr Baratron® Model 220 differential pressure transducer described in Subsection 3.5.3 was used. When the tests were above a Reynolds number of 250,000 based on airfoil chord, a non-temperature controlled 10-Torr Baratron® Model 221 differential pressure transducers was used. More information about the Baratron® Model 221 can be found on the MKS Instruments website [42].

The freestream velocity can be calculated by using

$$V_\infty = \sqrt{\frac{2q_\infty}{\rho}} \tag{3.2}$$

where q_∞ is the freestream dynamic pressure and ρ is the density. The density is dependent on the pressure and temperature and can be calculated from

$$\rho = \frac{P_{atm}}{RT} \tag{3.3}$$

where P_{atm} is the local atmospheric pressure and T is the ambient temperature. The temperature was determined using an Omega Model CJ thermocouple mounted to the side of the tunnel inlet at the elevation of the model. The thermocouple had an accuracy of $\pm 1\ ^oR$.

Since the pitot static probe was located relatively close to the leading edge of the airfoil model, the circulation created by the airfoil was taken into account to ensure accurate freestream velocity measurements. An in-depth discussion of the necessary corrections when using splitter plates can be found in Ref. 43.

3.5.5 Angle of Attack Determination

The performance of airfoils are generally viewed with respect to angle of attack. Therefore, it was important to know the angle at which the models were being tested. The angle of attack was determined using a Bourns 9545EP precision potentiometer located on the left side of the model seen in Fig. 3.19. The airfoil was connected to the angle of attack test apparatus using two steel pins described in Section 3.3. The voltage from the potentiometer was signal conditioned and then read into the data acquisition (DAQ) board. The potentiometer was calibrated after the LSATs test apparatus was installed to ensure accurate measurements. The uncertainty of the angle of attack measurement can be found in Section 3.7.

3.6 Data Acquisition and Reduction

All of the measurements taken during the experiments were recorded with a Dell 1.4-GHz Precision-330 computer. All measurements taken with LSATs setup were analog and required conversion to digital. The conversion was accomplished with a National Instruments NI PCI-6031E 16-bit analog-to-digital DAQ board. The resolution of the NI PCI-6031E DAQ board is 0.0015% of the full-scale reading. The board was capable of handling 32 differential input channels and two 16-bit digital-to-analog output channels. An accuracy of ±0.305 mV for a full-scale range of ±10 V was achieved using the 16-bit resolution of the DAQ board.

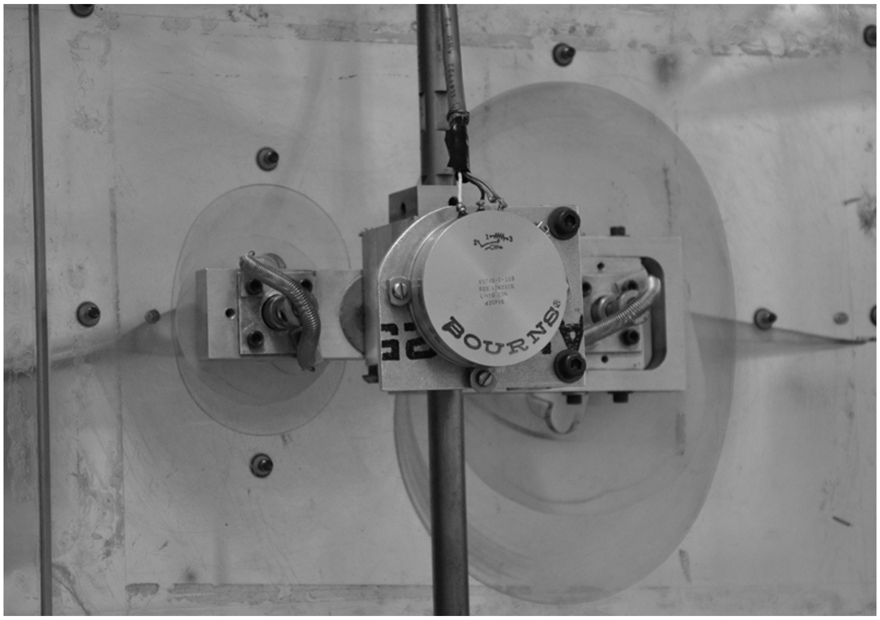

Figure 3.19: Photograph the angle of attack rig on the left side of the model.

After initial inputs into the LabWindows™ code, the entire data acquisition process was fully autonomous. The automation handled setting the speed of the wind tunnel to maintain a constant Reynolds number. It also plotted the raw data to the computer screen and recorded it for future data reduction. In order to remove any time-dependencies that occur with any wind tunnel experiment, all of the measurements were taken simultaneously.

Since wind tunnels have walls that bound the flow, they do not perfectly mimic nature. Therefore, corrections needed to be implemented to correct the raw data sets and create reduced data sets. The walls cause four phenomena to occur [37]: wake blockage, streamline curvature, buoyancy, and solid blockage. These effects were taken into account during the data reduction process. An in-depth discussion of each of the four effects can be found in Refs. 37 and 5. The splitter plates and LSATs hardware that were mounted in tunnel created more blockage that affected the freestream velocity as discussed in Subsection 3.5.4. Therefore, additional velocity corrections needed to be made. The additional corrections and further details can be found in Ref 5. The requisite equations to correct the measured quantities of C_d, C_l, C_m, and α can be found in Ref. 31.

3.7 Calibrations and Uncertainty

Calibration of instruments was necessary to ensure the experimental data was correct. The calibration process and uncertainty values for certain quantities will be presented in the following discussion. Detailed information regarding the processes used to determine the uncertainty values can be found in Ref. 41.

The first quantity of interest is the freestream velocity because it was used to determine the Reynolds number and to nondimensionalize the lift, drag, and moment forces. Therefore, it was extremely important that the freestream velocity was precise and accurate. The largest uncertainty with the freestream velocity was the variations in the flow angularity which was stated to be 1% [31]. If no errors associated with the pitot static probe are included, then the resulting uncertainty of the freestream velocity was determined to be 0.3% [41].

For the lift measurements, one of three load cells located in one of nine hole locations can be chosen based upon the testing conditions as discussed in Subsection 3.5.1. Each time a new load cell or new hole location was chosen, the load cell was calibrated to ensure accurate lift force measurements were taken. A load cell was calibrated by first loading it to its maximum capacity by adding extra weights to the counterweights section of the lift beam balance as seen in Fig. 3.16. Second, the load cell was unloaded and reloaded by adding and subtracting precision weights respectively. Data points were taken each time a precision weight was added or subtracted. The precision weights were chosen to provide a total of 14 to 18 data points that were used in a linear regression. The slope of the line from the linear regression was used to determine the lift force during experimental runs. The overall uncertainty for the lift coefficient was estimated to be 1.5% [31].

The moment load cell was calibrated in similar way to the lift load cells. The bi-directional load cell was loaded then unloaded by adding and subtracting precision weights respectively, and data points were taken each time a weight was added or subtracted. The weights were selected to provide a total 16 to 18 data points that were used in a linear regression. The slope of the line from the linear regression was used to determine the moment force during experimental runs. A photograph of the calibration process for the moment load cell can be seen in Fig. 3.20. Before each data set was taken, a moment tare was performed with increasing and decreasing values of angle of attack to remove variations in moment measurements owing to shifts in the airfoil center of gravity. A nonlinear fit was applied to the moment tare data to determine the tare value at any angle of attack.

For the drag measurement, differential pressure transducers were used to measure the pressure difference between an upstream location and the wake. A detailed discussion of this method can be found in Subsection 3.5.3. The differential pressure transducers come from the factory pre-calibrated. Therefore, no calibration could be done for the drag measurements. Each time the LSATs setup was installed, a pressure test was performed to check for leaks in the pressure tubing and connections. The leak check was done to minimize errors with the drag measurement. The spanwise variations in drag that occur at low Reynolds numbers, discussed in Subsection 3.5.3, introduced uncertainty in the drag measurement that was estimated to be 3% for a Reynolds number of 100,000 and 1.5% for $Re \geq 200{,}000$ [31].

The angle of attack was calibrated upon installation of the LSATs setup. It was calibrated by taking several angular measurements from approximately -10 to 25 deg with a vernier caliper. A linear fit of the data was performed using

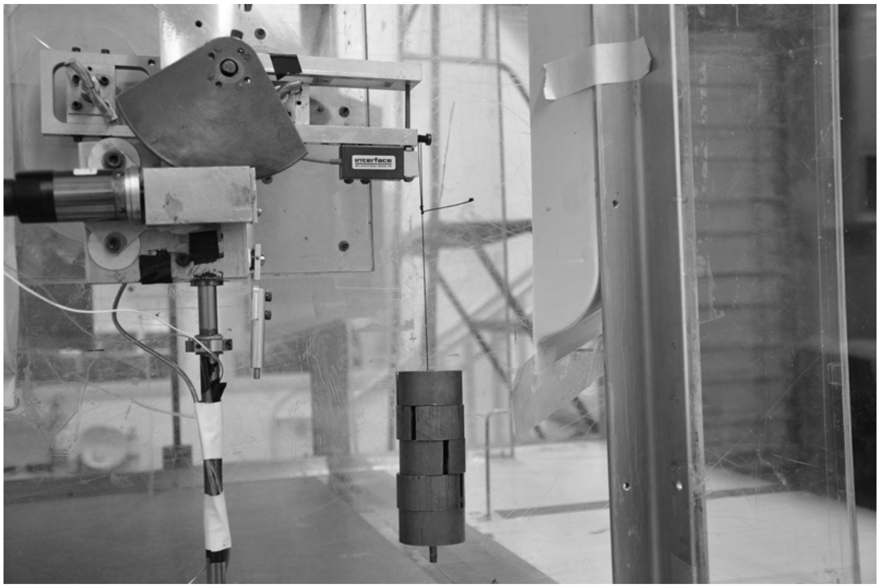

Figure 3.20: Photograph of moment load cell calibration.

linear regression, and the slope was used to determine the angle of attack. An initial offset angle was also measured with the vernier caliper to determine the 0-deg angle of attack. The overall uncertainty of the angle of attack was estimated to be 0.08 deg [31]. The uncertainty was determined using the calibration results.

Chapter 4

Data Validation

Instilling confidence in experimental results is an important aspect of any experiment. The simplest way to accomplish this goal is to compare data against a known standard. As stated in Section 3.1, the performance of low Reynolds number airfoils is highly dependent on the turbulence intensity levels in a wind tunnel. Thus, no one specific facility will provide perfect data, but there are those considered better than others. The Low-Turbulence Pressure Tunnel (LTPT) at NASA Langley Research Center is one of those tunnels. The LTPT tunnel has low turbulence, tall test section walls, and models that mount directly to the wind tunnel wall that all attribute to the high quality data produced by the tunnel [44]. Therefore, the standard for comparison will be the data from the NASA LTPT wind tunnel.

The LSATs apparatus was validated every time it was installed in the wind tunnel to ensure quality data was collected. Since the UIUC LSATs program was started in 1993, the check standard airfoil has been the E387. The E387 has been extensively studied by multiple facilities. For that reason, it serves as a good airfoil for the data validation process. Currently, there are five different version of the E387 available for data validation, but the third version, E387(C), was used for this research. The E387(C) was chosen because it was used extensively in past entries to perform the validation. By using the same airfoil, the repeatability of the LSATs apparatus can be examined as well as its agreement with the NASA LTPT data. Comprehensive discussions on data validation for the LSATs apparatus are presented in each of the LSATs books [5–9].

One of the most thorough ways to validate a wind tunnel setup in the low Reynolds number regime is to compare the laminar separation bubble. As previously discussed, the performance of low Reynolds number airfoils is directly affected by the laminar boundary layer. To be more specific, the performance is directly affected by the location and size of the laminar separation bubble. Therefore, the location of separation, transition, and reattachment of a laminar separation bubble are key driving factors in the performance of low Reynolds number airfoils. Laminar separation bubbles are affected by the turbulence levels in a wind tunnel. By comparing the location of separation, transition, and reattachment of the laminar separation bubbles, distinct difference in wind tunnel facilities can be determined. A common technique used to determine these locations is oil flow visualization. A comprehensive oil flow visualization comparison of the NASA LTPT data to the LSATs E387(E) was conducted and presented in Ref. 8. The conclusion of their study was that the two wind tunnel facilities produce air flows that are in close agreement.

In the next three sections, the moment, lift and drag data will be separately compared to the NASA LTPT E387 data found in Ref. 45. In the three sets of plots, four data sets are compared. The LTPT E387 data is compared to three validation runs performed at the beginning of three separate wind tunnel entries. The three wind tunnel entries took place in the Fall of 2010, Spring of 2011, and Fall of 2011.

4.1 Moment Data

The moment data comparison between the UIUC and LTPT data is shown in Fig. 4.1. A slight discrepancy with the LTPT data can be seen for a Reynolds number of 100,000. The discrepancy seen at a Reynolds number of 100,000 was more than likely due to measurement accuracy. At low Reynolds number and chosen moment load cell location, the forces were small when compared with higher Reynolds numbers and difficult to accurately capture. Besides the slight discrepancy at a Reynolds number of 100,000, the data for the three wind tunnel entries showed excellent agreement with the LTPT data even into stall.

4.2 Lift Data

The lift data comparison between the UIUC and LTPT data is shown in Fig. 4.2. The lift data from the three separate wind tunnel entries agreed well with the LTPT data for Reynolds number of 200,000 and higher. At a Reynolds number of 100,000, there were some discrepancies in the data. The discrepancies were more than likely due to measurement accuracy. The discrepancies could also be caused by slight variations in the laminar separation bubble between the two facilities that can cause slight shifts in the lift curve or slight offset in the angle of attack. For Reynolds numbers of 200,000 and higher, the data showed excellent agreement up to stall. For high angles of attack ($\alpha > 12$ deg), the airfoil entered stall and the data started to disagree. More than likely, the differences between the UIUC and LTPT data in the stall regime were due to three-dimensional end effects since the UIUC models do not mount directly to the wind tunnel walls.

The UIUC data contained increasing and decreasing angle of attack data to ensure the apparatus did not introduce hysteresis into to system. At low Reynolds numbers, the decreasing angle of attack data did not always follow the same linear fit as the increasing angle of attack data. This effect can be clearly seen in the Spring 2011 data at a Reynolds number of 100,000, but it visibly disappears for $Re \geq 200{,}000$. These variations were more than likely due to slight stiction in the system. It was more visible at low Reynolds numbers owing to lower ratio of lift force to stiction force. Even though slight discrepancies existed at a Reynolds number of 100,000, the data still showed acceptable agreement with the LTPT data.

4.3 Drag Data

The drag data comparison between the UIUC and LTPT data is shown in Fig. 4.3. The data showed good agreement for Reynolds numbers of 200,000 and higher. The slight discrepancies observed at the upper limits of all the drag polar can be attributed to the slightly less maximum lift coefficients obtained by the UIUC model, which can be seen in Fig. 4.2. The largest discrepancies occurred at a Reynolds number of 100,000 in the range of the polar dominated by a laminar separation bubble ($0.25 < C_l < 1.0$). The discrepancies at a Reynolds number of 100,000 could be caused by any number of issues. The drag measurements at the UIUC facility were taken 1.25 chord lengths downstream of the model trailing edge while the NASA took measurements 1.5 chord lengths downstream. The NASA study took one wake survey for drag while the UIUC studies took eight wake surveys in order to average out the spanwise variations at low Reynolds numbers documented in Ref. 40.

Comparing results from different facilities is useful, but it is also instructive to compare data sets taken at the same facility. This comparison sheds light on the wind tunnel and apparatus repeatability. Even though there were slight discrepancies with the LTPT benchmark data for $Re \geq$ 200,000, it was repeatable between wind tunnel entries. Even at a Reynolds number of 100,000, the large discrepancies with the LTPT data discussed above were also fairly repeatable with previous entries. This repeatability should instill confidence in the drag data taken during the three wind tunnel entries.

4.4 Summary

The accuracy of the data collected for this research was established to be acceptable. This conclusion was reached by observing three important points. First, the moment data had excellent agreement the NASA LTPT data except for a slight discrepancy at a Reynolds number of 100,000. Second, the lift data showed acceptable agreement up to stall for Reynolds numbers of 200,000 and higher. At a Reynolds number of 100,000, the lift data had some slight discrepancies that were more than likely due to measurement accuracy, but it showed satisfactory agreement. Lastly, the drag data showed acceptable agreement, but some discrepancies at a Reynolds number of 100,000 have yet to be fully explained. In conclusion, the ability of the LSATs apparatus to produce repeatable results from entry-to-entry that agrees with the NASA LTPT benchmark data validates the experimental data presented in this research.

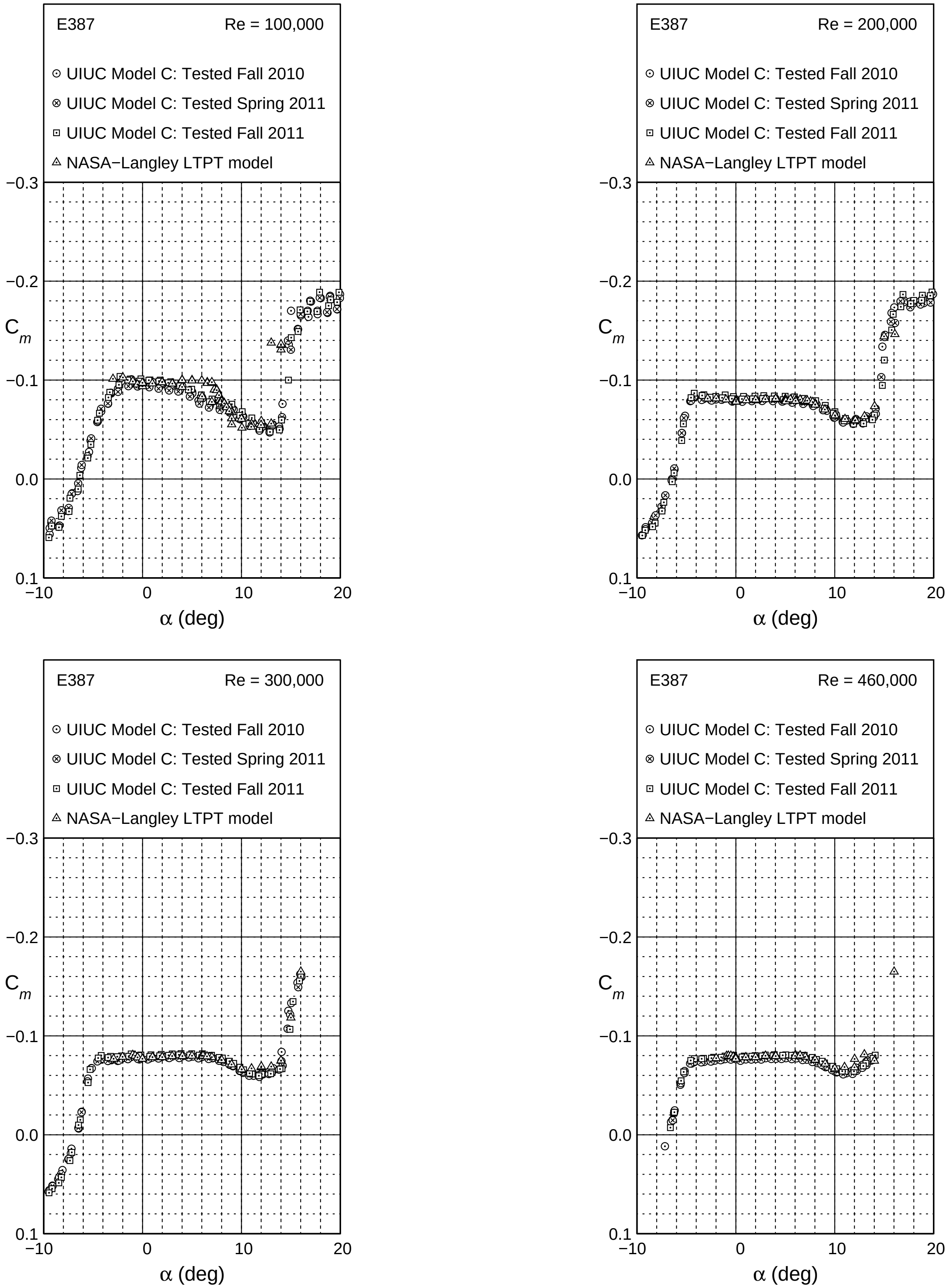

Figure 4.1: Comparison between UIUC and LTPT E387 moment coefficient data for Re = 100,000, 200,000, 300,000, and 460,000.

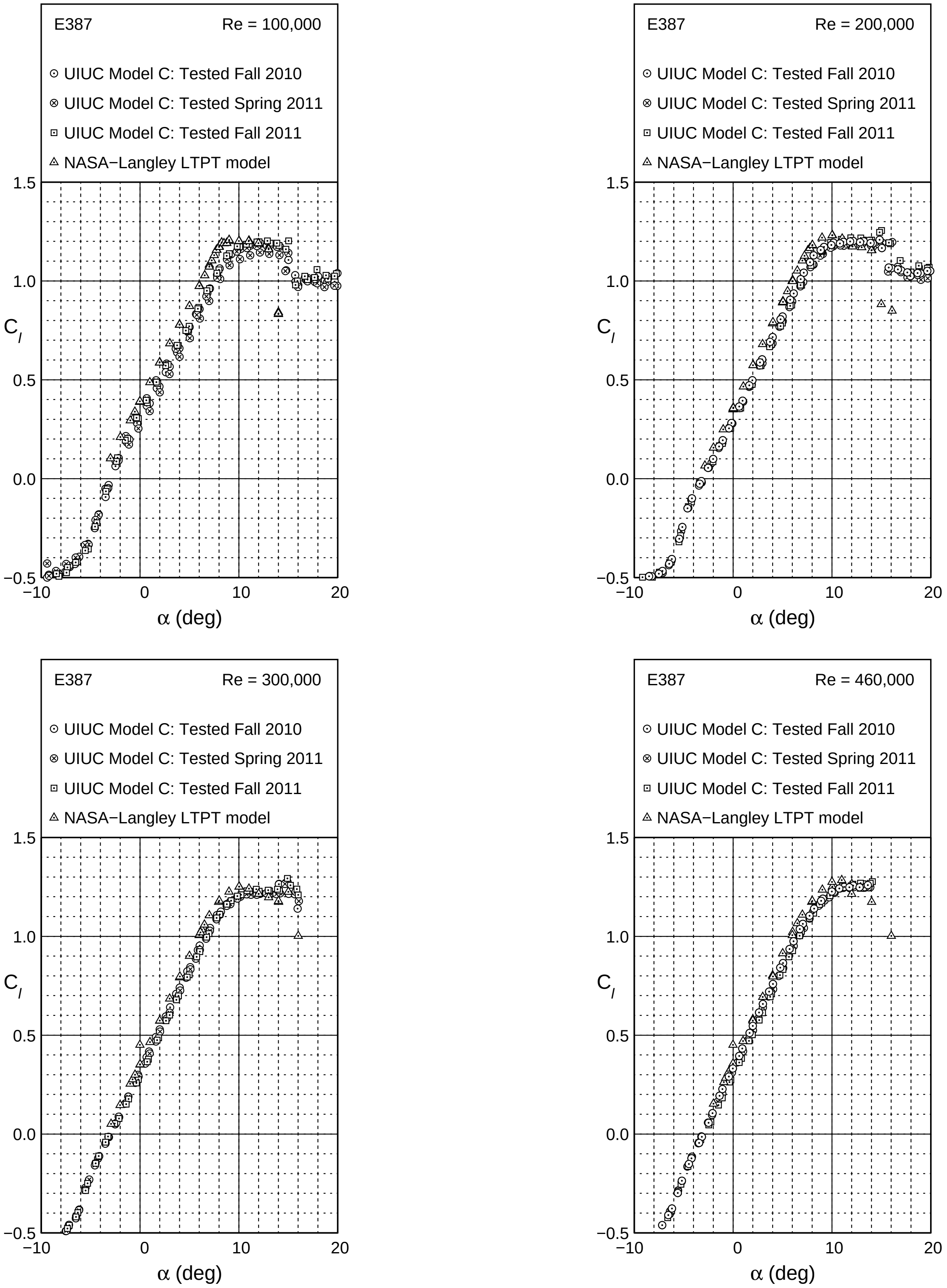

Figure 4.2: Comparison between UIUC and LTPT E387 lift coefficient data for Re = 100,000, 200,000, 300,000, and 460,000.

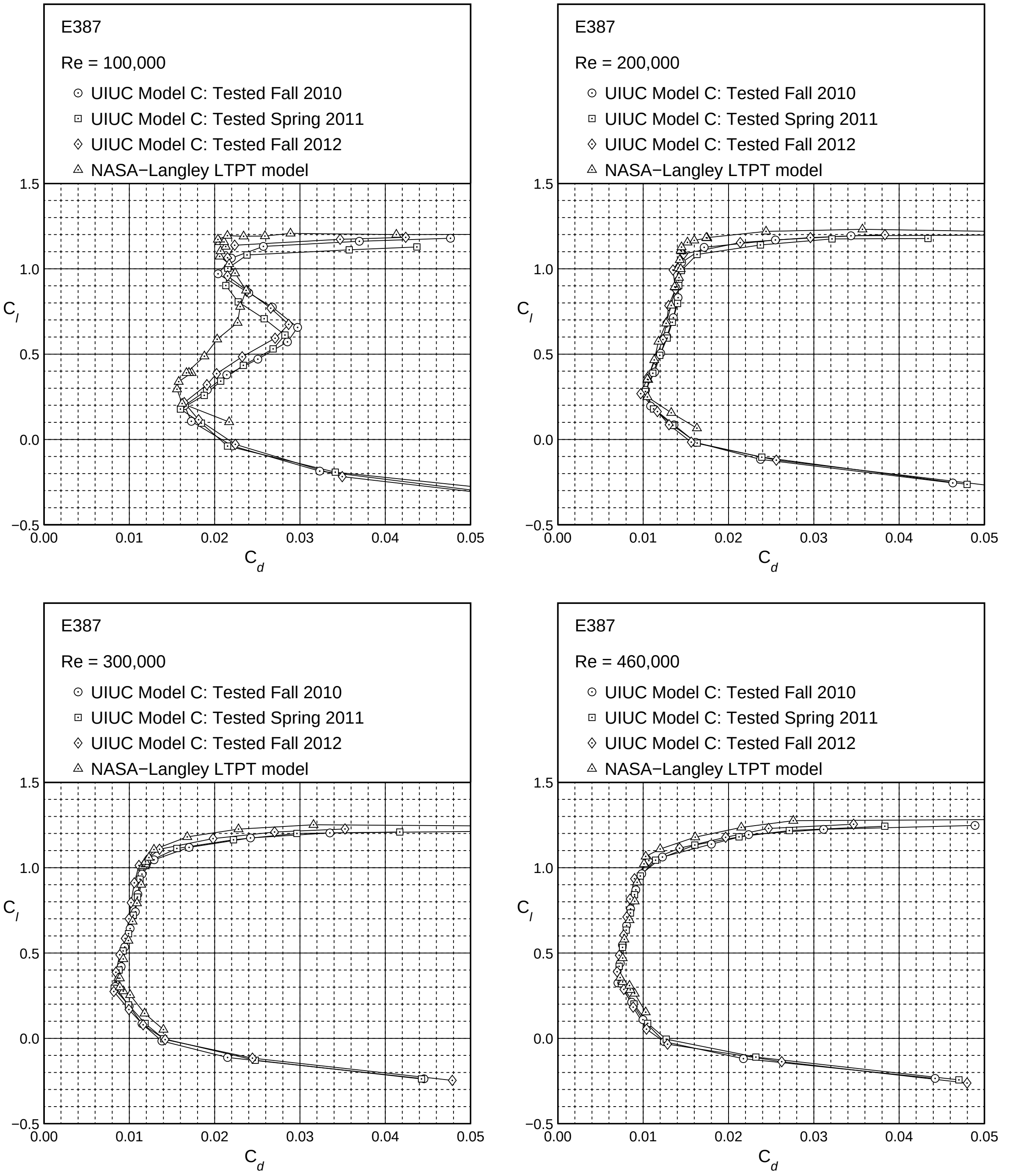

Figure 4.3: Comparison between UIUC and LTPT E387 drag coefficient data for Re = 100,000, 200,000, 300,000, and 460,000.

Chapter 5

Inverse Airfoil Design

Inverse design of airfoils is currently the most efficient method for designing airfoils to meet specific performance parameters. This chapter discusses the importance of inverse airfoil design, the inverse design approach, and the results of two symmetrical airfoils designed for this research. Special considerations exist for the design of low Reynolds airfoils, which will also be discussed.

5.1 Importance of Inverse Airfoil Design

Inverse design through conformal mapping provides enormous control over airfoil design, which is especially important for the design of low Reynolds number airfoils. Inverse airfoil design uses specific performance parameters to define the airfoil geometry. Thus, the airfoil can be tailored to specific aerodynamic needs. The inverse method can be seen pictorially in Fig. 5.1. It has proven to be an elegant and powerful method for airfoil design. Before proceeding with this discussion, a brief history of the inverse design code used for this research is presented. In the early 1990s, Selig [13, 14] drew upon Eppler's work in inverse design of airfoils through conformal mapping and created the inverse design code PROFOIL. PROFOIL differs from the Eppler code by incorporating the ability to control maximum thickness, thickness distribution, and others. More information regarding PROFOIL and the differences between it and the Eppler code can be found in Refs. 13, 14, and 29.

The need for inverse design of airfoils is evident at low Reynolds number where the adverse effects of laminar separation bubbles seen in Subsection 2.2.2 become increasingly apparent. With inverse airfoil design, the designer is given direct control over the boundary layer development that in turn allows for the mitigation of laminar separation bubbles. The mitigation of the laminar separation bubble is key to improving the performance and stability of a low Reynolds number airfoil [2]. The control of the boundary layer development does little good if only applied at one angle of attack. It would be desirable to control the boundary layer development at multiple angles of attack. This control at multiple angles of attack, called multi-point inverse design, enables the designer to come one step closer to the ideal outcome of direct prescription of the airfoil performance. The ability to easily control the performance of an airfoil is the main benefit and reason to utilize inverse methods for airfoil design.

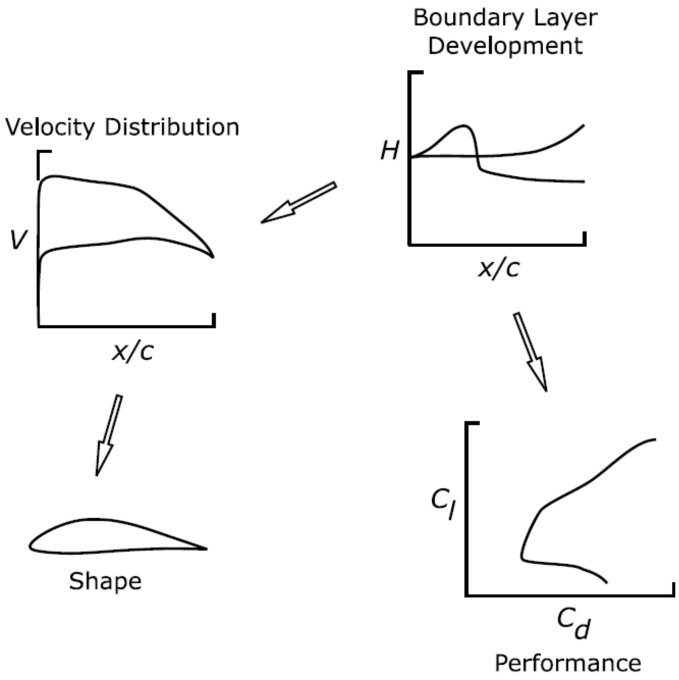

Figure 5.1: Inverse design method using boundary layer development (taken from Ref. 20).

5.2 Inverse Design Approach

For low Reynolds number airfoils, the ability to control the point of transition is instrumental to the inverse design process [20]. Therefore, in the following subsections, the topics of determining the location of transition, controlling the point of transition, and defining the transition curve will be discussed. The discussion will culminate with the knowledge of how to control the transition curve to improve airfoil designs at low Reynolds number. This knowledge is key to understanding the inverse design methodology presented here.

5.2.1 Transition Location

The performance of low Reynolds number airfoils is "strongly dependent on the location of transition as that sets the length of the laminar separation bubble and consequently the magnitude of the drag rise attributed to the bubble." [20] Therefore, the ability to control the point of transition is fundamentally key to improving airfoil performance through the mitigation of the laminar separation bubble [20]. Thus, the first step in designing low Reynolds number airfoils is accurately determining the point of transition. There are multiple ways to determine the point of transition, but the two most common methods, wind tunnel experiments and computational methods, are presented.

Wind tunnel experiments are used to accurately determine the point of transition on airfoils. With any experiment at low Reynolds numbers, the ability of the wind tunnel to obtain low levels of turbulence intensity is instrumental in obtaining good data as discussed in Section 3.1. It has been well documented that low Reynolds number airfoils are highly sensitive to turbulence intensity and in general, the tunnel flow quality [20]. Thus, the location of transition and the size of the laminar separation bubble are affected by the tunnel flow quality. One method commonly used to determine the locations of separation and reattachment of a laminar separation bubble is oil flow visualization. With oil flow visualization, a fluorescent pigment is suspended in a common household mineral oil that can be viewed under a black light to visually see the locations of separation and reattachment. This mixture is sprayed on the airfoil with an airbrush to give it an "orange-peel" look. The model is then run in the wind tunnel for approximately 20 to 45 min depending on the Reynolds number. When the tunnel is running, skin friction causes the oil to move in the direction of the flow. The bubble can be located by finding the places on the airfoil that retain the original "orange-peel" look. A detailed explanation of oil flow visualization and how to interpret the flow features can be found in Ref. 46.

Computational methods can also be used to predict the location of transition. XFOIL [47] is a panel method solver that couples a linear-vorticity second-order accurate inviscid solution with viscous integral boundary layer solution with an e^n-type transition amplification formulation. In order to couple the inviscid and viscous effects, a global Newton method is used. It has been found that XFOIL, written by Drela [47], is well suited for the analysis of low Reynolds number airfoils even with the presence of significant laminar separation bubbles [20]. Therefore, XFOIL was used to analyze low Reynolds number airfoils to predict the locations of separation, transition, and reattachment of a laminar separation bubble. To predict the location of transition of a smooth surface in low-turbulence, a n_{crit} value of 9 is typical [20] and was used in this research. XFOIL was also used to predict the lift, drag, and moment coefficients. It has its limitations and should not be blindly used for all situations. The advantage of XFOIL is that it takes approximately 20 sec to compute an airfoil polar. The latest version of XFOIL can be found on the XFOIL website [48].

5.2.2 Transition Control

There are two main methods for controlling the point of transition. The first is through the use of a boundary layer trip, and the second is through the use of a transition ramp. The topic of boundary layer trips was discussed in Subsection 2.2.3. From the previous discussion, it can be concluded that the employment of boundary layer trips is not the optimal solution for the mitigation of laminar separation bubbles and their effects on airfoil performance. A transition ramp is defined to be the chordwise extent the point of transition moves while operating in the low drag region [20]. A transition ramp promotes transition by introducing an instability region on the upper surface pressure gradient. With an effective transition ramp, the flow gradually transitions to a turbulent flow in a thin bubble instead of a thick bubble. Thick bubbles have a large pressure rise that lead to large increases in drag. The use of a long transition ramp is necessary at low Reynolds numbers but not as necessary at high Reynolds numbers. A good example that shows the effects of different transition ramps can be found in Ref 20. The transition ramp is more effective at controlling the point of transition than boundary layer trips and will be the focus of the inverse design approach.

A transition curve ($C_l - x_{tr}/c$ curve) is used in the design process to define the transition ramp. The transition curve graphically depicts the percent chord location of boundary layer transition from laminar-to-turbulent flow with respect to the lift coefficient. From the examples presented in Ref. 20, there is a noticeable correlation between the shape of transition curve on the upper surface and the drag polar. This correlation indicates that the steepness of the transition curve is a direct indication of the bubble drag. The transition curve is steeper when the bubble is larger. This trends leads to the conclusion that the airfoil performance can be controlled by prescribing the slope of the transition curve - a shallow curve implies smaller bubble drag and a steeper curve implies larger bubble drag. Therefore, the philosophy is to prescribe a transition curve from the leading edge to the trailing edge keeping in mind that the slope of the curve can be used to prescribe low drag regions in the polar.

5.2.3 Transition Curve Control

The ability to control the transition curve would provide the designer control over the boundary layer development at multiple angles. This control is critical when properly designing airfoils for low Reynolds numbers and is referred to as multi-point inverse design. A multi-point inverse design is the end goal of inverse airfoil design as discussed in Section 5.1. The capability of prescribing the transition curve is conveniently integrated in the inverse design process within PROFOIL [13–15], which is an inverse airfoil design code based on conformal mapping briefly discussed in Section 5.1.

The transition curve is prescribed in PROFOIL by defining the α^*-ϕ curve. The first variable, α^*, is the angle of attack with respect to the zero-lift angle of attack where the velocity is constant over a segment of an airfoil. The second variable, ϕ, is used for conformal mapping of a circle to the airfoil shape. The advantage of prescribing α^* is that the lift coefficient can be estimated by $C_l = 2\pi\alpha^*$. For example, an angle of attack with respect to the zero-lift line of 10 deg will approximately yield a lift coefficient of 1.0 ($C_l = 2\pi\alpha^* \approx 1.0$). The transition curve can be prescribed by defining the α^*-ϕ curve because (1) the boundary layer reacts mainly to the pressure gradient, (2) the pressure gradient is directly affected by the design angle of attack, α^*, and (3) multiple design angle of attacks can be prescribed that are used to define the shape of the airfoil [20]. These three facts lead to an elegant solution to the problem of having control over the transition curve. The PROFOIL code was integrated into a graphical user interface (GUI) using MATLAB, and it was given the name MFOIL. MFOIL [49] allows the user to modify the α^*-ϕ curve rapidly and see the changes of the resulting airfoil. The changes can be seen in two forms. First, the resultant airfoil shape is plotted allowing the designer to visually see if the airfoil is a plausible shape. Second, the resultant inviscid velocity distribution is plotted allowing the user to analyze the pressure recovery and tailor it to their specific needs. A

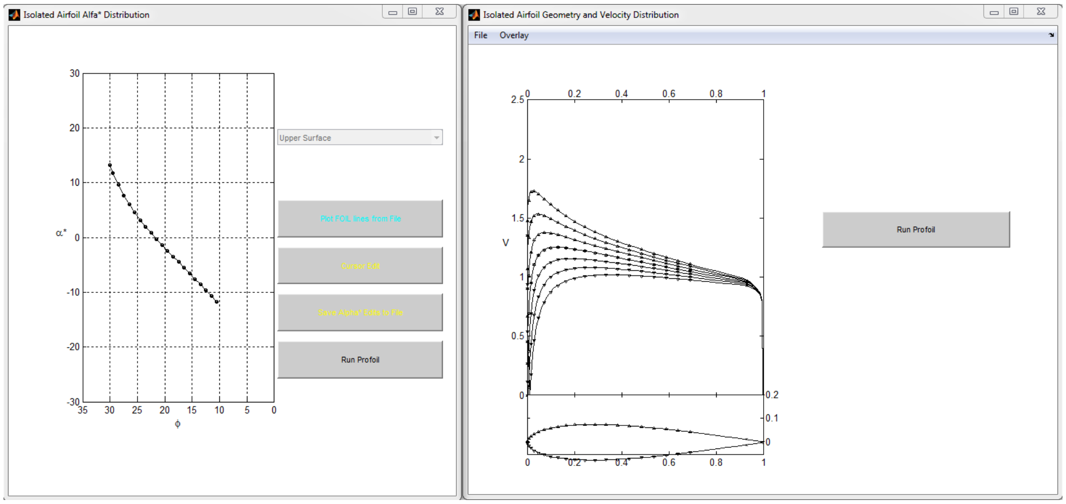

Figure 5.2: MFOIL graphical user interface (GUI) screen grab showing the interactive nature of MFOIL.

screen grab of the GUI can be seen in Fig. 5.2. The left plot in Fig. 5.2 shows the interactive window used to modify the α^*-ϕ curve. The right plot in Fig. 5.2 shows the results of the modified α^*-ϕ curve defined in the left plot. The main benefit of using MFOIL is that it allows for rapid design iterations. The designer has the ability to examine the inviscid velocity distribution and adjust the α^*-ϕ curve before using a viscous analysis tool to analyze the airfoil performance.

5.3 Symmetrical Airfoil Design

Two symmetrical airfoils with different thicknesses were designed to satisfy one of the goals of this research. In the following subsections, the design considerations, design process, and results will be discussed.

5.3.1 Design Considerations

The airfoils that were designed as part of this research had several design constraints and considerations that defined the final performance and geometry. The two airfoils were designed for use on aerobatic aircraft with large control surfaces. Thus, the airfoils were designed to be symmetrical. The two airfoils had a maximum thickness of 11% and 15% with respect to the airfoil chord. The two thicknesses were decided upon by examining typical airfoils used on current wings. It is desirable to have a thicker airfoil section near the root of the wing to provide more structural integrity and stiffness. Out toward the tip of the wing, thinner airfoil sections are more desirable to reduce drag where strength and stiffness are not as important. Thus, the two airfoils were designed specifically to create a family of airfoils with similar transition curves and performance characteristics so they could be used together on a wing with the 15% near the root and the 11% near the tip.

In order to create the family of airfoils, the performance characteristics needed to be similar. This similarity was accomplished through the α^*-ϕ curve because it sets the transition curve of the airfoil. Therefore, the two airfoils were designed with similar α^*-ϕ curves but not identical. Identical α^*-ϕ curves would not have been practical due to the way PROFOIL iterates on the α^*'s to set the thickness.

One important aspect of the design of these airfoils was the transition curve. With most airfoils designs, delaying transition is desirable due to low drag values that can be obtained with laminar flow. But with these airfoil designs, the transition curve was intentionally shifted forward toward the leading edge in order to promote early transition. The early promotion of transition was done to ensure the flow was turbulent before it encountered the control surface. A turbulent flow resists separation more than a laminar flow as discussed in Subsection 2.2.3. Therefore, a turbulent flow would help the flow stay attached to a deflected control surface and reduce the drag. By shifting the transition curve forward, airfoil performance becomes more resistant to defects and roughness on the airfoil surface, which is another added benefit.

In regard to performance, the design goal was to create an airfoil that had a wide performance range without much adverse effect to changes in Reynolds number. It is a known fact the maximum lift coefficient decreases as Reynolds number decreases [20]. One goal of these designs was to mitigate Reynolds number effects. With aerobatic airfoils, the stall is usually fairly sharp to aid in aerobatic maneuvers. Therefore, designing the airfoils to have a fairly sharp stall was a design consideration that was taken into account. As the Reynolds number decreases, the effects of laminar separation bubbles become more evident. Thus, a major design goal was to create an airfoil that had a wide performance range without much indication of a laminar separation bubble at a Reynolds number of 60,000. A wide range at such a low Reynolds number would ensure equal or better performance at higher Reynolds numbers.

5.3.2 Design Process

The design process was fairly straightforward and involved the programs MFOIL/PROFOIL, XFOIL, and MATLAB. MFOIL/PROFOIL was used to perform the inverse design, XFOIL was used to perform the viscous analysis, and MATLAB was used to interface with XFOIL to run batches of airfoils. In the next few paragraphs, the design process will be described in detail.

The first step in the design process was to define the airfoil using the inverse methods embedded in MFOIL. MFOIL is a convenient tool for rapid airfoil design owing to the nature of the graphical user interface. As discussed in Subsection 5.2.3, MFOIL allows the user to interactively modify the α^*-ϕ curve and visually see the changes that ensue. Notably, the inviscid velocity profile was extensively used to determine needed adjustments to the α^*-ϕ curve.

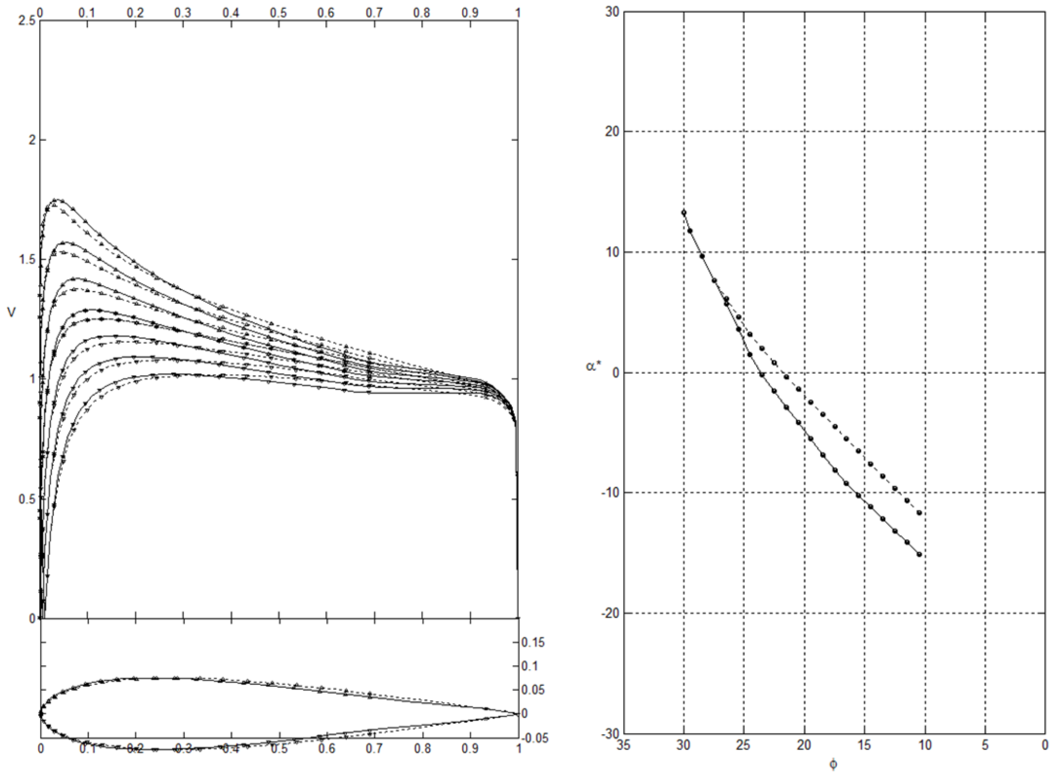

Figure 5.3: Example of an overly aggressive and proper pressure recovery with their respective α^* distributions.

For example, if the pressure recovery was too aggressive, the α^*'s on the right side of the α^*-ϕ curve were increased (less negative) to lessen the adverse pressure gradient. An example of an overly aggressive and proper pressure recovery can be seen in the left plot of Fig. 5.3. In Fig. 5.3, the solid line indicates the overly aggressive pressure recovery, and the dotted line indicates the proper pressure recovery. The respective α^*-ϕ curve for each pressure recovery can be seen in the right plot of Fig. 5.3. In the left plot of Fig. 5.3, the respective airfoil shapes can be seen. It can be seen that the overly aggressive pressure recovery produces an airfoil that has a concave surface in the pressure recover region.

After a suitable airfoil was designed in MFOIL, the coordinates were used in XFOIL to perform a viscous analysis of the airfoil. As discussed in Subsection 5.2.1, XFOIL can analyze airfoils at low Reynolds numbers even with significant laminar separation bubbles. After importing the coordinates into XFOIL, the airfoil was re-paneled to improve the solution accuracy. The airfoil was re-paneled because 60 coordinate points were determined using PROFOIL, which can lead to excessive panel angles in XFOIL. Excessive panel angles can cause computational errors leading to inaccurate results. Thus, the airfoil was re-paneled to 240 panels to provide accurate results. An adverse effect of increasing the number of panels is the increased computational time, but it was not noticeable. Increasing the number of panels too much can lead to inaccuracies as well and should be avoided.

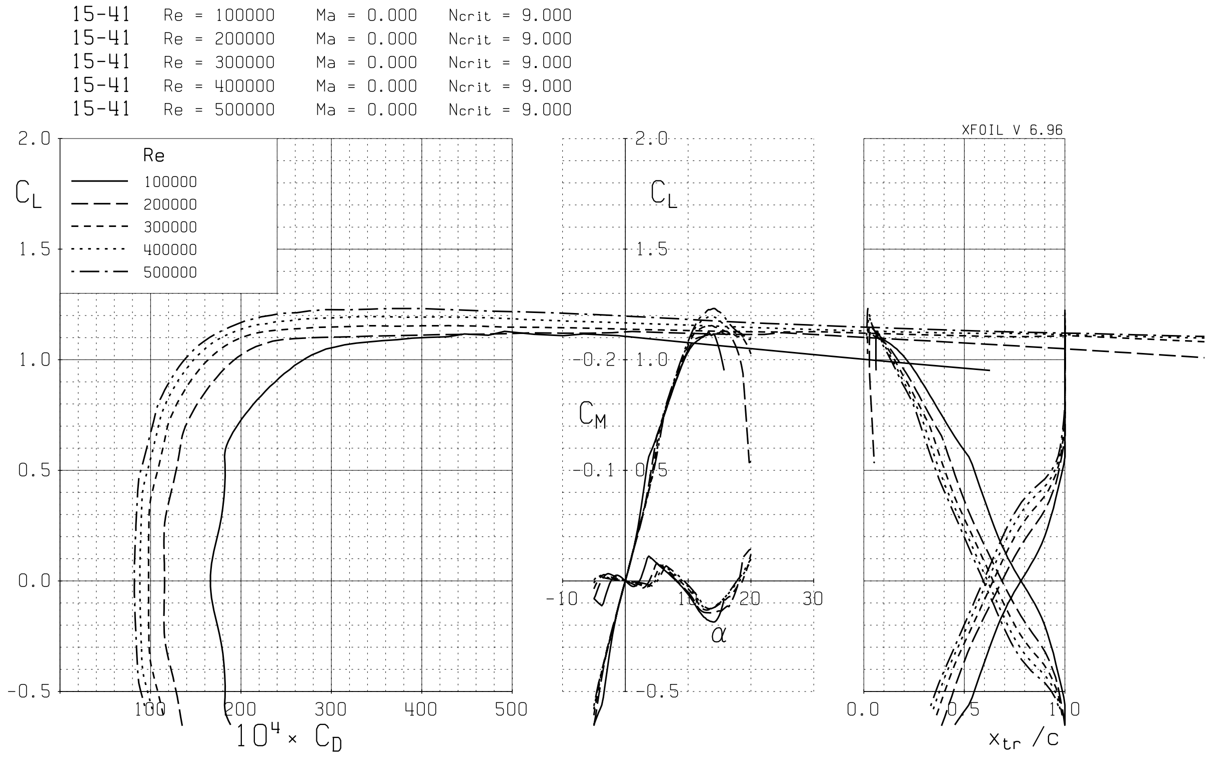

Figure 5.4: Example XFOIL plot showing drag polar, lift curve, moment curve, and transition curve.

After re-paneling, the airfoil was analyzed at the different Reynolds numbers of 100,000, 200,000, 300,000, 400,000, and 500,000. If the airfoil exhibited desired performance and transition curve qualities, the airfoil was re-analyzed at a Reynolds number of 60,000 and 100,000. This extra analysis was done in order to examine the performance and transition curve at the lower end of the Reynolds number range where airfoil performance is dictated by laminar separation bubbles. The upper bound of the angle of attack sweep was set to exceed the airfoil stall angle, and data was collected until XFOIL failed to converge. The post stall examination was done in order to inspect the type of stall the airfoil exhibited. The actual values from XFOIL are not reliable beyond the linear region of the lift curve, but stall trends are similar to the actual stall.

After the viscous analysis was performed, an XFOIL plot was created and exported from XFOIL. An example XFOIL plot can be seen in Fig. 5.4. At the top of the XFOIL plot, the analyzed airfoils and Reynolds numbers are listed. In this particular example, only one airfoil, "15-41," was examined but at five Reynolds numbers. At the far left of the XFOIL plot, the drag polar data is presented. The drag polar plots the lift coefficient against the drag coefficient. In the center of the XFOIL plot, the lift and moment data are presented. The lift and moment curves plot the lift and moment coefficients against the angle of attack, which occupies the x-axis. At the far right of the XFOIL plot, the transition curve is presented. The transition curve graphically depicts the percent chord location of boundary layer transition from laminar-to-turbulent flow with respect to the lift coefficient. In conjunction, the three plots can be used to fully examine airfoil performance. The drag polar was used to examine the low drag regions of the polar and provide indications of laminar separation bubbles as discussed in Subsection 2.2.2 and seen in Fig. 2.4. The lift curve was used to examine the stall characteristics as well as look for irregularities in the lift curve that may indicate a laminar separation bubble. The lift curve should be more or less linear below stall. The transition curve was extensively used to determine the quality of the airfoil. There are different types of transition curves depending on the desired type of airfoil. The transition curve in Fig. 5.4 is an example of the desired trends for the aerobatic airfoils designed for this research. There are interesting correlations between the transition curve and the drag polar which are discussed at length in Ref. 20.

Operating XFOIL can be time consuming and monotonous. It is much faster if run from an external program. For this research, MATLAB scripts were created to run XFOIL in a batch mode to analyze multiple airfoils simultaneously. The MATLAB scripts can be found in Appendix D. The scripts ran XFOIL through the Windows “DOS” command and received the run inputs from a Microsoft Excel file. The Microsoft Excel file contained information about the name of the airfoil coordinate file, angles of attack, and Reynolds number. A screen grab and brief description of the Microsoft Excel input file can be found in Appendix D. The typical analysis of one airfoil at five different Reynolds numbers took approximately 80 sec with the script. The same analysis performed by manual inputs took a minimum of 5 min. For each analyzed airfoil, the MATLAB script prompted XFOIL to output polar data for each Reynolds number and an XFOIL plot similar to Fig. 5.4.

5.3.3 Design Results

The design of the two airfoils took several iterations in order to find the optimum geometry. The 11%-thick airfoil took 72 iterations, and the 15%-thick airfoil took 48 iterations. In the following paragraphs, the two final airfoils will be discussed and plots for each airfoil will be presented. The 11%-thick airfoil will be discussed first.

11%-Thick Airfoil Design

The W1011 airfoil was the result of 72 iteration exploring different pressure recoveries and transition curves to find the optimum airfoil geometry. A considerable amount of time was spent of the pressure recovery region on the airfoil, which can be seen in the left plot of Fig. 5.5. The pressure recovery was designed to be slightly concave. The concavity increased the maximum C_l and made the stall slightly sharper as seen in Fig. 5.6. More performance results are discussed in the next paragraph. The resulting α^*-ϕ curve for the final airfoil can be seen in right plot of Fig. 5.5. A comparison of the pressure distribution and the α^*-ϕ curve reveals some interesting similarities. The shape of the

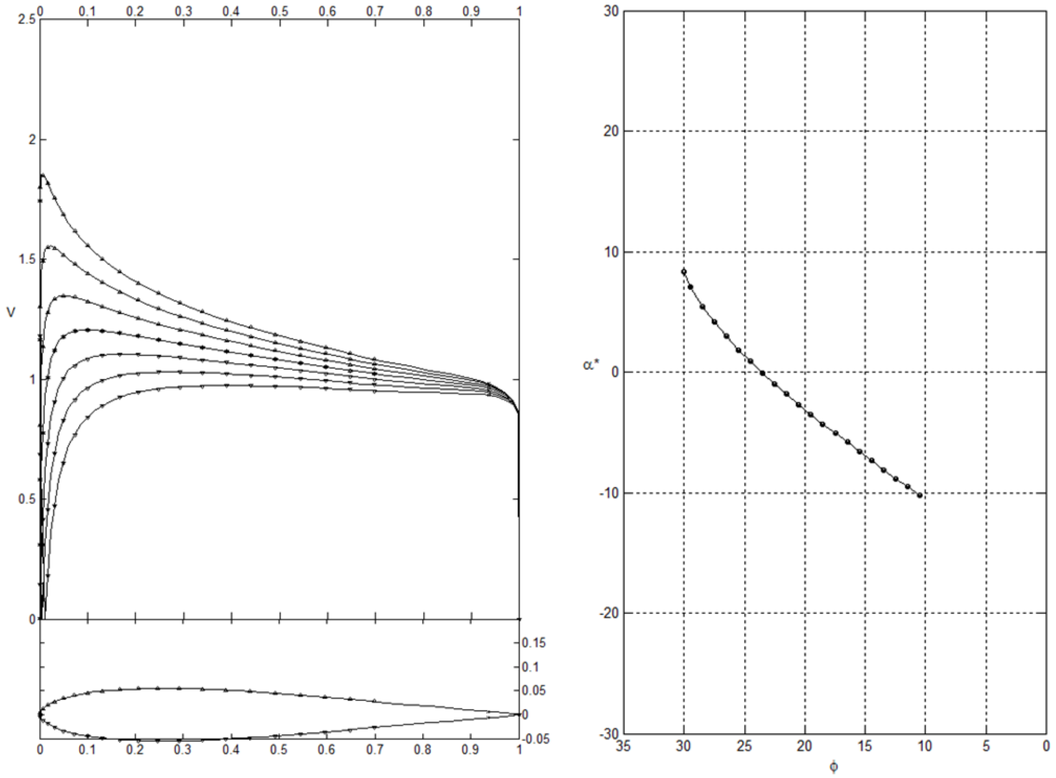

Figure 5.5: MFOIL results for the W1011 airfoil.

α^*-ϕ curve was mimicked in the pressure distribution. Therefore, to attain a slightly concave pressure recovery, the α^*-ϕ curve was designed to be slightly concave.

The XFOIL viscous analysis results for the W1011 airfoil can be seen in Fig. 5.6. It can be seen from the drag polar that the airfoil attained a wide range of low drag, but signs of a laminar separation bubble can be seen for Reynolds numbers of 60,000 and 100,000. After further examination of the drag polar, it can be seen that the size of the rightward bump at low lift coefficient values does not increase with a reduction of Reynolds number, which suggests the boundary layer is stable for low Reynolds numbers. Variations in the maximum lift coefficient were seen with changes in Reynolds number, which was to be expected. The variations in maximum lift coefficient are not excessive but typical for low Reynolds number airfoils. Above a Reynolds number of 200,000, the transition curve was fairly linear and shifted forward toward the leading edge in order to ensure the flow transitioned before the control surface for reasons discussed in Subsection 5.3.1. The airfoil was designed to handle control surfaces up to 30% of the chord in length. Therefore, it was beneficial to have transition before 70% of the chord. It can be seen that for two highest Reynolds numbers the flow transitioned around 70% of chord for a lift coefficient of zero and progressed toward the leading edge as the lift coefficient increased.

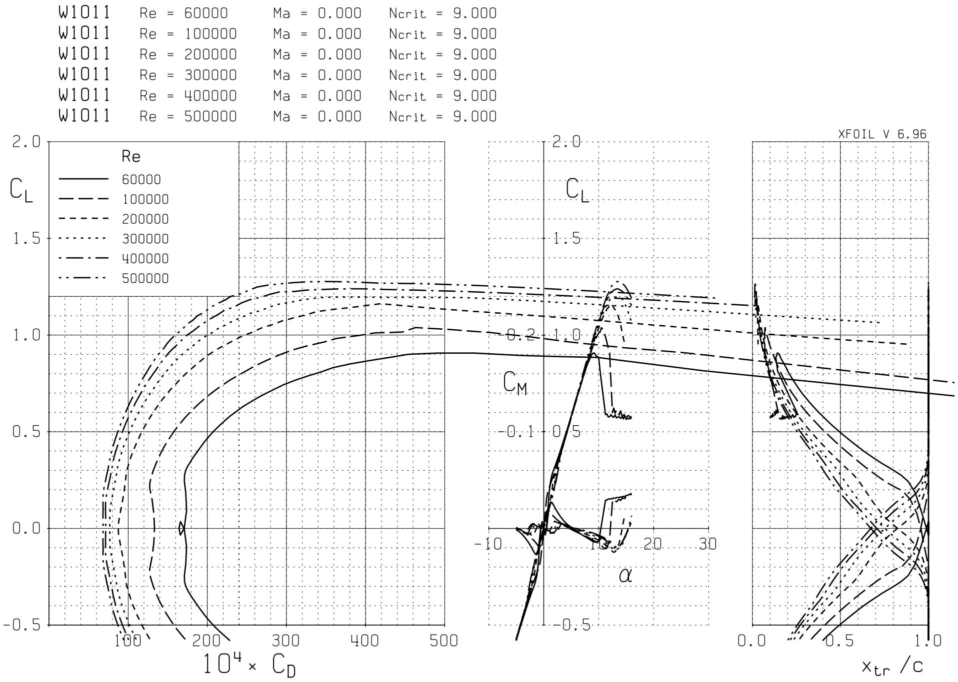

Figure 5.6: XFOIL viscous analysis for the W1011 airfoil.

15%-Thick Airfoil Design

The W1015 airfoil was the result of 48 iteration exploring different pressure recoveries and transition curves to find the optimum airfoil geometry. As with the W1011, a considerable amount of time was spent of the pressure recovery region of the airfoil, which can be seen in the left plot of Fig. 5.7. The pressure recover was also designed to be slightly concave to increase the maximum C_l and make the stall slightly sharper as seen in Fig. 5.8. More performance results are discussed in the next paragraph. The resulting α^*-ϕ curve for the final airfoil can be seen in right plot of Fig. 5.7. As with the W1011, the α^*-ϕ curve was designed to be slightly concave.

The XFOIL viscous analysis results for the W1015 airfoil can be seen in Fig. 5.8. It can be seen from the drag polar that the airfoil attained a wide range of low drag. The first indication of a laminar separation bubble occurred at the lowest analyzed Reynolds number of 60,000. Even though the airfoil showed signs of a laminar separation bubble at a Reynolds number of 60,000, it was deemed acceptable considering the Reynolds number and airfoil thickness. Except at Reynolds number of 60,000, the maximum lift coefficient had little variation with Reynolds number. The larger variation in maximum lift coefficient between a Reynolds number of 60,000 and 100,000 was not excessive but typical for low Reynolds number airfoils. The transition curve was near linear except for Reynolds number of 60,000. It is also worth noting that the transition curve was shifted forward toward the leading edge in order to ensure the flow transitioned before the control surface for reasons discussed in Subsection 5.3.1. As with the W1011, the airfoil

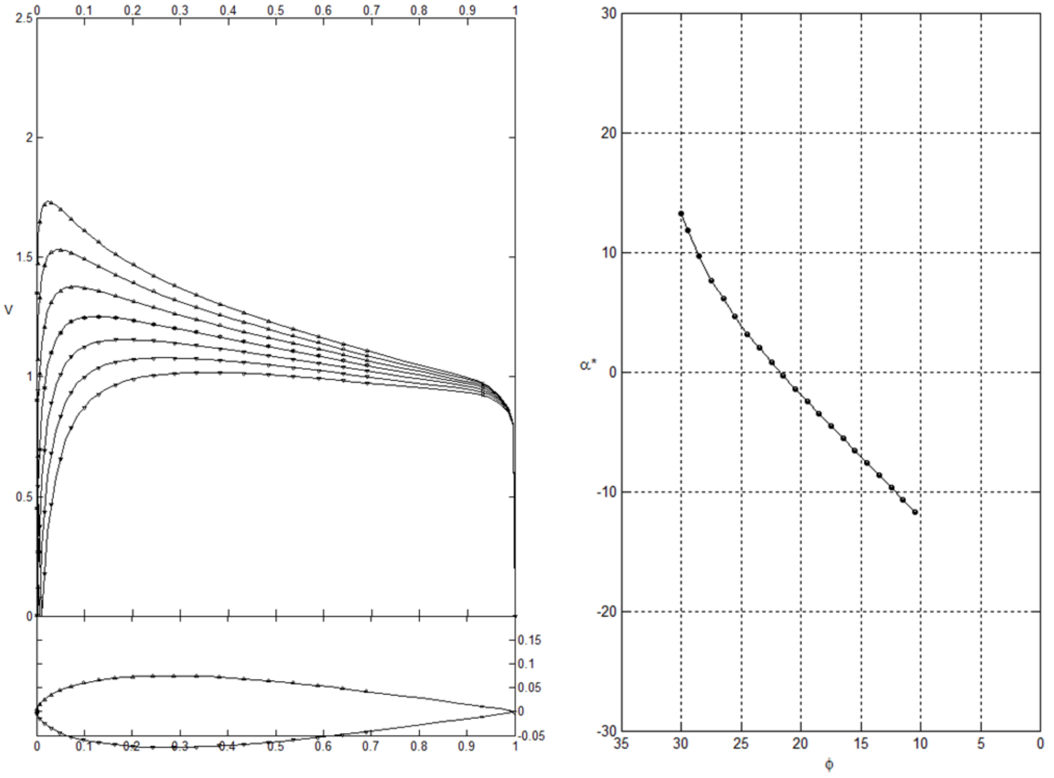

Figure 5.7: MFOIL results for the W1015 airfoil.

was designed to handle control surfaces up to 30% of the chord in length. For the four highest Reynolds numbers, the flow transitioned at or before 70% of the chord for a lift coefficient of zero. As the angle of attack was increased, the transition point moved toward the leading edge. Thus, transition occurred before the control surface, which is advantageous as mentioned previously.

Airfoil Comparison

By comparing these two airfoils, it can be seen that they exhibited similar characteristics. The α^*-ϕ curve were similar but not identical. As mentioned previously, identical α^*-ϕ curves would not have been possible due to the way PROFOIL iterates on the α^*'s to set the thickness. The α^*-ϕ curves were intentionally designed to be similar in order to create a family of airfoils. The family of airfoils should exhibit similar transition curves and performance as was observed for the two airfoils. The W1015 achieved higher maximum lift coefficients while the W1011 achieved lower drag coefficient, which was to be expected.

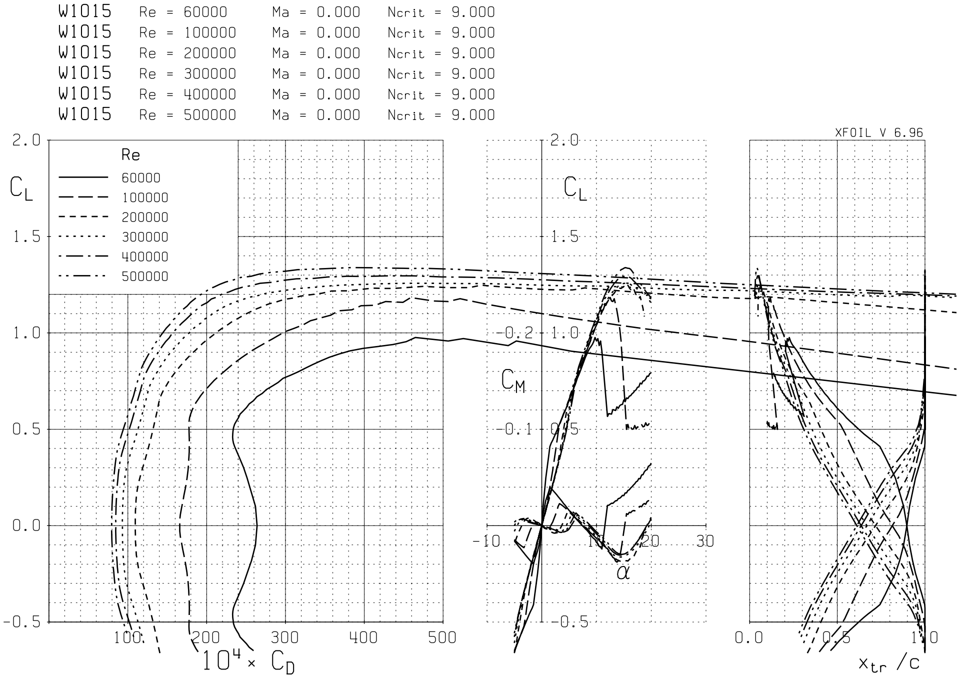

Figure 5.8: XFOIL viscous analysis for the W1015 airfoil.

Chapter 6

Results and Discussion

In this chapter, the results for the flapped airfoil wind tunnel tests are presented in five sections. In Section 6.1, the effects of the flaps on the lift and moment are studied and compared. Following in Section 6.2, the maximum lift coefficients with respect to flap deflection are presented. Section 6.3 examines and compares the effects of large flap deflections on drag. In Section 6.4, the maximum lift-to-drag ratios are analyzed with respect to flap deflection. Finally in Section 6.5, the performance of each airfoil configuration is plotted in a similar structure compared to the LSATs books seen in Refs. 4–9. For this research, a configuration is defined to be a unique combination of three variables that include the airfoil, flap-chord ratio (c_f/c), and flap deflection (δ_f). In total, 80 different configurations were tested with varying Reynolds numbers. Table 6.2 in Section 6.5 details all of the tested configurations. A summarized version of Table 6.2 can be seen in Table 6.1. In Table 6.1, important airfoil parameters are given along with the tested Reynolds numbers. In some cases with the AG40d-02r and AG455ct-02r, the highest Reynolds number (Re = 500,000) was not tested due to force measurement limitations of the LSATs setup. For more information on what was tested, see Table 6.2 on page 86.

Table 6.1: Summary of Airfoils Tested

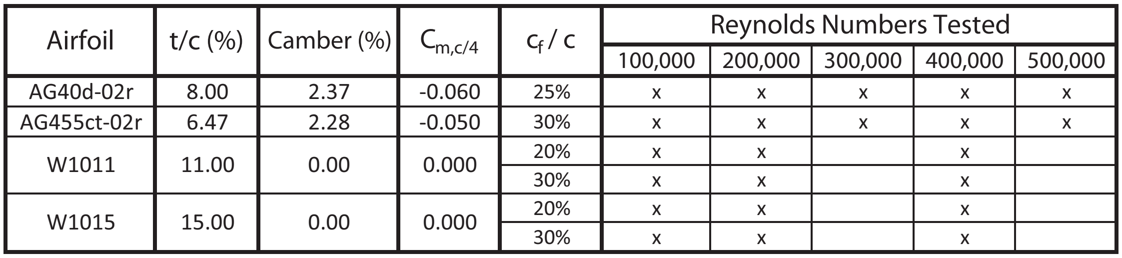

Airfoil	t/c (%)	Camber (%)	$C_{m,c/4}$	c_f / c	Reynolds Numbers Tested				
					100,000	200,000	300,000	400,000	500,000
AG40d-02r	8.00	2.37	-0.060	25%	x	x	x	x	x
AG455ct-02r	6.47	2.28	-0.050	30%	x	x	x	x	x
W1011	11.00	0.00	0.000	20%	x	x		x	
				30%	x	x		x	
W1015	15.00	0.00	0.000	20%	x	x		x	
				30%	x	x		x	

Throughout this chapter, a few variables will be frequently used for analysis and comparison. These variables are the airfoil thickness ratio (t/c), flap-chord ratio (c_f/c), and flap deflection (δ_f). Each of these parameters are shown schematically in Fig. 6.1.

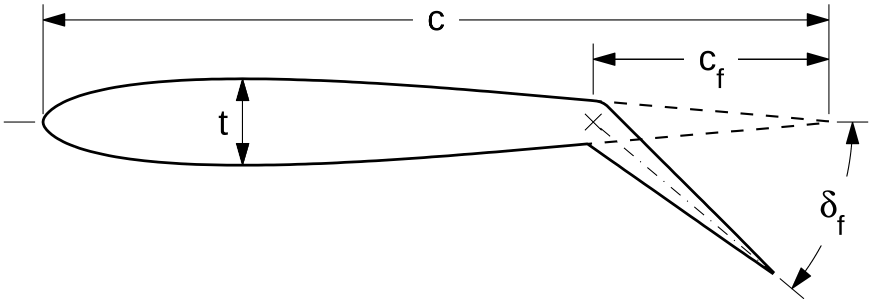

Figure 6.1: Schematic defining c, c_f, t, and δ_f.

6.1 Lift and Moment Increments Plots

When analyzing the performance of flapped airfoils, it is instructive to look at a lift increment plot. A lift increment (ΔC_l) represents the amount of lift that is gained or lost due to a flap deflection measured from a reference configuration. It is usually most instructive to take the unflapped airfoil ($\delta_f = 0$) as the reference configuration, which is done for this analysis. The lift increments are plotted against their respective flap deflection to create the lift increment plot. An example of a lift increment plot taken from Hoerner [50] can be seen in Fig. 6.2.

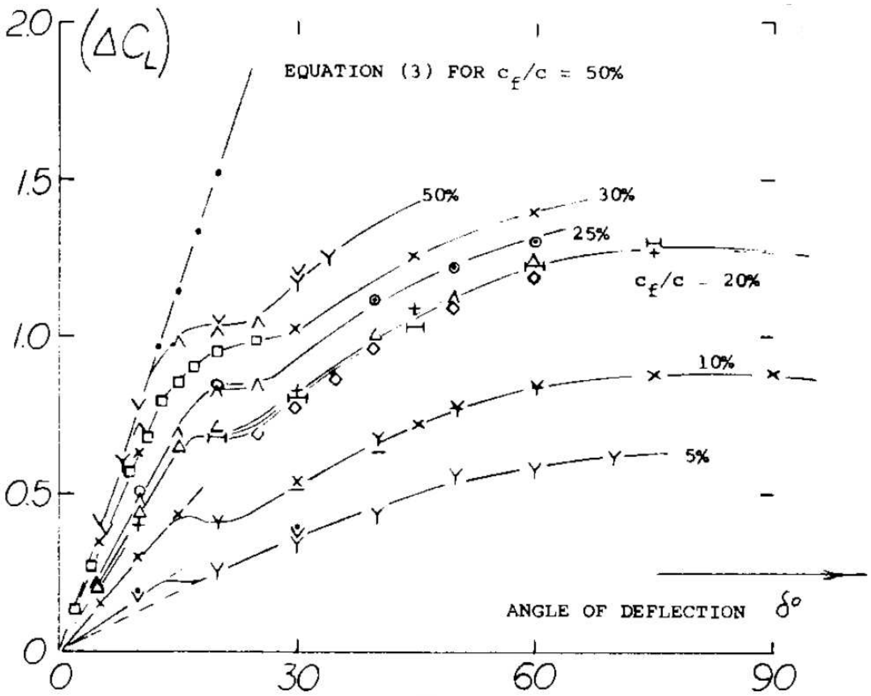

Figure 6.2: Lift increment plot taken from Hoerner [50].

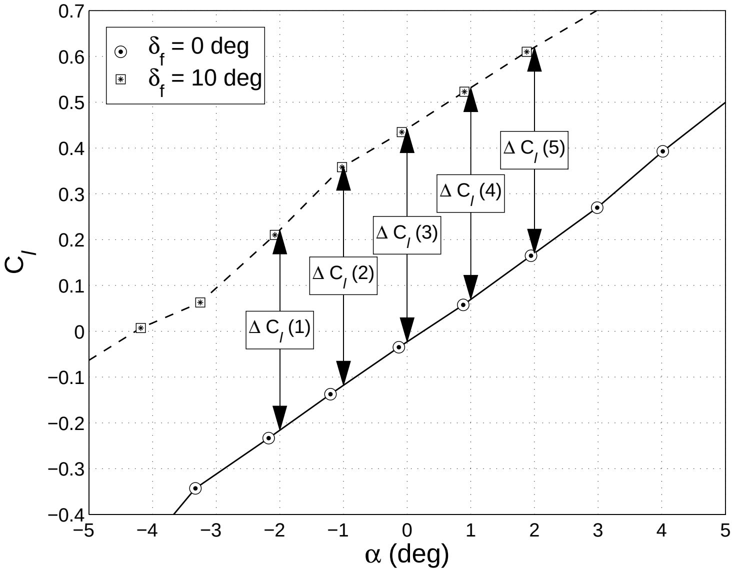

Figure 6.3: Example of a lift increment calculation using experimental data from the W1015 airfoil ($c_f/c = 0.20$) with a 0 and 10 deg flap.

The lift increments are calculated in a similar fashion as Hoerner but with a slight variation. In Hoerner's book, Fluid-Dynamic Lift [50], the lift increments (ΔC_l) were calculated at a single angle of attack. An angle of attack of 0 deg with respect to the undeflected airfoil was chosen by Hoerner since most flapped airfoils operate in this angle of attack region. The lift increments seen in Figs. 6.5–6.21 are an average of five lift increments calculated at different angle of attacks to help remove inconsistencies in lift data caused by low Reynolds number effects. Angles of attack of -2, -1, 0, 1, and 2 deg were chosen to best represent the operation region. A visual representation of the five lift increments can be seen in Fig. 6.3. The moment increments (ΔC_m) seen in Figs. 6.5–6.12 are calculated in the same manner as the lift increments.

In Fig. 6.3, experimental data points from the W1015 airfoil ($c_f/c = 0.20$) with a 0 and 10 deg flap deflection are plotted. It can be seen that the experimental data points do not exactly equal the values of interest for the lift increment analysis. Thus, a linear interpolation was performed to obtain the lift coefficient at the desired angles of attack. The same procedure was followed for the moment increment calculation.

In the lift increment plots seen in Figs. 6.5–6.21, there are three distinct regions (see Fig. 6.4) that define different trends of the ΔC_l values. The first (I) region is defined as the linear region and occupies the smaller flap deflections of 0 deg $\leq \delta_f \leq$ 10 to 20 deg. In this region, the performance is dominated by fully attached flow on the upper and lower surfaces, and the slope of the ΔC_l curve is constant. The second (II) region is defined as the transition region because it functions as a connection between the first and third regions. It is normally marked as the leveling or decreasing of ΔC_l values that is caused by the separation of flow from the upper surface of the flap. Separation from the upper

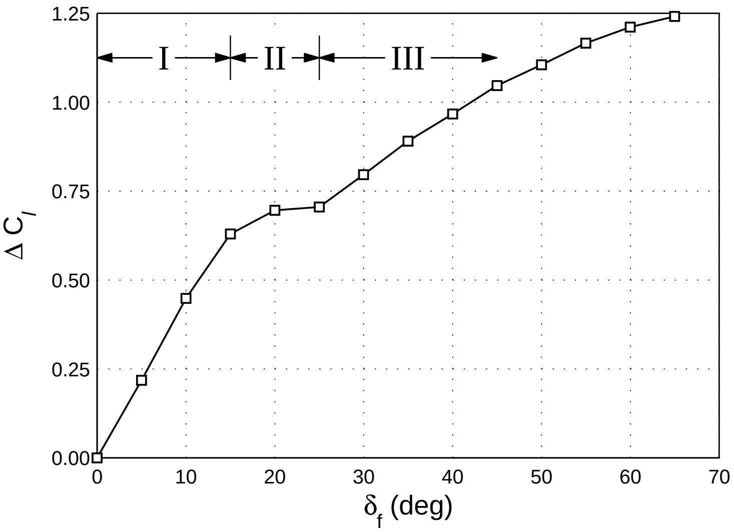

Figure 6.4: Conceptual drawing defining the linear (I), transition (II), and nonlinear (III) regions of the ΔC_l plot using data from the W1011 airfoil with $c_f/c = 0.20$ at $Re = 200{,}000$.

surface normally occurs around a flap deflection of 10 to 20 deg. The actual flap deflection for flow separation is dependent on Reynolds number, airfoil thickness, flap-chord ratio, angle of attack, and the size of the gap around the nose of the flap [50]. The third (III) region is defined as the nonlinear region because of the reduced nonlinear increase of ΔC_l values with flap deflection compared with the linear (I) region. The nonlinear region occupies everything after the transition region, and the start of the nonlinear region is marked by the increase in ΔC_l values. In this region, the flow is completely separated over the upper surface of the flap.

6.1.1 Individual Airfoil Results

The lift and moment increment results centered about $\alpha = 0$ deg are plotted below in Figs. 6.5–6.12 for each airfoil tested. The airfoil results are plotted in the following order: AG40d-02r, AG455ct-02r, W1011, and W1015. The first plot for each airfoil contains the lift increment results while the second plot contains the moment increment results. It is interesting to note that Reynolds number does not play a significant role in either the lift or moment increments since most of the results follow the same trends regardless of Reynolds number. Instead, the main driving factor for changes in ΔC_l is the flap-chord ratio, which was observed in Ref. 50. The Reynolds number does seem to affect the initiation and severity of the transition region.

From Figs. 6.5–6.12, it can be seen that some correlation exists between the lift and moment increments. In the linear region of the lift increment, the moment increment decreases linearly. In the transition region, the moment increment slope starts to increase as the lift increment slope decreases. This trend is evident in the AG455ct-02r plots found in Figs. 6.7 and 6.8. All of the airfoils exhibit these characteristics.

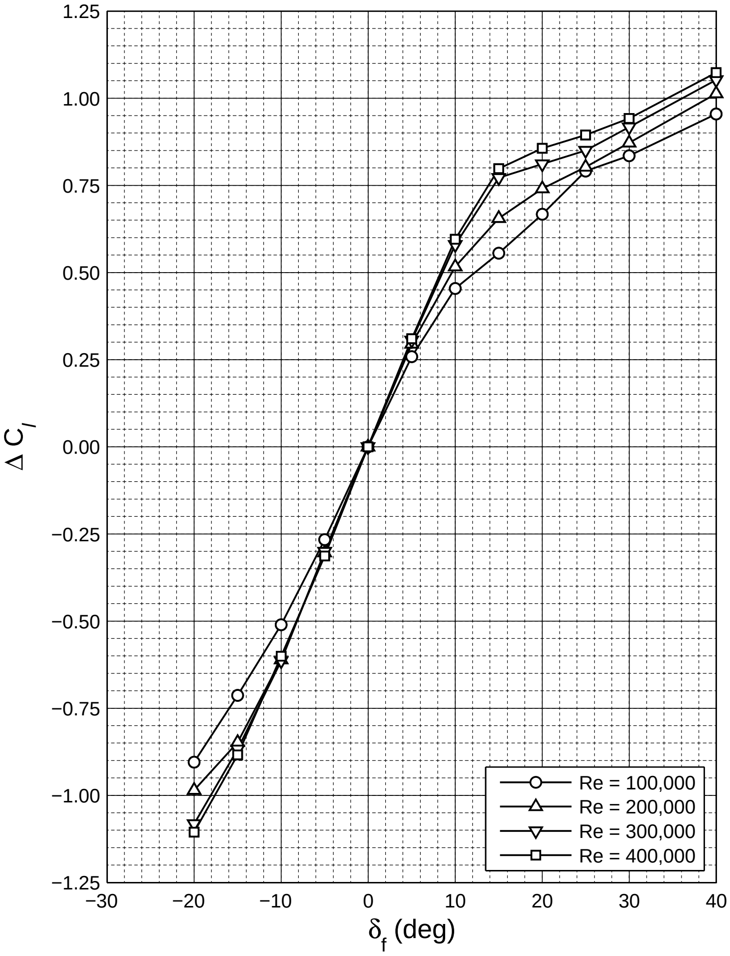

Figure 6.5: Effect of a flap on lift increment for the AG40d-02r airfoil with $c_f/c = 0.25$ centered about $\alpha = 0$ deg.

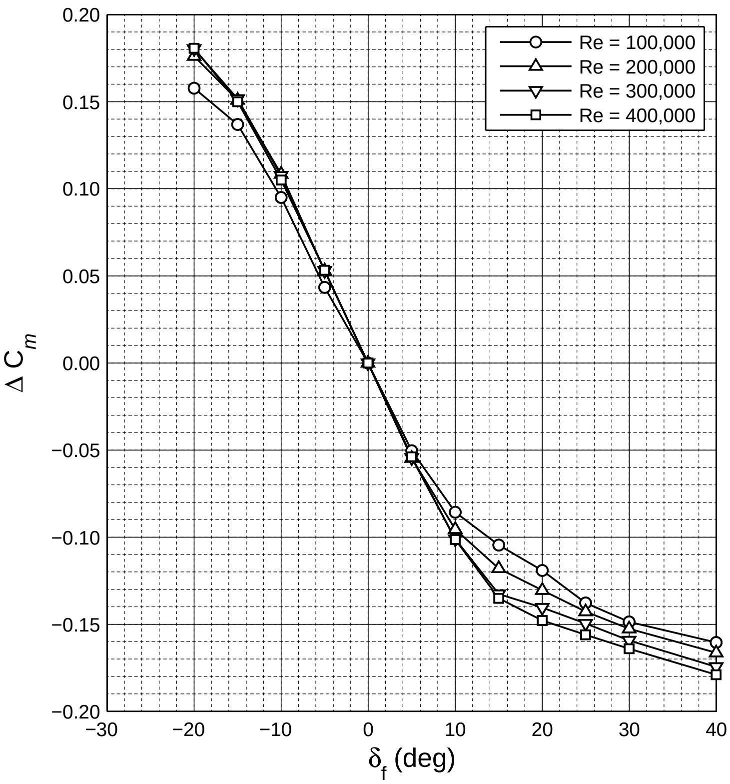

Figure 6.6: Effect of a flap on moment increment for the AG40d-02r airfoil with $c_f/c = 0.25$ centered about $\alpha = 0$ deg.

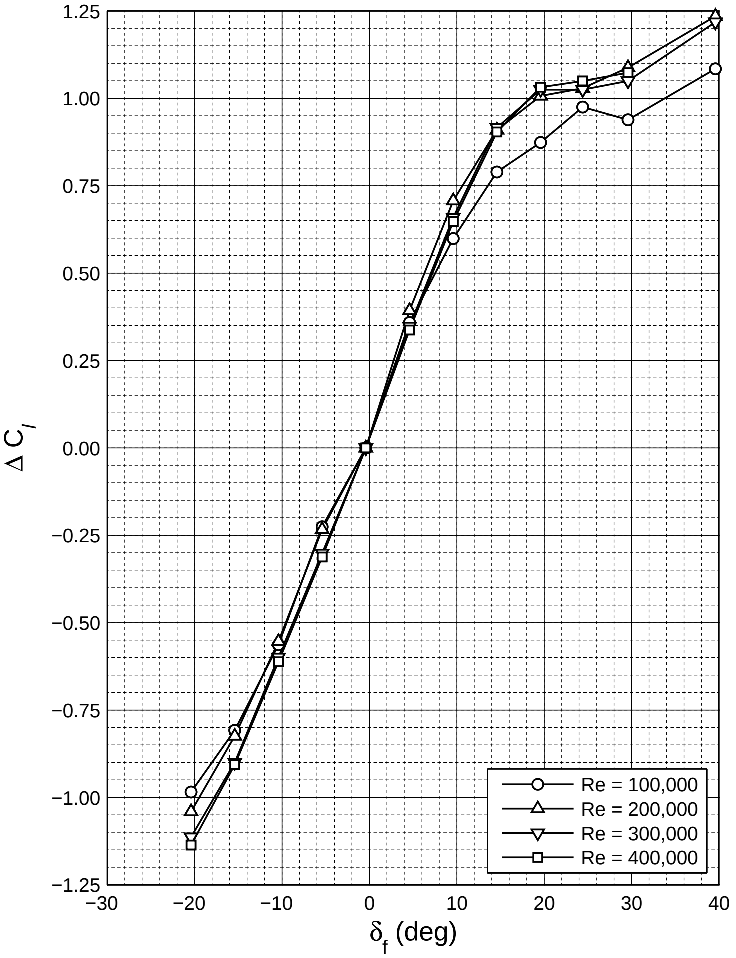

Figure 6.7: Effect of a flap on lift increment for the AG455ct-02r airfoil with $c_f/c\ =\ 0.30$ centered about $\alpha = 0$ deg.

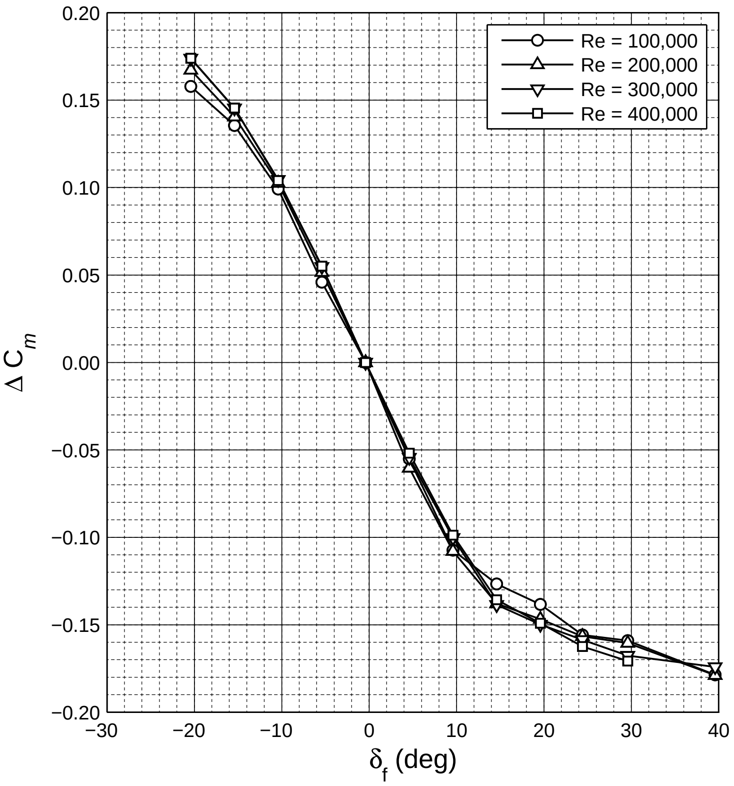

Figure 6.8: Effect of a flap on moment increment for the AG455ct-02r airfoil with $c_f/c = 0.30$ centered about $\alpha = 0$ deg.

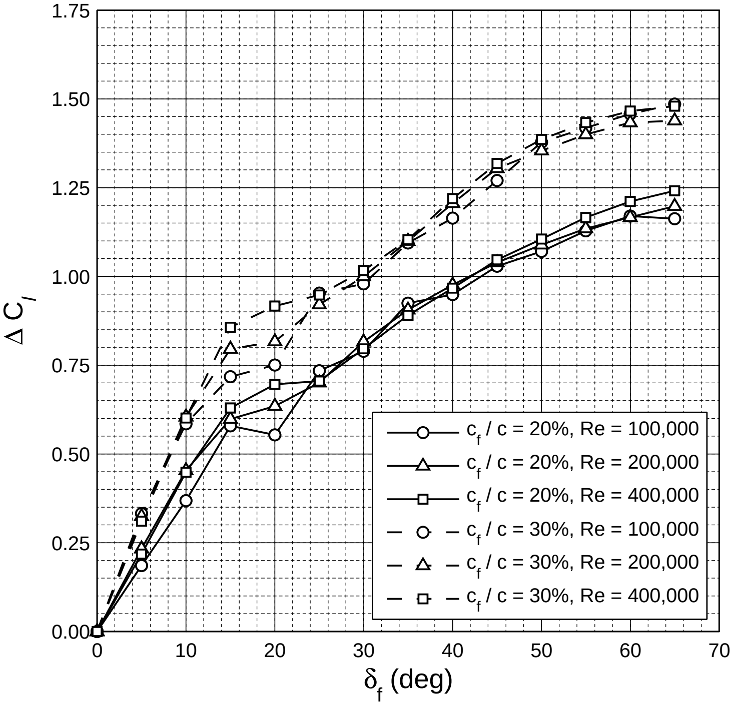

Figure 6.9: Effect of a flap on lift increment for the W1011 airfoil with two flap sizes centered about $\alpha = 0$ deg.

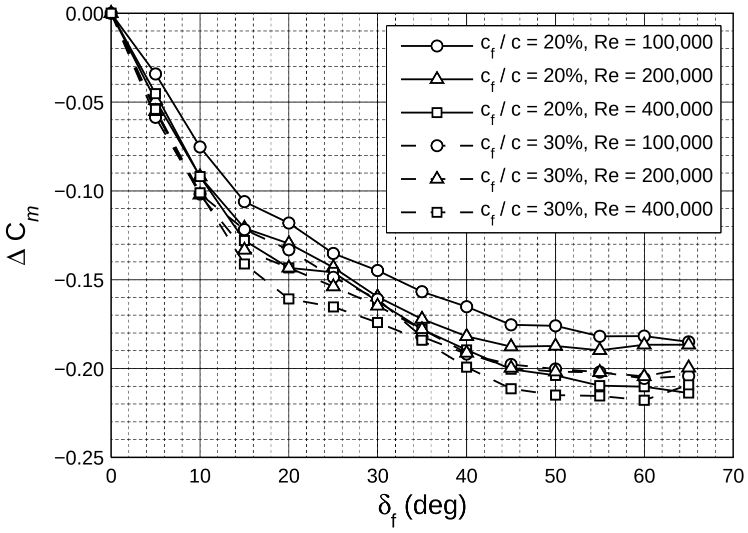

Figure 6.10: Effect of a flap on moment increment for the W1011 airfoil with two flap sizes centered about $\alpha = 0$ deg.

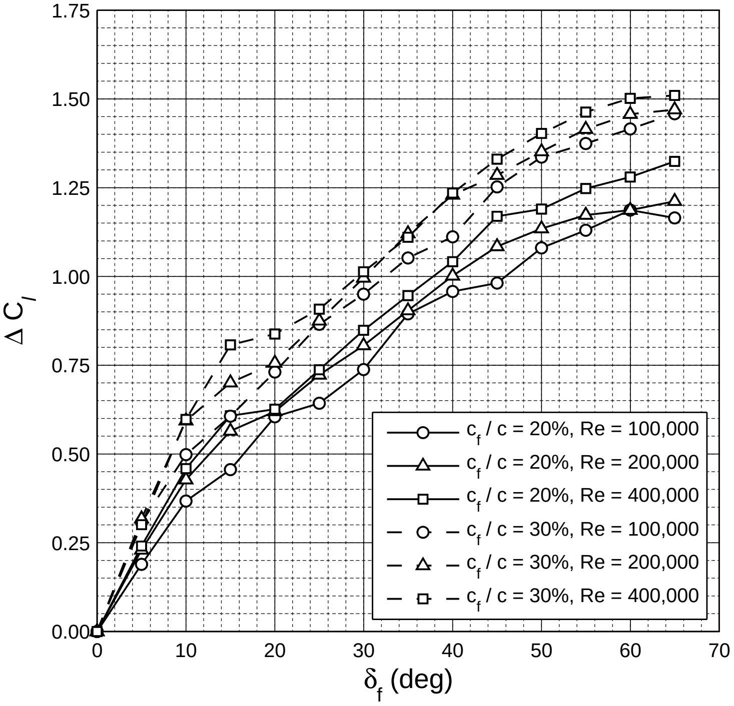

Figure 6.11: Effect of a flap on lift increment for the W1015 airfoil with two flap sizes centered about $\alpha = 0$ deg.

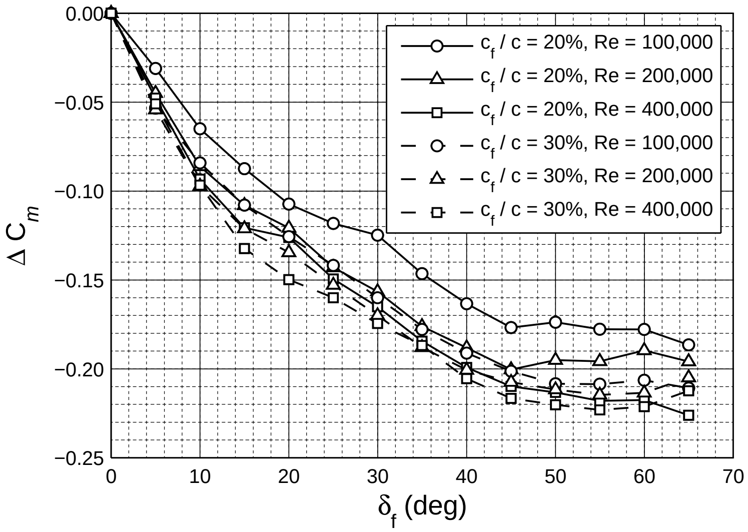

Figure 6.12: Effect of a flap on moment increment for the W1015 airfoil with two flap sizes centered about $\alpha = 0$ deg.

6.1.2 Cross Comparisons of Lift Increment

Cross comparisons of all the airfoil lift increment results centered about $\alpha = 0$ deg are plotted in Figs. 6.13–6.21. These figures are split up into three different sets to shed light on the trends in the lift increments with respect to flap deflection. Within each set, the results are plotted according to Reynolds number to better examine the results.

In the first set of plots (Figs. 6.13–6.15), the 20% of chord ($c_f/c = 0.20$) flapped airfoils are compared. The airfoils with a 20% of chord flap are the W1011 and W1015. Both airfoils are symmetrical and were designed to exhibit similar qualities, which was accomplished with the transition curve discussed in Chapter 5. The results for Reynolds numbers of 100,000 and 200,000 are consistent between the two airfoils, but the results for a Reynolds number of 400,000 show some discrepancy in the nonlinear region. The W1015 produces consistently more ΔC_l compared with the W1011 potentially owing to a thickness effect. As seen in all three plots, the W1015, which is the thicker airfoil (see Table 6.1), starts the transition region earlier and has a more severe degradation of ΔC_l.

In the second set of plots (Figs. 6.16–6.18), the 30% of chord ($c_f/c = 0.30$) flapped airfoils are compared. The airfoils with a 30% of chord flap are the AG455ct-02r, W1011, and W1015. As discussed previously, the W1011 and W1015 were designed to exhibit similar qualities. The AG455ct-02r is a non-symmetrical airfoil with a thickness of 6.47%. All of the results are consistent between the three airfoils besides in the transition region. As observed in the first (20% of chord flap) cross comparison, the thicker airfoils start the transition region earlier and have a more severe degradation of ΔC_l independent of Reynolds number.

In the third set of plots (Figs. 6.19–6.21), all of the airfoils are compared according to Reynolds number. These plots include results from the AG40d-02r, AG455ct-02r, W1011 with $c_f/c = 0.20$, W1011 with $c_f/c = 0.30$, W1015 with $c_f/c = 0.20$, and W1015 with $c_f/c = 0.30$. All of the airfoil results were plotted in either the first or second set of plots except the AG40d-02r. The AG40d-02r is a non-symmetrical airfoil with a thickness of 8.00% and 25% of chord flap. With a 25% of chord flap, it is expected that the lift increment values will fall between the 20% and 30% of chord flap results. As seen in Figs. 6.19–6.21, the AG40d-02r lift increment values fall between the 20% and 30% of chord flap results. This result confirms that the flap-chord ratio (c_f/c) is the major factor that drives the lift increment values.

From the results seen in Figs. 6.13–6.21, it can be concluded that airfoil thickness does not significantly affect the lift increment, but it does affect the initiation and severity of the transition region. This result agrees with an earlier statement that thickness (t/c) affects the flap deflection where the flow separates over the upper surface of the flap. Instead, the flap-chord ratio is the main cause for changes in lift increment when comparing different airfoils as seen in Figs. 6.19–6.21.

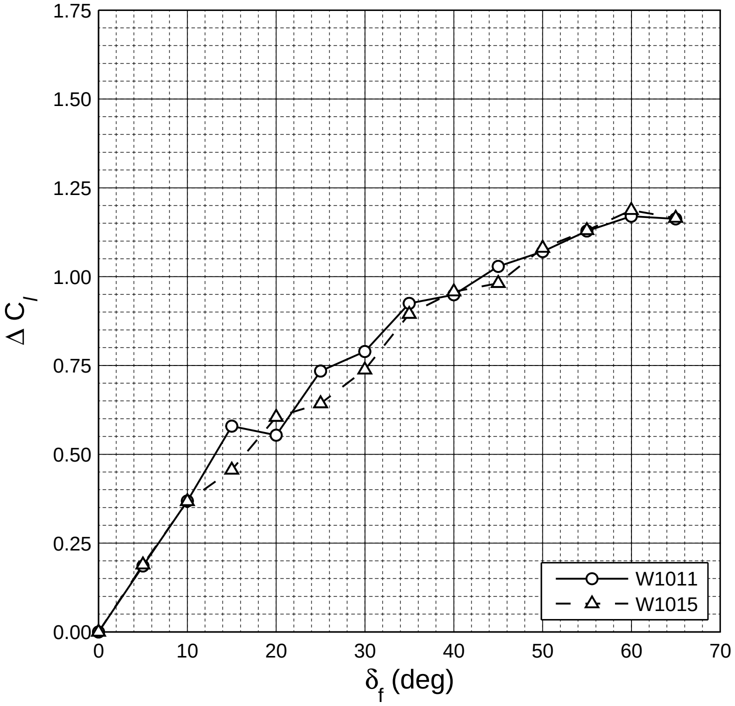

Figure 6.13: Effect of a flap on lift increment for a 20%-chord flap at Re = 100,000 centered about $\alpha = 0$ deg.

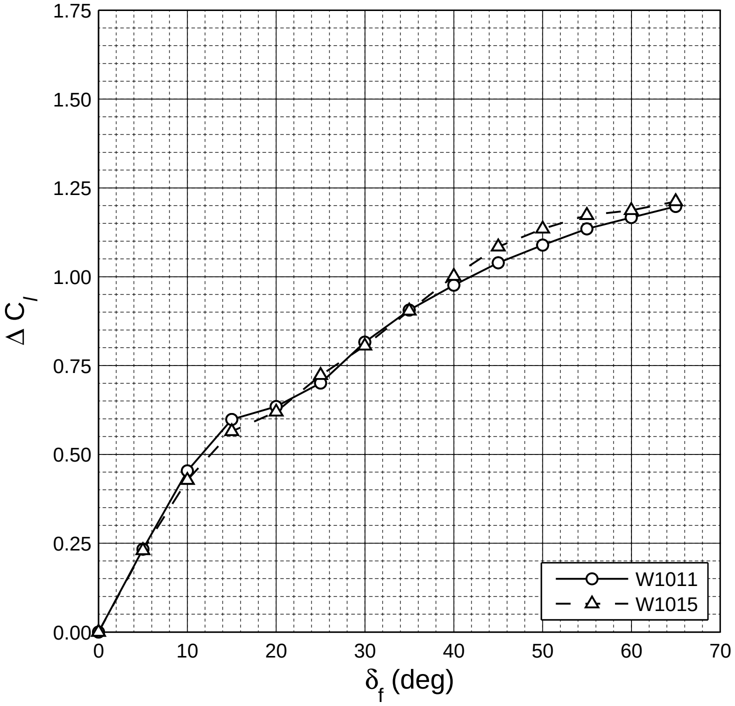

Figure 6.14: Effect of a flap on lift increment for a 20%-chord flap at Re = 200,000 centered about $\alpha = 0$ deg.

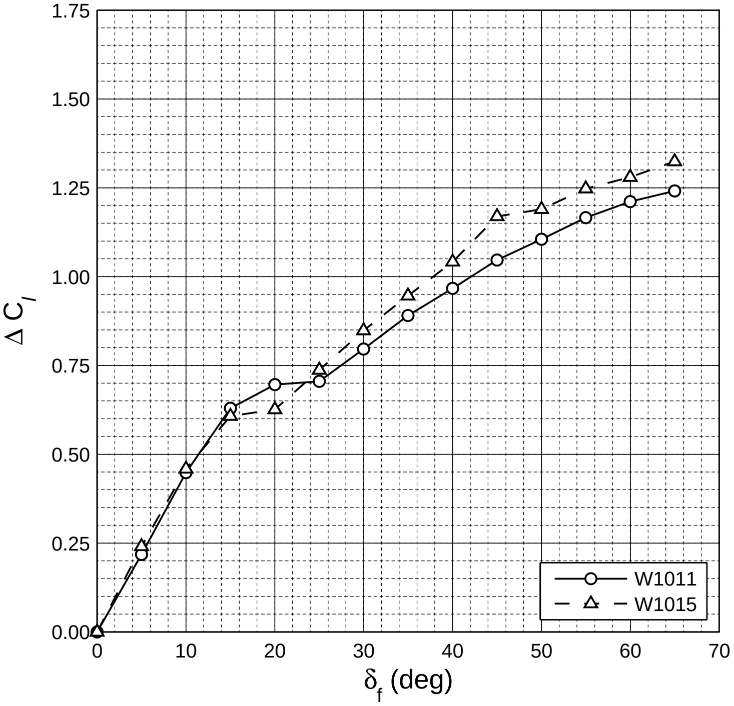

Figure 6.15: Effect of a flap on lift increment for a 20%-chord flap at Re = 400,000 centered about $\alpha = 0$ deg.

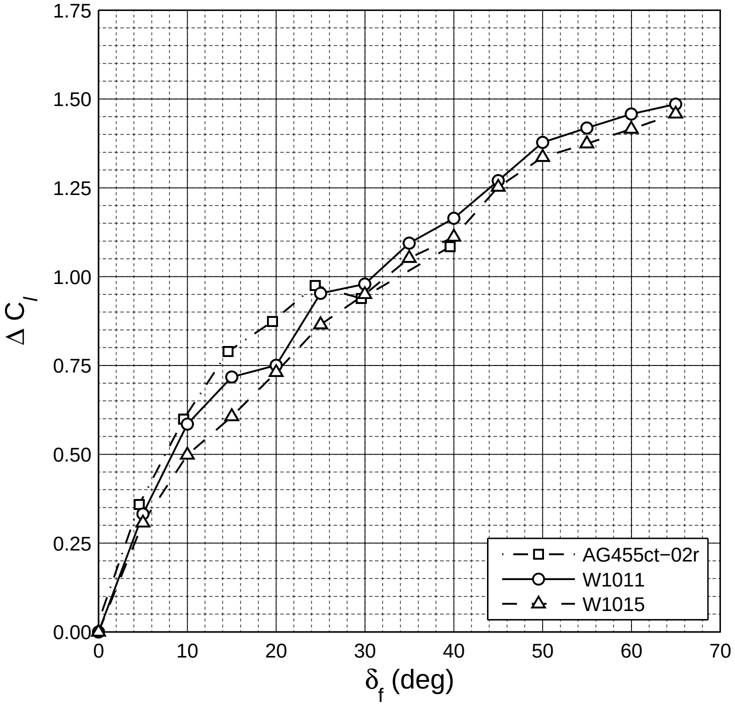

Figure 6.16: Effect of a flap on lift increment for a 30%-chord flap at Re = 100,000 centered about $\alpha = 0$ deg.

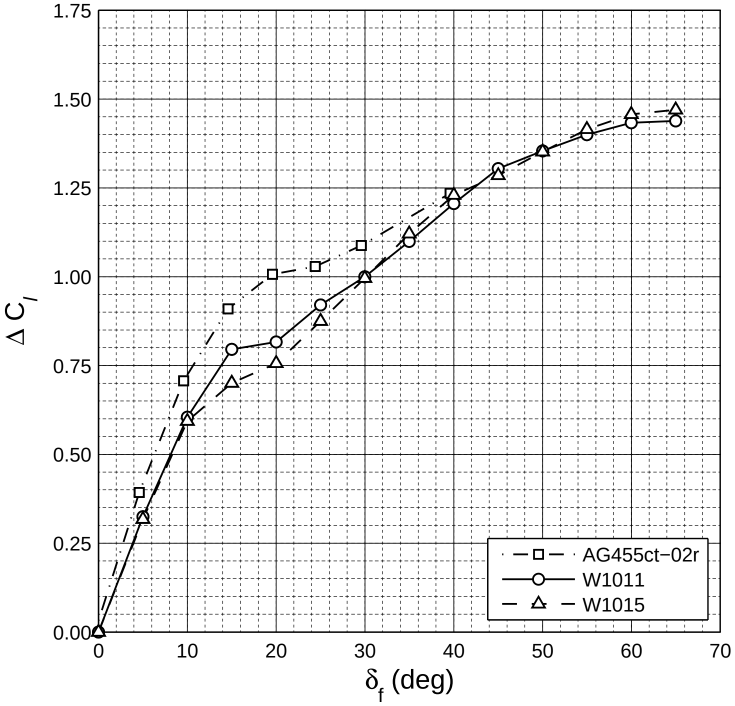

Figure 6.17: Effect of a flap on lift increment for a 30%-chord flap at Re = 200,000 centered about $\alpha = 0$ deg.

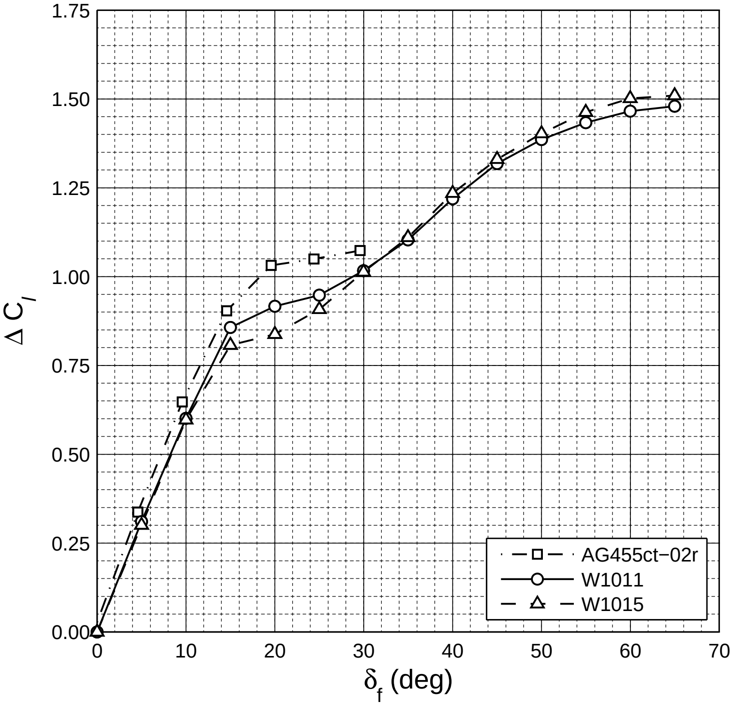

Figure 6.18: Effect of a flap on lift increment for a 30%-chord flap at Re = 400,000 centered about $\alpha = 0$ deg.

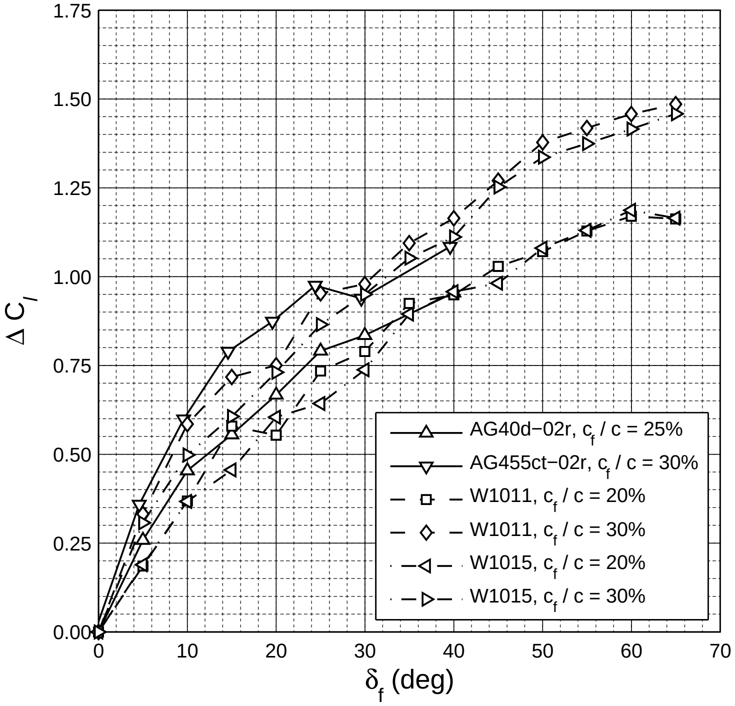

Figure 6.19: Effect of a flap on lift increment for all airfoils at Re = 100,000 centered about $\alpha = 0$ deg.

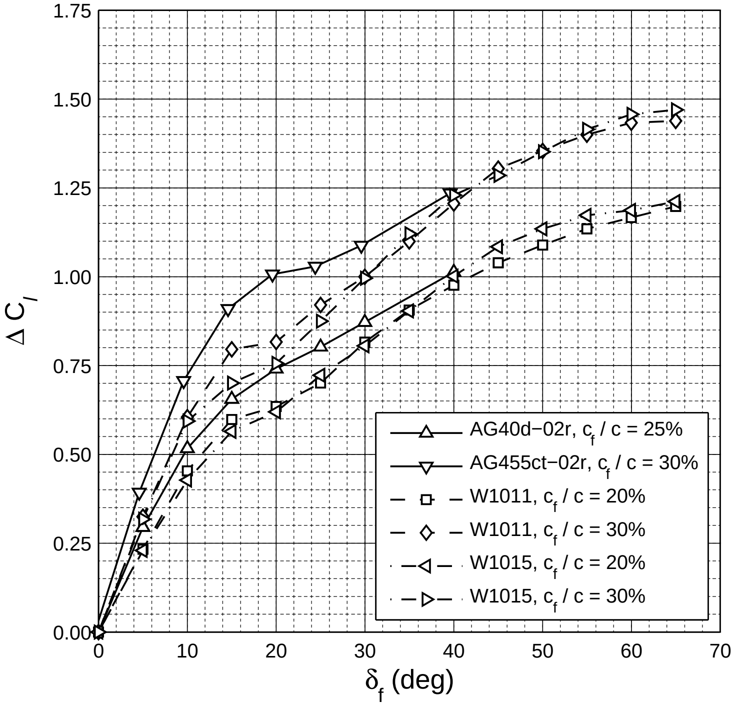

Figure 6.20: Effect of a flap on lift increment for all airfoils at Re = 200,000 centered about $\alpha = 0$ deg.

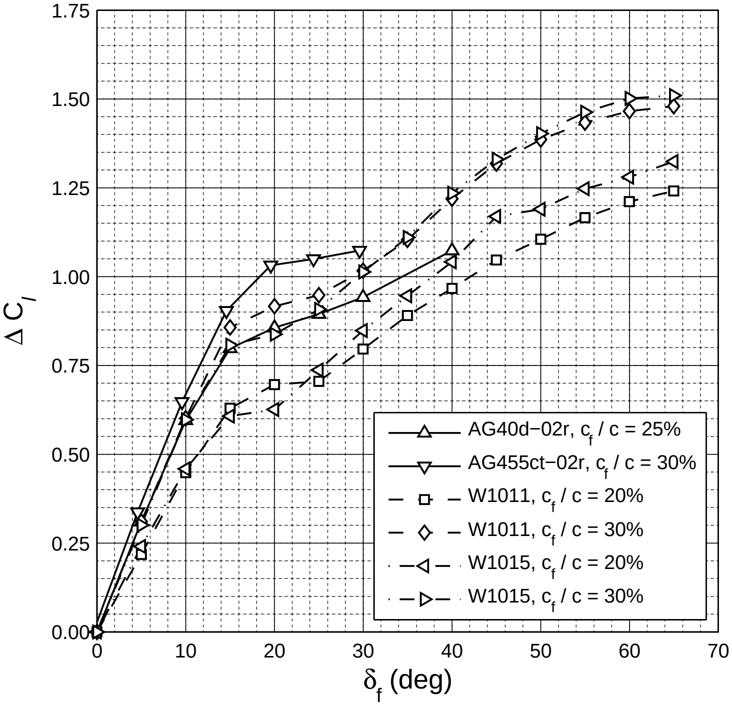

Figure 6.21: Effect of a flap on lift increment for all airfoils at Re = 400,000 centered about $\alpha = 0$ deg.

6.1.3 Effect of Flap-Chord Ratio on Lift Increment

The flap-chord ratio plays a crucial role in determining the effectiveness of a plain flap as seen in Figs. 6.19–6.21. In Ref. 50, it is suggested that the effectiveness of a plain flap is a function of the square root of the flap-chord ratio, viz

$$\Delta C_l \sim \sqrt{c_f/c} \tag{6.1}$$

Experimental lift increment values centered about $\alpha = 0$ deg for the W1011 airfoil with a 20% and 30% of chord flap at a Reynolds number of 400,000 with flap deflections of 40, 50, and 60 deg are plotted in Fig. 6.22. Along with the plotted data, scaled square root curves of the flap-chord ratio are also plotted to best fit the experimental data. The fitted curves agree well with the suggested relationship from Ref. 50. Similar results were seen with the W1015 airfoil. In aircraft design, flap-chord ratios of 20% are often used for control surfaces to obtain a modest lift increment with an acceptable structural penalty [50].

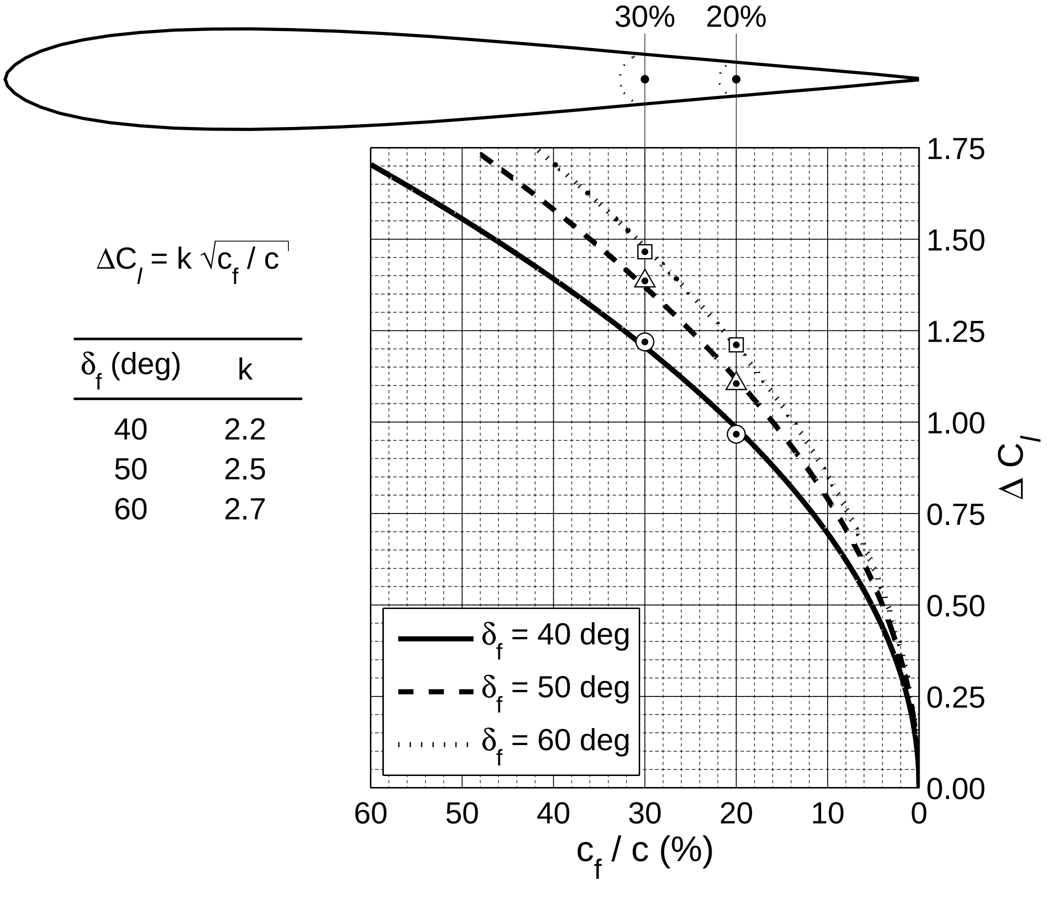

Figure 6.22: Scaled lift increment curves as a function of the square root of the flap-chord ratio to fit experimental lift increment values centered about α = 0 deg for the W1011 airfoil at Re = 400,000 with flap deflections of 40, 50, and 60 deg shown by markers.

6.2 Maximum Lift Coefficient for Varying Flap Deflections

Maximum lift coefficients for all configurations are presented in this section. In Figs. 6.23–6.26, the maximum lift coefficients for each configuration are plotted against their respective flap deflection. The results for each of the four airfoils are plotted separately for clarity. From Figs. 6.23–6.26, four main trends emerge. First, the Reynolds number affects the maximum lift coefficient. As the Reynolds number increases, the maximum lift coefficient also increases. From the discussion in Chapter 5, this result is not surprising. In fact for the W1011 and W1015 airfoils seen in Figs. 6.25 and 6.26, variations in the maximum lift coefficient for a 0-deg flap deflection can also be seen in the XFOIL viscous analysis presented in Chapter 5. The XFOIL viscous analysis for the W1011 and W1015 airfoils can be seen in Figs. 5.6 and 5.8. Second, the maximum lift coefficient increases linearly for small ($\delta_f \leq$ 10 to 20 deg) flap deflections. This result is not surprising since most of the flow is attached to the upper surface of the flap for these small flap deflections. The flap deflection at which the results deviate from the linear trend depends on Reynolds number, airfoil thickness, flap-chord ratio, and others. Third, the maximum lift coefficient plateaus between a flap deflection of 40 and 50 deg. Thus, it can be concluded that an additional deflection of the flap above 50 deg will provide no extra benefit in regard to the maximum lift coefficient. Fourth, the 30% of chord flap consistently produces a larger maximum lift coefficient compared with the 20% of chord flap for the W1011 and W1015 airfoils. This result is expected because of the larger size of the 30% of chord flap compared to the 20% of chord flap.

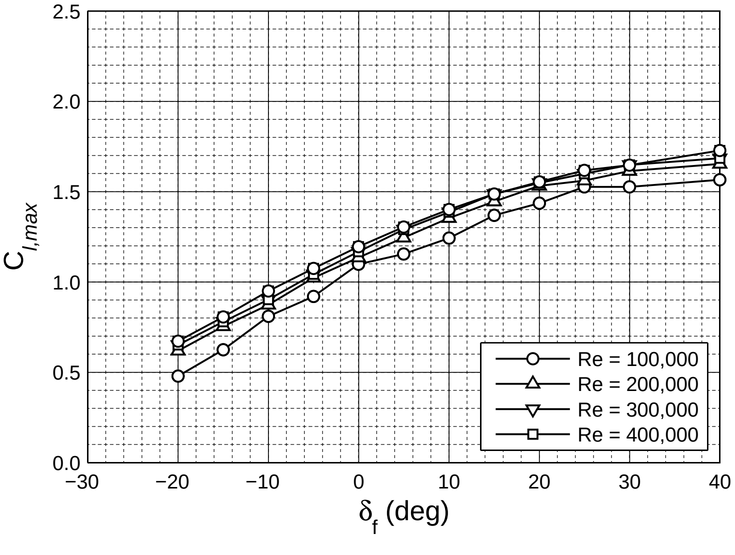

Figure 6.23: Effect of a flap on maximum lift coefficient for the AG40d-02r airfoil with $c_f/c = 0.25$.

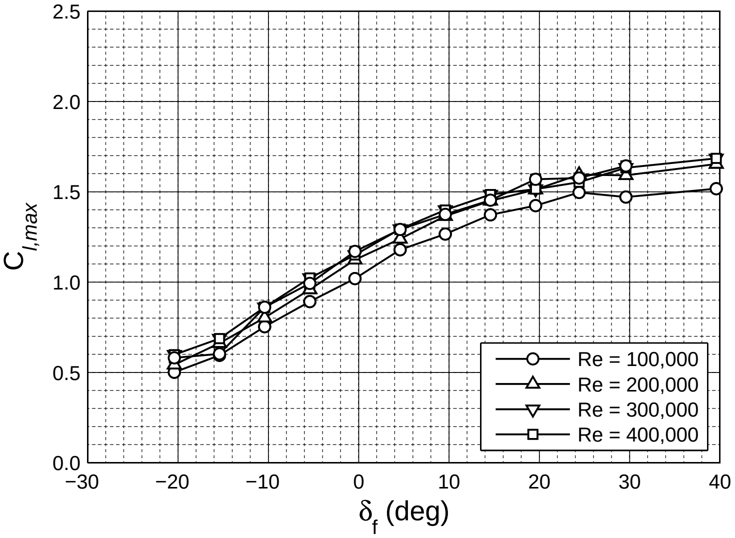

Figure 6.24: Effect of a flap on maximum lift coefficient for the AG455ct-02r airfoil with $c_f/c = 0.30$.

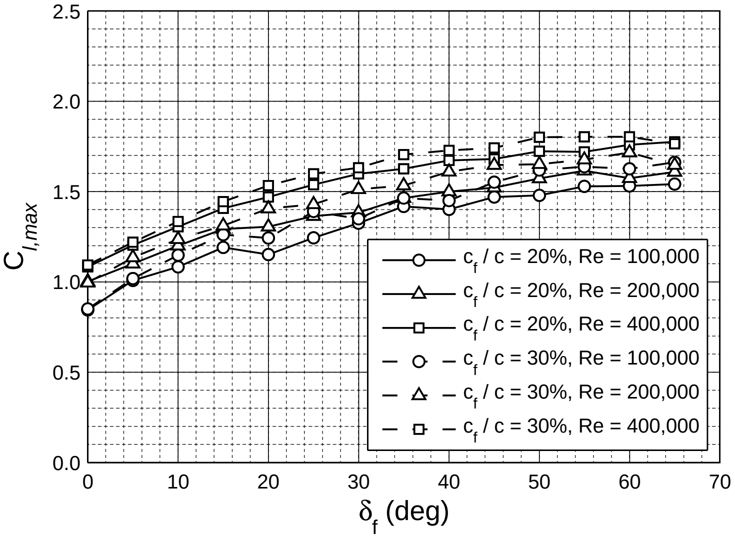

Figure 6.25: Effect of a flap on maximum lift coefficient for the W1011 airfoil with two flap sizes ($c_f/c = 0.20$ and 0.30).

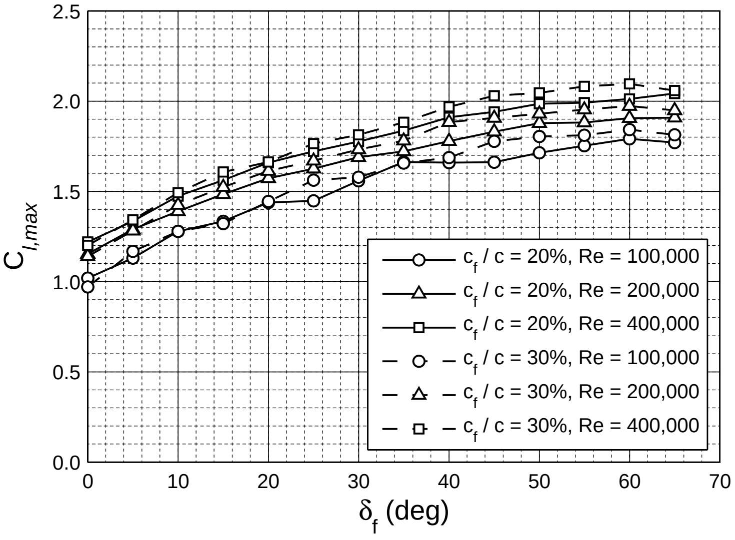

Figure 6.26: Effect of a flap on maximum lift coefficient for the W1015 airfoil with two flap sizes ($c_f/c = 0.20$ and 0.30).

6.3 Drag Polars for Large Flap Deflections

Drag data with highly deflected flaps ($\delta_f \geq 30$ deg) is presented in this section. There are three sets of plots contained in this section. The first set of plots (Figs. 6.28–6.32) shows the effect of flap deflections on the drag values for individual airfoils. Five airfoil drag polars are plotted with varying flap deflections while holding Reynolds number constant. The five airfoils are plotted in the following order: AG455ct-02r, W1011 with $c_f/c = 0.20$, W1011 with $c_f/c = 0.30$, W1015 with $c_f/c = 0.20$, and W1015 with $c_f/c = 0.30$.

The second set of plots (Figs. 6.33 and 6.34) shows the effect of the flap size on the drag values for flap deflections of 40, 50, and 60 deg. The first plot examines the flap size effects for the W1011 and the second plot for the W1015. From Figs. 6.33 and 6.34, it can be seen that the 30% of chord flap has more drag than the 20% of chord flap for the same flap deflection. For both the W1011 and W1015, the drag values for the 20% of chord flap with a 60-deg flap deflection are similar to the drag values for the 30% of chord flap with a 40-deg flap deflection. It can be seen in Fig. 6.27 that the projected areas of the two configurations in the freestream direction are almost the same. Thus, it can be concluded that the primary driving factor for drag with large flap deflections is the projected area of the flap in the freestream direction.

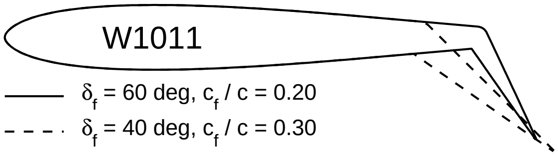

Figure 6.27: Projected area comparison of two flap deflections with different flap-chord ratios.

The third set of plots (Figs. 6.35 and 6.36) shows the effect of varying airfoil thickness while keeping the flap size constant. The first plot examines the 20% of chord flap and the second the 30% of chord flap. From Figs. 6.35 and 6.36, it can be concluded that the airfoil thickness does not significantly affect the drag for highly deflected flaps.

Drag data with highly deflected flaps was only taken at a Reynolds number of 200,000 owing to a combination of constraints. Lift data was taken at Reynolds numbers of 100,000, 200,000, and 400,000. Thus, the drag data had to be taken at one of those Reynolds numbers. It is advantageous to take drag data at the highest Reynolds number possible to mitigate measurement uncertainty associated with lower Reynolds numbers (see Section 4.3). At a Reynolds number of 400,000, the differential pressure modules described in Subsection 3.5.3 were exceeding their limit. This limit restricted the tests to a Reynolds number of 100,000 and 200,000. Time was a major constraint because the data was taken toward the end of the last wind tunnel entry. Observations from previous tests showed that collecting drag data for a 40 deg flap deflection took about 20% longer at a Reynolds number of 100,000 compared with 200,000. Thus, drag data with highly deflected flaps was only collected at a Reynolds number of 200,000.

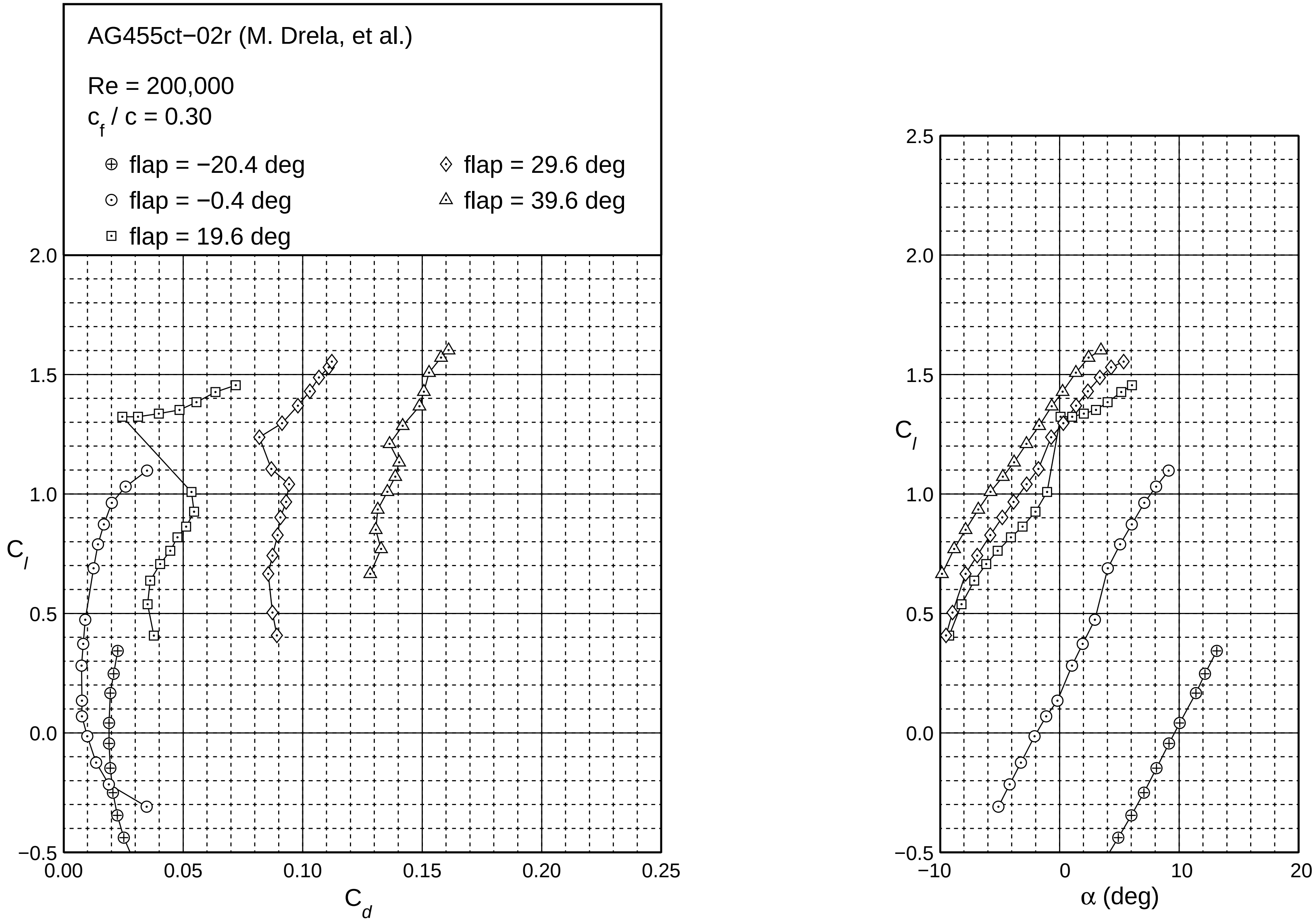

Figure 6.28: Drag polar with selected flap deflections for the AG455ct-02r airfoil.

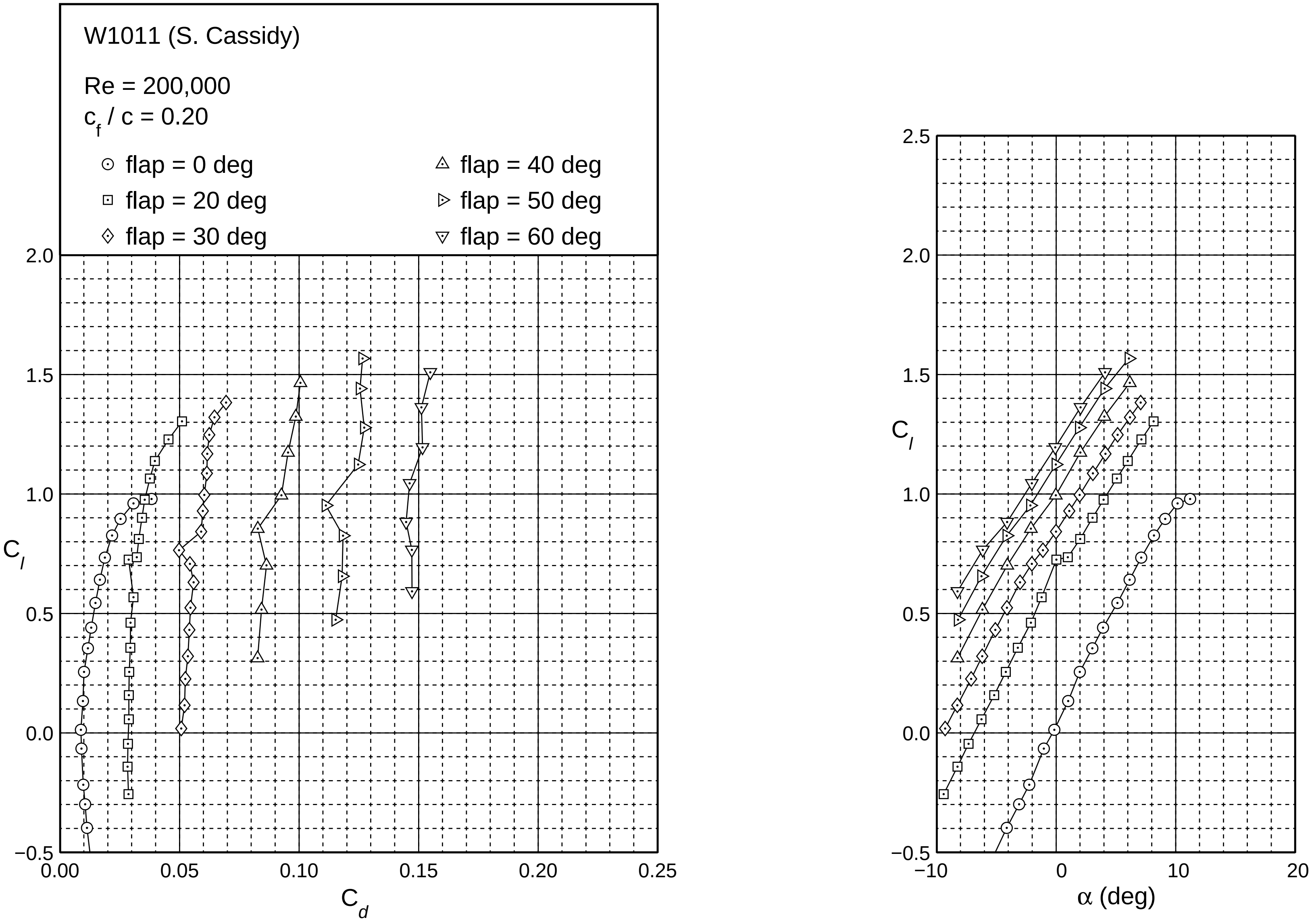

Figure 6.29: Drag polar with selected flap deflections for the W1011 airfoil with $c_f/c = 0.20$.

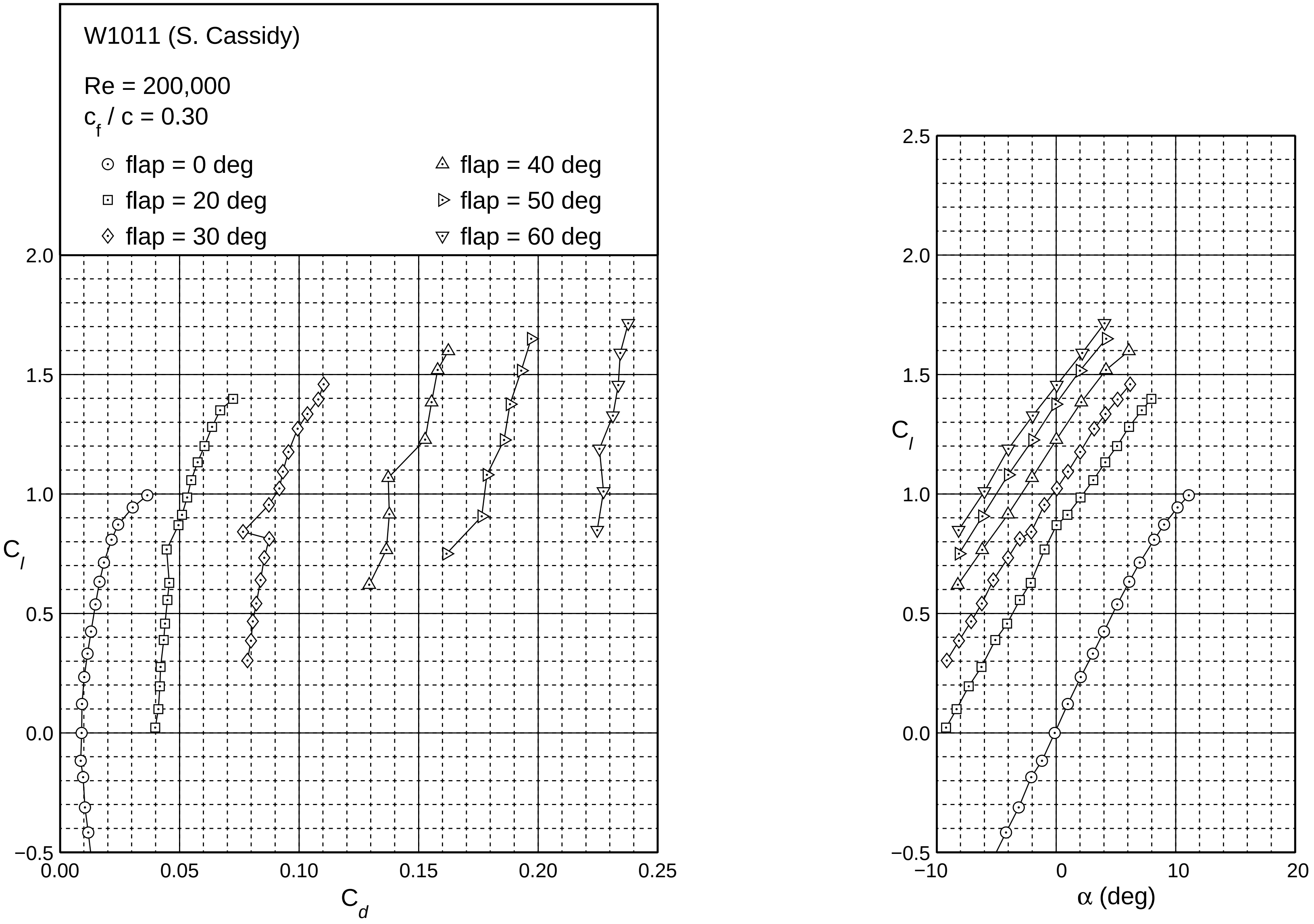

Figure 6.30: Drag polar with selected flap deflections for the W1011 airfoil with $c_f/c = 0.30$.

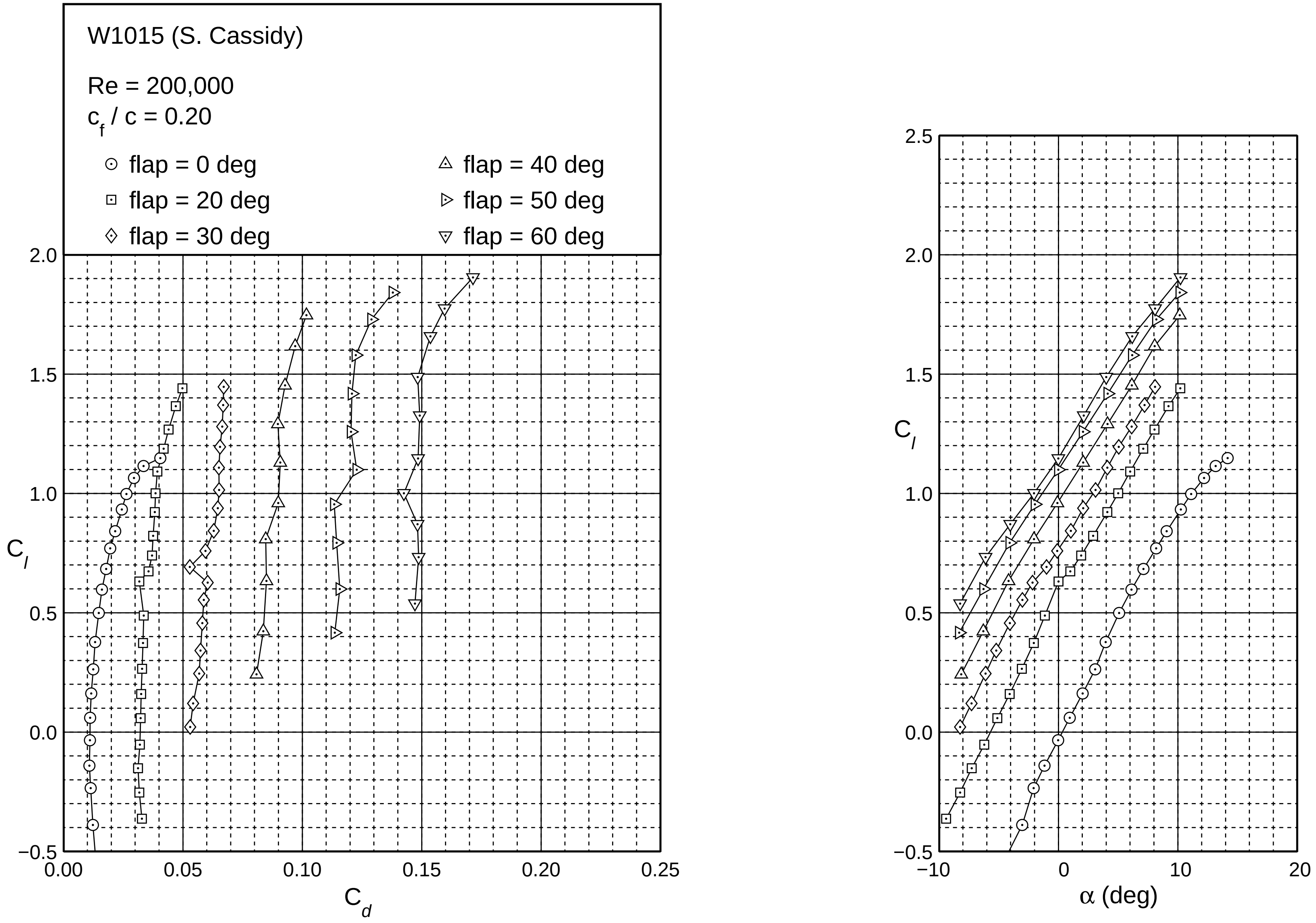

Figure 6.31: Drag polar with selected flap deflections for the W1015 airfoil with $c_f/c = 0.20$.

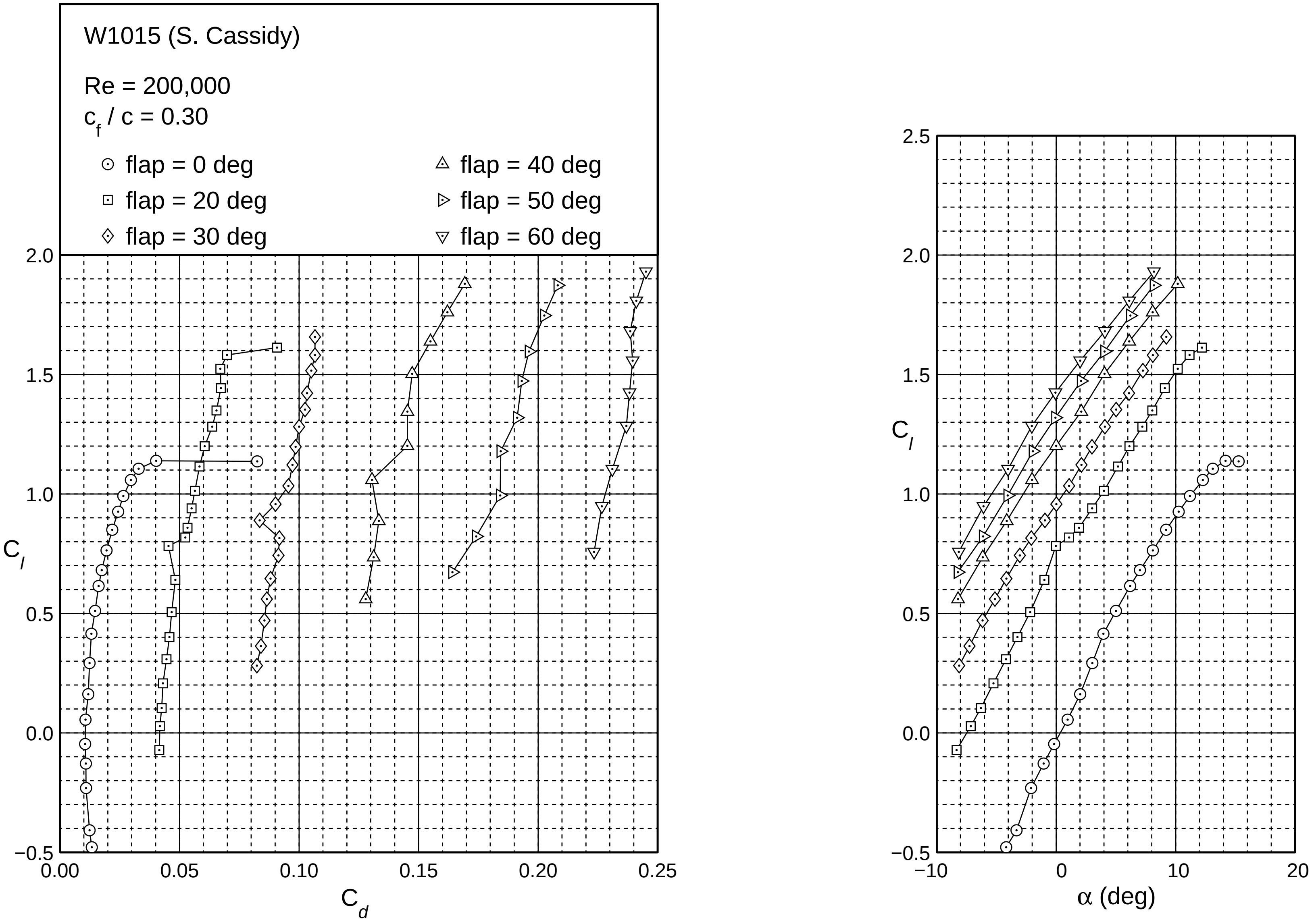

Figure 6.32: Drag polar with selected flap deflections for the W1015 airfoil with $c_f/c = 0.30$.

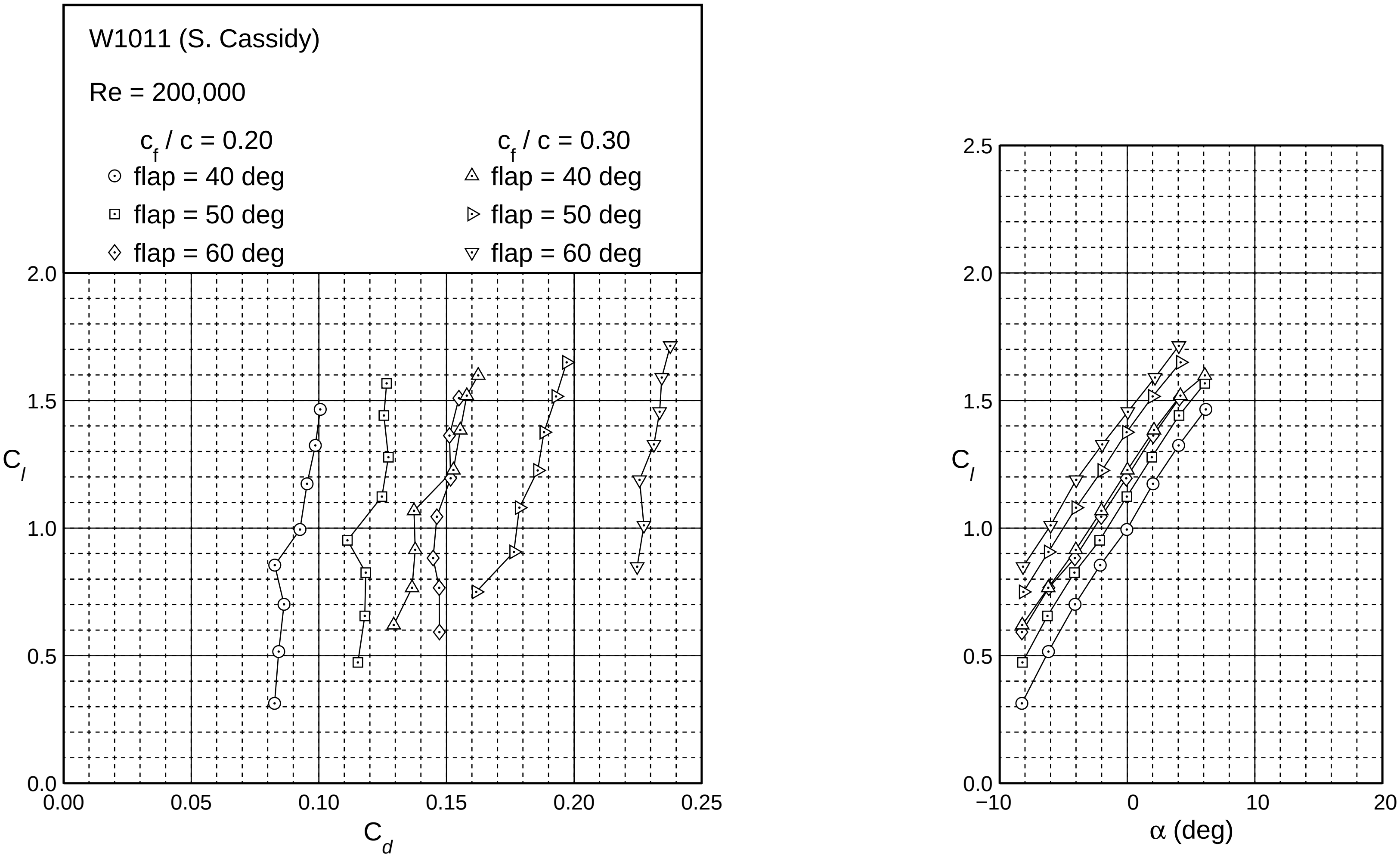

Figure 6.33: Comparison of drag polars with large flap deflections for the W1011 airfoil with two flap sizes (c_f/c = 0.20 and 0.30).

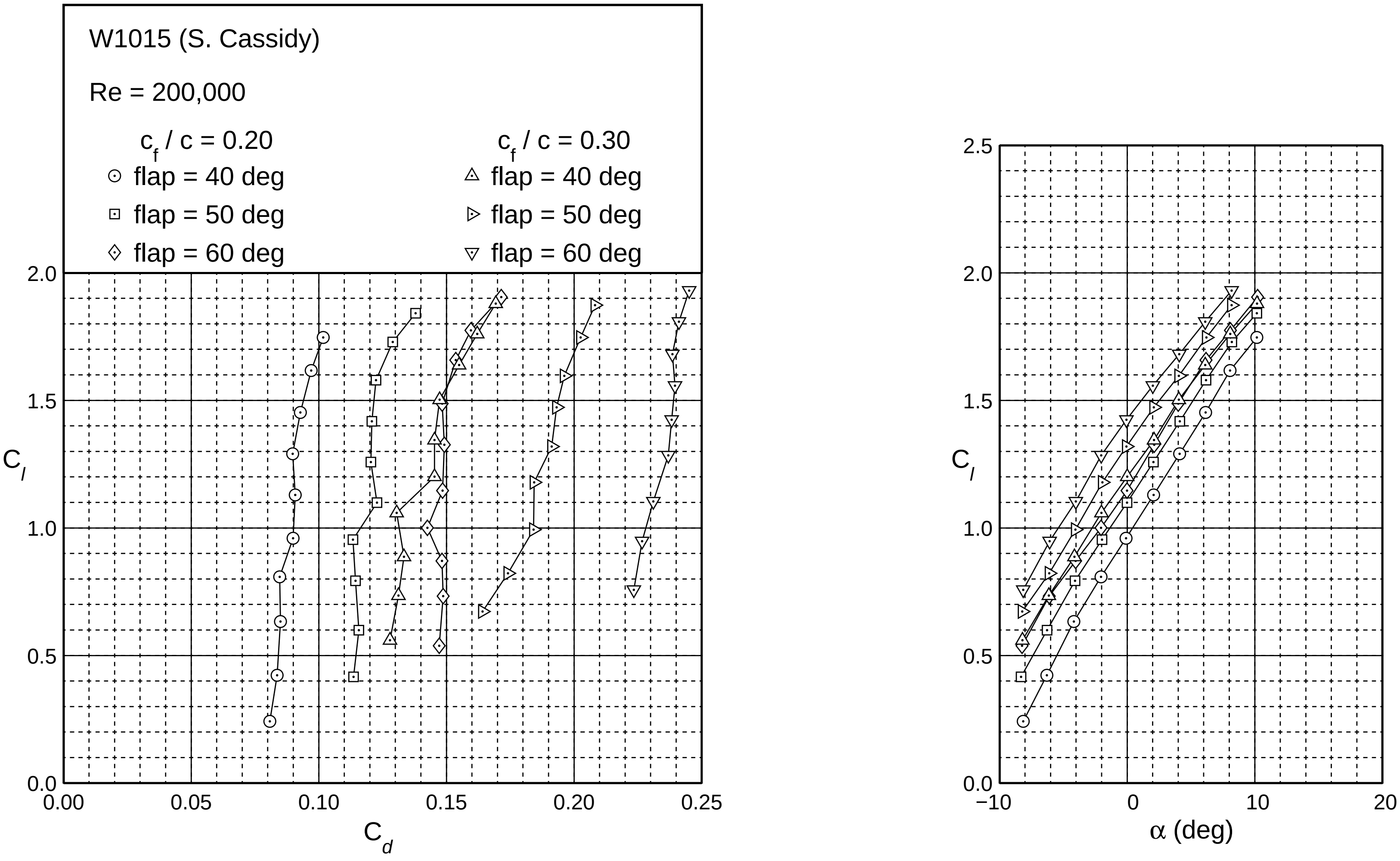

Figure 6.34: Comparison of drag polars with large flap deflections for the W1015 airfoil with two flap sizes (c_f/c = 0.20 and 0.30).

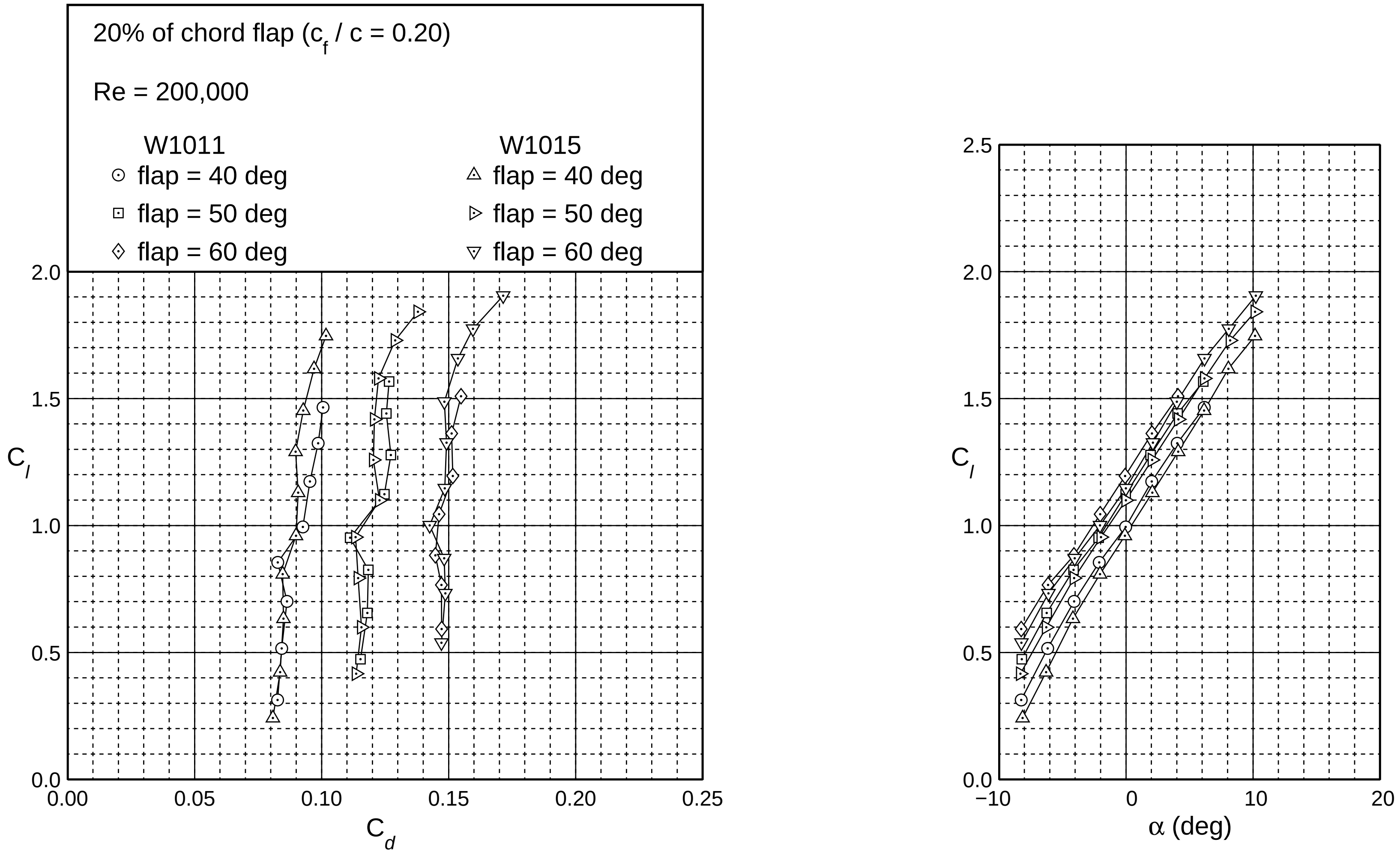

Figure 6.35: Comparison of drag polars for the W1015 and W1011 airfoils with $c_f/c = 0.20$.

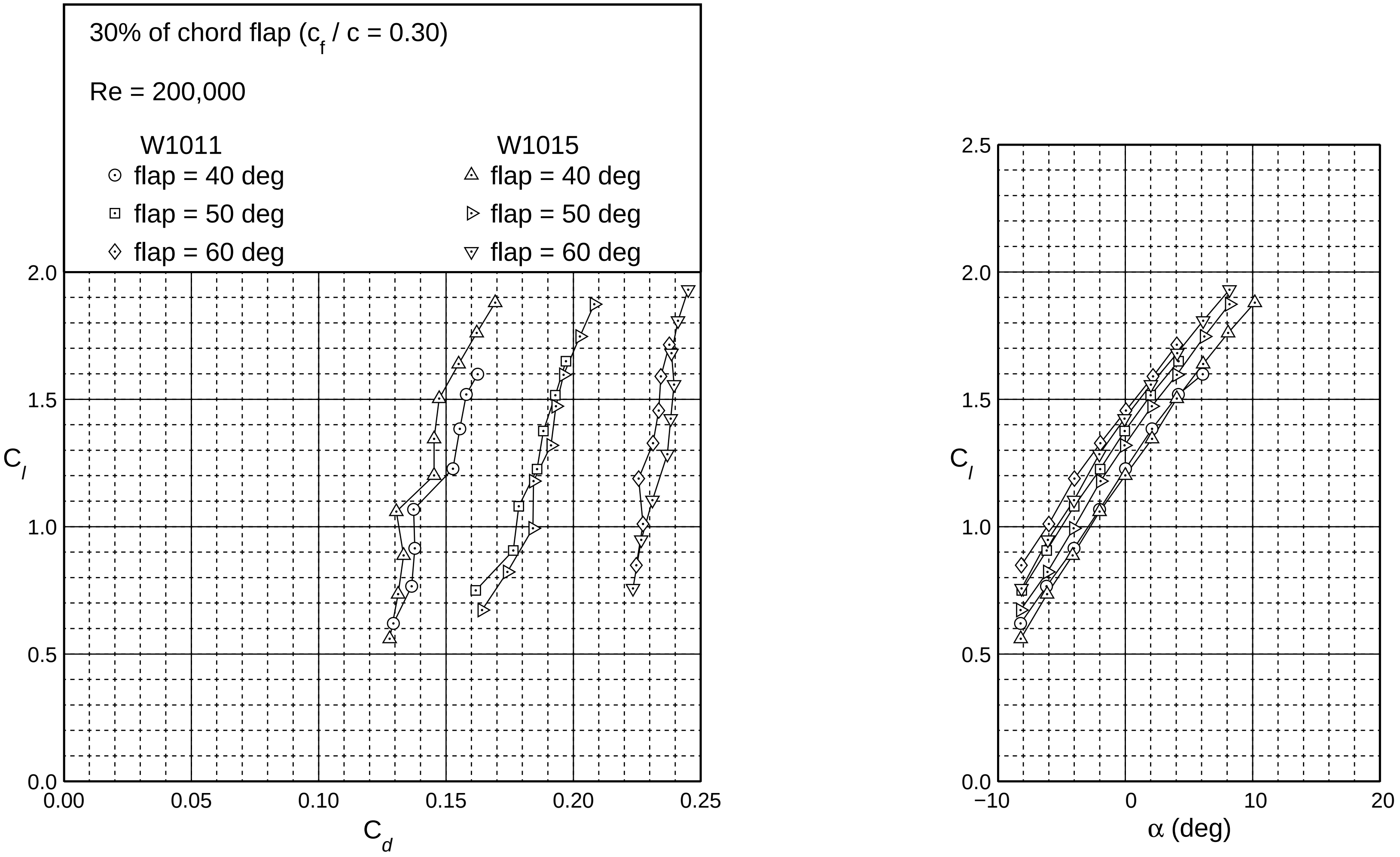

Figure 6.36: Comparison of drag polars for the W1015 and W1011 airfoils with $c_f/c = 0.30$.

6.4 Lift-to-Drag Ratio Characteristics

In this section, the lift-to-drag ratio characteristics of the flapped W1011 and W1015 airfoils are analyzed. The maximum lift-to-drag ratio was calculated for each configuration and plotted in Fig. 6.37 with respect to flap deflection. From Fig. 6.37, it can be seen that the maximum lift-to-drag ratio is obtained with a flap deflection of 10 deg except for the W1015 with a 20% of chord flap. Below a flap deflection of 20 deg, two trends emerge. First, the W1011 outperforms the W1015 independent of the flap-chord ratio. Second, the 30% of chord flap has better lift-to-drag ratios compared with the 20% of chord flap for both the W1011 and W1015 airfoils. Above a flap deflection of 20 deg, two trends emerge. First, the W1015 outperforms the W1011 when comparing the same flap-chord ratio. Second, the 20% of chord flap has better lift-to-drag ratios compared with the 30% of chord flap for both the W1011 and W1015 airfoils. From the above discussion and Fig. 6.37, it can be seen that the trends below a flap deflection of 20 deg are almost completely opposite compared with the trends above a flap deflection of 20 deg. It can be concluded that the maximum lift-to-drag ratio for flap deflections below 20 deg is a function of the airfoil thickness and above 20 deg is a function of flap-chord ratio.

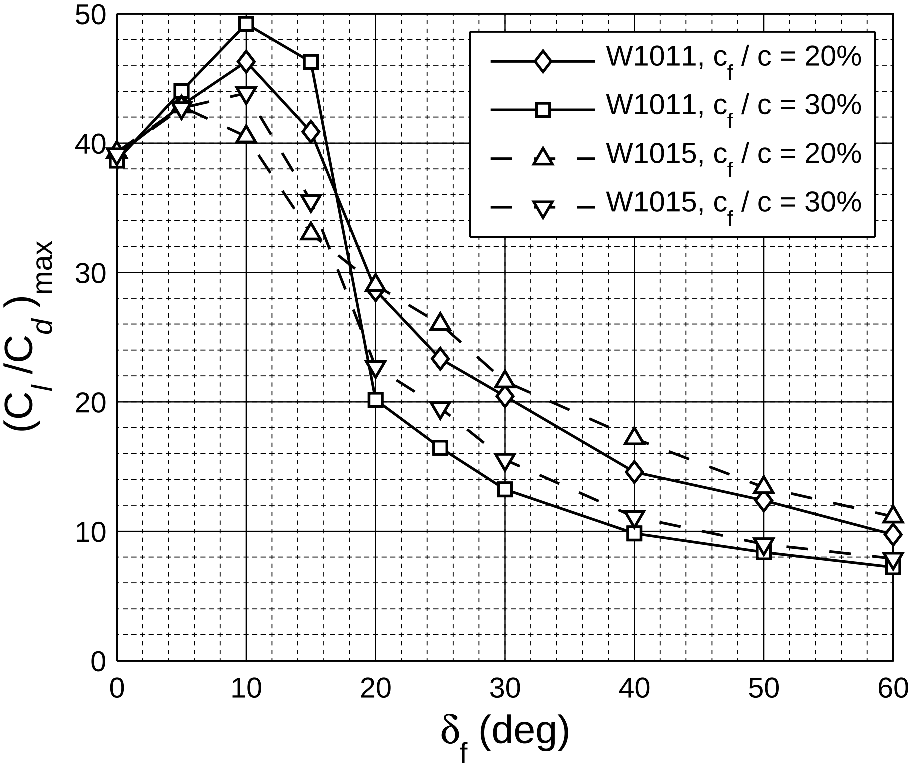

Figure 6.37: $(C_l/C_d)_{max}$ for the W1011 and W1015 airfoils each with two flap sizes ($c_f/c\ =\ 0.20$ and 0.30).

6.5 Performance Plots

In this section, the airfoil profiles, inviscid velocity profiles, and performance plots are presented for each configuration. A detailed table of all of the tested configurations is presented in Table 6.2. Table 6.2 lists all the data sets, associated figures, figure page numbers, and all associated run numbers for each configuration on the next few pages. The layout of data is consistent with the LSATs books seen in Refs. 4–9.

The accuracy of each model is graphically depicted in a difference plot before the data for that airfoil is presented. The tabulated airfoil coordinates can be found in Appendix A. The difference plot is made up of two subplots that show the accuracy of the model on different scales. The upper subplot shows the actual digitized airfoil (dotted line) co-plotted with the true as designed airfoil (solid line). This plot allows the reader to see the full scale error of the actual model, but normally the discrepancy between the actual and true airfoil cannot be seen with this plot. Therefore, the lower subplot was produced to show the discrepancies between the actual and true airfoil upper (solid line) and lower (dotted line) surfaces on a finer scale. The horizontal axis represents the true airfoil and the difference above or below the horizontal axis represents the error of the actual airfoil. For example, if the lower surface of the actual airfoil was thinner than the true airfoil, the dotted line would be above the horizontal axis and vice versa.

With trailing edge flap models, the airfoil model accuracy graphically depicted in the difference plot may include errors associated with a 0-deg flap offset. This effect can be identified by examining trailing edge portion of the lower subplot. If both lines (dotted and solid) are above/below the horizontal axis, the flap may be slightly deflected up/down respectively from the true configuration. Since all of the airfoils models tested for this research employed trailing edge flaps, slight deviations in the trailing edge portion of the lower subplot may be present. All of the airfoil models constrained the flap from rotating with machined aluminum flap endplates on each end of the model. The 0-deg flap deflection for the AG40d-02r and AG455ct-02r were preset by the builder. With the W1011 and W1015 airfoil models, the 0-deg flap deflection was set with an aluminum airfoil template. The template was necessary because the models employed an interchangeable flap system that required the rear $\approx$40% of the model to be disassembled to change the flap size. Therefore, errors associated with reassembly and part construction required the 0-deg flap deflection be set with a template.

As discussed in Section 3.2, the AG455ct-02r airfoil has a preset absolute flap deflection of -2 deg incorporated into the airfoil coordinates. As seen in Fig. 3.6, the chord line is referenced to this configuration. Thus, the angle of attack is also referenced to this configuration. The convention for defining the flap deflections used in this chapter can be seen in Fig. 3.6. The same flap and angle of attack conventions are used for the AG40d-02r airfoil.

For the data presented in the section, the following comments may be helpful:

- The inviscid velocity distributions shown for the true airfoil coordinates were calculated using XFOIL. The details of XFOIL can be found in Chapter 5.
- For the W1011 and W1015 airfoil models, the difference plots (see Figs. 6.110, 6.146, 6.182, and 6.218) show that models are consistently thin with respect to the true shape. Normally, airfoil models are thicker with respect to the true airfoil shape owing to paint and/or coverings, which add thickness.
- The figures list nominal Reynolds numbers. The actual Reynolds number can be found in Appendix B for the drag polar data and Appendix C for the lift and moment data. The difference between the nominal and actual Reynolds number is typically no larger than $\Delta Re = 100$ to 200.
- For the lift curves, increasing and decreasing angles of attack are denoted by solid triangles and open circles, respectively.
- For the moment curves, increasing and decreasing angles of attack are denoted by inverted solid triangles and open rectangles, respectively. In the lift and moment plots, the C_m axis has been inverted (positive values at the bottom of the plot) as is convention when plotting pitching-moment data.
- Drag data is presented on three different scales depending on the drag values being presented. Most of the data is shown on the standard scale of $C_d = 0$ to 0.05, but for large flap deflections, the scale is 2X ($C_d = 0$ to 0.10) or 5X ($C_d = 0$ to 0.25) the standard scale to best present the data.
- In some cases, additional drag runs were required to fill out the drag polars in the upper/lower regions. These additional runs normally only account for a few angles of attack and are documented in Table 6.2. In Appendix B, however, only the main file is listed, but it contains the data of the additional runs.

Table 6.2: Test Matrix and Run Number Index

Model (Builder) Designer	Configuration	V-dist & Profile		Drag Data				Lift & Moment Data			
		Fig.	**p.**	**Fig.**	**p.**	***Re***	**Run #**	**Fig.**	**p.**	***Re***	**Run #**
AG40d-02r	Clean	6.38	94	6.40	95	100,000	06824ga	6.41	96	100,000	06823ga
(M. Drela et al.)	0 deg flap	6.39				200,000	06826gw			200,000	06825ga
Drela	$c_f / c = 0.25$					300,000	06828gw	6.41	97	300,000	06827gw
						400,000	06830gw			400,000	06829gw
						500,000	06832gw	6.41	98	500,000	06831gw
	Clean	6.42	99	6.43	100	100,000	06916ga	6.44	101	100,000	06915ga
	-20 deg flap					200,000	06918gw			200,000	06917gw
	$c_f / c = 0.25$					300,000	06920gw	6.44	102	300,000	06919gw
						400,000	06922gw			400,000	06921gw
						500,000	06924gw	6.44	103	500,000	06923gw
	Clean	6.45	104	6.46	105	100,000	06834gw	6.47	106	100,000	06833gw
	-15 deg flap					200,000	06836gw			200,000	06835rd
	$c_f / c = 0.25$					300,000	06838gw	6.47	107	300,000	06837gw
						400,000	06840gw			400,000	06839gw
						500,000	06842gw	6.47	108	500,000	06841gw
	Clean	6.48	109	6.49	110	100,000	06844gw	6.50	111	100,000	06843gw
	-10 deg flap					200,000	06846ga			200,000	06845ga
	$c_f / c = 0.25$					300,000	06848ga	6.50	112	300,000	06847ga
						400,000	06850gw			400,000	06849gw
						500,000	06852gw	6.50	113	500,000	06851gw
	Clean	6.51	114	6.52	115	100,000	06854gw	6.53	116	100,000	06853gw
	-5 deg flap					200,000	06856gw			200,000	06855gw
	$c_f / c = 0.25$					300,000	06858gw	6.53	117	300,000	06857gw
						400,000	06860gw			400,000	06859gw
	Clean	6.54	118	6.55	119	100,000	06882gw	6.56	120	100,000	06881gw
	5 deg flap					200,000	06884gw			200,000	06883gw
	$c_f / c = 0.25$					300,000	06886gw	6.56	121	300,000	06885gw
						400,000	06888gw/06888gw_add			400,000	06887gw
						500,000	06890gw	6.56	122	500,000	06889gw
	Clean	6.57	123	6.58	124	100,000	06872ga	6.59	125	100,000	06871gw
	10 deg flap					200,000	06874gw			200,000	06873gw
	$c_f / c = 0.25$					300,000	06876ga	6.59	126	300,000	06875gw
						400,000	06878gw			400,000	06877gw
(continues)						500,000	06880gw	6.59	127	500,000	06879gw

Table 6.2: Continued

AG40d-02r (continued)	Clean 15 deg flap c_f / c = 0.25	6.60	128	6.61	129	100,000	06862ga	6.62	130	100,000	06861gw
						200,000	06864ga			200,000	06863ga
						300,000	06866gw	6.62	131	300,000	06865gw
						400,000	06868gw			400,000	06867rd
						500,000	06870gw	6.62	132	500,000	06869gw
	Clean 20 deg flap c_f / c = 0.25	6.63	133	6.64	134	100,000	06892ga	6.65	135	100,000	06891ga
						200,000	06894ga			200,000	06893ga
						300,000	06896gw	6.65	136	300,000	06895gw
						400,000	06898gw			400,000	06897gw
	Clean 25 deg flap c_f / c = 0.25	6.66	137	6.67	138	100,000	06900gw	6.68	139	100,000	06899gw
						200,000	06902gw			200,000	06901gw
						300,000	06904gw/06904gw_add	6.68	140	300,000	06903gw
						400,000	06906gw			400,000	06905gw
	Clean 30 deg flap c_f / c = 0.25	6.69	141					6.70	142	100,000	06907gw
										200,000	06908gw
								6.70	143	300,000	06909gw
										400,000	06910gw
	Clean 40 deg flap c_f / c = 0.25	6.71	144					6.72	145	100,000	06911gw
										200,000	06912gw
								6.72	146	300,000	06913gw
										400,000	06914gw
AG455ct-02r (M. Drela et al.) Drela	Clean -0.4 deg flap c_f / c = 0.30	6.73 6.74	147	6.75	148	100,000	06724gw	6.76	149	100,000	06723gw
						200,000	06726gw			200,000	06725gw
						300,000	06728gw	6.76	150	300,000	06727gw
						400,000	06732ga			400,000	06731gw
						500,000	06730gw	6.76	151	500,000	06729gw
	Clean -20.4 deg flap c_f / c = 0.30	6.77	152	6.78	153	100,000	06818gw	6.79	154	100,000	06813gw
						200,000	06819gw			200,000	06814gw
						300,000	06820ga	6.79	155	300,000	06815gw
						400,000	06821gw			400,000	06816gw
						500,000	06822gw	6.79	156	500,000	06817gw
	Clean -15.4 deg flap c_f / c = 0.30	6.80	157	6.81	158	100,000	06734gw	6.82	159	100,000	06733gw
						200,000	06736gw			200,000	06735gw
						300,000	06738rd	6.82	160	300,000	06737gw
						400,000	06740gw			400,000	06739gw
(continues)						500,000	06742gw	6.82	161	500,000	06741gw

Table 6.2: Continued

AG455ct-02r (continued)	Clean -10.4 deg flap c_f / c = 0.30	6.83	162	6.84	163	100,000	06744gw	6.85	164	100,000	06743gw
						200,000	06746gw			200,000	06745gw
						300,000	06748gw	6.85	165	300,000	06747gw
						400,000	06750gw			400,000	06749gw
						500,000	06752gw	6.85	166	500,000	06751gw
	Clean -5.4 deg flap c_f / c = 0.30	6.86	167	6.87	168	100,000	06754ga	6.88	169	100,000	06753ga
						200,000	06756ga			200,000	06755ga
						300,000	06758gw	6.88	170	300,000	06757gw
						400,000	06760gw			400,000	06759gw
						500,000	06762gw	6.88	171	500,000	06761gw
	Clean 4.6 deg flap c_f / c = 0.30	6.89	172	6.90	173	100,000	06784gw	6.91	174	100,000	06783gw
						200,000	06786gw			200,000	06785gw
						300,000	06788gw	6.91	175	300,000	06787gw
						400,000	06790ga			400,000	06789ga
						500,000	06792ga	6.91	176	500,000	06791ga
	Clean 9.6 deg flap c_f / c = 0.30	6.92	177	6.93	178	100,000	06778ga	6.94	179	100,000	06773gw
						200,000	06779ga			200,000	06774gw
						300,000	06780gw	6.94	180	300,000	06775gw
						400,000	06781gw			400,000	06776gw
						500,000	06782gw	6.94	181	500,000	06777gw
	Clean 14.6 deg flap c_f / c = 0.30	6.95	182	6.96	183	100,000	06764gw	6.97	184	100,000	06763gw
						200,000	06766gw			200,000	06765gw
						300,000	06768gw	6.97	185	300,000	06767rd
						400,000	06770gw			400,000	06769gw
						500,000	06772gw	6.97	186	500,000	06771gw
	Clean 19.6 deg flap c_f / c = 0.30	6.98	187	6.99	188	100,000	06794rd	6.100	189	100,000	06793gw
						200,000	06796gw			200,000	06795gw
						300,000	06798gw	6.100	190	300,000	06797gw
						400,000	06800gw			400,000	06799gw
	Clean 24.6 deg flap c_f / c = 0.30	6.101	191	6.102	192	100,000	06805gw	6.103	193	100,000	06801gw
						200,000	06806gw			200,000	06802gw
						300,000	06807gw	6.103	194	300,000	06803gw
						400,000	06808gw			400,000	06804gw
	Clean 29.6 deg flap c_f / c = 0.30	6.104	195	6.105	196	100,000	06611ga	6.106	197	100,000	06610ga
						200,000	06613gw			200,000	06612gw
						300,000	06811gw	6.106	198	300,000	06809gw
(continues)						400,000	06812gw			400,000	06810gw

Table 6.2: Continued

AG455ct-02r	Clean	6.107	199	6.108	200	100,000	06617gw	6.109	201	100,000	06616gw
(continued)	39.6 deg flap					200,000	06619ga			200,000	06618gw
	c_f / c = 0.30					300,000	06621ga	6.109	202	300,000	06620ga
W1011 (20%)	Clean	6.110	203	6.112	204	100,000	07069gw	6.113	205	100,000	07068gw
(S. Cassidy)	0 deg flap	6.111				200,000	07071sn			200,000	07070gw
Williamson	c_f / c = 0.20					400,000	07073sn	6.113	206	400,000	07072gw
	Clean	6.114	207	6.115	208			6.116	209	100,000	07084gw
	5 deg flap					200,000	07083gw			200,000	07082gw
	c_f / c = 0.20					400,000	07081gw	6.116	210	400,000	07080gw
	Clean	6.117	211	6.118	212	100,000	07086gw	6.119	213	100,000	07085gw
	10 deg flap					200,000	07088gw			200,000	07087gw
	c_f / c = 0.20					400,000	07090gw	6.119	214	400,000	07089gw
	Clean	6.120	215	6.121	216			6.122	217	100,000	07095gw
	15 deg flap					200,000	07094gw			200,000	07093gw
	c_f / c = 0.20					400,000	07092gw	6.122	218	400,000	07091gw
	Clean	6.123	219	6.124	220	100,000	07097sn	6.125	221	100,000	07096gw
	20 deg flap					200,000	07099sn			200,000	07098gw
	c_f / c = 0.20					400,000	07101sn	6.125	222	400,000	07100gw
	Clean	6.126	223	6.127	224			6.128	225	100,000	07106gw
	25 deg flap					200,000	07105sn			200,000	07104gw
	c_f / c = 0.20					400,000	07103sn	6.128	226	400,000	07102gw
	Clean	6.129	227	6.130	228	100,000	07075sn	6.131	229	100,000	07074sn
	30 deg flap					200,000	07077gw			200,000	07076sn
	c_f / c = 0.20					400,000	07079gw	6.131	230	400,000	07078gw
	Clean	6.132	231					6.133	232	100,000	07107sn
	35 deg flap									200,000	07108gw
	c_f / c = 0.20							6.133	233	400,000	07109gw
	Clean	6.134	234					6.135	235	100,000	07112gw
	40 deg flap			6.29	75	200,000	07257gw			200,000	07111gw
	c_f / c = 0.20							6.135	236	400,000	07110gw
	Clean	6.136	237					6.137	238	100,000	07113gw
	45 deg flap									200,000	07114gw
	c_f / c = 0.20							6.137	239	400,000	07115gw
	Clean	6.138	240					6.139	241	100,000	07125sn
	50 deg flap			6.29	75	200,000	07258gw			200,000	07126sn
(continues)	c_f / c = 0.20							6.139	242	400,000	07127sn

Table 6.2: Continued

W1011 (20%)	Clean	6.140	243					6.141	244	100,000	07124sn
(continued)	55 deg flap									200,000	07123sn
	c_f / c = 0.20							6.141	245	400,000	07122sn
	Clean	6.142	246					6.143	247	100,000	07119sn
	60 deg flap			6.29	75	200,000	07259gw			200,000	07120sn
	c_f / c = 0.20							6.143	248	400,000	07121sn
	Clean	6.144	249					6.145	250	100,000	07118gw
	65 deg flap									200,000	07117gw
	c_f / c = 0.20							6.145	251	400,000	07116gw
W1011 (30%)	Clean	6.146	252	6.148	253	100,000	07129sn	6.149	254	100,000	07128sn
(S. Cassidy)	0 deg flap	6.147				200,000	07131sn			200,000	07130sn
Williamson	c_f / c = 0.30					400,000	07133sn	6.149	255	400,000	07132sn
	Clean	6.150	256	6.151	257			6.152	258	100,000	07138gw
	5 deg flap					200,000	07137sn			200,000	07136gw
	c_f / c = 0.30					400,000	07135sn	6.152	259	400,000	07134gw
	Clean	6.153	260	6.154	261	100,000	07140gw	6.155	262	100,000	07139gw
	10 deg flap					200,000	07142gw			200,000	07141gw
	c_f / c = 0.30					400,000	07144sn	6.155	263	400,000	07143gw
	Clean	6.156	264	6.157	265			6.158	266	100,000	07145gw
	15 deg flap					200,000	07147gw			200,000	07146gw
	c_f / c = 0.30					400,000	07149gw	6.158	267	400,000	07148gw
	Clean	6.159	268	6.160	269	100,000	07155sn	6.161	270	100,000	07154gw
	20 deg flap					200,000	07153gw			200,000	07152gw
	c_f / c = 0.30					400,000	07151gw	6.161	271	400,000	07150gw
	Clean	6.162	272	6.163	273			6.164	274	100,000	07156sn
	25 deg flap					200,000	07158sn			200,000	07157sn
	c_f / c = 0.30					400,000	07160sn	6.164	275	400,000	07159sn
	Clean	6.165	276	6.166	277	100,000	07166gw	6.167	278	100,000	07165sn
	30 deg flap					200,000	07164gw			200,000	07163sn
	c_f / c = 0.30							6.167	279	400,000	07161sn
	Clean	6.168	280					6.169	281	100,000	07167sn
	35 deg flap									200,000	07168sn
	c_f / c = 0.30							6.169	282	400,000	07169sn
	Clean	6.170	283					6.171	284	100,000	07170sn
	40 deg flap			6.30	76	200,000	07251gw			200,000	07171sn
(continues)	c_f / c = 0.30							6.171	285	400,000	07172sn

Table 6.2: Continued

W1011 (30%) (continued)	Clean 45 deg flap $c_f / c = 0.30$	6.172	286					6.173	287	100,000	07173gw
										200,000	07174gw
								6.173	288	400,000	07175gw
	Clean 50 deg flap $c_f / c = 0.30$	6.174	289					6.175	290	100,000	07176gw
				6.30	76	200,000	07252gw			200,000	07177gw
								6.175	291	400,000	07178gw
	Clean 55 deg flap $c_f / c = 0.30$	6.176	292					6.177	293	100,000	07179gw
										200,000	07180gw
								6.177	294	400,000	07181gw
	Clean 60 deg flap $c_f / c = 0.30$	6.178	295					6.179	296	100,000	07182gw
				6.30	76	200,000	07253gw			200,000	07183gw
								6.179	297	400,000	07184gw
	Clean 65 deg flap $c_f / c = 0.30$	6.180	298					6.181	299	100,000	07185gw
										200,000	07186gw
								6.181	300	400,000	07187gw
W1015 (20%) (S. Cassidy) Williamson	Clean 0 deg flap $c_f / c = 0.20$	6.182	301	6.184	302	100,000	06997gw/07057gw	6.185	303	100,000	06996gw
		6.183				200,000	06999gw/07058gw			200,000	06998gw
						400,000	07001gw/07059gw	6.185	304	400,000	07000gw
	Clean 5 deg flap $c_f / c = 0.20$	6.186	305	6.187	306			6.188	307	100,000	07008gw
						200,000	07010gw/07060gw			200,000	07009gw
						400,000	07012gw/07061gw	6.188	308	400,000	07011gw
	Clean 10 deg flap $c_f / c = 0.20$	6.189	309	6.190	310	100,000	07014gw/07062gw	6.191	311	100,000	07013gw
						200,000	07016gw/07063gw			200,000	07015gw
						400,000	07018gw/07064gw	6.191	312	400,000	07017gw
	Clean 15 deg flap $c_f / c = 0.20$	6.192	313	6.193	314			6.194	315	100,000	07019gw
						200,000	07021gw/07065sn			200,000	07020gw
						400,000	07023sn/07066gw	6.194	316	400,000	07022gw
	Clean 20 deg flap $c_f / c = 0.20$	6.195	317	6.196	318	100,000	07025gw	6.197	319	100,000	07024gw
						200,000	07027gw			200,000	07026gw
						400,000	07029gw	6.197	320	400,000	07028gw
	Clean 25 deg flap $c_f / c = 0.20$	6.198	321	6.199	322			6.200	323	100,000	07030gw
						200,000	07032gw			200,000	07031gw
						400,000	07034gw	6.200	324	400,000	07033gw
	Clean 30 deg flap $c_f / c = 0.20$	6.201	325	6.202	326	100,000	07003gw	6.203	327	100,000	07002gw
						200,000	07005gw			200,000	07004gw
(continues)						400,000	07007gw	6.203	328	400,000	07006gw

Table 6.2: Continued

W1015 (20%)	Clean	6.204	329					6.205	330	100,000	07035sn
(continued)	35 deg flap									200,000	07036sn
	c_f / c = 0.20							6.205	331	400,000	07037sn
	Clean	6.206	332					6.207	333	100,000	07040gw
	40 deg flap			6.31	77	200,000	07248gw			200,000	07039gw
	c_f / c = 0.20							6.207	334	400,000	07038sn
	Clean	6.208	335					6.209	336	100,000	07042gw
	45 deg flap									200,000	07043gw
	c_f / c = 0.20							6.209	337	400,000	07246gw
	Clean	6.210	338					6.211	339	100,000	07054gw
	50 deg flap			6.31	77	200,000	07249gw			200,000	07055gw
	c_f / c = 0.20							6.211	340	400,000	07056gw
	Clean	6.212	341					6.213	342	100,000	07053gw
	55 deg flap									200,000	07052gw
	c_f / c = 0.20							6.213	343	400,000	07051gw
	Clean	6.214	344					6.215	345	100,000	07048gw
	60 deg flap			6.31	77	200,000	07250gw			200,000	07049gw
	c_f / c = 0.20							6.215	346	400,000	07050gw
	Clean	6.216	347					6.217	348	100,000	07047gw
	65 deg flap									200,000	07046gw
	c_f / c = 0.20							6.217	349	400,000	07045gw
W1015 (30%)	Clean	6.218	350	6.220	351	100,000	06936gw/07189sn	6.221	352	100,000	07188sn
(S. Cassidy)	0 deg flap	6.219				200,000	06940ga/07191sn/07244gw			200,000	07190sn
Williamson	c_f / c = 0.30					400,000	06939gw/07193sn/07245gw	6.221	353	400,000	07192sn
	Clean	6.222	354	6.223	355			6.224	356	100,000	07198sn
	5 deg flap					200,000	06949sn/07197sn			200,000	07196sn
	c_f / c = 0.30					400,000	06947sn/07195sn	6.224	357	400,000	07194sn
	Clean	6.225	358	6.226	359	100,000	06952gw/07200sn	6.227	360	100,000	07199sn
	10 deg flap					200,000	06954gw/07202sn			200,000	07201sn
	c_f / c = 0.30					400,000	06956sn/07204sn	6.227	361	400,000	07203sn
	Clean	6.228	362	6.229	363			6.230	364	100,000	07209sn
	15 deg flap					200,000	06959sn/07208sn			200,000	07207sn
	c_f / c = 0.30					400,000	06961sn/07206sn	6.230	365	400,000	07205sn
	Clean	6.231	366	6.232	367	100,000	06963sn	6.233	368	100,000	07210sn
	20 deg flap					200,000	06965sn/07212sn			200,000	07211sn
(continues)	c_f / c = 0.30					400,000	06967sn/072014sn	6.233	369	400,000	07213sn

Table 6.2: Continued

W1015 (30%)	Clean	6.234	370	6.235	371			6.236	372	100,000	07219sn
(continued)	25 deg flap					200,000	06071sn/07218sn			200,000	07217sn
	c_f / c = 0.30					400,000	06973sn/07216sn	6.236	373	400,000	07215sn
	Clean	6.237	374	6.238	375	100,000	06942gw	6.239	376	100,000	07220sn
	30 deg flap					200,000	06944sn			200,000	07221sn
	c_f / c = 0.30							6.239	377	400,000	07222sn
	Clean	6.240	378					6.241	379	100,000	07225sn
	35 deg flap									200,000	07224sn
	c_f / c = 0.30							6.241	380	400,000	07223sn
	Clean	6.242	381					6.243	382	100,000	07226sn
	40 deg flap			6.32	78	200,000	07254gw			200,000	07227sn
	c_f / c = 0.30							6.243	383	400,000	07228sn
	Clean	6.244	384					6.245	385	100,000	07231sn
	45 deg flap									200,000	07230sn
	c_f / c = 0.30							6.245	386	400,000	07229sn
	Clean	6.246	387					6.247	388	100,000	07232sn
	50 deg flap			6.32	78	200,000	07255gw			200,000	07233sn
	c_f / c = 0.30							6.247	389	400,000	07234sn
	Clean	6.248	390					6.249	391	100,000	07237sn
	55 deg flap									200,000	07236sn
	c_f / c = 0.30							6.249	392	400,000	07235sn
	Clean	6.250	393					6.251	394	100,000	07238sn
	60 deg flap			6.32	78	200,000	07256gw			200,000	07239sn
	c_f / c = 0.30							6.251	395	400,000	07240sn
	Clean	6.252	396					6.253	397	100,000	07243sn
	65 deg flap									200,000	07242sn
	c_f / c = 0.30							6.253	398	400,000	07241sn

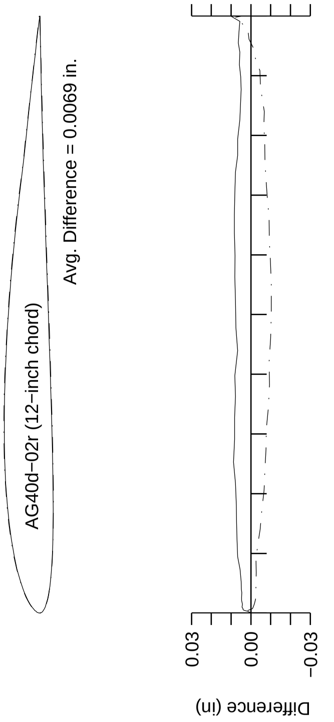

Figure 6.38: Comparison between the true and actual AG40d-02r.

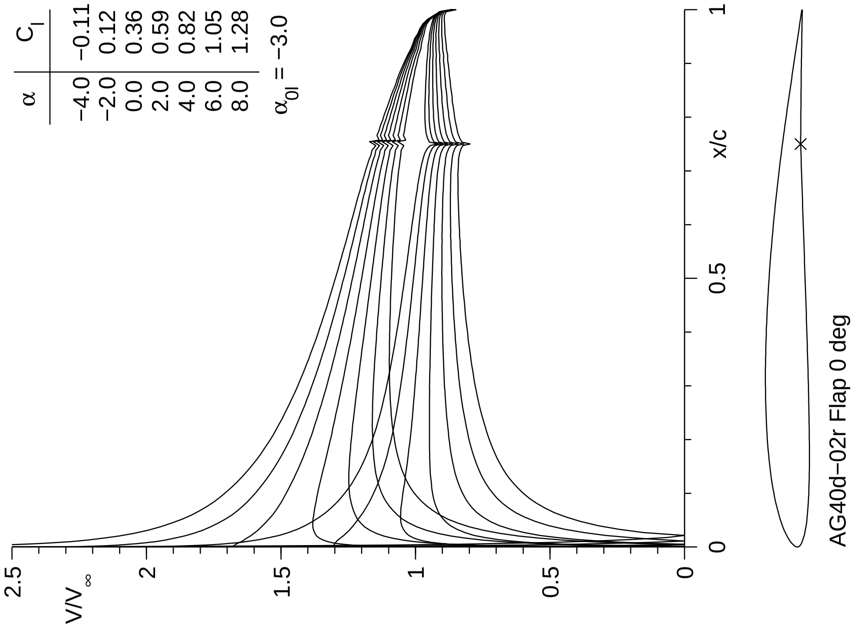

Figure 6.39: Inviscid velocity distributions for the AG40d-02r.

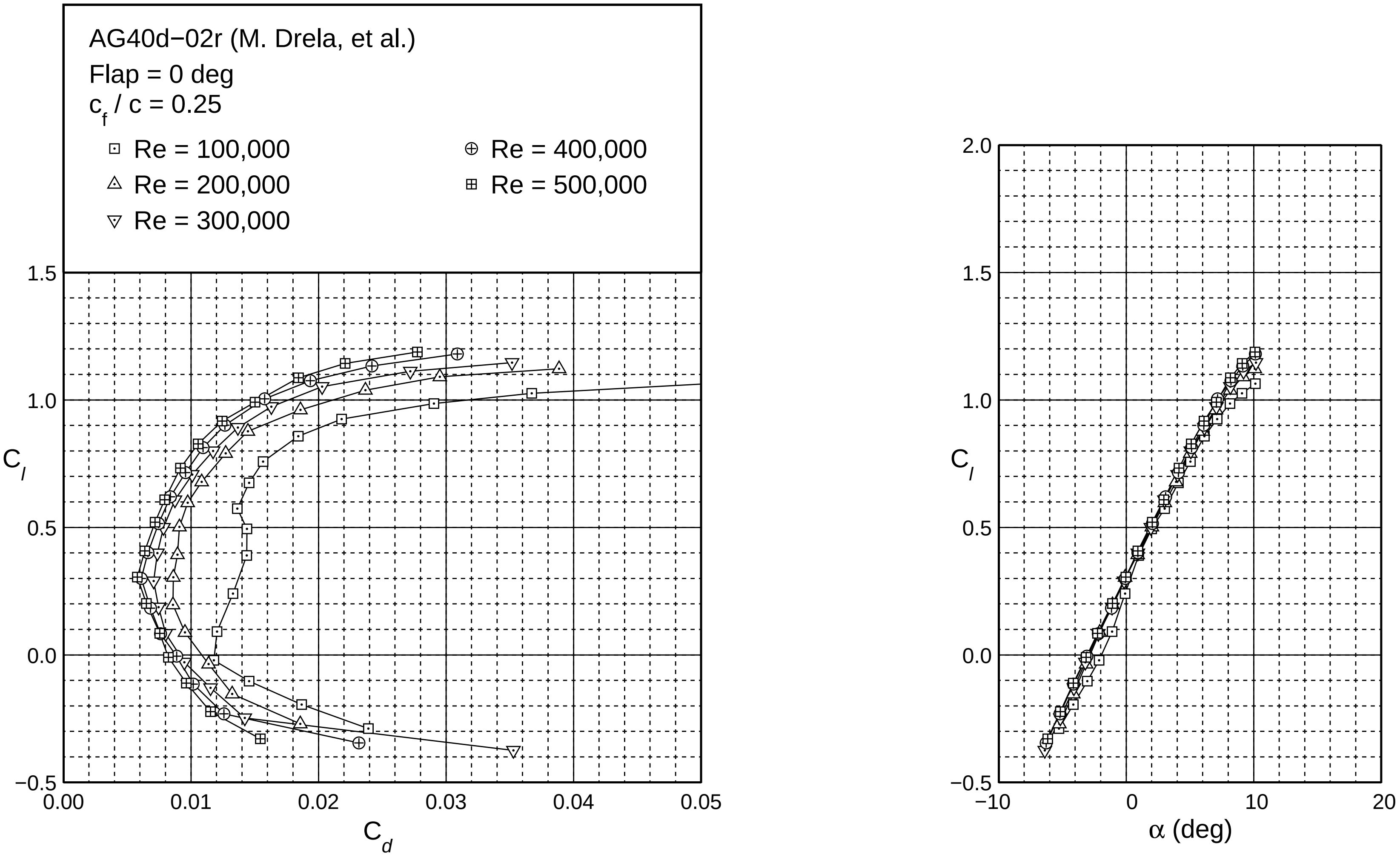

Figure 6.40: Drag polar for the AG40d-02r.

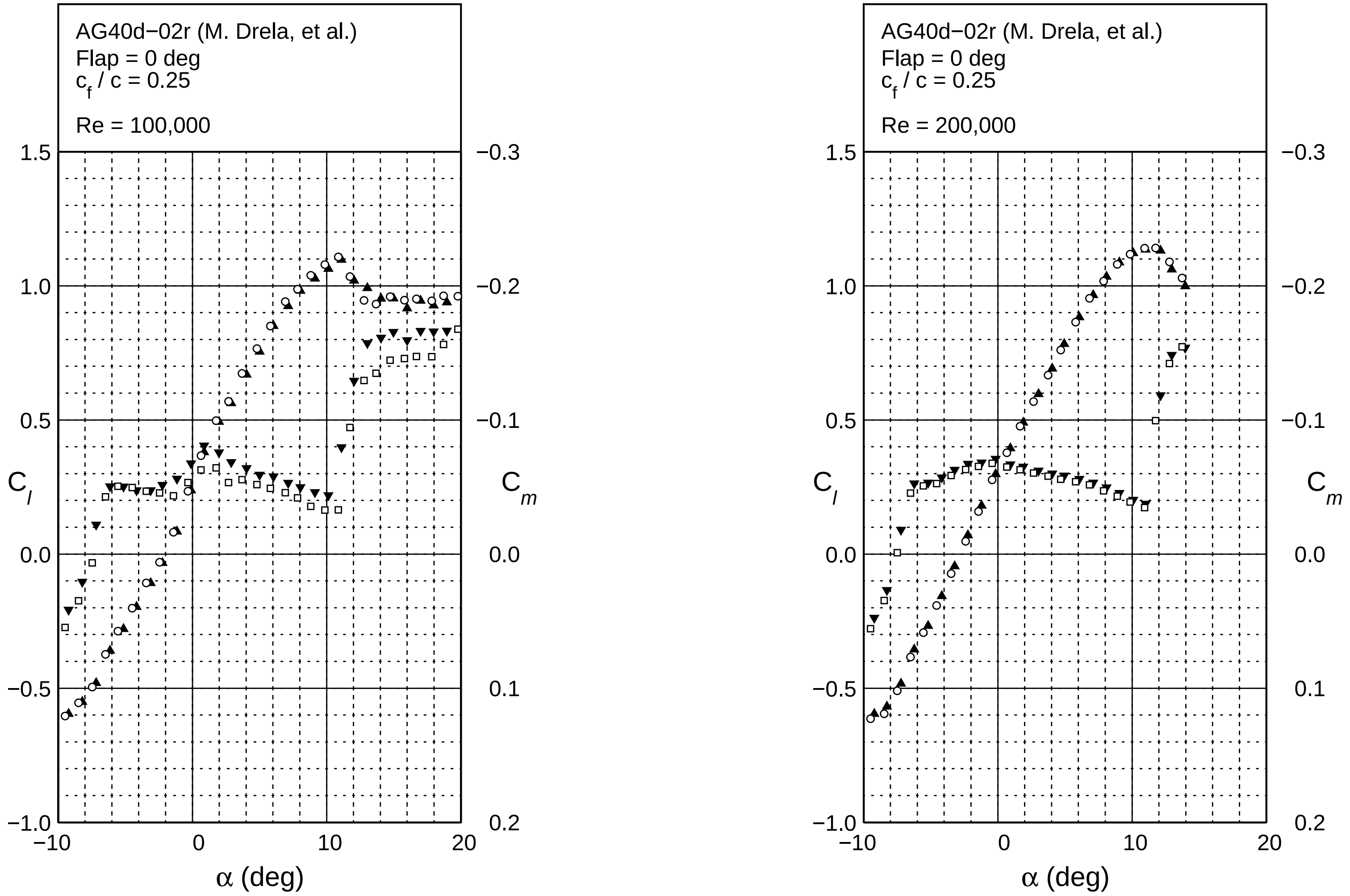

Figure 6.41: Lift and moment characteristics for the AG40d-02r.

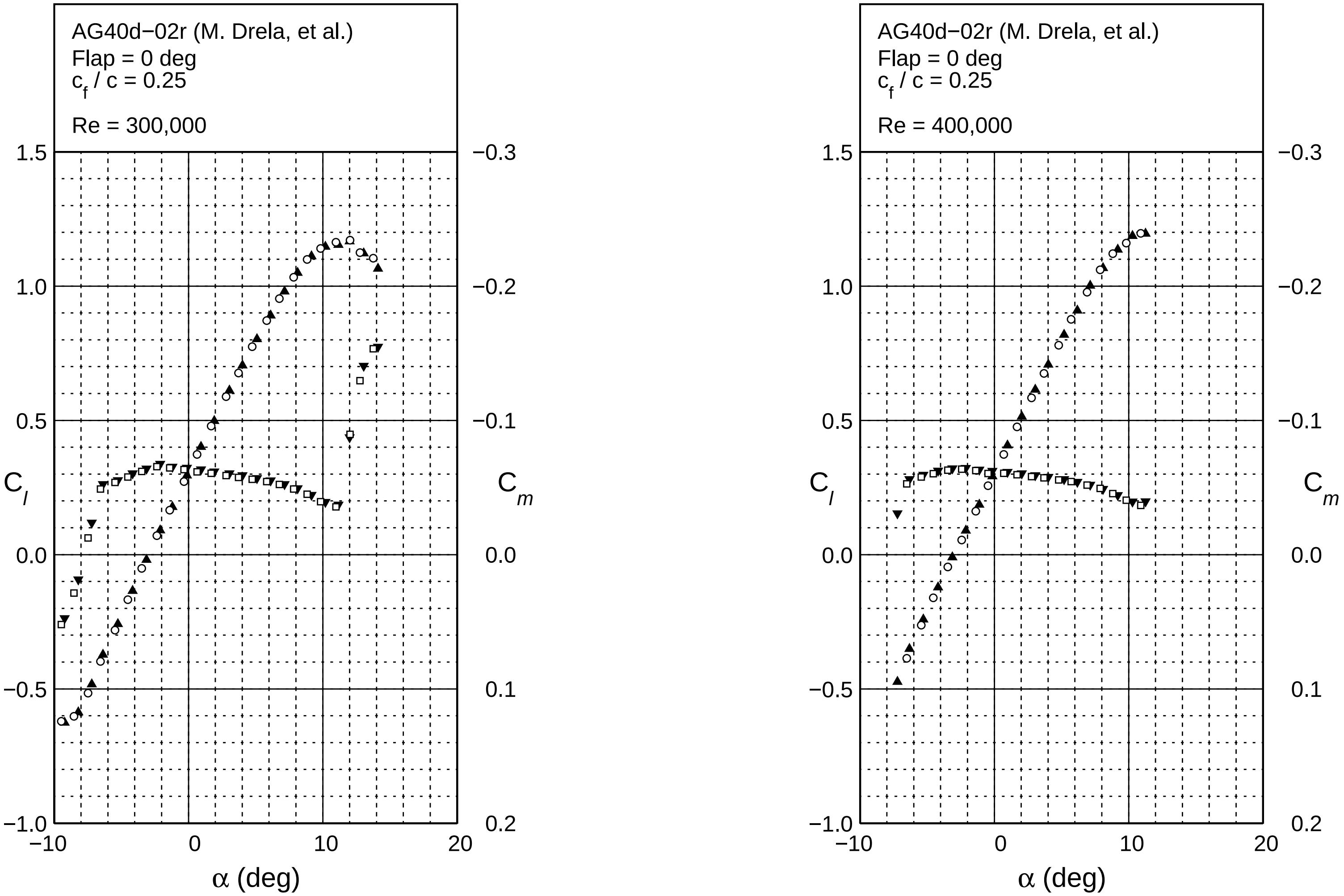

Figure 6.41: Continued.

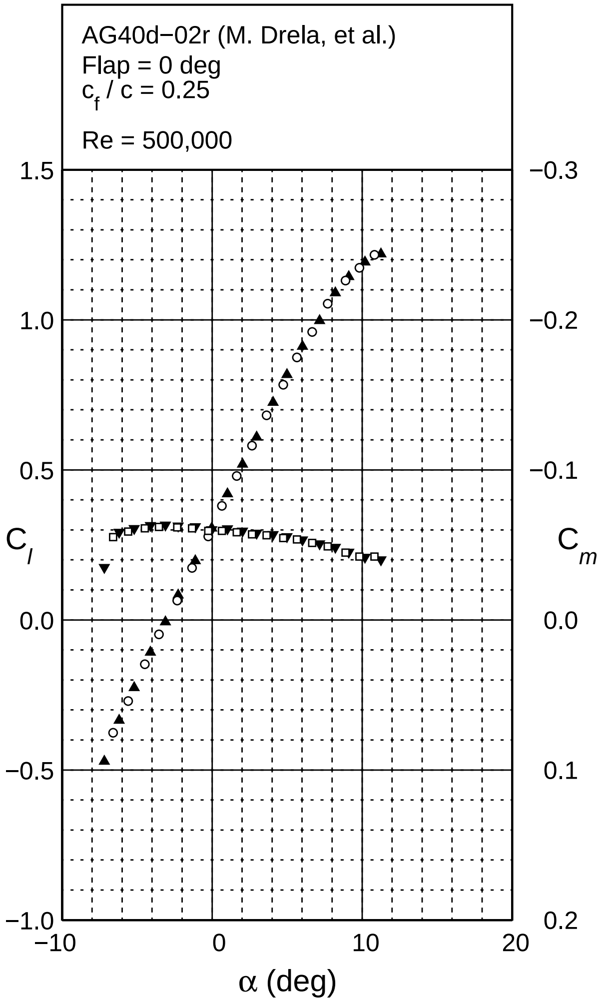

Figure 6.41: Continued.

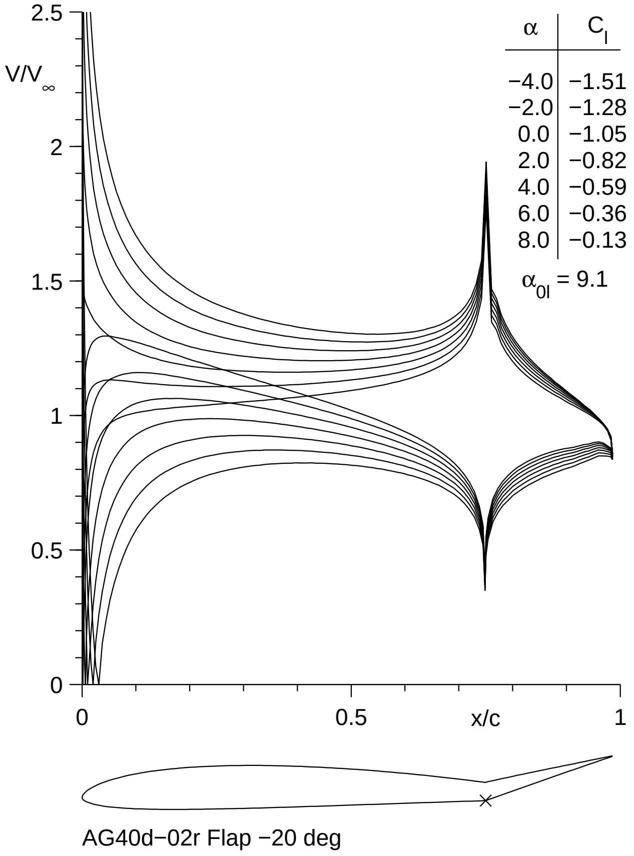

Figure 6.42: Inviscid velocity distributions for the AG40d-02r with a −20 deg flap.

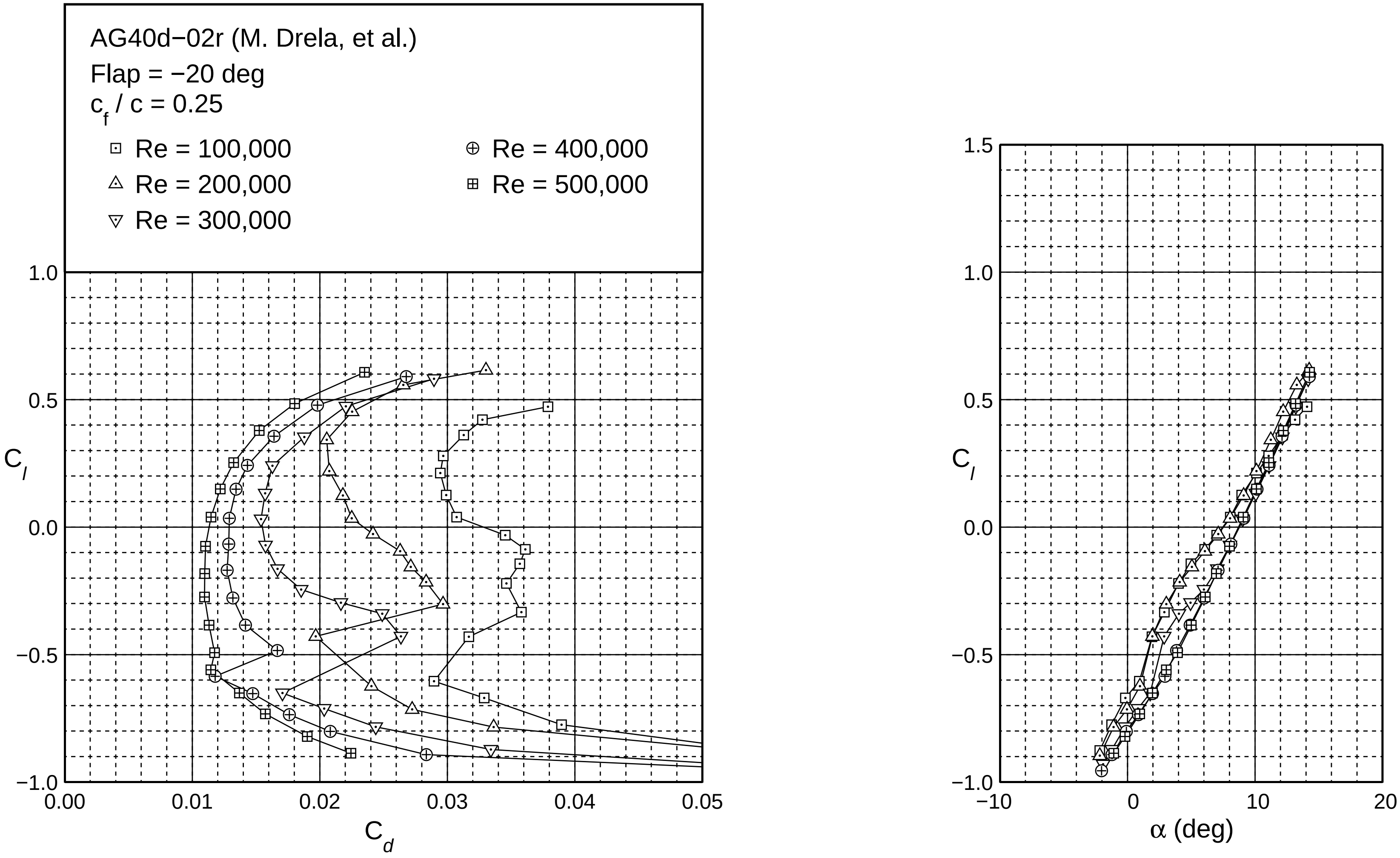

Figure 6.43: Drag polar for the AG40d-02r with a −20 deg flap.

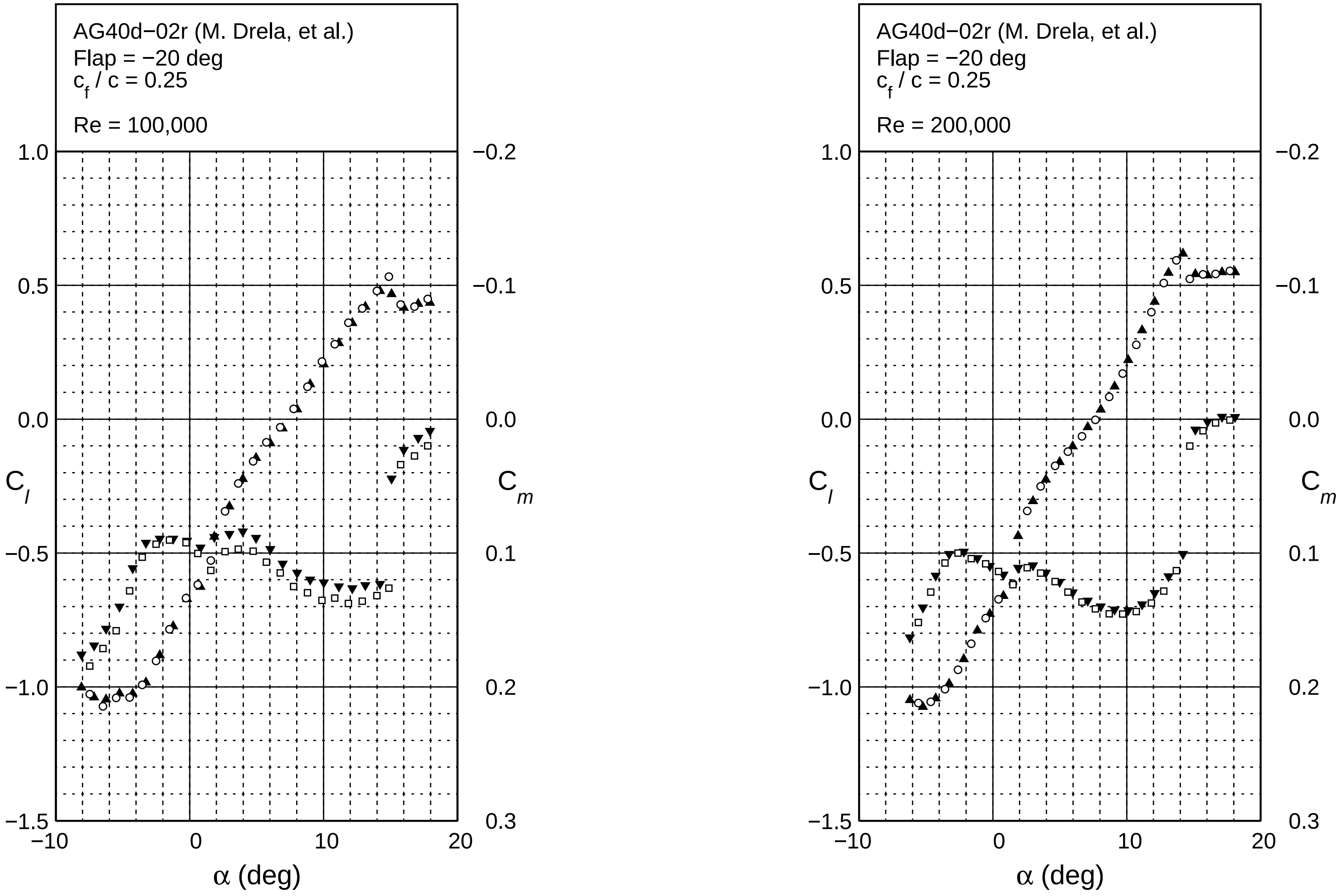

Figure 6.44: Lift and moment characteristics for the AG40d-02r with a −20 deg flap.

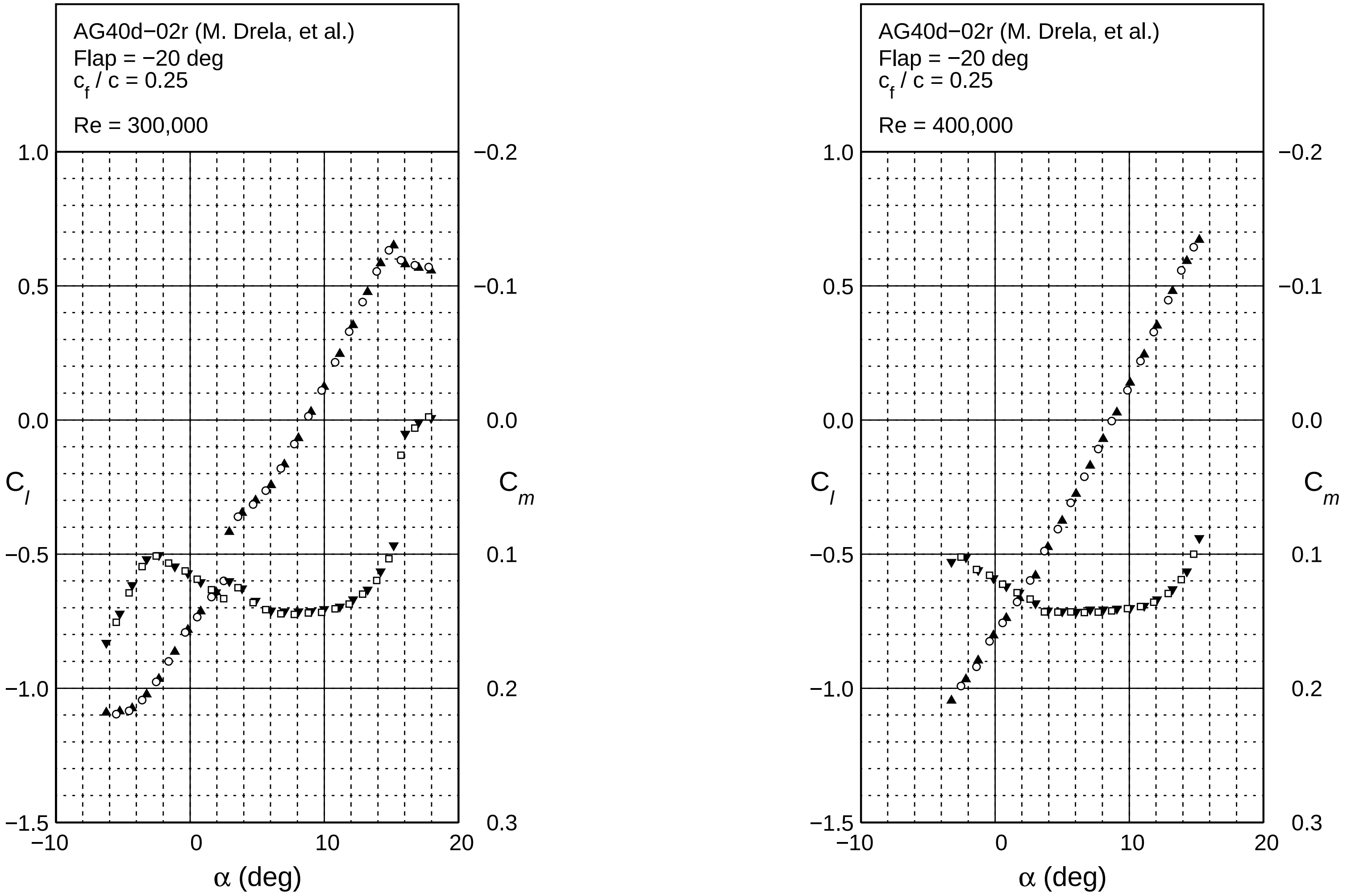

Figure 6.44: Continued.

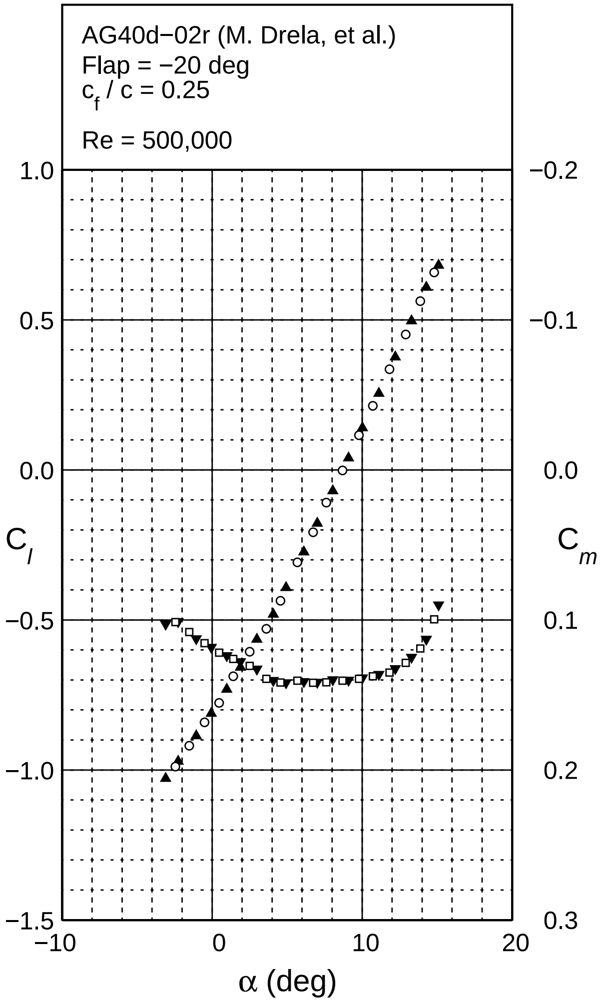

Figure 6.44: Continued.

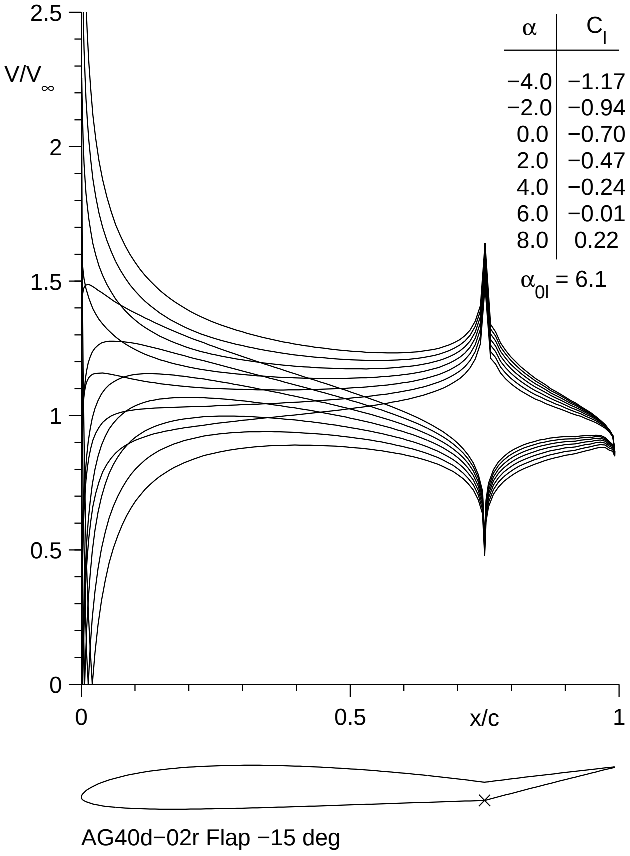

Figure 6.45: Inviscid velocity distributions for the AG40d-02r with a −15 deg flap.

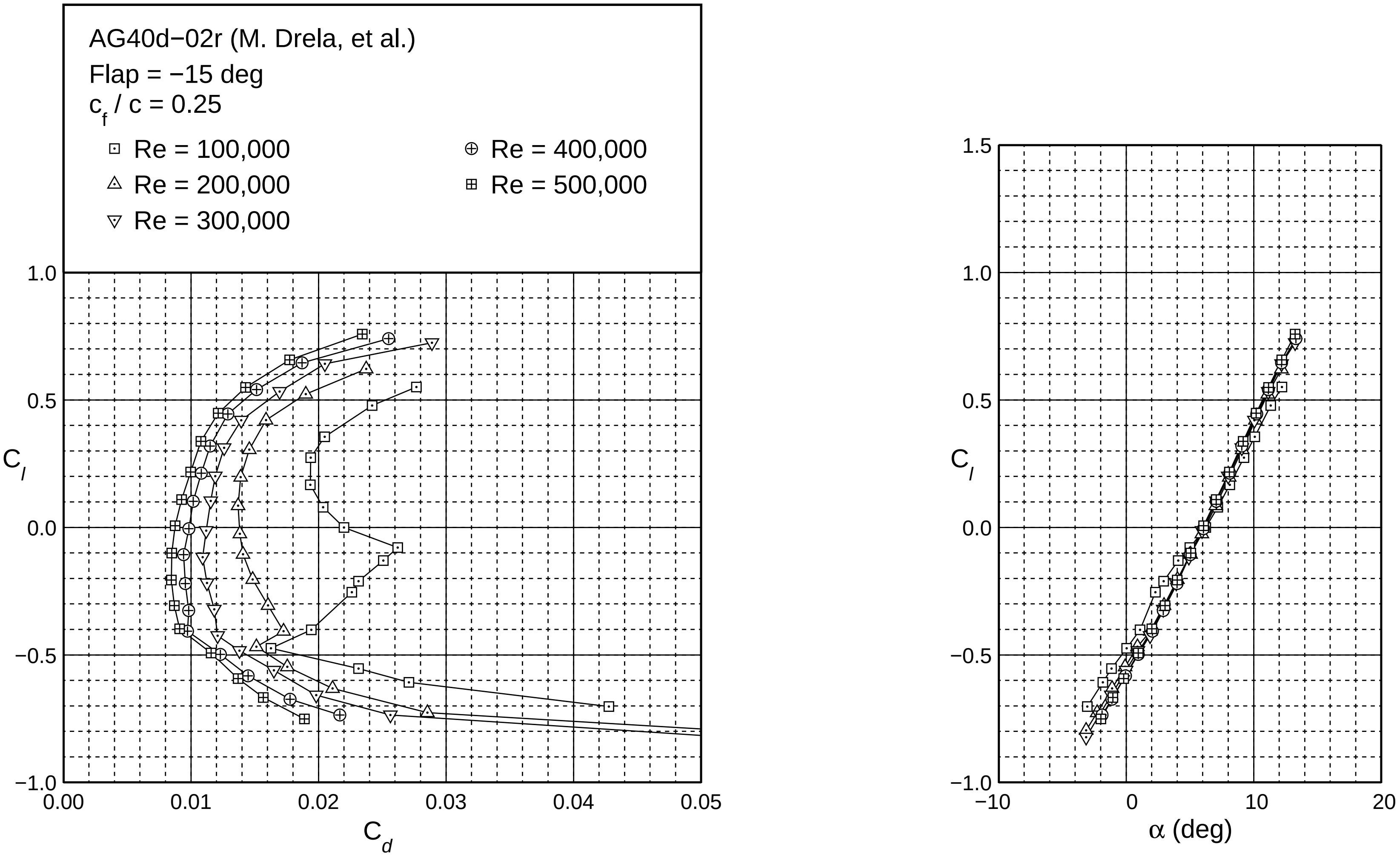

Figure 6.46: Drag polar for the AG40d-02r with a −15 deg flap.

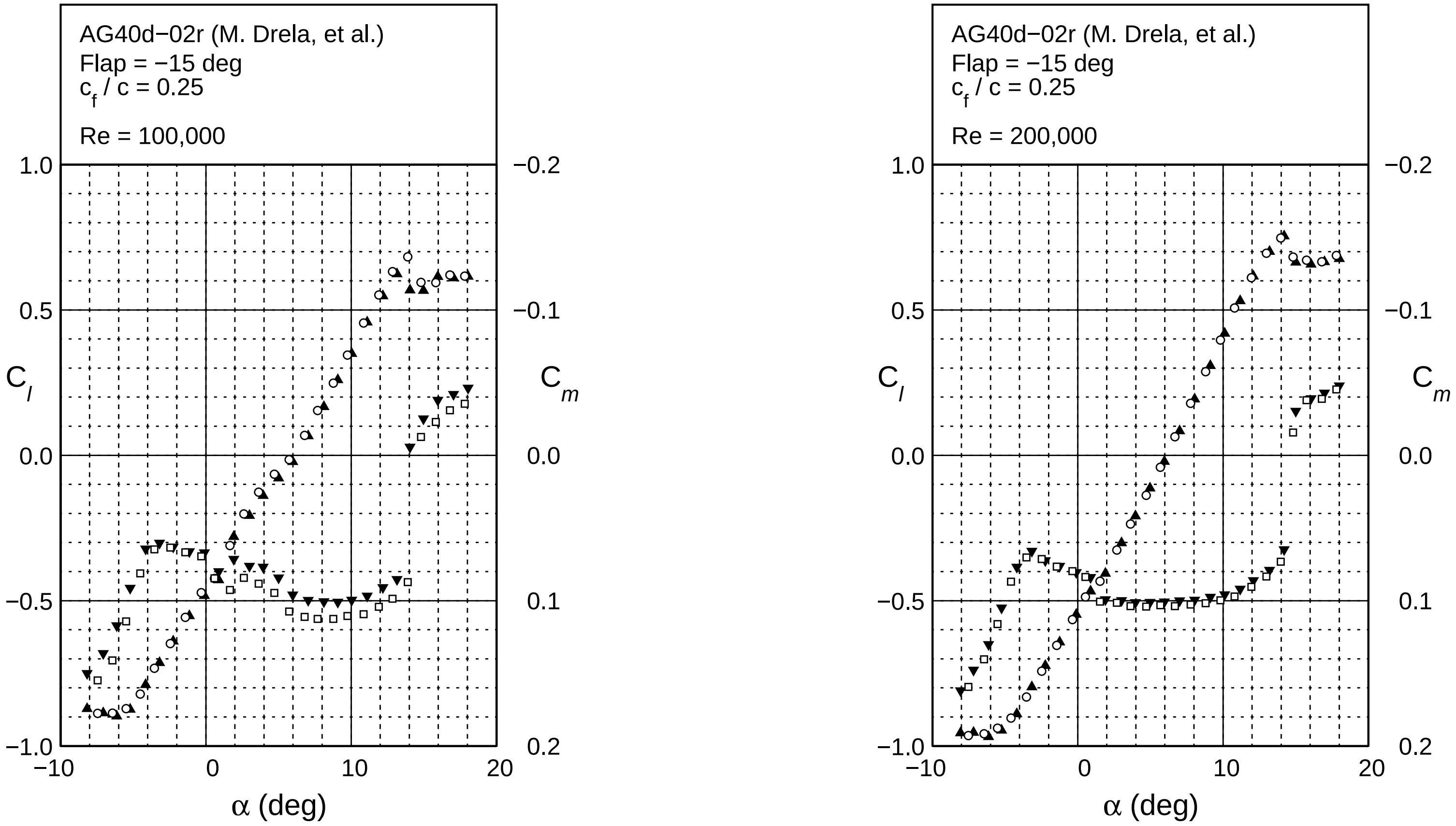

Figure 6.47: Lift and moment characteristics for the AG40d-02r with a −15 deg flap.

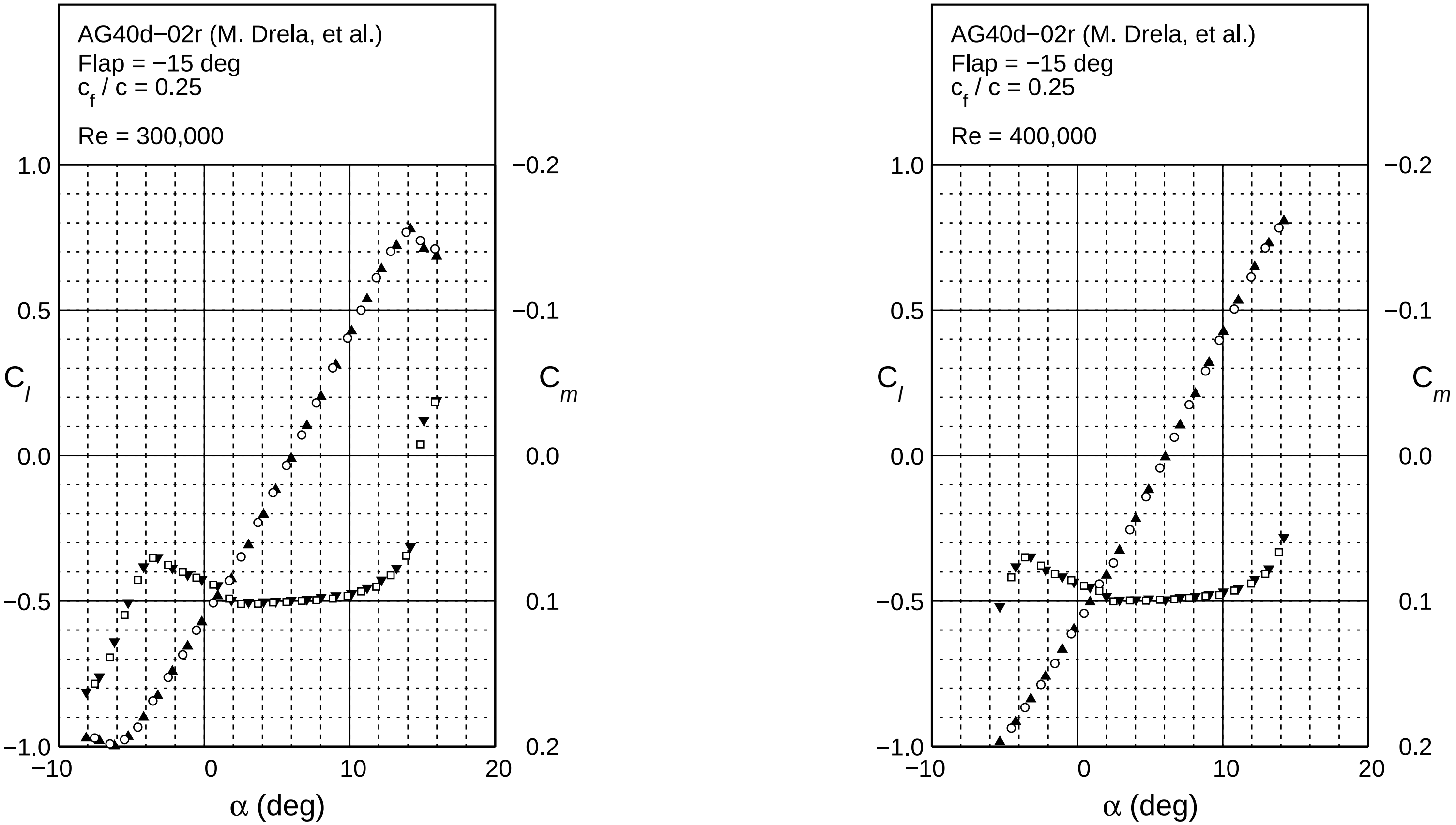

Figure 6.47: Continued.

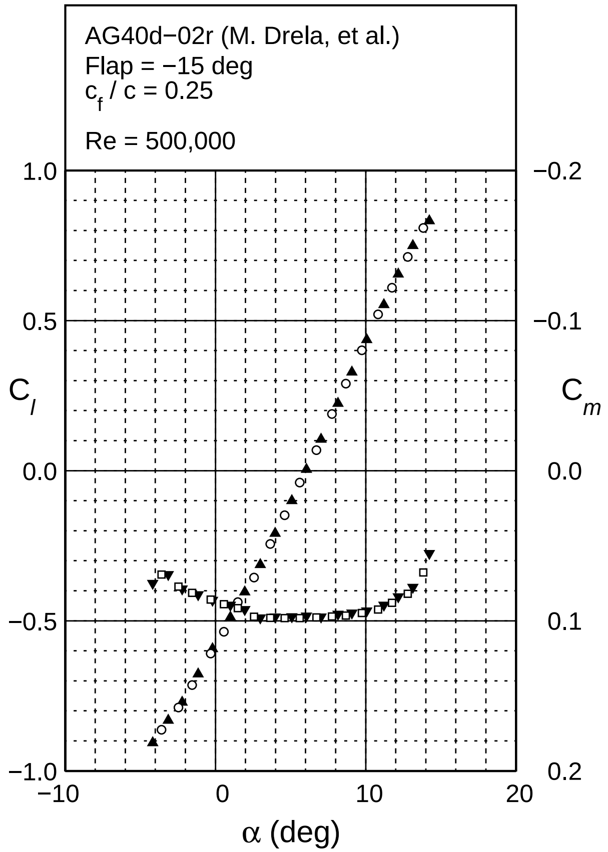

Figure 6.47: Continued.

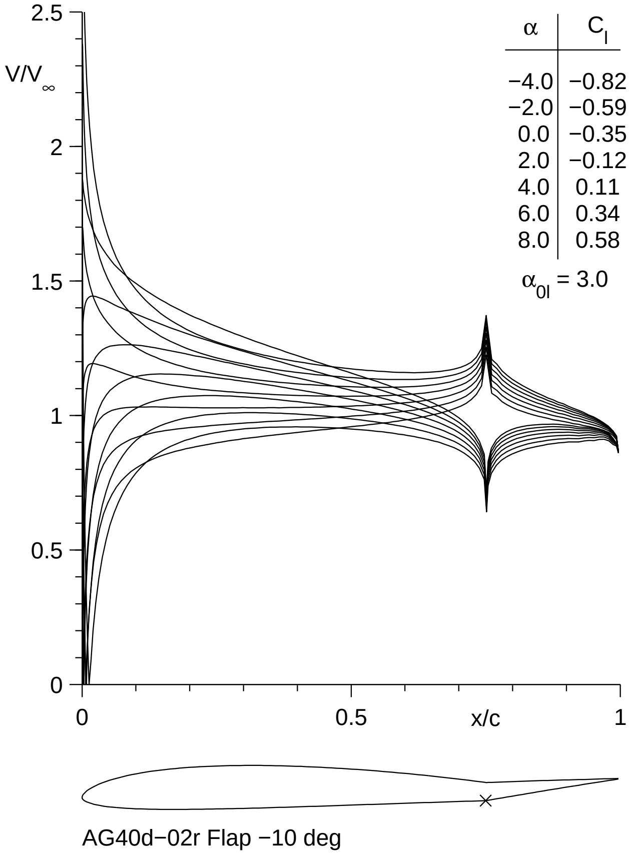

Figure 6.48: Inviscid velocity distributions for the AG40d-02r with a −10 deg flap.

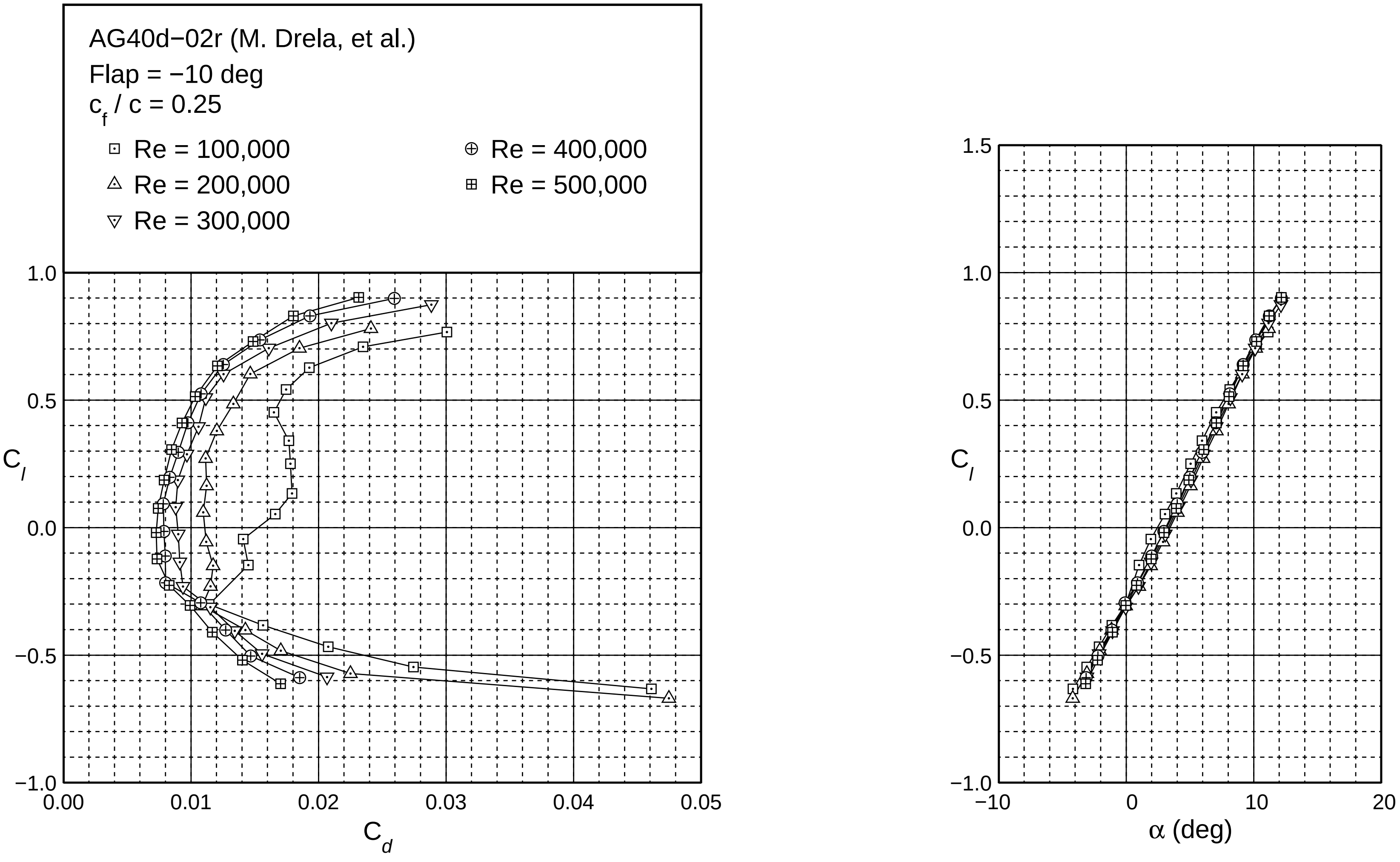

Figure 6.49: Drag polar for the AG40d-02r with a −10 deg flap.

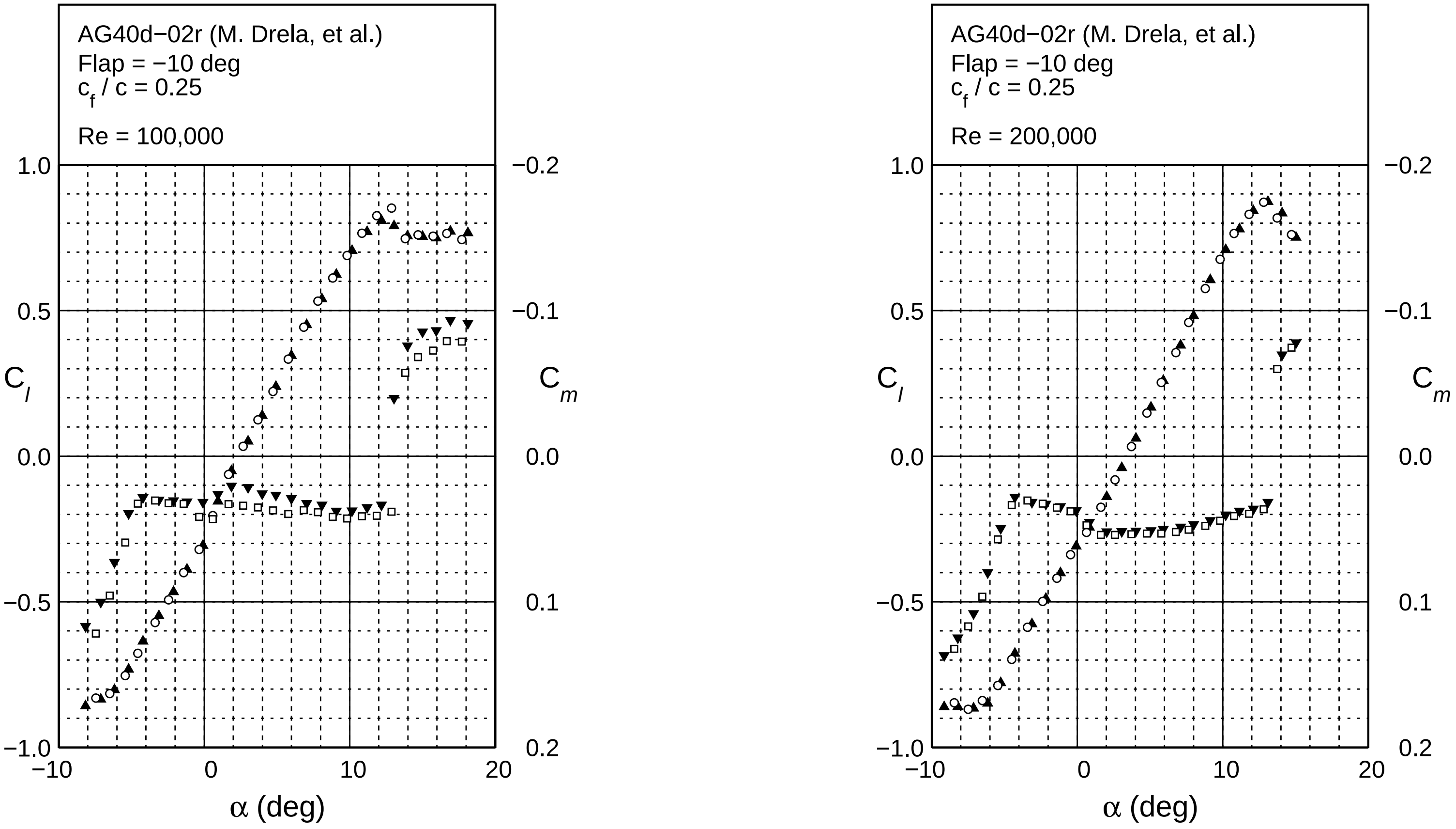

Figure 6.50: Lift and moment characteristics for the AG40d-02r with a −10 deg flap.

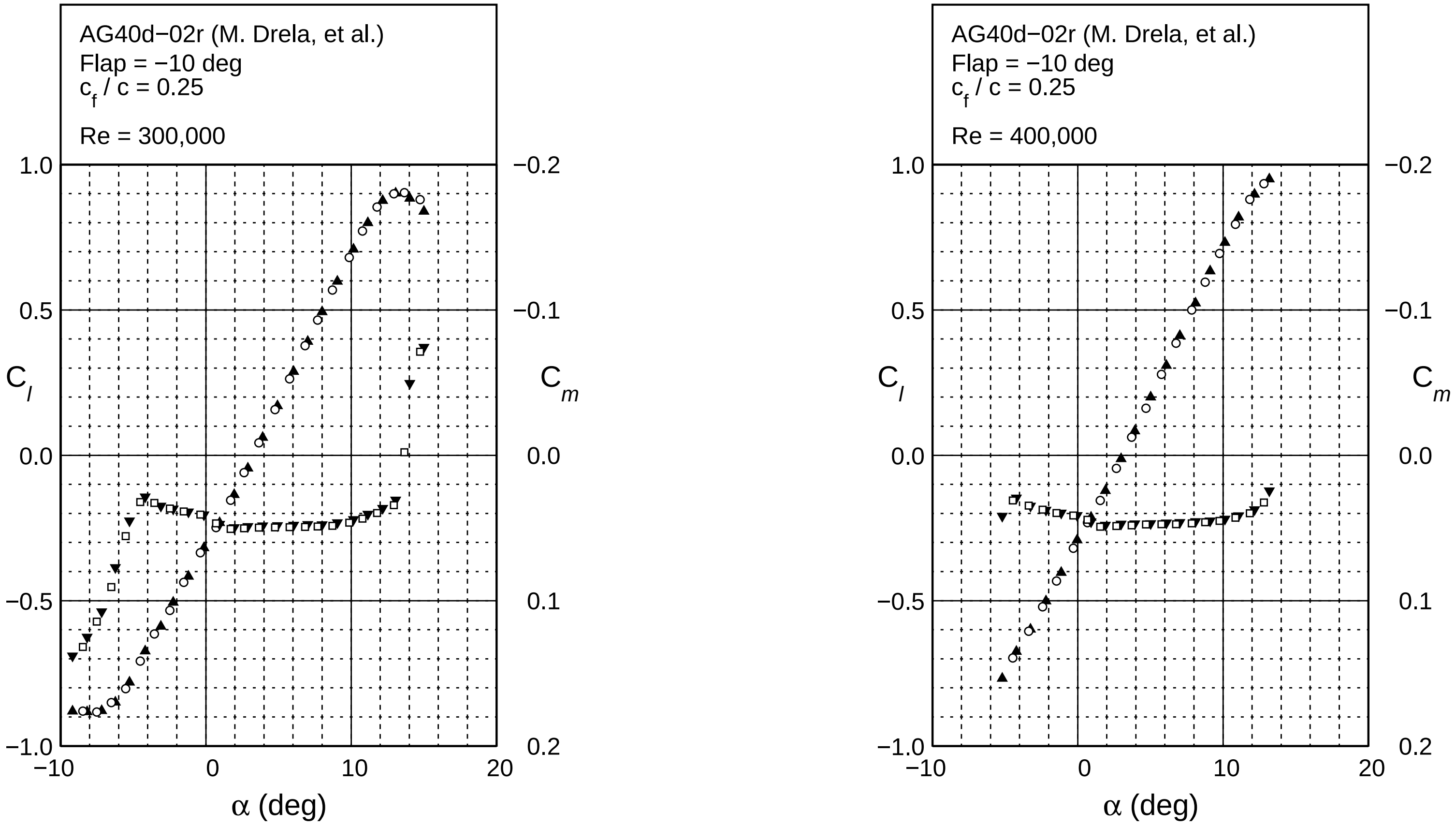

Figure 6.50: Continued.

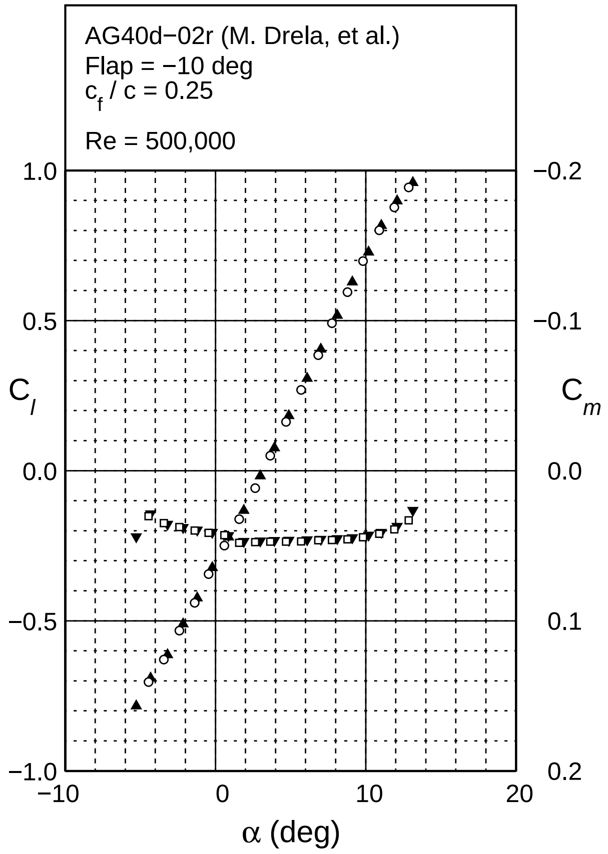

Figure 6.50: Continued.

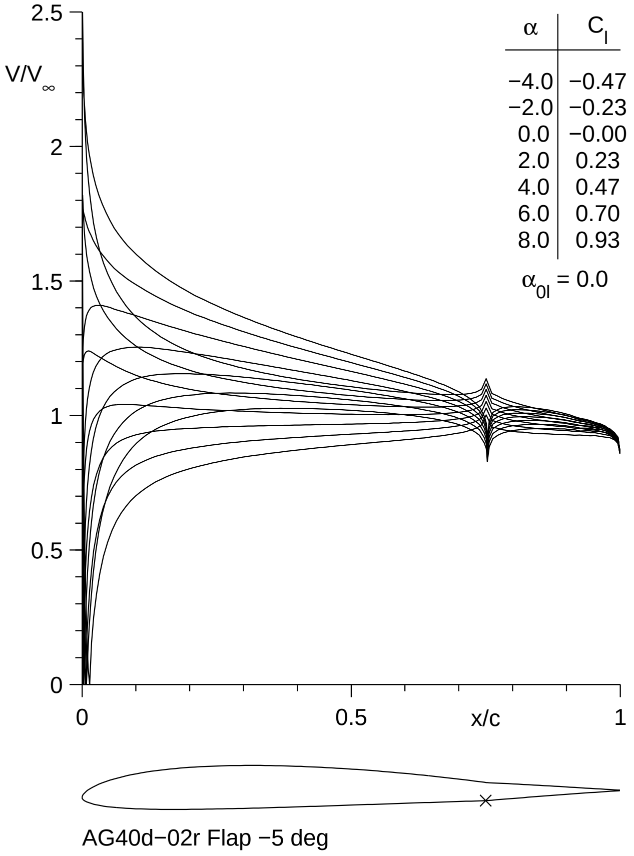

Figure 6.51: Inviscid velocity distributions for the AG40d-02r with a −5 deg flap.

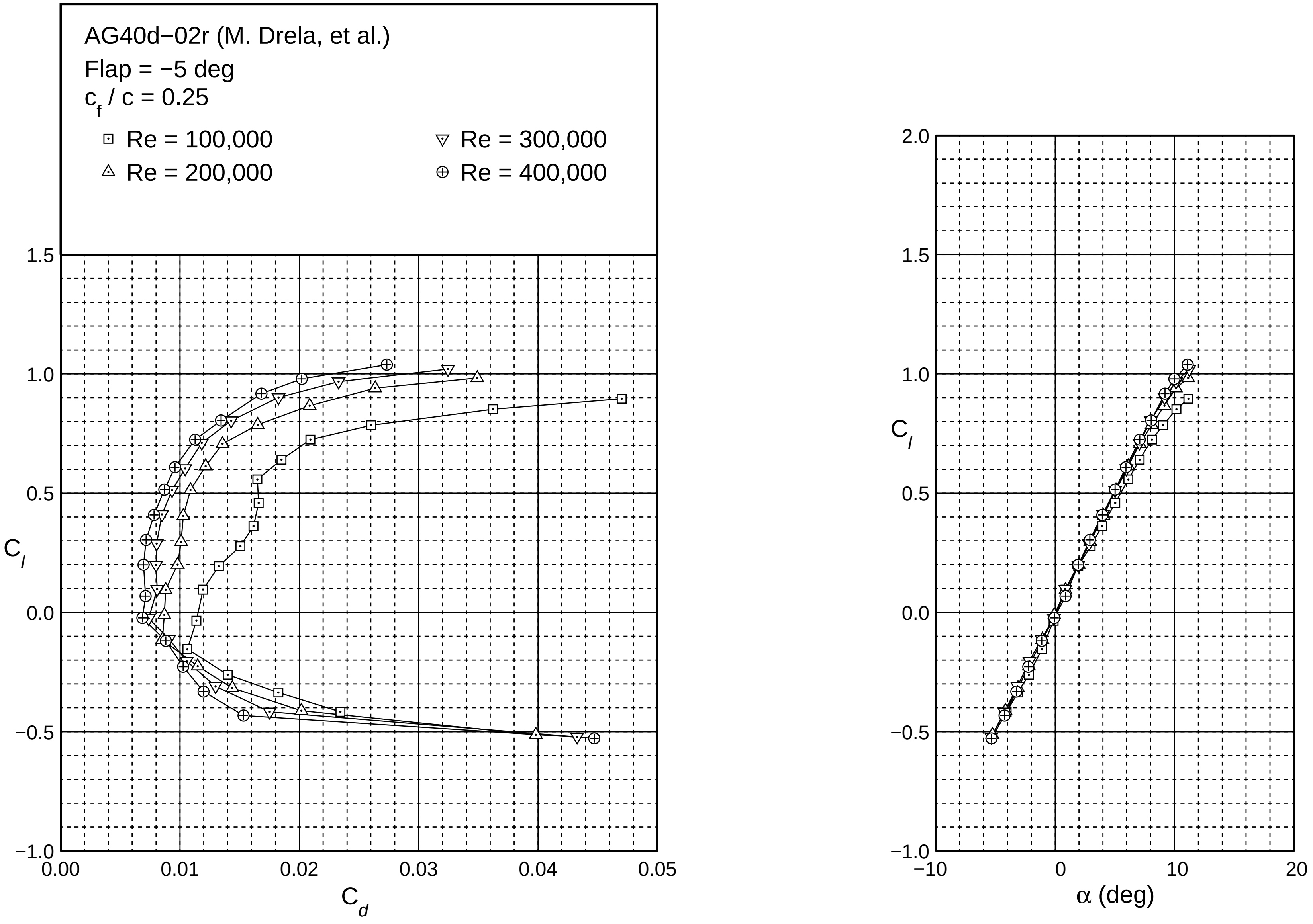

Figure 6.52: Drag polar for the AG40d-02r with a −5 deg flap.

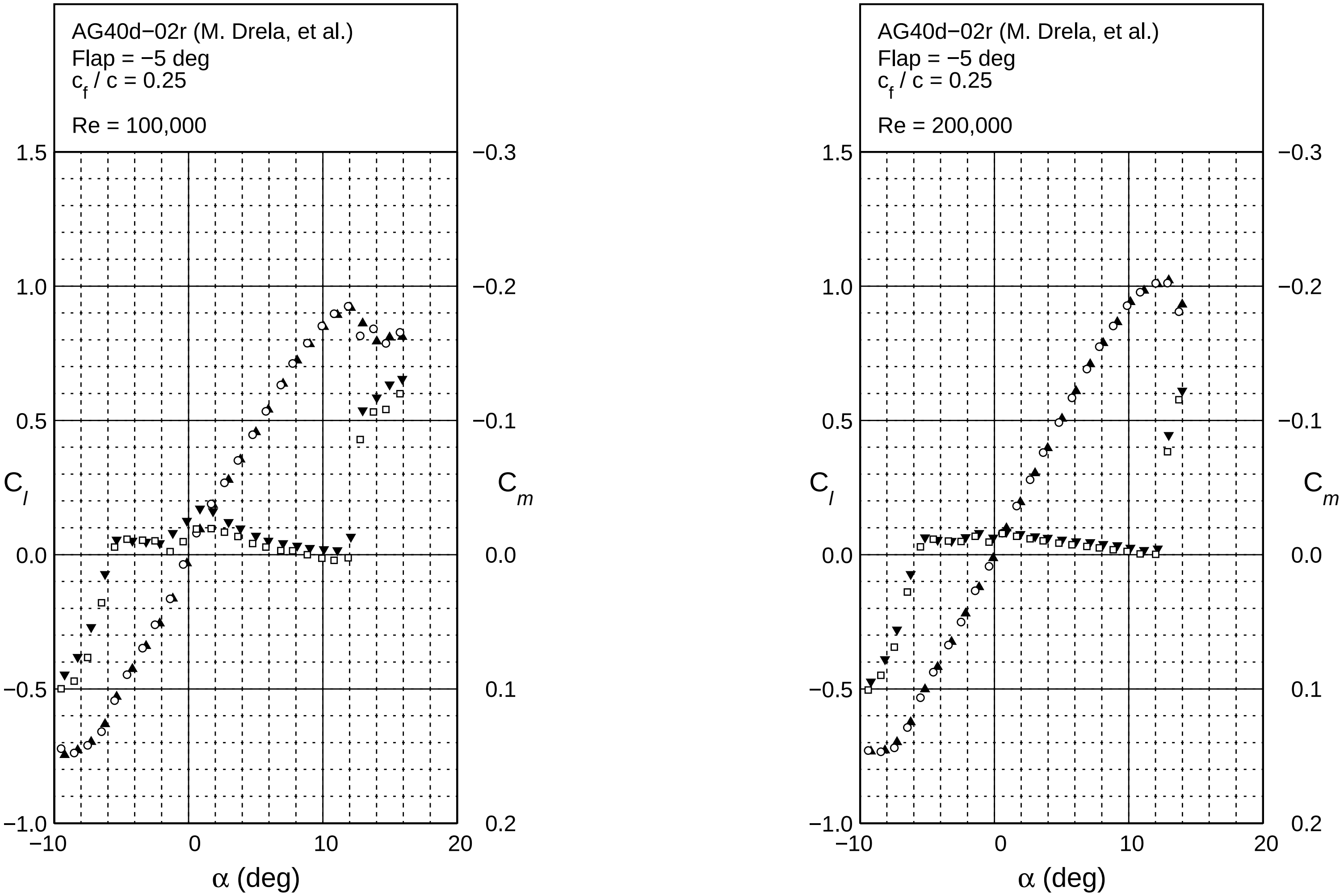

Figure 6.53: Lift and moment characteristics for the AG40d-02r with a −5 deg flap.

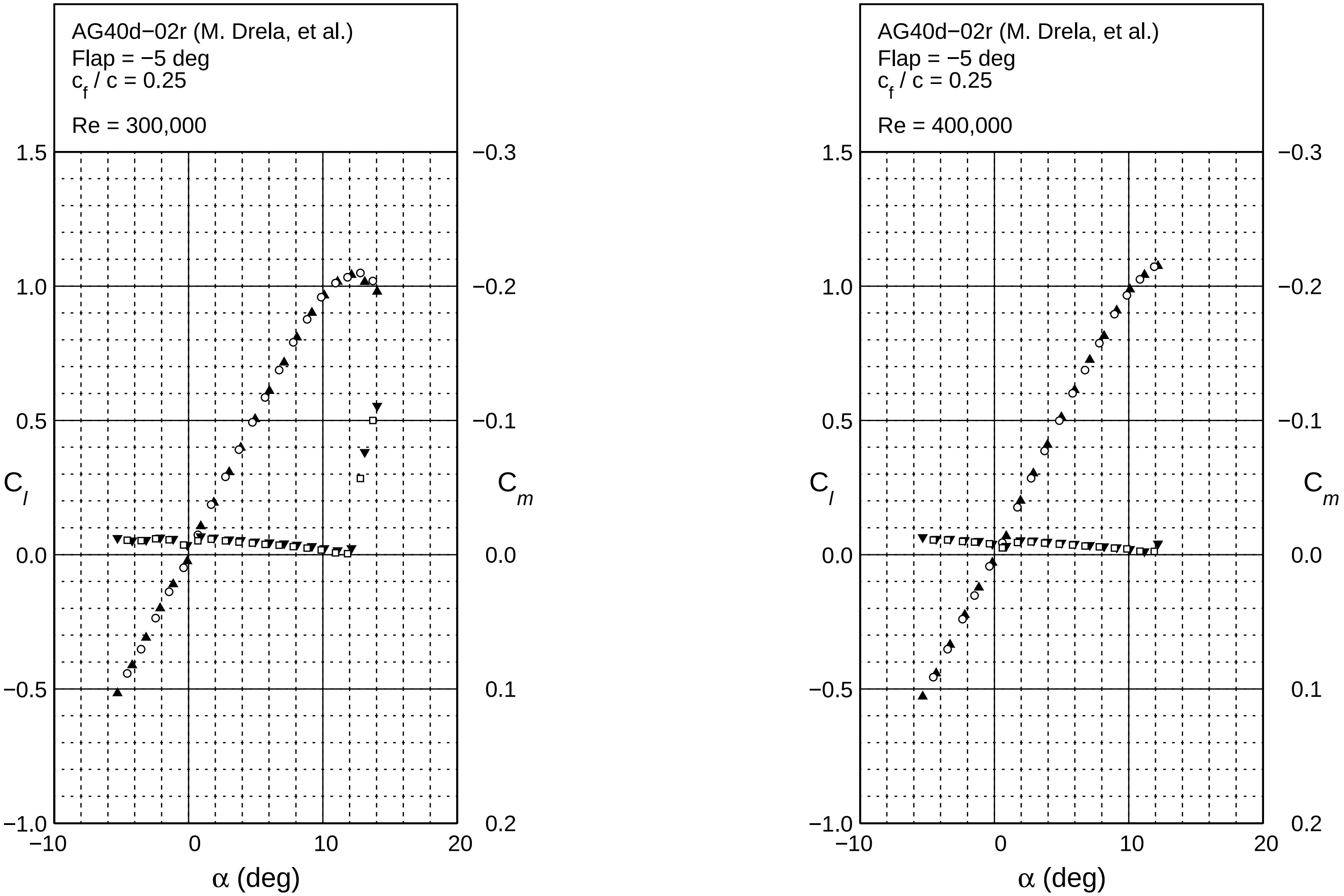

Figure 6.53: Continued.

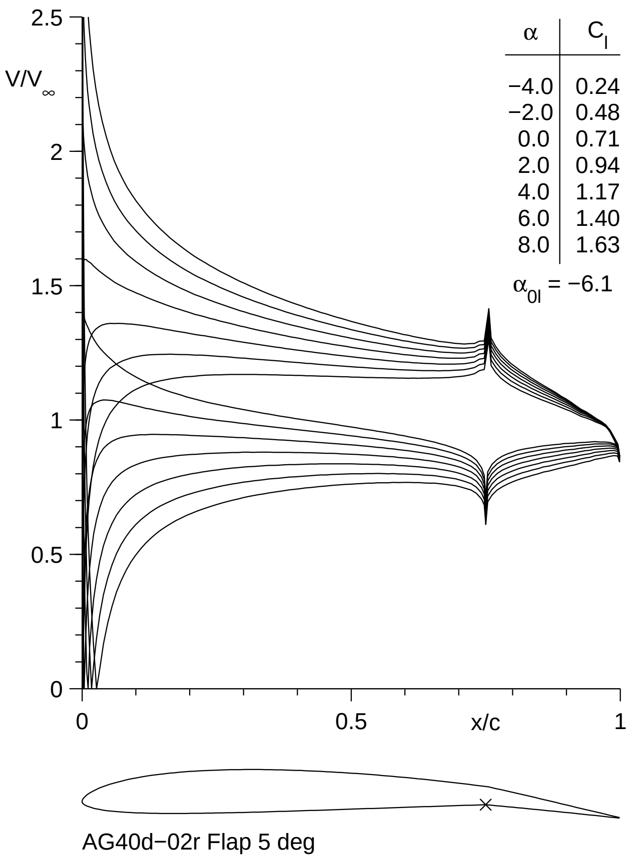

Figure 6.54: Inviscid velocity distributions for the AG40d-02r with a 5 deg flap.

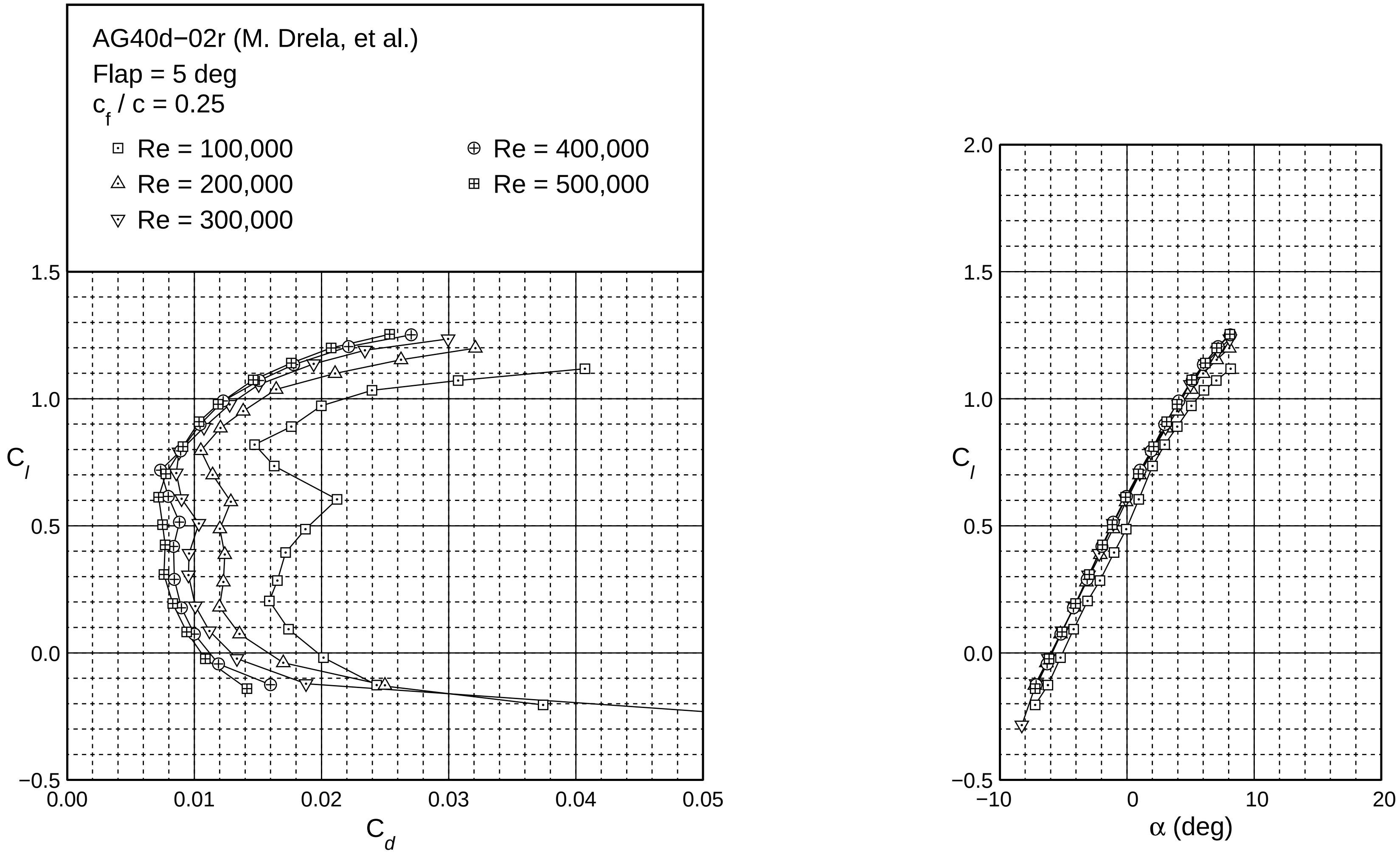

Figure 6.55: Drag polar for the AG40d-02r with a 5 deg flap.

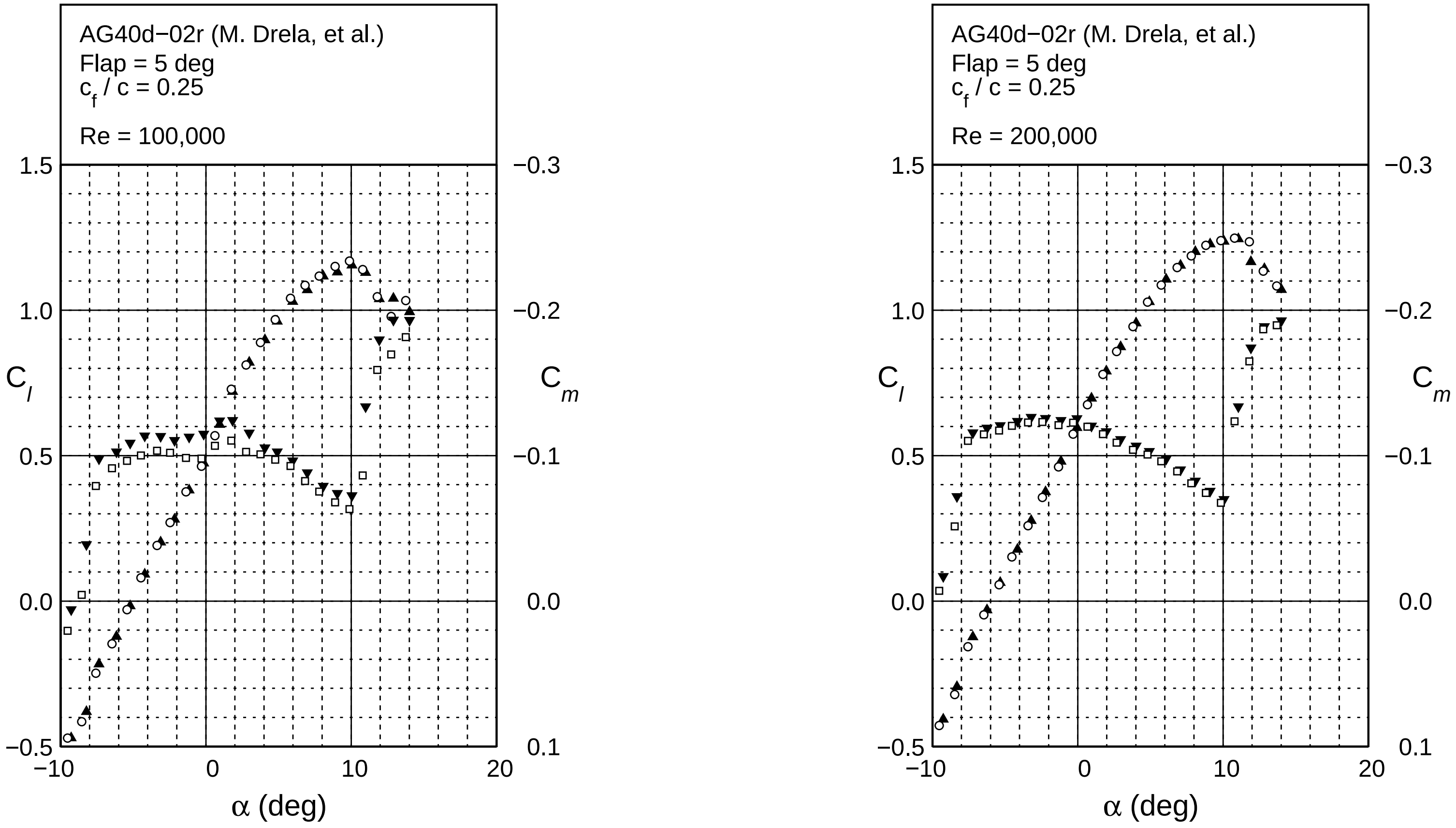

Figure 6.56: Lift and moment characteristics for the AG40d-02r with a 5 deg flap.

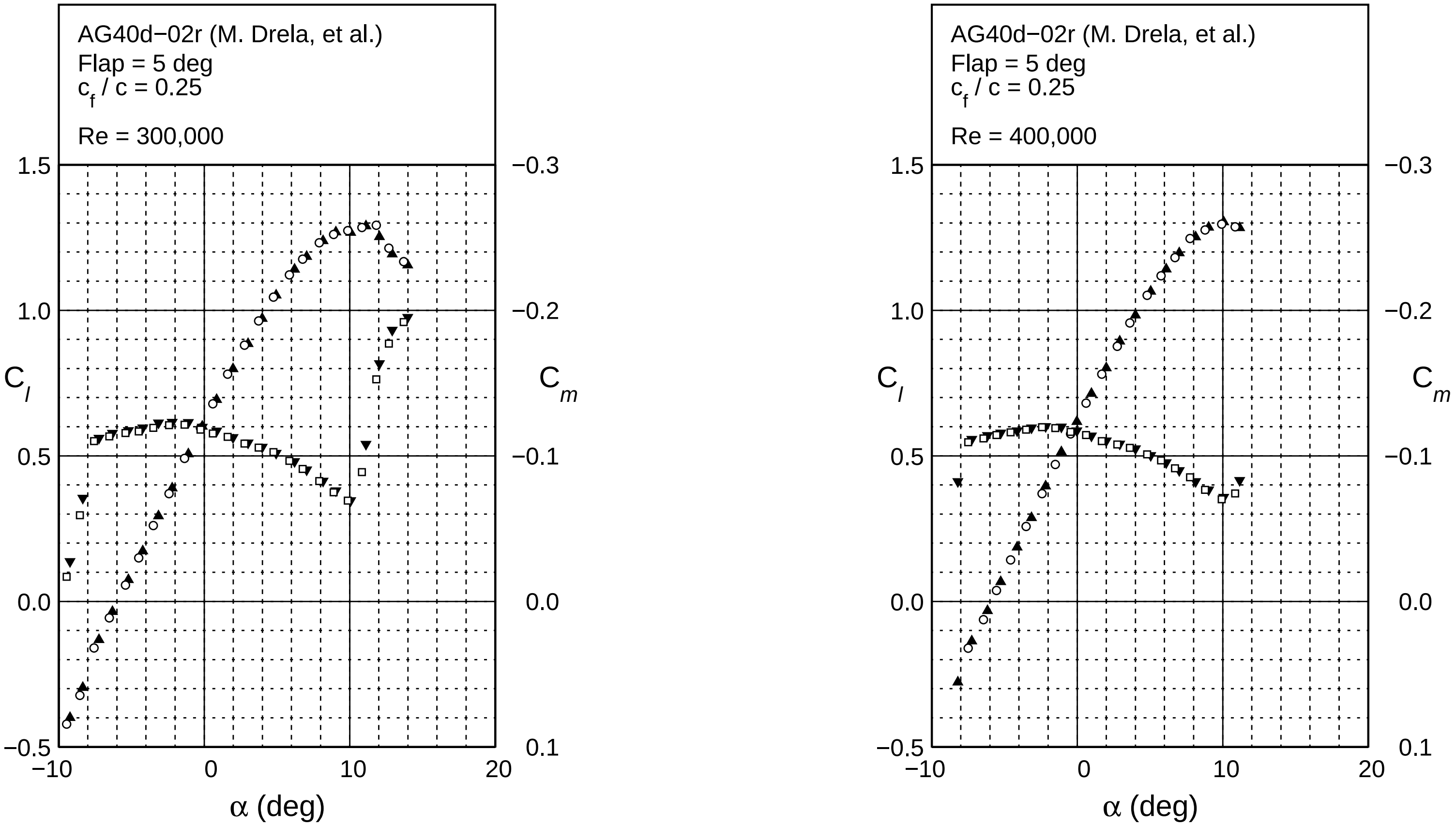

Figure 6.56: Continued.

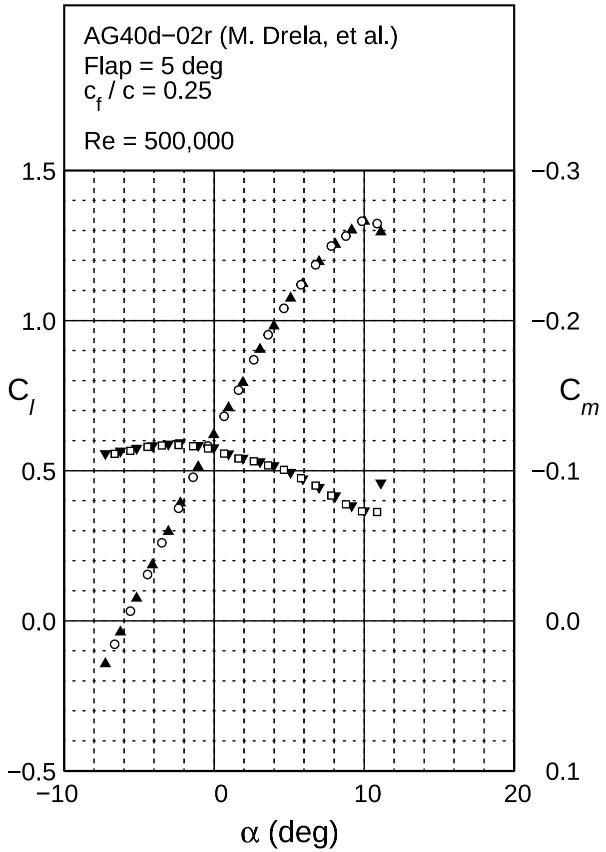

Figure 6.56: Continued.

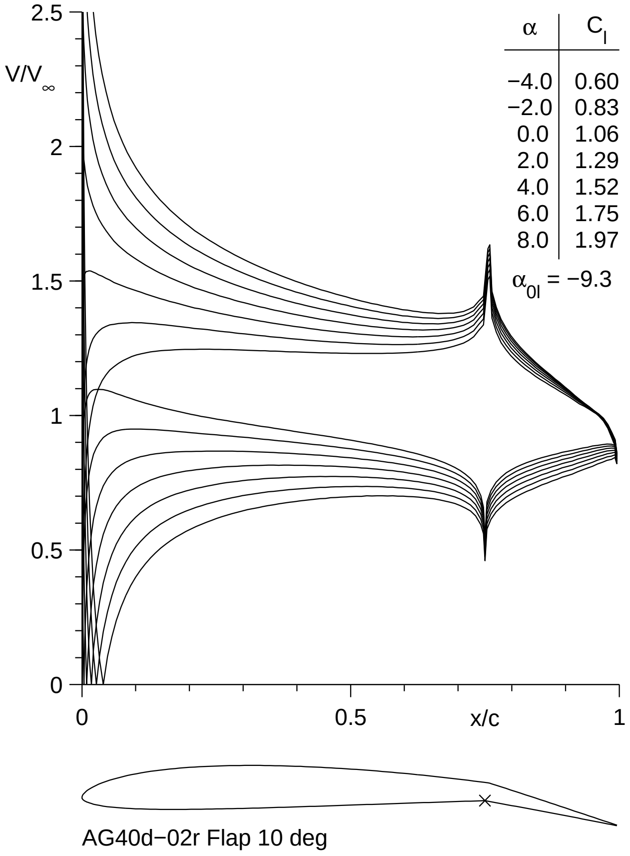

Figure 6.57: Inviscid velocity distributions for the AG40d-02r with a 10 deg flap.

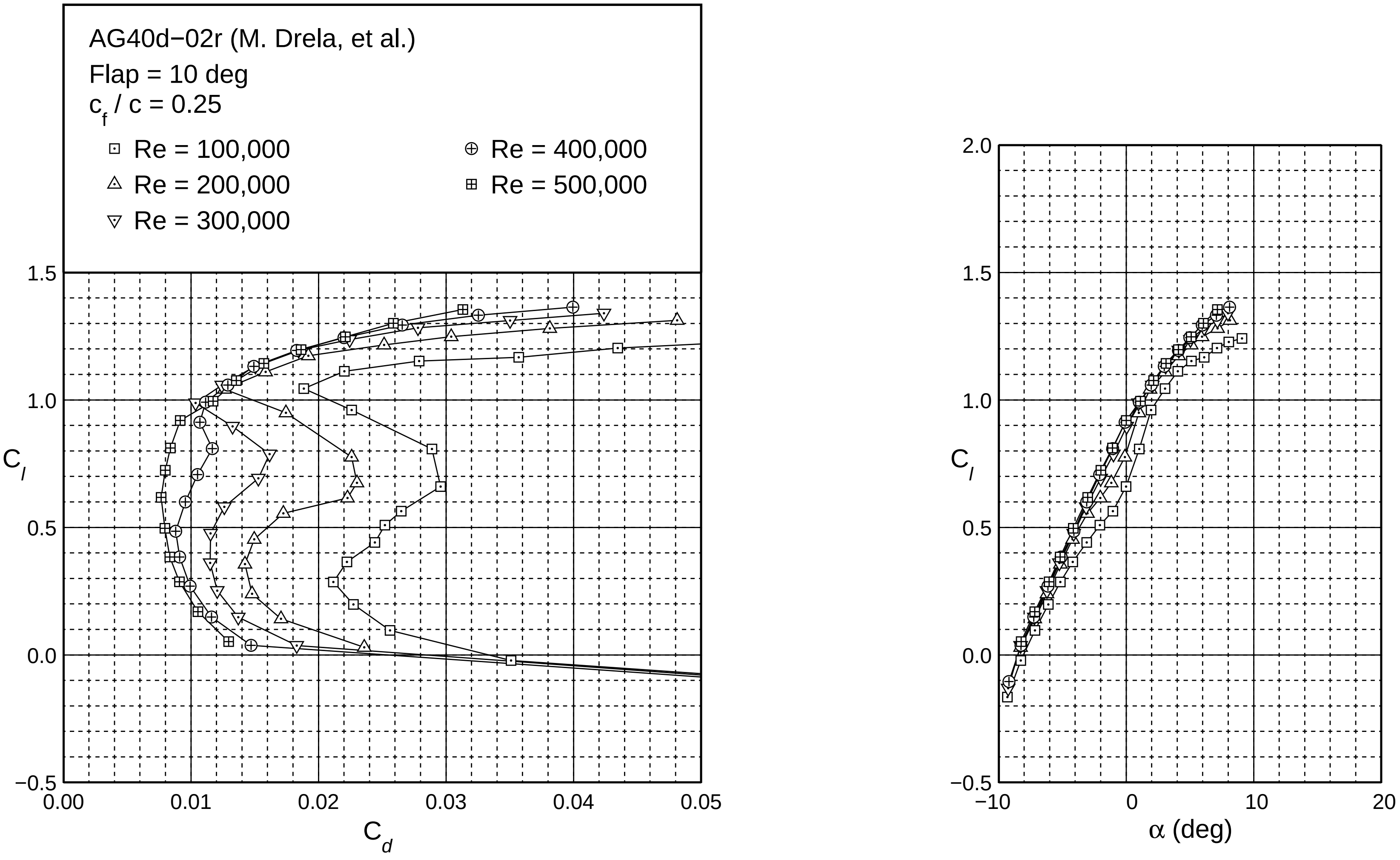

Figure 6.58: Drag polar for the AG40d-02r with a 10 deg flap.

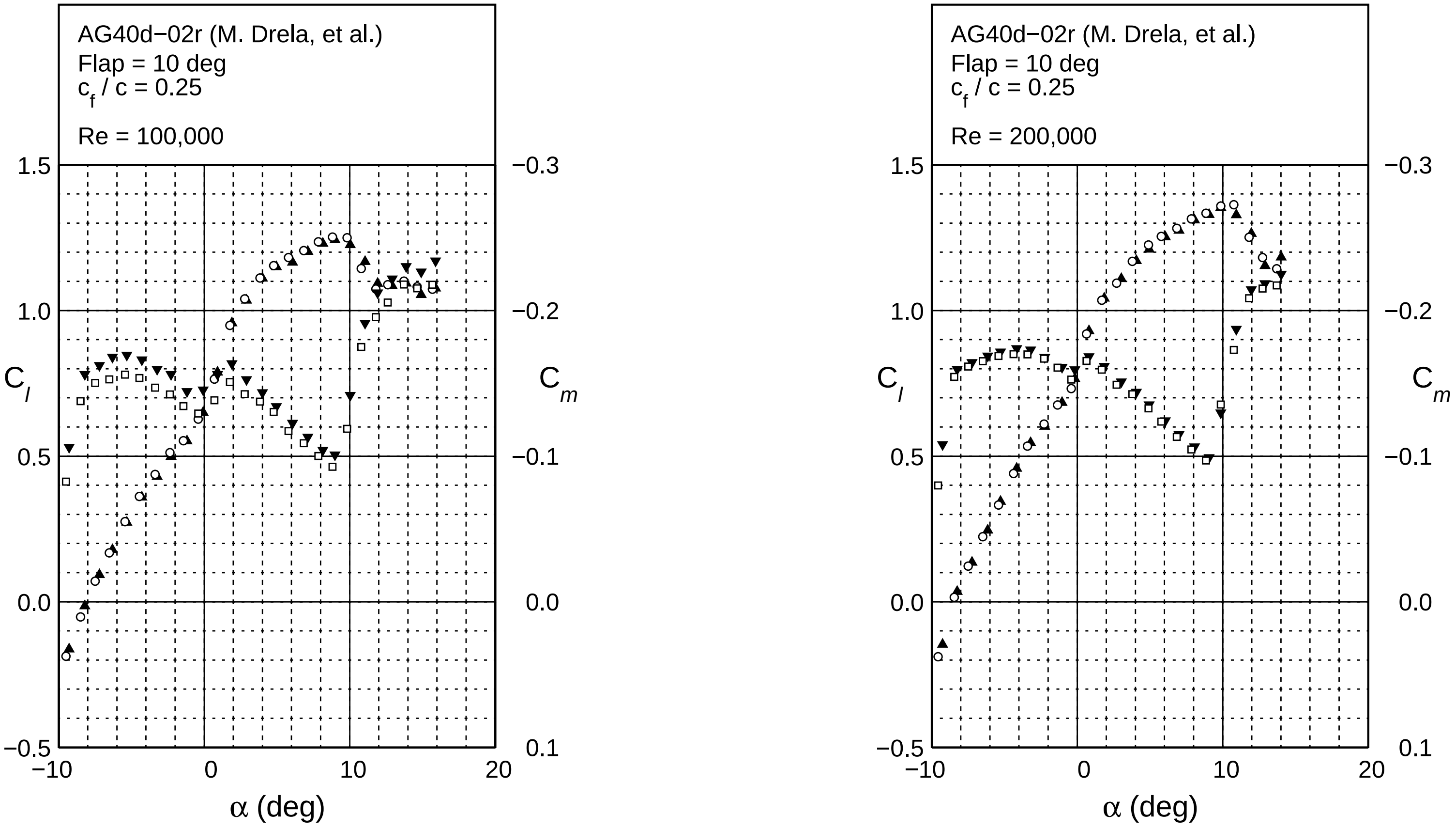

Figure 6.59: Lift and moment characteristics for the AG40d-02r with a 10 deg flap.

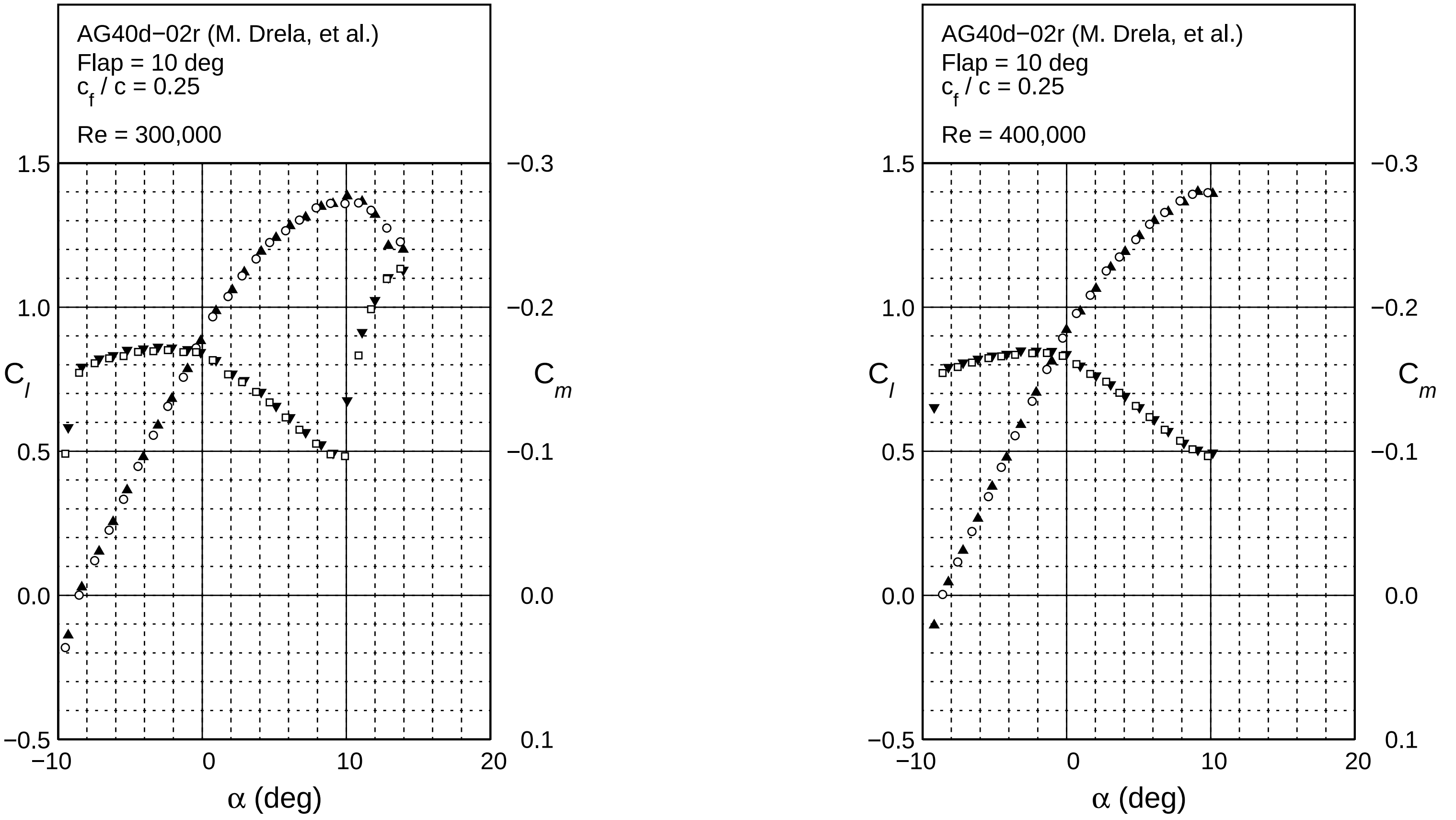

Figure 6.59: Continued.

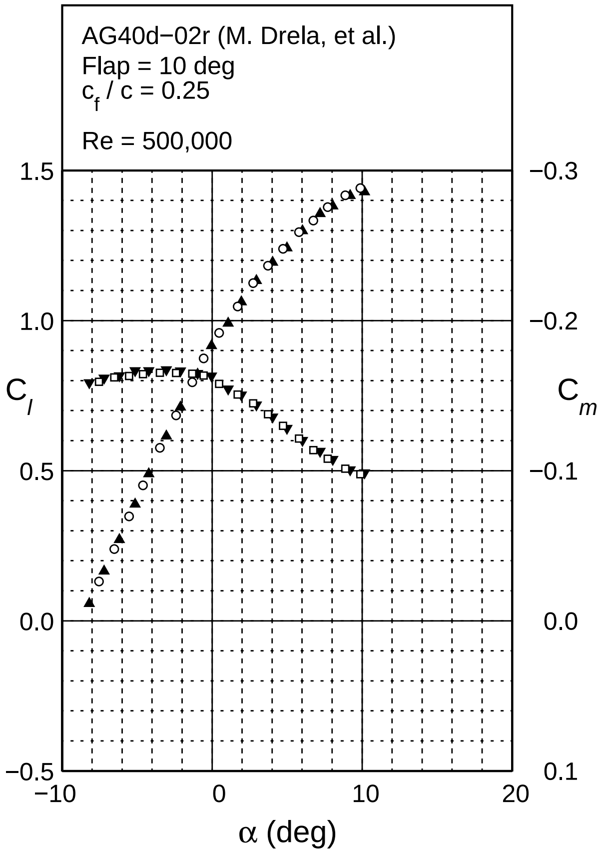

Figure 6.59: Continued.

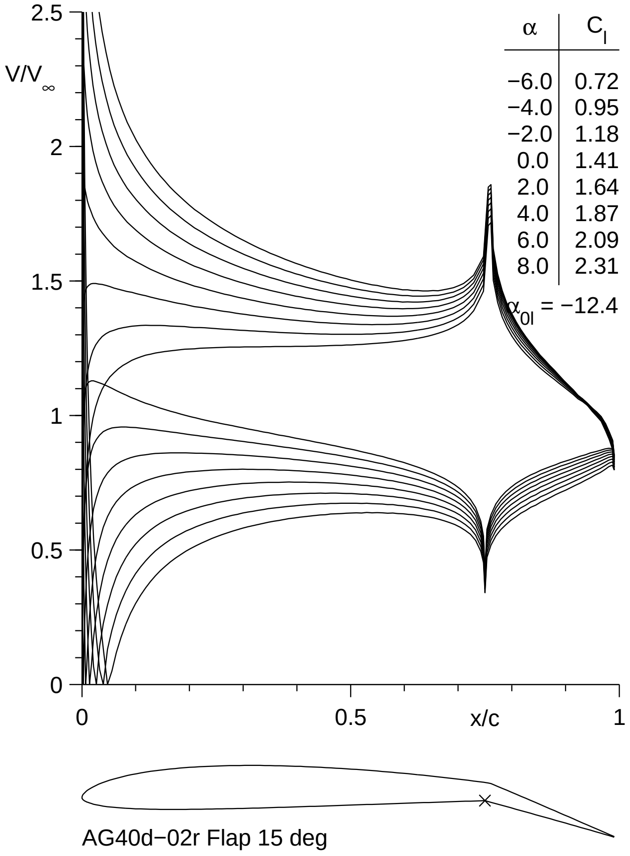

Figure 6.60: Inviscid velocity distributions for the AG40d-02r with a 15 deg flap.

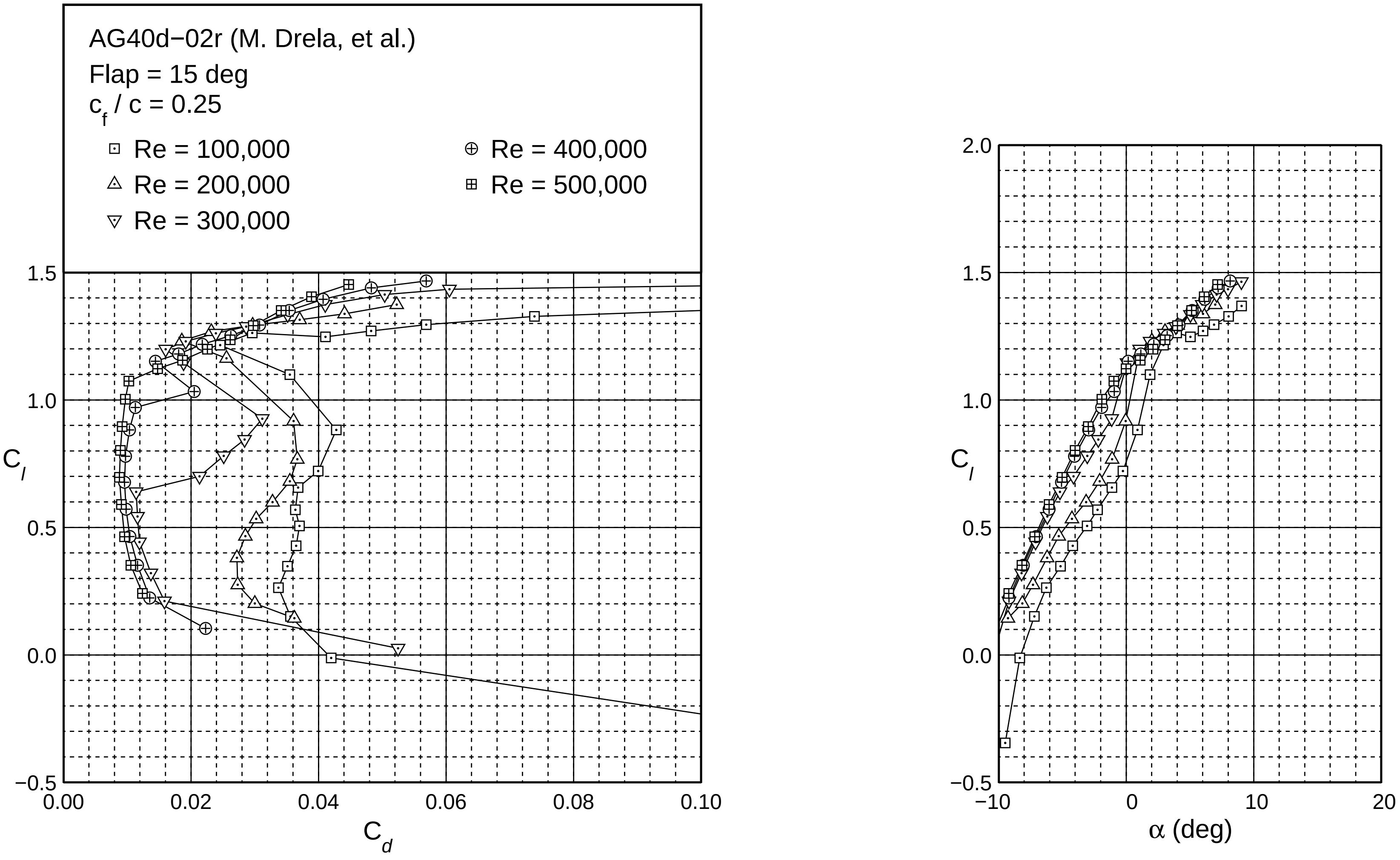

Figure 6.61: Drag polar for the AG40d-02r with a 15 deg flap.

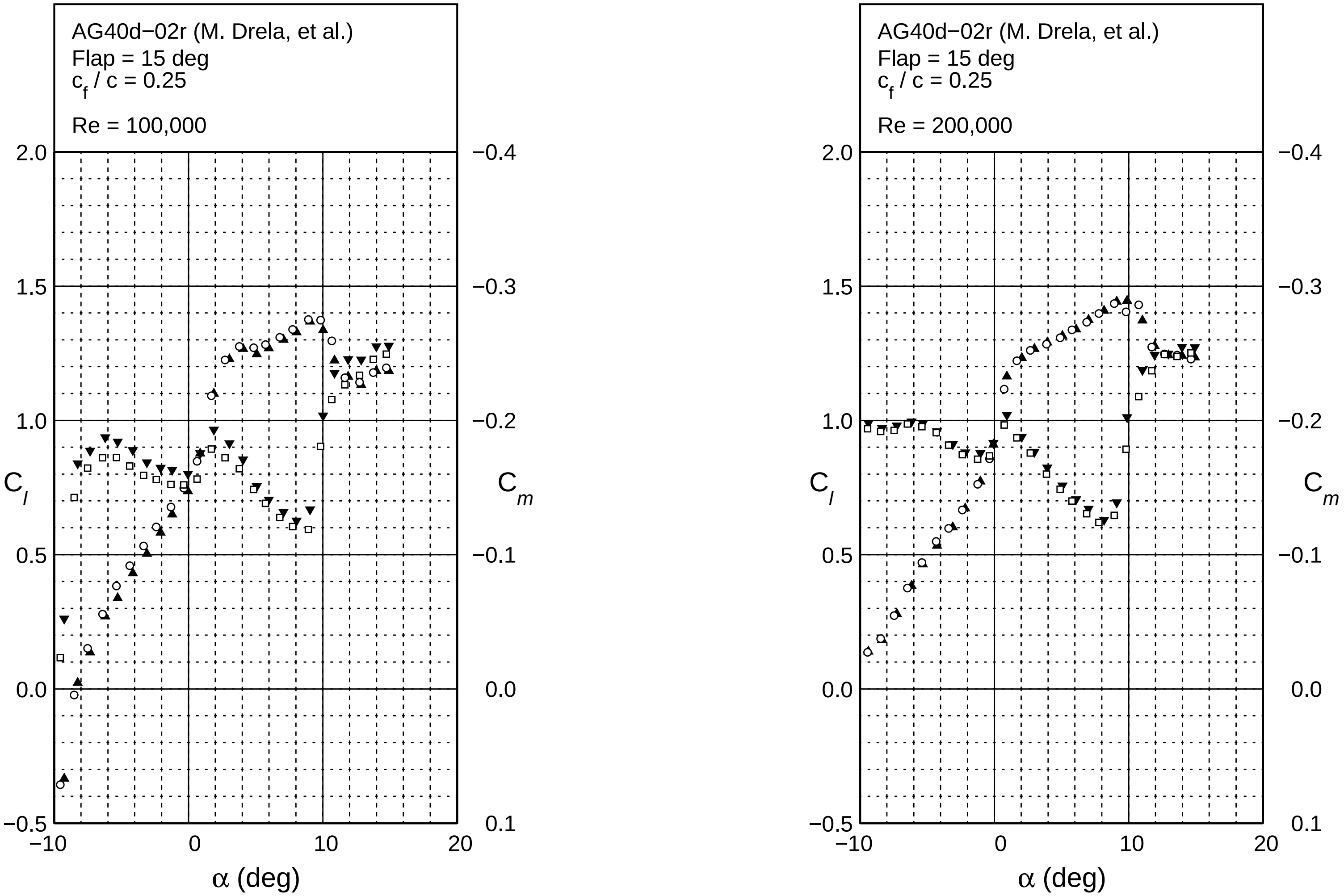

Figure 6.62: Lift and moment characteristics for the AG40d-02r with a 15 deg flap.

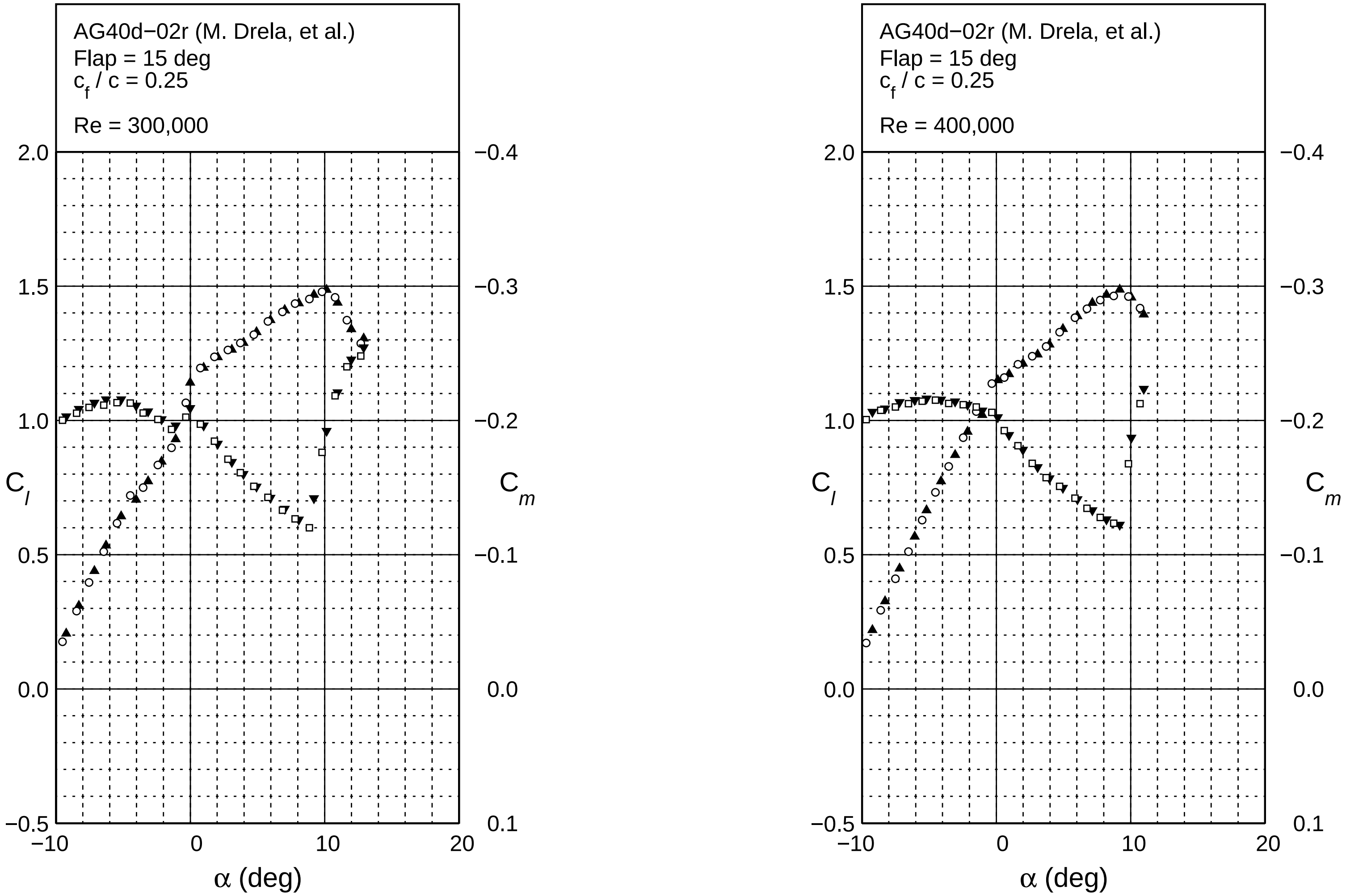

Figure 6.62: Continued.

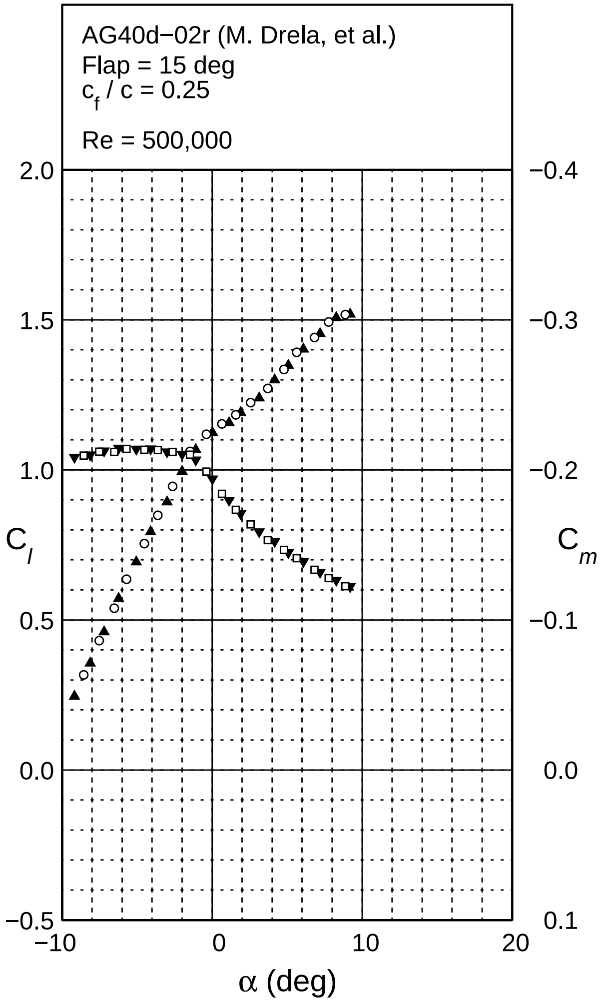

Figure 6.62: Continued.

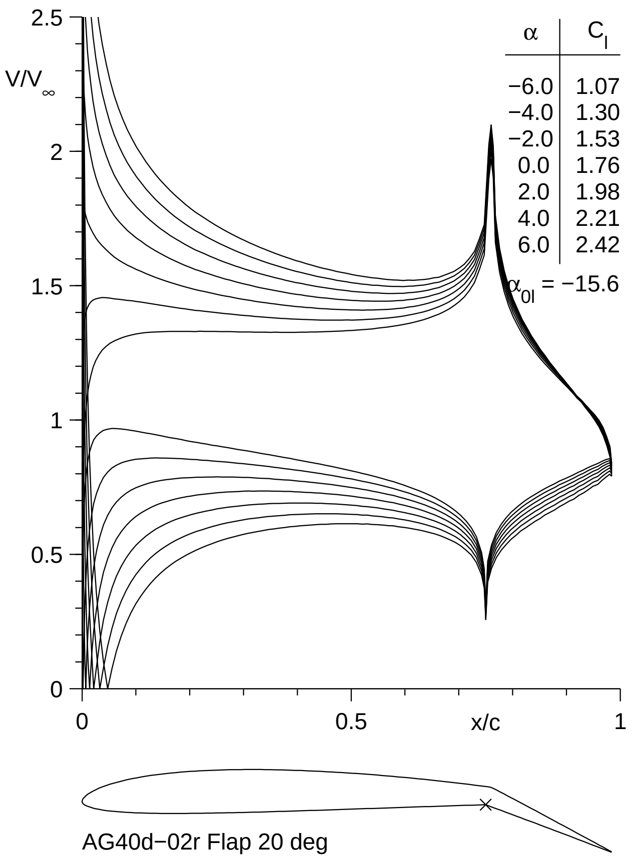

Figure 6.63: Inviscid velocity distributions for the AG40d-02r with a 20 deg flap.

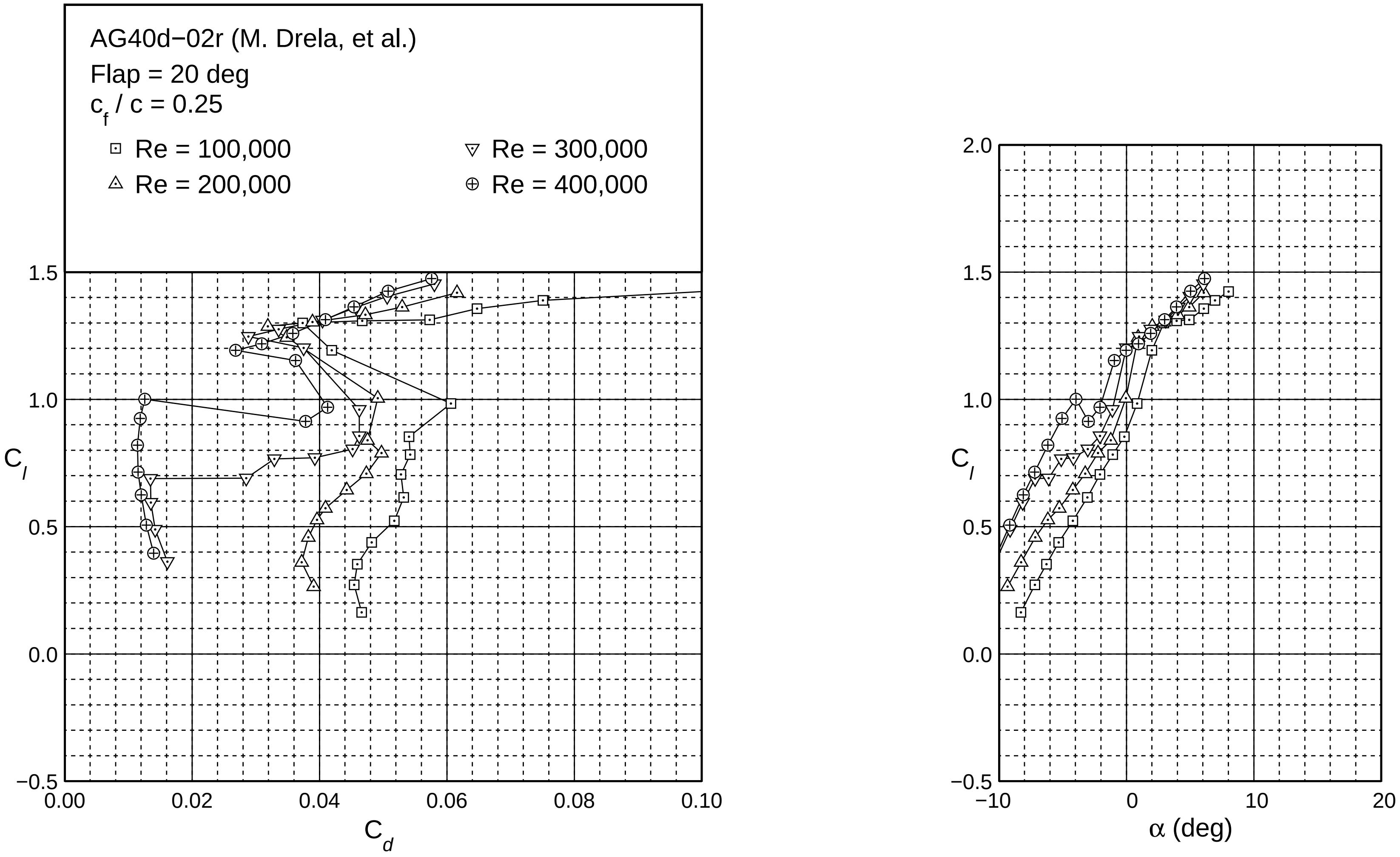

Figure 6.64: Drag polar for the AG40d-02r with a 20 deg flap.

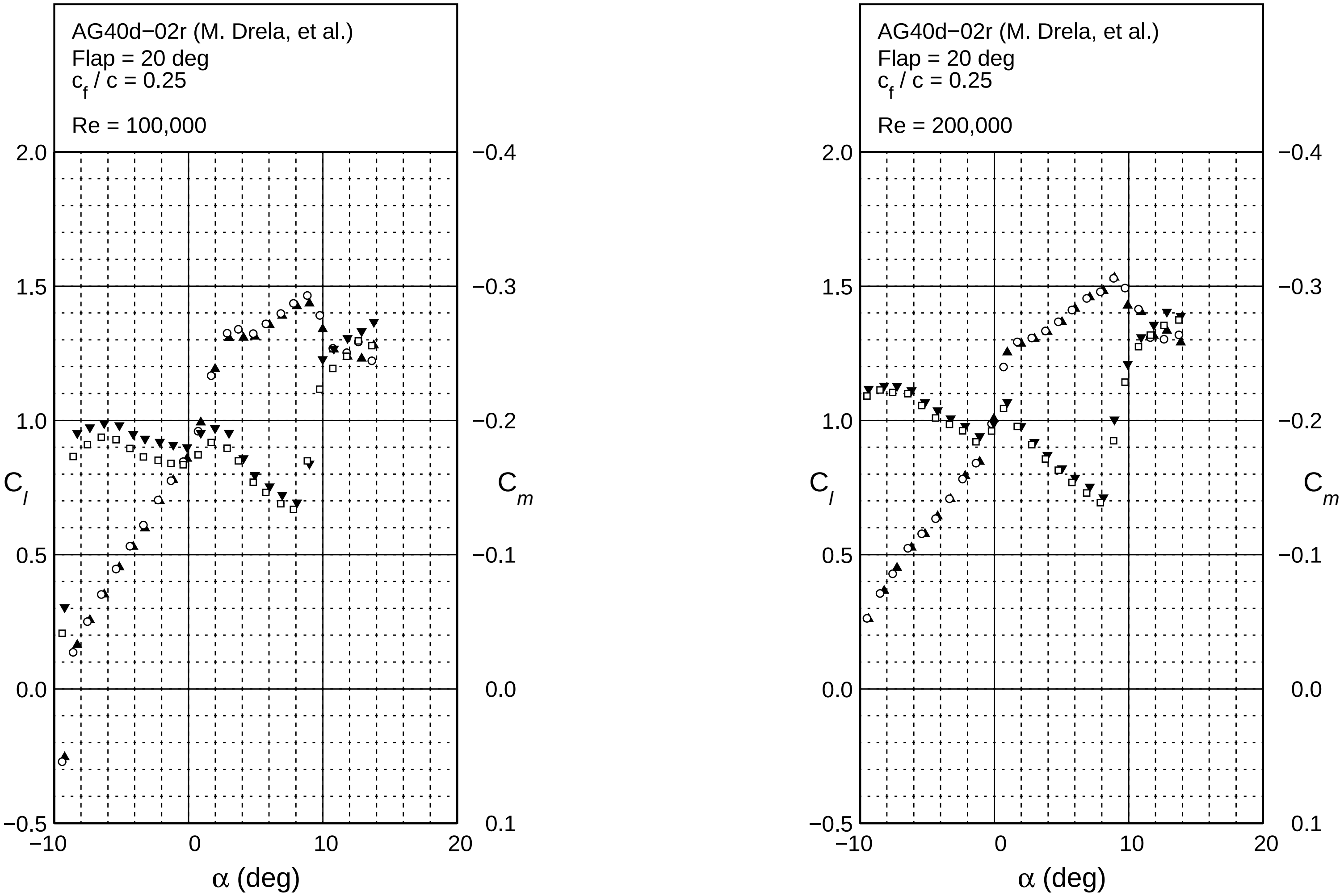

Figure 6.65: Lift and moment characteristics for the AG40d-02r with a 20 deg flap.

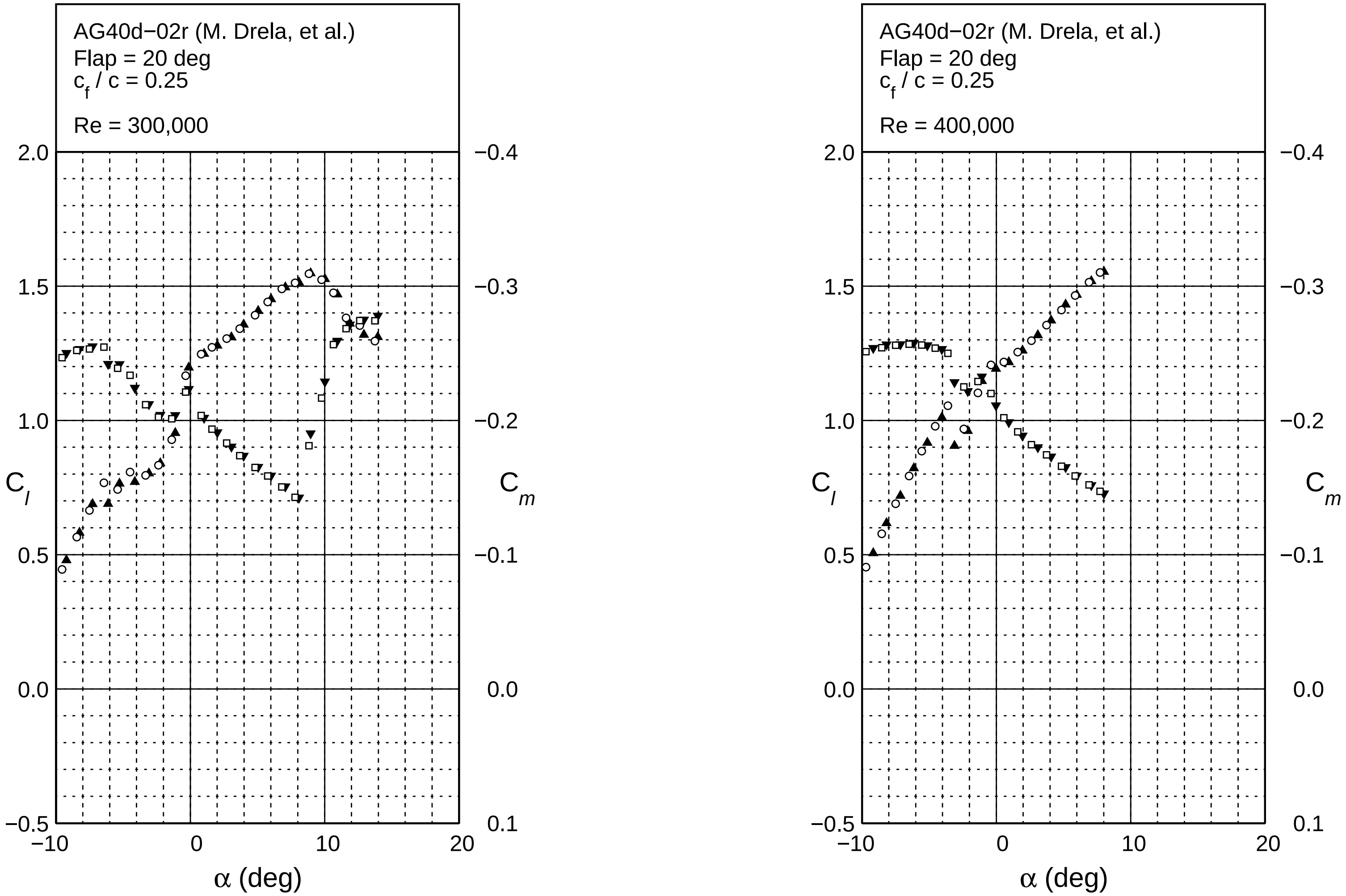

Figure 6.65: Continued.

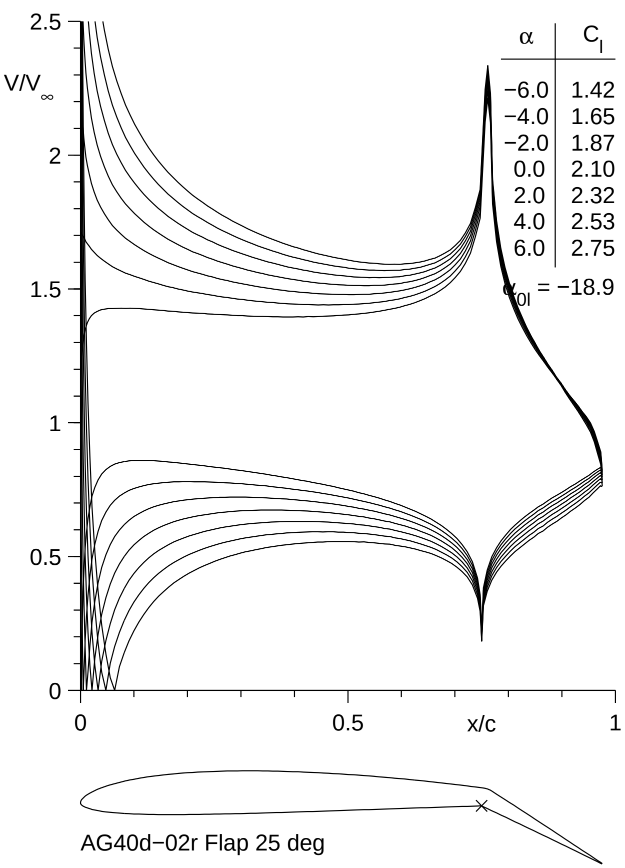

Figure 6.66: Inviscid velocity distributions for the AG40d-02r with a 25 deg flap.

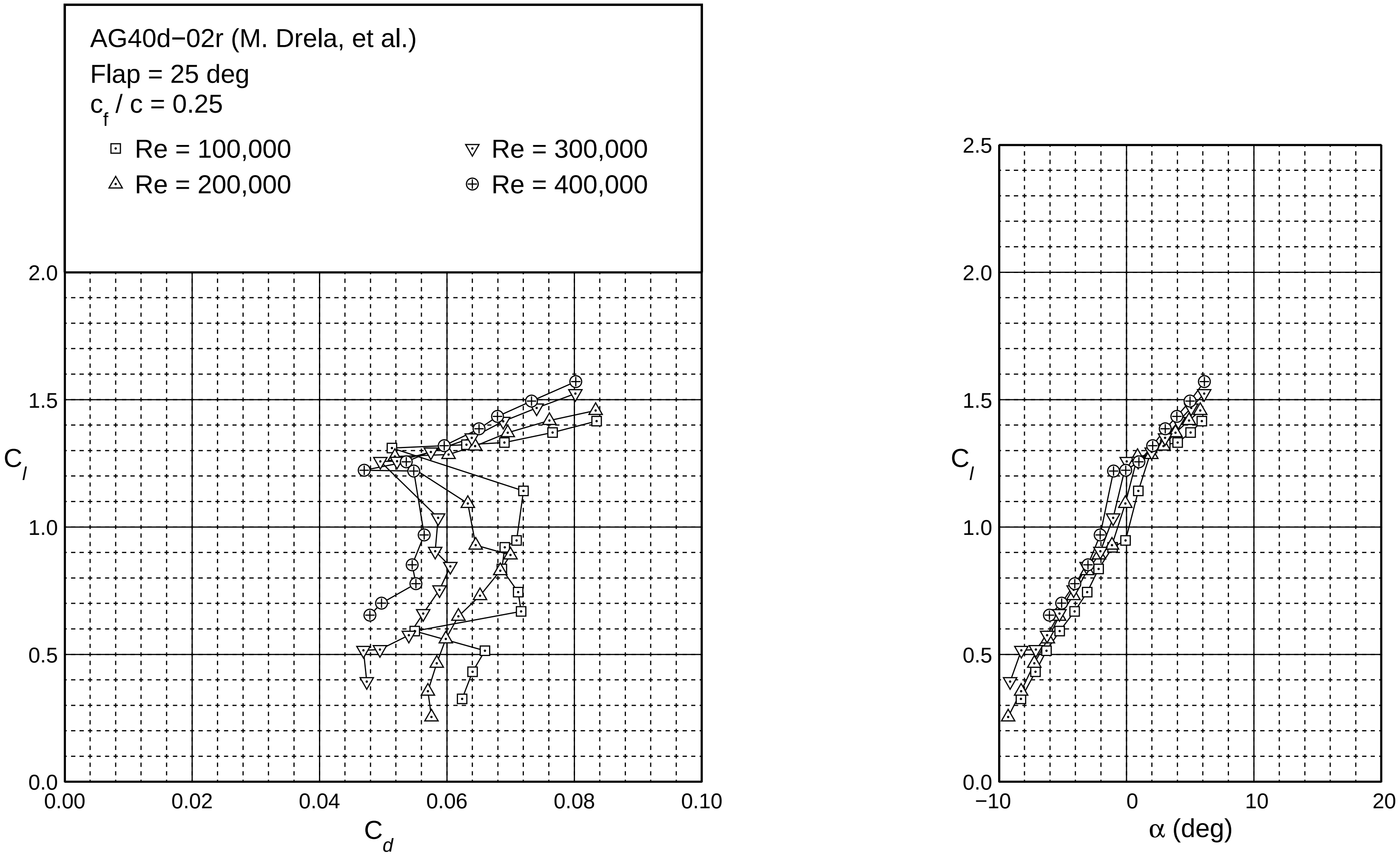

Figure 6.67: Drag polar for the AG40d-02r with a 25 deg flap.

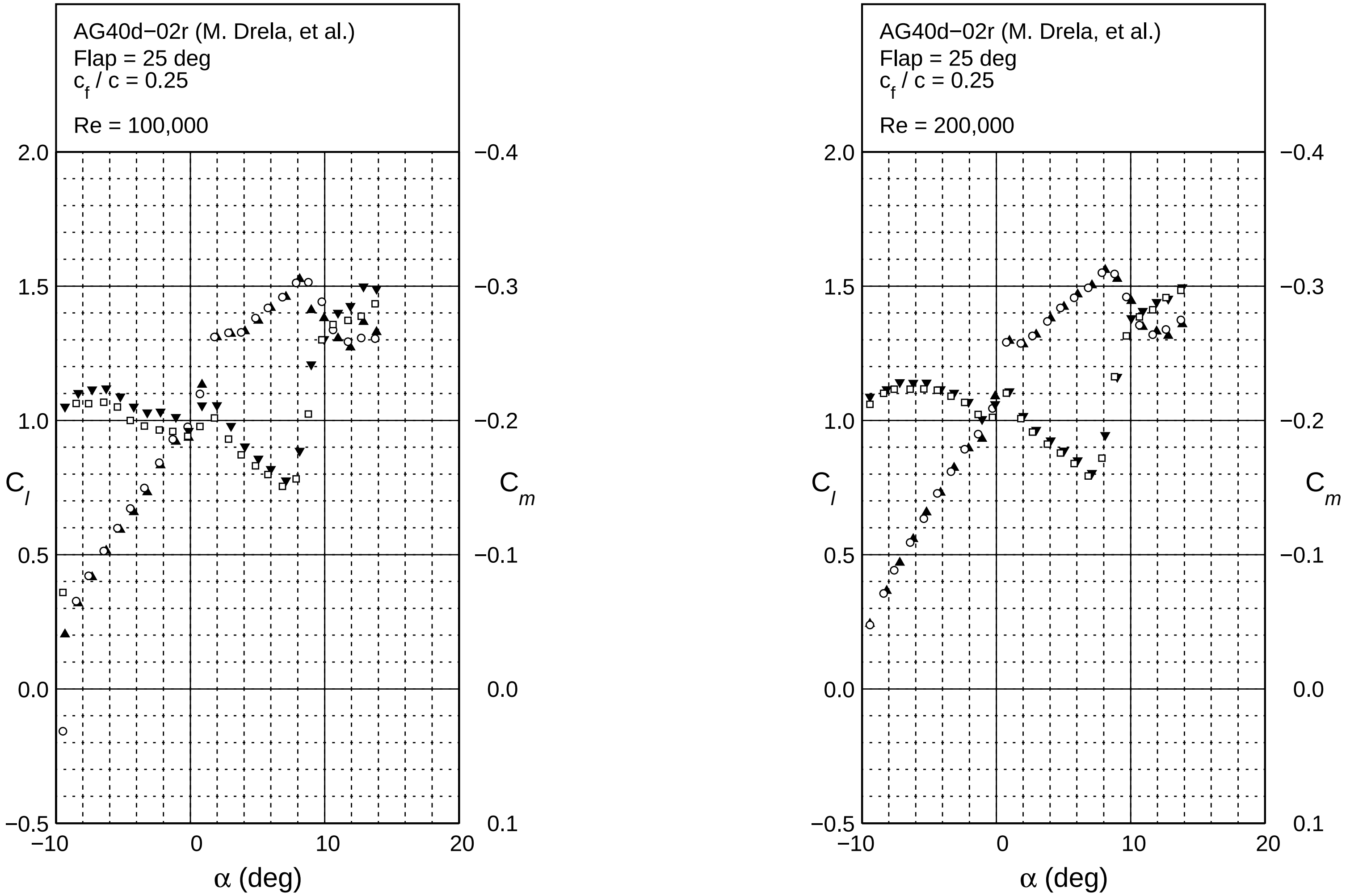

Figure 6.68: Lift and moment characteristics for the AG40d-02r with a 25 deg flap.

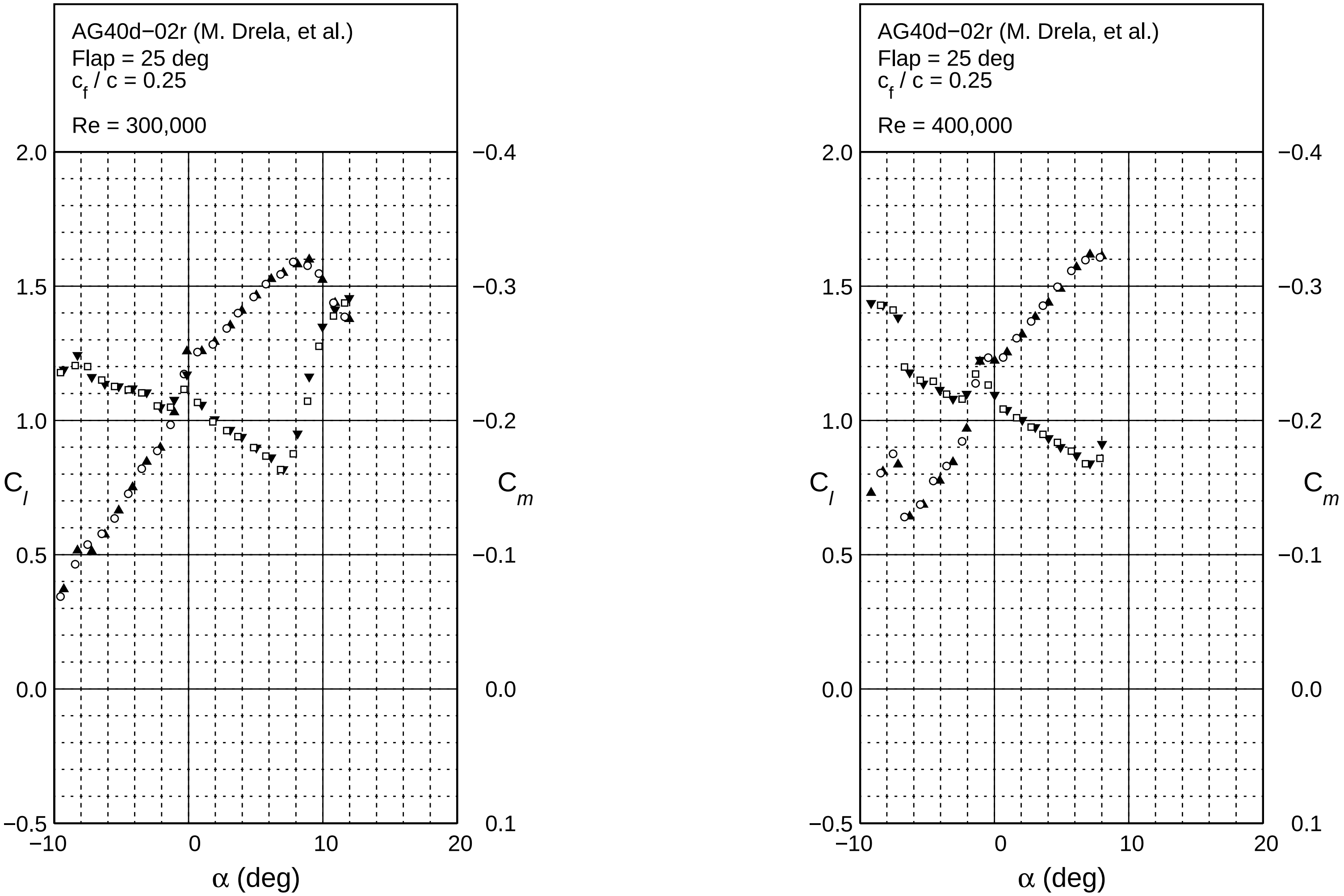

Figure 6.68: Continued.

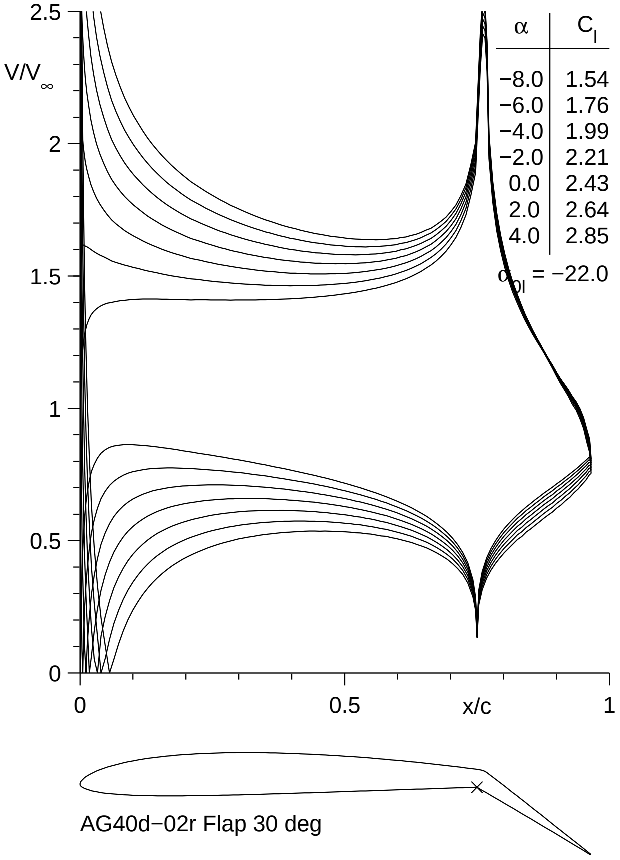

Figure 6.69: Inviscid velocity distributions for the AG40d-02r with a 30 deg flap.

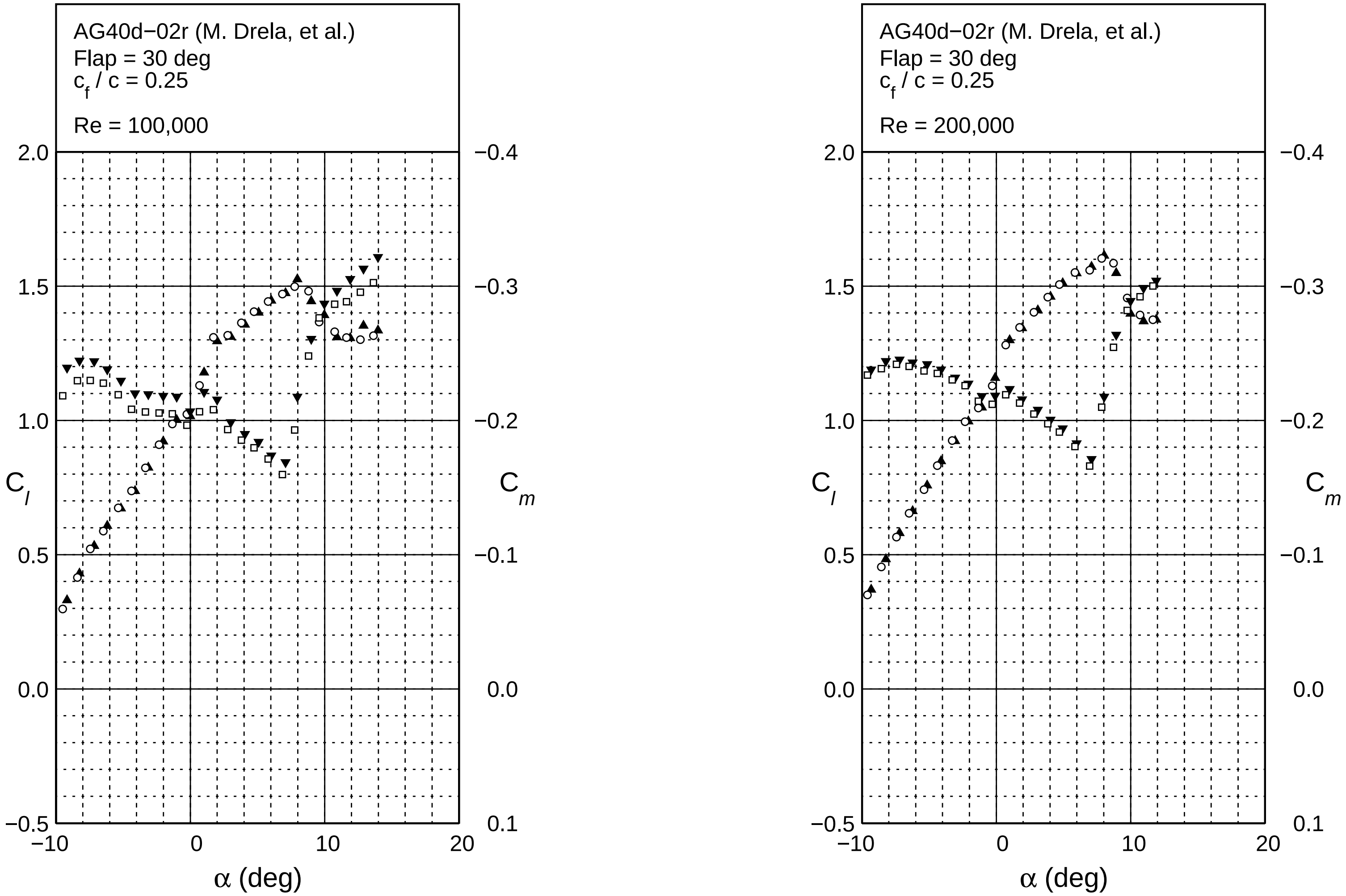

Figure 6.70: Lift and moment characteristics for the AG40d-02r with a 30 deg flap.

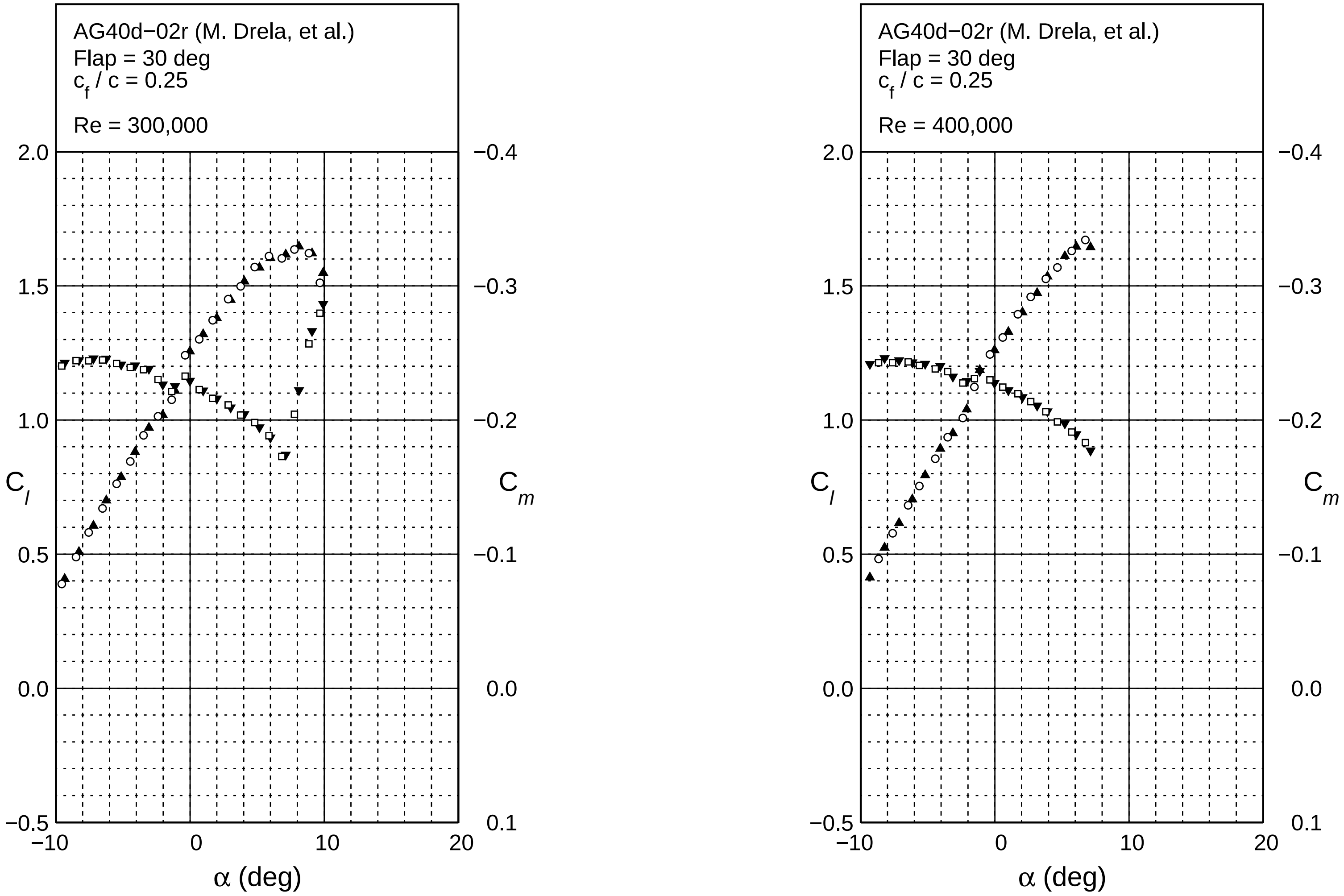

Figure 6.70: Continued.

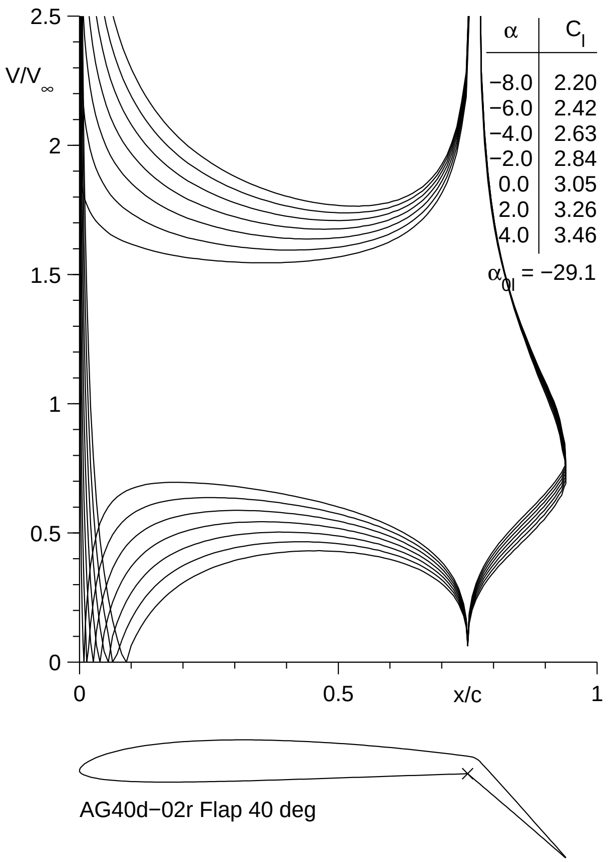

Figure 6.71: Inviscid velocity distributions for the AG40d-02r with a 40 deg flap.

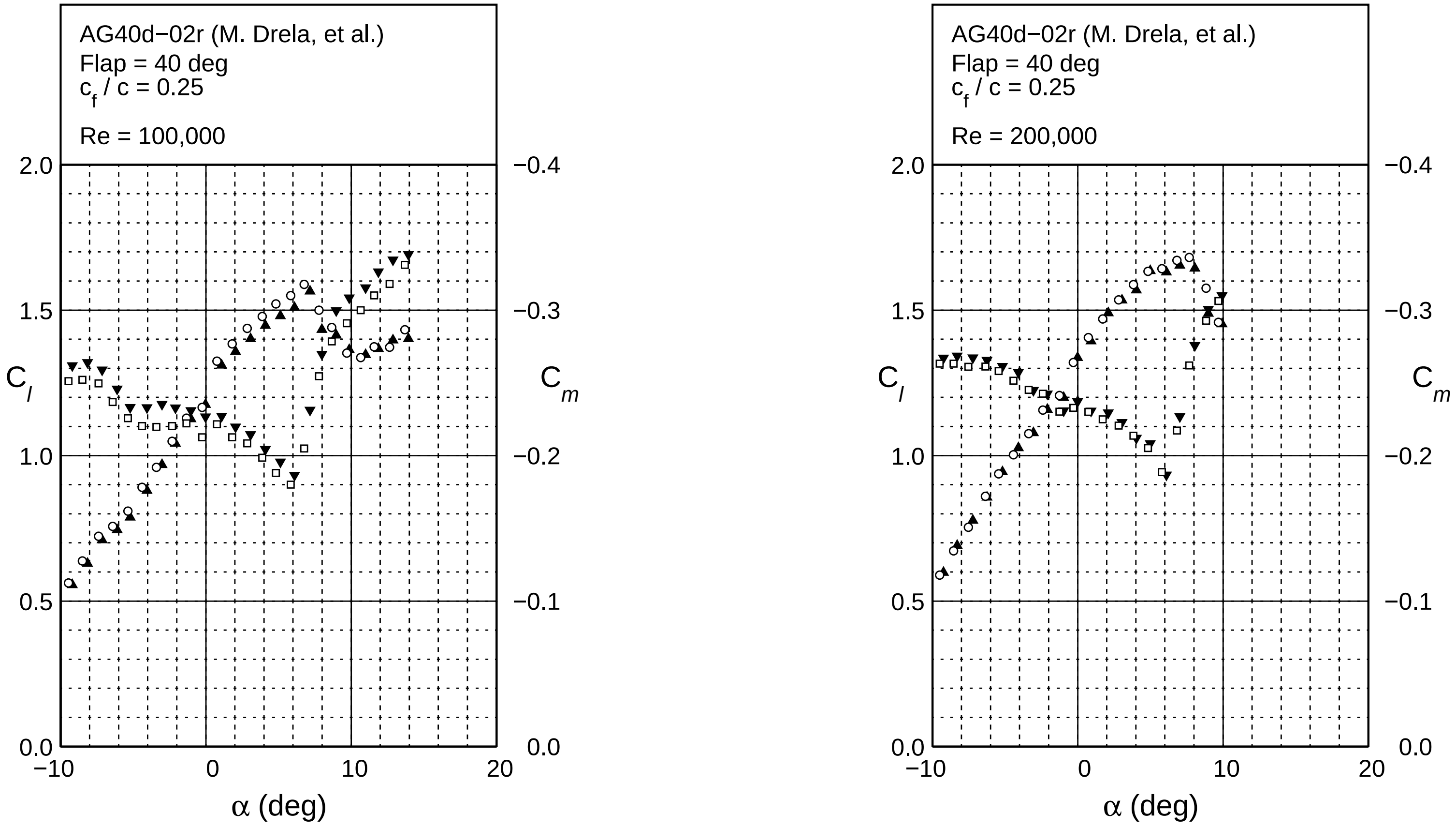

Figure 6.72: Lift and moment characteristics for the AG40d-02r with a 40 deg flap.

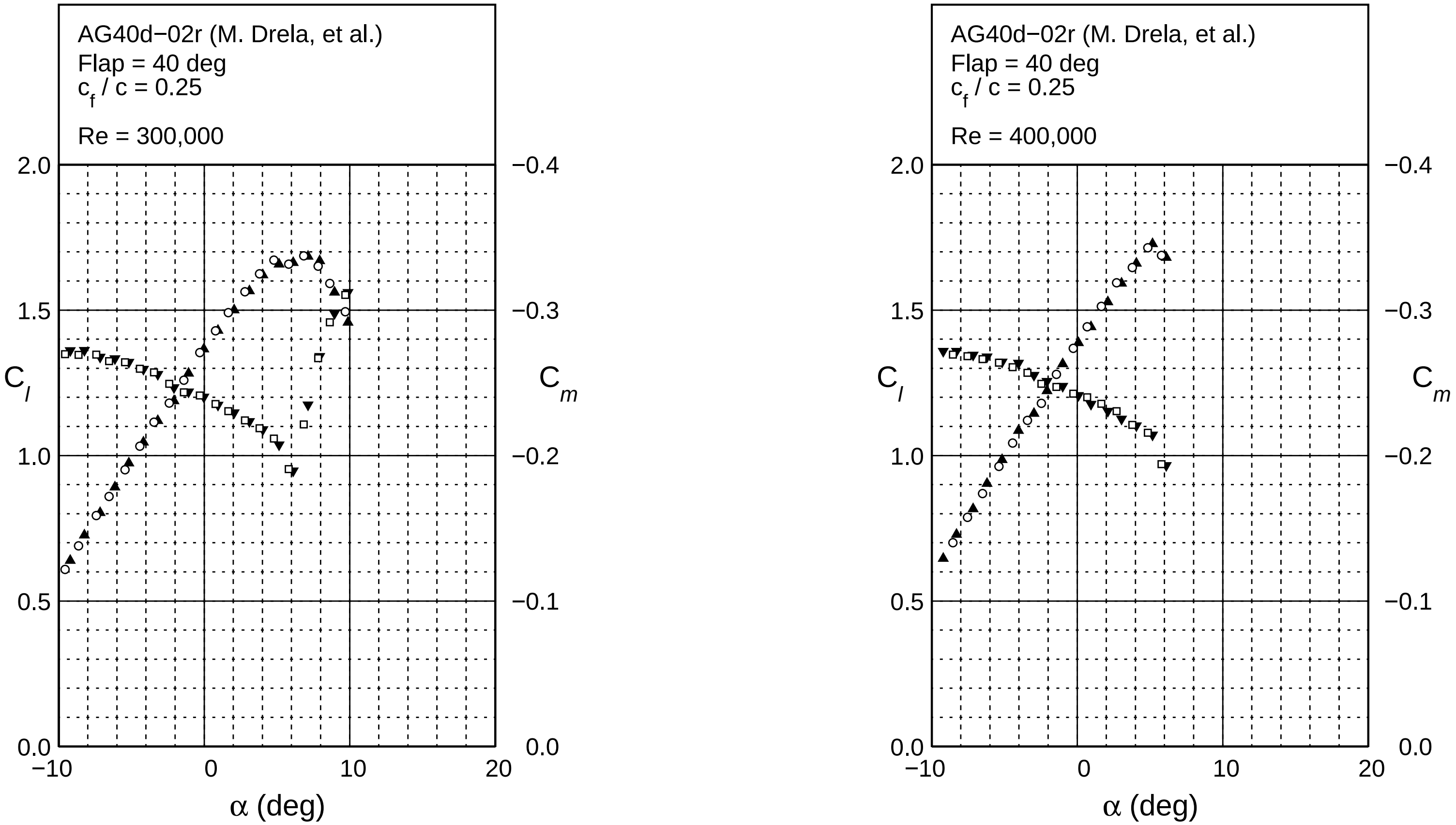

Figure 6.72: Continued.

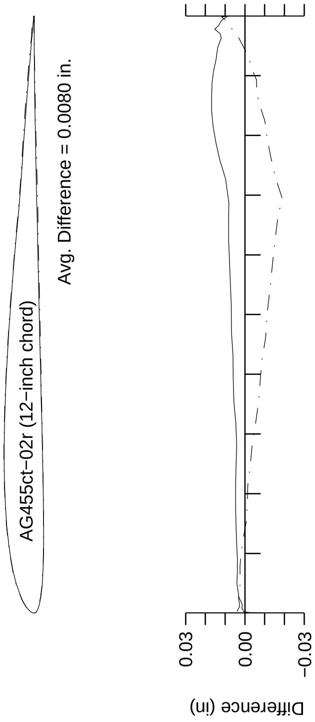

Figure 6.73: Comparison between the true and actual AG455ct-02r.

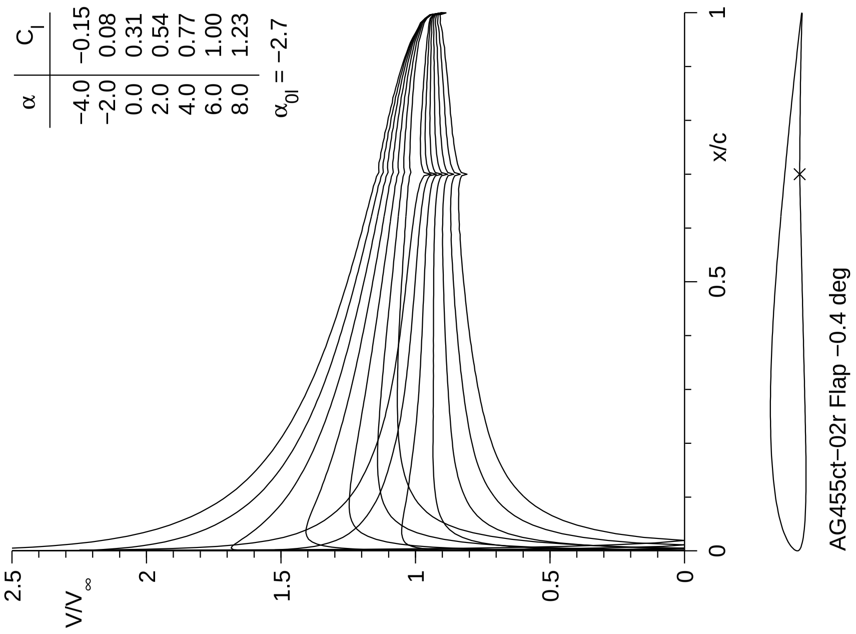

Figure 6.74: Inviscid velocity distributions for the AG455ct-02r with a −0.4 deg flap.

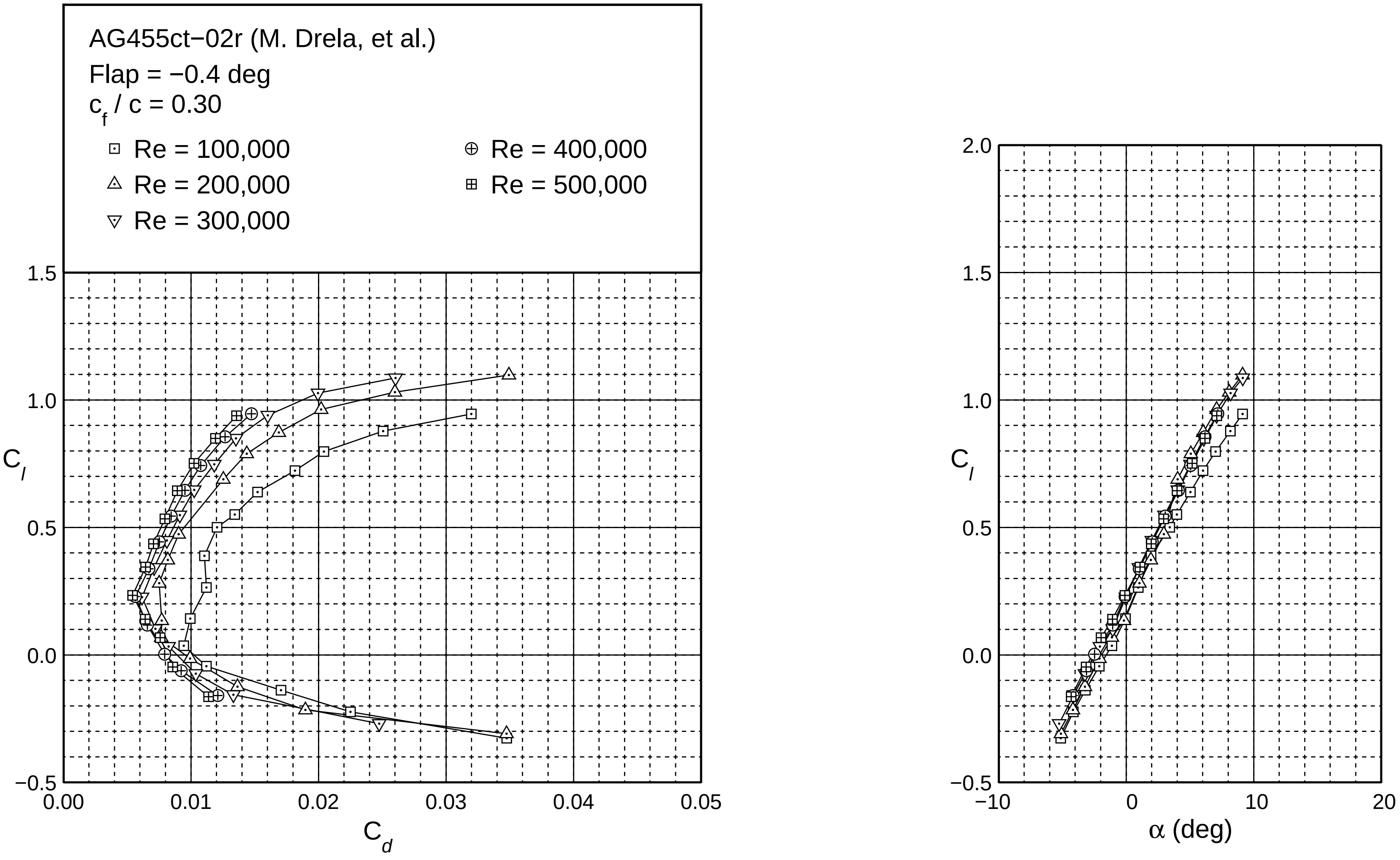

Figure 6.75: Drag polar for the AG455ct-02r with a −0.4 deg flap.

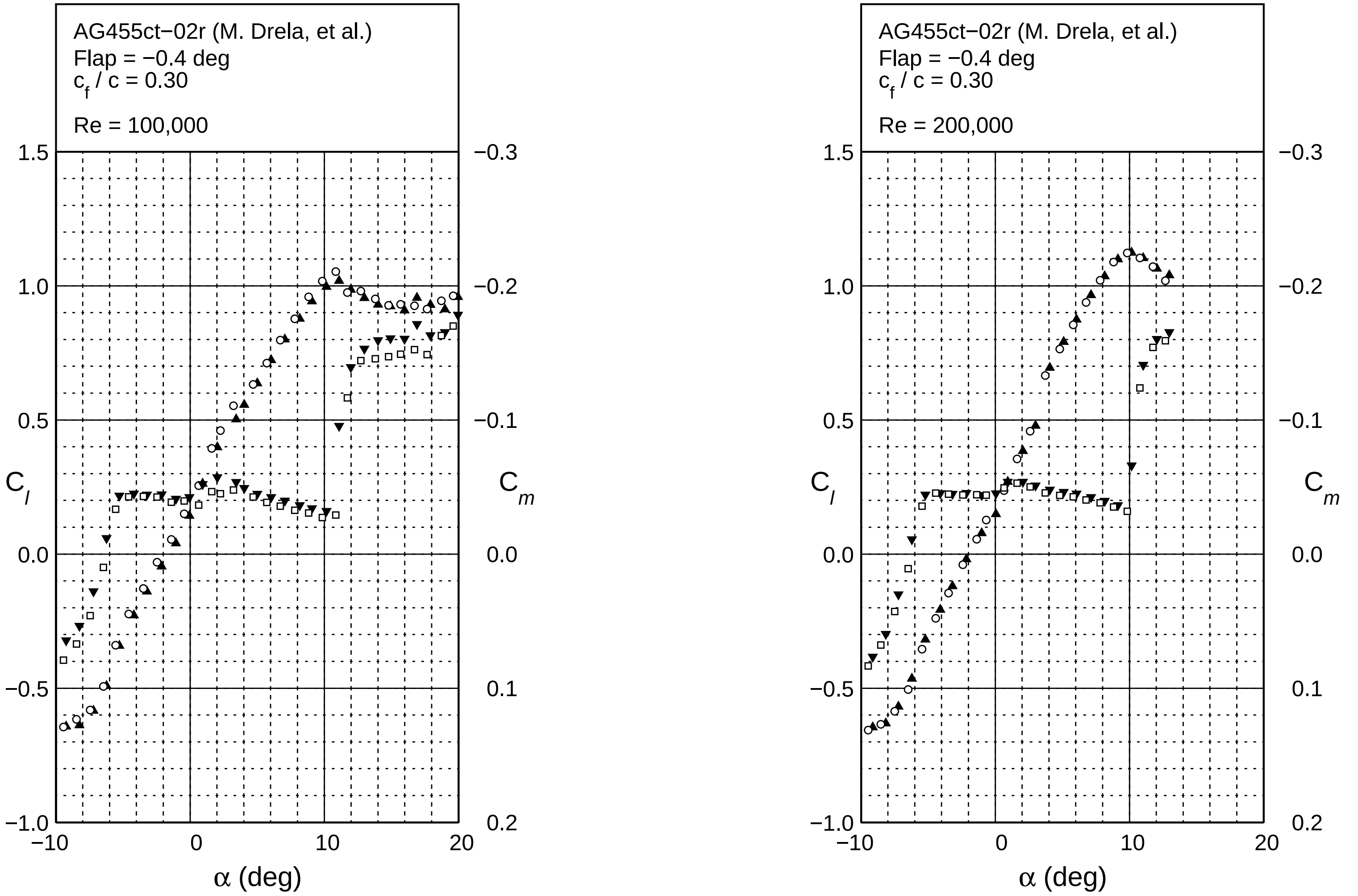

Figure 6.76: Lift and moment characteristics for the AG455ct-02r with a −0.4 deg flap.

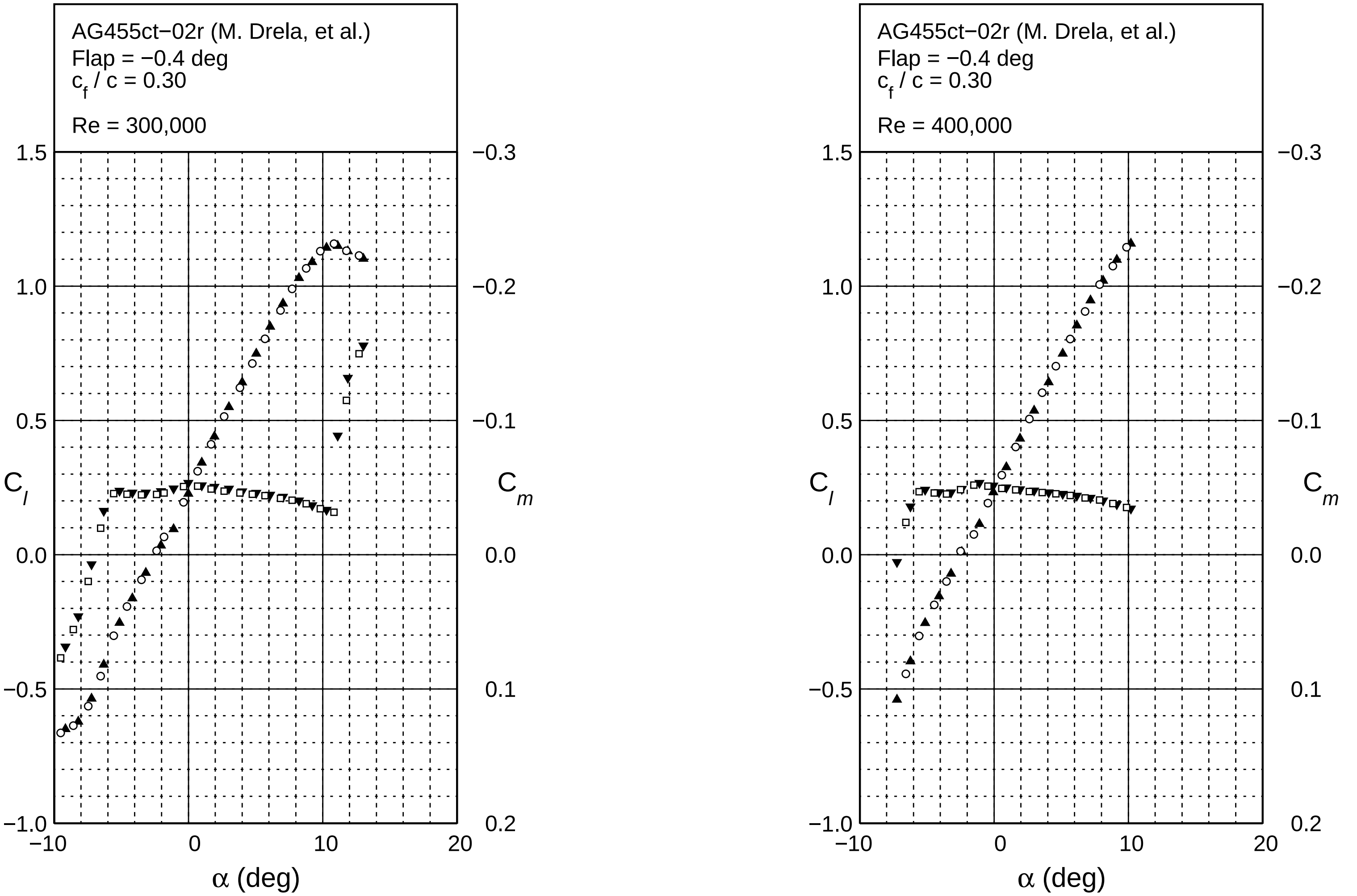

Figure 6.76: Continued.

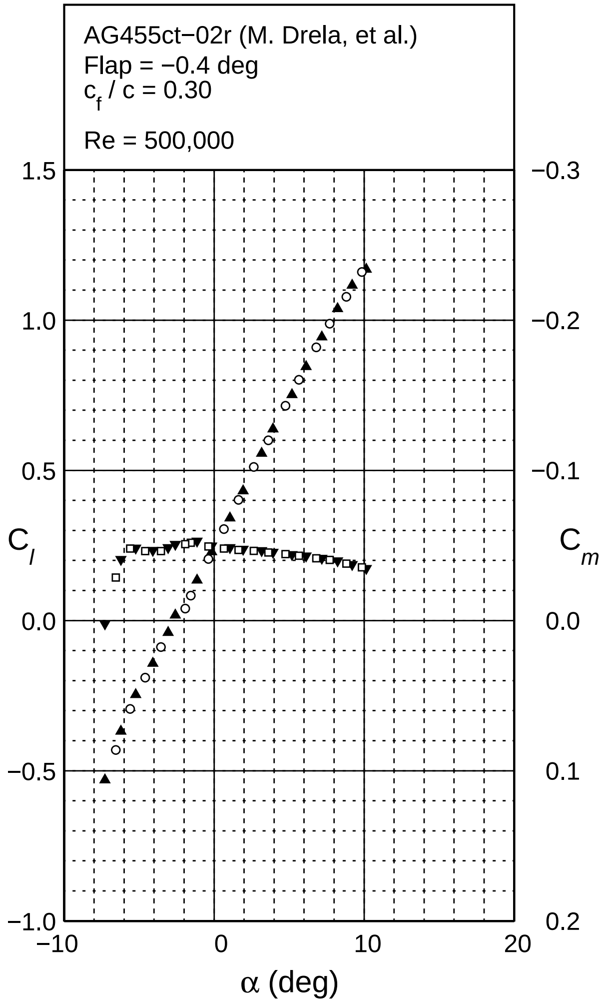

Figure 6.76: Continued.

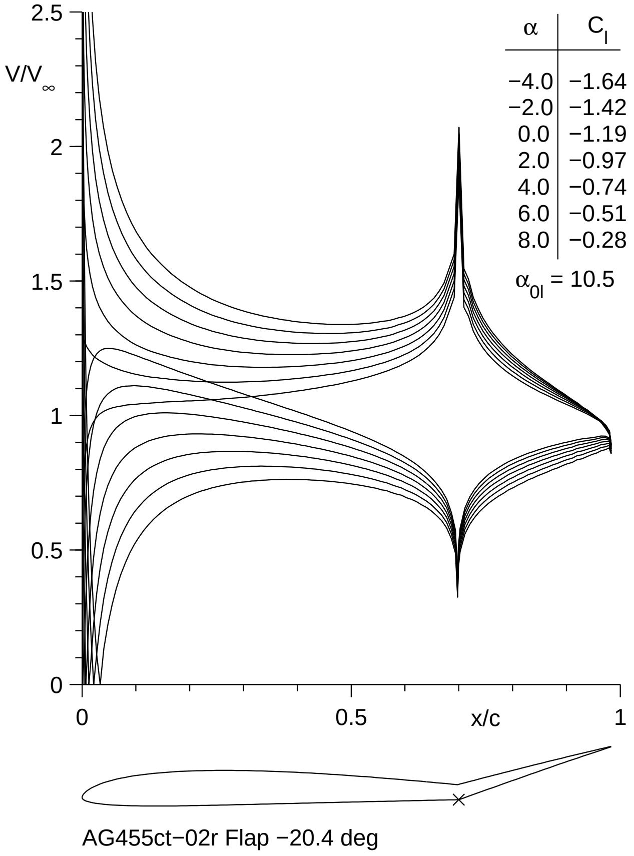

Figure 6.77: Inviscid velocity distributions for the AG455ct-02r with a −20.4 deg flap.

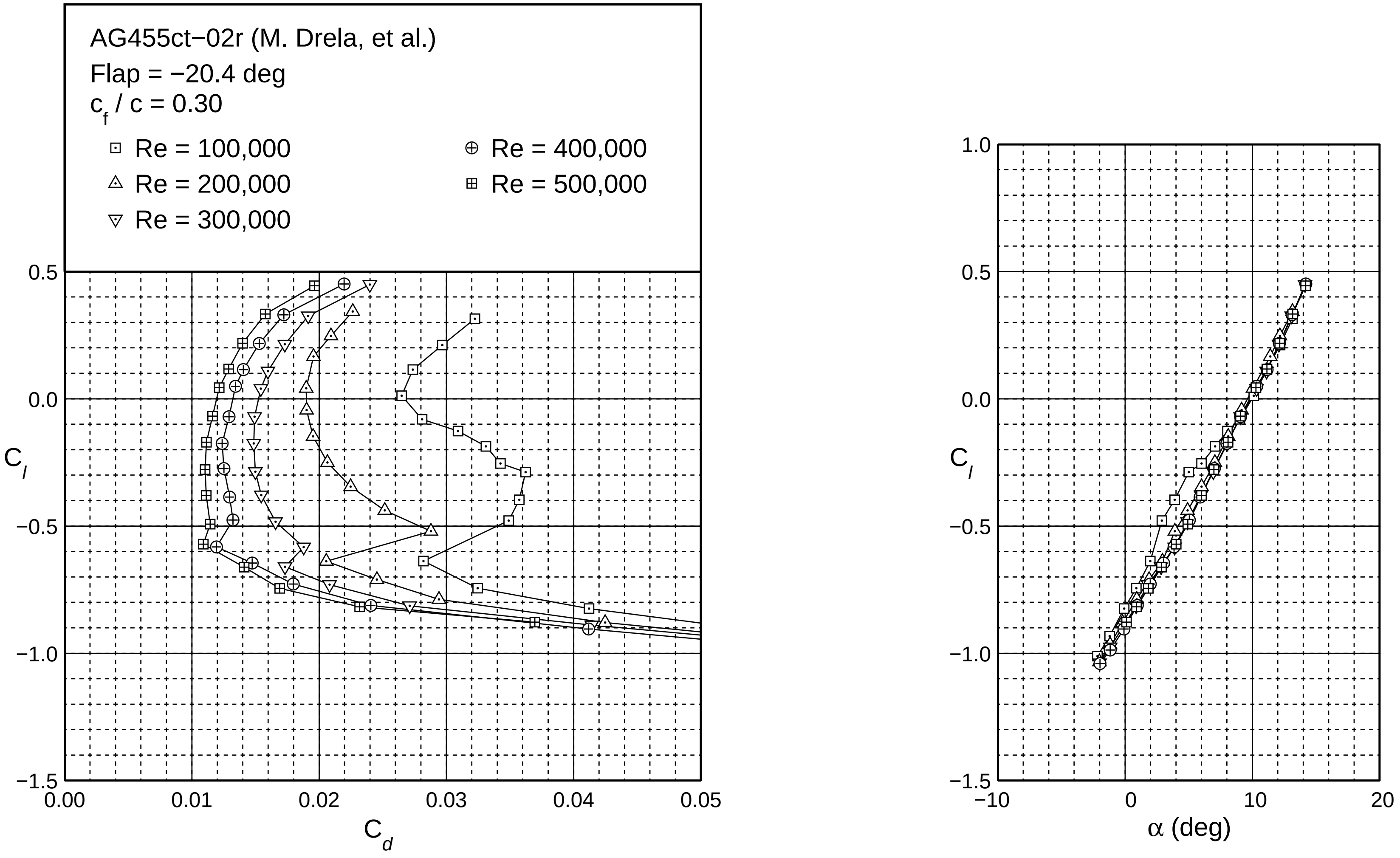

Figure 6.78: Drag polar for the AG455ct-02r with a −20.4 deg flap.

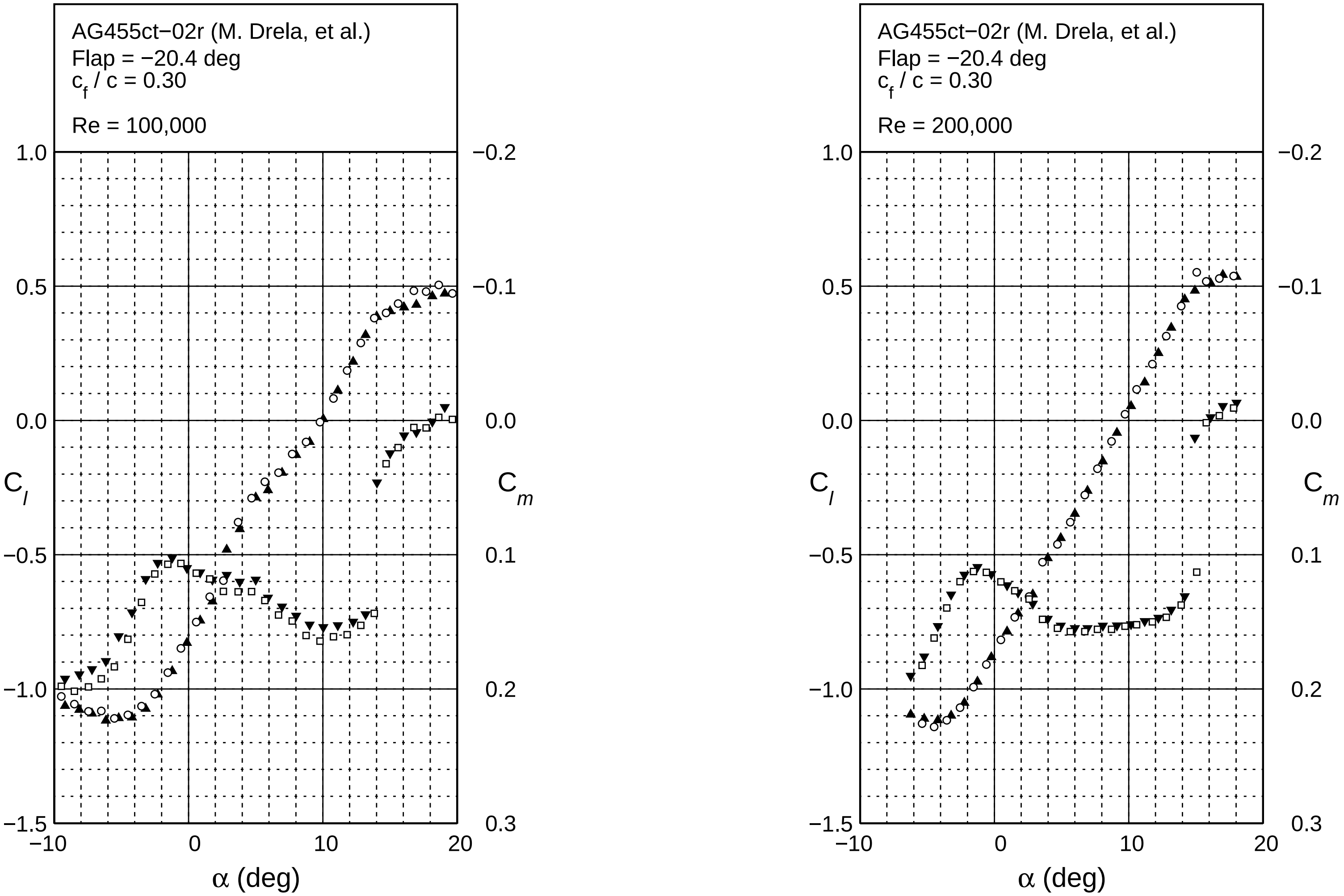

Figure 6.79: Lift and moment characteristics for the AG455ct-02r with a −20.4 deg flap.

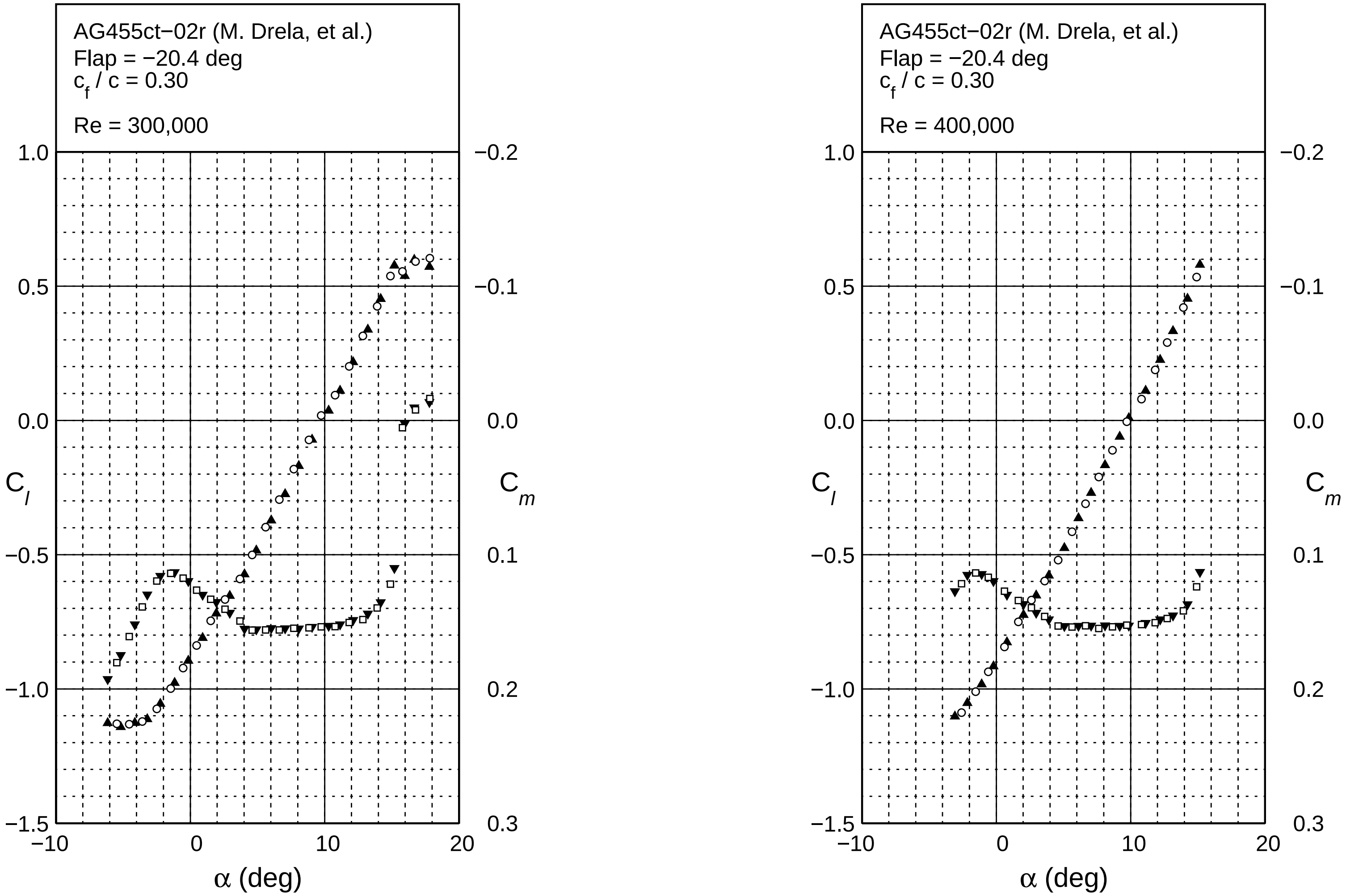

Figure 6.79: Continued.

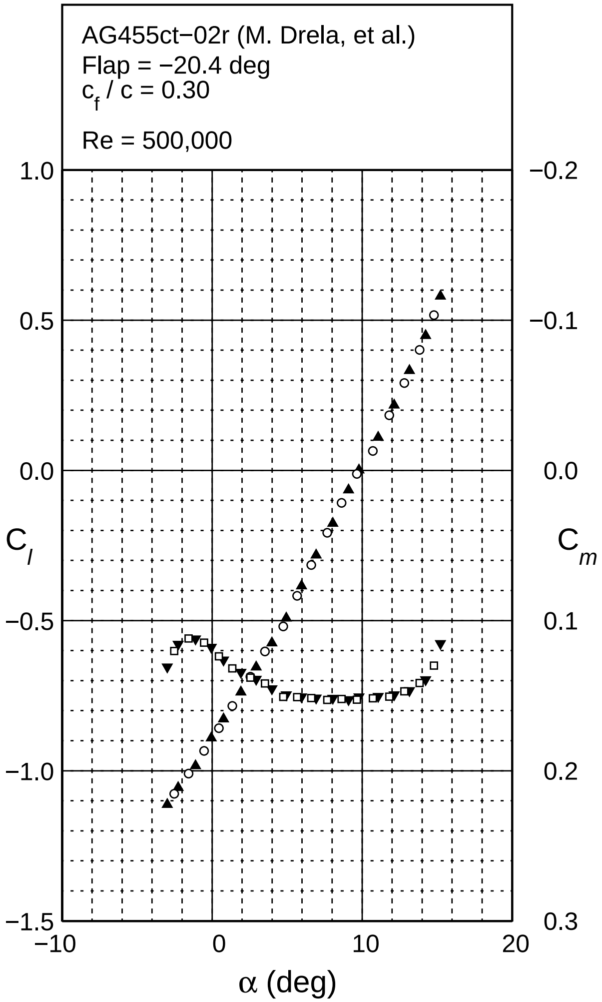

Figure 6.79: Continued.

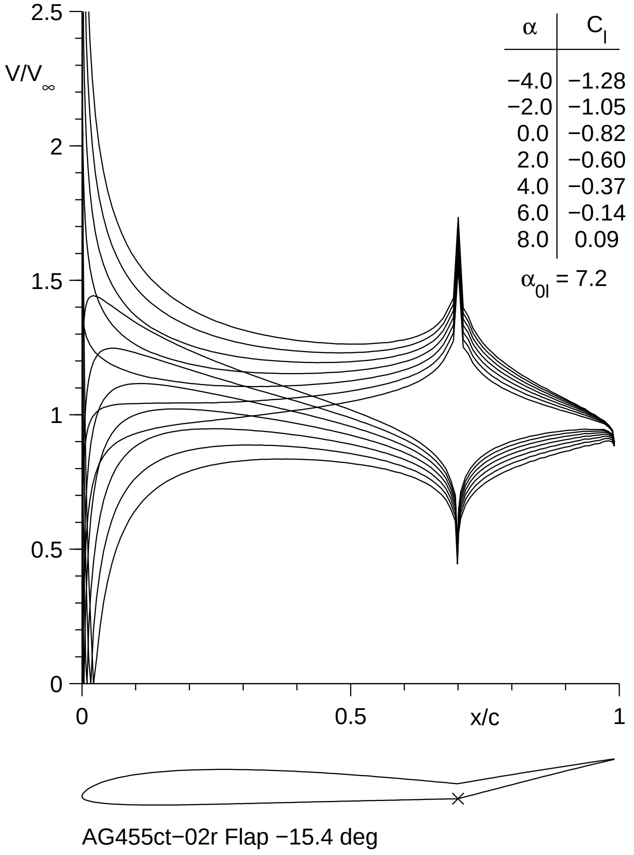

Figure 6.80: Inviscid velocity distributions for the AG455ct-02r with a −15.4 deg flap.

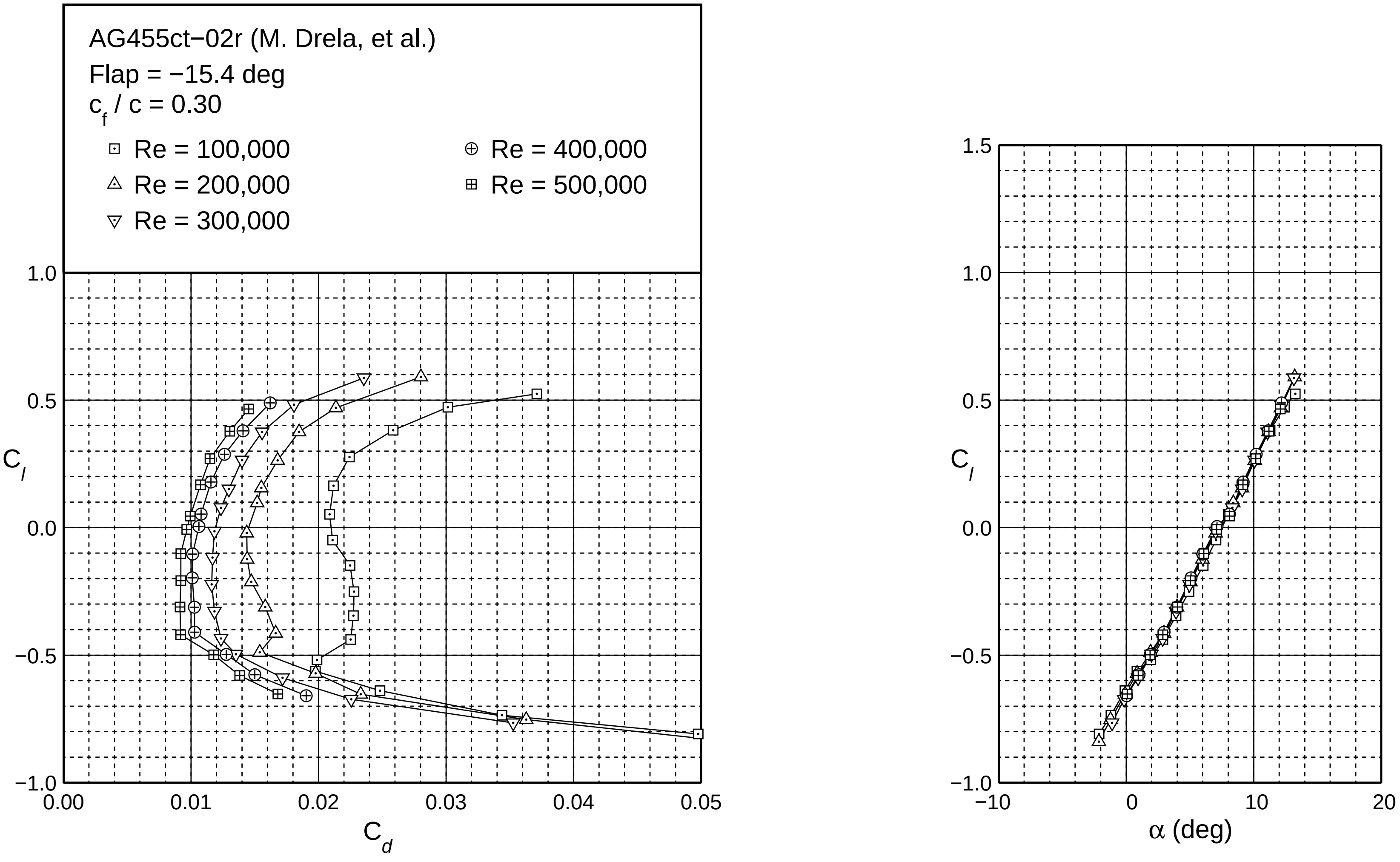

Figure 6.81: Drag polar for the AG455ct-02r with a −15.4 deg flap.

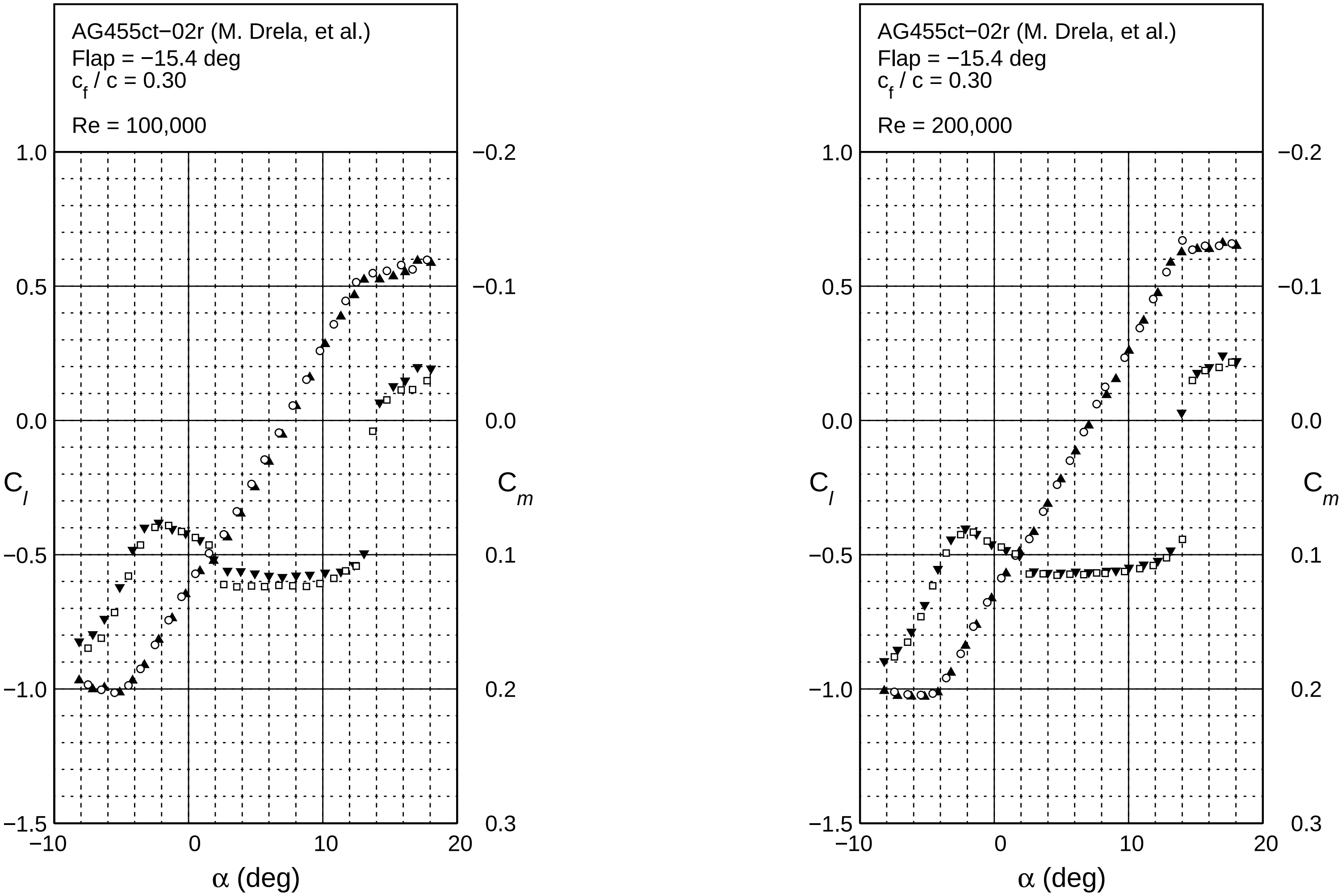

Figure 6.82: Lift and moment characteristics for the AG455ct-02r with a − 15.4 deg flap.

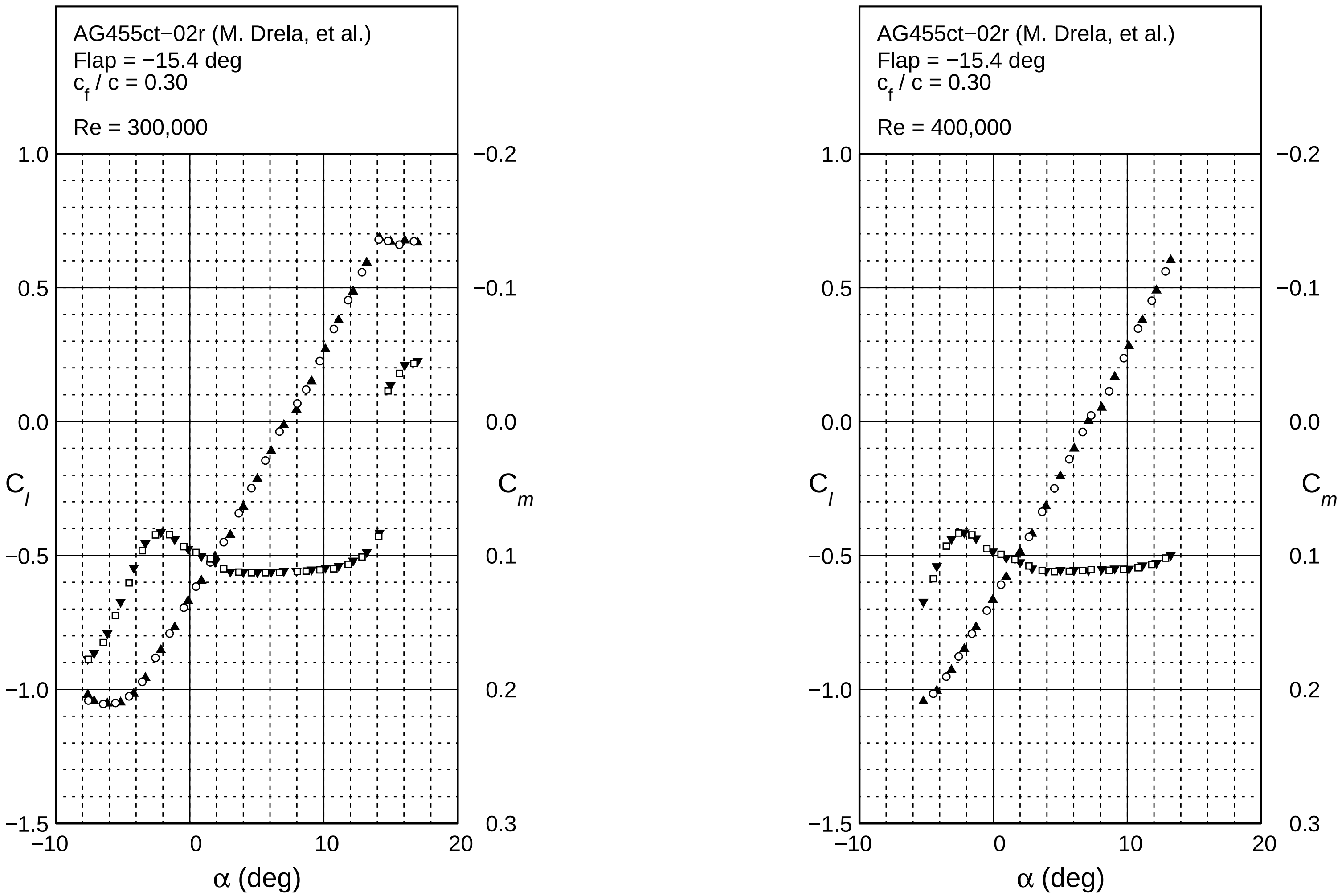

Figure 6.82: Continued.

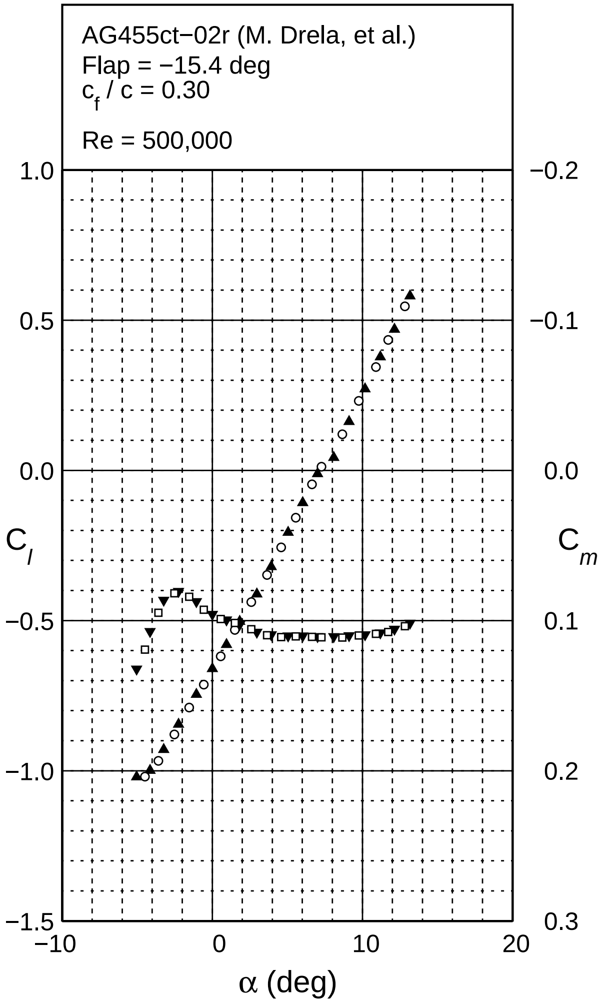

Figure 6.82: Continued.

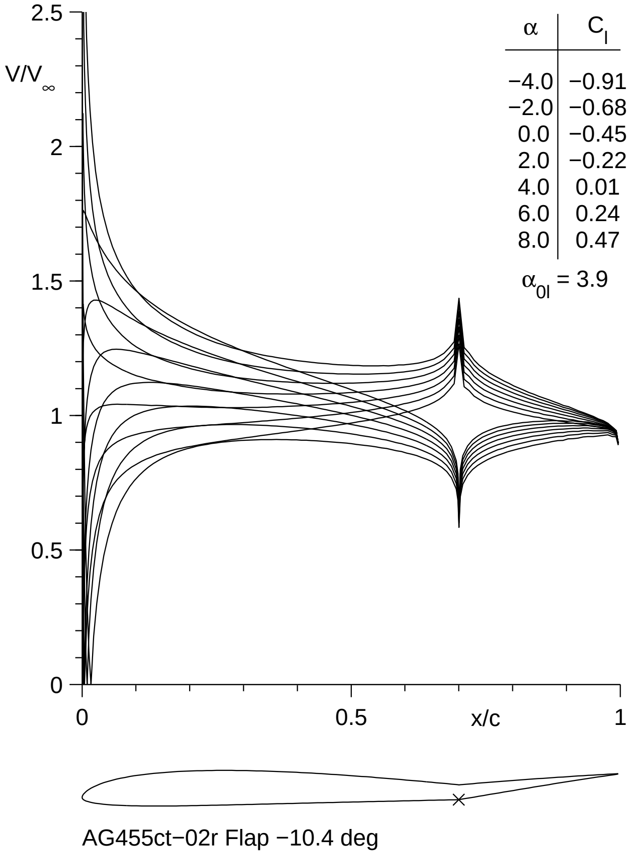

Figure 6.83: Inviscid velocity distributions for the AG455ct-02r with a −10.4 deg flap.

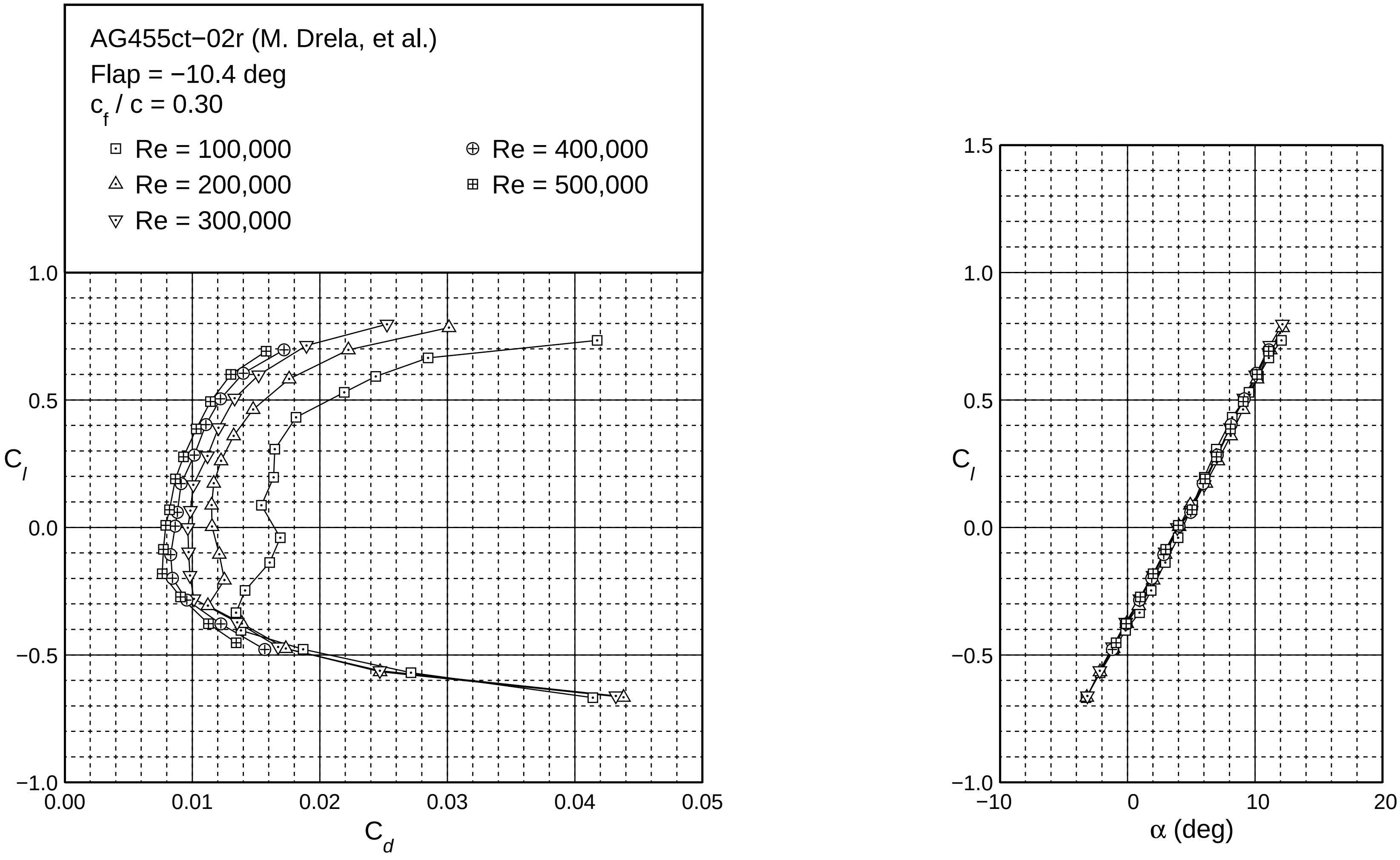

Figure 6.84: Drag polar for the AG455ct-02r with a −10.4 deg flap.

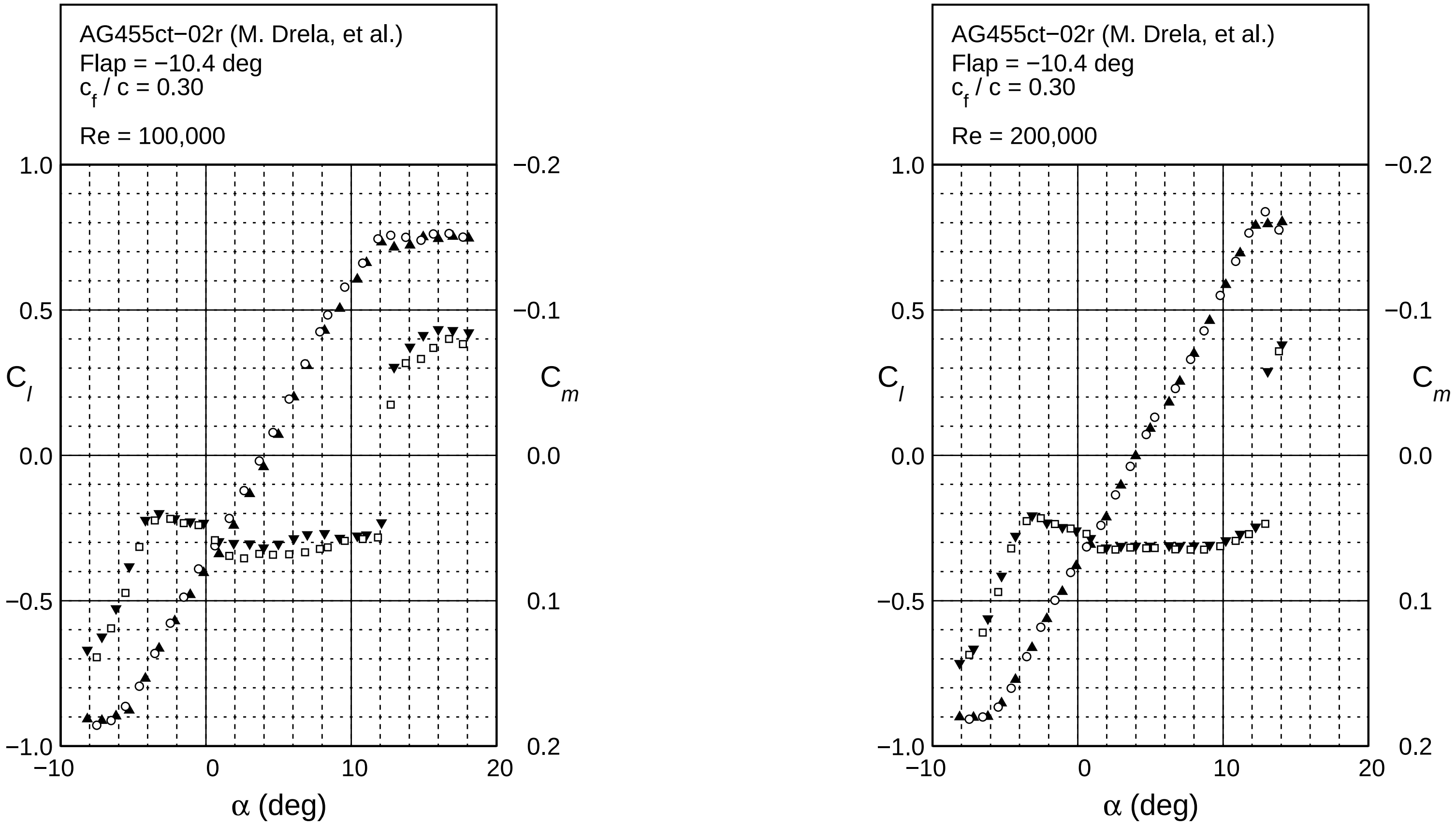

Figure 6.85: Lift and moment characteristics for the AG455ct-02r with a −10.4 deg flap.

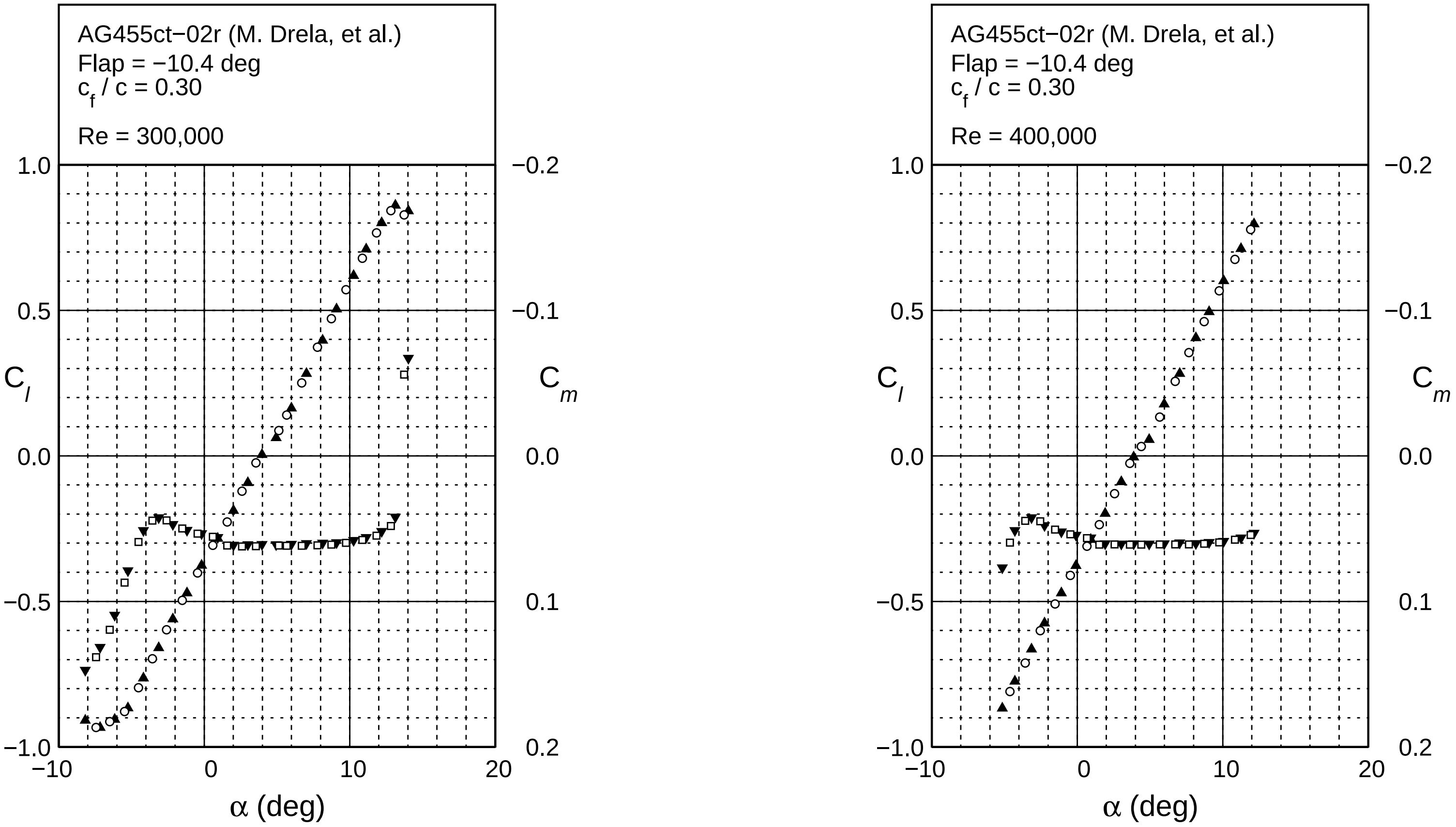

Figure 6.85: Continued.

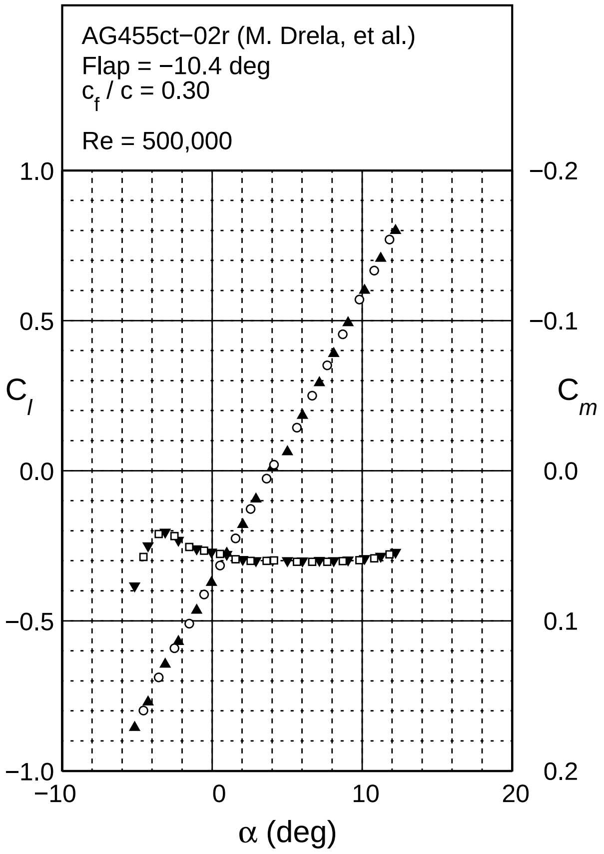

Figure 6.85: Continued.

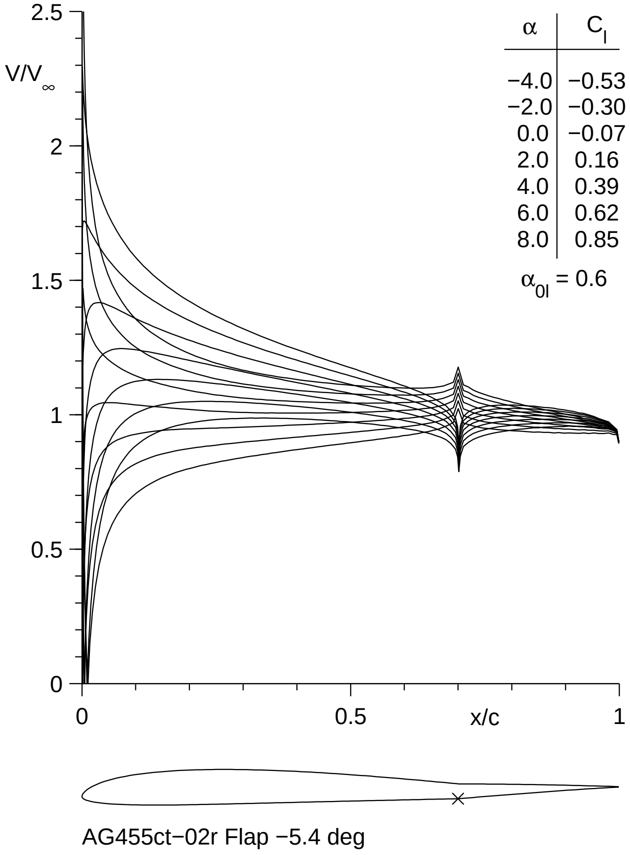

Figure 6.86: Inviscid velocity distributions for the AG455ct-02r with a −5.4 deg flap.

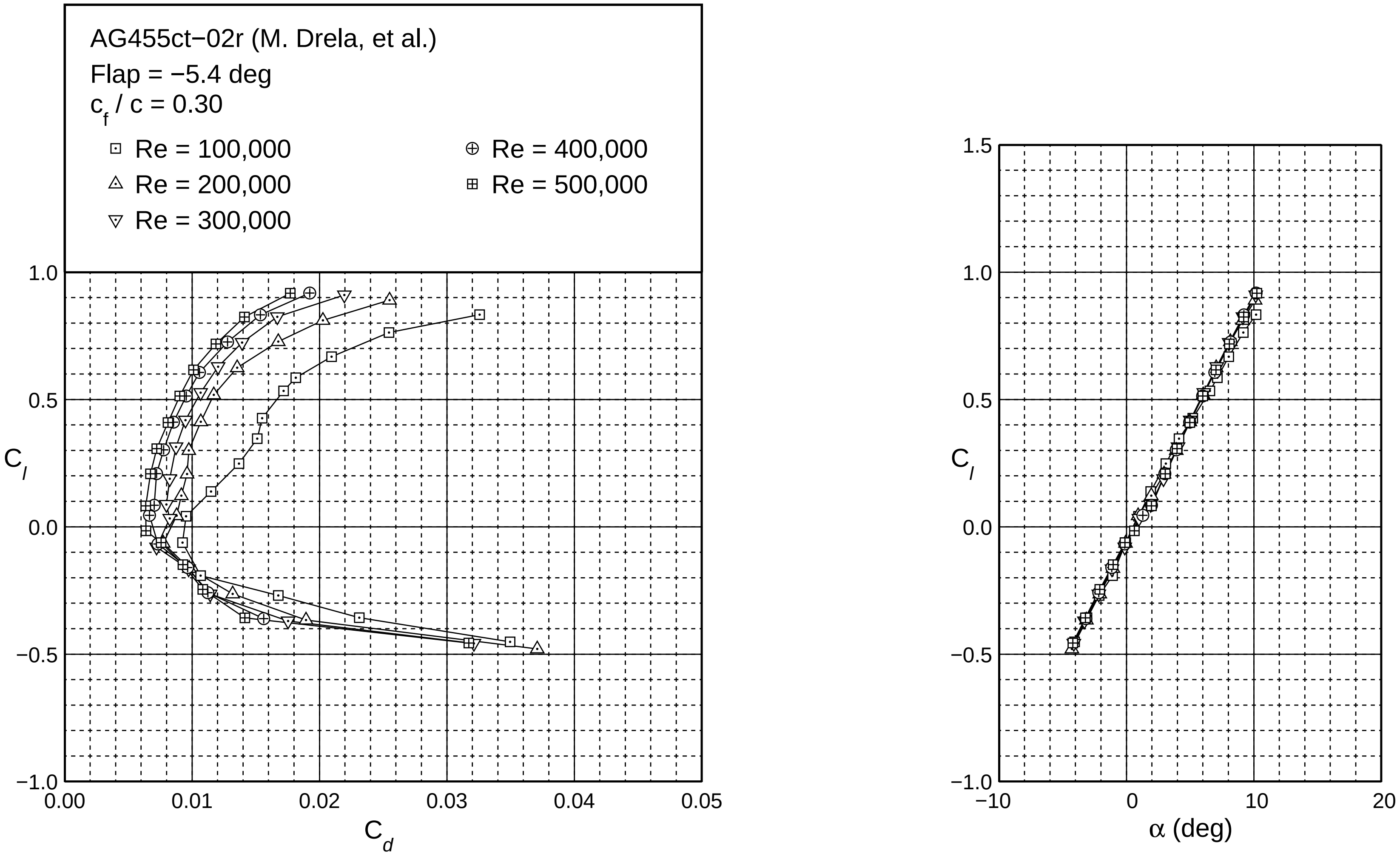

Figure 6.87: Drag polar for the AG455ct-02r with a −5.4 deg flap.

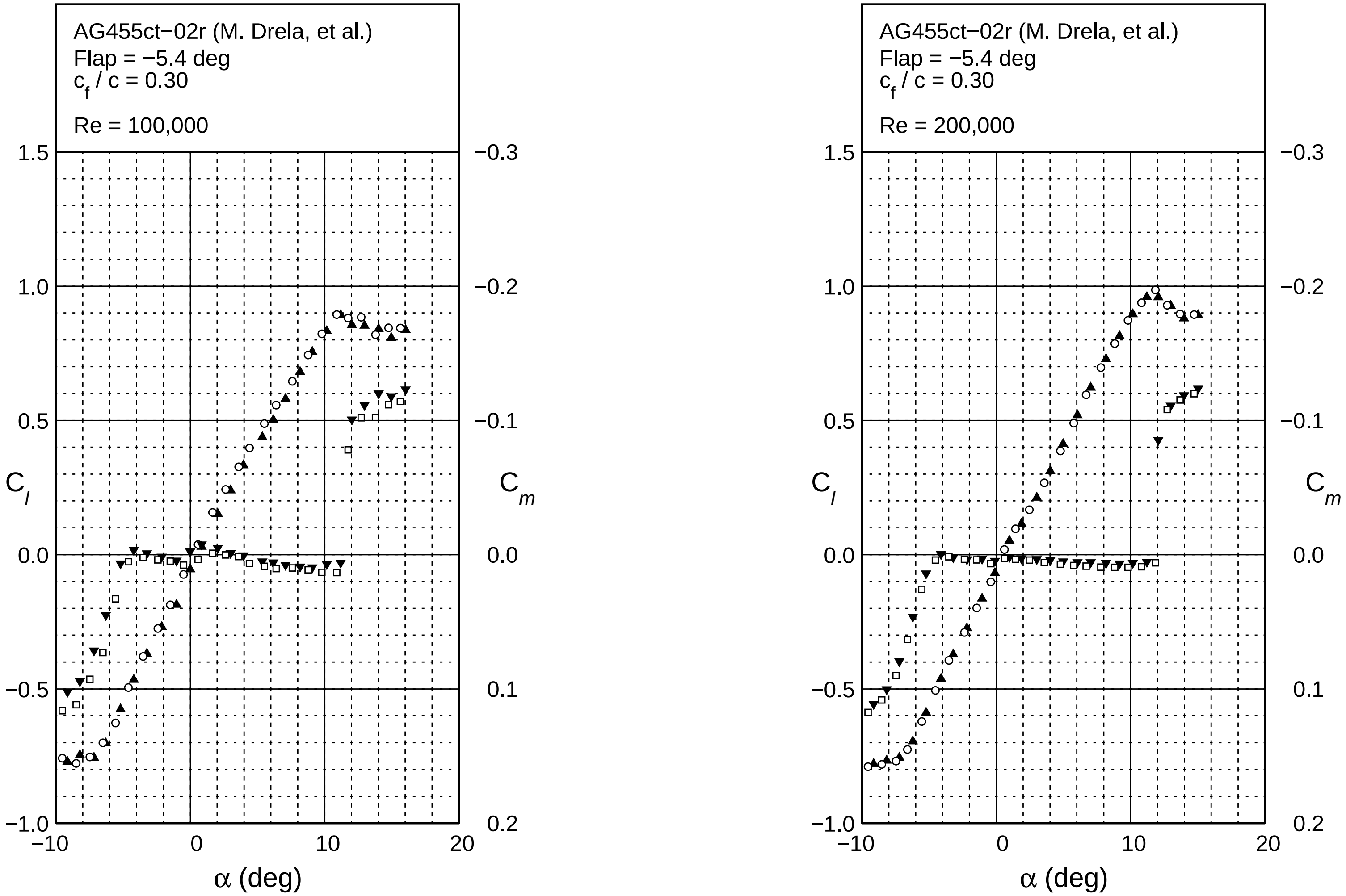

Figure 6.88: Lift and moment characteristics for the AG455ct-02r with a −5.4 deg flap.

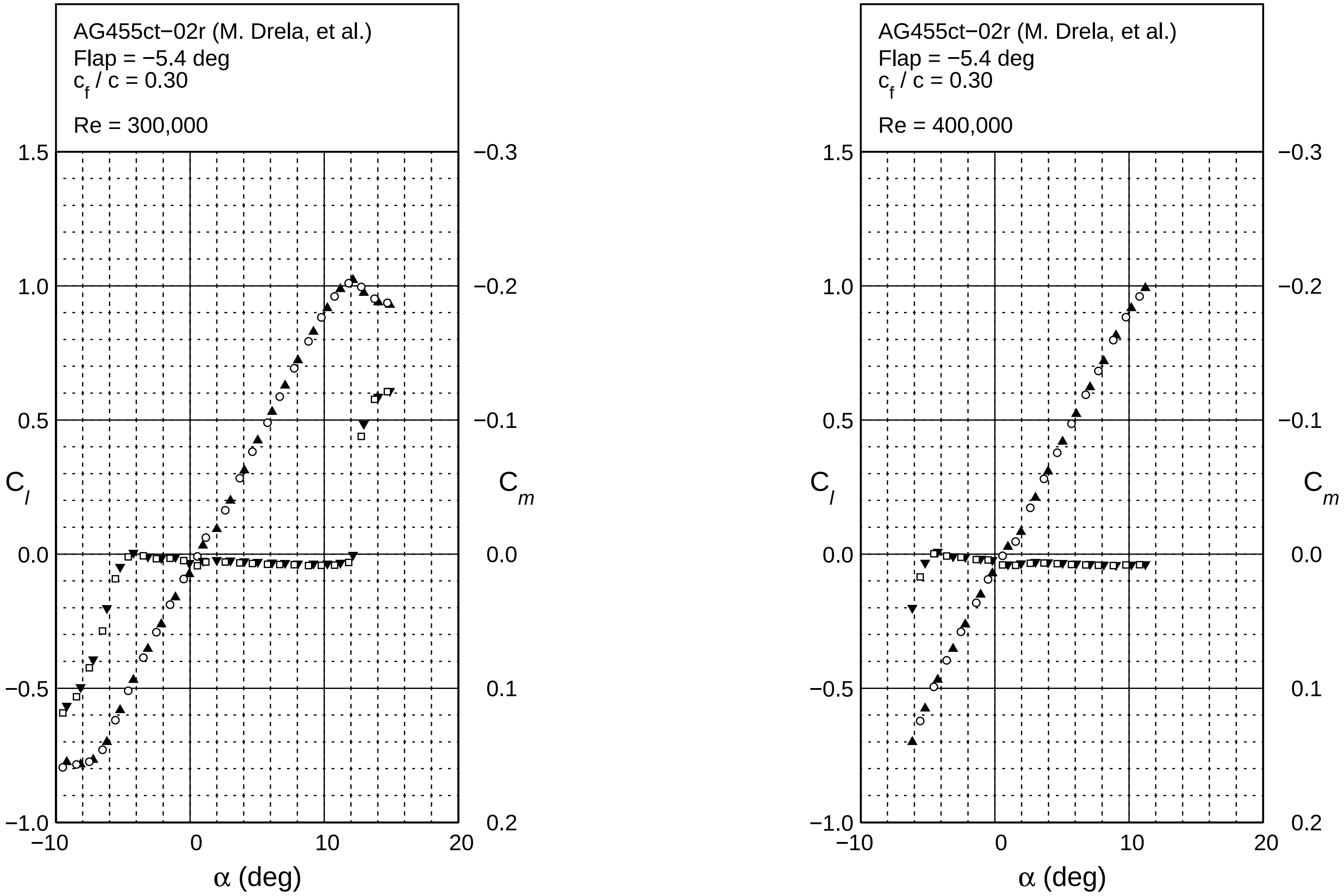

Figure 6.88: Continued.

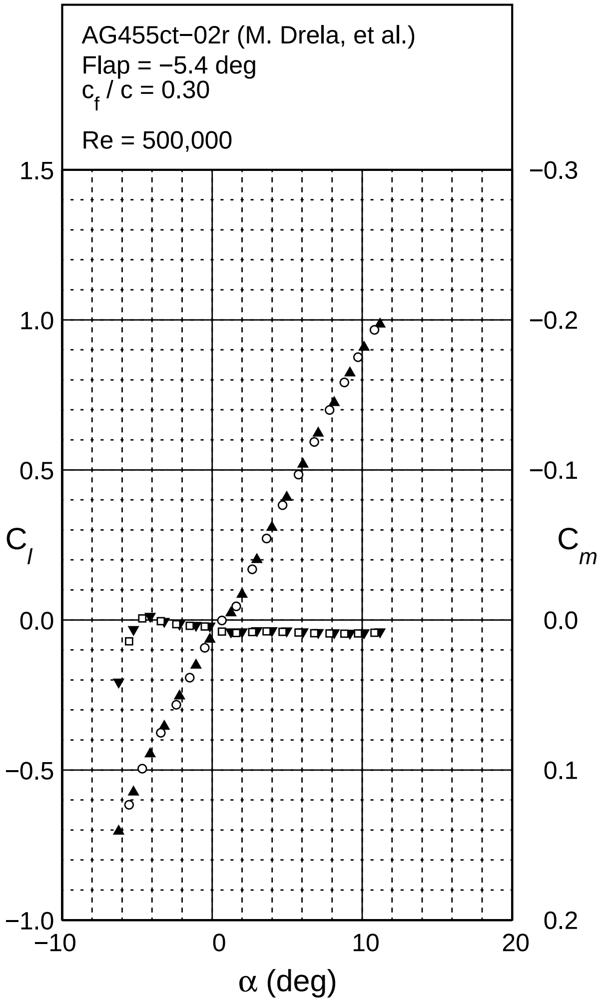

Figure 6.88: Continued.

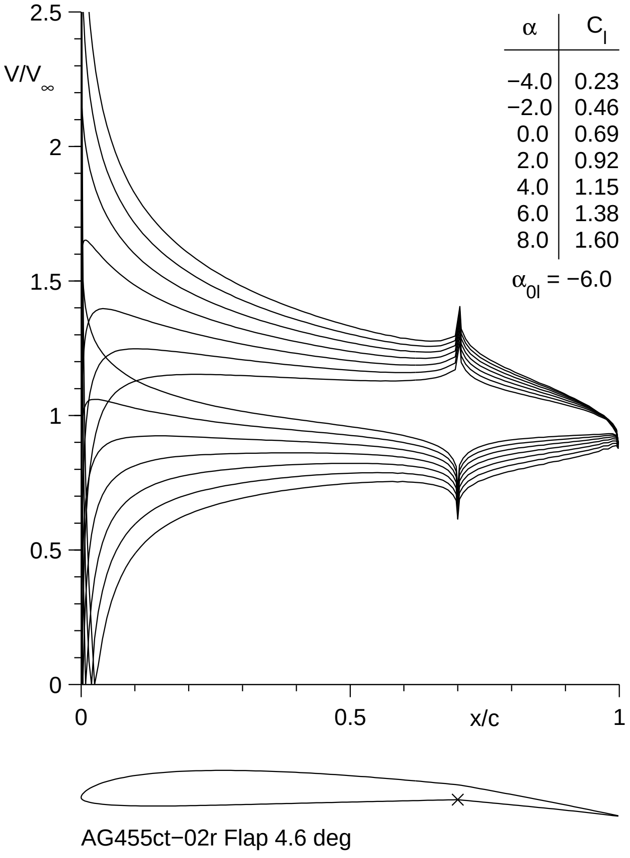

Figure 6.89: Inviscid velocity distributions for the AG455ct-02r with a 4.6 deg flap.

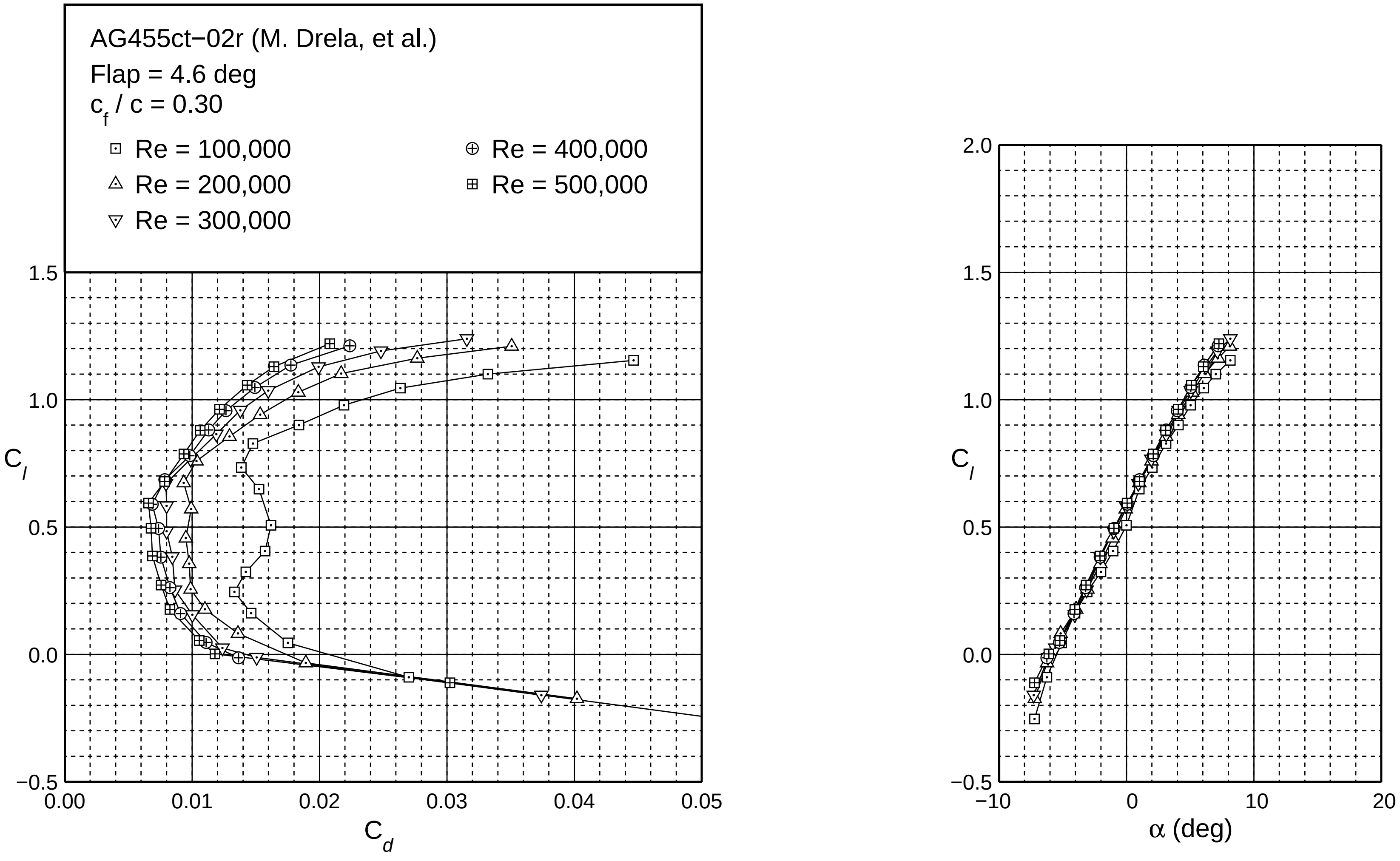

Figure 6.90: Drag polar for the AG455ct-02r with a 4.6 deg flap.

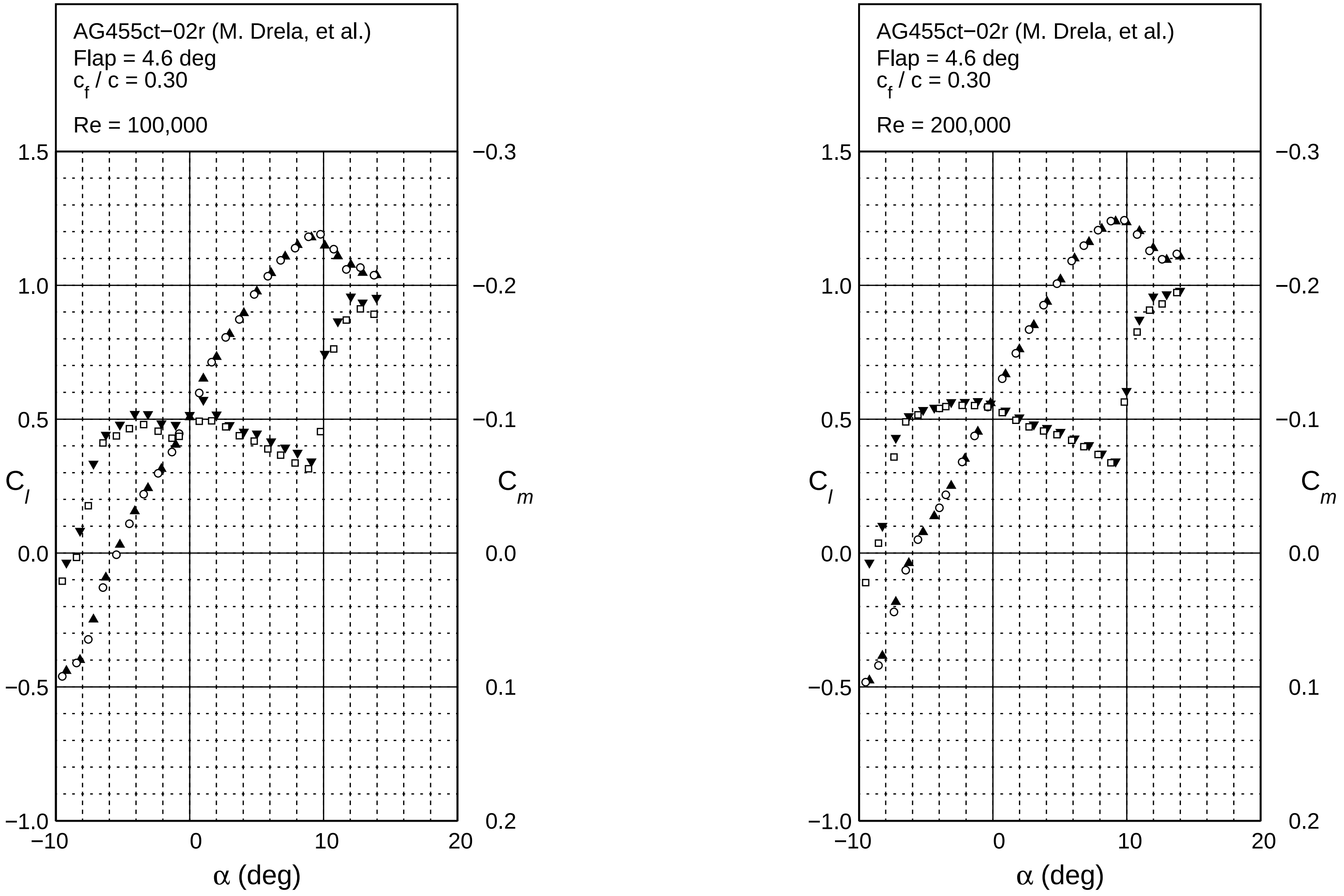

Figure 6.91: Lift and moment characteristics for the AG455ct-02r with a 4.6 deg flap.

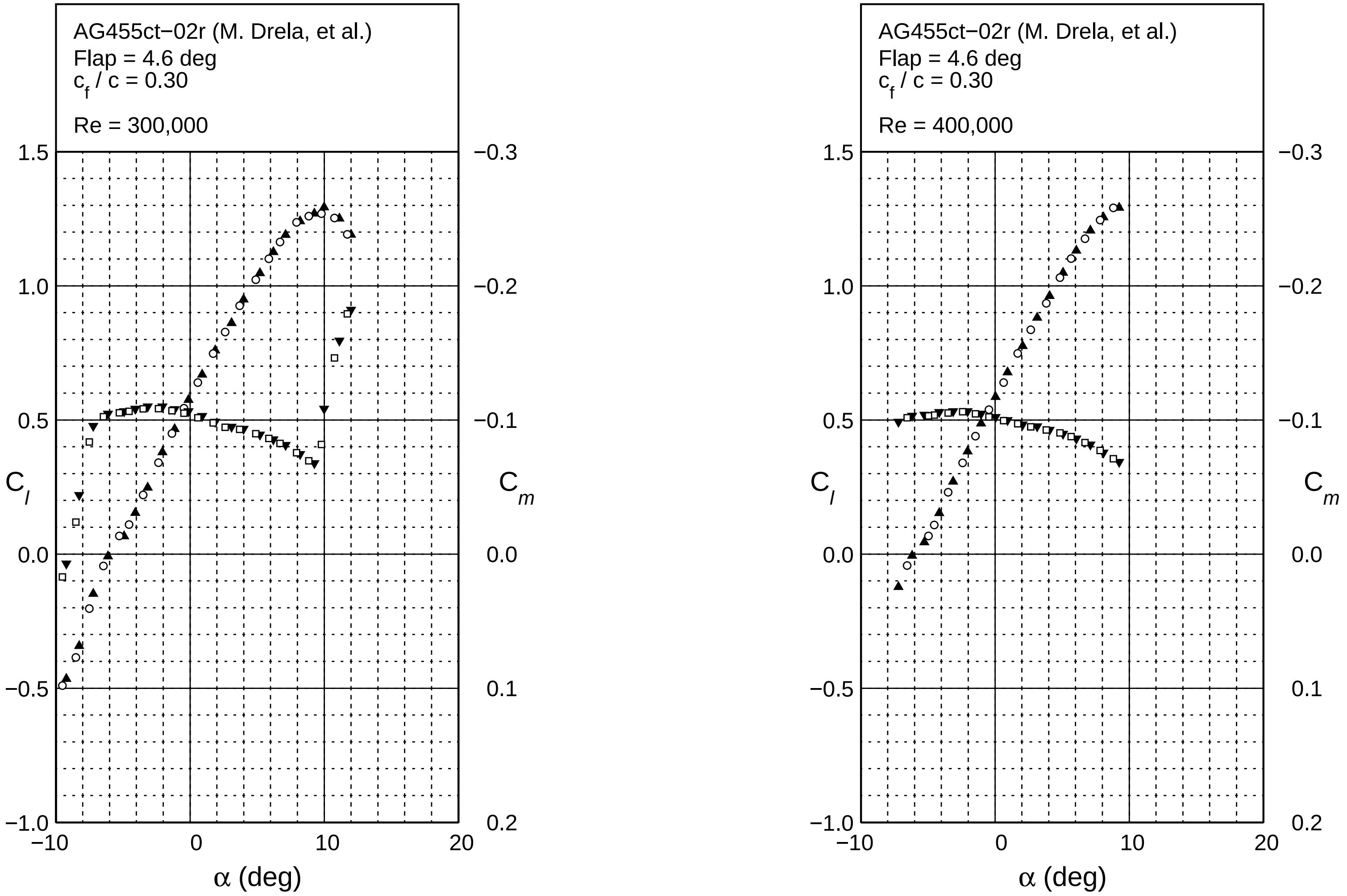

Figure 6.91: Continued.

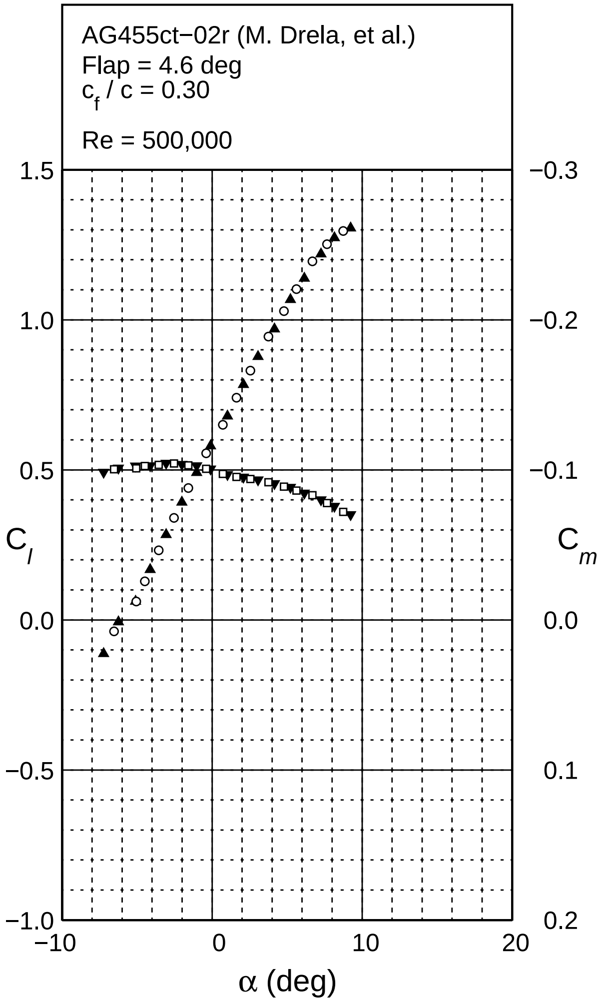

Figure 6.91: Continued.

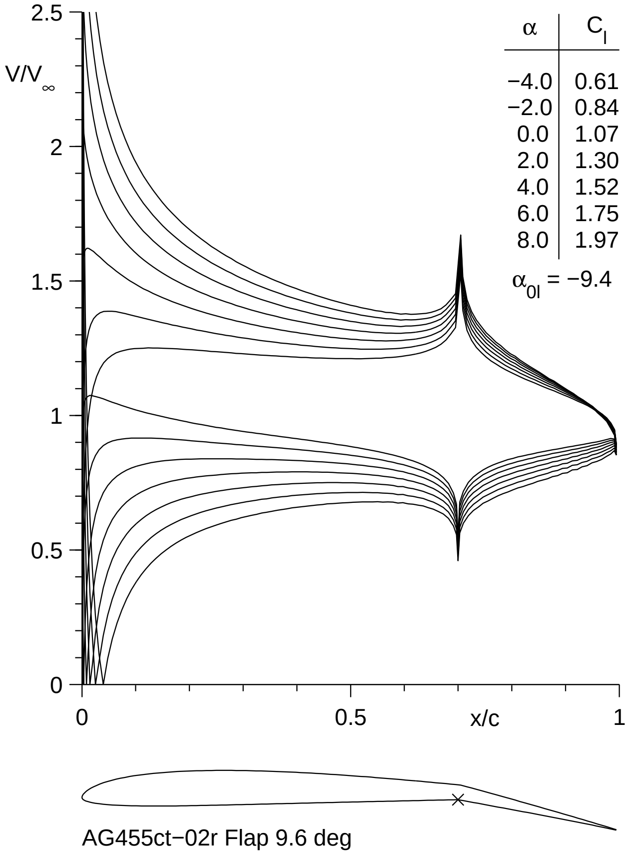

Figure 6.92: Inviscid velocity distributions for the AG455ct-02r with a 9.6 deg flap.

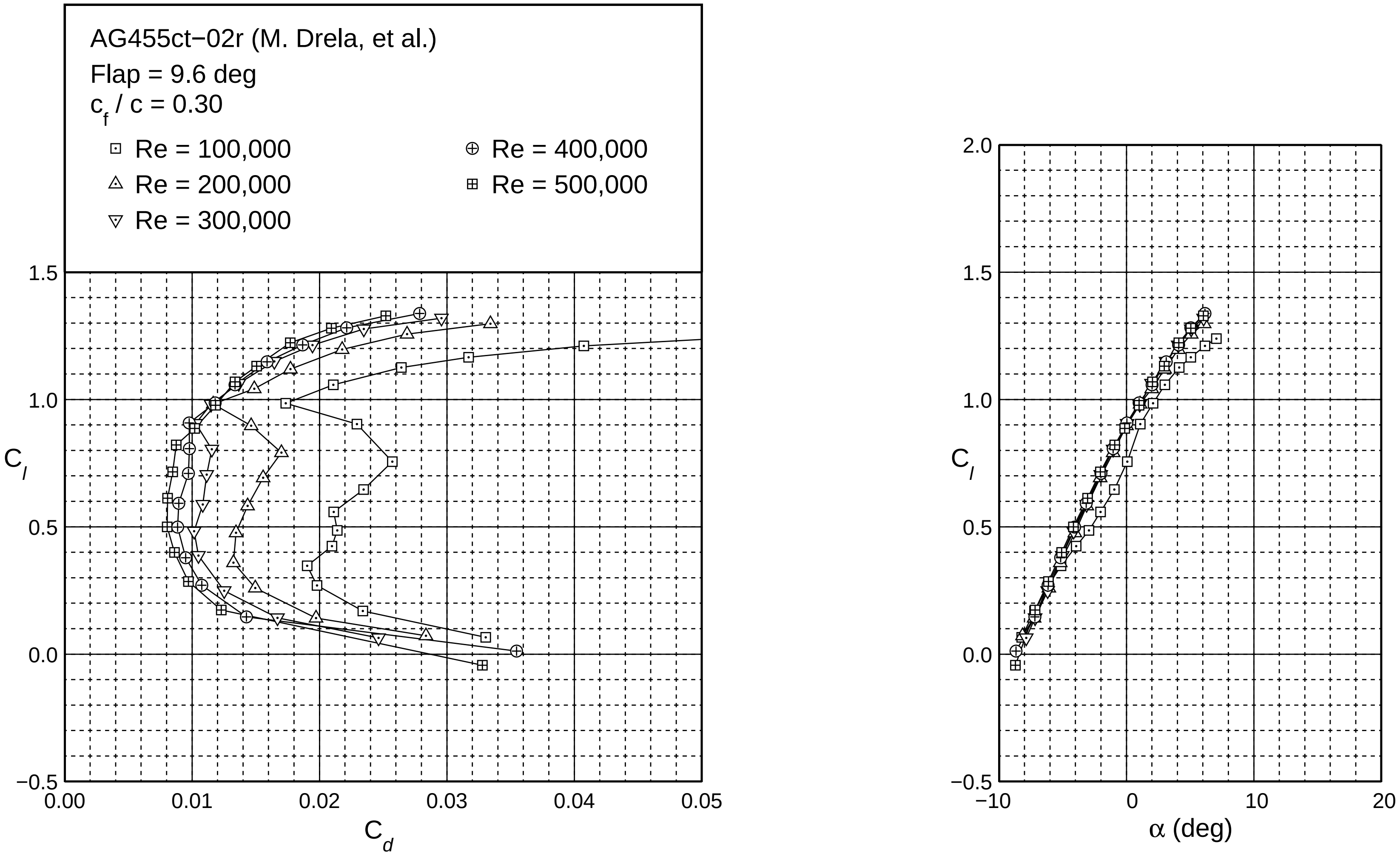

Figure 6.93: Drag polar for the AG455ct-02r with a 9.6 deg flap.

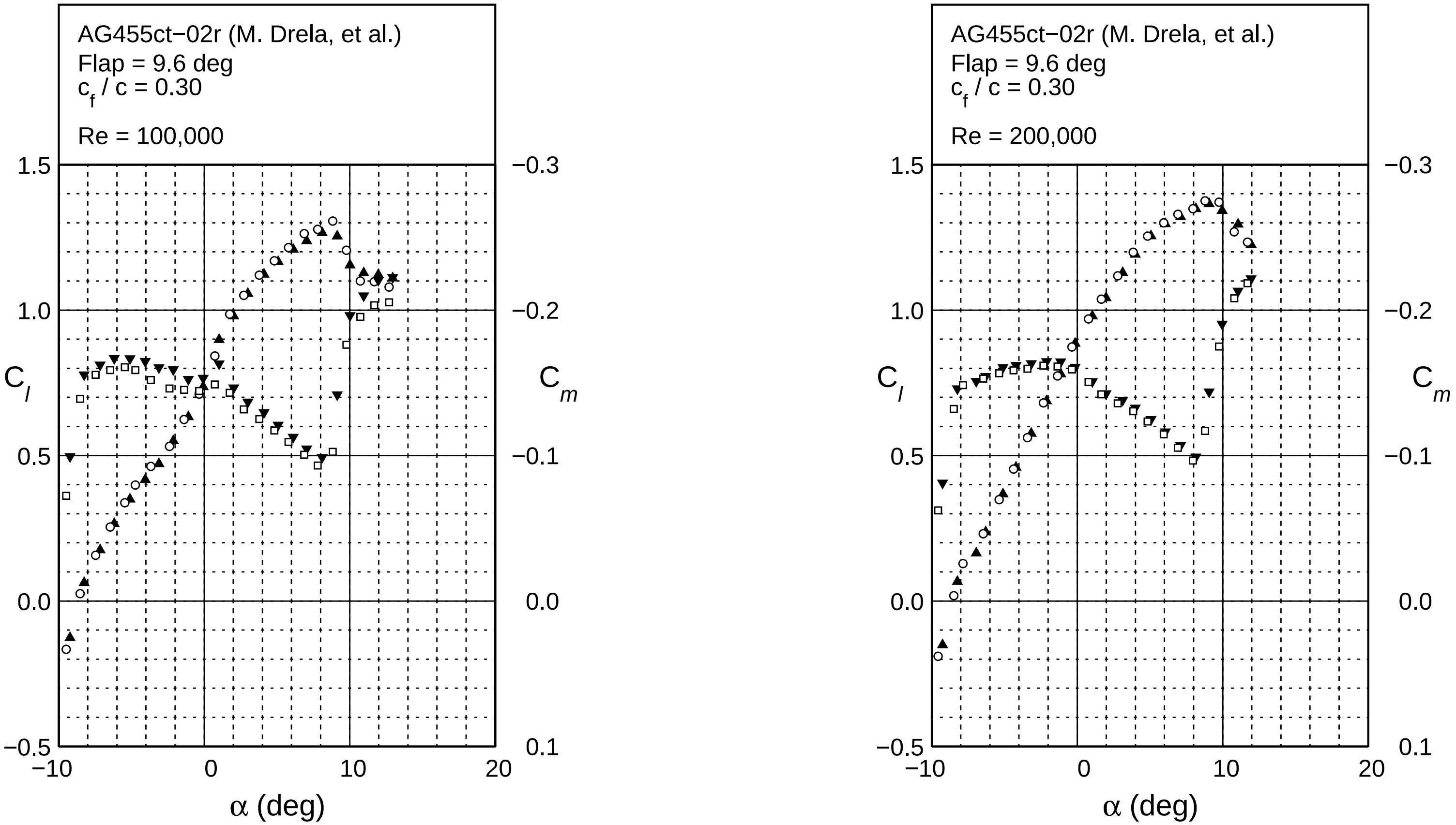

Figure 6.94: Lift and moment characteristics for the AG455ct-02r with a 9.6 deg flap.

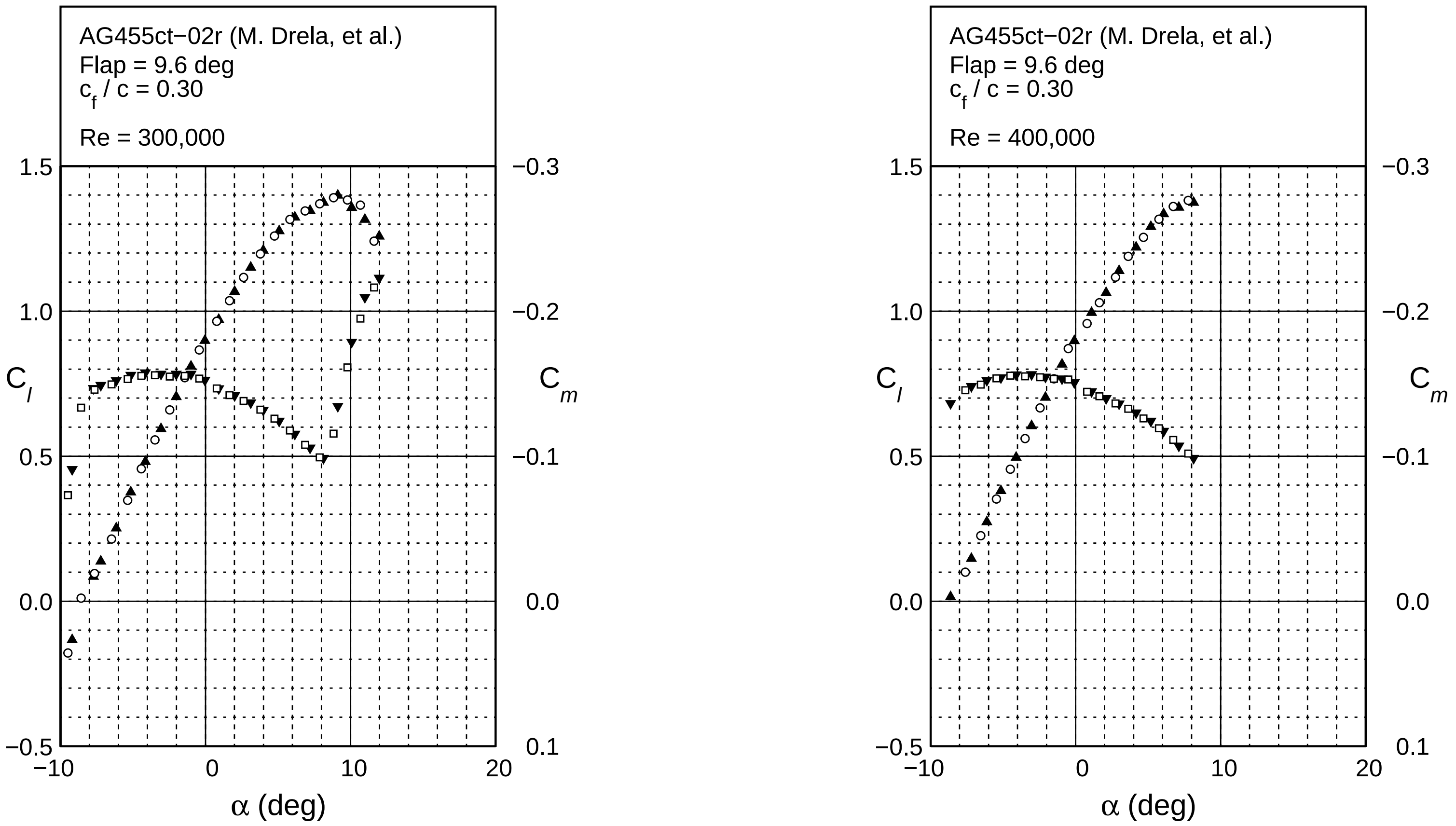

Figure 6.94: Continued.

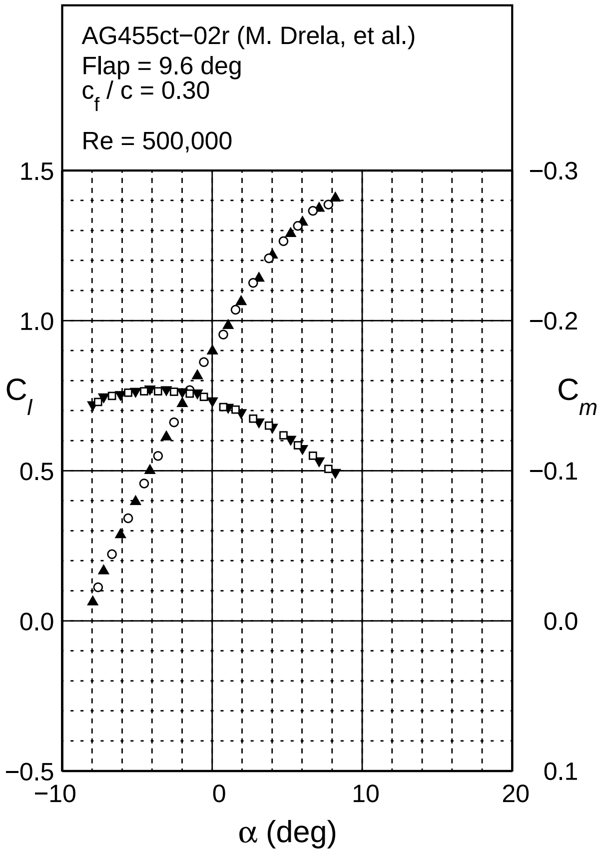

Figure 6.94: Continued.

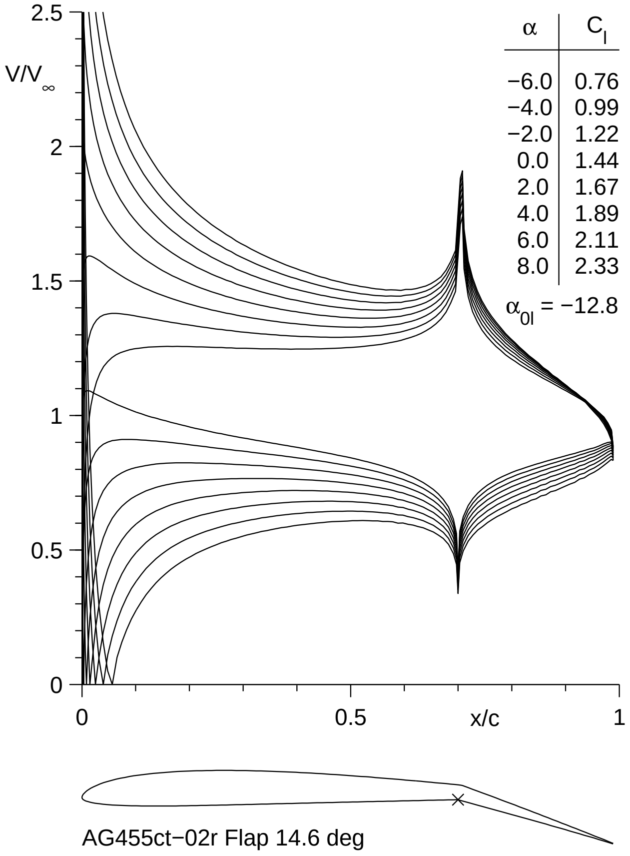

Figure 6.95: Inviscid velocity distributions for the AG455ct-02r with a 14.6 deg flap.

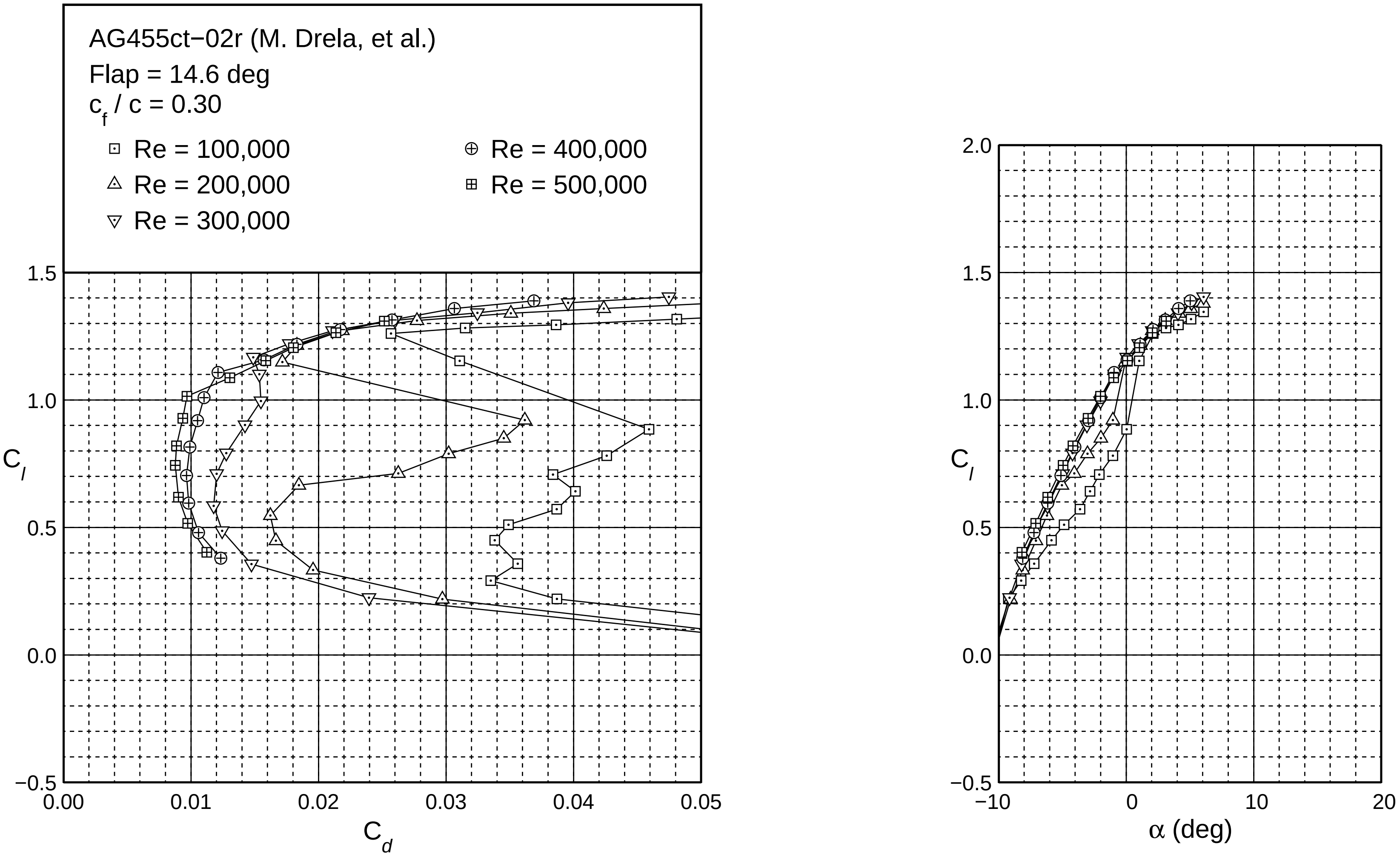

Figure 6.96: Drag polar for the AG455ct-02r with a 14.6 deg flap.

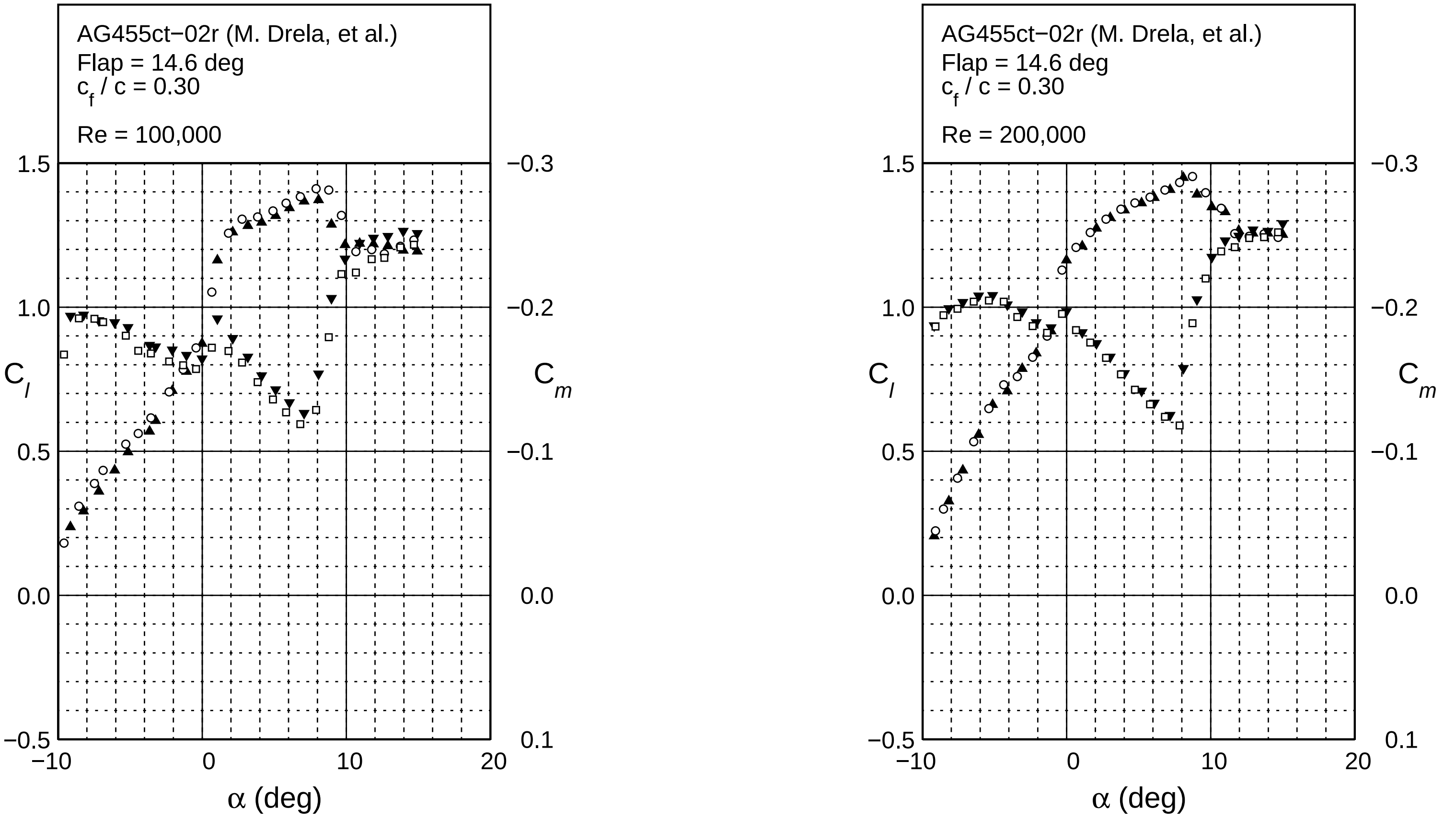

Figure 6.97: Lift and moment characteristics for the AG455ct-02r with a 14.6 deg flap.

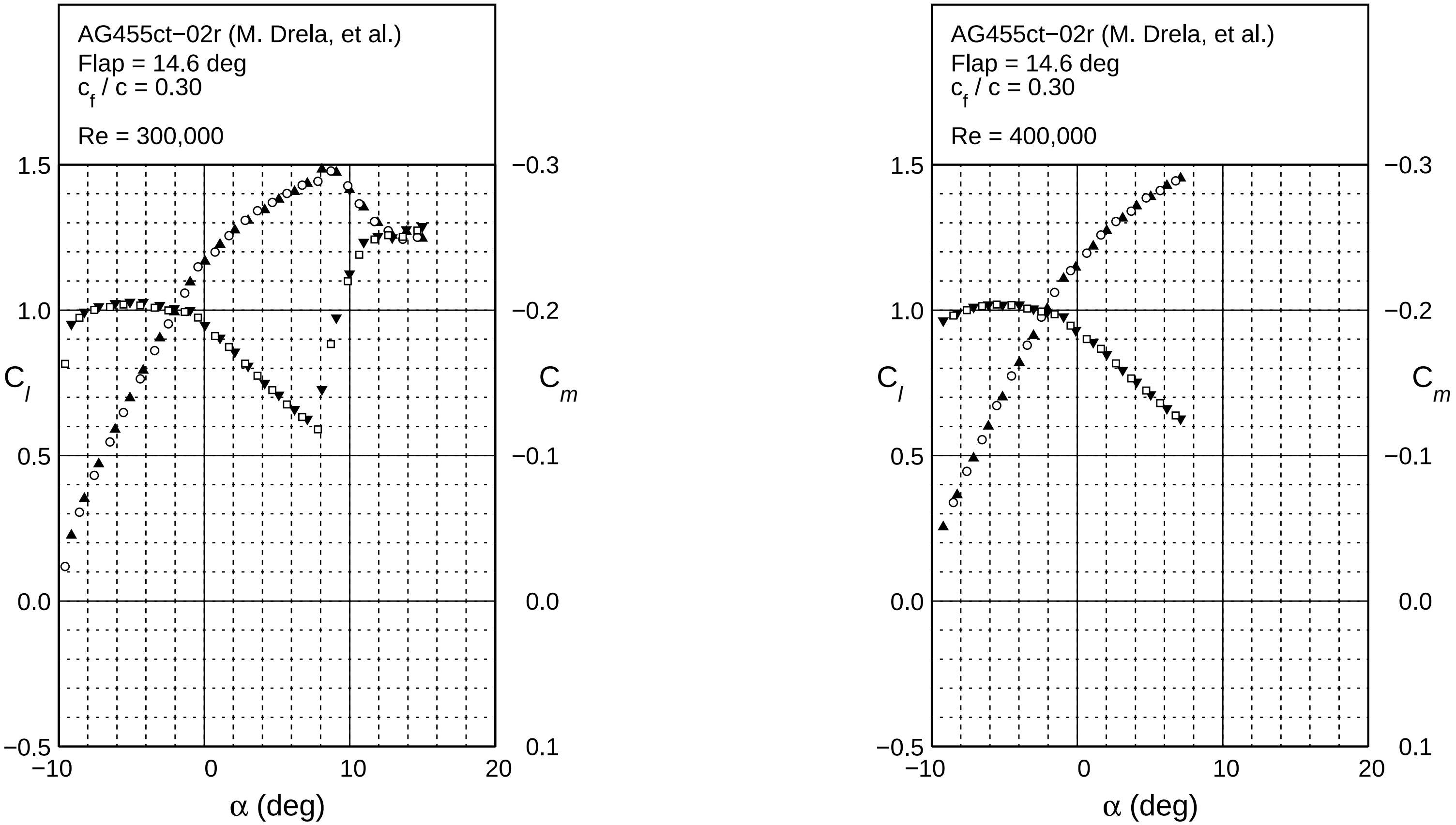

Figure 6.97: Continued.

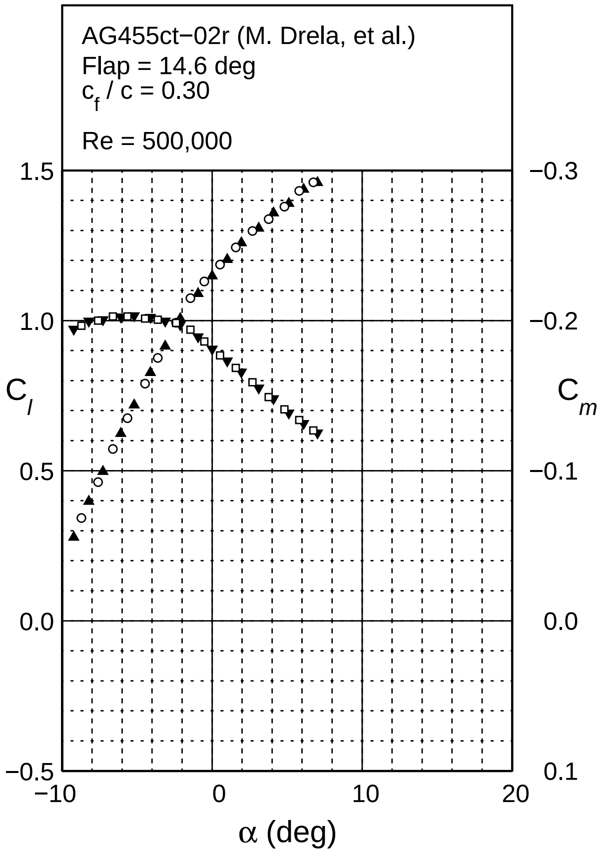

Figure 6.97: Continued.

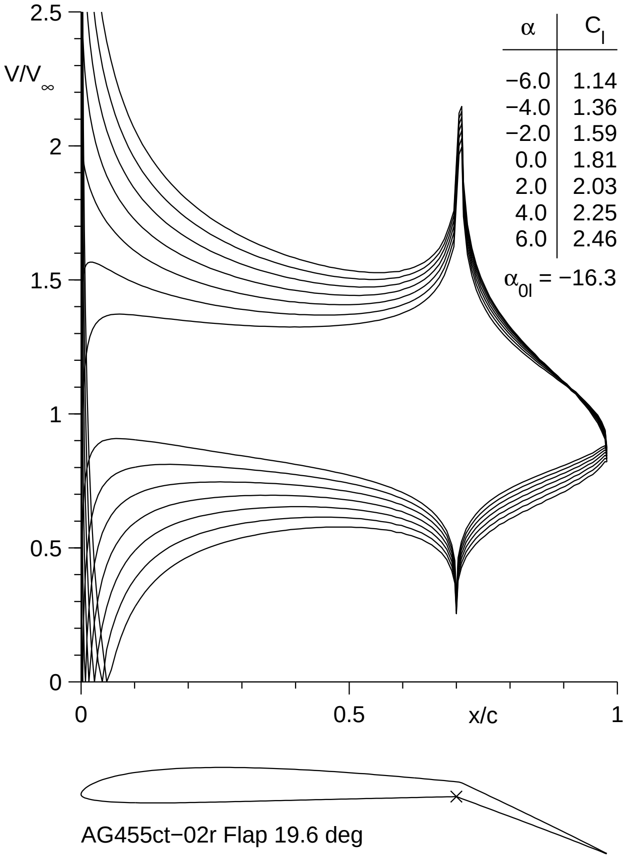

Figure 6.98: Inviscid velocity distributions for the AG455ct-02r with a 19.6 deg flap.

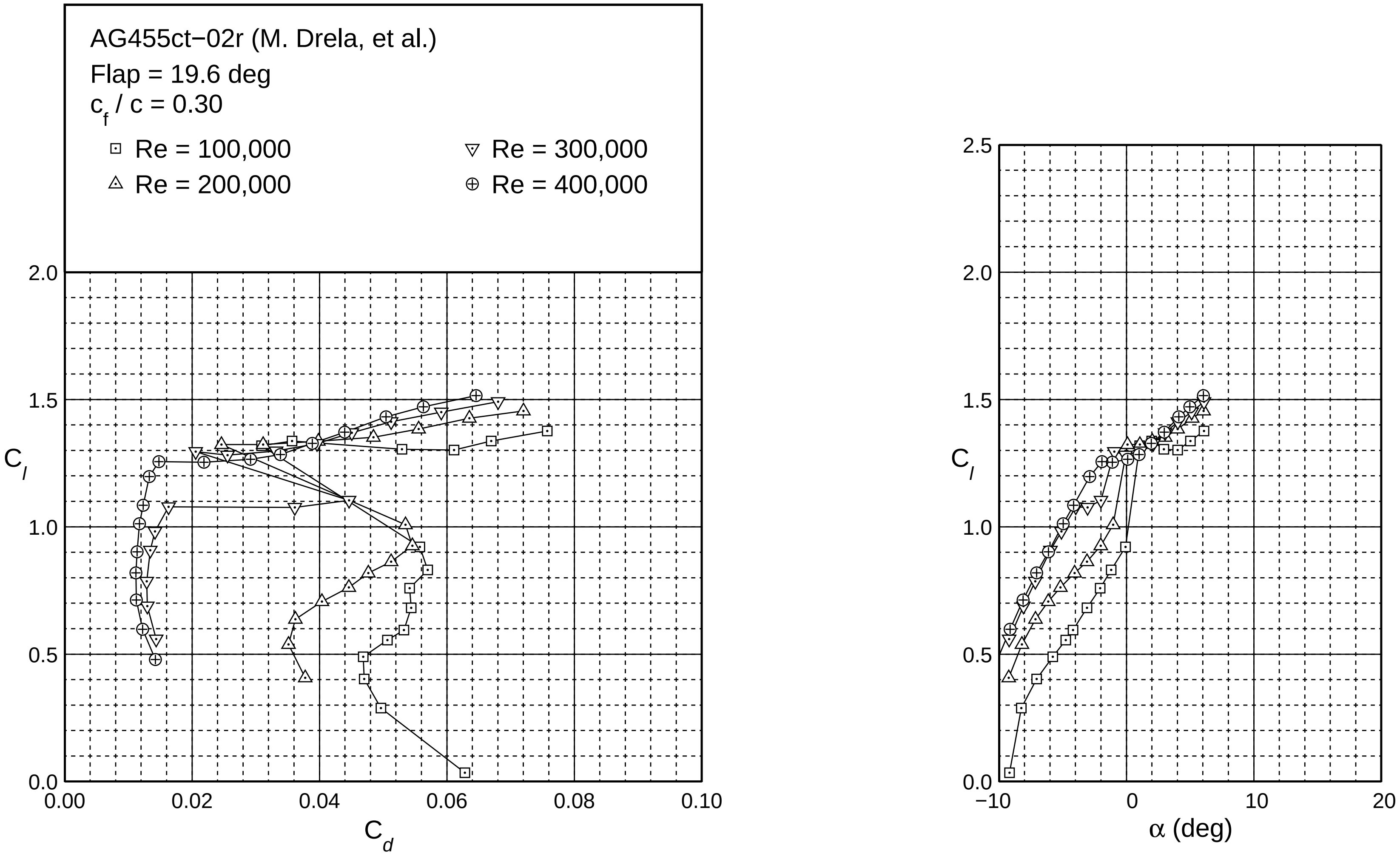

Figure 6.99: Drag polar for the AG455ct-02r with a 19.6 deg flap.

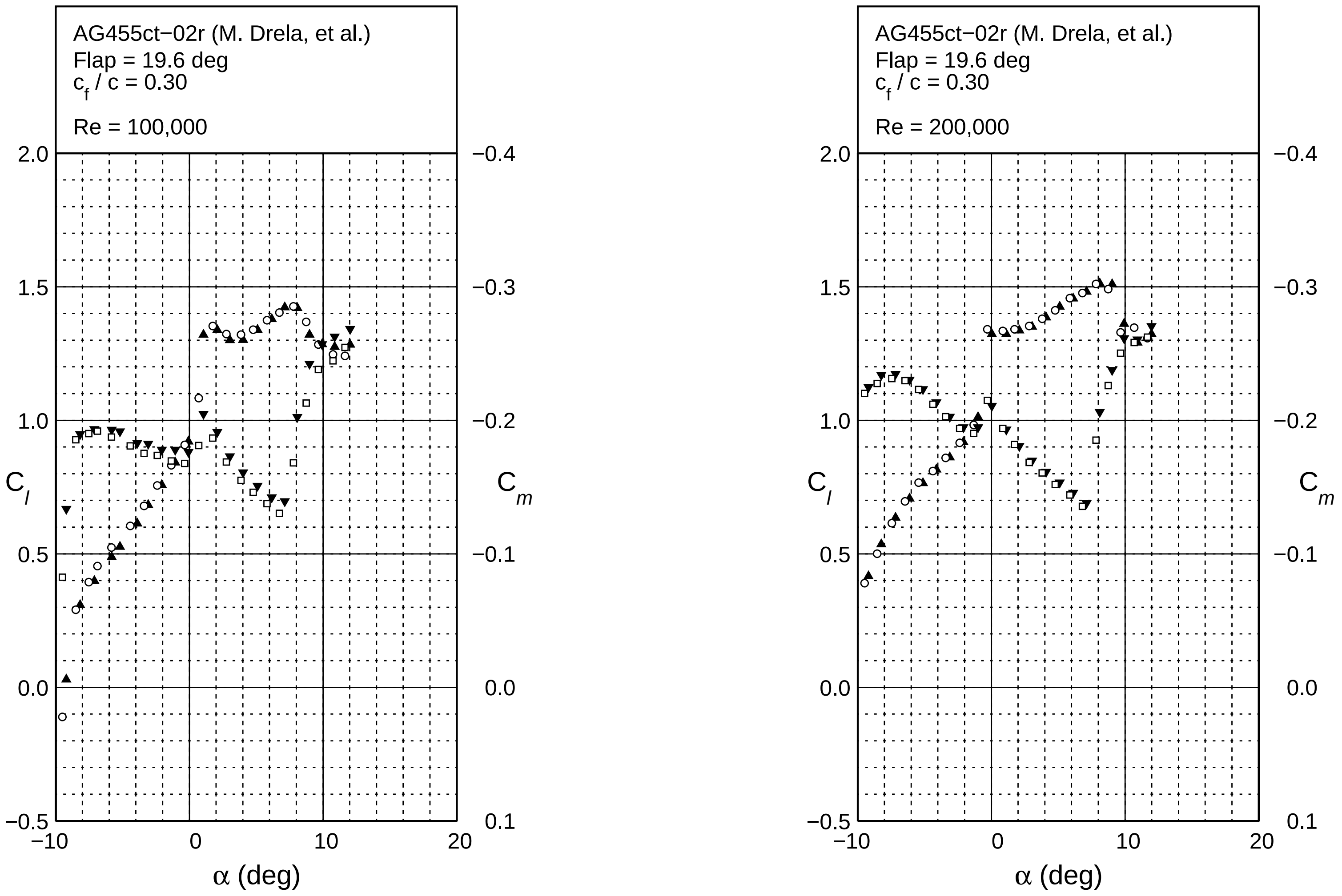

Figure 6.100: Lift and moment characteristics for the AG455ct-02r with a 19.6 deg flap.

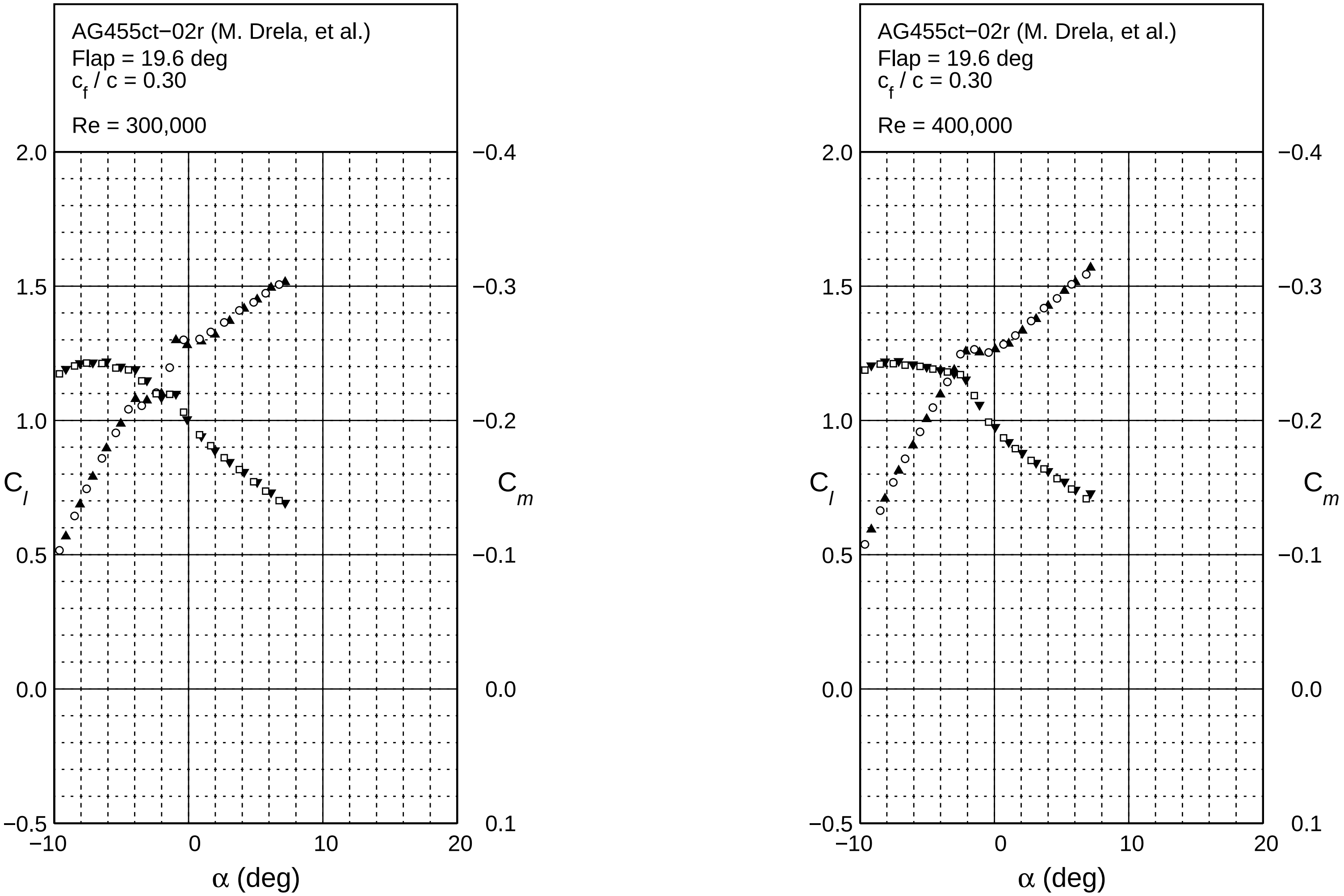

Figure 6.100: Continued.

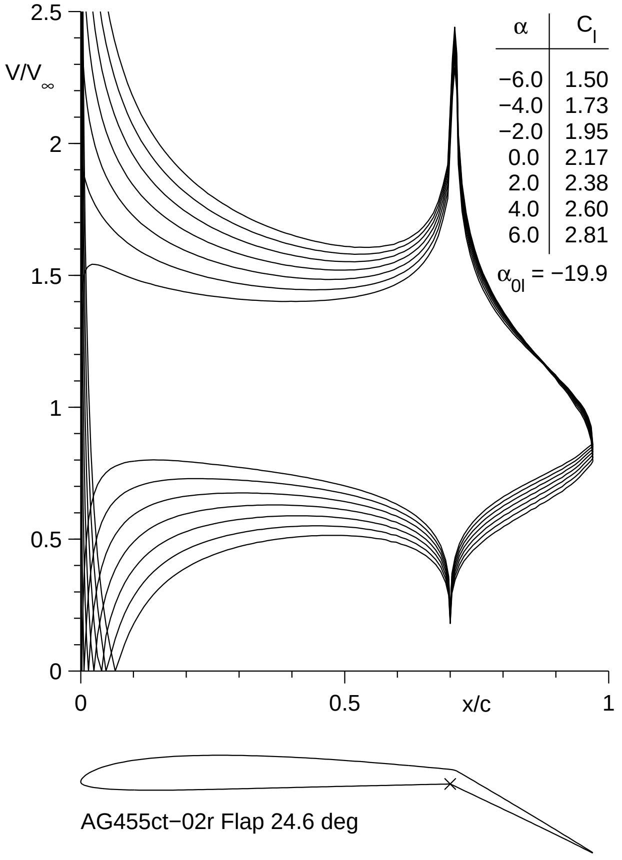

Figure 6.101: Inviscid velocity distributions for the AG455ct-02r with a 24.6 deg flap.

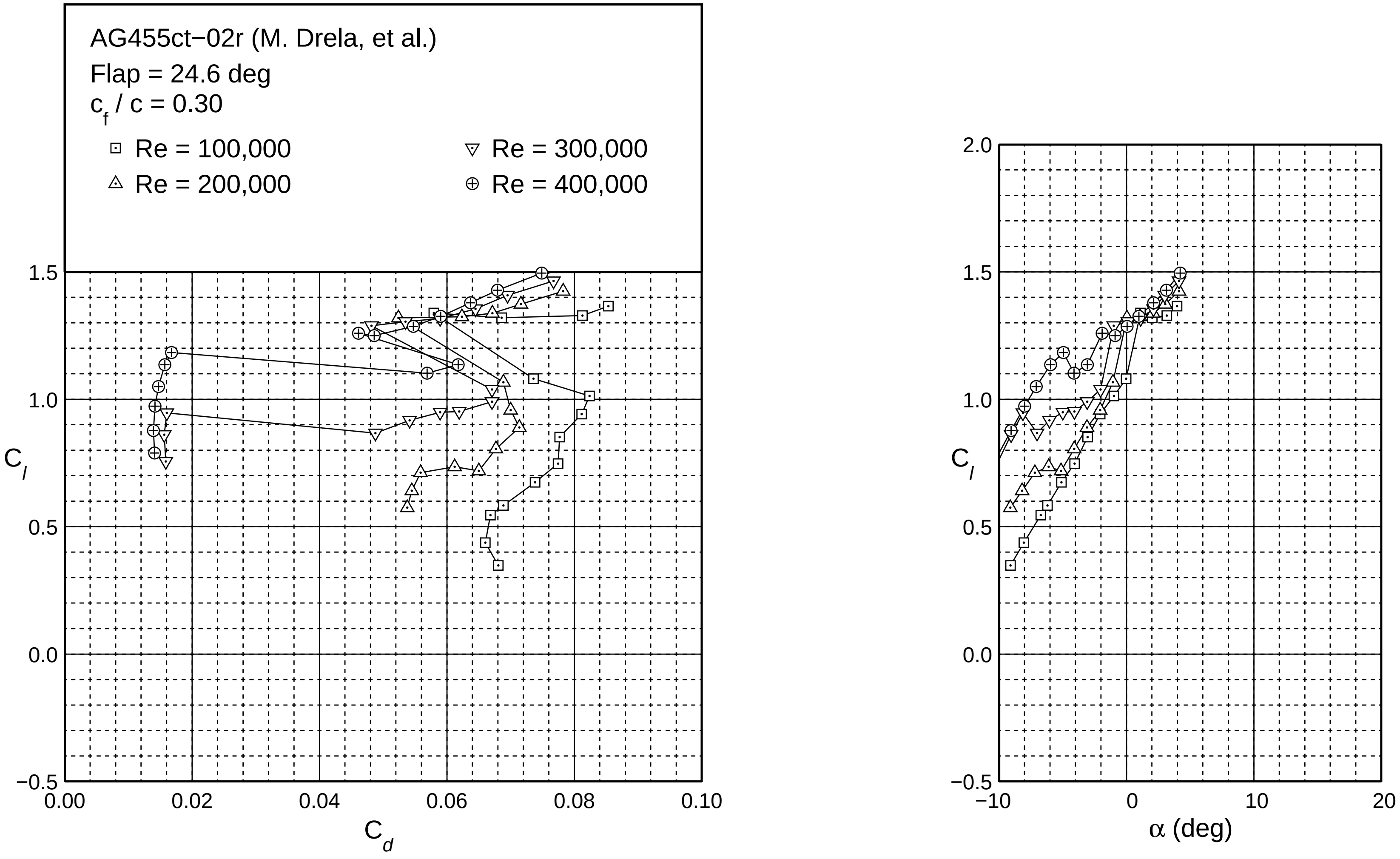

Figure 6.102: Drag polar for the AG455ct-02r with a 24.6 deg flap.

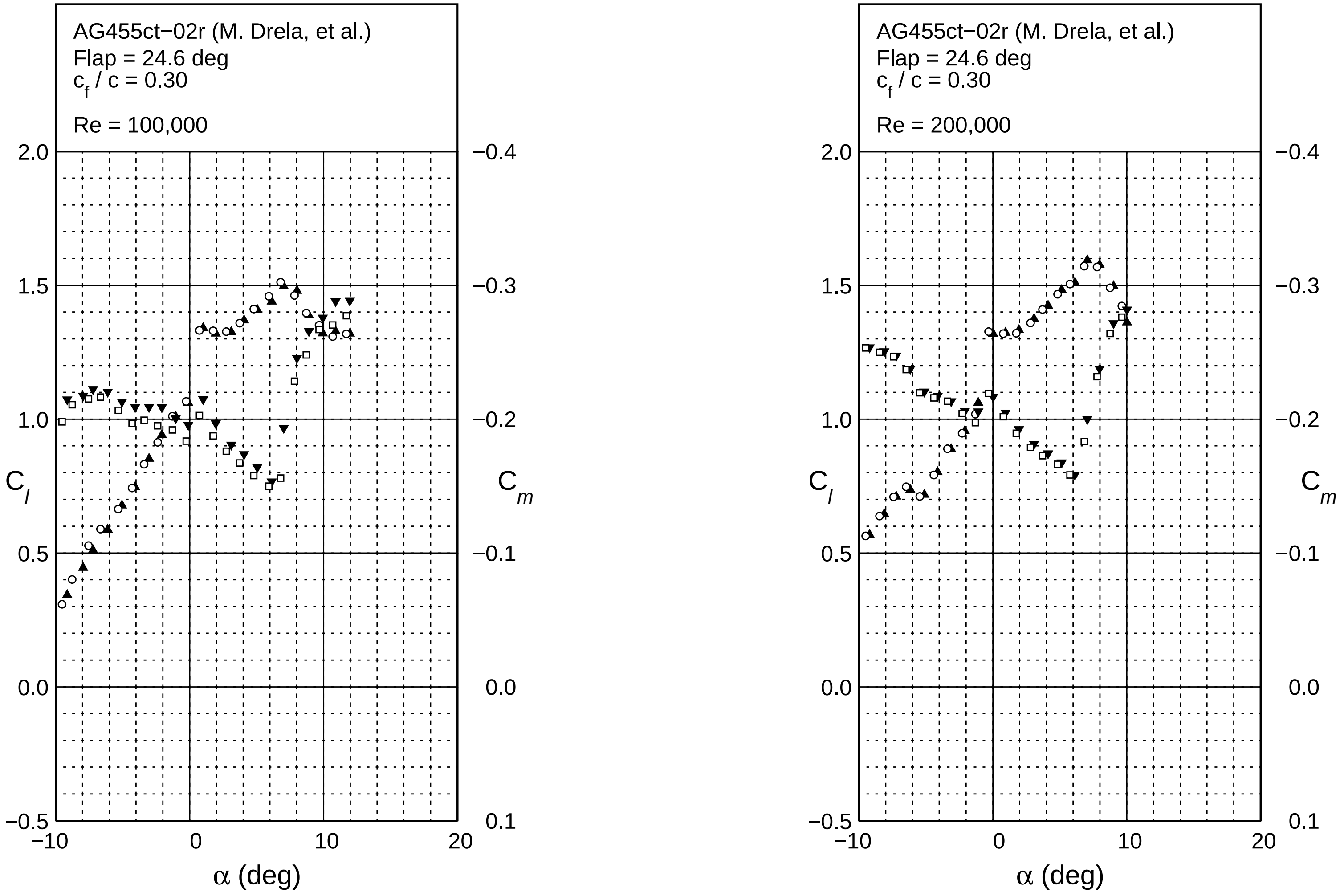

Figure 6.103: Lift and moment characteristics for the AG455ct-02r with a 24.6 deg flap.

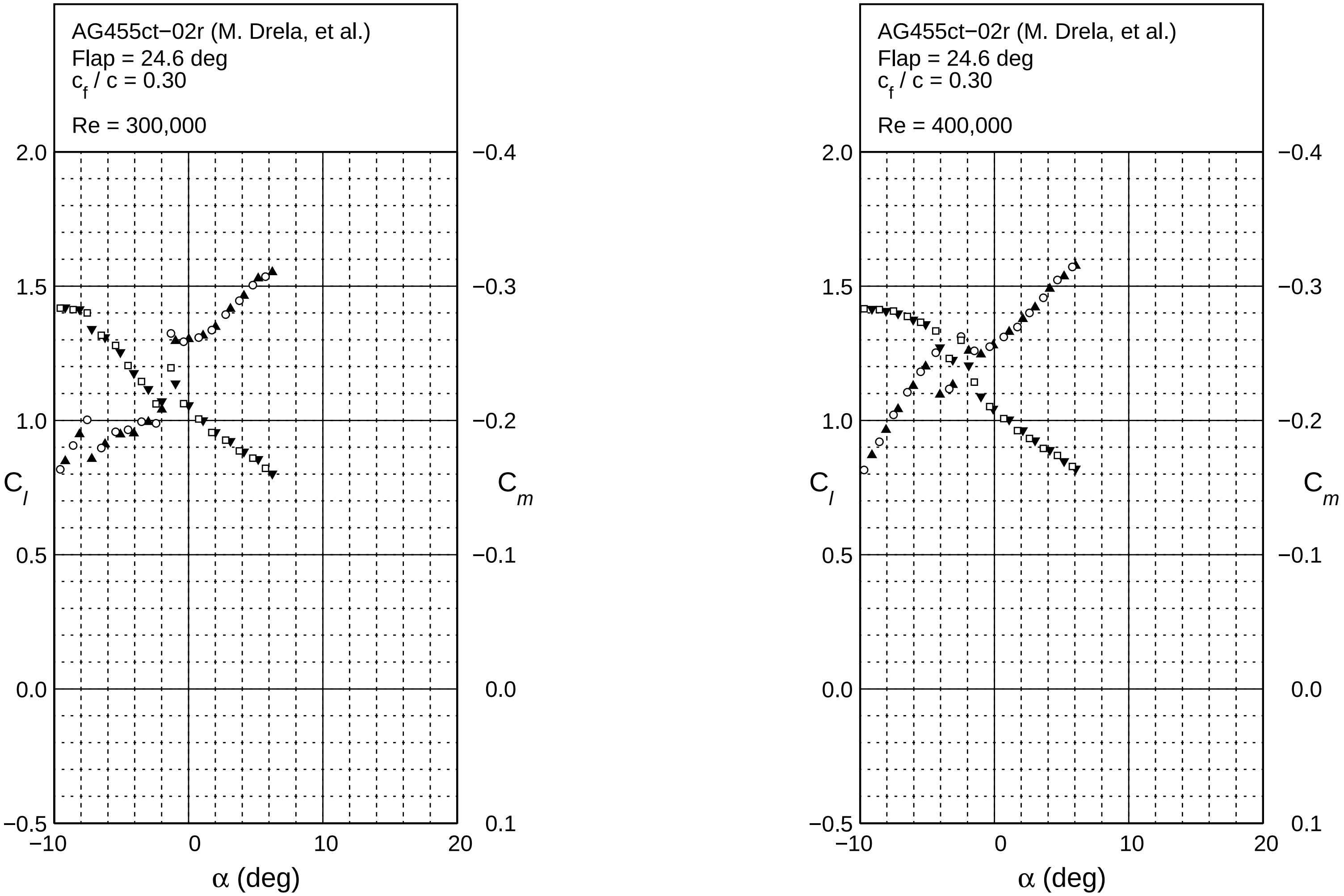

Figure 6.103: Continued.

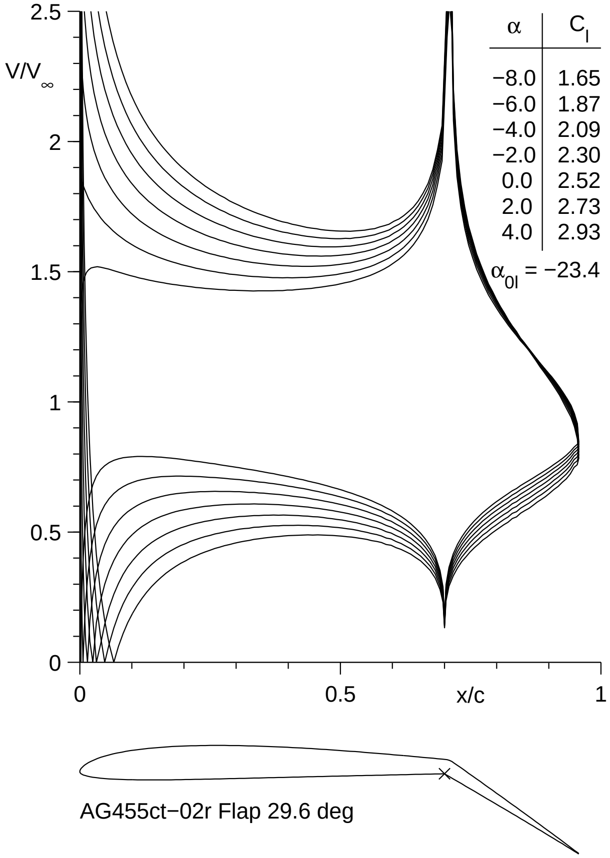

Figure 6.104: Inviscid velocity distributions for the AG455ct-02r with a 29.6 deg flap.

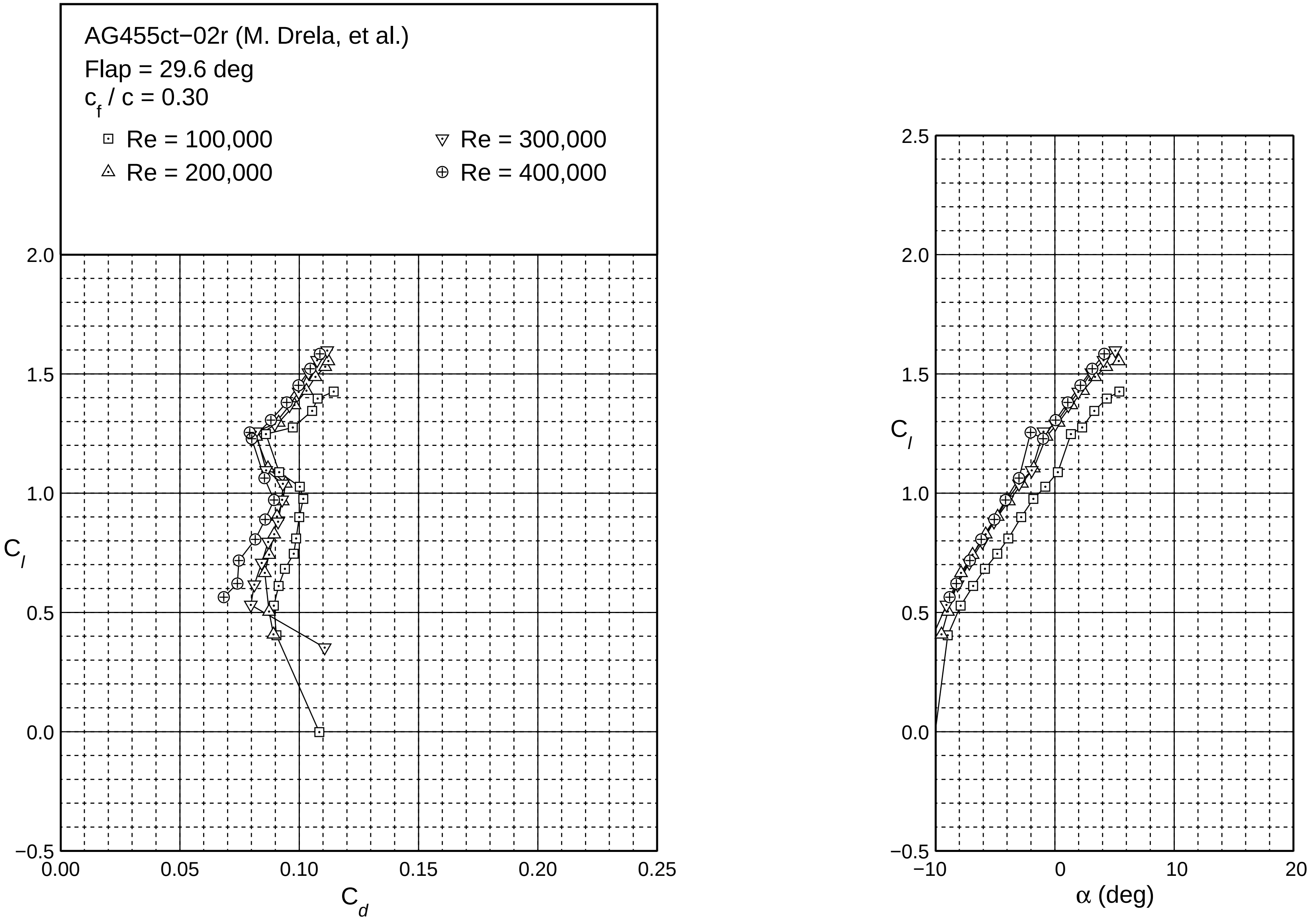

Figure 6.105: Drag polar for the AG455ct-02r with a 29.6 deg flap.

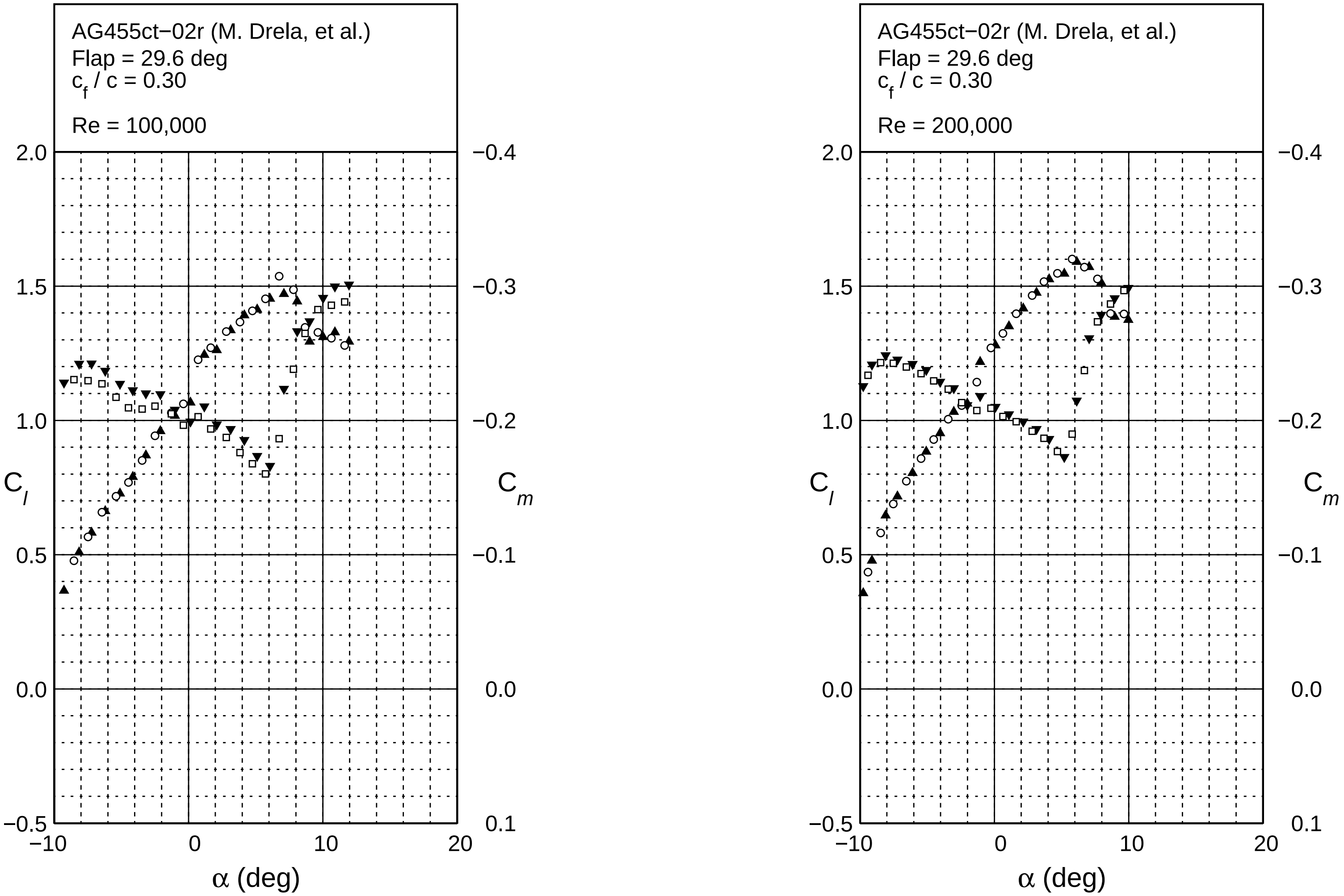

Figure 6.106: Lift and moment characteristics for the AG455ct-02r with a 29.6 deg flap.

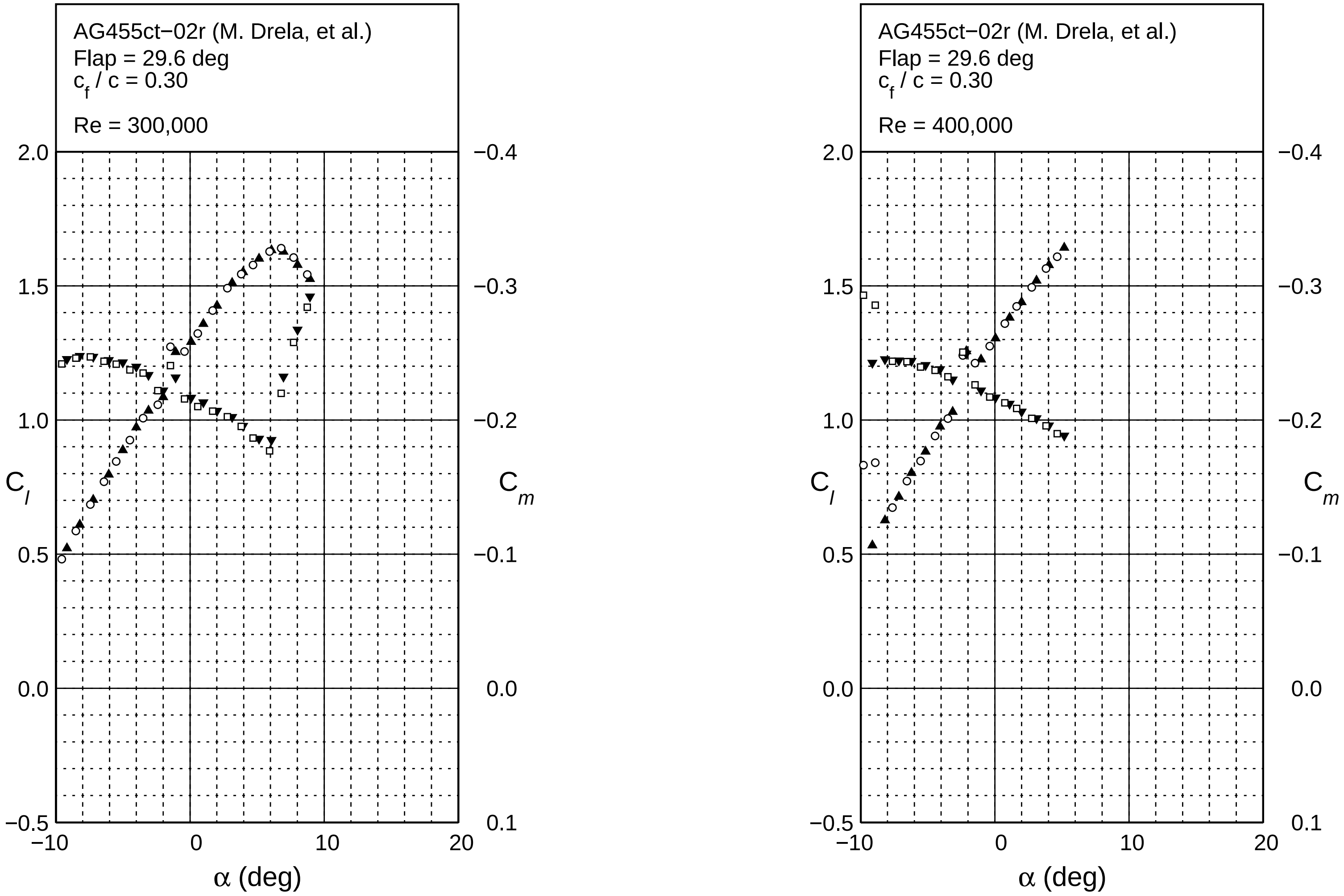

Figure 6.106: Continued.

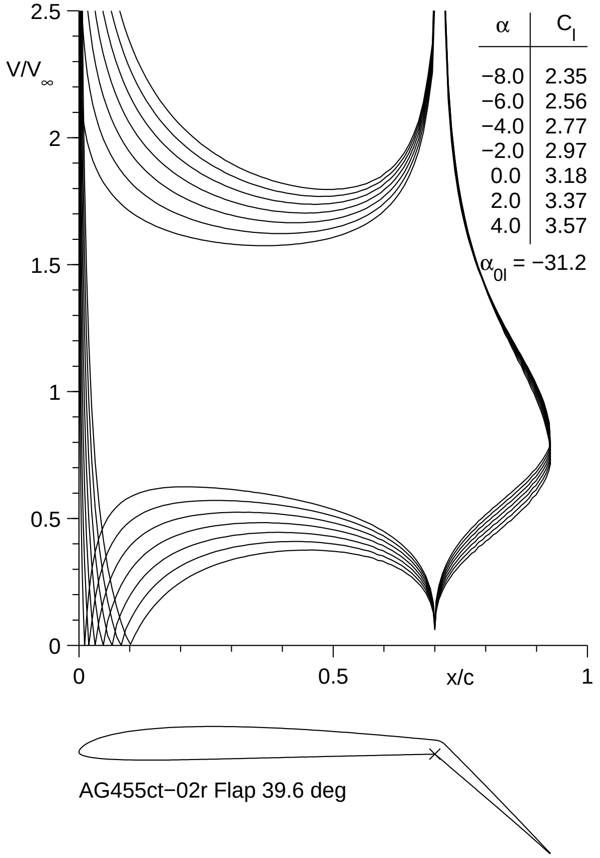

Figure 6.107: Inviscid velocity distributions for the AG455ct-02r with a 39.6 deg flap.

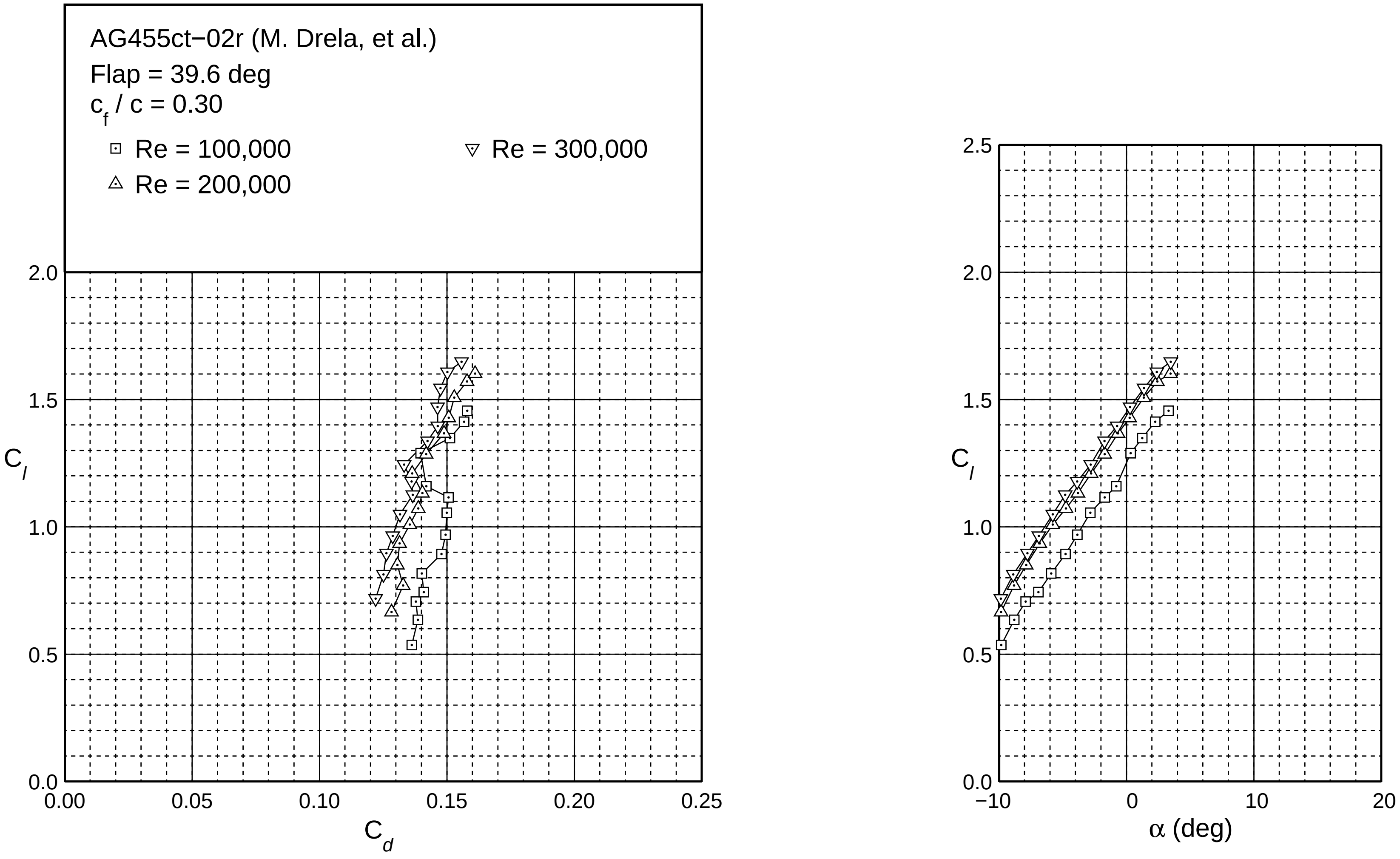

Figure 6.108: Drag polar for the AG455ct-02r with a 39.6 deg flap.

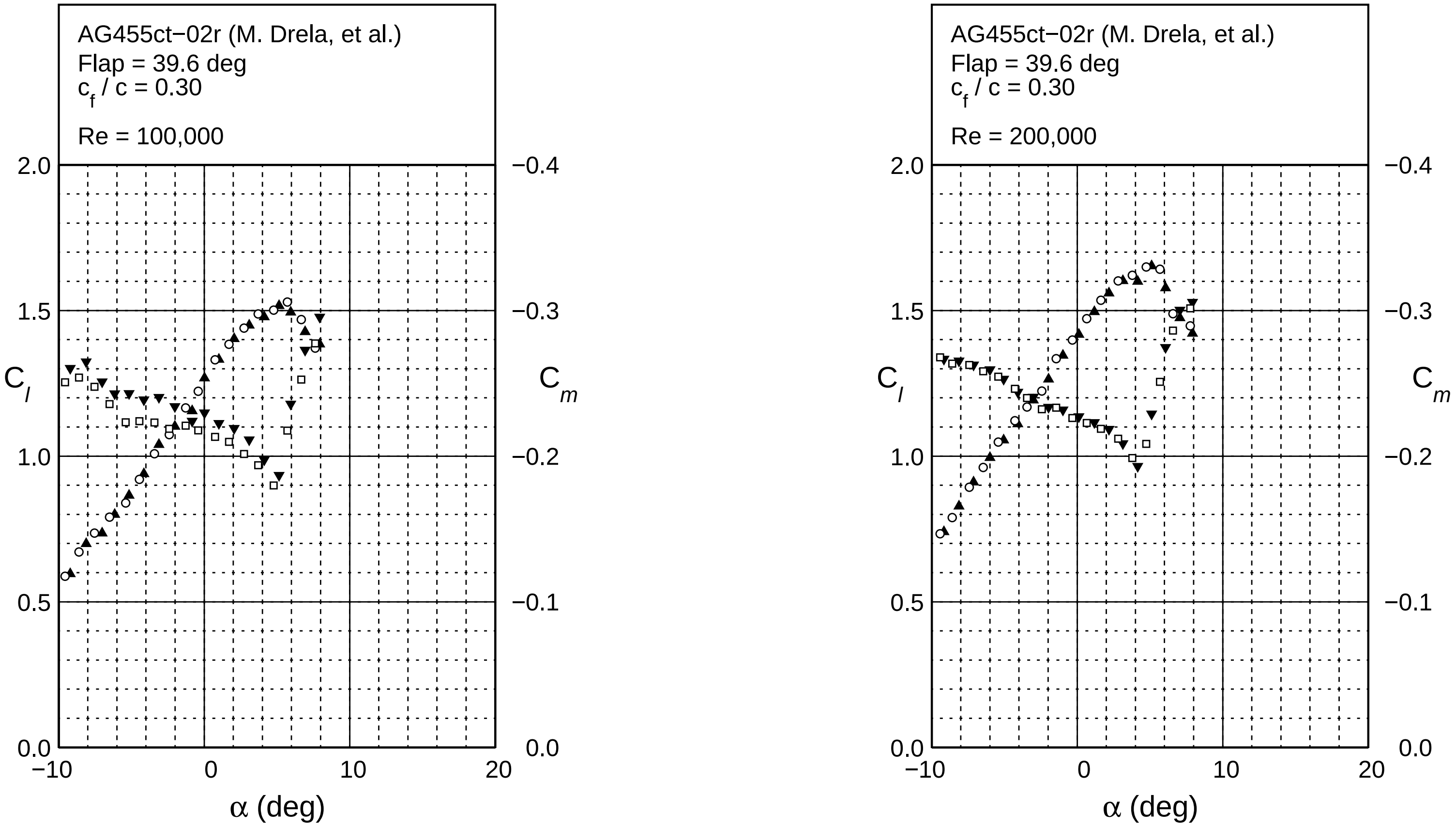

Figure 6.109: Lift and moment characteristics for the AG455ct-02r with a 39.6 deg flap.

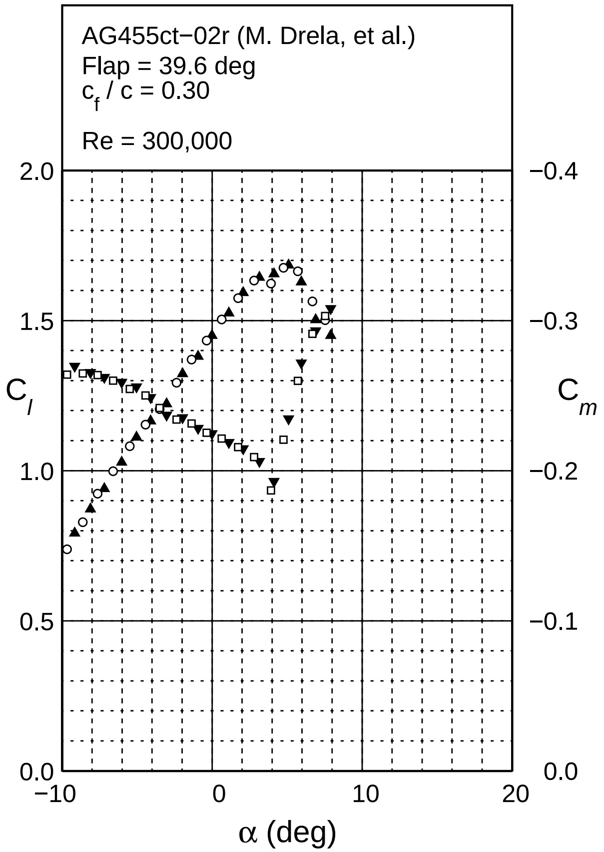

Figure 6.109: Continued.

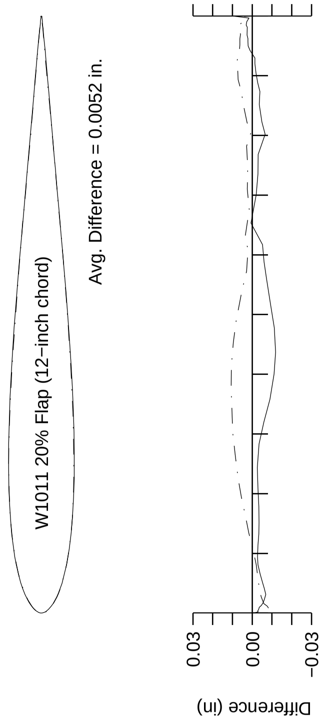

Figure 6.110: Comparison between the true and actual W1011 ($c_f/c\ =\ 20\%$).

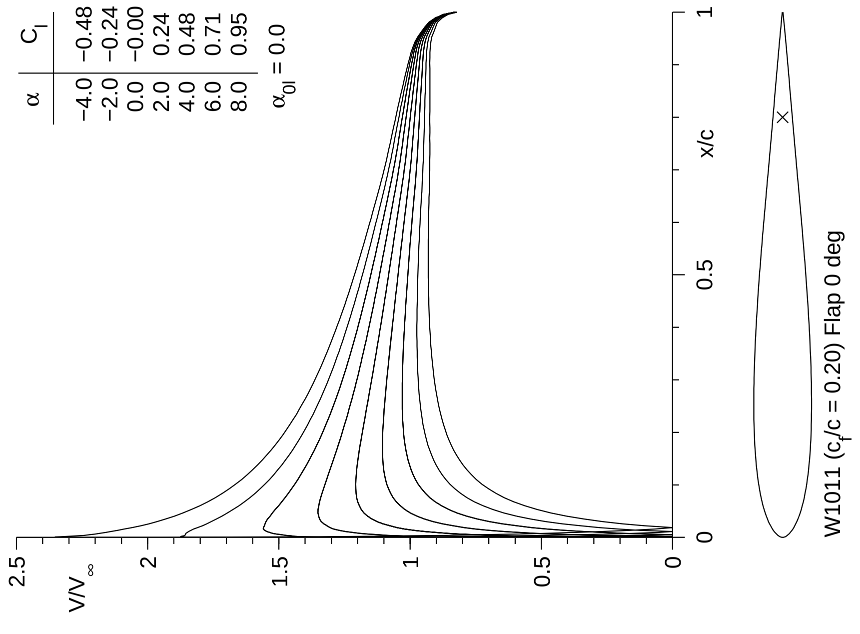

Figure 6.111: Inviscid velocity distribution for the W1011 ($c_f/c\ =\ 20\%$).

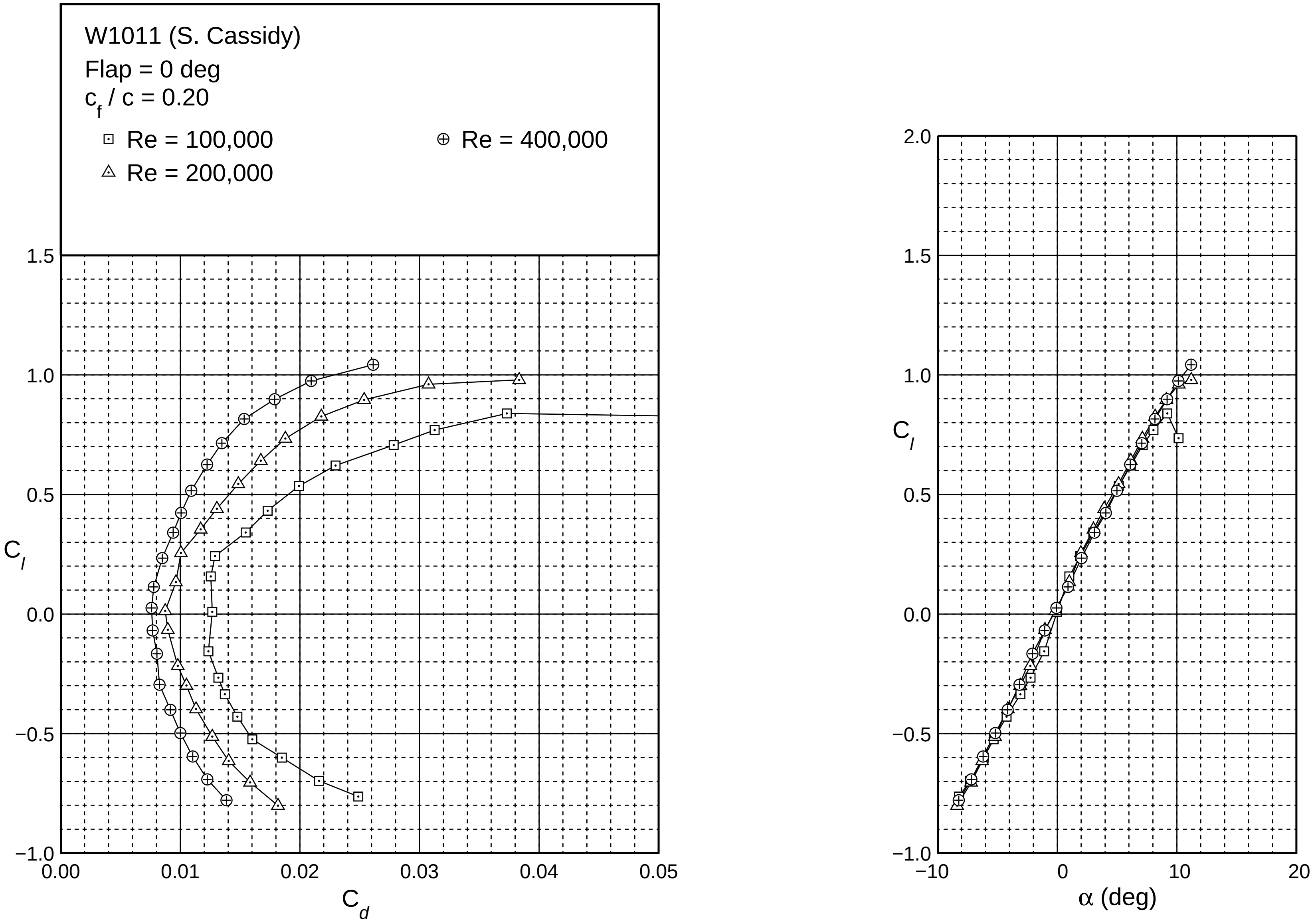

Figure 6.112: Drag polar for the W1011 ($c_f/c = 20\%$).

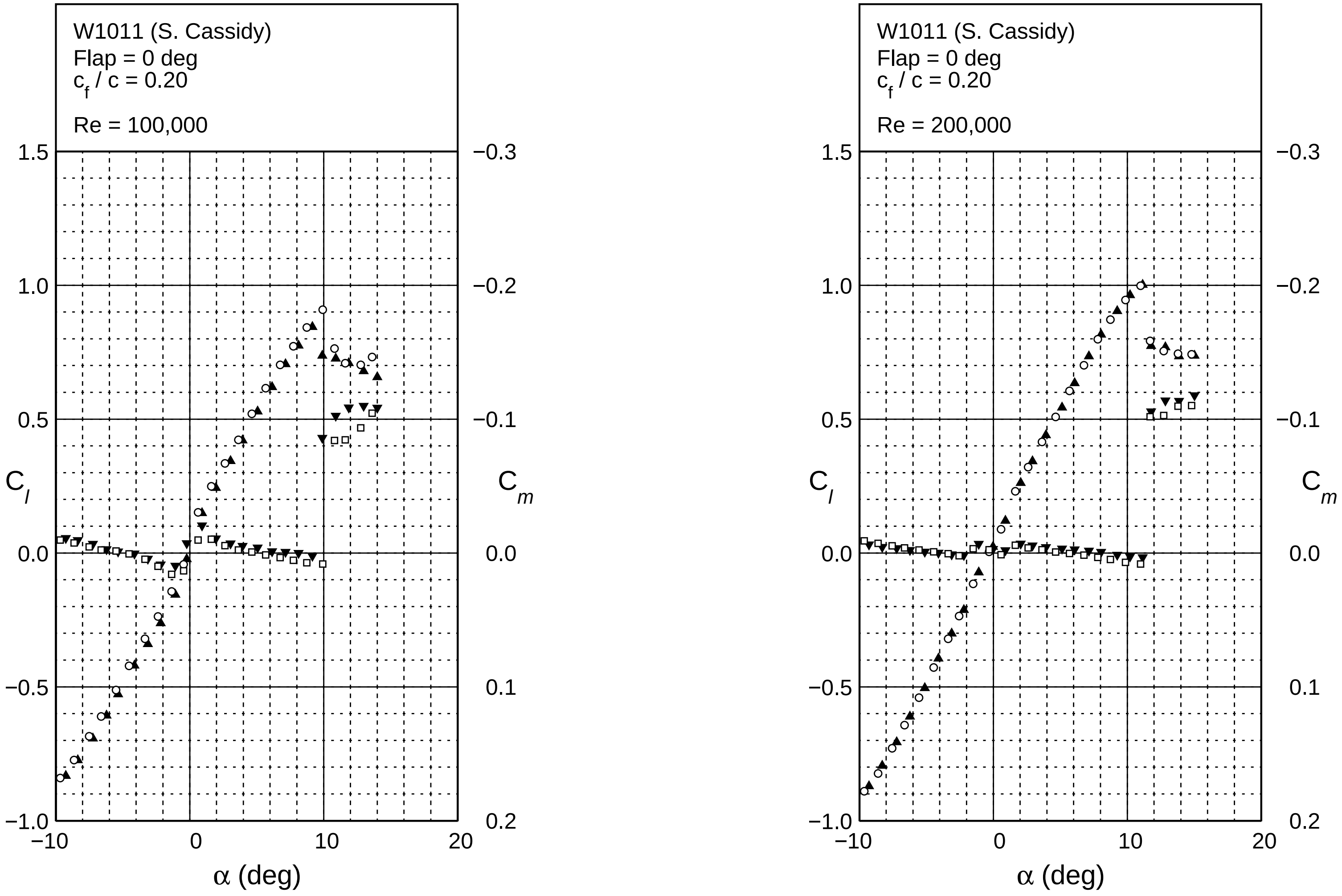

Figure 6.113: Lift and moment characteristics for the W1011 ($c_f/c = 20\%$).

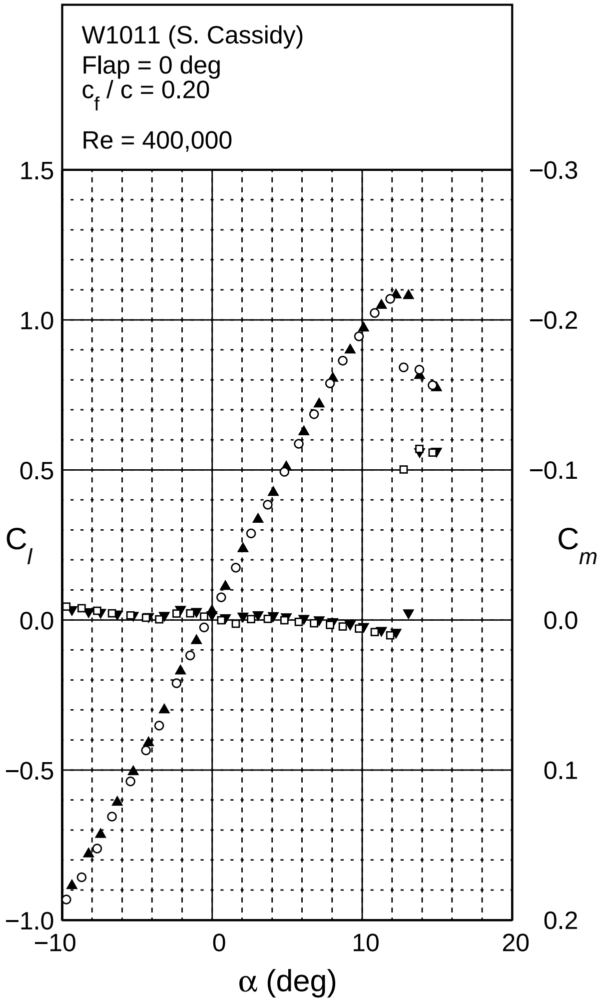

Figure 6.113: Continued.

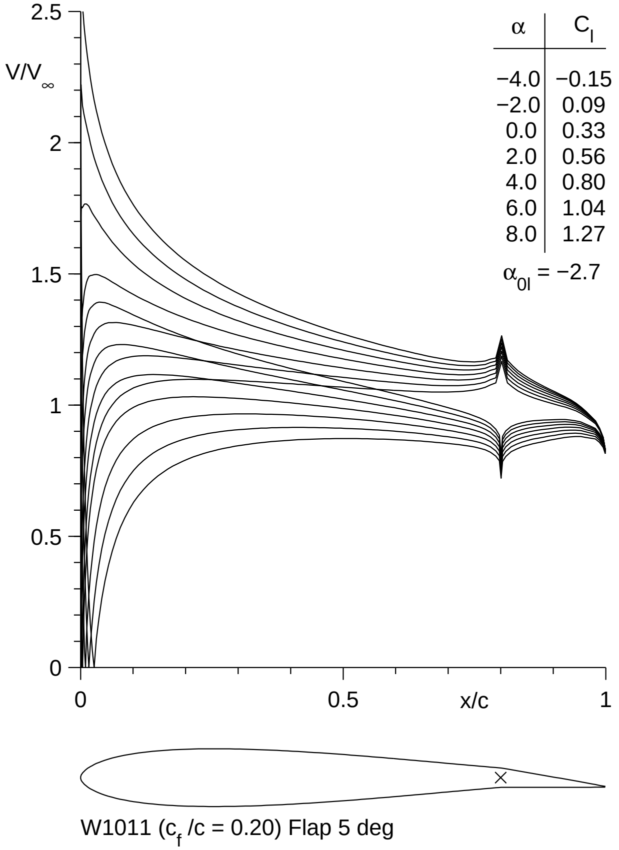

Figure 6.114: Inviscid velocity distribution for the W1011 $(c_f/c = 20\%)$ with a 5 deg flap.

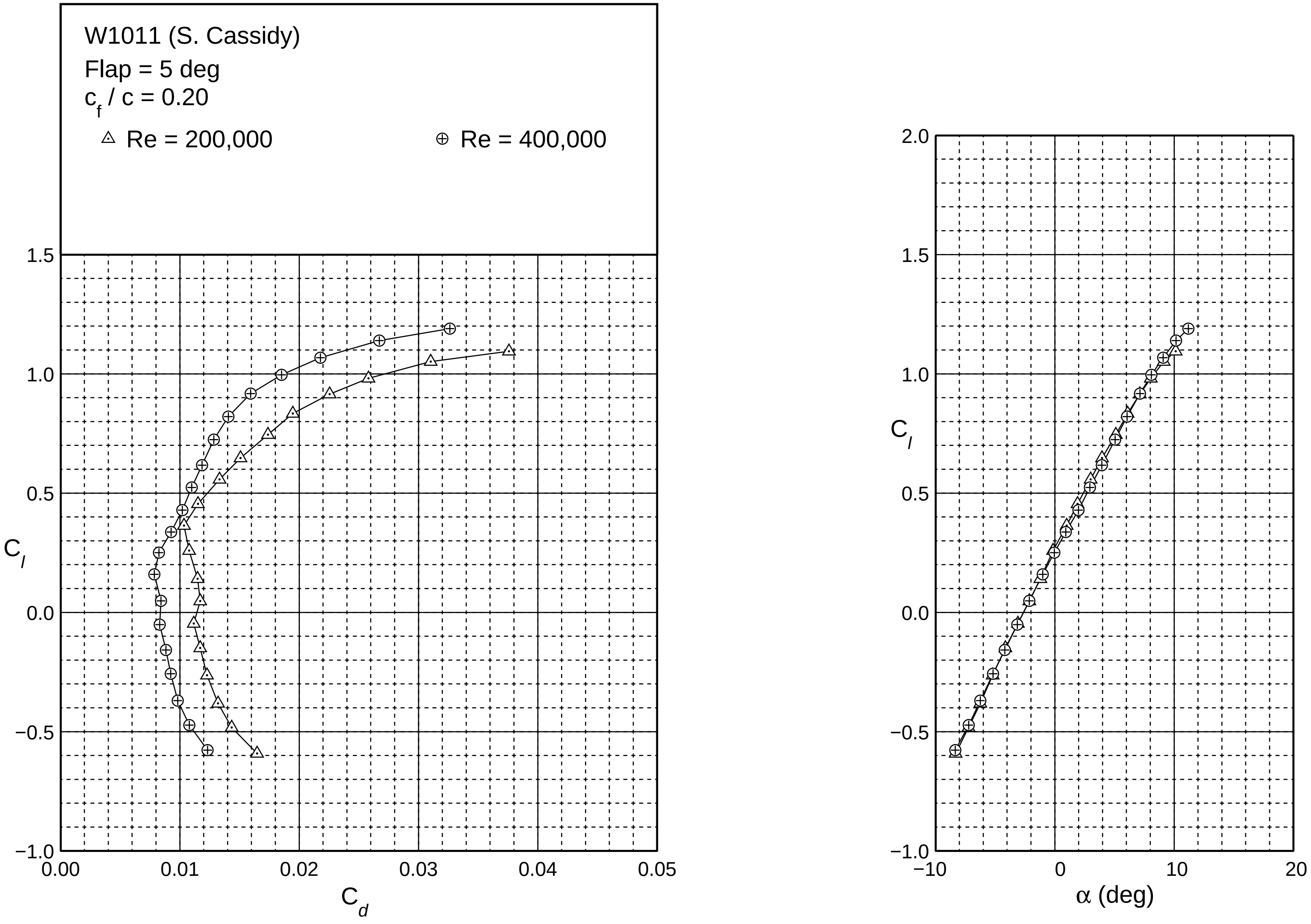

Figure 6.115: Drag polar for the W1011 ($c_f/c = 20\%$) with a 5 deg flap.

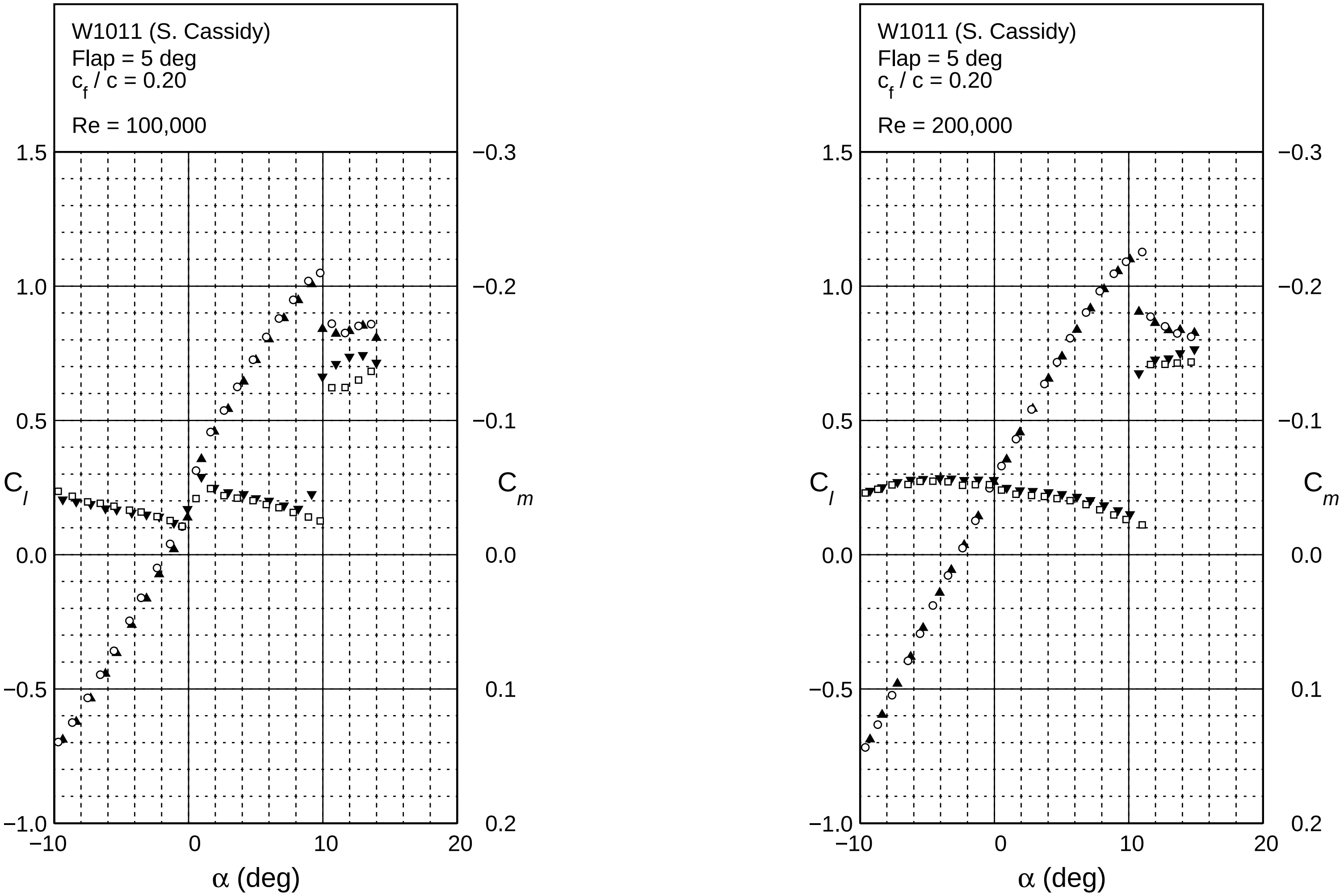

Figure 6.116: Lift and moment characteristics for the W1011 ($c_f/c = 20\%$) with a 5 deg flap.

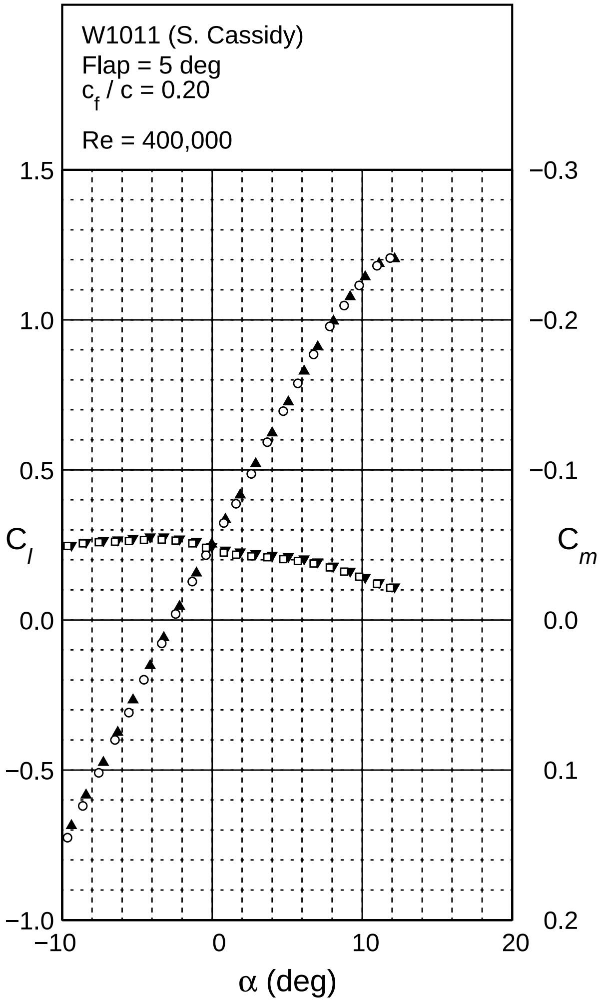

Figure 6.116: Continued.

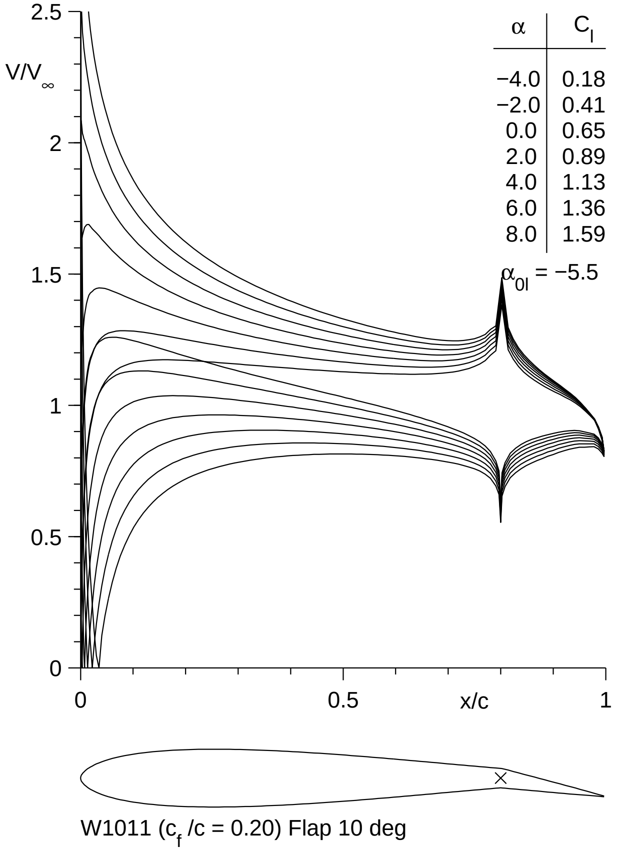

Figure 6.117: Inviscid velocity distribution for the W1011 ($c_f/c = 20\%$) with a 10 deg flap.

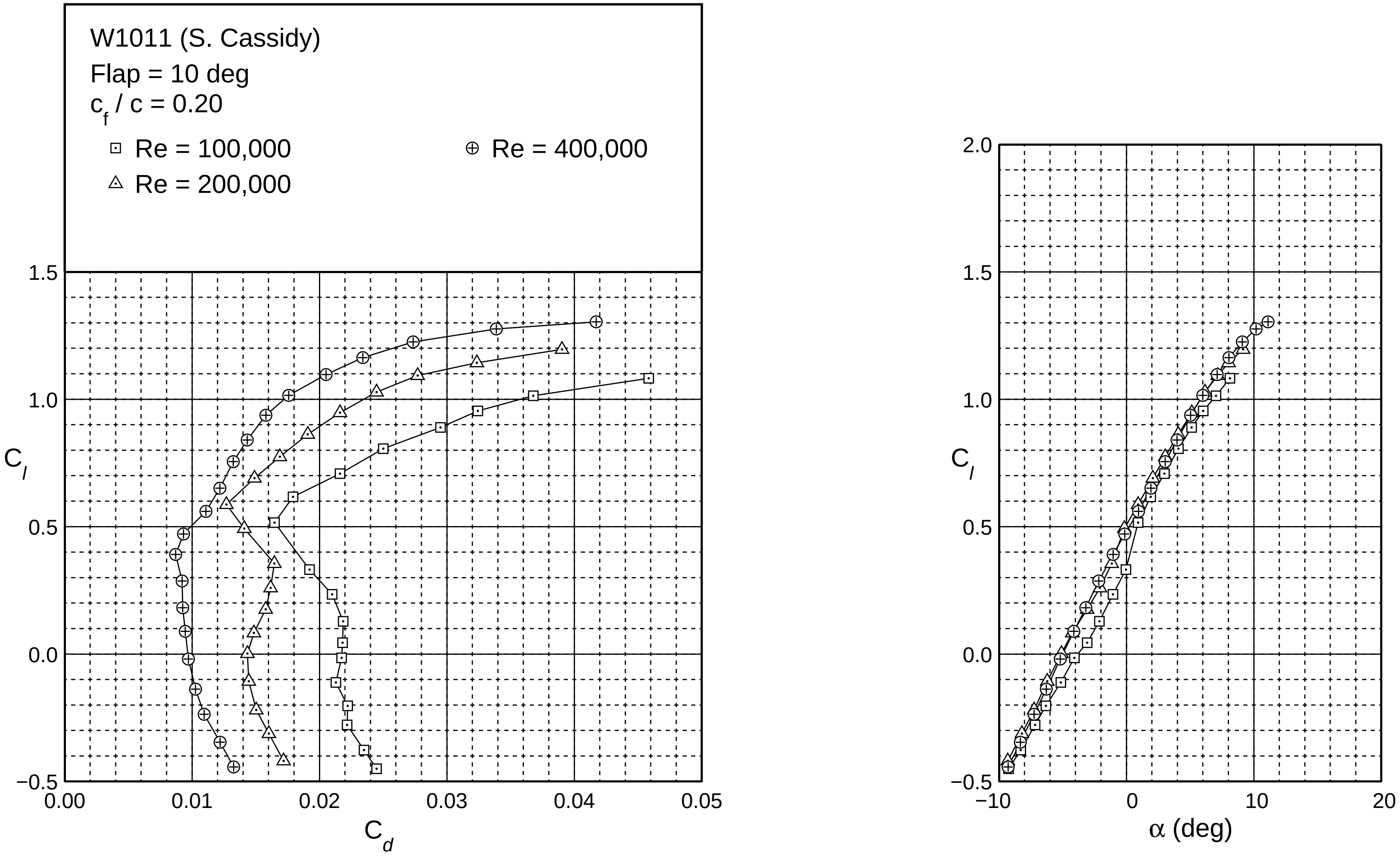

Figure 6.118: Drag polar for the W1011 ($c_f/c = 20\%$) with a 10 deg flap.

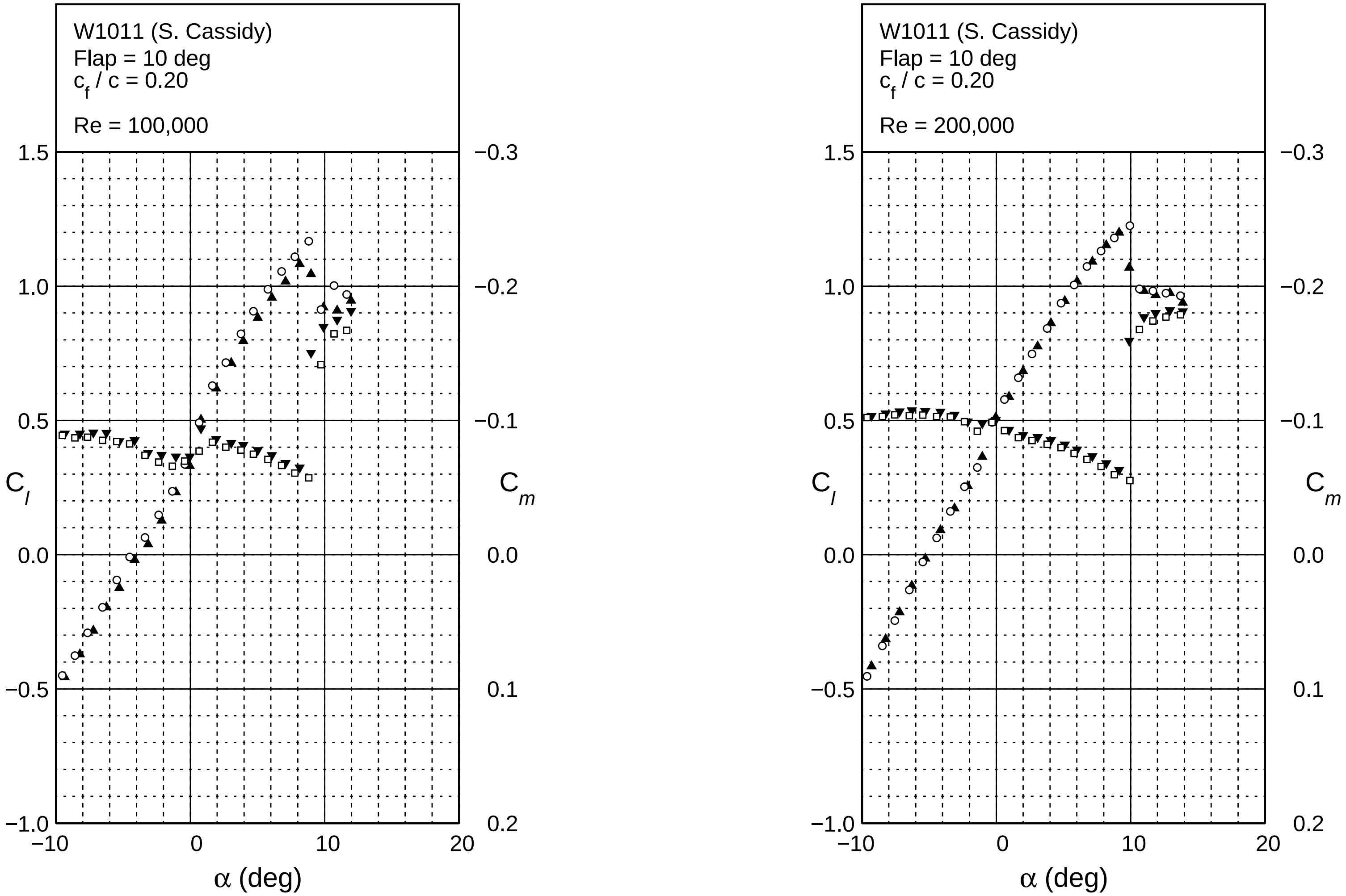

Figure 6.119: Lift and moment characteristics for the W1011 ($c_f/c = 20\%$) with a 10 deg flap.

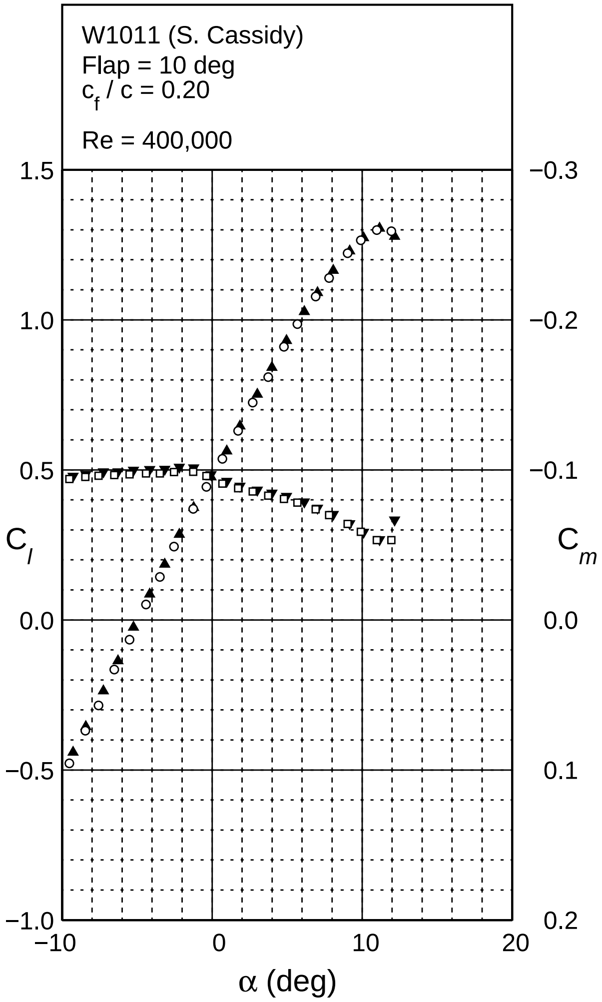

Figure 6.119: Continued.

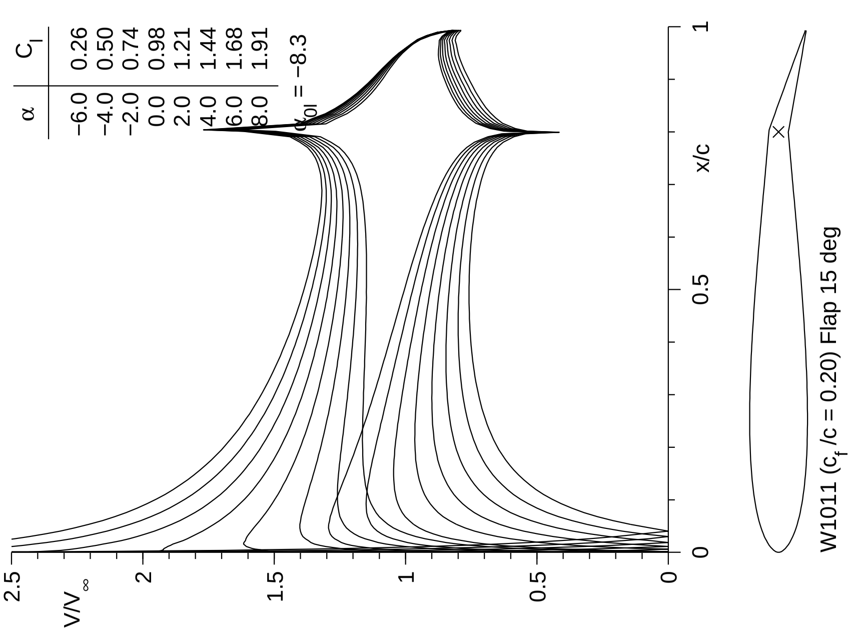

Figure 6.120: Inviscid velocity distribution for the W1011 $(c_f/c\ =\ 20\%)$ with a 15 deg flap.

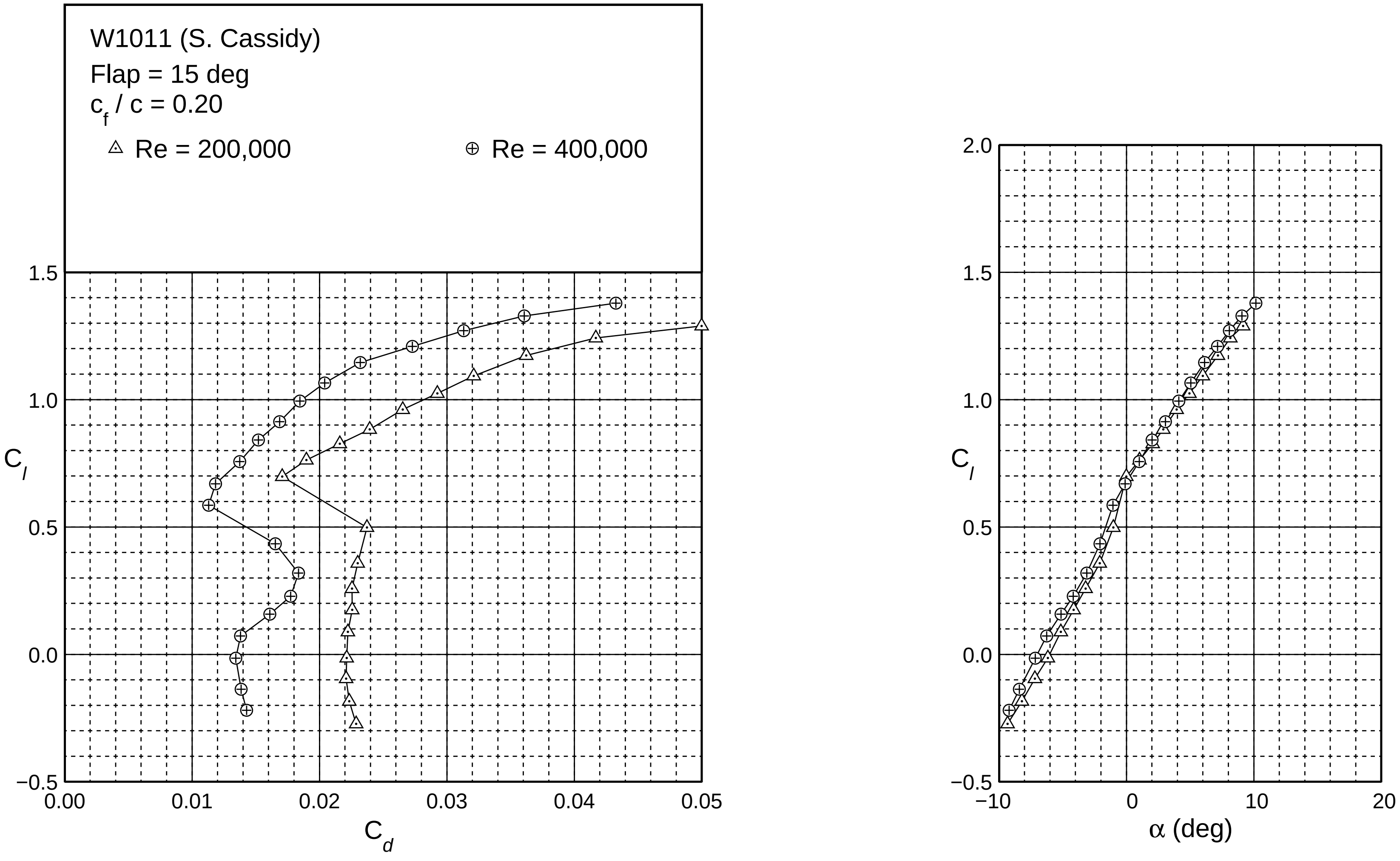

Figure 6.121: Drag polar for the W1011 ($c_f/c = 20\%$) with a 15 deg flap.

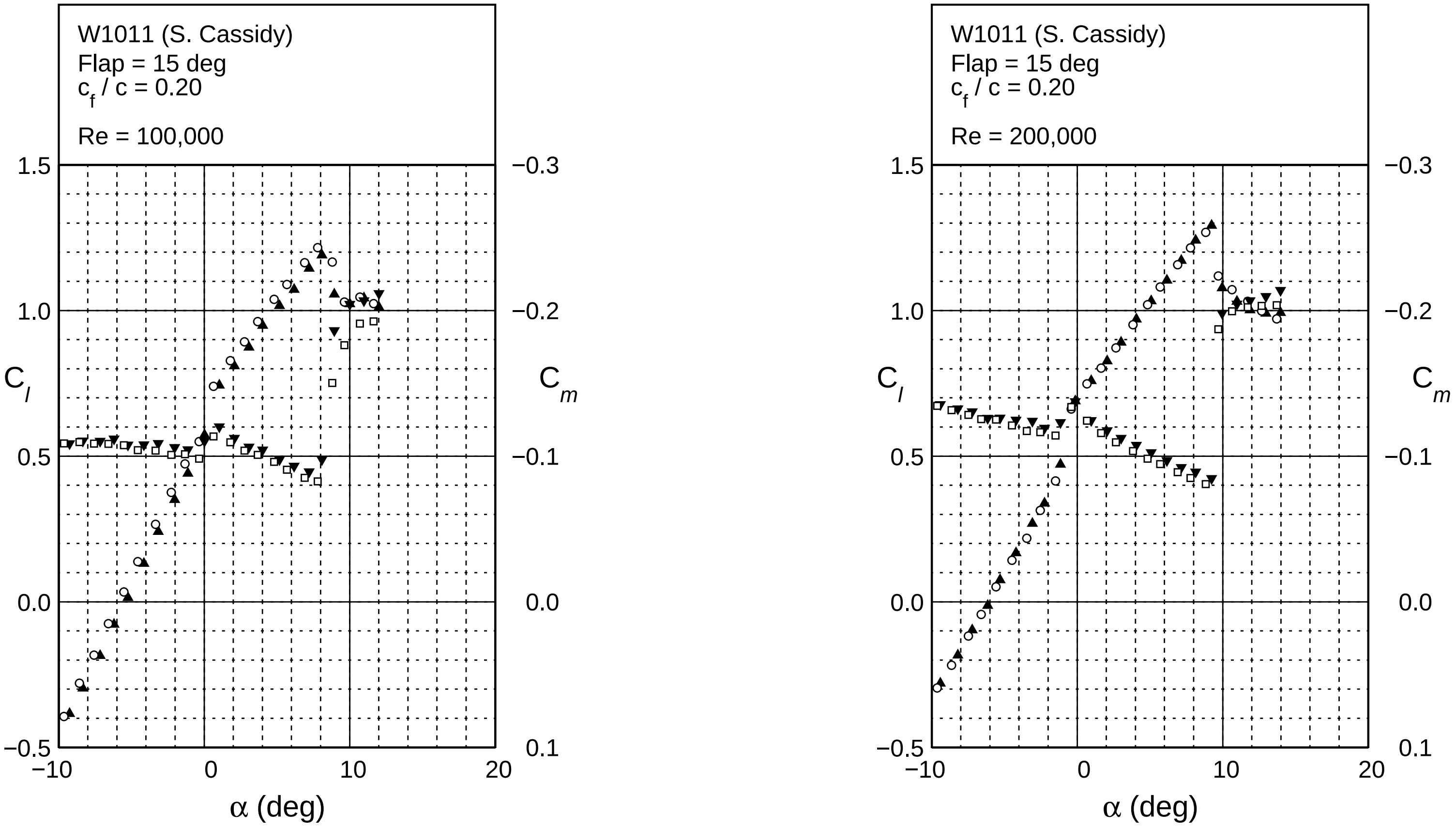

Figure 6.122: Lift and moment characteristics for the W1011 ($c_f/c = 20\%$) with a 15 deg flap.

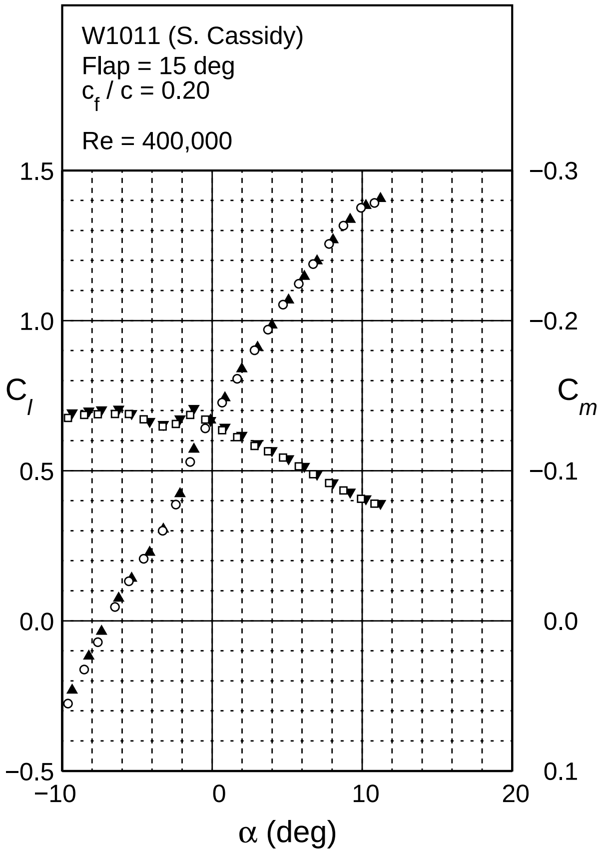

Figure 6.122: Continued.

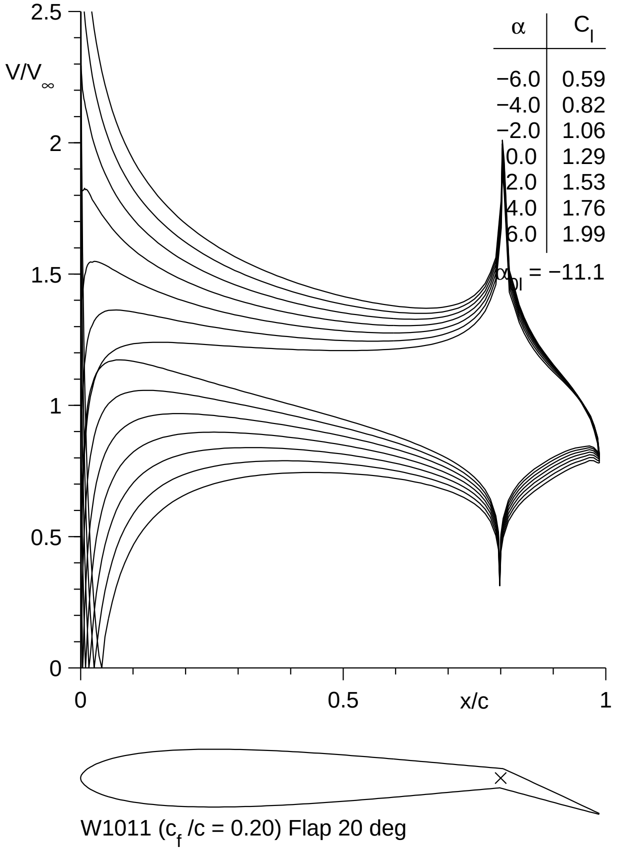

Figure 6.123: Inviscid velocity distribution for the W1011 ($c_f/c = 20\%$) with a 20 deg flap.

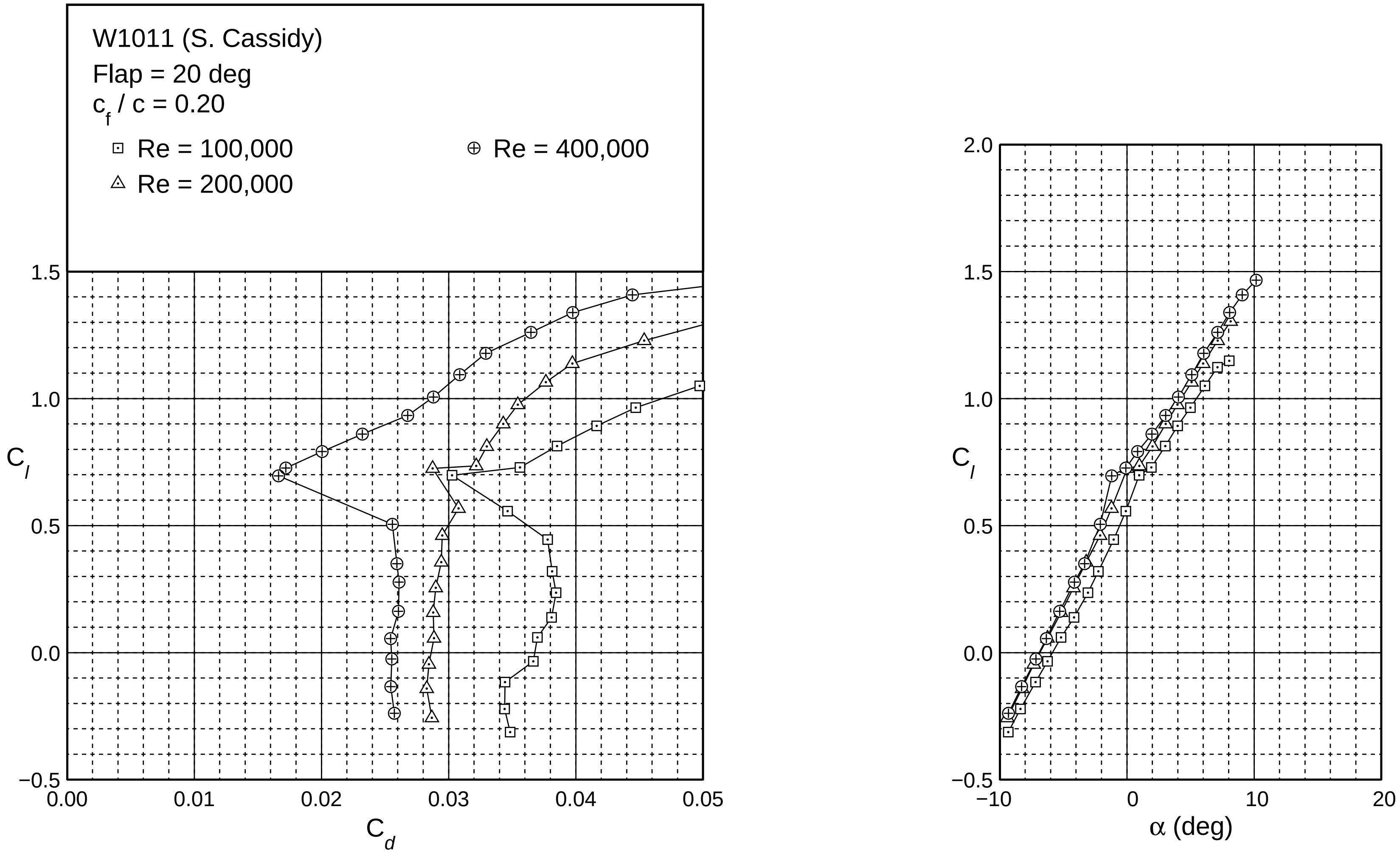

Figure 6.124: Drag polar for the W1011 ($c_f/c = 20\%$) with a 20 deg flap.

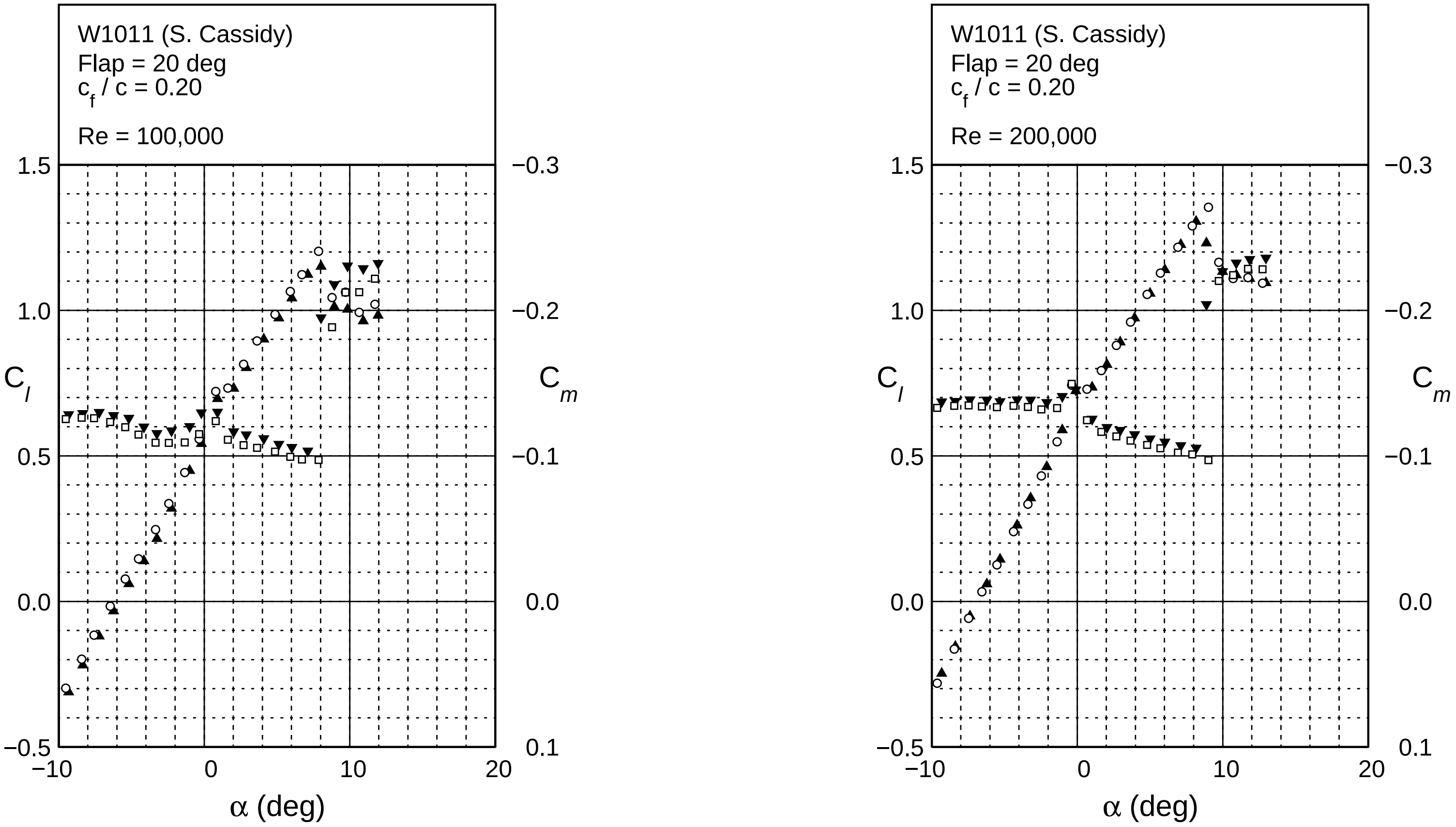

Figure 6.125: Lift and moment characteristics for the W1011 ($c_f/c = 20\%$) with a 20 deg flap.

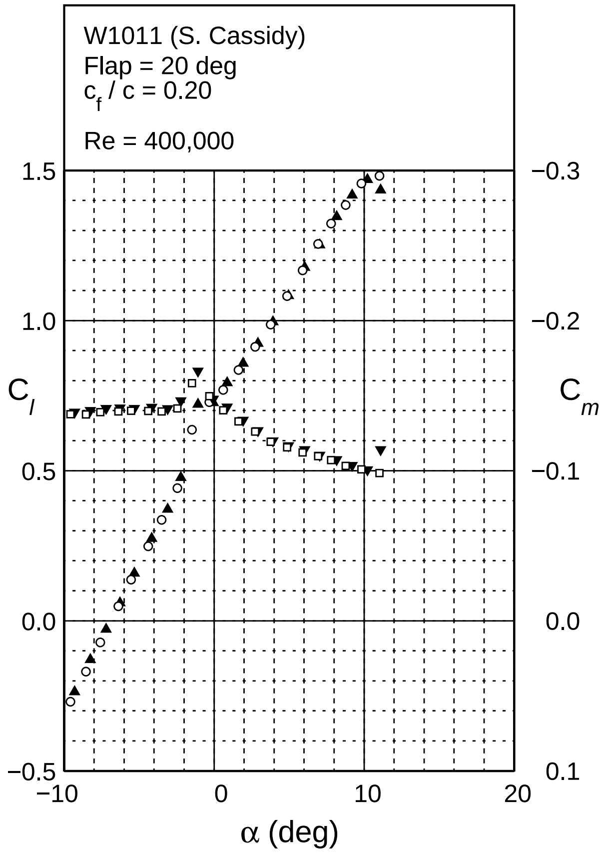

Figure 6.125: Continued.

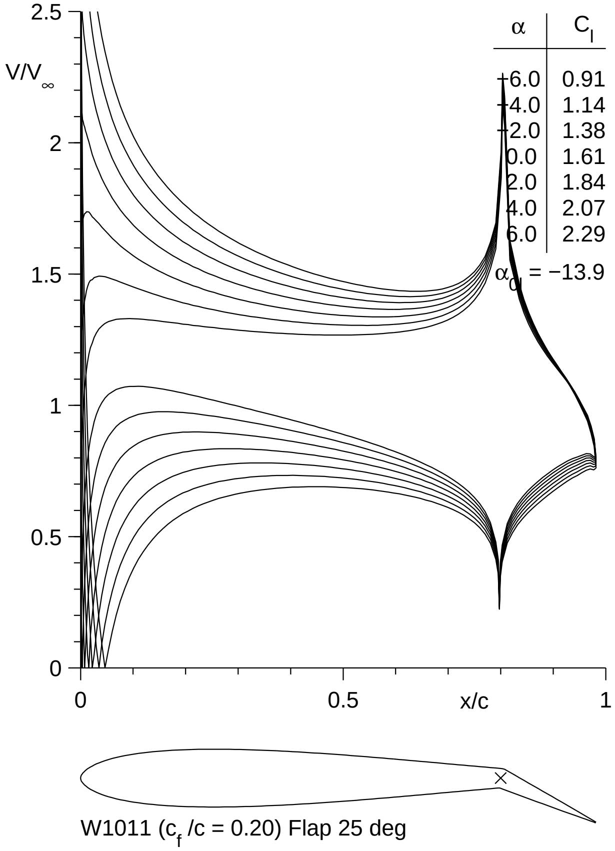

Figure 6.126: Inviscid velocity distribution for the W1011 ($c_f/c = 20\%$) with a 25 deg flap.

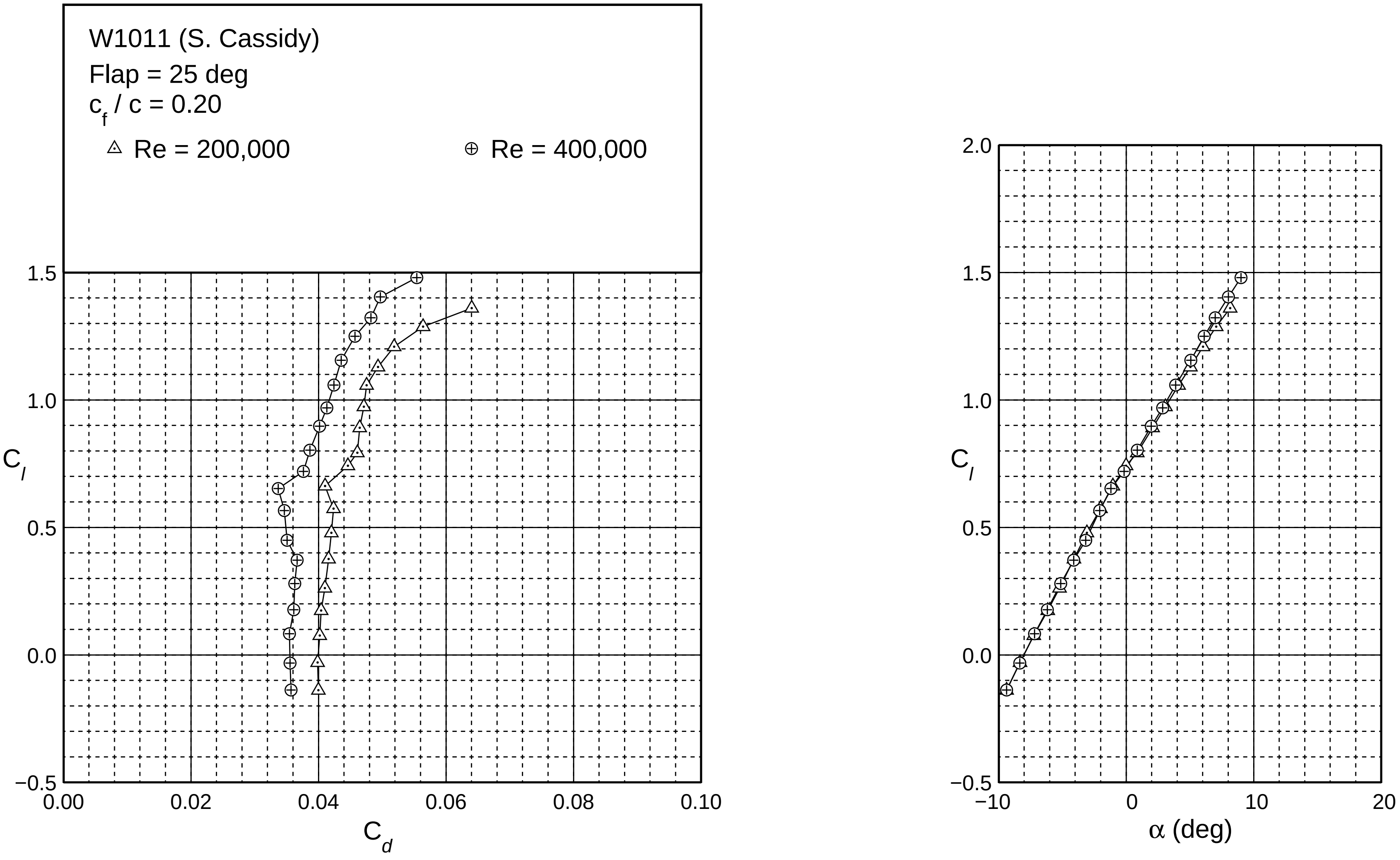

Figure 6.127: Drag polar for the W1011 ($c_f/c = 20\%$) with a 25 deg flap.

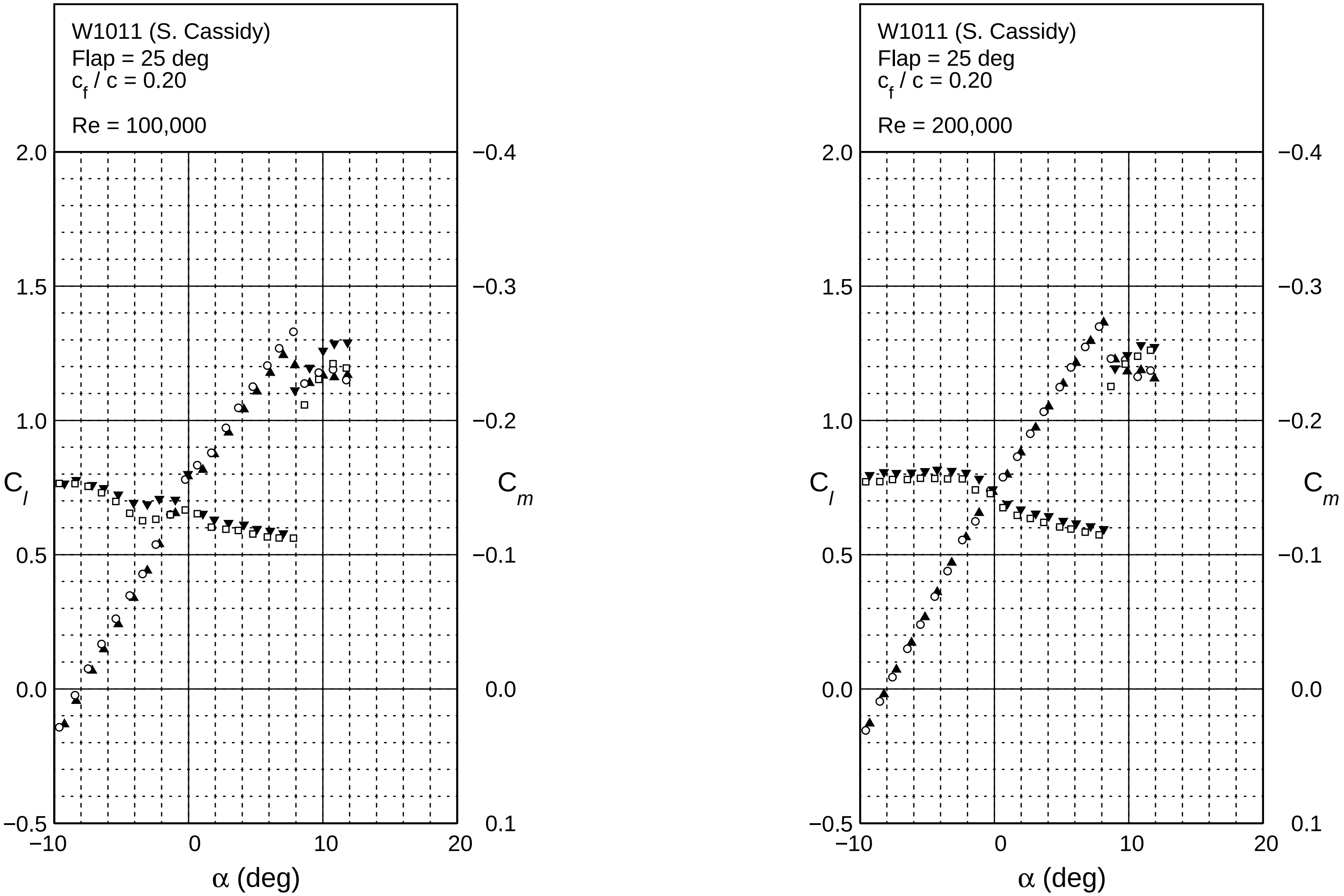

Figure 6.128: Lift and moment characteristics for the W1011 ($c_f/c = 20\%$) with a 25 deg flap.

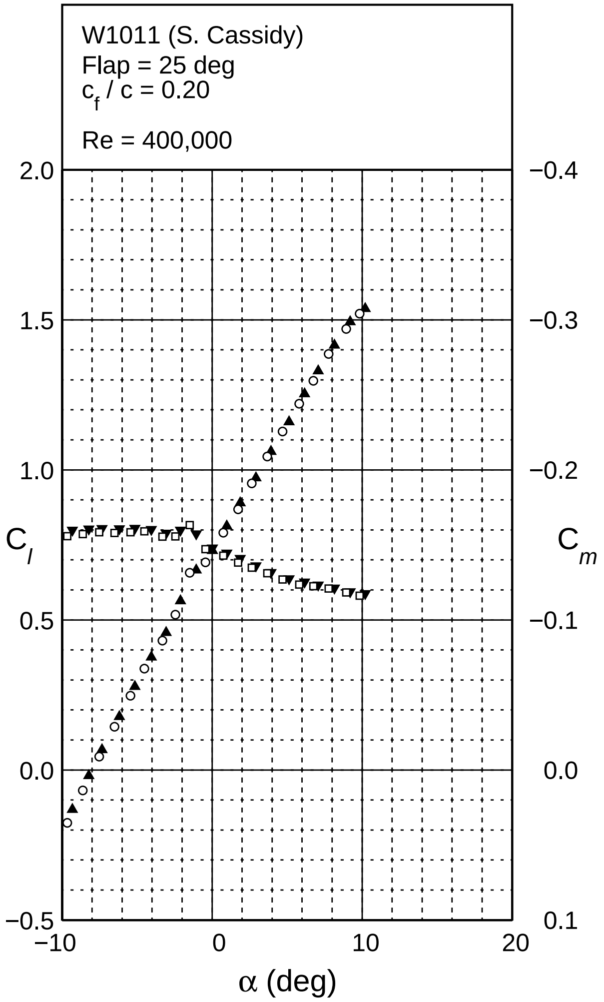

Figure 6.128: Continued.

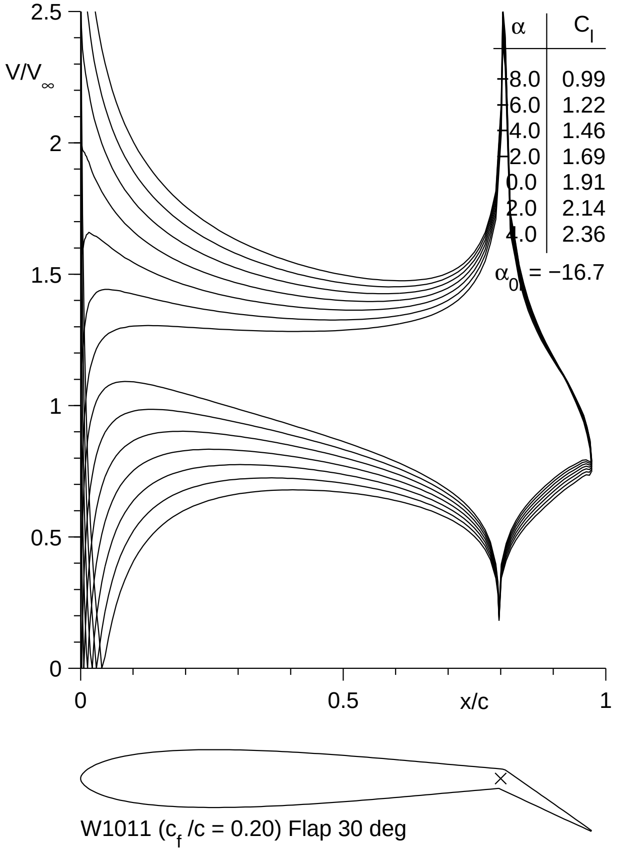

Figure 6.129: Inviscid velocity distribution for the W1011 ($c_f/c = 20\%$) with a 30 deg flap.

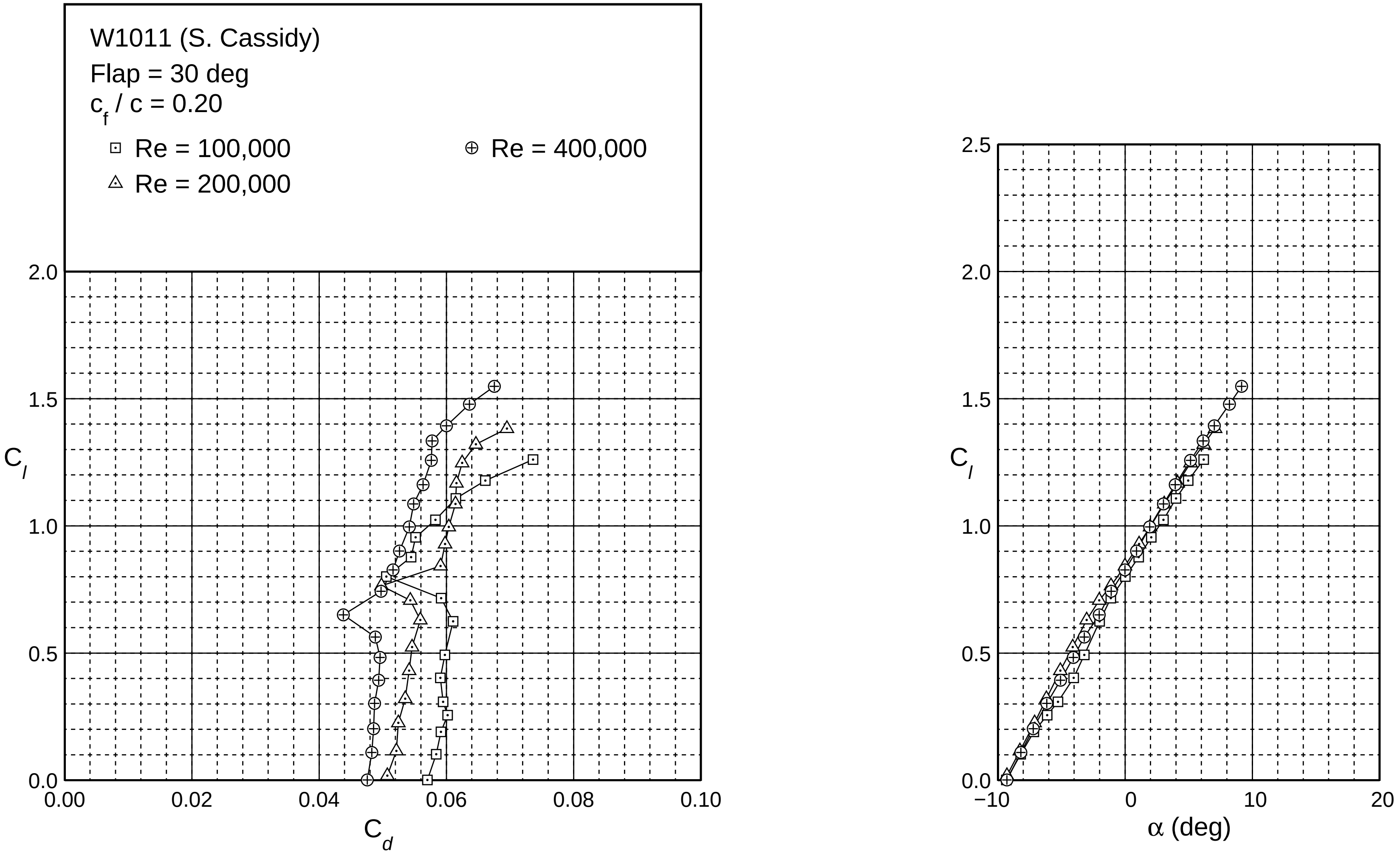

Figure 6.130: Drag polar for the W1011 ($c_f/c = 20\%$) with a 30 deg flap.

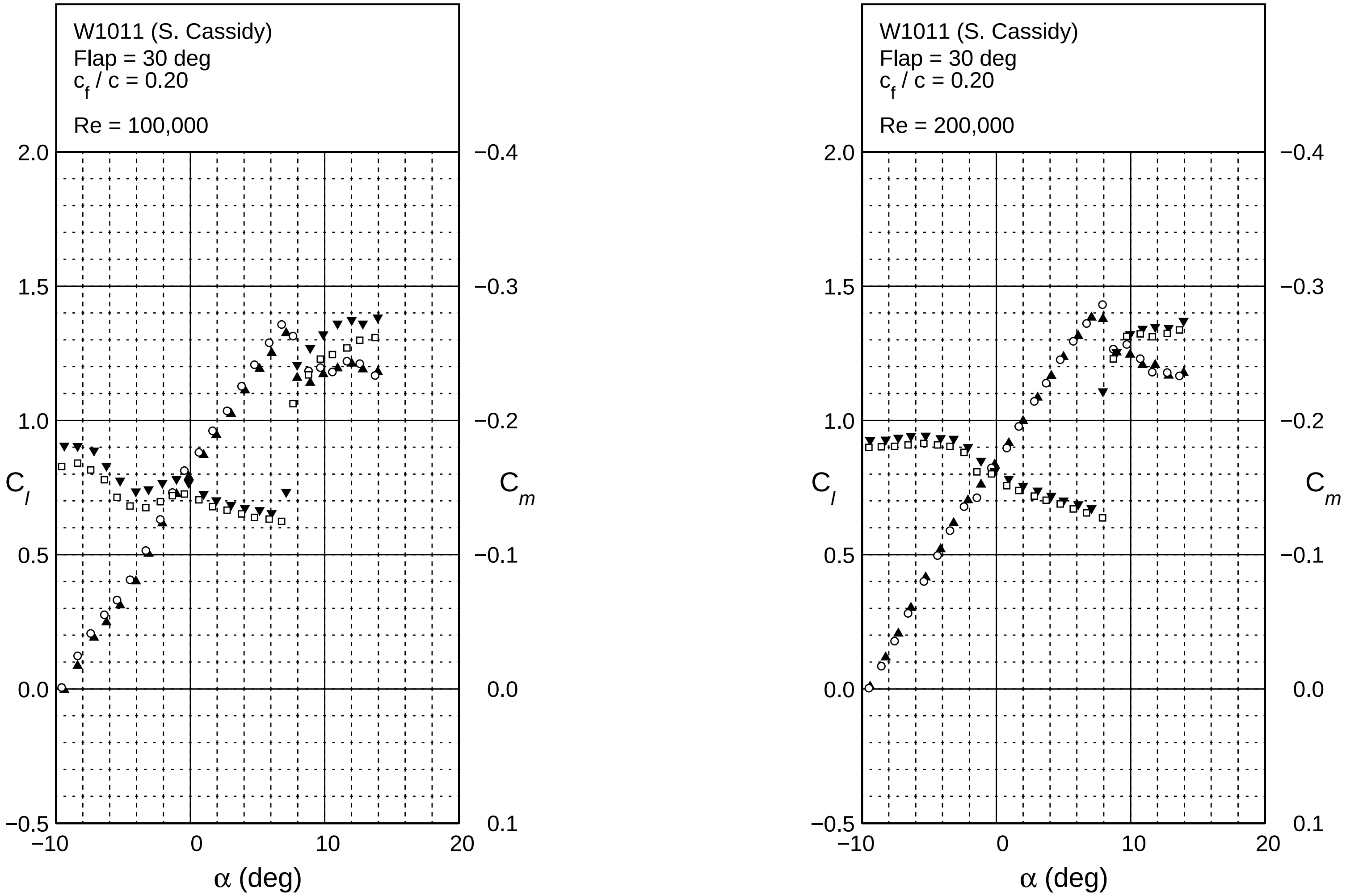

Figure 6.131: Lift and moment characteristics for the W1011 ($c_f/c = 20\%$) with a 30 deg flap.

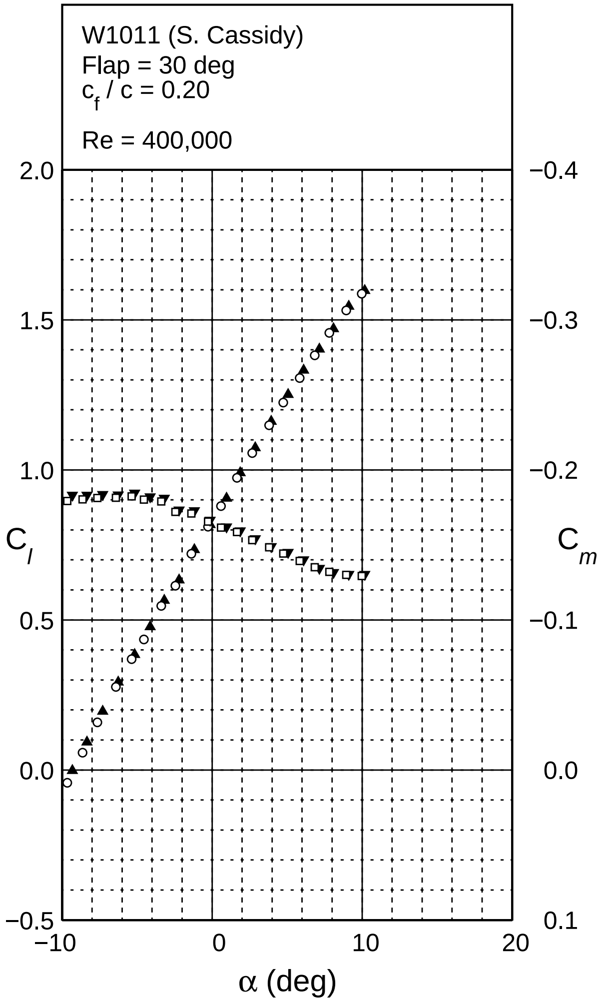

Figure 6.131: Continued.

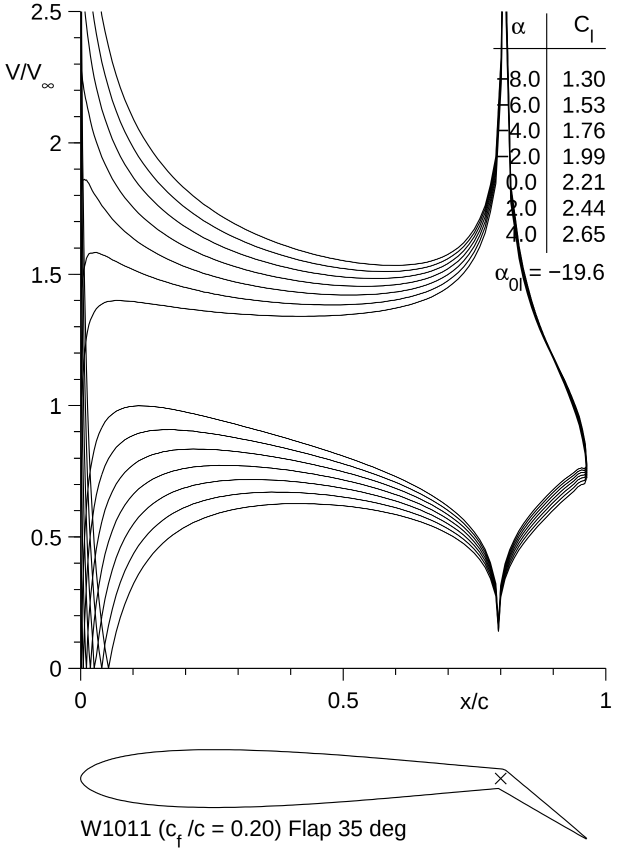

Figure 6.132: Inviscid velocity distribution for the W1011 ($c_f/c = 20\%$) with a 35 deg flap.

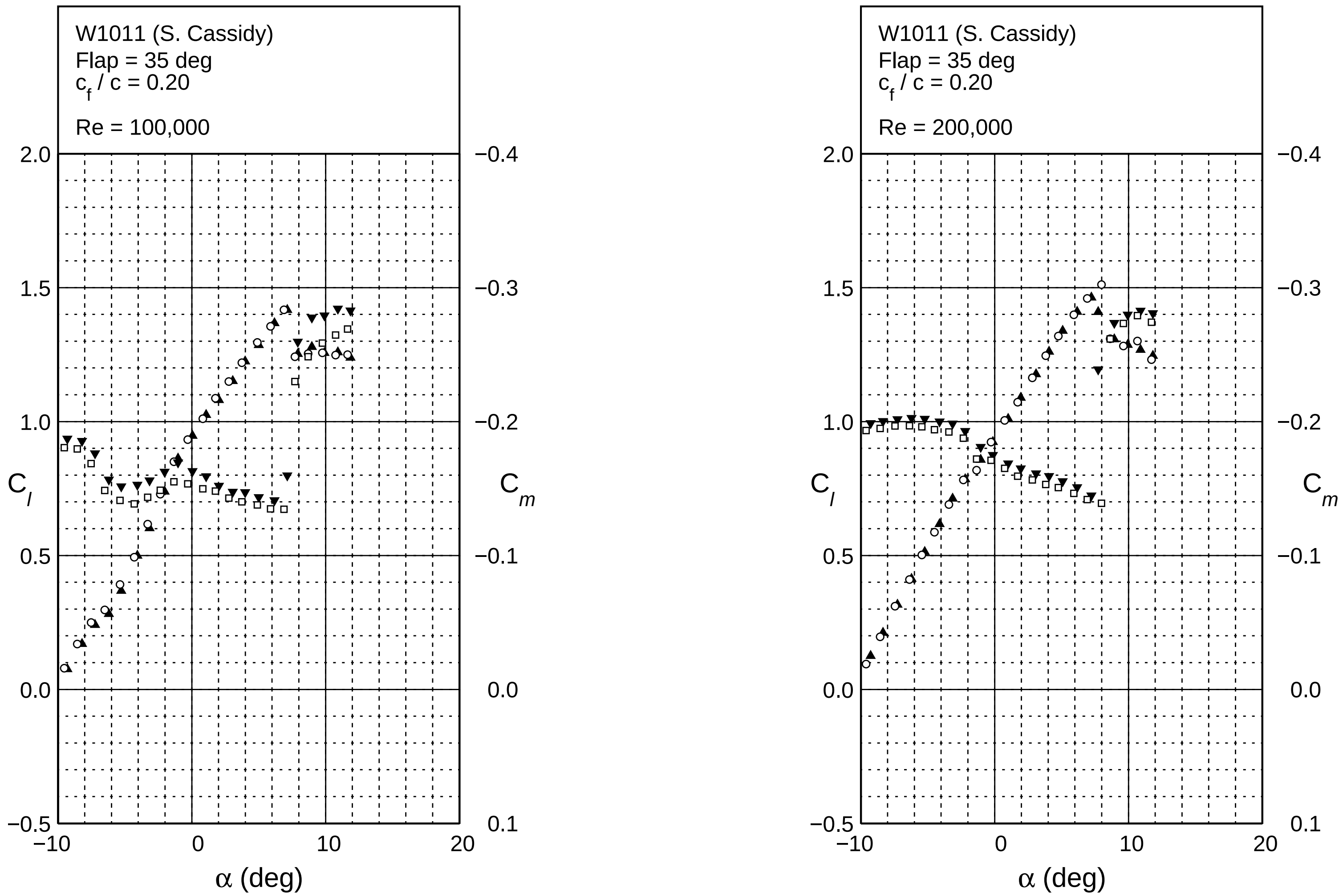

Figure 6.133: Lift and moment characteristics for the W1011 ($c_f/c = 20\%$) with a 35 deg flap.

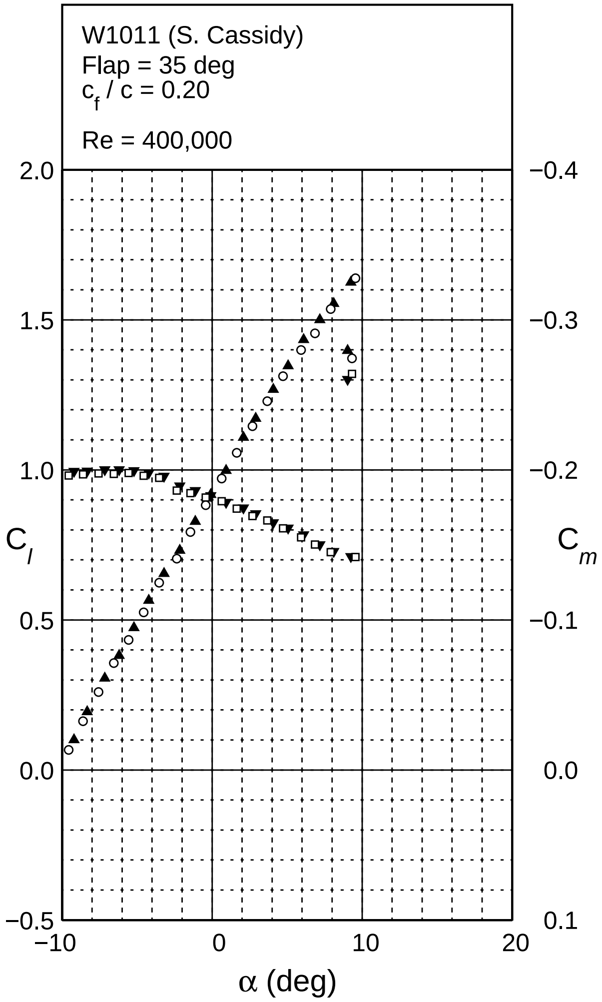

Figure 6.133: Continued.

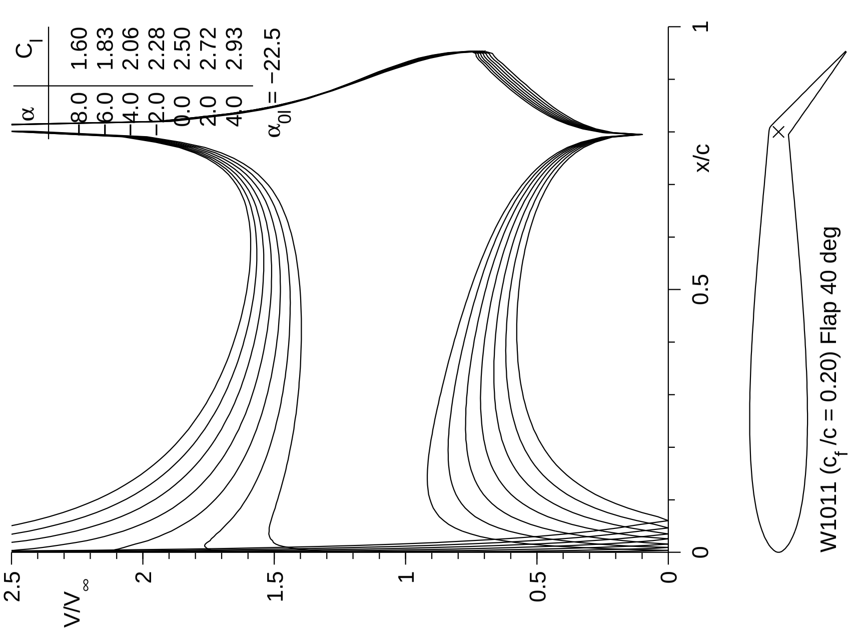

Figure 6.134: Inviscid velocity distribution for the W1011 $(c_f/c\ =\ 20\%)$ with a 40 deg flap.

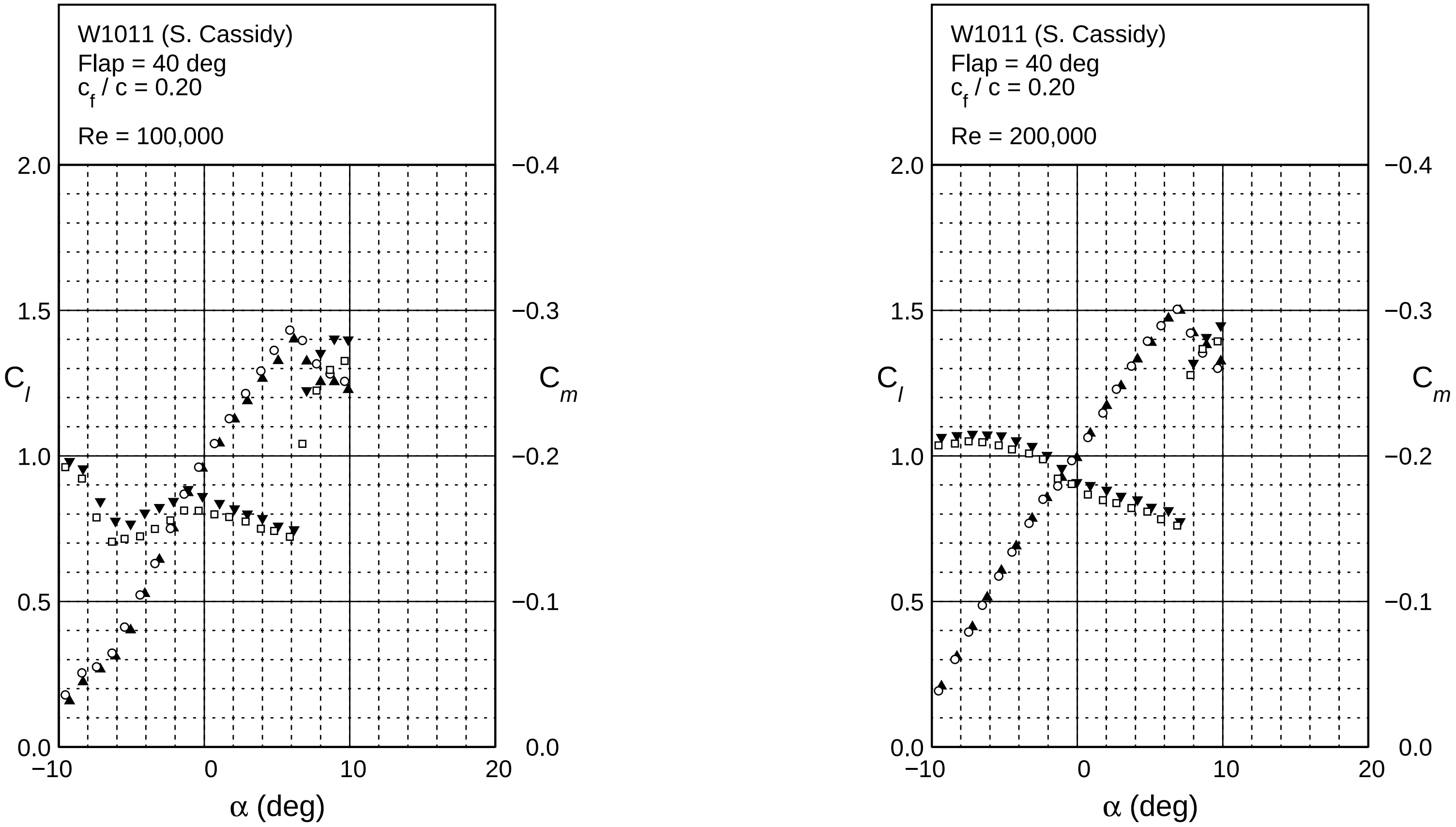

Figure 6.135: Lift and moment characteristics for the W1011 ($c_f/c = 20\%$) with a 40 deg flap.

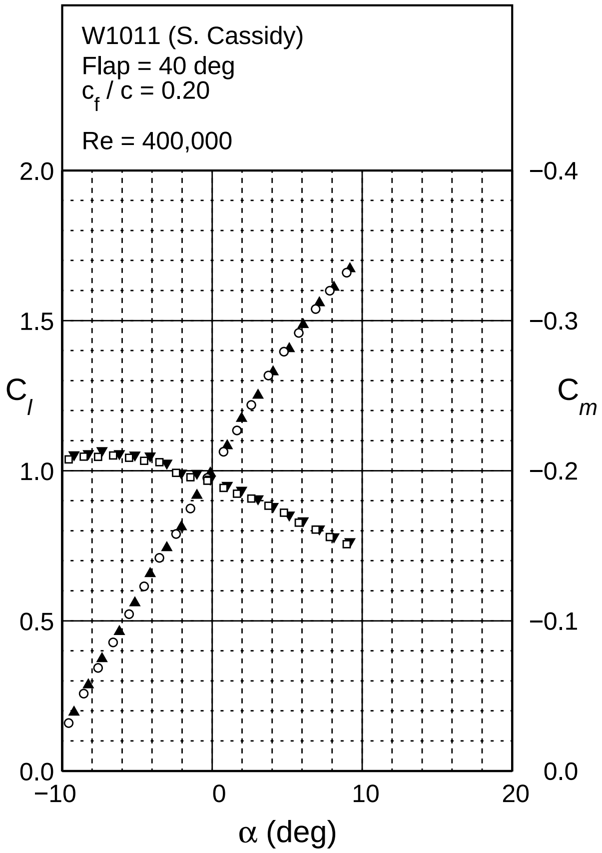

Figure 6.135: Continued.

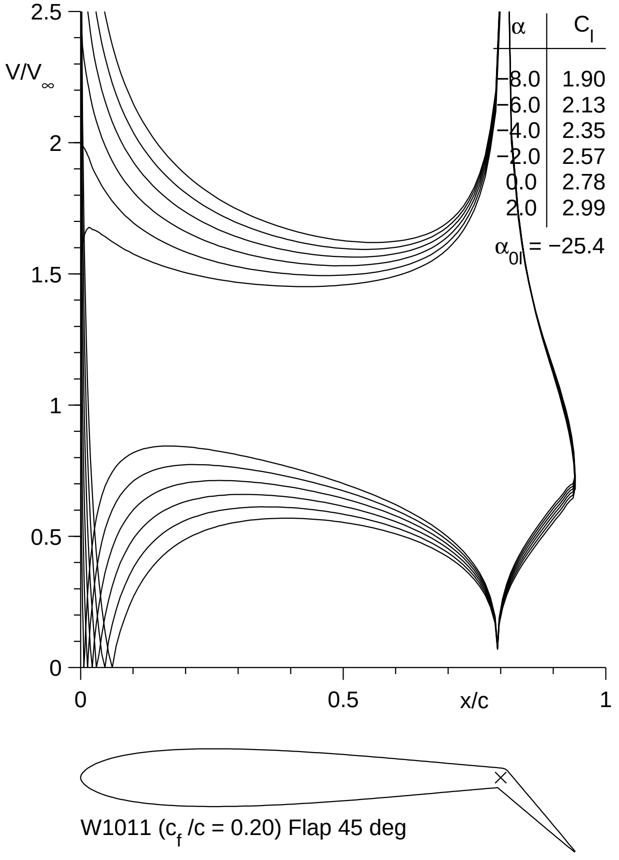

Figure 6.136: Inviscid velocity distribution for the W1011 ($c_f/c = 20\%$) with a 45 deg flap.

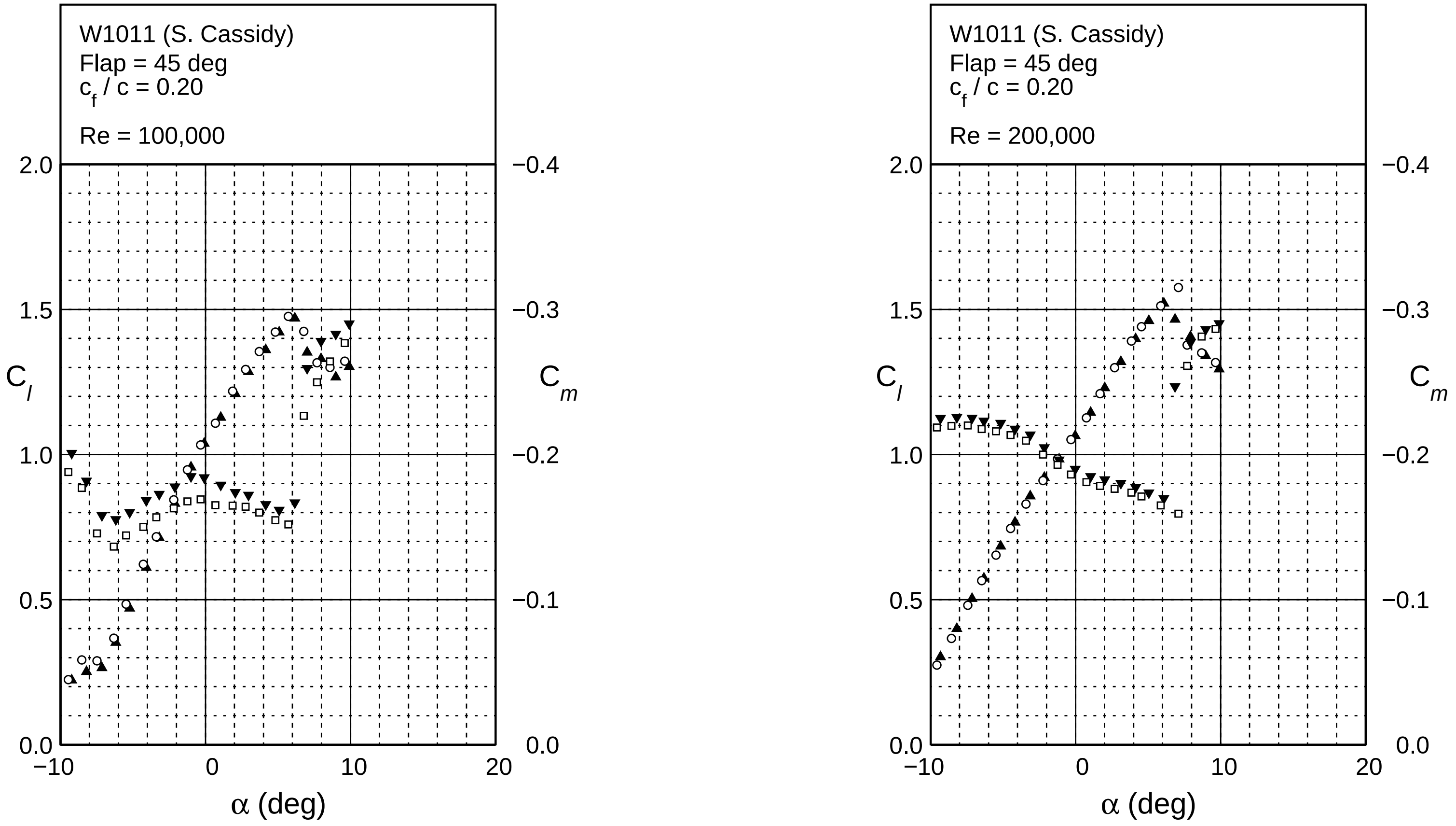

Figure 6.137: Lift and moment characteristics for the W1011 ($c_f/c = 20\%$) with a 45 deg flap.

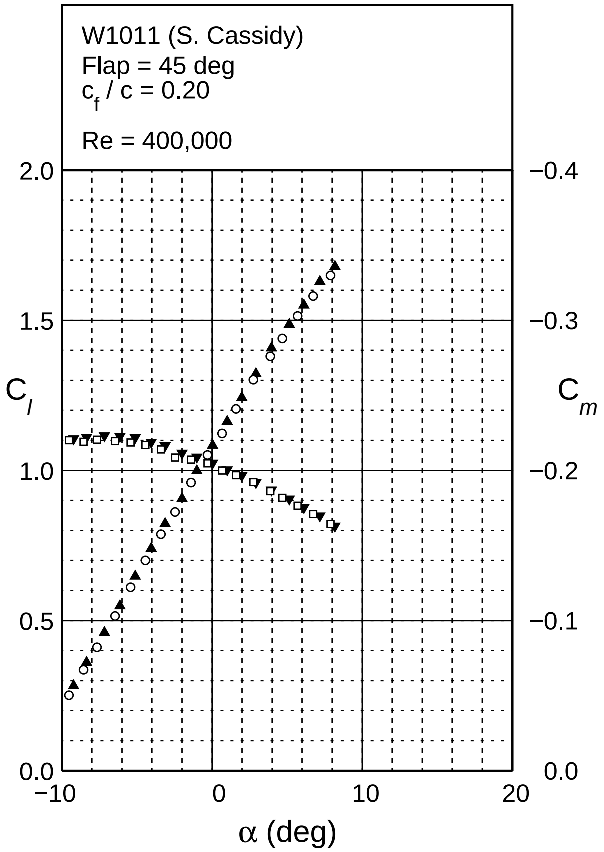

Figure 6.137: Continued.

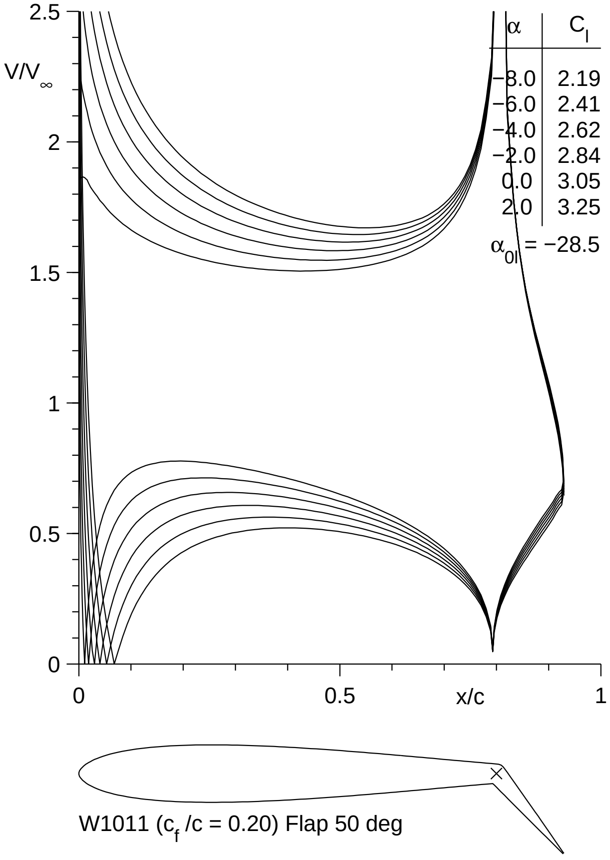

Figure 6.138: Inviscid velocity distribution for the W1011 ($c_f/c = 20\%$) with a 50 deg flap.

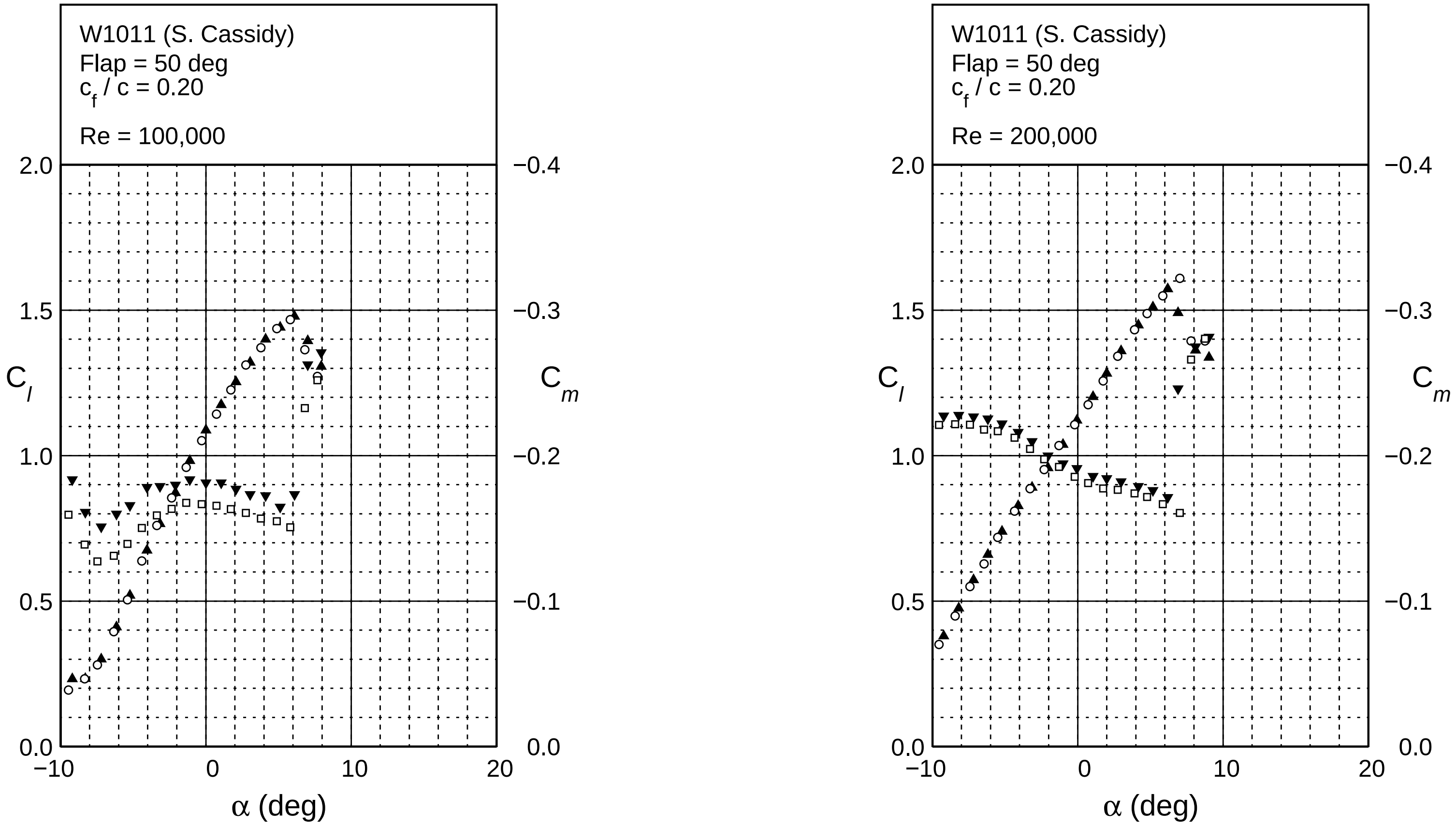

Figure 6.139: Lift and moment characteristics for the W1011 (c_f/c = 20%) with a 50 deg flap

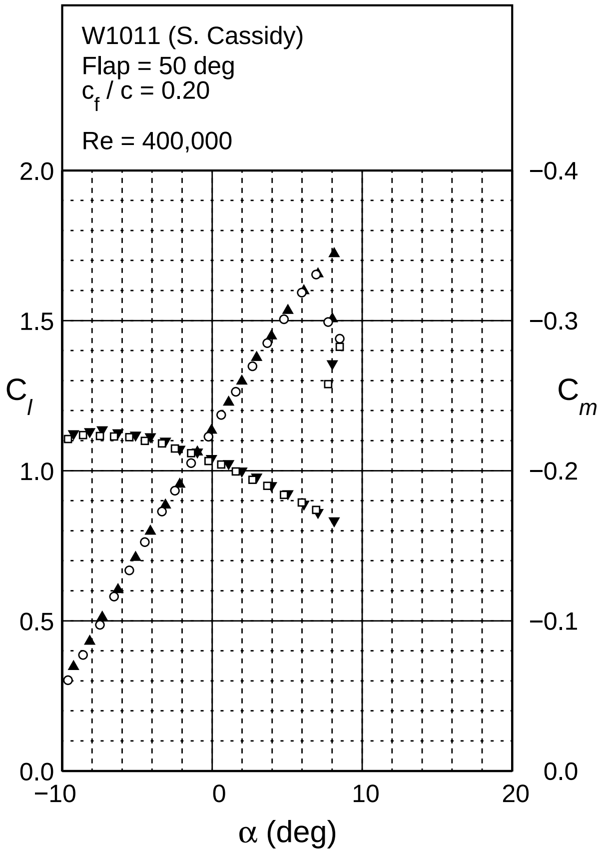

Figure 6.139: Continued.

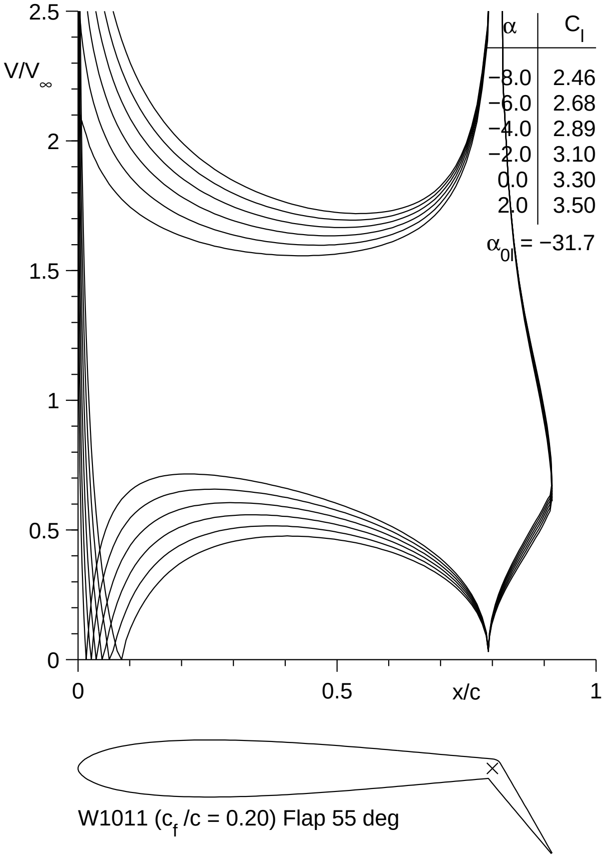

Figure 6.140: Inviscid velocity distribution for the W1011 ($c_f/c = 20\%$) with a 55 deg flap.

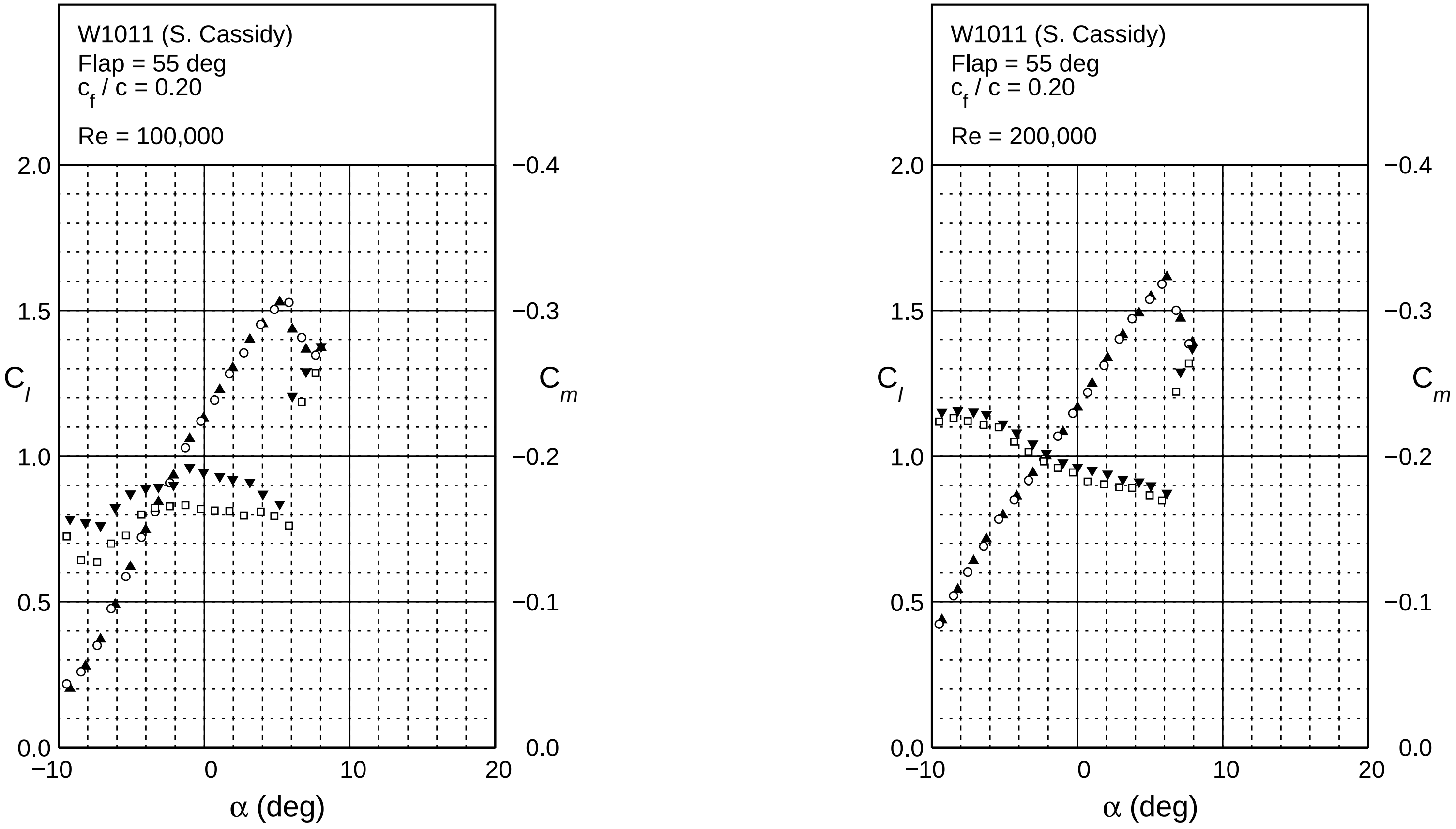

Figure 6.141: Lift and moment characteristics for the W1011 ($c_f/c = 20\%$) with a 55 deg flap.

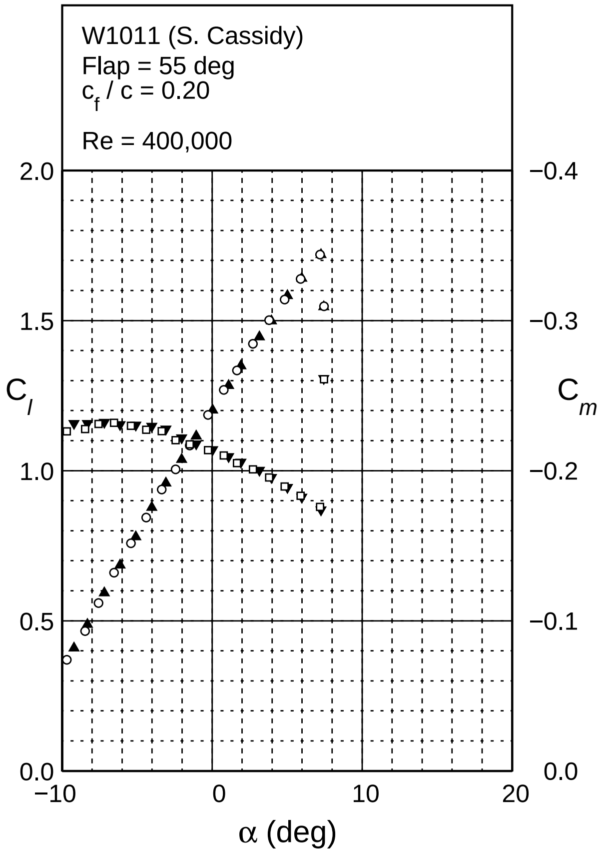

Figure 6.141: Continued.

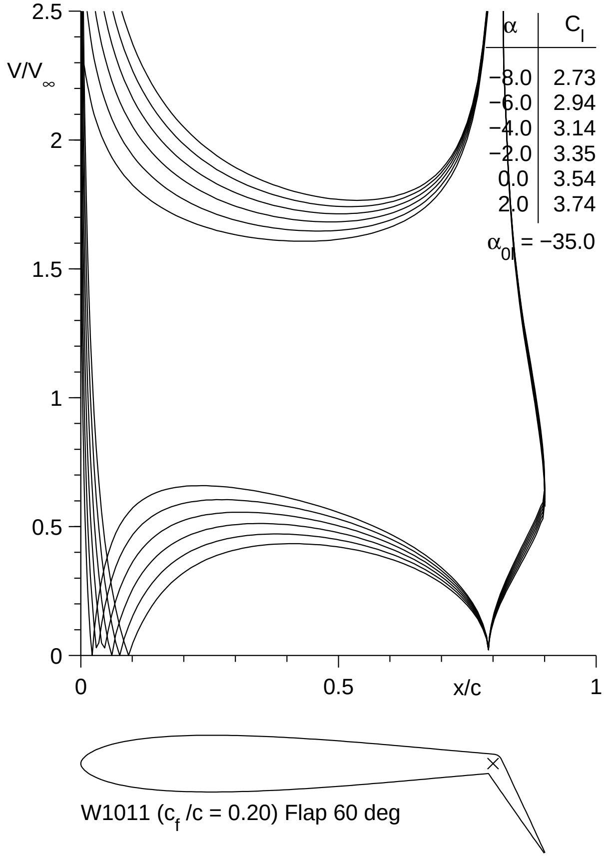

Figure 6.142: Inviscid velocity distribution for the W1011 ($c_f/c = 20\%$) with a 60 deg flap.

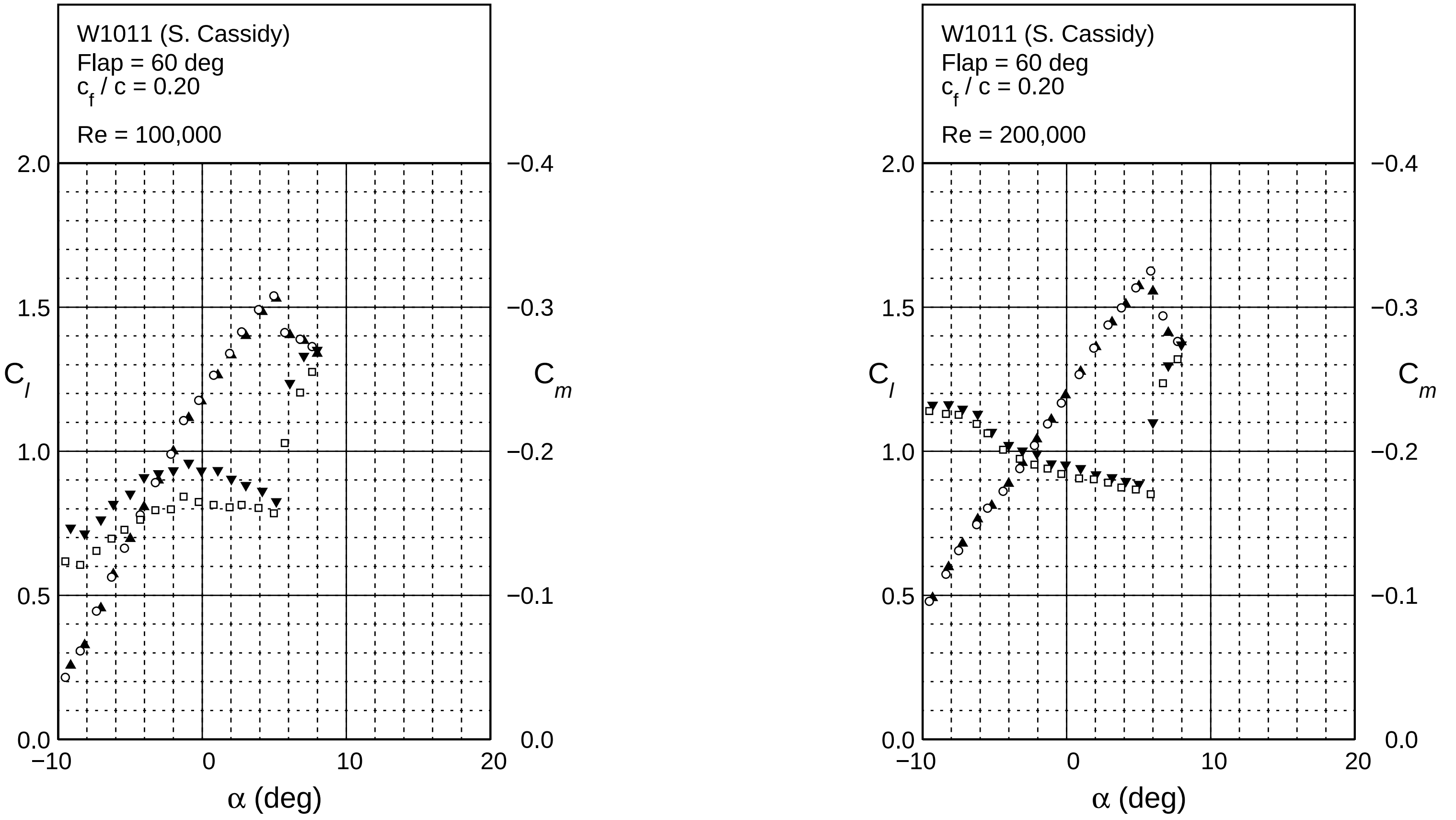

Figure 6.143: Lift and moment characteristics for the W1011 ($c_f/c = 20\%$) with a 60 deg flap.

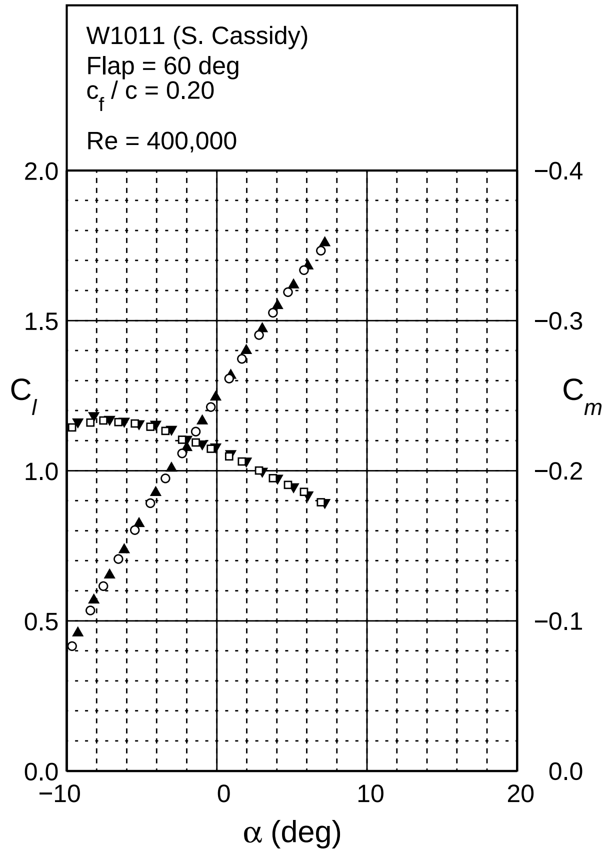

Figure 6.143: Continued.

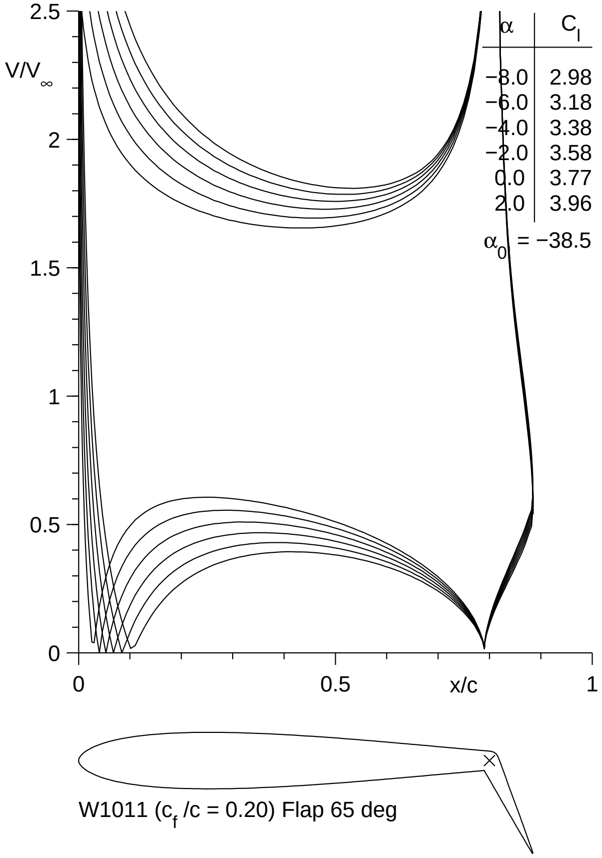

Figure 6.144: Inviscid velocity distribution for the W1011 ($c_f/c = 20\%$) with a 65 deg flap.

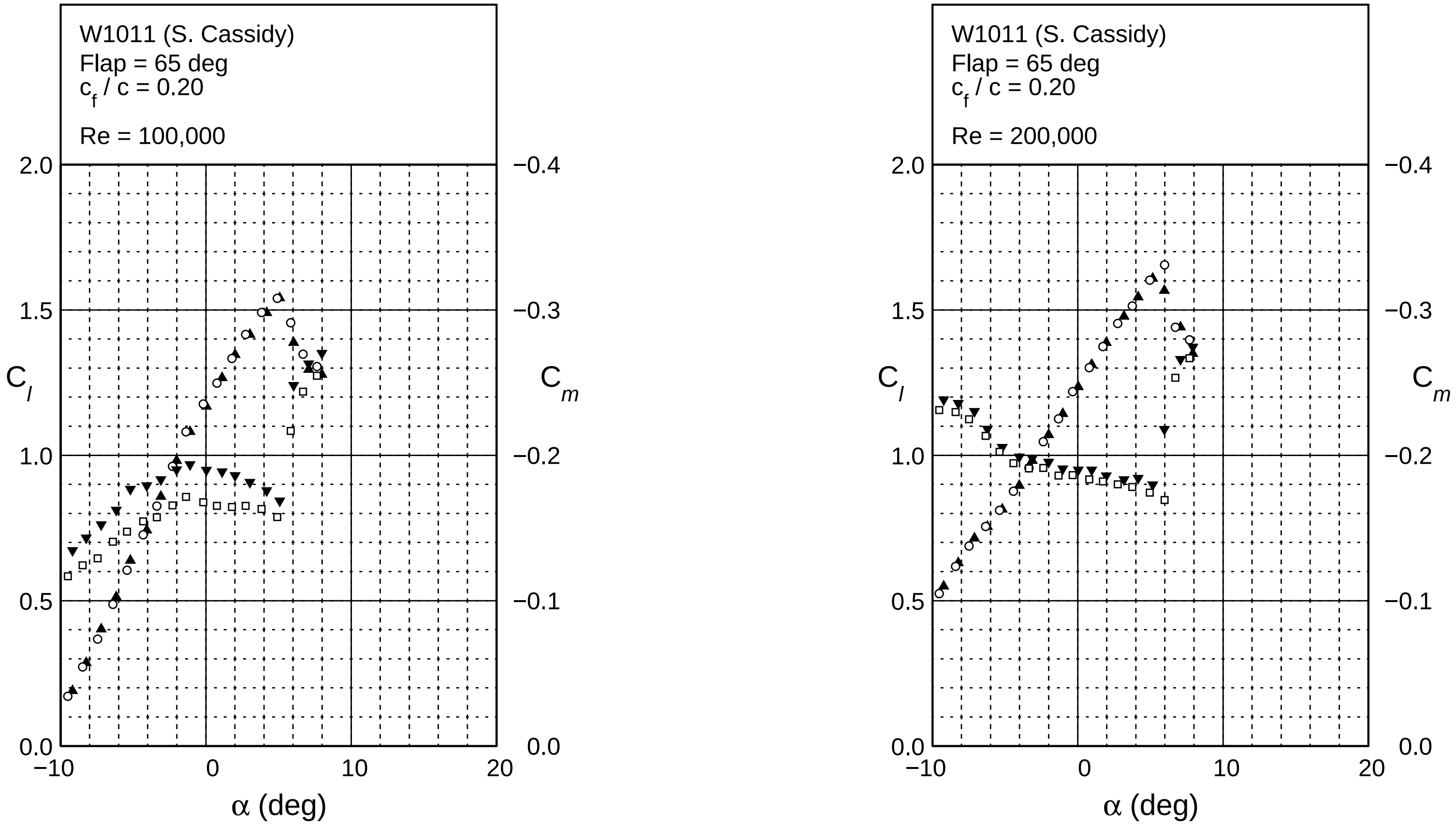

Figure 6.145: Lift and moment characteristics for the W1011 ($c_f/c = 20\%$) with a 65 deg flap.

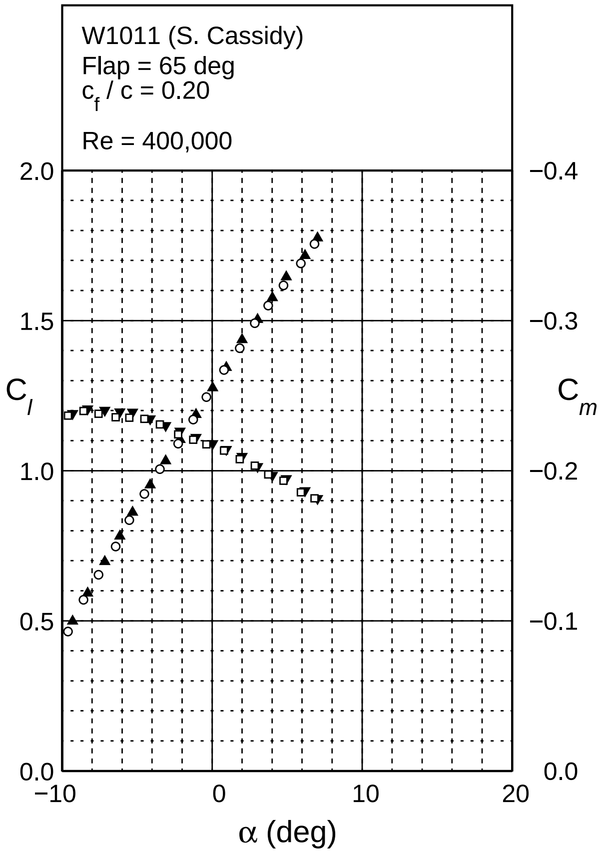

Figure 6.145: Continued.

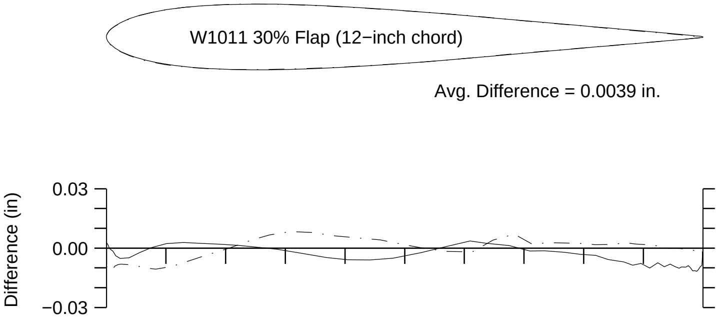

Figure 6.146: Comparison between the true and actual W1011 (c_f/c = 30%).

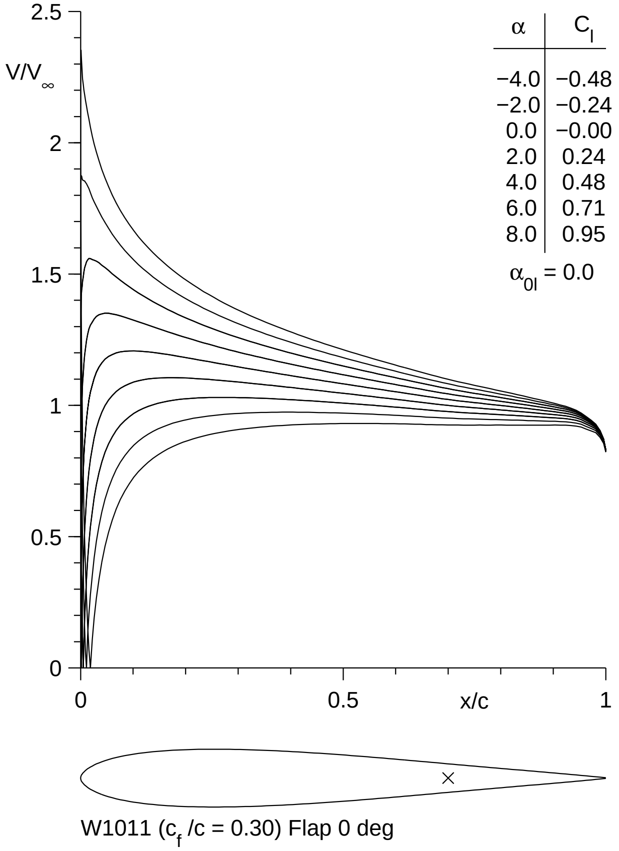

Figure 6.147: Inviscid velocity distribution for the W1011 (c_f/c = 30%).

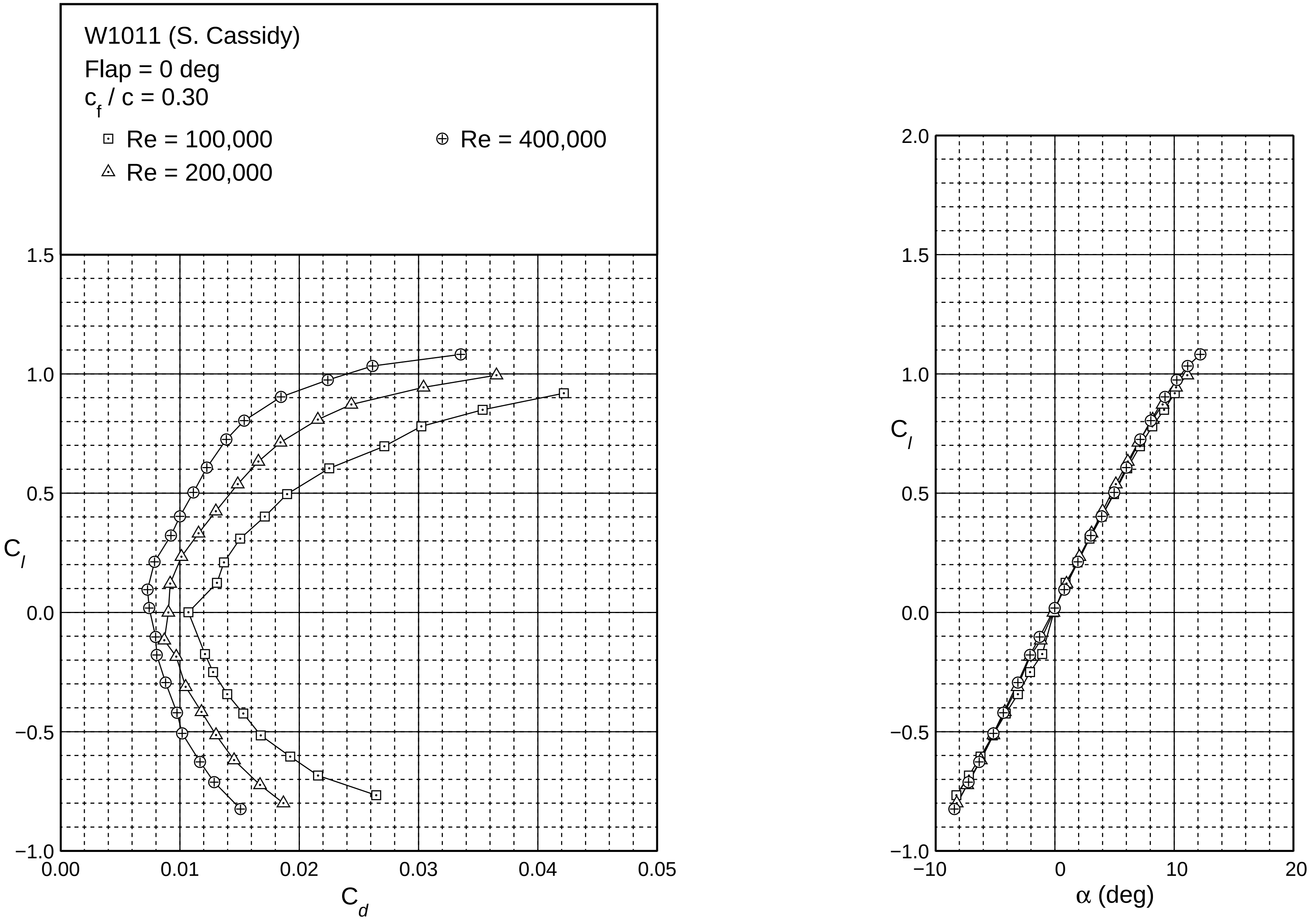

Figure 6.148: Drag polar for the W1011 ($c_f/c = 30\%$).

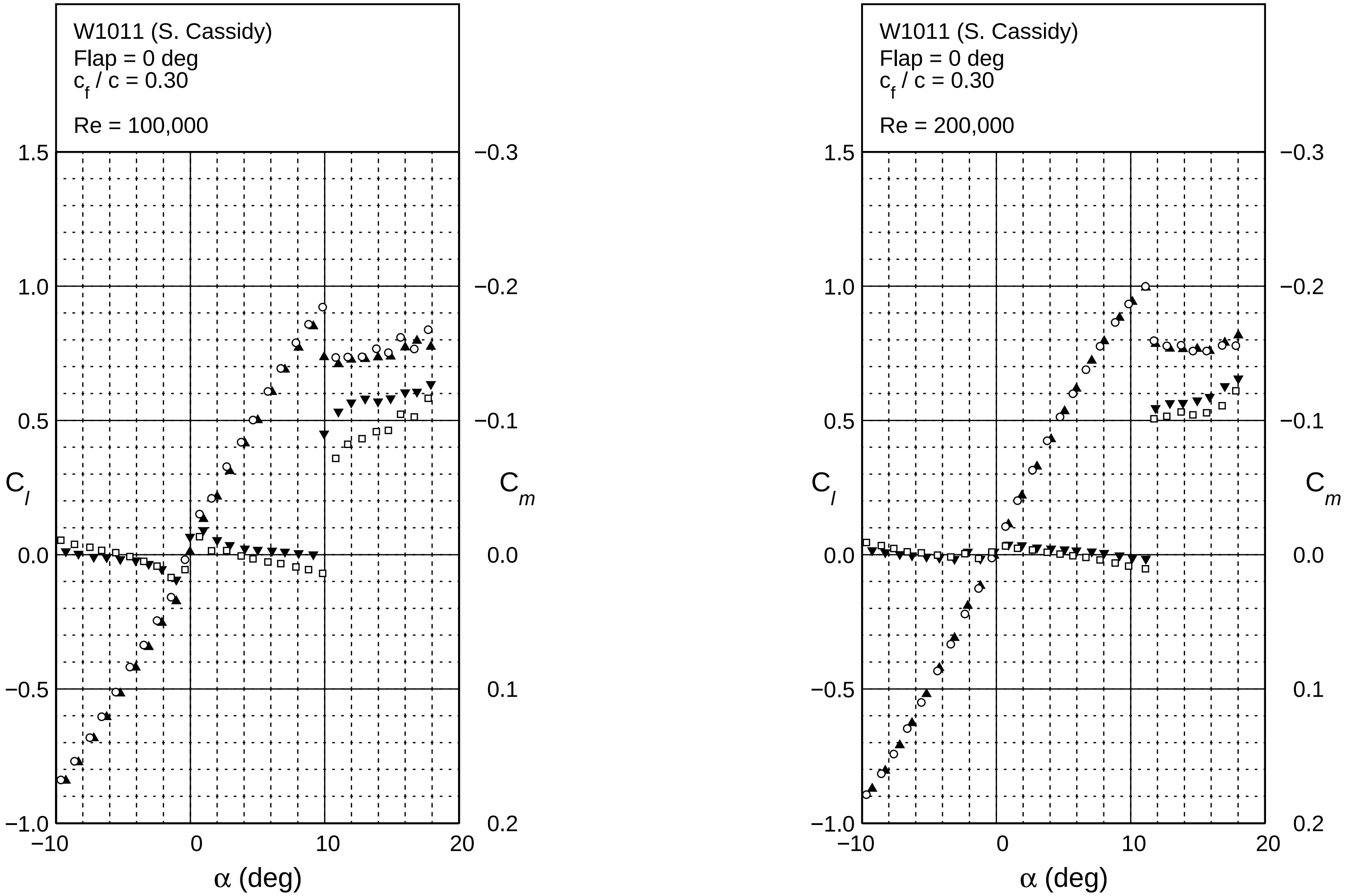

Figure 6.149: Lift and moment characteristics for the W1011 ($c_f/c = 30\%$).

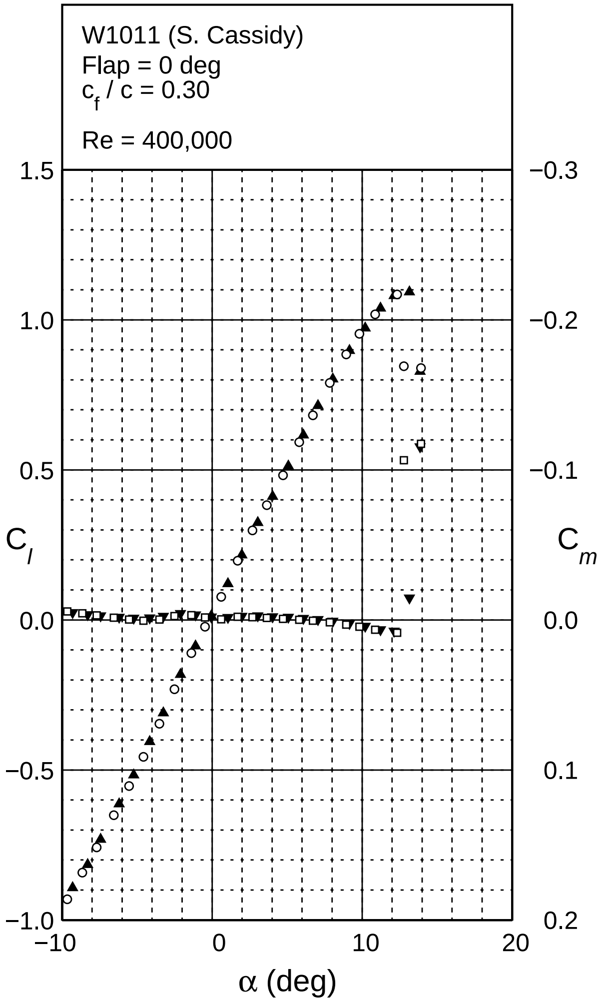

Figure 6.149: Continued.

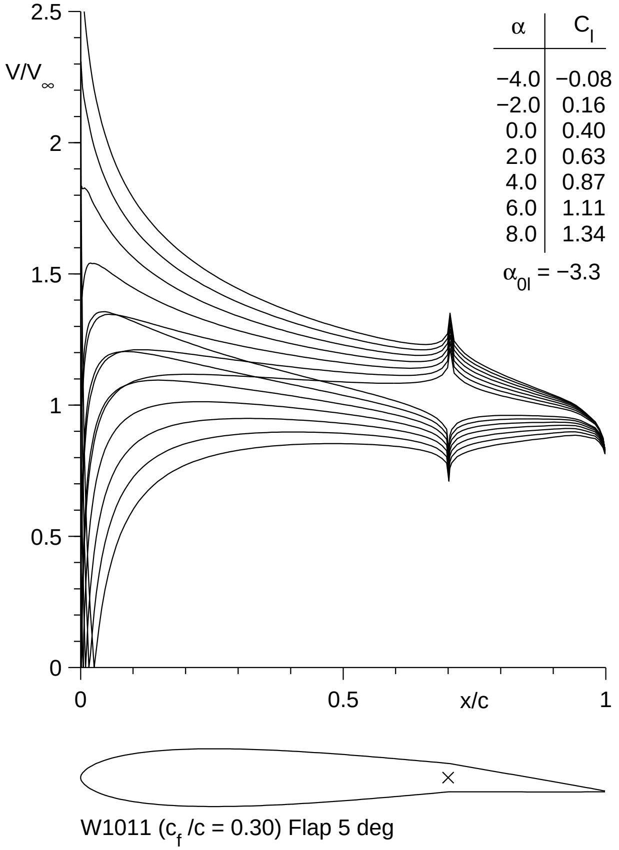

Figure 6.150: Inviscid velocity distribution for the W1011 ($c_f/c = 30\%$) with a 5 deg flap.

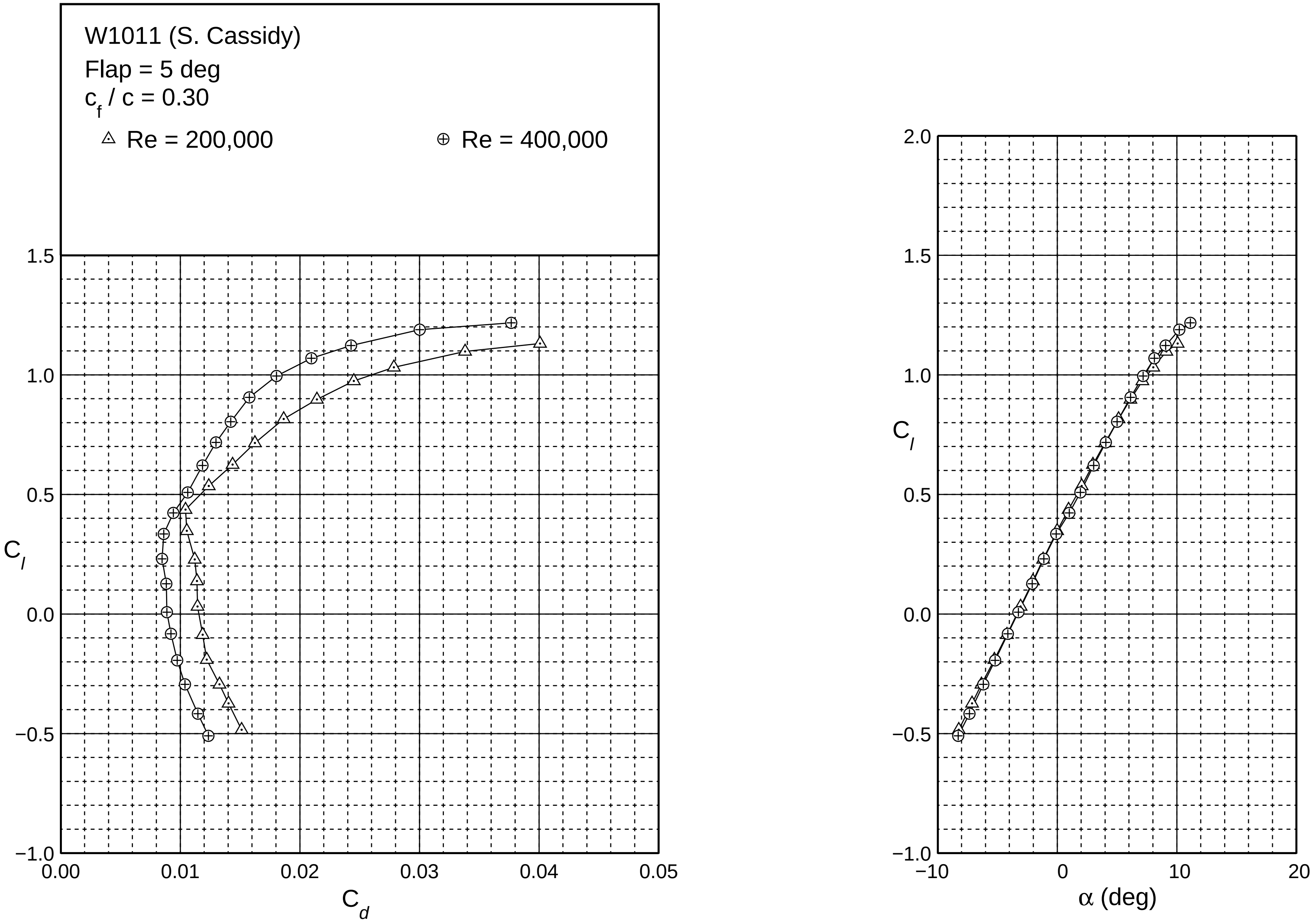

Figure 6.151: Drag polar for the W1011 ($c_f/c = 30\%$) with a 5 deg flap.

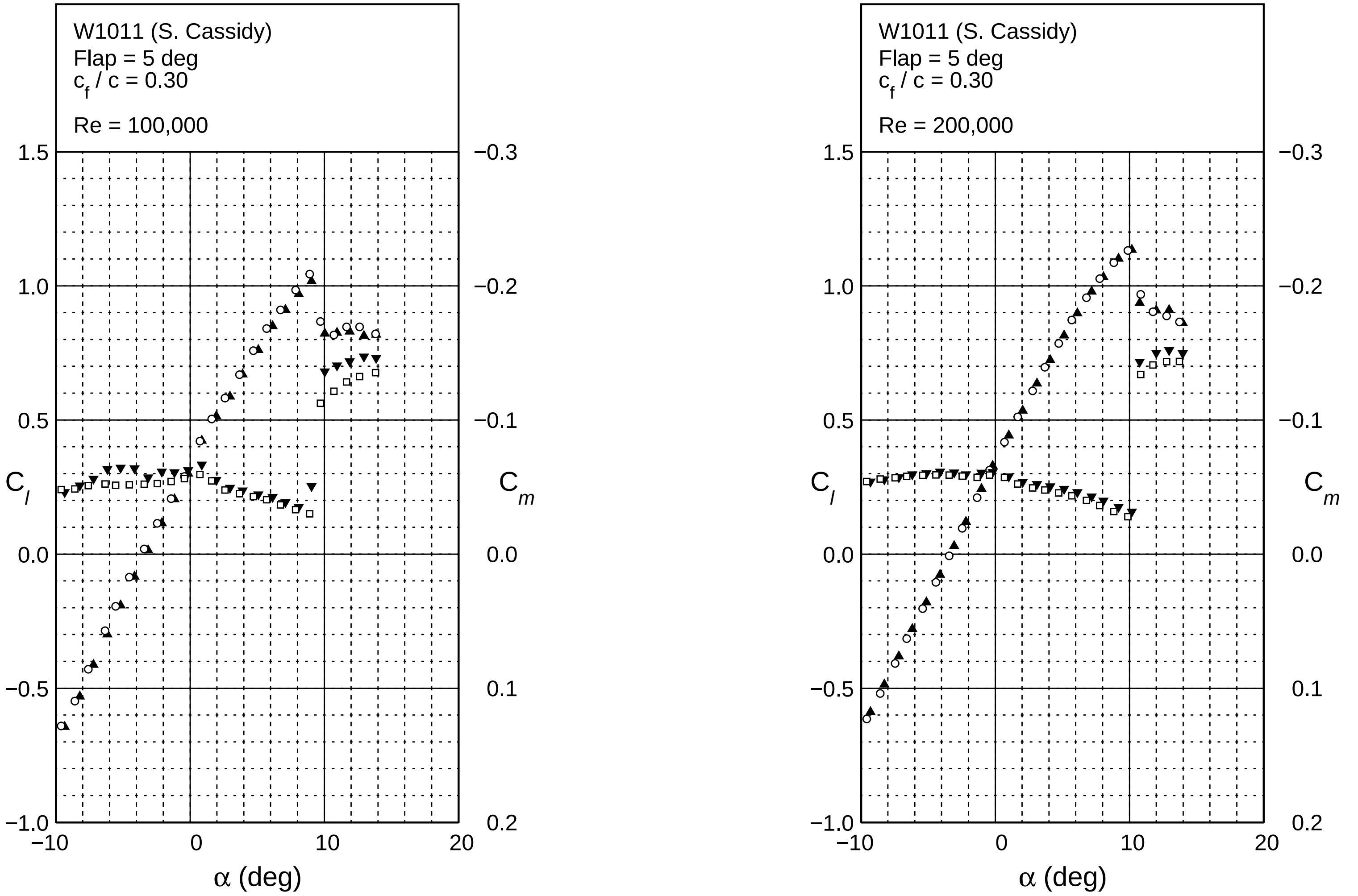

Figure 6.152: Lift and moment characteristics for the W1011 ($c_f/c = 30\%$) with a 5 deg flap.

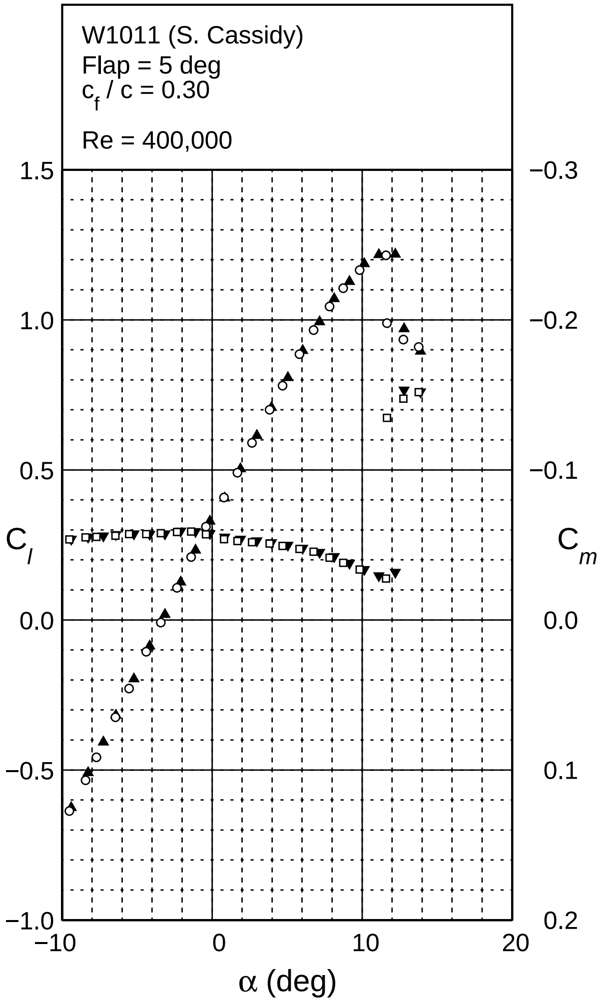

Figure 6.152: Continued.

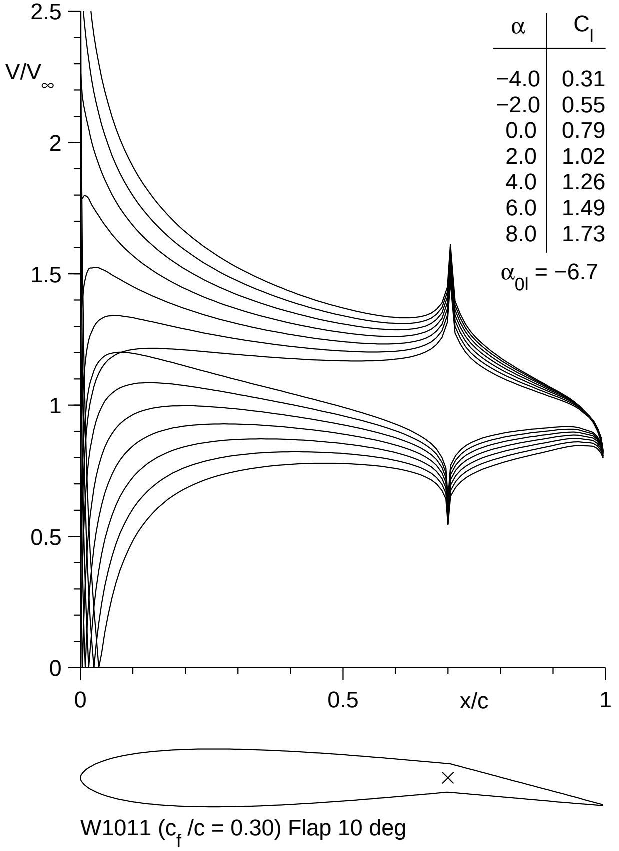

Figure 6.153: Inviscid velocity distribution for the W1011 ($c_f/c = 30\%$) with a 10 deg flap.

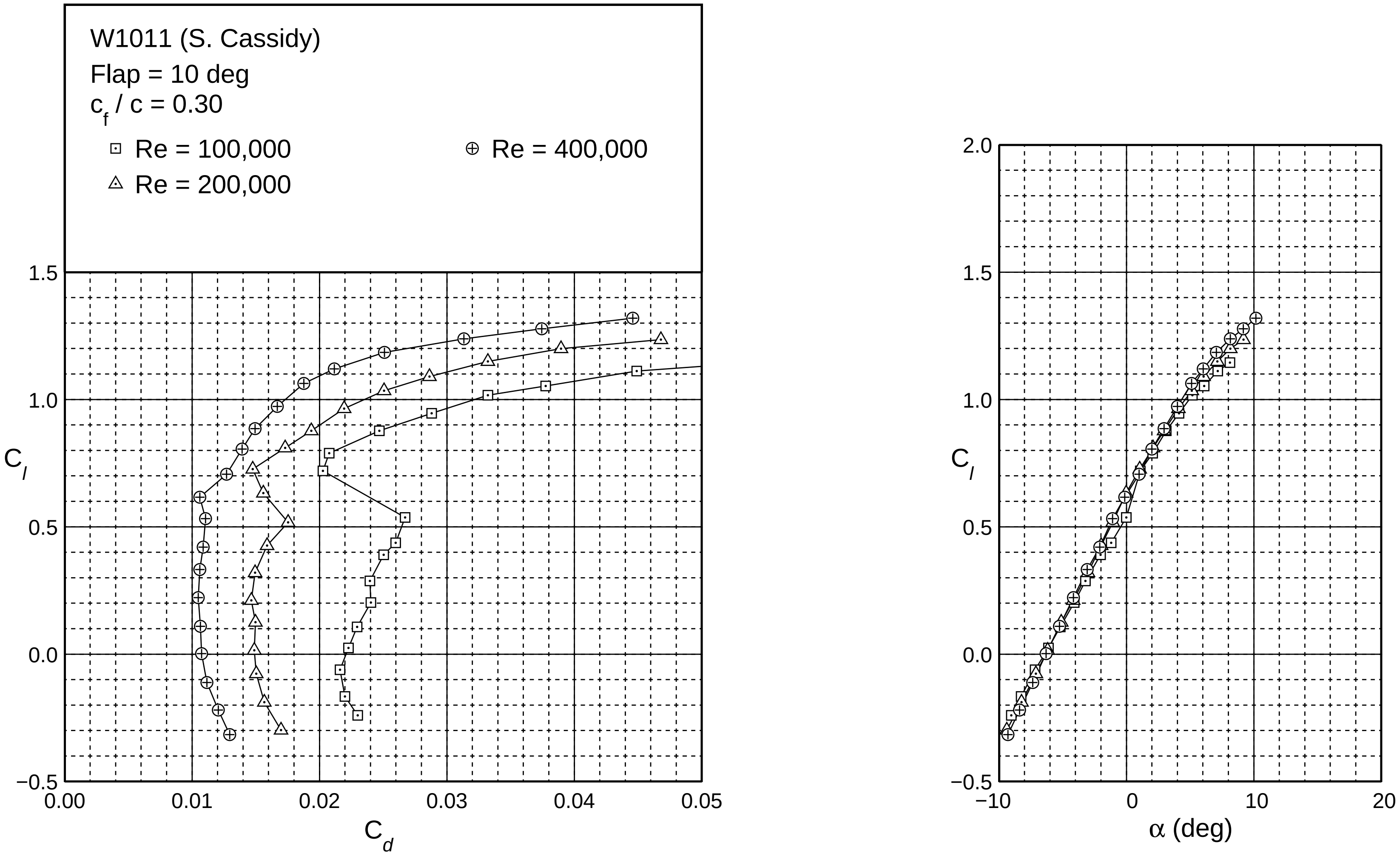

Figure 6.154: Drag polar for the W1011 (c_f/c = 30%) with a 10 deg flap.

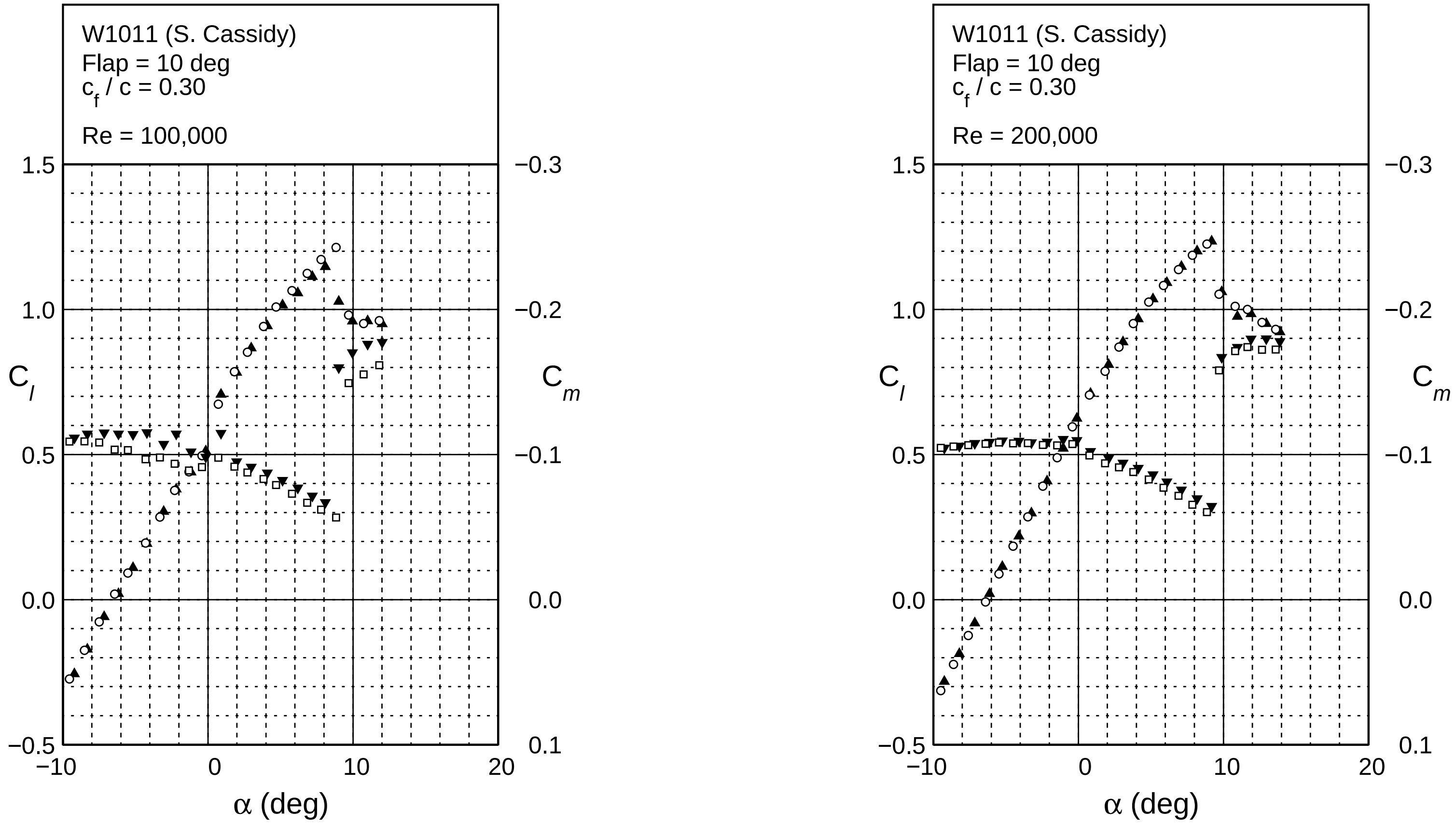

Figure 6.155: Lift and moment characteristics for the W1011 ($c_f/c = 30\%$) with a 10 deg flap.

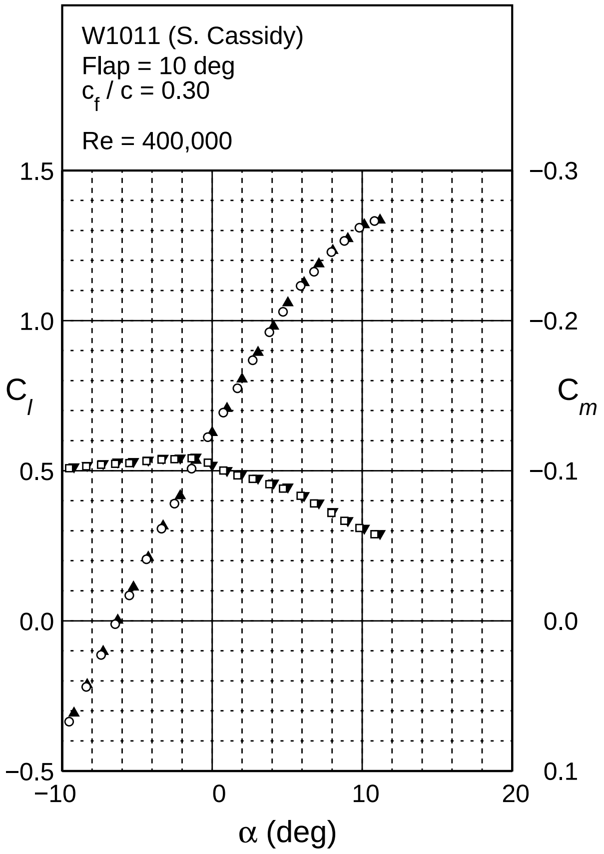

Figure 6.155: Continued.

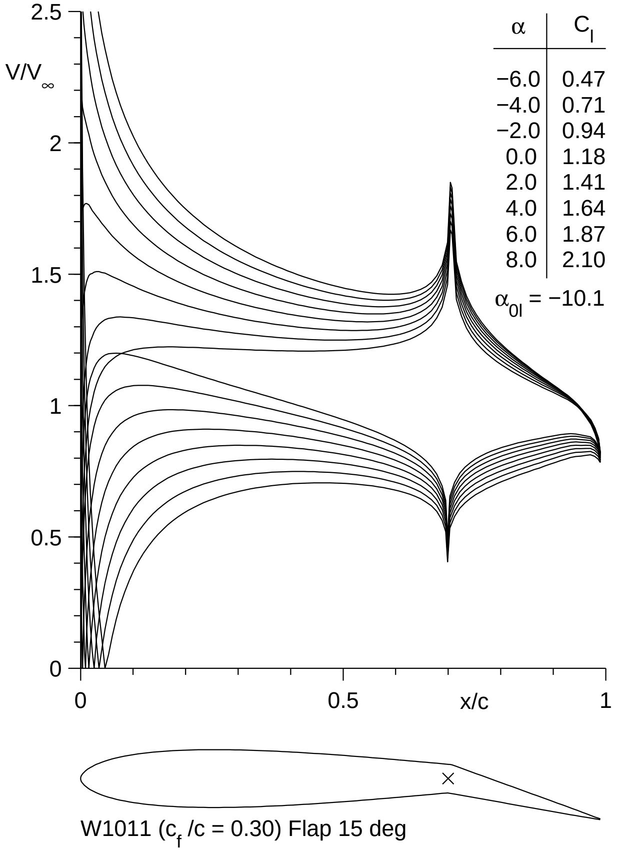

Figure 6.156: Inviscid velocity distribution for the W1011 ($c_f/c = 30\%$) with a 15 deg flap.

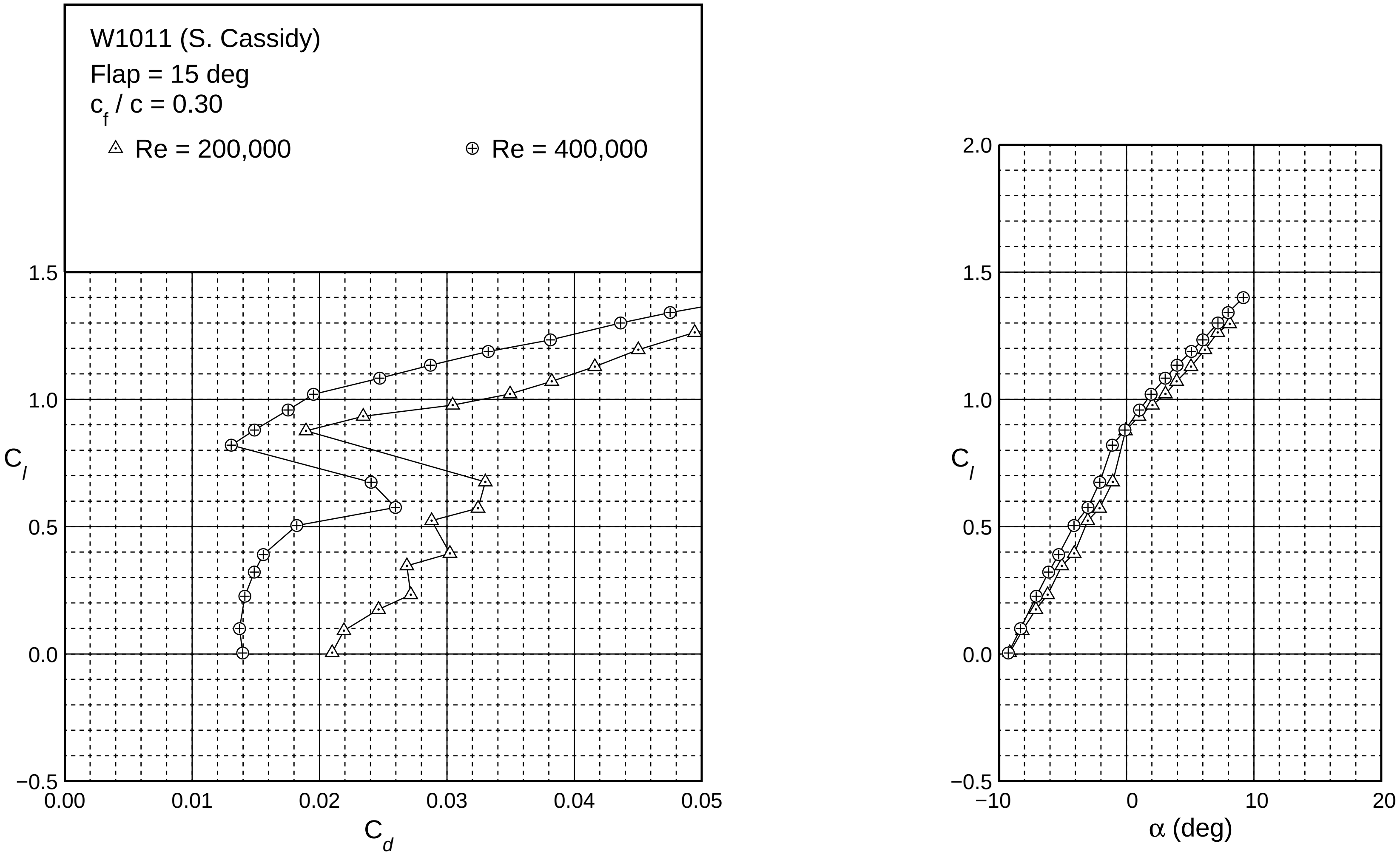

Figure 6.157: Drag polar for the W1011 ($c_f/c = 30\%$) with a 15 deg flap.

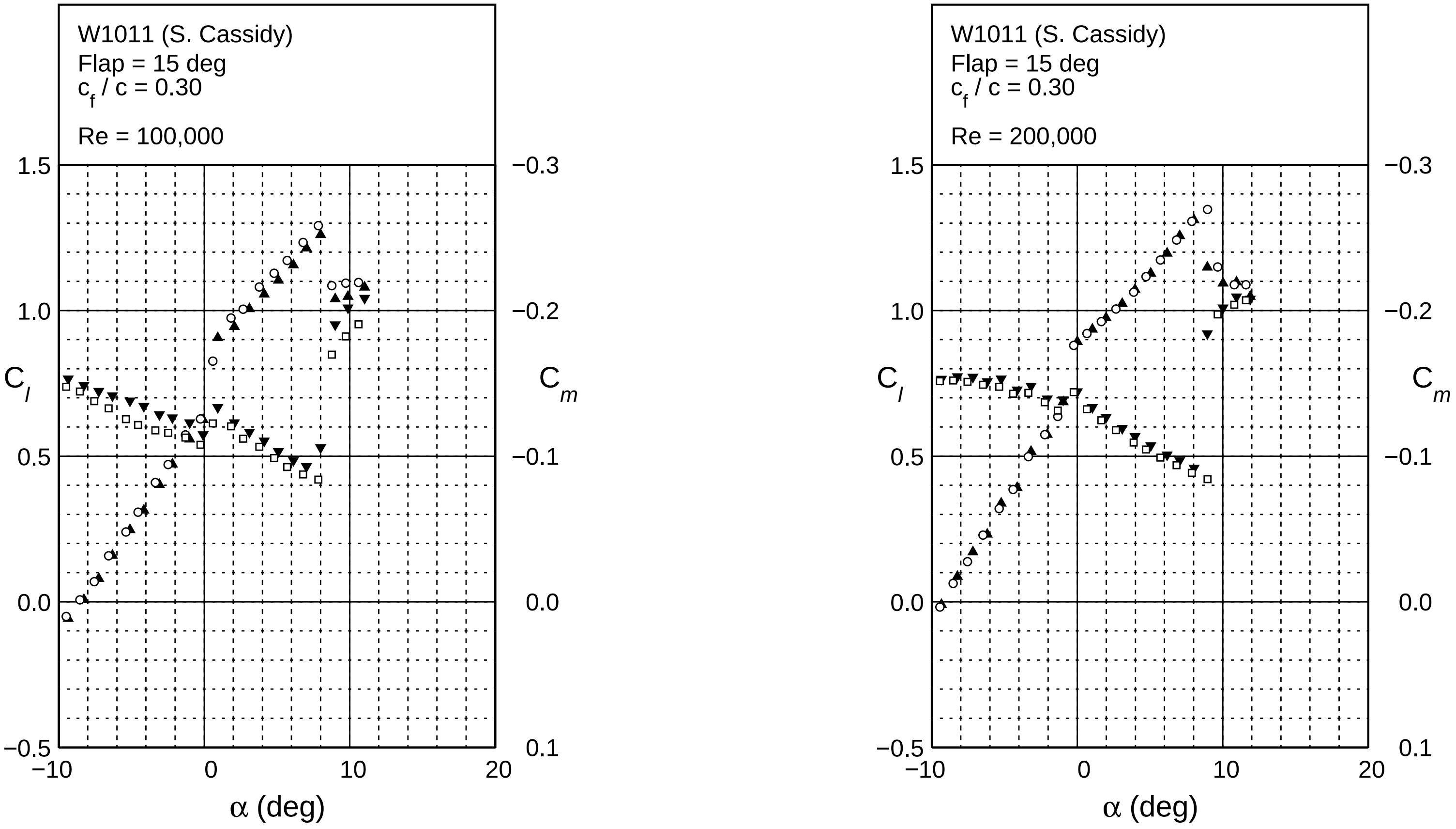

Figure 6.158: Lift and moment characteristics for the W1011 ($c_f/c = 30\%$) with a 15 deg flap.

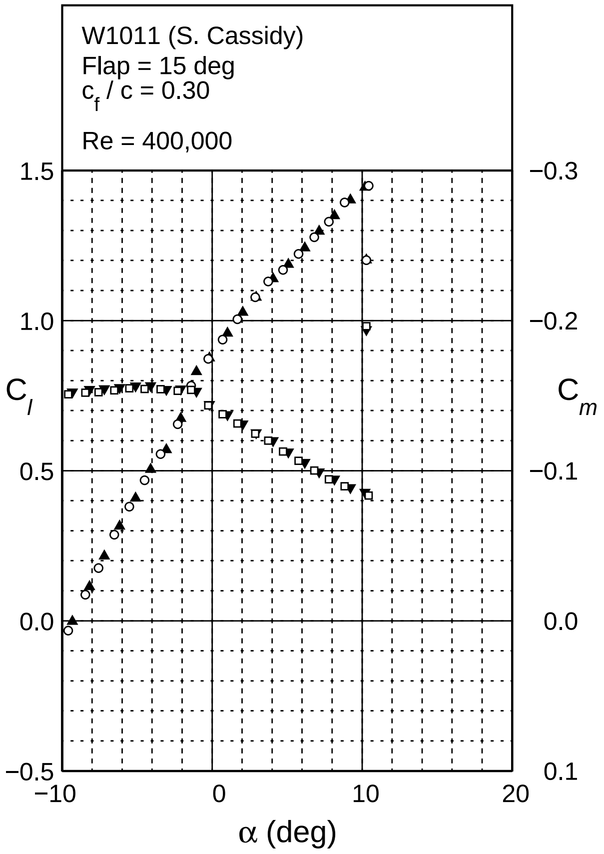

Figure 6.158: Continued.

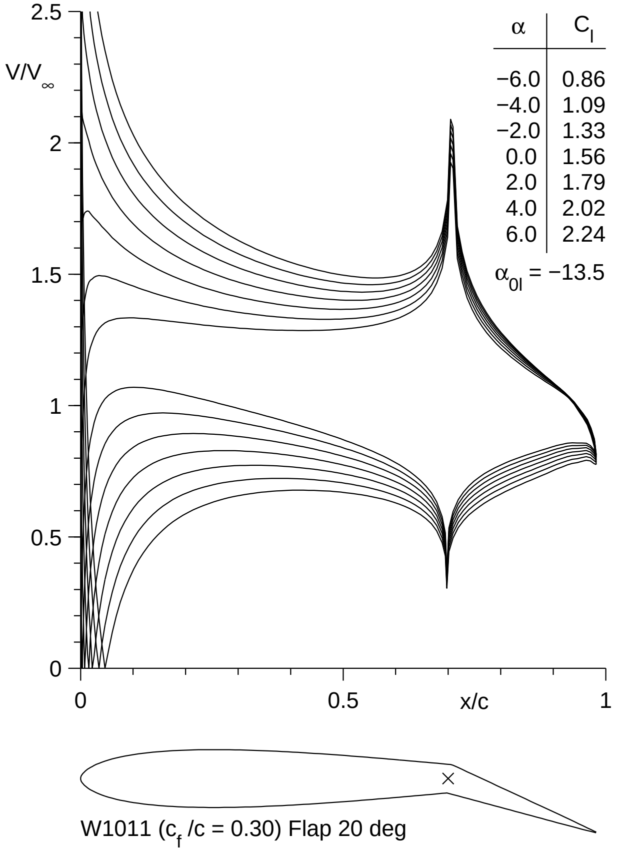

Figure 6.159: Inviscid velocity distribution for the W1011 ($c_f/c = 30\%$) with a 20 deg flap.

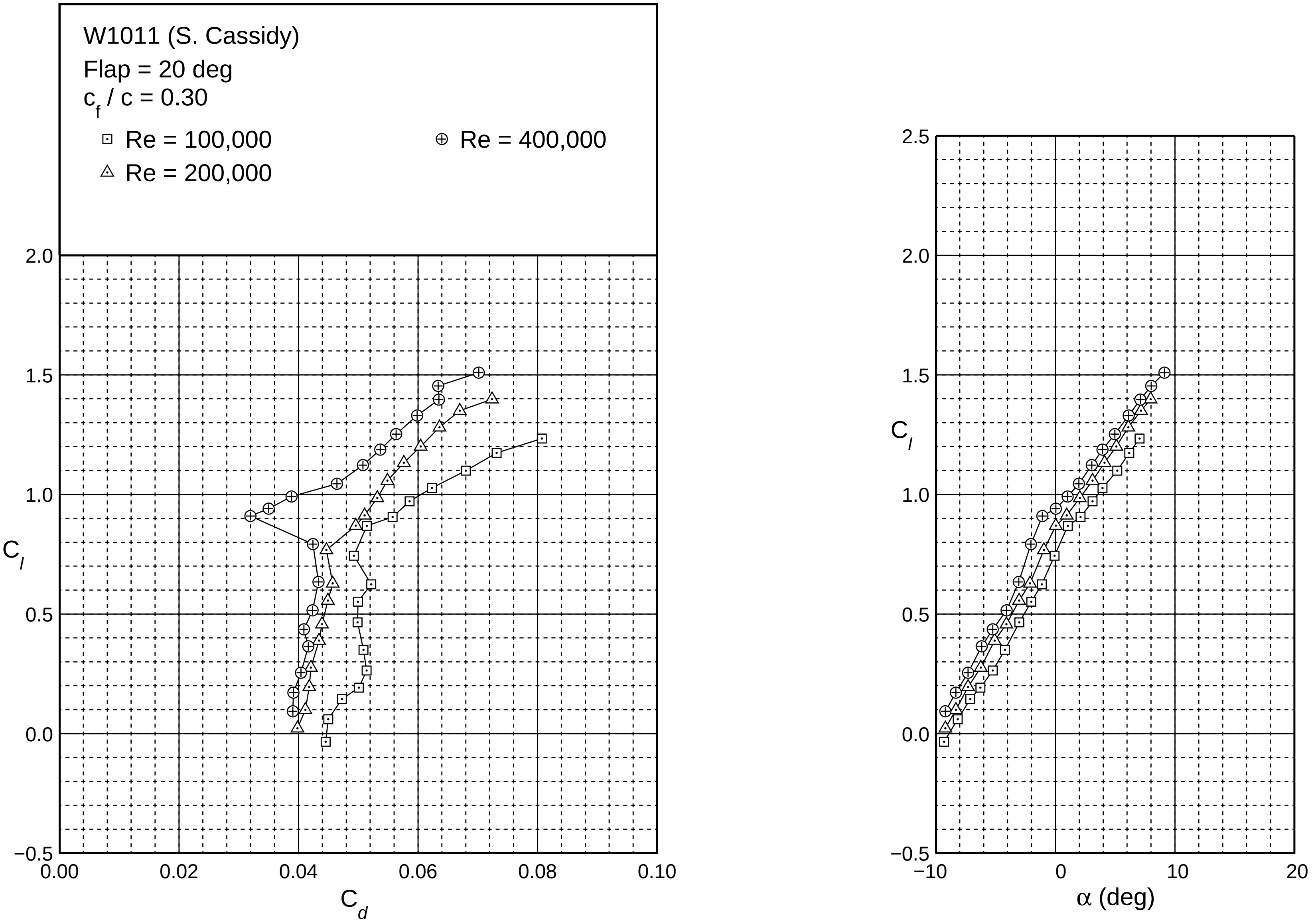

Figure 6.160: Drag polar for the W1011 ($c_f/c = 30\%$) with a 20 deg flap.

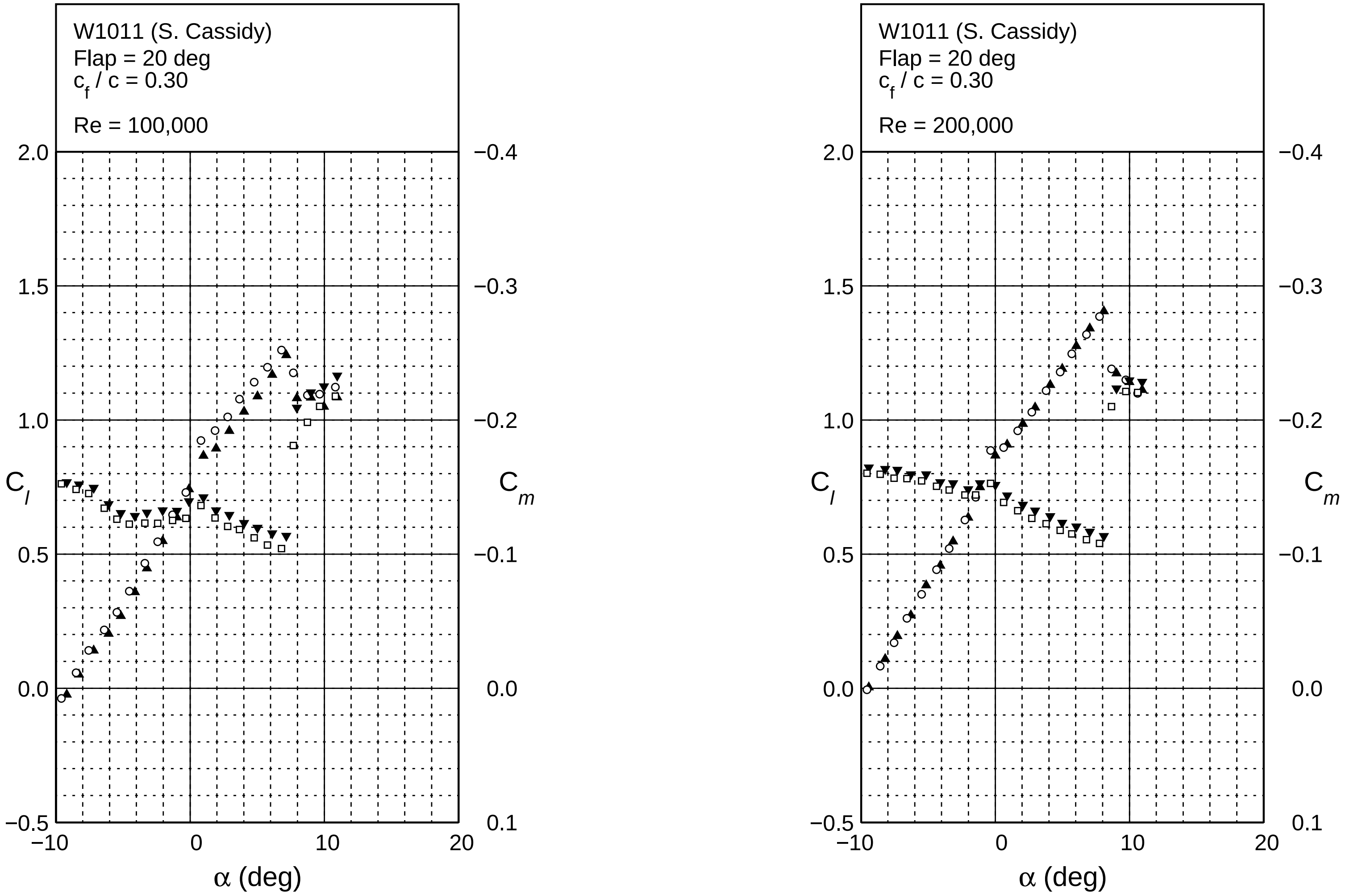

Figure 6.161: Lift and moment characteristics for the W1011 ($c_f/c = 30\%$) with a 20 deg flap.

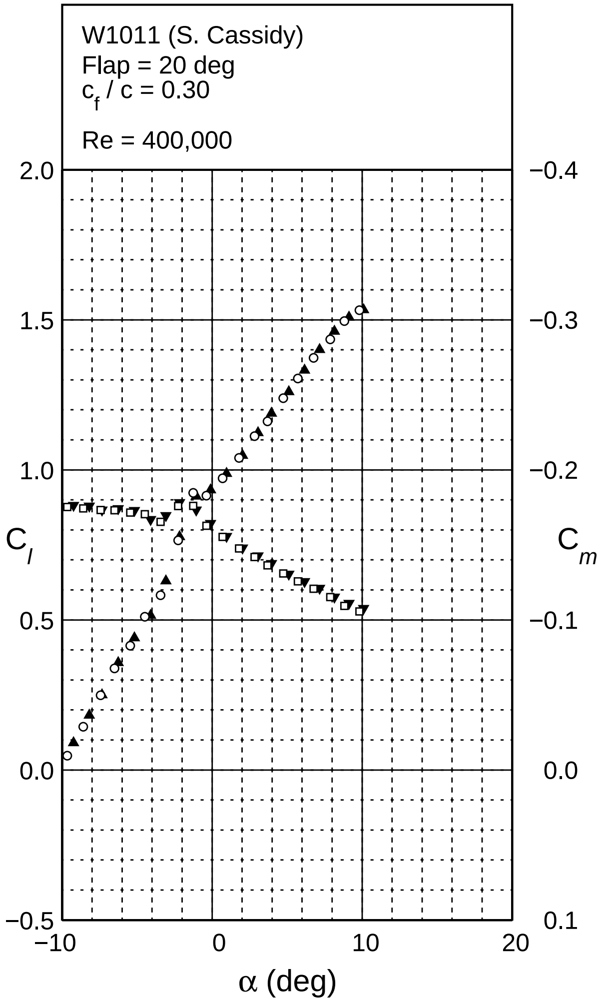

Figure 6.161: Continued.

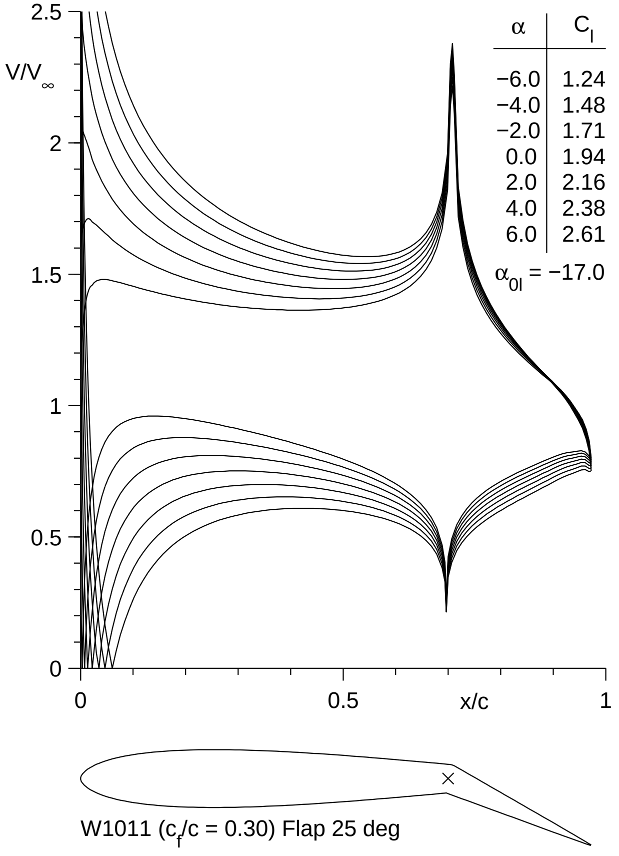

Figure 6.162: Inviscid velocity distribution for the W1011 ($c_f/c = 30\%$) with a 25 deg flap.

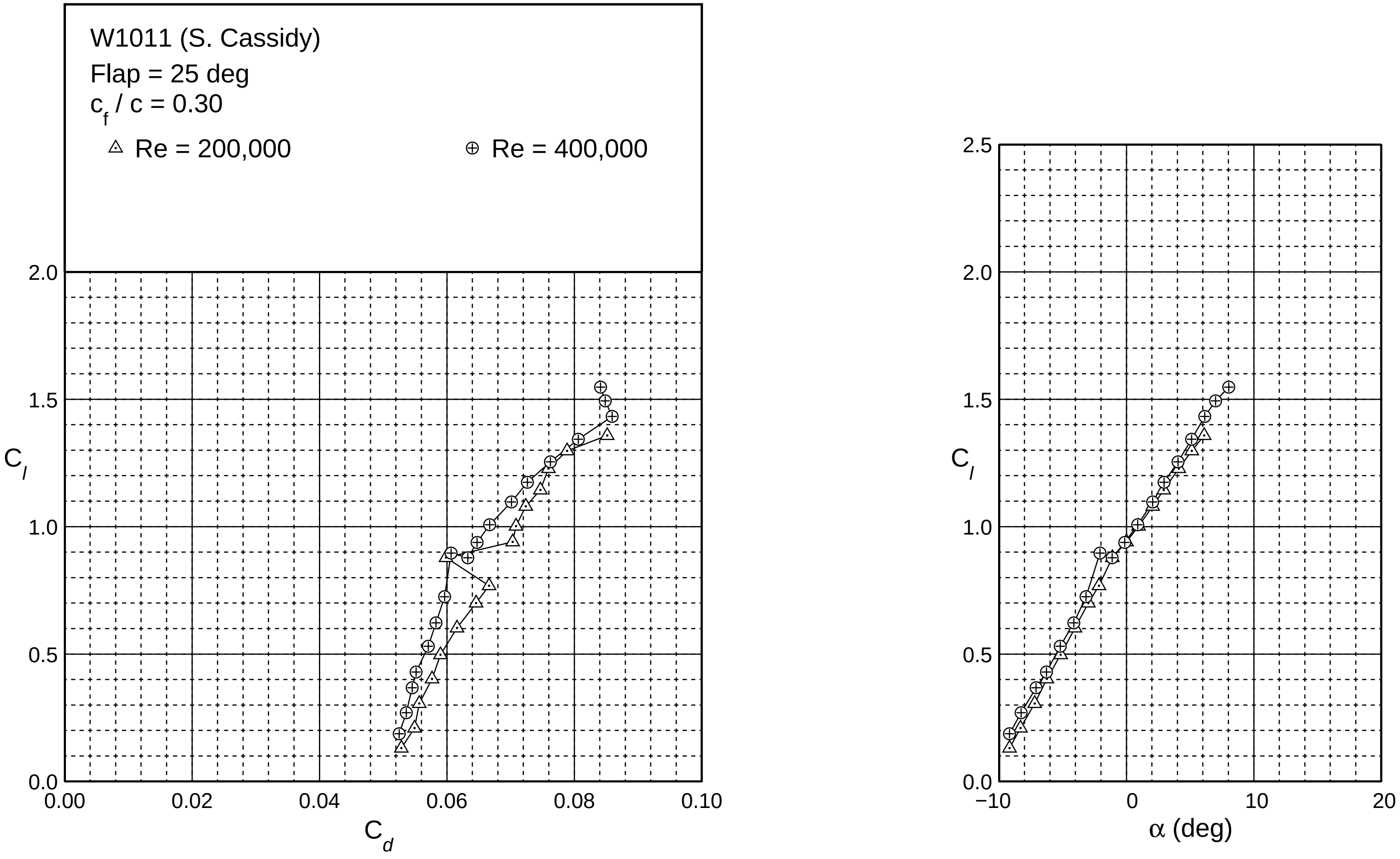

Figure 6.163: Drag polar for the W1011 ($c_f/c = 30\%$) with a 25 deg flap.

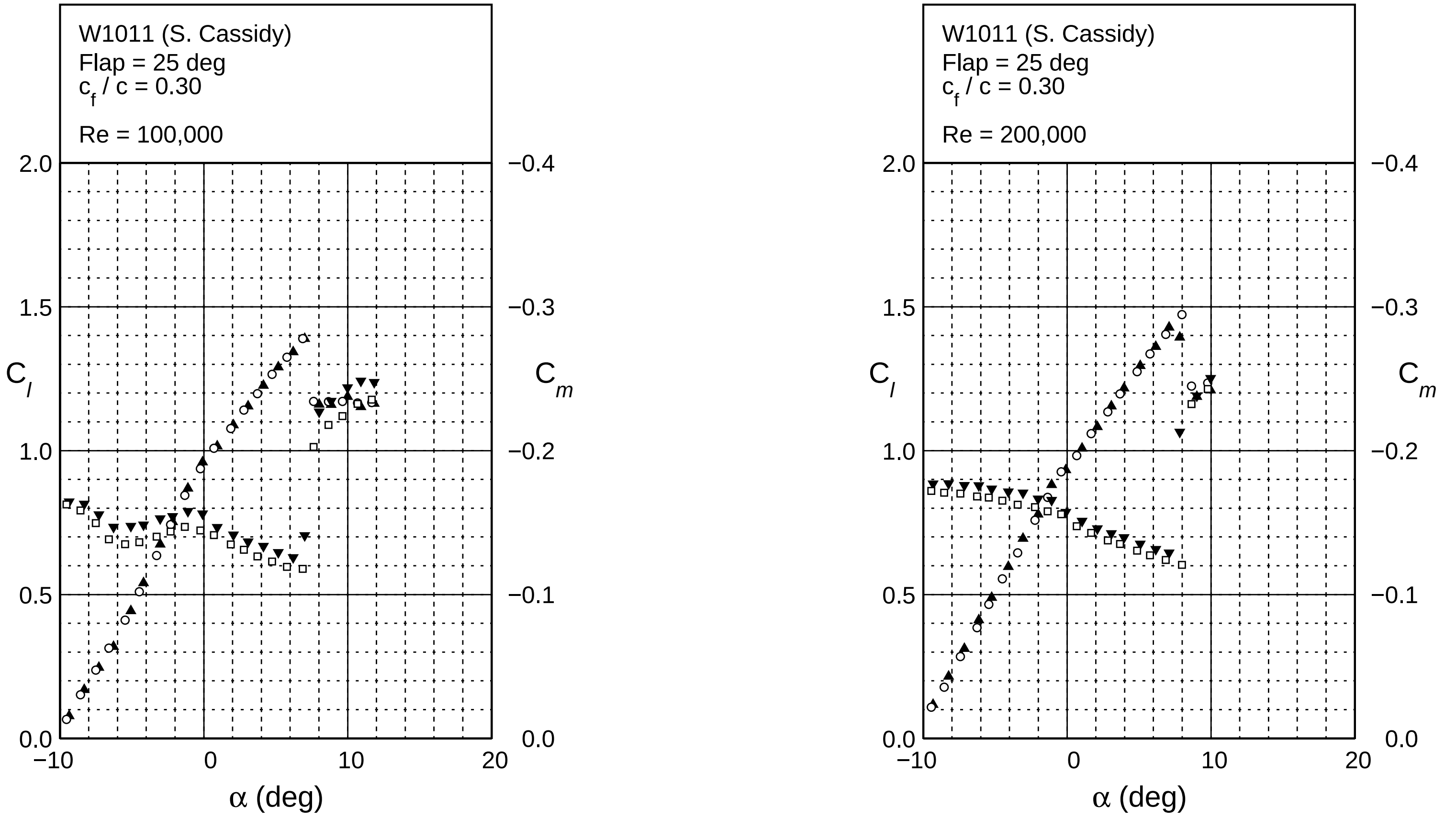

Figure 6.164: Lift and moment characteristics for the W1011 ($c_f/c = 30\%$) with a 25 deg flap.

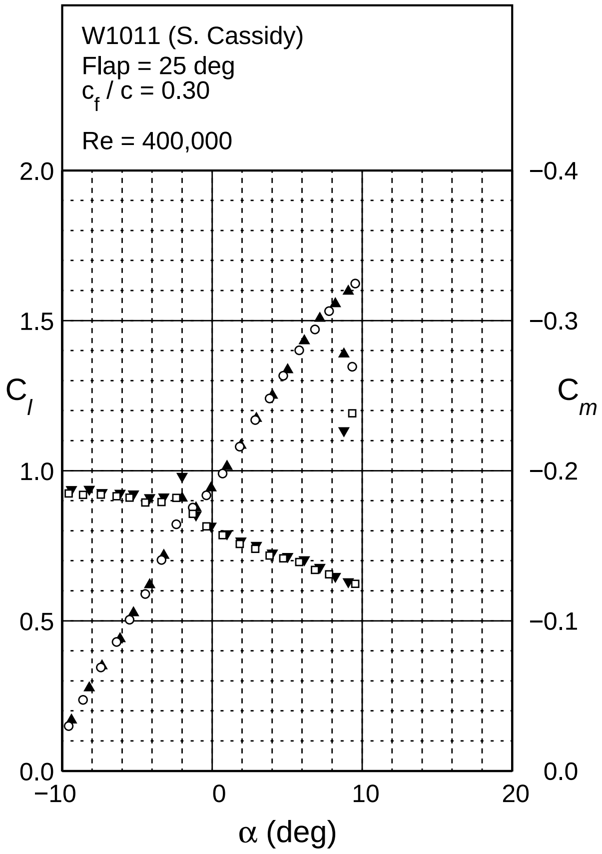

Figure 6.164: Continued.

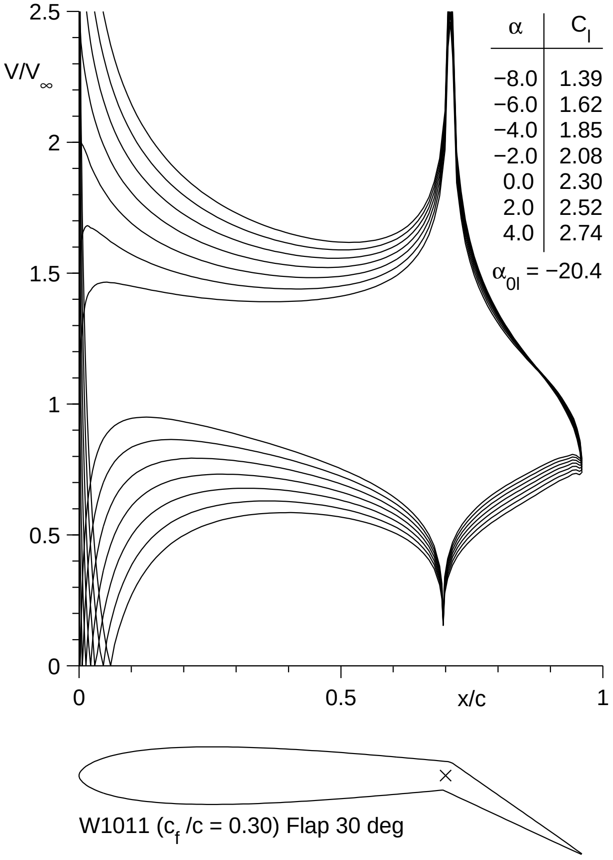

Figure 6.165: Inviscid velocity distribution for the W1011 ($c_f/c = 30\%$) with a 30 deg flap.

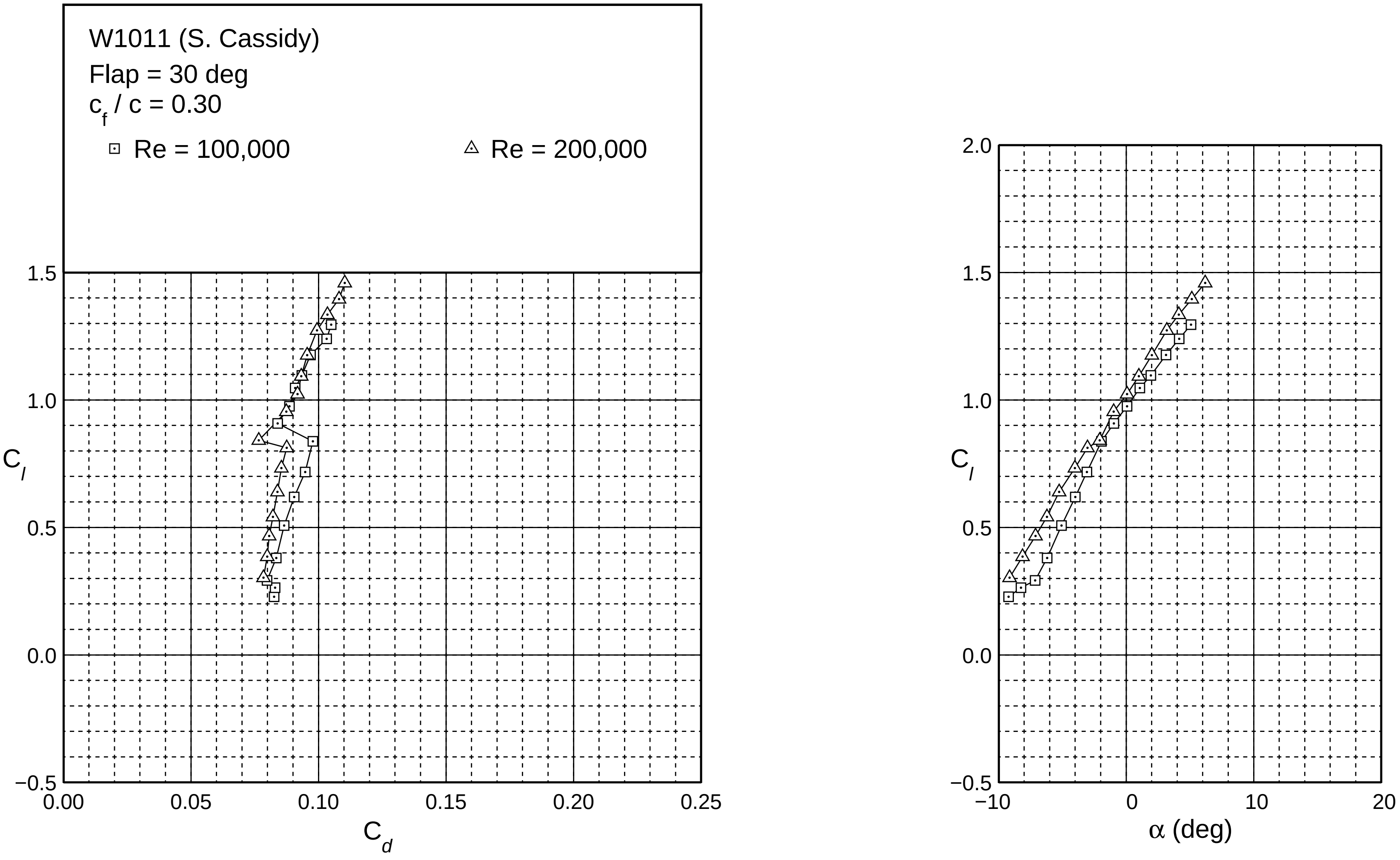

Figure 6.166: Drag polar for the W1011 (c_f/c = 30%) with a 30 deg flap.

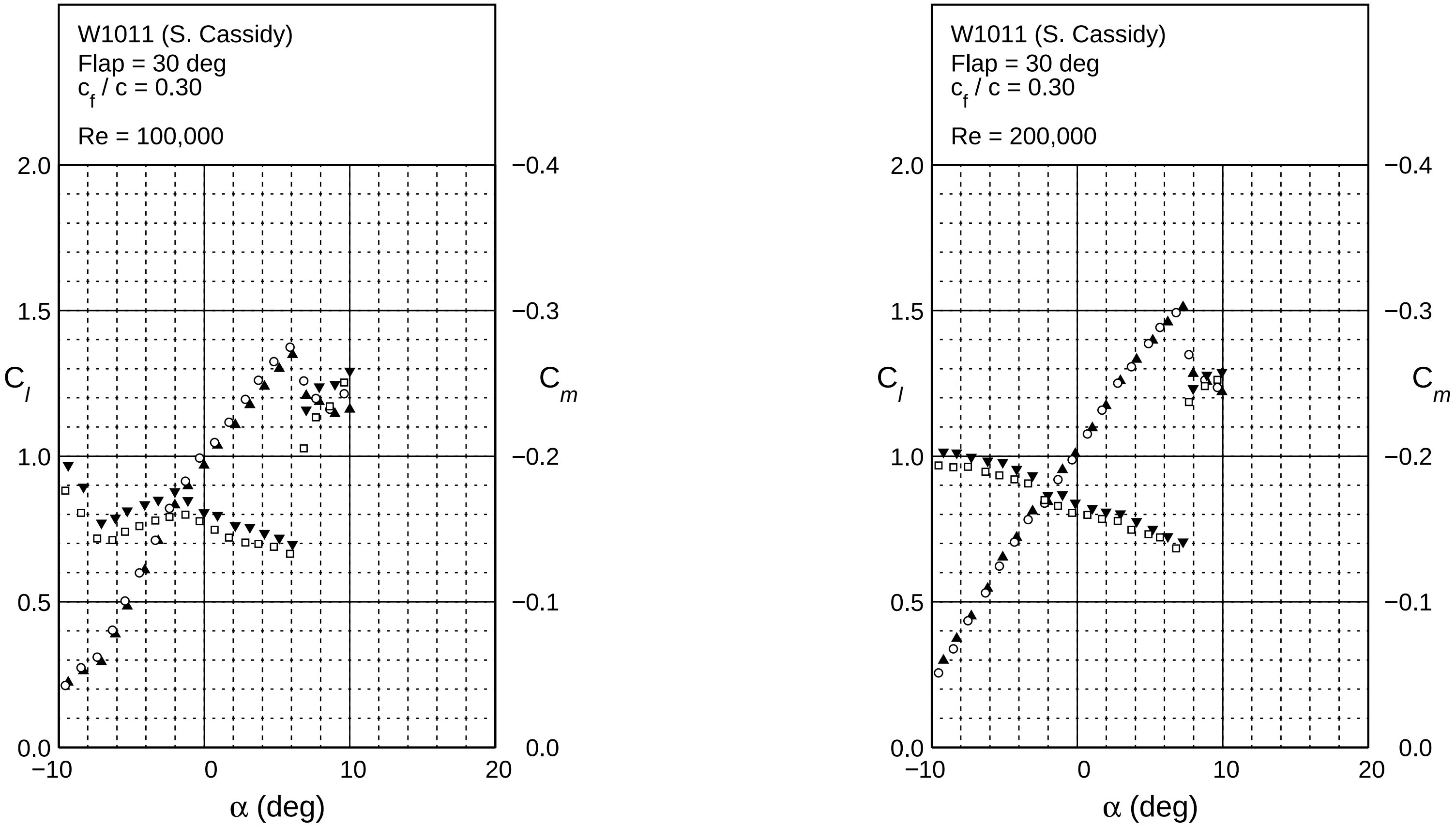

Figure 6.167: Lift and moment characteristics for the W1011 ($c_f/c = 30\%$) with a 30 deg flap.

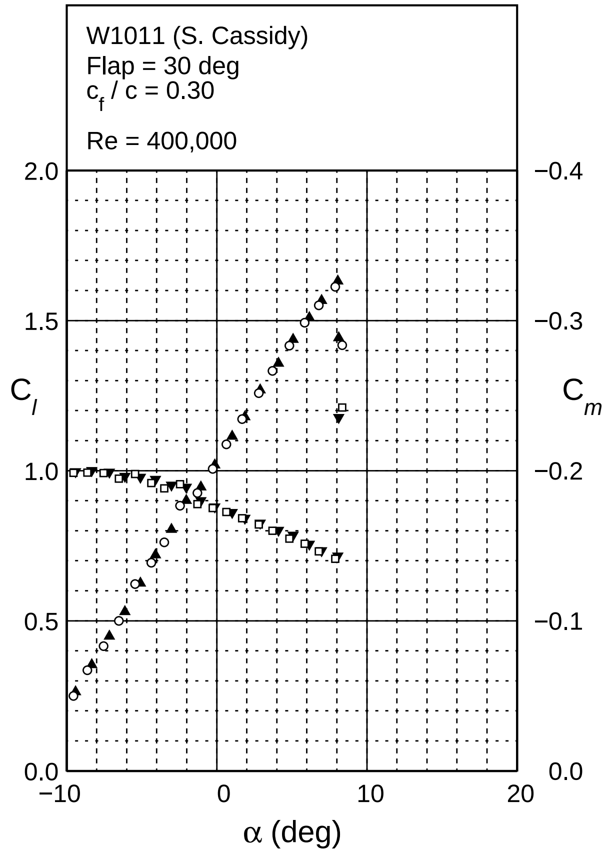

Figure 6.167: Continued.

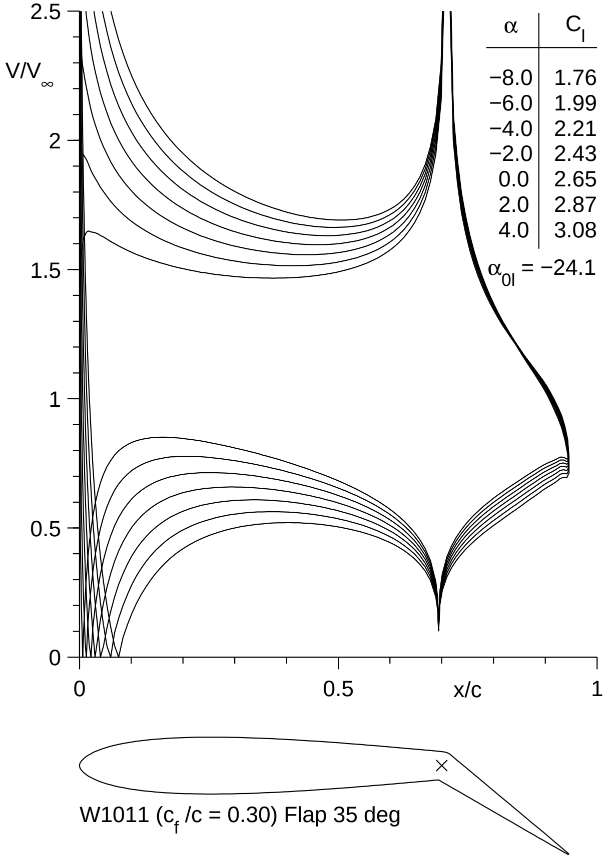

Figure 6.168: Inviscid velocity distribution for the W1011 ($c_f/c = 30\%$) with a 35 deg flap.

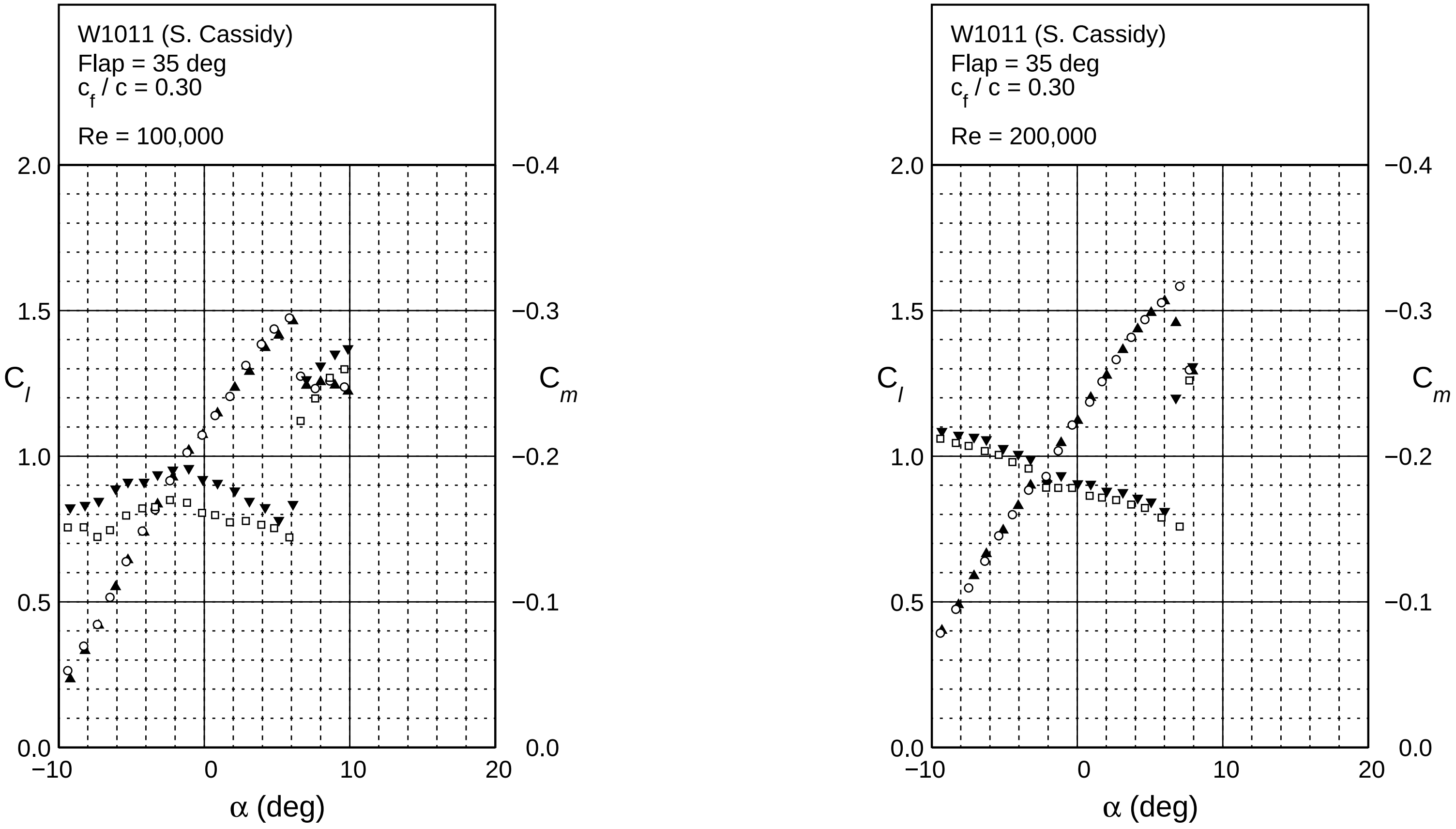

Figure 6.169: Lift and moment characteristics for the W1011 ($c_f/c = 30\%$) with a 35 deg flap.

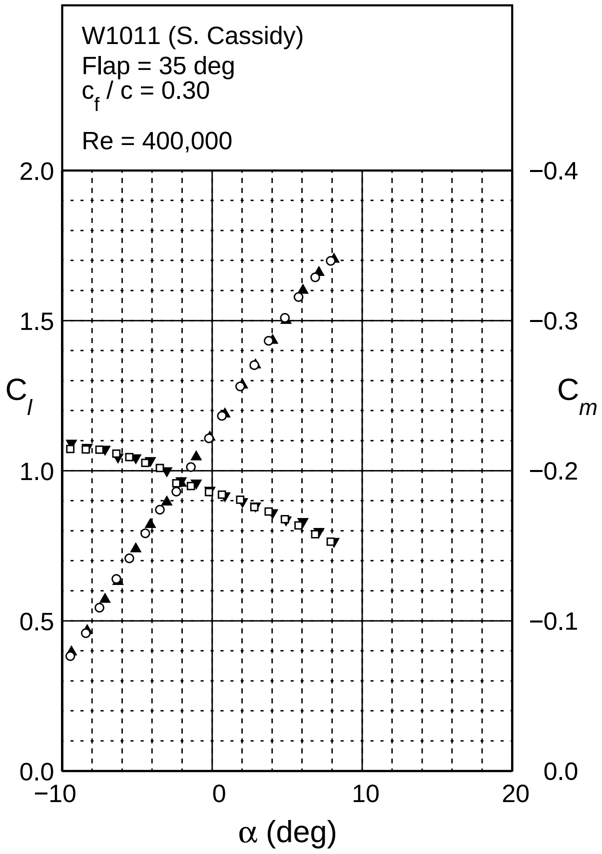

Figure 6.169: Continued.

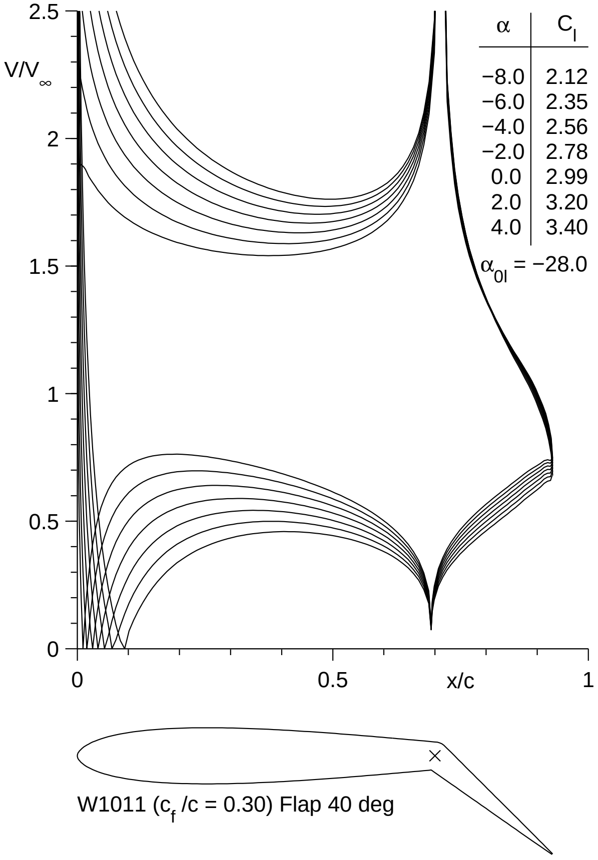

Figure 6.170: Inviscid velocity distribution for the W1011 ($c_f/c = 30\%$) with a 40 deg flap.

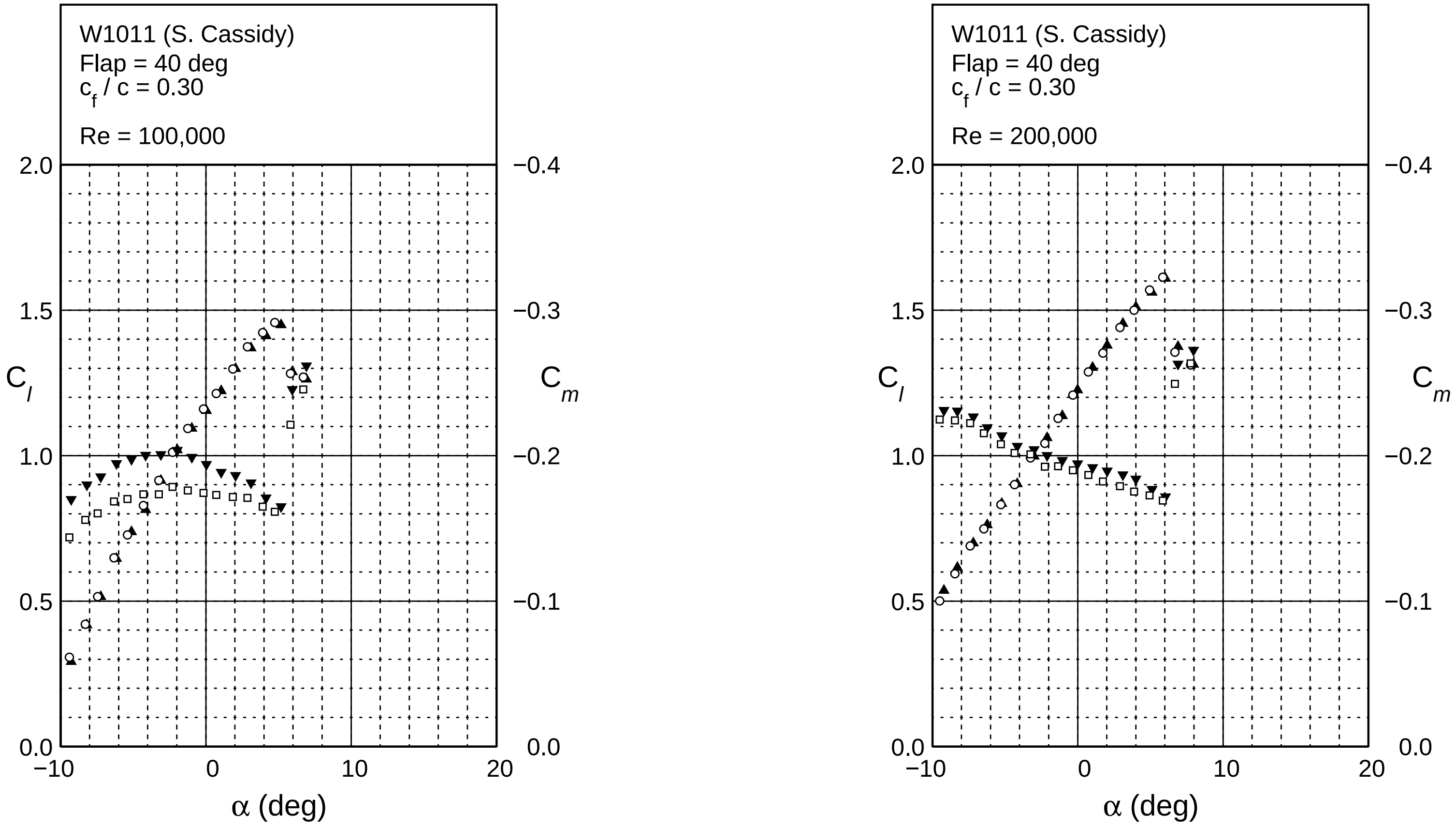

Figure 6.171: Lift and moment characteristics for the W1011 ($c_f/c = 30\%$) with a 40 deg flap.

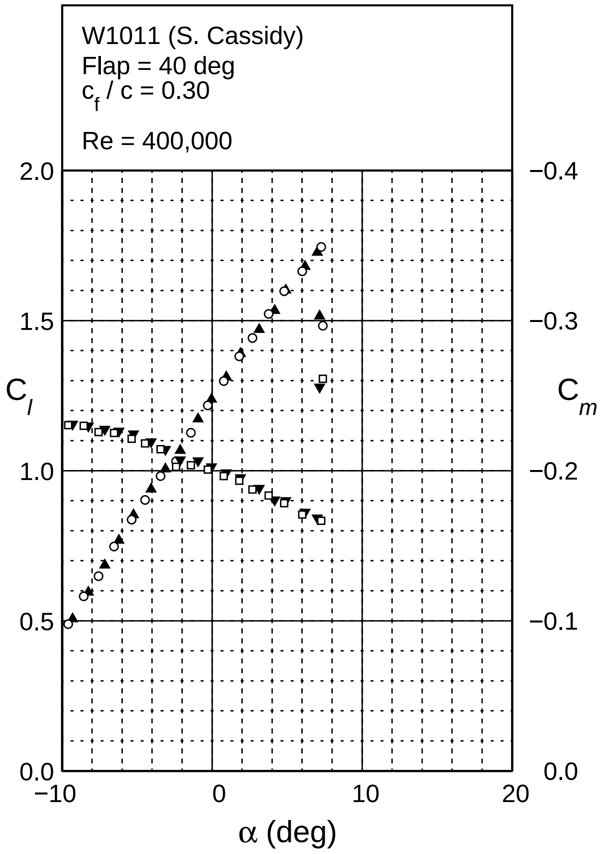

Figure 6.171: Continued.

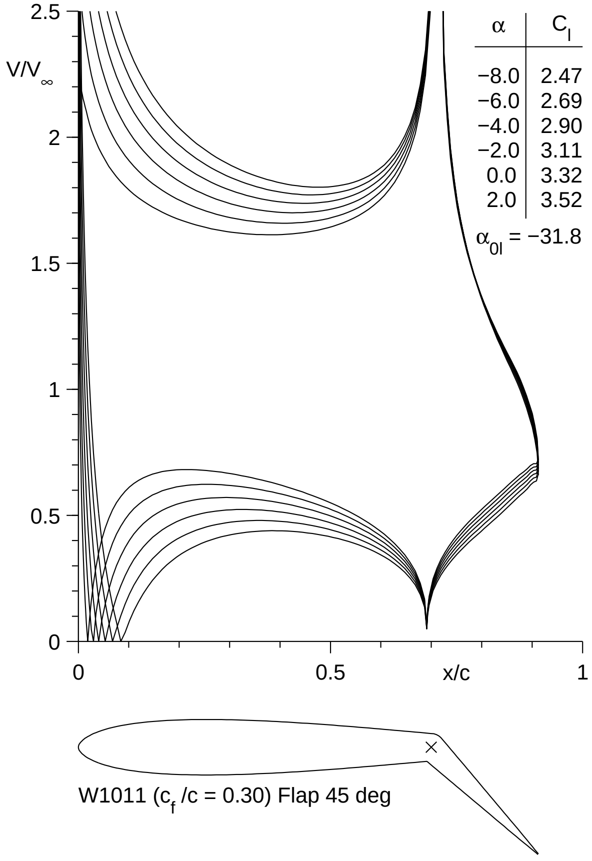

Figure 6.172: Inviscid velocity distribution for the W1011 ($c_f/c = 30\%$) with a 45 deg flap.

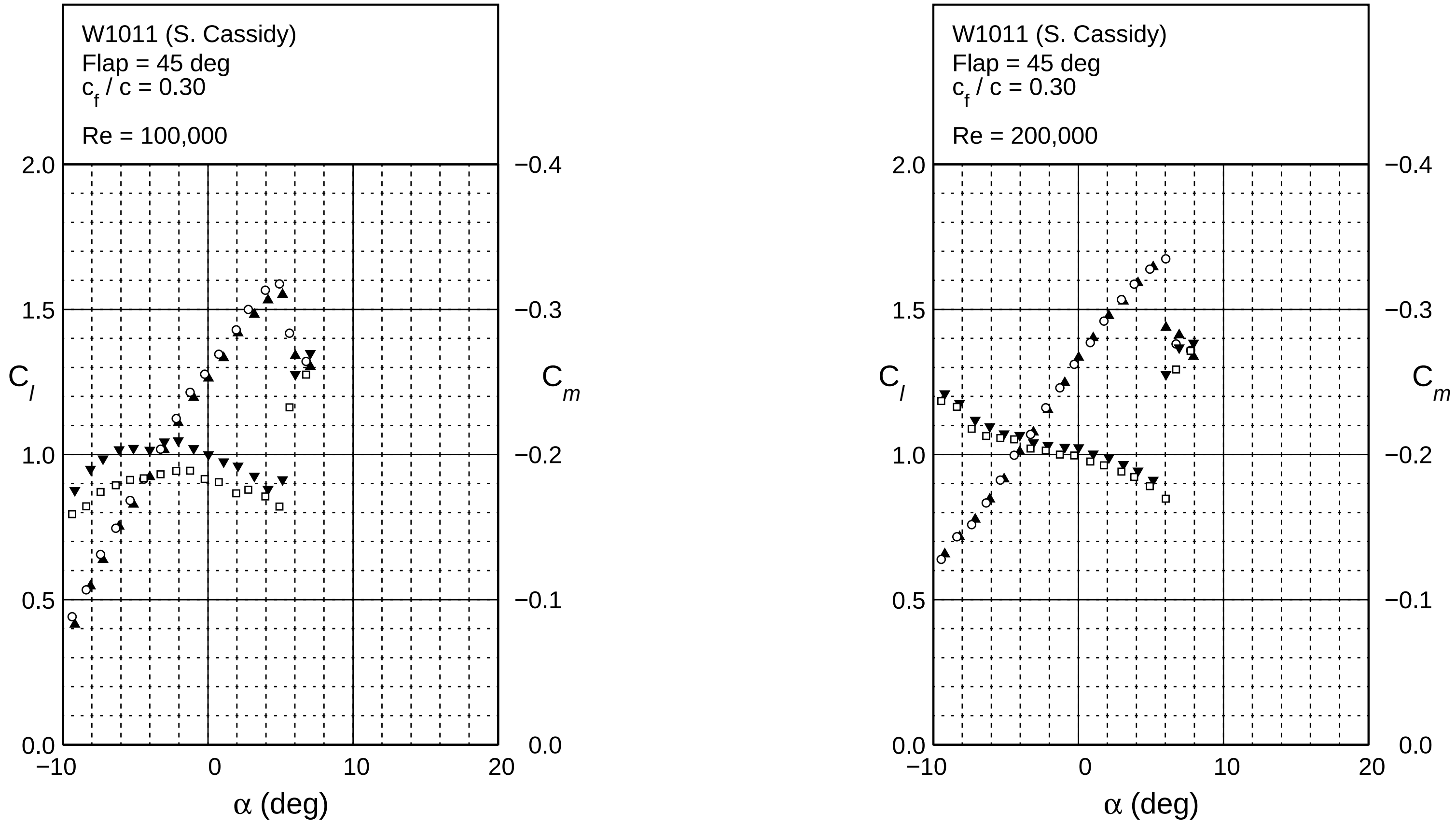

Figure 6.173: Lift and moment characteristics for the W1011 ($c_f/c = 30\%$) with a 45 deg flap.

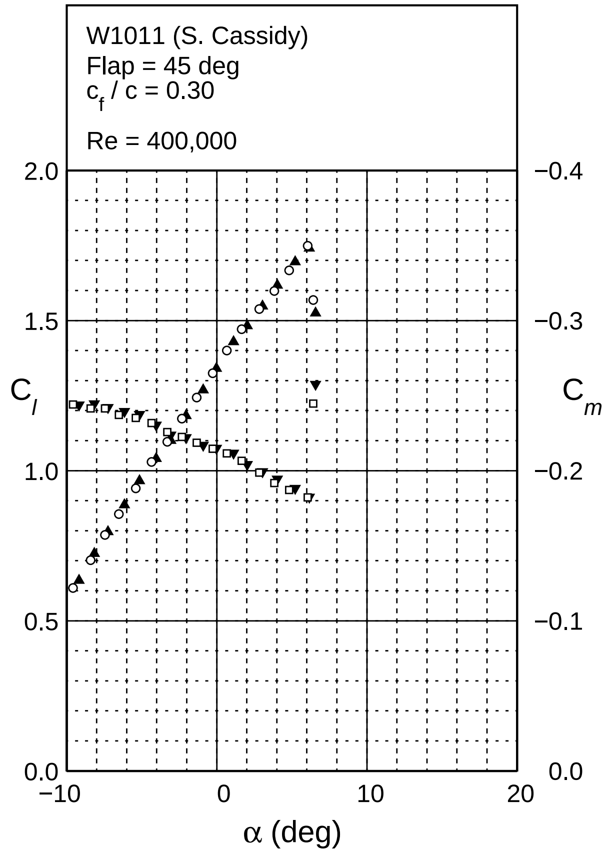

Figure 6.173: Continued.

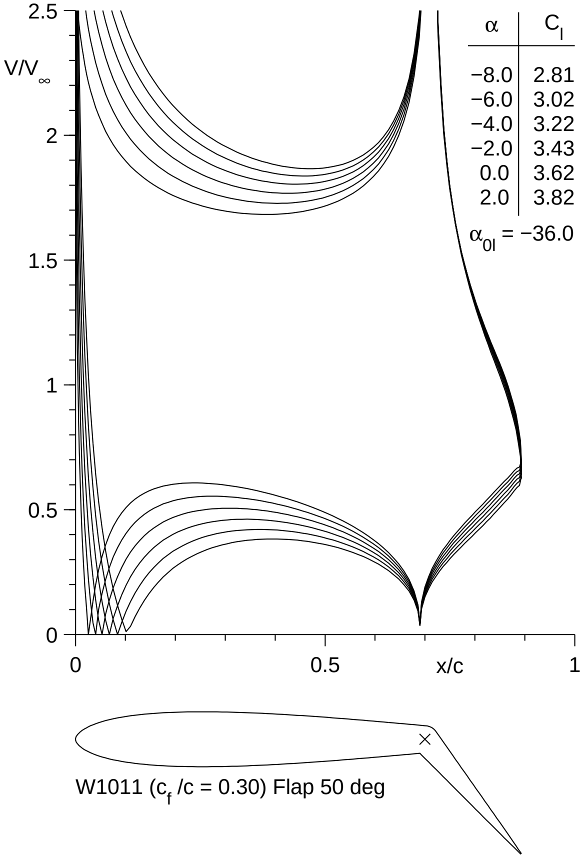

Figure 6.174: Inviscid velocity distribution for the W1011 ($c_f/c = 30\%$) with a 50 deg flap.

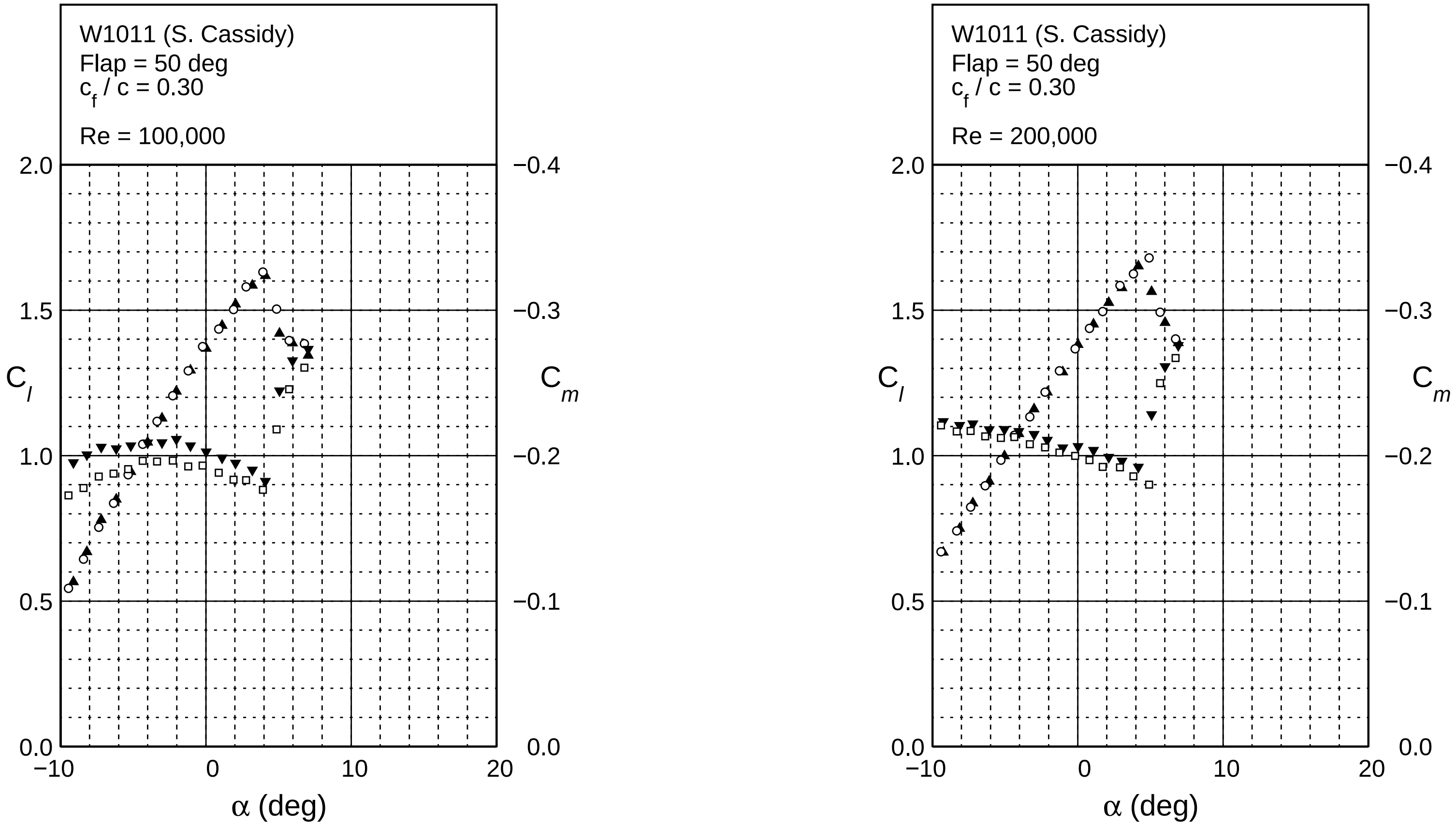

Figure 6.175: Lift and moment characteristics for the W1011 ($c_f/c = 30\%$) with a 50 deg flap.

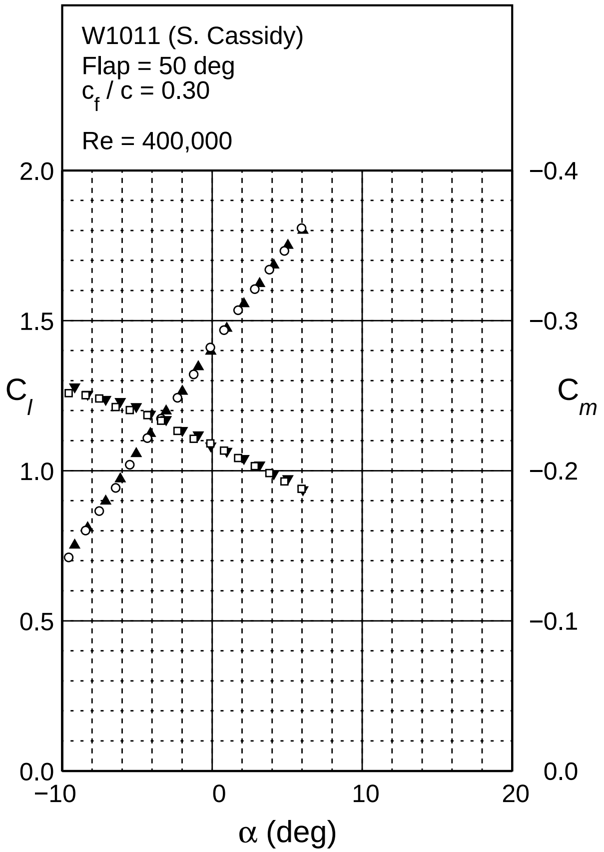

Figure 6.175: Continued.

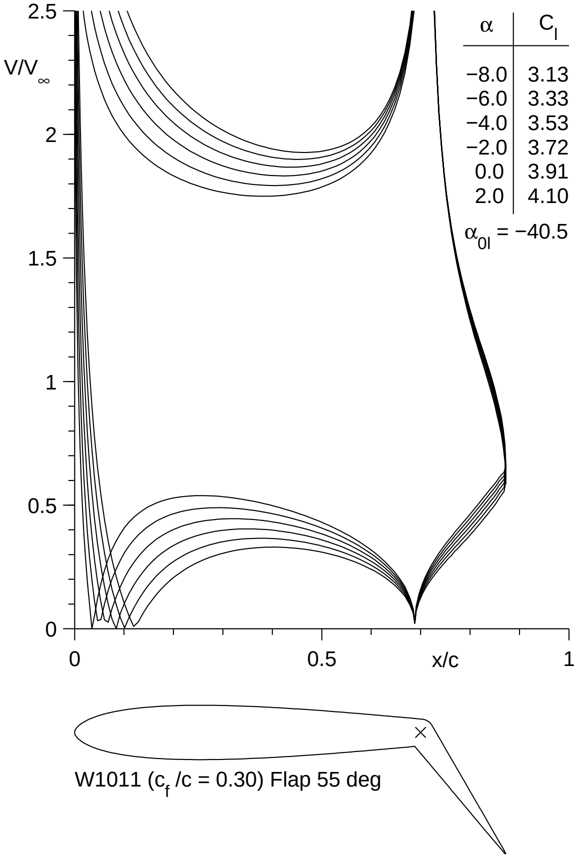

Figure 6.176: Inviscid velocity distribution for the W1011 ($c_f/c = 30\%$) with a 55 deg flap.

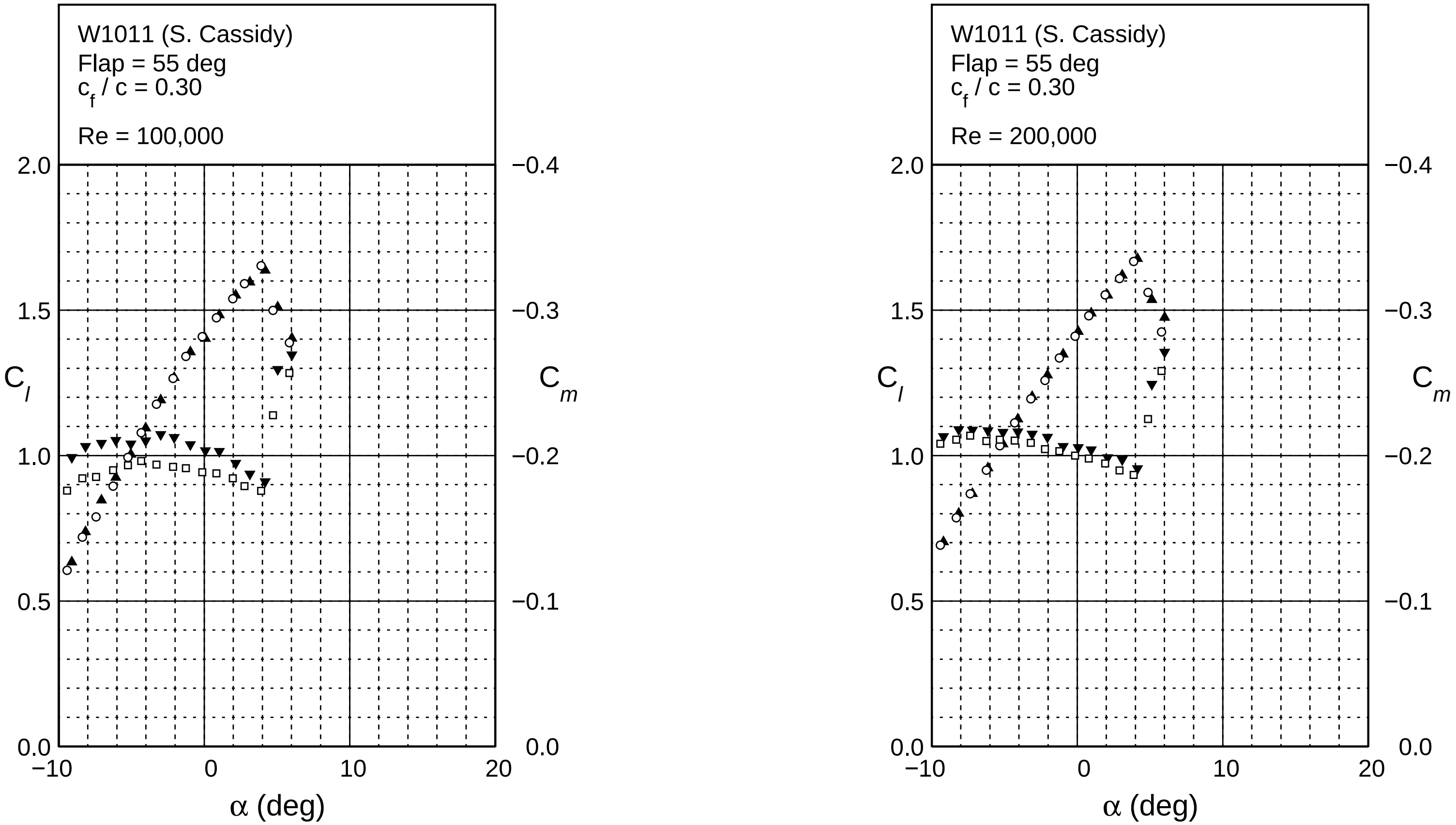

Figure 6.177: Lift and moment characteristics for the W1011 ($c_f/c = 30\%$) with a 55 deg flap.

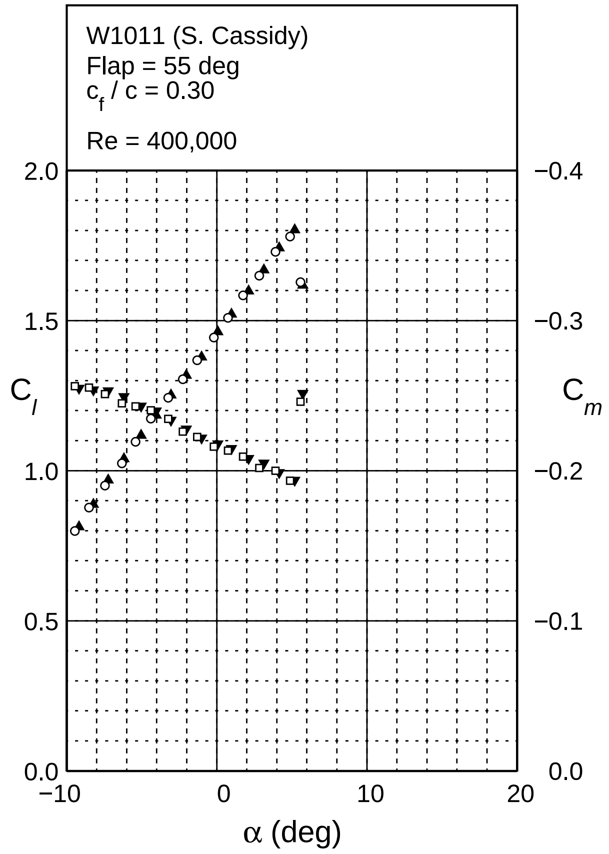

Figure 6.177: Continued.

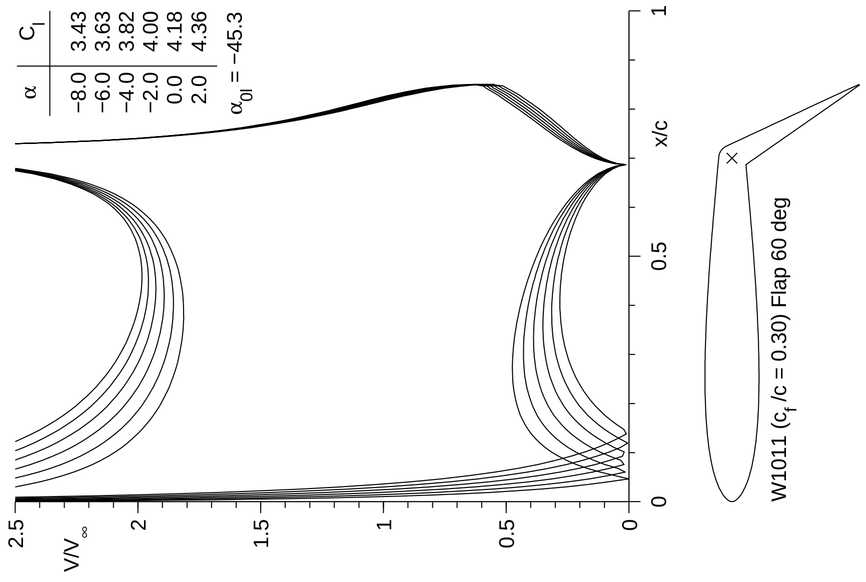

Figure 6.178: Inviscid velocity distribution for the W1011 $(c_f/c\ =\ 30\%)$ with a 60 deg flap.

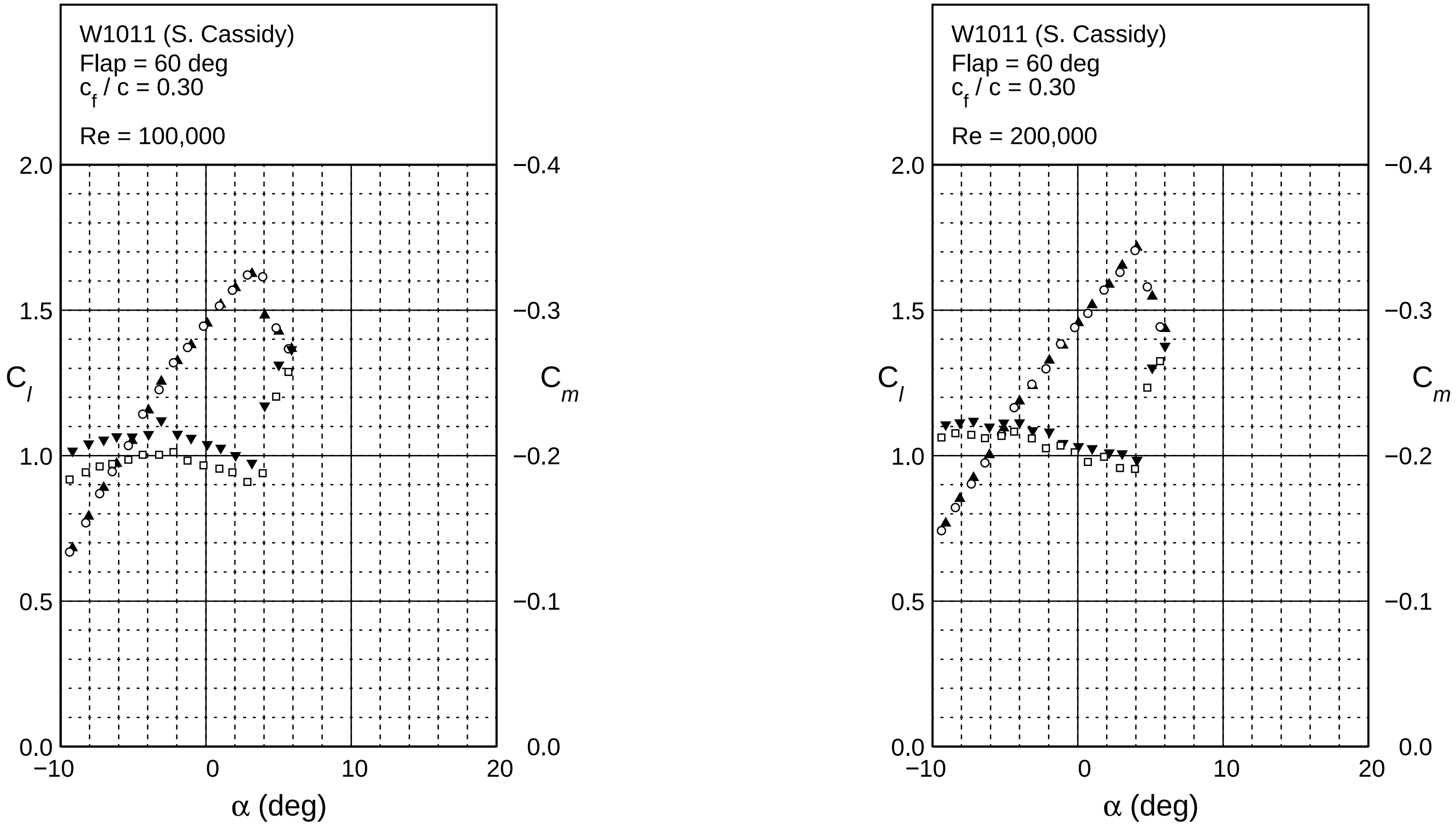

Figure 6.179: Lift and moment characteristics for the W1011 ($c_f/c = 30\%$) with a 60 deg flap.

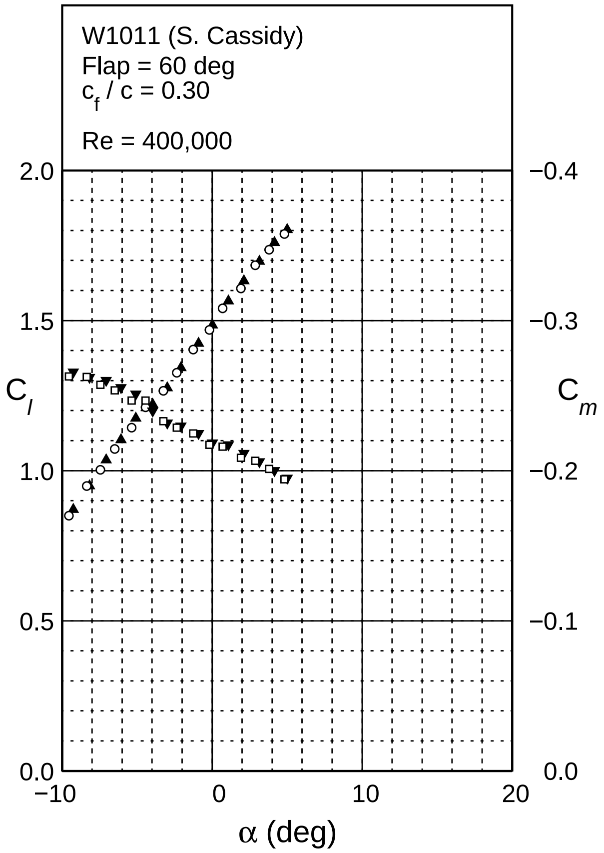

Figure 6.179: Continued.

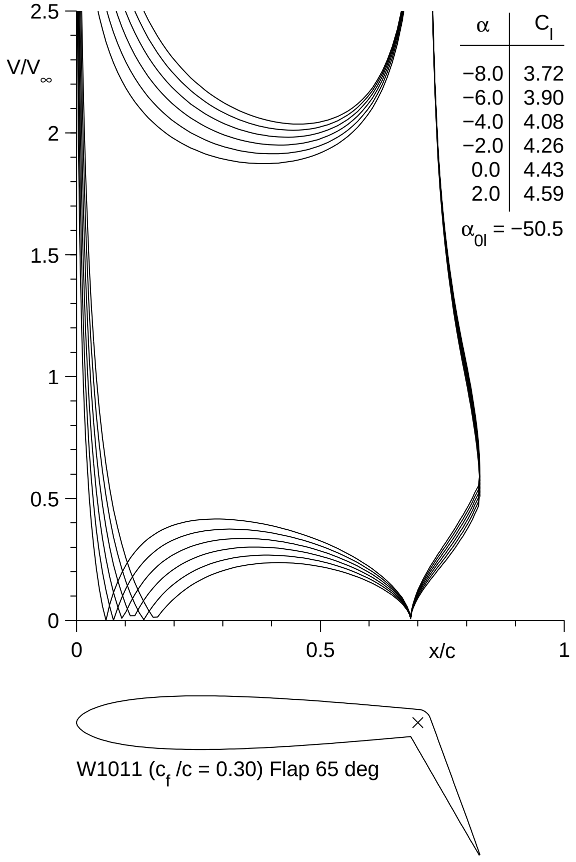

Figure 6.180: Inviscid velocity distribution for the W1011 ($c_f/c = 30\%$) with a 65 deg flap.

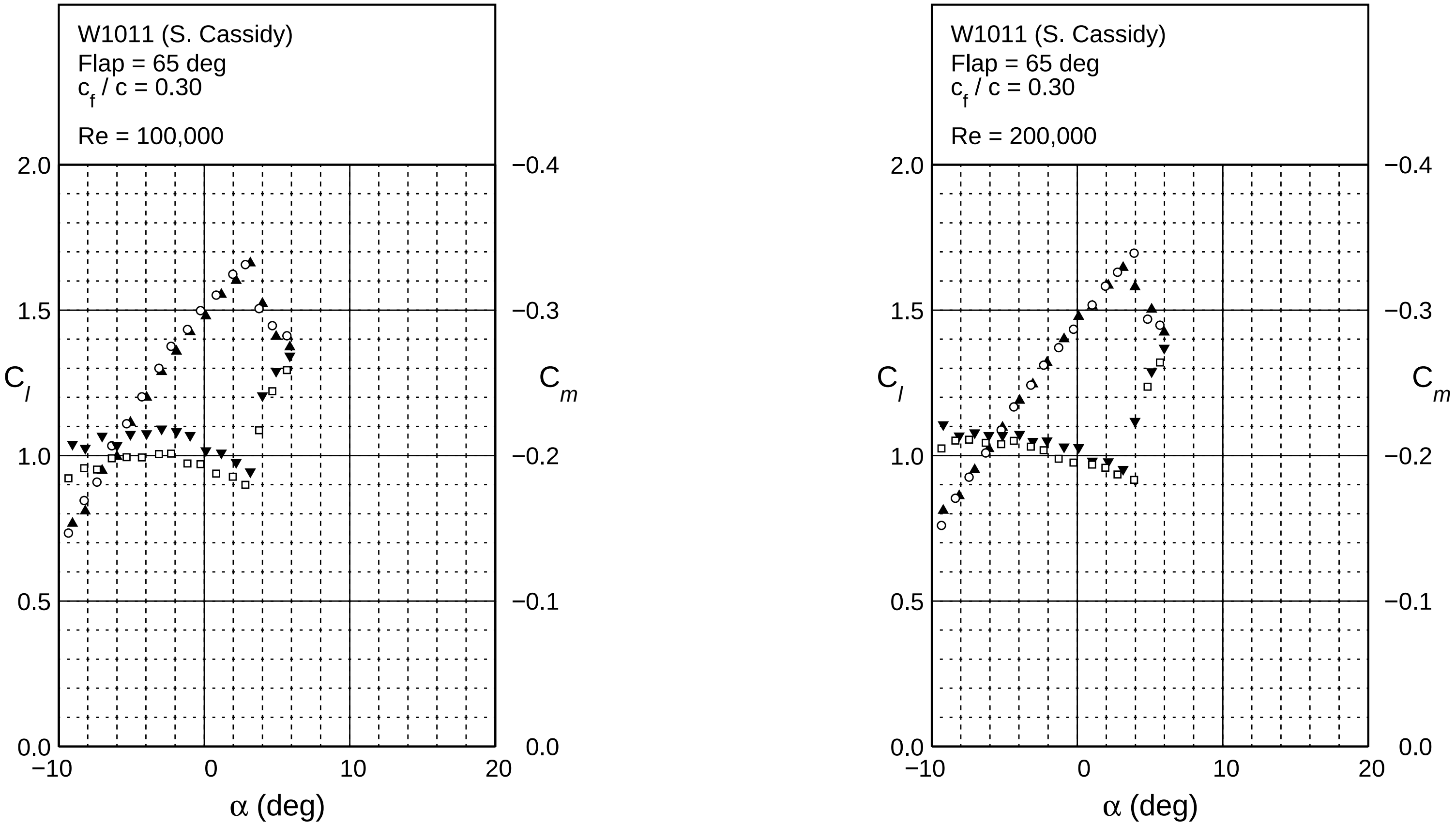

Figure 6.181: Lift and moment characteristics for the W1011 ($c_f/c = 30\%$) with a 65 deg flap.

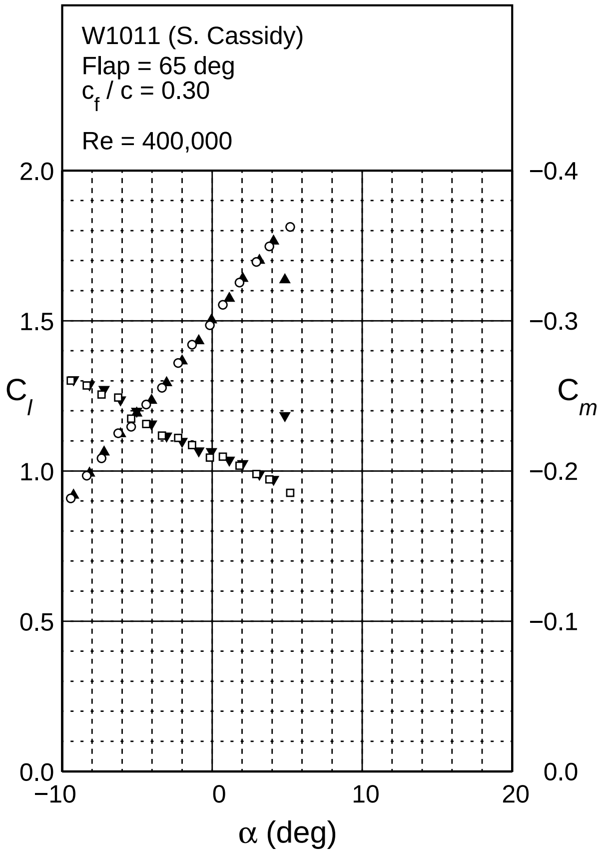

Figure 6.181: Continued.

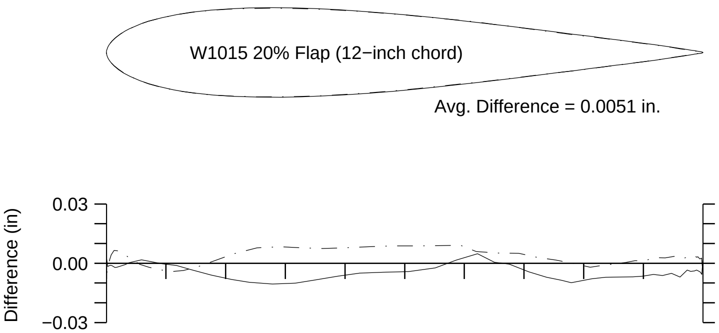

Figure 6.182: Comparison between the true and actual W1015 ($c_f/c = 20\%$).

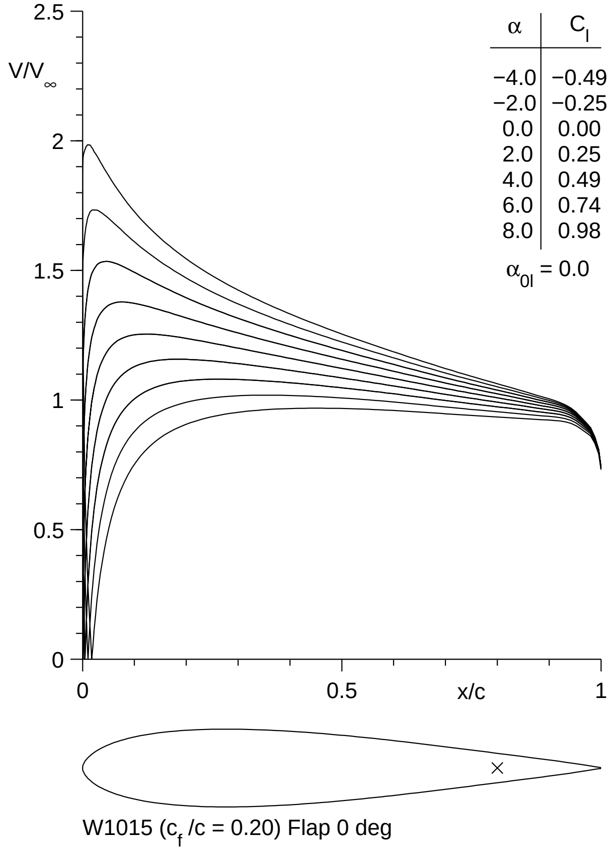

Figure 6.183: Inviscid velocity distribution for the W1015 ($c_f/c = 20\%$).

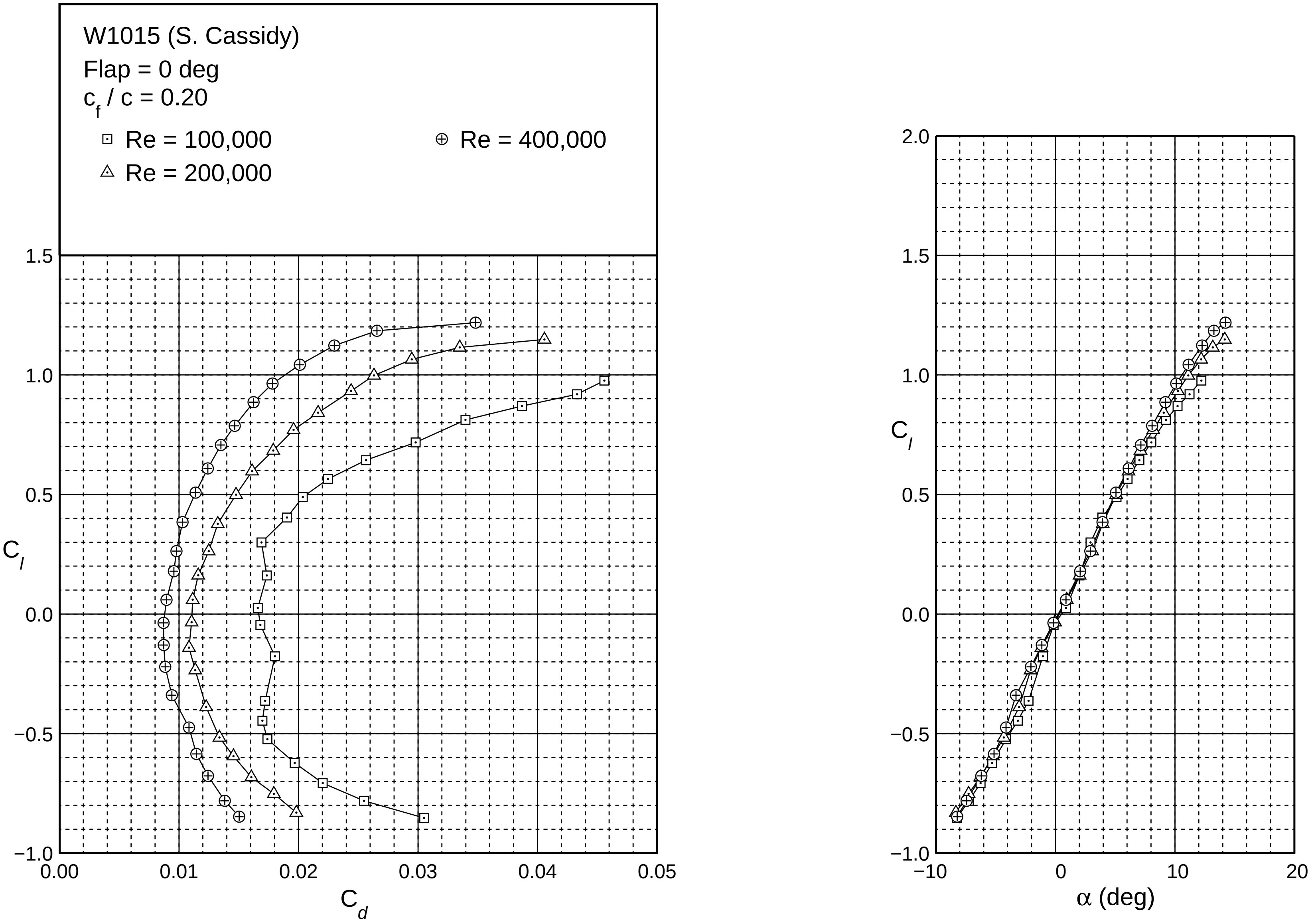

Figure 6.184: Drag polar for the W1015 ($c_f/c = 20\%$).

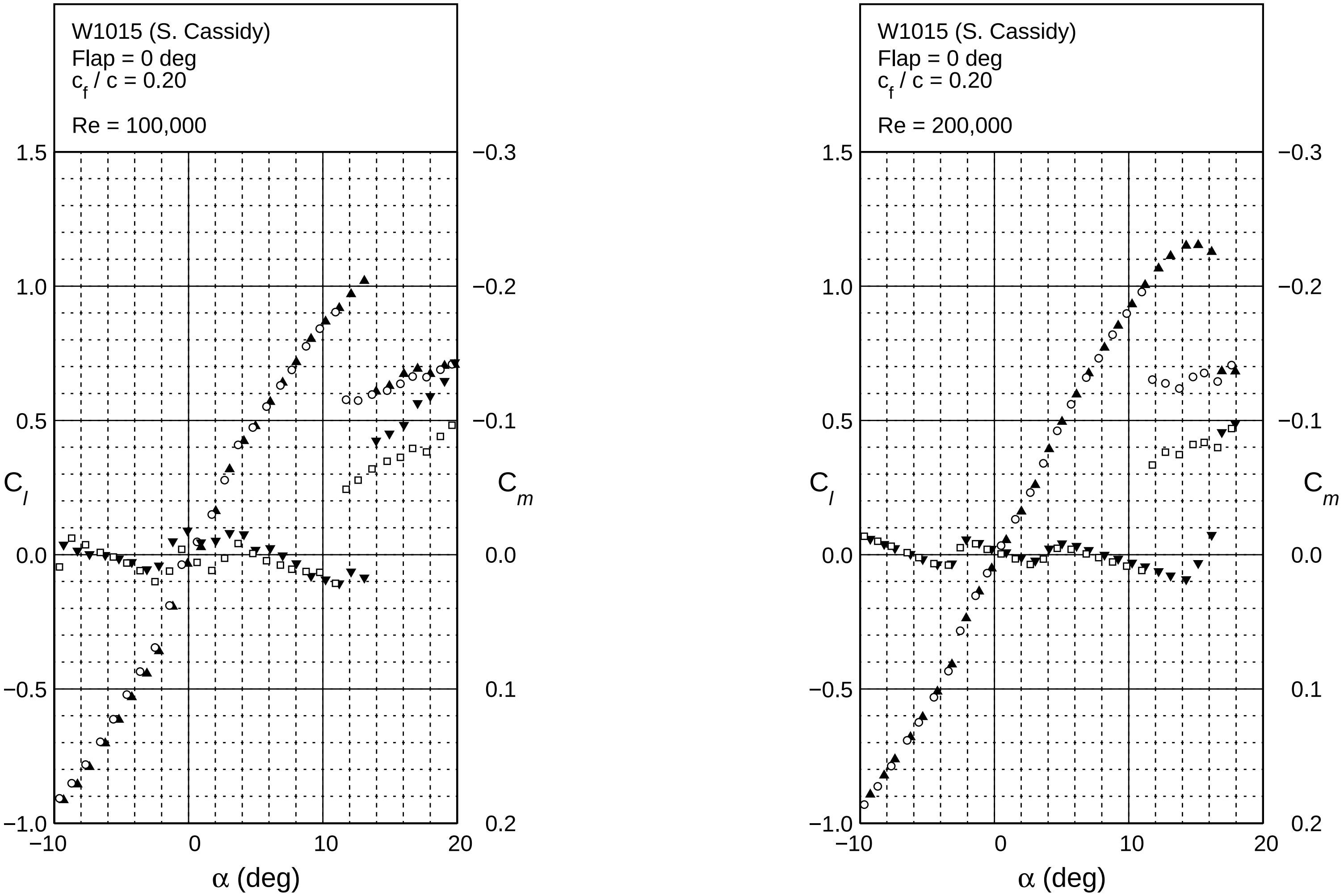

Figure 6.185: Lift and moment characteristics for the W1015 ($c_f/c = 20\%$).

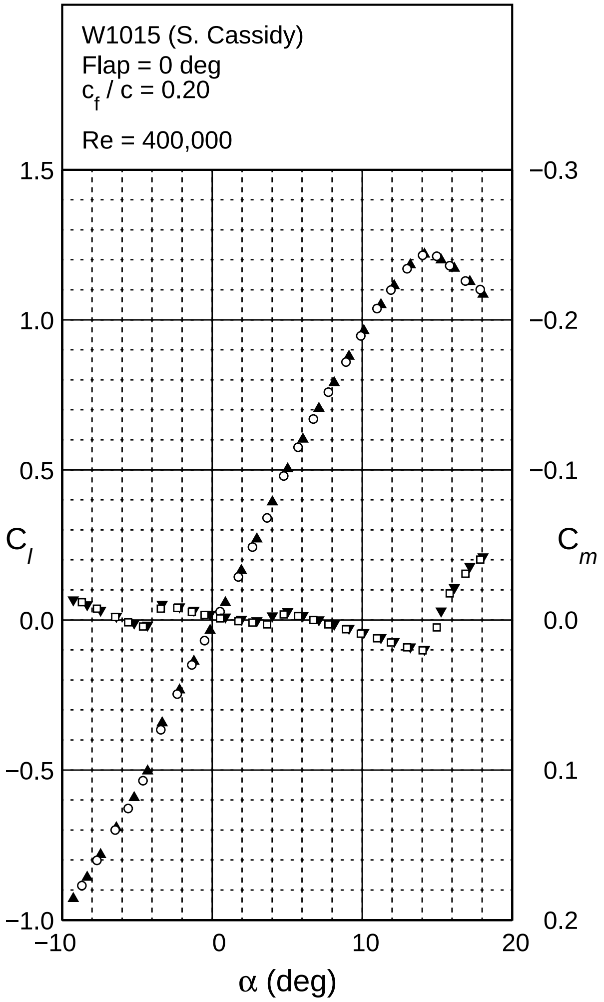

Figure 6.185: Continued.

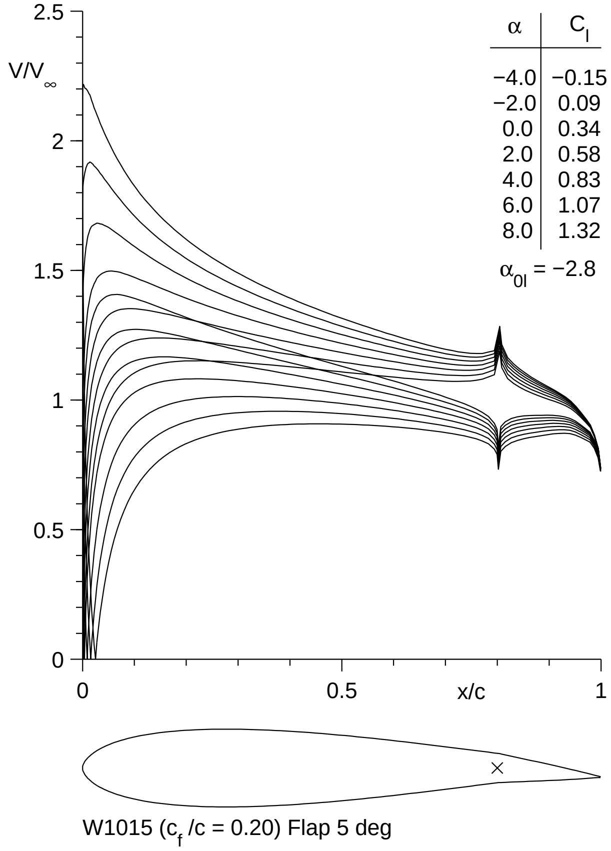

Figure 6.186: Inviscid velocity distribution for the W1015 ($c_f/c = 20\%$) with a 5 deg flap.

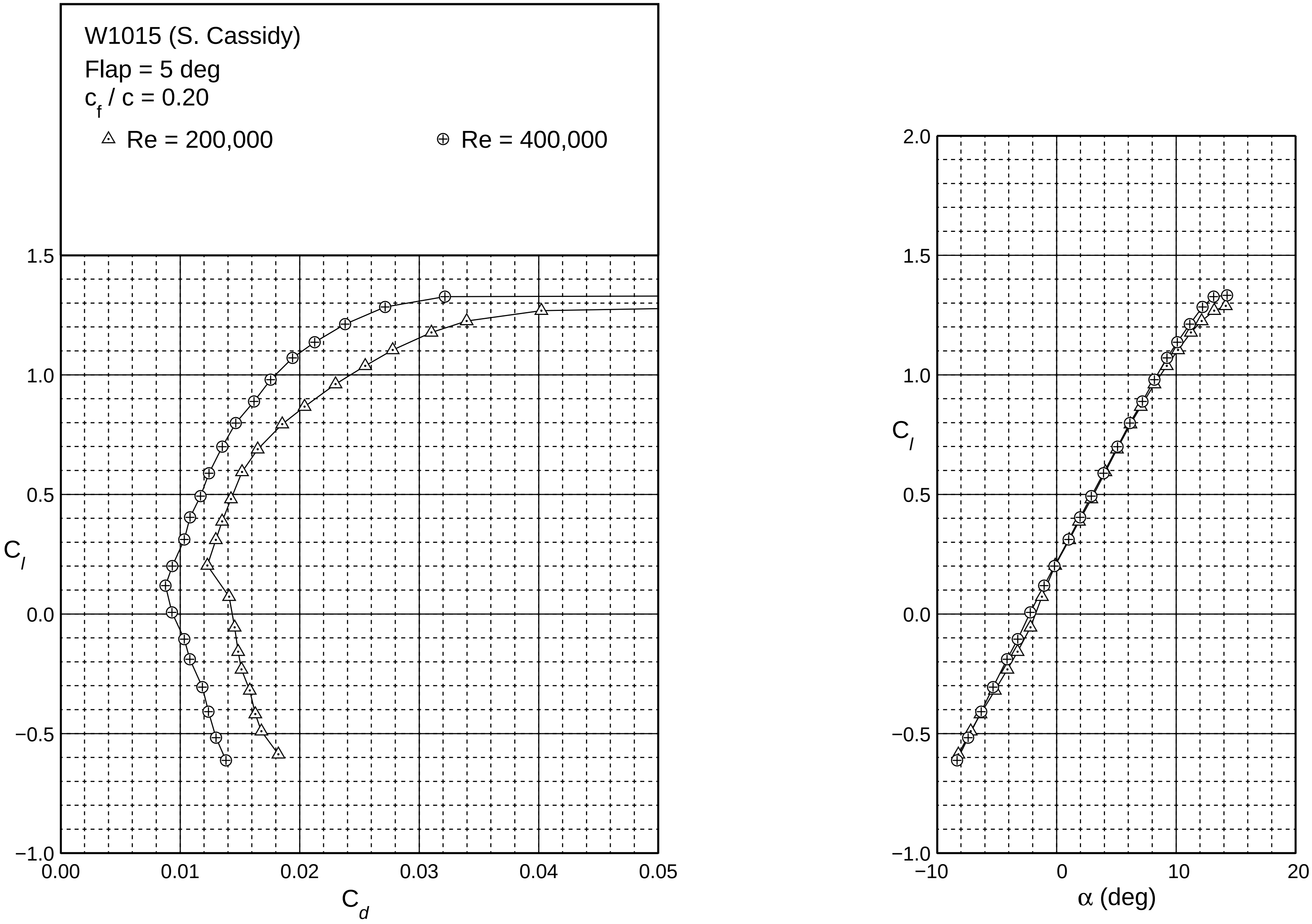

Figure 6.187: Drag polar for the W1015 ($c_f/c = 20\%$) with a 5 deg flap.

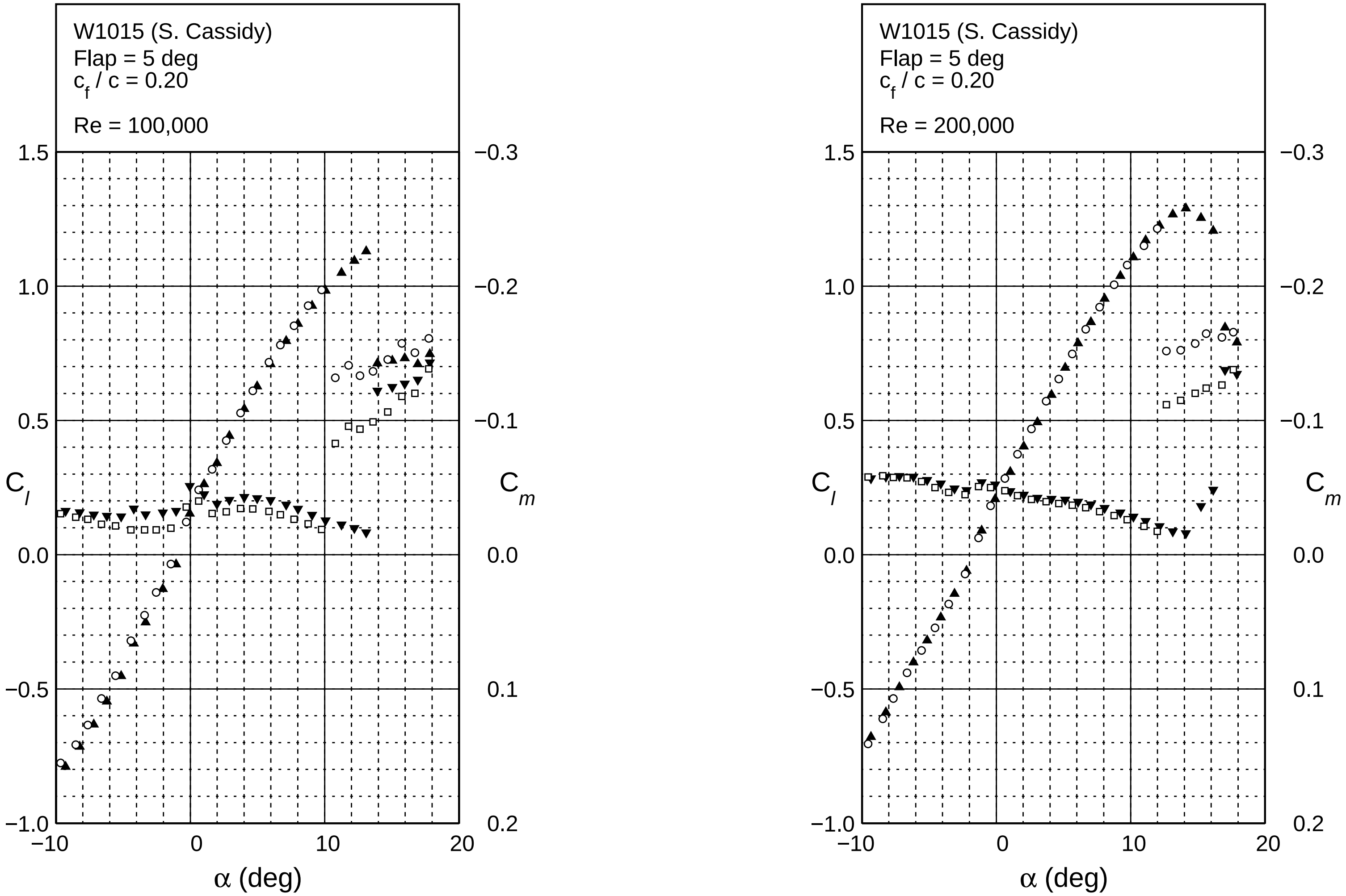

Figure 6.188: Lift and moment characteristics for the W1015 ($c_f/c = 20\%$) with a 5 deg flap.

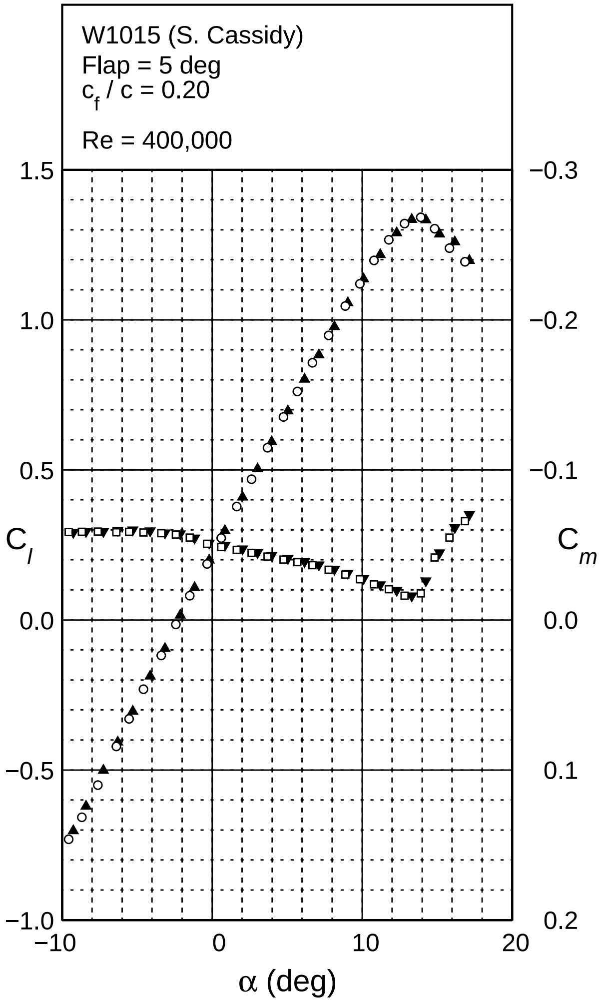

Figure 6.188: Continued.

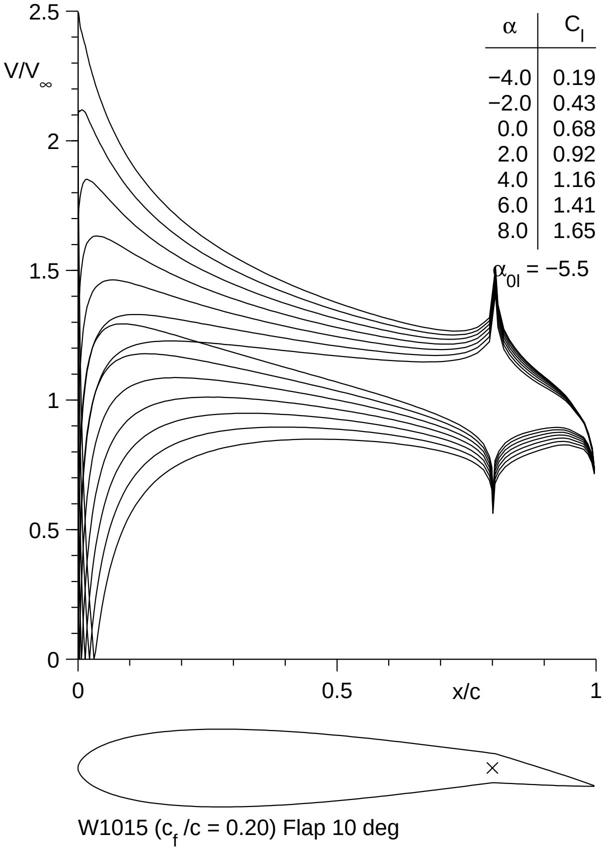

Figure 6.189: Inviscid velocity distribution for the W1015 ($c_f/c = 20\%$) with a 10 deg flap.

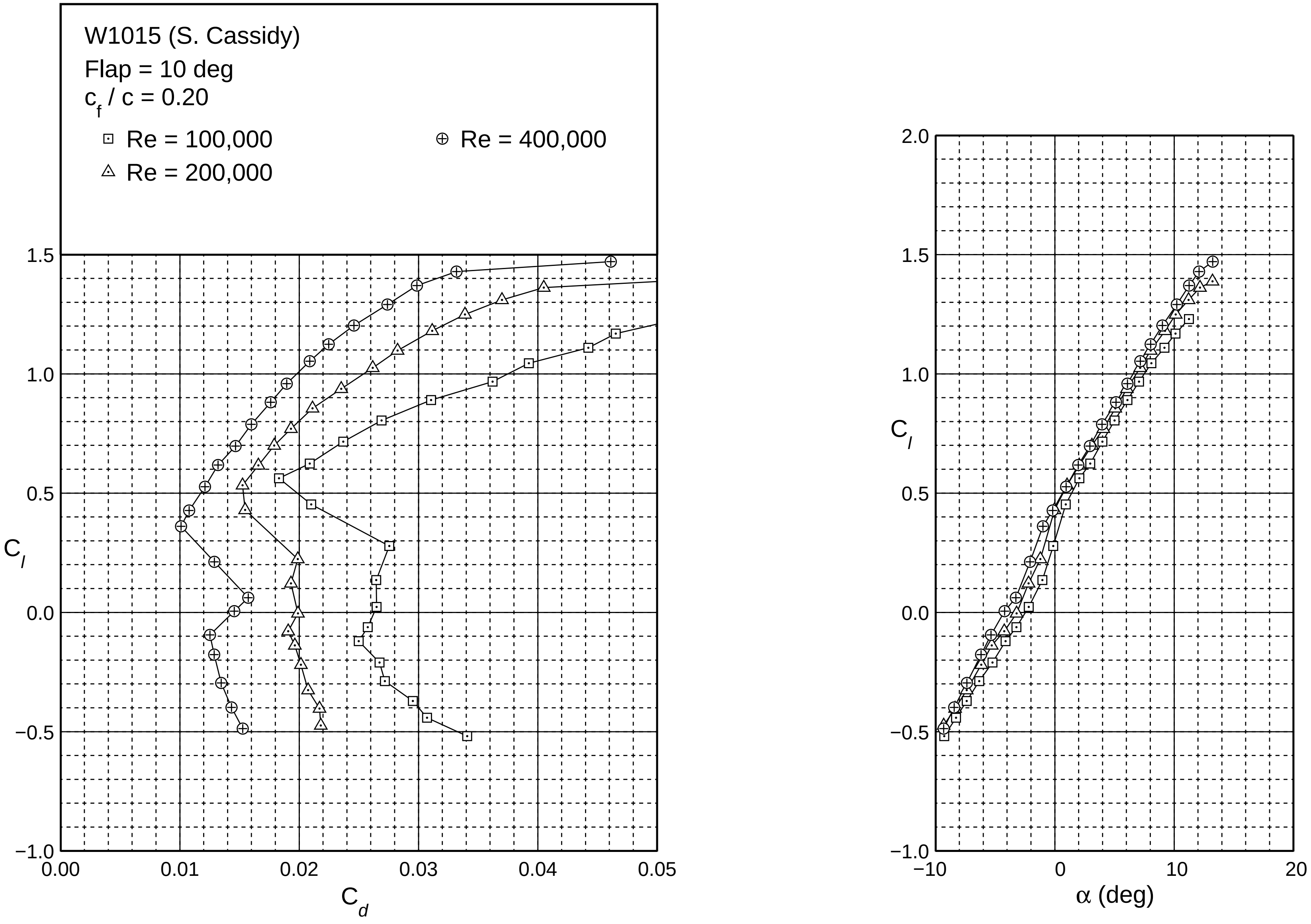

Figure 6.190: Drag polar for the W1015 ($c_f/c = 20\%$) with a 10 deg flap.

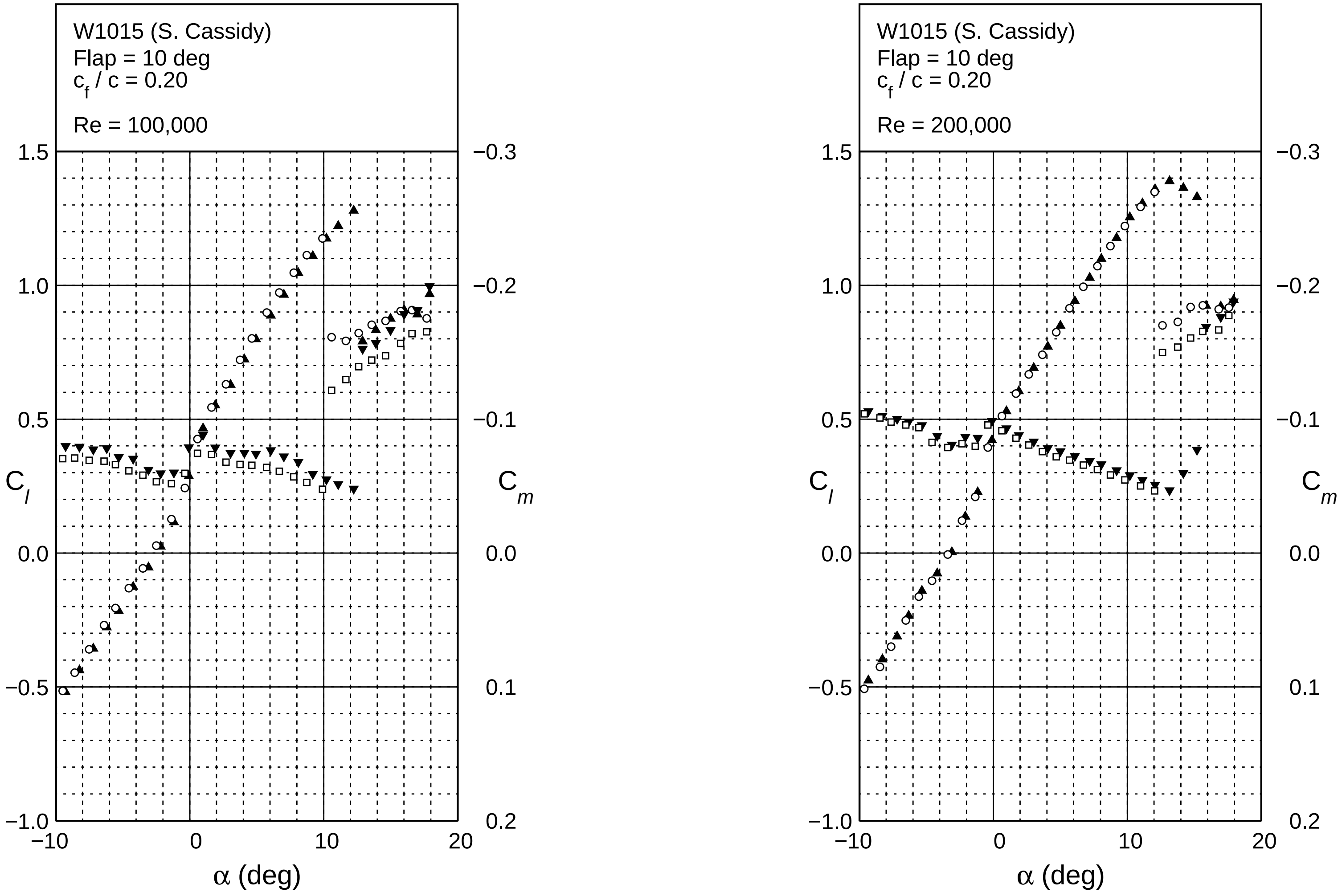

Figure 6.191: Lift and moment characteristics for the W1015 ($c_f/c = 20\%$) with a 10 deg flap.

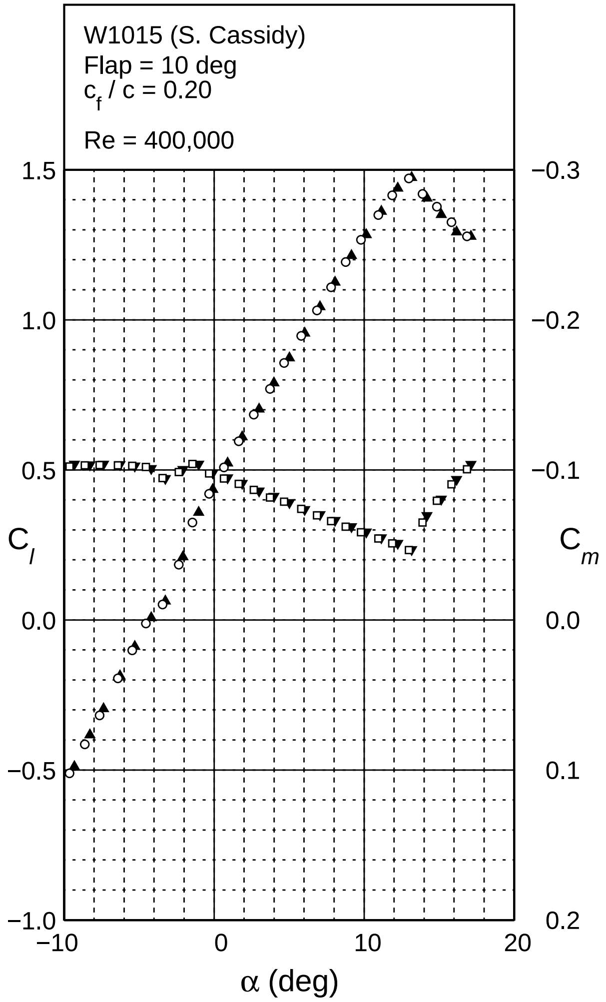

Figure 6.191: Continued.

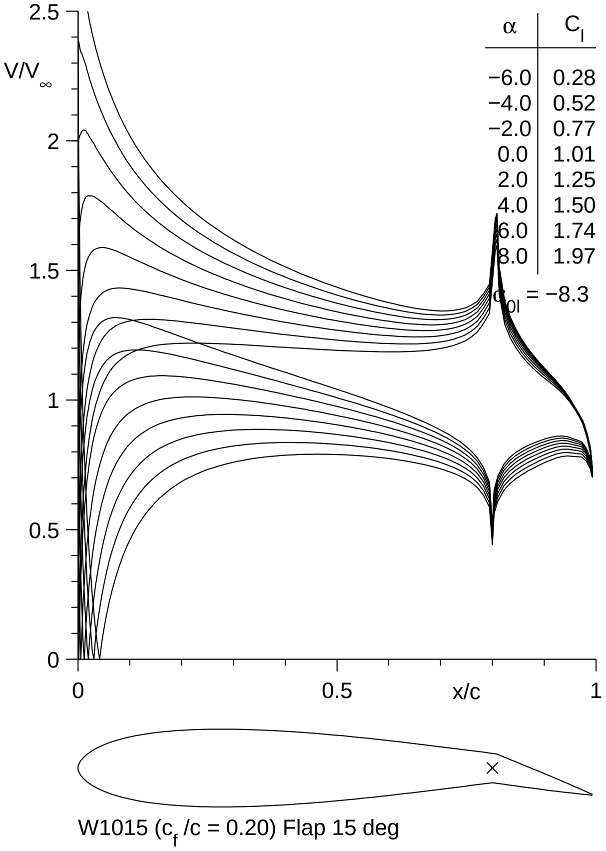

Figure 6.192: Inviscid velocity distribution for the W1015 ($c_f/c = 20\%$) with a 15 deg flap.

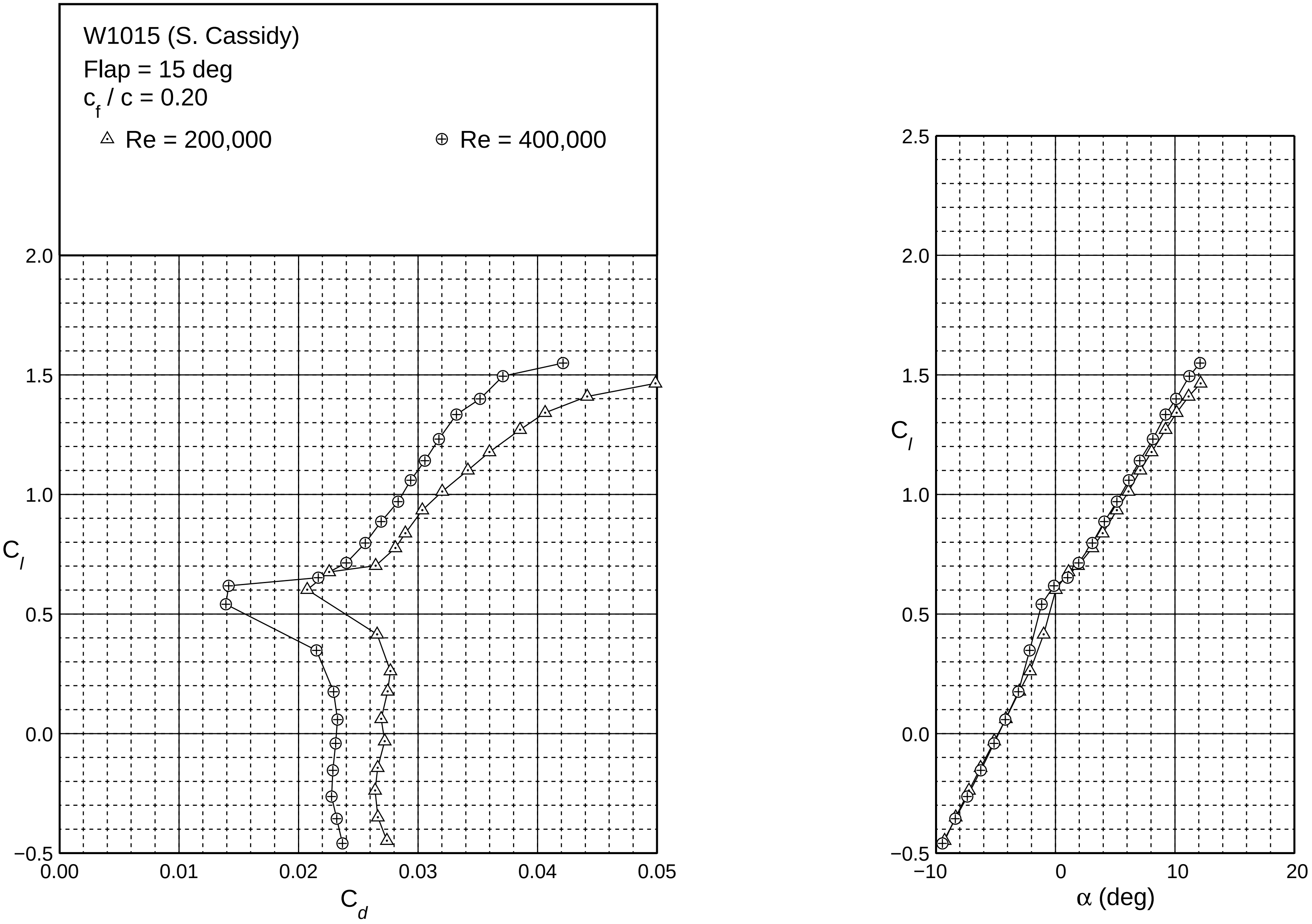

Figure 6.193: Drag polar for the W1015 ($c_f/c = 20\%$) with a 15 deg flap.

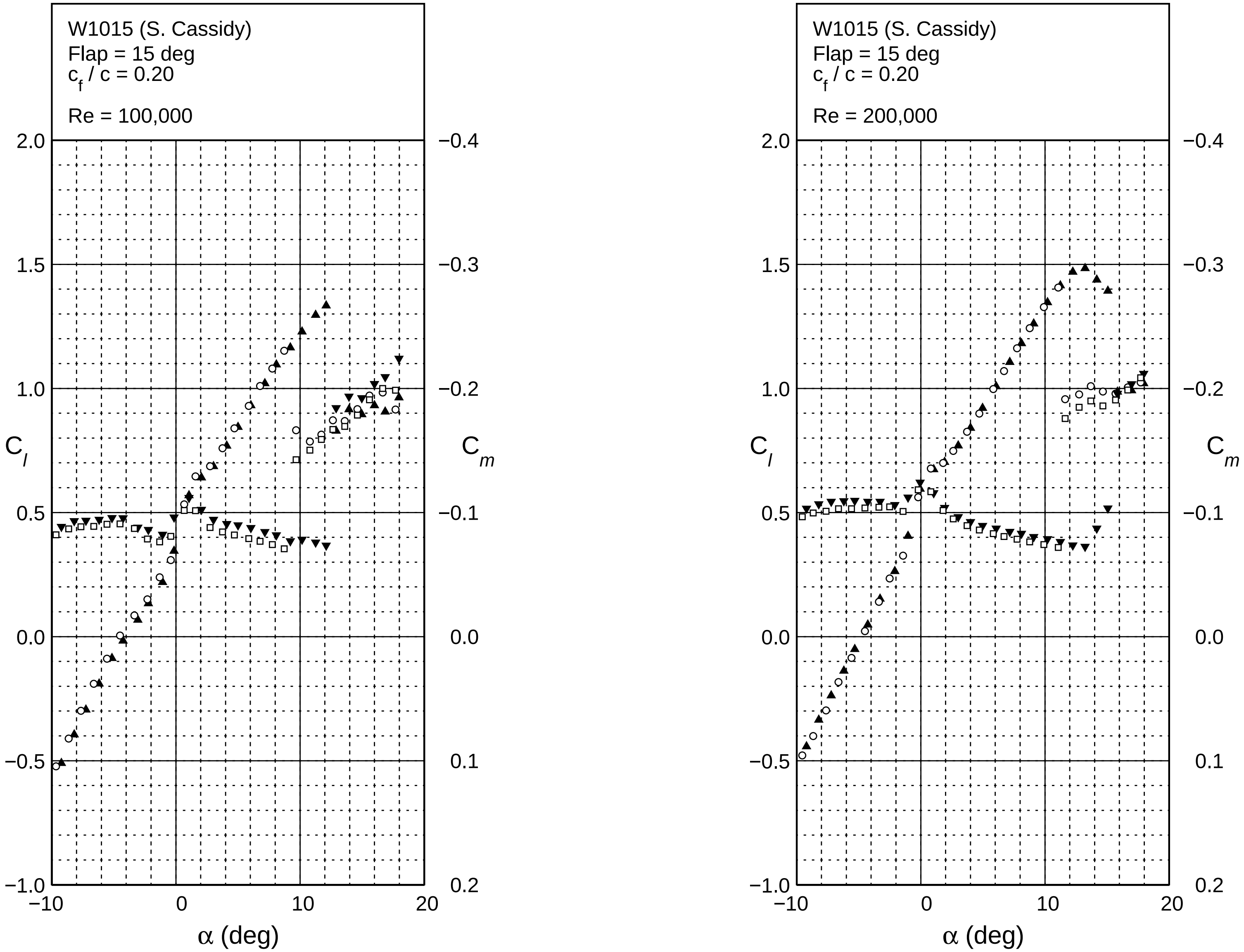

Figure 6.194: Lift and moment characteristics for the W1015 ($c_f/c = 20\%$) with a 15 deg flap.

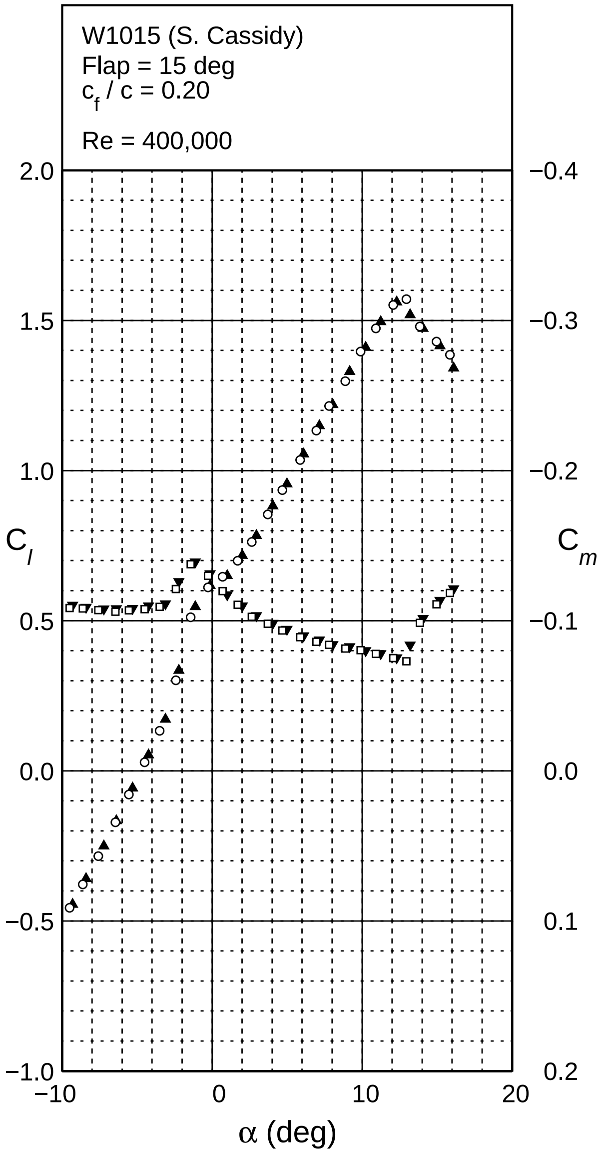

Figure 6.194: Continued.

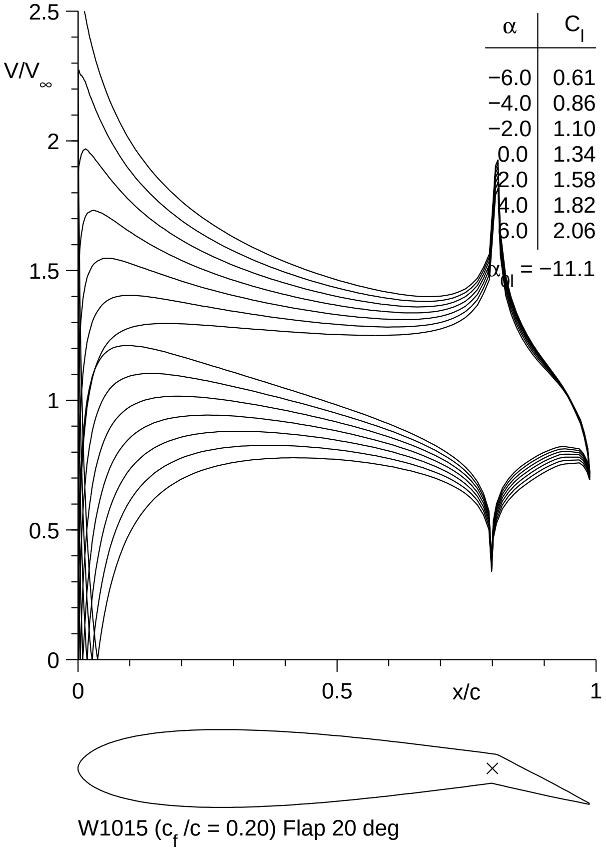

Figure 6.195: Inviscid velocity distribution for the W1015 ($c_f/c = 20\%$) with a 20 deg flap.

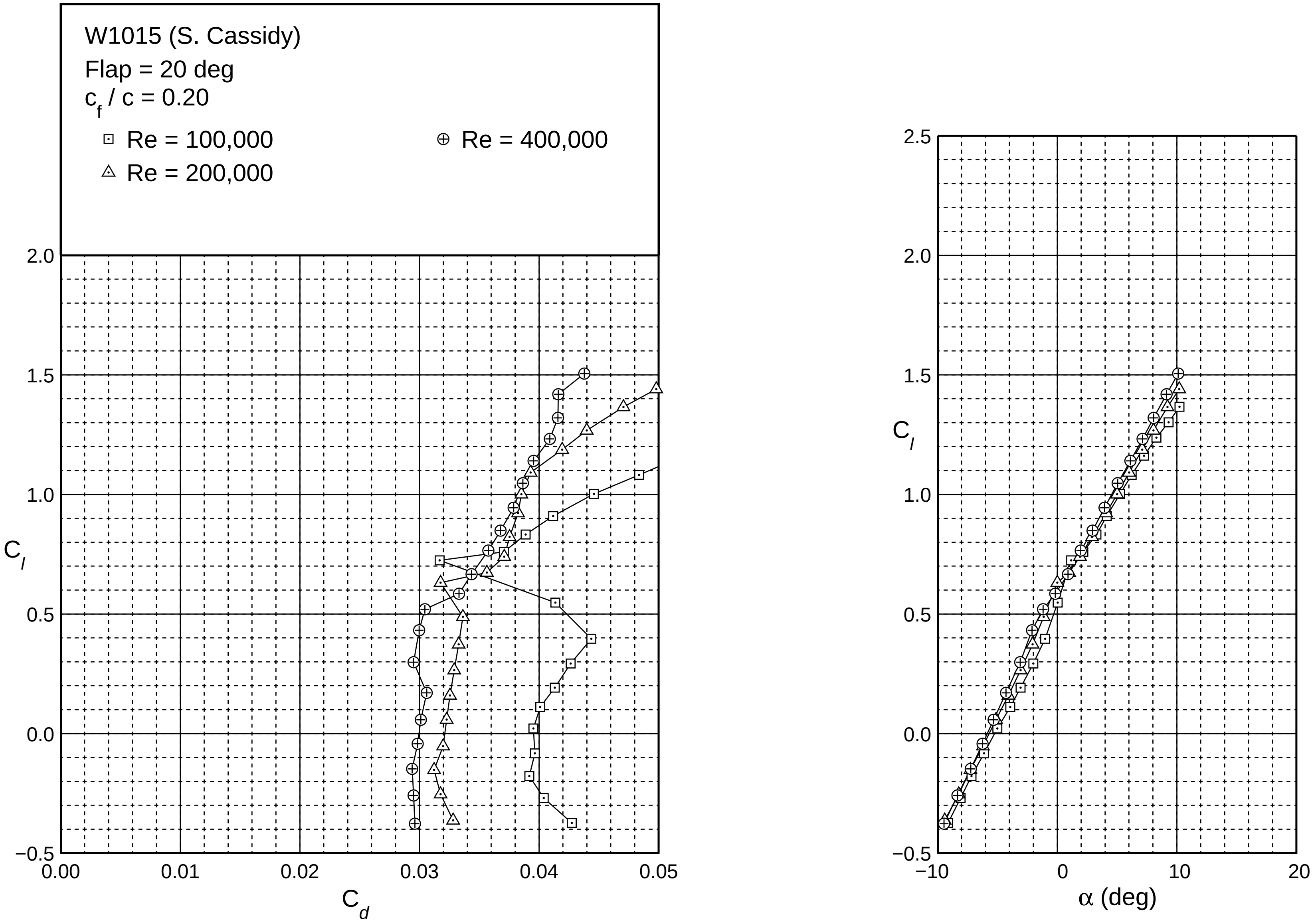

Figure 6.196: Drag polar for the W1015 ($c_f/c = 20\%$) with a 20 deg flap.

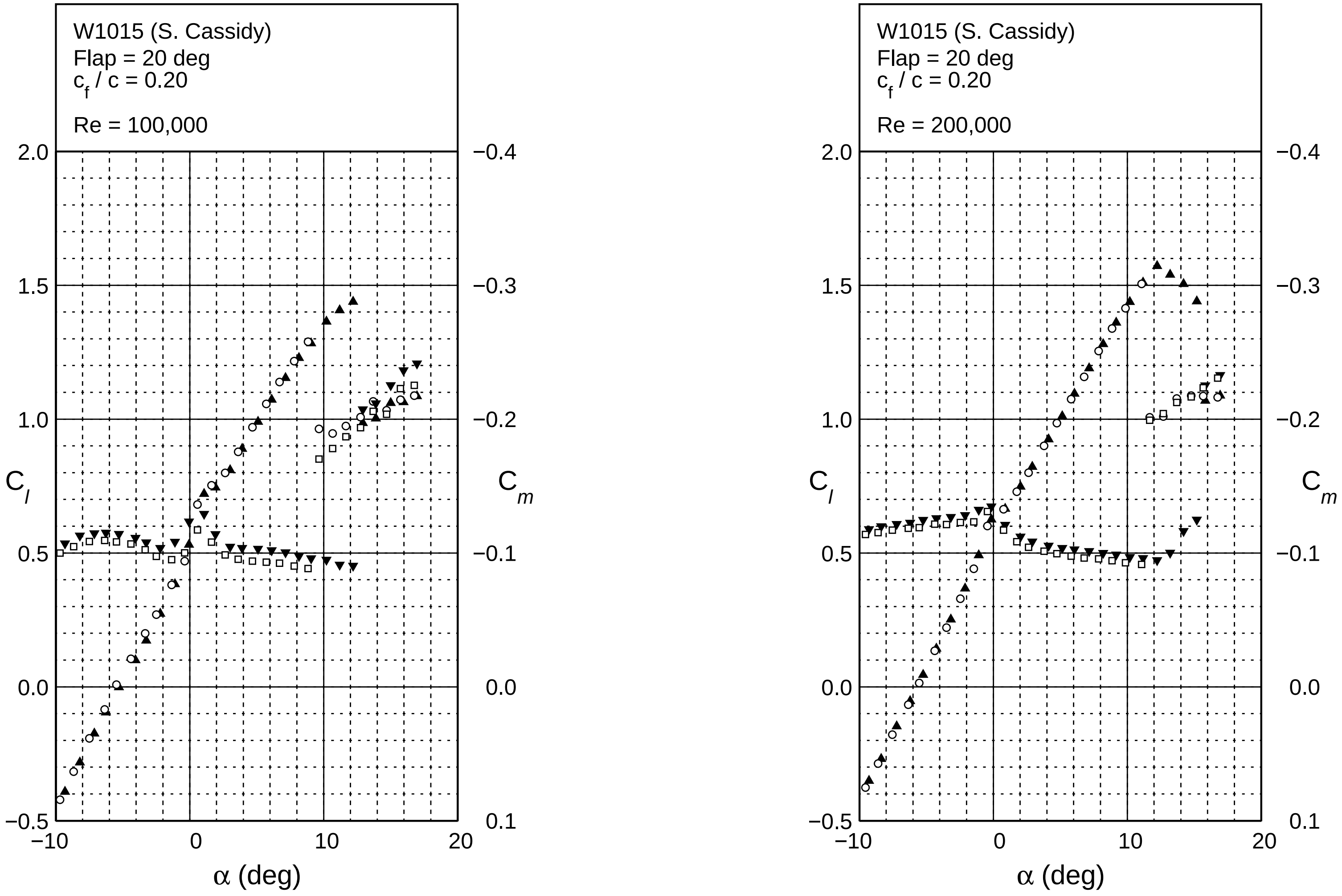

Figure 6.197: Lift and moment characteristics for the W1015 ($c_f/c = 20\%$) with a 20 deg flap.

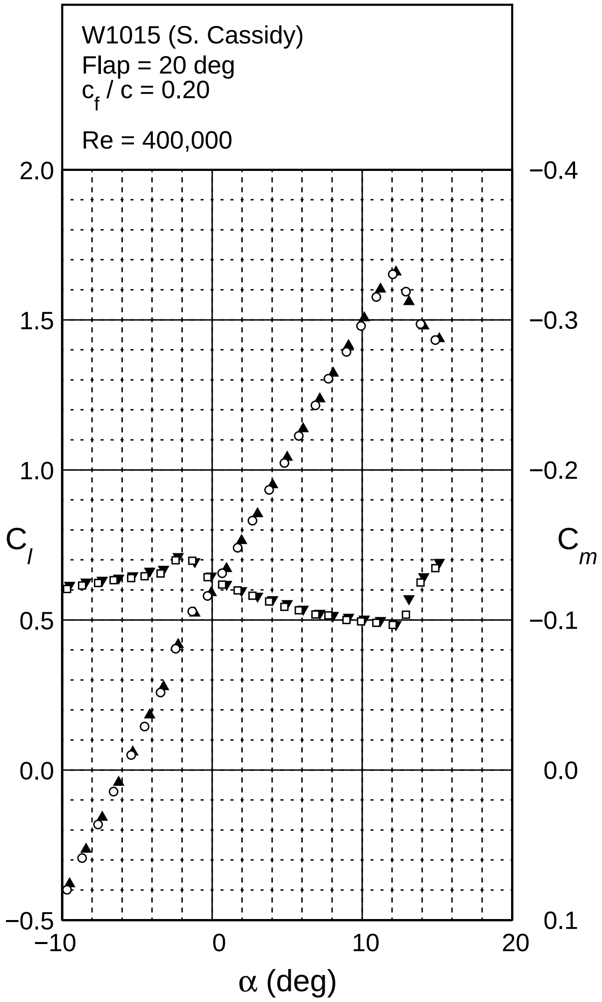

Figure 6.197: Continued.

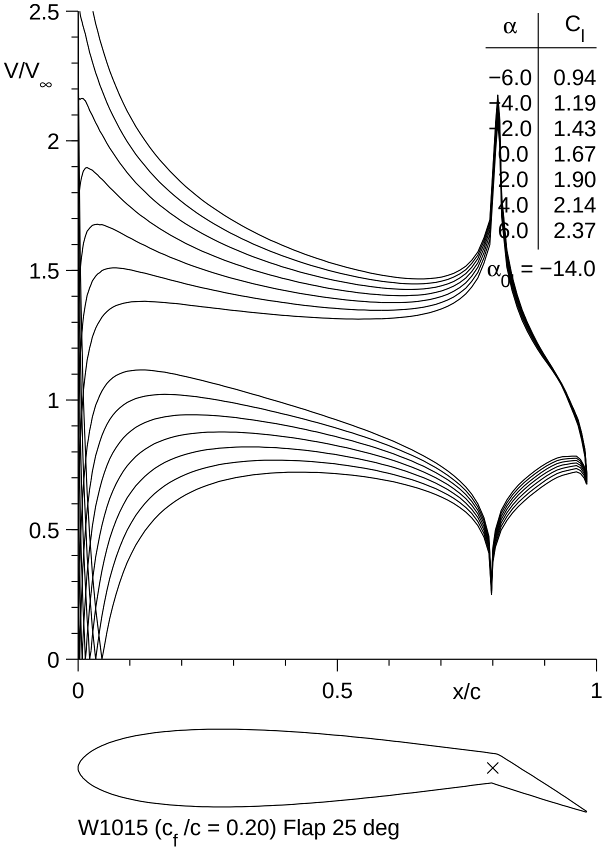

Figure 6.198: Inviscid velocity distribution for the W1015 ($c_f/c = 20\%$) with a 25 deg flap.

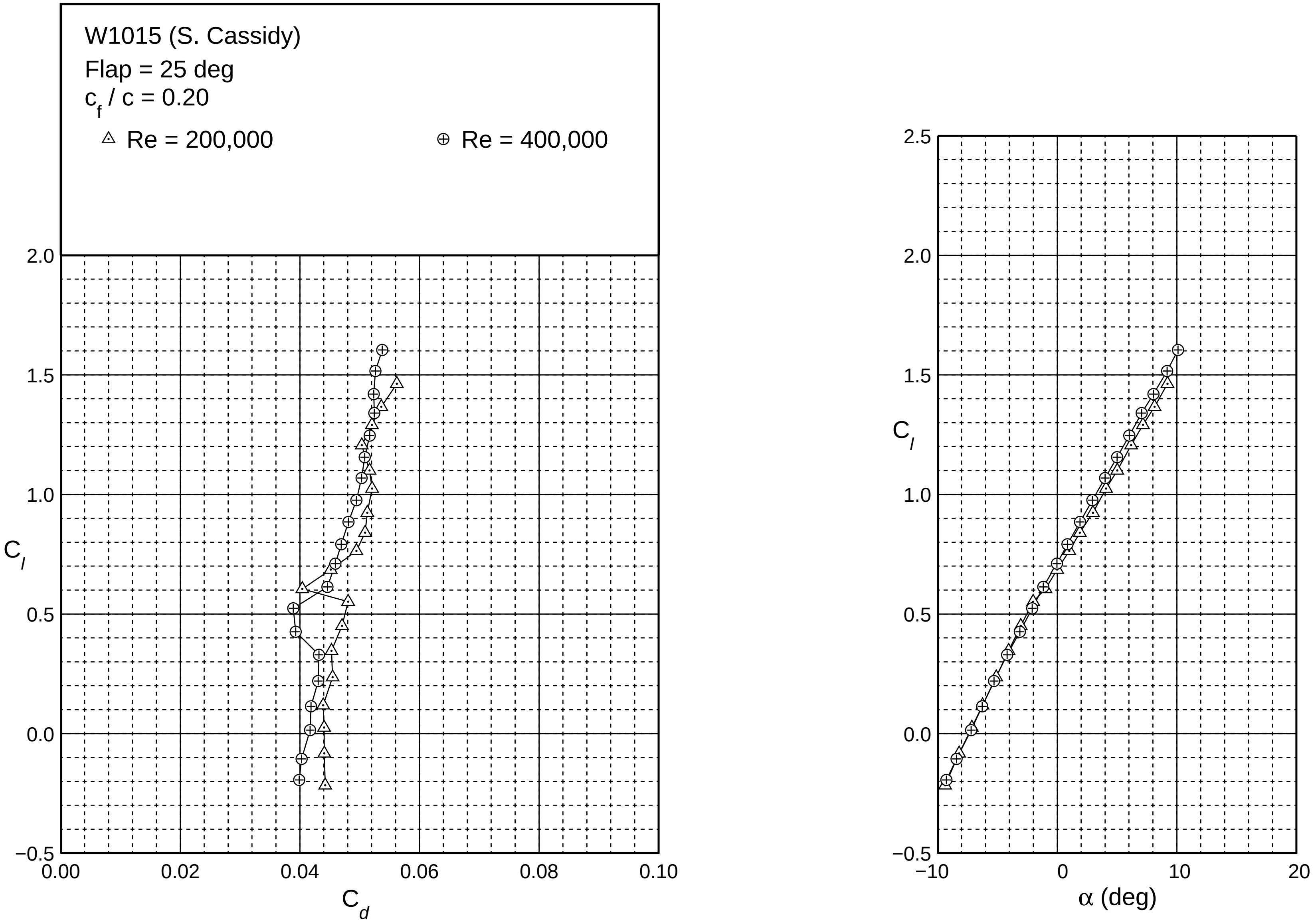

Figure 6.199: Drag polar for the W1015 ($c_f/c = 20\%$) with a 25 deg flap.

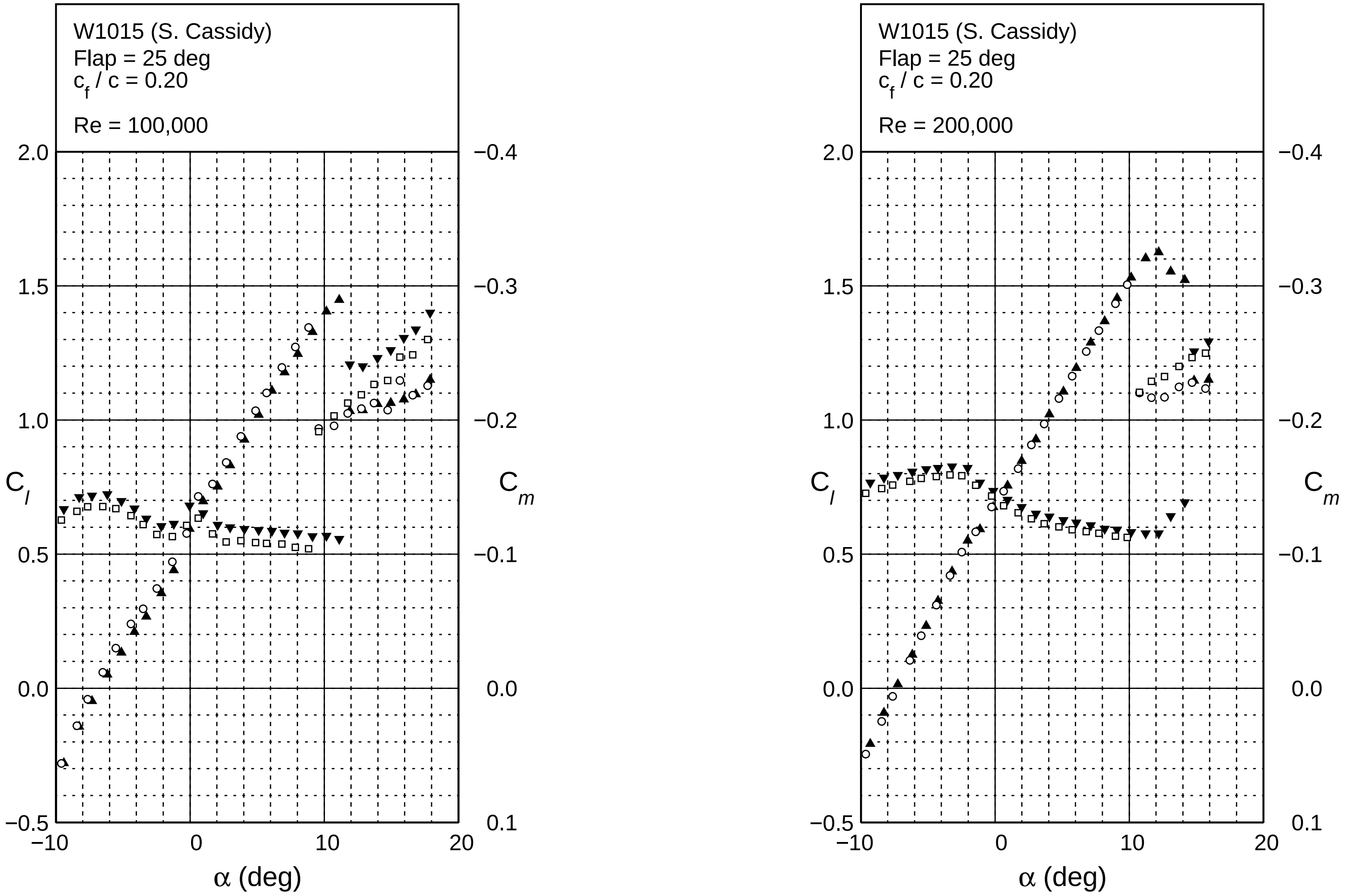

Figure 6.200: Lift and moment characteristics for the W1015 ($c_f/c = 20\%$) with a 25 deg flap.

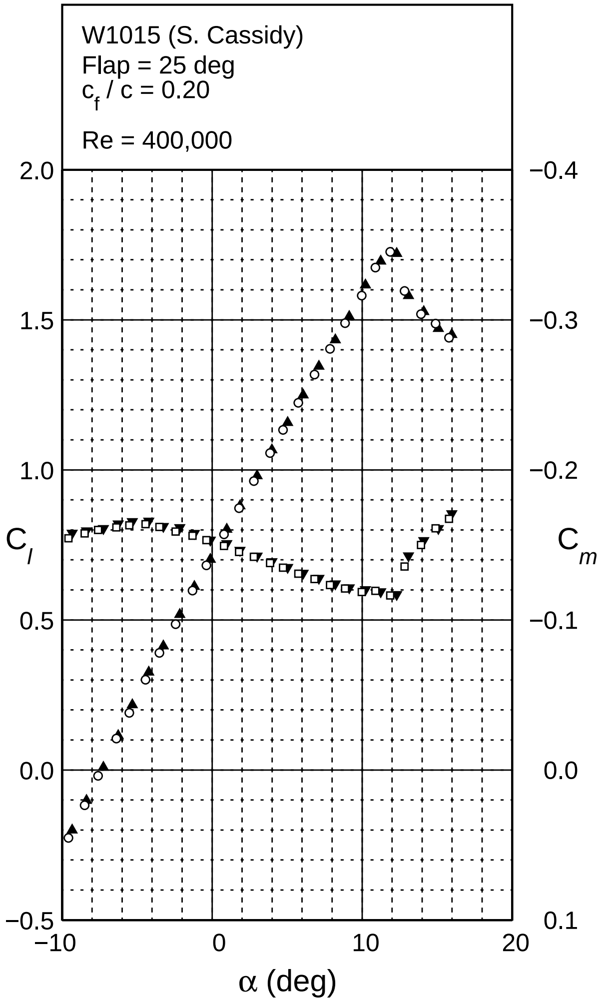

Figure 6.200: Continued.

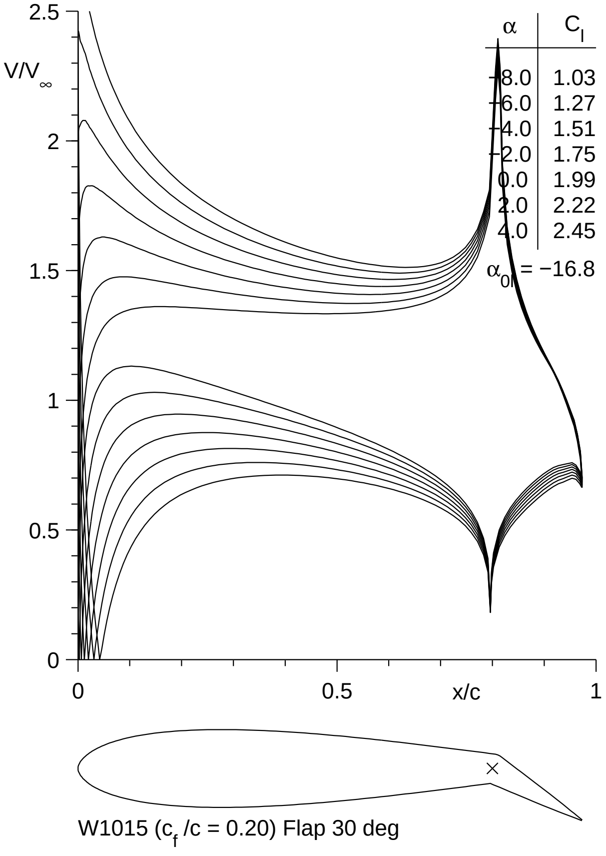

Figure 6.201: Inviscid velocity distribution for the W1015 ($c_f/c = 20\%$) with a 30 deg flap.

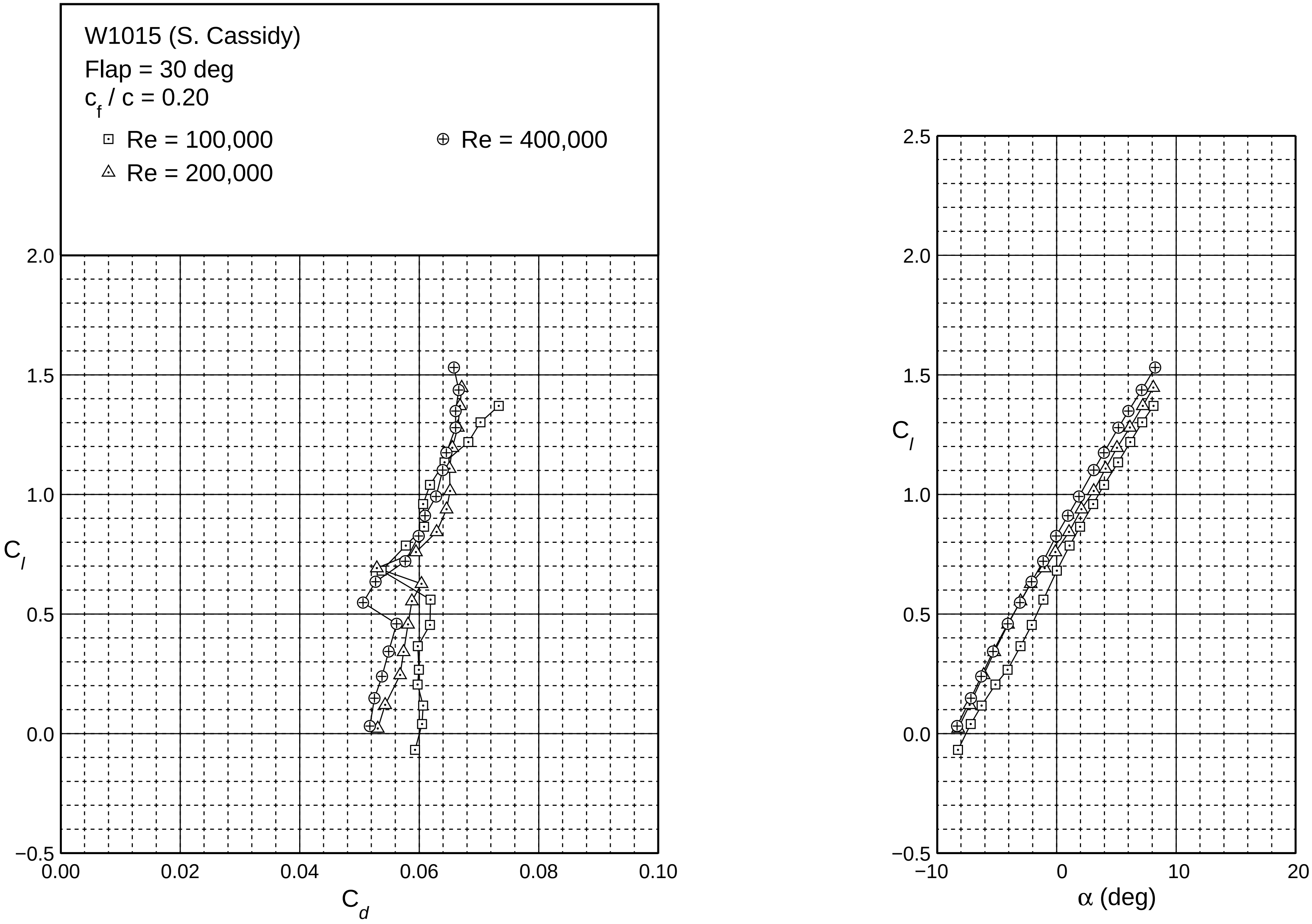

Figure 6.202: Drag polar for the W1015 ($c_f/c = 20\%$) with a 30 deg flap.

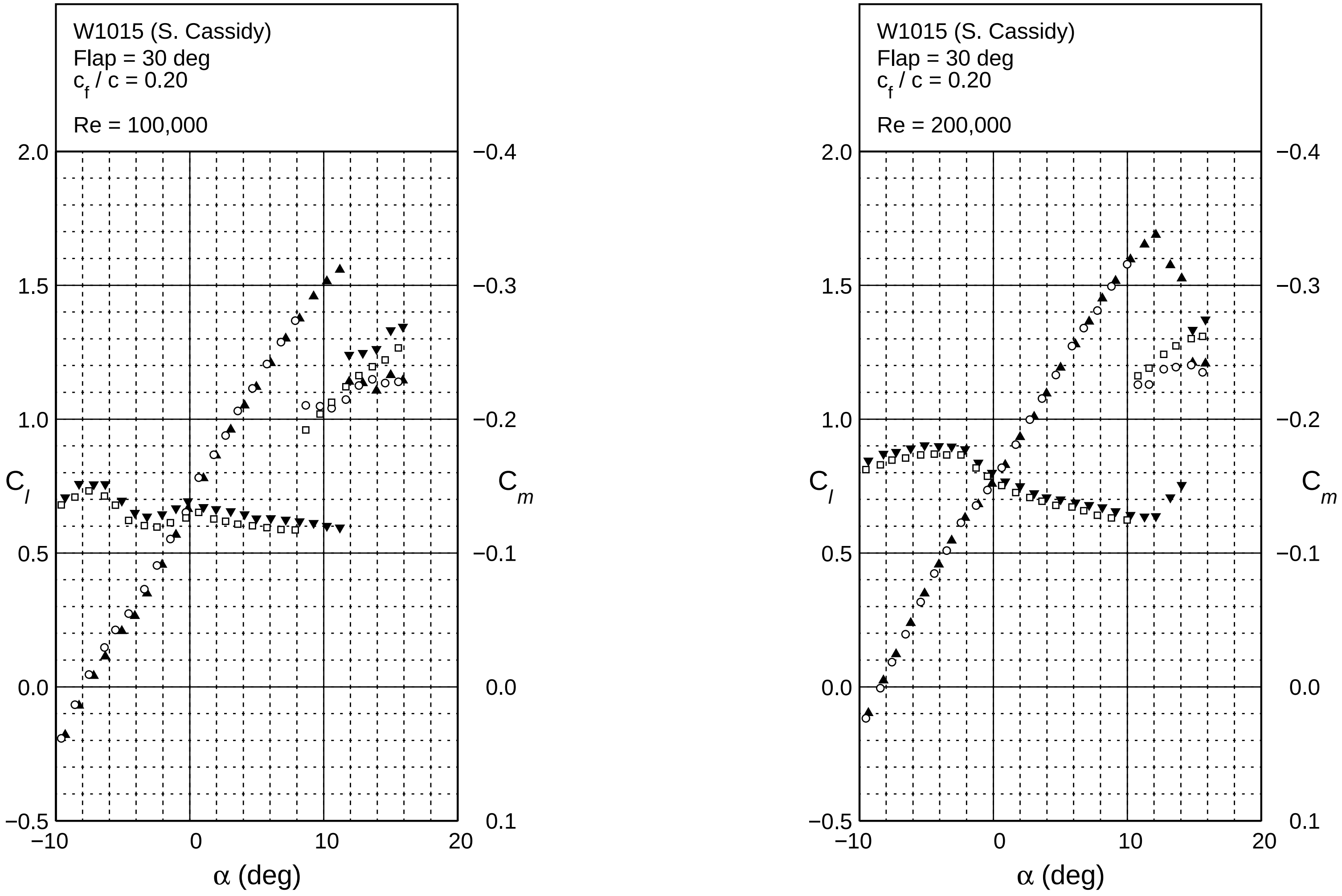

Figure 6.203: Lift and moment characteristics for the W1015 ($c_f/c = 20\%$) with a 30 deg flap.

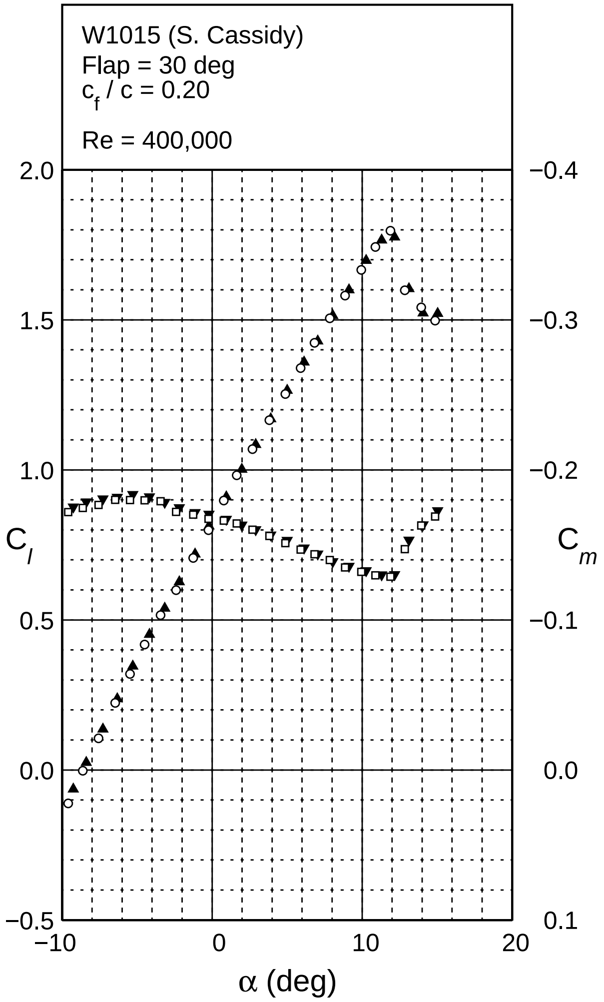

Figure 6.203: Continued.

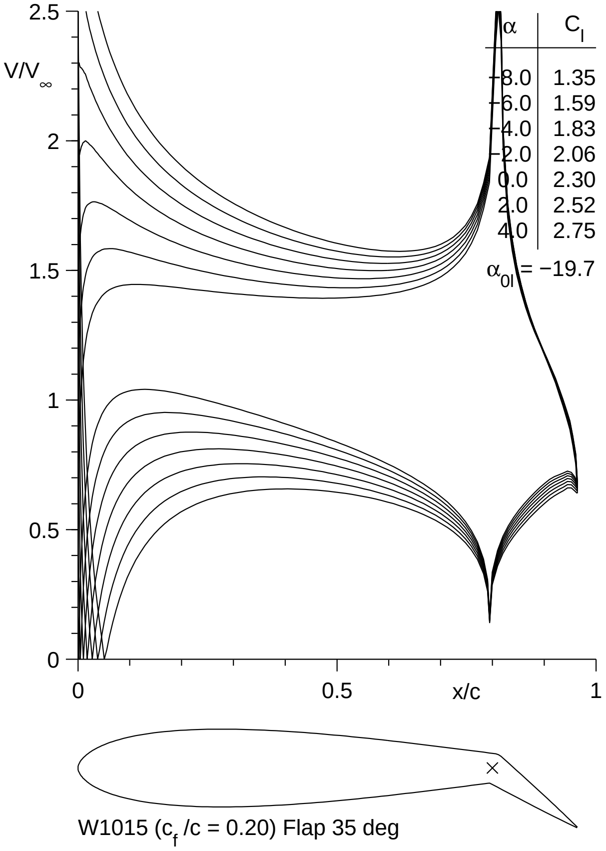

Figure 6.204: Inviscid velocity distribution for the W1015 ($c_f/c = 20\%$) with a 35 deg flap.

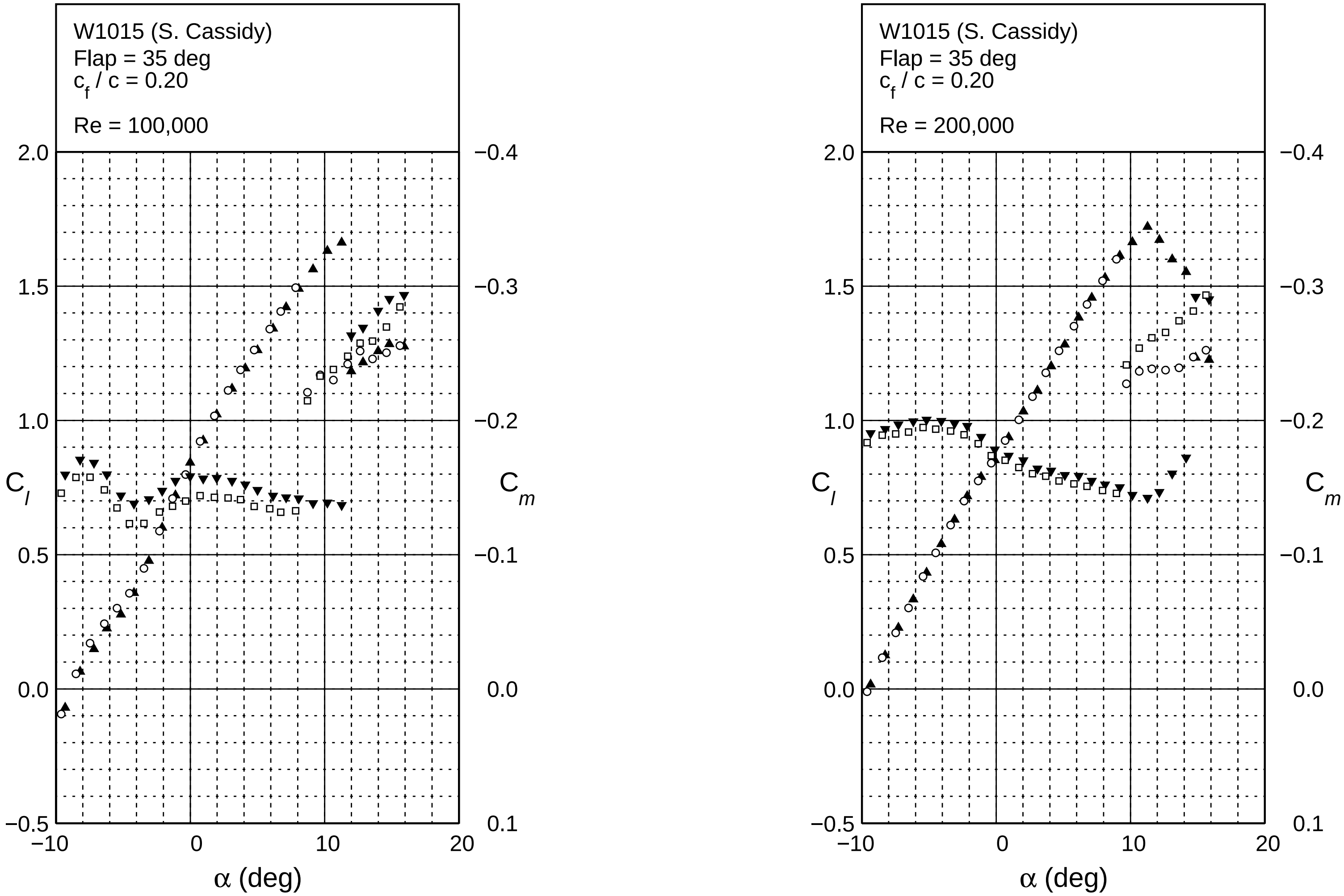

Figure 6.205: Lift and moment characteristics for the W1015 ($c_f/c = 20\%$) with a 35 deg flap.

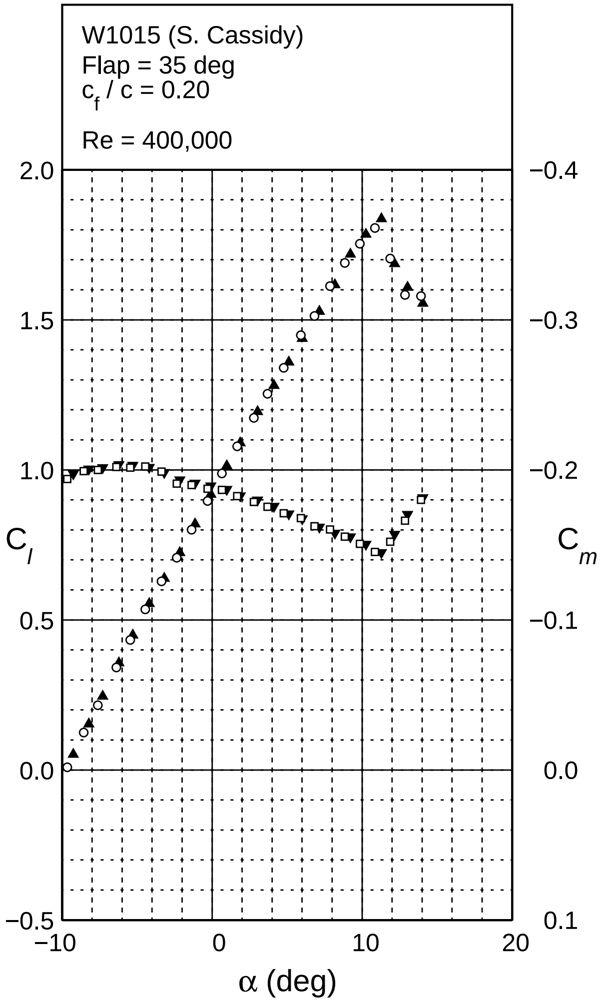

Figure 6.205: Continued.

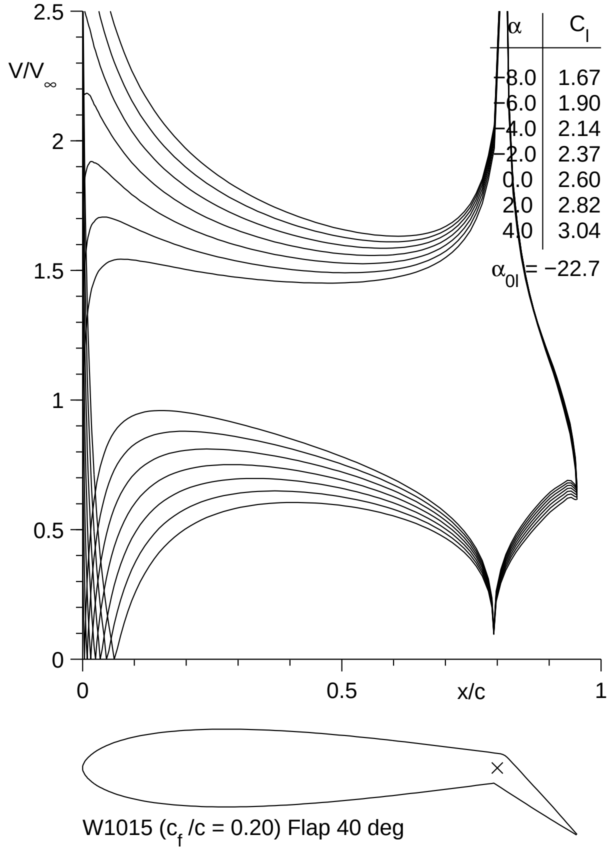

Figure 6.206: Inviscid velocity distribution for the W1015 $(c_f/c = 20\%)$ with a 40 deg flap.

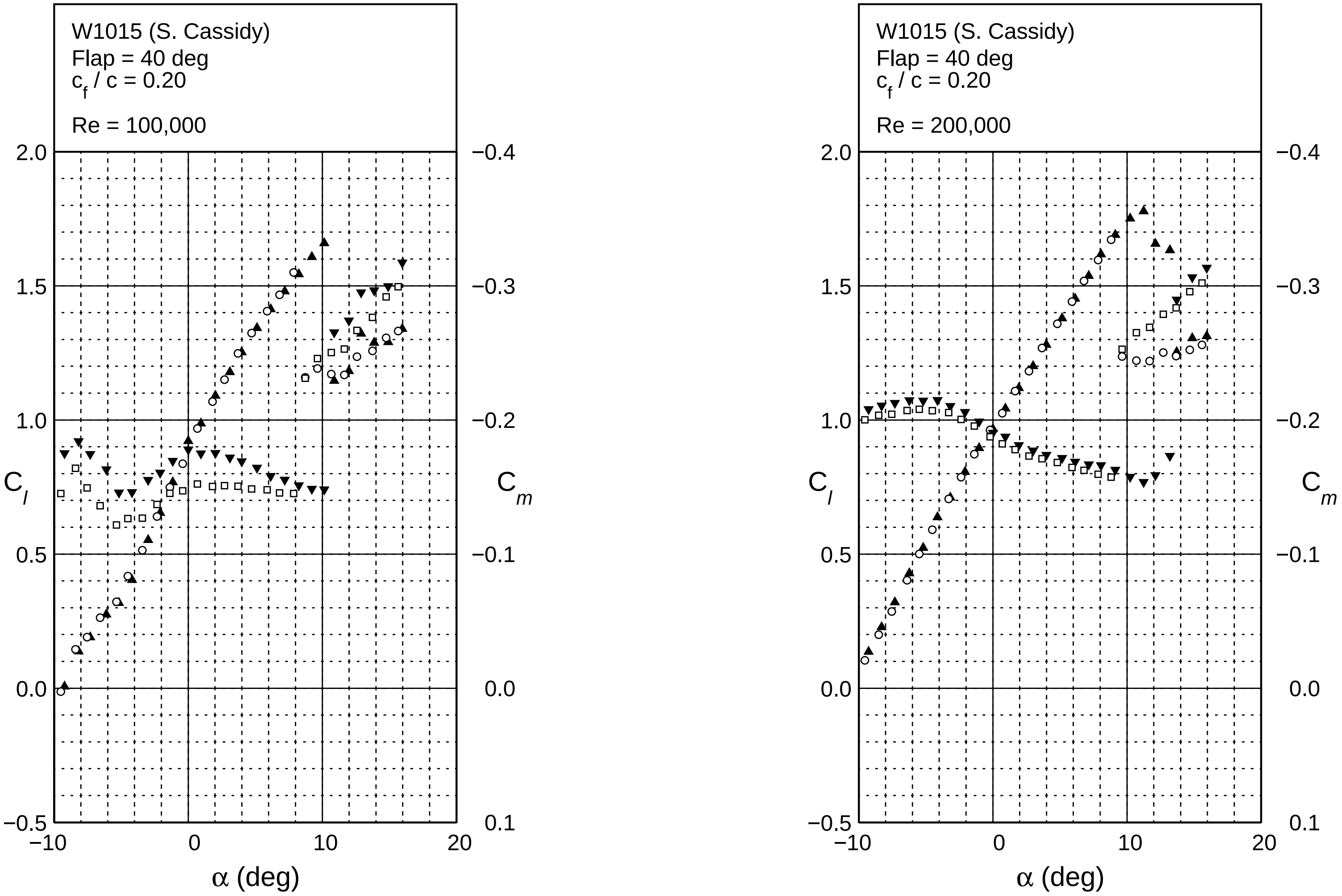

Figure 6.207: Lift and moment characteristics for the W1015 ($c_f/c = 20\%$) with a 40 deg flap.

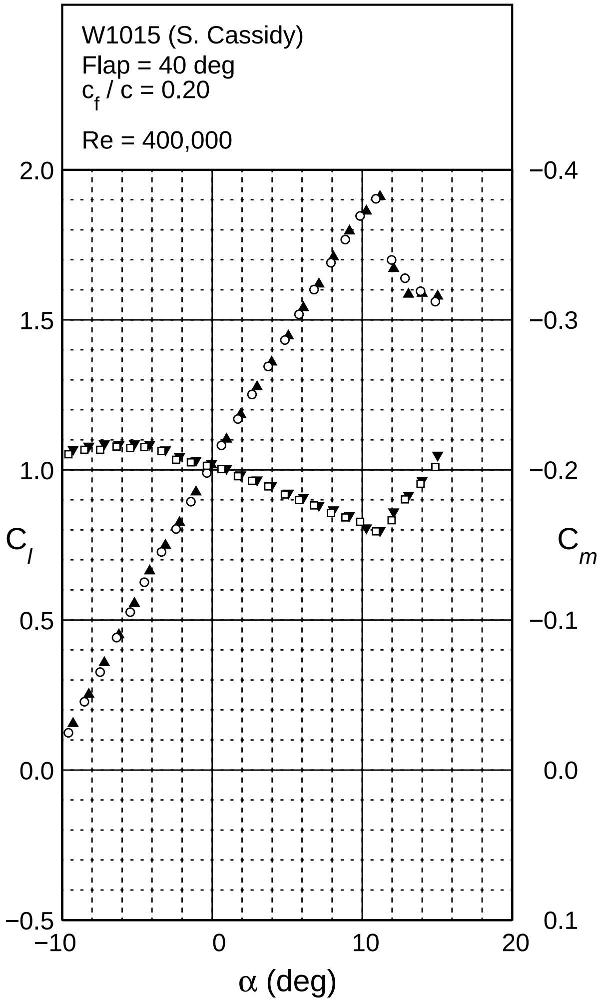

Figure 6.207: Continued.

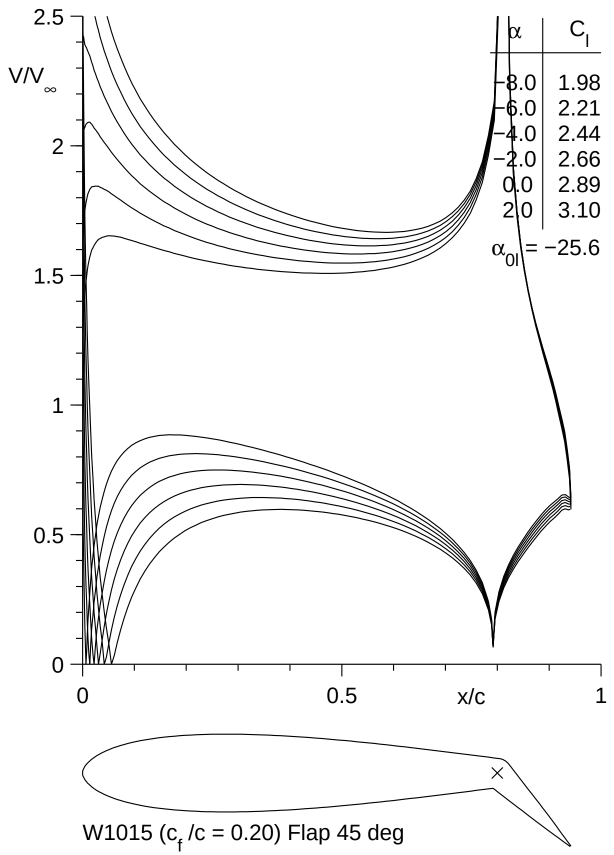

Figure 6.208: Inviscid velocity distribution for the W1015 ($c_f/c = 20\%$) with a 45 deg flap.

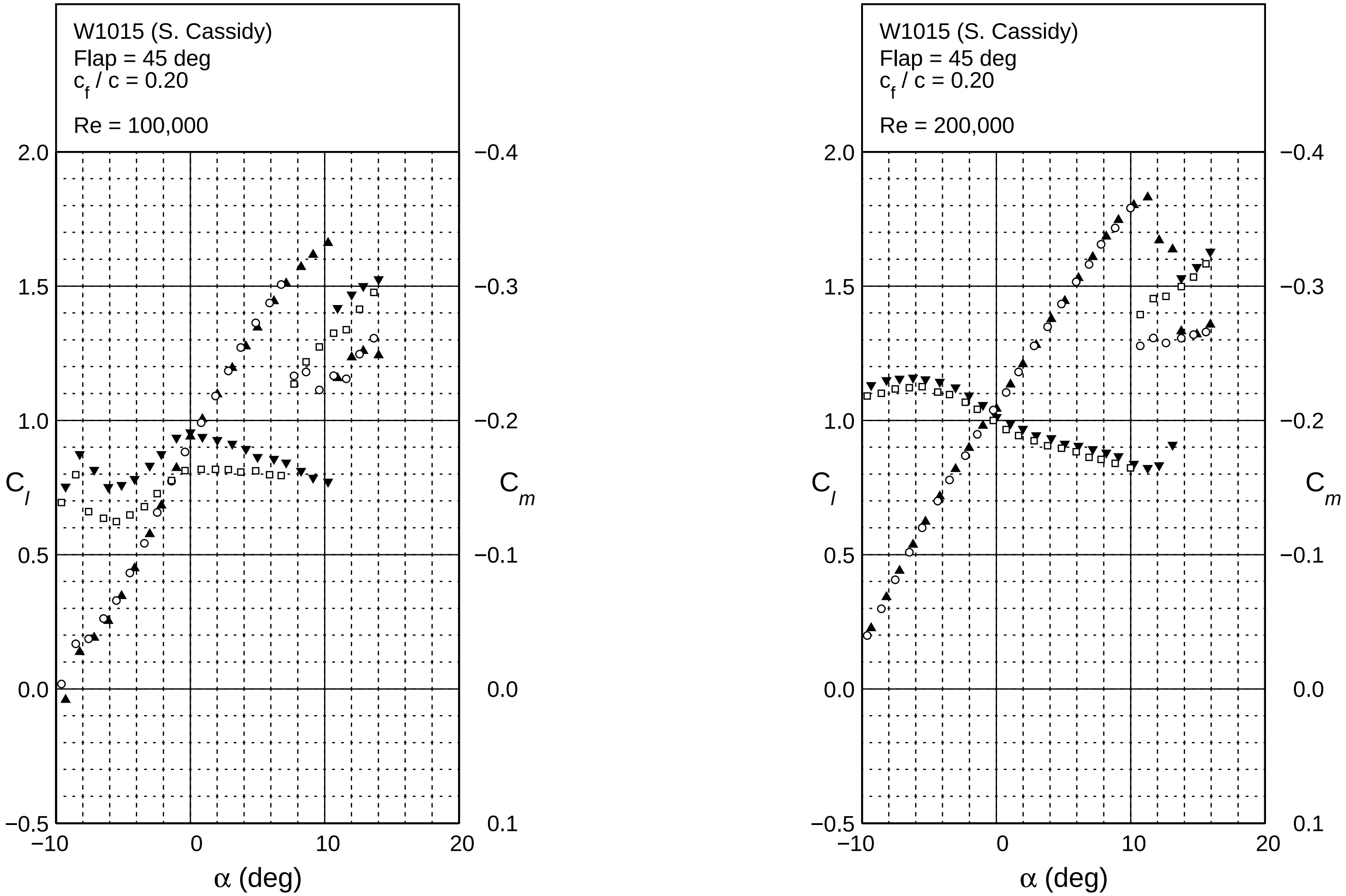

Figure 6.209: Lift and moment characteristics for the W1015 ($c_f/c = 20\%$) with a 45 deg flap.

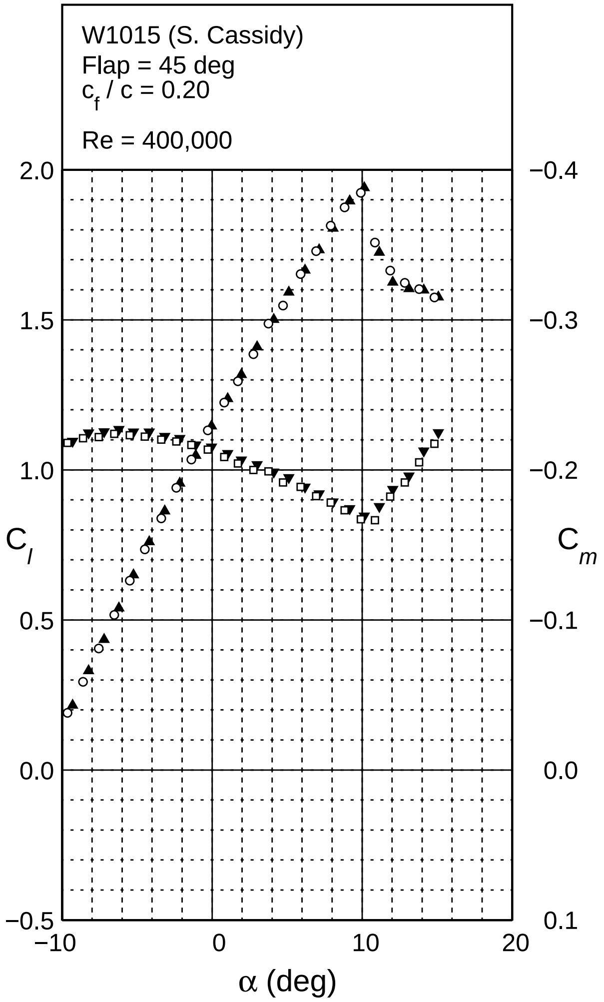

Figure 6.209: Continued.

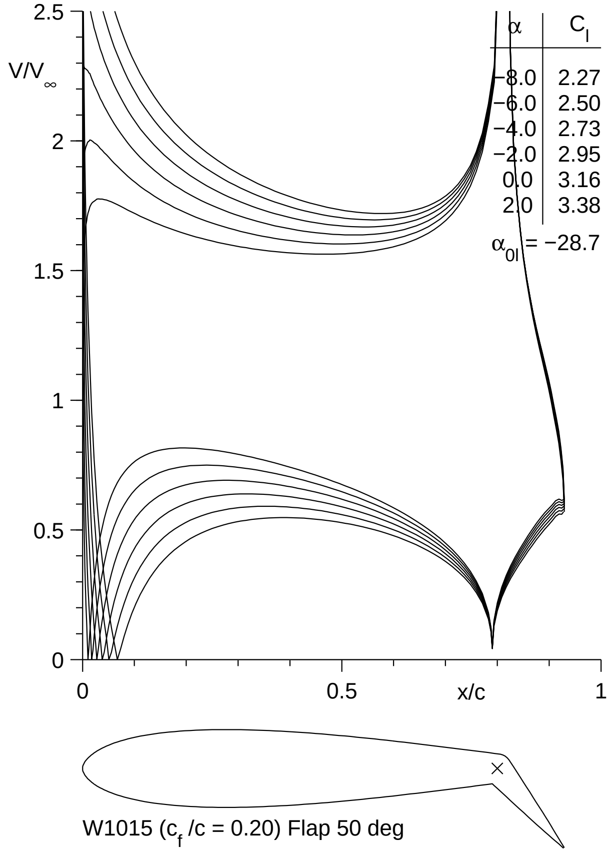

Figure 6.210: Inviscid velocity distribution for the W1015 ($c_f/c = 20\%$) with a 50 deg flap.

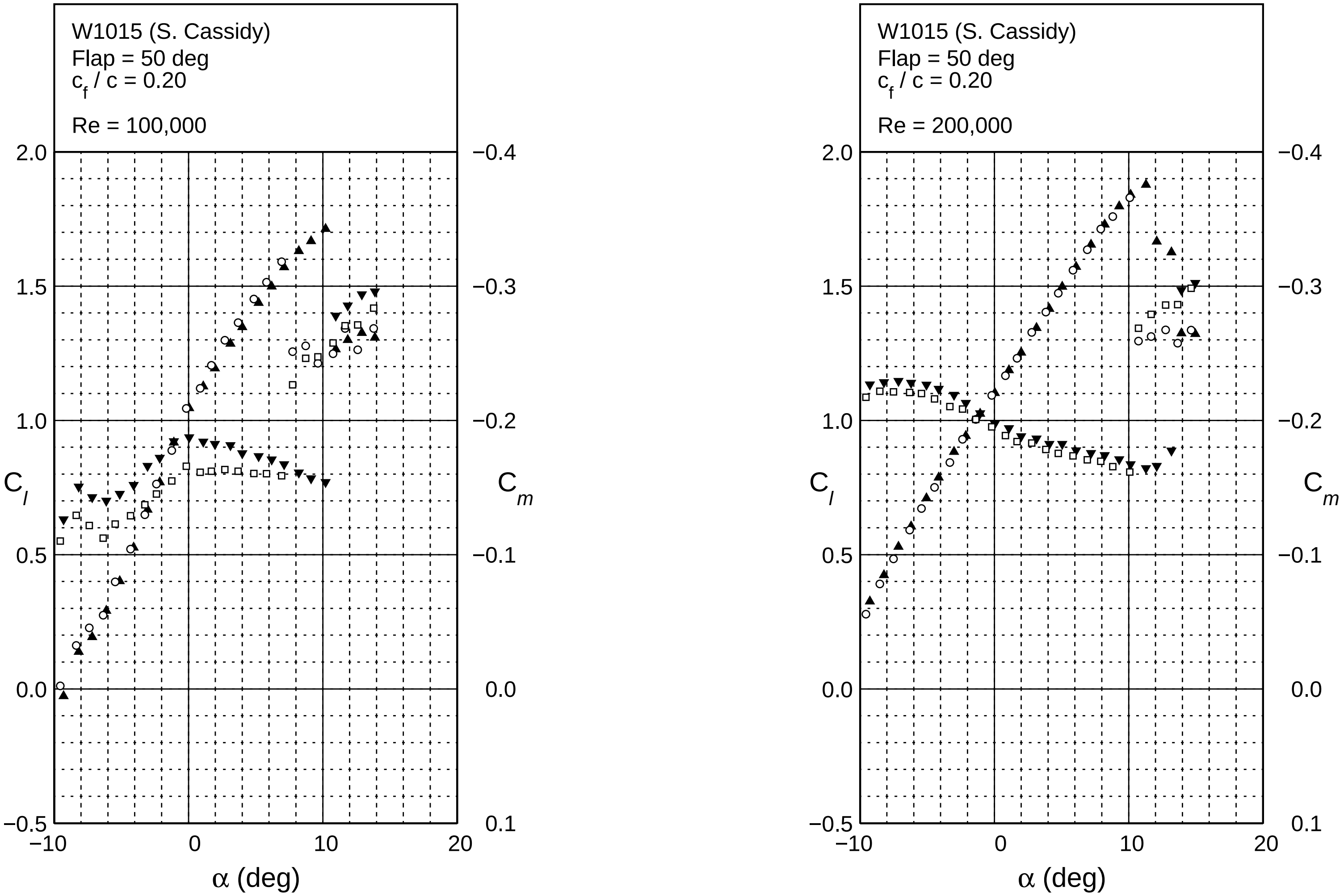

Figure 6.211: Lift and moment characteristics for the W1015 ($c_f/c = 20\%$) with a 50 deg flap.

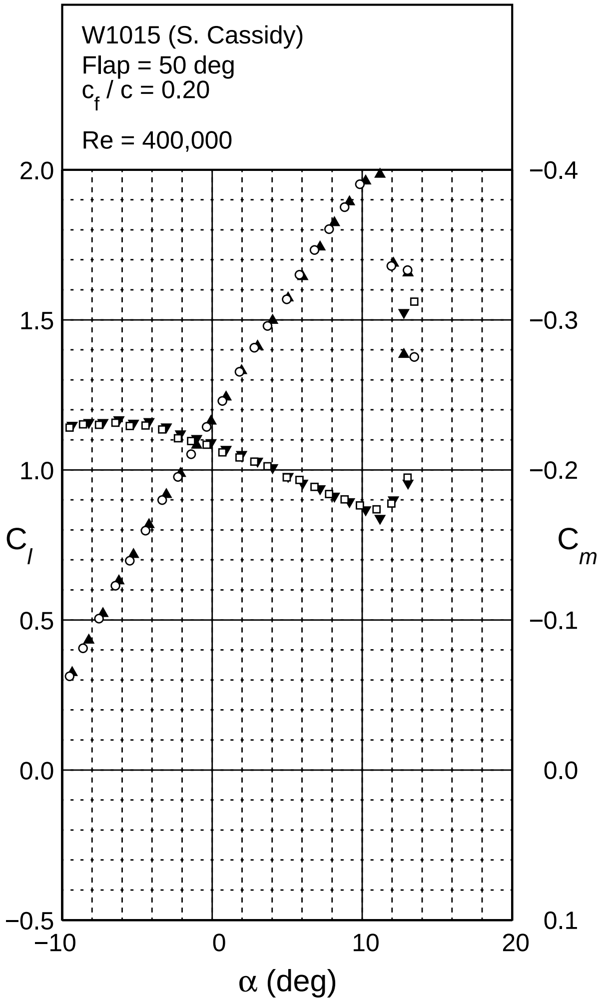

Figure 6.211: Continued.

Figure 6.212: Inviscid velocity distribution for the W1015 ($c_f/c = 20\%$) with a 55 deg flap.

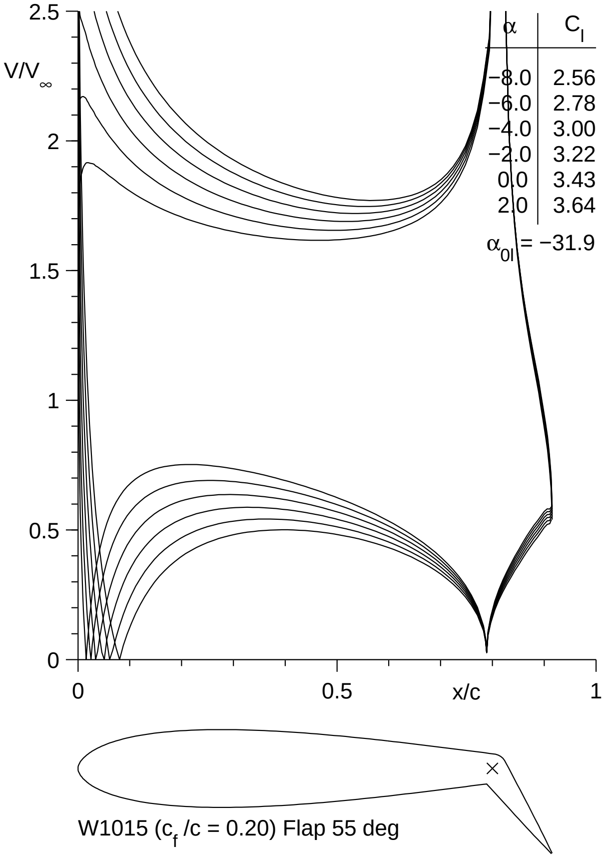

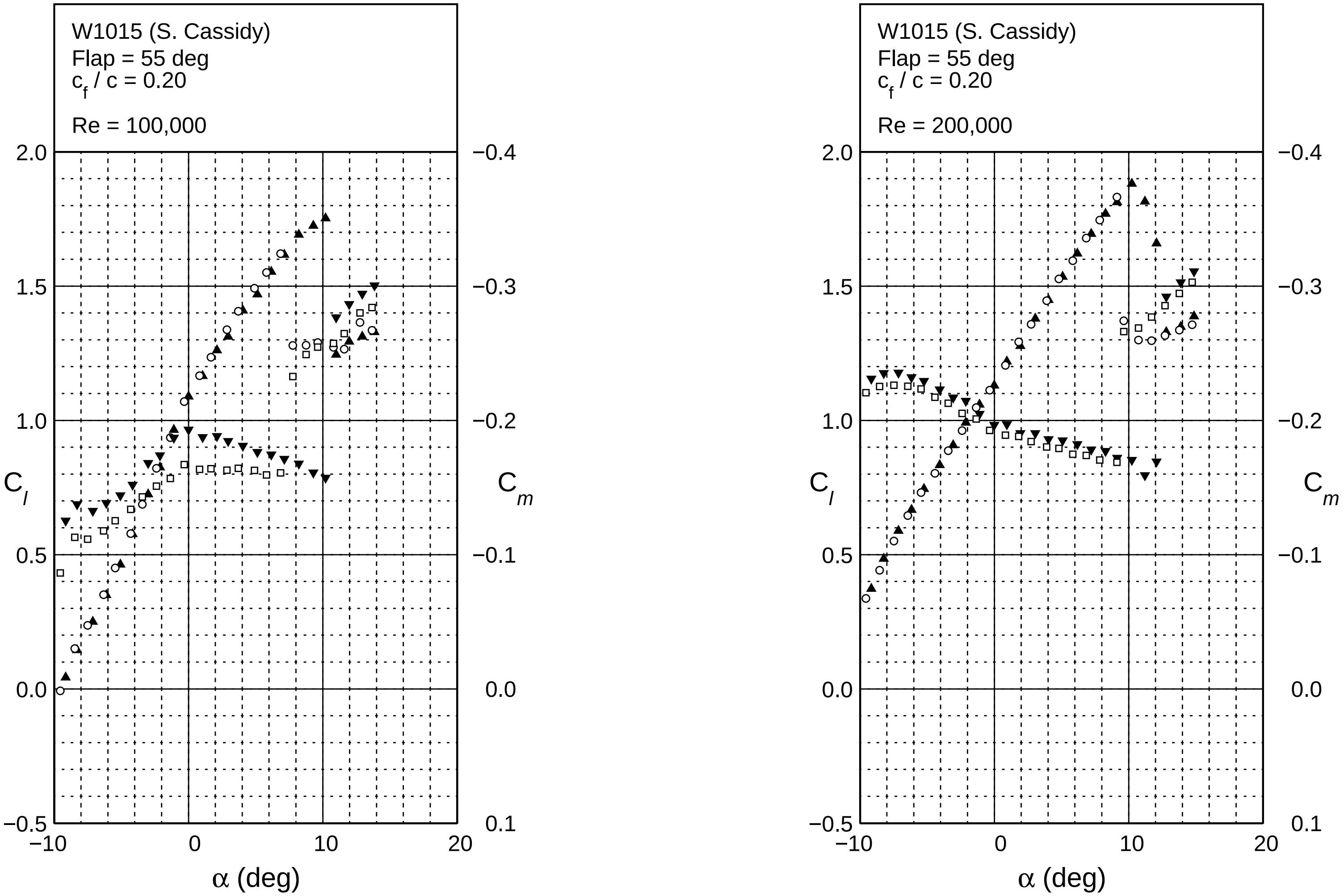

Figure 6.213: Lift and moment characteristics for the W1015 ($c_f/c = 20\%$) with a 55 deg flap.

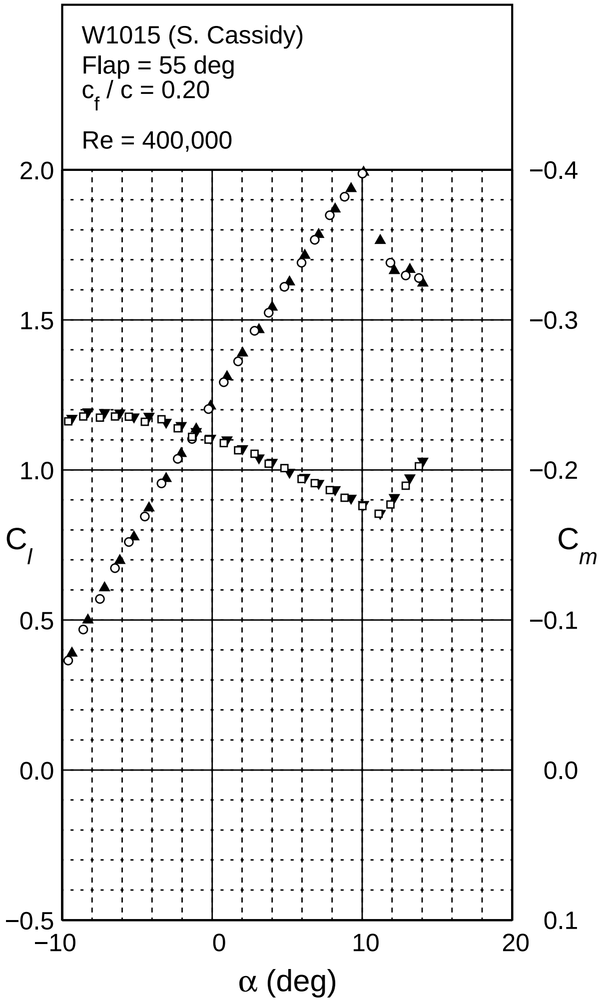

Figure 6.213: Continued.

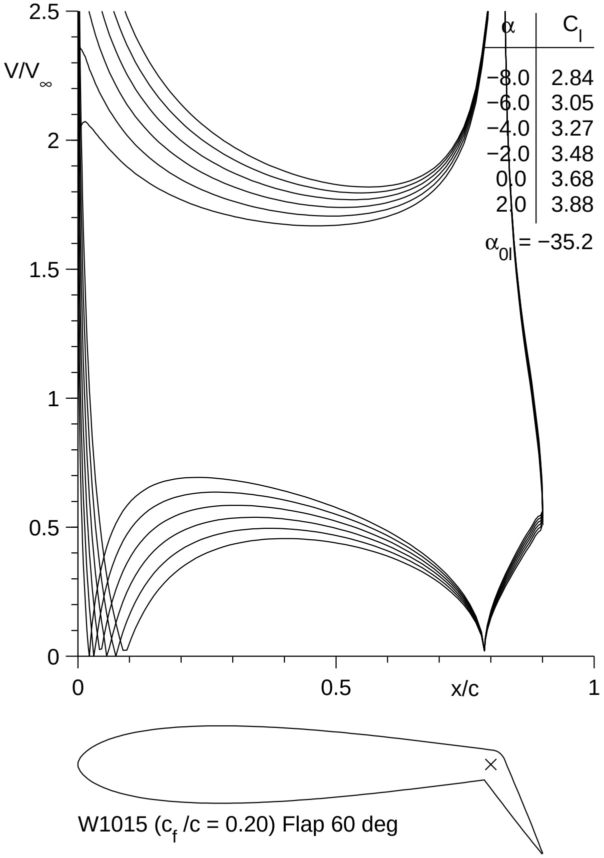

Figure 6.214: Inviscid velocity distribution for the W1015 ($c_f/c = 20\%$) with a 60 deg flap.

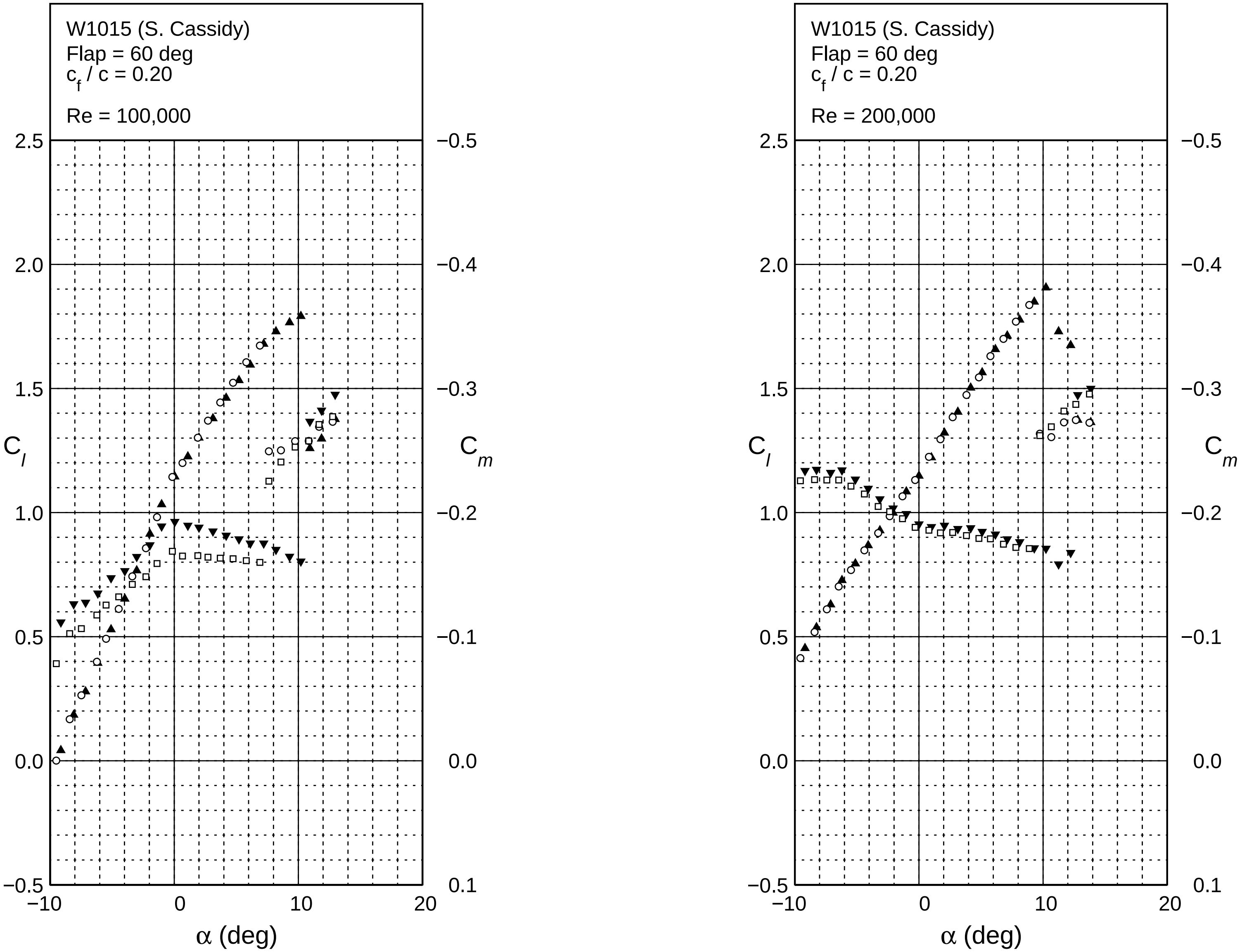

Figure 6.215: Lift and moment characteristics for the W1015 ($c_f/c = 20\%$) with a 60 deg flap.

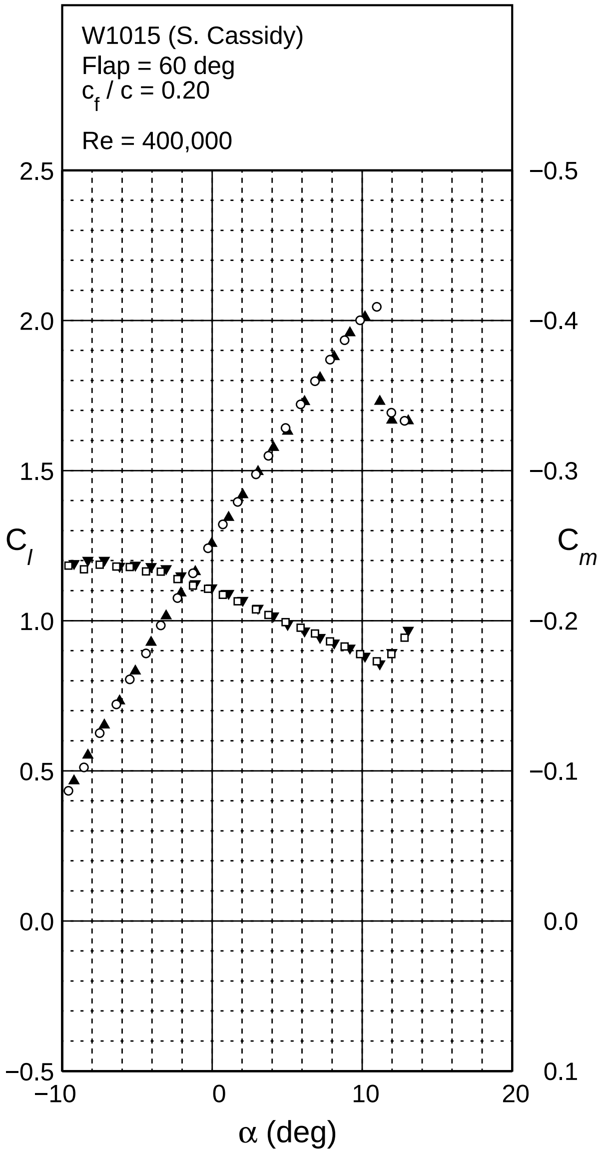

Figure 6.215: Continued.

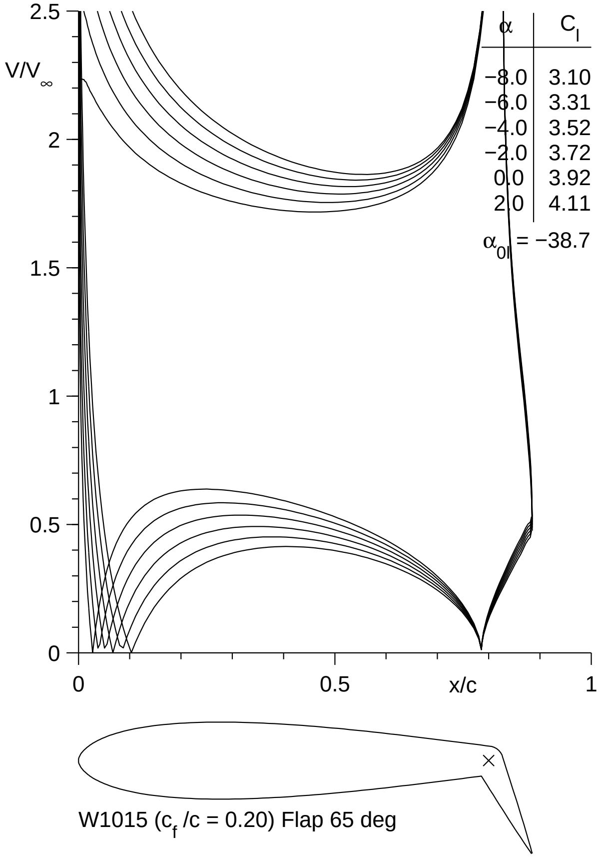

Figure 6.216: Inviscid velocity distribution for the W1015 ($c_f/c = 20\%$) with a 65 deg flap.

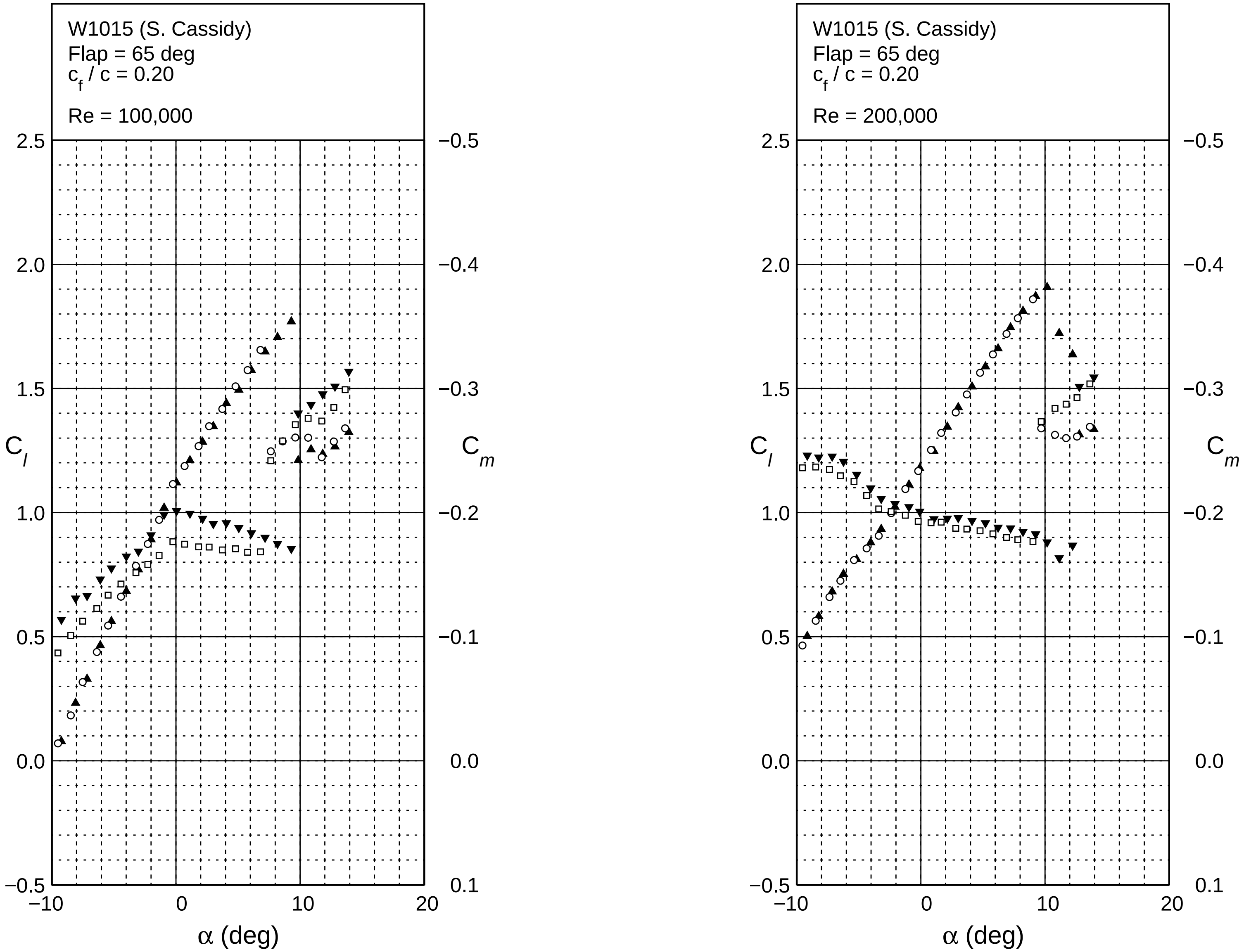

Figure 6.217: Lift and moment characteristics for the W1015 ($c_f/c = 20\%$) with a 65 deg flap.

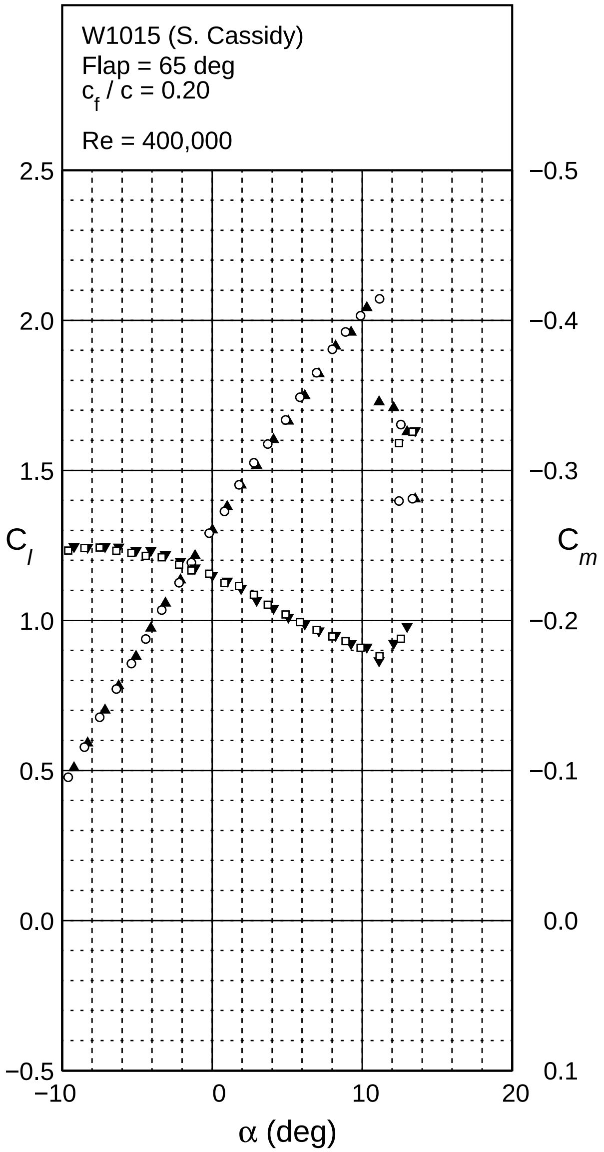

Figure 6.217: Continued.

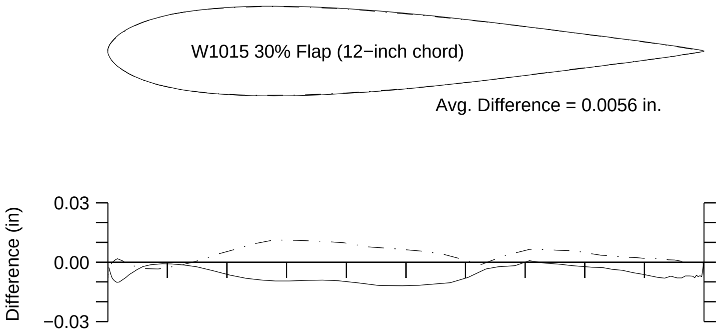

Figure 6.218: Comparison between the true and actual W1015 ($c_f/c = 30\%$).

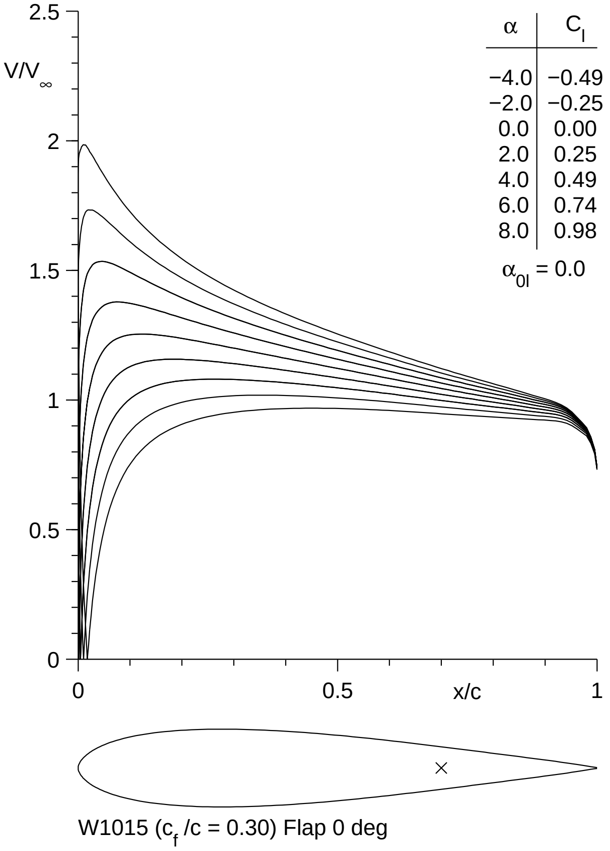

Figure 6.219: Inviscid velocity distribution for the W1015 ($c_f/c = 30\%$).

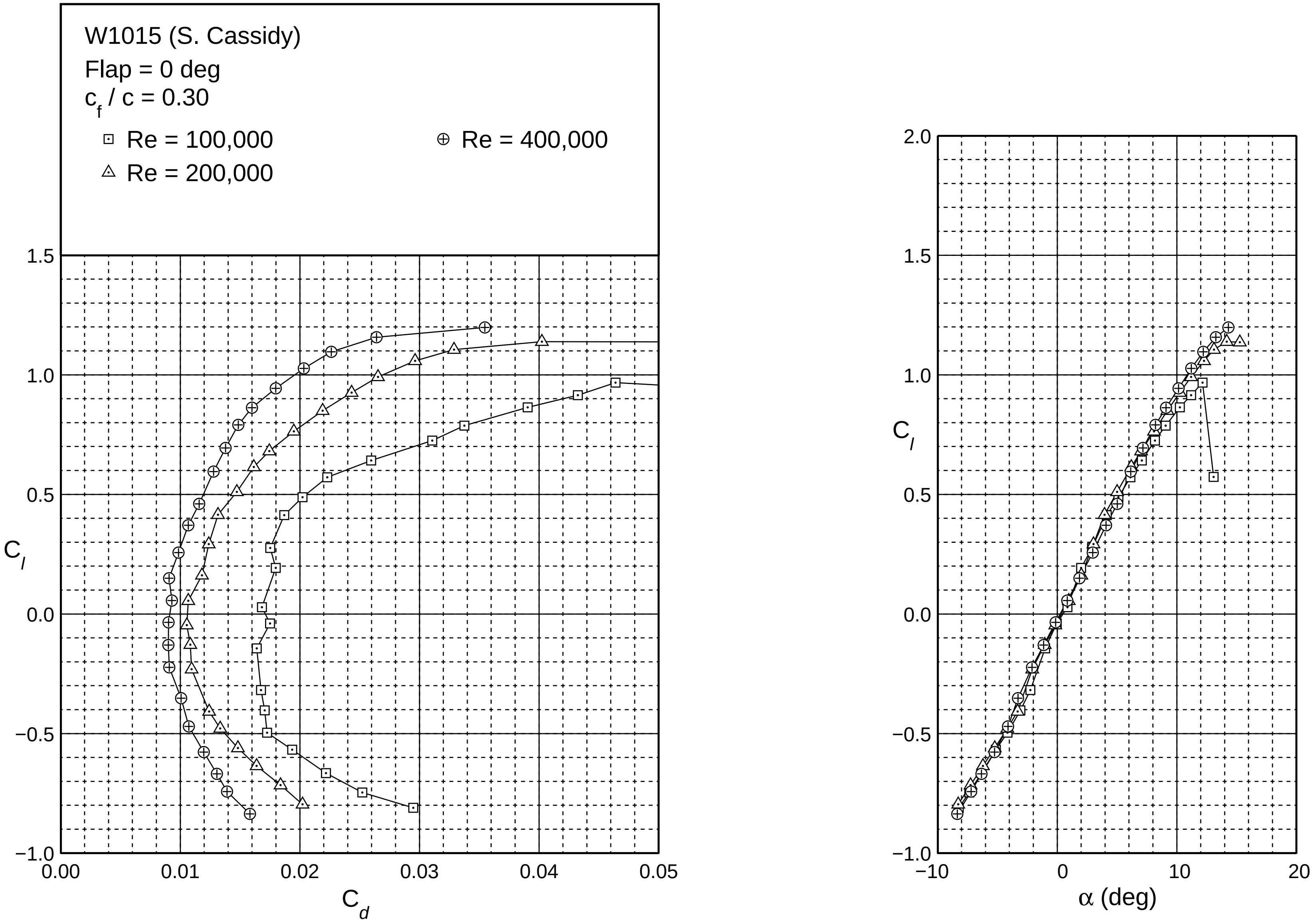

Figure 6.220: Drag polar for the W1015 ($c_f/c = 30\%$).

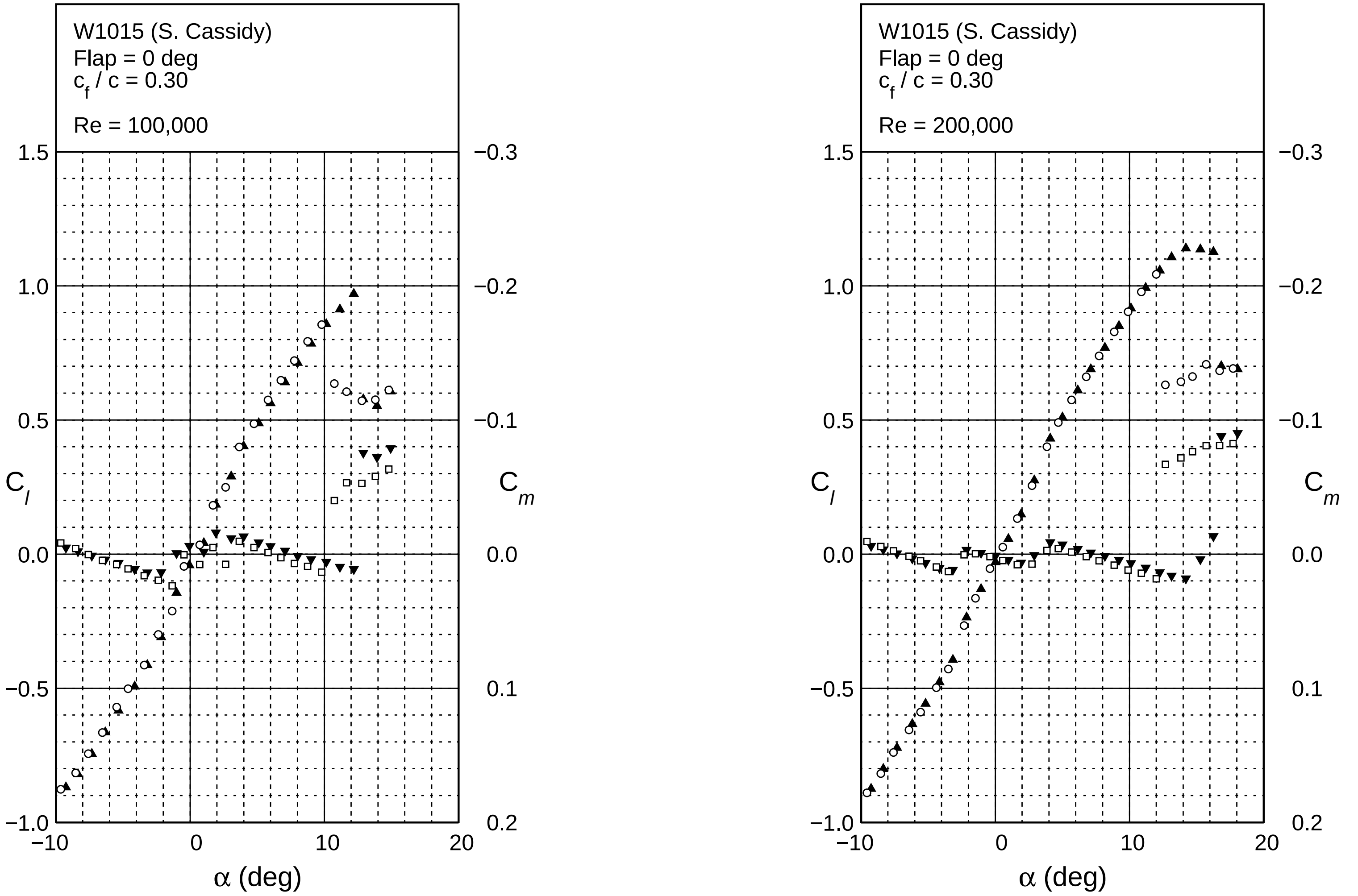

Figure 6.221: Lift and moment characteristics for the W1015 ($c_f/c = 30\%$).

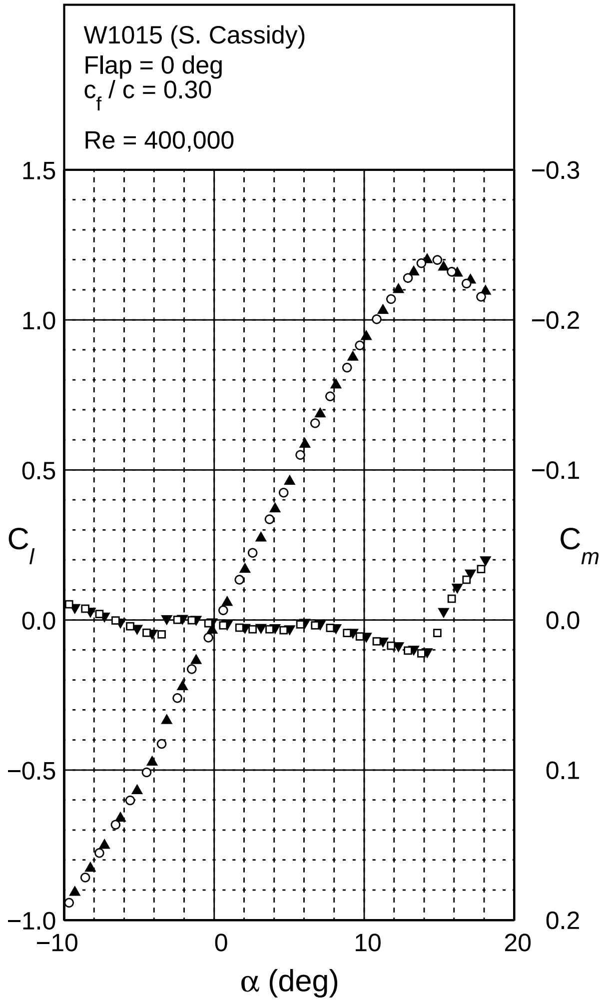

Figure 6.221: Continued.

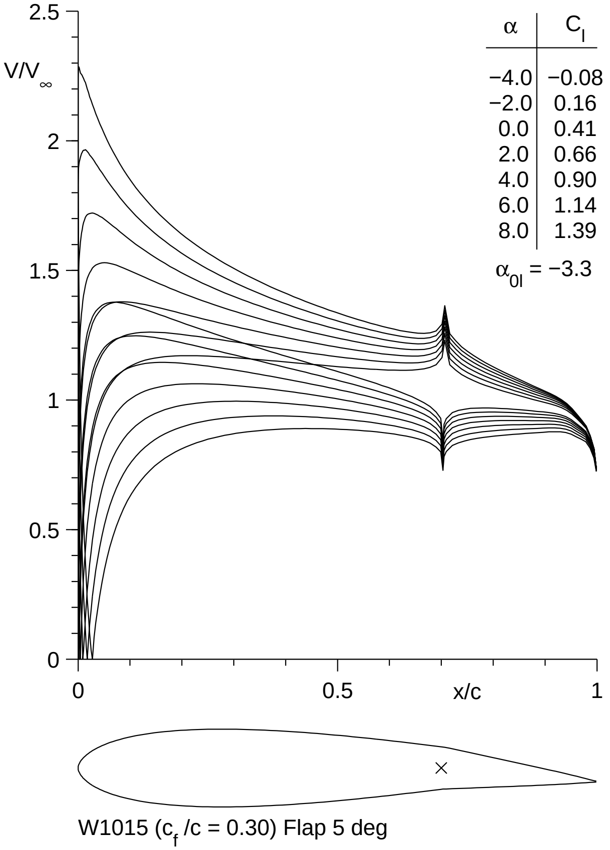

Figure 6.222: Inviscid velocity distribution for the W1015 $(c_f/c = 30\%)$ with a 5 deg flap.

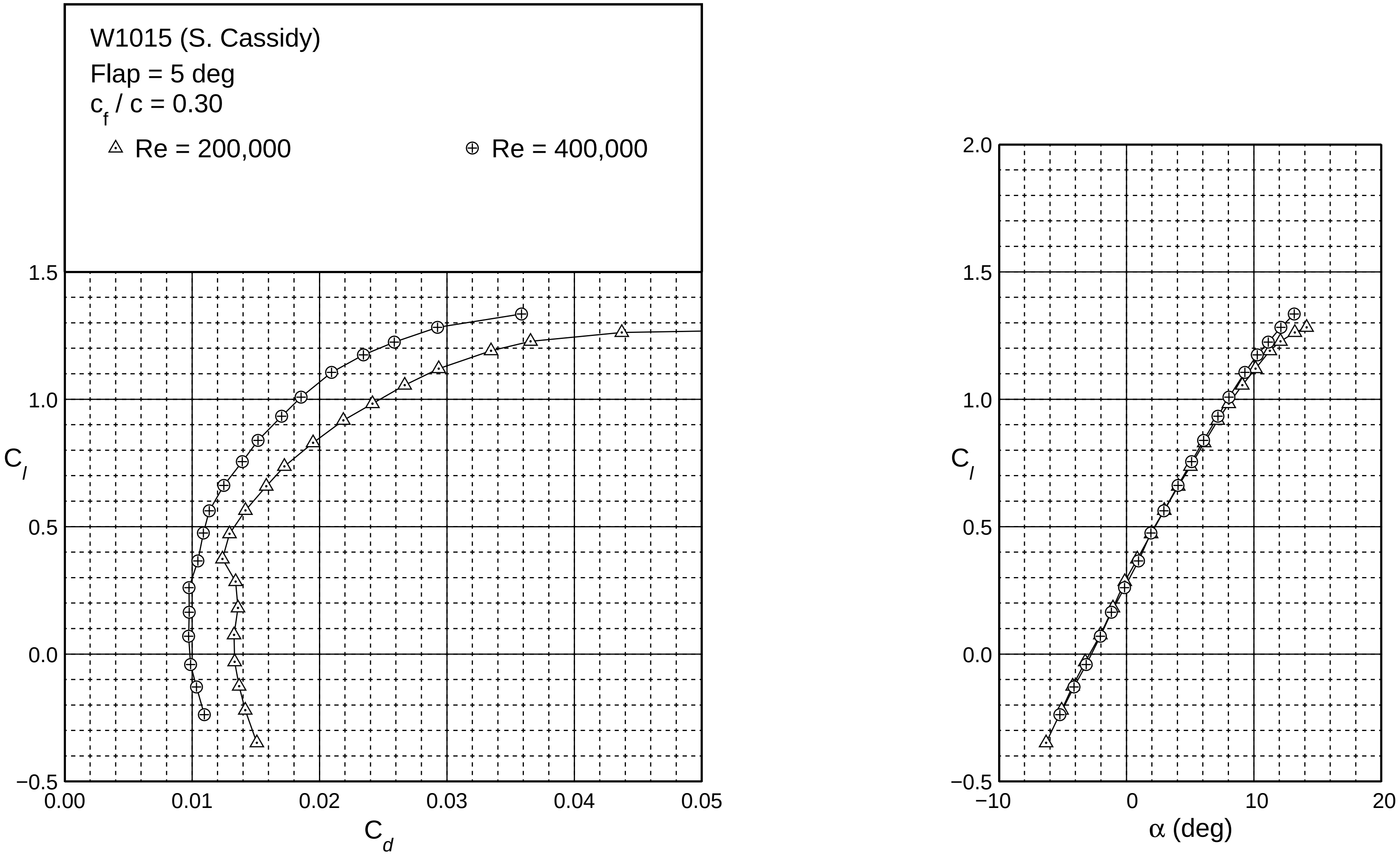

Figure 6.223: Drag polar for the W1015 ($c_f/c = 30\%$) with a 5 deg flap.

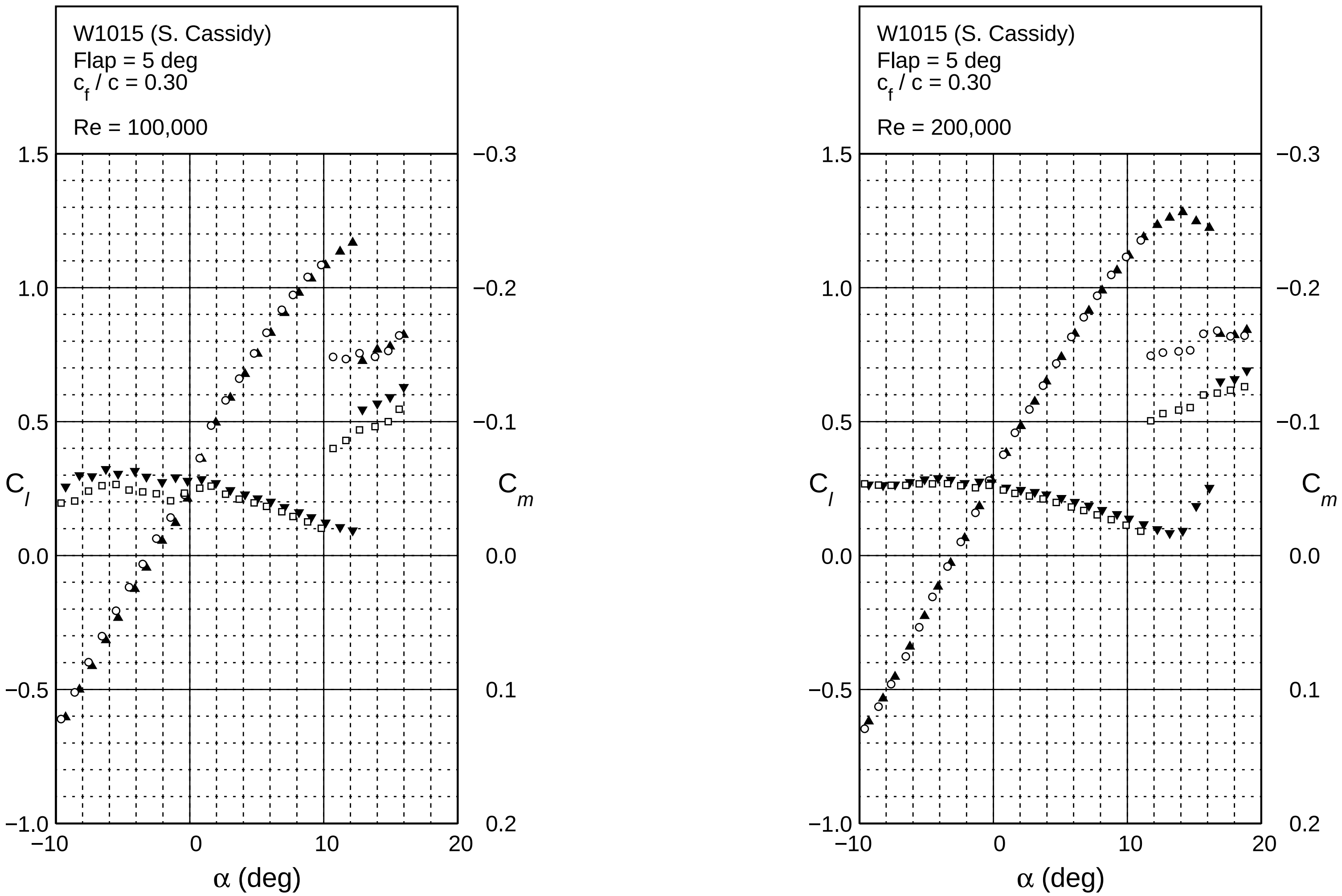

Figure 6.224: Lift and moment characteristics for the W1015 ($c_f/c = 30\%$) with a 5 deg flap.

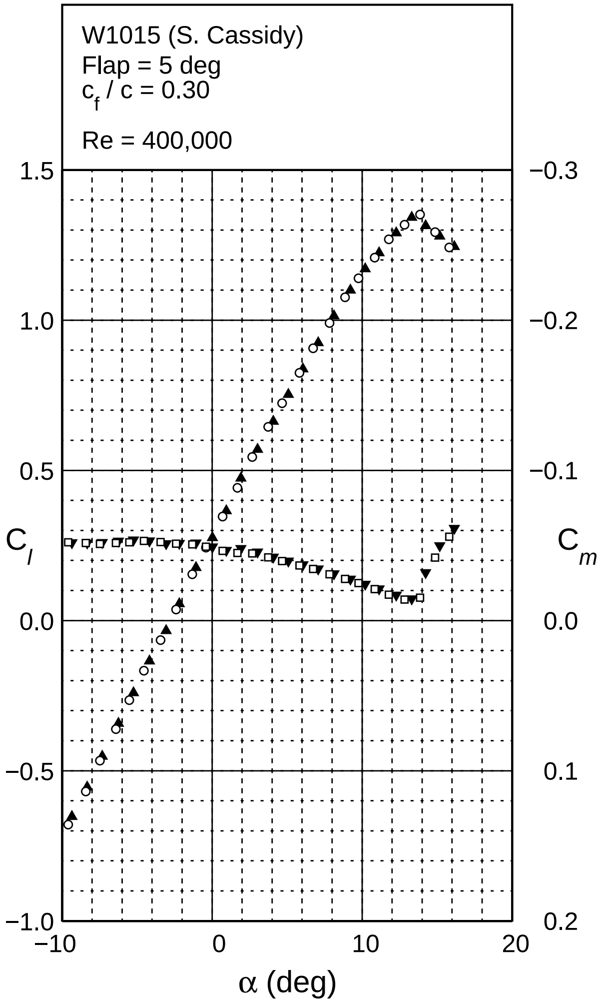

Figure 6.224: Continued.

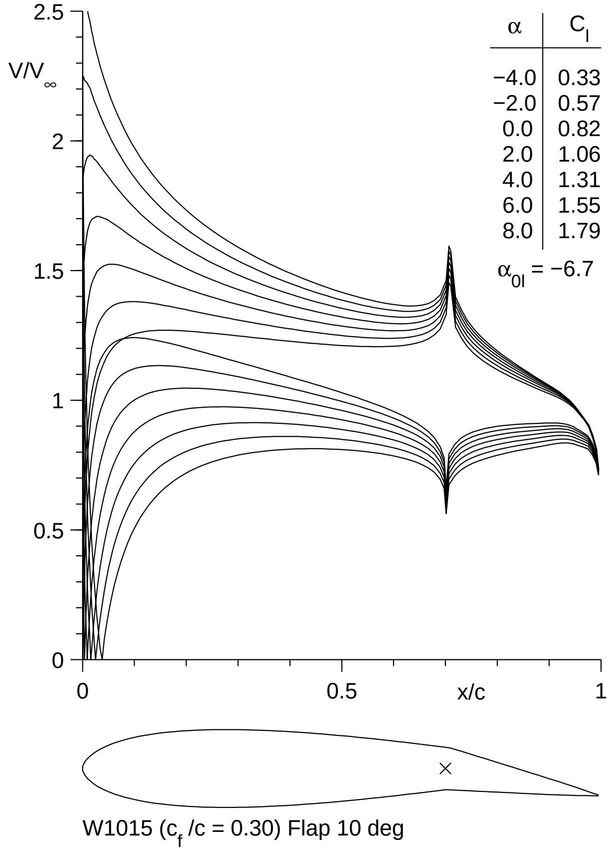

Figure 6.225: Inviscid velocity distribution for the W1015 ($c_f/c = 30\%$) with a 10 deg flap.

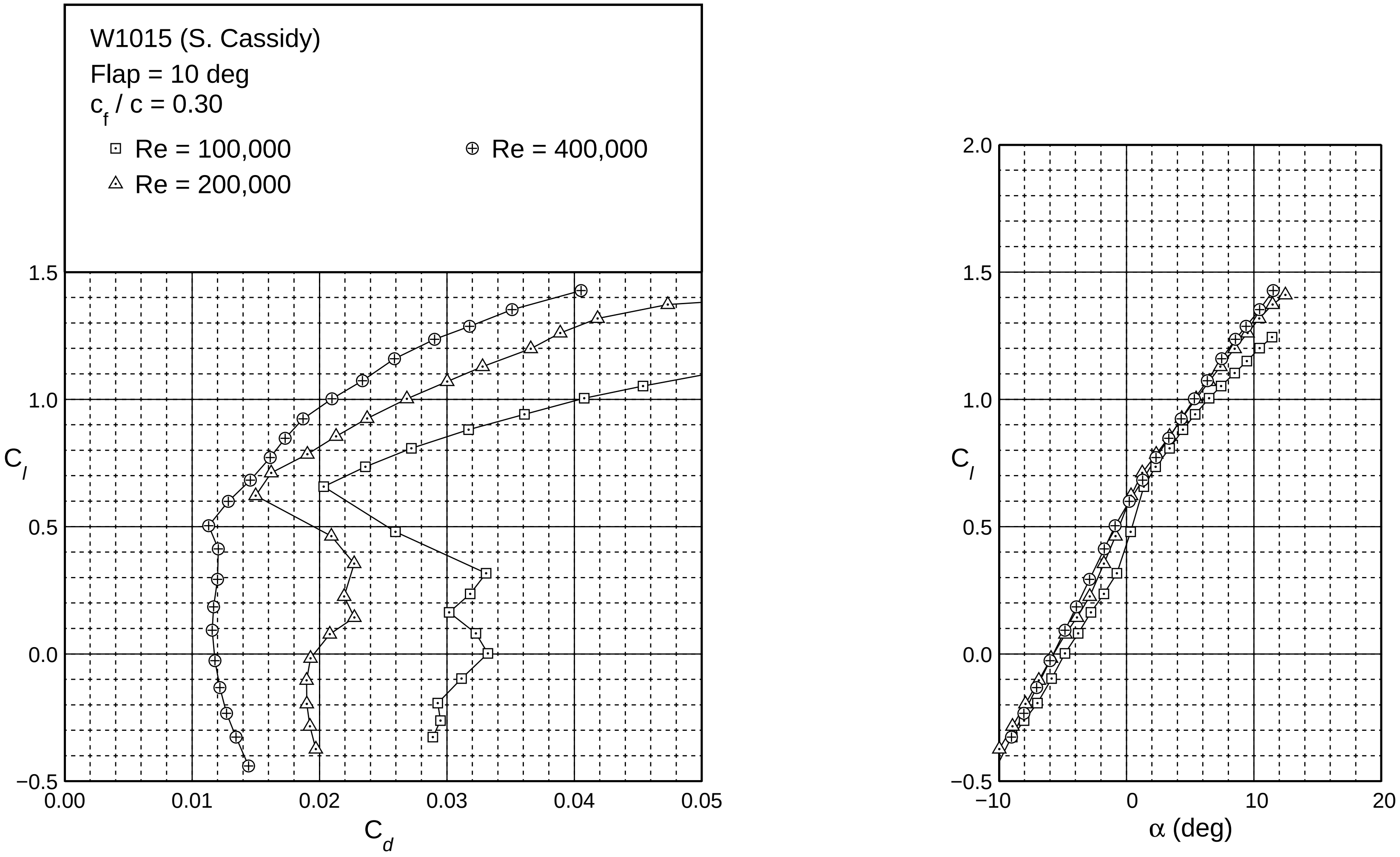

Figure 6.226: Drag polar for the W1015 ($c_f/c = 30\%$) with a 10 deg flap.

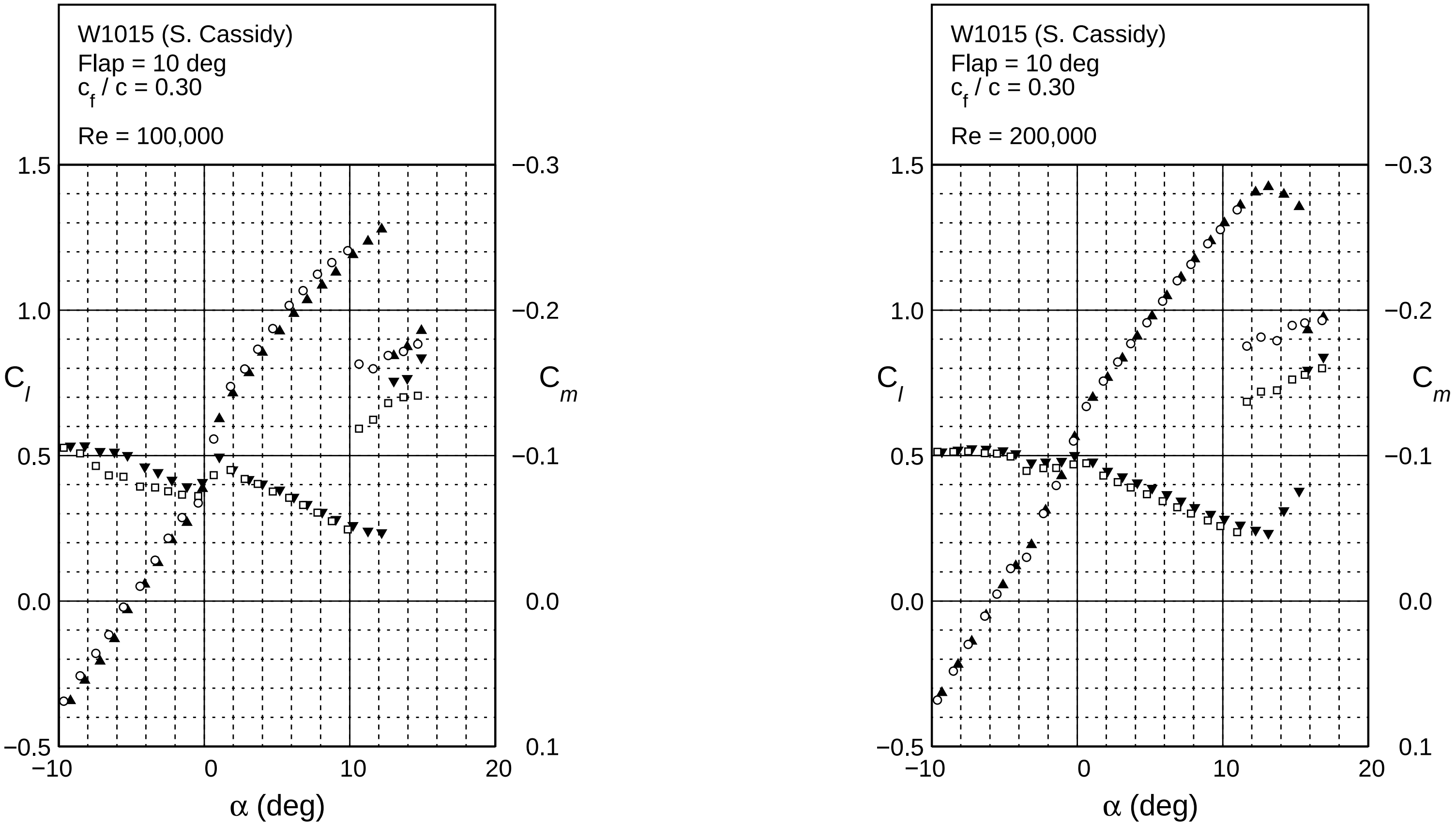

Figure 6.227: Lift and moment characteristics for the W1015 ($c_f/c = 30\%$) with a 10 deg flap.

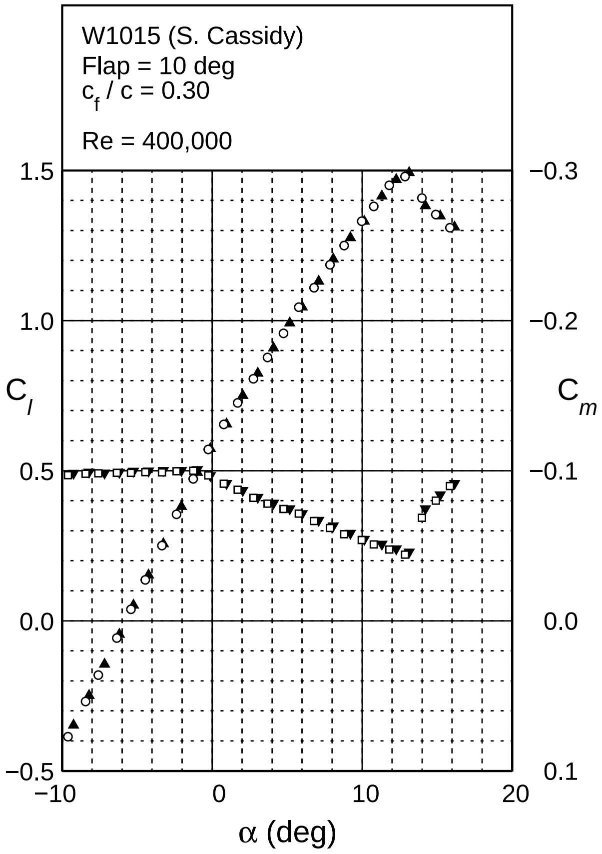

Figure 6.227: Continued.

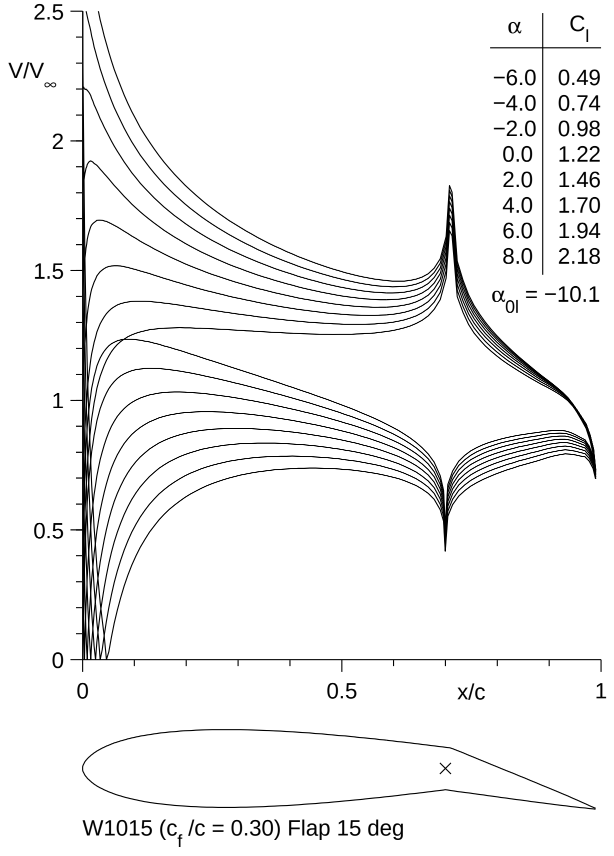

Figure 6.228: Inviscid velocity distribution for the W1015 ($c_f/c = 30\%$) with a 15 deg flap.

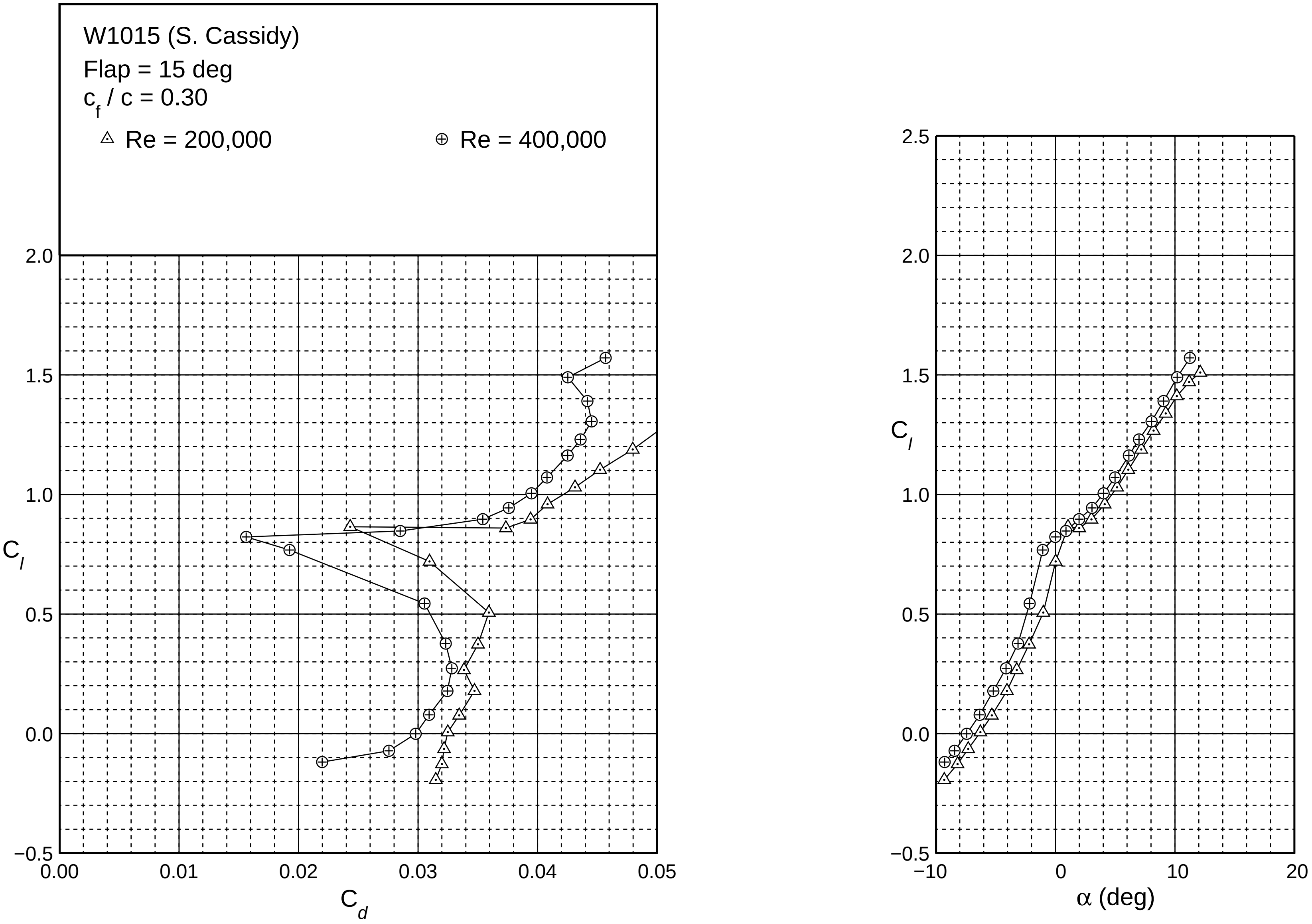

Figure 6.229: Drag polar for the W1015 ($c_f/c = 30\%$) with a 15 deg flap.

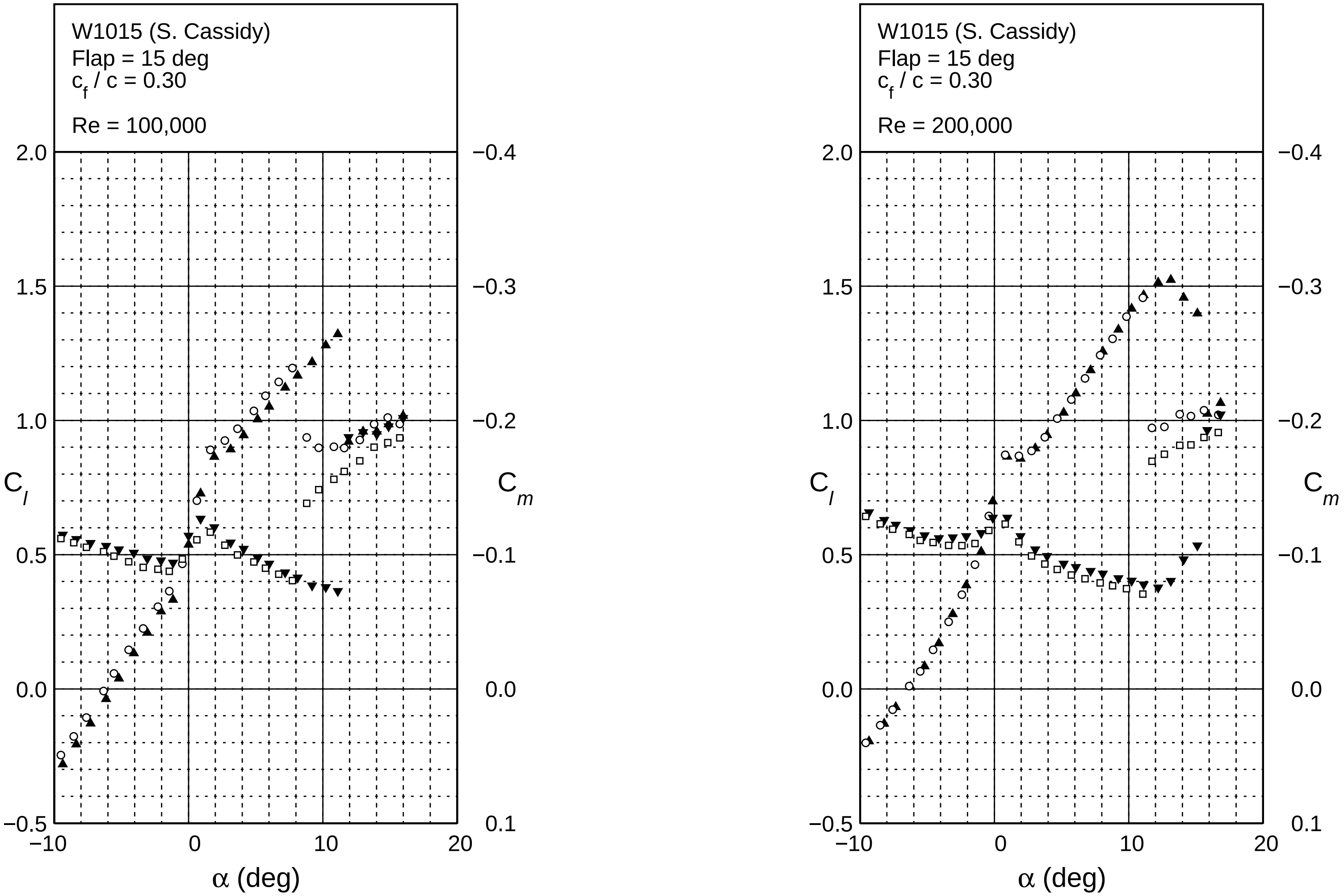

Figure 6.230: Lift and moment characteristics for the W1015 ($c_f/c = 30\%$) with a 15 deg flap.

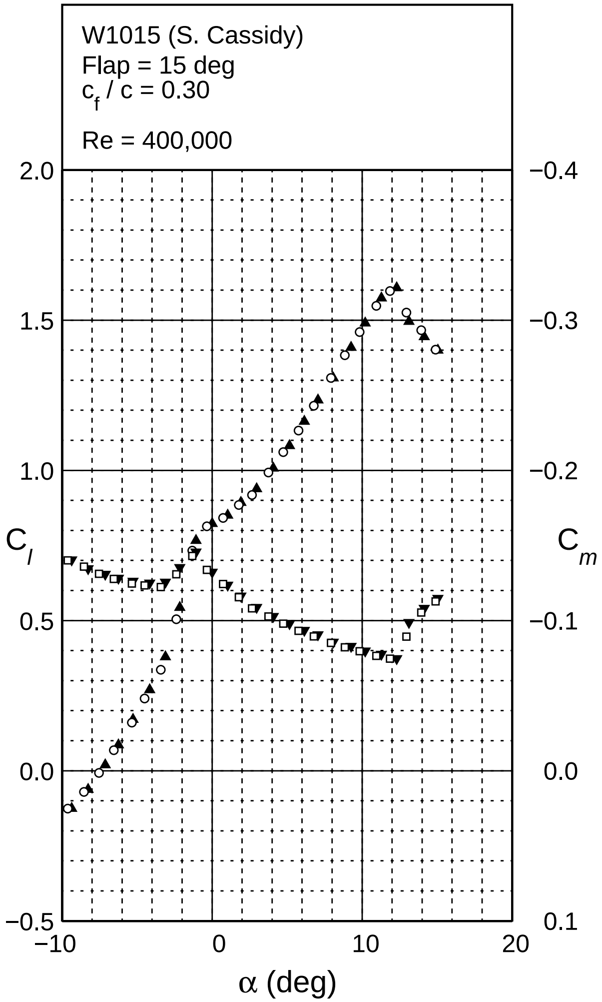

Figure 6.230: Continued.

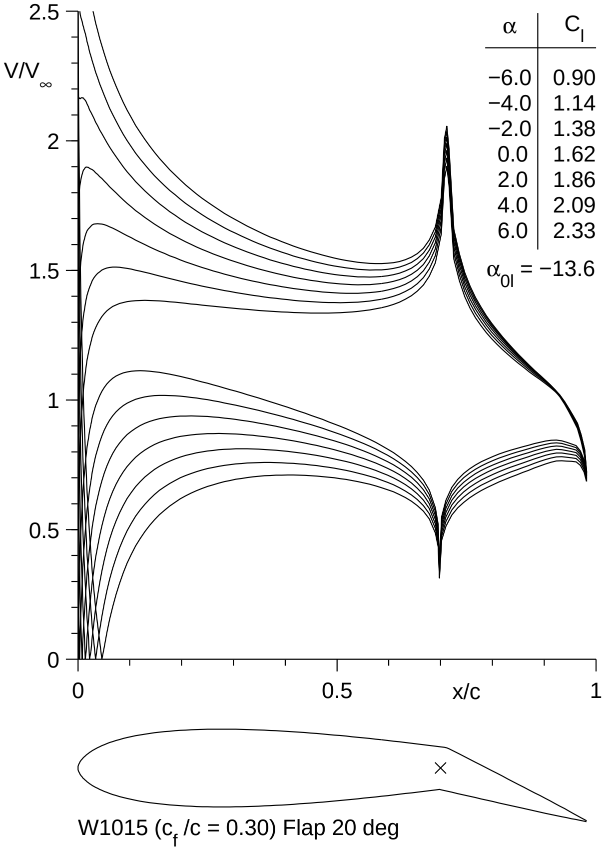

Figure 6.231: Inviscid velocity distribution for the W1015 $(c_f/c = 30\%)$ with a 20 deg flap.

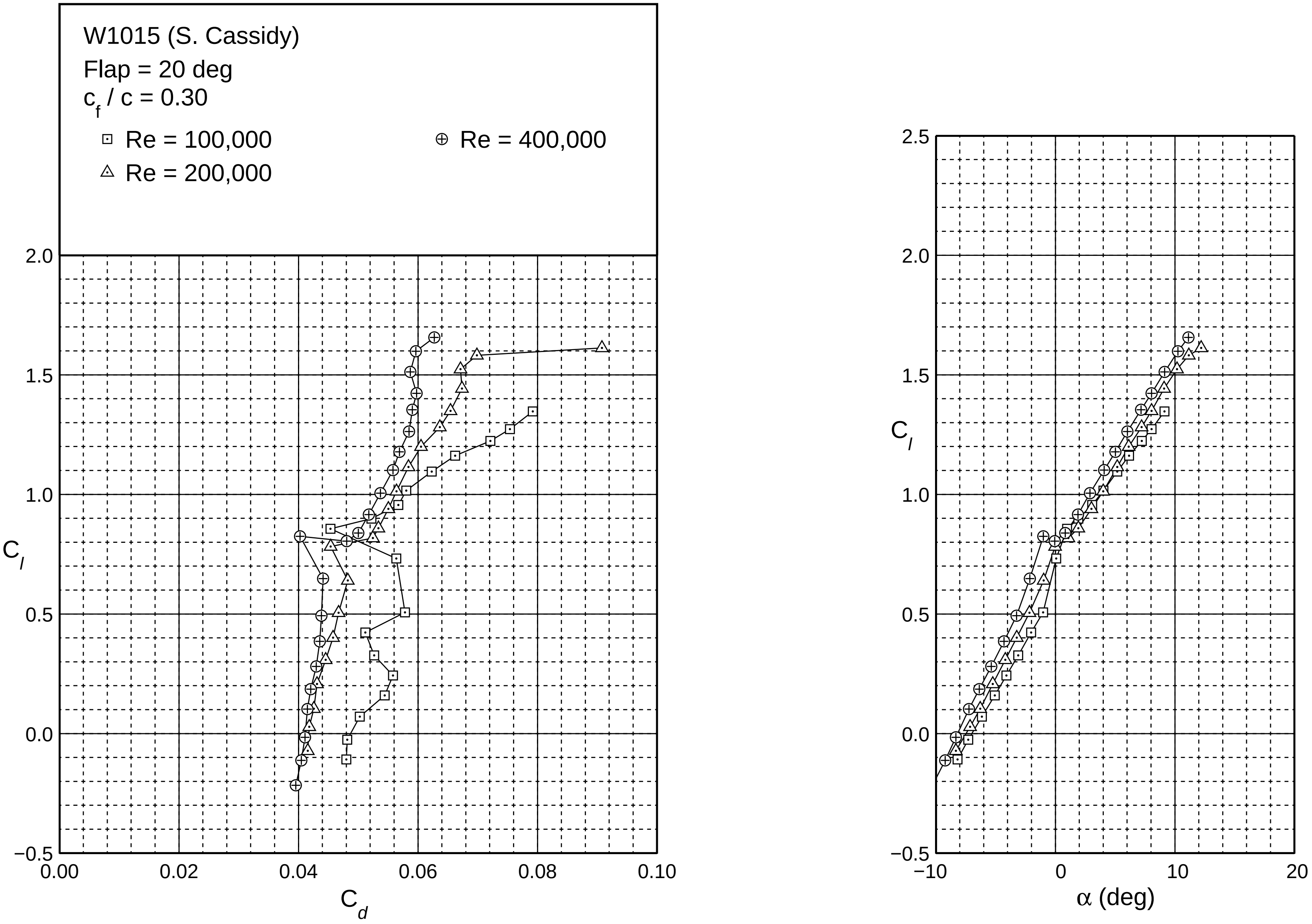

Figure 6.232: Drag polar for the W1015 ($c_f/c = 30\%$) with a 20 deg flap.

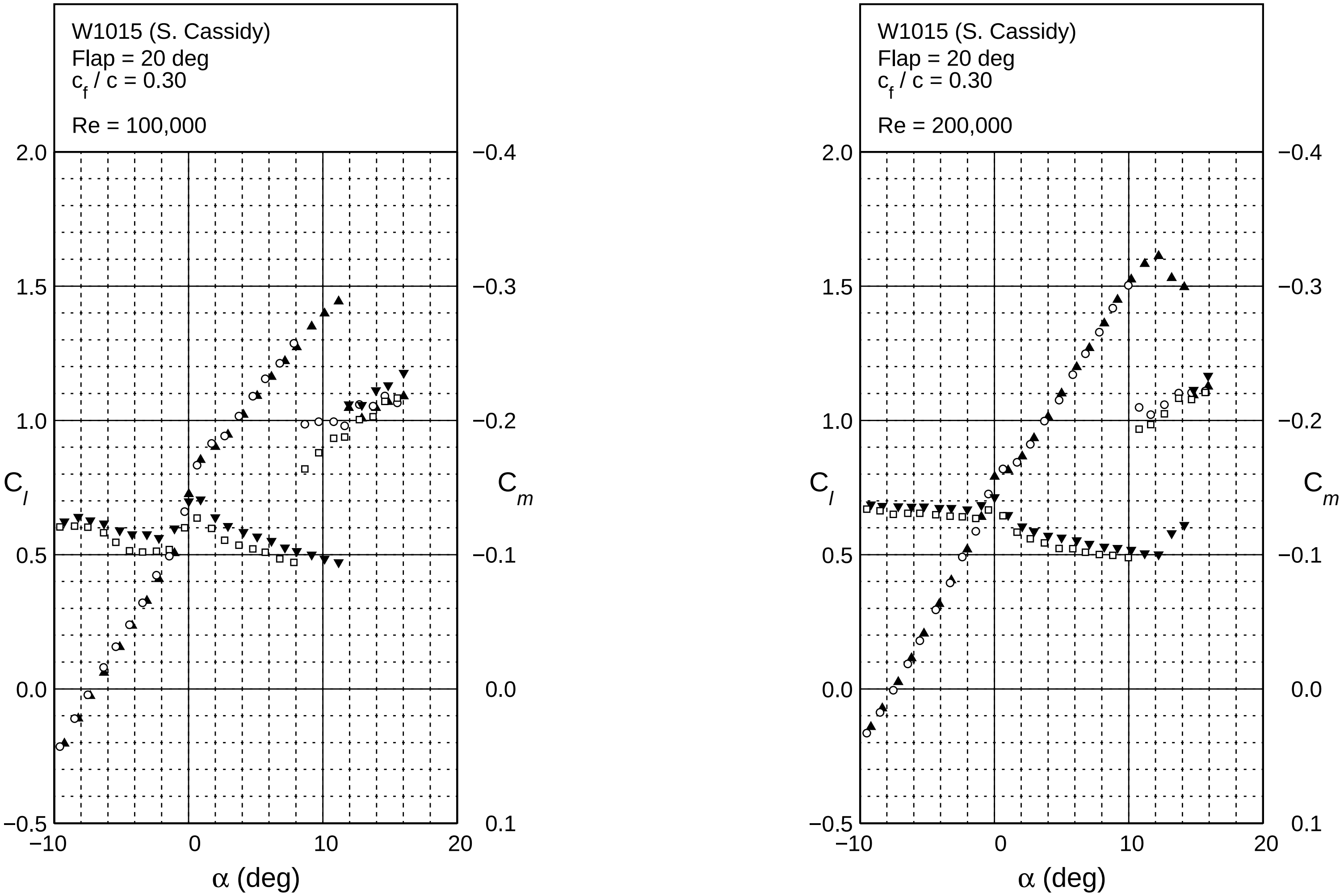

Figure 6.233: Lift and moment characteristics for the W1015 ($c_f/c = 30\%$) with a 20 deg flap.

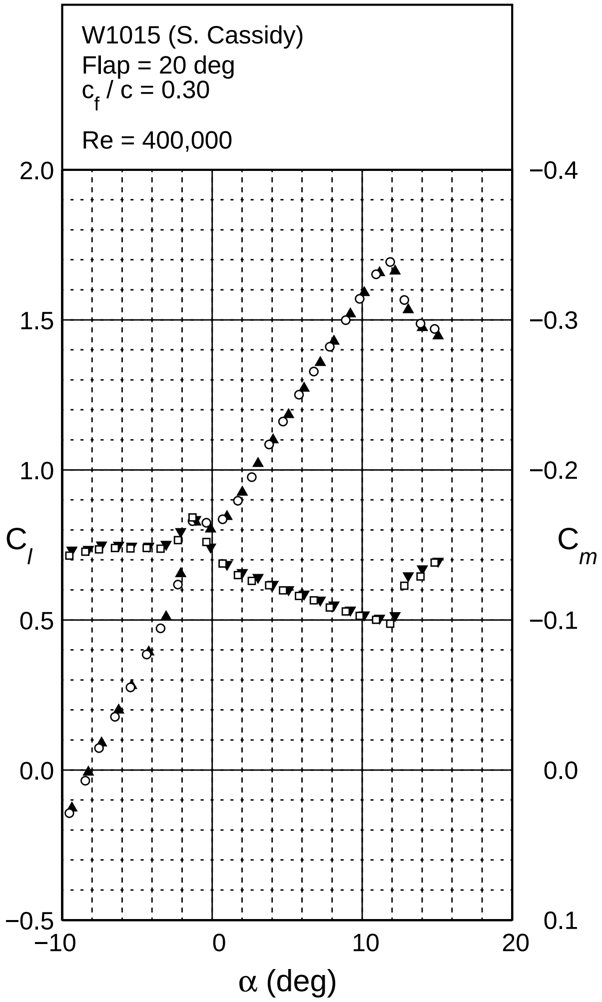

Figure 6.233: Continued.

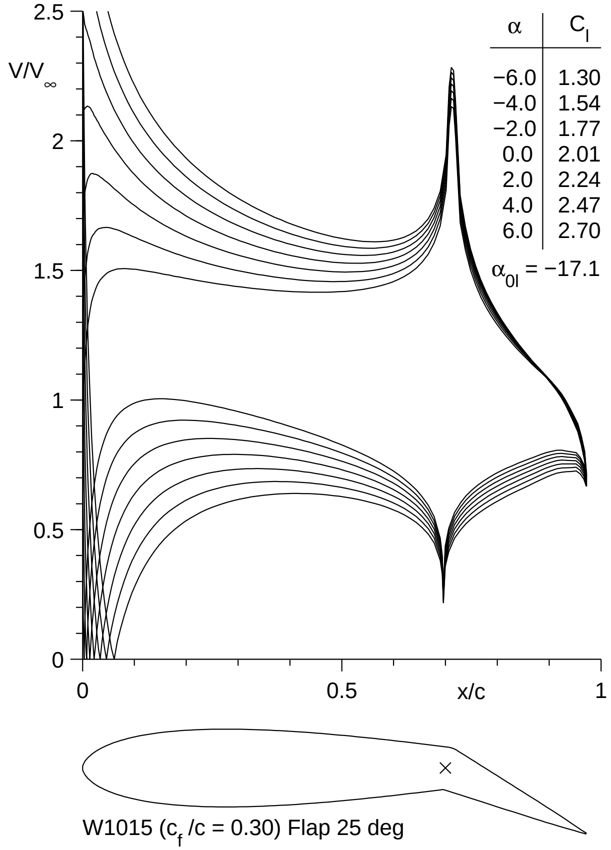

Figure 6.234: Inviscid velocity distribution for the W1015 ($c_f/c = 30\%$) with a 25 deg flap.

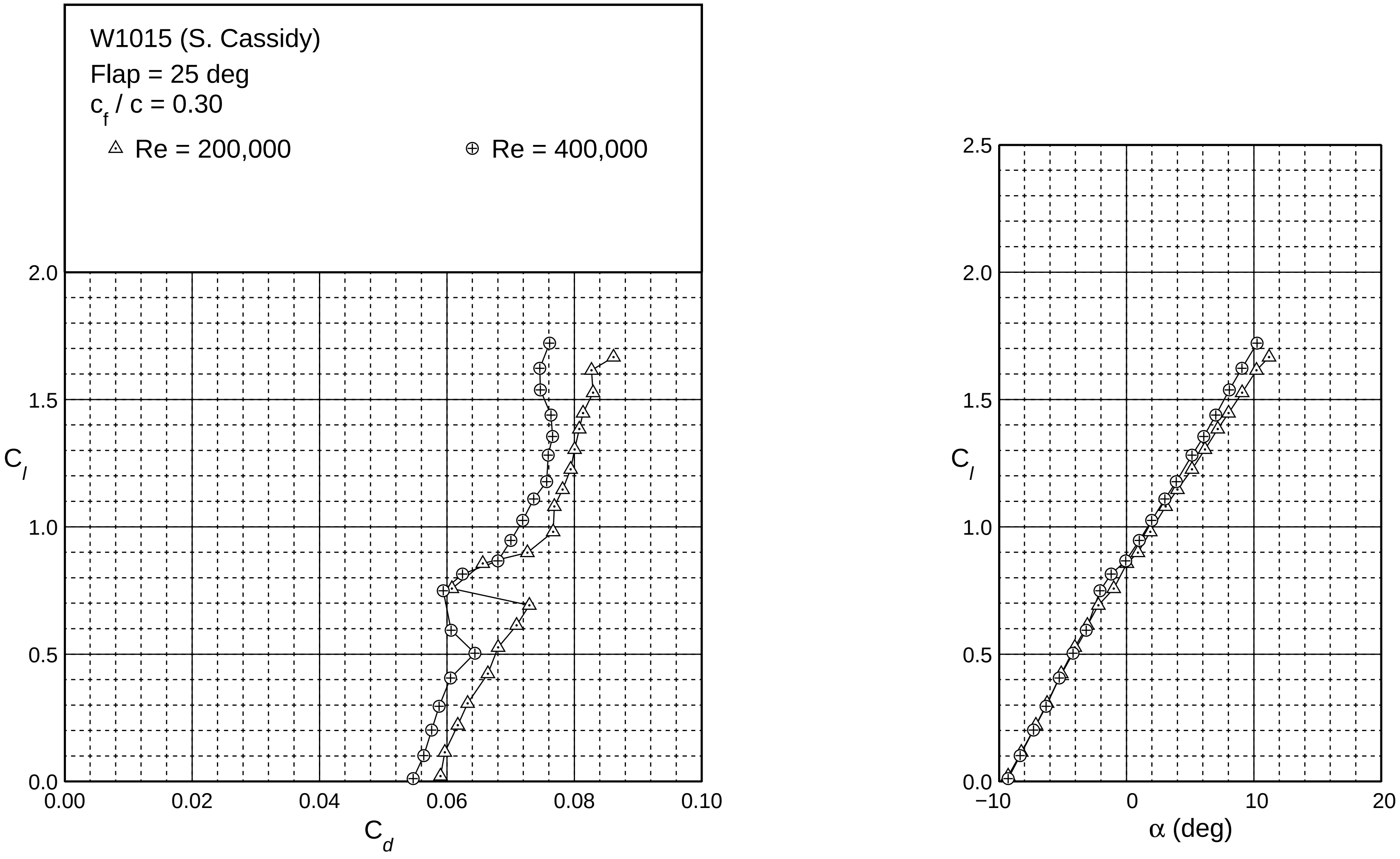

Figure 6.235: Drag polar for the W1015 ($c_f/c = 30\%$) with a 25 deg flap.

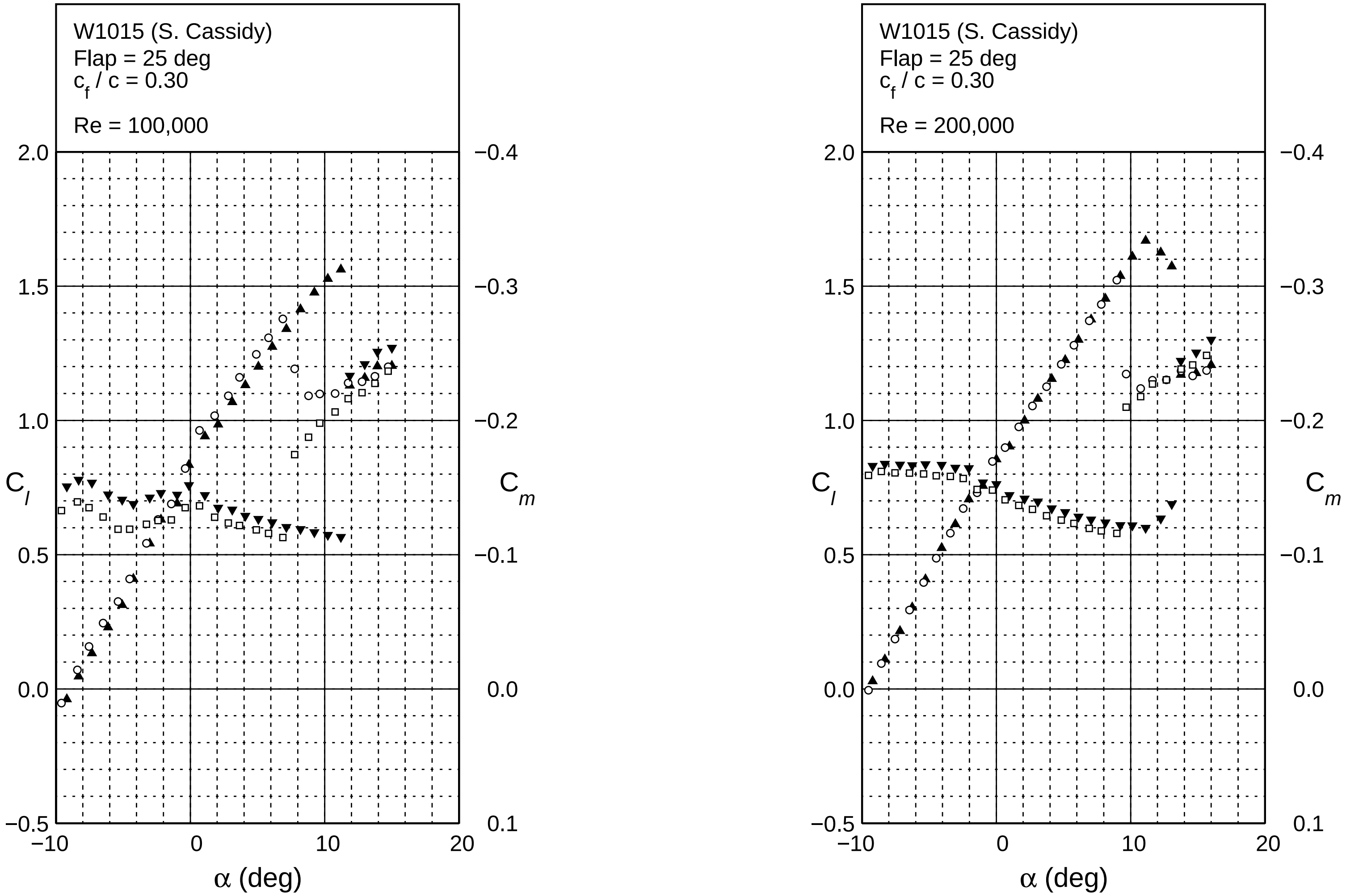

Figure 6.236: Lift and moment characteristics for the W1015 ($c_f/c = 30\%$) with a 25 deg flap.

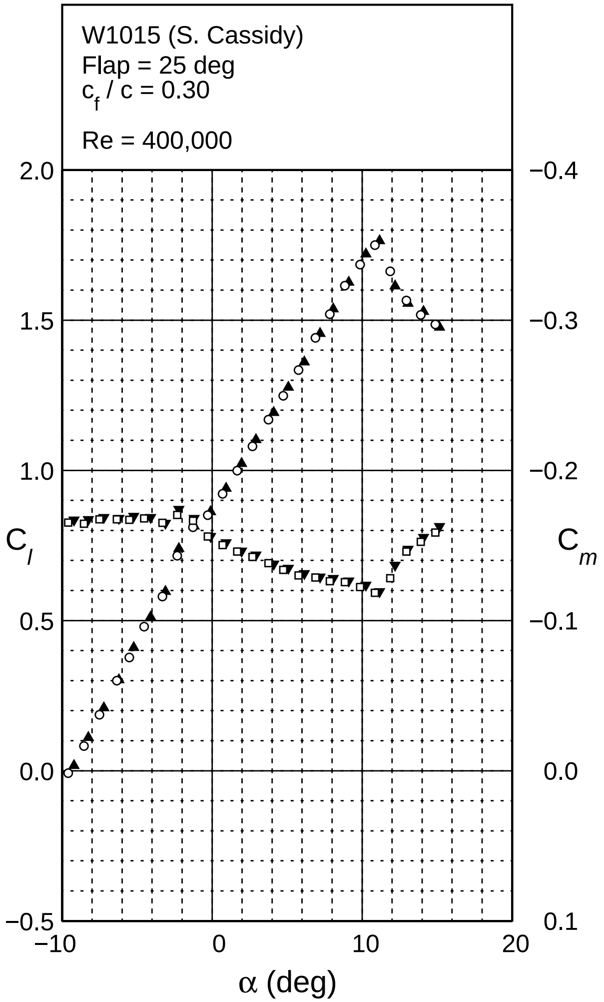

Figure 6.236: Continued.

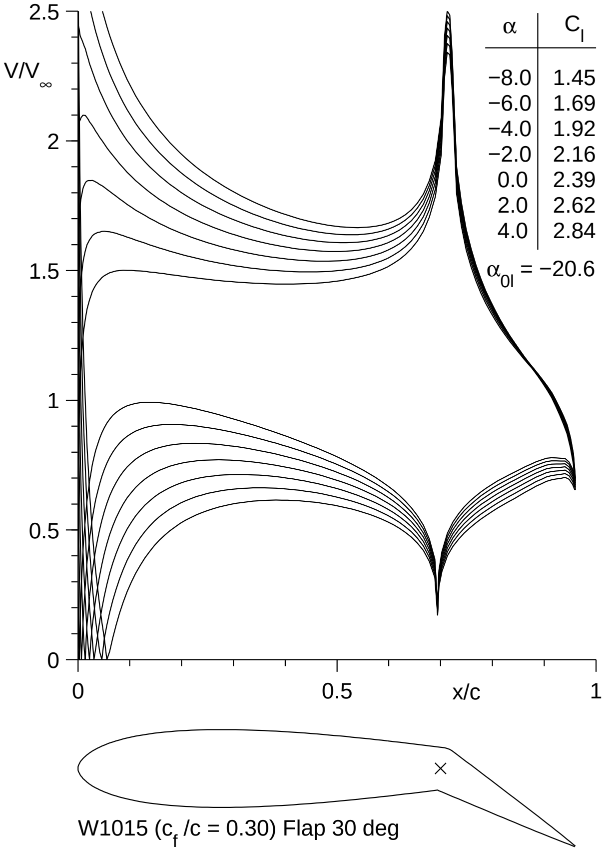

Figure 6.237: Inviscid velocity distribution for the W1015 ($c_f/c = 30\%$) with a 30 deg flap.

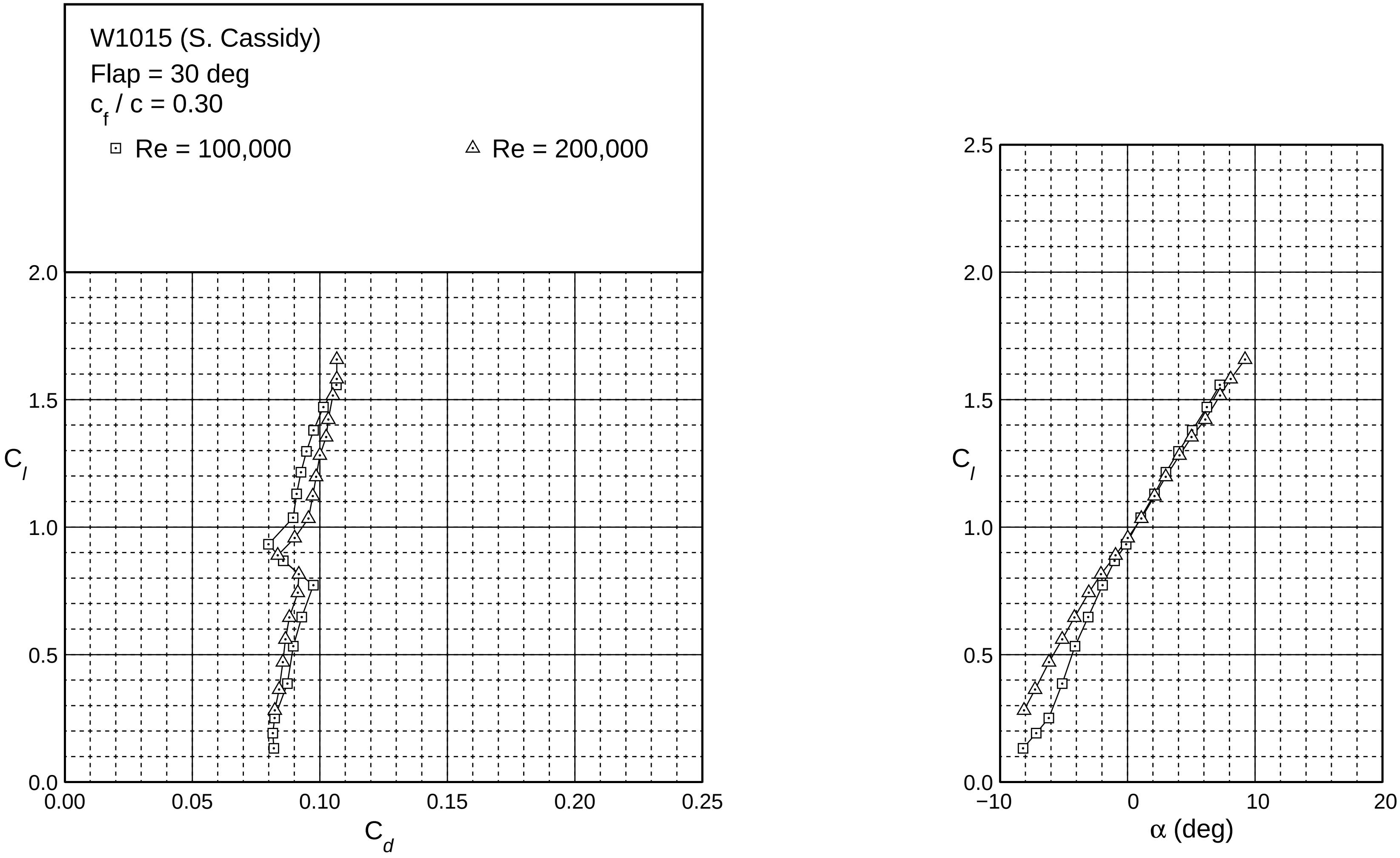

Figure 6.238: Drag polar for the W1015 ($c_f/c = 30\%$) with a 30 deg flap.

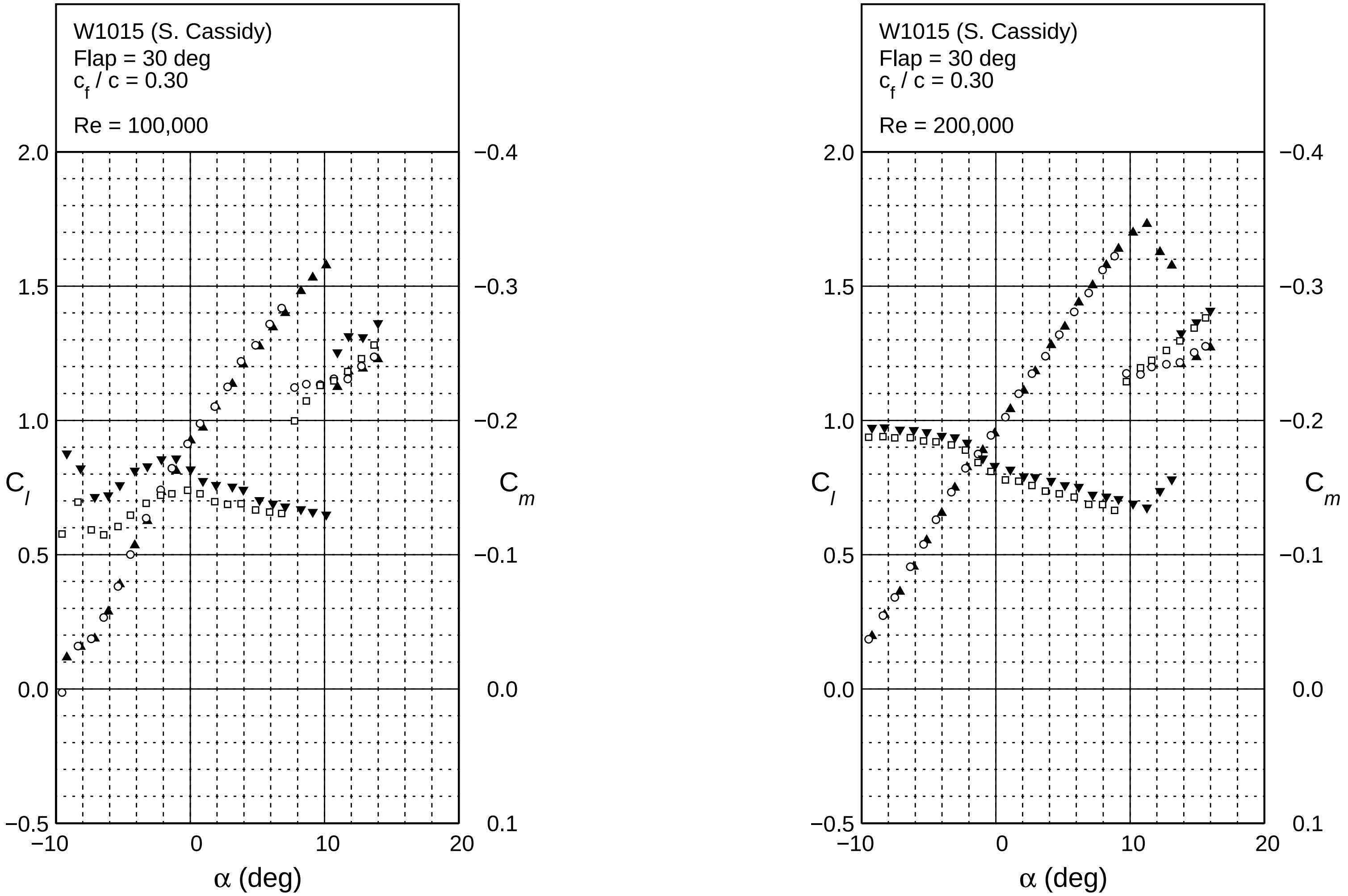

Figure 6.239: Lift and moment characteristics for the W1015 ($c_f/c = 30\%$) with a 30 deg flap.

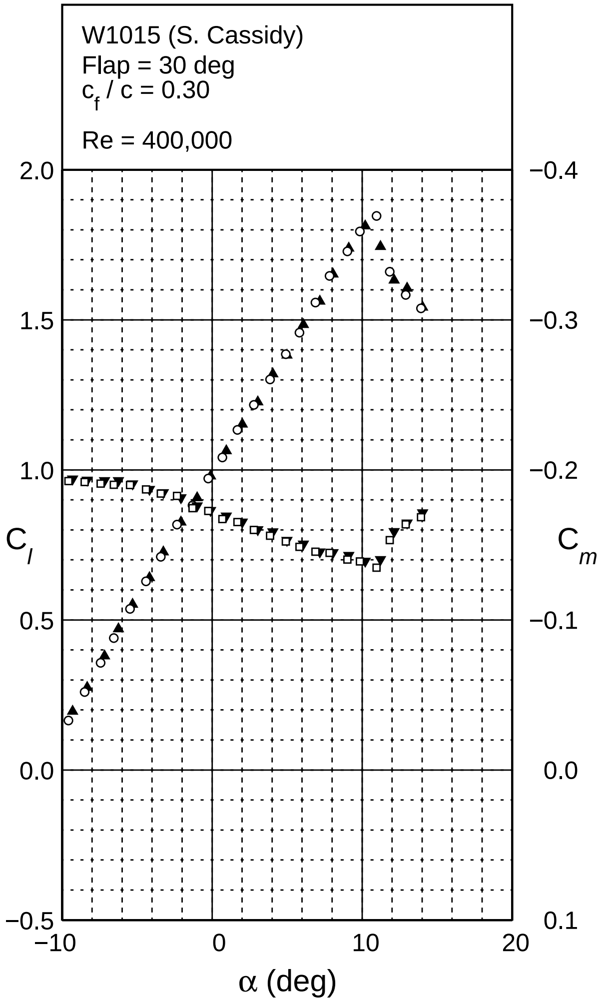

Figure 6.239: Continued.

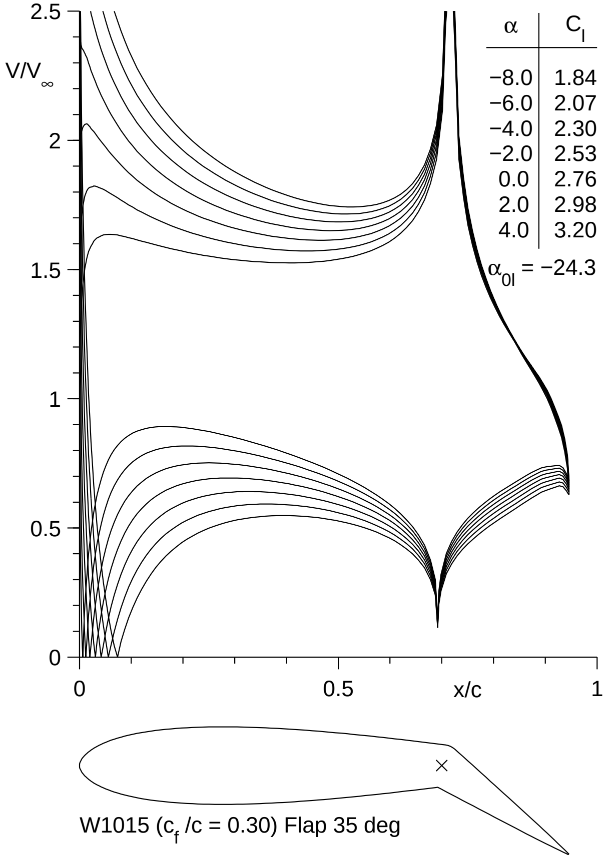

Figure 6.240: Inviscid velocity distribution for the W1015 ($c_f/c = 30\%$) with a 35 deg flap.

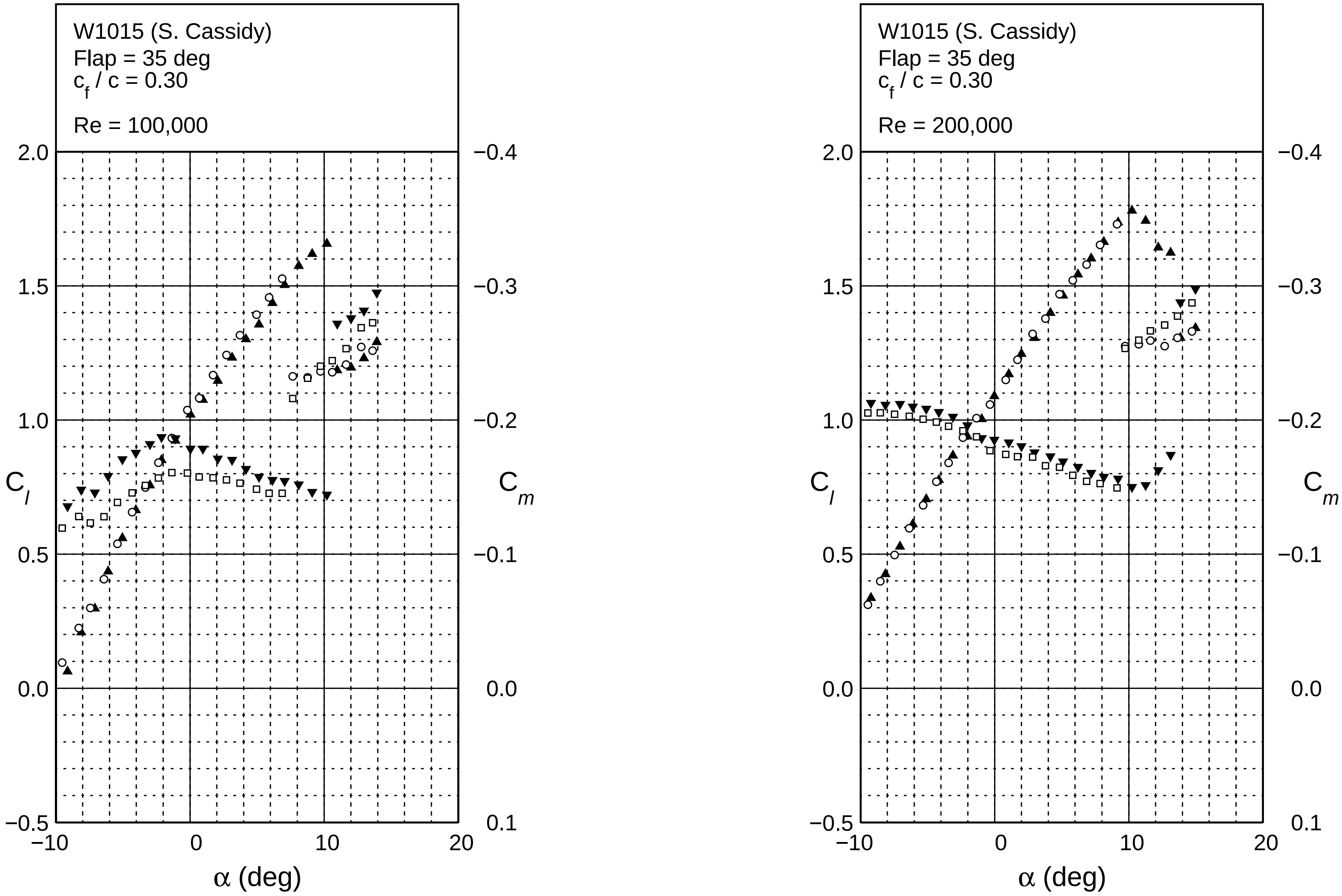

Figure 6.241: Lift and moment characteristics for the W1015 ($c_f/c = 30\%$) with a 35 deg flap.

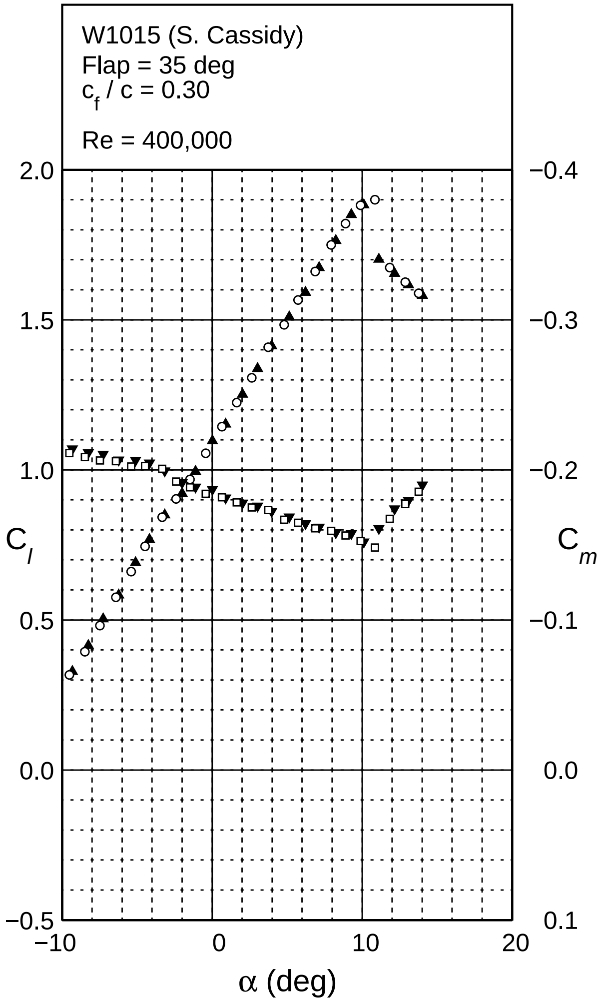

Figure 6.241: Continued.

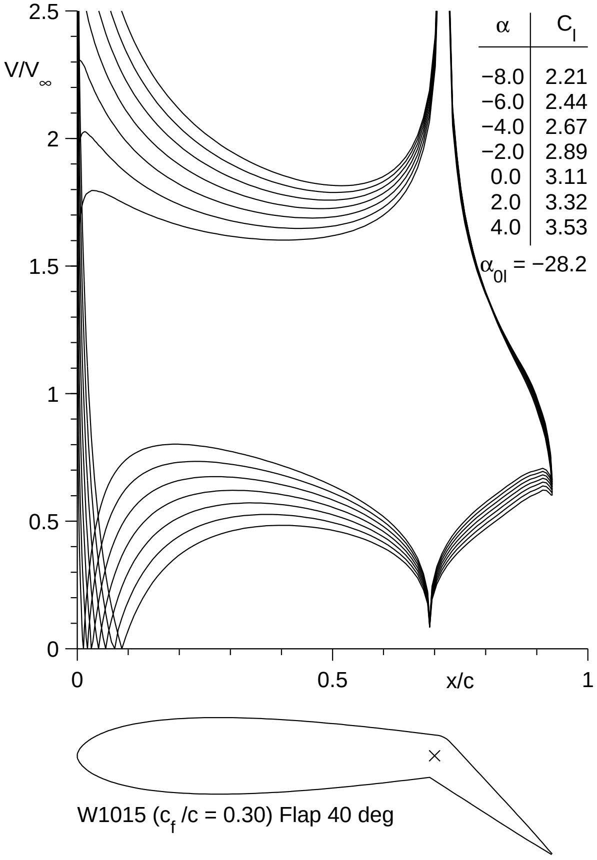

Figure 6.242: Inviscid velocity distribution for the W1015 ($c_f/c = 30\%$) with a 40 deg flap.

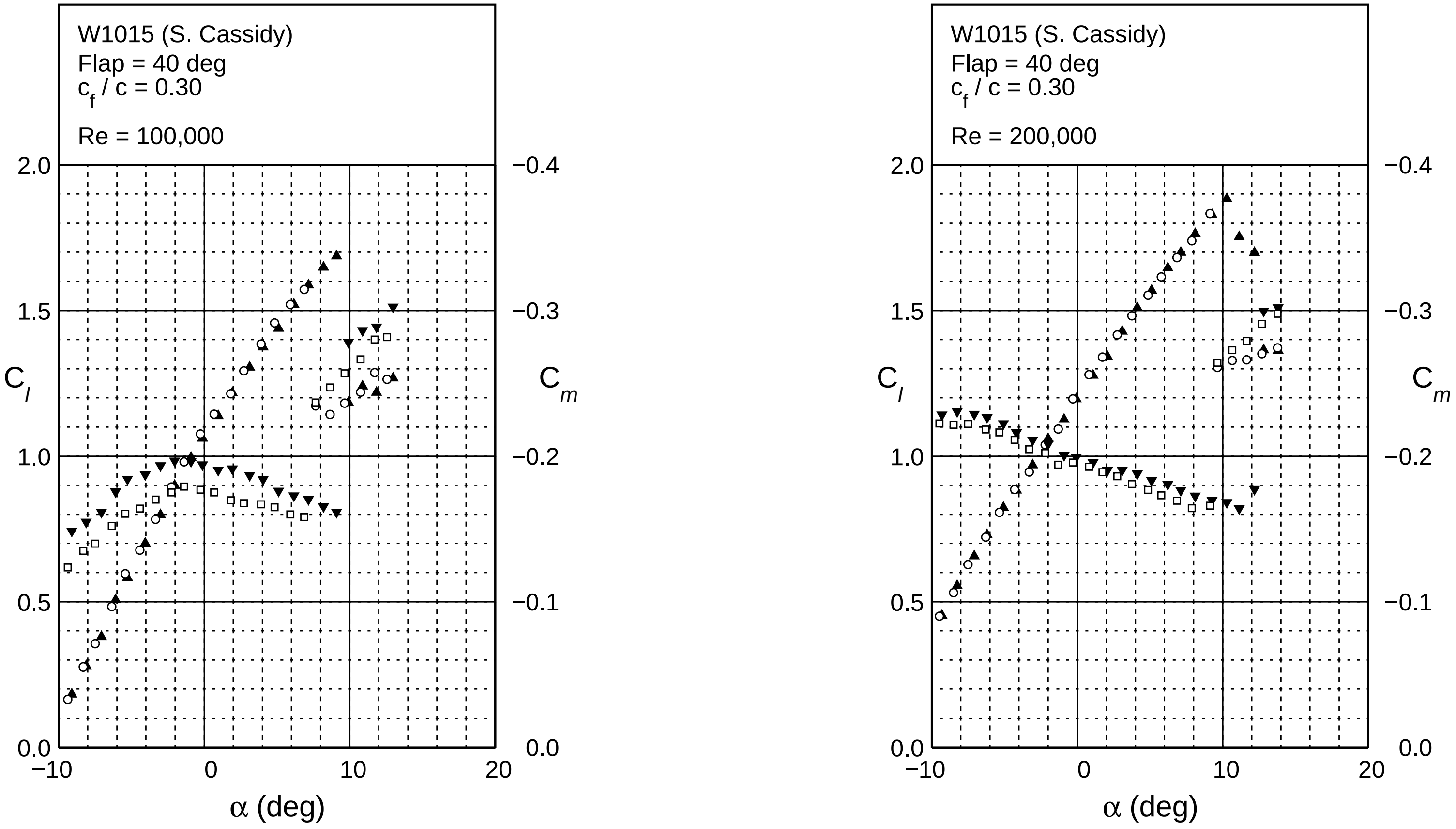

Figure 6.243: Lift and moment characteristics for the W1015 ($c_f/c = 30\%$) with a 40 deg flap.

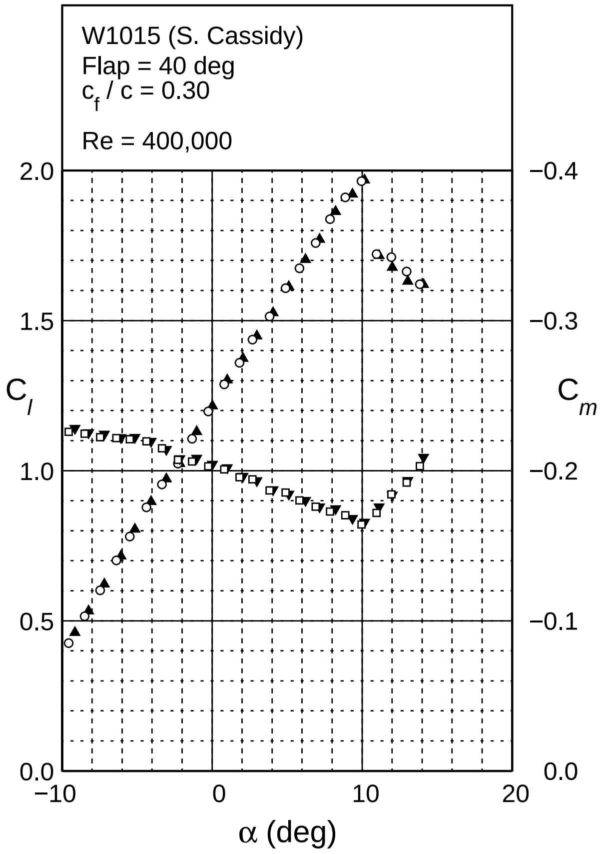

Figure 6.243: Continued.

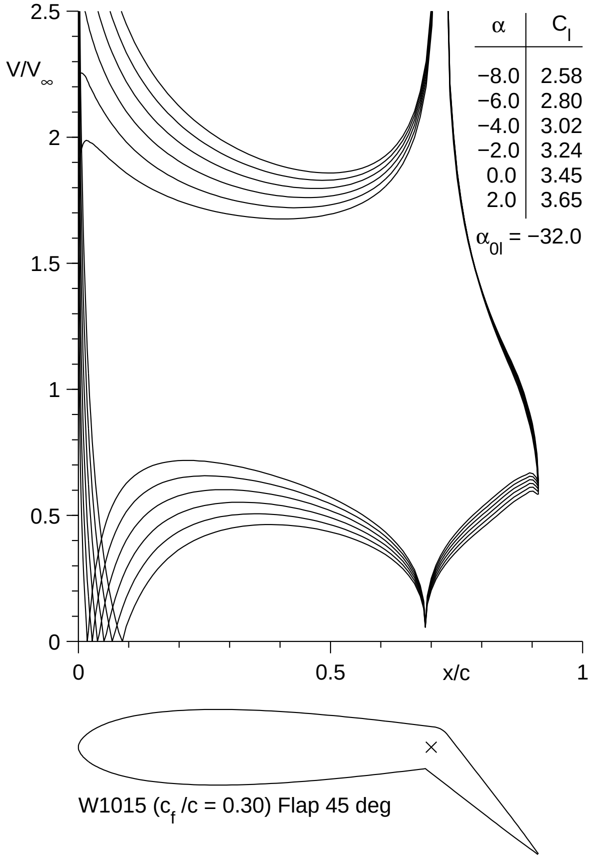

Figure 6.244: Inviscid velocity distribution for the W1015 $(c_f/c = 30\%)$ with a 45 deg flap.

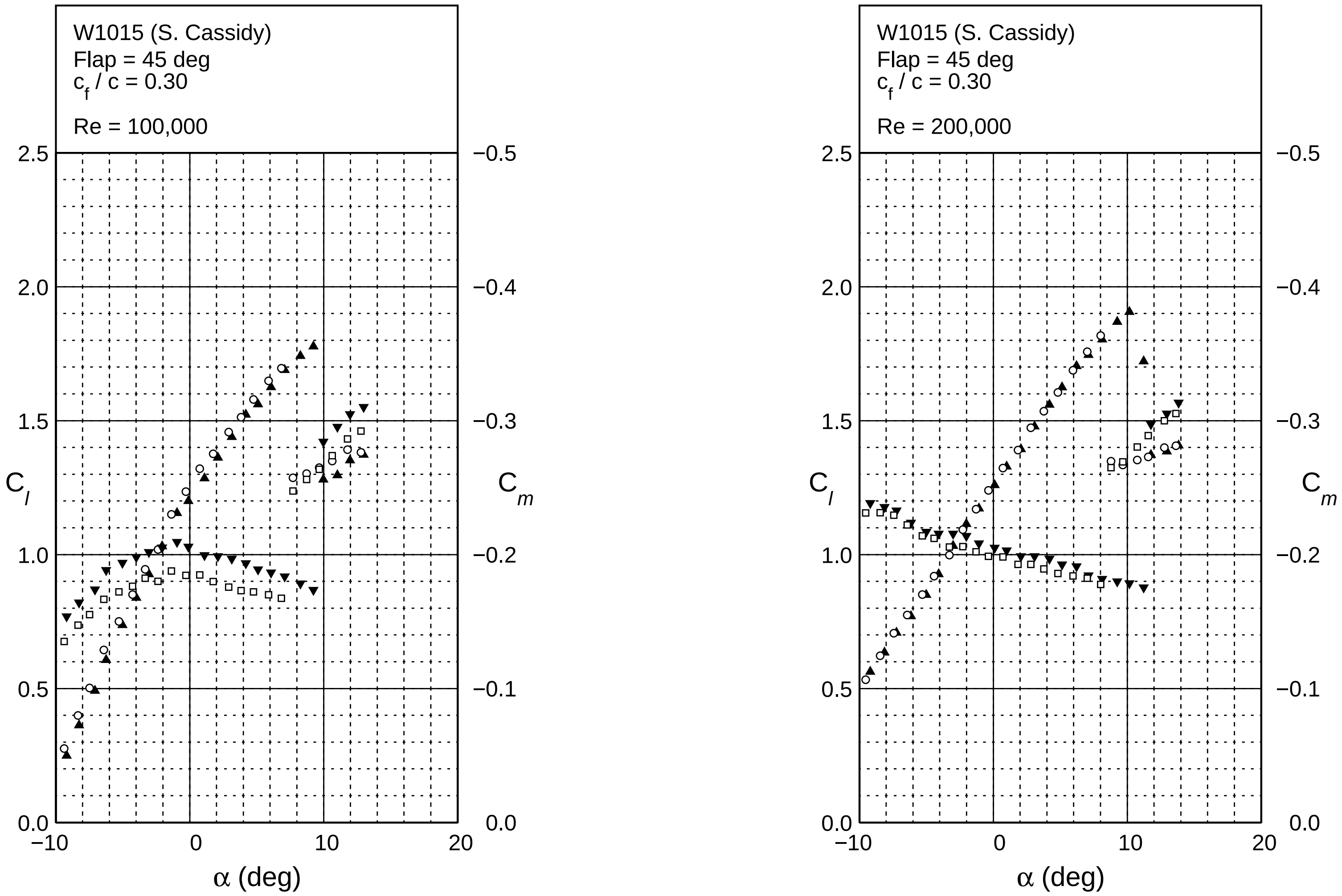

Figure 6.245: Lift and moment characteristics for the W1015 ($c_f/c = 30\%$) with a 45 deg flap.

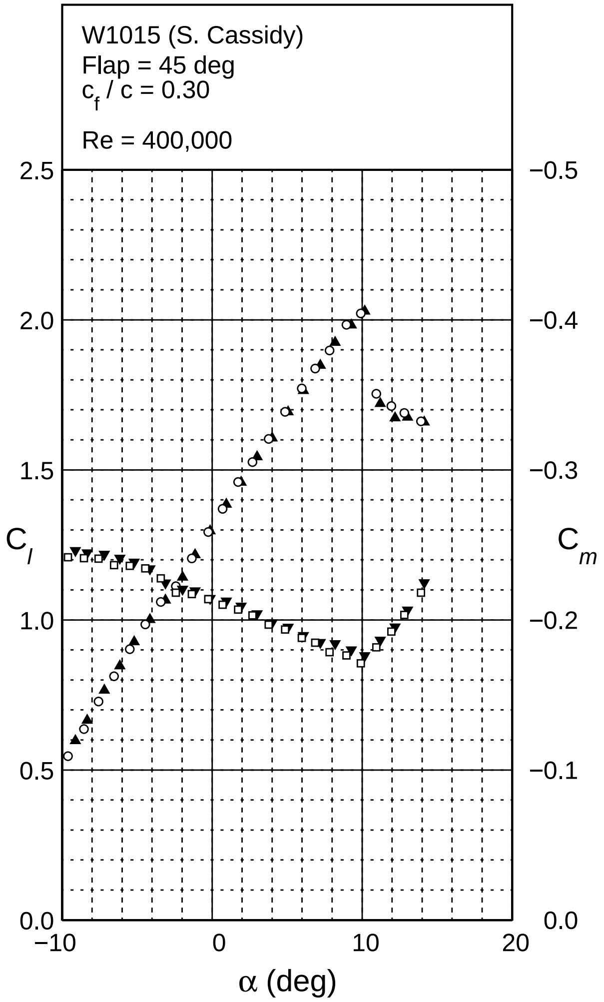

Figure 6.245: Continued.

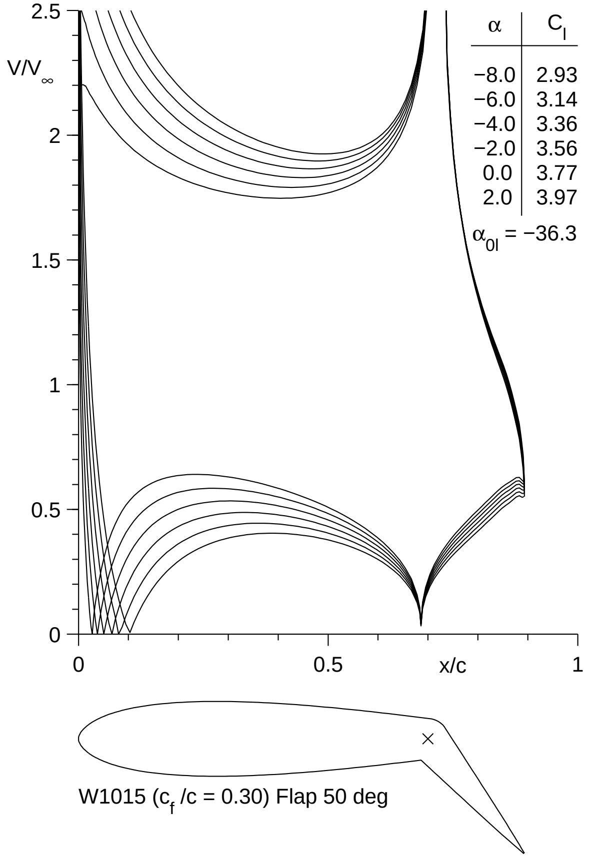

Figure 6.246: Inviscid velocity distribution for the W1015 ($c_f/c = 30\%$) with a 50 deg flap.

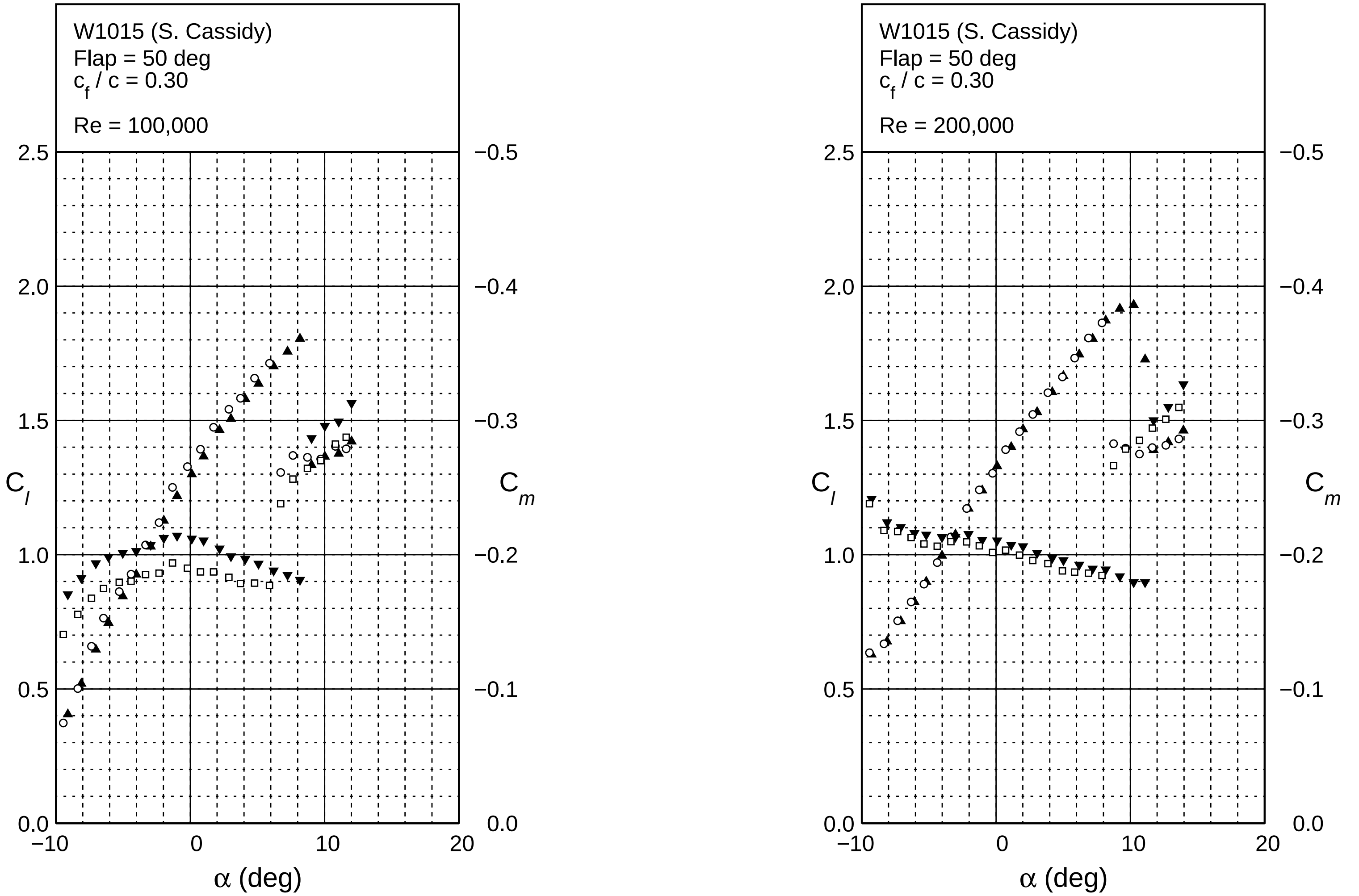

Figure 6.247: Lift and moment characteristics for the W1015 ($c_f/c = 30\%$) with a 50 deg flap.

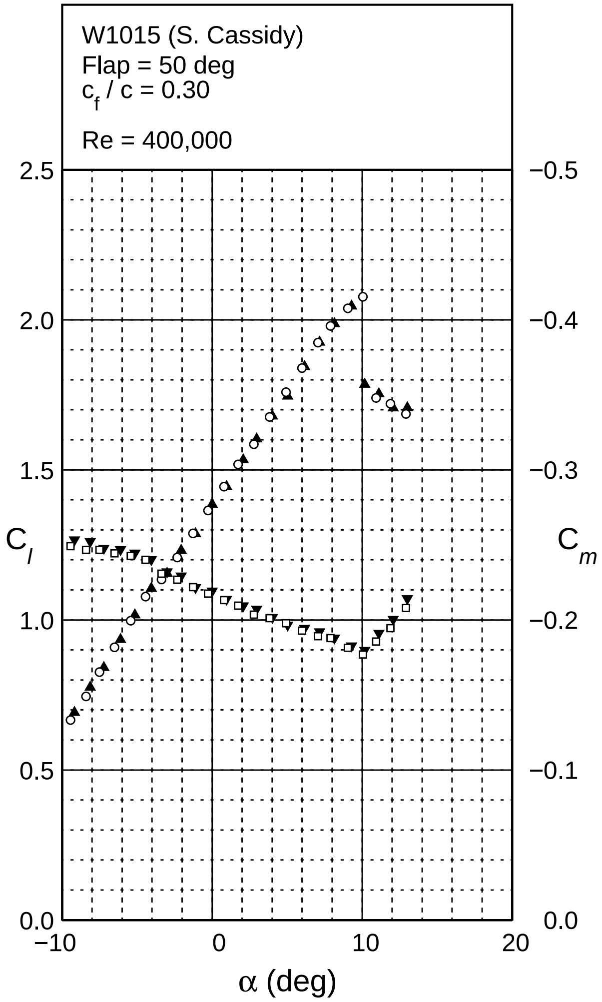

Figure 6.247: Continued.

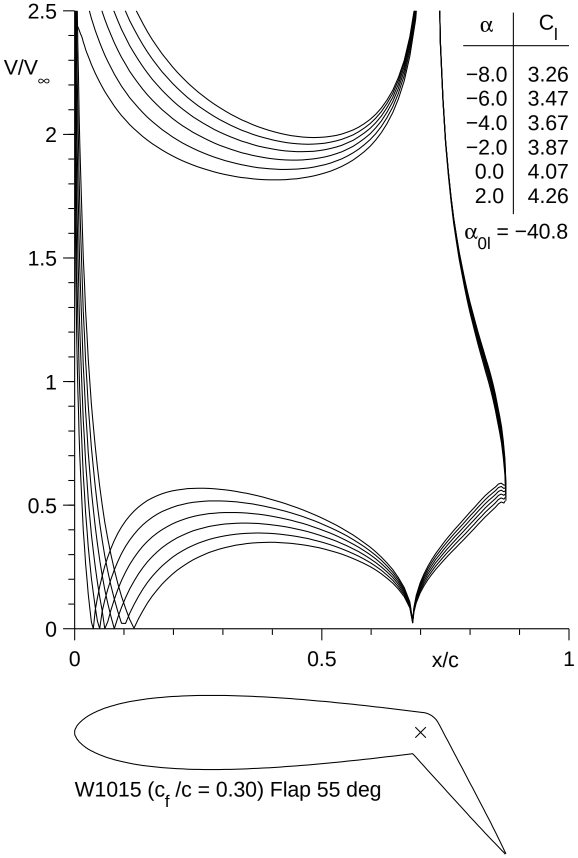

Figure 6.248: Inviscid velocity distribution for the W1015 ($c_f/c = 30\%$) with a 55 deg flap.

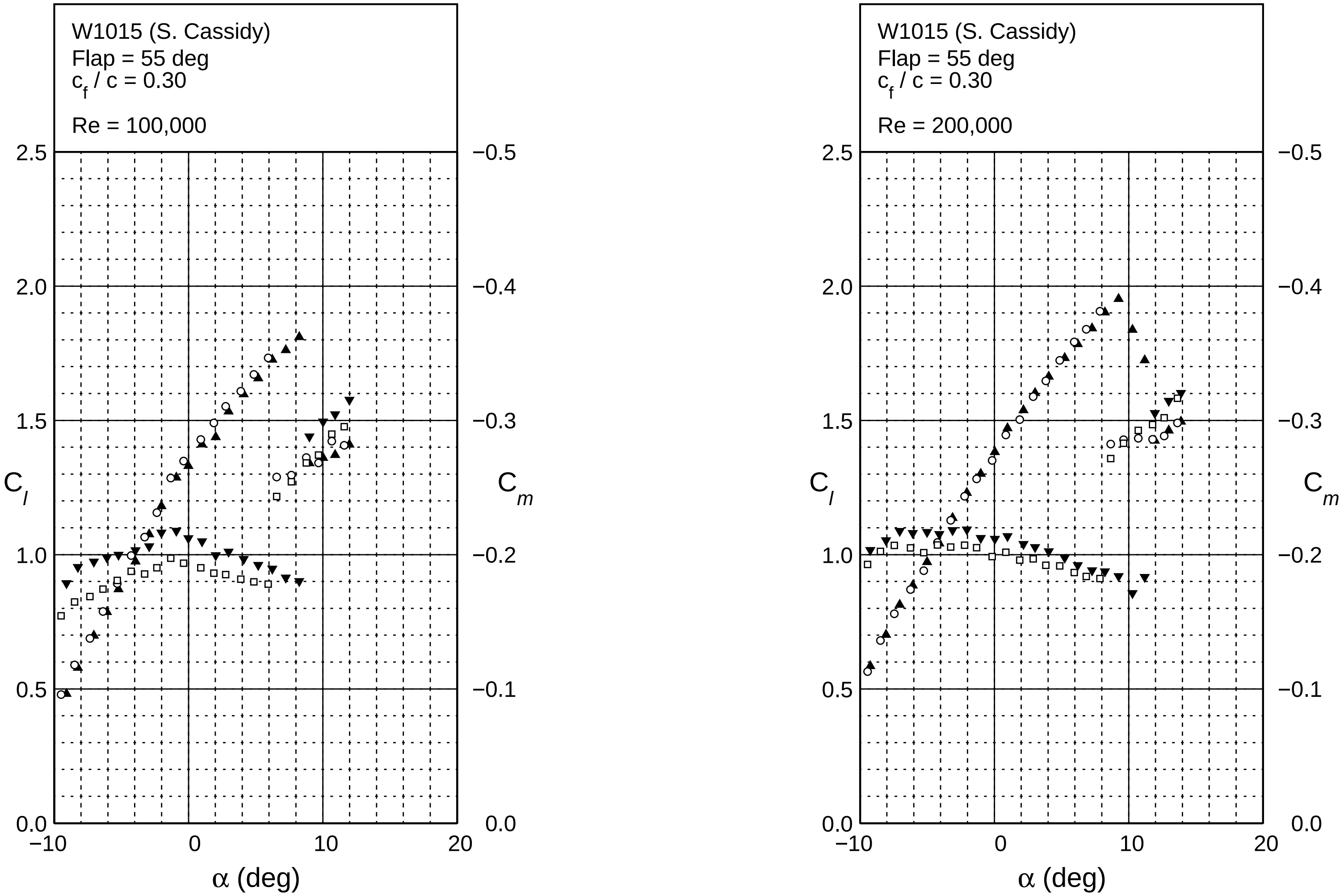

Figure 6.249: Lift and moment characteristics for the W1015 ($c_f/c = 30\%$) with a 55 deg flap.

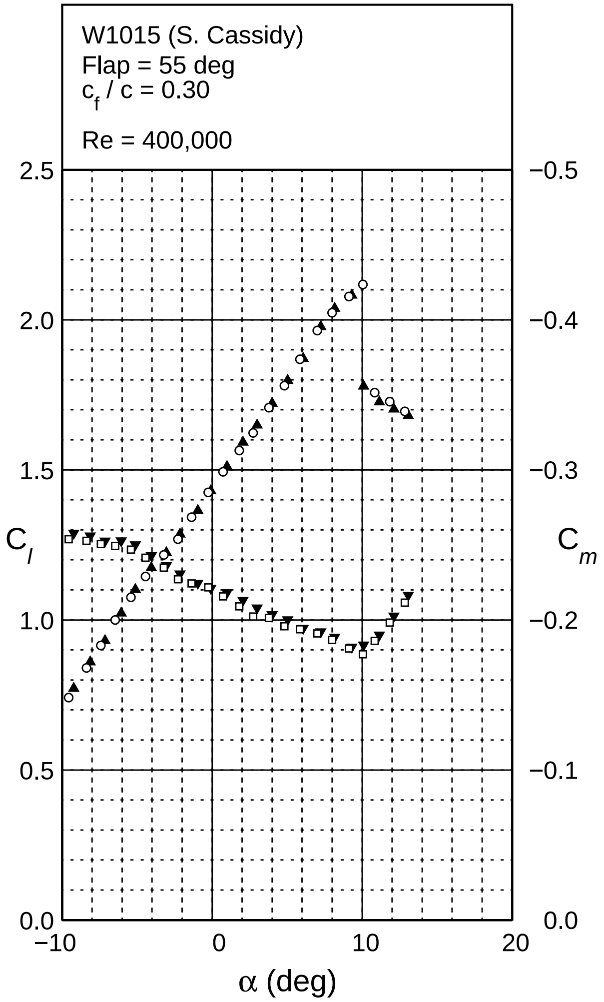

Figure 6.249: Continued.

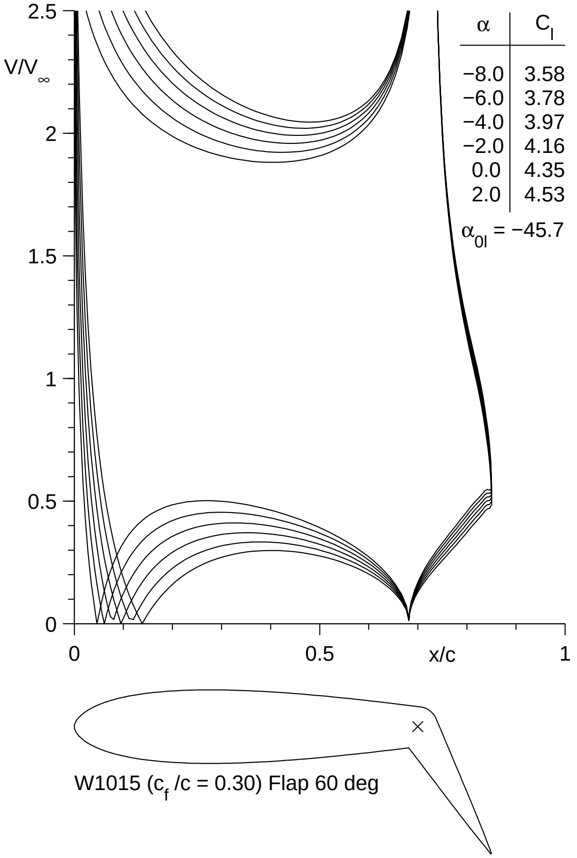

Figure 6.250: Inviscid velocity distribution for the W1015 ($c_f/c = 30\%$) with a 60 deg flap.

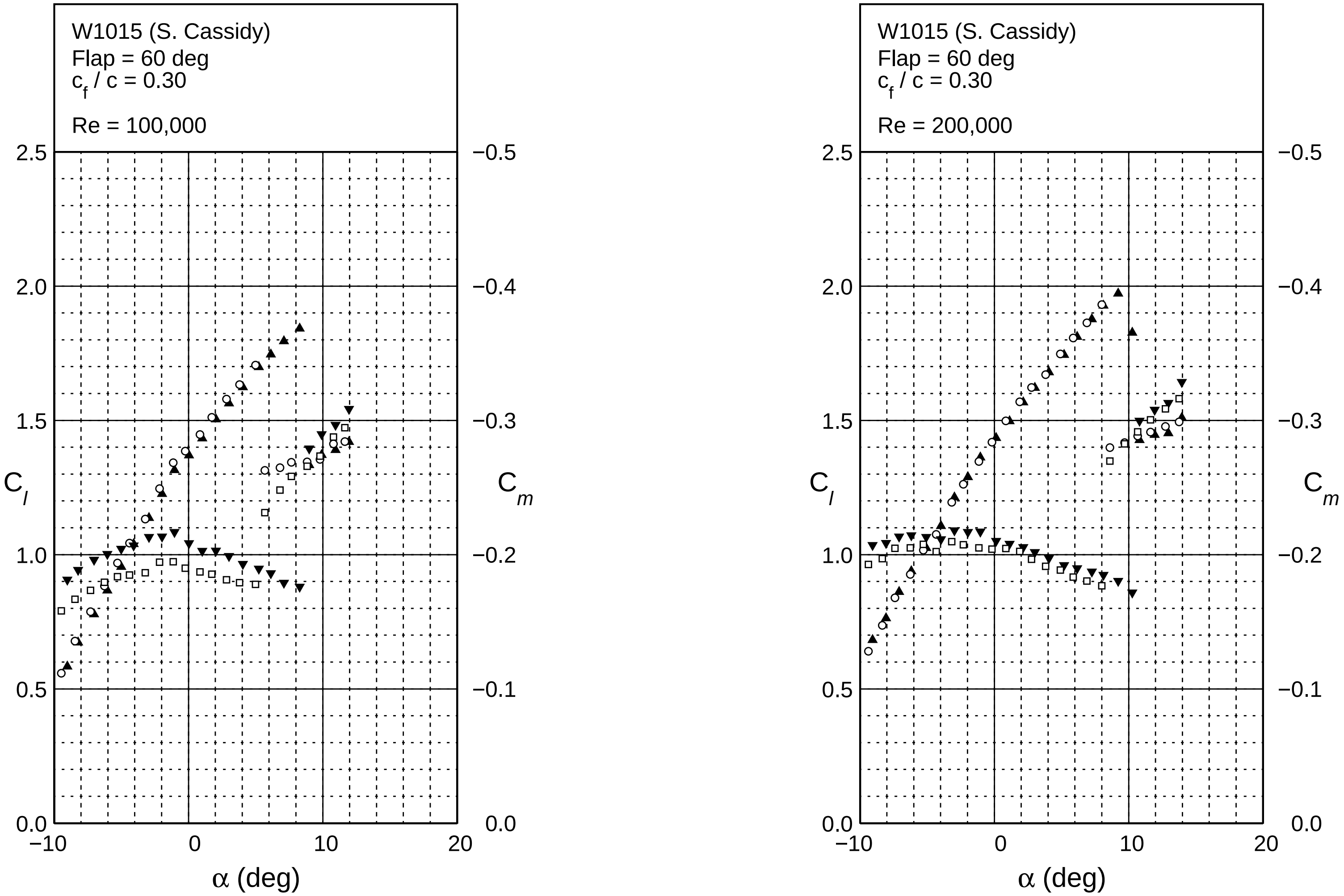

Figure 6.251: Lift and moment characteristics for the W1015 (c_f/c = 30%) with a 60 deg flap.

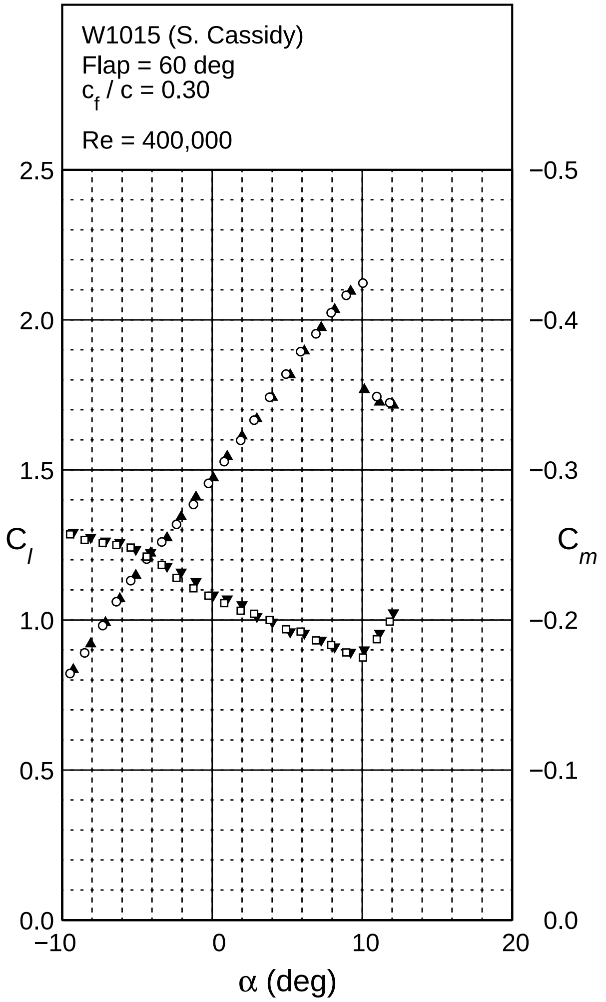

Figure 6.251: Continued.

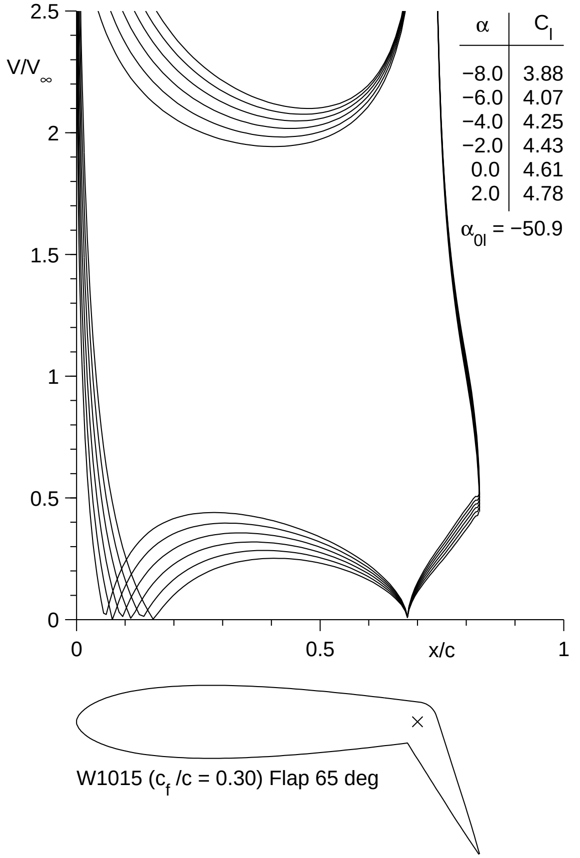

Figure 6.252: Inviscid velocity distribution for the W1015 ($c_f/c = 30\%$) with a 65 deg flap.

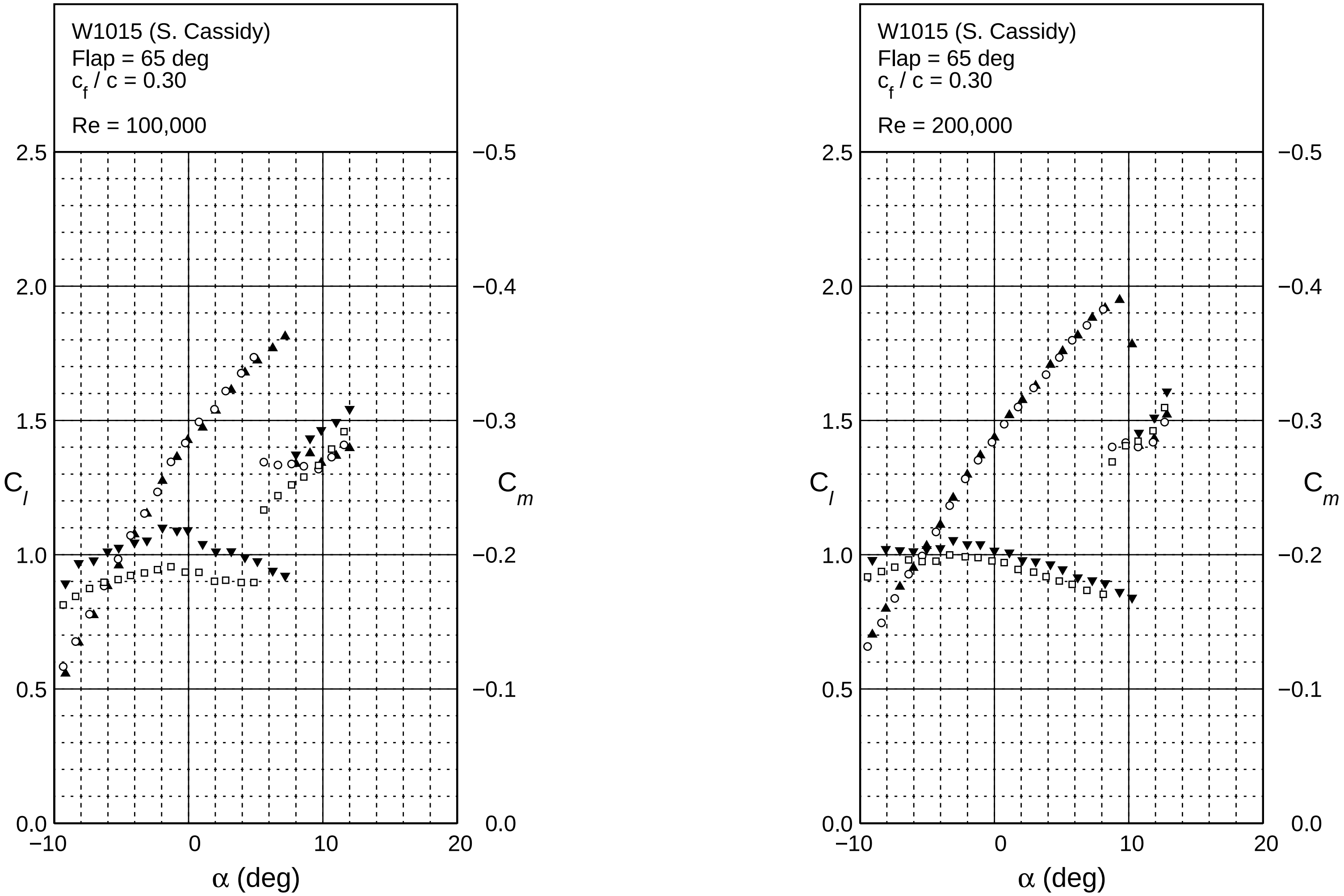

Figure 6.253: Lift and moment characteristics for the W1015 (c_f/c = 30%) with a 65 deg flap.

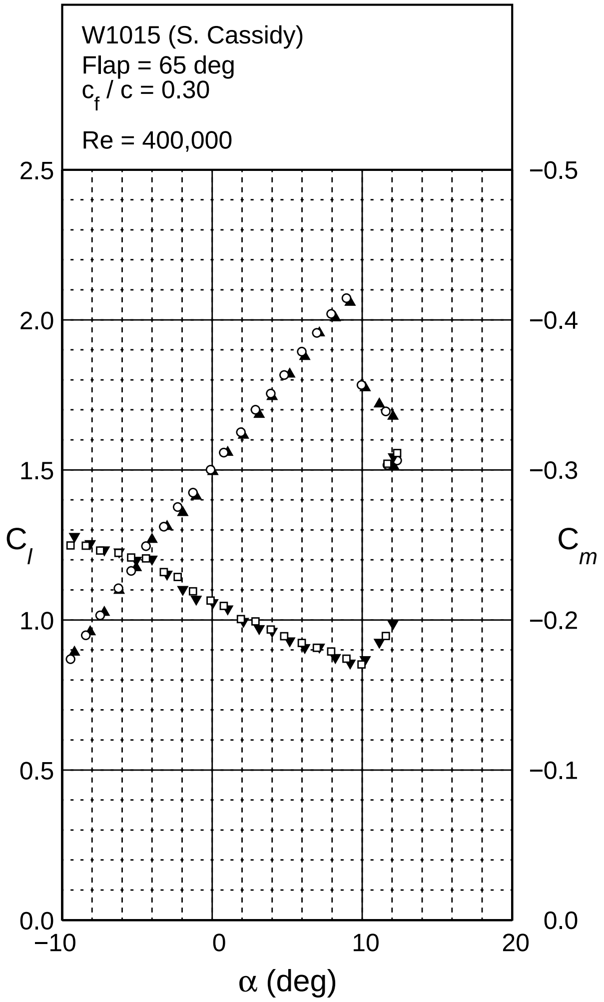

Figure 6.253: Continued.

Chapter 7

Conclusions

Four airfoils, AG40d-02r, AG455ct-02r, W1011, and W1015, with plain flaps were experimentally examined in the UIUC low-turbulence subsonic wind tunnel. The effects of plain flaps on lift, moment, and drag coefficients were examined in great detail. The effects of Reynolds number, thickness, flap-chord ratio, and flap deflection on the lift and moment increments were examined by creating various lift and moment increment plots.

Multiple difficulties were encountered when collecting data for large flap deflections. In some cases, lift and moment data was not collected because of excessive forces that would have exceeded load cell capacities. Collection of drag data was severely limited due to excessive pressure differentials at the higher Reynolds numbers and time constraints at lower Reynolds numbers. Unexpected difficulties were encountered with the W1011 and W1015 models. When fully assembled, the flap endplates, which constrained the flap from rotating, would rub against the Plexiglas® splitter plates causing erroneous lift and moment data. The problem was solved by reducing the thickness of the flap endplates with a grinder.

After analyzing the data, clear trends emerged in the lift and moment increments. The airfoil thickness did not play a crucial role in affecting lift increments, but it did affect the initiation and severity of the transition region (10 deg $\leq \delta_f \leq$ 30 deg). The Reynolds number also did not play a significant role in affecting the lift or the moment increments as most of the results followed the same trends independent of the Reynolds number, but it did seem to affect the initiation and severity of the transition region. Instead, the flap-chord ratio was the main cause for changes in lift increment. It was observed that some correlation existed between the lift and moment increments. In the linear region of the lift increment, the moment increment decreased linearly. In the transition region, the moment increment slope started to increase as the lift increment slope decreased. This trend was observed for all four airfoils.

When analyzing the effects of flap deflections on maximum lift coefficient for each configuration, four trends were revealed. First, the Reynolds number affected the maximum lift coefficient. As the Reynolds number increased, the maximum lift coefficient also increased. Second, the maximum lift coefficient increases linearly for small ($\delta_f \leq$ 10 to 20 deg) flap deflections. Third, the maximum lift coefficient plateaued between a flap deflection of 40 and 50 deg. Fourth and finally, the 30% of chord flap consistently produced a larger maximum lift coefficient compared with the 20% of chord flap for the W1011 and W1015 airfoils.

Drag data with large flap deflections ($\delta_f \geq 30$ deg) revealed two interesting conclusions. First, the airfoil thickness did not significantly affect the drag for highly deflected flaps. Second, the primary driving factor for drag values at large flap deflections was the projected area of the flap in the freestream direction. Therefore, the flap-chord ratio and flap deflection set the amount of airfoil drag.

The maximum lift-to-drag ratio (C_l/C_d) for the W1011 and W1015 airfoils with both flap-chord ratios (20% and 30%) and various flap deflections were calculated and compared revealing two interesting trends. First, the maximum lift-to-drag ratio for flapped airfoils was highly dependent on flap deflection. Second, the maximum lift-to-drag ratio for flap deflections below 20 deg was a function of the airfoil thickness and above 20 deg was a function of flap-chord ratio.

The effects of plain flaps on airfoil performance at low Reynolds numbers are still not fully understood. Future research in this area should focus on the effects of thickness, camber, flap-chord ratio, and flap deflection on the lift and moment increments especially for flap-chord ratios above and below the region examined in this research. Further exploration of the transition region (10 deg $\leq \delta_f \leq$ 30 deg) may reveal interesting trends of how thickness affects the flow separation from the upper surface of the flap. As computational tools become more accurate for low Reynolds number flows, the experimental data taken during this research could be used to validate new computational methods.

Appendix A

Tabulated Airfoil Coordinates

Appendix A contains both the true (as designed) coordinates and actual (as built) coordinates for the airfoils tested during this research. For any given airfoil, the true coordinates are listed first.

AG40d-02r

True

x/c	y/c
1.000000	0.000478
0.994054	0.001077
0.982165	0.002447
0.968707	0.004000
0.955028	0.005514
0.941303	0.007040
0.927596	0.008561
0.913882	0.010123
0.900153	0.011689
0.886424	0.013247
0.872689	0.014787
0.858978	0.016307
0.845256	0.017813
0.831558	0.019302
0.817862	0.020769
0.804186	0.022212
0.790513	0.023629
0.776850	0.025017
0.763195	0.026371
0.758006	0.026876
0.755235	0.027144
0.751672	0.027563
0.747315	0.028133
0.736722	0.029510
0.723013	0.031247
0.712660	0.032532
0.695454	0.034604
0.681588	0.036212
0.667686	0.037773
0.656489	0.038994
0.650920	0.039589
0.639796	0.040751
0.625817	0.042169
0.613984	0.043330
0.597880	0.044855
0.583944	0.046121
0.570012	0.047339
0.558942	0.048272
0.549985	0.049003
0.541959	0.049640
0.528043	0.050704
0.514128	0.051716
0.500179	0.052677
0.486200	0.053585
0.472209	0.054436
0.458206	0.055229
0.444178	0.055962
0.430126	0.056635
0.416049	0.057244
0.401961	0.057786
0.387896	0.058256
0.373869	0.058654
0.359878	0.058976
0.345919	0.059218
0.331997	0.059377
0.318109	0.059451
0.304252	0.059436
0.290430	0.059325
0.276625	0.059117
0.262828	0.058803
0.249051	0.058379
0.235294	0.057838
0.221551	0.057169
0.207837	0.056364
0.194155	0.055424
0.180501	0.054331
0.166900	0.053074
0.153345	0.051640
0.139858	0.050012
0.126454	0.048171
0.113141	0.046094
0.099962	0.043759
0.086936	0.041134
0.074119	0.038197
0.061549	0.034907
0.049346	0.031231
0.037694	0.027122
0.026971	0.022619
0.017869	0.017982
0.011096	0.013717
0.006584	0.010180
0.003679	0.007316
0.001804	0.004930
0.000652	0.002875
0.000091	0.001085
0.000013	-0.000428
0.000284	-0.001830
0.001126	-0.003269
0.002626	-0.004743
0.004894	-0.006315
0.008268	-0.008084
0.013250	-0.010082
0.020143	-0.012183
0.028974	-0.014226
0.039695	-0.016113
0.051627	-0.017698
0.064190	-0.018957
0.077232	-0.019943
0.090870	-0.020715
0.105062	-0.021304
0.119601	-0.021732
0.134234	-0.022023
0.148850	-0.022192
0.163428	-0.022266
0.177968	-0.022262
0.192444	-0.022190
0.206857	-0.022064
0.221090	-0.021895
0.235287	-0.021692
0.249436	-0.021456
0.263570	-0.021192
0.277689	-0.020900
0.291816	-0.020583
0.305952	-0.020243
0.320107	-0.019880
0.334290	-0.019499
0.348500	-0.019103
0.362730	-0.018690
0.377003	-0.018266
0.391304	-0.017831
0.405592	-0.017386
0.419896	-0.016934
0.434181	-0.016474
0.448442	-0.016011
0.462684	-0.015541
0.476907	-0.015066
0.491095	-0.014588
0.505262	-0.014108
0.519422	-0.013624
0.533574	-0.013141
0.547715	-0.012658
0.555357	-0.012396
0.565055	-0.012063
0.575458	-0.011709
0.589006	-0.011247
0.602553	-0.010788
0.608953	-0.010571
0.616233	-0.010326
0.629888	-0.009871
0.643526	-0.009420
0.653333	-0.009098
0.662365	-0.008801
0.670765	-0.008529
0.684400	-0.008091
0.698020	-0.007656
0.712999	-0.007185
0.724857	-0.006818
0.738189	-0.006409
0.743882	-0.006236
0.747950	-0.006114
0.753502	-0.005948
0.758125	-0.005810
0.765054	-0.005605
0.778506	-0.005211
0.791927	-0.004828

0.805336	-0.004452
0.818895	-0.004083
0.832453	-0.003724
0.846006	-0.003377
0.859583	-0.003045
0.873153	-0.002724
0.886712	-0.002420
0.900308	-0.002133
0.913918	-0.001852
0.927552	-0.001597
0.941205	-0.001354
0.954907	-0.001128
0.968612	-0.000909
0.982101	-0.000716
0.994042	-0.000557
1.000000	-0.000478

AG40d-02r
Actual

x/c	y/c
1.000000	0.000283
0.990989	0.001311
0.973043	0.003438
0.954935	0.005494
0.939409	0.007154
0.918306	0.009548
0.898215	0.011789
0.876763	0.014202
0.825857	0.019851
0.793702	0.023340
0.766521	0.026094
0.738633	0.029408
0.702342	0.033972
0.667117	0.038049
0.636811	0.041279
0.598439	0.045010
0.563137	0.048146
0.522877	0.051287
0.477931	0.054290
0.439679	0.056321
0.397393	0.058213
0.362714	0.059165
0.327708	0.059708
0.290868	0.059637
0.252756	0.058863
0.217607	0.057238
0.180313	0.054575
0.151338	0.051673
0.123842	0.048038
0.094467	0.042926
0.073206	0.038116
0.052963	0.032479
0.040003	0.028094
0.034163	0.025810
0.026938	0.022695
0.021327	0.019950
0.014666	0.016141
0.010001	0.013010
0.007804	0.011268
0.005521	0.009244
0.004708	0.008402
0.002975	0.006354
0.001462	0.004171
0.000457	0.002106
0.000105	0.000822
0.000004	-0.000161
0.000147	-0.000973
0.001486	-0.003520
0.003356	-0.005405
0.007541	-0.008100
0.010916	-0.009617
0.015749	-0.011365
0.023172	-0.013449
0.030185	-0.014966
0.045148	-0.017423
0.067756	-0.019799
0.090376	-0.021226
0.114505	-0.022217
0.140179	-0.022837
0.173693	-0.023085
0.205520	-0.022992
0.241251	-0.022557
0.274734	-0.021974
0.307351	-0.021237
0.345101	-0.020337
0.382510	-0.019287
0.420936	-0.018083
0.459624	-0.016904
0.498837	-0.015618
0.552033	-0.013818
0.590354	-0.012487
0.623461	-0.011327
0.661500	-0.010078
0.694860	-0.008938
0.725654	-0.007934
0.758741	-0.006892
0.788048	-0.006034
0.815384	-0.005249
0.840282	-0.004613
0.867870	-0.003841
0.886589	-0.003368
0.908515	-0.002887
0.925994	-0.002385
0.945888	-0.001952
0.960939	-0.001512
0.976995	-0.001229
0.989888	-0.000751
0.995443	-0.000551
0.997540	-0.000397
1.000000	-0.000237

AG455ct-02r
True

x/c	y/c
1.000000	0.000422
0.994170	0.000954
0.982316	0.002035
0.968892	0.003221
0.955202	0.004424
0.941444	0.005624
0.927663	0.006791
0.913863	0.007945
0.900051	0.009079
0.886239	0.010196
0.872425	0.011290
0.858612	0.012360
0.844813	0.013416
0.831008	0.014448
0.817215	0.015463
0.803422	0.016459
0.789639	0.017432
0.775854	0.018393
0.762077	0.019332
0.748302	0.020252
0.734533	0.021156
0.720760	0.022041
0.710075	0.022717
0.704818	0.023044
0.702188	0.023207
0.699579	0.023458
0.694361	0.023961
0.680231	0.025310
0.666108	0.026635
0.659173	0.027278
0.648776	0.028235
0.637922	0.029221
0.623855	0.030481
0.607516	0.031915
0.595808	0.032923
0.581851	0.034103
0.567919	0.035257
0.556858	0.036153
0.547916	0.036865
0.539911	0.037494
0.526047	0.038556
0.512218	0.039585
0.498385	0.040583

0.484548	0.041545
0.470723	0.042469
0.456908	0.043354
0.443086	0.044199
0.429265	0.045000
0.415452	0.045755
0.401634	0.046462
0.387821	0.047118
0.374011	0.047721
0.360206	0.048269
0.346397	0.048755
0.332597	0.049178
0.318804	0.049535
0.305013	0.049822
0.291233	0.050032
0.277461	0.050163
0.263691	0.050206
0.249936	0.050156
0.236200	0.050007
0.222471	0.049752
0.208767	0.049380
0.195088	0.048882
0.181432	0.048247
0.167822	0.047462
0.154250	0.046514
0.140736	0.045384
0.127294	0.044055
0.113930	0.042500
0.100688	0.040698
0.087581	0.038611
0.074669	0.036199
0.061994	0.033406
0.049680	0.030176
0.037910	0.026460
0.027072	0.022269
0.017878	0.017838
0.011050	0.013680
0.006524	0.010179
0.003631	0.007321
0.001787	0.004934
0.000668	0.002882
0.000113	0.001120
0.000013	-0.000359
0.000337	-0.001726
0.001239	-0.003095
0.002858	-0.004390
0.005244	-0.005665
0.008721	-0.007025
0.013948	-0.008549
0.021760	-0.010208
0.032064	-0.011783
0.043924	-0.013076
0.056554	-0.014057
0.069555	-0.014776
0.082773	-0.015286
0.096139	-0.015633
0.109606	-0.015854
0.123148	-0.015975
0.136750	-0.016013
0.150401	-0.015977
0.164083	-0.015879
0.177803	-0.015730
0.191544	-0.015537
0.205308	-0.015310
0.219101	-0.015056
0.232927	-0.014781
0.246776	-0.014488
0.260659	-0.014186
0.274574	-0.013872
0.288521	-0.013551
0.302495	-0.013226
0.316489	-0.012897
0.330500	-0.012566
0.344528	-0.012235
0.358569	-0.011904
0.372617	-0.011572
0.386681	-0.011241
0.400763	-0.010909
0.414858	-0.010579
0.428946	-0.010250
0.443025	-0.009923
0.457091	-0.009599
0.471152	-0.009274
0.485206	-0.008954
0.499244	-0.008636
0.513274	-0.008321
0.527300	-0.008006
0.541320	-0.007694
0.548893	-0.007526
0.558509	-0.007311
0.568829	-0.007080
0.582291	-0.006781
0.595470	-0.006488
0.609368	-0.006177
0.622968	-0.005875
0.636569	-0.005574
0.646155	-0.005363
0.655175	-0.005166
0.663777	-0.004978
0.677452	-0.004682
0.691121	-0.004388
0.696993	-0.004263
0.699968	-0.004200
0.702041	-0.004159
0.706272	-0.004069
0.718805	-0.003804
0.732681	-0.003515
0.746544	-0.003230
0.760397	-0.002950
0.774251	-0.002672
0.788103	-0.002399
0.801961	-0.002128
0.815822	-0.001864
0.829684	-0.001609
0.843548	-0.001374
0.857420	-0.001155
0.871290	-0.000956
0.885162	-0.000778
0.899044	-0.000622
0.912921	-0.000494
0.926805	-0.000391
0.940689	-0.000321
0.954576	-0.000285
0.968440	-0.000285
0.982058	-0.000332
0.994081	-0.000389
1.000000	-0.000422

AG455ct-02r

Actual

x/c	y/c
1.000000	0.000488
0.999334	0.000585
0.992577	0.001450
0.984324	0.002324
0.977756	0.003082
0.970349	0.003503
0.963038	0.004111
0.947330	0.005646
0.926492	0.007504
0.909954	0.008983
0.888459	0.010816
0.865706	0.012640
0.840791	0.014557
0.814702	0.016427
0.787289	0.018277
0.757929	0.020141
0.727475	0.021909
0.687524	0.024803
0.658313	0.027562
0.625135	0.030590
0.587918	0.033795
0.515952	0.039473
0.470748	0.042642
0.431370	0.045008
0.393190	0.047009
0.354360	0.048605
0.318301	0.049610

0.280791	0.050182
0.246697	0.050218
0.211778	0.049593
0.179151	0.048263
0.144672	0.045868
0.115528	0.042816
0.092142	0.039484
0.069824	0.035307
0.049584	0.030289
0.025383	0.021592
0.017818	0.017772
0.013341	0.015130
0.010813	0.013468
0.007720	0.011153
0.006007	0.009644
0.004424	0.008090
0.003229	0.006762
0.002505	0.005835
0.001340	0.003945
0.000677	0.002525
0.000104	0.000851
0.000005	-0.000189
0.000084	-0.000764
0.000052	-0.000681
0.000489	-0.001812
0.000913	-0.002499
0.001852	-0.003495
0.004680	-0.005268
0.010442	-0.007517
0.014862	-0.008725
0.021208	-0.010037
0.026771	-0.010951
0.035643	-0.012156
0.044735	-0.013133
0.056534	-0.014055
0.077638	-0.015109
0.099559	-0.015761
0.124306	-0.016145
0.153575	-0.016265
0.182524	-0.016032
0.214094	-0.015552
0.245662	-0.015023
0.282032	-0.014314
0.321311	-0.013571
0.352669	-0.012955
0.394479	-0.012070
0.423808	-0.011461
0.462308	-0.010743
0.498729	-0.009984
0.550621	-0.008999
0.598723	-0.008062
0.636002	-0.007367
0.669935	-0.006742
0.692137	-0.006452
0.729257	-0.005393
0.765908	-0.004445
0.797483	-0.003690
0.824447	-0.003099
0.849501	-0.002489
0.871630	-0.002033
0.892923	-0.001764
0.913887	-0.001355
0.931490	-0.001137
0.946132	-0.000884
0.966531	-0.000602
0.985756	-0.000272
0.991795	-0.000220
0.995876	-0.000128
0.998199	-0.000072
1.000000	0.000000

W1011
True

x/c	y/c
1.000000	0.000833
0.996554	0.001082
0.986588	0.002001
0.970666	0.003532
0.949180	0.005593
0.922446	0.008011
0.890721	0.010731
0.854380	0.013825
0.813920	0.017285
0.769876	0.021087
0.722822	0.025193
0.673411	0.029575
0.622352	0.034101
0.570291	0.038556
0.517819	0.042765
0.465516	0.046568
0.413946	0.049820
0.363647	0.052383
0.315132	0.054129
0.268880	0.054956
0.225330	0.054775
0.184879	0.053512
0.147864	0.051121
0.114572	0.047595
0.085238	0.042961
0.060051	0.037288
0.039145	0.030683
0.022599	0.023307
0.010453	0.015415
0.002742	0.007360
0.000000	-0.000000
0.002742	-0.007360
0.010454	-0.015415
0.022600	-0.023306
0.039147	-0.030681
0.060054	-0.037285
0.085242	-0.042956
0.114575	-0.047588
0.147868	-0.051111
0.184883	-0.053499
0.225334	-0.054759
0.268884	-0.054937
0.315136	-0.054106
0.363651	-0.052357
0.413950	-0.049791
0.465520	-0.046535
0.517822	-0.042728
0.570294	-0.038515
0.622354	-0.034056
0.673413	-0.029526
0.722824	-0.025141
0.769878	-0.021032
0.813921	-0.017227
0.854381	-0.013763
0.890722	-0.010667
0.922447	-0.007944
0.949180	-0.005525
0.970666	-0.003461
0.986589	-0.001930
0.996554	-0.001010
1.000000	-0.000760

W1011 20% Flap
Actual

x/c	y/c
1.000000	0.000371
0.996654	0.000725
0.994199	0.000970
0.990718	0.001343
0.989375	0.001479
0.984877	0.001936
0.981284	0.002234
0.968035	0.003537
0.962106	0.004075
0.957016	0.004569
0.949682	0.005267
0.942004	0.005901
0.929635	0.006828
0.920316	0.007656
0.904490	0.008987
0.887983	0.010334
0.873424	0.011487
0.851889	0.013365

0.822665	0.015780
0.801799	0.017453
0.768288	0.020668
0.735371	0.023575
0.700616	0.026747
0.653175	0.031224
0.617084	0.033947
0.588217	0.036396
0.560874	0.038603
0.518642	0.041834
0.477781	0.044726
0.436935	0.047426
0.400505	0.049650
0.358132	0.051908
0.319622	0.053575
0.283188	0.054609
0.243419	0.054901
0.209312	0.054335
0.178787	0.053114
0.151565	0.051341
0.132446	0.049630
0.113365	0.047434
0.094364	0.044628
0.081258	0.042217
0.065429	0.038626
0.051338	0.034669
0.041358	0.031289
0.031102	0.027175
0.022425	0.023027
0.017628	0.020339
0.013140	0.017424
0.009858	0.014979
0.006202	0.011731
0.003761	0.008935
0.002300	0.006746
0.001064	0.004501
0.000193	0.001868
0.000002	0.000203
0.000142	-0.001607
0.000446	-0.003115
0.000871	-0.004296
0.002518	-0.007510
0.004084	-0.009674
0.006482	-0.012298
0.009264	-0.014805
0.011842	-0.016816
0.016069	-0.019662
0.022338	-0.023273
0.027303	-0.025763
0.033212	-0.028383
0.038862	-0.030598
0.049972	-0.034368
0.081159	-0.042068
0.107198	-0.046372
0.134173	-0.049487
0.161888	-0.051699
0.193966	-0.053267
0.225597	-0.054026
0.263759	-0.054145
0.303116	-0.053509
0.336752	-0.052520
0.374259	-0.050963
0.413952	-0.048924
0.452988	-0.046625
0.489588	-0.044236
0.538924	-0.040750
0.572877	-0.038201
0.607753	-0.035316
0.632208	-0.033090
0.675932	-0.029401
0.710202	-0.026303
0.742631	-0.023499
0.761096	-0.021887
0.782259	-0.020033
0.804733	-0.018300
0.821705	-0.016684
0.848039	-0.014318
0.874197	-0.012003
0.893663	-0.010226
0.910952	-0.008753
0.922713	-0.007713
0.932074	-0.006912
0.941432	-0.006144
0.951626	-0.005226
0.961678	-0.004267
0.969367	-0.003560
0.974496	-0.003034
0.978958	-0.002664
0.984542	-0.002074
0.988549	-0.001765
0.991066	-0.001594
0.994432	-0.001265
0.996614	-0.001042
0.999030	-0.000858
1.000000	-0.000750

W1011 30% Flap
Actual

x/c	y/c
1.000000	0.000549
0.998032	0.000691
0.995497	0.000830
0.991465	0.001043
0.989460	0.001193
0.985927	0.001558
0.982702	0.001861
0.979076	0.002330
0.975453	0.002776
0.971081	0.003132
0.963899	0.003836
0.960137	0.004141
0.951803	0.005023
0.945169	0.005728
0.935285	0.006519
0.924178	0.007672
0.910852	0.008610
0.895905	0.010079
0.882132	0.011176
0.867364	0.012562
0.840946	0.014911
0.820187	0.016866
0.793702	0.019180
0.768279	0.021464
0.734147	0.024490
0.709839	0.026617
0.675053	0.029938
0.637430	0.033364
0.609600	0.035896
0.567299	0.039241
0.528272	0.042139
0.480297	0.045483
0.441891	0.047988
0.404572	0.050211
0.368912	0.052098
0.326506	0.053920
0.286226	0.055043
0.250553	0.055385
0.220148	0.055122
0.191172	0.054277
0.158562	0.052474
0.129570	0.049929
0.101131	0.046188
0.076322	0.041512
0.056190	0.036351
0.038148	0.030203
0.023046	0.023420
0.015750	0.019269
0.010990	0.016023
0.008314	0.013884
0.006451	0.012175
0.005008	0.010678
0.002279	0.007097
0.000889	0.004409
0.000350	0.002760
0.000168	0.001837
0.000005	0.000329
0.000433	-0.002964
0.001245	-0.005156

0.002763	-0.008005
0.004473	-0.010336
0.006773	-0.012820
0.010270	-0.015857
0.014575	-0.018949
0.019939	-0.022232
0.024827	-0.024846
0.039551	-0.031227
0.049494	-0.034674
0.065145	-0.039133
0.082971	-0.043097
0.098258	-0.045745
0.114947	-0.048055
0.144331	-0.050986
0.171733	-0.052745
0.205957	-0.053986
0.243029	-0.054292
0.274071	-0.053999
0.309077	-0.053229
0.343701	-0.052164
0.384037	-0.050539
0.417183	-0.048809
0.458963	-0.046270
0.500825	-0.043505
0.535665	-0.040979
0.571658	-0.038165
0.613580	-0.034591
0.648037	-0.031055
0.683859	-0.027612
0.712731	-0.025449
0.744869	-0.022577
0.762630	-0.021035
0.792435	-0.018466
0.819329	-0.016197
0.848527	-0.013689
0.870541	-0.011736
0.886596	-0.010416
0.905419	-0.008839
0.922274	-0.007421
0.942907	-0.005680
0.955826	-0.004453
0.968299	-0.003291
0.983045	-0.001908
0.992722	-0.001077
0.995760	-0.000757
0.998587	-0.000495
1.000000	-0.000312

W1015
True

x/c	y/c
1.000000	0.000833
0.996172	0.001317
0.985342	0.003004
0.968435	0.005676
0.945984	0.009146
0.918334	0.013081
0.885688	0.017388
0.848447	0.022191
0.807188	0.027465
0.762511	0.033137
0.715057	0.039101
0.665492	0.045205
0.614480	0.051243
0.562630	0.056981
0.510516	0.062211
0.458700	0.066753
0.407723	0.070435
0.358096	0.073108
0.310302	0.074643
0.264788	0.074936
0.221965	0.073911
0.182203	0.071519
0.145825	0.067739
0.113101	0.062584
0.084253	0.056119
0.059460	0.048438
0.038838	0.039685
0.022468	0.030089
0.010419	0.019937
0.002741	0.009615
0.000000	-0.000000
0.002741	-0.009615
0.010419	-0.019937
0.022468	-0.030089
0.038838	-0.039685
0.059460	-0.048438
0.084253	-0.056119
0.113101	-0.062584
0.145825	-0.067739
0.182203	-0.071519
0.221965	-0.073911
0.264788	-0.074936
0.310302	-0.074643
0.358096	-0.073108
0.407723	-0.070435
0.458700	-0.066753
0.510516	-0.062211
0.562630	-0.056981
0.614480	-0.051242
0.665492	-0.045205
0.715057	-0.039101
0.762511	-0.033137
0.807188	-0.027465
0.848447	-0.022191
0.885688	-0.017388
0.918334	-0.013080
0.945984	-0.009145
0.968435	-0.005675
0.985342	-0.003004
0.996172	-0.001316
1.000000	-0.000833

W1015 20% Flap
Actual

x/c	y/c
1.000000	0.000450
0.998056	0.000734
0.995887	0.001106
0.993436	0.001500
0.989299	0.002207
0.985422	0.002802
0.979311	0.003751
0.973408	0.004737
0.961623	0.006297
0.947319	0.008654
0.932406	0.010739
0.917063	0.012925
0.898922	0.015272
0.882568	0.017370
0.860129	0.020265
0.836642	0.023274
0.813483	0.026165
0.779298	0.030355
0.763105	0.032511
0.737906	0.035820
0.708075	0.039786
0.675491	0.044131
0.650450	0.047252
0.622347	0.050926
0.586900	0.054681
0.551417	0.058160
0.506413	0.062457
0.463297	0.066218
0.424473	0.069125
0.387934	0.071303
0.348620	0.073028
0.316886	0.073905
0.278437	0.074358
0.239430	0.073955
0.209693	0.072914
0.175959	0.070758

0.142069	0.067248
0.117890	0.063649
0.093275	0.058649
0.070759	0.052626
0.059079	0.048728
0.038714	0.039943
0.031562	0.036066
0.023526	0.031006
0.017546	0.026568
0.014366	0.023881
0.009650	0.019337
0.006954	0.016282
0.003721	0.011610
0.002235	0.008772
0.000479	0.004115
0.000052	0.001245
0.000011	-0.000552
0.000759	-0.004709
0.001476	-0.006772
0.003054	-0.010073
0.005506	-0.013674
0.008185	-0.016868
0.013084	-0.021733
0.020212	-0.027652
0.029071	-0.033681
0.040374	-0.039952
0.056548	-0.047124
0.071265	-0.052285
0.089920	-0.057569
0.112692	-0.062573
0.129177	-0.065392
0.152294	-0.068438
0.179487	-0.070945
0.213715	-0.072878
0.252388	-0.073881
0.292430	-0.073969
0.327481	-0.073329
0.362407	-0.072056
0.399507	-0.070068
0.438303	-0.067415
0.479965	-0.064034
0.518292	-0.060532
0.556872	-0.056642
0.593358	-0.052684
0.620135	-0.049907
0.657516	-0.045556
0.691059	-0.041480
0.722685	-0.037726
0.753310	-0.033999
0.784581	-0.030200
0.810968	-0.026991
0.832577	-0.024150
0.853795	-0.021372
0.870536	-0.019166
0.885786	-0.017120
0.900637	-0.015202
0.920062	-0.012460
0.936624	-0.010144
0.952080	-0.007793
0.964340	-0.005994
0.973401	-0.004500
0.982342	-0.003101
0.985969	-0.002459
0.989088	-0.002012
0.991566	-0.001602
0.994848	-0.001193
0.997675	-0.000775
1.000000	-0.000422

W1015 30% Flap

Actual

x/c	y/c
1.000000	0.000702
0.996340	0.001260
0.993420	0.001726
0.989993	0.002220
0.987264	0.002718
0.984660	0.003029
0.980970	0.003680
0.975597	0.004537
0.968870	0.005603
0.962501	0.006517
0.954800	0.007712
0.944243	0.009380
0.934022	0.010786
0.923425	0.012300
0.910569	0.014114
0.898630	0.015749
0.881025	0.018115
0.862744	0.020570
0.846706	0.022666
0.830691	0.024790
0.812126	0.027172
0.779441	0.031389
0.757021	0.034292
0.732029	0.037481
0.707384	0.040655
0.682813	0.043474
0.654844	0.046828
0.634092	0.049198
0.603831	0.052337
0.574470	0.055366
0.547843	0.058119
0.520772	0.060767
0.494193	0.063227
0.455534	0.066525
0.420940	0.069183
0.387125	0.071371
0.360304	0.072745
0.337699	0.073621
0.304400	0.074441
0.280889	0.074662
0.258728	0.074594
0.232612	0.074086
0.204833	0.072998
0.176622	0.071152
0.149346	0.068446
0.127992	0.065514
0.107003	0.061773
0.091399	0.058313
0.071395	0.052781
0.058862	0.048482
0.049181	0.044566
0.041798	0.041148
0.036412	0.038387
0.030548	0.035049
0.023567	0.030542
0.019340	0.027441
0.015070	0.023973
0.011072	0.020289
0.008036	0.017112
0.006329	0.015101
0.003495	0.011110
0.002815	0.009932
0.002441	0.009225
0.001261	0.006453
0.000345	0.003204
0.000261	-0.002709
0.000657	-0.004322
0.001604	-0.007063
0.002929	-0.009801
0.005124	-0.013235
0.007063	-0.015758
0.012102	-0.021106
0.016206	-0.024746
0.024893	-0.031241
0.035280	-0.037481
0.045000	-0.042325
0.058398	-0.047872
0.070270	-0.051925
0.084711	-0.056074
0.099713	-0.059637
0.122338	-0.063913
0.140077	-0.066537
0.163321	-0.069166
0.185771	-0.070989
0.220484	-0.072800
0.242549	-0.073356

0.278906	-0.073574
0.316772	-0.073109
0.358503	-0.071724
0.395926	-0.069849
0.437615	-0.067245
0.479417	-0.063951
0.529448	-0.059413
0.563336	-0.056059
0.596528	-0.052658
0.626978	-0.049367
0.665155	-0.044445
0.707573	-0.038957
0.733450	-0.035733
0.760265	-0.032385
0.784232	-0.029360
0.803528	-0.026999
0.826962	-0.024103
0.845358	-0.021772
0.867742	-0.018944
0.886526	-0.016529
0.901848	-0.014566
0.923958	-0.011573
0.940159	-0.009332
0.950914	-0.007737
0.963061	-0.005915
0.973015	-0.004395
0.980736	-0.003167
0.984968	-0.002515
0.990190	-0.001720
0.993841	-0.001145
0.998467	-0.000427
1.000000	-0.000199

Appendix B

Tabulated Drag Polar Data

Appendix B contains all of the polar data seen in Chapter 6. The data presented in this appendix is identified by airfoil name, figure number, and run number. The same data along with all eight spanwise C_d values used to calculate the average C_d is available upon request. As a note, the flap deflections are defined with the following notation: “p” is positive and “n” is negative. For example, the AG40d-02r with a -10 deg flap would have identified as “AG40d-02r fn10”.

AG40d-02r

Fig. 6.40

Run: 06824ga_interp

Re = 99839.9

α	C_l	C_d
-5.26	-0.289	0.0239
-4.14	-0.195	0.0187
-3.05	-0.103	0.0146
-2.12	-0.021	0.0118
-1.10	0.092	0.0120
-0.09	0.240	0.0133
0.98	0.390	0.0144
1.99	0.494	0.0144
3.01	0.574	0.0136
4.10	0.675	0.0146
5.04	0.758	0.0157
6.14	0.858	0.0184
7.14	0.925	0.0218
8.13	0.986	0.0290
9.09	1.026	0.0367
10.13	1.064	0.0506

Run: 06826gw_interp

Re = 199652.6

α	C_l	C_d
-5.24	-0.271	0.0186
-4.14	-0.153	0.0132
-3.14	-0.036	0.0114
-2.07	0.088	0.0095
-1.07	0.196	0.0086
-0.09	0.305	0.0086
0.91	0.393	0.0089
2.01	0.502	0.0091
3.03	0.597	0.0097
3.91	0.679	0.0108
5.02	0.790	0.0127
6.00	0.877	0.0145
7.04	0.961	0.0186
8.15	1.038	0.0237
9.16	1.091	0.0295
10.09	1.122	0.0389

Run: 06828gw_interp

Re = 299954.3

α	C_l	C_d
-6.39	-0.375	0.0353
-5.16	-0.247	0.0142
-4.10	-0.129	0.0115
-3.21	-0.029	0.0095
-2.18	0.083	0.0080
-1.10	0.187	0.0075
-0.16	0.290	0.0071
0.92	0.399	0.0074
1.93	0.499	0.0079
3.01	0.607	0.0087
4.04	0.707	0.0101
5.07	0.800	0.0117
6.13	0.892	0.0137
7.07	0.973	0.0163
8.16	1.052	0.0203
9.20	1.112	0.0272
10.18	1.146	0.0352

Run: 06830gw_interp

Re = 399756.8

α	C_l	C_d
-6.27	-0.345	0.0232
-5.19	-0.231	0.0126
-4.13	-0.115	0.0102
-3.08	-0.005	0.0089
-2.19	0.083	0.0076
-1.15	0.183	0.0068
-0.07	0.300	0.0061
0.91	0.401	0.0066
2.06	0.515	0.0075
3.10	0.620	0.0084
4.09	0.715	0.0096
5.13	0.813	0.0110
6.10	0.901	0.0127
7.16	1.004	0.0158
8.22	1.075	0.0194
9.15	1.133	0.0242
10.12	1.180	0.0309

Run: 06832gw_interp

Re = 499203.9

α	C_l	C_d
-6.15	-0.329	0.0154
-5.17	-0.222	0.0115
-4.14	-0.110	0.0096
-3.15	-0.010	0.0082
-2.24	0.084	0.0076
-1.07	0.202	0.0065
-0.03	0.305	0.0058
0.92	0.408	0.0064
2.04	0.520	0.0072
2.96	0.609	0.0079
4.15	0.733	0.0092
5.11	0.828	0.0106
6.10	0.917	0.0125
7.08	0.991	0.0150
8.17	1.086	0.0184
9.10	1.143	0.0221
10.10	1.188	0.0277

AG40d-02r fn20

Fig. 6.43

Run: 06916ga_interp

Re = 100039.5

α	C_l	C_d
-2.17	-0.876	0.0544
-1.24	-0.775	0.0390
-0.15	-0.670	0.0329
0.94	-0.604	0.0290
1.92	-0.430	0.0317
2.89	-0.334	0.0358
4.00	-0.221	0.0346
4.97	-0.144	0.0357
6.06	-0.088	0.0361
6.99	-0.032	0.0345
8.06	0.039	0.0307
8.95	0.126	0.0299
10.11	0.212	0.0295
11.07	0.279	0.0297
12.18	0.360	0.0313
13.14	0.421	0.0327
14.09	0.472	0.0379

Run: 06918gw_interp

Re = 199940.9

α	C_l	C_d
-2.17	-0.896	0.0572
-1.08	-0.784	0.0336
-0.04	-0.715	0.0272
0.97	-0.624	0.0241
1.96	-0.428	0.0197
3.05	-0.302	0.0297
4.10	-0.216	0.0283
5.05	-0.156	0.0271
6.08	-0.094	0.0263
7.12	-0.028	0.0242
8.05	0.035	0.0225
9.11	0.124	0.0218
10.11	0.220	0.0207
11.24	0.342	0.0205
12.22	0.452	0.0225
13.28	0.557	0.0265
14.24	0.615	0.0330

Run: 06920gw_interp

Re = 299845.8

α	C_l	C_d
-1.91	-0.930	0.0520
-1.23	-0.872	0.0334
-0.18	-0.784	0.0244
0.82	-0.712	0.0204

1.78	-0.651	0.0171
2.87	-0.429	0.0264
4.03	-0.340	0.0249
4.95	-0.297	0.0217
6.00	-0.245	0.0185
7.04	-0.164	0.0167
8.03	-0.072	0.0158
9.03	0.031	0.0154
10.07	0.132	0.0157
11.11	0.241	0.0163
12.15	0.353	0.0188
13.20	0.473	0.0220
14.18	0.582	0.0290

Run: 06922gw_interp
Re = 399872.3

α	C_l	C_d
-2.03	-0.956	0.0570
-1.21	-0.893	0.0284
-0.09	-0.801	0.0208
0.86	-0.736	0.0176
1.97	-0.653	0.0148
2.94	-0.585	0.0118
3.85	-0.484	0.0167
4.91	-0.385	0.0142
6.01	-0.278	0.0132
7.10	-0.170	0.0127
8.10	-0.067	0.0129
9.13	0.034	0.0129
10.16	0.148	0.0134
11.10	0.242	0.0143
12.11	0.356	0.0164
13.21	0.478	0.0198
14.27	0.590	0.0268

Run: 06924gw_interp
Re = 499695.7

α	C_l	C_d
-1.08	-0.887	0.0224
-0.19	-0.822	0.0190
0.96	-0.733	0.0157
1.97	-0.651	0.0137
3.06	-0.560	0.0115
3.93	-0.493	0.0118
5.01	-0.385	0.0113
6.10	-0.274	0.0110
6.98	-0.183	0.0110
8.00	-0.075	0.0110
9.09	0.039	0.0115
10.11	0.149	0.0122
11.10	0.253	0.0133
12.24	0.378	0.0152
13.18	0.484	0.0180
14.28	0.607	0.0235

AG40d-02r fn15

Fig. 6.46

Run: 06834gw_interp
Re = 99936.9

α	C_l	C_d
-3.05	-0.702	0.0428
-1.84	-0.607	0.0271
-1.16	-0.554	0.0231
0.05	-0.474	0.0163
1.08	-0.402	0.0194
2.29	-0.255	0.0226
2.94	-0.211	0.0231
4.09	-0.130	0.0251
5.00	-0.079	0.0262
6.24	-0.000	0.0220
7.19	0.079	0.0204
8.13	0.167	0.0194
9.24	0.274	0.0194
10.09	0.355	0.0205
11.34	0.478	0.0242
12.22	0.550	0.0277

Run: 06836gw_interp
Re = 200255.7

α	C_l	C_d
-3.14	-0.796	0.0518
-2.27	-0.726	0.0285
-1.11	-0.631	0.0211
-0.08	-0.546	0.0175
0.89	-0.468	0.0151
1.90	-0.407	0.0173
2.97	-0.306	0.0160
4.01	-0.204	0.0148
5.06	-0.106	0.0141
5.93	-0.025	0.0138
7.03	0.085	0.0137
8.08	0.197	0.0139
9.10	0.305	0.0146
10.13	0.421	0.0159
11.10	0.523	0.0190
12.16	0.621	0.0237

Run: 06838gw_interp
Re = 299156.9

α	C_l	C_d
-3.14	-0.823	0.0523
-2.11	-0.736	0.0256
-1.17	-0.658	0.0198
-0.01	-0.560	0.0165
0.92	-0.484	0.0138
1.87	-0.424	0.0121
2.90	-0.322	0.0118
3.93	-0.218	0.0113
4.92	-0.117	0.0109
5.95	-0.012	0.0112
7.07	0.104	0.0115
8.00	0.201	0.0119
9.06	0.312	0.0126
10.06	0.420	0.0139
11.14	0.533	0.0170
12.18	0.642	0.0205
13.25	0.724	0.0289

Run: 06840gw_interp
Re = 400030.0

α	C_l	C_d
-1.89	-0.736	0.0217
-1.12	-0.674	0.0178
-0.05	-0.582	0.0145
0.95	-0.498	0.0123
2.07	-0.407	0.0097
2.91	-0.326	0.0098
3.99	-0.221	0.0096
5.02	-0.107	0.0094
6.06	-0.005	0.0098
7.05	0.102	0.0102
8.12	0.213	0.0108
9.07	0.319	0.0115
10.24	0.445	0.0129
11.15	0.541	0.0151
12.18	0.646	0.0187
13.31	0.740	0.0255

Run: 06842gw_interp
Re = 500304.7

α	C_l	C_d
-1.98	-0.751	0.0189
-1.05	-0.667	0.0157
-0.19	-0.593	0.0137
0.94	-0.493	0.0116
2.01	-0.398	0.0091
3.05	-0.307	0.0087
4.00	-0.207	0.0085
5.07	-0.101	0.0085
6.08	0.007	0.0088
7.07	0.109	0.0093
8.09	0.218	0.0100
9.17	0.338	0.0108
10.19	0.448	0.0121
11.17	0.549	0.0143
12.19	0.657	0.0177
13.25	0.758	0.0234

AG40d-02r fn10
Fig. 6.49

Run: 06844gw_interp
Re = 100010.7

α	C_l	C_d
-4.17	-0.632	0.0461
-3.09	-0.546	0.0274
-2.12	-0.467	0.0208
-1.11	-0.383	0.0157
-0.04	-0.301	0.0114
1.02	-0.147	0.0145
1.93	-0.045	0.0141
3.04	0.053	0.0166
3.93	0.134	0.0179
5.05	0.250	0.0178
5.95	0.341	0.0177
7.06	0.452	0.0165
8.12	0.542	0.0175
9.13	0.627	0.0193
10.22	0.709	0.0235
11.13	0.766	0.0301

Run: 06846ga_interp
Re = 199900.8

α	C_l	C_d
-4.19	-0.669	0.0475
-3.07	-0.572	0.0225
-2.08	-0.483	0.0170
-1.15	-0.401	0.0143
-0.04	-0.307	0.0109
1.00	-0.230	0.0115
1.92	-0.149	0.0117
2.90	-0.056	0.0112
4.03	0.060	0.0110
5.03	0.164	0.0112
6.03	0.271	0.0112
7.08	0.379	0.0120
8.03	0.485	0.0133
9.11	0.602	0.0147
10.16	0.703	0.0185
11.16	0.781	0.0241

Run: 06848ga_interp
Re = 299567.2

α	C_l	C_d
-3.08	-0.586	0.0207
-2.12	-0.495	0.0156
-1.07	-0.404	0.0134
-0.04	-0.312	0.0115
0.97	-0.231	0.0094
1.95	-0.136	0.0091
3.07	-0.026	0.0090
4.08	0.080	0.0088
5.09	0.187	0.0090
6.04	0.288	0.0097
7.05	0.395	0.0106
8.17	0.509	0.0112
9.09	0.602	0.0126
10.12	0.704	0.0161
11.16	0.801	0.0210
12.14	0.874	0.0289

Run: 06850gw_interp
Re = 399642.1

α	C_l	C_d
-3.14	-0.589	0.0185
-2.21	-0.504	0.0147
-1.12	-0.402	0.0127
-0.08	-0.295	0.0108
0.88	-0.216	0.0080
2.00	-0.112	0.0080
2.95	-0.015	0.0079
4.01	0.093	0.0078
5.00	0.197	0.0083
5.96	0.295	0.0090
7.03	0.411	0.0098
8.12	0.524	0.0108
9.17	0.639	0.0125
10.17	0.736	0.0154
11.23	0.830	0.0193
12.17	0.898	0.0260

Run: 06852gw_interp
Re = 499080.9

α	C_l	C_d
-3.18	-0.612	0.0170
-2.24	-0.519	0.0140
-1.07	-0.410	0.0117
-0.03	-0.305	0.0099
0.81	-0.227	0.0083
1.97	-0.123	0.0073
2.97	-0.020	0.0073
3.93	0.075	0.0074
4.92	0.186	0.0079
6.09	0.306	0.0085
7.07	0.410	0.0093
8.07	0.513	0.0103
9.17	0.634	0.0121
10.22	0.730	0.0149
11.21	0.830	0.0180
12.17	0.902	0.0232

AG40d-02r fn5
Fig. 6.52

Run: 06854gw_interp
Re = 100020.6

α	C_l	C_d
-4.07	-0.417	0.0235
-3.10	-0.336	0.0182
-2.20	-0.261	0.0140
-1.10	-0.154	0.0106
-0.13	-0.035	0.0114
0.87	0.096	0.0119
1.93	0.194	0.0133
2.97	0.277	0.0151
3.95	0.362	0.0162
5.04	0.459	0.0166
6.14	0.557	0.0165
7.08	0.640	0.0185
8.11	0.724	0.0209
9.04	0.784	0.0260
10.16	0.852	0.0362
11.16	0.895	0.0470

Run: 06856gw_interp
Re = 199972.3

α	C_l	C_d
-5.26	-0.513	0.0398
-4.15	-0.413	0.0202
-3.11	-0.317	0.0144
-2.20	-0.225	0.0115
-1.07	-0.114	0.0085
-0.07	-0.011	0.0087
0.87	0.095	0.0088
1.99	0.200	0.0098
2.95	0.296	0.0101
4.05	0.404	0.0103
5.10	0.512	0.0109
6.12	0.613	0.0122
7.09	0.706	0.0136
8.10	0.787	0.0165
9.16	0.866	0.0209
10.12	0.940	0.0264
11.14	0.983	0.0349

Run: 06858gw_interp
Re = 299742.0

α	C_l	C_d
-5.35	-0.522	0.0433
-4.26	-0.417	0.0175
-3.15	-0.310	0.0130
-2.15	-0.205	0.0106
-1.15	-0.111	0.0091

-0.10	-0.026	0.0074
0.85	0.097	0.0081
1.94	0.199	0.0080
2.83	0.288	0.0081
4.02	0.411	0.0085
5.03	0.512	0.0094
5.96	0.603	0.0104
7.06	0.710	0.0118
8.02	0.804	0.0143
9.18	0.901	0.0183
10.13	0.967	0.0233
11.24	1.020	0.0325

Run: 06860gw_interp
Re = 399771.9

α	C_l	C_d
-5.33	-0.528	0.0447
-4.24	-0.433	0.0153
-3.26	-0.332	0.0120
-2.24	-0.228	0.0103
-1.11	-0.119	0.0088
-0.08	-0.023	0.0069
0.88	0.069	0.0071
1.94	0.199	0.0069
2.91	0.304	0.0072
3.95	0.408	0.0078
5.02	0.514	0.0087
5.94	0.608	0.0096
7.10	0.724	0.0113
8.05	0.805	0.0134
9.21	0.917	0.0168
9.99	0.979	0.0202
11.11	1.038	0.0273

AG40d-02r fp5
Fig. 6.55

Run: 06882gw_interp
Re = 99914.3

α	C_l	C_d
-7.21	-0.205	0.0374
-6.22	-0.127	0.0243
-5.23	-0.019	0.0202
-4.19	0.093	0.0174
-3.10	0.204	0.0159
-2.12	0.284	0.0165
-1.01	0.394	0.0172
-0.05	0.486	0.0187
0.93	0.604	0.0212
2.01	0.735	0.0163
2.98	0.819	0.0148
3.96	0.890	0.0176
5.07	0.972	0.0200
6.05	1.032	0.0240
7.03	1.072	0.0307
8.15	1.118	0.0407

Run: 06884gw_interp
Re = 200045.5

α	C_l	C_d
-7.25	-0.128	0.0250
-6.34	-0.039	0.0170
-5.22	0.075	0.0136
-4.12	0.180	0.0120
-3.18	0.279	0.0123
-2.10	0.387	0.0124
-1.08	0.488	0.0120
-0.08	0.594	0.0129
0.98	0.700	0.0114
2.03	0.796	0.0105
3.08	0.884	0.0121
3.95	0.951	0.0138
5.05	1.036	0.0164
5.99	1.099	0.0211
7.05	1.153	0.0263
8.05	1.199	0.0321

Run: 06886gw_interp
Re = 299606.8

α	C_l	C_d
-8.27	-0.284	0.0653
-7.14	-0.122	0.0188
-6.18	-0.022	0.0134
-5.10	0.086	0.0112
-4.13	0.184	0.0101
-3.01	0.306	0.0095
-2.19	0.391	0.0096
-1.07	0.509	0.0104
-0.08	0.606	0.0090
1.01	0.707	0.0086
1.88	0.790	0.0088
3.03	0.887	0.0108
4.06	0.978	0.0128
4.99	1.055	0.0151
6.17	1.137	0.0194
7.15	1.190	0.0234
8.09	1.235	0.0300

Run: 06888gw_interp
Re = 399192.4

α	C_l	C_d
-7.13	-0.125	0.0160
-6.28	-0.044	0.0119
-5.20	0.074	0.0100
-4.21	0.177	0.0090
-3.13	0.289	0.0084
-1.96	0.419	0.0084
-1.08	0.514	0.0088
-0.05	0.615	0.0080
1.04	0.719	0.0074
1.90	0.794	0.0089
2.98	0.898	0.0105
4.09	0.991	0.0123
5.13	1.071	0.0151
6.02	1.134	0.0178
7.17	1.205	0.0221
8.12	1.251	0.0271

Run: 06890gw_interp
Re = 499053.7

α	C_l	C_d
-7.22	-0.141	0.0141
-6.11	-0.024	0.0109
-5.10	0.082	0.0094
-4.03	0.194	0.0083
-2.96	0.308	0.0076
-1.93	0.425	0.0077
-1.14	0.504	0.0075
-0.10	0.613	0.0072
0.90	0.704	0.0078
2.11	0.811	0.0091
3.13	0.909	0.0104
3.95	0.978	0.0119
5.10	1.073	0.0146
6.17	1.140	0.0176
7.05	1.199	0.0208
8.09	1.253	0.0254

AG40d-02r fp10
Fig. 6.58

Run: 06872ga_interp
Re = 99795.6

α	C_l	C_d
-9.32	-0.165	0.0765
-8.26	-0.022	0.0351
-7.16	0.096	0.0256
-6.11	0.198	0.0227
-5.16	0.286	0.0212
-4.19	0.365	0.0222
-3.09	0.441	0.0244
-2.06	0.509	0.0252
-1.05	0.564	0.0265
-0.01	0.660	0.0296
1.03	0.808	0.0289
1.96	0.961	0.0226
3.05	1.044	0.0188

4.05	1.112	0.0220
5.12	1.152	0.0279
6.12	1.167	0.0357
7.13	1.203	0.0435
8.05	1.227	0.0530
9.08	1.241	0.0678

Run: 06874gw_interp
Re = 199968.2

α	C_l	C_d
-8.27	0.030	0.0236
-7.17	0.141	0.0171
-6.21	0.240	0.0148
-5.16	0.356	0.0142
-4.21	0.453	0.0150
-3.04	0.555	0.0172
-2.04	0.615	0.0223
-1.16	0.675	0.0230
-0.11	0.776	0.0226
0.99	0.949	0.0174
1.88	1.042	0.0126
3.06	1.110	0.0159
4.12	1.173	0.0192
5.10	1.216	0.0251
5.95	1.248	0.0304
7.17	1.281	0.0381
8.14	1.312	0.0481

Run: 06876ga_interp
Re = 304588.0

α	C_l	C_d
-9.25	-0.131	0.0641
-8.28	0.036	0.0183
-7.20	0.148	0.0137
-6.21	0.252	0.0121
-5.25	0.360	0.0115
-4.12	0.476	0.0115
-3.15	0.581	0.0126
-2.00	0.693	0.0153
-1.00	0.787	0.0162
0.03	0.896	0.0133
0.97	0.988	0.0104
2.04	1.057	0.0124
3.10	1.133	0.0151
4.13	1.194	0.0185
5.03	1.237	0.0224
6.12	1.283	0.0278
7.15	1.311	0.0350
7.98	1.340	0.0424

Run: 06878gw_interp
Re = 399910.9

α	C_l	C_d
-9.20	-0.105	0.0551
-8.26	0.038	0.0147
-7.24	0.149	0.0116
-6.13	0.270	0.0099
-5.10	0.384	0.0091
-4.10	0.485	0.0088
-3.10	0.600	0.0096
-2.07	0.707	0.0105
-1.06	0.809	0.0117
-0.09	0.912	0.0107
1.02	0.991	0.0112
1.96	1.058	0.0129
2.98	1.132	0.0149
4.09	1.194	0.0183
4.99	1.244	0.0220
5.96	1.293	0.0266
7.08	1.332	0.0325
8.11	1.364	0.0400

Run: 06880gw_interp
Re = 499894.6

α	C_l	C_d
-8.23	0.052	0.0130
-7.17	0.169	0.0105
-6.04	0.287	0.0091
-5.18	0.384	0.0083
-4.15	0.496	0.0080
-3.02	0.618	0.0077
-1.99	0.724	0.0080
-1.07	0.811	0.0084
0.01	0.920	0.0092
1.12	0.995	0.0117
2.15	1.076	0.0136
3.13	1.143	0.0157
4.10	1.197	0.0186
5.09	1.247	0.0221
6.05	1.300	0.0259
7.16	1.355	0.0313

AG40d-02r fp15

Fig. 6.61

Run: 06862ga_interp
Re = 100083.9

α	C_l	C_d
-9.49	-0.345	0.1302
-8.35	-0.012	0.0420
-7.20	0.151	0.0356
-6.26	0.264	0.0337
-5.15	0.347	0.0351
-4.19	0.428	0.0365
-3.06	0.506	0.0370
-2.24	0.569	0.0364
-1.12	0.656	0.0368
-0.25	0.721	0.0400
0.89	0.883	0.0428
1.88	1.099	0.0355
2.93	1.215	0.0246
3.96	1.263	0.0296
5.03	1.247	0.0411
6.03	1.270	0.0483
6.89	1.295	0.0569
8.04	1.328	0.0739
9.04	1.368	0.1207

Run: 06864ga_interp
Re = 199529.0

α	C_l	C_d
-9.27	0.144	0.0362
-8.14	0.202	0.0300
-7.31	0.275	0.0273
-6.19	0.381	0.0272
-5.29	0.466	0.0285
-4.25	0.534	0.0302
-3.14	0.599	0.0328
-2.07	0.681	0.0355
-1.11	0.767	0.0367
-0.04	0.917	0.0361
0.93	1.163	0.0256
2.02	1.231	0.0186
3.05	1.268	0.0232
4.04	1.293	0.0297
5.01	1.314	0.0371
6.02	1.338	0.0441
6.98	1.374	0.0523

Run: 06866gw_interp
Re = 300159.5

α	C_l	C_d
-10.27	0.026	0.0525
-9.20	0.211	0.0158
-8.19	0.320	0.0137
-7.11	0.443	0.0119
-6.18	0.543	0.0116
-5.19	0.639	0.0114
-4.12	0.700	0.0213
-3.05	0.780	0.0251
-2.18	0.844	0.0284
-1.13	0.927	0.0312
0.07	1.145	0.0189
1.06	1.198	0.0160
1.88	1.230	0.0192

2.99	1.261	0.0239
3.90	1.288	0.0286
5.04	1.334	0.0352
5.96	1.374	0.0411
7.09	1.413	0.0504
7.99	1.434	0.0605
9.04	1.463	0.1515

Run: 06868gw_interp
Re = 399759.2

α	C_l	C_d
-10.19	0.104	0.0223
-9.18	0.224	0.0135
-8.06	0.351	0.0116
-7.05	0.464	0.0104
-6.04	0.571	0.0098
-5.07	0.677	0.0096
-4.04	0.779	0.0097
-2.95	0.882	0.0104
-1.93	0.970	0.0113
-0.93	1.032	0.0205
0.16	1.152	0.0144
1.15	1.180	0.0181
2.18	1.218	0.0218
3.22	1.252	0.0263
4.15	1.293	0.0308
5.18	1.351	0.0354
6.17	1.394	0.0407
7.21	1.439	0.0483
8.16	1.466	0.0569

Run: 06870gw_interp
Re = 499259.7

α	C_l	C_d
-9.21	0.241	0.0124
-8.17	0.352	0.0106
-7.17	0.463	0.0096
-6.05	0.590	0.0091
-5.03	0.696	0.0088
-4.01	0.802	0.0089
-2.97	0.896	0.0092
-1.90	1.003	0.0097
-0.96	1.074	0.0103
-0.01	1.123	0.0148
1.10	1.156	0.0187
2.10	1.199	0.0226
3.04	1.236	0.0262
4.02	1.291	0.0298
5.12	1.351	0.0342
6.12	1.405	0.0389
7.16	1.453	0.0447

AG40d-02r fp20

Fig. 6.64

Run: 06892ga_interp
Re = 100077.5

α	C_l	C_d
-8.27	0.164	0.0466
-7.18	0.271	0.0454
-6.28	0.353	0.0459
-5.32	0.438	0.0482
-4.20	0.523	0.0517
-3.07	0.614	0.0532
-2.08	0.705	0.0528
-1.08	0.783	0.0543
-0.17	0.853	0.0541
0.84	0.983	0.0606
1.99	1.193	0.0419
2.95	1.300	0.0374
3.94	1.308	0.0467
4.93	1.312	0.0573
6.07	1.356	0.0647
6.95	1.389	0.0751
8.02	1.423	0.1002

Run: 06894ga_interp
Re = 199902.6

α	C_l	C_d
-9.33	0.264	0.0391
-8.27	0.360	0.0372
-7.15	0.458	0.0383
-6.17	0.527	0.0396
-5.27	0.572	0.0409
-4.20	0.644	0.0443
-3.24	0.708	0.0474
-2.23	0.789	0.0497
-1.23	0.839	0.0475
-0.04	1.005	0.0491
0.92	1.243	0.0349
2.03	1.287	0.0319
2.94	1.304	0.0389
4.03	1.332	0.0472
4.93	1.362	0.0530
6.07	1.418	0.0616

Run: 06896gw_interp
Re = 299482.0

α	C_l	C_d
-10.28	0.362	0.0161
-9.14	0.489	0.0142
-8.14	0.595	0.0135
-7.17	0.689	0.0135
-6.10	0.691	0.0285
-5.12	0.766	0.0329
-4.15	0.771	0.0393
-3.03	0.805	0.0452
-2.08	0.856	0.0462
-1.10	0.960	0.0462
-0.01	1.202	0.0375
1.00	1.247	0.0288
1.90	1.275	0.0336
3.08	1.310	0.0405
4.07	1.361	0.0457
4.97	1.404	0.0506
6.05	1.454	0.0581

Run: 06898gw_interp
Re = 399591.3

α	C_l	C_d
-10.15	0.396	0.0140
-9.17	0.506	0.0128
-8.10	0.625	0.0120
-7.19	0.714	0.0115
-6.16	0.820	0.0114
-5.05	0.925	0.0119
-3.95	1.000	0.0126
-2.98	0.913	0.0378
-2.08	0.969	0.0413
-0.94	1.152	0.0362
-0.02	1.192	0.0268
0.95	1.218	0.0309
1.90	1.259	0.0358
2.99	1.313	0.0409
3.93	1.363	0.0454
5.04	1.425	0.0508
6.13	1.474	0.0576

AG40d-02r fp25

Fig. 6.67

Run: 06900gw_interp
Re = 99904.2

α	C_l	C_d
-8.28	0.325	0.0624
-7.14	0.432	0.0640
-6.27	0.514	0.0660
-5.23	0.591	0.0550
-4.07	0.669	0.0716
-3.08	0.745	0.0712
-2.19	0.835	0.0686
-1.08	0.920	0.0691
-0.06	0.947	0.0709
0.93	1.142	0.0720
2.02	1.310	0.0514
3.05	1.323	0.0631

4.03	1.332	0.0690
5.04	1.371	0.0766
5.92	1.416	0.0835

Run: 06902gw_interp
Re = 200268.6

α	C_l	C_d
-9.29	0.255	0.0576
-8.26	0.356	0.0570
-7.23	0.465	0.0584
-6.16	0.561	0.0598
-5.28	0.649	0.0618
-4.16	0.730	0.0652
-3.07	0.828	0.0684
-2.15	0.890	0.0700
-1.13	0.929	0.0645
-0.08	1.092	0.0633
0.88	1.277	0.0518
1.95	1.284	0.0603
2.91	1.318	0.0644
3.86	1.370	0.0695
4.92	1.418	0.0761
5.79	1.458	0.0833

Run: 06904gw_interp
Re = 300752.0

α	C_l	C_d
-9.13	0.393	0.0474
-8.25	0.516	0.0469
-7.11	0.519	0.0495
-6.23	0.575	0.0540
-5.25	0.660	0.0563
-4.14	0.754	0.0588
-3.13	0.845	0.0605
-2.05	0.905	0.0582
-1.04	1.036	0.0586
0.02	1.258	0.0495
0.92	1.258	0.0522
1.98	1.294	0.0575
3.04	1.350	0.0639
4.09	1.415	0.0688
5.08	1.468	0.0741
6.11	1.523	0.0802

Run: 06906gw_interp
Re = 400126.2

α	C_l	C_d
-6.04	0.654	0.0479
-5.09	0.701	0.0497
-4.05	0.777	0.0551
-3.02	0.852	0.0546
-2.06	0.969	0.0564
-1.01	1.219	0.0548
-0.05	1.222	0.0470
0.99	1.256	0.0536
2.06	1.319	0.0596
3.04	1.385	0.0650
3.95	1.434	0.0680
4.99	1.494	0.0733
6.12	1.571	0.0802

AG455ct-02r fn0.4

Fig. 6.75

Run: 06724gw_interp
Re = 99989.3

α	C_l	C_d
-5.13	-0.327	0.0348
-4.14	-0.223	0.0225
-3.20	-0.138	0.0171
-2.10	-0.044	0.0112
-1.12	0.036	0.0094
-0.06	0.142	0.0100
0.95	0.264	0.0112
1.95	0.389	0.0111
3.41	0.500	0.0120
3.97	0.551	0.0134
5.03	0.639	0.0152
6.03	0.722	0.0182
7.02	0.797	0.0204
8.18	0.877	0.0251
9.13	0.945	0.0320

Run: 06726gw_interp
Re = 199803.2

α	C_l	C_d
-5.11	-0.309	0.0347
-4.18	-0.215	0.0190
-3.24	-0.124	0.0137
-2.09	-0.014	0.0099
-1.12	0.069	0.0077
-0.17	0.135	0.0077
1.04	0.281	0.0075
1.94	0.372	0.0082
2.95	0.473	0.0090
4.04	0.688	0.0125
5.07	0.789	0.0144
6.03	0.872	0.0169
7.10	0.963	0.0202
8.07	1.030	0.0260
9.13	1.098	0.0349

Run: 06728gw_interp
Re = 300280.5

α	C_l	C_d
-5.25	-0.270	0.0248
-4.11	-0.156	0.0133
-3.23	-0.073	0.0104
-2.07	0.033	0.0083
-1.05	0.102	0.0072
-0.02	0.226	0.0062
0.99	0.342	0.0071
2.02	0.448	0.0081
3.01	0.548	0.0091
4.05	0.647	0.0102
5.04	0.747	0.0118
6.08	0.849	0.0135
7.09	0.940	0.0160
8.18	1.027	0.0200
9.15	1.086	0.0260

Run: 06732ga_interp
Re = 400350.5

α	C_l	C_d
-4.16	-0.160	0.0121
-3.12	-0.062	0.0092
-2.48	0.003	0.0079
-1.06	0.117	0.0066
-0.08	0.229	0.0056
1.02	0.337	0.0067
2.04	0.444	0.0075
3.06	0.545	0.0085
4.09	0.645	0.0095
5.05	0.743	0.0108
6.19	0.855	0.0127
7.18	0.946	0.0147

Run: 06730gw_interp
Re = 499662.2

α	C_l	C_d
-4.31	-0.164	0.0114
-3.14	-0.048	0.0086
-1.97	0.067	0.0076
-1.06	0.140	0.0064
-0.10	0.233	0.0054
1.08	0.345	0.0064
1.96	0.435	0.0071
2.94	0.533	0.0080
4.00	0.644	0.0089
5.18	0.751	0.0102
6.18	0.849	0.0119
7.11	0.938	0.0136

AG455ct-02r fn20.4

Fig. 6.78

Run: 06818gw_interp

Re = 99905.9

α	C_l	C_d
-2.17	-1.011	0.0785
-1.21	-0.933	0.0580
-0.07	-0.825	0.0412
0.89	-0.744	0.0325
1.98	-0.638	0.0282
2.89	-0.479	0.0349
3.90	-0.397	0.0357
5.00	-0.288	0.0362
6.01	-0.254	0.0343
7.08	-0.187	0.0331
8.05	-0.127	0.0309
9.01	-0.080	0.0281
10.11	0.012	0.0265
11.15	0.114	0.0274
12.18	0.211	0.0297
13.15	0.315	0.0323

Run: 06819gw_interp

Re = 199775.1

α	C_l	C_d
-2.01	-1.033	0.0761
-1.18	-0.966	0.0601
-0.20	-0.879	0.0425
0.92	-0.788	0.0294
1.89	-0.710	0.0245
2.94	-0.639	0.0206
3.91	-0.521	0.0288
4.92	-0.439	0.0252
6.02	-0.346	0.0225
7.05	-0.251	0.0206
8.12	-0.148	0.0195
9.15	-0.044	0.0190
10.05	0.041	0.0190
11.42	0.166	0.0196
12.17	0.247	0.0209
13.15	0.343	0.0226

Run: 06820ga_interp

Re = 299633.4

α	C_l	C_d
-2.00	-1.038	0.0762
-1.16	-0.976	0.0602
-0.07	-0.889	0.0414
0.87	-0.814	0.0271
1.82	-0.730	0.0208
2.83	-0.660	0.0173
3.89	-0.583	0.0188
4.92	-0.483	0.0166
5.97	-0.378	0.0155
6.93	-0.286	0.0150
8.01	-0.176	0.0149
9.08	-0.070	0.0149
10.34	0.040	0.0154
11.12	0.108	0.0160
12.09	0.214	0.0173
13.10	0.325	0.0191
14.15	0.449	0.0240

Run: 06821gw_interp

Re = 398796.0

α	C_l	C_d
-1.97	-1.040	0.0766
-1.16	-0.987	0.0594
-0.09	-0.905	0.0412
0.96	-0.812	0.0241
1.98	-0.728	0.0180
3.04	-0.646	0.0148
3.85	-0.582	0.0119
5.05	-0.477	0.0132
5.91	-0.386	0.0130
7.01	-0.274	0.0125
7.99	-0.176	0.0124
9.09	-0.070	0.0129
10.35	0.049	0.0134
11.16	0.115	0.0140
12.12	0.217	0.0153
13.12	0.330	0.0172
14.21	0.451	0.0220

Run: 06822gw_interp

Re = 499548.5

α	C_l	C_d
0.12	-0.877	0.0370
0.90	-0.817	0.0232
1.83	-0.745	0.0169
2.86	-0.662	0.0141
4.02	-0.571	0.0109
4.93	-0.493	0.0114
6.01	-0.380	0.0111
6.98	-0.278	0.0110
8.09	-0.171	0.0111
9.07	-0.068	0.0116
10.29	0.043	0.0122
11.15	0.117	0.0129
12.15	0.218	0.0140
13.17	0.333	0.0158
14.19	0.444	0.0196

AG455ct-02r fn15.4

Fig. 6.81

Run: 06734gw_interp

Re = 100005.3

α	C_l	C_d
-2.12	-0.809	0.0498
-1.20	-0.736	0.0344
-0.11	-0.639	0.0248
0.85	-0.563	0.0198
1.92	-0.519	0.0199
2.88	-0.439	0.0225
3.91	-0.345	0.0227
4.92	-0.251	0.0228
6.04	-0.149	0.0225
7.04	-0.049	0.0211
7.99	0.052	0.0209
9.07	0.164	0.0212
10.11	0.276	0.0224
11.29	0.382	0.0259
12.42	0.472	0.0302
13.27	0.525	0.0371

Run: 06736gw_interp

Re = 200034.0

α	C_l	C_d
-2.13	-0.839	0.0522
-1.22	-0.752	0.0363
-0.08	-0.653	0.0233
0.86	-0.572	0.0198
1.90	-0.489	0.0154
2.97	-0.414	0.0166
3.98	-0.311	0.0158
5.04	-0.213	0.0147
5.98	-0.124	0.0144
7.02	-0.021	0.0144
8.41	0.097	0.0152
9.08	0.155	0.0155
10.08	0.264	0.0168
11.17	0.376	0.0185
12.13	0.469	0.0214
13.22	0.591	0.0280

Run: 06738rd_interp

Re = 300010.4

α	C_l	C_d
-1.10	-0.766	0.0353
-0.16	-0.674	0.0226
0.93	-0.589	0.0172
1.99	-0.497	0.0135
2.87	-0.435	0.0124
3.91	-0.329	0.0119

4.96	-0.223	0.0116
6.02	-0.117	0.0117
7.01	-0.014	0.0118
8.32	0.077	0.0124
9.09	0.151	0.0130
10.08	0.264	0.0140
11.08	0.375	0.0156
12.16	0.482	0.0181
13.16	0.587	0.0236

Run: 06740gw_interp
Re = 399112.4

α	C_l	C_d
0.04	-0.659	0.0190
1.00	-0.576	0.0150
1.88	-0.497	0.0128
2.97	-0.410	0.0103
3.97	-0.312	0.0103
5.08	-0.197	0.0101
6.00	-0.104	0.0101
7.12	0.004	0.0106
8.10	0.053	0.0108
9.18	0.179	0.0116
10.19	0.287	0.0126
11.14	0.379	0.0141
12.18	0.489	0.0162

Run: 06742gw_interp
Re = 499329.7

α	C_l	C_d
0.09	-0.653	0.0168
0.95	-0.580	0.0138
1.87	-0.499	0.0118
2.87	-0.420	0.0092
4.02	-0.312	0.0091
5.04	-0.208	0.0092
6.09	-0.102	0.0092
7.09	-0.007	0.0097
8.11	0.045	0.0100
9.16	0.168	0.0107
10.16	0.270	0.0115
11.20	0.378	0.0130
12.09	0.465	0.0145

AG455ct-02r fn10.4

Fig. 6.84

Run: 06744gw_interp
Re = 100098.2

α	C_l	C_d
-3.25	-0.668	0.0414
-2.14	-0.570	0.0272
-1.06	-0.478	0.0187
-0.14	-0.404	0.0138
0.95	-0.334	0.0134
1.86	-0.247	0.0141
2.97	-0.138	0.0161
3.97	-0.040	0.0169
5.11	0.087	0.0154
6.03	0.196	0.0164
6.97	0.307	0.0165
8.21	0.432	0.0181
9.53	0.530	0.0219
10.27	0.592	0.0244
11.08	0.665	0.0285
12.08	0.733	0.0417

Run: 06746gw_interp
Re = 199975.9

α	C_l	C_d
-3.19	-0.666	0.0438
-2.16	-0.566	0.0247
-1.13	-0.475	0.0173
-0.05	-0.377	0.0139
0.89	-0.307	0.0112
2.02	-0.207	0.0125
2.96	-0.106	0.0121
4.05	0.003	0.0115
4.94	0.088	0.0115
6.15	0.173	0.0117
7.10	0.261	0.0123
8.09	0.359	0.0132
9.07	0.462	0.0148
10.15	0.582	0.0176
11.20	0.697	0.0222
12.17	0.784	0.0301

Run: 06748gw_interp
Re = 299755.7

α	C_l	C_d
-3.14	-0.661	0.0432
-2.17	-0.562	0.0247
-1.16	-0.469	0.0167
-0.13	-0.372	0.0135
0.98	-0.280	0.0101
2.01	-0.189	0.0098
2.95	-0.097	0.0097
3.92	-0.002	0.0097
4.99	0.066	0.0099
6.01	0.167	0.0101
7.01	0.281	0.0112
8.07	0.391	0.0121
9.13	0.507	0.0133
10.05	0.597	0.0152
11.16	0.713	0.0190
12.15	0.797	0.0253

Run: 06750gw_interp
Re = 400039.9

α	C_l	C_d
-1.18	-0.479	0.0157
-0.09	-0.378	0.0122
0.95	-0.285	0.0096
1.91	-0.199	0.0084
2.85	-0.107	0.0083
4.05	0.005	0.0087
4.97	0.059	0.0088
5.93	0.172	0.0091
7.05	0.284	0.0102
8.13	0.403	0.0111
9.16	0.504	0.0122
10.10	0.604	0.0140
11.09	0.697	0.0172

Run: 06752gw_interp
Re = 499978.9

α	C_l	C_d
-0.89	-0.452	0.0135
-0.09	-0.377	0.0113
1.01	-0.273	0.0091
2.02	-0.182	0.0076
3.01	-0.086	0.0077
3.99	0.008	0.0079
5.07	0.069	0.0082
6.08	0.190	0.0087
6.99	0.276	0.0093
8.08	0.386	0.0103
9.08	0.494	0.0114
10.16	0.600	0.0130
11.08	0.691	0.0158

AG455ct-02r fn5.4

Fig. 6.87

Run: 06754ga_interp
Re = 99982.9

α	C_l	C_d
-4.07	-0.452	0.0350
-3.10	-0.357	0.0231
-2.13	-0.270	0.0168
-1.09	-0.192	0.0107
-0.06	-0.062	0.0093
0.95	0.041	0.0095
1.91	0.138	0.0115
3.09	0.248	0.0137
4.13	0.346	0.0151
5.21	0.426	0.0155

6.54	0.534	0.0172
7.14	0.585	0.0181
8.03	0.668	0.0210
9.18	0.763	0.0255
10.17	0.833	0.0326

Run: 06756ga_interp
Re = 199784.3

α	C_l	C_d
-4.28	-0.480	0.0371
-3.15	-0.366	0.0189
-2.09	-0.264	0.0132
-1.05	-0.163	0.0098
-0.06	-0.064	0.0077
0.91	0.044	0.0088
1.96	0.122	0.0092
2.96	0.207	0.0096
3.90	0.299	0.0097
4.97	0.413	0.0107
6.02	0.518	0.0117
7.05	0.625	0.0135
8.16	0.727	0.0168
9.12	0.811	0.0203
10.10	0.890	0.0255

Run: 06758gw_interp
Re = 299892.1

α	C_l	C_d
-4.12	-0.458	0.0321
-3.29	-0.370	0.0175
-2.17	-0.264	0.0114
-1.13	-0.166	0.0097
-0.12	-0.080	0.0072
0.98	0.033	0.0083
1.90	0.088	0.0080
2.91	0.189	0.0082
4.05	0.313	0.0087
5.01	0.419	0.0095
6.08	0.527	0.0107
7.09	0.628	0.0121
8.06	0.723	0.0139
9.15	0.824	0.0167
10.15	0.910	0.0219

Run: 06760gw_interp
Re = 400204.0

α	C_l	C_d
-3.19	-0.361	0.0156
-2.17	-0.259	0.0112
-1.15	-0.160	0.0096
-0.13	-0.068	0.0073
1.30	0.045	0.0067
1.97	0.085	0.0070
3.02	0.209	0.0072
3.92	0.302	0.0078
4.96	0.411	0.0085
5.98	0.513	0.0095
6.94	0.606	0.0106
8.18	0.726	0.0128
9.23	0.832	0.0154
10.18	0.918	0.0192

Run: 06762gw_interp
Re = 499686.1

α	C_l	C_d
-4.21	-0.457	0.0317
-3.22	-0.357	0.0141
-2.09	-0.246	0.0108
-1.04	-0.149	0.0093
-0.12	-0.062	0.0076
0.63	-0.016	0.0064
1.97	0.082	0.0064
3.05	0.208	0.0067
3.98	0.307	0.0072
4.98	0.409	0.0081
6.00	0.514	0.0090
7.02	0.616	0.0101
8.08	0.718	0.0119
9.21	0.824	0.0141
10.25	0.917	0.0177

AG455ct-02r fp4.6

Fig. 6.90

Run: 06784gw_interp
Re = 99825.3

α	C_l	C_d
-7.21	-0.254	0.0515
-6.25	-0.090	0.0270
-5.09	0.045	0.0175
-4.04	0.161	0.0146
-3.08	0.245	0.0133
-2.00	0.324	0.0142
-1.04	0.405	0.0157
0.01	0.506	0.0162
1.00	0.648	0.0152
2.03	0.734	0.0139
3.11	0.828	0.0148
4.09	0.900	0.0184
5.04	0.978	0.0219
6.07	1.045	0.0264
7.01	1.100	0.0332
8.16	1.154	0.0446

Run: 06786gw_interp
Re = 200308.1

α	C_l	C_d
-7.19	-0.174	0.0402
-6.23	-0.033	0.0189
-5.16	0.082	0.0136
-3.94	0.177	0.0110
-3.06	0.256	0.0099
-2.05	0.356	0.0098
-1.08	0.456	0.0095
-0.05	0.570	0.0099
1.01	0.673	0.0093
1.96	0.759	0.0104
3.11	0.855	0.0129
4.07	0.941	0.0153
5.15	1.029	0.0183
6.14	1.102	0.0217
7.20	1.163	0.0277
8.10	1.209	0.0351

Run: 06788gw_interp
Re = 299835.0

α	C_l	C_d
-7.28	-0.160	0.0374
-6.15	-0.012	0.0151
-5.59	0.025	0.0124
-4.06	0.156	0.0100
-3.12	0.253	0.0087
-2.03	0.383	0.0084
-1.00	0.483	0.0080
-0.03	0.583	0.0080
0.93	0.671	0.0080
1.96	0.766	0.0099
3.12	0.864	0.0119
4.09	0.958	0.0138
5.06	1.035	0.0160
6.25	1.129	0.0199
7.14	1.191	0.0248
8.16	1.239	0.0316

Run: 06790ga_interp
Re = 399827.8

α	C_l	C_d
-6.24	-0.014	0.0137
-5.26	0.046	0.0111
-4.11	0.160	0.0091
-3.20	0.262	0.0083
-2.06	0.382	0.0076
-0.97	0.494	0.0074
0.07	0.589	0.0069
1.03	0.685	0.0079
2.10	0.780	0.0098
3.12	0.880	0.0113

3.99	0.957	0.0127
5.06	1.047	0.0149
6.11	1.135	0.0178
7.20	1.211	0.0224

Run: 06792ga_interp
Re = 499619.5

α	C_l	C_d
-7.21	-0.111	0.0302
-6.09	0.002	0.0118
-5.23	0.054	0.0106
-4.05	0.176	0.0083
-3.18	0.272	0.0076
-2.07	0.386	0.0069
-0.98	0.495	0.0068
0.06	0.594	0.0066
1.03	0.679	0.0078
2.11	0.787	0.0094
3.08	0.879	0.0106
4.06	0.962	0.0121
5.10	1.057	0.0143
6.04	1.130	0.0164
7.27	1.219	0.0208

AG455ct-02r fp9.6

Fig. 6.93

Run: 06778ga_interp
Re = 100000.3

α	C_l	C_d
-8.21	0.066	0.0330
-7.21	0.169	0.0234
-6.13	0.270	0.0198
-5.14	0.346	0.0190
-3.94	0.424	0.0210
-2.94	0.486	0.0214
-2.02	0.559	0.0211
-0.95	0.646	0.0235
0.07	0.756	0.0257
1.09	0.903	0.0229
2.10	0.985	0.0174
3.02	1.058	0.0211
4.15	1.125	0.0264
5.06	1.165	0.0317
6.16	1.210	0.0407
7.06	1.239	0.0511

Run: 06779ga_interp
Re = 200019.1

α	C_l	C_d
-8.16	0.072	0.0284
-7.24	0.141	0.0197
-6.09	0.259	0.0150
-5.19	0.359	0.0133
-4.05	0.476	0.0134
-3.10	0.582	0.0144
-2.05	0.692	0.0156
-1.04	0.791	0.0170
0.00	0.897	0.0146
1.07	0.982	0.0117
1.98	1.042	0.0149
3.00	1.119	0.0177
4.06	1.196	0.0218
5.09	1.256	0.0269
6.10	1.297	0.0334

Run: 06780gw_interp
Re = 300015.3

α	C_l	C_d
-7.86	0.064	0.0246
-7.17	0.142	0.0167
-6.19	0.249	0.0125
-5.04	0.387	0.0105
-4.14	0.483	0.0102
-3.13	0.587	0.0108
-2.01	0.705	0.0112
-1.04	0.804	0.0116
0.05	0.905	0.0103
1.04	0.981	0.0115
1.97	1.063	0.0137
3.11	1.149	0.0165
4.06	1.214	0.0195
5.09	1.276	0.0235
6.05	1.319	0.0296

Run: 06781gw_interp
Re = 400036.6

α	C_l	C_d
-8.66	0.012	0.0355
-7.19	0.146	0.0143
-6.15	0.270	0.0108
-5.16	0.379	0.0095
-4.07	0.499	0.0089
-3.15	0.592	0.0090
-2.00	0.709	0.0097
-1.04	0.807	0.0098
0.04	0.907	0.0098
1.00	0.986	0.0118
2.01	1.057	0.0134
3.13	1.148	0.0159
4.09	1.214	0.0187
5.05	1.282	0.0221
6.16	1.337	0.0279

Run: 06782gw_interp
Re = 499508.0

α	C_l	C_d
-8.71	-0.044	0.0328
-7.17	0.173	0.0123
-6.12	0.285	0.0097
-5.08	0.399	0.0086
-4.15	0.500	0.0081
-3.05	0.613	0.0081
-2.05	0.716	0.0085
-0.91	0.821	0.0088
-0.13	0.886	0.0102
0.99	0.977	0.0118
2.05	1.069	0.0134
2.98	1.131	0.0151
4.11	1.223	0.0177
5.06	1.279	0.0209
6.05	1.328	0.0252

AG455ct-02r fp14.6

Fig. 6.96

Run: 06764gw_interp
Re = 100064.4

α	C_l	C_d
-10.22	0.025	0.0737
-9.23	0.220	0.0387
-8.24	0.291	0.0335
-7.21	0.358	0.0356
-5.86	0.449	0.0338
-4.87	0.511	0.0349
-3.62	0.571	0.0387
-2.83	0.642	0.0402
-2.11	0.707	0.0384
-1.04	0.781	0.0426
0.04	0.885	0.0459
1.03	1.153	0.0311
2.12	1.260	0.0257
3.12	1.282	0.0315
4.10	1.294	0.0386
5.08	1.317	0.0481
6.08	1.345	0.0593

Run: 06766gw_interp
Re = 200191.1

α	C_l	C_d
-10.29	0.013	0.0655
-9.07	0.219	0.0297
-8.11	0.333	0.0196
-7.08	0.448	0.0167
-6.20	0.547	0.0162
-5.04	0.666	0.0185

-4.07	0.712	0.0263
-3.03	0.789	0.0302
-1.98	0.850	0.0345
-1.05	0.921	0.0362
-0.07	1.149	0.0172
1.13	1.214	0.0183
2.04	1.272	0.0219
3.07	1.312	0.0277
4.15	1.340	0.0351
5.05	1.358	0.0424
6.05	1.379	0.0508

Run: 06768gw_interp
Re = 299912.8

α	C_l	C_d
-10.14	0.068	0.0539
-9.15	0.224	0.0240
-8.20	0.356	0.0147
-7.09	0.487	0.0125
-6.17	0.585	0.0118
-4.98	0.710	0.0120
-4.20	0.791	0.0128
-3.07	0.902	0.0142
-2.01	0.996	0.0155
-0.90	1.100	0.0154
0.04	1.167	0.0149
0.98	1.220	0.0177
2.04	1.272	0.0211
3.14	1.312	0.0260
4.07	1.341	0.0325
5.14	1.381	0.0396
6.08	1.404	0.0475

Run: 06770gw_interp
Re = 399705.1

α	C_l	C_d
-8.11	0.379	0.0123
-7.22	0.480	0.0106
-6.16	0.596	0.0098
-5.11	0.704	0.0097
-4.02	0.815	0.0099
-2.94	0.919	0.0105
-2.01	1.009	0.0110
-0.95	1.107	0.0121
0.07	1.157	0.0157
1.09	1.218	0.0183
2.11	1.276	0.0217
3.06	1.313	0.0258
4.12	1.358	0.0307
5.02	1.389	0.0369

Run: 06772gw_interp
Re = 499715.4

α	C_l	C_d
-8.17	0.402	0.0112
-7.10	0.516	0.0098
-6.14	0.619	0.0090
-4.95	0.744	0.0088
-4.18	0.820	0.0089
-2.98	0.928	0.0094
-2.02	1.014	0.0097
-0.97	1.087	0.0131
0.10	1.154	0.0159
1.04	1.205	0.0180
2.06	1.264	0.0214
3.14	1.309	0.0252

AG455ct-02r fp19.6
Fig. 6.99

Run: 06794rd_interp
Re = 100171.8

α	C_l	C_d
-9.18	0.034	0.0628
-8.24	0.288	0.0496
-7.04	0.403	0.0470
-5.78	0.489	0.0469
-4.76	0.556	0.0507
-4.19	0.595	0.0532
-3.10	0.682	0.0544
-2.07	0.759	0.0541
-1.20	0.831	0.0570
-0.06	0.921	0.0558
1.04	1.318	0.0309
1.99	1.337	0.0357
2.93	1.304	0.0529
4.02	1.302	0.0611
5.02	1.337	0.0670
6.08	1.376	0.0757

Run: 06796gw_interp
Re = 199964.4

α	C_l	C_d
-9.23	0.407	0.0378
-8.20	0.538	0.0351
-7.14	0.637	0.0362
-6.13	0.706	0.0404
-5.17	0.762	0.0446
-4.07	0.818	0.0477
-3.09	0.863	0.0512
-2.02	0.925	0.0546
-1.03	1.008	0.0535
0.09	1.323	0.0246
1.06	1.323	0.0312
2.03	1.336	0.0398
3.05	1.351	0.0485
4.03	1.384	0.0556
5.16	1.426	0.0635
6.05	1.455	0.0720

Run: 06798gw_interp
Re = 300435.6

α	C_l	C_d
-9.20	0.559	0.0144
-8.07	0.688	0.0130
-7.16	0.786	0.0129
-5.97	0.908	0.0134
-5.10	0.982	0.0142
-3.97	1.078	0.0163
-3.05	1.076	0.0361
-2.00	1.104	0.0447
-0.95	1.295	0.0206
-0.08	1.281	0.0256
1.09	1.297	0.0332
2.11	1.326	0.0396
3.04	1.369	0.0451
4.04	1.412	0.0512
5.11	1.450	0.0591
6.08	1.491	0.0680

Run: 06800gw_interp
Re = 400106.5

α	C_l	C_d
-10.13	0.479	0.0142
-9.13	0.597	0.0122
-8.10	0.712	0.0112
-7.05	0.819	0.0112
-6.12	0.902	0.0114
-4.96	1.012	0.0117
-4.15	1.085	0.0123
-2.87	1.197	0.0133
-1.92	1.256	0.0148
-1.10	1.253	0.0219
0.10	1.265	0.0292
1.00	1.284	0.0339
1.95	1.327	0.0389
2.97	1.372	0.0440
4.12	1.432	0.0504
4.97	1.471	0.0563
6.04	1.515	0.0646

AG455ct-02r fp24.6

Fig. 6.102

Run: 06805gw_interp
Re = 100085.4

α	C_l	C_d
-9.10	0.348	0.0681
-8.04	0.437	0.0660
-6.72	0.545	0.0668
-6.19	0.583	0.0689
-5.11	0.674	0.0739
-4.06	0.747	0.0774
-3.05	0.852	0.0777
-2.05	0.942	0.0811
-0.99	1.013	0.0824
-0.02	1.081	0.0736
1.10	1.339	0.0579
2.02	1.320	0.0686
3.17	1.328	0.0813
3.98	1.365	0.0853

Run: 06806gw_interp
Re = 200173.1

α	C_l	C_d
-9.12	0.574	0.0538
-8.18	0.640	0.0545
-7.18	0.712	0.0559
-6.10	0.735	0.0612
-5.14	0.719	0.0650
-4.10	0.805	0.0677
-3.09	0.889	0.0714
-2.07	0.957	0.0700
-1.06	1.067	0.0689
0.05	1.319	0.0524
1.07	1.324	0.0624
2.09	1.338	0.0671
3.04	1.373	0.0716
4.14	1.424	0.0782

Run: 06807gw_interp
Re = 299715.8

α	C_l	C_d
-10.07	0.756	0.0159
-9.05	0.861	0.0156
-8.13	0.946	0.0160
-7.02	0.867	0.0488
-6.04	0.917	0.0541
-4.99	0.948	0.0589
-4.08	0.951	0.0619
-3.07	0.991	0.0671
-2.03	1.039	0.0671
-0.99	1.288	0.0482
0.12	1.304	0.0535
1.12	1.317	0.0589
2.13	1.355	0.0645
3.01	1.408	0.0695
4.13	1.464	0.0767

Run: 06808gw_interp
Re = 400728.7

α	C_l	C_d
-10.00	0.789	0.0141
-9.04	0.877	0.0139
-7.98	0.972	0.0142
-7.07	1.050	0.0147
-5.95	1.135	0.0157
-4.94	1.183	0.0168
-4.11	1.102	0.0569
-3.07	1.136	0.0618
-1.90	1.259	0.0461
-0.88	1.250	0.0486
0.05	1.286	0.0547
0.98	1.325	0.0590
2.14	1.378	0.0637
3.15	1.428	0.0680
4.22	1.495	0.0749

AG455ct-02r fp29.6

Fig. 6.105

Run: 06611ga_interp
Re = 100161.8

α	C_l	C_d
-10.03	-0.002	0.1085
-8.97	0.404	0.0904
-7.90	0.528	0.0894
-6.85	0.611	0.0914
-5.86	0.682	0.0940
-4.83	0.746	0.0977
-3.90	0.810	0.0987
-2.82	0.899	0.1000
-1.80	0.976	0.1017
-0.79	1.027	0.1003
0.26	1.087	0.0917
1.35	1.247	0.0861
2.29	1.275	0.0973
3.30	1.345	0.1054
4.37	1.396	0.1077
5.41	1.426	0.1145

Run: 06613gw_interp
Re = 200224.6

α	C_l	C_d
-9.50	0.407	0.0892
-8.97	0.503	0.0874
-7.86	0.665	0.0856
-6.89	0.742	0.0874
-5.80	0.827	0.0895
-4.80	0.902	0.0907
-3.86	0.966	0.0931
-2.75	1.040	0.0943
-1.76	1.104	0.0869
-0.71	1.237	0.0819
0.31	1.296	0.0914
1.38	1.369	0.0980
2.37	1.430	0.1030
3.36	1.487	0.1068
4.32	1.530	0.1109
5.36	1.554	0.1122

Run: 06811gw_interp
Re = 300110.6

α	C_l	C_d
-10.66	0.352	0.1107
-9.08	0.531	0.0797
-8.16	0.616	0.0812
-7.16	0.707	0.0843
-6.08	0.795	0.0870
-5.10	0.880	0.0912
-4.01	0.972	0.0929
-3.00	1.039	0.0932
-1.94	1.095	0.0861
-0.95	1.258	0.0818
0.04	1.289	0.0898
1.14	1.368	0.0960
1.97	1.424	0.0998
3.06	1.505	0.1039
4.08	1.557	0.1075
5.07	1.598	0.1117

Run: 06812gw_interp
Re = 399801.9

α	C_l	C_d
-8.82	0.564	0.0684
-8.25	0.621	0.0741
-7.11	0.717	0.0748
-6.16	0.806	0.0816
-5.08	0.889	0.0858
-4.13	0.971	0.0895
-3.00	1.063	0.0854
-2.02	1.254	0.0793
-0.99	1.228	0.0801
0.07	1.306	0.0882

1.09	1.380	0.0948
2.16	1.452	0.0998
3.14	1.521	0.1047
4.15	1.584	0.1087

AG455ct-02r fp39.6

Fig. 6.108

Run: 06617gw_interp

Re = 100590.9

α	C_l	C_d
-9.82	0.536	0.1362
-8.80	0.635	0.1386
-7.91	0.706	0.1379
-6.91	0.744	0.1409
-5.90	0.817	0.1402
-4.78	0.893	0.1478
-3.84	0.969	0.1495
-2.84	1.055	0.1500
-1.71	1.116	0.1507
-0.79	1.160	0.1420
0.34	1.289	0.1397
1.25	1.349	0.1512
2.26	1.412	0.1567
3.31	1.456	0.1580

Run: 06619ga_interp

Re = 200664.4

α	C_l	C_d
-9.84	0.665	0.1283
-8.82	0.770	0.1329
-7.86	0.850	0.1306
-6.80	0.935	0.1314
-5.79	1.008	0.1355
-4.75	1.072	0.1388
-3.80	1.133	0.1404
-2.77	1.210	0.1364
-1.71	1.285	0.1419
-0.66	1.367	0.1489
0.26	1.428	0.1507
1.37	1.508	0.1529
2.43	1.571	0.1579
3.46	1.601	0.1611

Run: 06621ga_interp

Re = 300397.1

α	C_l	C_d
-9.86	0.718	0.1220
-8.88	0.813	0.1251
-7.78	0.897	0.1263
-6.87	0.964	0.1288
-5.79	1.049	0.1316
-4.80	1.125	0.1366
-3.87	1.178	0.1361
-2.81	1.244	0.1332
-1.72	1.337	0.1424
-0.74	1.396	0.1464
0.29	1.471	0.1464
1.38	1.545	0.1475
2.39	1.608	0.1502
3.49	1.648	0.1557

W1011 (20%) **fp0**

Fig. 6.112

Run: 07069gw_interp

Re = 100114.9

α	C_l	C_d
-8.22	-0.764	0.0249
-7.29	-0.698	0.0216
-6.15	-0.601	0.0185
-5.31	-0.524	0.0160
-4.23	-0.430	0.0148
-3.08	-0.336	0.0137
-2.23	-0.266	0.0132
-1.09	-0.157	0.0123
-0.01	0.009	0.0127
1.01	0.157	0.0126
1.93	0.242	0.0129
3.02	0.341	0.0155
4.05	0.431	0.0173
5.15	0.535	0.0199
6.16	0.621	0.0230
7.15	0.706	0.0278
8.04	0.769	0.0313
9.20	0.839	0.0373
10.14	0.735	0.1607

Run: 07071sn_interp

Re = 199995.0

α	C_l	C_d
-8.38	-0.801	0.0182
-7.20	-0.704	0.0158
-6.27	-0.615	0.0140
-5.21	-0.513	0.0127
-4.13	-0.398	0.0113
-3.10	-0.299	0.0105
-2.25	-0.217	0.0098
-1.02	-0.066	0.0090
-0.15	0.013	0.0087
1.01	0.133	0.0096
1.99	0.255	0.0101
3.04	0.354	0.0117
3.92	0.440	0.0131
5.13	0.544	0.0149
6.14	0.641	0.0167
7.12	0.733	0.0188
8.18	0.826	0.0218
9.13	0.895	0.0254
10.16	0.961	0.0308
11.21	0.979	0.0383

Run: 07073sn_interp

Re = 399111.7

α	C_l	C_d
-8.23	-0.779	0.0139
-7.19	-0.692	0.0123
-6.19	-0.596	0.0110
-5.17	-0.498	0.0100
-4.15	-0.400	0.0092
-3.15	-0.296	0.0083
-2.07	-0.166	0.0080
-1.04	-0.069	0.0077
-0.06	0.025	0.0076
0.90	0.113	0.0078
2.02	0.233	0.0085
3.11	0.340	0.0094
4.06	0.423	0.0101
5.00	0.515	0.0109
6.10	0.625	0.0122
7.07	0.714	0.0135
8.17	0.816	0.0153
9.19	0.898	0.0179
10.13	0.974	0.0209
11.20	1.042	0.0261

W1011 (20%) **fp5**

Fig. 6.115

Run: 07083gw_interp

Re = 200075.3

α	C_l	C_d
-8.31	-0.591	0.0165
-7.24	-0.483	0.0143
-6.24	-0.381	0.0132
-5.22	-0.264	0.0123
-4.14	-0.149	0.0117
-3.10	-0.047	0.0112
-2.13	0.048	0.0117
-1.22	0.141	0.0115
-0.15	0.259	0.0108
1.00	0.364	0.0103
1.90	0.455	0.0115
3.01	0.557	0.0133
3.95	0.647	0.0151
5.12	0.745	0.0174

6.10	0.834	0.0195
7.13	0.915	0.0226
8.06	0.981	0.0258
9.13	1.051	0.0310
10.12	1.095	0.0376

Run: 07081gw_interp
Re = 399694.6

α	C_l	C_d
-8.34	-0.577	0.0123
-7.22	-0.472	0.0108
-6.24	-0.370	0.0098
-5.17	-0.257	0.0092
-4.19	-0.158	0.0088
-3.14	-0.051	0.0083
-2.14	0.048	0.0084
-1.00	0.159	0.0079
-0.05	0.250	0.0082
0.91	0.337	0.0093
1.99	0.429	0.0102
2.94	0.523	0.0110
3.94	0.617	0.0119
5.06	0.724	0.0129
6.05	0.821	0.0141
7.13	0.917	0.0159
8.09	0.996	0.0185
9.08	1.067	0.0218
10.16	1.139	0.0267
11.19	1.189	0.0326

W1011 (20%) **fp10**

Fig. 6.118

Run: 07086gw_interp
Re = 99982.1

α	C_l	C_d
-9.26	-0.450	0.0245
-8.30	-0.377	0.0235
-7.16	-0.278	0.0222
-6.32	-0.203	0.0222
-5.15	-0.111	0.0213
-4.08	-0.015	0.0217
-3.07	0.045	0.0218
-2.12	0.129	0.0219
-1.06	0.234	0.0210
-0.04	0.331	0.0192
0.92	0.516	0.0165
1.90	0.617	0.0179
2.98	0.708	0.0216
4.08	0.806	0.0250
5.12	0.889	0.0295
6.03	0.954	0.0324
7.02	1.014	0.0368
8.13	1.082	0.0458

Run: 07088gw_interp
Re = 199990.5

α	C_l	C_d
-9.32	-0.419	0.0172
-8.21	-0.312	0.0160
-7.25	-0.219	0.0150
-6.21	-0.107	0.0145
-5.11	0.002	0.0143
-4.25	0.083	0.0149
-3.07	0.176	0.0158
-2.08	0.260	0.0162
-1.15	0.355	0.0165
-0.16	0.493	0.0141
0.92	0.587	0.0127
2.07	0.690	0.0149
3.05	0.774	0.0169
4.07	0.862	0.0191
5.13	0.947	0.0216
6.17	1.028	0.0245
7.17	1.093	0.0277
8.02	1.143	0.0324
9.16	1.195	0.0390

Run: 07090gw_interp
Re = 399397.9

α	C_l	C_d
-9.28	-0.443	0.0133
-8.32	-0.346	0.0122
-7.24	-0.236	0.0110
-6.28	-0.138	0.0103
-5.19	-0.020	0.0097
-4.12	0.089	0.0095
-3.19	0.182	0.0093
-2.17	0.286	0.0092
-1.04	0.391	0.0087
-0.13	0.471	0.0093
0.95	0.560	0.0111
1.91	0.651	0.0122
3.04	0.755	0.0132
3.98	0.840	0.0143
5.04	0.937	0.0158
6.00	1.015	0.0176
7.13	1.097	0.0205
8.06	1.163	0.0234
9.10	1.225	0.0273
10.18	1.276	0.0339
11.12	1.303	0.0417

W1011 (20%) **fp15**

Fig. 6.121

Run: 07094gw_interp
Re = 199972.6

α	C_l	C_d
-9.32	-0.273	0.0229
-8.21	-0.184	0.0223
-7.19	-0.095	0.0221
-6.17	-0.014	0.0221
-5.15	0.088	0.0222
-4.14	0.175	0.0226
-3.20	0.258	0.0225
-2.08	0.358	0.0230
-1.02	0.498	0.0237
-0.01	0.698	0.0171
1.03	0.763	0.0190
2.06	0.827	0.0216
2.89	0.883	0.0239
3.94	0.961	0.0265
4.95	1.024	0.0292
6.00	1.093	0.0321
7.18	1.174	0.0362
8.16	1.242	0.0417
9.17	1.289	0.0500

Run: 07092gw_interp
Re = 399291.9

α	C_l	C_d
-9.21	-0.220	0.0143
-8.40	-0.137	0.0138
-7.16	-0.015	0.0134
-6.25	0.072	0.0138
-5.14	0.158	0.0161
-4.17	0.228	0.0177
-3.12	0.319	0.0184
-2.07	0.434	0.0165
-1.05	0.586	0.0113
-0.09	0.669	0.0118
1.02	0.757	0.0137
2.02	0.841	0.0152
3.06	0.913	0.0169
4.11	0.995	0.0185
5.06	1.065	0.0204
6.14	1.146	0.0232
7.15	1.209	0.0273
8.08	1.270	0.0313
9.06	1.329	0.0361
10.16	1.379	0.0433

W1011 (20%) **fp20**

Fig. 6.124

Run: 07097sn_interp

Re = 99968.8

α	C_l	C_d
-9.33	-0.313	0.0348
-8.38	-0.222	0.0344
-7.18	-0.116	0.0344
-6.24	-0.034	0.0367
-5.18	0.060	0.0370
-4.16	0.138	0.0381
-3.06	0.236	0.0384
-2.24	0.320	0.0381
-1.04	0.445	0.0378
-0.09	0.557	0.0346
0.96	0.698	0.0303
1.92	0.728	0.0356
3.01	0.813	0.0385
3.99	0.893	0.0416
5.00	0.964	0.0447
6.13	1.050	0.0497
7.12	1.123	0.0568
8.05	1.149	0.0705

Run: 07099sn_interp

Re = 199804.8

α	C_l	C_d
-9.41	-0.256	0.0287
-8.25	-0.141	0.0283
-7.32	-0.046	0.0284
-6.24	0.056	0.0288
-5.17	0.158	0.0288
-4.20	0.255	0.0290
-3.20	0.356	0.0294
-2.10	0.461	0.0295
-1.21	0.568	0.0308
0.03	0.725	0.0287
0.97	0.735	0.0322
2.02	0.811	0.0330
3.05	0.900	0.0343
3.98	0.976	0.0354
5.09	1.065	0.0376
6.00	1.137	0.0397
7.14	1.228	0.0454
8.15	1.304	0.0510

Run: 07101sn_interp

Re = 399799.5

α	C_l	C_d
-9.32	-0.239	0.0257
-8.28	-0.134	0.0255
-7.16	-0.025	0.0255
-6.33	0.055	0.0254
-5.28	0.162	0.0261
-4.13	0.277	0.0261
-3.32	0.350	0.0259
-2.09	0.505	0.0256
-1.19	0.696	0.0166
-0.08	0.726	0.0172
0.84	0.791	0.0201
1.96	0.860	0.0232
3.06	0.933	0.0268
4.05	1.006	0.0288
5.09	1.094	0.0309
6.04	1.178	0.0329
7.14	1.260	0.0365
8.08	1.338	0.0398
9.07	1.408	0.0445
10.15	1.466	0.0541

W1011 (20%) **fp25**

Fig. 6.127

Run: 07105sn_interp

Re = 199731.5

α	C_l	C_d
-9.38	-0.138	0.0400
-8.32	-0.030	0.0399
-7.25	0.076	0.0402
-6.15	0.174	0.0404
-5.23	0.262	0.0410
-4.10	0.376	0.0416
-3.08	0.479	0.0420
-2.02	0.573	0.0424
-1.04	0.663	0.0410
-0.00	0.742	0.0446
0.87	0.793	0.0461
2.08	0.891	0.0465
3.07	0.974	0.0471
4.12	1.057	0.0476
5.04	1.129	0.0493
6.02	1.209	0.0519
7.06	1.288	0.0564
8.16	1.360	0.0640

Run: 07103sn_interp

Re = 400067.2

α	C_l	C_d
-9.37	-0.137	0.0357
-8.34	-0.032	0.0355
-7.18	0.083	0.0354
-6.19	0.177	0.0361
-5.13	0.279	0.0363
-4.11	0.371	0.0366
-3.17	0.449	0.0351
-2.08	0.566	0.0346
-1.20	0.652	0.0337
-0.17	0.720	0.0376
0.87	0.803	0.0386
1.97	0.897	0.0402
2.87	0.968	0.0413
3.89	1.058	0.0424
5.07	1.156	0.0436
6.12	1.250	0.0457
6.98	1.322	0.0482
8.01	1.404	0.0497
9.01	1.479	0.0554

W1011 (20%) **fp30**

Fig. 6.130

Run: 07075sn_interp

Re = 99860.1

α	C_l	C_d
-9.33	0.001	0.0570
-8.20	0.102	0.0584
-7.17	0.190	0.0592
-6.11	0.256	0.0602
-5.27	0.308	0.0595
-4.04	0.403	0.0591
-3.20	0.493	0.0598
-2.00	0.624	0.0611
-1.13	0.716	0.0592
0.03	0.800	0.0506
1.07	0.877	0.0544
2.05	0.955	0.0552
3.01	1.023	0.0583
4.00	1.107	0.0615
4.96	1.178	0.0661
6.19	1.260	0.0736

Run: 07077gw_interp

Re = 199900.0

α	C_l	C_d
-9.29	0.018	0.0507
-8.26	0.115	0.0522
-7.10	0.226	0.0524
-6.17	0.320	0.0535
-5.09	0.431	0.0542
-4.11	0.524	0.0546
-3.02	0.630	0.0559
-2.03	0.707	0.0543
-1.11	0.764	0.0498
-0.01	0.843	0.0591
1.10	0.929	0.0598

1.97	0.995	0.0604
3.08	1.086	0.0614
4.13	1.168	0.0616
5.15	1.247	0.0625
6.18	1.321	0.0646
7.08	1.383	0.0695

Run: 07079gw_interp
Re = 399758.0

α	C_l	C_d
-9.28	0.001	0.0476
-8.19	0.109	0.0483
-7.21	0.203	0.0486
-6.15	0.302	0.0487
-5.06	0.393	0.0494
-4.07	0.483	0.0496
-3.21	0.563	0.0488
-2.03	0.650	0.0438
-1.09	0.742	0.0497
-0.01	0.827	0.0516
0.90	0.901	0.0526
1.94	0.996	0.0542
3.02	1.086	0.0548
3.94	1.162	0.0563
5.14	1.257	0.0576
6.13	1.334	0.0578
7.01	1.393	0.0600
8.20	1.478	0.0636
9.16	1.548	0.0675

W1011 (20%) **fp40**

Fig. 6.29

Run: 07257gw_interp
Re = 199809.3

α	C_l	C_d
-8.25	0.313	0.0827
-6.17	0.516	0.0843
-4.08	0.701	0.0864
-2.11	0.854	0.0828
-0.02	0.994	0.0926
2.04	1.173	0.0954
4.04	1.323	0.0986
6.17	1.465	0.1006

W1011 (20%) **fp50**

Fig. 6.29

Run: 07258gw_interp
Re = 199842.0

α	C_l	C_d
-8.21	0.474	0.1153
-6.24	0.655	0.1180
-4.12	0.825	0.1184
-2.15	0.952	0.1112
-0.03	1.123	0.1247
1.94	1.277	0.1273
4.07	1.441	0.1255
6.09	1.566	0.1266

W1011 (20%) **fp60**

Fig. 6.29

Run: 07259gw_interp
Re = 199892.9

α	C_l	C_d
-8.25	0.592	0.1473
-6.13	0.766	0.1472
-4.10	0.883	0.1448
-2.03	1.044	0.1463
-0.07	1.195	0.1516
2.05	1.362	0.1512
4.09	1.509	0.1549

W1011 (30%) **fp0**

Fig. 6.148

Run: 07129sn_interp
Re = 100108.2

α	C_l	C_d
-8.25	-0.767	0.0265
-7.20	-0.684	0.0216
-6.23	-0.604	0.0192
-5.20	-0.516	0.0168
-4.12	-0.424	0.0153
-3.09	-0.343	0.0140
-2.08	-0.250	0.0128
-1.06	-0.175	0.0121
-0.08	0.001	0.0107
0.90	0.124	0.0131
1.91	0.210	0.0137
2.91	0.309	0.0150
3.92	0.402	0.0171
4.97	0.496	0.0190
6.07	0.604	0.0225
7.14	0.696	0.0271
8.17	0.780	0.0302
9.15	0.850	0.0354
10.06	0.918	0.0422

Run: 07131sn_interp
Re = 199881.6

α	C_l	C_d
-8.21	-0.800	0.0187
-7.34	-0.723	0.0167
-6.19	-0.619	0.0145
-5.15	-0.514	0.0130
-4.19	-0.417	0.0118
-3.13	-0.312	0.0105
-2.07	-0.186	0.0097
-1.18	-0.117	0.0087
-0.11	-0.000	0.0090
0.98	0.121	0.0092
2.05	0.234	0.0101
3.07	0.331	0.0116
4.01	0.424	0.0130
5.12	0.538	0.0148
6.12	0.632	0.0166
7.00	0.713	0.0184
8.20	0.809	0.0216
9.03	0.871	0.0244
10.16	0.943	0.0304
11.10	0.994	0.0365

Run: 07133sn_interp
Re = 399951.9

α	C_l	C_d
-8.41	-0.824	0.0151
-7.22	-0.712	0.0129
-6.34	-0.627	0.0117
-5.14	-0.507	0.0102
-4.31	-0.421	0.0098
-3.10	-0.294	0.0088
-2.07	-0.179	0.0081
-1.28	-0.103	0.0080
-0.01	0.018	0.0074
0.80	0.096	0.0073
1.94	0.212	0.0079
3.02	0.322	0.0093
3.93	0.403	0.0100
4.98	0.503	0.0111
5.99	0.607	0.0123
7.17	0.725	0.0139
8.05	0.803	0.0154
9.23	0.903	0.0185
10.22	0.974	0.0224
11.13	1.033	0.0262
12.20	1.081	0.0335

W1011 (30%) **fp5**
Fig. 6.151

Run: 07137sn_interp
Re = 199863.1

α	C_l	C_d
-8.24	-0.484	0.0151
-7.12	-0.374	0.0140
-6.34	-0.294	0.0133
-5.26	-0.191	0.0122
-4.21	-0.087	0.0119
-3.06	0.031	0.0114
-2.02	0.138	0.0114
-1.18	0.228	0.0112
-0.00	0.347	0.0106
0.95	0.437	0.0104
2.04	0.535	0.0124
2.98	0.625	0.0144
3.99	0.715	0.0162
5.13	0.815	0.0186
6.11	0.897	0.0214
7.11	0.974	0.0245
8.03	1.031	0.0279
9.13	1.098	0.0338
10.07	1.131	0.0401

Run: 07135sn_interp
Re = 399050.6

α	C_l	C_d
-8.28	-0.510	0.0124
-7.34	-0.417	0.0115
-6.17	-0.294	0.0104
-5.19	-0.194	0.0097
-4.12	-0.083	0.0092
-3.24	0.007	0.0089
-2.10	0.126	0.0088
-1.12	0.231	0.0085
-0.09	0.334	0.0086
1.01	0.423	0.0094
1.93	0.508	0.0106
3.05	0.620	0.0119
4.06	0.717	0.0130
5.01	0.804	0.0142
6.14	0.905	0.0158
7.19	0.995	0.0181
8.12	1.069	0.0210
9.06	1.122	0.0243
10.21	1.189	0.0300
11.14	1.217	0.0377

W1011 (30%) **fp10**
Fig. 6.154

Run: 07140gw_interp
Re = 100018.8

α	C_l	C_d
-9.04	-0.240	0.0230
-8.26	-0.167	0.0220
-7.17	-0.061	0.0216
-6.12	0.025	0.0223
-5.20	0.107	0.0230
-4.10	0.203	0.0240
-3.22	0.287	0.0240
-2.03	0.390	0.0250
-1.20	0.437	0.0260
-0.01	0.537	0.0267
1.08	0.719	0.0203
2.06	0.789	0.0208
3.13	0.877	0.0247
4.13	0.946	0.0288
5.18	1.016	0.0332
6.10	1.053	0.0378
7.17	1.112	0.0449
8.12	1.145	0.0539

Run: 07142gw_interp
Re = 199510.2

α	C_l	C_d
-9.39	-0.298	0.0170
-8.23	-0.188	0.0157
-7.11	-0.077	0.0150
-6.17	0.015	0.0149
-5.11	0.126	0.0150
-4.18	0.211	0.0146
-3.02	0.320	0.0150
-1.98	0.426	0.0159
-1.08	0.517	0.0175
-0.02	0.632	0.0156
1.04	0.726	0.0148
2.10	0.810	0.0173
2.95	0.877	0.0194
4.08	0.964	0.0219
5.13	1.034	0.0251
6.06	1.090	0.0286
7.14	1.149	0.0332
8.16	1.200	0.0390
9.19	1.235	0.0468

Run: 07144sn_interp
Re = 399888.4

α	C_l	C_d
-9.30	-0.316	0.0130
-8.39	-0.220	0.0121
-7.35	-0.112	0.0112
-6.30	0.002	0.0107
-5.26	0.110	0.0107
-4.16	0.222	0.0105
-3.08	0.332	0.0106
-2.09	0.420	0.0109
-1.09	0.532	0.0111
-0.13	0.616	0.0106
1.00	0.707	0.0127
2.00	0.805	0.0139
2.95	0.885	0.0149
4.00	0.972	0.0167
5.12	1.063	0.0188
6.03	1.120	0.0212
7.06	1.185	0.0251
8.16	1.238	0.0313
9.17	1.277	0.0374
10.16	1.319	0.0446

W1011 (30%) **fp15**
Fig. 6.157

Run: 07147gw_interp
Re = 200178.3

α	C_l	C_d
-9.16	0.005	0.0210
-8.17	0.091	0.0219
-7.11	0.174	0.0246
-6.17	0.233	0.0272
-5.07	0.346	0.0269
-4.10	0.395	0.0302
-3.04	0.523	0.0288
-2.10	0.572	0.0324
-1.07	0.676	0.0330
-0.07	0.876	0.0189
0.98	0.933	0.0234
2.05	0.977	0.0304
3.06	1.021	0.0350
3.94	1.070	0.0382
5.06	1.128	0.0416
6.16	1.195	0.0450
7.16	1.263	0.0495
8.11	1.297	0.0551

Run: 07149gw_interp
Re = 399283.5

α	C_l	C_d
-9.26	0.003	0.0140
-8.31	0.099	0.0137
-7.07	0.227	0.0141
-6.10	0.322	0.0149
-5.32	0.390	0.0156
-4.11	0.504	0.0182
-3.01	0.575	0.0260
-2.09	0.674	0.0240
-1.11	0.820	0.0131
-0.11	0.879	0.0149
1.03	0.958	0.0175
1.93	1.020	0.0195
3.05	1.083	0.0247
3.97	1.134	0.0287
5.10	1.188	0.0333
6.00	1.233	0.0381
7.18	1.300	0.0436
7.98	1.341	0.0475
9.17	1.399	0.0540

W1011 (30%) **fp20**

Fig. 6.160

Run: 07155sn_interp
Re = 100069.6

α	C_l	C_d
-9.32	-0.034	0.0446
-8.17	0.060	0.0450
-7.12	0.144	0.0473
-6.28	0.191	0.0501
-5.25	0.263	0.0514
-4.22	0.350	0.0509
-3.02	0.465	0.0499
-2.02	0.552	0.0499
-1.14	0.624	0.0522
-0.06	0.744	0.0493
1.04	0.868	0.0514
2.11	0.905	0.0557
3.10	0.971	0.0586
3.95	1.027	0.0623
5.17	1.099	0.0680
6.19	1.173	0.0732
7.05	1.234	0.0807

Run: 07153gw_interp
Re = 200013.9

α	C_l	C_d
-9.21	0.022	0.0398
-8.32	0.099	0.0412
-7.30	0.195	0.0418
-6.24	0.276	0.0421
-5.08	0.389	0.0434
-4.10	0.457	0.0439
-3.03	0.556	0.0449
-2.13	0.627	0.0457
-0.96	0.767	0.0447
0.03	0.869	0.0496
0.95	0.913	0.0511
2.05	0.985	0.0532
3.11	1.057	0.0549
4.11	1.132	0.0576
5.10	1.200	0.0604
6.11	1.280	0.0636
7.17	1.350	0.0670
7.98	1.398	0.0724

Run: 07151gw_interp
Re = 399558.3

α	C_l	C_d
-9.21	0.093	0.0391
-8.32	0.171	0.0392
-7.30	0.254	0.0404
-6.17	0.365	0.0417
-5.23	0.436	0.0409
-4.09	0.515	0.0423
-3.06	0.634	0.0433
-2.04	0.792	0.0424
-1.08	0.910	0.0319
0.03	0.940	0.0350
1.03	0.991	0.0388
1.96	1.045	0.0464
3.05	1.123	0.0508
3.95	1.187	0.0537
4.98	1.252	0.0564
6.13	1.330	0.0598
7.10	1.396	0.0635
8.02	1.453	0.0634
9.12	1.509	0.0702

W1011 (30%) **fp25**

Fig. 6.163

Run: 07158sn_interp
Re = 200014.4

α	C_l	C_d
-9.18	0.131	0.0529
-8.31	0.209	0.0549
-7.20	0.306	0.0557
-6.23	0.402	0.0577
-5.15	0.497	0.0590
-4.03	0.602	0.0616
-2.99	0.700	0.0646
-2.15	0.768	0.0666
-1.10	0.878	0.0598
0.01	0.940	0.0703
0.95	1.002	0.0708
2.05	1.080	0.0724
2.93	1.144	0.0747
4.11	1.228	0.0759
5.13	1.298	0.0789
6.10	1.357	0.0852

Run: 07160sn_interp
Re = 399632.2

α	C_l	C_d
-9.17	0.187	0.0525
-8.26	0.269	0.0536
-7.09	0.368	0.0545
-6.27	0.430	0.0552
-5.19	0.530	0.0571
-4.13	0.622	0.0583
-3.17	0.725	0.0596
-2.08	0.897	0.0607
-1.13	0.878	0.0633
-0.13	0.938	0.0647
0.89	1.007	0.0667
2.06	1.097	0.0701
2.96	1.174	0.0726
4.06	1.254	0.0762
5.11	1.343	0.0806
6.15	1.433	0.0859
7.00	1.494	0.0849
8.04	1.548	0.0841

W1011 (30%) **fp30**

Fig. 6.166

Run: 07166gw_interp
Re = 100201.0

α	C_l	C_d
-9.23	0.228	0.0826
-8.25	0.264	0.0830
-7.13	0.292	0.0798
-6.19	0.380	0.0834
-5.07	0.507	0.0866
-3.99	0.619	0.0904
-3.09	0.717	0.0948
-1.94	0.838	0.0978
-0.96	0.908	0.0840
0.07	0.975	0.0886
1.08	1.047	0.0909
1.94	1.096	0.0935
3.13	1.176	0.0969

4.16	1.240	0.1032
5.09	1.295	0.1050

Run: 07164gw_interp
Re = 200077.9

α	C_l	C_d
-9.14	0.303	0.0785
-8.13	0.386	0.0799
-7.10	0.467	0.0807
-6.21	0.542	0.0821
-5.25	0.639	0.0839
-4.02	0.733	0.0855
-3.03	0.812	0.0876
-2.08	0.842	0.0766
-0.99	0.954	0.0873
0.07	1.023	0.0918
0.99	1.093	0.0932
2.01	1.176	0.0956
3.18	1.273	0.0994
4.13	1.335	0.1035
5.15	1.395	0.1081
6.20	1.459	0.1103

W1011 (30%) **fp40**

Fig. 6.30

Run: 07251gw_interp
Re = 200978.3

α	C_l	C_d
-8.22	0.620	0.1293
-6.18	0.766	0.1365
-4.02	0.915	0.1378
-2.02	1.068	0.1373
0.02	1.228	0.1527
2.10	1.384	0.1554
4.18	1.519	0.1580
6.08	1.598	0.1624

W1011 (30%) **fp50**

Fig. 6.30

Run: 07252gw_interp
Re = 200588.5

α	C_l	C_d
-8.12	0.750	0.1617
-6.17	0.906	0.1764
-4.00	1.080	0.1786
-1.97	1.226	0.1858
-0.04	1.376	0.1882
2.00	1.516	0.1930
4.19	1.649	0.1971

W1011 (30%) **fp60**

Fig. 6.30

Run: 07253gw_interp
Re = 201397.0

α	C_l	C_d
-8.15	0.848	0.2247
-5.99	1.010	0.2274
-3.99	1.188	0.2257
-1.95	1.328	0.2313
0.06	1.456	0.2335
2.18	1.590	0.2344
4.06	1.714	0.2377

W1015 (20%) **fp0**

Fig. 6.184

Run: 06997gw_interp
Re = 99896.6

α	C_l	C_d
-8.24	-0.853	0.0305
-7.25	-0.782	0.0255
-6.25	-0.707	0.0220
-5.28	-0.623	0.0197
-4.13	-0.523	0.0174
-3.14	-0.446	0.0170
-2.24	-0.363	0.0172
-1.05	-0.177	0.0180
-0.15	-0.046	0.0168
0.88	0.025	0.0166
2.02	0.161	0.0173
2.93	0.299	0.0169
3.93	0.403	0.0190
5.12	0.489	0.0204
6.04	0.564	0.0225
7.03	0.643	0.0257
8.04	0.717	0.0298
9.25	0.811	0.0340
10.23	0.869	0.0387
11.23	0.919	0.0433
12.22	0.976	0.0456

Run: 06999gw_interp
Re = 200163.0

α	C_l	C_d
-8.33	-0.831	0.0198
-7.26	-0.752	0.0179
-6.29	-0.682	0.0161
-5.22	-0.595	0.0146
-4.31	-0.516	0.0134
-3.03	-0.389	0.0123
-2.08	-0.235	0.0114
-1.17	-0.141	0.0108
-0.02	-0.034	0.0111
0.94	0.060	0.0111
2.03	0.161	0.0116
3.08	0.263	0.0125
3.96	0.377	0.0132
5.09	0.499	0.0148
6.12	0.597	0.0161
7.12	0.683	0.0179
8.18	0.770	0.0196
9.07	0.842	0.0217
10.25	0.933	0.0244
11.13	0.997	0.0263
12.20	1.064	0.0295
13.17	1.114	0.0335
14.17	1.147	0.0406

Run: 07001gw_interp
Re = 399599.8

α	C_l	C_d
-8.21	-0.847	0.0150
-7.43	-0.782	0.0138
-6.19	-0.677	0.0124
-5.13	-0.585	0.0115
-4.12	-0.475	0.0108
-3.29	-0.340	0.0094
-2.05	-0.221	0.0088
-1.13	-0.130	0.0087
-0.16	-0.038	0.0087
0.89	0.059	0.0090
2.08	0.179	0.0096
2.92	0.263	0.0098
3.94	0.384	0.0103
5.08	0.507	0.0114
6.13	0.609	0.0124
7.15	0.707	0.0135
8.09	0.786	0.0147
9.21	0.886	0.0162
10.11	0.963	0.0178
11.15	1.042	0.0201
12.28	1.123	0.0230
13.26	1.184	0.0266
14.24	1.218	0.0348

W1015 (**20**%) **fp5**

Fig. 6.187

Run: 07010gw_interp

Re = 200180.1

α	C_l	C_d
-8.22	-0.586	0.0182
-7.18	-0.490	0.0168
-6.37	-0.419	0.0163
-5.16	-0.320	0.0158
-4.12	-0.232	0.0151
-3.26	-0.158	0.0149
-2.19	-0.056	0.0146
-1.22	0.072	0.0141
-0.12	0.203	0.0123
1.06	0.310	0.0130
1.88	0.387	0.0135
2.91	0.480	0.0143
4.09	0.594	0.0152
5.06	0.688	0.0165
6.18	0.794	0.0185
7.05	0.867	0.0204
8.18	0.961	0.0230
9.23	1.037	0.0255
10.16	1.104	0.0278
11.24	1.177	0.0310
12.13	1.225	0.0340
13.19	1.268	0.0402
14.16	1.288	0.0633

Run: 07012sn_interp

Re = 399462.5

α	C_l	C_d
-8.32	-0.612	0.0138
-7.40	-0.517	0.0130
-6.30	-0.409	0.0124
-5.31	-0.306	0.0119
-4.14	-0.189	0.0108
-3.25	-0.105	0.0103
-2.20	0.006	0.0093
-1.05	0.119	0.0088
-0.18	0.201	0.0093
1.01	0.311	0.0103
1.97	0.404	0.0108
2.91	0.493	0.0117
3.92	0.589	0.0124
5.09	0.700	0.0135
6.13	0.798	0.0147
7.18	0.889	0.0162
8.18	0.979	0.0176
9.24	1.071	0.0194
10.10	1.136	0.0213
11.14	1.212	0.0238
12.22	1.284	0.0271
13.14	1.327	0.0321
14.27	1.332	0.0782

W1015 (**20**%) **fp10**

Fig. 6.190

Run: 07014gw_interp

Re = 99973.1

α	C_l	C_d
-9.26	-0.519	0.0341
-8.27	-0.441	0.0307
-7.38	-0.371	0.0295
-6.34	-0.288	0.0272
-5.22	-0.210	0.0267
-4.13	-0.120	0.0250
-3.21	-0.062	0.0258
-2.19	0.022	0.0265
-1.04	0.136	0.0265
-0.12	0.278	0.0275
0.91	0.453	0.0210
2.06	0.562	0.0183
2.97	0.624	0.0209
4.00	0.716	0.0237
5.01	0.804	0.0269
6.09	0.890	0.0311
7.06	0.967	0.0362
8.09	1.044	0.0393
9.19	1.109	0.0442
10.11	1.169	0.0465
11.24	1.229	0.0518

Run: 07016gw_interp

Re = 199801.2

α	C_l	C_d
-9.31	-0.474	0.0218
-8.36	-0.403	0.0217
-7.38	-0.326	0.0208
-6.16	-0.219	0.0202
-5.29	-0.139	0.0196
-4.24	-0.079	0.0191
-3.20	-0.004	0.0199
-2.19	0.122	0.0193
-1.20	0.224	0.0199
-0.02	0.430	0.0155
1.02	0.533	0.0153
2.05	0.616	0.0166
3.12	0.700	0.0179
4.06	0.770	0.0193
5.08	0.855	0.0211
6.05	0.937	0.0235
7.15	1.025	0.0262
8.04	1.097	0.0282
9.24	1.180	0.0312
10.13	1.249	0.0339
11.21	1.310	0.0370
12.17	1.361	0.0405
13.21	1.388	0.0503

Run: 07018gw_interp

Re = 400017.1

α	C_l	C_d
-9.31	-0.487	0.0153
-8.43	-0.399	0.0143
-7.37	-0.296	0.0135
-6.18	-0.177	0.0129
-5.35	-0.094	0.0125
-4.21	0.005	0.0146
-3.27	0.062	0.0157
-2.07	0.212	0.0129
-0.99	0.361	0.0101
-0.18	0.427	0.0108
0.94	0.527	0.0121
1.97	0.618	0.0132
2.94	0.697	0.0147
3.96	0.788	0.0160
5.13	0.881	0.0176
6.08	0.959	0.0190
7.17	1.053	0.0209
8.04	1.124	0.0225
9.02	1.203	0.0246
10.23	1.291	0.0274
11.26	1.370	0.0299
12.10	1.429	0.0332
13.23	1.471	0.0461

W1015 (**20**%) **fp15**

Fig. 6.193

Run: 07021gw_interp

Re = 199852.3

α	C_l	C_d
-9.27	-0.448	0.0274
-8.35	-0.350	0.0266
-7.22	-0.238	0.0264
-6.25	-0.143	0.0266
-5.12	-0.032	0.0272
-4.15	0.061	0.0269
-3.02	0.176	0.0275
-2.12	0.261	0.0277
-0.97	0.415	0.0266
0.03	0.601	0.0207
1.10	0.676	0.0226

1.89	0.702	0.0265
3.10	0.776	0.0281
3.96	0.837	0.0289
5.14	0.934	0.0304
6.11	1.012	0.0320
7.11	1.101	0.0342
8.05	1.177	0.0360
9.22	1.270	0.0385
10.15	1.341	0.0406
11.16	1.409	0.0442
12.15	1.464	0.0499

Run: 07023sn_interp
Re = 400406.9

α	C_l	C_d
-9.46	-0.459	0.0237
-8.37	-0.356	0.0232
-7.36	-0.264	0.0228
-6.25	-0.154	0.0229
-5.13	-0.041	0.0231
-4.18	0.059	0.0233
-3.09	0.175	0.0229
-2.15	0.348	0.0215
-1.15	0.541	0.0139
-0.12	0.618	0.0142
1.03	0.651	0.0217
1.95	0.713	0.0240
3.09	0.797	0.0256
4.10	0.886	0.0269
5.14	0.970	0.0283
6.15	1.059	0.0294
7.07	1.141	0.0306
8.16	1.231	0.0318
9.22	1.334	0.0332
10.10	1.400	0.0352
11.22	1.494	0.0371
12.11	1.549	0.0421

W1015 (20%) **fp20**

Fig. 6.196

Run: 07025gw_interp
Re = 99982.9

α	C_l	C_d
-9.13	-0.374	0.0427
-8.08	-0.270	0.0404
-7.17	-0.178	0.0392
-6.12	-0.083	0.0397
-5.01	0.022	0.0395
-3.93	0.111	0.0401
-3.06	0.191	0.0413
-2.01	0.293	0.0426
-1.01	0.396	0.0444
0.05	0.547	0.0414
1.17	0.724	0.0317
2.18	0.760	0.0371
3.27	0.832	0.0389
4.15	0.909	0.0412
5.25	1.002	0.0446
6.23	1.081	0.0484
7.26	1.161	0.0521
8.30	1.237	0.0552
9.31	1.301	0.0590
10.23	1.366	0.0618

Run: 07027gw_interp
Re = 199856.2

α	C_l	C_d
-9.40	-0.363	0.0328
-8.23	-0.254	0.0318
-7.27	-0.152	0.0312
-6.20	-0.053	0.0320
-5.12	0.058	0.0323
-4.09	0.160	0.0326
-3.06	0.265	0.0329
-2.07	0.373	0.0333
-1.13	0.488	0.0336
0.00	0.631	0.0318
0.99	0.673	0.0356
1.90	0.740	0.0371
2.91	0.822	0.0375
4.09	0.921	0.0382
5.01	1.000	0.0385
6.02	1.091	0.0393
7.11	1.187	0.0419
8.04	1.267	0.0440
9.23	1.365	0.0471
10.21	1.440	0.0498

Run: 07029gw_interp
Re = 399533.6

α	C_l	C_d
-9.47	-0.377	0.0296
-8.35	-0.259	0.0295
-7.22	-0.148	0.0294
-6.24	-0.043	0.0299
-5.31	0.058	0.0301
-4.28	0.170	0.0306
-3.09	0.298	0.0295
-2.11	0.432	0.0300
-1.18	0.520	0.0305
-0.16	0.584	0.0333
0.90	0.666	0.0344
1.97	0.765	0.0358
2.96	0.848	0.0368
3.96	0.944	0.0379
5.06	1.047	0.0386
6.11	1.140	0.0395
7.13	1.232	0.0409
8.06	1.320	0.0416
9.15	1.419	0.0416
10.12	1.505	0.0438

W1015 (20%) **fp25**

Fig. 6.199

Run: 07032gw_interp
Re = 199999.1

α	C_l	C_d
-9.38	-0.216	0.0442
-8.20	-0.083	0.0441
-7.14	0.025	0.0441
-6.24	0.119	0.0439
-5.10	0.236	0.0455
-4.06	0.346	0.0453
-3.04	0.451	0.0470
-2.02	0.551	0.0481
-0.99	0.605	0.0404
-0.00	0.685	0.0452
1.02	0.763	0.0495
1.89	0.840	0.0509
2.98	0.923	0.0513
4.09	1.024	0.0521
5.03	1.100	0.0517
6.19	1.205	0.0504
7.17	1.291	0.0521
8.14	1.366	0.0536
9.21	1.462	0.0562

Run: 07034gw_interp
Re = 399974.8

α	C_l	C_d
-9.27	-0.194	0.0399
-8.42	-0.106	0.0403
-7.20	0.015	0.0417
-6.27	0.113	0.0419
-5.28	0.220	0.0431
-4.19	0.329	0.0432
-3.12	0.425	0.0393
-2.10	0.524	0.0389
-1.16	0.613	0.0446
-0.03	0.711	0.0459
0.85	0.791	0.0469
1.91	0.884	0.0481
2.94	0.976	0.0494
4.01	1.068	0.0503
5.01	1.155	0.0509

6.03	1.246	0.0517
7.06	1.340	0.0525
8.04	1.420	0.0524
9.19	1.516	0.0526
10.10	1.603	0.0538

W1015 (20%) **fp30**

Fig. 6.202

Run: 07003gw_interp

Re = 99900.8

α	C_l	C_d
-8.25	-0.068	0.0593
-7.18	0.039	0.0605
-6.27	0.117	0.0607
-5.12	0.205	0.0597
-4.09	0.266	0.0599
-3.02	0.365	0.0598
-2.07	0.454	0.0618
-1.10	0.560	0.0619
0.02	0.681	0.0537
1.09	0.786	0.0578
1.96	0.864	0.0608
3.06	0.960	0.0607
3.98	1.040	0.0618
5.14	1.134	0.0642
6.17	1.219	0.0682
7.17	1.302	0.0703
8.11	1.370	0.0733

Run: 07005gw_interp

Re = 199907.4

α	C_l	C_d
-8.23	0.021	0.0531
-7.28	0.120	0.0543
-6.11	0.245	0.0568
-5.21	0.341	0.0574
-4.07	0.457	0.0581
-3.02	0.554	0.0588
-2.17	0.626	0.0604
-1.00	0.692	0.0529
-0.10	0.759	0.0595
1.04	0.843	0.0629
2.08	0.938	0.0646
3.10	1.015	0.0652
4.10	1.107	0.0651
5.05	1.195	0.0655
6.13	1.279	0.0665
7.21	1.370	0.0668
8.09	1.446	0.0671

Run: 07007gw_interp

Re = 399654.9

α	C_l	C_d
-8.32	0.031	0.0517
-7.16	0.148	0.0525
-6.30	0.239	0.0538
-5.32	0.343	0.0549
-4.08	0.459	0.0562
-3.07	0.547	0.0506
-2.09	0.634	0.0527
-1.12	0.720	0.0577
-0.04	0.826	0.0599
0.95	0.911	0.0610
1.87	0.991	0.0628
3.11	1.102	0.0639
3.95	1.174	0.0646
5.18	1.279	0.0661
6.01	1.349	0.0661
7.13	1.437	0.0666
8.25	1.531	0.0658

W1015 (20%) **fp40**

Fig. 6.31

Run: 07248gw_interp

Re = 199781.6

α	C_l	C_d
-8.15	0.242	0.0808
-6.29	0.423	0.0836
-4.17	0.633	0.0850
-2.05	0.808	0.0847
-0.09	0.960	0.0899
2.07	1.130	0.0907
4.11	1.290	0.0898
6.14	1.452	0.0928
8.06	1.617	0.0971
10.16	1.747	0.1017

W1015 (20%) **fp50**

Fig. 6.31

Run: 07249gw_interp

Re = 199964.0

α	C_l	C_d
-8.30	0.416	0.1136
-6.28	0.599	0.1157
-4.08	0.793	0.1144
-1.97	0.954	0.1134
-0.00	1.099	0.1228
2.07	1.258	0.1204
4.13	1.418	0.1208
6.18	1.579	0.1224
8.20	1.729	0.1290
10.15	1.841	0.1380

W1015 (20%) **fp60**

Fig. 6.31

Run: 07250gw_interp

Re = 200134.8

α	C_l	C_d
-8.24	0.538	0.1472
-6.11	0.732	0.1487
-4.03	0.871	0.1483
-2.05	1.001	0.1426
-0.01	1.146	0.1485
2.12	1.326	0.1492
4.01	1.488	0.1484
6.18	1.658	0.1536
8.09	1.775	0.1596
10.22	1.905	0.1715

W1015 (30%) **fp0**

Fig. 6.220

Run: 06936gw_interp

Re = 99952.2

α	C_l	C_d
-8.23	-0.811	0.0295
-7.36	-0.747	0.0252
-6.34	-0.665	0.0222
-5.13	-0.567	0.0194
-4.16	-0.497	0.0173
-3.08	-0.403	0.0171
-2.24	-0.318	0.0167
-1.02	-0.144	0.0164
-0.03	-0.040	0.0175
0.85	0.028	0.0168
2.00	0.192	0.0180
2.91	0.276	0.0175
4.14	0.413	0.0187
5.12	0.488	0.0202
6.11	0.572	0.0223
7.08	0.641	0.0260
8.17	0.725	0.0311
9.06	0.788	0.0338
10.25	0.863	0.0391
11.19	0.915	0.0432
12.15	0.967	0.0464
13.07	0.573	0.1883

Run: 06940ga_interp
Re = 199911.7

α	C_l	C_d
-8.27	-0.796	0.0202
-7.25	-0.716	0.0184
-6.20	-0.635	0.0164
-5.23	-0.561	0.0148
-4.17	-0.478	0.0133
-3.32	-0.408	0.0124
-2.09	-0.231	0.0109
-1.05	-0.128	0.0108
-0.16	-0.046	0.0105
0.96	0.055	0.0107
2.02	0.162	0.0118
3.03	0.292	0.0124
3.97	0.414	0.0132
5.02	0.510	0.0147
6.20	0.615	0.0161
7.02	0.681	0.0175
8.09	0.763	0.0195
9.20	0.850	0.0219
10.25	0.926	0.0243
11.19	0.991	0.0265
12.27	1.058	0.0296
13.11	1.105	0.0329
14.17	1.139	0.0402
15.27	1.136	0.0825

Run: 06939gw_interp
Re = 399414.2

α	C_l	C_d
-8.36	-0.836	0.0158
-7.20	-0.742	0.0139
-6.34	-0.669	0.0131
-5.24	-0.578	0.0120
-4.11	-0.471	0.0107
-3.28	-0.353	0.0101
-2.11	-0.223	0.0091
-1.13	-0.130	0.0090
-0.13	-0.035	0.0090
0.84	0.056	0.0093
1.85	0.150	0.0091
2.96	0.256	0.0098
4.08	0.371	0.0107
5.02	0.460	0.0116
6.15	0.596	0.0128
7.16	0.694	0.0138
8.22	0.790	0.0149
9.10	0.862	0.0160
10.14	0.943	0.0180
11.21	1.027	0.0203
12.21	1.096	0.0226
13.27	1.157	0.0264
14.32	1.198	0.0355

W1015 (30%) **fp5**

Fig. 6.223

Run: 06949sn_interp
Re = 199795.8

α	C_l	C_d
-6.30	-0.348	0.0151
-5.08	-0.220	0.0142
-4.22	-0.126	0.0137
-3.23	-0.031	0.0133
-2.04	0.075	0.0133
-1.06	0.181	0.0136
-0.13	0.285	0.0134
0.86	0.373	0.0124
1.94	0.472	0.0129
2.97	0.563	0.0142
4.07	0.659	0.0158
5.02	0.736	0.0172
6.10	0.829	0.0195
7.17	0.917	0.0219
8.03	0.983	0.0242
9.09	1.055	0.0267
10.14	1.120	0.0294
11.26	1.190	0.0335
12.08	1.227	0.0366
13.21	1.262	0.0437
14.14	1.282	0.0691

Run: 06947sn_interp
Re = 399160.4

α	C_l	C_d
-5.22	-0.238	0.0110
-4.11	-0.129	0.0104
-3.15	-0.041	0.0099
-2.05	0.070	0.0097
-1.18	0.164	0.0098
-0.15	0.261	0.0098
0.95	0.365	0.0105
1.93	0.475	0.0109
2.94	0.562	0.0114
4.06	0.661	0.0125
5.11	0.755	0.0139
6.06	0.838	0.0152
7.18	0.933	0.0170
8.05	1.008	0.0186
9.30	1.106	0.0210
10.27	1.174	0.0235
11.13	1.224	0.0259
12.13	1.282	0.0293
13.17	1.335	0.0359

W1015 (30%) **fp10**

Fig. 6.226

Run: 06952gw_interp
Re = 100140.7

α	C_l	C_d
-8.96	-0.327	0.0289
-8.03	-0.262	0.0295
-6.98	-0.193	0.0293
-5.87	-0.097	0.0312
-4.83	0.002	0.0332
-3.79	0.081	0.0323
-2.79	0.163	0.0302
-1.76	0.236	0.0318
-0.75	0.316	0.0331
0.34	0.480	0.0260
1.36	0.657	0.0203
2.29	0.735	0.0236
3.38	0.807	0.0272
4.44	0.881	0.0317
5.40	0.941	0.0361
6.48	1.004	0.0408
7.43	1.052	0.0454
8.49	1.103	0.0509
9.45	1.150	0.0546
10.46	1.201	0.0585
11.43	1.244	0.0634

Run: 06954gw_interp
Re = 200107.6

α	C_l	C_d
-9.97	-0.374	0.0197
-8.95	-0.284	0.0192
-7.93	-0.196	0.0190
-6.87	-0.104	0.0190
-5.91	-0.017	0.0193
-4.79	0.078	0.0208
-3.88	0.143	0.0227
-2.88	0.225	0.0219
-1.77	0.354	0.0227
-0.86	0.463	0.0209
0.36	0.622	0.0150
1.24	0.711	0.0162
2.34	0.784	0.0190
3.39	0.855	0.0213
4.35	0.925	0.0237
5.47	1.002	0.0269
6.49	1.070	0.0300
7.37	1.129	0.0328
8.50	1.199	0.0366
9.52	1.261	0.0389
10.43	1.317	0.0418

11.48	1.372	0.0473
12.48	1.410	0.0593

Run: 06956sn_interp
Re = 399777.0

α	C_l	C_d
-10.17	-0.440	0.0144
-9.01	-0.327	0.0134
-8.05	-0.234	0.0127
-7.05	-0.132	0.0122
-6.00	-0.027	0.0118
-4.83	0.093	0.0116
-3.93	0.185	0.0117
-2.90	0.293	0.0120
-1.74	0.413	0.0121
-0.88	0.503	0.0113
0.22	0.599	0.0129
1.27	0.682	0.0146
2.33	0.771	0.0161
3.33	0.847	0.0173
4.29	0.923	0.0187
5.33	1.002	0.0210
6.36	1.073	0.0234
7.47	1.159	0.0259
8.56	1.236	0.0290
9.40	1.287	0.0318
10.45	1.353	0.0351
11.53	1.427	0.0405

W1015 (30%) **fp15**

Fig. 6.229

Run: 06959sn_interp
Re = 200077.1

α	C_l	C_d
-9.30	-0.193	0.0315
-8.18	-0.128	0.0320
-7.29	-0.064	0.0322
-6.28	0.006	0.0325
-5.31	0.076	0.0334
-4.05	0.179	0.0347
-3.23	0.266	0.0339
-2.20	0.373	0.0350
-1.02	0.506	0.0359
0.02	0.720	0.0310
1.06	0.864	0.0243
2.00	0.859	0.0374
3.02	0.895	0.0394
4.12	0.959	0.0408
5.17	1.030	0.0431
6.10	1.103	0.0452
7.18	1.188	0.0480
8.22	1.267	0.0501
9.24	1.339	0.0502
10.17	1.411	0.0515
11.20	1.470	0.0547
12.12	1.510	0.0616

Run: 06961sn_interp
Re = 399734.7

α	C_l	C_d
-9.26	-0.119	0.0220
-8.44	-0.072	0.0276
-7.42	-0.001	0.0298
-6.34	0.078	0.0309
-5.19	0.178	0.0325
-4.13	0.273	0.0328
-3.13	0.377	0.0323
-2.15	0.543	0.0305
-1.05	0.767	0.0193
-0.01	0.822	0.0156
0.89	0.847	0.0285
1.99	0.896	0.0354
3.06	0.944	0.0376
4.04	1.004	0.0395
4.99	1.071	0.0408
6.14	1.162	0.0425
7.00	1.230	0.0436
8.05	1.305	0.0445
9.05	1.390	0.0442
10.19	1.489	0.0425
11.25	1.571	0.0457

W1015 (30%) **fp20**

Fig. 6.232

Run: 06963sn_interp
Re = 100003.6

α	C_l	C_d
-8.18	-0.108	0.0480
-7.30	-0.026	0.0482
-6.16	0.071	0.0503
-5.07	0.160	0.0544
-4.10	0.243	0.0558
-3.11	0.327	0.0527
-2.03	0.423	0.0512
-1.03	0.507	0.0578
0.06	0.732	0.0564
0.98	0.856	0.0454
1.93	0.899	0.0522
3.08	0.956	0.0567
4.02	1.016	0.0580
5.18	1.095	0.0623
6.17	1.161	0.0662
7.23	1.223	0.0721
8.05	1.272	0.0754
9.13	1.347	0.0792

Run: 06965sn_interp
Re = 199777.7

α	C_l	C_d
-8.33	-0.072	0.0416
-7.14	0.028	0.0418
-6.29	0.104	0.0426
-5.23	0.207	0.0431
-4.18	0.308	0.0446
-3.24	0.400	0.0458
-2.17	0.505	0.0467
-0.98	0.640	0.0483
-0.03	0.782	0.0454
1.09	0.817	0.0525
1.92	0.858	0.0534
3.02	0.939	0.0551
4.00	1.013	0.0564
5.17	1.114	0.0584
6.14	1.200	0.0605
7.22	1.281	0.0637
8.05	1.350	0.0655
9.09	1.442	0.0673
10.18	1.524	0.0671
11.16	1.581	0.0699
12.21	1.612	0.0908

Run: 06967sn_interp
Re = 400348.9

α	C_l	C_d
-10.30	-0.217	0.0396
-9.22	-0.113	0.0405
-8.32	-0.016	0.0411
-7.24	0.102	0.0415
-6.37	0.185	0.0421
-5.37	0.281	0.0430
-4.30	0.385	0.0436
-3.24	0.493	0.0438
-2.13	0.648	0.0441
-1.02	0.824	0.0402
-0.05	0.804	0.0481
0.82	0.838	0.0500
1.88	0.915	0.0518
2.89	1.005	0.0537
4.08	1.101	0.0558
5.02	1.178	0.0569
6.02	1.263	0.0585
7.17	1.354	0.0591
8.05	1.423	0.0598
9.14	1.512	0.0587
10.26	1.598	0.0596

11.14	1.656	0.0627

W1015 (30%) **fp25**

Fig. 6.235

Run: 06971sn_interp
Re = 199830.5

α	C_l	C_d
-9.28	0.021	0.0590
-8.25	0.114	0.0597
-7.11	0.221	0.0617
-6.22	0.307	0.0633
-5.12	0.423	0.0664
-4.05	0.526	0.0680
-3.06	0.613	0.0709
-2.20	0.691	0.0730
-1.00	0.757	0.0608
0.03	0.856	0.0656
0.90	0.899	0.0726
1.88	0.980	0.0767
3.08	1.080	0.0769
4.01	1.146	0.0782
5.14	1.226	0.0794
6.16	1.304	0.0800
7.17	1.384	0.0808
8.02	1.446	0.0814
9.08	1.527	0.0829
10.21	1.615	0.0827
11.19	1.667	0.0862

Run: 06973sn_interp
Re = 399569.9

α	C_l	C_d
-9.29	0.011	0.0547
-8.35	0.102	0.0564
-7.29	0.201	0.0576
-6.30	0.295	0.0588
-5.27	0.406	0.0606
-4.19	0.504	0.0644
-3.15	0.594	0.0607
-2.07	0.749	0.0594
-1.19	0.815	0.0625
-0.06	0.866	0.0680
1.01	0.946	0.0700
1.99	1.025	0.0719
3.01	1.109	0.0736
3.91	1.177	0.0757
5.15	1.281	0.0759
6.08	1.355	0.0766
7.01	1.439	0.0763
8.07	1.538	0.0747
9.07	1.622	0.0746

10.26	1.721	0.0761

W1015 (30%) **fp30**

Fig. 6.238

Run: 06942gw_interp
Re = 100332.1

α	C_l	C_d
-8.19	0.132	0.0820
-7.15	0.192	0.0816
-6.16	0.251	0.0823
-5.12	0.386	0.0873
-4.11	0.532	0.0896
-3.08	0.647	0.0929
-1.95	0.772	0.0975
-1.01	0.868	0.0857
-0.09	0.933	0.0799
1.04	1.036	0.0895
2.13	1.130	0.0909
3.02	1.215	0.0927
4.00	1.296	0.0948
5.08	1.379	0.0976
6.22	1.470	0.1014
7.24	1.558	0.1065

Run: 06944sn_interp
Re = 200105.5

α	C_l	C_d
-8.12	0.281	0.0824
-7.24	0.363	0.0841
-6.14	0.471	0.0856
-5.12	0.559	0.0865
-4.15	0.646	0.0881
-3.04	0.743	0.0914
-2.07	0.816	0.0918
-0.94	0.889	0.0835
0.03	0.957	0.0901
1.09	1.034	0.0956
2.12	1.122	0.0972
3.00	1.197	0.0986
4.08	1.281	0.1001
5.02	1.353	0.1025
6.10	1.421	0.1034
7.27	1.516	0.1051
8.09	1.581	0.1067
9.22	1.657	0.1067

W1015 (30%) **fp40**

Fig. 6.32

Run: 07254gw_interp
Re = 200311.3

α	C_l	C_d
-8.20	0.560	0.1279
-6.14	0.735	0.1312
-4.13	0.887	0.1333
-2.01	1.059	0.1305
0.01	1.201	0.1454
2.11	1.345	0.1453
4.04	1.503	0.1473
6.12	1.638	0.1550
8.07	1.760	0.1621
10.18	1.879	0.1693

W1015 (30%) **fp50**

Fig. 6.32

Run: 07255gw_interp
Re = 200547.6

α	C_l	C_d
-8.21	0.673	0.1641
-6.10	0.822	0.1741
-4.06	0.993	0.1841
-1.94	1.178	0.1844
-0.06	1.319	0.1913
2.09	1.472	0.1932
4.04	1.596	0.1962
6.21	1.747	0.2026
8.19	1.873	0.2082

W1015 (30%) **fp60**

Fig. 6.32

Run: 07256gw_interp
Re = 201379.8

α	C_l	C_d
-8.15	0.757	0.2234
-6.07	0.948	0.2267
-4.01	1.104	0.2311
-2.03	1.284	0.2369
-0.06	1.424	0.2383
2.01	1.558	0.2395
4.09	1.681	0.2386
6.13	1.808	0.2411
8.19	1.930	0.2451

Appendix C

Tabulated Lift and Moment Data

Appendix C contains all of the lift and moment data seen in Chapter 6. The data presented in this appendix is identified by airfoil name, figure number, and run number. As a note, the flap deflections are defined with the following notation: “p” is positive and “n” is negative. For example, the AG40d-02r with a -10 deg flap would have identified as “AG40d-02r fn10”.

AG40d-02r
Fig. 6.41

Run: 06823ga
Re = 99994.8

α	C_l	C_m
-10.10	-0.574	0.0494
-9.23	-0.595	0.0415
-8.20	-0.551	0.0208
-7.18	-0.480	-0.0219
-6.13	-0.360	-0.0504
-5.13	-0.279	-0.0503
-4.16	-0.196	-0.0474
-3.10	-0.108	-0.0475
-2.22	-0.033	-0.0514
-1.15	0.085	-0.0561
-0.10	0.238	-0.0675
0.87	0.380	-0.0808
1.98	0.493	-0.0756
2.89	0.563	-0.0684
4.03	0.669	-0.0639
5.01	0.755	-0.0590
6.04	0.851	-0.0577
7.14	0.925	-0.0531
8.04	0.982	-0.0498
9.13	1.028	-0.0461
10.14	1.064	-0.0437
11.11	1.097	-0.0795
12.04	1.020	-0.1291
13.03	0.992	-0.1571
14.05	0.953	-0.1612
14.97	0.954	-0.1655
16.00	0.916	-0.1593
17.00	0.945	-0.1662
17.97	0.927	-0.1658
18.96	0.938	-0.1665
20.03	0.999	-0.1714
19.77	0.961	-0.1676
18.70	0.963	-0.1562
17.83	0.944	-0.1472
16.68	0.951	-0.1473
15.79	0.946	-0.1457
14.72	0.959	-0.1445
13.69	0.932	-0.1348
12.78	0.946	-0.1294
11.74	1.034	-0.0944
10.87	1.108	-0.0330
9.87	1.079	-0.0328
8.81	1.039	-0.0356
7.83	0.987	-0.0419
6.92	0.941	-0.0457
5.81	0.850	-0.0491
4.81	0.766	-0.0518
3.69	0.673	-0.0555
2.69	0.569	-0.0533
1.77	0.497	-0.0642
0.64	0.367	-0.0627
-0.34	0.234	-0.0533
-1.41	0.081	-0.0435
-2.44	-0.030	-0.0456
-3.43	-0.108	-0.0468
-4.49	-0.201	-0.0496
-5.54	-0.287	-0.0506
-6.48	-0.374	-0.0427
-7.47	-0.496	0.0066
-8.48	-0.554	0.0348
-9.48	-0.604	0.0547

Run: 06825ga
Re = 199925.3

α	C_l	C_m
-10.09	-0.615	0.0599
-9.21	-0.595	0.0476
-8.26	-0.568	0.0269
-7.22	-0.482	-0.0179
-6.23	-0.355	-0.0526
-5.20	-0.267	-0.0531
-4.17	-0.156	-0.0570
-3.22	-0.045	-0.0628
-2.23	0.071	-0.0672
-1.21	0.181	-0.0682
-0.16	0.298	-0.0710
0.93	0.395	-0.0667
1.89	0.490	-0.0650
3.03	0.596	-0.0621
4.05	0.692	-0.0599
4.94	0.783	-0.0584
6.08	0.883	-0.0560
7.11	0.966	-0.0531
8.09	1.035	-0.0496
9.05	1.087	-0.0454
10.08	1.122	-0.0404
11.02	1.135	-0.0374
12.12	1.132	-0.1182
12.96	1.061	-0.1484
13.96	0.999	-0.1538
13.73	1.029	-0.1546
12.79	1.089	-0.1421
11.74	1.141	-0.0994
10.93	1.140	-0.0346
9.85	1.118	-0.0388
8.90	1.080	-0.0431
7.87	1.017	-0.0471
6.83	0.953	-0.0516
5.80	0.865	-0.0539
4.68	0.760	-0.0558
3.74	0.667	-0.0581
2.66	0.569	-0.0604
1.66	0.476	-0.0628
0.68	0.378	-0.0649
-0.43	0.277	-0.0676
-1.45	0.159	-0.0653
-2.39	0.047	-0.0630
-3.48	-0.073	-0.0585
-4.57	-0.192	-0.0525
-5.54	-0.293	-0.0508
-6.51	-0.384	-0.0454
-7.49	-0.510	-0.0010
-8.47	-0.596	0.0346
-9.48	-0.614	0.0556

Run: 06827gw
Re = 300042.4

α	C_l	C_m
-10.14	-0.636	0.0618
-9.21	-0.625	0.0474
-8.20	-0.586	0.0186
-7.20	-0.483	-0.0237
-6.37	-0.372	-0.0523
-5.26	-0.258	-0.0553
-4.16	-0.135	-0.0604
-3.12	-0.019	-0.0639
-2.11	0.091	-0.0675
-1.19	0.178	-0.0654
-0.11	0.295	-0.0645
0.94	0.402	-0.0634
1.92	0.498	-0.0618
3.05	0.611	-0.0604
4.02	0.705	-0.0590
5.11	0.803	-0.0569
6.11	0.890	-0.0552
7.16	0.980	-0.0524
8.12	1.049	-0.0493
9.16	1.111	-0.0443
10.20	1.147	-0.0391
11.17	1.154	-0.0371
12.00	1.167	-0.0873
13.05	1.122	-0.1405
14.11	1.065	-0.1548
13.76	1.104	-0.1534
12.77	1.124	-0.1295
12.04	1.171	-0.0897
10.98	1.163	-0.0356
9.83	1.140	-0.0394
8.84	1.099	-0.0449
7.83	1.033	-0.0488
6.76	0.954	-0.0523
5.82	0.871	-0.0544

4.75	0.774	-0.0561
3.73	0.677	-0.0574
2.79	0.588	-0.0589
1.69	0.479	-0.0606
0.65	0.373	-0.0616
-0.33	0.272	-0.0633
-1.40	0.165	-0.0646
-2.35	0.071	-0.0656
-3.48	-0.051	-0.0619
-4.51	-0.168	-0.0578
-5.47	-0.281	-0.0538
-6.56	-0.398	-0.0488
-7.48	-0.516	-0.0124
-8.53	-0.602	0.0287
-9.47	-0.621	0.0521

Run: 06829gw
Re = 400101.1

α	C_l	C_m
-7.22	-0.473	-0.0306
-6.32	-0.351	-0.0561
-5.28	-0.241	-0.0593
-4.19	-0.121	-0.0624
-3.13	-0.009	-0.0641
-2.12	0.090	-0.0644
-1.12	0.186	-0.0632
-0.15	0.292	-0.0622
0.98	0.407	-0.0616
2.05	0.514	-0.0604
3.04	0.614	-0.0591
4.02	0.708	-0.0577
5.20	0.819	-0.0561
6.19	0.909	-0.0541
7.14	1.002	-0.0519
8.10	1.067	-0.0488
9.19	1.136	-0.0442
10.28	1.187	-0.0394
11.26	1.195	-0.0396
10.91	1.196	-0.0367
9.82	1.160	-0.0406
8.83	1.120	-0.0455
7.88	1.061	-0.0493
6.91	0.977	-0.0518
5.72	0.876	-0.0545
4.79	0.780	-0.0556
3.69	0.675	-0.0572
2.77	0.584	-0.0582
1.69	0.475	-0.0595
0.71	0.373	-0.0605
-0.47	0.257	-0.0604
-1.39	0.162	-0.0626
-2.44	0.055	-0.0637
-3.47	-0.046	-0.0629
-4.54	-0.161	-0.0602
-5.43	-0.262	-0.0578
-6.53	-0.386	-0.0527

Run: 06831gw
Re = 499634.3

α	C_l	C_m
-7.18	-0.471	-0.0350
-6.20	-0.335	-0.0584
-5.20	-0.226	-0.0609
-4.11	-0.108	-0.0628
-3.11	-0.006	-0.0632
-2.25	0.083	-0.0626
-1.12	0.197	-0.0621
-0.02	0.306	-0.0601
1.03	0.420	-0.0607
2.03	0.519	-0.0592
2.96	0.609	-0.0578
4.07	0.725	-0.0569
5.00	0.818	-0.0554
6.02	0.911	-0.0533
7.17	0.997	-0.0507
8.21	1.090	-0.0483
9.11	1.144	-0.0451
10.20	1.193	-0.0417
11.26	1.220	-0.0401
10.83	1.216	-0.0422
9.83	1.173	-0.0422
8.89	1.131	-0.0449
7.71	1.053	-0.0490
6.67	0.959	-0.0513
5.66	0.875	-0.0537
4.74	0.784	-0.0546
3.63	0.682	-0.0564
2.66	0.581	-0.0571
1.65	0.480	-0.0584
0.65	0.380	-0.0593
-0.25	0.278	-0.0593
-1.33	0.174	-0.0611
-2.33	0.064	-0.0617
-3.54	-0.048	-0.0620
-4.48	-0.148	-0.0611
-5.60	-0.270	-0.0589
-6.60	-0.376	-0.0551

AG40d-02r fn20

Fig. 6.44

Run: 06915ga
Re = 100029.0

α	C_l	C_m
-8.07	-1.002	0.1760
-7.14	-1.039	0.1692
-6.24	-1.046	0.1567
-5.24	-1.024	0.1403
-4.25	-1.025	0.1116
-3.27	-0.983	0.0926
-2.22	-0.882	0.0894
-1.23	-0.773	0.0895
-0.20	-0.672	0.0909
0.82	-0.626	0.0961
1.84	-0.439	0.0881
2.97	-0.326	0.0859
3.97	-0.224	0.0841
4.96	-0.145	0.0887
6.02	-0.090	0.0971
6.96	-0.035	0.1081
8.03	0.037	0.1148
9.01	0.131	0.1200
10.02	0.205	0.1221
11.14	0.284	0.1251
12.15	0.359	0.1264
13.13	0.420	0.1242
14.22	0.479	0.1233
15.09	0.467	0.0445
16.00	0.416	0.0231
17.07	0.431	0.0141
17.96	0.435	0.0089
17.79	0.449	0.0200
16.80	0.420	0.0275
15.77	0.427	0.0340
14.88	0.532	0.1263
13.98	0.479	0.1318
12.89	0.413	0.1360
11.85	0.360	0.1377
10.84	0.280	0.1337
9.89	0.215	0.1355
8.81	0.121	0.1298
7.77	0.038	0.1251
6.76	-0.031	0.1150
5.73	-0.087	0.1069
4.75	-0.158	0.0987
3.63	-0.240	0.0972
2.64	-0.344	0.0989
1.58	-0.528	0.1131
0.61	-0.619	0.1004
-0.27	-0.669	0.0924

-1.51	-0.785	0.0903
-2.50	-0.903	0.0934
-3.55	-0.993	0.1032
-4.48	-1.040	0.1283
-5.49	-1.041	0.1581
-6.47	-1.073	0.1713
-7.47	-1.027	0.1845

Run: 06917gw
Re = 199782.1

α	C_l	C_m
-6.19	-1.049	0.1632
-5.23	-1.075	0.1408
-4.26	-1.043	0.1171
-3.27	-0.988	0.1008
-2.17	-0.897	0.0991
-1.16	-0.789	0.1039
-0.22	-0.727	0.1099
0.79	-0.660	0.1163
1.89	-0.436	0.1112
3.01	-0.306	0.1094
3.95	-0.225	0.1149
4.99	-0.160	0.1217
5.97	-0.101	0.1295
7.09	-0.030	0.1357
8.07	0.036	0.1400
9.10	0.122	0.1424
10.12	0.221	0.1428
11.16	0.332	0.1385
12.09	0.439	0.1300
13.12	0.547	0.1175
14.20	0.619	0.1008
15.13	0.542	0.0080
16.04	0.538	0.0021
17.12	0.549	-0.0015
18.09	0.549	-0.0014
17.71	0.554	0.0007
16.64	0.542	0.0029
15.70	0.540	0.0088
14.71	0.523	0.0201
13.71	0.593	0.1132
12.77	0.508	0.1285
11.85	0.399	0.1375
10.71	0.278	0.1438
9.70	0.170	0.1456
8.70	0.083	0.1454
7.66	-0.003	0.1418
6.66	-0.065	0.1367
5.61	-0.121	0.1293
4.65	-0.175	0.1214
3.58	-0.251	0.1151
2.57	-0.343	0.1110
1.51	-0.614	0.1237

0.42	-0.673	0.1139
-0.53	-0.743	0.1080
-1.62	-0.839	0.1043
-2.59	-0.936	0.1001
-3.57	-1.009	0.1075
-4.64	-1.056	0.1293
-5.56	-1.060	0.1519

Run: 06919gw
Re = 300366.5

α	C_l	C_m
-6.24	-1.091	0.1663
-5.24	-1.086	0.1445
-4.31	-1.075	0.1233
-3.24	-1.022	0.1040
-2.32	-0.965	0.1009
-1.13	-0.864	0.1093
-0.16	-0.782	0.1144
0.80	-0.713	0.1211
1.94	-0.641	0.1286
2.92	-0.417	0.1203
3.88	-0.346	0.1257
4.89	-0.300	0.1350
6.04	-0.243	0.1422
7.03	-0.165	0.1427
8.07	-0.067	0.1429
9.02	0.030	0.1427
9.99	0.124	0.1411
11.17	0.247	0.1393
12.16	0.354	0.1338
13.23	0.477	0.1267
14.20	0.584	0.1131
15.17	0.651	0.0937
16.04	0.580	0.0105
17.05	0.567	0.0018
17.96	0.557	-0.0013
17.78	0.570	-0.0022
16.74	0.577	0.0061
15.71	0.595	0.0263
14.82	0.633	0.1035
13.91	0.554	0.1196
12.86	0.439	0.1298
11.86	0.329	0.1373
10.81	0.215	0.1409
9.80	0.110	0.1434
8.82	0.013	0.1439
7.77	-0.090	0.1451
6.77	-0.181	0.1445
5.63	-0.263	0.1414
4.70	-0.315	0.1361
3.58	-0.361	0.1251
2.51	-0.600	0.1333
1.59	-0.660	0.1266

0.53	-0.735	0.1188
-0.37	-0.792	0.1126
-1.60	-0.900	0.1068
-2.52	-0.976	0.1015
-3.58	-1.045	0.1093
-4.55	-1.085	0.1289
-5.50	-1.097	0.1508

Run: 06921gw
Re = 399938.9

α	C_l	C_m
-3.25	-1.046	0.1059
-2.17	-0.967	0.1025
-1.26	-0.897	0.1121
-0.12	-0.803	0.1182
0.84	-0.738	0.1241
1.82	-0.664	0.1290
3.02	-0.580	0.1369
3.94	-0.473	0.1422
5.01	-0.375	0.1428
6.04	-0.275	0.1432
7.10	-0.170	0.1414
8.07	-0.070	0.1415
9.08	0.029	0.1408
10.07	0.139	0.1403
11.12	0.244	0.1387
12.08	0.352	0.1338
13.24	0.481	0.1264
14.30	0.593	0.1131
15.23	0.671	0.0882
14.81	0.644	0.1001
13.89	0.558	0.1190
12.91	0.447	0.1294
11.83	0.328	0.1359
10.84	0.219	0.1391
9.87	0.110	0.1407
8.69	-0.004	0.1423
7.70	-0.108	0.1432
6.66	-0.212	0.1435
5.64	-0.309	0.1431
4.68	-0.407	0.1432
3.69	-0.489	0.1432
2.62	-0.599	0.1336
1.64	-0.678	0.1288
0.56	-0.757	0.1225
-0.41	-0.826	0.1158
-1.39	-0.920	0.1114
-2.54	-0.992	0.1023

Run: 06923gw
Re = 500098.0

α	C_l	C_m
-3.10	-1.028	0.1029
-2.26	-0.971	0.1012
-1.06	-0.886	0.1125
-0.05	-0.811	0.1182
0.98	-0.731	0.1239
1.89	-0.658	0.1278
2.99	-0.565	0.1329
4.07	-0.481	0.1404
4.93	-0.393	0.1419
6.11	-0.273	0.1412
7.02	-0.178	0.1416
8.04	-0.070	0.1399
9.10	0.040	0.1402
10.03	0.140	0.1387
11.12	0.255	0.1363
12.22	0.376	0.1326
13.29	0.496	0.1249
14.29	0.608	0.1128
15.09	0.682	0.0900
14.81	0.657	0.0996
13.89	0.562	0.1191
12.91	0.451	0.1287
11.83	0.335	0.1351
10.73	0.213	0.1376
9.79	0.116	0.1392
8.69	-0.002	0.1404
7.61	-0.109	0.1416
6.73	-0.208	0.1419
5.69	-0.309	0.1405
4.56	-0.436	0.1417
3.61	-0.529	0.1393
2.51	-0.606	0.1306
1.42	-0.688	0.1260
0.46	-0.777	0.1218
-0.50	-0.841	0.1156
-1.52	-0.920	0.1082
-2.45	-0.989	0.1015

AG40d-02r fn15

Fig. 6.47

Run: 06833gw
Re = 99930.7

α	C_l	C_m
-8.17	-0.872	0.1500
-7.06	-0.886	0.1363
-6.13	-0.897	0.1172
-5.20	-0.874	0.0914
-4.15	-0.789	0.0644
-3.19	-0.714	0.0605
-2.24	-0.639	0.0630
-1.13	-0.552	0.0663
-0.11	-0.482	0.0671
0.89	-0.429	0.0801
1.92	-0.280	0.0715
2.99	-0.207	0.0762
3.95	-0.138	0.0770
5.01	-0.078	0.0844
5.98	-0.022	0.0960
7.05	0.066	0.0997
8.13	0.167	0.1007
9.09	0.259	0.1010
10.03	0.350	0.0997
11.10	0.458	0.0969
12.19	0.548	0.0909
13.16	0.624	0.0854
14.06	0.569	-0.0057
14.98	0.567	-0.0250
15.97	0.614	-0.0379
17.04	0.610	-0.0420
18.05	0.616	-0.0462
17.82	0.616	-0.0355
16.80	0.620	-0.0309
15.82	0.594	-0.0230
14.81	0.594	-0.0126
13.89	0.683	0.0872
12.85	0.632	0.0987
11.91	0.551	0.1042
10.85	0.455	0.1093
9.75	0.345	0.1105
8.77	0.248	0.1125
7.69	0.154	0.1125
6.80	0.068	0.1112
5.73	-0.015	0.1075
4.71	-0.065	0.0947
3.64	-0.127	0.0883
2.62	-0.202	0.0844
1.66	-0.311	0.0926
0.60	-0.424	0.0847
-0.32	-0.473	0.0696
-1.41	-0.558	0.0667
-2.44	-0.648	0.0634
-3.54	-0.733	0.0647
-4.51	-0.821	0.0812
-5.48	-0.872	0.1142
-6.43	-0.887	0.1411
-7.45	-0.888	0.1548

Run: 06835rd
Re = 200009.5

α	C_l	C_m
-8.07	-0.955	0.1620
-7.16	-0.953	0.1478
-6.14	-0.968	0.1302
-5.24	-0.945	0.1051
-4.19	-0.889	0.0769
-3.15	-0.797	0.0660
-2.23	-0.723	0.0725
-1.24	-0.642	0.0763
-0.10	-0.548	0.0806
0.89	-0.467	0.0841
1.91	-0.407	0.0993
3.02	-0.301	0.1000
3.97	-0.209	0.1014
4.98	-0.113	0.1012
5.97	-0.021	0.1008
7.02	0.084	0.1001
8.05	0.194	0.0996
9.13	0.308	0.0976
10.11	0.419	0.0960
11.18	0.531	0.0920
12.09	0.616	0.0862
13.20	0.701	0.0790
14.20	0.754	0.0648
15.01	0.664	-0.0302
16.05	0.657	-0.0390
16.99	0.666	-0.0429
18.00	0.677	-0.0478
17.79	0.687	-0.0453
16.80	0.665	-0.0389
15.74	0.671	-0.0379
14.82	0.682	-0.0157
13.97	0.747	0.0733
12.98	0.695	0.0833
11.95	0.610	0.0905
10.80	0.506	0.0972
9.82	0.396	0.0998
8.80	0.287	0.1018
7.77	0.179	0.1027
6.69	0.063	0.1038
5.69	-0.041	0.1032
4.72	-0.137	0.1041
3.63	-0.236	0.1037
2.70	-0.326	0.1015
1.53	-0.433	0.1006
0.53	-0.487	0.0837
-0.36	-0.565	0.0796
-1.45	-0.654	0.0766
-2.48	-0.742	0.0713
-3.53	-0.831	0.0703
-4.59	-0.904	0.0869

-5.52	-0.939	0.1161
-6.44	-0.958	0.1404
-7.52	-0.964	0.1593

Run: 06837gw
Re = 299948.8

α	C_l	C_m
-8.11	-0.971	0.1626
-7.21	-0.981	0.1522
-6.16	-0.998	0.1281
-5.22	-0.966	0.1012
-4.17	-0.900	0.0765
-3.18	-0.826	0.0701
-2.18	-0.742	0.0774
-1.14	-0.655	0.0820
-0.16	-0.572	0.0852
0.93	-0.482	0.0895
1.87	-0.424	0.0994
3.04	-0.308	0.1009
4.08	-0.203	0.1005
4.91	-0.117	0.1002
5.97	-0.010	0.0994
7.06	0.102	0.0988
8.03	0.203	0.0974
9.05	0.312	0.0964
10.13	0.428	0.0950
11.19	0.538	0.0910
12.18	0.642	0.0855
13.21	0.722	0.0774
14.18	0.779	0.0627
15.10	0.711	-0.0242
15.99	0.685	-0.0379
15.86	0.710	-0.0367
14.86	0.739	-0.0076
13.88	0.768	0.0689
12.82	0.702	0.0823
11.82	0.611	0.0902
10.78	0.500	0.0935
9.85	0.404	0.0966
8.84	0.301	0.0984
7.72	0.181	0.0995
6.71	0.071	0.0999
5.65	-0.034	0.1007
4.73	-0.128	0.1010
3.70	-0.230	0.1020
2.54	-0.348	0.1021
1.72	-0.430	0.0984
0.63	-0.507	0.0889
-0.53	-0.601	0.0841
-1.47	-0.684	0.0800
-2.48	-0.763	0.0753
-3.53	-0.843	0.0704
-4.56	-0.934	0.0856
-5.46	-0.977	0.1096
-6.48	-0.991	0.1388
-7.53	-0.971	0.1568

Run: 06839gw
Re = 400084.9

α	C_l	C_m
-5.32	-0.984	0.1039
-4.22	-0.915	0.0765
-3.18	-0.837	0.0697
-2.18	-0.759	0.0786
-1.03	-0.667	0.0834
-0.23	-0.597	0.0869
0.88	-0.504	0.0905
2.02	-0.411	0.0969
2.91	-0.326	0.0993
4.03	-0.217	0.0992
4.92	-0.118	0.0985
6.06	-0.005	0.0992
7.08	0.105	0.0977
8.12	0.212	0.0966
9.07	0.320	0.0956
10.06	0.426	0.0937
11.07	0.533	0.0912
12.21	0.649	0.0851
13.17	0.730	0.0778
14.20	0.806	0.0563
13.86	0.783	0.0664
12.92	0.713	0.0814
11.95	0.614	0.0880
10.80	0.503	0.0929
9.75	0.396	0.0959
8.82	0.291	0.0966
7.70	0.175	0.0979
6.67	0.063	0.0989
5.68	-0.043	0.0991
4.73	-0.141	0.0998
3.63	-0.255	0.0997
2.50	-0.369	0.1003
1.53	-0.441	0.0932
0.48	-0.543	0.0897
-0.40	-0.613	0.0857
-1.54	-0.715	0.0815
-2.50	-0.788	0.0757
-3.58	-0.866	0.0700
-4.54	-0.937	0.0837

Run: 06841gw
Re = 500080.8

α	C_l	C_m
-4.18	-0.906	0.0751
-3.14	-0.832	0.0691
-2.21	-0.772	0.0788
-1.15	-0.677	0.0826
-0.20	-0.593	0.0864
1.00	-0.488	0.0895
1.94	-0.404	0.0925
2.99	-0.313	0.0981
3.98	-0.209	0.0974
5.08	-0.100	0.0973
6.05	0.004	0.0969
7.02	0.105	0.0975
8.15	0.224	0.0956
9.08	0.328	0.0949
10.07	0.436	0.0935
11.21	0.553	0.0896
12.17	0.655	0.0841
13.13	0.749	0.0778
14.23	0.833	0.0551
13.83	0.808	0.0678
12.80	0.712	0.0821
11.74	0.609	0.0880
10.83	0.521	0.0924
9.75	0.401	0.0948
8.69	0.290	0.0965
7.76	0.189	0.0971
6.71	0.068	0.0978
5.61	-0.040	0.0982
4.60	-0.148	0.0983
3.65	-0.244	0.0981
2.57	-0.356	0.0972
1.49	-0.438	0.0916
0.56	-0.536	0.0890
-0.32	-0.609	0.0859
-1.55	-0.714	0.0814
-2.46	-0.789	0.0772
-3.60	-0.863	0.0692

AG40d-02r fn10
Fig. 6.50

Run: 06843gw
Re = 99982.8

α	C_l	C_m
-8.16	-0.857	0.1168
-7.11	-0.834	0.1002
-6.16	-0.802	0.0729
-5.19	-0.732	0.0395
-4.20	-0.635	0.0285
-3.11	-0.548	0.0302
-2.11	-0.466	0.0307
-1.18	-0.388	0.0314
-0.08	-0.307	0.0317
0.95	-0.155	0.0262
1.87	-0.051	0.0205

3.02	0.051	0.0216
4.00	0.140	0.0259
4.93	0.239	0.0268
6.00	0.345	0.0292
7.05	0.451	0.0324
8.10	0.540	0.0336
9.09	0.624	0.0377
10.16	0.705	0.0376
11.20	0.771	0.0353
12.18	0.809	0.0336
13.05	0.790	-0.0398
13.98	0.756	-0.0757
15.01	0.754	-0.0852
15.95	0.749	-0.0861
16.92	0.772	-0.0934
18.12	0.766	-0.0912
17.71	0.743	-0.0787
16.68	0.764	-0.0789
15.73	0.755	-0.0725
14.70	0.760	-0.0679
13.81	0.747	-0.0572
12.87	0.851	0.0382
11.85	0.826	0.0410
10.84	0.765	0.0413
9.82	0.689	0.0428
8.84	0.611	0.0417
7.81	0.532	0.0385
6.85	0.442	0.0371
5.77	0.333	0.0397
4.74	0.222	0.0373
3.69	0.124	0.0352
2.68	0.033	0.0340
1.68	-0.063	0.0329
0.59	-0.204	0.0432
-0.35	-0.321	0.0418
-1.42	-0.400	0.0328
-2.45	-0.493	0.0324
-3.37	-0.571	0.0304
-4.56	-0.677	0.0327
-5.42	-0.753	0.0594
-6.49	-0.815	0.0958
-7.45	-0.831	0.1218

Run: 06845ga
Re = 200145.6

α	C_l	C_m
-9.14	-0.860	0.1370
-8.21	-0.860	0.1248
-7.12	-0.866	0.1081
-6.15	-0.848	0.0801
-5.25	-0.778	0.0496
-4.28	-0.677	0.0281
-3.11	-0.576	0.0317

-2.15	-0.489	0.0329
-1.15	-0.401	0.0346
-0.07	-0.309	0.0374
0.84	-0.244	0.0454
2.03	-0.139	0.0520
3.07	-0.040	0.0518
4.04	0.062	0.0515
5.07	0.168	0.0512
5.92	0.260	0.0503
7.10	0.381	0.0487
8.00	0.482	0.0470
9.14	0.605	0.0443
10.21	0.708	0.0404
11.14	0.780	0.0377
12.10	0.842	0.0363
13.11	0.874	0.0317
14.08	0.834	-0.0695
15.04	0.751	-0.0779
14.73	0.760	-0.0745
13.74	0.818	-0.0598
12.82	0.871	0.0366
11.81	0.830	0.0395
10.79	0.764	0.0411
9.81	0.675	0.0444
8.81	0.575	0.0479
7.67	0.458	0.0505
6.78	0.355	0.0521
5.78	0.253	0.0532
4.79	0.148	0.0532
3.73	0.033	0.0537
2.61	-0.081	0.0541
1.63	-0.175	0.0541
0.64	-0.262	0.0474
-0.46	-0.338	0.0379
-1.40	-0.419	0.0355
-2.37	-0.499	0.0326
-3.41	-0.588	0.0305
-4.50	-0.698	0.0335
-5.45	-0.788	0.0572
-6.52	-0.839	0.0966
-7.50	-0.869	0.1168
-8.44	-0.847	0.1323

Run: 06847ga
Re = 300113.3

α	C_l	C_m
-9.17	-0.880	0.1380
-8.17	-0.882	0.1251
-7.16	-0.878	0.1076
-6.23	-0.849	0.0773
-5.25	-0.781	0.0451
-4.17	-0.673	0.0286
-3.10	-0.589	0.0349

-2.24	-0.506	0.0370
-1.19	-0.416	0.0390
-0.12	-0.319	0.0409
0.96	-0.232	0.0475
1.95	-0.136	0.0497
2.90	-0.044	0.0490
3.91	0.062	0.0485
4.93	0.170	0.0484
6.04	0.288	0.0481
7.02	0.391	0.0476
8.01	0.493	0.0477
9.06	0.598	0.0464
10.17	0.709	0.0442
11.14	0.800	0.0405
12.17	0.876	0.0366
13.06	0.902	0.0308
14.04	0.884	-0.0494
15.00	0.839	-0.0743
14.74	0.880	-0.0712
13.67	0.903	-0.0021
12.94	0.899	0.0343
11.78	0.854	0.0397
10.79	0.771	0.0436
9.86	0.681	0.0463
8.71	0.568	0.0485
7.70	0.465	0.0491
6.82	0.377	0.0494
5.77	0.262	0.0495
4.76	0.157	0.0496
3.65	0.043	0.0498
2.63	-0.060	0.0502
1.70	-0.155	0.0508
0.71	-0.249	0.0469
-0.39	-0.335	0.0408
-1.51	-0.437	0.0387
-2.47	-0.533	0.0366
-3.55	-0.614	0.0328
-4.52	-0.708	0.0323
-5.51	-0.803	0.0557
-6.51	-0.851	0.0907
-7.50	-0.883	0.1145
-8.46	-0.880	0.1319

Run: 06849gw
Re = 400196.8

α	C_l	C_m
-5.19	-0.767	0.0419
-4.22	-0.675	0.0293
-3.25	-0.599	0.0350
-2.19	-0.501	0.0378
-1.13	-0.403	0.0397
-0.04	-0.291	0.0415
0.92	-0.213	0.0457

1.90	-0.122	0.0481
2.98	-0.012	0.0472
3.92	0.084	0.0472
5.03	0.200	0.0470
6.10	0.309	0.0465
7.03	0.411	0.0462
8.12	0.523	0.0456
9.11	0.634	0.0451
10.13	0.732	0.0439
11.07	0.819	0.0416
12.17	0.898	0.0375
13.19	0.950	0.0245
12.81	0.934	0.0325
11.84	0.880	0.0399
10.85	0.795	0.0429
9.77	0.694	0.0452
8.77	0.595	0.0460
7.84	0.500	0.0468
6.77	0.385	0.0474
5.76	0.278	0.0474
4.70	0.162	0.0476
3.72	0.062	0.0482
2.66	-0.046	0.0487
1.56	-0.155	0.0492
0.67	-0.232	0.0444
-0.31	-0.320	0.0415
-1.46	-0.432	0.0397
-2.42	-0.521	0.0374
-3.37	-0.605	0.0347
-4.46	-0.697	0.0311

Run: 06851gw
Re = 499801.2

α	C_l	C_m
-5.27	-0.784	0.0440
-4.31	-0.691	0.0288
-3.18	-0.613	0.0357
-2.15	-0.510	0.0378
-1.21	-0.424	0.0396
-0.21	-0.323	0.0411
0.87	-0.221	0.0433
1.89	-0.133	0.0472
2.99	-0.018	0.0468
3.93	0.076	0.0465
4.89	0.183	0.0464
6.10	0.307	0.0461
7.01	0.405	0.0457
8.11	0.517	0.0453
9.11	0.628	0.0446
10.20	0.728	0.0430
11.04	0.817	0.0411
12.10	0.898	0.0372
13.14	0.959	0.0264
12.86	0.943	0.0332
11.91	0.877	0.0392
10.90	0.801	0.0420
9.82	0.698	0.0444
8.78	0.595	0.0457
7.75	0.491	0.0462
6.84	0.385	0.0464
5.70	0.269	0.0472
4.70	0.162	0.0474
3.65	0.050	0.0474
2.64	-0.058	0.0477
1.58	-0.162	0.0481
0.59	-0.250	0.0429
-0.45	-0.345	0.0414
-1.39	-0.440	0.0398
-2.40	-0.533	0.0376
-3.43	-0.629	0.0349
-4.45	-0.704	0.0303

AG40d-02r fn5
Fig. 6.53

Run: 06853gw
Re = 99988.5

α	C_l	C_m
-10.24	-0.762	0.0987
-9.21	-0.746	0.0894
-8.25	-0.728	0.0762
-7.24	-0.697	0.0541
-6.21	-0.631	0.0146
-5.35	-0.529	-0.0111
-4.18	-0.425	-0.0103
-3.15	-0.340	-0.0094
-2.14	-0.256	-0.0084
-1.17	-0.163	-0.0159
-0.11	-0.032	-0.0251
0.86	0.095	-0.0341
1.83	0.186	-0.0322
2.99	0.279	-0.0242
3.87	0.355	-0.0194
5.02	0.456	-0.0140
5.95	0.541	-0.0103
7.04	0.637	-0.0085
8.09	0.723	-0.0065
9.04	0.784	-0.0049
10.08	0.848	-0.0039
11.09	0.893	-0.0031
12.08	0.919	-0.0132
12.98	0.861	-0.1074
14.02	0.794	-0.1170
14.97	0.809	-0.1266
15.92	0.812	-0.1307
15.74	0.828	-0.1198
14.69	0.786	-0.1081
13.78	0.841	-0.1063
12.79	0.815	-0.0858
11.89	0.925	0.0023
10.83	0.897	0.0042
9.94	0.851	0.0027
8.85	0.787	0.0000
7.76	0.712	-0.0028
6.87	0.631	-0.0030
5.77	0.534	-0.0056
4.78	0.446	-0.0083
3.68	0.351	-0.0135
2.68	0.267	-0.0167
1.69	0.188	-0.0193
0.60	0.080	-0.0191
-0.39	-0.037	-0.0097
-1.37	-0.165	-0.0023
-2.49	-0.262	-0.0103
-3.42	-0.349	-0.0108
-4.57	-0.447	-0.0116
-5.51	-0.544	-0.0057
-6.47	-0.659	0.0358
-7.51	-0.710	0.0766
-8.51	-0.739	0.0942
-9.48	-0.722	0.0999

Run: 06855gw
Re = 200128.9

α	C_l	C_m
-10.26	-0.738	0.1035
-9.18	-0.732	0.0946
-8.14	-0.729	0.0780
-7.24	-0.698	0.0559
-6.22	-0.624	0.0146
-5.16	-0.501	-0.0128
-4.22	-0.418	-0.0109
-3.19	-0.324	-0.0101
-2.14	-0.219	-0.0129
-1.14	-0.121	-0.0159
-0.09	-0.013	-0.0127
0.90	0.098	-0.0169
1.94	0.195	-0.0152
3.03	0.304	-0.0135
3.98	0.397	-0.0124
5.04	0.507	-0.0111
6.08	0.609	-0.0098
7.13	0.710	-0.0091
8.11	0.788	-0.0078
9.16	0.866	-0.0068
10.13	0.941	-0.0050
11.16	0.983	-0.0032
12.17	1.008	-0.0044

12.99	1.022	-0.0890
13.99	0.932	-0.1220
13.74	0.905	-0.1154
12.89	1.011	-0.0766
12.01	1.011	-0.0002
10.85	0.977	-0.0005
9.88	0.927	-0.0024
8.85	0.852	-0.0036
7.81	0.775	-0.0050
6.89	0.691	-0.0061
5.77	0.584	-0.0073
4.81	0.492	-0.0085
3.64	0.380	-0.0103
2.67	0.279	-0.0118
1.66	0.181	-0.0136
0.60	0.080	-0.0157
-0.40	-0.044	-0.0094
-1.42	-0.134	-0.0136
-2.47	-0.251	-0.0098
-3.41	-0.337	-0.0101
-4.55	-0.438	-0.0115
-5.50	-0.532	-0.0058
-6.48	-0.644	0.0278
-7.44	-0.720	0.0690
-8.45	-0.734	0.0899
-9.39	-0.729	0.1008

Run: 06857gw
Re = 300124.6

α	C_l	C_m
-5.28	-0.516	-0.0122
-4.20	-0.412	-0.0104
-3.15	-0.309	-0.0109
-2.10	-0.200	-0.0126
-1.14	-0.110	-0.0116
-0.08	-0.024	-0.0070
0.92	0.106	-0.0134
1.90	0.194	-0.0126
3.03	0.307	-0.0112
3.90	0.399	-0.0107
4.95	0.505	-0.0097
6.03	0.610	-0.0090
7.12	0.716	-0.0082
8.07	0.809	-0.0073
9.18	0.901	-0.0062
10.11	0.966	-0.0047
11.10	1.016	-0.0032
12.13	1.042	-0.0047
13.12	1.016	-0.0763
14.05	0.980	-0.1107
13.73	1.019	-0.0999
12.81	1.049	-0.0567
11.85	1.032	-0.0006
10.95	1.011	-0.0014
9.89	0.958	-0.0035
8.83	0.876	-0.0049
7.80	0.790	-0.0060
6.74	0.687	-0.0070
5.71	0.585	-0.0077
4.76	0.493	-0.0086
3.75	0.391	-0.0093
2.76	0.290	-0.0102
1.68	0.186	-0.0114
0.70	0.074	-0.0102
-0.36	-0.049	-0.0072
-1.44	-0.139	-0.0111
-2.45	-0.237	-0.0119
-3.52	-0.352	-0.0104
-4.55	-0.442	-0.0107

Run: 06859gw
Re = 400182.4

α	C_l	C_m
-5.33	-0.528	-0.0129
-4.32	-0.442	-0.0117
-3.29	-0.335	-0.0116
-2.20	-0.224	-0.0107
-1.15	-0.123	-0.0102
-0.14	-0.030	-0.0079
0.88	0.069	-0.0064
1.95	0.201	-0.0106
2.91	0.303	-0.0104
3.96	0.409	-0.0095
5.00	0.512	-0.0087
5.98	0.613	-0.0079
7.11	0.726	-0.0071
8.17	0.815	-0.0062
9.11	0.910	-0.0054
10.10	0.988	-0.0042
11.18	1.042	-0.0024
12.19	1.075	-0.0080
11.91	1.072	-0.0024
10.85	1.025	-0.0026
9.87	0.966	-0.0042
8.94	0.895	-0.0049
7.81	0.788	-0.0058
6.75	0.688	-0.0065
5.82	0.600	-0.0071
4.85	0.499	-0.0079
3.74	0.386	-0.0086
2.73	0.285	-0.0094
1.72	0.176	-0.0091
0.60	0.044	-0.0050
-0.36	-0.043	-0.0081
-1.48	-0.153	-0.0094
-2.36	-0.240	-0.0098
-3.48	-0.352	-0.0109
-4.55	-0.457	-0.0109

AG40d-02r fp5
Fig. 6.56

Run: 06881gw
Re = 100071.2

α	C_l	C_m
-10.20	-0.469	0.0120
-9.27	-0.471	0.0060
-8.22	-0.380	-0.0387
-7.35	-0.216	-0.0978
-6.15	-0.121	-0.1025
-5.21	-0.016	-0.1086
-4.20	0.092	-0.1136
-3.11	0.203	-0.1132
-2.15	0.281	-0.1105
-1.15	0.381	-0.1128
-0.15	0.474	-0.1148
0.96	0.607	-0.1238
1.84	0.720	-0.1242
2.99	0.821	-0.1155
4.06	0.898	-0.1053
4.92	0.962	-0.1025
5.99	1.030	-0.0963
6.98	1.070	-0.0883
8.08	1.117	-0.0790
9.05	1.131	-0.0741
10.06	1.154	-0.0725
10.99	1.129	-0.1336
11.93	1.039	-0.1795
12.90	1.041	-0.1932
14.01	0.994	-0.1930
13.75	1.033	-0.1814
12.75	0.978	-0.1695
11.80	1.046	-0.1590
10.79	1.139	-0.0863
9.88	1.169	-0.0631
8.90	1.150	-0.0678
7.81	1.117	-0.0752
6.83	1.085	-0.0825
5.83	1.040	-0.0928
4.77	0.967	-0.0972
3.76	0.889	-0.1009
2.76	0.812	-0.1025
1.75	0.728	-0.1103
0.63	0.568	-0.1067
-0.30	0.463	-0.0979
-1.37	0.376	-0.0984
-2.46	0.269	-0.1019
-3.35	0.191	-0.1033

-4.46	0.080	-0.1000
-5.43	-0.029	-0.0964
-6.45	-0.147	-0.0913
-7.58	-0.248	-0.0792
-8.54	-0.415	-0.0043
-9.52	-0.471	0.0205

Run: 06883gw

Re = 200061.6

α	C_l	C_m
-10.24	-0.463	0.0097
-9.24	-0.407	-0.0169
-8.30	-0.294	-0.0718
-7.22	-0.123	-0.1156
-6.24	-0.030	-0.1189
-5.34	0.063	-0.1207
-4.15	0.177	-0.1235
-3.20	0.277	-0.1264
-2.21	0.375	-0.1255
-1.15	0.480	-0.1242
-0.06	0.596	-0.1255
0.95	0.697	-0.1204
1.97	0.790	-0.1164
2.95	0.874	-0.1111
4.02	0.956	-0.1066
4.93	1.029	-0.1029
6.09	1.106	-0.0976
7.07	1.154	-0.0902
8.09	1.201	-0.0824
9.12	1.227	-0.0755
10.08	1.237	-0.0698
11.06	1.245	-0.1336
11.92	1.167	-0.1739
12.85	1.142	-0.1887
14.02	1.071	-0.1926
13.69	1.083	-0.1897
12.76	1.134	-0.1868
11.81	1.235	-0.1647
10.79	1.248	-0.1235
9.86	1.239	-0.0676
8.82	1.223	-0.0744
7.82	1.186	-0.0810
6.84	1.147	-0.0891
5.75	1.086	-0.0960
4.80	1.027	-0.1006
3.81	0.943	-0.1040
2.68	0.858	-0.1089
1.73	0.779	-0.1147
0.67	0.675	-0.1198
-0.31	0.573	-0.1226
-1.32	0.461	-0.1209
-2.43	0.356	-0.1230
-3.42	0.259	-0.1228

-4.53	0.152	-0.1204
-5.40	0.056	-0.1171
-6.46	-0.048	-0.1146
-7.55	-0.157	-0.1102
-8.46	-0.321	-0.0514
-9.52	-0.428	-0.0070

Run: 06885gw

Re = 299880.1

α	C_l	C_m
-10.32	-0.455	0.0069
-9.23	-0.399	-0.0273
-8.35	-0.296	-0.0709
-7.23	-0.132	-0.1121
-6.31	-0.035	-0.1155
-5.21	0.074	-0.1174
-4.23	0.173	-0.1193
-3.14	0.293	-0.1226
-2.20	0.390	-0.1231
-1.09	0.506	-0.1230
-0.13	0.601	-0.1198
0.86	0.693	-0.1170
1.98	0.799	-0.1126
3.01	0.885	-0.1089
3.99	0.972	-0.1059
4.95	1.052	-0.1017
6.21	1.141	-0.0960
7.05	1.185	-0.0904
8.18	1.239	-0.0827
9.04	1.269	-0.0760
10.06	1.267	-0.0692
11.11	1.290	-0.1080
12.04	1.253	-0.1633
12.92	1.193	-0.1864
13.99	1.156	-0.1952
13.71	1.167	-0.1919
12.70	1.213	-0.1771
11.83	1.292	-0.1525
10.84	1.285	-0.0889
9.87	1.274	-0.0692
8.89	1.261	-0.0749
7.90	1.232	-0.0826
6.76	1.176	-0.0910
5.85	1.121	-0.0966
4.77	1.045	-0.1026
3.75	0.964	-0.1057
2.77	0.880	-0.1084
1.61	0.780	-0.1131
0.60	0.679	-0.1154
-0.25	0.595	-0.1180
-1.35	0.491	-0.1213
-2.42	0.370	-0.1211
-3.49	0.260	-0.1193

-4.50	0.149	-0.1167
-5.41	0.056	-0.1157
-6.52	-0.057	-0.1133
-7.58	-0.160	-0.1101
-8.54	-0.323	-0.0592
-9.45	-0.422	-0.0169

Run: 06887gw

Re = 399973.5

α	C_l	C_m
-8.20	-0.277	-0.0823
-7.25	-0.136	-0.1113
-6.16	-0.032	-0.1139
-5.26	0.067	-0.1156
-4.12	0.186	-0.1172
-3.15	0.288	-0.1192
-2.18	0.396	-0.1201
-1.08	0.514	-0.1198
-0.02	0.618	-0.1172
0.98	0.714	-0.1137
2.00	0.802	-0.1103
2.93	0.894	-0.1081
4.00	0.984	-0.1049
5.05	1.065	-0.1002
6.12	1.141	-0.0953
7.02	1.197	-0.0898
8.14	1.252	-0.0823
9.04	1.285	-0.0766
10.06	1.303	-0.0715
11.17	1.283	-0.0830
10.85	1.287	-0.0741
9.93	1.296	-0.0701
8.79	1.276	-0.0766
7.76	1.246	-0.0853
6.72	1.181	-0.0915
5.76	1.118	-0.0969
4.81	1.051	-0.1011
3.63	0.956	-0.1055
2.76	0.876	-0.1078
1.69	0.781	-0.1101
0.61	0.681	-0.1143
-0.46	0.575	-0.1164
-1.50	0.471	-0.1190
-2.42	0.370	-0.1196
-3.52	0.257	-0.1180
-4.58	0.142	-0.1161
-5.55	0.038	-0.1143
-6.45	-0.063	-0.1119
-7.49	-0.161	-0.1094

Run: 06889gw
Re = 499607.6

α	C_l	C_m
-7.25	-0.143	-0.1113
-6.24	-0.037	-0.1130
-5.16	0.075	-0.1149
-4.11	0.186	-0.1166
-3.05	0.297	-0.1177
-2.25	0.392	-0.1185
-1.06	0.513	-0.1168
-0.02	0.620	-0.1152
0.96	0.709	-0.1112
1.92	0.793	-0.1083
3.07	0.904	-0.1060
3.99	0.982	-0.1032
5.10	1.074	-0.0989
5.92	1.123	-0.0945
6.99	1.196	-0.0889
8.09	1.253	-0.0832
9.18	1.302	-0.0766
10.02	1.331	-0.0732
11.12	1.295	-0.0918
10.87	1.323	-0.0725
9.86	1.330	-0.0730
8.78	1.281	-0.0776
7.81	1.248	-0.0834
6.77	1.186	-0.0901
5.79	1.119	-0.0950
4.65	1.040	-0.1005
3.60	0.953	-0.1035
2.65	0.869	-0.1063
1.63	0.768	-0.1082
0.67	0.681	-0.1114
-0.41	0.582	-0.1147
-1.39	0.478	-0.1162
-2.36	0.375	-0.1171
-3.47	0.259	-0.1167
-4.43	0.154	-0.1158
-5.58	0.032	-0.1132
-6.63	-0.078	-0.1112

AG40d-02r fp10

Fig. 6.59

Run: 06871gw
Re = 99852.1

α	C_l	C_m
-10.28	-0.237	-0.0708
-9.28	-0.162	-0.1061
-8.21	-0.014	-0.1560
-7.20	0.093	-0.1623
-6.31	0.179	-0.1681
-5.32	0.273	-0.1694
-4.28	0.359	-0.1662
-3.23	0.430	-0.1597
-2.27	0.499	-0.1560
-1.18	0.552	-0.1444
-0.08	0.650	-0.1455
0.91	0.788	-0.1561
1.91	0.957	-0.1634
2.91	1.035	-0.1525
4.01	1.110	-0.1437
4.96	1.150	-0.1341
6.07	1.165	-0.1226
7.12	1.203	-0.1131
8.15	1.230	-0.1041
8.99	1.243	-0.1008
10.03	1.226	-0.1417
11.06	1.168	-0.1913
11.93	1.093	-0.2120
12.92	1.084	-0.2217
13.88	1.094	-0.2301
14.92	1.054	-0.2265
15.91	1.077	-0.2340
15.68	1.073	-0.2177
14.64	1.081	-0.2152
13.72	1.100	-0.2179
12.62	1.089	-0.2054
11.79	1.074	-0.1955
10.80	1.144	-0.1749
9.83	1.250	-0.1187
8.81	1.252	-0.0927
7.85	1.236	-0.1000
6.84	1.205	-0.1089
5.80	1.182	-0.1172
4.78	1.154	-0.1303
3.84	1.112	-0.1374
2.78	1.040	-0.1424
1.76	0.949	-0.1509
0.70	0.765	-0.1383
-0.41	0.627	-0.1293
-1.42	0.553	-0.1343
-2.36	0.512	-0.1423
-3.37	0.437	-0.1470
-4.45	0.361	-0.1536
-5.44	0.275	-0.1560
-6.53	0.168	-0.1527
-7.50	0.070	-0.1503
-8.49	-0.052	-0.1377
-9.50	-0.187	-0.0825

Run: 06873gw
Re = 200169.4

α	C_l	C_m
-10.26	-0.252	-0.0553
-9.25	-0.147	-0.1080
-8.24	0.035	-0.1597
-7.23	0.135	-0.1642
-6.15	0.246	-0.1687
-5.27	0.344	-0.1716
-4.16	0.458	-0.1739
-3.20	0.546	-0.1730
-2.23	0.602	-0.1678
-1.03	0.684	-0.1611
-0.16	0.766	-0.1593
0.82	0.930	-0.1683
1.87	1.042	-0.1617
3.04	1.109	-0.1510
4.07	1.171	-0.1439
4.95	1.210	-0.1353
6.06	1.252	-0.1243
6.99	1.275	-0.1148
8.07	1.311	-0.1064
9.07	1.329	-0.0990
9.87	1.354	-0.1298
10.94	1.328	-0.1872
11.97	1.264	-0.2142
12.91	1.154	-0.2184
14.02	1.183	-0.2249
13.71	1.143	-0.2171
12.74	1.182	-0.2151
11.81	1.251	-0.2084
10.76	1.363	-0.1729
9.87	1.358	-0.1354
8.85	1.334	-0.0970
7.85	1.315	-0.1045
6.84	1.282	-0.1132
5.78	1.254	-0.1237
4.90	1.225	-0.1328
3.79	1.168	-0.1424
2.71	1.094	-0.1490
1.69	1.035	-0.1593
0.65	0.920	-0.1654
-0.41	0.732	-0.1526
-1.35	0.675	-0.1608
-2.28	0.610	-0.1669
-3.41	0.534	-0.1699
-4.38	0.441	-0.1699
-5.41	0.332	-0.1688
-6.48	0.223	-0.1652
-7.50	0.123	-0.1616
-8.45	0.015	-0.1544
-9.56	-0.189	-0.0799

Run: 06875gw
Re = 299967.9

α	C_l	C_m
-10.25	-0.259	-0.0620
-9.30	-0.139	-0.1165
-8.36	0.028	-0.1584
-7.16	0.152	-0.1641
-6.18	0.255	-0.1664
-5.20	0.365	-0.1702
-4.08	0.480	-0.1711
-3.06	0.590	-0.1723
-2.11	0.683	-0.1717
-1.01	0.786	-0.1707
-0.10	0.883	-0.1686
0.96	0.988	-0.1631
2.09	1.060	-0.1536
2.92	1.122	-0.1492
4.10	1.193	-0.1409
5.13	1.241	-0.1313
6.10	1.282	-0.1233
7.18	1.312	-0.1130
8.26	1.349	-0.1045
9.08	1.359	-0.0987
10.07	1.386	-0.1351
11.10	1.367	-0.1824
11.99	1.321	-0.2047
12.92	1.214	-0.2206
13.96	1.200	-0.2256
13.77	1.227	-0.2267
12.82	1.274	-0.2195
11.73	1.336	-0.1985
10.85	1.362	-0.1664
9.92	1.360	-0.0965
8.91	1.360	-0.0977
7.91	1.345	-0.1052
6.75	1.302	-0.1150
5.79	1.265	-0.1234
4.69	1.225	-0.1338
3.73	1.167	-0.1411
2.77	1.109	-0.1480
1.79	1.037	-0.1534
0.73	0.966	-0.1633
-0.42	0.858	-0.1687
-1.30	0.756	-0.1688
-2.38	0.656	-0.1701
-3.38	0.555	-0.1694
-4.45	0.447	-0.1690
-5.46	0.333	-0.1660
-6.46	0.226	-0.1644
-7.46	0.120	-0.1610
-8.54	0.001	-0.1544
-9.50	-0.182	-0.0982

Run: 06877gw
Re = 399909.0

α	C_l	C_m
-9.19	-0.104	-0.1303
-8.20	0.046	-0.1583
-7.18	0.155	-0.1613
-6.16	0.267	-0.1640
-5.16	0.378	-0.1661
-4.16	0.478	-0.1673
-3.16	0.593	-0.1697
-2.11	0.704	-0.1696
-1.02	0.812	-0.1694
-0.00	0.922	-0.1673
0.95	0.986	-0.1592
2.05	1.064	-0.1524
3.07	1.138	-0.1462
4.06	1.193	-0.1381
5.06	1.247	-0.1303
6.08	1.300	-0.1220
7.06	1.331	-0.1138
8.13	1.365	-0.1057
9.11	1.401	-0.1008
10.14	1.394	-0.0989
9.81	1.397	-0.0966
8.75	1.392	-0.1013
7.88	1.369	-0.1072
6.82	1.328	-0.1149
5.76	1.288	-0.1237
4.81	1.234	-0.1314
3.67	1.174	-0.1405
2.75	1.126	-0.1482
1.65	1.041	-0.1536
0.69	0.978	-0.1605
-0.27	0.893	-0.1661
-1.37	0.784	-0.1682
-2.38	0.673	-0.1680
-3.57	0.554	-0.1668
-4.53	0.444	-0.1659
-5.43	0.342	-0.1646
-6.57	0.221	-0.1614
-7.56	0.116	-0.1584
-8.61	0.003	-0.1543

Run: 06879gw
Re = 499995.4

α	C_l	C_m
-8.18	0.057	-0.1585
-7.20	0.166	-0.1616
-6.18	0.270	-0.1631
-5.13	0.389	-0.1666
-4.21	0.489	-0.1667
-3.04	0.616	-0.1671
-2.11	0.712	-0.1664
-0.97	0.821	-0.1647
-0.04	0.916	-0.1631
1.08	0.991	-0.1545
1.96	1.062	-0.1504
2.95	1.133	-0.1438
4.04	1.194	-0.1357
4.99	1.242	-0.1281
6.03	1.299	-0.1202
7.19	1.356	-0.1128
8.05	1.381	-0.1075
9.21	1.416	-0.1006
10.16	1.428	-0.0985
9.88	1.441	-0.0976
8.87	1.417	-0.1013
7.71	1.378	-0.1080
6.76	1.333	-0.1136
5.80	1.294	-0.1214
4.73	1.239	-0.1299
3.73	1.182	-0.1376
2.74	1.124	-0.1448
1.71	1.047	-0.1507
0.47	0.959	-0.1578
-0.57	0.874	-0.1633
-1.32	0.795	-0.1646
-2.40	0.684	-0.1651
-3.48	0.576	-0.1653
-4.60	0.451	-0.1643
-5.53	0.348	-0.1631
-6.52	0.239	-0.1621
-7.53	0.131	-0.1592

AG40d-02r fp15

Fig. 6.62

Run: 06861gw
Re = 100010.9

α	C_l	C_m
-10.22	-0.384	-0.0295
-9.25	-0.333	-0.0522
-8.25	0.023	-0.1679
-7.32	0.137	-0.1773
-6.20	0.271	-0.1873
-5.26	0.338	-0.1840
-4.14	0.431	-0.1777
-3.09	0.503	-0.1686
-2.07	0.582	-0.1646
-1.21	0.650	-0.1630
-0.04	0.736	-0.1601
0.86	0.877	-0.1753
1.89	1.100	-0.1930
3.05	1.228	-0.1827
4.07	1.267	-0.1708

5.08	1.247	-0.1508
5.98	1.269	-0.1409
7.07	1.301	-0.1318
8.05	1.328	-0.1252
9.05	1.368	-0.1336
10.03	1.336	-0.2035
10.86	1.224	-0.2353
11.89	1.163	-0.2455
12.87	1.132	-0.2452
13.99	1.184	-0.2550
14.92	1.185	-0.2555
14.72	1.196	-0.2493
13.76	1.178	-0.2455
12.74	1.142	-0.2335
11.65	1.159	-0.2264
10.67	1.296	-0.2156
9.83	1.373	-0.1806
8.93	1.375	-0.1187
7.76	1.338	-0.1210
6.79	1.309	-0.1277
5.73	1.282	-0.1381
4.86	1.270	-0.1486
3.79	1.275	-0.1640
2.72	1.225	-0.1722
1.71	1.092	-0.1786
0.65	0.848	-0.1562
-0.35	0.748	-0.1519
-1.30	0.677	-0.1523
-2.39	0.603	-0.1559
-3.34	0.532	-0.1590
-4.37	0.459	-0.1659
-5.36	0.383	-0.1722
-6.40	0.279	-0.1722
-7.50	0.151	-0.1644
-8.51	-0.023	-0.1424
-9.55	-0.357	-0.0233

Run: 06863ga
Re = 200055.3

α	C_l	C_m
-10.26	-0.046	-0.1246
-9.38	0.139	-0.1979
-8.35	0.183	-0.1941
-7.26	0.279	-0.1961
-6.16	0.384	-0.1990
-5.31	0.464	-0.1978
-4.26	0.534	-0.1917
-3.09	0.602	-0.1822
-2.17	0.672	-0.1761
-1.04	0.772	-0.1755
-0.07	0.910	-0.1831
0.94	1.164	-0.2039
2.05	1.233	-0.1877
2.98	1.266	-0.1764
3.95	1.291	-0.1647
5.07	1.315	-0.1513
6.09	1.339	-0.1411
7.01	1.375	-0.1340
8.16	1.408	-0.1259
9.11	1.442	-0.1388
9.88	1.445	-0.2022
11.03	1.372	-0.2375
11.94	1.277	-0.2487
12.95	1.242	-0.2496
13.97	1.241	-0.2546
14.93	1.235	-0.2544
14.64	1.228	-0.2502
13.61	1.243	-0.2476
12.67	1.248	-0.2491
11.72	1.272	-0.2369
10.75	1.430	-0.2177
9.81	1.404	-0.1785
8.93	1.435	-0.1293
7.79	1.398	-0.1240
6.87	1.365	-0.1306
5.78	1.337	-0.1399
4.89	1.308	-0.1487
3.88	1.284	-0.1600
2.68	1.261	-0.1757
1.67	1.222	-0.1870
0.73	1.116	-0.1966
-0.36	0.857	-0.1736
-1.24	0.762	-0.1711
-2.38	0.667	-0.1744
-3.41	0.597	-0.1816
-4.33	0.549	-0.1909
-5.39	0.470	-0.1953
-6.47	0.376	-0.1974
-7.46	0.272	-0.1926
-8.46	0.187	-0.1918
-9.43	0.136	-0.1938

Run: 06865gw
Re = 299859.3

α	C_l	C_m
-10.23	0.034	-0.1665
-9.24	0.206	-0.2029
-8.29	0.310	-0.2084
-7.14	0.440	-0.2130
-6.27	0.535	-0.2155
-5.15	0.643	-0.2155
-4.03	0.705	-0.2108
-3.14	0.774	-0.2066
-2.14	0.847	-0.2007
-1.09	0.930	-0.1961
-0.01	1.141	-0.2091
0.99	1.196	-0.1960
2.04	1.236	-0.1825
3.09	1.264	-0.1689
3.96	1.289	-0.1600
4.93	1.329	-0.1506
5.96	1.374	-0.1422
7.03	1.412	-0.1341
8.08	1.436	-0.1260
9.21	1.468	-0.1418
10.15	1.487	-0.1920
10.96	1.439	-0.2207
11.98	1.340	-0.2452
12.91	1.305	-0.2542
12.69	1.286	-0.2479
11.66	1.373	-0.2399
10.78	1.458	-0.2183
9.81	1.479	-0.1761
8.87	1.452	-0.1200
7.80	1.435	-0.1266
6.86	1.404	-0.1330
5.78	1.369	-0.1427
4.74	1.319	-0.1509
3.72	1.289	-0.1610
2.81	1.262	-0.1711
1.79	1.236	-0.1845
0.74	1.195	-0.1972
-0.33	1.065	-0.2024
-1.39	0.897	-0.1932
-2.41	0.833	-0.2008
-3.51	0.750	-0.2055
-4.46	0.720	-0.2129
-5.46	0.617	-0.2131
-6.45	0.511	-0.2114
-7.53	0.396	-0.2097
-8.46	0.290	-0.2054
-9.51	0.175	-0.2001

Run: 06867rd
Re = 399677.0

α	C_l	C_m
-10.23	0.099	-0.1944
-9.22	0.219	-0.2063
-8.28	0.327	-0.2087
-7.20	0.448	-0.2135
-6.07	0.568	-0.2151
-5.19	0.666	-0.2161
-4.11	0.773	-0.2153
-3.06	0.871	-0.2140
-2.14	0.958	-0.2115
-1.04	1.020	-0.2071
0.11	1.150	-0.2022
0.95	1.172	-0.1890
1.99	1.212	-0.1780

3.07	1.246	-0.1651
3.96	1.283	-0.1566
4.96	1.341	-0.1496
6.04	1.389	-0.1412
7.15	1.438	-0.1329
8.20	1.468	-0.1262
9.18	1.487	-0.1222
10.06	1.458	-0.1870
10.98	1.395	-0.2234
10.70	1.418	-0.2124
9.83	1.461	-0.1676
8.75	1.463	-0.1234
7.74	1.448	-0.1278
6.74	1.415	-0.1345
5.85	1.382	-0.1421
4.71	1.328	-0.1508
3.71	1.275	-0.1573
2.68	1.239	-0.1679
1.62	1.209	-0.1811
0.59	1.160	-0.1924
-0.33	1.137	-0.2059
-1.49	1.033	-0.2099
-2.47	0.936	-0.2117
-3.55	0.828	-0.2126
-4.53	0.732	-0.2150
-5.51	0.628	-0.2143
-6.53	0.511	-0.2125
-7.51	0.410	-0.2100
-8.60	0.293	-0.2074
-9.68	0.171	-0.2005

Run: 06869gw
Re = 500554.6

α	C_l	C_m
-9.17	0.246	-0.2084
-8.13	0.356	-0.2100
-7.19	0.460	-0.2125
-6.22	0.571	-0.2145
-5.06	0.693	-0.2138
-4.10	0.794	-0.2140
-3.00	0.893	-0.2119
-2.00	0.995	-0.2104
-1.09	1.067	-0.2066
0.02	1.124	-0.1939
1.14	1.157	-0.1797
1.91	1.191	-0.1708
3.13	1.239	-0.1587
4.17	1.300	-0.1523
5.08	1.349	-0.1449
6.08	1.403	-0.1389
7.20	1.454	-0.1317
8.27	1.507	-0.1265
9.21	1.519	-0.1222
8.88	1.517	-0.1225
7.78	1.492	-0.1278
6.84	1.441	-0.1334
5.64	1.392	-0.1411
4.79	1.334	-0.1467
3.70	1.272	-0.1532
2.58	1.224	-0.1636
1.58	1.183	-0.1733
0.66	1.153	-0.1841
-0.38	1.118	-0.1988
-1.47	1.061	-0.2101
-2.64	0.945	-0.2120
-3.62	0.849	-0.2132
-4.51	0.754	-0.2134
-5.70	0.636	-0.2140
-6.52	0.539	-0.2120
-7.52	0.431	-0.2122
-8.56	0.317	-0.2095

AG40d-02r fp20
Fig. 6.65

Run: 06891ga
Re = 100011.0

α	C_l	C_m
-10.28	-0.363	-0.0233
-9.22	-0.254	-0.0607
-8.27	0.164	-0.1903
-7.34	0.257	-0.1946
-6.28	0.353	-0.1978
-5.15	0.453	-0.1963
-4.11	0.530	-0.1897
-3.24	0.599	-0.1862
-2.14	0.700	-0.1840
-1.14	0.778	-0.1817
-0.10	0.858	-0.1799
0.92	0.993	-0.1905
1.99	1.192	-0.1940
3.02	1.307	-0.1905
4.09	1.308	-0.1717
4.94	1.312	-0.1593
6.04	1.355	-0.1506
6.99	1.390	-0.1444
8.07	1.425	-0.1386
9.01	1.436	-0.1677
9.99	1.340	-0.2455
10.82	1.264	-0.2534
11.85	1.238	-0.2611
12.89	1.230	-0.2663
13.80	1.280	-0.2732
13.66	1.222	-0.2557
12.65	1.292	-0.2592
11.78	1.252	-0.2477
10.74	1.268	-0.2386
9.77	1.391	-0.2232
8.85	1.465	-0.1698
7.82	1.436	-0.1338
6.87	1.398	-0.1379
5.76	1.359	-0.1464
4.83	1.323	-0.1540
3.70	1.339	-0.1698
2.87	1.324	-0.1793
1.69	1.166	-0.1836
0.71	0.960	-0.1743
-0.40	0.846	-0.1669
-1.30	0.775	-0.1680
-2.26	0.703	-0.1703
-3.36	0.610	-0.1728
-4.36	0.531	-0.1790
-5.40	0.447	-0.1856
-6.49	0.352	-0.1874
-7.53	0.250	-0.1819
-8.59	0.136	-0.1731
-9.40	-0.272	-0.0415

Run: 06893ga
Re = 200066.0

α	C_l	C_m
-10.24	-0.058	-0.1215
-9.36	0.261	-0.2234
-8.21	0.365	-0.2257
-7.25	0.451	-0.2256
-6.16	0.527	-0.2222
-5.16	0.578	-0.2133
-4.22	0.643	-0.2073
-3.25	0.708	-0.2014
-2.17	0.794	-0.1958
-1.09	0.846	-0.1880
-0.03	1.006	-0.1979
0.96	1.254	-0.2135
1.99	1.286	-0.1957
2.98	1.304	-0.1838
3.96	1.330	-0.1742
5.03	1.366	-0.1641
6.01	1.416	-0.1571
7.10	1.459	-0.1505
8.13	1.483	-0.1425
8.95	1.532	-0.2005
9.93	1.428	-0.2418
10.93	1.404	-0.2618
11.88	1.315	-0.2710
12.84	1.335	-0.2808
13.88	1.290	-0.2778
13.74	1.318	-0.2747
12.63	1.302	-0.2708

11.62	1.308	-0.2636
10.73	1.414	-0.2548
9.74	1.493	-0.2285
8.88	1.529	-0.1848
7.89	1.479	-0.1387
6.88	1.454	-0.1459
5.79	1.411	-0.1537
4.76	1.367	-0.1628
3.80	1.333	-0.1712
2.78	1.306	-0.1819
1.71	1.292	-0.1955
0.69	1.199	-0.2090
-0.20	0.987	-0.1921
-1.36	0.840	-0.1840
-2.37	0.781	-0.1922
-3.34	0.708	-0.1969
-4.37	0.634	-0.2018
-5.41	0.577	-0.2110
-6.44	0.523	-0.2199
-7.57	0.429	-0.2207
-8.52	0.355	-0.2226
-9.48	0.262	-0.2182

Run: 06895gw
Re = 299794.9

α	C_l	C_m
-10.23	0.368	-0.2447
-9.23	0.479	-0.2500
-8.26	0.582	-0.2531
-7.27	0.688	-0.2549
-6.12	0.689	-0.2418
-5.27	0.765	-0.2417
-4.12	0.771	-0.2241
-3.07	0.803	-0.2120
-2.22	0.841	-0.2039
-1.12	0.953	-0.2038
-0.12	1.197	-0.2232
1.02	1.248	-0.2017
2.02	1.279	-0.1910
3.07	1.309	-0.1803
3.97	1.357	-0.1735
5.05	1.408	-0.1652
6.00	1.452	-0.1587
7.08	1.496	-0.1507
8.10	1.514	-0.1423
8.96	1.548	-0.1902
10.02	1.526	-0.2288
10.96	1.470	-0.2591
11.88	1.360	-0.2713
12.92	1.319	-0.2749
13.96	1.311	-0.2779
13.75	1.295	-0.2741
12.61	1.353	-0.2743

11.60	1.381	-0.2683
10.65	1.475	-0.2564
9.78	1.524	-0.2166
8.84	1.546	-0.1811
7.79	1.512	-0.1427
6.81	1.489	-0.1503
5.77	1.441	-0.1586
4.82	1.392	-0.1648
3.69	1.342	-0.1736
2.71	1.305	-0.1830
1.61	1.272	-0.1934
0.80	1.247	-0.2037
-0.34	1.166	-0.2210
-1.37	0.928	-0.2012
-2.36	0.833	-0.2024
-3.32	0.795	-0.2116
-4.49	0.807	-0.2336
-5.40	0.743	-0.2388
-6.43	0.767	-0.2545
-7.50	0.665	-0.2532
-8.46	0.565	-0.2521
-9.55	0.445	-0.2467

Run: 06897gw
Re = 399618.1

α	C_l	C_m
-10.20	0.390	-0.2497
-9.16	0.506	-0.2537
-8.17	0.618	-0.2564
-7.14	0.720	-0.2566
-6.14	0.822	-0.2576
-5.14	0.917	-0.2558
-4.05	1.011	-0.2531
-3.12	0.906	-0.2283
-2.12	0.961	-0.2217
-1.07	1.147	-0.2324
-0.02	1.192	-0.2110
0.93	1.217	-0.1986
1.95	1.261	-0.1885
3.10	1.318	-0.1798
4.09	1.372	-0.1729
5.16	1.432	-0.1651
6.00	1.468	-0.1587
7.07	1.519	-0.1515
8.02	1.554	-0.1455
7.72	1.550	-0.1471
6.90	1.514	-0.1519
5.87	1.465	-0.1586
4.86	1.411	-0.1658
3.74	1.354	-0.1744
2.61	1.297	-0.1819
1.59	1.254	-0.1914
0.56	1.217	-0.2019

-0.40	1.206	-0.2200
-1.36	1.102	-0.2290
-2.41	0.968	-0.2249
-3.61	1.055	-0.2500
-4.54	0.978	-0.2538
-5.55	0.886	-0.2561
-6.49	0.793	-0.2568
-7.50	0.689	-0.2560
-8.52	0.578	-0.2542
-9.70	0.453	-0.2512

AG40d-02r fp25
Fig. 6.68

Run: 06899gw
Re = 100558.3

α	C_l	C_m
-10.29	-0.291	-0.0426
-9.33	0.203	-0.2101
-8.35	0.319	-0.2204
-7.31	0.416	-0.2229
-6.26	0.515	-0.2237
-5.21	0.593	-0.2177
-4.21	0.659	-0.2102
-3.20	0.733	-0.2058
-2.21	0.833	-0.2064
-1.07	0.921	-0.2024
-0.12	0.936	-0.1920
0.88	1.133	-0.2111
1.99	1.309	-0.2112
3.02	1.323	-0.1957
4.07	1.332	-0.1805
5.06	1.371	-0.1714
6.00	1.420	-0.1637
7.12	1.460	-0.1552
8.14	1.526	-0.1773
9.01	1.411	-0.2416
9.96	1.381	-0.2604
10.99	1.306	-0.2800
11.92	1.272	-0.2852
12.89	1.367	-0.2997
13.86	1.329	-0.2979
13.75	1.304	-0.2869
12.73	1.307	-0.2776
11.73	1.293	-0.2744
10.62	1.337	-0.2714
9.78	1.442	-0.2599
8.78	1.514	-0.2047
7.88	1.512	-0.1564
6.86	1.459	-0.1508
5.79	1.419	-0.1597
4.86	1.380	-0.1662

3.79	1.328	-0.1743
2.84	1.326	-0.1861
1.80	1.310	-0.2017
0.71	1.098	-0.1954
-0.19	0.976	-0.1883
-1.30	0.930	-0.1917
-2.31	0.842	-0.1929
-3.42	0.748	-0.1958
-4.47	0.672	-0.2000
-5.42	0.599	-0.2099
-6.44	0.513	-0.2135
-7.57	0.421	-0.2125
-8.50	0.327	-0.2126
-9.48	-0.158	-0.0718

Run: 06901gw
Re = 201161.0

α	C_l	C_m
-10.28	-0.320	-0.0404
-9.41	0.243	-0.2175
-8.16	0.365	-0.2230
-7.18	0.470	-0.2283
-6.18	0.558	-0.2278
-5.19	0.658	-0.2280
-4.14	0.731	-0.2230
-3.14	0.823	-0.2205
-2.06	0.896	-0.2137
-1.06	0.932	-0.2009
-0.09	1.090	-0.2120
0.98	1.297	-0.2215
2.01	1.283	-0.2032
2.97	1.320	-0.1928
4.05	1.380	-0.1850
5.04	1.423	-0.1773
6.05	1.469	-0.1702
7.12	1.504	-0.1608
8.10	1.561	-0.1889
9.00	1.528	-0.2323
10.05	1.445	-0.2759
10.91	1.348	-0.2813
11.94	1.331	-0.2880
12.80	1.315	-0.2905
13.85	1.359	-0.2990
13.74	1.373	-0.2968
12.63	1.338	-0.2915
11.65	1.319	-0.2823
10.65	1.355	-0.2771
9.69	1.460	-0.2629
8.81	1.545	-0.2324
7.86	1.550	-0.1719
6.85	1.493	-0.1586
5.79	1.456	-0.1678
4.78	1.419	-0.1757

3.80	1.368	-0.1824
2.69	1.314	-0.1913
1.82	1.287	-0.2013
0.75	1.291	-0.2203
-0.29	1.044	-0.2022
-1.35	0.949	-0.2043
-2.35	0.893	-0.2134
-3.37	0.809	-0.2180
-4.38	0.728	-0.2224
-5.39	0.634	-0.2234
-6.42	0.545	-0.2233
-7.60	0.442	-0.2232
-8.39	0.355	-0.2202
-9.40	0.238	-0.2119

Run: 06903gw
Re = 301395.6

α	C_l	C_m
-10.08	0.367	-0.2458
-9.29	0.372	-0.2378
-8.26	0.516	-0.2486
-7.20	0.513	-0.2321
-6.23	0.575	-0.2270
-5.19	0.664	-0.2252
-4.16	0.751	-0.2237
-3.12	0.846	-0.2208
-2.10	0.899	-0.2096
-1.06	1.030	-0.2152
-0.12	1.257	-0.2340
0.99	1.258	-0.2115
1.94	1.292	-0.2007
3.11	1.354	-0.1928
3.97	1.409	-0.1875
5.05	1.466	-0.1795
6.17	1.526	-0.1724
7.06	1.550	-0.1635
8.12	1.581	-0.1900
8.99	1.599	-0.2325
9.97	1.523	-0.2697
10.92	1.438	-0.2824
11.97	1.378	-0.2909
11.63	1.385	-0.2874
10.80	1.438	-0.2777
9.71	1.546	-0.2552
8.86	1.576	-0.2142
7.80	1.590	-0.1751
6.86	1.543	-0.1633
5.77	1.508	-0.1734
4.85	1.459	-0.1797
3.69	1.400	-0.1879
2.85	1.343	-0.1923
1.82	1.283	-0.1988
0.67	1.255	-0.2134

-0.33	1.172	-0.2230
-1.34	0.984	-0.2098
-2.32	0.886	-0.2107
-3.48	0.820	-0.2205
-4.48	0.726	-0.2227
-5.50	0.635	-0.2253
-6.47	0.578	-0.2300
-7.51	0.538	-0.2400
-8.44	0.464	-0.2408
-9.52	0.344	-0.2356

Run: 06905gw
Re = 401769.5

α	C_l	C_m
-9.17	0.730	-0.2873
-8.29	0.810	-0.2859
-7.17	0.836	-0.2765
-6.31	0.643	-0.2356
-5.29	0.687	-0.2273
-4.06	0.776	-0.2226
-3.08	0.844	-0.2159
-2.06	0.969	-0.2196
-1.08	1.219	-0.2451
0.02	1.223	-0.2189
0.95	1.253	-0.2076
2.08	1.320	-0.2002
3.05	1.386	-0.1949
4.03	1.438	-0.1867
4.93	1.490	-0.1801
6.12	1.571	-0.1739
7.12	1.617	-0.1678
8.01	1.611	-0.1824
7.86	1.607	-0.1717
6.79	1.597	-0.1677
5.73	1.557	-0.1770
4.70	1.497	-0.1835
3.61	1.427	-0.1897
2.75	1.368	-0.1949
1.66	1.306	-0.2019
0.65	1.235	-0.2084
-0.46	1.233	-0.2263
-1.39	1.138	-0.2345
-2.40	0.922	-0.2158
-3.55	0.830	-0.2195
-4.54	0.774	-0.2292
-5.52	0.686	-0.2298
-6.68	0.640	-0.2397
-7.53	0.876	-0.2822
-8.47	0.803	-0.2858

AG40d-02r fp30
Fig. 6.70

Run: 06907gw
Re = 100953.9

α	C_l	C_m
-10.23	-0.250	-0.0735
-9.17	0.330	-0.2391
-8.25	0.430	-0.2444
-7.16	0.533	-0.2439
-6.19	0.607	-0.2379
-5.16	0.672	-0.2295
-4.12	0.737	-0.2200
-3.13	0.824	-0.2194
-2.01	0.921	-0.2181
-1.01	1.002	-0.2175
-0.00	1.016	-0.2066
1.02	1.179	-0.2210
2.00	1.295	-0.2153
3.02	1.311	-0.1986
4.06	1.357	-0.1897
5.08	1.402	-0.1839
6.03	1.446	-0.1737
7.09	1.474	-0.1688
7.98	1.526	-0.2176
9.00	1.444	-0.2606
9.97	1.392	-0.2867
10.92	1.310	-0.2964
11.91	1.307	-0.3051
12.90	1.353	-0.3128
13.98	1.335	-0.3215
13.64	1.316	-0.3026
12.66	1.300	-0.2955
11.63	1.308	-0.2884
10.74	1.330	-0.2865
9.59	1.366	-0.2762
8.80	1.481	-0.2480
7.77	1.498	-0.1928
6.86	1.470	-0.1597
5.80	1.443	-0.1713
4.75	1.405	-0.1795
3.80	1.363	-0.1853
2.78	1.317	-0.1932
1.72	1.309	-0.2079
0.69	1.130	-0.2064
-0.26	1.022	-0.1965
-1.33	0.987	-0.2048
-2.32	0.909	-0.2055
-3.34	0.823	-0.2062
-4.37	0.737	-0.2083
-5.36	0.674	-0.2191
-6.48	0.588	-0.2278
-7.45	0.521	-0.2297
-8.41	0.415	-0.2296
-9.50	0.297	-0.2184

Run: 06908gw
Re = 201947.9

α	C_l	C_m
-10.21	-0.239	-0.0631
-9.31	0.370	-0.2377
-8.22	0.484	-0.2441
-7.21	0.581	-0.2452
-6.23	0.662	-0.2430
-5.14	0.758	-0.2417
-4.11	0.848	-0.2377
-3.07	0.923	-0.2317
-2.08	0.997	-0.2272
-1.08	1.048	-0.2179
-0.08	1.159	-0.2183
0.99	1.299	-0.2232
1.92	1.343	-0.2155
3.09	1.410	-0.2078
4.04	1.461	-0.2004
4.95	1.511	-0.1939
5.98	1.548	-0.1827
7.09	1.572	-0.1710
8.03	1.613	-0.2175
8.92	1.549	-0.2637
9.99	1.398	-0.2889
10.96	1.369	-0.2985
11.91	1.375	-0.3039
11.66	1.375	-0.3000
10.70	1.392	-0.2920
9.75	1.456	-0.2818
8.72	1.586	-0.2545
7.84	1.603	-0.2099
6.96	1.559	-0.1660
5.86	1.551	-0.1804
4.70	1.506	-0.1912
3.84	1.459	-0.1974
2.80	1.403	-0.2047
1.73	1.346	-0.2129
0.70	1.281	-0.2190
-0.30	1.128	-0.2119
-1.33	1.046	-0.2144
-2.32	0.995	-0.2258
-3.28	0.924	-0.2302
-4.39	0.831	-0.2349
-5.38	0.742	-0.2369
-6.48	0.654	-0.2402
-7.43	0.565	-0.2417
-8.56	0.454	-0.2384
-9.60	0.350	-0.2338

Run: 06909gw
Re = 302356.7

α	C_l	C_m
-10.29	-0.179	-0.0827
-9.34	0.408	-0.2425
-8.29	0.508	-0.2444
-7.21	0.606	-0.2457
-6.24	0.700	-0.2456
-5.13	0.787	-0.2411
-4.09	0.881	-0.2405
-3.06	0.971	-0.2380
-2.02	1.019	-0.2263
-1.12	1.109	-0.2251
-0.01	1.256	-0.2291
0.97	1.320	-0.2219
2.01	1.380	-0.2158
3.03	1.448	-0.2092
4.06	1.517	-0.2042
5.17	1.569	-0.1943
5.99	1.603	-0.1868
7.14	1.617	-0.1741
8.12	1.647	-0.2220
9.10	1.622	-0.2662
9.93	1.549	-0.2863
9.69	1.511	-0.2796
8.86	1.622	-0.2567
7.79	1.635	-0.2042
6.85	1.602	-0.1727
5.89	1.610	-0.1882
4.82	1.570	-0.1980
3.78	1.498	-0.2037
2.85	1.450	-0.2111
1.69	1.371	-0.2161
0.68	1.300	-0.2226
-0.36	1.241	-0.2327
-1.37	1.075	-0.2212
-2.38	1.014	-0.2302
-3.46	0.942	-0.2375
-4.45	0.846	-0.2392
-5.48	0.762	-0.2421
-6.52	0.670	-0.2446
-7.55	0.580	-0.2440
-8.50	0.489	-0.2443
-9.57	0.388	-0.2401

Run: 06910gw
Re = 403208.1

α	C_l	C_m
-9.31	0.413	-0.2415
-8.22	0.525	-0.2460
-7.14	0.616	-0.2444
-6.16	0.704	-0.2428
-5.19	0.794	-0.2417

-4.07	0.893	-0.2400
-3.13	0.951	-0.2322
-2.09	1.040	-0.2289
-1.11	1.186	-0.2364
-0.02	1.261	-0.2274
1.01	1.328	-0.2220
2.05	1.402	-0.2169
3.15	1.474	-0.2106
3.93	1.535	-0.2062
5.22	1.611	-0.1974
6.08	1.646	-0.1893
7.14	1.644	-0.1771
6.76	1.671	-0.1832
5.74	1.630	-0.1910
4.68	1.568	-0.1985
3.81	1.526	-0.2061
2.67	1.458	-0.2136
1.72	1.394	-0.2195
0.59	1.307	-0.2245
-0.36	1.244	-0.2299
-1.52	1.123	-0.2308
-2.38	1.007	-0.2275
-3.51	0.936	-0.2360
-4.44	0.855	-0.2380
-5.62	0.754	-0.2407
-6.45	0.681	-0.2434
-7.61	0.578	-0.2426
-8.66	0.482	-0.2427

AG40d-02r fp40

Fig. 6.72

Run: 06911gw

Re = 101890.3

α	C_l	C_m
-10.24	0.454	-0.2586
-9.19	0.556	-0.2618
-8.13	0.630	-0.2640
-7.14	0.710	-0.2589
-6.11	0.745	-0.2458
-5.20	0.788	-0.2330
-4.05	0.880	-0.2330
-3.02	0.968	-0.2352
-2.09	1.042	-0.2328
-1.03	1.126	-0.2309
-0.02	1.175	-0.2266
1.08	1.311	-0.2271
2.04	1.357	-0.2197
3.07	1.402	-0.2144
4.10	1.447	-0.2042
5.14	1.480	-0.1956
6.10	1.509	-0.1865
7.17	1.565	-0.2312
7.98	1.433	-0.2697
8.98	1.414	-0.2997
9.88	1.364	-0.3083
11.00	1.347	-0.3153
11.88	1.368	-0.3263
12.87	1.397	-0.3345
13.95	1.402	-0.3382
13.70	1.432	-0.3311
12.65	1.372	-0.3180
11.58	1.373	-0.3102
10.66	1.337	-0.3000
9.70	1.352	-0.2910
8.67	1.440	-0.2785
7.79	1.499	-0.2546
6.76	1.588	-0.2048
5.84	1.550	-0.1801
4.82	1.521	-0.1880
3.88	1.478	-0.1985
2.85	1.437	-0.2084
1.81	1.384	-0.2126
0.76	1.324	-0.2216
-0.26	1.165	-0.2126
-1.34	1.128	-0.2221
-2.32	1.049	-0.2203
-3.40	0.960	-0.2197
-4.40	0.891	-0.2203
-5.37	0.809	-0.2257
-6.42	0.756	-0.2368
-7.38	0.722	-0.2496
-8.49	0.638	-0.2521
-9.45	0.562	-0.2512

Run: 06912gw

Re = 203894.4

α	C_l	C_m
-10.26	0.502	-0.2629
-9.24	0.598	-0.2671
-8.29	0.691	-0.2684
-7.21	0.777	-0.2672
-6.25	0.857	-0.2656
-5.18	0.944	-0.2614
-4.08	1.026	-0.2571
-3.04	1.078	-0.2448
-2.09	1.159	-0.2423
-0.97	1.199	-0.2307
-0.01	1.337	-0.2371
0.92	1.394	-0.2306
2.10	1.491	-0.2294
3.05	1.534	-0.2228
4.04	1.569	-0.2119
4.99	1.635	-0.2082
6.10	1.631	-0.1867
7.03	1.654	-0.2268
8.06	1.644	-0.2757
8.99	1.489	-0.3005
9.92	1.452	-0.3100
9.69	1.458	-0.3062
8.84	1.575	-0.2926
7.68	1.681	-0.2619
6.83	1.671	-0.2171
5.80	1.642	-0.1887
4.84	1.633	-0.2051
3.83	1.588	-0.2136
2.82	1.535	-0.2206
1.72	1.470	-0.2249
0.74	1.405	-0.2300
-0.30	1.320	-0.2329
-1.26	1.206	-0.2302
-2.40	1.156	-0.2426
-3.37	1.075	-0.2451
-4.42	1.002	-0.2515
-5.43	0.937	-0.2581
-6.35	0.860	-0.2612
-7.52	0.754	-0.2610
-8.54	0.673	-0.2633
-9.50	0.589	-0.2632

Run: 06913gw

Re = 305697.5

α	C_l	C_m
-10.22	0.551	-0.2698
-9.20	0.639	-0.2722
-8.23	0.726	-0.2724
-7.15	0.804	-0.2677
-6.14	0.891	-0.2665
-5.17	0.974	-0.2641
-4.18	1.046	-0.2594
-3.18	1.120	-0.2558
-2.07	1.188	-0.2467
-1.07	1.283	-0.2438
-0.03	1.366	-0.2401
0.96	1.430	-0.2346
2.07	1.501	-0.2294
3.12	1.566	-0.2234
4.04	1.620	-0.2179
5.15	1.658	-0.2074
6.12	1.663	-0.1895
7.14	1.685	-0.2348
7.93	1.669	-0.2681
8.96	1.562	-0.2976
9.89	1.458	-0.3121
9.71	1.494	-0.3104
8.63	1.591	-0.2916
7.84	1.650	-0.2669
6.84	1.686	-0.2214

5.81	1.658	-0.1906
4.79	1.672	-0.2116
3.80	1.625	-0.2187
2.81	1.563	-0.2242
1.66	1.491	-0.2305
0.77	1.428	-0.2355
-0.30	1.354	-0.2412
-1.39	1.259	-0.2434
-2.39	1.180	-0.2493
-3.44	1.114	-0.2571
-4.42	1.032	-0.2597
-5.44	0.951	-0.2642
-6.54	0.859	-0.2649
-7.41	0.794	-0.2694
-8.63	0.689	-0.2692
-9.56	0.609	-0.2697

Run: 06914gw
Re = 407704.6

α	C_l	C_m
-9.20	0.646	-0.2717
-8.29	0.729	-0.2717
-7.15	0.816	-0.2691
-6.20	0.904	-0.2679
-5.16	0.985	-0.2643
-4.03	1.086	-0.2636
-2.97	1.144	-0.2551
-2.07	1.222	-0.2510
-1.00	1.315	-0.2476
0.08	1.388	-0.2414
0.94	1.442	-0.2352
2.11	1.528	-0.2305
3.05	1.592	-0.2251
4.07	1.661	-0.2205
5.17	1.728	-0.2142
6.12	1.681	-0.1932
5.79	1.688	-0.1941
4.85	1.714	-0.2157
3.78	1.646	-0.2211
2.71	1.594	-0.2304
1.65	1.513	-0.2355
0.69	1.442	-0.2400
-0.27	1.369	-0.2426
-1.43	1.279	-0.2471
-2.46	1.180	-0.2493
-3.42	1.121	-0.2569
-4.44	1.043	-0.2608
-5.38	0.963	-0.2639
-6.51	0.869	-0.2662
-7.53	0.787	-0.2684
-8.53	0.700	-0.2694

AG455ct-02r fn0.4
Fig. 6.76

Run: 06723gw
Re = 100019.1

α	C_l	C_m
-10.31	-0.692	0.0783
-9.23	-0.643	0.0644
-8.24	-0.638	0.0536
-7.20	-0.584	0.0278
-6.23	-0.491	-0.0118
-5.27	-0.341	-0.0435
-4.19	-0.228	-0.0450
-3.21	-0.140	-0.0443
-2.13	-0.046	-0.0443
-1.06	0.040	-0.0411
-0.05	0.143	-0.0424
0.94	0.263	-0.0520
2.03	0.398	-0.0571
3.44	0.502	-0.0536
4.04	0.557	-0.0492
5.01	0.637	-0.0448
6.04	0.723	-0.0423
7.06	0.800	-0.0397
8.17	0.877	-0.0364
9.09	0.942	-0.0340
10.17	0.996	-0.0320
11.10	1.019	-0.0955
11.99	0.986	-0.1393
12.98	0.955	-0.1530
14.01	0.930	-0.1593
14.94	0.924	-0.1607
15.98	0.909	-0.1604
16.91	0.955	-0.1713
17.92	0.929	-0.1630
18.98	0.912	-0.1654
19.96	0.959	-0.1783
19.60	0.963	-0.1700
18.73	0.944	-0.1629
17.66	0.913	-0.1487
16.73	0.925	-0.1523
15.69	0.931	-0.1490
14.79	0.927	-0.1472
13.81	0.951	-0.1455
12.72	0.980	-0.1442
11.72	0.975	-0.1165
10.86	1.053	-0.0291
9.85	1.017	-0.0272
8.83	0.958	-0.0306
7.80	0.877	-0.0326
6.73	0.797	-0.0358
5.71	0.712	-0.0386
4.70	0.633	-0.0426
3.23	0.553	-0.0477
2.26	0.461	-0.0450
1.62	0.394	-0.0465
0.65	0.255	-0.0365
-0.43	0.150	-0.0395
-1.40	0.054	-0.0386
-2.46	-0.031	-0.0425
-3.49	-0.128	-0.0430
-4.57	-0.223	-0.0426
-5.54	-0.340	-0.0334
-6.45	-0.493	0.0100
-7.44	-0.582	0.0460
-8.46	-0.616	0.0670
-9.43	-0.645	0.0791

Run: 06725gw
Re = 199810.4

α	C_l	C_m
-10.15	-0.649	0.0852
-9.13	-0.645	0.0766
-8.16	-0.630	0.0596
-7.22	-0.569	0.0302
-6.21	-0.464	-0.0110
-5.20	-0.318	-0.0442
-4.10	-0.207	-0.0452
-3.19	-0.119	-0.0448
-2.15	-0.019	-0.0454
-1.01	0.078	-0.0439
0.05	0.150	-0.0452
0.93	0.270	-0.0537
2.06	0.385	-0.0538
3.01	0.479	-0.0510
4.07	0.695	-0.0479
5.10	0.791	-0.0462
6.06	0.875	-0.0449
7.13	0.966	-0.0424
8.15	1.036	-0.0395
9.15	1.099	-0.0363
10.16	1.124	-0.0659
11.03	1.104	-0.1409
12.04	1.065	-0.1603
12.97	1.039	-0.1654
12.68	1.019	-0.1590
11.75	1.072	-0.1541
10.78	1.104	-0.1239
9.84	1.122	-0.0318
8.82	1.088	-0.0351
7.81	1.021	-0.0382
6.77	0.938	-0.0404
5.81	0.854	-0.0426
4.81	0.764	-0.0438
3.73	0.665	-0.0456

2.60	0.458	-0.0500
1.62	0.355	-0.0529
0.66	0.236	-0.0493
-0.68	0.127	-0.0438
-1.38	0.055	-0.0442
-2.42	-0.040	-0.0441
-3.47	-0.146	-0.0446
-4.44	-0.239	-0.0455
-5.45	-0.354	-0.0357
-6.49	-0.505	0.0109
-7.49	-0.586	0.0429
-8.53	-0.635	0.0678
-9.46	-0.656	0.0835

Run: 06727gw
Re = 300226.2

α	C_l	C_m
-10.10	-0.654	0.0829
-9.16	-0.649	0.0687
-8.21	-0.622	0.0461
-7.21	-0.536	0.0073
-6.31	-0.409	-0.0324
-5.13	-0.253	-0.0474
-4.17	-0.162	-0.0461
-3.16	-0.067	-0.0461
-2.05	0.034	-0.0471
-1.11	0.095	-0.0491
-0.02	0.227	-0.0534
1.00	0.343	-0.0514
1.93	0.440	-0.0503
3.02	0.550	-0.0489
4.00	0.642	-0.0470
5.05	0.749	-0.0460
6.09	0.850	-0.0446
7.04	0.935	-0.0429
8.23	1.030	-0.0401
9.21	1.090	-0.0367
10.28	1.143	-0.0332
11.12	1.150	-0.0885
11.88	1.130	-0.1316
13.04	1.102	-0.1556
12.71	1.114	-0.1496
11.76	1.131	-0.1148
10.84	1.158	-0.0316
9.82	1.130	-0.0341
8.78	1.066	-0.0378
7.72	0.990	-0.0405
6.85	0.909	-0.0419
5.71	0.803	-0.0439
4.77	0.712	-0.0450
3.83	0.621	-0.0459
2.66	0.514	-0.0473
1.69	0.411	-0.0488

0.68	0.310	-0.0510
-0.37	0.195	-0.0508
-1.81	0.066	-0.0459
-2.38	0.014	-0.0448
-3.50	-0.094	-0.0445
-4.58	-0.193	-0.0450
-5.57	-0.302	-0.0455
-6.53	-0.452	-0.0197
-7.47	-0.565	0.0199
-8.57	-0.637	0.0558
-9.51	-0.664	0.0770

Run: 06731gw
Re = 399969.8

α	C_l	C_m
-7.22	-0.539	0.0056
-6.23	-0.397	-0.0357
-5.13	-0.254	-0.0482
-4.10	-0.154	-0.0464
-3.21	-0.071	-0.0462
-2.40	0.011	-0.0489
-1.09	0.115	-0.0533
-0.05	0.232	-0.0513
0.91	0.326	-0.0499
1.93	0.433	-0.0486
2.98	0.537	-0.0476
4.06	0.642	-0.0462
5.11	0.749	-0.0451
6.17	0.854	-0.0438
7.19	0.947	-0.0423
8.13	1.021	-0.0402
9.15	1.098	-0.0375
10.19	1.159	-0.0341
9.86	1.145	-0.0351
8.85	1.074	-0.0381
7.86	1.006	-0.0407
6.78	0.905	-0.0422
5.66	0.803	-0.0441
4.60	0.702	-0.0452
3.59	0.603	-0.0462
2.63	0.505	-0.0471
1.61	0.401	-0.0482
0.57	0.296	-0.0493
-0.45	0.191	-0.0510
-1.50	0.075	-0.0518
-2.49	0.013	-0.0484
-3.54	-0.100	-0.0452
-4.45	-0.187	-0.0460
-5.58	-0.303	-0.0469
-6.57	-0.444	-0.0240

Run: 06729gw
Re = 500541.5

α	C_l	C_m
-7.27	-0.531	0.0023
-6.21	-0.368	-0.0407
-5.22	-0.247	-0.0482
-4.08	-0.143	-0.0467
-3.07	-0.040	-0.0486
-2.59	0.018	-0.0508
-1.13	0.134	-0.0528
-0.16	0.229	-0.0496
1.06	0.342	-0.0485
1.93	0.432	-0.0474
3.17	0.556	-0.0465
3.93	0.638	-0.0454
5.19	0.752	-0.0439
6.14	0.845	-0.0429
7.18	0.944	-0.0414
8.23	1.038	-0.0397
9.21	1.116	-0.0373
10.14	1.169	-0.0346
9.86	1.160	-0.0354
8.82	1.077	-0.0379
7.71	0.988	-0.0403
6.82	0.909	-0.0415
5.66	0.801	-0.0431
4.75	0.715	-0.0442
3.62	0.600	-0.0453
2.65	0.511	-0.0464
1.63	0.401	-0.0470
0.65	0.304	-0.0479
-0.38	0.205	-0.0494
-1.55	0.083	-0.0518
-1.92	0.040	-0.0509
-3.54	-0.088	-0.0462
-4.60	-0.190	-0.0463
-5.60	-0.294	-0.0478
-6.56	-0.431	-0.0286

AG455ct-02r fn20.4

Fig. 6.79

Run: 06813gw
Re = 100124.4

α	C_l	C_m
-10.21	-1.053	0.1976
-9.19	-1.063	0.1925
-8.12	-1.077	0.1893
-7.18	-1.092	0.1854
-6.15	-1.118	0.1795
-5.19	-1.108	0.1609
-4.20	-1.106	0.1431

-3.19	-1.074	0.1183
-2.28	-1.021	0.1062
-1.21	-0.933	0.1024
-0.11	-0.828	0.1100
0.88	-0.745	0.1133
1.78	-0.674	0.1187
2.85	-0.481	0.1152
3.82	-0.405	0.1203
5.01	-0.287	0.1188
5.92	-0.260	0.1321
6.96	-0.195	0.1388
8.02	-0.129	0.1456
9.03	-0.080	0.1522
10.04	0.005	0.1541
11.12	0.111	0.1526
12.26	0.219	0.1500
13.19	0.318	0.1445
14.04	0.385	0.0463
15.01	0.407	0.0247
16.06	0.421	0.0113
16.97	0.431	0.0089
18.15	0.463	0.0009
19.08	0.473	-0.0098
20.19	0.501	-0.0148
19.66	0.472	-0.0007
18.64	0.504	-0.0023
17.70	0.480	0.0056
16.79	0.483	0.0054
15.61	0.435	0.0202
14.72	0.400	0.0324
13.84	0.381	0.1437
12.84	0.288	0.1527
11.82	0.186	0.1597
10.80	0.081	0.1612
9.79	-0.007	0.1644
8.76	-0.080	0.1602
7.72	-0.125	0.1495
6.70	-0.195	0.1450
5.69	-0.229	0.1342
4.70	-0.290	0.1276
3.69	-0.379	0.1277
2.60	-0.597	0.1274
1.58	-0.657	0.1182
0.58	-0.751	0.1138
-0.56	-0.849	0.1066
-1.53	-0.940	0.1072
-2.51	-1.020	0.1145
-3.50	-1.064	0.1355
-4.51	-1.097	0.1630
-5.51	-1.110	0.1836
-6.48	-1.082	0.1925
-7.44	-1.084	0.1985
-8.50	-1.057	0.2017
-9.47	-1.028	0.1980

Run: 06814gw
Re = 199899.1

α	C_l	C_m
-6.23	-1.095	0.1903
-5.22	-1.111	0.1760
-4.20	-1.116	0.1533
-3.22	-1.099	0.1299
-2.23	-1.051	0.1151
-1.26	-0.973	0.1093
-0.23	-0.881	0.1146
0.95	-0.786	0.1229
1.76	-0.719	0.1284
2.87	-0.648	0.1366
3.97	-0.513	0.1479
4.94	-0.438	0.1530
5.99	-0.348	0.1549
6.93	-0.262	0.1549
8.07	-0.152	0.1530
9.13	-0.046	0.1528
10.18	0.053	0.1520
11.19	0.142	0.1496
12.21	0.251	0.1472
13.17	0.345	0.1411
14.18	0.451	0.1311
14.92	0.483	0.0130
16.10	0.511	-0.0023
17.01	0.542	-0.0106
18.02	0.535	-0.0131
17.81	0.537	-0.0091
16.74	0.528	-0.0034
15.77	0.517	0.0018
15.07	0.552	0.1131
13.92	0.425	0.1376
12.81	0.314	0.1467
11.77	0.209	0.1501
10.60	0.115	0.1522
9.73	0.023	0.1533
8.72	-0.078	0.1556
7.67	-0.180	0.1557
6.73	-0.278	0.1573
5.66	-0.379	0.1573
4.70	-0.462	0.1548
3.59	-0.528	0.1482
2.58	-0.656	0.1332
1.52	-0.734	0.1269
0.49	-0.817	0.1202
-0.60	-0.910	0.1132
-1.55	-0.993	0.1127
-2.55	-1.070	0.1201
-3.55	-1.117	0.1397
-4.48	-1.142	0.1622
-5.38	-1.129	0.1826

Run: 06815gw
Re = 300196.1

α	C_l	C_m
-6.15	-1.127	0.1928
-5.18	-1.142	0.1749
-4.14	-1.126	0.1521
-3.21	-1.113	0.1298
-2.23	-1.055	0.1160
-1.17	-0.977	0.1131
-0.14	-0.895	0.1199
0.92	-0.810	0.1301
1.94	-0.719	0.1354
2.94	-0.653	0.1434
4.03	-0.573	0.1553
4.91	-0.484	0.1557
6.03	-0.373	0.1549
7.06	-0.274	0.1551
8.07	-0.170	0.1552
9.07	-0.071	0.1540
10.31	0.037	0.1532
11.15	0.111	0.1520
12.12	0.217	0.1489
13.22	0.339	0.1441
14.18	0.452	0.1355
15.19	0.576	0.1101
15.97	0.538	0.0025
16.67	0.598	-0.0095
17.80	0.572	-0.0136
17.83	0.604	-0.0163
16.77	0.591	-0.0077
15.80	0.554	0.0055
14.90	0.538	0.1220
13.91	0.425	0.1398
12.84	0.315	0.1483
11.82	0.201	0.1505
10.78	0.094	0.1536
9.74	0.018	0.1538
8.84	-0.073	0.1546
7.71	-0.181	0.1549
6.63	-0.295	0.1562
5.62	-0.397	0.1561
4.61	-0.501	0.1562
3.70	-0.590	0.1495
2.59	-0.667	0.1407
1.52	-0.746	0.1333
0.47	-0.838	0.1265
-0.52	-0.922	0.1175
-1.45	-0.999	0.1139
-2.50	-1.074	0.1197
-3.57	-1.121	0.1390
-4.54	-1.132	0.1610

-5.47	-1.130	0.1805

Run: 06816gw
Re = 400274.3

α	C_l	C_m
-3.08	-1.102	0.1274
-2.15	-1.052	0.1153
-1.10	-0.983	0.1146
-0.21	-0.916	0.1199
0.79	-0.826	0.1300
2.02	-0.724	0.1369
2.97	-0.651	0.1435
3.91	-0.577	0.1484
5.07	-0.475	0.1533
6.12	-0.364	0.1531
7.06	-0.269	0.1531
8.09	-0.166	0.1528
9.19	-0.061	0.1531
9.86	0.009	0.1530
11.12	0.110	0.1510
12.20	0.225	0.1484
13.15	0.333	0.1454
14.23	0.454	0.1371
15.17	0.580	0.1131
14.91	0.534	0.1241
13.93	0.420	0.1418
12.72	0.290	0.1476
11.83	0.188	0.1507
10.81	0.079	0.1521
9.71	-0.005	0.1525
8.65	-0.111	0.1538
7.64	-0.211	0.1549
6.64	-0.311	0.1530
5.64	-0.415	0.1540
4.61	-0.520	0.1532
3.61	-0.599	0.1460
2.62	-0.670	0.1396
1.64	-0.750	0.1341
0.60	-0.844	0.1272
-0.59	-0.936	0.1170
-1.54	-1.011	0.1137
-2.59	-1.088	0.1217

Run: 06817gw
Re = 500043.2

α	C_l	C_m
-2.99	-1.112	0.1309
-2.26	-1.056	0.1158
-1.11	-0.983	0.1122
-0.06	-0.891	0.1179
0.77	-0.828	0.1263
1.92	-0.738	0.1345
2.95	-0.655	0.1392
3.98	-0.574	0.1455
4.94	-0.492	0.1495
5.97	-0.384	0.1509
6.94	-0.282	0.1516
8.04	-0.176	0.1518
9.09	-0.065	0.1526
9.79	0.001	0.1509
11.08	0.110	0.1505
12.14	0.217	0.1494
13.16	0.332	0.1467
14.23	0.448	0.1395
15.23	0.580	0.1153
14.79	0.516	0.1301
13.84	0.401	0.1416
12.82	0.290	0.1472
11.81	0.183	0.1508
10.72	0.065	0.1518
9.65	-0.012	0.1527
8.64	-0.109	0.1523
7.68	-0.208	0.1529
6.62	-0.315	0.1517
5.67	-0.418	0.1511
4.74	-0.519	0.1509
3.53	-0.603	0.1419
2.55	-0.687	0.1380
1.35	-0.784	0.1318
0.45	-0.858	0.1238
-0.53	-0.934	0.1147
-1.57	-1.010	0.1120
-2.52	-1.077	0.1203

AG455ct-02r fn15.4

Fig. 6.82

Run: 06733gw
Re = 99985.8

α	C_l	C_m
-8.14	-0.968	0.1648
-7.13	-1.001	0.1594
-6.26	-0.995	0.1480
-5.12	-1.012	0.1243
-4.16	-0.969	0.0965
-3.28	-0.911	0.0800
-2.21	-0.816	0.0764
-1.21	-0.737	0.0810
-0.21	-0.647	0.0842
0.86	-0.562	0.0892
1.87	-0.523	0.1037
2.92	-0.436	0.1121
3.90	-0.347	0.1124
4.94	-0.249	0.1141
5.99	-0.154	0.1158
7.00	-0.053	0.1167
8.01	0.054	0.1157
9.04	0.160	0.1150
10.18	0.284	0.1135
11.35	0.387	0.1127
12.36	0.467	0.1078
13.08	0.525	0.0992
14.24	0.525	-0.0132
15.25	0.537	-0.0253
16.14	0.552	-0.0296
17.06	0.595	-0.0396
18.06	0.587	-0.0386
17.77	0.597	-0.0296
16.69	0.562	-0.0230
15.84	0.579	-0.0226
14.78	0.556	-0.0153
13.73	0.548	0.0082
12.49	0.514	0.1086
11.70	0.445	0.1122
10.82	0.358	0.1177
9.79	0.259	0.1215
8.78	0.151	0.1237
7.77	0.055	0.1233
6.73	-0.046	0.1229
5.67	-0.146	0.1238
4.71	-0.238	0.1234
3.60	-0.339	0.1241
2.64	-0.425	0.1222
1.54	-0.495	0.0929
0.51	-0.571	0.0873
-0.52	-0.657	0.0828
-1.47	-0.744	0.0784
-2.49	-0.836	0.0798
-3.58	-0.925	0.0929
-4.47	-0.987	0.1159
-5.50	-1.014	0.1431
-6.49	-1.004	0.1623
-7.47	-0.984	0.1697

Run: 06735gw
Re = 199989.9

α	C_l	C_m
-8.18	-1.007	0.1794
-7.20	-1.026	0.1709
-6.17	-1.028	0.1574
-5.18	-1.029	0.1376
-4.20	-1.013	0.1107
-3.22	-0.939	0.0888
-2.13	-0.839	0.0806
-1.33	-0.761	0.0846
-0.19	-0.663	0.0923
0.89	-0.570	0.0967
1.89	-0.489	0.1009

2.95	-0.415	0.1125
3.98	-0.311	0.1137
4.97	-0.219	0.1135
6.07	-0.115	0.1127
7.04	-0.019	0.1131
8.37	0.094	0.1122
9.07	0.154	0.1119
10.04	0.260	0.1098
11.13	0.372	0.1075
12.18	0.474	0.1047
13.14	0.587	0.0970
13.96	0.626	-0.0057
15.11	0.638	-0.0352
16.02	0.639	-0.0396
17.02	0.661	-0.0482
18.05	0.650	-0.0440
17.69	0.658	-0.0433
16.76	0.650	-0.0394
15.71	0.650	-0.0371
14.76	0.635	-0.0297
14.02	0.670	0.0887
12.84	0.552	0.1023
11.85	0.452	0.1081
10.84	0.344	0.1105
9.71	0.233	0.1126
8.26	0.124	0.1140
7.63	0.060	0.1136
6.68	-0.044	0.1148
5.63	-0.150	0.1147
4.69	-0.239	0.1153
3.65	-0.340	0.1143
2.62	-0.441	0.1145
1.58	-0.504	0.0995
0.53	-0.588	0.0944
-0.52	-0.678	0.0899
-1.55	-0.768	0.0833
-2.50	-0.870	0.0851
-3.57	-0.959	0.0989
-4.58	-1.017	0.1232
-5.46	-1.023	0.1462
-6.45	-1.020	0.1652
-7.43	-1.011	0.1762

Run: 06737gw

Re = 300020.1

α	C_l	C_m
-7.62	-1.020	0.1775
-7.14	-1.044	0.1730
-6.16	-1.052	0.1583
-5.16	-1.048	0.1347
-4.18	-1.016	0.1094
-3.30	-0.956	0.0910
-2.15	-0.853	0.0826
-1.12	-0.768	0.0881
-0.11	-0.669	0.0953
0.88	-0.594	0.1006
1.90	-0.503	0.1048
3.03	-0.423	0.1122
4.01	-0.318	0.1124
5.06	-0.213	0.1126
6.09	-0.110	0.1123
7.03	-0.013	0.1116
7.97	0.044	0.1117
9.09	0.151	0.1105
10.13	0.270	0.1092
11.12	0.379	0.1078
12.19	0.486	0.1040
13.22	0.594	0.0976
14.17	0.687	0.0831
15.00	0.672	-0.0271
16.05	0.676	-0.0421
17.02	0.669	-0.0450
16.73	0.673	-0.0434
15.65	0.660	-0.0359
14.80	0.674	-0.0228
14.11	0.680	0.0857
12.86	0.558	0.1012
11.83	0.453	0.1066
10.76	0.345	0.1100
9.71	0.226	0.1107
8.70	0.120	0.1116
8.04	0.067	0.1119
6.71	-0.037	0.1126
5.66	-0.145	0.1128
4.60	-0.249	0.1129
3.66	-0.343	0.1124
2.54	-0.450	0.1099
1.53	-0.526	0.1026
0.47	-0.616	0.0978
-0.44	-0.695	0.0934
-1.50	-0.792	0.0845
-2.55	-0.882	0.0847
-3.55	-0.972	0.0963
-4.53	-1.026	0.1205
-5.55	-1.050	0.1449
-6.46	-1.054	0.1650
-7.57	-1.042	0.1775

Run: 06739gw

Re = 400205.3

α	C_l	C_m
-5.22	-1.045	0.1347
-4.22	-1.005	0.1081
-3.13	-0.928	0.0877
-2.17	-0.849	0.0830
-1.29	-0.768	0.0872
-0.04	-0.666	0.0972
0.97	-0.580	0.1018
2.00	-0.487	0.1052
2.89	-0.419	0.1099
3.93	-0.316	0.1116
5.01	-0.204	0.1111
6.04	-0.100	0.1107
7.10	0.003	0.1112
8.09	0.052	0.1102
9.07	0.167	0.1098
10.13	0.281	0.1100
11.13	0.379	0.1075
12.18	0.489	0.1056
13.24	0.602	0.0997
12.86	0.560	0.1020
11.82	0.451	0.1068
10.82	0.347	0.1092
9.75	0.237	0.1103
8.65	0.113	0.1111
7.31	0.022	0.1106
6.67	-0.039	0.1111
5.67	-0.141	0.1118
4.57	-0.250	0.1121
3.65	-0.337	0.1112
2.67	-0.431	0.1079
1.61	-0.513	0.1030
0.59	-0.609	0.0992
-0.49	-0.706	0.0949
-1.59	-0.792	0.0846
-2.58	-0.877	0.0832
-3.51	-0.952	0.0930
-4.48	-1.016	0.1174

Run: 06741gw

Re = 499873.6

α	C_l	C_m
-5.04	-1.020	0.1324
-4.14	-0.999	0.1074
-3.23	-0.929	0.0865
-2.24	-0.845	0.0806
-1.06	-0.746	0.0874
0.00	-0.660	0.0959
0.94	-0.580	0.0996
1.83	-0.502	0.1027
2.98	-0.412	0.1078
3.93	-0.321	0.1095
5.06	-0.206	0.1102
6.03	-0.108	0.1103
7.01	-0.011	0.1107
8.09	0.043	0.1107
9.11	0.162	0.1101
10.17	0.271	0.1095
11.19	0.377	0.1082

12.13	0.469	0.1058
13.17	0.581	0.1017
12.84	0.546	0.1038
11.73	0.434	0.1077
10.90	0.344	0.1089
9.76	0.231	0.1100
8.66	0.120	0.1113
7.28	0.012	0.1111
6.64	-0.047	0.1109
5.56	-0.158	0.1106
4.59	-0.257	0.1110
3.66	-0.348	0.1097
2.60	-0.439	0.1057
1.50	-0.531	0.1016
0.56	-0.619	0.0989
-0.56	-0.714	0.0928
-1.53	-0.789	0.0842
-2.52	-0.879	0.0819
-3.59	-0.967	0.0948
-4.48	-1.020	0.1193

AG455ct-02r fn10.4

Fig. 6.85

Run: 06743gw
Re = 100089.2

α	C_l	C_m
-8.16	-0.907	0.1341
-7.15	-0.913	0.1250
-6.17	-0.897	0.1055
-5.27	-0.877	0.0766
-4.15	-0.767	0.0447
-3.22	-0.664	0.0400
-2.13	-0.570	0.0436
-1.08	-0.480	0.0458
-0.14	-0.404	0.0467
0.91	-0.339	0.0594
1.93	-0.241	0.0606
3.02	-0.133	0.0608
3.97	-0.040	0.0637
4.99	0.071	0.0610
6.06	0.201	0.0573
6.98	0.308	0.0545
8.18	0.430	0.0537
9.23	0.505	0.0570
10.43	0.605	0.0555
11.05	0.663	0.0548
12.08	0.734	0.0463
12.95	0.716	-0.0606
14.05	0.722	-0.0744
14.97	0.752	-0.0824
16.00	0.745	-0.0865
17.00	0.753	-0.0858
18.09	0.746	-0.0844
17.69	0.750	-0.0765
16.74	0.763	-0.0801
15.65	0.761	-0.0739
14.81	0.740	-0.0662
13.76	0.750	-0.0633
12.73	0.757	-0.0348
11.84	0.744	0.0565
10.79	0.660	0.0576
9.55	0.578	0.0588
8.39	0.482	0.0634
7.85	0.425	0.0644
6.83	0.314	0.0668
5.74	0.193	0.0681
4.63	0.078	0.0685
3.68	-0.020	0.0678
2.63	-0.121	0.0708
1.61	-0.217	0.0692
0.62	-0.311	0.0584
-0.51	-0.391	0.0481
-1.52	-0.488	0.0467
-2.44	-0.578	0.0437
-3.51	-0.682	0.0449
-4.57	-0.795	0.0630
-5.53	-0.864	0.0947
-6.52	-0.912	0.1191
-7.51	-0.929	0.1390

Run: 06745gw
Re = 199807.6

α	C_l	C_m
-8.13	-0.900	0.1431
-7.17	-0.902	0.1333
-6.18	-0.899	0.1124
-5.23	-0.853	0.0831
-4.29	-0.771	0.0556
-3.14	-0.662	0.0417
-2.12	-0.562	0.0465
-1.06	-0.469	0.0496
-0.10	-0.380	0.0519
0.89	-0.307	0.0572
1.96	-0.213	0.0637
2.98	-0.103	0.0625
3.99	-0.002	0.0624
4.99	0.092	0.0625
6.29	0.182	0.0621
7.03	0.254	0.0625
8.01	0.350	0.0623
9.08	0.464	0.0617
10.20	0.587	0.0588
11.19	0.695	0.0543
12.24	0.790	0.0493
13.08	0.796	-0.0577
14.07	0.803	-0.0760
13.85	0.775	-0.0715
12.91	0.837	0.0471
11.79	0.764	0.0543
10.87	0.667	0.0589
9.80	0.550	0.0626
8.69	0.428	0.0648
7.77	0.330	0.0649
6.72	0.229	0.0647
5.30	0.131	0.0637
4.72	0.071	0.0639
3.61	-0.038	0.0635
2.60	-0.136	0.0648
1.59	-0.241	0.0648
0.60	-0.315	0.0541
-0.49	-0.403	0.0503
-1.56	-0.499	0.0473
-2.54	-0.591	0.0432
-3.52	-0.692	0.0452
-4.57	-0.802	0.0640
-5.46	-0.866	0.0940
-6.53	-0.900	0.1220
-7.47	-0.908	0.1373

Run: 06747gw
Re = 299856.5

α	C_l	C_m
-8.17	-0.909	0.1473
-7.15	-0.933	0.1316
-6.16	-0.905	0.1095
-5.23	-0.866	0.0789
-4.18	-0.764	0.0513
-3.13	-0.660	0.0426
-2.15	-0.560	0.0471
-1.18	-0.471	0.0511
-0.18	-0.376	0.0534
0.94	-0.283	0.0561
2.02	-0.188	0.0614
3.00	-0.093	0.0610
3.98	0.005	0.0609
4.95	0.062	0.0610
5.99	0.164	0.0608
7.03	0.283	0.0603
8.13	0.397	0.0600
9.10	0.504	0.0597
10.27	0.619	0.0581
11.13	0.710	0.0561
12.20	0.801	0.0520
13.14	0.861	0.0420
14.03	0.841	-0.0670
13.75	0.828	-0.0557
12.82	0.842	0.0482

11.84	0.766	0.0548
10.87	0.679	0.0577
9.75	0.570	0.0598
8.74	0.471	0.0610
7.78	0.373	0.0616
6.70	0.251	0.0617
5.67	0.140	0.0618
5.14	0.087	0.0617
3.56	-0.024	0.0621
2.60	-0.122	0.0623
1.57	-0.227	0.0616
0.60	-0.307	0.0557
-0.45	-0.402	0.0534
-1.50	-0.497	0.0499
-2.58	-0.598	0.0444
-3.55	-0.697	0.0446
-4.51	-0.796	0.0592
-5.48	-0.878	0.0872
-6.49	-0.913	0.1196
-7.44	-0.933	0.1383

Run: 06749gw
Re = 399895.3

α	C_l	C_m
-5.14	-0.867	0.0770
-4.28	-0.775	0.0513
-3.14	-0.664	0.0426
-2.24	-0.575	0.0478
-1.09	-0.471	0.0522
-0.08	-0.377	0.0545
0.93	-0.287	0.0564
1.92	-0.198	0.0605
3.03	-0.089	0.0606
3.88	-0.004	0.0604
4.94	0.056	0.0606
5.98	0.178	0.0604
7.04	0.283	0.0599
8.16	0.406	0.0603
9.07	0.495	0.0595
10.07	0.601	0.0587
11.25	0.712	0.0563
12.15	0.797	0.0531
11.92	0.778	0.0543
10.84	0.675	0.0576
9.76	0.567	0.0595
8.73	0.461	0.0604
7.68	0.354	0.0609
6.74	0.256	0.0609
5.68	0.133	0.0609
4.40	0.032	0.0611
3.62	-0.026	0.0610
2.57	-0.130	0.0609
1.53	-0.236	0.0610
0.67	-0.311	0.0566
-0.46	-0.411	0.0539
-1.52	-0.509	0.0507
-2.54	-0.601	0.0451
-3.57	-0.711	0.0447
-4.62	-0.810	0.0597

Run: 06751gw
Re = 499972.4

α	C_l	C_m
-5.17	-0.856	0.0767
-4.26	-0.770	0.0500
-3.12	-0.645	0.0410
-2.25	-0.569	0.0464
-1.02	-0.465	0.0521
-0.04	-0.372	0.0542
0.98	-0.275	0.0558
2.05	-0.179	0.0591
2.92	-0.095	0.0600
4.04	0.013	0.0596
5.02	0.063	0.0600
6.03	0.184	0.0601
7.15	0.293	0.0597
8.12	0.390	0.0599
9.07	0.493	0.0596
10.16	0.600	0.0586
11.24	0.707	0.0570
12.22	0.800	0.0545
11.83	0.770	0.0558
10.81	0.666	0.0584
9.82	0.570	0.0596
8.71	0.454	0.0603
7.67	0.351	0.0607
6.67	0.249	0.0607
5.66	0.143	0.0608
4.13	0.020	0.0597
3.64	-0.027	0.0601
2.58	-0.127	0.0601
1.56	-0.225	0.0590
0.53	-0.316	0.0554
-0.53	-0.412	0.0534
-1.52	-0.510	0.0508
-2.50	-0.592	0.0437
-3.56	-0.689	0.0422
-4.58	-0.799	0.0575

AG455ct-02r fn5.4

Fig. 6.88

Run: 06753ga
Re = 99955.9

α	C_l	C_m
-10.08	-0.768	0.1073
-9.14	-0.771	0.1023
-8.22	-0.747	0.0944
-7.17	-0.756	0.0715
-6.28	-0.703	0.0452
-5.20	-0.575	0.0067
-4.21	-0.465	-0.0033
-3.23	-0.368	-0.0008
-2.12	-0.269	0.0017
-1.02	-0.187	0.0045
-0.00	-0.055	-0.0022
0.84	0.030	-0.0075
2.05	0.152	-0.0048
3.00	0.239	-0.0010
3.96	0.333	0.0008
5.37	0.438	0.0052
6.18	0.502	0.0060
7.09	0.581	0.0078
8.17	0.681	0.0090
9.08	0.756	0.0096
10.17	0.833	0.0072
11.20	0.892	0.0061
12.03	0.856	-0.1006
12.97	0.853	-0.1114
14.02	0.841	-0.1200
14.96	0.808	-0.1179
16.03	0.837	-0.1230
15.64	0.844	-0.1141
14.76	0.845	-0.1117
13.79	0.819	-0.1022
12.72	0.884	-0.1019
11.75	0.881	-0.0781
10.90	0.894	0.0133
9.79	0.822	0.0132
8.78	0.744	0.0113
7.60	0.645	0.0100
6.40	0.557	0.0104
5.51	0.488	0.0086
4.41	0.397	0.0066
3.61	0.326	0.0015
2.63	0.243	0.0002
1.66	0.157	-0.0010
0.58	0.038	0.0037
-0.51	-0.074	0.0077
-1.49	-0.187	0.0048
-2.41	-0.275	0.0040

-3.51	-0.379	0.0023
-4.60	-0.495	0.0053
-5.57	-0.627	0.0330
-6.51	-0.701	0.0729
-7.48	-0.753	0.0928
-8.50	-0.777	0.1118
-9.52	-0.758	0.1162

Run: 06755ga
Re = 199921.2

α	C_l	C_m
-10.06	-0.763	0.1166
-9.12	-0.779	0.1114
-8.15	-0.767	0.1004
-7.21	-0.756	0.0795
-6.21	-0.695	0.0464
-5.23	-0.589	0.0141
-4.12	-0.462	-0.0003
-3.20	-0.371	0.0021
-2.19	-0.274	0.0037
-1.06	-0.163	0.0031
-0.10	-0.068	0.0047
0.99	0.052	0.0018
1.88	0.115	0.0028
3.02	0.212	0.0035
4.02	0.311	0.0041
4.97	0.412	0.0052
6.04	0.520	0.0058
7.02	0.623	0.0057
8.17	0.729	0.0064
9.17	0.815	0.0066
10.16	0.895	0.0063
11.21	0.959	0.0054
12.06	0.959	-0.0853
12.98	0.927	-0.1109
13.97	0.880	-0.1186
15.02	0.892	-0.1236
14.72	0.894	-0.1198
13.69	0.896	-0.1152
12.72	0.929	-0.1081
11.84	0.986	0.0061
10.81	0.938	0.0090
9.81	0.872	0.0096
8.82	0.786	0.0094
7.78	0.697	0.0093
6.68	0.595	0.0086
5.77	0.489	0.0082
4.77	0.386	0.0072
3.57	0.267	0.0060
2.46	0.167	0.0041
1.43	0.096	0.0034
0.60	0.019	0.0027
-0.41	-0.102	0.0067
-1.46	-0.199	0.0040
-2.37	-0.290	0.0035
-3.52	-0.394	0.0015
-4.54	-0.506	0.0040
-5.54	-0.622	0.0258
-6.61	-0.725	0.0631
-7.45	-0.769	0.0900
-8.52	-0.781	0.1082
-9.54	-0.789	0.1176

Run: 06757gw
Re = 300065.6

α	C_l	C_m
-10.10	-0.786	0.1208
-9.20	-0.775	0.1132
-8.16	-0.784	0.0993
-7.21	-0.766	0.0786
-6.19	-0.700	0.0404
-5.20	-0.581	0.0097
-4.23	-0.469	-0.0009
-3.14	-0.353	0.0020
-2.14	-0.261	0.0031
-1.09	-0.161	0.0023
-0.06	-0.074	0.0067
0.97	0.032	0.0052
2.01	0.094	0.0045
3.02	0.200	0.0049
4.05	0.312	0.0055
5.06	0.424	0.0060
6.12	0.531	0.0064
7.09	0.628	0.0068
8.05	0.723	0.0071
9.20	0.829	0.0072
10.24	0.917	0.0073
11.20	0.988	0.0065
12.16	1.022	0.0008
12.96	0.974	-0.0970
14.03	0.939	-0.1171
14.91	0.930	-0.1216
14.72	0.936	-0.1211
13.76	0.952	-0.1153
12.76	0.996	-0.0877
11.84	1.009	0.0062
10.78	0.960	0.0082
9.79	0.882	0.0084
8.83	0.793	0.0085
7.76	0.693	0.0080
6.69	0.587	0.0077
5.78	0.489	0.0077
4.65	0.381	0.0070
3.71	0.283	0.0066
2.64	0.163	0.0060
1.17	0.061	0.0059
0.55	-0.009	0.0088
-0.47	-0.093	0.0049
-1.49	-0.189	0.0031
-2.51	-0.291	0.0034
-3.48	-0.386	0.0014
-4.60	-0.509	0.0021
-5.56	-0.619	0.0185
-6.51	-0.729	0.0573
-7.51	-0.774	0.0848
-8.46	-0.784	0.1064
-9.48	-0.795	0.1185

Run: 06759gw
Re = 399849.8

α	C_l	C_m
-6.14	-0.700	0.0402
-5.20	-0.576	0.0066
-4.25	-0.468	-0.0017
-3.11	-0.353	0.0018
-2.20	-0.262	0.0022
-1.05	-0.151	0.0036
-0.17	-0.071	0.0046
0.98	0.027	0.0078
1.96	0.083	0.0070
3.04	0.210	0.0060
3.98	0.308	0.0062
5.05	0.419	0.0067
6.08	0.523	0.0072
7.11	0.622	0.0075
8.12	0.719	0.0079
9.04	0.815	0.0082
10.17	0.917	0.0080
11.22	0.992	0.0077
10.79	0.960	0.0080
9.78	0.883	0.0082
8.83	0.797	0.0085
7.73	0.683	0.0084
6.78	0.594	0.0082
5.72	0.485	0.0077
4.65	0.378	0.0072
3.67	0.281	0.0068
2.65	0.173	0.0068
1.56	0.047	0.0084
0.58	-0.006	0.0080
-0.50	-0.095	0.0044
-1.38	-0.182	0.0040
-2.52	-0.290	0.0024
-3.58	-0.396	0.0014
-4.55	-0.495	-0.0002
-5.56	-0.623	0.0170

Run: 06761gw
Re = 499778.0

α	C_l	C_m
-6.22	-0.704	0.0414
-5.23	-0.573	0.0064
-4.12	-0.447	-0.0024
-3.19	-0.354	0.0010
-2.17	-0.254	0.0028
-1.07	-0.151	0.0037
-0.15	-0.064	0.0042
1.25	0.023	0.0079
2.00	0.085	0.0080
2.99	0.201	0.0072
3.99	0.308	0.0071
4.98	0.409	0.0073
6.05	0.519	0.0080
7.08	0.622	0.0084
8.14	0.724	0.0085
9.19	0.823	0.0088
10.13	0.908	0.0086
11.20	0.986	0.0079
10.82	0.967	0.0085
9.73	0.875	0.0090
8.82	0.791	0.0092
7.83	0.699	0.0091
6.81	0.593	0.0089
5.76	0.484	0.0083
4.69	0.382	0.0080
3.63	0.271	0.0076
2.68	0.168	0.0081
1.62	0.045	0.0086
0.66	-0.002	0.0078
-0.48	-0.093	0.0045
-1.49	-0.193	0.0040
-2.38	-0.283	0.0029
-3.43	-0.376	0.0008
-4.65	-0.496	-0.0010
-5.53	-0.616	0.0143

AG455ct-02r fp4.6

Fig. 6.91

Run: 06783gw
Re = 100028.0

α	C_l	C_m
-10.13	-0.488	0.0243
-9.20	-0.440	0.0073
-8.18	-0.399	-0.0164
-7.18	-0.248	-0.0667
-6.26	-0.091	-0.0882
-5.21	0.031	-0.0958
-4.10	0.156	-0.1038
-3.11	0.243	-0.1036
-2.11	0.315	-0.0968
-1.04	0.405	-0.0957
0.01	0.507	-0.1030
1.03	0.651	-0.1143
2.02	0.732	-0.1033
2.99	0.818	-0.0954
4.05	0.896	-0.0906
5.02	0.977	-0.0891
6.08	1.046	-0.0832
7.14	1.108	-0.0786
8.07	1.151	-0.0747
9.10	1.179	-0.0684
10.10	1.148	-0.1488
11.08	1.108	-0.1730
12.05	1.077	-0.1915
12.93	1.047	-0.1870
13.96	1.038	-0.1905
13.77	1.037	-0.1783
12.76	1.066	-0.1823
11.71	1.059	-0.1740
10.76	1.134	-0.1524
9.78	1.190	-0.0907
8.88	1.181	-0.0629
7.88	1.139	-0.0673
6.79	1.093	-0.0731
5.84	1.034	-0.0777
4.83	0.966	-0.0836
3.72	0.872	-0.0876
2.70	0.805	-0.0942
1.64	0.713	-0.0987
0.72	0.597	-0.0984
-0.78	0.446	-0.0872
-1.33	0.377	-0.0857
-2.36	0.297	-0.0910
-3.43	0.219	-0.0960
-4.49	0.109	-0.0929
-5.47	-0.007	-0.0875
-6.47	-0.129	-0.0822
-7.57	-0.323	-0.0352
-8.46	-0.411	0.0033
-9.52	-0.461	0.0211

Run: 06785gw
Re = 199901.6

α	C_l	C_m
-10.16	-0.507	0.0300
-9.23	-0.475	0.0073
-8.25	-0.384	-0.0202
-7.25	-0.182	-0.0858
-6.27	-0.038	-0.1020
-5.21	0.078	-0.1067
-4.38	0.137	-0.1084
-3.10	0.251	-0.1126
-2.09	0.352	-0.1128
-1.11	0.453	-0.1133
-0.16	0.560	-0.1115
0.95	0.668	-0.1063
1.99	0.761	-0.1011
3.06	0.852	-0.0959
4.05	0.939	-0.0932
5.06	1.022	-0.0903
6.11	1.101	-0.0854
7.18	1.162	-0.0805
8.14	1.211	-0.0741
9.18	1.239	-0.0682
9.99	1.236	-0.1209
10.95	1.202	-0.1742
11.99	1.139	-0.1915
12.98	1.095	-0.1931
13.98	1.107	-0.1958
13.74	1.117	-0.1945
12.65	1.097	-0.1860
11.71	1.128	-0.1814
10.78	1.189	-0.1651
9.82	1.242	-0.1127
8.82	1.240	-0.0673
7.86	1.206	-0.0736
6.79	1.148	-0.0794
5.88	1.091	-0.0842
4.79	1.006	-0.0883
3.80	0.926	-0.0912
2.71	0.834	-0.0943
1.73	0.746	-0.0992
0.71	0.651	-0.1049
-0.39	0.545	-0.1090
-1.37	0.437	-0.1102
-2.29	0.340	-0.1102
-3.50	0.217	-0.1094
-3.99	0.169	-0.1079
-5.60	0.049	-0.1031
-6.51	-0.065	-0.0979
-7.38	-0.220	-0.0717
-8.54	-0.420	-0.0074
-9.50	-0.483	0.0222

Run: 06787gw
Re = 299945.0

α	C_l	C_m
-10.15	-0.505	0.0303
-9.22	-0.465	0.0072
-8.27	-0.343	-0.0438
-7.21	-0.148	-0.0954
-6.12	-0.008	-0.1046
-4.91	0.067	-0.1064
-4.08	0.154	-0.1082

-3.16	0.248	-0.1100
-2.07	0.380	-0.1099
-1.16	0.467	-0.1079
-0.11	0.575	-0.1064
0.91	0.669	-0.1029
1.87	0.759	-0.0985
3.10	0.862	-0.0948
3.99	0.950	-0.0932
5.21	1.047	-0.0890
6.21	1.126	-0.0854
7.13	1.190	-0.0812
8.20	1.241	-0.0744
9.27	1.270	-0.0676
9.99	1.293	-0.1082
11.14	1.251	-0.1590
11.99	1.191	-0.1820
11.73	1.192	-0.1792
10.76	1.252	-0.1462
9.78	1.269	-0.0817
8.85	1.260	-0.0695
7.93	1.236	-0.0755
6.71	1.163	-0.0825
5.87	1.100	-0.0862
4.91	1.023	-0.0897
3.69	0.926	-0.0930
2.62	0.828	-0.0945
1.72	0.747	-0.0978
0.58	0.639	-0.1017
-0.45	0.543	-0.1050
-1.36	0.449	-0.1069
-2.35	0.341	-0.1084
-3.49	0.221	-0.1083
-4.54	0.110	-0.1064
-5.27	0.068	-0.1054
-6.46	-0.044	-0.1024
-7.50	-0.203	-0.0836
-8.51	-0.385	-0.0238
-9.51	-0.491	0.0170

Run: 06789ga

Re = 399460.7

α	C_l	C_m
-7.21	-0.122	-0.0986
-6.18	-0.006	-0.1030
-5.28	0.045	-0.1038
-4.16	0.153	-0.1058
-3.12	0.270	-0.1064
-2.05	0.383	-0.1064
-1.04	0.487	-0.1046
0.04	0.586	-0.1020
0.93	0.677	-0.0997
2.06	0.776	-0.0965
3.14	0.882	-0.0951
4.07	0.963	-0.0925
5.07	1.049	-0.0896
6.06	1.132	-0.0861
7.10	1.206	-0.0815
8.08	1.256	-0.0756
9.25	1.291	-0.0686
8.82	1.290	-0.0710
7.83	1.245	-0.0772
6.71	1.176	-0.0831
5.68	1.102	-0.0876
4.83	1.030	-0.0904
3.82	0.935	-0.0925
2.66	0.836	-0.0949
1.70	0.748	-0.0971
0.64	0.640	-0.0995
-0.45	0.538	-0.1022
-1.46	0.440	-0.1045
-2.41	0.340	-0.1061
-3.50	0.230	-0.1052
-4.53	0.108	-0.1036
-4.96	0.067	-0.1030
-6.55	-0.043	-0.1016

Run: 06791ga

Re = 500321.8

α	C_l	C_m
-7.22	-0.112	-0.0984
-6.24	-0.007	-0.1012
-5.10	0.062	-0.1025
-4.13	0.168	-0.1027
-3.06	0.284	-0.1043
-2.02	0.392	-0.1037
-1.03	0.491	-0.1027
-0.10	0.580	-0.1006
1.03	0.679	-0.0969
2.09	0.784	-0.0951
3.06	0.878	-0.0933
4.15	0.969	-0.0908
5.22	1.068	-0.0884
6.15	1.138	-0.0845
7.27	1.219	-0.0801
8.16	1.273	-0.0758
9.24	1.306	-0.0702
8.74	1.296	-0.0720
7.66	1.252	-0.0778
6.69	1.195	-0.0830
5.63	1.103	-0.0862
4.79	1.029	-0.0888
3.75	0.944	-0.0917
2.55	0.831	-0.0939
1.62	0.740	-0.0953
0.72	0.650	-0.0974
-0.39	0.555	-0.1007
-1.59	0.440	-0.1030
-2.54	0.340	-0.1042
-3.56	0.232	-0.1034
-4.48	0.128	-0.1025
-5.06	0.061	-0.1010
-6.54	-0.038	-0.1004

AG455ct-02r fp9.6

Fig. 6.94

Run: 06773gw

Re = 99990.9

α	C_l	C_m
-10.24	-0.238	-0.0542
-9.22	-0.127	-0.0992
-8.25	0.063	-0.1555
-7.15	0.176	-0.1623
-6.18	0.266	-0.1667
-5.10	0.350	-0.1666
-4.05	0.417	-0.1648
-3.11	0.472	-0.1604
-2.13	0.550	-0.1590
-1.09	0.633	-0.1523
-0.06	0.737	-0.1532
1.03	0.898	-0.1630
2.03	0.979	-0.1465
3.00	1.056	-0.1368
4.11	1.123	-0.1296
5.08	1.167	-0.1210
6.13	1.209	-0.1126
7.04	1.238	-0.1045
8.11	1.266	-0.0987
9.14	1.254	-0.1417
10.03	1.155	-0.1962
10.96	1.127	-0.2097
11.96	1.121	-0.2205
12.96	1.110	-0.2224
12.71	1.079	-0.2054
11.69	1.098	-0.2032
10.73	1.100	-0.1953
9.78	1.206	-0.1762
8.84	1.306	-0.1025
7.81	1.277	-0.0931
6.88	1.263	-0.1006
5.80	1.215	-0.1094
4.82	1.170	-0.1172
3.79	1.120	-0.1250
2.72	1.050	-0.1317
1.76	0.986	-0.1431
0.74	0.842	-0.1488
-0.35	0.711	-0.1444
-1.38	0.624	-0.1451

-2.38	0.531	-0.1461
-3.67	0.463	-0.1519
-4.73	0.398	-0.1588
-5.46	0.337	-0.1608
-6.45	0.254	-0.1587
-7.46	0.157	-0.1555
-8.52	0.025	-0.1390
-9.48	-0.166	-0.0722

Run: 06774gw
Re = 199843.1

α	C_l	C_m
-10.15	-0.259	-0.0415
-9.25	-0.151	-0.0810
-8.23	0.067	-0.1459
-6.93	0.165	-0.1511
-6.29	0.238	-0.1544
-5.11	0.368	-0.1605
-4.20	0.460	-0.1619
-3.16	0.576	-0.1633
-2.10	0.688	-0.1645
-1.14	0.781	-0.1645
-0.14	0.885	-0.1606
1.04	0.979	-0.1509
1.98	1.042	-0.1425
3.12	1.129	-0.1381
3.99	1.192	-0.1326
5.06	1.255	-0.1247
6.06	1.296	-0.1164
7.10	1.320	-0.1069
8.16	1.349	-0.0989
9.07	1.366	-0.1437
9.96	1.343	-0.1903
11.05	1.295	-0.2131
11.96	1.226	-0.2215
11.71	1.233	-0.2184
10.79	1.269	-0.2080
9.75	1.371	-0.1749
8.79	1.375	-0.1168
7.96	1.348	-0.0966
6.93	1.329	-0.1053
5.95	1.300	-0.1146
4.83	1.254	-0.1235
3.85	1.199	-0.1305
2.78	1.118	-0.1359
1.66	1.038	-0.1420
0.77	0.970	-0.1505
-0.37	0.873	-0.1591
-1.35	0.774	-0.1612
-2.32	0.681	-0.1619
-3.42	0.561	-0.1596
-4.37	0.453	-0.1585
-5.36	0.349	-0.1566
-6.45	0.231	-0.1529
-7.84	0.129	-0.1484
-8.48	0.018	-0.1321
-9.55	-0.190	-0.0622

Run: 06775gw
Re = 300149.8

α	C_l	C_m
-10.14	-0.264	-0.0432
-9.19	-0.133	-0.0909
-7.72	0.085	-0.1467
-7.21	0.137	-0.1488
-6.16	0.252	-0.1520
-5.14	0.376	-0.1558
-4.15	0.481	-0.1575
-3.06	0.595	-0.1566
-2.01	0.705	-0.1565
-1.00	0.809	-0.1566
-0.03	0.899	-0.1524
0.92	0.971	-0.1465
2.02	1.067	-0.1418
3.13	1.151	-0.1368
3.99	1.209	-0.1317
5.09	1.276	-0.1241
6.16	1.324	-0.1152
7.22	1.347	-0.1056
8.14	1.375	-0.0985
9.14	1.399	-0.1343
10.09	1.357	-0.1787
11.00	1.316	-0.2094
11.98	1.258	-0.2228
11.63	1.241	-0.2162
10.69	1.365	-0.1948
9.80	1.383	-0.1612
8.83	1.391	-0.1155
7.88	1.370	-0.0991
6.87	1.345	-0.1077
5.83	1.316	-0.1176
4.75	1.259	-0.1259
3.79	1.197	-0.1320
2.64	1.116	-0.1381
1.66	1.036	-0.1421
0.78	0.965	-0.1467
-0.42	0.866	-0.1535
-1.43	0.771	-0.1553
-2.46	0.660	-0.1549
-3.47	0.556	-0.1558
-4.42	0.456	-0.1554
-5.36	0.348	-0.1532
-6.47	0.214	-0.1494
-7.64	0.095	-0.1458
-8.57	0.011	-0.1334
-9.49	-0.179	-0.0731

Run: 06776gw
Re = 400441.2

α	C_l	C_m
-8.62	0.015	-0.1364
-7.18	0.147	-0.1480
-6.12	0.274	-0.1523
-5.14	0.381	-0.1541
-4.10	0.496	-0.1561
-3.03	0.605	-0.1563
-2.07	0.703	-0.1546
-0.94	0.817	-0.1534
-0.08	0.898	-0.1507
1.10	0.995	-0.1445
2.11	1.064	-0.1398
3.00	1.139	-0.1360
4.18	1.220	-0.1299
5.19	1.292	-0.1241
6.07	1.335	-0.1172
7.12	1.358	-0.1070
8.14	1.375	-0.0986
7.78	1.382	-0.1017
6.74	1.361	-0.1111
5.75	1.317	-0.1193
4.68	1.254	-0.1261
3.64	1.189	-0.1327
2.76	1.117	-0.1364
1.64	1.029	-0.1414
0.80	0.958	-0.1443
-0.50	0.871	-0.1528
-1.49	0.767	-0.1533
-2.45	0.666	-0.1544
-3.48	0.561	-0.1550
-4.50	0.455	-0.1554
-5.46	0.353	-0.1537
-6.54	0.226	-0.1493
-7.61	0.100	-0.1454

Run: 06777gw
Re = 499919.8

α	C_l	C_m
-7.95	0.063	-0.1439
-7.23	0.167	-0.1491
-6.10	0.287	-0.1507
-5.10	0.397	-0.1529
-4.14	0.501	-0.1544
-3.05	0.612	-0.1540
-1.98	0.723	-0.1526
-0.97	0.816	-0.1517
0.02	0.899	-0.1465
1.07	0.983	-0.1422
1.94	1.063	-0.1386
3.13	1.141	-0.1325
4.02	1.218	-0.1290

5.23	1.290	-0.1208
6.03	1.328	-0.1147
7.13	1.374	-0.1066
8.21	1.408	-0.0989
7.75	1.386	-0.1012
6.73	1.366	-0.1100
5.72	1.315	-0.1169
4.77	1.264	-0.1235
3.79	1.207	-0.1301
2.74	1.125	-0.1346
1.56	1.036	-0.1407
0.75	0.954	-0.1424
-0.54	0.861	-0.1491
-1.48	0.768	-0.1513
-2.53	0.661	-0.1526
-3.60	0.549	-0.1529
-4.52	0.457	-0.1529
-5.59	0.341	-0.1519
-6.67	0.222	-0.1497
-7.61	0.112	-0.1458

AG455ct-02r fp14.6

Fig. 6.97

Run: 06763gw
Re = 99980.2

α	C_l	C_m
-10.20	0.031	-0.1296
-9.14	0.237	-0.1937
-8.23	0.292	-0.1945
-7.17	0.361	-0.1907
-6.08	0.434	-0.1892
-5.14	0.497	-0.1858
-3.65	0.569	-0.1735
-3.23	0.606	-0.1724
-2.08	0.710	-0.1702
-1.09	0.777	-0.1666
-0.00	0.874	-0.1641
1.06	1.163	-0.1919
2.11	1.260	-0.1784
3.18	1.283	-0.1653
4.13	1.294	-0.1524
5.10	1.317	-0.1427
6.05	1.345	-0.1338
7.08	1.368	-0.1263
8.08	1.372	-0.1536
8.98	1.288	-0.2061
9.91	1.216	-0.2334
10.93	1.221	-0.2444
11.89	1.219	-0.2479
12.90	1.212	-0.2492
13.96	1.197	-0.2527
14.93	1.194	-0.2512
14.70	1.233	-0.2434
13.76	1.211	-0.2415
12.64	1.185	-0.2342
11.76	1.200	-0.2332
10.67	1.193	-0.2240
9.66	1.318	-0.2229
8.79	1.406	-0.1791
7.90	1.411	-0.1286
6.81	1.383	-0.1187
5.82	1.361	-0.1270
4.91	1.334	-0.1359
3.85	1.313	-0.1479
2.77	1.305	-0.1616
1.83	1.256	-0.1695
0.67	1.052	-0.1718
-0.42	0.859	-0.1570
-1.33	0.784	-0.1596
-2.29	0.706	-0.1623
-3.56	0.615	-0.1678
-4.43	0.561	-0.1697
-5.31	0.524	-0.1801
-6.87	0.433	-0.1897
-7.48	0.388	-0.1918
-8.56	0.309	-0.1922
-9.58	0.181	-0.1670

Run: 06765gw
Re = 199916.5

α	C_l	C_m
-10.15	0.038	-0.1296
-9.18	0.205	-0.1872
-8.16	0.327	-0.1991
-7.20	0.434	-0.2034
-6.11	0.557	-0.2078
-5.13	0.661	-0.2082
-4.12	0.708	-0.2016
-3.08	0.786	-0.1968
-2.10	0.840	-0.1893
-1.07	0.917	-0.1857
-0.01	1.163	-0.1970
1.09	1.212	-0.1824
2.07	1.274	-0.1748
3.03	1.311	-0.1653
4.02	1.337	-0.1540
5.22	1.362	-0.1417
6.08	1.380	-0.1335
7.18	1.408	-0.1250
8.10	1.449	-0.1576
9.05	1.392	-0.2052
10.09	1.347	-0.2346
11.01	1.331	-0.2460
11.96	1.266	-0.2493
12.94	1.256	-0.2537
13.98	1.256	-0.2527
15.00	1.252	-0.2579
14.68	1.242	-0.2519
13.71	1.254	-0.2486
12.67	1.246	-0.2478
11.68	1.255	-0.2416
10.73	1.343	-0.2386
9.65	1.397	-0.2198
8.75	1.453	-0.1888
7.85	1.433	-0.1178
6.82	1.406	-0.1239
5.79	1.381	-0.1326
4.75	1.362	-0.1427
3.78	1.340	-0.1533
2.74	1.306	-0.1647
1.64	1.259	-0.1753
0.66	1.207	-0.1840
-0.31	1.129	-0.1953
-1.35	0.899	-0.1822
-2.35	0.826	-0.1869
-3.41	0.759	-0.1931
-4.37	0.731	-0.2037
-5.40	0.648	-0.2046
-6.44	0.533	-0.2038
-7.56	0.407	-0.1988
-8.54	0.299	-0.1943
-9.09	0.223	-0.1865

Run: 06767rd
Re = 300014.0

α	C_l	C_m
-10.16	0.064	-0.1464
-9.14	0.226	-0.1903
-8.23	0.352	-0.1987
-7.24	0.471	-0.2024
-6.12	0.590	-0.2045
-5.10	0.698	-0.2055
-4.19	0.793	-0.2053
-3.05	0.904	-0.2034
-2.04	0.993	-0.2011
-0.96	1.096	-0.2000
0.05	1.168	-0.1897
1.09	1.226	-0.1808
2.11	1.275	-0.1712
3.02	1.308	-0.1615
4.16	1.344	-0.1498
5.12	1.381	-0.1416
6.21	1.407	-0.1317
7.09	1.436	-0.1250
8.09	1.484	-0.1454
9.07	1.473	-0.1947
10.00	1.414	-0.2249

10.96	1.354	-0.2467
11.94	1.300	-0.2506
12.92	1.256	-0.2497
13.89	1.270	-0.2554
14.99	1.247	-0.2575
14.65	1.251	-0.2547
13.64	1.244	-0.2504
12.65	1.273	-0.2515
11.70	1.305	-0.2485
10.66	1.366	-0.2380
9.86	1.427	-0.2198
8.71	1.478	-0.1766
7.82	1.442	-0.1179
6.74	1.430	-0.1264
5.69	1.401	-0.1352
4.68	1.370	-0.1449
3.66	1.341	-0.1549
2.81	1.308	-0.1631
1.70	1.256	-0.1746
0.74	1.199	-0.1823
-0.43	1.149	-0.1949
-1.34	1.058	-0.1987
-2.46	0.953	-0.1998
-3.41	0.860	-0.2016
-4.39	0.763	-0.2031
-5.54	0.648	-0.2038
-6.47	0.547	-0.2020
-7.56	0.432	-0.2000
-8.57	0.305	-0.1947
-9.56	0.118	-0.1630

Run: 06769gw
Re = 400197.7

α	C_l	C_m
-9.21	0.254	-0.1926
-8.24	0.365	-0.1979
-7.12	0.491	-0.2020
-6.11	0.601	-0.2036
-5.14	0.701	-0.2035
-3.98	0.819	-0.2036
-3.00	0.912	-0.2009
-2.06	1.005	-0.1985
-0.94	1.108	-0.1955
-0.09	1.147	-0.1860
1.10	1.219	-0.1779
2.03	1.273	-0.1695
3.13	1.316	-0.1587
4.09	1.357	-0.1505
5.05	1.390	-0.1419
6.17	1.428	-0.1324
7.10	1.453	-0.1252
6.77	1.444	-0.1276
5.71	1.411	-0.1360
4.75	1.385	-0.1446
3.71	1.340	-0.1530
2.66	1.304	-0.1633
1.63	1.258	-0.1733
0.66	1.195	-0.1801
-0.46	1.135	-0.1892
-1.55	1.061	-0.1971
-2.46	0.975	-0.1989
-3.44	0.879	-0.2010
-4.51	0.773	-0.2034
-5.54	0.672	-0.2037
-6.54	0.554	-0.2027
-7.59	0.446	-0.2000
-8.51	0.339	-0.1962

Run: 06771gw
Re = 499798.7

α	C_l	C_m
-9.22	0.278	-0.1942
-8.21	0.397	-0.1997
-7.27	0.498	-0.2005
-6.09	0.624	-0.2024
-5.20	0.719	-0.2031
-4.11	0.826	-0.2021
-3.13	0.914	-0.1996
-2.12	1.007	-0.1972
-0.93	1.090	-0.1892
0.01	1.149	-0.1809
1.01	1.203	-0.1731
1.96	1.259	-0.1657
3.11	1.308	-0.1551
4.09	1.359	-0.1479
5.12	1.390	-0.1384
6.10	1.437	-0.1314
7.03	1.460	-0.1251
6.76	1.460	-0.1268
5.80	1.432	-0.1338
4.82	1.379	-0.1409
3.77	1.338	-0.1490
2.70	1.298	-0.1589
1.59	1.244	-0.1685
0.53	1.186	-0.1769
-0.51	1.130	-0.1860
-1.44	1.075	-0.1940
-2.41	0.993	-0.1983
-3.61	0.875	-0.2005
-4.47	0.790	-0.2012
-5.64	0.675	-0.2027
-6.61	0.572	-0.2027
-7.60	0.461	-0.1999
-8.70	0.343	-0.1966

AG455ct-02r fp19.6
Fig. 6.100

Run: 06793gw
Re = 100084.1

α	C_l	C_m
-10.20	-0.249	-0.0625
-9.20	0.029	-0.1336
-8.17	0.308	-0.1896
-7.11	0.398	-0.1933
-5.80	0.488	-0.1928
-5.19	0.527	-0.1916
-3.90	0.614	-0.1829
-3.08	0.684	-0.1823
-2.07	0.758	-0.1778
-1.06	0.842	-0.1779
-0.06	0.921	-0.1762
1.05	1.320	-0.2047
2.09	1.338	-0.1911
3.04	1.300	-0.1730
4.02	1.302	-0.1609
5.10	1.339	-0.1509
6.16	1.379	-0.1422
7.13	1.423	-0.1393
8.08	1.421	-0.2024
8.99	1.320	-0.2422
9.92	1.285	-0.2569
10.87	1.275	-0.2626
12.02	1.284	-0.2683
11.64	1.241	-0.2546
10.75	1.247	-0.2446
9.66	1.284	-0.2380
8.74	1.369	-0.2129
7.79	1.426	-0.1681
6.74	1.403	-0.1303
5.81	1.374	-0.1375
4.77	1.339	-0.1461
3.87	1.321	-0.1549
2.77	1.323	-0.1687
1.75	1.353	-0.1866
0.70	1.083	-0.1811
-0.34	0.908	-0.1677
-1.35	0.832	-0.1696
-2.39	0.756	-0.1737
-3.39	0.679	-0.1753
-4.42	0.604	-0.1808
-5.83	0.524	-0.1874
-6.88	0.454	-0.1919
-7.52	0.394	-0.1900
-8.50	0.290	-0.1854
-9.50	-0.111	-0.0825

Run: 06795gw
Re = 199840.1

α	C_l	C_m
-10.58	0.141	-0.1547
-9.18	0.416	-0.2248
-8.23	0.536	-0.2338
-7.16	0.636	-0.2346
-6.12	0.707	-0.2303
-5.11	0.765	-0.2232
-4.11	0.816	-0.2134
-3.12	0.861	-0.2026
-2.10	0.919	-0.1946
-0.99	1.012	-0.1947
0.04	1.323	-0.2107
1.12	1.323	-0.1930
2.09	1.337	-0.1806
3.04	1.351	-0.1697
4.09	1.386	-0.1613
5.12	1.425	-0.1533
6.11	1.457	-0.1456
7.13	1.482	-0.1379
8.11	1.513	-0.2061
9.03	1.510	-0.2376
9.92	1.361	-0.2614
10.93	1.292	-0.2605
11.98	1.323	-0.2705
11.67	1.307	-0.2623
10.68	1.347	-0.2582
9.67	1.329	-0.2502
8.74	1.491	-0.2260
7.83	1.511	-0.1851
6.82	1.476	-0.1356
5.87	1.457	-0.1441
4.77	1.412	-0.1519
3.81	1.380	-0.1605
2.83	1.353	-0.1684
1.74	1.340	-0.1818
0.85	1.335	-0.1939
-0.31	1.340	-0.2149
-1.32	0.983	-0.1902
-2.36	0.915	-0.1940
-3.42	0.859	-0.2027
-4.38	0.810	-0.2120
-5.44	0.767	-0.2231
-6.46	0.697	-0.2297
-7.45	0.615	-0.2312
-8.55	0.501	-0.2275
-9.48	0.390	-0.2201

Run: 06797gw
Re = 299895.0

α	C_l	C_m
-10.17	0.448	-0.2331
-9.12	0.568	-0.2383
-8.08	0.687	-0.2425
-7.12	0.790	-0.2430
-6.10	0.896	-0.2438
-5.03	0.988	-0.2399
-3.95	1.080	-0.2380
-3.09	1.075	-0.2297
-2.02	1.100	-0.2170
-0.93	1.299	-0.2197
-0.10	1.281	-0.2006
0.97	1.294	-0.1880
1.96	1.320	-0.1775
3.07	1.371	-0.1689
4.14	1.417	-0.1615
5.12	1.450	-0.1539
6.15	1.494	-0.1463
7.19	1.515	-0.1384
6.75	1.506	-0.1402
5.75	1.474	-0.1473
4.85	1.440	-0.1543
3.79	1.409	-0.1634
2.66	1.364	-0.1722
1.66	1.329	-0.1810
0.83	1.303	-0.1893
-0.36	1.300	-0.2060
-1.39	1.197	-0.2194
-2.41	1.103	-0.2199
-3.47	1.054	-0.2294
-4.46	1.041	-0.2376
-5.41	0.953	-0.2390
-6.44	0.859	-0.2424
-7.59	0.745	-0.2426
-8.48	0.644	-0.2405
-9.60	0.516	-0.2347

Run: 06799gw
Re = 400432.0

α	C_l	C_m
-10.17	0.475	-0.2347
-9.16	0.594	-0.2409
-8.14	0.709	-0.2437
-7.12	0.813	-0.2440
-6.06	0.907	-0.2415
-5.04	1.005	-0.2397
-4.02	1.097	-0.2373
-2.99	1.188	-0.2347
-2.12	1.257	-0.2304
-1.10	1.253	-0.2115
0.07	1.265	-0.1949
1.07	1.286	-0.1837
2.09	1.334	-0.1757
3.11	1.378	-0.1682
4.01	1.427	-0.1621
5.22	1.482	-0.1542
6.04	1.515	-0.1482
7.17	1.569	-0.1456
6.85	1.544	-0.1416
5.75	1.507	-0.1488
4.67	1.454	-0.1565
3.70	1.418	-0.1638
2.75	1.370	-0.1701
1.57	1.316	-0.1789
0.69	1.283	-0.1870
-0.43	1.253	-0.1986
-1.49	1.264	-0.2184
-2.52	1.247	-0.2340
-3.50	1.143	-0.2361
-4.57	1.047	-0.2382
-5.53	0.957	-0.2403
-6.64	0.857	-0.2411
-7.52	0.769	-0.2422
-8.50	0.664	-0.2420
-9.64	0.538	-0.2374

AG455ct-02r fp24.6
Fig. 6.103

Run: 06801gw
Re = 100445.3

α	C_l	C_m
-10.22	-0.145	-0.0852
-9.15	0.344	-0.2146
-7.95	0.445	-0.2174
-7.21	0.510	-0.2223
-6.13	0.588	-0.2203
-5.06	0.678	-0.2129
-4.07	0.747	-0.2089
-3.04	0.852	-0.2089
-2.07	0.941	-0.2087
-1.05	1.010	-0.2005
-0.10	1.061	-0.1956
1.01	1.341	-0.2148
1.96	1.320	-0.1969
3.11	1.326	-0.1808
4.06	1.369	-0.1736
5.06	1.409	-0.1639
6.13	1.440	-0.1533
7.02	1.496	-0.1932
8.01	1.480	-0.2456
8.90	1.388	-0.2656
9.95	1.320	-0.2757

10.91	1.328	-0.2879
11.96	1.320	-0.2884
11.71	1.318	-0.2772
10.68	1.308	-0.2702
9.67	1.351	-0.2669
8.70	1.396	-0.2479
7.83	1.462	-0.2283
6.80	1.511	-0.1560
5.92	1.459	-0.1499
4.79	1.411	-0.1578
3.75	1.359	-0.1672
2.73	1.327	-0.1761
1.74	1.330	-0.1874
0.73	1.331	-0.2028
-0.25	1.066	-0.1836
-1.29	1.010	-0.1920
-2.38	0.914	-0.1950
-3.40	0.831	-0.1992
-4.30	0.743	-0.1969
-5.33	0.664	-0.2065
-6.65	0.589	-0.2165
-7.55	0.527	-0.2150
-8.78	0.401	-0.2107
-9.53	0.308	-0.1980

Run: 06802gw
Re = 201194.9

α	C_l	C_m
-10.04	0.483	-0.2501
-9.20	0.569	-0.2535
-8.12	0.645	-0.2505
-7.21	0.711	-0.2473
-6.17	0.736	-0.2375
-5.11	0.718	-0.2204
-4.13	0.802	-0.2171
-3.11	0.888	-0.2132
-2.08	0.955	-0.2060
-1.08	1.062	-0.2056
0.02	1.319	-0.2165
0.95	1.323	-0.2048
1.96	1.333	-0.1924
3.08	1.375	-0.1814
4.13	1.424	-0.1743
5.15	1.483	-0.1675
6.13	1.510	-0.1584
7.06	1.594	-0.2000
7.97	1.577	-0.2376
9.02	1.496	-0.2715
10.02	1.361	-0.2817
9.63	1.422	-0.2761
8.75	1.490	-0.2639
7.79	1.568	-0.2318
6.82	1.571	-0.1833
5.76	1.504	-0.1582
4.84	1.467	-0.1662
3.72	1.409	-0.1725
2.81	1.359	-0.1790
1.75	1.321	-0.1894
0.78	1.319	-0.2017
-0.32	1.327	-0.2192
-1.31	1.018	-0.1974
-2.29	0.947	-0.2042
-3.39	0.889	-0.2134
-4.40	0.791	-0.2158
-5.46	0.711	-0.2197
-6.47	0.747	-0.2370
-7.42	0.709	-0.2466
-8.46	0.638	-0.2500
-9.50	0.563	-0.2532

Run: 06803gw
Re = 301335.0

α	C_l	C_m
-10.25	0.737	-0.2808
-9.18	0.848	-0.2840
-8.10	0.949	-0.2827
-7.20	0.857	-0.2679
-6.21	0.912	-0.2618
-5.07	0.948	-0.2507
-4.07	0.952	-0.2350
-2.98	0.994	-0.2232
-1.98	1.041	-0.2141
-0.96	1.296	-0.2274
0.02	1.303	-0.2112
1.09	1.316	-0.1999
2.02	1.348	-0.1911
3.13	1.415	-0.1844
4.12	1.464	-0.1767
5.19	1.529	-0.1711
6.24	1.552	-0.1603
5.73	1.535	-0.1642
4.79	1.503	-0.1718
3.78	1.445	-0.1772
2.77	1.394	-0.1852
1.73	1.336	-0.1910
0.76	1.309	-0.2010
-0.36	1.293	-0.2125
-1.31	1.323	-0.2392
-2.42	0.989	-0.2122
-3.49	0.995	-0.2289
-4.49	0.965	-0.2408
-5.43	0.957	-0.2557
-6.49	0.897	-0.2633
-7.53	1.002	-0.2800
-8.59	0.906	-0.2825
-9.54	0.818	-0.2835

Run: 06804gw
Re = 402141.2

α	C_l	C_m
-10.11	0.778	-0.2833
-9.11	0.871	-0.2829
-8.07	0.965	-0.2814
-7.16	1.042	-0.2795
-6.04	1.129	-0.2748
-5.12	1.201	-0.2715
-4.05	1.096	-0.2543
-3.10	1.132	-0.2450
-1.91	1.259	-0.2408
-0.99	1.246	-0.2176
-0.09	1.280	-0.2085
1.10	1.330	-0.2006
2.13	1.378	-0.1925
3.04	1.421	-0.1849
4.13	1.491	-0.1779
5.20	1.537	-0.1696
6.05	1.576	-0.1640
5.81	1.571	-0.1657
4.70	1.522	-0.1739
3.65	1.457	-0.1791
2.62	1.400	-0.1865
1.72	1.348	-0.1923
0.71	1.310	-0.2012
-0.35	1.274	-0.2102
-1.49	1.259	-0.2285
-2.47	1.312	-0.2597
-3.36	1.117	-0.2461
-4.36	1.252	-0.2666
-5.49	1.181	-0.2731
-6.47	1.105	-0.2774
-7.50	1.020	-0.2814
-8.56	0.920	-0.2824
-9.70	0.815	-0.2831

AG455ct-02r fp29.6

Fig. 6.106

Run: 06610ga
Re = 100949.2

α	C_l	C_m
-10.18	-0.075	-0.1024
-9.27	0.366	-0.2280
-8.14	0.509	-0.2420
-7.21	0.582	-0.2422
-6.20	0.662	-0.2369
-5.10	0.728	-0.2271
-4.15	0.790	-0.2223
-3.17	0.870	-0.2199
-2.09	0.960	-0.2194

-1.01	1.017	-0.2077
0.14	1.067	-0.1991
1.17	1.244	-0.2102
2.10	1.262	-0.1968
3.14	1.336	-0.1934
4.16	1.392	-0.1853
5.11	1.414	-0.1734
6.08	1.453	-0.1660
7.11	1.471	-0.2235
8.09	1.443	-0.2663
9.02	1.294	-0.2737
10.03	1.311	-0.2912
10.90	1.329	-0.2996
11.95	1.293	-0.3010
11.63	1.279	-0.2883
10.64	1.306	-0.2857
9.63	1.328	-0.2824
8.68	1.346	-0.2648
7.81	1.487	-0.2381
6.74	1.537	-0.1863
5.73	1.453	-0.1601
4.75	1.408	-0.1676
3.83	1.366	-0.1759
2.82	1.331	-0.1872
1.66	1.270	-0.1935
0.72	1.226	-0.2027
-0.38	1.061	-0.1965
-1.27	1.028	-0.2049
-2.49	0.943	-0.2106
-3.45	0.851	-0.2084
-4.47	0.769	-0.2093
-5.40	0.717	-0.2173
-6.44	0.658	-0.2273
-7.48	0.566	-0.2296
-8.53	0.477	-0.2304
-10.12	-0.045	-0.0925

Run: 06612gw

Re = 201766.8

α	C_l	C_m
-9.77	0.357	-0.2253
-9.12	0.478	-0.2414
-8.10	0.646	-0.2485
-7.21	0.717	-0.2451
-6.10	0.805	-0.2419
-5.07	0.884	-0.2374
-4.03	0.953	-0.2286
-3.01	1.032	-0.2238
-2.02	1.063	-0.2112
-1.06	1.218	-0.2180
0.08	1.280	-0.2099
1.09	1.351	-0.2045
2.16	1.417	-0.1990
3.14	1.475	-0.1934
4.09	1.526	-0.1860
5.21	1.547	-0.1726
6.13	1.590	-0.2146
7.06	1.572	-0.2611
7.96	1.514	-0.2785
8.96	1.386	-0.2909
9.97	1.374	-0.2985
9.65	1.396	-0.2966
8.64	1.398	-0.2867
7.67	1.526	-0.2735
6.70	1.571	-0.2371
5.79	1.601	-0.1898
4.70	1.547	-0.1768
3.69	1.517	-0.1867
2.81	1.465	-0.1918
1.63	1.397	-0.1991
0.64	1.324	-0.2029
-0.25	1.269	-0.2091
-1.30	1.142	-0.2073
-2.43	1.055	-0.2131
-3.43	1.004	-0.2232
-4.51	0.929	-0.2294
-5.46	0.858	-0.2348
-6.56	0.774	-0.2397
-7.53	0.688	-0.2426
-8.46	0.581	-0.2430
-9.41	0.435	-0.2336

Run: 06809gw

Re = 302715.5

α	C_l	C_m
-10.23	0.401	-0.2376
-9.18	0.522	-0.2453
-8.22	0.610	-0.2477
-7.22	0.703	-0.2470
-6.06	0.796	-0.2445
-5.02	0.888	-0.2428
-4.00	0.972	-0.2396
-3.09	1.035	-0.2334
-2.00	1.085	-0.2219
-1.07	1.254	-0.2316
0.09	1.291	-0.2165
1.00	1.358	-0.2130
2.01	1.426	-0.2068
3.15	1.511	-0.2021
3.96	1.552	-0.1955
5.15	1.601	-0.1859
6.07	1.633	-0.1849
6.97	1.628	-0.2321
8.02	1.578	-0.2672
8.94	1.526	-0.2918
8.75	1.542	-0.2841
7.72	1.606	-0.2577
6.80	1.640	-0.2198
5.94	1.628	-0.1769
4.70	1.577	-0.1865
3.82	1.544	-0.1952
2.78	1.491	-0.2024
1.68	1.408	-0.2066
0.57	1.322	-0.2099
-0.42	1.255	-0.2157
-1.47	1.273	-0.2405
-2.40	1.057	-0.2218
-3.49	1.007	-0.2349
-4.48	0.925	-0.2373
-5.51	0.846	-0.2415
-6.42	0.770	-0.2438
-7.44	0.684	-0.2470
-8.52	0.586	-0.2460
-9.55	0.481	-0.2417

Run: 06810gw

Re = 403001.1

α	C_l	C_m
-10.31	0.137	-0.1619
-9.13	0.533	-0.2426
-8.19	0.627	-0.2452
-7.15	0.714	-0.2442
-6.20	0.803	-0.2439
-5.16	0.882	-0.2408
-4.08	0.976	-0.2377
-3.14	1.031	-0.2301
-2.12	1.257	-0.2494
-1.02	1.226	-0.2219
0.05	1.305	-0.2166
1.11	1.381	-0.2119
1.99	1.440	-0.2061
3.12	1.520	-0.2011
4.04	1.578	-0.1958
5.18	1.642	-0.1882
4.65	1.608	-0.1897
3.81	1.565	-0.1957
2.76	1.494	-0.2012
1.63	1.423	-0.2086
0.75	1.359	-0.2127
-0.38	1.275	-0.2171
-1.48	1.212	-0.2262
-2.39	1.241	-0.2506
-3.49	1.005	-0.2322
-4.46	0.940	-0.2369
-5.53	0.847	-0.2394
-6.54	0.772	-0.2434
-7.63	0.673	-0.2437
-8.91	0.841	-0.2856
-9.79	0.831	-0.2930

AG455ct-02r fp39.6

Fig. 6.109

Run: 06616gw

Re = 101960.8

α	C_l	C_m
-10.12	0.505	-0.2539
-9.21	0.596	-0.2603
-8.11	0.700	-0.2647
-7.01	0.736	-0.2510
-6.16	0.800	-0.2428
-5.15	0.866	-0.2430
-4.15	0.940	-0.2386
-3.11	1.040	-0.2403
-2.01	1.102	-0.2340
-0.82	1.156	-0.2239
0.02	1.268	-0.2297
1.00	1.332	-0.2224
2.06	1.403	-0.2190
3.09	1.450	-0.2112
4.12	1.478	-0.1974
5.15	1.517	-0.1868
5.95	1.494	-0.2358
6.93	1.427	-0.2727
7.94	1.384	-0.2954
7.64	1.371	-0.2774
6.67	1.469	-0.2525
5.71	1.529	-0.2176
4.78	1.502	-0.1799
3.72	1.488	-0.1937
2.74	1.439	-0.2015
1.70	1.384	-0.2099
0.75	1.331	-0.2131
-0.41	1.222	-0.2176
-1.28	1.165	-0.2209
-2.40	1.074	-0.2187
-3.41	1.008	-0.2230
-4.45	0.920	-0.2240
-5.39	0.839	-0.2232
-6.50	0.790	-0.2357
-7.53	0.736	-0.2476
-8.60	0.671	-0.2539
-9.55	0.588	-0.2506

Run: 06618gw

Re = 203813.6

α	C_l	C_m
-10.21	0.625	-0.2635
-9.16	0.741	-0.2666
-8.13	0.828	-0.2653
-7.12	0.911	-0.2626
-6.00	0.995	-0.2593
-5.05	1.055	-0.2529
-4.08	1.111	-0.2439
-3.02	1.193	-0.2405
-1.96	1.265	-0.2336
-0.98	1.346	-0.2316
0.12	1.418	-0.2270
1.18	1.496	-0.2231
2.18	1.560	-0.2184
3.14	1.602	-0.2086
4.15	1.600	-0.1929
5.12	1.653	-0.2289
6.07	1.578	-0.2746
7.07	1.475	-0.3003
7.92	1.422	-0.3057
7.78	1.447	-0.3015
6.58	1.488	-0.2863
5.69	1.642	-0.2510
4.74	1.650	-0.2084
3.78	1.621	-0.1987
2.81	1.601	-0.2120
1.62	1.535	-0.2188
0.65	1.472	-0.2227
-0.33	1.398	-0.2261
-1.45	1.334	-0.2332
-2.43	1.224	-0.2322
-3.44	1.169	-0.2399
-4.29	1.122	-0.2463
-5.43	1.048	-0.2546
-6.46	0.961	-0.2582
-7.42	0.893	-0.2626
-8.59	0.789	-0.2636
-9.42	0.733	-0.2678

Run: 06620ga

Re = 305953.4

α	C_l	C_m
-10.13	0.690	-0.2653
-9.15	0.792	-0.2695
-8.10	0.872	-0.2653
-7.18	0.940	-0.2621
-6.03	1.028	-0.2588
-5.04	1.111	-0.2558
-4.09	1.166	-0.2487
-3.03	1.223	-0.2369
-1.96	1.323	-0.2352
-0.94	1.380	-0.2281
-0.01	1.450	-0.2246
1.11	1.525	-0.2187
2.07	1.593	-0.2146
3.16	1.644	-0.2060
4.13	1.656	-0.1928
5.09	1.685	-0.2344
5.95	1.629	-0.2717
6.90	1.503	-0.2931
7.91	1.450	-0.3080
7.53	1.501	-0.3030
6.69	1.564	-0.2912
5.71	1.664	-0.2598
4.76	1.675	-0.2206
3.93	1.623	-0.1868
2.80	1.633	-0.2091
1.73	1.575	-0.2156
0.63	1.504	-0.2213
-0.37	1.433	-0.2253
-1.37	1.370	-0.2314
-2.36	1.293	-0.2341
-3.50	1.205	-0.2418
-4.44	1.153	-0.2501
-5.48	1.082	-0.2544
-6.60	0.998	-0.2600
-7.63	0.923	-0.2636
-8.62	0.828	-0.2648
-9.66	0.738	-0.2639

W1011 (20%) fp0

Fig. 6.113

Run: 07068gw

Re = 100055.6

α	C_l	C_m
-10.27	-0.892	-0.0132
-9.25	-0.832	-0.0110
-8.36	-0.773	-0.0095
-7.22	-0.693	-0.0067
-6.22	-0.607	-0.0027
-5.35	-0.527	-0.0009
-4.13	-0.420	0.0006
-3.12	-0.340	0.0043
-2.17	-0.262	0.0088
-1.07	-0.155	0.0096
-0.23	-0.023	-0.0072
0.92	0.149	-0.0205
1.95	0.243	-0.0107
3.05	0.344	-0.0070
3.94	0.421	-0.0052
5.07	0.529	-0.0039
6.15	0.620	-0.0012
7.15	0.706	-0.0007
8.13	0.775	0.0001
9.16	0.844	0.0022
9.90	0.738	-0.0859
10.90	0.727	-0.1024
11.87	0.709	-0.1086
12.99	0.679	-0.1098
14.00	0.657	-0.1085

13.61	0.732	-0.1045
12.77	0.703	-0.0935
11.61	0.709	-0.0845
10.82	0.763	-0.0841
9.94	0.908	0.0083
8.74	0.842	0.0073
7.73	0.772	0.0055
6.75	0.702	0.0035
5.68	0.615	0.0015
4.63	0.520	-0.0006
3.64	0.423	-0.0022
2.62	0.334	-0.0055
1.62	0.249	-0.0103
0.62	0.151	-0.0096
-0.46	-0.043	0.0134
-1.35	-0.144	0.0159
-2.37	-0.237	0.0100
-3.34	-0.321	0.0047
-4.53	-0.422	0.0007
-5.50	-0.512	-0.0014
-6.61	-0.611	-0.0022
-7.50	-0.685	-0.0045
-8.64	-0.773	-0.0075
-9.67	-0.840	-0.0096

Run: 07070gw
Re = 199933.7

α	C_l	C_m
-10.21	-0.929	-0.0081
-9.28	-0.871	-0.0062
-8.29	-0.795	-0.0044
-7.22	-0.706	-0.0035
-6.23	-0.611	-0.0020
-5.12	-0.504	-0.0008
-4.09	-0.394	-0.0001
-3.11	-0.300	0.0012
-2.21	-0.213	0.0016
-1.09	-0.072	-0.0068
-0.03	0.024	-0.0029
0.91	0.121	-0.0020
2.04	0.262	-0.0068
2.93	0.343	-0.0055
3.92	0.440	-0.0043
5.12	0.544	-0.0032
6.07	0.634	-0.0025
7.14	0.735	-0.0016
8.05	0.816	-0.0006
9.25	0.904	0.0014
10.20	0.963	0.0028
11.15	1.002	0.0033
11.78	0.773	-0.1056
12.85	0.769	-0.1138
13.86	0.735	-0.1136

15.03	0.738	-0.1176
14.81	0.742	-0.1101
13.80	0.745	-0.1097
12.72	0.755	-0.1027
11.71	0.792	-0.1019
10.99	0.998	0.0083
9.87	0.945	0.0070
8.74	0.872	0.0048
7.80	0.798	0.0034
6.77	0.701	0.0016
5.69	0.605	0.0004
4.65	0.508	-0.0008
3.63	0.414	-0.0023
2.60	0.321	-0.0037
1.64	0.230	-0.0058
0.58	0.088	0.0013
-0.32	0.004	-0.0023
-1.51	-0.115	-0.0032
-2.55	-0.236	0.0020
-3.37	-0.320	0.0006
-4.45	-0.428	-0.0008
-5.54	-0.540	-0.0022
-6.63	-0.643	-0.0037
-7.55	-0.730	-0.0053
-8.61	-0.824	-0.0071
-9.63	-0.890	-0.0090

Run: 07072gw
Re = 399867.3

α	C_l	C_m
-10.27	-0.957	-0.0083
-9.35	-0.885	-0.0068
-8.24	-0.780	-0.0054
-7.43	-0.715	-0.0051
-6.31	-0.608	-0.0040
-5.25	-0.506	-0.0030
-4.24	-0.410	-0.0022
-3.18	-0.300	-0.0029
-2.11	-0.171	-0.0071
-1.04	-0.069	-0.0057
-0.01	0.030	-0.0035
0.88	0.111	-0.0015
2.07	0.237	-0.0026
3.06	0.335	-0.0035
4.09	0.425	-0.0028
4.94	0.509	-0.0021
6.13	0.627	-0.0011
7.13	0.719	-0.0001
8.05	0.805	0.0012
9.21	0.899	0.0029
10.11	0.972	0.0044
11.30	1.048	0.0070
12.27	1.083	0.0083

13.09	1.081	-0.0047
13.84	0.815	-0.1121
14.96	0.773	-0.1125
14.70	0.782	-0.1115
13.82	0.833	-0.1139
12.77	0.841	-0.1002
11.88	1.070	0.0102
10.84	1.023	0.0081
9.80	0.945	0.0058
8.72	0.864	0.0044
7.87	0.789	0.0033
6.81	0.686	0.0022
5.78	0.586	0.0013
4.82	0.494	0.0003
3.70	0.384	-0.0006
2.60	0.288	-0.0005
1.58	0.174	0.0025
0.62	0.075	0.0003
-0.53	-0.025	-0.0023
-1.45	-0.118	-0.0043
-2.37	-0.211	-0.0043
-3.53	-0.352	-0.0004
-4.40	-0.435	-0.0015
-5.45	-0.538	-0.0030
-6.67	-0.656	-0.0044
-7.66	-0.762	-0.0060
-8.69	-0.858	-0.0078
-9.71	-0.932	-0.0089

W1011 (20%) **fp5**

Fig. 6.116

Run: 07084gw
Re = 99950.8

α	C_l	C_m
-10.45	-0.756	-0.0436
-9.36	-0.689	-0.0410
-8.35	-0.622	-0.0394
-7.27	-0.535	-0.0376
-6.18	-0.443	-0.0344
-5.35	-0.366	-0.0334
-4.22	-0.261	-0.0312
-3.12	-0.163	-0.0297
-2.19	-0.073	-0.0282
-1.09	0.021	-0.0235
-0.07	0.138	-0.0340
0.97	0.356	-0.0578
1.92	0.459	-0.0496
2.95	0.543	-0.0464
4.11	0.645	-0.0449
5.02	0.725	-0.0420
6.00	0.802	-0.0401

7.11	0.881	-0.0365
8.17	0.948	-0.0340
9.17	1.007	-0.0450
9.97	0.841	-0.1325
10.98	0.823	-0.1419
11.98	0.833	-0.1474
12.98	0.853	-0.1485
13.99	0.807	-0.1429
13.60	0.859	-0.1365
12.66	0.851	-0.1300
11.66	0.825	-0.1244
10.67	0.860	-0.1243
9.81	1.049	-0.0251
8.92	1.019	-0.0281
7.80	0.949	-0.0314
6.73	0.879	-0.0350
5.80	0.810	-0.0372
4.80	0.725	-0.0401
3.64	0.625	-0.0420
2.65	0.537	-0.0439
1.64	0.457	-0.0491
0.56	0.313	-0.0418
-0.47	0.104	-0.0210
-1.37	0.039	-0.0253
-2.34	-0.049	-0.0284
-3.52	-0.161	-0.0316
-4.40	-0.247	-0.0332
-5.55	-0.358	-0.0360
-6.57	-0.447	-0.0383
-7.51	-0.533	-0.0394
-8.66	-0.625	-0.0434
-9.69	-0.698	-0.0472

Run: 07082gw
Re = 200027.0

α	C_l	C_m
-10.30	-0.774	-0.0440
-9.25	-0.688	-0.0475
-8.35	-0.596	-0.0502
-7.21	-0.480	-0.0540
-6.22	-0.380	-0.0556
-5.30	-0.273	-0.0563
-4.07	-0.141	-0.0569
-3.20	-0.057	-0.0566
-2.25	0.036	-0.0554
-1.20	0.143	-0.0558
-0.04	0.271	-0.0554
0.91	0.355	-0.0496
1.91	0.455	-0.0477
2.87	0.544	-0.0473
4.03	0.655	-0.0464
5.04	0.738	-0.0450
6.15	0.838	-0.0430

7.15	0.917	-0.0405
8.17	0.989	-0.0367
9.20	1.056	-0.0329
10.11	1.100	-0.0300
10.76	0.905	-0.1349
11.97	0.863	-0.1451
12.98	0.836	-0.1461
13.83	0.837	-0.1499
14.91	0.826	-0.1528
14.65	0.811	-0.1434
13.62	0.823	-0.1427
12.70	0.850	-0.1418
11.63	0.886	-0.1416
11.01	1.127	-0.0222
9.81	1.091	-0.0261
8.89	1.046	-0.0295
7.85	0.981	-0.0335
6.82	0.902	-0.0373
5.65	0.806	-0.0402
4.67	0.717	-0.0418
3.73	0.636	-0.0433
2.76	0.540	-0.0441
1.61	0.430	-0.0450
0.54	0.330	-0.0480
-0.36	0.247	-0.0520
-1.41	0.126	-0.0520
-2.37	0.024	-0.0516
-3.46	-0.078	-0.0543
-4.58	-0.189	-0.0546
-5.54	-0.294	-0.0545
-6.43	-0.396	-0.0522
-7.62	-0.523	-0.0520
-8.67	-0.633	-0.0487
-9.60	-0.718	-0.0459

Run: 07080gw
Re = 399973.8

α	C_l	C_m
-10.32	-0.774	-0.0472
-9.37	-0.686	-0.0497
-8.41	-0.584	-0.0517
-7.25	-0.475	-0.0528
-6.29	-0.374	-0.0532
-5.27	-0.267	-0.0543
-4.13	-0.152	-0.0553
-3.22	-0.059	-0.0554
-2.17	0.045	-0.0539
-1.04	0.156	-0.0525
-0.02	0.253	-0.0489
0.89	0.335	-0.0465
1.87	0.416	-0.0454
2.91	0.521	-0.0442
4.01	0.623	-0.0431

5.08	0.727	-0.0422
6.14	0.829	-0.0407
7.05	0.910	-0.0387
8.09	0.996	-0.0359
9.21	1.077	-0.0325
10.22	1.143	-0.0283
11.13	1.188	-0.0248
12.17	1.203	-0.0220
11.88	1.206	-0.0213
10.99	1.180	-0.0240
9.81	1.114	-0.0287
8.80	1.047	-0.0322
7.84	0.978	-0.0350
6.77	0.885	-0.0376
5.71	0.788	-0.0393
4.75	0.696	-0.0406
3.68	0.592	-0.0417
2.62	0.486	-0.0423
1.60	0.387	-0.0434
0.78	0.323	-0.0448
-0.41	0.215	-0.0481
-1.32	0.127	-0.0509
-2.43	0.019	-0.0528
-3.36	-0.078	-0.0535
-4.54	-0.199	-0.0533
-5.55	-0.309	-0.0526
-6.48	-0.400	-0.0521
-7.55	-0.510	-0.0517
-8.62	-0.620	-0.0510
-9.64	-0.725	-0.0493

W1011 (20%) **fp10**

Fig. 6.119

Run: 07085gw
Re = 100002.8

α	C_l	C_m
-10.23	-0.525	-0.0891
-9.34	-0.457	-0.0900
-8.21	-0.370	-0.0901
-7.22	-0.283	-0.0908
-6.24	-0.196	-0.0907
-5.29	-0.124	-0.0843
-4.15	-0.019	-0.0852
-3.14	0.039	-0.0757
-2.14	0.127	-0.0741
-1.07	0.232	-0.0730
-0.04	0.331	-0.0730
0.80	0.503	-0.0940
1.92	0.619	-0.0861
3.05	0.714	-0.0831
3.95	0.796	-0.0816

5.02	0.882	-0.0777
6.07	0.957	-0.0740
7.09	1.017	-0.0681
8.14	1.082	-0.0647
8.99	1.045	-0.1503
9.91	0.921	-0.1695
10.93	0.910	-0.1750
11.97	0.947	-0.1814
11.64	0.969	-0.1670
10.70	1.002	-0.1644
9.72	0.912	-0.1415
8.83	1.167	-0.0571
7.79	1.109	-0.0607
6.79	1.054	-0.0665
5.79	0.988	-0.0709
4.69	0.906	-0.0748
3.77	0.822	-0.0779
2.64	0.715	-0.0800
1.64	0.629	-0.0837
0.65	0.491	-0.0771
-0.41	0.336	-0.0696
-1.33	0.236	-0.0658
-2.35	0.148	-0.0689
-3.38	0.063	-0.0739
-4.51	-0.009	-0.0825
-5.47	-0.095	-0.0841
-6.54	-0.197	-0.0851
-7.65	-0.291	-0.0874
-8.59	-0.377	-0.0870
-9.52	-0.450	-0.0888

Run: 07087gw

Re = 199889.5

α	C_l	C_m
-10.27	-0.510	-0.1005
-9.28	-0.415	-0.1034
-8.24	-0.315	-0.1050
-7.20	-0.214	-0.1066
-6.29	-0.115	-0.1073
-5.28	-0.014	-0.1067
-4.16	0.091	-0.1063
-3.11	0.173	-0.1041
-2.12	0.255	-0.0990
-1.05	0.365	-0.0977
-0.03	0.511	-0.1003
0.94	0.589	-0.0929
1.99	0.683	-0.0889
3.07	0.776	-0.0874
4.07	0.862	-0.0852
5.11	0.945	-0.0819
6.01	1.017	-0.0782
7.15	1.092	-0.0733
8.18	1.153	-0.0679

9.14	1.199	-0.0631
9.90	1.069	-0.1592
10.99	0.983	-0.1768
11.86	0.967	-0.1799
12.92	0.975	-0.1819
13.88	0.939	-0.1811
13.71	0.964	-0.1786
12.63	0.974	-0.1770
11.67	0.982	-0.1740
10.66	0.990	-0.1677
9.95	1.225	-0.0552
8.80	1.180	-0.0596
7.80	1.131	-0.0657
6.75	1.073	-0.0708
5.80	1.004	-0.0755
4.82	0.936	-0.0797
3.79	0.842	-0.0822
2.66	0.748	-0.0850
1.65	0.659	-0.0871
0.61	0.578	-0.0924
-0.31	0.492	-0.0985
-1.41	0.325	-0.0919
-2.37	0.253	-0.0989
-3.42	0.161	-0.1025
-4.44	0.062	-0.1029
-5.47	-0.028	-0.1040
-6.47	-0.132	-0.1035
-7.55	-0.246	-0.1040
-8.47	-0.340	-0.1029
-9.62	-0.453	-0.1021

Run: 07089gw

Re = 399786.1

α	C_l	C_m
-10.31	-0.546	-0.0934
-9.26	-0.441	-0.0958
-8.41	-0.355	-0.0971
-7.24	-0.236	-0.0987
-6.27	-0.136	-0.0987
-5.24	-0.025	-0.0998
-4.15	0.086	-0.1002
-3.16	0.185	-0.1005
-2.19	0.285	-0.1017
-1.23	0.375	-0.1013
-0.07	0.476	-0.0968
0.99	0.563	-0.0924
1.87	0.647	-0.0892
3.02	0.752	-0.0865
3.99	0.842	-0.0844
4.96	0.931	-0.0824
6.15	1.027	-0.0786
7.04	1.090	-0.0745
8.08	1.165	-0.0703

9.17	1.230	-0.0641
10.10	1.273	-0.0584
11.17	1.305	-0.0535
12.17	1.278	-0.0666
11.96	1.295	-0.0532
10.98	1.299	-0.0531
9.92	1.265	-0.0587
9.03	1.222	-0.0640
7.80	1.139	-0.0698
6.90	1.078	-0.0737
5.69	0.985	-0.0781
4.80	0.910	-0.0807
3.74	0.809	-0.0828
2.70	0.724	-0.0856
1.74	0.630	-0.0878
0.69	0.537	-0.0909
-0.38	0.444	-0.0959
-1.26	0.370	-0.0986
-2.53	0.244	-0.0985
-3.47	0.143	-0.0977
-4.41	0.051	-0.0976
-5.50	-0.066	-0.0969
-6.52	-0.166	-0.0966
-7.58	-0.285	-0.0960
-8.45	-0.369	-0.0954
-9.51	-0.478	-0.0940

W1011 (20%) **fp15**

Fig. 6.122

Run: 07095gw

Re = 100049.7

α	C_l	C_m
-10.30	-0.484	-0.1057
-9.25	-0.384	-0.1086
-8.34	-0.296	-0.1104
-7.16	-0.184	-0.1103
-6.20	-0.078	-0.1119
-5.23	0.014	-0.1077
-4.15	0.132	-0.1079
-3.16	0.241	-0.1087
-2.02	0.351	-0.1059
-1.12	0.441	-0.1043
0.02	0.573	-0.1103
1.03	0.743	-0.1201
2.07	0.810	-0.1123
3.08	0.874	-0.1063
4.02	0.949	-0.1043
5.18	1.016	-0.0976
6.18	1.072	-0.0931
7.21	1.144	-0.0892
8.10	1.190	-0.0976

8.94	1.056	-0.1861
10.01	1.022	-0.2042
10.98	1.043	-0.2067
12.01	1.011	-0.2117
11.64	1.024	-0.1925
10.70	1.046	-0.1910
9.64	1.029	-0.1762
8.80	1.166	-0.1502
7.81	1.216	-0.0826
6.91	1.164	-0.0851
5.69	1.089	-0.0907
4.81	1.038	-0.0960
3.68	0.962	-0.1008
2.77	0.892	-0.1038
1.80	0.827	-0.1096
0.64	0.740	-0.1135
-0.34	0.550	-0.0982
-1.32	0.473	-0.1013
-2.26	0.375	-0.1009
-3.35	0.266	-0.1037
-4.55	0.138	-0.1041
-5.51	0.034	-0.1075
-6.58	-0.075	-0.1084
-7.57	-0.183	-0.1086
-8.57	-0.279	-0.1097
-9.64	-0.394	-0.1087

Run: 07093gw
Re = 199955.7

α	C_l	C_m
-10.26	-0.348	-0.1358
-9.40	-0.280	-0.1354
-8.20	-0.183	-0.1325
-7.21	-0.097	-0.1305
-6.15	-0.013	-0.1260
-5.30	0.075	-0.1261
-4.21	0.168	-0.1248
-3.08	0.269	-0.1239
-2.24	0.339	-0.1192
-1.15	0.472	-0.1230
-0.14	0.690	-0.1374
0.97	0.759	-0.1244
2.06	0.827	-0.1176
3.01	0.891	-0.1123
4.07	0.970	-0.1075
5.09	1.033	-0.1024
6.16	1.104	-0.0970
7.15	1.172	-0.0922
8.15	1.242	-0.0891
9.24	1.292	-0.0847
9.96	1.078	-0.1981
10.98	1.032	-0.2044
11.88	1.002	-0.2068

12.97	0.990	-0.2097
13.98	0.992	-0.2138
13.71	0.971	-0.2036
12.68	0.998	-0.2032
11.72	1.032	-0.2023
10.64	1.071	-0.1994
9.70	1.118	-0.1872
8.83	1.268	-0.0809
7.79	1.215	-0.0850
6.90	1.157	-0.0889
5.70	1.081	-0.0945
4.83	1.019	-0.0982
3.83	0.951	-0.1034
2.67	0.871	-0.1095
1.64	0.802	-0.1158
0.68	0.748	-0.1243
-0.40	0.661	-0.1338
-1.49	0.415	-0.1141
-2.53	0.314	-0.1164
-3.47	0.218	-0.1172
-4.48	0.143	-0.1211
-5.57	0.051	-0.1250
-6.60	-0.043	-0.1253
-7.47	-0.117	-0.1283
-8.63	-0.218	-0.1315
-9.63	-0.296	-0.1345

Run: 07091gw
Re = 399834.9

α	C_l	C_m
-10.25	-0.326	-0.1366
-9.32	-0.231	-0.1386
-8.21	-0.118	-0.1398
-7.36	-0.035	-0.1404
-6.22	0.075	-0.1410
-5.36	0.141	-0.1381
-4.16	0.228	-0.1329
-3.24	0.305	-0.1307
-2.14	0.423	-0.1344
-1.22	0.571	-0.1414
-0.10	0.669	-0.1335
0.86	0.743	-0.1289
1.99	0.839	-0.1236
3.03	0.911	-0.1180
3.99	0.985	-0.1133
5.10	1.069	-0.1079
6.15	1.147	-0.1029
7.00	1.199	-0.0977
8.06	1.269	-0.0919
9.21	1.337	-0.0858
10.26	1.383	-0.0813
11.23	1.406	-0.0781
10.82	1.392	-0.0781

9.94	1.375	-0.0813
8.77	1.316	-0.0868
7.79	1.255	-0.0918
6.74	1.188	-0.0977
5.78	1.122	-0.1028
4.73	1.053	-0.1088
3.73	0.969	-0.1128
2.84	0.901	-0.1164
1.68	0.806	-0.1223
0.68	0.727	-0.1270
-0.46	0.641	-0.1340
-1.46	0.529	-0.1371
-2.42	0.387	-0.1311
-3.30	0.299	-0.1294
-4.56	0.207	-0.1341
-5.55	0.131	-0.1377
-6.47	0.046	-0.1378
-7.61	-0.071	-0.1375
-8.53	-0.163	-0.1371
-9.61	-0.276	-0.1351

W1011 (20%) **fp20**

Fig. 6.125

Run: 07096gw
Re = 99889.4

α	C_l	C_m
-10.27	-0.410	-0.1236
-9.32	-0.311	-0.1283
-8.34	-0.219	-0.1290
-7.22	-0.119	-0.1298
-6.23	-0.033	-0.1278
-5.17	0.060	-0.1258
-4.15	0.140	-0.1199
-3.25	0.216	-0.1154
-2.24	0.320	-0.1172
-0.99	0.450	-0.1202
-0.20	0.542	-0.1295
0.92	0.697	-0.1300
2.03	0.732	-0.1165
2.89	0.803	-0.1144
4.09	0.901	-0.1119
5.13	0.973	-0.1080
6.03	1.042	-0.1058
7.12	1.123	-0.1033
8.03	1.151	-0.1948
8.94	1.012	-0.2177
9.85	1.004	-0.2305
10.93	0.963	-0.2286
11.96	0.983	-0.2322
11.73	1.020	-0.2217
10.66	0.993	-0.2124

9.71	1.062	-0.2123
8.79	1.044	-0.1884
7.86	1.203	-0.0972
6.72	1.122	-0.0975
5.91	1.065	-0.0994
4.87	0.986	-0.1029
3.64	0.894	-0.1056
2.70	0.815	-0.1073
1.63	0.733	-0.1110
0.80	0.721	-0.1238
-0.35	0.557	-0.1149
-1.34	0.442	-0.1092
-2.44	0.336	-0.1090
-3.35	0.247	-0.1090
-4.52	0.146	-0.1147
-5.43	0.077	-0.1197
-6.46	-0.016	-0.1233
-7.57	-0.116	-0.1258
-8.42	-0.199	-0.1262
-9.52	-0.298	-0.1253

Run: 07098gw

Re = 199936.0

α	C_l	C_m
-10.46	-0.355	-0.1337
-9.32	-0.247	-0.1370
-8.37	-0.155	-0.1375
-7.37	-0.050	-0.1386
-6.20	0.060	-0.1383
-5.30	0.145	-0.1373
-4.13	0.262	-0.1384
-3.21	0.355	-0.1384
-2.09	0.462	-0.1367
-1.03	0.589	-0.1408
-0.10	0.723	-0.1453
1.02	0.736	-0.1252
2.05	0.814	-0.1195
2.95	0.891	-0.1174
3.94	0.973	-0.1146
5.01	1.059	-0.1116
6.03	1.140	-0.1095
7.11	1.226	-0.1071
8.17	1.305	-0.1053
8.89	1.231	-0.2040
9.99	1.133	-0.2267
10.93	1.122	-0.2324
11.85	1.109	-0.2350
12.97	1.095	-0.2358
12.74	1.093	-0.2281
11.74	1.112	-0.2284
10.71	1.109	-0.2242
9.74	1.164	-0.2202
9.01	1.354	-0.0970

7.90	1.290	-0.1010
6.93	1.216	-0.1023
5.72	1.128	-0.1051
4.81	1.054	-0.1074
3.66	0.959	-0.1104
2.69	0.879	-0.1133
1.66	0.793	-0.1164
0.67	0.729	-0.1245
-0.39	0.743	-0.1494
-1.38	0.548	-0.1327
-2.46	0.431	-0.1319
-3.39	0.334	-0.1336
-4.37	0.240	-0.1344
-5.51	0.126	-0.1335
-6.56	0.033	-0.1339
-7.45	-0.058	-0.1347
-8.45	-0.164	-0.1343
-9.62	-0.281	-0.1330

Run: 07100gw

Re = 400055.6

α	C_l	C_m
-10.25	-0.336	-0.1366
-9.29	-0.236	-0.1390
-8.24	-0.129	-0.1400
-7.19	-0.028	-0.1414
-6.27	0.060	-0.1417
-5.32	0.158	-0.1414
-4.16	0.274	-0.1422
-3.09	0.371	-0.1413
-2.22	0.477	-0.1466
-1.07	0.721	-0.1662
-0.05	0.726	-0.1476
0.87	0.793	-0.1423
1.93	0.858	-0.1335
2.92	0.924	-0.1266
3.93	0.996	-0.1198
4.97	1.083	-0.1167
6.03	1.177	-0.1140
7.04	1.252	-0.1103
8.17	1.346	-0.1073
9.21	1.417	-0.1034
10.23	1.470	-0.1005
11.11	1.435	-0.1139
11.02	1.482	-0.0984
9.82	1.457	-0.1009
8.77	1.384	-0.1032
7.80	1.323	-0.1070
6.94	1.255	-0.1097
5.91	1.167	-0.1122
4.87	1.081	-0.1154
3.77	0.987	-0.1193
2.74	0.912	-0.1260

1.62	0.836	-0.1328
0.61	0.769	-0.1403
-0.32	0.728	-0.1496
-1.47	0.636	-0.1582
-2.44	0.442	-0.1414
-3.49	0.336	-0.1394
-4.39	0.248	-0.1398
-5.53	0.137	-0.1399
-6.39	0.049	-0.1395
-7.59	-0.072	-0.1390
-8.55	-0.169	-0.1375
-9.57	-0.270	-0.1375

W1011 (20%) **fp25**

Fig. 6.128

Run: 07106gw

Re = 100066.9

α	C_l	C_m
-10.25	-0.243	-0.1498
-9.23	-0.132	-0.1528
-8.36	-0.045	-0.1555
-7.17	0.068	-0.1518
-6.30	0.147	-0.1494
-5.23	0.241	-0.1447
-4.08	0.339	-0.1385
-3.07	0.441	-0.1374
-2.17	0.540	-0.1414
-0.98	0.655	-0.1408
-0.03	0.792	-0.1599
1.07	0.816	-0.1303
1.92	0.875	-0.1260
2.98	0.955	-0.1235
4.13	1.041	-0.1223
5.10	1.108	-0.1190
6.09	1.177	-0.1177
7.06	1.243	-0.1159
7.93	1.206	-0.2223
9.01	1.139	-0.2391
10.02	1.167	-0.2518
10.86	1.161	-0.2571
11.85	1.169	-0.2580
11.75	1.150	-0.2390
10.76	1.190	-0.2422
9.69	1.177	-0.2304
8.63	1.137	-0.2115
7.82	1.330	-0.1123
6.76	1.268	-0.1124
5.88	1.204	-0.1132
4.79	1.126	-0.1153
3.71	1.047	-0.1181
2.78	0.972	-0.1189

1.71	0.879	-0.1204
0.66	0.833	-0.1305
-0.24	0.780	-0.1332
-1.35	0.650	-0.1297
-2.42	0.537	-0.1263
-3.42	0.427	-0.1252
-4.38	0.348	-0.1307
-5.41	0.261	-0.1397
-6.47	0.167	-0.1460
-7.48	0.075	-0.1509
-8.45	-0.024	-0.1528
-9.62	-0.143	-0.1530

Run: 07104gw
Re = 199974.5

α	C_l	C_m
-10.42	-0.238	-0.1553
-9.28	-0.128	-0.1592
-8.22	-0.020	-0.1613
-7.29	0.072	-0.1608
-6.17	0.172	-0.1611
-5.17	0.267	-0.1621
-4.25	0.361	-0.1632
-3.18	0.471	-0.1622
-2.11	0.565	-0.1608
-1.13	0.655	-0.1565
-0.12	0.735	-0.1486
0.97	0.799	-0.1377
1.97	0.881	-0.1335
3.07	0.974	-0.1305
4.05	1.052	-0.1286
5.13	1.137	-0.1251
6.08	1.214	-0.1232
7.17	1.296	-0.1211
8.14	1.364	-0.1189
8.98	1.227	-0.2386
9.90	1.182	-0.2485
10.92	1.187	-0.2560
11.92	1.156	-0.2546
11.63	1.186	-0.2522
10.67	1.163	-0.2478
9.75	1.225	-0.2418
8.68	1.230	-0.2253
7.80	1.349	-0.1147
6.77	1.273	-0.1167
5.70	1.197	-0.1191
4.87	1.124	-0.1206
3.68	1.032	-0.1241
2.68	0.950	-0.1269
1.70	0.864	-0.1293
0.64	0.788	-0.1349
-0.30	0.738	-0.1455
-1.41	0.624	-0.1483

-2.39	0.554	-0.1564
-3.48	0.439	-0.1564
-4.44	0.344	-0.1568
-5.51	0.239	-0.1569
-6.47	0.149	-0.1559
-7.58	0.043	-0.1559
-8.52	-0.047	-0.1545
-9.58	-0.155	-0.1542

Run: 07102gw
Re = 399965.2

α	C_l	C_m
-10.25	-0.222	-0.1580
-9.31	-0.131	-0.1598
-8.21	-0.019	-0.1605
-7.33	0.068	-0.1608
-6.18	0.178	-0.1607
-5.15	0.278	-0.1611
-4.05	0.376	-0.1603
-3.07	0.458	-0.1579
-2.11	0.563	-0.1598
-1.06	0.666	-0.1573
0.02	0.731	-0.1479
0.99	0.813	-0.1445
1.88	0.890	-0.1410
2.93	0.973	-0.1360
3.93	1.062	-0.1316
5.12	1.160	-0.1274
6.16	1.254	-0.1252
7.08	1.330	-0.1232
8.16	1.416	-0.1212
9.20	1.494	-0.1188
10.22	1.538	-0.1175
9.84	1.521	-0.1161
8.95	1.470	-0.1183
7.77	1.386	-0.1209
6.75	1.297	-0.1224
5.81	1.220	-0.1236
4.70	1.128	-0.1270
3.69	1.044	-0.1310
2.64	0.955	-0.1348
1.73	0.869	-0.1383
0.75	0.790	-0.1429
-0.44	0.691	-0.1472
-1.50	0.657	-0.1633
-2.45	0.517	-0.1556
-3.32	0.431	-0.1555
-4.52	0.338	-0.1590
-5.44	0.248	-0.1583
-6.51	0.144	-0.1580
-7.52	0.044	-0.1584
-8.62	-0.068	-0.1572
-9.65	-0.176	-0.1558

W1011 (20%) **fp30**

Fig. 6.131

Run: 07074sn
Re = 100034.8

α	C_l	C_m
-10.28	-0.101	-0.1761
-9.38	-0.004	-0.1812
-8.39	0.086	-0.1808
-7.16	0.191	-0.1774
-6.24	0.248	-0.1662
-5.22	0.312	-0.1550
-4.06	0.401	-0.1470
-3.11	0.503	-0.1485
-2.07	0.617	-0.1533
-1.03	0.726	-0.1563
-0.12	0.790	-0.1534
0.99	0.871	-0.1451
1.93	0.947	-0.1404
3.04	1.025	-0.1370
4.06	1.112	-0.1346
5.16	1.192	-0.1331
6.05	1.251	-0.1308
7.14	1.325	-0.1465
7.96	1.159	-0.2413
8.93	1.140	-0.2539
9.89	1.173	-0.2639
10.97	1.194	-0.2720
12.01	1.212	-0.2747
12.85	1.190	-0.2720
13.96	1.181	-0.2765
13.75	1.167	-0.2617
12.62	1.211	-0.2596
11.65	1.220	-0.2539
10.59	1.180	-0.2491
9.69	1.197	-0.2455
8.80	1.184	-0.2338
7.65	1.314	-0.2124
6.81	1.357	-0.1248
5.88	1.289	-0.1265
4.78	1.208	-0.1277
3.82	1.127	-0.1304
2.73	1.035	-0.1331
1.67	0.961	-0.1357
0.64	0.881	-0.1409
-0.45	0.813	-0.1451
-1.33	0.731	-0.1439
-2.23	0.631	-0.1394
-3.31	0.515	-0.1349
-4.48	0.406	-0.1361
-5.46	0.330	-0.1427
-6.40	0.276	-0.1558

-7.42	0.206	-0.1631
-8.39	0.123	-0.1681
-9.58	0.005	-0.1657

Run: 07076sn
Re = 200004.6

α	C_l	C_m
-10.31	-0.081	-0.1818
-9.38	0.009	-0.1851
-8.24	0.117	-0.1855
-7.30	0.206	-0.1869
-6.35	0.302	-0.1882
-5.25	0.416	-0.1886
-4.15	0.520	-0.1867
-3.18	0.618	-0.1862
-2.11	0.703	-0.1800
-1.14	0.761	-0.1698
-0.11	0.835	-0.1621
0.93	0.915	-0.1565
2.00	0.998	-0.1512
3.07	1.086	-0.1475
4.10	1.166	-0.1438
5.01	1.237	-0.1402
6.10	1.315	-0.1374
7.09	1.383	-0.1346
7.94	1.378	-0.2215
8.96	1.253	-0.2507
9.97	1.245	-0.2641
10.89	1.206	-0.2681
11.83	1.206	-0.2695
12.84	1.167	-0.2690
13.95	1.177	-0.2739
13.63	1.166	-0.2673
12.72	1.178	-0.2648
11.61	1.180	-0.2623
10.72	1.229	-0.2644
9.72	1.283	-0.2625
8.71	1.265	-0.2458
7.91	1.431	-0.1274
6.72	1.361	-0.1310
5.73	1.295	-0.1341
4.76	1.225	-0.1377
3.70	1.138	-0.1405
2.83	1.071	-0.1436
1.68	0.977	-0.1478
0.77	0.897	-0.1514
-0.37	0.823	-0.1602
-1.44	0.712	-0.1616
-2.41	0.678	-0.1762
-3.45	0.589	-0.1807
-4.38	0.496	-0.1818
-5.40	0.400	-0.1828
-6.56	0.281	-0.1817

-7.57	0.178	-0.1807
-8.56	0.084	-0.1803
-9.49	0.002	-0.1799

Run: 07078gw
Re = 399954.0

α	C_l	C_m
-10.32	-0.109	-0.1797
-9.32	-0.002	-0.1832
-8.35	0.093	-0.1831
-7.29	0.196	-0.1835
-6.26	0.293	-0.1833
-5.16	0.385	-0.1845
-4.13	0.477	-0.1820
-3.18	0.565	-0.1810
-2.20	0.633	-0.1733
-1.19	0.734	-0.1728
-0.12	0.818	-0.1664
0.96	0.906	-0.1620
1.87	0.991	-0.1593
2.87	1.073	-0.1541
3.94	1.162	-0.1489
5.07	1.251	-0.1450
6.10	1.332	-0.1400
7.15	1.403	-0.1343
8.10	1.470	-0.1316
9.11	1.545	-0.1303
10.17	1.598	-0.1303
9.98	1.587	-0.1293
8.94	1.531	-0.1300
7.82	1.457	-0.1320
6.84	1.381	-0.1351
5.83	1.306	-0.1393
4.75	1.224	-0.1442
3.80	1.149	-0.1484
2.68	1.056	-0.1532
1.65	0.974	-0.1585
0.60	0.879	-0.1615
-0.27	0.810	-0.1655
-1.38	0.720	-0.1709
-2.44	0.614	-0.1720
-3.39	0.547	-0.1789
-4.55	0.435	-0.1802
-5.36	0.369	-0.1824
-6.41	0.276	-0.1815
-7.64	0.158	-0.1812
-8.63	0.057	-0.1803
-9.65	-0.043	-0.1792

W1011 (20%) **fp35**

Fig. 6.133

Run: 07107sn
Re = 100027.5

α	C_l	C_m
-10.22	-0.011	-0.1854
-9.30	0.076	-0.1871
-8.21	0.170	-0.1853
-7.24	0.241	-0.1761
-6.19	0.282	-0.1565
-5.27	0.369	-0.1515
-4.06	0.500	-0.1527
-3.15	0.602	-0.1560
-2.04	0.739	-0.1625
-1.03	0.862	-0.1694
0.06	0.947	-0.1629
1.07	1.025	-0.1590
2.02	1.080	-0.1519
3.07	1.152	-0.1474
3.99	1.225	-0.1471
5.01	1.286	-0.1434
6.19	1.368	-0.1411
7.13	1.417	-0.1596
7.92	1.252	-0.2595
8.97	1.279	-0.2775
9.91	1.257	-0.2791
10.92	1.259	-0.2842
11.85	1.239	-0.2828
11.64	1.250	-0.2691
10.74	1.248	-0.2646
9.76	1.257	-0.2585
8.70	1.254	-0.2484
7.71	1.242	-0.2299
6.89	1.417	-0.1345
5.89	1.355	-0.1347
4.90	1.295	-0.1378
3.75	1.220	-0.1400
2.77	1.149	-0.1428
1.76	1.087	-0.1480
0.82	1.011	-0.1497
-0.30	0.932	-0.1535
-1.34	0.850	-0.1550
-2.36	0.729	-0.1486
-3.30	0.617	-0.1434
-4.30	0.494	-0.1384
-5.37	0.392	-0.1412
-6.50	0.297	-0.1485
-7.52	0.249	-0.1687
-8.55	0.169	-0.1796
-9.53	0.079	-0.1805

Run: 07108gw
Re = 199968.9

α	C_l	C_m
-10.37	0.008	-0.1954
-9.26	0.126	-0.1987
-8.35	0.212	-0.2003
-7.26	0.317	-0.2016
-6.21	0.413	-0.2025
-5.22	0.514	-0.2019
-4.11	0.618	-0.1999
-3.14	0.712	-0.1984
-2.20	0.785	-0.1928
-1.04	0.858	-0.1809
-0.13	0.924	-0.1749
1.02	1.010	-0.1686
1.95	1.089	-0.1649
3.10	1.177	-0.1612
4.07	1.261	-0.1592
5.09	1.339	-0.1554
6.16	1.410	-0.1509
7.24	1.463	-0.1446
7.74	1.410	-0.2389
8.95	1.308	-0.2736
9.95	1.287	-0.2797
10.91	1.268	-0.2826
11.84	1.246	-0.2808
11.72	1.231	-0.2741
10.67	1.300	-0.2791
9.63	1.282	-0.2732
8.63	1.309	-0.2616
7.99	1.511	-0.1389
6.92	1.459	-0.1417
5.91	1.398	-0.1465
4.77	1.319	-0.1506
3.82	1.246	-0.1530
2.81	1.163	-0.1564
1.73	1.072	-0.1592
0.75	1.004	-0.1650
-0.27	0.923	-0.1711
-1.36	0.818	-0.1720
-2.34	0.782	-0.1875
-3.41	0.690	-0.1922
-4.50	0.587	-0.1938
-5.45	0.502	-0.1961
-6.37	0.410	-0.1969
-7.44	0.310	-0.1966
-8.56	0.196	-0.1949
-9.60	0.094	-0.1933

Run: 07109gw
Re = 399986.2

α	C_l	C_m
-10.35	-0.002	-0.1973
-9.21	0.101	-0.1990
-8.32	0.194	-0.1992
-7.15	0.306	-0.2001
-6.19	0.381	-0.2001
-5.21	0.474	-0.1994
-4.21	0.565	-0.1980
-3.21	0.655	-0.1957
-2.16	0.732	-0.1893
-1.12	0.828	-0.1862
-0.09	0.918	-0.1827
0.93	0.998	-0.1784
2.10	1.108	-0.1746
2.91	1.172	-0.1707
4.08	1.268	-0.1648
5.07	1.347	-0.1611
6.10	1.434	-0.1567
7.18	1.500	-0.1501
8.11	1.554	-0.1456
9.26	1.625	-0.1421
9.04	1.398	-0.2603
9.33	1.371	-0.2640
9.55	1.638	-0.1419
7.91	1.536	-0.1451
6.85	1.455	-0.1502
5.94	1.400	-0.1550
4.72	1.312	-0.1610
3.68	1.229	-0.1662
2.70	1.145	-0.1692
1.64	1.057	-0.1741
0.64	0.971	-0.1790
-0.42	0.882	-0.1815
-1.44	0.793	-0.1845
-2.35	0.704	-0.1862
-3.53	0.624	-0.1947
-4.55	0.525	-0.1961
-5.57	0.434	-0.1978
-6.55	0.356	-0.1972
-7.57	0.260	-0.1977
-8.61	0.163	-0.1971
-9.55	0.067	-0.1962

W1011 (20%) **fp40**

Fig. 6.135

Run: 07112gw
Re = 100074.2

α	C_l	C_m
-10.23	0.073	-0.1980
-9.25	0.158	-0.1962
-8.33	0.223	-0.1911
-7.14	0.268	-0.1686
-6.11	0.312	-0.1551
-5.06	0.402	-0.1532
-4.08	0.527	-0.1607
-3.08	0.644	-0.1645
-2.10	0.752	-0.1688
-1.10	0.873	-0.1770
-0.11	0.957	-0.1721
1.05	1.044	-0.1674
2.09	1.126	-0.1637
2.97	1.189	-0.1601
4.00	1.266	-0.1571
5.09	1.327	-0.1518
6.18	1.401	-0.1492
7.04	1.325	-0.2448
8.00	1.254	-0.2704
8.94	1.254	-0.2803
9.90	1.228	-0.2796
9.65	1.256	-0.2652
8.65	1.281	-0.2590
7.72	1.316	-0.2448
6.76	1.396	-0.2082
5.89	1.432	-0.1444
4.81	1.362	-0.1484
3.90	1.291	-0.1500
2.84	1.214	-0.1548
1.73	1.128	-0.1580
0.71	1.042	-0.1598
-0.38	0.961	-0.1623
-1.37	0.869	-0.1624
-2.33	0.750	-0.1556
-3.39	0.630	-0.1497
-4.40	0.522	-0.1447
-5.47	0.411	-0.1430
-6.34	0.322	-0.1410
-7.39	0.275	-0.1576
-8.40	0.254	-0.1843
-9.54	0.178	-0.1922

Run: 07111gw

Re = 200073.1

α	C_l	C_m
-10.33	0.105	-0.2094
-9.33	0.209	-0.2128
-8.27	0.311	-0.2140
-7.21	0.413	-0.2149
-6.18	0.515	-0.2144
-5.22	0.606	-0.2139
-4.20	0.690	-0.2103
-3.10	0.785	-0.2066
-2.08	0.856	-0.2004
-1.06	0.925	-0.1914
-0.03	0.994	-0.1817
0.91	1.077	-0.1797
2.03	1.173	-0.1764
3.02	1.240	-0.1723
4.15	1.332	-0.1699
5.09	1.389	-0.1647
6.27	1.473	-0.1624
7.07	1.500	-0.1548
7.98	1.423	-0.2637
8.88	1.381	-0.2814
9.87	1.325	-0.2894
9.65	1.301	-0.2786
8.62	1.353	-0.2734
7.79	1.421	-0.2555
6.88	1.503	-0.1520
5.77	1.447	-0.1565
4.82	1.394	-0.1616
3.73	1.308	-0.1641
2.69	1.229	-0.1674
1.76	1.147	-0.1694
0.73	1.063	-0.1734
-0.37	0.983	-0.1806
-1.34	0.897	-0.1843
-2.36	0.851	-0.1976
-3.31	0.768	-0.2017
-4.48	0.669	-0.2043
-5.39	0.587	-0.2072
-6.52	0.487	-0.2093
-7.47	0.394	-0.2100
-8.41	0.300	-0.2084
-9.52	0.193	-0.2072

Run: 07110gw

Re = 399955.5

α	C_l	C_m
-10.43	0.083	-0.2100
-9.21	0.196	-0.2106
-8.24	0.287	-0.2114
-7.34	0.373	-0.2133
-6.17	0.464	-0.2113
-5.14	0.560	-0.2104
-4.13	0.657	-0.2099
-3.02	0.744	-0.2049
-2.04	0.813	-0.1984
-1.01	0.918	-0.1983
-0.11	0.992	-0.1944
1.01	1.083	-0.1901
1.97	1.174	-0.1870
3.06	1.251	-0.1813
4.07	1.329	-0.1761
5.15	1.406	-0.1704
6.07	1.486	-0.1666
7.16	1.559	-0.1612
8.12	1.610	-0.1559
9.19	1.672	-0.1527
8.98	1.659	-0.1510
7.85	1.599	-0.1558
6.91	1.538	-0.1608
5.77	1.459	-0.1654
4.79	1.396	-0.1719
3.76	1.317	-0.1766
2.61	1.219	-0.1814
1.65	1.134	-0.1846
0.76	1.063	-0.1885
-0.31	0.976	-0.1933
-1.45	0.873	-0.1957
-2.40	0.789	-0.1986
-3.51	0.710	-0.2057
-4.53	0.615	-0.2065
-5.53	0.522	-0.2086
-6.60	0.428	-0.2101
-7.61	0.343	-0.2092
-8.55	0.257	-0.2093
-9.56	0.159	-0.2075

W1011 (20%) **fp45**

Fig. 6.137

Run: 07113gw

Re = 100035.1

α	C_l	C_m
-10.20	0.157	-0.2087
-9.21	0.223	-0.2008
-8.20	0.252	-0.1818
-7.14	0.265	-0.1580
-6.18	0.352	-0.1552
-5.22	0.470	-0.1601
-4.08	0.611	-0.1682
-3.19	0.713	-0.1727
-2.10	0.832	-0.1777
-1.00	0.956	-0.1849
-0.09	1.038	-0.1840
1.06	1.128	-0.1789
2.06	1.209	-0.1739
2.97	1.285	-0.1719
4.16	1.360	-0.1655
5.08	1.421	-0.1616
6.17	1.469	-0.1667
7.02	1.352	-0.2593
7.97	1.330	-0.2780
8.99	1.266	-0.2829
9.92	1.303	-0.2900
9.61	1.321	-0.2767
8.59	1.300	-0.2641
7.69	1.316	-0.2498
6.78	1.424	-0.2266
5.72	1.476	-0.1518
4.83	1.422	-0.1547
3.72	1.355	-0.1599
2.77	1.293	-0.1639
1.88	1.218	-0.1647
0.68	1.107	-0.1651
-0.34	1.033	-0.1691
-1.25	0.947	-0.1677
-2.19	0.844	-0.1629
-3.39	0.717	-0.1568
-4.28	0.622	-0.1501
-5.47	0.484	-0.1443
-6.32	0.367	-0.1366
-7.48	0.289	-0.1456
-8.53	0.292	-0.1769
-9.44	0.224	-0.1879

Run: 07114gw

Re = 199988.2

α	C_l	C_m
-10.22	0.212	-0.2217
-9.31	0.302	-0.2249
-8.19	0.400	-0.2256
-7.14	0.503	-0.2251
-6.32	0.574	-0.2230
-5.16	0.684	-0.2215
-4.17	0.767	-0.2175
-3.12	0.857	-0.2135
-2.15	0.921	-0.2047
-1.13	0.984	-0.1963
-0.03	1.065	-0.1899
1.05	1.145	-0.1848
2.01	1.229	-0.1826
3.12	1.320	-0.1801
4.15	1.398	-0.1773
5.05	1.461	-0.1735
6.09	1.521	-0.1696
6.85	1.465	-0.2468
7.92	1.407	-0.2771

8.98	1.340	-0.2862
9.90	1.294	-0.2903
9.65	1.317	-0.2865
8.70	1.350	-0.2812
7.69	1.377	-0.2611
7.09	1.575	-0.1592
5.87	1.512	-0.1649
4.54	1.441	-0.1711
3.84	1.391	-0.1737
2.69	1.299	-0.1762
1.69	1.210	-0.1784
0.74	1.126	-0.1810
-0.32	1.051	-0.1862
-1.24	0.985	-0.1928
-2.25	0.910	-0.1999
-3.42	0.829	-0.2095
-4.48	0.745	-0.2134
-5.48	0.653	-0.2160
-6.48	0.565	-0.2175
-7.44	0.480	-0.2199
-8.56	0.366	-0.2198
-9.56	0.275	-0.2186

Run: 07115gw
Re = 399945.7

α	C_l	C_m
-10.27	0.181	-0.2200
-9.22	0.283	-0.2211
-8.36	0.361	-0.2220
-7.17	0.461	-0.2230
-6.13	0.549	-0.2227
-5.11	0.648	-0.2218
-4.05	0.741	-0.2188
-3.13	0.823	-0.2164
-2.00	0.906	-0.2115
-1.01	0.999	-0.2089
0.04	1.084	-0.2048
1.00	1.163	-0.2004
1.98	1.243	-0.1966
2.93	1.322	-0.1919
3.96	1.408	-0.1870
5.14	1.487	-0.1809
6.12	1.551	-0.1752
7.19	1.629	-0.1697
8.19	1.680	-0.1629
7.89	1.649	-0.1643
6.73	1.581	-0.1708
5.69	1.514	-0.1765
4.68	1.439	-0.1817
3.88	1.380	-0.1862
2.75	1.302	-0.1922
1.60	1.205	-0.1969
0.67	1.123	-0.1999
-0.29	1.051	-0.2047
-1.39	0.959	-0.2072
-2.46	0.861	-0.2086
-3.40	0.787	-0.2140
-4.44	0.700	-0.2169
-5.42	0.611	-0.2187
-6.46	0.515	-0.2195
-7.66	0.411	-0.2205
-8.56	0.336	-0.2190
-9.53	0.251	-0.2201

W1011 (20%) **fp50**

Fig. 6.139

Run: 07125sn
Re = 99882.8

α	C_l	C_m
-10.25	0.191	-0.2047
-9.19	0.233	-0.1834
-8.29	0.233	-0.1611
-7.20	0.301	-0.1509
-6.15	0.411	-0.1598
-5.23	0.520	-0.1656
-4.05	0.674	-0.1781
-3.15	0.765	-0.1788
-2.09	0.872	-0.1796
-1.11	0.983	-0.1834
0.01	1.087	-0.1813
1.06	1.174	-0.1813
2.08	1.254	-0.1769
3.04	1.321	-0.1732
4.11	1.400	-0.1725
5.12	1.441	-0.1646
6.11	1.478	-0.1732
7.01	1.394	-0.2625
7.94	1.307	-0.2707
7.68	1.272	-0.2517
6.81	1.364	-0.2327
5.81	1.467	-0.1506
4.88	1.436	-0.1548
3.79	1.371	-0.1567
2.75	1.311	-0.1606
1.72	1.225	-0.1632
0.73	1.142	-0.1655
-0.29	1.051	-0.1666
-1.34	0.960	-0.1676
-2.36	0.854	-0.1633
-3.36	0.759	-0.1589
-4.40	0.637	-0.1503
-5.40	0.504	-0.1393
-6.33	0.395	-0.1311
-7.46	0.280	-0.1273
-8.34	0.233	-0.1388
-9.45	0.194	-0.1593

Run: 07126sn
Re = 199781.8

α	C_l	C_m
-10.26	0.274	-0.2244
-9.22	0.380	-0.2273
-8.19	0.476	-0.2277
-7.17	0.573	-0.2266
-6.18	0.660	-0.2253
-5.21	0.740	-0.2219
-4.10	0.828	-0.2159
-3.15	0.891	-0.2096
-2.05	0.958	-0.1997
-1.01	1.038	-0.1943
-0.05	1.122	-0.1912
1.06	1.203	-0.1857
2.00	1.283	-0.1842
2.98	1.360	-0.1820
4.17	1.449	-0.1787
5.18	1.511	-0.1759
6.20	1.573	-0.1713
6.91	1.491	-0.2459
8.11	1.362	-0.2748
9.03	1.337	-0.2815
8.75	1.394	-0.2803
7.80	1.394	-0.2660
7.02	1.609	-0.1606
5.85	1.549	-0.1666
4.78	1.488	-0.1715
3.91	1.432	-0.1740
2.75	1.341	-0.1765
1.75	1.257	-0.1774
0.71	1.175	-0.1811
-0.21	1.106	-0.1854
-1.28	1.034	-0.1923
-2.31	0.952	-0.1974
-3.27	0.886	-0.2046
-4.35	0.809	-0.2122
-5.50	0.719	-0.2167
-6.44	0.628	-0.2178
-7.42	0.550	-0.2213
-8.44	0.449	-0.2215
-9.54	0.351	-0.2211

Run: 07127sn
Re = 399897.3

α	C_l	C_m
-10.20	0.257	-0.2248
-9.23	0.348	-0.2247
-8.16	0.432	-0.2260
-7.32	0.512	-0.2272

-6.28	0.603	-0.2252
-5.10	0.711	-0.2238
-4.11	0.798	-0.2227
-3.11	0.885	-0.2197
-2.16	0.955	-0.2142
-0.98	1.062	-0.2125
-0.04	1.135	-0.2082
1.10	1.228	-0.2047
1.99	1.298	-0.1998
2.96	1.377	-0.1958
3.96	1.449	-0.1900
5.06	1.533	-0.1846
6.12	1.599	-0.1776
7.06	1.655	-0.1721
8.14	1.722	-0.1666
8.01	1.505	-0.2712
8.52	1.439	-0.2825
7.74	1.495	-0.2576
6.94	1.653	-0.1738
5.97	1.593	-0.1788
4.80	1.504	-0.1838
3.68	1.424	-0.1899
2.69	1.347	-0.1938
1.58	1.263	-0.1995
0.61	1.186	-0.2041
-0.23	1.113	-0.2064
-1.39	1.025	-0.2117
-2.48	0.933	-0.2148
-3.34	0.864	-0.2182
-4.48	0.762	-0.2198
-5.52	0.668	-0.2223
-6.54	0.581	-0.2227
-7.48	0.486	-0.2231
-8.60	0.386	-0.2236
-9.61	0.302	-0.2210

W1011 (20%) **fp55**

Fig. 6.141

Run: 07124sn

Re = 100006.4

α	C_l	C_m
-10.32	0.205	-0.1889
-9.22	0.203	-0.1569
-8.16	0.279	-0.1543
-7.12	0.371	-0.1523
-6.11	0.491	-0.1646
-5.06	0.620	-0.1742
-4.01	0.748	-0.1778
-3.14	0.843	-0.1787
-2.11	0.935	-0.1802
-1.00	1.060	-0.1922
-0.04	1.131	-0.1888
1.08	1.228	-0.1860
1.96	1.303	-0.1840
3.14	1.400	-0.1821
4.04	1.454	-0.1741
5.19	1.529	-0.1672
6.06	1.436	-0.2412
7.00	1.367	-0.2580
8.03	1.373	-0.2752
7.66	1.347	-0.2570
6.70	1.407	-0.2373
5.83	1.527	-0.1523
4.82	1.504	-0.1589
3.88	1.452	-0.1617
2.73	1.354	-0.1591
1.73	1.283	-0.1623
0.72	1.192	-0.1626
-0.23	1.120	-0.1637
-1.29	1.029	-0.1663
-2.36	0.909	-0.1655
-3.38	0.810	-0.1644
-4.32	0.721	-0.1598
-5.38	0.587	-0.1456
-6.40	0.476	-0.1399
-7.35	0.350	-0.1273
-8.46	0.259	-0.1286
-9.45	0.218	-0.1449

Run: 07123sn

Re = 200046.1

α	C_l	C_m
-10.25	0.350	-0.2289
-9.30	0.438	-0.2301
-8.19	0.542	-0.2313
-7.12	0.641	-0.2303
-6.24	0.716	-0.2286
-5.10	0.797	-0.2221
-4.15	0.863	-0.2160
-3.05	0.942	-0.2085
-2.12	1.000	-0.2020
-0.98	1.083	-0.1954
0.02	1.168	-0.1923
1.03	1.250	-0.1902
2.08	1.338	-0.1877
3.14	1.416	-0.1841
4.26	1.491	-0.1823
5.07	1.548	-0.1797
6.16	1.616	-0.1746
7.10	1.473	-0.2578
7.91	1.390	-0.2739
7.68	1.386	-0.2636
6.80	1.501	-0.2442
5.82	1.591	-0.1695
4.97	1.538	-0.1731
3.78	1.472	-0.1782
2.90	1.401	-0.1785
1.84	1.311	-0.1806
0.72	1.219	-0.1826
-0.30	1.147	-0.1888
-1.33	1.068	-0.1919
-2.30	0.989	-0.1963
-3.34	0.917	-0.2028
-4.33	0.850	-0.2099
-5.39	0.784	-0.2199
-6.43	0.691	-0.2213
-7.52	0.602	-0.2239
-8.49	0.521	-0.2262
-9.48	0.423	-0.2237

Run: 07122sn

Re = 399804.6

α	C_l	C_m
-10.36	0.313	-0.2277
-9.21	0.410	-0.2314
-8.31	0.488	-0.2314
-7.18	0.593	-0.2321
-6.14	0.685	-0.2306
-5.08	0.780	-0.2304
-4.02	0.877	-0.2295
-3.09	0.959	-0.2277
-2.03	1.038	-0.2218
-1.06	1.116	-0.2178
0.03	1.202	-0.2140
1.10	1.283	-0.2094
1.92	1.349	-0.2056
3.16	1.446	-0.2002
3.96	1.499	-0.1955
5.02	1.583	-0.1888
5.98	1.641	-0.1823
7.25	1.719	-0.1738
7.45	1.546	-0.2614
7.47	1.548	-0.2609
7.20	1.720	-0.1758
5.90	1.639	-0.1832
4.83	1.570	-0.1895
3.80	1.501	-0.1955
2.73	1.422	-0.2008
1.67	1.334	-0.2049
0.77	1.269	-0.2102
-0.27	1.186	-0.2136
-1.49	1.083	-0.2175
-2.43	1.004	-0.2203
-3.36	0.937	-0.2264
-4.39	0.844	-0.2272
-5.40	0.758	-0.2298
-6.53	0.660	-0.2318

-7.57	0.559	-0.2311
-8.47	0.466	-0.2276
-9.68	0.370	-0.2262

W1011 (20%) **fp60**

Fig. 6.143

Run: 07119sn

Re = 100007.1

α	C_l	C_m
-10.12	0.213	-0.1632
-9.13	0.256	-0.1467
-8.15	0.327	-0.1427
-7.04	0.456	-0.1524
-6.17	0.574	-0.1632
-4.99	0.696	-0.1702
-4.04	0.807	-0.1818
-3.04	0.899	-0.1844
-1.99	1.001	-0.1865
-0.94	1.116	-0.1918
-0.05	1.174	-0.1863
1.08	1.264	-0.1866
2.04	1.334	-0.1807
3.03	1.401	-0.1762
4.18	1.484	-0.1723
5.14	1.530	-0.1650
6.09	1.404	-0.2471
7.06	1.384	-0.2659
7.98	1.339	-0.2702
7.63	1.363	-0.2551
6.80	1.389	-0.2407
5.73	1.411	-0.2056
4.97	1.539	-0.1569
3.91	1.491	-0.1605
2.74	1.414	-0.1627
1.90	1.339	-0.1610
0.80	1.263	-0.1627
-0.24	1.176	-0.1647
-1.29	1.106	-0.1684
-2.16	0.990	-0.1597
-3.25	0.891	-0.1591
-4.29	0.779	-0.1524
-5.40	0.663	-0.1455
-6.29	0.563	-0.1393
-7.34	0.444	-0.1307
-8.46	0.307	-0.1210
-9.51	0.215	-0.1236

Run: 07120sn

Re = 199968.9

α	C_l	C_m
-10.27	0.411	-0.2329
-9.30	0.491	-0.2321
-8.18	0.599	-0.2323
-7.21	0.680	-0.2293
-6.16	0.764	-0.2257
-5.19	0.811	-0.2132
-4.02	0.888	-0.2041
-3.06	0.960	-0.2003
-2.06	1.042	-0.1983
-1.06	1.110	-0.1913
-0.06	1.195	-0.1905
0.99	1.276	-0.1880
2.05	1.362	-0.1837
3.15	1.448	-0.1818
4.11	1.510	-0.1790
5.03	1.574	-0.1771
5.99	1.555	-0.2198
7.06	1.412	-0.2593
7.97	1.379	-0.2738
7.71	1.381	-0.2638
6.69	1.470	-0.2472
5.84	1.626	-0.1702
4.81	1.567	-0.1733
3.80	1.498	-0.1748
2.88	1.438	-0.1781
1.89	1.357	-0.1805
0.87	1.266	-0.1811
-0.36	1.167	-0.1841
-1.33	1.094	-0.1880
-2.23	1.020	-0.1907
-3.25	0.940	-0.1947
-4.41	0.861	-0.2010
-5.48	0.802	-0.2125
-6.24	0.745	-0.2188
-7.50	0.655	-0.2253
-8.38	0.573	-0.2258
-9.53	0.479	-0.2279

Run: 07121sn

Re = 399963.3

α	C_l	C_m
-10.39	0.365	-0.2309
-9.25	0.459	-0.2325
-8.19	0.569	-0.2366
-7.14	0.652	-0.2342
-6.16	0.737	-0.2329
-5.18	0.824	-0.2313
-4.06	0.927	-0.2309
-3.01	1.008	-0.2276
-2.00	1.076	-0.2208
-0.97	1.166	-0.2178
-0.07	1.245	-0.2158
0.94	1.317	-0.2114
1.96	1.400	-0.2064
3.04	1.473	-0.1995
4.05	1.550	-0.1949
5.12	1.618	-0.1893
6.08	1.682	-0.1838
7.20	1.759	-0.1787
6.93	1.732	-0.1789
5.81	1.668	-0.1859
4.75	1.595	-0.1906
3.74	1.526	-0.1950
2.82	1.452	-0.2001
1.68	1.372	-0.2062
0.83	1.307	-0.2095
-0.39	1.212	-0.2146
-1.40	1.130	-0.2187
-2.30	1.058	-0.2206
-3.42	0.974	-0.2265
-4.42	0.891	-0.2293
-5.45	0.802	-0.2314
-6.55	0.705	-0.2324
-7.55	0.615	-0.2335
-8.42	0.535	-0.2321
-9.64	0.415	-0.2287

W1011 (20%) **fp65**

Fig. 6.145

Run: 07118gw

Re = 99968.8

α	C_l	C_m
-10.23	0.141	-0.1456
-9.17	0.190	-0.1345
-8.23	0.286	-0.1432
-7.20	0.403	-0.1523
-6.17	0.513	-0.1623
-5.19	0.638	-0.1766
-4.07	0.743	-0.1790
-3.10	0.859	-0.1833
-2.01	0.982	-0.1901
-1.09	1.081	-0.1936
0.03	1.168	-0.1897
1.12	1.266	-0.1887
2.01	1.346	-0.1860
3.02	1.416	-0.1814
4.18	1.490	-0.1757
5.09	1.541	-0.1686
6.04	1.388	-0.2480
7.08	1.295	-0.2628
7.99	1.278	-0.2702

7.65	1.305	-0.2547
6.69	1.347	-0.2437
5.84	1.455	-0.2167
4.91	1.540	-0.1575
3.83	1.491	-0.1630
2.73	1.416	-0.1652
1.80	1.333	-0.1644
0.77	1.248	-0.1653
-0.17	1.176	-0.1676
-1.37	1.081	-0.1713
-2.30	0.962	-0.1655
-3.36	0.825	-0.1574
-4.32	0.727	-0.1546
-5.42	0.604	-0.1475
-6.40	0.487	-0.1405
-7.44	0.368	-0.1291
-8.47	0.272	-0.1244
-9.50	0.171	-0.1168

Run: 07117gw
Re = 199996.0

α	C_l	C_m
-10.25	0.456	-0.2369
-9.22	0.550	-0.2382
-8.21	0.630	-0.2357
-7.11	0.715	-0.2302
-6.21	0.755	-0.2180
-5.19	0.815	-0.2054
-4.03	0.896	-0.1988
-3.12	0.982	-0.1979
-1.99	1.071	-0.1952
-1.03	1.143	-0.1907
0.04	1.235	-0.1898
0.96	1.312	-0.1899
1.97	1.388	-0.1860
3.19	1.478	-0.1833
4.15	1.544	-0.1842
5.17	1.609	-0.1797
5.97	1.567	-0.2178
7.07	1.441	-0.2659
7.92	1.350	-0.2745
7.70	1.397	-0.2668
6.72	1.440	-0.2532
5.98	1.654	-0.1693
4.97	1.602	-0.1743
3.76	1.513	-0.1782
2.76	1.453	-0.1801
1.73	1.374	-0.1820
0.80	1.301	-0.1834
-0.34	1.218	-0.1864
-1.33	1.126	-0.1861
-2.37	1.047	-0.1913
-3.35	0.956	-0.1910
-4.42	0.876	-0.1945
-5.38	0.811	-0.2024
-6.34	0.755	-0.2133
-7.48	0.688	-0.2248
-8.40	0.618	-0.2297
-9.54	0.525	-0.2310

Run: 07116gw
Re = 399793.1

α	C_l	C_m
-10.16	0.417	-0.2368
-9.29	0.499	-0.2381
-8.29	0.592	-0.2411
-7.16	0.697	-0.2403
-6.15	0.782	-0.2392
-5.29	0.861	-0.2389
-4.12	0.952	-0.2345
-3.10	1.033	-0.2300
-2.14	1.104	-0.2262
-1.08	1.187	-0.2221
0.04	1.276	-0.2180
0.94	1.344	-0.2142
2.00	1.436	-0.2095
3.03	1.504	-0.2027
4.02	1.576	-0.1969
4.94	1.646	-0.1946
6.19	1.716	-0.1866
7.03	1.775	-0.1814
6.83	1.755	-0.1816
5.93	1.690	-0.1856
4.76	1.617	-0.1933
3.75	1.549	-0.1974
2.84	1.491	-0.2033
1.84	1.407	-0.2076
0.80	1.335	-0.2134
-0.37	1.245	-0.2175
-1.26	1.170	-0.2206
-2.27	1.090	-0.2242
-3.48	1.005	-0.2308
-4.51	0.922	-0.2346
-5.51	0.835	-0.2353
-6.42	0.747	-0.2355
-7.58	0.653	-0.2379
-8.58	0.570	-0.2397
-9.61	0.464	-0.2366

W1011 (30%) **fp0**

Fig. 6.149

Run: 07128sn
Re = 99952.5

α	C_l	C_m
-10.25	-0.900	-0.0039
-9.27	-0.842	-0.0023
-8.32	-0.773	-0.0006
-7.19	-0.683	0.0017
-6.22	-0.604	0.0021
-5.20	-0.517	0.0035
-4.07	-0.420	0.0045
-3.10	-0.344	0.0069
-2.13	-0.253	0.0109
-1.04	-0.173	0.0188
-0.03	0.010	-0.0133
0.98	0.133	-0.0181
1.99	0.217	-0.0107
2.93	0.311	-0.0071
4.06	0.414	-0.0045
5.03	0.501	-0.0035
6.09	0.606	-0.0029
7.05	0.689	-0.0021
8.06	0.772	-0.0010
9.17	0.850	-0.0001
9.96	0.736	-0.0901
11.02	0.709	-0.1065
11.98	0.726	-0.1132
13.01	0.729	-0.1161
13.98	0.735	-0.1140
14.91	0.738	-0.1163
16.00	0.772	-0.1207
16.88	0.797	-0.1212
17.90	0.775	-0.1270
17.70	0.837	-0.1165
16.68	0.766	-0.1026
15.65	0.809	-0.1046
14.75	0.752	-0.0925
13.85	0.766	-0.0916
12.79	0.737	-0.0863
11.73	0.736	-0.0823
10.82	0.734	-0.0717
9.86	0.922	0.0139
8.81	0.858	0.0112
7.86	0.789	0.0091
6.74	0.693	0.0066
5.79	0.608	0.0055
4.66	0.501	0.0032
3.78	0.418	0.0010
2.70	0.327	-0.0029
1.59	0.210	-0.0029

0.69	0.151	-0.0134
-0.39	-0.019	0.0111
-1.43	-0.158	0.0171
-2.48	-0.246	0.0085
-3.46	-0.337	0.0050
-4.49	-0.419	0.0014
-5.55	-0.512	-0.0014
-6.60	-0.604	-0.0032
-7.47	-0.682	-0.0055
-8.62	-0.770	-0.0076
-9.64	-0.839	-0.0107

Run: 07130sn
Re = 199916.4

α	C_l	C_m
-10.35	-0.936	-0.0056
-9.24	-0.871	-0.0032
-8.27	-0.804	-0.0017
-7.19	-0.710	-0.0003
-6.27	-0.627	0.0006
-5.20	-0.519	0.0016
-4.24	-0.422	0.0024
-3.11	-0.310	0.0033
-2.12	-0.190	-0.0020
-1.18	-0.116	0.0031
-0.14	-0.004	-0.0021
0.91	0.113	-0.0074
1.91	0.220	-0.0069
3.04	0.328	-0.0052
4.08	0.430	-0.0044
5.09	0.535	-0.0037
5.97	0.618	-0.0030
7.11	0.723	-0.0023
8.02	0.795	-0.0011
9.17	0.882	0.0007
10.13	0.942	0.0024
11.13	0.995	0.0031
11.86	0.785	-0.1090
12.93	0.767	-0.1128
13.90	0.766	-0.1129
14.96	0.767	-0.1148
15.89	0.759	-0.1174
17.01	0.790	-0.1254
18.02	0.817	-0.1311
17.84	0.778	-0.1220
16.82	0.779	-0.1109
15.66	0.758	-0.1056
14.64	0.758	-0.1041
13.75	0.780	-0.1063
12.70	0.777	-0.1030
11.74	0.797	-0.1011
11.10	0.999	0.0106
9.85	0.934	0.0086
8.86	0.864	0.0063
7.73	0.776	0.0039
6.67	0.689	0.0020
5.70	0.599	0.0008
4.74	0.513	-0.0003
3.80	0.424	-0.0018
2.70	0.315	-0.0034
1.59	0.201	-0.0047
0.69	0.105	-0.0064
-0.34	-0.013	-0.0019
-1.31	-0.126	0.0029
-2.33	-0.221	-0.0006
-3.38	-0.333	0.0018
-4.38	-0.433	0.0004
-5.58	-0.550	-0.0013
-6.62	-0.648	-0.0020
-7.63	-0.743	-0.0046
-8.56	-0.816	-0.0068
-9.66	-0.894	-0.0090

Run: 07132sn
Re = 400024.8

α	C_l	C_m
-10.29	-0.974	-0.0067
-9.30	-0.892	-0.0049
-8.29	-0.815	-0.0034
-7.42	-0.731	-0.0027
-6.19	-0.613	-0.0018
-5.23	-0.516	-0.0011
-4.17	-0.406	-0.0013
-3.24	-0.310	-0.0024
-2.10	-0.182	-0.0043
-1.11	-0.087	-0.0034
-0.06	0.013	-0.0019
1.05	0.121	-0.0016
1.98	0.216	-0.0023
3.05	0.324	-0.0026
4.03	0.411	-0.0021
5.08	0.513	-0.0018
6.08	0.616	-0.0011
7.06	0.714	-0.0003
8.04	0.803	0.0008
9.16	0.898	0.0024
10.20	0.973	0.0043
11.23	1.039	0.0066
12.14	1.080	0.0075
13.15	1.093	-0.0146
13.87	0.829	-0.1153
13.93	0.839	-0.1173
12.78	0.845	-0.1064
12.34	1.085	0.0086
10.87	1.018	0.0065
9.82	0.953	0.0046
8.95	0.884	0.0032
7.85	0.790	0.0017
6.72	0.681	0.0005
5.81	0.592	-0.0001
4.73	0.482	-0.0007
3.65	0.382	-0.0012
2.70	0.298	-0.0017
1.71	0.197	-0.0021
0.61	0.077	-0.0004
-0.48	-0.023	-0.0016
-1.38	-0.111	-0.0031
-2.50	-0.231	-0.0026
-3.51	-0.346	-0.0002
-4.57	-0.457	0.0005
-5.54	-0.554	-0.0002
-6.54	-0.651	-0.0015
-7.69	-0.758	-0.0030
-8.65	-0.842	-0.0044
-9.66	-0.931	-0.0056

W1011 (30%) **fp5**

Fig. 6.152

Run: 07138gw
Re = 99986.5

α	C_l	C_m
-10.35	-0.720	-0.0469
-9.35	-0.644	-0.0460
-8.22	-0.531	-0.0509
-7.19	-0.412	-0.0561
-6.16	-0.299	-0.0634
-5.18	-0.191	-0.0643
-4.15	-0.084	-0.0638
-3.13	0.015	-0.0570
-2.10	0.115	-0.0614
-1.16	0.205	-0.0609
-0.15	0.300	-0.0624
0.88	0.423	-0.0665
1.95	0.515	-0.0551
2.97	0.588	-0.0493
3.92	0.670	-0.0474
5.08	0.761	-0.0443
6.14	0.850	-0.0426
7.11	0.911	-0.0387
8.10	0.970	-0.0349
9.05	1.018	-0.0505
10.04	0.822	-0.1361
10.94	0.825	-0.1406
11.89	0.830	-0.1435
12.96	0.814	-0.1472
13.87	0.818	-0.1461
13.82	0.821	-0.1352

12.63	0.847	-0.1324
11.66	0.847	-0.1284
10.72	0.817	-0.1213
9.71	0.867	-0.1124
8.91	1.043	-0.0300
7.86	0.984	-0.0332
6.73	0.910	-0.0367
5.70	0.840	-0.0405
4.71	0.758	-0.0429
3.68	0.669	-0.0450
2.60	0.581	-0.0478
1.62	0.503	-0.0546
0.73	0.421	-0.0593
-0.43	0.289	-0.0562
-1.41	0.206	-0.0541
-2.44	0.115	-0.0525
-3.41	0.019	-0.0520
-4.52	-0.086	-0.0516
-5.54	-0.195	-0.0513
-6.34	-0.286	-0.0522
-7.58	-0.430	-0.0510
-8.59	-0.548	-0.0486
-9.60	-0.641	-0.0481

Run: 07136gw
Re = 200225.2

α	C_l	C_m
-10.26	-0.681	-0.0505
-9.30	-0.588	-0.0539
-8.26	-0.486	-0.0557
-7.18	-0.380	-0.0572
-6.19	-0.279	-0.0593
-5.14	-0.179	-0.0601
-4.11	-0.077	-0.0613
-3.07	0.031	-0.0607
-2.19	0.121	-0.0593
-1.03	0.243	-0.0605
-0.20	0.329	-0.0610
1.02	0.442	-0.0578
2.04	0.535	-0.0536
3.11	0.636	-0.0521
4.09	0.724	-0.0504
5.13	0.815	-0.0485
6.12	0.897	-0.0461
7.18	0.979	-0.0428
8.06	1.033	-0.0397
9.19	1.101	-0.0351
10.18	1.134	-0.0316
10.76	0.936	-0.1432
11.99	0.909	-0.1500
12.95	0.910	-0.1520
13.97	0.861	-0.1496
13.73	0.865	-0.1436

12.76	0.888	-0.1434
11.74	0.903	-0.1409
10.84	0.968	-0.1338
9.89	1.131	-0.0279
8.84	1.086	-0.0317
7.79	1.027	-0.0361
6.80	0.955	-0.0400
5.70	0.872	-0.0435
4.74	0.785	-0.0455
3.70	0.696	-0.0478
2.78	0.609	-0.0492
1.67	0.511	-0.0523
0.69	0.417	-0.0572
-0.42	0.313	-0.0588
-1.35	0.211	-0.0571
-2.45	0.096	-0.0581
-3.43	-0.007	-0.0588
-4.42	-0.106	-0.0590
-5.41	-0.203	-0.0587
-6.59	-0.315	-0.0580
-7.46	-0.408	-0.0568
-8.57	-0.520	-0.0559
-9.57	-0.615	-0.0541

Run: 07134gw
Re = 399798.9

α	C_l	C_m
-10.33	-0.709	-0.0522
-9.39	-0.625	-0.0537
-8.27	-0.509	-0.0552
-7.25	-0.407	-0.0560
-6.41	-0.318	-0.0569
-5.21	-0.197	-0.0574
-4.17	-0.087	-0.0571
-3.13	0.018	-0.0574
-2.10	0.126	-0.0592
-1.10	0.233	-0.0589
-0.15	0.329	-0.0575
0.84	0.407	-0.0552
1.89	0.504	-0.0537
2.99	0.615	-0.0527
3.96	0.708	-0.0515
5.06	0.808	-0.0497
6.05	0.898	-0.0478
7.17	0.993	-0.0450
8.14	1.070	-0.0422
9.17	1.128	-0.0378
10.14	1.187	-0.0336
11.12	1.217	-0.0294
12.21	1.219	-0.0317
12.80	0.971	-0.1532
13.89	0.895	-0.1520
13.78	0.909	-0.1518

12.75	0.934	-0.1475
11.66	0.989	-0.1346
11.60	1.215	-0.0275
9.84	1.165	-0.0335
8.74	1.105	-0.0380
7.83	1.044	-0.0415
6.77	0.965	-0.0454
5.83	0.885	-0.0474
4.70	0.781	-0.0493
3.83	0.700	-0.0508
2.66	0.590	-0.0518
1.69	0.490	-0.0526
0.80	0.408	-0.0538
-0.41	0.311	-0.0571
-1.39	0.209	-0.0588
-2.33	0.107	-0.0585
-3.43	-0.009	-0.0578
-4.40	-0.106	-0.0573
-5.53	-0.229	-0.0572
-6.45	-0.324	-0.0561
-7.70	-0.458	-0.0554
-8.44	-0.534	-0.0549
-9.52	-0.637	-0.0536

W1011 (30%) fp10

Fig. 6.155

Run: 07139gw
Re = 99983.3

α	C_l	C_m
-10.19	-0.349	-0.1075
-9.20	-0.256	-0.1114
-8.31	-0.171	-0.1141
-7.15	-0.059	-0.1149
-6.17	0.020	-0.1142
-5.16	0.110	-0.1138
-4.20	0.193	-0.1150
-3.05	0.304	-0.1070
-2.19	0.381	-0.1142
-1.16	0.439	-0.1018
-0.15	0.512	-0.0983
0.90	0.707	-0.1145
1.98	0.782	-0.0950
2.98	0.867	-0.0913
4.09	0.943	-0.0873
5.15	1.015	-0.0822
6.19	1.057	-0.0769
7.19	1.113	-0.0714
8.10	1.147	-0.0668
9.02	1.027	-0.1597
9.96	0.959	-0.1702
11.01	0.961	-0.1760

12.02	0.950	-0.1773
11.82	0.961	-0.1614
10.73	0.951	-0.1552
9.69	0.980	-0.1491
8.84	1.213	-0.0566
7.80	1.171	-0.0619
6.84	1.124	-0.0667
5.80	1.065	-0.0729
4.70	1.008	-0.0790
3.83	0.941	-0.0832
2.73	0.852	-0.0876
1.83	0.785	-0.0915
0.71	0.674	-0.0978
-0.41	0.496	-0.0912
-1.31	0.440	-0.0890
-2.30	0.376	-0.0935
-3.32	0.284	-0.0979
-4.30	0.195	-0.0967
-5.51	0.091	-0.1030
-6.43	0.019	-0.1034
-7.49	-0.076	-0.1083
-8.51	-0.175	-0.1090
-9.54	-0.273	-0.1089

Run: 07141gw
Re = 200087.8

α	C_l	C_m
-10.20	-0.384	-0.1028
-9.24	-0.282	-0.1043
-8.21	-0.186	-0.1058
-7.14	-0.080	-0.1076
-6.11	0.021	-0.1084
-5.24	0.114	-0.1094
-4.10	0.219	-0.1091
-3.24	0.298	-0.1081
-2.15	0.408	-0.1086
-1.04	0.521	-0.1104
-0.10	0.625	-0.1097
0.84	0.710	-0.1021
2.09	0.809	-0.0973
3.08	0.887	-0.0940
4.12	0.967	-0.0905
5.15	1.036	-0.0861
6.11	1.092	-0.0811
7.11	1.147	-0.0755
8.19	1.201	-0.0696
9.19	1.235	-0.0643
9.89	1.061	-0.1669
10.97	0.976	-0.1739
11.90	0.985	-0.1796
12.95	0.951	-0.1796
13.89	0.923	-0.1778
13.61	0.931	-0.1723

12.66	0.955	-0.1721
11.67	0.999	-0.1740
10.80	1.010	-0.1712
9.69	1.052	-0.1579
8.86	1.225	-0.0602
7.87	1.186	-0.0654
6.91	1.137	-0.0715
5.87	1.082	-0.0771
4.85	1.025	-0.0829
3.79	0.951	-0.0878
2.80	0.870	-0.0912
1.84	0.787	-0.0940
0.76	0.705	-0.0994
-0.42	0.596	-0.1072
-1.45	0.489	-0.1063
-2.44	0.391	-0.1065
-3.48	0.285	-0.1078
-4.50	0.184	-0.1077
-5.47	0.089	-0.1083
-6.40	-0.008	-0.1073
-7.59	-0.124	-0.1064
-8.60	-0.224	-0.1055
-9.49	-0.313	-0.1045

Run: 07143gw
Re = 399714.0

α	C_l	C_m
-10.49	-0.434	-0.1006
-9.21	-0.307	-0.1026
-8.32	-0.213	-0.1035
-7.27	-0.102	-0.1046
-6.30	0.002	-0.1058
-5.23	0.112	-0.1061
-4.26	0.212	-0.1071
-3.26	0.316	-0.1083
-2.13	0.416	-0.1084
-1.07	0.534	-0.1090
0.00	0.627	-0.1037
1.00	0.707	-0.1000
2.00	0.805	-0.0981
3.06	0.894	-0.0951
4.10	0.981	-0.0918
5.05	1.059	-0.0892
6.13	1.126	-0.0834
7.12	1.189	-0.0785
8.04	1.234	-0.0728
9.06	1.273	-0.0667
10.15	1.319	-0.0616
11.20	1.334	-0.0581
10.83	1.331	-0.0577
9.82	1.309	-0.0617
8.82	1.265	-0.0667
7.95	1.228	-0.0719

6.79	1.162	-0.0782
5.90	1.116	-0.0833
4.74	1.029	-0.0880
3.83	0.961	-0.0910
2.71	0.868	-0.0945
1.69	0.775	-0.0968
0.75	0.693	-0.1000
-0.29	0.612	-0.1053
-1.37	0.507	-0.1082
-2.50	0.390	-0.1077
-3.37	0.306	-0.1073
-4.38	0.205	-0.1065
-5.51	0.084	-0.1050
-6.46	-0.011	-0.1045
-7.40	-0.114	-0.1040
-8.39	-0.220	-0.1029
-9.54	-0.336	-0.1016

W1011 (30%) **fp15**

Fig. 6.158

Run: 07145gw
Re = 100051.1

α	C_l	C_m
-10.19	-0.111	-0.1528
-9.35	-0.058	-0.1530
-8.27	0.007	-0.1485
-7.24	0.080	-0.1445
-6.31	0.159	-0.1414
-5.11	0.247	-0.1379
-4.14	0.315	-0.1342
-3.08	0.402	-0.1285
-2.18	0.473	-0.1263
-1.00	0.559	-0.1230
-0.07	0.626	-0.1147
0.94	0.906	-0.1335
2.07	0.945	-0.1230
3.11	1.006	-0.1164
4.12	1.056	-0.1104
5.10	1.104	-0.1032
6.13	1.156	-0.0970
7.03	1.214	-0.0928
8.00	1.261	-0.1058
9.01	1.040	-0.1902
9.88	1.048	-0.2017
11.03	1.080	-0.2084
10.60	1.096	-0.1906
9.72	1.093	-0.1822
8.77	1.085	-0.1697
7.84	1.292	-0.0839
6.80	1.234	-0.0874
5.70	1.172	-0.0925

4.81	1.128	-0.0986
3.79	1.081	-0.1065
2.68	1.004	-0.1119
1.84	0.974	-0.1204
0.60	0.826	-0.1225
-0.26	0.627	-0.1077
-1.29	0.573	-0.1127
-2.47	0.471	-0.1159
-3.36	0.410	-0.1177
-4.55	0.307	-0.1213
-5.37	0.239	-0.1254
-6.57	0.158	-0.1328
-7.56	0.069	-0.1377
-8.55	0.007	-0.1444
-9.48	-0.050	-0.1477

Run: 07146gw
Re = 199965.7

α	C_l	C_m
-10.30	-0.105	-0.1504
-9.33	-0.010	-0.1529
-8.23	0.087	-0.1545
-7.17	0.171	-0.1543
-6.18	0.232	-0.1511
-5.22	0.338	-0.1530
-4.12	0.392	-0.1454
-3.18	0.516	-0.1481
-2.06	0.575	-0.1393
-0.97	0.686	-0.1386
0.01	0.893	-0.1442
1.04	0.935	-0.1334
1.99	0.975	-0.1267
3.10	1.023	-0.1191
3.97	1.072	-0.1135
5.05	1.128	-0.1071
6.18	1.196	-0.1009
7.05	1.256	-0.0970
8.03	1.311	-0.0917
8.94	1.149	-0.1841
10.02	1.094	-0.2018
10.95	1.098	-0.2094
11.89	1.048	-0.2077
11.60	1.088	-0.2070
10.80	1.089	-0.2040
9.65	1.149	-0.1973
8.96	1.347	-0.0841
7.88	1.306	-0.0885
6.83	1.242	-0.0937
5.72	1.174	-0.0990
4.72	1.116	-0.1046
3.88	1.063	-0.1093
2.66	1.005	-0.1179
1.66	0.962	-0.1247
0.68	0.921	-0.1322
-0.24	0.880	-0.1439
-1.33	0.636	-0.1313
-2.23	0.573	-0.1369
-3.35	0.498	-0.1434
-4.40	0.385	-0.1428
-5.36	0.320	-0.1475
-6.47	0.229	-0.1490
-7.54	0.138	-0.1510
-8.52	0.063	-0.1519
-9.44	-0.018	-0.1515

Run: 07148gw
Re = 399924.8

α	C_l	C_m
-10.25	-0.096	-0.1512
-9.32	-0.002	-0.1524
-8.17	0.114	-0.1541
-7.18	0.216	-0.1545
-6.17	0.315	-0.1554
-5.11	0.409	-0.1564
-4.10	0.505	-0.1565
-3.06	0.570	-0.1541
-2.08	0.674	-0.1544
-1.04	0.830	-0.1529
-0.17	0.876	-0.1441
1.03	0.958	-0.1373
2.05	1.028	-0.1311
2.94	1.077	-0.1252
4.07	1.139	-0.1200
5.08	1.187	-0.1124
6.18	1.242	-0.1055
7.14	1.298	-0.0992
8.15	1.349	-0.0944
9.21	1.402	-0.0887
10.20	1.444	-0.0856
10.28	1.202	-0.1939
10.28	1.201	-0.1963
10.44	1.449	-0.0833
8.83	1.393	-0.0896
7.79	1.329	-0.0943
6.81	1.278	-0.1000
5.76	1.222	-0.1065
4.73	1.168	-0.1127
3.74	1.130	-0.1200
2.88	1.078	-0.1246
1.69	1.004	-0.1314
0.70	0.936	-0.1375
-0.26	0.873	-0.1435
-1.39	0.783	-0.1537
-2.29	0.655	-0.1531
-3.44	0.555	-0.1543
-4.49	0.468	-0.1544
-5.52	0.380	-0.1548
-6.52	0.287	-0.1535
-7.56	0.176	-0.1522
-8.44	0.086	-0.1520
-9.59	-0.033	-0.1509

W1011 (30%) **fp20**

Fig. 6.161

Run: 07154gw
Re = 99998.5

α	C_l	C_m
-10.34	-0.121	-0.1545
-9.19	-0.023	-0.1535
-8.28	0.051	-0.1517
-7.18	0.141	-0.1492
-6.07	0.203	-0.1371
-5.16	0.270	-0.1305
-4.12	0.359	-0.1283
-3.22	0.447	-0.1308
-2.05	0.549	-0.1326
-0.99	0.637	-0.1321
-0.08	0.742	-0.1393
0.99	0.867	-0.1422
1.93	0.894	-0.1325
2.93	0.959	-0.1291
4.01	1.031	-0.1231
5.02	1.089	-0.1196
6.12	1.169	-0.1154
7.17	1.242	-0.1136
7.96	1.081	-0.2090
9.01	1.084	-0.2205
9.97	1.050	-0.2249
10.97	1.084	-0.2329
10.83	1.122	-0.2177
9.66	1.096	-0.2100
8.74	1.092	-0.1982
7.69	1.175	-0.1809
6.81	1.260	-0.1041
5.76	1.196	-0.1067
4.78	1.141	-0.1121
3.68	1.078	-0.1183
2.79	1.011	-0.1206
1.85	0.960	-0.1270
0.81	0.923	-0.1362
-0.31	0.729	-0.1266
-1.30	0.646	-0.1252
-2.42	0.546	-0.1229
-3.37	0.466	-0.1230
-4.53	0.362	-0.1223
-5.46	0.283	-0.1260
-6.40	0.217	-0.1341

-7.55	0.141	-0.1451
-8.49	0.058	-0.1482
-9.59	-0.038	-0.1524

Run: 07152gw
Re = 199821.3

α	C_l	C_m
-10.24	-0.065	-0.1656
-9.42	0.004	-0.1644
-8.20	0.109	-0.1634
-7.30	0.195	-0.1627
-6.29	0.272	-0.1594
-5.15	0.384	-0.1594
-4.09	0.457	-0.1534
-3.13	0.547	-0.1527
-2.02	0.636	-0.1482
-1.13	0.750	-0.1527
0.01	0.868	-0.1515
0.88	0.908	-0.1437
2.06	0.985	-0.1367
2.97	1.047	-0.1324
4.09	1.131	-0.1281
4.99	1.191	-0.1232
6.04	1.276	-0.1205
7.04	1.342	-0.1166
8.10	1.405	-0.1133
9.03	1.174	-0.2233
9.99	1.142	-0.2294
10.95	1.112	-0.2284
10.61	1.099	-0.2205
9.73	1.149	-0.2212
8.66	1.190	-0.2100
7.77	1.385	-0.1079
6.80	1.319	-0.1107
5.70	1.246	-0.1151
4.84	1.178	-0.1177
3.79	1.109	-0.1226
2.72	1.029	-0.1266
1.67	0.960	-0.1323
0.63	0.897	-0.1386
-0.35	0.887	-0.1527
-1.45	0.712	-0.1440
-2.26	0.627	-0.1440
-3.44	0.520	-0.1477
-4.37	0.441	-0.1505
-5.48	0.350	-0.1545
-6.58	0.261	-0.1562
-7.54	0.169	-0.1565
-8.58	0.082	-0.1595
-9.56	-0.006	-0.1603

Run: 07150gw
Re = 400167.6

α	C_l	C_m
-10.18	-0.001	-0.1750
-9.24	0.091	-0.1764
-8.19	0.183	-0.1759
-7.34	0.250	-0.1733
-6.26	0.357	-0.1741
-5.17	0.440	-0.1729
-4.09	0.515	-0.1669
-3.08	0.630	-0.1696
-2.16	0.777	-0.1782
-1.06	0.913	-0.1732
-0.10	0.933	-0.1643
0.97	0.988	-0.1556
2.03	1.049	-0.1479
3.07	1.124	-0.1427
3.96	1.188	-0.1376
5.11	1.260	-0.1305
6.16	1.332	-0.1256
7.17	1.401	-0.1211
8.15	1.462	-0.1152
9.12	1.509	-0.1111
10.10	1.533	-0.1077
9.82	1.532	-0.1057
8.82	1.496	-0.1094
7.88	1.435	-0.1151
6.77	1.373	-0.1207
5.71	1.305	-0.1257
4.74	1.239	-0.1310
3.70	1.162	-0.1363
2.83	1.112	-0.1419
1.80	1.040	-0.1477
0.71	0.972	-0.1554
-0.38	0.914	-0.1627
-1.26	0.923	-0.1760
-2.26	0.765	-0.1758
-3.43	0.582	-0.1653
-4.48	0.510	-0.1705
-5.46	0.414	-0.1715
-6.50	0.339	-0.1731
-7.43	0.249	-0.1732
-8.59	0.144	-0.1744
-9.65	0.048	-0.1752

W1011 (30%) **fp25**
Fig. 6.164

Run: 07156sn
Re = 99951.4

α	C_l	C_m
-10.22	0.012	-0.1668
-9.36	0.079	-0.1644
-8.32	0.169	-0.1628
-7.29	0.246	-0.1555
-6.28	0.319	-0.1469
-5.07	0.443	-0.1475
-4.19	0.540	-0.1483
-3.04	0.674	-0.1527
-2.16	0.752	-0.1543
-1.10	0.869	-0.1577
-0.08	0.960	-0.1561
0.94	1.016	-0.1467
2.06	1.089	-0.1414
3.08	1.154	-0.1367
4.14	1.227	-0.1336
5.17	1.291	-0.1293
6.21	1.343	-0.1258
7.02	1.389	-0.1409
8.01	1.161	-0.2270
8.86	1.160	-0.2343
10.00	1.188	-0.2437
10.92	1.152	-0.2484
11.84	1.164	-0.2475
11.67	1.167	-0.2355
10.69	1.165	-0.2325
9.64	1.171	-0.2240
8.66	1.170	-0.2179
7.63	1.171	-0.2026
6.88	1.390	-0.1178
5.78	1.325	-0.1192
4.74	1.265	-0.1228
3.73	1.198	-0.1265
2.78	1.141	-0.1311
1.87	1.077	-0.1348
0.70	1.008	-0.1413
-0.24	0.937	-0.1445
-1.32	0.844	-0.1470
-2.30	0.742	-0.1438
-3.29	0.635	-0.1402
-4.48	0.510	-0.1364
-5.47	0.411	-0.1350
-6.59	0.313	-0.1383
-7.51	0.238	-0.1496
-8.58	0.152	-0.1584
-9.55	0.066	-0.1626

Run: 07157sn
Re = 199952.6

α	C_l	C_m
-10.32	0.026	-0.1771
-9.32	0.118	-0.1769
-8.24	0.216	-0.1772
-7.13	0.312	-0.1758
-6.14	0.412	-0.1757
-5.24	0.490	-0.1734
-4.09	0.597	-0.1714
-3.06	0.695	-0.1707
-2.02	0.779	-0.1664
-1.07	0.882	-0.1655
-0.09	0.933	-0.1572
1.04	1.008	-0.1510
2.10	1.083	-0.1457
3.08	1.155	-0.1424
3.96	1.218	-0.1396
5.09	1.295	-0.1351
6.17	1.362	-0.1314
7.09	1.428	-0.1289
7.84	1.394	-0.2128
9.01	1.188	-0.2381
9.98	1.210	-0.2503
9.78	1.235	-0.2429
8.65	1.225	-0.2323
7.99	1.473	-0.1206
6.86	1.404	-0.1241
5.77	1.336	-0.1272
4.86	1.274	-0.1305
3.68	1.197	-0.1352
2.83	1.135	-0.1376
1.68	1.059	-0.1428
0.67	0.983	-0.1475
-0.41	0.927	-0.1558
-1.35	0.837	-0.1578
-2.24	0.758	-0.1607
-3.43	0.644	-0.1625
-4.50	0.554	-0.1653
-5.43	0.466	-0.1674
-6.26	0.385	-0.1681
-7.42	0.285	-0.1701
-8.55	0.178	-0.1707
-9.44	0.108	-0.1719

Run: 07159sn
Re = 400077.2

α	C_l	C_m
-10.17	0.095	-0.1863
-9.37	0.170	-0.1875
-8.18	0.277	-0.1876
-7.33	0.350	-0.1853
-6.13	0.440	-0.1850
-5.24	0.526	-0.1845
-4.15	0.620	-0.1820
-3.21	0.718	-0.1825
-2.00	0.909	-0.1962
-1.07	0.876	-0.1705
-0.06	0.943	-0.1631
1.00	1.015	-0.1580
1.92	1.085	-0.1532
2.96	1.174	-0.1502
4.02	1.251	-0.1451
5.03	1.336	-0.1428
6.15	1.432	-0.1407
7.19	1.507	-0.1356
8.22	1.556	-0.1295
9.09	1.598	-0.1260
8.79	1.388	-0.2266
9.34	1.346	-0.2383
9.54	1.623	-0.1246
7.80	1.531	-0.1309
6.87	1.471	-0.1339
5.81	1.401	-0.1391
4.75	1.316	-0.1415
3.83	1.241	-0.1435
2.88	1.169	-0.1479
1.85	1.080	-0.1512
0.69	0.991	-0.1570
-0.38	0.918	-0.1629
-1.29	0.877	-0.1713
-2.38	0.821	-0.1818
-3.38	0.703	-0.1790
-4.46	0.589	-0.1787
-5.50	0.503	-0.1820
-6.36	0.429	-0.1829
-7.42	0.345	-0.1840
-8.60	0.237	-0.1839
-9.56	0.149	-0.1848

W1011 (30%) fp30

Fig. 6.167

Run: 07165sn
Re = 99984.9

α	C_l	C_m
-10.23	0.156	-0.1962
-9.34	0.224	-0.1937
-8.29	0.263	-0.1787
-7.06	0.293	-0.1541
-6.10	0.389	-0.1575
-5.28	0.485	-0.1624
-4.09	0.609	-0.1667
-3.16	0.709	-0.1699
-2.02	0.832	-0.1757
-1.12	0.898	-0.1695
-0.01	0.969	-0.1611
0.91	1.038	-0.1594
2.13	1.108	-0.1522
3.13	1.176	-0.1512
4.15	1.239	-0.1470
5.17	1.300	-0.1437
6.07	1.349	-0.1394
7.01	1.208	-0.2317
7.91	1.187	-0.2477
8.99	1.145	-0.2494
10.01	1.161	-0.2585
9.62	1.214	-0.2505
8.64	1.161	-0.2342
7.67	1.198	-0.2266
6.85	1.258	-0.2053
5.90	1.374	-0.1329
4.79	1.325	-0.1377
3.72	1.261	-0.1398
2.83	1.195	-0.1406
1.70	1.116	-0.1441
0.71	1.047	-0.1494
-0.32	0.994	-0.1553
-1.29	0.914	-0.1598
-2.38	0.821	-0.1583
-3.35	0.711	-0.1558
-4.46	0.599	-0.1519
-5.45	0.502	-0.1480
-6.31	0.403	-0.1424
-7.36	0.309	-0.1434
-8.47	0.274	-0.1610
-9.55	0.213	-0.1763

Run: 07163sn
Re = 200000.9

α	C_l	C_m
-10.19	0.210	-0.2013
-9.19	0.299	-0.2028
-8.28	0.374	-0.2022
-7.28	0.451	-0.1993
-6.16	0.546	-0.1968
-5.12	0.653	-0.1957
-4.16	0.721	-0.1910
-3.07	0.811	-0.1866
-2.01	0.843	-0.1731
-1.01	0.953	-0.1735
-0.12	1.008	-0.1679
1.04	1.097	-0.1641
1.98	1.173	-0.1616
2.97	1.259	-0.1605
4.08	1.332	-0.1552
5.19	1.398	-0.1500
6.22	1.460	-0.1449

7.28	1.512	-0.1411
7.96	1.283	-0.2463
8.92	1.257	-0.2556
9.95	1.221	-0.2576
9.63	1.236	-0.2524
8.77	1.261	-0.2480
7.67	1.348	-0.2371
6.80	1.492	-0.1366
5.69	1.442	-0.1442
4.90	1.386	-0.1464
3.72	1.307	-0.1495
2.78	1.250	-0.1555
1.70	1.158	-0.1569
0.70	1.076	-0.1596
-0.35	0.987	-0.1611
-1.33	0.919	-0.1658
-2.25	0.838	-0.1699
-3.38	0.782	-0.1813
-4.31	0.705	-0.1840
-5.34	0.622	-0.1868
-6.31	0.531	-0.1893
-7.51	0.435	-0.1927
-8.52	0.338	-0.1923
-9.53	0.256	-0.1936

Run: 07161sn
Re = 399750.6

α	C_l	C_m
-10.27	0.198	-0.2029
-9.41	0.263	-0.1993
-8.33	0.354	-0.2000
-7.15	0.449	-0.1990
-6.11	0.531	-0.1963
-5.09	0.625	-0.1956
-4.08	0.719	-0.1943
-3.01	0.805	-0.1903
-2.02	0.901	-0.1889
-1.05	0.946	-0.1800
-0.14	1.019	-0.1759
1.03	1.115	-0.1722
1.87	1.179	-0.1684
2.90	1.269	-0.1650
4.11	1.358	-0.1602
5.08	1.437	-0.1570
6.17	1.510	-0.1511
6.98	1.566	-0.1467
8.07	1.631	-0.1431
8.12	1.442	-0.2353
8.36	1.418	-0.2421
7.89	1.612	-0.1413
6.80	1.550	-0.1463
5.86	1.493	-0.1513
4.84	1.416	-0.1547
3.71	1.332	-0.1599
2.80	1.258	-0.1641
1.69	1.172	-0.1683
0.64	1.087	-0.1725
-0.27	1.006	-0.1751
-1.29	0.926	-0.1777
-2.44	0.883	-0.1909
-3.50	0.761	-0.1882
-4.36	0.693	-0.1917
-5.44	0.622	-0.1977
-6.52	0.500	-0.1947
-7.53	0.415	-0.1984
-8.62	0.335	-0.1988
-9.55	0.250	-0.1985

W1011 (30%) **fp35**

Fig. 6.169

Run: 07167sn
Re = 99916.4

α	C_l	C_m
-10.37	0.254	-0.2000
-9.21	0.235	-0.1646
-8.18	0.332	-0.1663
-7.24	0.419	-0.1691
-6.09	0.552	-0.1775
-5.24	0.644	-0.1822
-4.12	0.739	-0.1821
-3.20	0.835	-0.1873
-2.15	0.928	-0.1906
-1.05	1.020	-0.1916
-0.11	1.074	-0.1840
0.92	1.148	-0.1814
2.11	1.235	-0.1761
3.11	1.290	-0.1690
4.19	1.372	-0.1647
5.13	1.415	-0.1559
6.10	1.464	-0.1668
7.03	1.243	-0.2525
8.00	1.255	-0.2620
8.99	1.244	-0.2701
9.88	1.222	-0.2738
9.63	1.238	-0.2596
8.63	1.258	-0.2538
7.63	1.232	-0.2396
6.62	1.274	-0.2241
5.85	1.474	-0.1442
4.81	1.436	-0.1506
3.92	1.384	-0.1529
2.86	1.311	-0.1555
1.76	1.205	-0.1546
0.74	1.139	-0.1595
-0.15	1.072	-0.1611
-1.18	1.012	-0.1680
-2.35	0.916	-0.1699
-3.37	0.816	-0.1650
-4.25	0.743	-0.1641
-5.36	0.638	-0.1592
-6.47	0.515	-0.1491
-7.34	0.422	-0.1445
-8.28	0.347	-0.1511
-9.38	0.263	-0.1510

Run: 07168sn
Re = 199975.6

α	C_l	C_m
-10.18	0.314	-0.2149
-9.30	0.402	-0.2170
-8.16	0.490	-0.2145
-7.09	0.589	-0.2131
-6.24	0.664	-0.2113
-5.08	0.746	-0.2053
-4.06	0.830	-0.2013
-3.20	0.900	-0.1980
-2.07	0.921	-0.1811
-1.10	1.046	-0.1866
0.04	1.122	-0.1811
0.94	1.201	-0.1808
2.03	1.277	-0.1761
3.14	1.365	-0.1751
4.17	1.437	-0.1712
5.09	1.493	-0.1687
6.01	1.533	-0.1621
6.79	1.458	-0.2399
7.93	1.292	-0.2615
7.71	1.296	-0.2519
7.05	1.583	-0.1516
5.79	1.526	-0.1577
4.65	1.469	-0.1644
3.71	1.408	-0.1668
2.67	1.331	-0.1698
1.70	1.256	-0.1715
0.85	1.186	-0.1728
-0.35	1.107	-0.1782
-1.31	1.018	-0.1782
-2.14	0.930	-0.1783
-3.34	0.883	-0.1915
-4.45	0.799	-0.1958
-5.40	0.726	-0.2009
-6.35	0.639	-0.2035
-7.46	0.547	-0.2070
-8.34	0.474	-0.2091
-9.40	0.392	-0.2120

Run: 07169sn
Re = 400013.9

α	C_l	C_m
-10.22	0.331	-0.2189
-9.37	0.396	-0.2183
-8.32	0.467	-0.2156
-7.14	0.571	-0.2142
-6.27	0.631	-0.2090
-5.09	0.740	-0.2085
-4.12	0.820	-0.2067
-3.02	0.895	-0.1999
-2.07	0.958	-0.1933
-1.06	1.046	-0.1918
-0.15	1.111	-0.1869
0.86	1.188	-0.1833
2.03	1.285	-0.1794
2.89	1.352	-0.1765
4.03	1.434	-0.1720
4.94	1.501	-0.1672
6.05	1.601	-0.1661
7.13	1.660	-0.1595
8.12	1.704	-0.1529
7.91	1.698	-0.1528
6.88	1.644	-0.1577
5.76	1.578	-0.1635
4.86	1.509	-0.1677
3.78	1.433	-0.1727
2.82	1.352	-0.1757
1.87	1.280	-0.1807
0.66	1.183	-0.1841
-0.22	1.108	-0.1857
-1.42	1.012	-0.1898
-2.39	0.930	-0.1916
-3.47	0.870	-0.2018
-4.46	0.792	-0.2052
-5.51	0.708	-0.2091
-6.38	0.639	-0.2113
-7.50	0.544	-0.2140
-8.43	0.459	-0.2141
-9.46	0.383	-0.2144

W1011 (30%) fp40

Fig. 6.171

Run: 07170sn
Re = 99924.6

α	C_l	C_m
-10.14	0.263	-0.1808
-9.26	0.292	-0.1698
-8.18	0.417	-0.1799
-7.23	0.515	-0.1854
-6.15	0.646	-0.1945
-5.12	0.738	-0.1975
-4.14	0.815	-0.2003
-3.10	0.914	-0.2007
-1.97	1.020	-0.2036
-0.96	1.094	-0.1988
0.04	1.155	-0.1939
1.06	1.223	-0.1885
2.05	1.299	-0.1863
3.11	1.370	-0.1812
4.15	1.411	-0.1709
5.17	1.449	-0.1650
5.96	1.289	-0.2455
6.93	1.262	-0.2617
6.71	1.270	-0.2454
5.82	1.282	-0.2213
4.75	1.457	-0.1613
3.91	1.422	-0.1649
2.86	1.374	-0.1709
1.85	1.297	-0.1716
0.71	1.213	-0.1729
-0.16	1.160	-0.1743
-1.25	1.093	-0.1761
-2.29	1.012	-0.1784
-3.23	0.915	-0.1734
-4.29	0.828	-0.1733
-5.40	0.727	-0.1702
-6.32	0.649	-0.1685
-7.45	0.515	-0.1602
-8.30	0.420	-0.1558
-9.39	0.306	-0.1437

Run: 07171sn
Re = 199942.0

α	C_l	C_m
-10.26	0.444	-0.2325
-9.21	0.537	-0.2311
-8.28	0.615	-0.2306
-7.18	0.700	-0.2266
-6.23	0.762	-0.2192
-5.22	0.836	-0.2137
-4.15	0.904	-0.2064
-3.01	0.998	-0.2041
-2.11	1.061	-0.2001
-1.05	1.137	-0.1966
-0.00	1.225	-0.1944
1.03	1.303	-0.1918
2.03	1.379	-0.1894
3.11	1.454	-0.1868
4.01	1.511	-0.1838
5.12	1.561	-0.1767
6.04	1.610	-0.1717
6.91	1.374	-0.2630
7.97	1.314	-0.2725
7.77	1.311	-0.2633
6.69	1.355	-0.2494
5.86	1.613	-0.1690
4.95	1.569	-0.1726
3.88	1.499	-0.1752
2.91	1.440	-0.1790
1.74	1.352	-0.1822
0.74	1.287	-0.1867
-0.32	1.208	-0.1898
-1.35	1.128	-0.1926
-2.27	1.042	-0.1924
-3.25	0.992	-0.2009
-4.34	0.900	-0.2018
-5.29	0.831	-0.2078
-6.47	0.748	-0.2153
-7.39	0.690	-0.2223
-8.45	0.594	-0.2242
-9.49	0.501	-0.2248

Run: 07172sn
Re = 399747.3

α	C_l	C_m
-10.41	0.416	-0.2308
-9.30	0.507	-0.2309
-8.25	0.595	-0.2297
-7.15	0.685	-0.2275
-6.21	0.768	-0.2263
-5.23	0.853	-0.2244
-4.06	0.939	-0.2192
-3.12	1.005	-0.2142
-2.12	1.067	-0.2072
-0.93	1.172	-0.2066
-0.04	1.238	-0.2025
0.94	1.312	-0.1986
1.89	1.390	-0.1954
3.14	1.470	-0.1881
4.18	1.533	-0.1805
4.92	1.601	-0.1799
6.20	1.680	-0.1723
7.02	1.727	-0.1684
7.17	1.515	-0.2556
7.39	1.482	-0.2613
7.28	1.745	-0.1666
6.00	1.664	-0.1708
4.81	1.598	-0.1784
3.77	1.522	-0.1835
2.69	1.442	-0.1875
1.81	1.381	-0.1932
0.77	1.298	-0.1964
-0.29	1.217	-0.2006
-1.41	1.126	-0.2037
-2.40	1.031	-0.2025
-3.44	0.982	-0.2142

-4.46	0.903	-0.2181
-5.37	0.837	-0.2212
-6.53	0.748	-0.2251
-7.57	0.648	-0.2257
-8.56	0.582	-0.2298
-9.59	0.489	-0.2304

W1011 (30%) **fp45**

Fig. 6.173

Run: 07173gw

Re = 99963.0

α	C_l	C_m
-10.30	0.328	-0.1774
-9.17	0.415	-0.1753
-8.09	0.547	-0.1900
-7.22	0.638	-0.1969
-6.12	0.753	-0.2033
-5.12	0.829	-0.2042
-4.00	0.923	-0.2029
-3.00	1.016	-0.2087
-2.04	1.109	-0.2094
-0.97	1.196	-0.2041
0.03	1.263	-0.2000
1.09	1.333	-0.1950
2.07	1.418	-0.1921
3.20	1.482	-0.1851
4.14	1.532	-0.1760
5.14	1.552	-0.1827
6.03	1.341	-0.2552
7.05	1.303	-0.2696
6.76	1.321	-0.2550
5.62	1.418	-0.2324
4.92	1.588	-0.1641
3.95	1.566	-0.1711
2.78	1.500	-0.1757
1.95	1.429	-0.1733
0.75	1.345	-0.1809
-0.23	1.277	-0.1831
-1.23	1.214	-0.1888
-2.19	1.124	-0.1887
-3.26	1.018	-0.1863
-4.42	0.915	-0.1836
-5.36	0.842	-0.1825
-6.34	0.746	-0.1788
-7.40	0.655	-0.1742
-8.39	0.534	-0.1643
-9.36	0.441	-0.1588

Run: 07174gw

Re = 200000.2

α	C_l	C_m
-10.17	0.584	-0.2453
-9.20	0.657	-0.2419
-8.19	0.716	-0.2352
-7.10	0.777	-0.2238
-6.10	0.846	-0.2193
-5.11	0.915	-0.2142
-4.03	1.009	-0.2132
-3.10	1.076	-0.2081
-2.09	1.154	-0.2063
-0.94	1.247	-0.2050
0.02	1.334	-0.2047
1.03	1.401	-0.2005
2.11	1.478	-0.1978
3.10	1.528	-0.1931
4.11	1.592	-0.1887
5.16	1.646	-0.1824
6.04	1.438	-0.2552
6.95	1.412	-0.2736
7.94	1.338	-0.2767
7.75	1.358	-0.2714
6.74	1.381	-0.2585
6.02	1.674	-0.1696
4.94	1.638	-0.1781
3.85	1.587	-0.1844
2.97	1.534	-0.1882
1.76	1.459	-0.1925
0.82	1.385	-0.1951
-0.28	1.311	-0.1993
-1.28	1.230	-0.1999
-2.24	1.161	-0.2028
-3.30	1.069	-0.2041
-4.42	0.997	-0.2104
-5.38	0.911	-0.2114
-6.36	0.833	-0.2128
-7.35	0.758	-0.2177
-8.37	0.716	-0.2328
-9.45	0.638	-0.2368

Run: 07175gw

Re = 399797.3

α	C_l	C_m
-10.33	0.547	-0.2464
-9.17	0.635	-0.2438
-8.16	0.724	-0.2445
-7.24	0.797	-0.2420
-6.16	0.886	-0.2394
-5.15	0.966	-0.2374
-4.03	1.041	-0.2304
-3.06	1.101	-0.2237
-2.05	1.184	-0.2220
-0.90	1.269	-0.2169
-0.02	1.341	-0.2150
1.12	1.430	-0.2116
2.03	1.483	-0.2041
3.04	1.549	-0.1993
4.04	1.618	-0.1944
5.22	1.696	-0.1883
6.17	1.741	-0.1823
6.58	1.525	-0.2574
6.42	1.569	-0.2447
6.06	1.749	-0.1822
4.83	1.667	-0.1872
3.84	1.599	-0.1917
2.83	1.538	-0.1986
1.66	1.471	-0.2066
0.67	1.400	-0.2115
-0.27	1.324	-0.2146
-1.34	1.244	-0.2187
-2.33	1.173	-0.2225
-3.30	1.096	-0.2256
-4.34	1.029	-0.2317
-5.39	0.941	-0.2352
-6.52	0.855	-0.2371
-7.44	0.785	-0.2414
-8.41	0.702	-0.2415
-9.57	0.609	-0.2441

W1011 (30%) **fp50**

Fig. 6.175

Run: 07176gw

Re = 100034.6

α	C_l	C_m
-10.19	0.433	-0.1788
-9.12	0.566	-0.1951
-8.18	0.669	-0.2005
-7.20	0.780	-0.2058
-6.16	0.850	-0.2047
-5.16	0.945	-0.2068
-4.00	1.046	-0.2087
-3.02	1.129	-0.2088
-2.03	1.221	-0.2112
-1.05	1.294	-0.2068
0.02	1.368	-0.2025
1.12	1.447	-0.1983
2.05	1.520	-0.1948
3.21	1.585	-0.1900
4.10	1.619	-0.1823
5.07	1.420	-0.2445
5.97	1.387	-0.2652
7.05	1.344	-0.2731
6.78	1.384	-0.2603

5.73	1.396	-0.2455
4.87	1.504	-0.2179
3.93	1.630	-0.1765
2.76	1.580	-0.1831
1.91	1.502	-0.1834
0.89	1.435	-0.1882
-0.22	1.375	-0.1931
-1.22	1.292	-0.1926
-2.27	1.206	-0.1966
-3.35	1.118	-0.1960
-4.34	1.039	-0.1964
-5.35	0.934	-0.1907
-6.35	0.836	-0.1876
-7.36	0.754	-0.1856
-8.42	0.644	-0.1777
-9.46	0.543	-0.1726

Run: 07177gw
Re = 199897.4

α	C_l	C_m
-10.27	0.659	-0.2472
-9.24	0.668	-0.2234
-8.12	0.750	-0.2208
-7.22	0.837	-0.2219
-6.09	0.912	-0.2178
-5.04	0.999	-0.2180
-4.06	1.076	-0.2165
-3.00	1.160	-0.2145
-2.09	1.218	-0.2106
-1.03	1.288	-0.2054
0.03	1.382	-0.2062
1.08	1.452	-0.2036
2.13	1.526	-0.1988
3.05	1.577	-0.1962
4.17	1.652	-0.1921
5.08	1.564	-0.2281
6.02	1.457	-0.2613
6.92	1.388	-0.2757
6.73	1.401	-0.2670
5.66	1.493	-0.2497
4.92	1.680	-0.1800
3.83	1.625	-0.1858
2.91	1.584	-0.1919
1.72	1.495	-0.1922
0.80	1.437	-0.1968
-0.17	1.367	-0.1997
-1.26	1.292	-0.2021
-2.24	1.218	-0.2057
-3.30	1.133	-0.2077
-4.36	1.070	-0.2128
-5.28	0.984	-0.2121
-6.37	0.896	-0.2132
-7.37	0.823	-0.2168
-8.33	0.741	-0.2167
-9.40	0.670	-0.2208

Run: 07178gw
Re = 399768.9

α	C_l	C_m
-10.18	0.666	-0.2550
-9.17	0.752	-0.2557
-8.29	0.810	-0.2509
-7.09	0.898	-0.2475
-6.12	0.973	-0.2460
-5.06	1.057	-0.2426
-4.12	1.123	-0.2376
-3.06	1.199	-0.2341
-1.99	1.265	-0.2267
-0.92	1.346	-0.2239
-0.08	1.398	-0.2164
0.97	1.474	-0.2128
2.12	1.556	-0.2082
3.17	1.623	-0.2038
4.12	1.684	-0.1980
5.05	1.751	-0.1948
6.06	1.801	-0.1873
5.97	1.807	-0.1880
4.82	1.732	-0.1928
3.82	1.669	-0.1984
2.85	1.605	-0.2029
1.73	1.534	-0.2084
0.80	1.468	-0.2133
-0.12	1.410	-0.2181
-1.23	1.321	-0.2212
-2.30	1.242	-0.2265
-3.40	1.173	-0.2333
-4.31	1.108	-0.2369
-5.49	1.020	-0.2404
-6.44	0.943	-0.2424
-7.53	0.865	-0.2481
-8.44	0.800	-0.2502
-9.55	0.711	-0.2516

W1011 (30%) **fp55**

Fig. 6.177

Run: 07179gw
Re = 100076.3

α	C_l	C_m
-10.08	0.557	-0.1945
-9.10	0.634	-0.1987
-8.16	0.738	-0.2062
-7.05	0.846	-0.2084
-6.07	0.925	-0.2105
-5.04	1.004	-0.2079
-4.02	1.095	-0.2101
-2.98	1.191	-0.2144
-2.06	1.268	-0.2124
-0.96	1.356	-0.2075
0.08	1.403	-0.2033
1.04	1.484	-0.2029
2.17	1.552	-0.1947
3.14	1.596	-0.1873
4.19	1.637	-0.1820
5.05	1.510	-0.2592
6.02	1.403	-0.2692
5.86	1.388	-0.2567
4.73	1.499	-0.2277
3.92	1.652	-0.1757
2.77	1.591	-0.1789
1.97	1.539	-0.1843
0.84	1.473	-0.1877
-0.14	1.408	-0.1885
-1.25	1.341	-0.1912
-2.14	1.265	-0.1922
-3.28	1.176	-0.1938
-4.33	1.078	-0.1962
-5.24	0.993	-0.1932
-6.26	0.894	-0.1899
-7.44	0.789	-0.1853
-8.38	0.719	-0.1843
-9.43	0.606	-0.1758

Run: 07180gw
Re = 200011.8

α	C_l	C_m
-10.18	0.619	-0.2130
-9.19	0.703	-0.2130
-8.15	0.802	-0.2178
-7.21	0.869	-0.2175
-6.14	0.958	-0.2170
-5.10	1.040	-0.2160
-4.09	1.125	-0.2162
-3.10	1.203	-0.2147
-2.05	1.277	-0.2126
-0.96	1.348	-0.2062
0.06	1.426	-0.2055
0.97	1.489	-0.2039
2.10	1.552	-0.1985
3.10	1.620	-0.1971
4.14	1.677	-0.1909
5.13	1.536	-0.2489
6.01	1.475	-0.2710
5.80	1.425	-0.2581
4.87	1.560	-0.2251
3.89	1.667	-0.1866
2.90	1.608	-0.1897
1.93	1.552	-0.1945

0.80	1.480	-0.1979
-0.15	1.410	-0.2000
-1.22	1.335	-0.2029
-2.21	1.258	-0.2044
-3.19	1.195	-0.2087
-4.30	1.113	-0.2103
-5.31	1.033	-0.2109
-6.25	0.950	-0.2100
-7.36	0.869	-0.2137
-8.32	0.786	-0.2109
-9.40	0.692	-0.2082

Run: 07181gw
Re = 399741.2

α	C_l	C_m
-10.29	0.730	-0.2562
-9.17	0.813	-0.2548
-8.21	0.888	-0.2538
-7.23	0.969	-0.2531
-6.19	1.040	-0.2493
-5.05	1.118	-0.2429
-4.04	1.185	-0.2397
-3.06	1.252	-0.2336
-2.03	1.318	-0.2277
-1.02	1.379	-0.2217
0.06	1.463	-0.2179
0.98	1.521	-0.2147
2.12	1.598	-0.2081
3.13	1.669	-0.2050
4.17	1.742	-0.1987
5.19	1.802	-0.1936
5.74	1.618	-0.2514
5.58	1.627	-0.2460
4.88	1.780	-0.1933
3.92	1.729	-0.1999
2.83	1.649	-0.2018
1.75	1.584	-0.2094
0.75	1.509	-0.2134
-0.19	1.443	-0.2159
-1.30	1.368	-0.2224
-2.26	1.304	-0.2260
-3.24	1.242	-0.2345
-4.39	1.173	-0.2402
-5.41	1.096	-0.2429
-6.32	1.025	-0.2448
-7.45	0.950	-0.2511
-8.51	0.877	-0.2554
-9.45	0.799	-0.2562

W1011 (30%) **fp60**
Fig. 6.179

Run: 07182gw
Re = 100051.0

α	C_l	C_m
-10.27	0.567	-0.1930
-9.17	0.683	-0.2032
-8.06	0.791	-0.2081
-7.02	0.890	-0.2107
-6.14	0.972	-0.2130
-5.06	1.051	-0.2129
-3.95	1.156	-0.2146
-3.06	1.255	-0.2240
-1.96	1.326	-0.2147
-1.00	1.381	-0.2120
0.11	1.455	-0.2077
1.03	1.520	-0.2052
2.04	1.577	-0.2001
3.17	1.626	-0.1949
4.06	1.482	-0.2342
5.03	1.427	-0.2623
5.91	1.368	-0.2729
5.69	1.367	-0.2575
4.83	1.439	-0.2405
3.92	1.615	-0.1878
2.87	1.620	-0.1819
1.83	1.568	-0.1884
0.93	1.515	-0.1909
-0.16	1.445	-0.1933
-1.25	1.371	-0.1965
-2.23	1.319	-0.2024
-3.21	1.227	-0.2005
-4.34	1.142	-0.2005
-5.34	1.034	-0.1971
-6.44	0.945	-0.1943
-7.30	0.869	-0.1924
-8.27	0.769	-0.1885
-9.38	0.669	-0.1835

Run: 07183gw
Re = 199976.7

α	C_l	C_m
-10.22	0.665	-0.2166
-9.08	0.767	-0.2212
-8.11	0.852	-0.2226
-7.17	0.924	-0.2238
-6.08	1.003	-0.2197
-5.09	1.095	-0.2224
-4.01	1.187	-0.2226
-3.09	1.240	-0.2172
-1.96	1.327	-0.2163
-1.00	1.379	-0.2084
0.06	1.456	-0.2063
1.00	1.518	-0.2049
2.17	1.588	-0.2019
3.07	1.654	-0.2013
4.08	1.716	-0.1968
5.13	1.548	-0.2602
6.01	1.436	-0.2753
5.66	1.442	-0.2649
4.80	1.580	-0.2466
3.95	1.705	-0.1909
2.90	1.630	-0.1914
1.81	1.569	-0.1991
0.71	1.489	-0.1956
-0.22	1.440	-0.2022
-1.18	1.384	-0.2069
-2.18	1.298	-0.2050
-3.16	1.245	-0.2119
-4.38	1.165	-0.2164
-5.24	1.073	-0.2135
-6.38	0.975	-0.2120
-7.33	0.902	-0.2143
-8.42	0.822	-0.2153
-9.37	0.742	-0.2125

Run: 07184gw
Re = 399808.1

α	C_l	C_m
-10.21	0.807	-0.2680
-9.26	0.871	-0.2657
-8.18	0.949	-0.2621
-7.06	1.036	-0.2601
-6.07	1.103	-0.2554
-5.08	1.175	-0.2510
-3.95	1.221	-0.2398
-2.99	1.276	-0.2317
-2.08	1.343	-0.2296
-0.90	1.424	-0.2248
0.03	1.485	-0.2185
1.09	1.565	-0.2172
2.12	1.632	-0.2115
3.16	1.697	-0.2060
4.16	1.759	-0.2001
5.01	1.803	-0.1950
4.82	1.788	-0.1943
3.80	1.736	-0.2011
2.88	1.684	-0.2065
1.92	1.607	-0.2086
0.70	1.541	-0.2159
-0.17	1.469	-0.2171
-1.25	1.403	-0.2247
-2.36	1.326	-0.2287
-3.25	1.266	-0.2329

-4.44	1.211	-0.2467
-5.37	1.143	-0.2467
-6.49	1.072	-0.2535
-7.44	1.003	-0.2571
-8.36	0.949	-0.2624
-9.55	0.850	-0.2627

W1011 (30%) **fp65**

Fig. 6.181

Run: 07185gw

Re = 100044.3

α	C_l	C_m
-10.09	0.619	-0.1903
-9.06	0.767	-0.2078
-8.17	0.809	-0.2051
-7.01	0.949	-0.2134
-5.99	0.996	-0.2069
-5.07	1.114	-0.2145
-3.96	1.200	-0.2150
-2.92	1.288	-0.2183
-1.90	1.358	-0.2164
-0.96	1.426	-0.2139
0.11	1.479	-0.2033
1.18	1.554	-0.2018
2.19	1.602	-0.1954
3.17	1.662	-0.1888
4.00	1.522	-0.2411
4.95	1.409	-0.2579
5.89	1.373	-0.2685
5.68	1.412	-0.2587
4.69	1.447	-0.2443
3.78	1.505	-0.2173
2.84	1.656	-0.1799
1.97	1.623	-0.1855
0.82	1.551	-0.1876
-0.26	1.498	-0.1940
-1.15	1.434	-0.1946
-2.28	1.375	-0.2013
-3.10	1.300	-0.2011
-4.28	1.202	-0.1988
-5.34	1.109	-0.1988
-6.36	1.033	-0.1981
-7.37	0.909	-0.1903
-8.25	0.845	-0.1912
-9.32	0.733	-0.1844

Run: 07186gw

Re = 199997.9

α	C_l	C_m
-10.17	0.698	-0.2103
-9.20	0.812	-0.2212
-8.11	0.861	-0.2135
-7.04	0.951	-0.2157
-6.08	1.024	-0.2137
-5.13	1.097	-0.2138
-3.95	1.189	-0.2145
-3.06	1.246	-0.2098
-2.08	1.320	-0.2101
-0.90	1.401	-0.2059
0.10	1.478	-0.2054
1.05	1.513	-0.1963
2.14	1.585	-0.1958
3.16	1.646	-0.1905
3.98	1.580	-0.2235
5.12	1.502	-0.2576
5.99	1.424	-0.2738
5.68	1.448	-0.2640
4.84	1.469	-0.2474
3.91	1.695	-0.1832
2.78	1.630	-0.1870
1.93	1.582	-0.1916
1.02	1.517	-0.1938
-0.25	1.434	-0.1951
-1.27	1.371	-0.1977
-2.31	1.310	-0.2036
-3.18	1.242	-0.2060
-4.36	1.167	-0.2102
-5.23	1.087	-0.2078
-6.29	1.009	-0.2088
-7.43	0.925	-0.2109
-8.38	0.853	-0.2102
-9.34	0.760	-0.2049

Run: 07187gw

Re = 400031.8

α	C_l	C_m
-10.15	0.859	-0.2634
-9.24	0.919	-0.2608
-8.18	0.993	-0.2573
-7.20	1.063	-0.2542
-6.10	1.124	-0.2472
-5.03	1.192	-0.2397
-4.03	1.235	-0.2313
-3.03	1.293	-0.2232
-1.99	1.366	-0.2196
-0.89	1.433	-0.2134
-0.03	1.503	-0.2130
1.14	1.575	-0.2072
2.05	1.641	-0.2049
3.16	1.701	-0.1977
4.10	1.765	-0.1944
4.85	1.636	-0.2368
5.22	1.812	-0.1854
3.82	1.747	-0.1943
2.96	1.696	-0.1980
1.83	1.627	-0.2034
0.71	1.553	-0.2095
-0.15	1.485	-0.2089
-1.33	1.420	-0.2172
-2.26	1.359	-0.2219
-3.34	1.277	-0.2235
-4.39	1.221	-0.2312
-5.40	1.147	-0.2348
-6.25	1.125	-0.2488
-7.37	1.042	-0.2508
-8.36	0.984	-0.2569
-9.42	0.908	-0.2601

W1015 (20%) **fp0**

Fig. 6.185

Run: 06996gw

Re = 99988.1

α	C_l	C_m
-10.23	-0.786	0.0386
-9.30	-0.914	-0.0074
-8.27	-0.855	-0.0028
-7.37	-0.791	-0.0002
-6.19	-0.703	0.0005
-5.18	-0.614	0.0030
-4.23	-0.531	0.0056
-3.10	-0.443	0.0111
-2.20	-0.359	0.0082
-1.16	-0.194	-0.0098
-0.06	-0.033	-0.0178
0.93	0.028	-0.0091
2.03	0.163	-0.0103
3.06	0.318	-0.0160
4.13	0.423	-0.0150
5.00	0.479	-0.0034
6.09	0.569	-0.0047
7.01	0.641	0.0007
8.04	0.717	0.0066
9.12	0.804	0.0160
10.21	0.868	0.0185
11.23	0.919	0.0215
12.11	0.970	0.0127
13.10	1.019	0.0172
13.97	0.608	-0.0849
14.96	0.629	-0.0900
16.05	0.673	-0.0965
17.06	0.692	-0.1128
17.99	0.673	-0.1180
19.07	0.703	-0.1292
19.84	0.707	-0.1432
19.62	0.709	-0.0964

18.76	0.689	-0.0881
17.72	0.661	-0.0765
16.69	0.663	-0.0791
15.78	0.636	-0.0724
14.79	0.611	-0.0695
13.66	0.596	-0.0639
12.62	0.574	-0.0554
11.73	0.577	-0.0486
10.96	0.903	0.0215
9.78	0.841	0.0132
8.75	0.776	0.0126
7.69	0.688	0.0109
6.84	0.630	0.0078
5.81	0.551	0.0046
4.80	0.473	-0.0008
3.69	0.409	-0.0083
2.69	0.277	0.0027
1.73	0.149	0.0118
0.64	0.048	0.0057
-0.51	-0.038	-0.0039
-1.41	-0.190	0.0123
-2.49	-0.346	0.0202
-3.60	-0.436	0.0120
-4.59	-0.521	0.0062
-5.60	-0.613	0.0017
-6.56	-0.697	-0.0016
-7.66	-0.782	-0.0074
-8.69	-0.852	-0.0122
-9.61	-0.908	0.0091

Run: 06998gw
Re = 200084.1

α	C_l	C_m
-10.38	-0.967	-0.0154
-9.24	-0.893	-0.0117
-8.21	-0.822	-0.0079
-7.40	-0.762	-0.0047
-6.25	-0.680	-0.0003
-5.33	-0.605	0.0035
-4.23	-0.510	0.0073
-3.15	-0.408	0.0066
-2.10	-0.236	-0.0111
-1.13	-0.137	-0.0086
-0.19	-0.051	-0.0043
0.89	0.055	-0.0015
2.02	0.161	0.0021
3.06	0.259	0.0046
4.08	0.393	-0.0044
5.04	0.495	-0.0082
6.12	0.597	-0.0063
7.02	0.675	-0.0033
8.20	0.771	0.0002
9.22	0.853	0.0032
10.25	0.932	0.0060
11.22	1.004	0.0089
12.22	1.066	0.0124
13.12	1.112	0.0157
14.28	1.151	0.0185
15.18	1.154	0.0065
16.19	1.128	-0.0145
16.94	0.683	-0.0912
17.94	0.683	-0.0976
17.66	0.706	-0.0939
16.64	0.644	-0.0798
15.62	0.677	-0.0836
14.79	0.661	-0.0821
13.77	0.619	-0.0745
12.74	0.638	-0.0763
11.77	0.652	-0.0668
10.98	0.978	0.0117
9.86	0.897	0.0085
8.80	0.819	0.0054
7.77	0.731	0.0023
6.85	0.659	-0.0006
5.72	0.560	-0.0040
4.68	0.461	-0.0048
3.65	0.340	0.0033
2.68	0.231	0.0073
1.56	0.131	0.0031
0.51	0.033	-0.0005
-0.53	-0.069	-0.0039
-1.40	-0.153	-0.0081
-2.54	-0.284	-0.0052
-3.42	-0.434	0.0078
-4.50	-0.531	0.0067
-5.62	-0.625	0.0023
-6.49	-0.692	-0.0014
-7.68	-0.787	-0.0063
-8.68	-0.863	-0.0100
-9.68	-0.931	-0.0136

Run: 07000gw
Re = 399875.2

α	C_l	C_m
-9.25	-0.929	-0.0134
-8.33	-0.857	-0.0100
-7.44	-0.782	-0.0064
-6.37	-0.693	-0.0022
-5.20	-0.592	0.0021
-4.29	-0.504	0.0035
-3.33	-0.343	-0.0104
-2.18	-0.233	-0.0087
-1.20	-0.137	-0.0065
-0.13	-0.035	-0.0038
0.88	0.058	-0.0019
1.95	0.165	-0.0003
2.99	0.270	0.0006
4.02	0.393	-0.0027
5.03	0.503	-0.0056
6.06	0.602	-0.0029
7.13	0.705	-0.0001
8.14	0.791	0.0028
9.13	0.879	0.0056
10.12	0.964	0.0084
11.26	1.051	0.0118
12.14	1.114	0.0145
13.22	1.183	0.0180
14.15	1.219	0.0197
15.27	1.199	-0.0059
16.15	1.171	-0.0215
17.18	1.127	-0.0357
18.06	1.085	-0.0420
17.88	1.101	-0.0401
16.89	1.130	-0.0308
15.84	1.180	-0.0177
14.97	1.212	0.0050
14.03	1.215	0.0203
13.00	1.170	0.0183
11.92	1.099	0.0151
10.99	1.038	0.0123
9.91	0.946	0.0092
8.93	0.859	0.0062
7.76	0.759	0.0030
6.75	0.670	0.0001
5.74	0.575	-0.0025
4.77	0.480	-0.0036
3.67	0.340	0.0030
2.70	0.243	0.0018
1.75	0.143	0.0008
0.53	0.027	-0.0011
-0.50	-0.069	-0.0033
-1.35	-0.150	-0.0053
-2.32	-0.247	-0.0079
-3.42	-0.366	-0.0076
-4.61	-0.536	0.0044
-5.60	-0.628	0.0016
-6.45	-0.700	-0.0019
-7.67	-0.801	-0.0074
-8.68	-0.886	-0.0118

W1015 (20%) **fp5**

Fig. 6.188

Run: 07008gw
Re = 100028.8

α	C_l	C_m
-10.35	-0.835	-0.0362
-9.28	-0.790	-0.0325

-8.24	-0.715	-0.0314
-7.19	-0.633	-0.0298
-6.21	-0.546	-0.0288
-5.14	-0.451	-0.0283
-4.21	-0.331	-0.0342
-3.32	-0.252	-0.0299
-2.05	-0.128	-0.0313
-1.06	-0.036	-0.0325
-0.04	0.153	-0.0510
1.02	0.263	-0.0448
1.98	0.342	-0.0377
2.91	0.442	-0.0407
4.02	0.543	-0.0429
4.98	0.627	-0.0419
5.98	0.710	-0.0405
7.13	0.796	-0.0371
8.02	0.860	-0.0341
9.07	0.927	-0.0295
10.07	0.983	-0.0254
11.25	1.050	-0.0222
12.21	1.094	-0.0196
13.10	1.130	-0.0165
13.93	0.713	-0.1220
15.05	0.723	-0.1248
15.97	0.732	-0.1272
16.94	0.709	-0.1302
17.84	0.747	-0.1429
17.76	0.805	-0.1384
16.72	0.752	-0.1202
15.75	0.787	-0.1177
14.69	0.726	-0.1063
13.60	0.682	-0.0988
12.64	0.666	-0.0934
11.79	0.705	-0.0956
10.80	0.658	-0.0828
9.77	0.986	-0.0188
8.77	0.927	-0.0230
7.73	0.852	-0.0263
6.70	0.781	-0.0297
5.86	0.716	-0.0321
4.65	0.610	-0.0340
3.74	0.527	-0.0343
2.67	0.425	-0.0319
1.63	0.318	-0.0306
0.62	0.241	-0.0399
-0.30	0.122	-0.0353
-1.44	-0.035	-0.0196
-2.54	-0.141	-0.0185
-3.40	-0.226	-0.0184
-4.43	-0.321	-0.0185
-5.57	-0.451	-0.0213
-6.62	-0.536	-0.0226
-7.63	-0.635	-0.0263
-8.52	-0.708	-0.0278
-9.66	-0.776	-0.0304

Run: 07009gw

Re = 200063.3

α	C_l	C_m
-10.39	-0.775	-0.0557
-9.32	-0.679	-0.0567
-8.22	-0.587	-0.0580
-7.22	-0.493	-0.0585
-6.16	-0.401	-0.0579
-5.15	-0.319	-0.0555
-4.13	-0.233	-0.0529
-3.11	-0.145	-0.0492
-2.22	-0.060	-0.0479
-1.09	0.090	-0.0538
-0.08	0.207	-0.0521
1.04	0.309	-0.0472
2.05	0.403	-0.0445
3.06	0.494	-0.0422
4.11	0.596	-0.0415
5.14	0.696	-0.0408
6.09	0.787	-0.0393
7.04	0.866	-0.0373
8.07	0.953	-0.0347
9.24	1.038	-0.0313
10.22	1.108	-0.0281
11.13	1.171	-0.0249
12.15	1.226	-0.0211
13.14	1.267	-0.0171
14.12	1.290	-0.0159
15.24	1.254	-0.0360
16.15	1.206	-0.0482
17.03	0.846	-0.1374
17.92	0.791	-0.1346
17.64	0.828	-0.1377
16.81	0.809	-0.1262
15.63	0.823	-0.1240
14.81	0.786	-0.1202
13.73	0.761	-0.1149
12.66	0.758	-0.1117
11.98	1.214	-0.0173
11.00	1.150	-0.0211
9.75	1.078	-0.0260
8.77	1.005	-0.0292
7.69	0.922	-0.0321
6.66	0.839	-0.0349
5.66	0.747	-0.0368
4.65	0.654	-0.0381
3.72	0.571	-0.0394
2.62	0.468	-0.0412
1.58	0.374	-0.0439
0.63	0.284	-0.0476
-0.42	0.182	-0.0499
-1.31	0.062	-0.0508
-2.33	-0.072	-0.0447
-3.54	-0.184	-0.0464
-4.56	-0.273	-0.0499
-5.57	-0.357	-0.0545
-6.64	-0.440	-0.0572
-7.66	-0.536	-0.0575
-8.45	-0.611	-0.0587
-9.55	-0.705	-0.0578

Run: 07011gw

Re = 400204.9

α	C_l	C_m
-10.27	-0.796	-0.0582
-9.25	-0.702	-0.0583
-8.41	-0.621	-0.0588
-7.24	-0.501	-0.0588
-6.29	-0.407	-0.0596
-5.29	-0.304	-0.0599
-4.13	-0.187	-0.0593
-3.14	-0.095	-0.0580
-2.12	0.016	-0.0574
-1.16	0.108	-0.0545
-0.19	0.199	-0.0511
0.86	0.297	-0.0496
2.03	0.410	-0.0473
3.03	0.504	-0.0449
3.98	0.594	-0.0430
5.06	0.696	-0.0409
6.17	0.802	-0.0389
7.12	0.883	-0.0366
8.16	0.977	-0.0338
9.05	1.057	-0.0311
10.10	1.136	-0.0276
11.21	1.217	-0.0234
12.30	1.289	-0.0197
13.30	1.335	-0.0159
14.25	1.333	-0.0261
15.17	1.286	-0.0447
16.18	1.259	-0.0614
17.16	1.198	-0.0702
16.86	1.194	-0.0658
15.83	1.238	-0.0548
14.84	1.303	-0.0416
13.91	1.341	-0.0176
12.84	1.320	-0.0160
11.79	1.266	-0.0205
10.80	1.198	-0.0238
9.86	1.120	-0.0271
8.89	1.046	-0.0302
7.77	0.948	-0.0334
6.69	0.857	-0.0365

5.68	0.762	-0.0386
4.76	0.676	-0.0403
3.69	0.574	-0.0421
2.64	0.469	-0.0447
1.64	0.378	-0.0468
0.61	0.273	-0.0485
-0.34	0.186	-0.0506
-1.49	0.081	-0.0548
-2.42	-0.015	-0.0568
-3.39	-0.118	-0.0577
-4.58	-0.231	-0.0583
-5.54	-0.330	-0.0587
-6.39	-0.422	-0.0584
-7.62	-0.551	-0.0590
-8.68	-0.658	-0.0587
-9.56	-0.731	-0.0586

W1015 (20%) **fp10**

Fig. 6.191

Run: 07013gw

Re = 100060.5

α	C_l	C_m
-10.30	-0.601	-0.0803
-9.27	-0.520	-0.0797
-8.23	-0.438	-0.0793
-7.20	-0.357	-0.0773
-6.20	-0.277	-0.0782
-5.30	-0.216	-0.0715
-4.22	-0.126	-0.0702
-3.08	-0.053	-0.0621
-2.17	0.024	-0.0593
-1.18	0.115	-0.0599
-0.06	0.287	-0.0788
0.99	0.466	-0.0882
1.91	0.552	-0.0786
3.04	0.629	-0.0746
4.07	0.723	-0.0748
4.94	0.799	-0.0740
6.05	0.887	-0.0766
7.03	0.965	-0.0720
8.11	1.046	-0.0678
9.19	1.109	-0.0589
10.20	1.175	-0.0549
11.09	1.222	-0.0512
12.24	1.279	-0.0478
12.91	0.790	-0.1524
13.89	0.833	-0.1568
14.99	0.875	-0.1665
16.00	0.908	-0.1783
17.00	0.892	-0.1813
17.91	0.968	-0.1991
17.69	0.876	-0.1653
16.60	0.907	-0.1639
15.75	0.903	-0.1565
14.63	0.867	-0.1473
13.58	0.853	-0.1440
12.61	0.822	-0.1392
11.65	0.792	-0.1296
10.59	0.806	-0.1215
9.92	1.175	-0.0476
8.74	1.113	-0.0528
7.77	1.047	-0.0569
6.68	0.972	-0.0610
5.75	0.898	-0.0639
4.64	0.801	-0.0656
3.76	0.721	-0.0662
2.71	0.630	-0.0678
1.62	0.543	-0.0736
0.58	0.426	-0.0745
-0.36	0.243	-0.0595
-1.37	0.126	-0.0517
-2.50	0.027	-0.0532
-3.49	-0.058	-0.0581
-4.54	-0.132	-0.0613
-5.55	-0.206	-0.0660
-6.40	-0.270	-0.0686
-7.50	-0.360	-0.0693
-8.59	-0.447	-0.0709
-9.48	-0.515	-0.0704

Run: 07015gw

Re = 200044.6

α	C_l	C_m
-10.41	-0.560	-0.1055
-9.33	-0.475	-0.1058
-8.28	-0.397	-0.1024
-7.19	-0.312	-0.1001
-6.32	-0.234	-0.0979
-5.33	-0.141	-0.0954
-4.19	-0.076	-0.0874
-3.09	0.003	-0.0808
-2.08	0.136	-0.0867
-1.17	0.227	-0.0859
-0.10	0.422	-0.0986
0.98	0.530	-0.0930
1.91	0.604	-0.0878
3.01	0.692	-0.0830
4.07	0.771	-0.0782
5.00	0.849	-0.0758
6.09	0.941	-0.0723
7.20	1.028	-0.0687
8.06	1.099	-0.0661
9.20	1.177	-0.0617
10.20	1.254	-0.0580
11.13	1.306	-0.0544
12.08	1.359	-0.0508
13.15	1.389	-0.0467
14.20	1.364	-0.0596
15.21	1.330	-0.0769
15.89	0.924	-0.1688
16.98	0.921	-0.1762
17.94	0.945	-0.1877
17.59	0.916	-0.1773
16.82	0.910	-0.1665
15.64	0.925	-0.1655
14.73	0.919	-0.1606
13.78	0.863	-0.1538
12.63	0.850	-0.1498
12.04	1.348	-0.0463
10.99	1.293	-0.0500
9.82	1.221	-0.0546
8.74	1.146	-0.0582
7.78	1.071	-0.0623
6.72	0.994	-0.0656
5.68	0.914	-0.0694
4.70	0.824	-0.0718
3.66	0.740	-0.0757
2.64	0.667	-0.0807
1.69	0.595	-0.0857
0.64	0.511	-0.0913
-0.41	0.394	-0.0955
-1.36	0.210	-0.0796
-2.34	0.121	-0.0816
-3.41	-0.006	-0.0788
-4.57	-0.104	-0.0827
-5.56	-0.163	-0.0936
-6.54	-0.252	-0.0955
-7.64	-0.350	-0.0977
-8.47	-0.425	-0.1009
-9.64	-0.507	-0.1040

Run: 07017gw

Re = 399990.0

α	C_l	C_m
-10.35	-0.585	-0.1023
-9.32	-0.489	-0.1038
-8.28	-0.383	-0.1033
-7.36	-0.296	-0.1038
-6.27	-0.187	-0.1034
-5.29	-0.088	-0.1026
-4.18	0.007	-0.1009
-3.25	0.063	-0.0943
-2.08	0.210	-0.1002
-1.02	0.358	-0.1037
-0.08	0.435	-0.0980
0.90	0.523	-0.0948
1.88	0.610	-0.0910

3.00	0.702	-0.0858
3.98	0.790	-0.0823
5.03	0.873	-0.0781
6.05	0.956	-0.0736
7.06	1.044	-0.0702
8.06	1.126	-0.0662
9.16	1.214	-0.0621
10.14	1.284	-0.0585
11.15	1.362	-0.0548
12.24	1.439	-0.0510
13.18	1.475	-0.0468
14.18	1.406	-0.0695
15.14	1.350	-0.0805
16.17	1.293	-0.0936
17.11	1.278	-0.1036
16.86	1.278	-0.1003
15.82	1.325	-0.0903
14.86	1.377	-0.0794
13.89	1.419	-0.0649
12.98	1.471	-0.0465
11.87	1.415	-0.0511
10.95	1.350	-0.0543
9.80	1.267	-0.0583
8.78	1.193	-0.0622
7.80	1.108	-0.0658
6.85	1.031	-0.0697
5.81	0.946	-0.0740
4.67	0.856	-0.0787
3.73	0.770	-0.0816
2.64	0.684	-0.0866
1.64	0.596	-0.0907
0.65	0.508	-0.0942
-0.33	0.420	-0.0977
-1.45	0.324	-0.1040
-2.36	0.184	-0.0985
-3.44	0.051	-0.0946
-4.54	-0.012	-0.1019
-5.46	-0.101	-0.1027
-6.42	-0.195	-0.1030
-7.63	-0.318	-0.1031
-8.62	-0.415	-0.1030
-9.64	-0.512	-0.1022

W1015 (20%) **fp15**

Fig. 6.194

Run: 07019gw
Re = 99973.4

α	C_l	C_m
-10.38	-0.635	-0.0829
-9.22	-0.510	-0.0886
-8.19	-0.395	-0.0932
-7.24	-0.294	-0.0935
-6.18	-0.189	-0.0943
-5.15	-0.087	-0.0955
-4.26	-0.016	-0.0955
-3.06	0.068	-0.0879
-2.21	0.134	-0.0860
-1.06	0.219	-0.0822
-0.15	0.345	-0.0960
1.05	0.569	-0.1118
2.06	0.641	-0.1023
3.03	0.687	-0.0941
4.10	0.769	-0.0908
5.01	0.845	-0.0898
6.04	0.932	-0.0876
7.17	1.021	-0.0843
8.10	1.096	-0.0818
9.22	1.165	-0.0770
10.16	1.229	-0.0782
11.26	1.296	-0.0758
12.11	1.334	-0.0734
12.91	0.829	-0.1842
13.95	0.916	-0.1934
14.98	0.896	-0.1922
16.00	0.932	-0.2037
16.86	0.906	-0.2091
17.97	0.963	-0.2240
17.69	0.915	-0.1985
16.66	0.984	-0.1999
15.60	0.971	-0.1909
14.62	0.916	-0.1784
13.60	0.869	-0.1693
12.65	0.872	-0.1669
11.73	0.814	-0.1588
10.79	0.786	-0.1502
9.69	0.832	-0.1426
8.73	1.151	-0.0708
7.76	1.080	-0.0742
6.79	1.009	-0.0767
5.87	0.930	-0.0790
4.72	0.839	-0.0819
3.76	0.759	-0.0843
2.75	0.686	-0.0879
1.59	0.645	-0.1015
0.68	0.533	-0.1016
-0.40	0.308	-0.0808
-1.31	0.239	-0.0763
-2.29	0.150	-0.0786
-3.34	0.085	-0.0871
-4.50	0.004	-0.0908
-5.55	-0.089	-0.0905
-6.61	-0.190	-0.0888
-7.65	-0.299	-0.0886
-8.64	-0.411	-0.0868
-9.66	-0.523	-0.0820

Run: 07020gw
Re = 199992.1

α	C_l	C_m
-10.33	-0.550	-0.1007
-9.21	-0.442	-0.1032
-8.21	-0.336	-0.1066
-7.22	-0.238	-0.1088
-6.20	-0.138	-0.1092
-5.32	-0.051	-0.1095
-4.27	0.049	-0.1087
-3.27	0.152	-0.1087
-2.09	0.263	-0.1060
-1.02	0.405	-0.1122
-0.05	0.595	-0.1242
1.05	0.674	-0.1157
1.92	0.703	-0.1038
3.02	0.770	-0.0964
4.01	0.841	-0.0923
4.98	0.921	-0.0893
6.07	1.008	-0.0871
7.18	1.106	-0.0845
8.10	1.182	-0.0829
9.10	1.261	-0.0803
10.22	1.346	-0.0786
11.24	1.415	-0.0763
12.25	1.470	-0.0736
13.23	1.484	-0.0724
14.17	1.438	-0.0872
15.06	1.393	-0.1033
15.83	0.986	-0.1957
16.98	0.992	-0.2034
17.96	1.020	-0.2118
17.70	1.025	-0.2086
16.67	1.004	-0.1986
15.68	0.979	-0.1907
14.68	0.987	-0.1859
13.70	1.009	-0.1898
12.76	0.976	-0.1848
11.62	0.956	-0.1757
11.07	1.406	-0.0719
9.91	1.328	-0.0741
8.78	1.243	-0.0762
7.76	1.161	-0.0785
6.70	1.070	-0.0807
5.85	0.997	-0.0830
4.71	0.898	-0.0859
3.72	0.825	-0.0895
2.62	0.748	-0.0948
1.80	0.699	-0.1017
0.81	0.677	-0.1168
-0.21	0.561	-0.1183

-1.43	0.326	-0.1008
-2.51	0.234	-0.1046
-3.37	0.140	-0.1043
-4.50	0.022	-0.1036
-5.58	-0.086	-0.1030
-6.63	-0.183	-0.1030
-7.63	-0.298	-0.1010
-8.66	-0.401	-0.0997
-9.55	-0.479	-0.0965

Run: 07022gw
Re = 399992.0

α	C_l	C_m
-10.29	-0.533	-0.1114
-9.29	-0.445	-0.1102
-8.40	-0.359	-0.1089
-7.22	-0.250	-0.1079
-6.37	-0.166	-0.1080
-5.29	-0.058	-0.1081
-4.24	0.053	-0.1098
-3.11	0.172	-0.1113
-2.22	0.334	-0.1259
-1.12	0.547	-0.1391
-0.14	0.617	-0.1312
1.01	0.650	-0.1172
2.01	0.717	-0.1098
2.95	0.784	-0.1034
4.05	0.883	-0.0982
4.99	0.956	-0.0943
6.11	1.055	-0.0899
7.16	1.149	-0.0871
8.04	1.219	-0.0840
9.17	1.330	-0.0827
10.24	1.410	-0.0800
11.24	1.496	-0.0779
12.31	1.562	-0.0753
13.20	1.519	-0.0837
14.07	1.473	-0.1014
15.19	1.416	-0.1136
16.11	1.342	-0.1213
15.86	1.386	-0.1184
14.95	1.429	-0.1109
13.85	1.480	-0.0986
12.95	1.571	-0.0728
12.07	1.551	-0.0751
10.92	1.473	-0.0778
9.89	1.397	-0.0803
8.88	1.297	-0.0815
7.81	1.215	-0.0839
6.95	1.133	-0.0859
5.88	1.035	-0.0890
4.68	0.935	-0.0935
3.72	0.854	-0.0978
2.64	0.762	-0.1025
1.70	0.699	-0.1105
0.70	0.646	-0.1197
-0.27	0.611	-0.1298
-1.43	0.511	-0.1376
-2.41	0.301	-0.1210
-3.50	0.133	-0.1092
-4.50	0.028	-0.1077
-5.54	-0.079	-0.1069
-6.45	-0.172	-0.1060
-7.58	-0.284	-0.1070
-8.62	-0.378	-0.1081
-9.51	-0.456	-0.1085

W1015 (20%) fp20

Fig. 6.197

Run: 07024gw
Re = 100063.0

α	C_l	C_m
-10.34	-0.498	-0.1002
-9.31	-0.392	-0.1070
-8.20	-0.282	-0.1129
-7.13	-0.174	-0.1146
-6.25	-0.095	-0.1151
-5.29	-0.001	-0.1141
-4.05	0.100	-0.1112
-3.25	0.173	-0.1078
-2.20	0.274	-0.1036
-1.10	0.384	-0.1083
-0.05	0.531	-0.1234
1.07	0.721	-0.1291
1.92	0.745	-0.1140
3.02	0.810	-0.1046
3.92	0.889	-0.1036
5.10	0.990	-0.1030
6.13	1.073	-0.1019
7.15	1.154	-0.1003
8.16	1.228	-0.0976
9.06	1.284	-0.0959
10.21	1.365	-0.0948
11.20	1.407	-0.0911
12.20	1.438	-0.0903
12.92	0.986	-0.2071
13.89	1.003	-0.2117
15.00	1.060	-0.2253
15.96	1.064	-0.2363
16.96	1.086	-0.2414
16.76	1.088	-0.2252
15.73	1.072	-0.2227
14.70	1.033	-0.2036
13.70	1.066	-0.2057
12.75	1.008	-0.1935
11.65	0.974	-0.1868
10.68	0.946	-0.1781
9.66	0.964	-0.1701
8.84	1.289	-0.0884
7.80	1.216	-0.0902
6.70	1.138	-0.0923
5.72	1.057	-0.0931
4.69	0.969	-0.0940
3.62	0.877	-0.0954
2.64	0.799	-0.0985
1.63	0.752	-0.1081
0.58	0.681	-0.1172
-0.39	0.470	-0.1001
-1.36	0.381	-0.0950
-2.49	0.270	-0.0974
-3.32	0.199	-0.1025
-4.39	0.105	-0.1067
-5.47	0.008	-0.1082
-6.35	-0.084	-0.1094
-7.49	-0.192	-0.1085
-8.66	-0.317	-0.1048
-9.68	-0.422	-0.1000

Run: 07026gw
Re = 200111.3

α	C_l	C_m
-10.28	-0.448	-0.1154
-9.28	-0.351	-0.1176
-8.38	-0.269	-0.1198
-7.22	-0.147	-0.1216
-6.21	-0.053	-0.1224
-5.25	0.045	-0.1246
-4.25	0.143	-0.1258
-3.18	0.252	-0.1268
-2.11	0.368	-0.1281
-1.10	0.492	-0.1322
-0.15	0.625	-0.1346
0.88	0.666	-0.1210
2.02	0.748	-0.1121
2.91	0.822	-0.1084
4.13	0.925	-0.1054
5.14	1.012	-0.1037
6.06	1.096	-0.1025
7.15	1.190	-0.1013
8.20	1.280	-0.0999
9.17	1.360	-0.0987
10.19	1.438	-0.0969
11.18	1.510	-0.0961
12.23	1.572	-0.0946
13.20	1.540	-0.1002
14.20	1.505	-0.1163
15.20	1.440	-0.1248

15.83	1.069	-0.2251
16.94	1.088	-0.2328
16.75	1.081	-0.2307
15.67	1.086	-0.2234
14.77	1.088	-0.2165
13.69	1.077	-0.2124
12.69	1.009	-0.2041
11.67	1.007	-0.1992
11.07	1.505	-0.0915
9.87	1.414	-0.0926
8.87	1.338	-0.0943
7.86	1.254	-0.0955
6.79	1.158	-0.0962
5.81	1.075	-0.0977
4.75	0.985	-0.0994
3.80	0.900	-0.1013
2.62	0.800	-0.1043
1.76	0.729	-0.1084
0.76	0.663	-0.1171
-0.44	0.601	-0.1310
-1.46	0.441	-0.1232
-2.47	0.329	-0.1228
-3.50	0.221	-0.1212
-4.38	0.135	-0.1215
-5.53	0.015	-0.1189
-6.34	-0.067	-0.1185
-7.53	-0.179	-0.1171
-8.61	-0.287	-0.1152
-9.54	-0.376	-0.1137

Run: 07028gw
Re = 399954.5

α	C_l	C_m
-10.28	-0.468	-0.1206
-9.49	-0.379	-0.1231
-8.40	-0.264	-0.1252
-7.32	-0.158	-0.1265
-6.22	-0.041	-0.1279
-5.29	0.060	-0.1293
-4.16	0.183	-0.1326
-3.24	0.277	-0.1337
-2.27	0.418	-0.1422
-1.15	0.523	-0.1388
-0.06	0.590	-0.1292
0.96	0.671	-0.1236
1.96	0.764	-0.1196
3.03	0.854	-0.1158
4.03	0.951	-0.1135
5.00	1.042	-0.1109
6.07	1.137	-0.1072
7.18	1.237	-0.1043
8.08	1.322	-0.1031
9.10	1.414	-0.1018
10.14	1.507	-0.1005
11.22	1.602	-0.0995
12.26	1.659	-0.0968
13.12	1.561	-0.1142
14.11	1.479	-0.1288
15.15	1.437	-0.1384
14.88	1.433	-0.1345
13.90	1.486	-0.1249
12.92	1.593	-0.1035
12.04	1.652	-0.0967
10.95	1.576	-0.0981
9.93	1.480	-0.0991
8.96	1.393	-0.1000
7.76	1.304	-0.1030
6.89	1.215	-0.1036
5.78	1.113	-0.1065
4.83	1.023	-0.1087
3.81	0.933	-0.1123
2.70	0.830	-0.1161
1.71	0.740	-0.1197
0.67	0.655	-0.1235
-0.30	0.579	-0.1284
-1.32	0.528	-0.1395
-2.43	0.404	-0.1397
-3.43	0.258	-0.1309
-4.50	0.145	-0.1290
-5.40	0.049	-0.1278
-6.57	-0.072	-0.1265
-7.60	-0.182	-0.1246
-8.66	-0.293	-0.1230
-9.67	-0.399	-0.1206

W1015 (20%) **fp25**

Fig. 6.200

Run: 07030gw
Re = 99987.8

α	C_l	C_m
-10.41	-0.415	-0.1240
-9.41	-0.279	-0.1333
-8.26	-0.143	-0.1424
-7.30	-0.048	-0.1434
-6.17	0.051	-0.1445
-5.11	0.133	-0.1394
-4.14	0.211	-0.1339
-3.27	0.267	-0.1263
-2.13	0.355	-0.1207
-1.22	0.440	-0.1224
-0.04	0.594	-0.1360
0.98	0.697	-0.1304
2.06	0.752	-0.1217
2.99	0.832	-0.1199
4.05	0.927	-0.1186
5.12	1.020	-0.1178
6.11	1.109	-0.1173
7.04	1.178	-0.1158
8.03	1.247	-0.1153
9.13	1.329	-0.1132
10.15	1.404	-0.1135
11.12	1.448	-0.1112
11.90	1.034	-0.2413
12.88	1.037	-0.2399
13.97	1.060	-0.2461
14.96	1.063	-0.2520
15.94	1.077	-0.2611
16.83	1.096	-0.2673
17.89	1.150	-0.2798
17.71	1.128	-0.2600
16.60	1.092	-0.2485
15.63	1.147	-0.2468
14.73	1.036	-0.2295
13.70	1.063	-0.2265
12.77	1.042	-0.2187
11.76	1.024	-0.2126
10.74	0.978	-0.2030
9.60	0.968	-0.1912
8.84	1.345	-0.1040
7.85	1.272	-0.1050
6.85	1.196	-0.1074
5.71	1.101	-0.1079
4.89	1.035	-0.1086
3.79	0.938	-0.1100
2.69	0.842	-0.1091
1.67	0.761	-0.1150
0.61	0.715	-0.1267
-0.26	0.577	-0.1213
-1.31	0.471	-0.1130
-2.48	0.372	-0.1147
-3.50	0.296	-0.1220
-4.41	0.240	-0.1286
-5.54	0.149	-0.1340
-6.51	0.059	-0.1354
-7.63	-0.042	-0.1352
-8.43	-0.140	-0.1318
-9.60	-0.280	-0.1255

Run: 07031gw
Re = 199920.6

α	C_l	C_m
-10.38	-0.327	-0.1481
-9.30	-0.207	-0.1532
-8.29	-0.092	-0.1568
-7.24	0.015	-0.1589
-6.17	0.126	-0.1614
-5.13	0.233	-0.1633

-4.25	0.326	-0.1641
-3.20	0.435	-0.1653
-2.04	0.550	-0.1641
-1.13	0.593	-0.1531
-0.13	0.676	-0.1470
0.93	0.755	-0.1403
1.98	0.848	-0.1349
3.04	0.928	-0.1299
4.05	1.021	-0.1278
5.10	1.106	-0.1252
6.05	1.194	-0.1233
7.14	1.289	-0.1213
8.17	1.369	-0.1188
9.10	1.454	-0.1182
10.14	1.532	-0.1163
11.23	1.603	-0.1154
12.20	1.626	-0.1153
13.09	1.553	-0.1281
14.14	1.522	-0.1385
14.84	1.147	-0.2510
15.91	1.150	-0.2585
15.68	1.117	-0.2497
14.69	1.139	-0.2465
13.72	1.123	-0.2398
12.63	1.084	-0.2323
11.66	1.083	-0.2288
10.76	1.101	-0.2206
9.85	1.504	-0.1125
8.98	1.433	-0.1133
7.74	1.333	-0.1155
6.80	1.255	-0.1168
5.74	1.163	-0.1181
4.76	1.080	-0.1203
3.67	0.985	-0.1226
2.71	0.907	-0.1263
1.71	0.818	-0.1308
0.63	0.734	-0.1360
-0.26	0.676	-0.1432
-1.45	0.583	-0.1513
-2.48	0.508	-0.1584
-3.35	0.420	-0.1591
-4.37	0.310	-0.1578
-5.50	0.196	-0.1564
-6.35	0.104	-0.1543
-7.63	-0.030	-0.1515
-8.46	-0.124	-0.1488
-9.64	-0.246	-0.1452

Run: 07033gw
Re = 400007.8

α	C_l	C_m
-10.32	-0.311	-0.1528
-9.33	-0.200	-0.1577
-8.38	-0.101	-0.1593
-7.25	0.009	-0.1609
-6.26	0.115	-0.1639
-5.31	0.217	-0.1655
-4.22	0.326	-0.1658
-3.25	0.413	-0.1622
-2.15	0.518	-0.1615
-1.18	0.612	-0.1576
-0.12	0.702	-0.1532
0.97	0.802	-0.1509
1.86	0.880	-0.1463
3.00	0.980	-0.1425
3.99	1.067	-0.1389
5.04	1.158	-0.1350
6.08	1.250	-0.1311
7.12	1.345	-0.1277
8.21	1.433	-0.1240
9.14	1.511	-0.1214
10.23	1.616	-0.1202
11.24	1.695	-0.1188
12.30	1.721	-0.1169
13.10	1.581	-0.1427
14.12	1.528	-0.1529
15.08	1.471	-0.1609
15.98	1.451	-0.1707
15.80	1.440	-0.1674
14.90	1.487	-0.1611
13.93	1.519	-0.1500
12.83	1.596	-0.1355
11.88	1.727	-0.1163
10.88	1.674	-0.1193
9.97	1.581	-0.1187
8.86	1.489	-0.1210
7.87	1.403	-0.1232
6.84	1.318	-0.1273
5.75	1.223	-0.1308
4.73	1.133	-0.1348
3.87	1.056	-0.1379
2.78	0.963	-0.1421
1.79	0.872	-0.1453
0.80	0.785	-0.1493
-0.37	0.682	-0.1532
-1.30	0.597	-0.1561
-2.43	0.486	-0.1589
-3.51	0.390	-0.1620
-4.44	0.301	-0.1638
-5.52	0.190	-0.1631
-6.38	0.105	-0.1616
-7.60	-0.019	-0.1600
-8.50	-0.118	-0.1576
-9.57	-0.226	-0.1544

W1015 (20%) **fp30**
Fig. 6.203

Run: 07002gw
Re = 99588.7

α	C_l	C_m
-10.32	-0.310	-0.1355
-9.30	-0.180	-0.1414
-8.26	-0.069	-0.1514
-7.16	0.041	-0.1512
-6.31	0.114	-0.1514
-5.07	0.208	-0.1390
-4.10	0.265	-0.1298
-3.19	0.349	-0.1271
-2.06	0.456	-0.1288
-1.02	0.569	-0.1333
-0.14	0.665	-0.1384
1.02	0.780	-0.1342
1.97	0.865	-0.1326
3.07	0.961	-0.1311
4.10	1.051	-0.1288
4.98	1.121	-0.1257
6.05	1.209	-0.1259
7.16	1.301	-0.1248
8.20	1.376	-0.1236
9.25	1.458	-0.1224
10.24	1.515	-0.1201
11.22	1.558	-0.1189
11.90	1.140	-0.2480
12.92	1.135	-0.2492
13.95	1.107	-0.2523
15.01	1.164	-0.2663
15.93	1.144	-0.2689
15.58	1.139	-0.2531
14.59	1.134	-0.2442
13.63	1.148	-0.2391
12.63	1.125	-0.2326
11.66	1.073	-0.2242
10.59	1.041	-0.2126
9.73	1.048	-0.2037
8.66	1.051	-0.1919
7.88	1.367	-0.1172
6.81	1.287	-0.1176
5.77	1.206	-0.1190
4.68	1.114	-0.1203
3.59	1.030	-0.1215
2.67	0.938	-0.1237
1.80	0.867	-0.1254
0.67	0.781	-0.1303
-0.29	0.652	-0.1262
-1.44	0.552	-0.1227
-2.45	0.454	-0.1194

-3.39	0.364	-0.1204
-4.56	0.274	-0.1244
-5.54	0.212	-0.1358
-6.36	0.147	-0.1425
-7.53	0.046	-0.1464
-8.57	-0.066	-0.1417
-9.58	-0.192	-0.1359

Run: 07004gw
Re = 199372.7

α	C_l	C_m
-10.36	-0.207	-0.1646
-9.34	-0.097	-0.1689
-8.21	0.024	-0.1739
-7.26	0.122	-0.1754
-6.17	0.239	-0.1780
-5.14	0.349	-0.1803
-4.06	0.457	-0.1797
-3.11	0.546	-0.1795
-2.11	0.631	-0.1774
-1.12	0.682	-0.1673
-0.10	0.759	-0.1598
0.88	0.829	-0.1534
2.00	0.933	-0.1498
3.04	1.009	-0.1445
3.98	1.096	-0.1415
5.02	1.193	-0.1399
6.13	1.280	-0.1376
7.15	1.364	-0.1358
8.15	1.451	-0.1341
9.12	1.517	-0.1310
10.23	1.597	-0.1283
11.29	1.652	-0.1271
12.14	1.689	-0.1274
13.22	1.575	-0.1414
14.06	1.526	-0.1507
14.89	1.211	-0.2666
15.84	1.208	-0.2744
15.63	1.175	-0.2618
14.77	1.202	-0.2601
13.64	1.194	-0.2547
12.72	1.186	-0.2484
11.62	1.129	-0.2380
10.79	1.128	-0.2323
9.99	1.578	-0.1247
8.82	1.496	-0.1262
7.76	1.406	-0.1281
6.75	1.340	-0.1316
5.87	1.273	-0.1344
4.68	1.165	-0.1356
3.64	1.077	-0.1386
2.72	0.998	-0.1414
1.68	0.905	-0.1452
0.63	0.818	-0.1504
-0.43	0.735	-0.1573
-1.28	0.677	-0.1635
-2.42	0.613	-0.1732
-3.48	0.509	-0.1732
-4.40	0.423	-0.1738
-5.43	0.317	-0.1733
-6.55	0.197	-0.1710
-7.57	0.092	-0.1694
-8.44	-0.005	-0.1658
-9.52	-0.118	-0.1623

Run: 07006gw
Re = 398440.4

α	C_l	C_m
-10.45	-0.193	-0.1718
-9.24	-0.064	-0.1752
-8.39	0.025	-0.1787
-7.27	0.136	-0.1806
-6.32	0.237	-0.1818
-5.29	0.346	-0.1836
-4.17	0.452	-0.1820
-3.16	0.539	-0.1784
-2.18	0.627	-0.1747
-1.13	0.719	-0.1715
-0.20	0.813	-0.1704
0.94	0.910	-0.1671
1.99	1.002	-0.1632
2.92	1.085	-0.1601
3.91	1.170	-0.1566
5.01	1.265	-0.1530
6.14	1.359	-0.1480
7.04	1.429	-0.1439
8.05	1.514	-0.1388
9.12	1.600	-0.1357
10.28	1.698	-0.1329
11.30	1.766	-0.1301
12.17	1.776	-0.1302
13.12	1.604	-0.1531
14.06	1.523	-0.1633
15.04	1.521	-0.1727
14.87	1.497	-0.1690
13.94	1.541	-0.1629
12.85	1.598	-0.1472
11.89	1.797	-0.1288
10.88	1.742	-0.1297
9.94	1.667	-0.1320
8.86	1.581	-0.1350
7.85	1.505	-0.1398
6.82	1.423	-0.1437
5.90	1.339	-0.1468
4.88	1.253	-0.1512
3.82	1.166	-0.1559
2.69	1.069	-0.1601
1.65	0.982	-0.1643
0.78	0.898	-0.1661
-0.23	0.799	-0.1674
-1.25	0.706	-0.1702
-2.40	0.599	-0.1720
-3.43	0.516	-0.1791
-4.49	0.418	-0.1798
-5.47	0.320	-0.1799
-6.46	0.224	-0.1800
-7.57	0.105	-0.1766
-8.62	-0.003	-0.1746
-9.60	-0.112	-0.1718

W1015 (20%) fp35

Fig. 6.205

Run: 07035sn
Re = 100036.2

α	C_l	C_m
-10.26	-0.174	-0.1583
-9.32	-0.069	-0.1594
-8.20	0.064	-0.1706
-7.17	0.148	-0.1683
-6.20	0.226	-0.1596
-5.16	0.277	-0.1439
-4.19	0.357	-0.1379
-3.08	0.477	-0.1412
-2.08	0.600	-0.1474
-1.11	0.721	-0.1549
-0.01	0.843	-0.1583
0.97	0.926	-0.1566
1.97	1.022	-0.1571
3.12	1.118	-0.1549
4.10	1.194	-0.1520
5.01	1.262	-0.1481
6.16	1.343	-0.1438
7.13	1.422	-0.1424
8.09	1.490	-0.1418
9.15	1.563	-0.1382
10.21	1.632	-0.1387
11.28	1.663	-0.1368
11.99	1.183	-0.2632
12.86	1.217	-0.2689
13.98	1.258	-0.2816
14.82	1.284	-0.2904
15.92	1.276	-0.2933
15.61	1.278	-0.2846
14.61	1.252	-0.2695
13.58	1.229	-0.2591
12.64	1.258	-0.2575
11.72	1.209	-0.2477

10.66	1.150	-0.2378
9.67	1.169	-0.2329
8.72	1.105	-0.2145
7.85	1.494	-0.1326
6.74	1.406	-0.1316
5.91	1.340	-0.1341
4.76	1.262	-0.1359
3.74	1.188	-0.1409
2.81	1.112	-0.1421
1.79	1.017	-0.1427
0.74	0.922	-0.1440
-0.34	0.798	-0.1399
-1.33	0.709	-0.1360
-2.29	0.588	-0.1318
-3.45	0.449	-0.1232
-4.53	0.356	-0.1231
-5.45	0.301	-0.1348
-6.39	0.243	-0.1482
-7.46	0.170	-0.1577
-8.52	0.056	-0.1574
-9.60	-0.093	-0.1457

Run: 07036sn

Re = 200068.7

α	C_l	C_m
-10.29	-0.091	-0.1867
-9.35	0.016	-0.1903
-8.27	0.126	-0.1935
-7.27	0.228	-0.1968
-6.17	0.333	-0.1992
-5.17	0.434	-0.2004
-4.09	0.540	-0.1994
-3.09	0.631	-0.1977
-2.15	0.718	-0.1958
-1.12	0.790	-0.1876
-0.10	0.852	-0.1781
0.94	0.937	-0.1735
2.03	1.033	-0.1702
3.08	1.112	-0.1640
4.10	1.202	-0.1624
5.12	1.283	-0.1592
6.15	1.383	-0.1586
7.12	1.457	-0.1549
8.12	1.531	-0.1521
9.20	1.614	-0.1500
10.14	1.664	-0.1444
11.27	1.721	-0.1422
12.15	1.673	-0.1465
13.11	1.600	-0.1603
14.14	1.553	-0.1721
14.86	1.234	-0.2919
15.85	1.225	-0.2900
15.63	1.261	-0.2933
14.69	1.236	-0.2814
13.62	1.196	-0.2742
12.62	1.187	-0.2656
11.60	1.191	-0.2614
10.66	1.182	-0.2537
9.69	1.136	-0.2413
8.95	1.600	-0.1456
7.92	1.519	-0.1477
6.77	1.432	-0.1509
5.79	1.350	-0.1527
4.68	1.259	-0.1549
3.70	1.177	-0.1584
2.70	1.088	-0.1603
1.69	1.002	-0.1649
0.67	0.924	-0.1703
-0.36	0.840	-0.1737
-1.34	0.775	-0.1826
-2.39	0.699	-0.1893
-3.39	0.610	-0.1920
-4.50	0.507	-0.1935
-5.44	0.419	-0.1946
-6.51	0.301	-0.1913
-7.48	0.209	-0.1898
-8.48	0.116	-0.1890
-9.60	-0.011	-0.1835

Run: 07037sn

Re = 400056.8

α	C_l	C_m
-10.26	-0.048	-0.1964
-9.25	0.052	-0.1973
-8.21	0.153	-0.2005
-7.30	0.246	-0.2014
-6.21	0.357	-0.2035
-5.29	0.450	-0.2029
-4.19	0.554	-0.2016
-3.19	0.639	-0.1982
-2.16	0.724	-0.1933
-1.13	0.820	-0.1912
-0.08	0.919	-0.1893
0.98	1.013	-0.1870
1.88	1.090	-0.1826
3.03	1.194	-0.1799
4.12	1.282	-0.1756
5.11	1.359	-0.1707
6.01	1.438	-0.1673
7.15	1.528	-0.1618
8.18	1.617	-0.1578
9.22	1.719	-0.1554
10.26	1.785	-0.1504
11.29	1.837	-0.1448
12.17	1.687	-0.1571
13.04	1.609	-0.1704
14.05	1.555	-0.1815
13.92	1.579	-0.1800
12.86	1.583	-0.1661
11.88	1.704	-0.1521
10.85	1.806	-0.1453
9.86	1.753	-0.1507
8.85	1.689	-0.1555
7.86	1.613	-0.1603
6.84	1.513	-0.1624
5.93	1.449	-0.1679
4.77	1.340	-0.1710
3.70	1.253	-0.1753
2.78	1.173	-0.1786
1.68	1.078	-0.1825
0.66	0.988	-0.1866
-0.30	0.896	-0.1875
-1.37	0.800	-0.1899
-2.35	0.708	-0.1908
-3.38	0.629	-0.1988
-4.45	0.535	-0.2023
-5.46	0.433	-0.2015
-6.38	0.342	-0.2019
-7.62	0.216	-0.2000
-8.56	0.125	-0.1991
-9.65	0.009	-0.1940

W1015 (20%) **fp40**

Fig. 6.207

Run: 07040gw

Re = 100006.4

α	C_l	C_m
-10.24	-0.094	-0.1730
-9.22	0.006	-0.1751
-8.17	0.138	-0.1840
-7.31	0.190	-0.1745
-6.11	0.275	-0.1631
-5.16	0.318	-0.1458
-4.19	0.404	-0.1460
-2.98	0.553	-0.1552
-2.09	0.654	-0.1605
-1.15	0.768	-0.1694
0.00	0.922	-0.1779
0.95	0.987	-0.1749
2.02	1.091	-0.1753
3.11	1.179	-0.1718
3.99	1.253	-0.1691
5.13	1.343	-0.1644
6.14	1.413	-0.1581
7.20	1.479	-0.1554
8.24	1.543	-0.1512
9.22	1.608	-0.1485

10.14	1.659	-0.1480
10.88	1.146	-0.2652
11.98	1.182	-0.2740
12.90	1.322	-0.2949
13.87	1.289	-0.2965
14.92	1.290	-0.2996
15.96	1.340	-0.3172
15.65	1.332	-0.2994
14.76	1.306	-0.2917
13.74	1.257	-0.2764
12.59	1.236	-0.2667
11.65	1.167	-0.2529
10.68	1.171	-0.2502
9.64	1.192	-0.2458
8.73	1.158	-0.2312
7.87	1.550	-0.1452
6.81	1.466	-0.1456
5.89	1.406	-0.1479
4.74	1.324	-0.1485
3.71	1.248	-0.1506
2.71	1.150	-0.1510
1.81	1.068	-0.1504
0.69	0.968	-0.1523
-0.40	0.836	-0.1472
-1.37	0.749	-0.1453
-2.32	0.640	-0.1369
-3.42	0.514	-0.1268
-4.50	0.418	-0.1264
-5.35	0.322	-0.1217
-6.57	0.263	-0.1360
-7.54	0.190	-0.1493
-8.40	0.145	-0.1640
-9.50	-0.013	-0.1452

Run: 07039gw
Re = 199971.2

α	C_l	C_m
-10.25	0.027	-0.2037
-9.27	0.136	-0.2079
-8.30	0.228	-0.2106
-7.30	0.321	-0.2126
-6.23	0.429	-0.2147
-5.19	0.523	-0.2143
-4.12	0.638	-0.2147
-3.17	0.711	-0.2103
-2.07	0.806	-0.2059
-1.03	0.896	-0.1988
0.01	0.967	-0.1904
0.94	1.042	-0.1874
1.93	1.119	-0.1811
3.00	1.201	-0.1771
4.00	1.280	-0.1739
5.16	1.379	-0.1715
6.14	1.452	-0.1688
7.15	1.538	-0.1668
8.07	1.617	-0.1662
9.13	1.690	-0.1627
10.24	1.751	-0.1575
11.24	1.778	-0.1536
12.13	1.657	-0.1588
13.21	1.633	-0.1730
13.71	1.253	-0.2896
14.86	1.305	-0.3063
15.95	1.313	-0.3133
15.59	1.280	-0.3021
14.69	1.261	-0.2956
13.67	1.238	-0.2836
12.71	1.251	-0.2787
11.70	1.219	-0.2691
10.70	1.221	-0.2651
9.64	1.236	-0.2527
8.82	1.671	-0.1573
7.84	1.596	-0.1594
6.80	1.518	-0.1623
5.90	1.441	-0.1646
4.81	1.358	-0.1682
3.67	1.268	-0.1710
2.69	1.182	-0.1730
1.66	1.107	-0.1779
0.71	1.025	-0.1821
-0.21	0.963	-0.1874
-1.38	0.872	-0.1955
-2.36	0.786	-0.2004
-3.29	0.706	-0.2055
-4.51	0.591	-0.2068
-5.48	0.500	-0.2079
-6.39	0.403	-0.2070
-7.54	0.286	-0.2042
-8.50	0.199	-0.2035
-9.54	0.103	-0.2001

Run: 07038sn
Re = 400014.0

α	C_l	C_m
-10.35	0.039	-0.2098
-9.26	0.154	-0.2137
-8.21	0.252	-0.2159
-7.19	0.358	-0.2174
-6.21	0.450	-0.2167
-5.18	0.555	-0.2173
-4.16	0.663	-0.2171
-3.11	0.749	-0.2134
-2.17	0.824	-0.2089
-1.07	0.926	-0.2064
-0.03	1.016	-0.2042
0.96	1.102	-0.2010
1.90	1.185	-0.1966
3.00	1.277	-0.1932
3.97	1.359	-0.1898
5.08	1.447	-0.1844
6.09	1.540	-0.1817
7.12	1.619	-0.1763
8.10	1.710	-0.1733
9.16	1.796	-0.1698
10.29	1.862	-0.1613
11.20	1.911	-0.1595
12.10	1.671	-0.1720
13.10	1.585	-0.1831
14.00	1.588	-0.1930
15.04	1.579	-0.2098
14.89	1.561	-0.2019
13.89	1.595	-0.1906
12.86	1.638	-0.1803
11.97	1.699	-0.1664
10.92	1.903	-0.1590
9.87	1.846	-0.1653
8.88	1.768	-0.1684
7.92	1.690	-0.1713
6.79	1.601	-0.1763
5.79	1.518	-0.1799
4.85	1.433	-0.1836
3.75	1.345	-0.1890
2.66	1.251	-0.1927
1.72	1.169	-0.1958
0.62	1.082	-0.2005
-0.34	0.990	-0.2028
-1.42	0.894	-0.2050
-2.40	0.803	-0.2067
-3.38	0.726	-0.2126
-4.52	0.625	-0.2152
-5.45	0.526	-0.2145
-6.37	0.441	-0.2155
-7.47	0.326	-0.2134
-8.51	0.227	-0.2134
-9.58	0.124	-0.2105

W1015 (20%) **fp45**

Fig. 6.209

Run: 07042gw
Re = 100033.7

α	C_l	C_m
-10.23	-0.016	-0.1838
-9.28	-0.040	-0.1505
-8.23	0.138	-0.1747
-7.15	0.191	-0.1631
-6.10	0.253	-0.1502
-5.12	0.346	-0.1519

-4.15	0.450	-0.1562
-3.02	0.576	-0.1662
-2.15	0.684	-0.1748
-1.03	0.823	-0.1870
0.01	0.940	-0.1909
0.91	1.005	-0.1876
2.02	1.098	-0.1853
3.13	1.195	-0.1825
4.14	1.276	-0.1787
5.01	1.346	-0.1726
6.23	1.444	-0.1713
7.14	1.510	-0.1685
8.25	1.571	-0.1623
9.14	1.617	-0.1572
10.26	1.661	-0.1543
10.96	1.158	-0.2835
12.02	1.235	-0.2935
12.88	1.259	-0.2999
14.01	1.243	-0.3051
13.67	1.306	-0.2953
12.60	1.247	-0.2827
11.62	1.155	-0.2676
10.67	1.167	-0.2648
9.61	1.113	-0.2547
8.63	1.180	-0.2436
7.72	1.166	-0.2271
6.77	1.506	-0.1589
5.90	1.437	-0.1595
4.87	1.363	-0.1624
3.76	1.271	-0.1615
2.83	1.184	-0.1634
1.87	1.091	-0.1634
0.81	0.991	-0.1636
-0.39	0.883	-0.1626
-1.40	0.774	-0.1552
-2.47	0.657	-0.1455
-3.41	0.542	-0.1358
-4.50	0.432	-0.1295
-5.50	0.329	-0.1246
-6.46	0.262	-0.1271
-7.57	0.187	-0.1320
-8.53	0.168	-0.1594
-9.59	0.018	-0.1388

Run: 07043gw
Re = 199935.4

α	C_l	C_m
-10.15	0.149	-0.2251
-9.32	0.227	-0.2261
-8.16	0.343	-0.2299
-7.21	0.440	-0.2310
-6.20	0.538	-0.2316
-5.27	0.623	-0.2305
-4.20	0.717	-0.2287
-3.04	0.819	-0.2245
-2.03	0.897	-0.2185
-1.00	0.980	-0.2114
0.03	1.044	-0.2024
1.06	1.134	-0.1976
1.98	1.209	-0.1936
2.97	1.281	-0.1887
4.10	1.378	-0.1866
5.10	1.445	-0.1824
6.12	1.530	-0.1809
7.19	1.608	-0.1785
8.19	1.684	-0.1759
9.10	1.747	-0.1732
10.25	1.802	-0.1675
11.27	1.831	-0.1645
12.12	1.671	-0.1665
13.12	1.637	-0.1817
13.77	1.332	-0.3058
14.94	1.321	-0.3141
15.93	1.357	-0.3256
15.61	1.329	-0.3166
14.68	1.319	-0.3068
13.77	1.306	-0.2996
12.63	1.289	-0.2923
11.68	1.307	-0.2907
10.71	1.278	-0.2788
9.99	1.790	-0.1646
8.85	1.716	-0.1680
7.81	1.655	-0.1710
6.91	1.581	-0.1724
5.94	1.516	-0.1767
4.85	1.433	-0.1793
3.82	1.348	-0.1812
2.81	1.277	-0.1848
1.65	1.180	-0.1887
0.73	1.104	-0.1932
-0.22	1.038	-0.1999
-1.40	0.948	-0.2082
-2.30	0.869	-0.2135
-3.48	0.778	-0.2192
-4.36	0.699	-0.2211
-5.52	0.600	-0.2251
-6.48	0.509	-0.2243
-7.52	0.406	-0.2233
-8.56	0.298	-0.2202
-9.60	0.198	-0.2181

Run: 07246gw
Re = 399916.8

α	C_l	C_m
-10.31	0.113	-0.2171
-9.30	0.216	-0.2191
-8.23	0.330	-0.2247
-7.20	0.435	-0.2253
-6.21	0.540	-0.2270
-5.24	0.650	-0.2253
-4.18	0.760	-0.2252
-3.15	0.863	-0.2223
-2.15	0.956	-0.2209
-1.08	1.048	-0.2166
-0.04	1.146	-0.2152
1.05	1.237	-0.2109
1.95	1.318	-0.2065
3.01	1.410	-0.2035
4.11	1.501	-0.1985
5.12	1.592	-0.1948
6.20	1.666	-0.1885
7.13	1.734	-0.1840
8.06	1.805	-0.1787
9.18	1.897	-0.1742
10.14	1.940	-0.1692
11.15	1.725	-0.1756
12.05	1.625	-0.1870
13.13	1.604	-0.1960
14.11	1.599	-0.2127
15.08	1.576	-0.2248
14.82	1.574	-0.2174
13.80	1.602	-0.2051
12.85	1.623	-0.1916
11.87	1.664	-0.1822
10.86	1.757	-0.1665
9.92	1.923	-0.1671
8.83	1.875	-0.1730
7.91	1.814	-0.1782
6.94	1.729	-0.1825
5.90	1.652	-0.1886
4.74	1.548	-0.1915
3.75	1.487	-0.1989
2.75	1.385	-0.1999
1.73	1.295	-0.2043
0.81	1.224	-0.2085
-0.29	1.132	-0.2136
-1.38	1.034	-0.2166
-2.39	0.940	-0.2189
-3.39	0.838	-0.2201
-4.48	0.735	-0.2221
-5.48	0.631	-0.2230
-6.53	0.517	-0.2241
-7.55	0.405	-0.2218
-8.60	0.294	-0.2210
-9.64	0.190	-0.2180

W1015 (20%) **fp50**
Fig. 6.211

Run: 07054gw
Re = 99972.7

α	C_l	C_m
-10.28	-0.068	-0.1412
-9.30	-0.026	-0.1262
-8.17	0.139	-0.1506
-7.17	0.194	-0.1427
-6.12	0.291	-0.1401
-5.11	0.402	-0.1451
-4.09	0.527	-0.1518
-3.05	0.668	-0.1659
-2.14	0.769	-0.1721
-1.08	0.918	-0.1844
0.06	1.046	-0.1873
1.11	1.127	-0.1840
1.96	1.194	-0.1823
3.12	1.286	-0.1815
4.00	1.348	-0.1754
5.22	1.438	-0.1732
6.20	1.499	-0.1708
7.12	1.571	-0.1673
8.23	1.631	-0.1611
9.13	1.668	-0.1568
10.21	1.714	-0.1539
10.96	1.265	-0.2778
11.86	1.300	-0.2854
12.91	1.326	-0.2937
13.89	1.309	-0.2959
13.78	1.342	-0.2835
12.60	1.263	-0.2711
11.66	1.342	-0.2705
10.76	1.248	-0.2576
9.64	1.212	-0.2473
8.73	1.277	-0.2463
7.76	1.256	-0.2264
6.94	1.590	-0.1588
5.80	1.514	-0.1603
4.88	1.451	-0.1603
3.70	1.364	-0.1622
2.72	1.298	-0.1634
1.70	1.205	-0.1621
0.87	1.119	-0.1613
-0.16	1.044	-0.1658
-1.24	0.888	-0.1548
-2.39	0.763	-0.1451
-3.25	0.649	-0.1371
-4.32	0.521	-0.1290
-5.46	0.398	-0.1227
-6.35	0.274	-0.1123
-7.38	0.227	-0.1216
-8.35	0.161	-0.1293
-9.54	0.012	-0.1101

Run: 07055gw
Re = 199905.3

α	C_l	C_m
-10.30	0.207	-0.2208
-9.27	0.326	-0.2266
-8.22	0.424	-0.2283
-7.13	0.530	-0.2292
-6.20	0.605	-0.2278
-5.06	0.710	-0.2264
-4.14	0.788	-0.2234
-3.00	0.883	-0.2189
-2.13	0.942	-0.2128
-1.05	1.025	-0.2052
0.04	1.102	-0.1975
1.09	1.187	-0.1941
2.00	1.253	-0.1881
3.14	1.344	-0.1864
4.10	1.416	-0.1823
5.06	1.498	-0.1823
6.09	1.572	-0.1775
7.20	1.655	-0.1755
8.21	1.730	-0.1739
9.29	1.798	-0.1710
10.14	1.841	-0.1671
11.29	1.878	-0.1643
12.09	1.667	-0.1659
13.18	1.626	-0.1774
13.93	1.325	-0.2969
14.97	1.322	-0.3022
14.66	1.336	-0.2983
13.64	1.288	-0.2862
12.75	1.337	-0.2858
11.68	1.312	-0.2789
10.74	1.295	-0.2687
10.08	1.829	-0.1614
8.81	1.759	-0.1655
7.93	1.713	-0.1695
6.92	1.635	-0.1706
5.85	1.559	-0.1736
4.76	1.473	-0.1754
3.84	1.403	-0.1784
2.78	1.327	-0.1830
1.69	1.231	-0.1842
0.82	1.166	-0.1887
-0.20	1.093	-0.1951
-1.38	1.003	-0.2008
-2.37	0.929	-0.2084
-3.31	0.843	-0.2103
-4.45	0.750	-0.2160
-5.43	0.671	-0.2199
-6.30	0.591	-0.2208
-7.51	0.485	-0.2213
-8.53	0.391	-0.2216
-9.57	0.279	-0.2173

Run: 07056gw
Re = 400267.9

α	C_l	C_m
-10.20	0.231	-0.2256
-9.32	0.324	-0.2297
-8.22	0.432	-0.2316
-7.28	0.521	-0.2315
-6.22	0.630	-0.2334
-5.25	0.718	-0.2312
-4.21	0.817	-0.2322
-3.04	0.918	-0.2286
-2.10	0.988	-0.2239
-1.03	1.082	-0.2210
-0.07	1.162	-0.2182
0.94	1.243	-0.2137
1.97	1.331	-0.2103
3.03	1.413	-0.2058
4.03	1.498	-0.2014
5.07	1.573	-0.1955
6.04	1.644	-0.1911
7.20	1.743	-0.1875
8.16	1.824	-0.1824
9.16	1.893	-0.1788
10.24	1.962	-0.1734
11.20	1.985	-0.1677
12.09	1.688	-0.1800
13.07	1.656	-0.1911
12.78	1.384	-0.3048
13.48	1.376	-0.3121
13.03	1.666	-0.1948
11.96	1.679	-0.1776
10.97	2.015	-0.1737
9.85	1.952	-0.1762
8.83	1.875	-0.1803
7.80	1.802	-0.1838
6.82	1.733	-0.1887
5.83	1.650	-0.1933
4.97	1.568	-0.1949
3.69	1.480	-0.2025
2.82	1.407	-0.2055
1.83	1.326	-0.2082
0.69	1.229	-0.2117
-0.36	1.143	-0.2168
-1.40	1.052	-0.2192
-2.28	0.976	-0.2210
-3.32	0.900	-0.2270
-4.44	0.798	-0.2295

-5.48	0.697	-0.2293
-6.44	0.614	-0.2313
-7.54	0.505	-0.2300
-8.60	0.405	-0.2303
-9.50	0.312	-0.2281

W1015 (20%) **fp55**

Fig. 6.213

Run: 07053gw
Re = 99904.7

α	C_l	C_m
-10.12	-0.083	-0.1118
-9.15	0.043	-0.1253
-8.29	0.145	-0.1375
-7.12	0.250	-0.1326
-6.12	0.350	-0.1383
-5.07	0.463	-0.1440
-4.16	0.577	-0.1520
-3.01	0.725	-0.1682
-2.12	0.825	-0.1739
-1.09	0.965	-0.1870
0.00	1.089	-0.1930
1.06	1.165	-0.1874
2.12	1.261	-0.1882
2.95	1.312	-0.1845
4.05	1.409	-0.1809
5.13	1.469	-0.1763
6.17	1.554	-0.1744
7.14	1.617	-0.1712
8.21	1.691	-0.1677
9.29	1.725	-0.1611
10.21	1.753	-0.1571
11.00	1.245	-0.2766
11.97	1.294	-0.2865
12.94	1.312	-0.2942
13.85	1.329	-0.3004
13.66	1.335	-0.2840
12.77	1.364	-0.2801
11.60	1.265	-0.2646
10.79	1.272	-0.2573
9.62	1.290	-0.2546
8.76	1.280	-0.2489
7.77	1.279	-0.2326
6.85	1.621	-0.1609
5.81	1.550	-0.1593
4.91	1.492	-0.1628
3.71	1.407	-0.1642
2.87	1.337	-0.1628
1.67	1.235	-0.1639
0.83	1.166	-0.1636
-0.31	1.070	-0.1670
-1.35	0.936	-0.1567
-2.38	0.821	-0.1511
-3.44	0.687	-0.1429
-4.30	0.578	-0.1338
-5.46	0.450	-0.1252
-6.32	0.351	-0.1177
-7.52	0.237	-0.1114
-8.47	0.150	-0.1129
-9.54	-0.007	-0.0864

Run: 07052gw
Re = 200036.3

α	C_l	C_m
-10.20	0.268	-0.2278
-9.16	0.373	-0.2309
-8.23	0.485	-0.2351
-7.13	0.589	-0.2354
-6.16	0.667	-0.2320
-5.23	0.745	-0.2292
-4.06	0.834	-0.2229
-3.06	0.908	-0.2168
-2.13	0.992	-0.2144
-1.10	1.059	-0.2047
-0.01	1.130	-0.1966
0.94	1.220	-0.1970
1.93	1.278	-0.1903
3.04	1.379	-0.1904
4.04	1.449	-0.1858
5.08	1.535	-0.1850
6.17	1.622	-0.1822
7.21	1.695	-0.1782
8.27	1.770	-0.1770
9.14	1.813	-0.1720
10.24	1.882	-0.1704
11.21	1.815	-0.1590
12.07	1.659	-0.1692
12.81	1.329	-0.2921
13.88	1.349	-0.3027
14.88	1.388	-0.3109
14.73	1.356	-0.3029
13.78	1.336	-0.2945
12.70	1.316	-0.2854
11.70	1.297	-0.2769
10.73	1.299	-0.2688
9.64	1.371	-0.2661
9.12	1.832	-0.1688
7.85	1.746	-0.1705
6.85	1.678	-0.1739
5.84	1.594	-0.1748
4.81	1.527	-0.1791
3.89	1.446	-0.1801
2.74	1.358	-0.1842
1.81	1.292	-0.1880
0.82	1.205	-0.1889
-0.35	1.112	-0.1925
-1.34	1.048	-0.2010
-2.40	0.961	-0.2052
-3.43	0.887	-0.2127
-4.42	0.803	-0.2172
-5.46	0.731	-0.2234
-6.44	0.646	-0.2253
-7.48	0.551	-0.2262
-8.55	0.441	-0.2252
-9.56	0.337	-0.2206

Run: 07051gw
Re = 400093.7

α	C_l	C_m
-10.22	0.306	-0.2332
-9.35	0.389	-0.2344
-8.28	0.499	-0.2386
-7.16	0.606	-0.2381
-6.14	0.698	-0.2379
-5.21	0.777	-0.2352
-4.21	0.873	-0.2358
-3.07	0.971	-0.2317
-2.06	1.055	-0.2295
-1.06	1.137	-0.2256
-0.10	1.213	-0.2210
1.00	1.311	-0.2200
2.03	1.389	-0.2141
3.12	1.467	-0.2080
4.01	1.542	-0.2050
5.17	1.626	-0.1984
6.18	1.715	-0.1950
7.11	1.785	-0.1909
8.19	1.869	-0.1868
9.27	1.937	-0.1811
10.10	1.992	-0.1769
11.21	1.764	-0.1709
12.15	1.664	-0.1815
13.18	1.668	-0.1946
14.05	1.622	-0.2058
13.79	1.639	-0.2023
12.90	1.648	-0.1894
11.90	1.690	-0.1770
11.11	2.022	-0.1708
10.02	1.987	-0.1758
8.84	1.910	-0.1814
7.84	1.848	-0.1865
6.85	1.767	-0.1912
5.97	1.690	-0.1938
4.82	1.610	-0.2012
3.77	1.523	-0.2041
2.84	1.464	-0.2107
1.74	1.362	-0.2130

0.78	1.292	-0.2179
-0.23	1.203	-0.2201
-1.34	1.103	-0.2220
-2.29	1.037	-0.2277
-3.38	0.955	-0.2337
-4.48	0.844	-0.2321
-5.55	0.760	-0.2354
-6.48	0.672	-0.2356
-7.48	0.570	-0.2349
-8.58	0.468	-0.2356
-9.59	0.364	-0.2324

W1015 (20%) **fp60**

Fig. 6.215

Run: 07048gw
Re = 100032.6

α	C_l	C_m
-10.24	-0.086	-0.0988
-9.13	0.042	-0.1115
-8.10	0.185	-0.1262
-7.14	0.279	-0.1274
-6.16	0.394	-0.1348
-5.09	0.529	-0.1472
-3.98	0.653	-0.1529
-3.02	0.767	-0.1642
-1.95	0.914	-0.1737
-1.02	1.033	-0.1888
0.05	1.145	-0.1925
1.11	1.225	-0.1894
2.00	1.302	-0.1879
3.12	1.379	-0.1848
4.19	1.462	-0.1814
5.23	1.533	-0.1784
6.13	1.595	-0.1750
7.21	1.679	-0.1751
8.21	1.730	-0.1700
9.30	1.766	-0.1645
10.22	1.792	-0.1606
10.93	1.259	-0.2732
11.88	1.297	-0.2821
12.96	1.376	-0.2950
12.77	1.365	-0.2772
11.67	1.345	-0.2709
10.83	1.288	-0.2577
9.74	1.288	-0.2527
8.61	1.250	-0.2407
7.63	1.246	-0.2252
6.90	1.672	-0.1597
5.81	1.605	-0.1612
4.74	1.523	-0.1627
3.71	1.443	-0.1633

2.72	1.370	-0.1640
1.91	1.301	-0.1652
0.67	1.200	-0.1650
-0.15	1.143	-0.1688
-1.39	0.981	-0.1588
-2.28	0.856	-0.1482
-3.37	0.743	-0.1421
-4.46	0.611	-0.1320
-5.49	0.491	-0.1254
-6.23	0.398	-0.1173
-7.47	0.263	-0.1064
-8.42	0.167	-0.1024
-9.50	0.000	-0.0782

Run: 07049gw
Re = 200108.0

α	C_l	C_m
-10.20	0.347	-0.2302
-9.17	0.453	-0.2335
-8.26	0.537	-0.2345
-7.11	0.629	-0.2320
-6.19	0.727	-0.2340
-5.12	0.795	-0.2267
-4.08	0.868	-0.2192
-3.14	0.928	-0.2108
-2.07	0.999	-0.2034
-1.02	1.084	-0.1988
0.01	1.148	-0.1905
1.00	1.222	-0.1883
2.06	1.321	-0.1895
3.14	1.406	-0.1868
4.17	1.503	-0.1874
5.10	1.564	-0.1845
6.17	1.657	-0.1824
7.12	1.713	-0.1785
8.13	1.777	-0.1762
9.30	1.849	-0.1712
10.24	1.906	-0.1709
11.25	1.729	-0.1582
12.23	1.674	-0.1675
12.81	1.373	-0.2946
13.85	1.364	-0.2997
13.74	1.362	-0.2955
12.65	1.373	-0.2872
11.68	1.363	-0.2818
10.68	1.304	-0.2690
9.75	1.317	-0.2620
8.89	1.836	-0.1709
7.82	1.769	-0.1718
6.82	1.700	-0.1745
5.76	1.630	-0.1788
4.83	1.544	-0.1792
3.84	1.474	-0.1814

2.73	1.384	-0.1839
1.73	1.295	-0.1836
0.81	1.224	-0.1858
-0.30	1.131	-0.1880
-1.32	1.065	-0.1950
-2.35	0.985	-0.2007
-3.28	0.917	-0.2048
-4.39	0.847	-0.2148
-5.46	0.768	-0.2212
-6.46	0.702	-0.2261
-7.42	0.610	-0.2262
-8.40	0.518	-0.2265
-9.54	0.413	-0.2256

Run: 07050gw
Re = 400265.9

α	C_l	C_m
-10.35	0.353	-0.2361
-9.20	0.466	-0.2381
-8.28	0.552	-0.2402
-7.18	0.652	-0.2402
-6.17	0.733	-0.2362
-5.12	0.833	-0.2370
-4.06	0.928	-0.2360
-3.06	1.016	-0.2346
-2.08	1.092	-0.2299
-1.11	1.163	-0.2247
-0.02	1.258	-0.2219
1.10	1.343	-0.2182
2.04	1.420	-0.2135
3.06	1.497	-0.2082
4.10	1.577	-0.2031
5.04	1.631	-0.1975
6.16	1.729	-0.1931
7.19	1.809	-0.1888
8.15	1.879	-0.1851
9.19	1.959	-0.1817
10.19	2.012	-0.1764
11.19	1.730	-0.1713
11.99	1.668	-0.1788
13.07	1.665	-0.1936
12.84	1.665	-0.1886
11.96	1.693	-0.1777
10.98	2.045	-0.1729
9.87	2.000	-0.1778
8.84	1.934	-0.1828
7.87	1.869	-0.1862
6.86	1.798	-0.1915
5.90	1.720	-0.1953
4.90	1.642	-0.1991
3.75	1.549	-0.2037
2.92	1.487	-0.2075
1.71	1.396	-0.2129

0.72	1.320	-0.2173
-0.26	1.241	-0.2212
-1.27	1.158	-0.2234
-2.31	1.075	-0.2276
-3.42	0.984	-0.2327
-4.40	0.891	-0.2328
-5.48	0.804	-0.2358
-6.38	0.721	-0.2360
-7.50	0.625	-0.2373
-8.54	0.511	-0.2342
-9.58	0.433	-0.2367

W1015 (20%) **fp65**

Fig. 6.217

Run: 07047gw
Re = 100026.9

α	C_l	C_m
-10.27	-0.071	-0.1021
-9.22	0.078	-0.1137
-8.08	0.233	-0.1307
-7.15	0.330	-0.1328
-6.09	0.465	-0.1460
-5.19	0.562	-0.1550
-3.98	0.683	-0.1646
-3.02	0.770	-0.1686
-2.00	0.891	-0.1817
-0.96	1.019	-0.1983
0.05	1.121	-0.2012
1.13	1.210	-0.1992
2.15	1.284	-0.1950
3.01	1.347	-0.1908
4.07	1.441	-0.1915
5.08	1.494	-0.1876
6.09	1.573	-0.1834
7.19	1.648	-0.1798
8.18	1.707	-0.1747
9.29	1.770	-0.1707
9.85	1.210	-0.2799
10.89	1.254	-0.2868
11.82	1.236	-0.2953
12.82	1.265	-0.3015
13.93	1.324	-0.3135
13.64	1.339	-0.2990
12.73	1.286	-0.2847
11.75	1.222	-0.2736
10.65	1.302	-0.2758
9.63	1.302	-0.2708
8.60	1.287	-0.2576
7.65	1.247	-0.2418
6.82	1.655	-0.1682
5.77	1.574	-0.1680

4.81	1.508	-0.1708
3.75	1.417	-0.1698
2.67	1.348	-0.1722
1.82	1.268	-0.1723
0.70	1.187	-0.1745
-0.24	1.115	-0.1764
-1.35	0.970	-0.1653
-2.26	0.873	-0.1580
-3.21	0.785	-0.1515
-4.42	0.661	-0.1423
-5.45	0.544	-0.1335
-6.37	0.438	-0.1226
-7.51	0.317	-0.1125
-8.47	0.183	-0.1009
-9.50	0.070	-0.0868

Run: 07046gw
Re = 199991.4

α	C_l	C_m
-10.31	0.384	-0.2427
-9.15	0.502	-0.2459
-8.22	0.582	-0.2444
-7.13	0.681	-0.2451
-6.23	0.752	-0.2410
-5.17	0.811	-0.2304
-4.04	0.880	-0.2195
-3.19	0.933	-0.2110
-2.07	1.023	-0.2069
-0.95	1.112	-0.2043
-0.08	1.179	-0.2006
1.06	1.247	-0.1947
2.14	1.345	-0.1952
3.02	1.424	-0.1956
4.13	1.507	-0.1932
5.21	1.589	-0.1914
6.23	1.661	-0.1879
7.23	1.746	-0.1872
8.24	1.812	-0.1845
9.25	1.871	-0.1824
10.18	1.908	-0.1760
11.15	1.723	-0.1632
12.24	1.637	-0.1734
12.77	1.315	-0.3014
13.94	1.335	-0.3090
13.62	1.345	-0.3036
12.58	1.306	-0.2925
11.71	1.300	-0.2873
10.81	1.313	-0.2838
9.70	1.339	-0.2732
9.03	1.859	-0.1766
7.82	1.783	-0.1781
6.90	1.720	-0.1798
5.81	1.637	-0.1827

4.78	1.563	-0.1853
3.71	1.475	-0.1867
2.81	1.403	-0.1873
1.65	1.320	-0.1922
0.82	1.252	-0.1918
-0.21	1.167	-0.1928
-1.24	1.094	-0.1977
-2.39	0.997	-0.2006
-3.39	0.906	-0.2028
-4.36	0.855	-0.2136
-5.38	0.809	-0.2250
-6.47	0.725	-0.2296
-7.35	0.660	-0.2347
-8.46	0.563	-0.2366
-9.53	0.464	-0.2361

Run: 07045gw
Re = 399878.1

α	C_l	C_m
-10.19	0.422	-0.2491
-9.21	0.509	-0.2492
-8.29	0.591	-0.2487
-7.14	0.701	-0.2491
-6.22	0.782	-0.2488
-5.07	0.880	-0.2466
-4.08	0.974	-0.2465
-3.11	1.058	-0.2437
-2.11	1.135	-0.2392
-1.13	1.216	-0.2350
0.02	1.301	-0.2300
1.01	1.379	-0.2262
1.94	1.451	-0.2213
2.97	1.517	-0.2134
4.09	1.602	-0.2081
5.09	1.664	-0.2021
6.19	1.749	-0.1976
7.12	1.822	-0.1930
8.24	1.914	-0.1900
9.26	1.961	-0.1845
10.31	2.042	-0.1821
11.14	1.728	-0.1731
12.11	1.709	-0.1848
13.01	1.629	-0.1959
13.55	1.405	-0.3265
13.36	1.405	-0.3256
12.46	1.398	-0.3181
12.59	1.652	-0.1878
11.17	2.071	-0.1762
9.91	2.015	-0.1817
8.90	1.961	-0.1861
8.01	1.903	-0.1892
6.97	1.825	-0.1937
5.86	1.743	-0.1989

4.91	1.668	-0.2039
3.72	1.588	-0.2104
2.78	1.525	-0.2171
1.80	1.452	-0.2230
0.83	1.363	-0.2250
-0.20	1.290	-0.2312
-1.38	1.193	-0.2333
-2.21	1.125	-0.2371
-3.36	1.035	-0.2421
-4.42	0.938	-0.2430
-5.37	0.856	-0.2450
-6.38	0.772	-0.2464
-7.49	0.677	-0.2485
-8.52	0.577	-0.2482
-9.59	0.477	-0.2465

W1015 (30%) **fp0**

Fig. 6.221

Run: 07188sn

Re = 100074.6

α	C_l	C_m
-10.31	-0.913	-0.0082
-9.25	-0.869	-0.0047
-8.35	-0.820	-0.0019
-7.33	-0.744	0.0013
-6.32	-0.664	0.0043
-5.34	-0.583	0.0067
-4.12	-0.494	0.0113
-3.18	-0.413	0.0139
-2.16	-0.310	0.0137
-1.02	-0.144	-0.0006
-0.05	-0.041	-0.0060
1.02	0.041	-0.0017
1.92	0.185	-0.0159
3.06	0.290	-0.0116
4.00	0.402	-0.0130
5.12	0.488	-0.0085
6.00	0.563	-0.0057
7.07	0.640	-0.0024
8.02	0.714	0.0014
9.03	0.785	0.0040
10.14	0.858	0.0059
11.16	0.913	0.0097
12.20	0.970	0.0114
12.91	0.577	-0.0754
13.92	0.553	-0.0721
14.95	0.607	-0.0789
14.81	0.612	-0.0633
13.81	0.575	-0.0579
12.80	0.571	-0.0527
11.66	0.606	-0.0532
10.75	0.636	-0.0398
9.81	0.856	0.0136
8.76	0.793	0.0092
7.76	0.721	0.0070
6.76	0.648	0.0027
5.81	0.575	-0.0012
4.76	0.486	-0.0048
3.67	0.400	-0.0094
2.64	0.249	0.0076
1.71	0.182	-0.0049
0.72	0.035	0.0078
-0.45	-0.046	0.0005
-1.34	-0.212	0.0238
-2.38	-0.300	0.0195
-3.41	-0.414	0.0162
-4.62	-0.502	0.0111
-5.48	-0.571	0.0078
-6.54	-0.666	0.0046
-7.58	-0.744	0.0004
-8.53	-0.816	-0.0042
-9.63	-0.877	-0.0082

Run: 07190sn

Re = 200060.0

α	C_l	C_m
-10.28	-0.940	-0.0086
-9.25	-0.875	-0.0059
-8.34	-0.801	-0.0033
-7.32	-0.722	-0.0004
-6.18	-0.633	0.0033
-5.19	-0.558	0.0068
-4.16	-0.477	0.0105
-3.15	-0.394	0.0118
-2.14	-0.235	-0.0030
-1.06	-0.130	-0.0008
0.02	-0.029	0.0014
0.98	0.057	0.0044
1.91	0.148	0.0066
2.91	0.275	0.0009
4.09	0.431	-0.0086
5.01	0.510	-0.0070
6.15	0.611	-0.0038
7.13	0.690	-0.0010
8.17	0.770	0.0015
9.21	0.851	0.0044
10.12	0.917	0.0069
11.22	0.993	0.0102
12.26	1.058	0.0136
13.14	1.107	0.0163
14.21	1.140	0.0183
15.29	1.136	0.0039
16.25	1.127	-0.0132
16.84	0.701	-0.0878
18.07	0.690	-0.0900
17.72	0.692	-0.0824
16.72	0.683	-0.0809
15.72	0.707	-0.0808
14.71	0.662	-0.0764
13.84	0.642	-0.0717
12.67	0.631	-0.0669
11.99	1.042	0.0184
10.88	0.977	0.0143
9.90	0.903	0.0119
8.87	0.829	0.0082
7.74	0.739	0.0051
6.78	0.661	0.0019
5.69	0.574	-0.0015
4.71	0.490	-0.0041
3.86	0.400	-0.0026
2.74	0.255	0.0074
1.64	0.132	0.0079
0.56	0.026	0.0048
-0.40	-0.054	0.0019
-1.47	-0.165	-0.0002
-2.33	-0.266	0.0005
-3.50	-0.428	0.0131
-4.40	-0.498	0.0097
-5.56	-0.589	0.0051
-6.42	-0.656	0.0016
-7.58	-0.740	-0.0023
-8.53	-0.819	-0.0056
-9.56	-0.890	-0.0094

Run: 07192sn

Re = 400089.4

α	C_l	C_m
-10.25	-0.978	-0.0109
-9.29	-0.908	-0.0083
-8.25	-0.827	-0.0058
-7.31	-0.752	-0.0026
-6.25	-0.661	0.0014
-5.13	-0.569	0.0056
-4.13	-0.474	0.0089
-3.16	-0.336	-0.0009
-2.11	-0.223	-0.0010
-1.19	-0.135	-0.0004
-0.13	-0.035	0.0013
0.87	0.058	0.0029
2.06	0.169	0.0050
3.13	0.273	0.0051
4.07	0.370	0.0052
5.04	0.462	0.0060
6.05	0.586	0.0017
7.08	0.686	0.0027
8.12	0.783	0.0052
9.25	0.875	0.0083

10.15	0.944	0.0108
11.26	1.031	0.0141
12.29	1.101	0.0171
13.32	1.159	0.0195
14.21	1.201	0.0213
15.31	1.176	-0.0056
16.20	1.156	-0.0219
17.09	1.133	-0.0312
18.09	1.095	-0.0401
17.80	1.077	-0.0339
16.83	1.120	-0.0268
15.84	1.160	-0.0141
14.88	1.200	0.0088
13.82	1.189	0.0223
12.93	1.139	0.0204
11.80	1.069	0.0172
10.84	1.002	0.0142
9.72	0.915	0.0111
8.86	0.841	0.0087
7.75	0.745	0.0054
6.73	0.656	0.0037
5.75	0.550	0.0029
4.64	0.424	0.0069
3.70	0.335	0.0063
2.57	0.223	0.0062
1.68	0.134	0.0052
0.61	0.032	0.0037
-0.37	-0.059	0.0022
-1.49	-0.164	0.0002
-2.45	-0.260	-0.0000
-3.49	-0.413	0.0096
-4.49	-0.508	0.0086
-5.60	-0.602	0.0043
-6.57	-0.682	0.0004
-7.64	-0.776	-0.0039
-8.59	-0.859	-0.0075
-9.67	-0.943	-0.0105

W1015 (30%) **fp5**

Fig. 6.224

Run: 07198sn

Re = 99956.2

α	C_l	C_m
-10.33	-0.688	-0.0441
-9.27	-0.604	-0.0513
-8.24	-0.500	-0.0599
-7.30	-0.413	-0.0591
-6.25	-0.316	-0.0644
-5.34	-0.232	-0.0609
-4.09	-0.125	-0.0630
-3.23	-0.045	-0.0588
-2.07	0.055	-0.0547
-1.06	0.122	-0.0583
-0.16	0.213	-0.0556
0.88	0.362	-0.0569
1.95	0.497	-0.0540
3.04	0.589	-0.0487
4.12	0.678	-0.0455
5.07	0.753	-0.0426
6.06	0.831	-0.0400
7.07	0.905	-0.0361
8.15	0.981	-0.0321
9.09	1.034	-0.0285
10.15	1.084	-0.0244
11.23	1.135	-0.0210
12.16	1.168	-0.0186
12.89	0.727	-0.1089
14.00	0.769	-0.1133
14.96	0.781	-0.1181
15.97	0.824	-0.1257
15.63	0.822	-0.1093
14.82	0.763	-0.1000
13.84	0.742	-0.0961
12.67	0.755	-0.0938
11.66	0.734	-0.0859
10.71	0.741	-0.0798
9.82	1.085	-0.0203
8.80	1.040	-0.0250
7.71	0.972	-0.0291
6.87	0.917	-0.0326
5.73	0.831	-0.0367
4.81	0.754	-0.0393
3.69	0.660	-0.0420
2.67	0.579	-0.0458
1.59	0.485	-0.0518
0.76	0.363	-0.0502
-0.39	0.227	-0.0466
-1.42	0.142	-0.0409
-2.50	0.063	-0.0460
-3.52	-0.032	-0.0475
-4.53	-0.119	-0.0488
-5.50	-0.206	-0.0531
-6.55	-0.301	-0.0522
-7.56	-0.399	-0.0481
-8.58	-0.512	-0.0406
-9.61	-0.611	-0.0391

Run: 07196sn

Re = 200192.7

α	C_l	C_m
-10.30	-0.709	-0.0522
-9.29	-0.619	-0.0528
-8.24	-0.534	-0.0524
-7.33	-0.453	-0.0529
-6.22	-0.340	-0.0546
-5.13	-0.226	-0.0568
-4.13	-0.116	-0.0577
-3.19	-0.028	-0.0564
-2.14	0.065	-0.0539
-1.04	0.184	-0.0551
-0.14	0.284	-0.0544
0.97	0.383	-0.0506
2.06	0.483	-0.0488
3.10	0.574	-0.0472
3.96	0.650	-0.0454
5.08	0.741	-0.0428
6.09	0.828	-0.0399
7.14	0.914	-0.0371
8.12	0.990	-0.0339
9.23	1.064	-0.0308
10.14	1.120	-0.0274
11.22	1.189	-0.0232
12.25	1.234	-0.0196
13.17	1.261	-0.0166
14.15	1.282	-0.0182
15.15	1.248	-0.0369
16.13	1.223	-0.0503
16.95	0.827	-0.1298
18.01	0.823	-0.1316
18.92	0.842	-0.1380
18.76	0.820	-0.1260
17.70	0.818	-0.1234
16.72	0.839	-0.1212
15.69	0.827	-0.1198
14.70	0.766	-0.1104
13.83	0.762	-0.1085
12.67	0.757	-0.1060
11.75	0.746	-0.1005
11.02	1.176	-0.0181
9.91	1.114	-0.0226
8.80	1.048	-0.0267
7.75	0.970	-0.0304
6.76	0.889	-0.0335
5.83	0.816	-0.0362
4.69	0.717	-0.0395
3.71	0.634	-0.0422
2.69	0.545	-0.0443
1.62	0.458	-0.0464
0.75	0.376	-0.0488
-0.32	0.280	-0.0523
-1.34	0.159	-0.0505
-2.42	0.050	-0.0522
-3.42	-0.041	-0.0536
-4.54	-0.155	-0.0535
-5.53	-0.268	-0.0535
-6.54	-0.377	-0.0524
-7.64	-0.480	-0.0524

-8.58	-0.564	-0.0526
-9.60	-0.647	-0.0535

Run: 07194sn
Re = 400019.4

α	C_l	C_m
-10.40	-0.750	-0.0520
-9.35	-0.652	-0.0518
-8.33	-0.554	-0.0517
-7.32	-0.452	-0.0520
-6.24	-0.343	-0.0528
-5.24	-0.240	-0.0536
-4.17	-0.135	-0.0530
-3.07	-0.034	-0.0512
-2.18	0.056	-0.0513
-1.07	0.176	-0.0517
0.02	0.276	-0.0490
0.95	0.365	-0.0467
1.93	0.474	-0.0480
3.03	0.570	-0.0457
4.08	0.664	-0.0422
5.09	0.753	-0.0396
6.06	0.838	-0.0371
7.08	0.924	-0.0343
8.13	1.014	-0.0311
9.22	1.100	-0.0275
10.21	1.171	-0.0241
11.13	1.224	-0.0211
12.28	1.290	-0.0169
13.32	1.342	-0.0144
14.24	1.314	-0.0319
15.18	1.279	-0.0498
16.15	1.245	-0.0613
15.80	1.242	-0.0558
14.87	1.293	-0.0419
13.86	1.352	-0.0152
12.83	1.317	-0.0140
11.79	1.269	-0.0171
10.85	1.208	-0.0209
9.76	1.139	-0.0249
8.87	1.076	-0.0278
7.83	0.990	-0.0308
6.73	0.906	-0.0344
5.82	0.825	-0.0367
4.67	0.723	-0.0396
3.75	0.645	-0.0421
2.68	0.544	-0.0446
1.69	0.442	-0.0451
0.70	0.346	-0.0464
-0.40	0.242	-0.0492
-1.32	0.154	-0.0507
-2.41	0.036	-0.0511
-3.44	-0.065	-0.0522
-4.54	-0.167	-0.0530
-5.52	-0.265	-0.0521
-6.41	-0.361	-0.0516
-7.47	-0.466	-0.0510
-8.42	-0.569	-0.0517
-9.59	-0.679	-0.0521

W1015 (30%) **fp10**
Fig. 6.227

Run: 07199sn
Re = 100002.0

α	C_l	C_m
-10.33	-0.427	-0.1033
-9.19	-0.343	-0.1066
-8.20	-0.273	-0.1068
-7.16	-0.207	-0.1029
-6.17	-0.130	-0.1024
-5.27	-0.030	-0.1000
-4.08	0.058	-0.0922
-3.17	0.132	-0.0883
-2.21	0.210	-0.0830
-1.17	0.270	-0.0786
-0.11	0.386	-0.0816
1.04	0.627	-0.0990
1.97	0.715	-0.0903
3.07	0.784	-0.0836
4.01	0.854	-0.0805
5.19	0.928	-0.0763
6.16	0.988	-0.0713
7.07	1.035	-0.0664
8.12	1.085	-0.0611
9.06	1.130	-0.0561
10.23	1.190	-0.0519
11.25	1.237	-0.0481
12.21	1.278	-0.0470
13.03	0.843	-0.1511
13.97	0.874	-0.1530
14.93	0.929	-0.1672
14.69	0.883	-0.1412
13.70	0.858	-0.1400
12.65	0.844	-0.1360
11.61	0.798	-0.1246
10.64	0.814	-0.1185
9.88	1.204	-0.0491
8.77	1.163	-0.0549
7.78	1.123	-0.0607
6.79	1.067	-0.0659
5.83	1.016	-0.0709
4.71	0.936	-0.0752
3.69	0.865	-0.0805
2.78	0.798	-0.0839
1.81	0.737	-0.0900
0.65	0.556	-0.0865
-0.41	0.337	-0.0721
-1.52	0.287	-0.0731
-2.47	0.216	-0.0753
-3.37	0.140	-0.0780
-4.41	0.051	-0.0786
-5.54	-0.021	-0.0854
-6.55	-0.116	-0.0863
-7.44	-0.180	-0.0928
-8.53	-0.257	-0.1015
-9.65	-0.345	-0.1054

Run: 07201sn
Re = 200028.2

α	C_l	C_m
-10.29	-0.402	-0.1017
-9.30	-0.315	-0.1025
-8.19	-0.218	-0.1039
-7.25	-0.139	-0.1047
-6.26	-0.048	-0.1044
-5.09	0.055	-0.1033
-4.22	0.120	-0.1013
-3.14	0.193	-0.0950
-2.17	0.312	-0.0956
-1.07	0.430	-0.0960
-0.17	0.564	-0.1001
1.08	0.700	-0.0956
2.10	0.768	-0.0893
3.12	0.835	-0.0854
4.13	0.910	-0.0813
5.14	0.979	-0.0776
6.16	1.049	-0.0733
7.13	1.113	-0.0688
8.09	1.175	-0.0643
9.18	1.238	-0.0597
10.11	1.300	-0.0563
11.22	1.361	-0.0523
12.25	1.406	-0.0487
13.13	1.424	-0.0466
14.21	1.398	-0.0622
15.25	1.355	-0.0756
15.84	0.932	-0.1587
16.92	0.975	-0.1677
16.82	0.964	-0.1599
15.64	0.956	-0.1554
14.77	0.947	-0.1523
13.72	0.895	-0.1448
12.62	0.907	-0.1439
11.65	0.877	-0.1369
11.00	1.345	-0.0474
9.84	1.276	-0.0515
8.97	1.228	-0.0553

7.82	1.157	-0.0601
6.88	1.101	-0.0645
5.87	1.030	-0.0686
4.79	0.957	-0.0734
3.68	0.885	-0.0780
2.79	0.821	-0.0817
1.80	0.756	-0.0862
0.63	0.669	-0.0946
-0.26	0.550	-0.0940
-1.45	0.397	-0.0914
-2.32	0.300	-0.0913
-3.48	0.150	-0.0894
-4.57	0.111	-0.0994
-5.52	0.024	-0.1013
-6.35	-0.052	-0.1016
-7.49	-0.149	-0.1029
-8.51	-0.241	-0.1025
-9.60	-0.341	-0.1025

Run: 07203sn
Re = 400137.5

α	C_l	C_m
-10.42	-0.465	-0.0972
-9.23	-0.348	-0.0983
-8.20	-0.249	-0.0989
-7.17	-0.145	-0.0983
-6.18	-0.045	-0.0989
-5.24	0.052	-0.0996
-4.24	0.153	-0.0998
-3.25	0.257	-0.1002
-2.05	0.380	-0.1001
-0.98	0.494	-0.1007
-0.12	0.573	-0.0966
0.96	0.655	-0.0915
2.04	0.750	-0.0868
3.05	0.825	-0.0822
4.10	0.908	-0.0783
5.17	0.992	-0.0746
6.00	1.045	-0.0713
7.10	1.131	-0.0668
8.07	1.205	-0.0633
9.21	1.276	-0.0583
10.15	1.331	-0.0543
11.31	1.415	-0.0510
12.28	1.470	-0.0479
13.14	1.493	-0.0458
14.23	1.382	-0.0745
15.21	1.349	-0.0839
16.17	1.311	-0.0914
15.85	1.309	-0.0897
14.91	1.353	-0.0800
13.99	1.408	-0.0686
12.86	1.479	-0.0440
11.82	1.450	-0.0474
10.78	1.380	-0.0508
9.98	1.331	-0.0537
8.81	1.249	-0.0576
7.86	1.186	-0.0618
6.80	1.109	-0.0664
5.78	1.045	-0.0713
4.76	0.957	-0.0745
3.69	0.877	-0.0781
2.75	0.806	-0.0818
1.71	0.726	-0.0873
0.78	0.654	-0.0913
-0.26	0.571	-0.0968
-1.26	0.473	-0.1000
-2.37	0.354	-0.0997
-3.35	0.250	-0.0989
-4.45	0.136	-0.0989
-5.41	0.038	-0.0985
-6.35	-0.058	-0.0986
-7.58	-0.181	-0.0982
-8.43	-0.269	-0.0979
-9.61	-0.386	-0.0970

W1015 (30%) **fp15**

Fig. 6.230

Run: 07209sn
Re = 100045.8

α	C_l	C_m
-10.42	-0.344	-0.1158
-9.36	-0.281	-0.1147
-8.35	-0.206	-0.1115
-7.29	-0.128	-0.1085
-6.13	-0.037	-0.1064
-5.17	0.039	-0.1038
-4.07	0.133	-0.1014
-3.06	0.210	-0.0970
-2.05	0.289	-0.0956
-1.15	0.332	-0.0940
0.00	0.537	-0.1139
0.90	0.728	-0.1266
1.92	0.865	-0.1203
3.14	0.892	-0.1089
4.12	0.945	-0.1043
5.15	1.004	-0.0974
6.01	1.051	-0.0931
7.20	1.122	-0.0867
8.12	1.167	-0.0828
9.21	1.218	-0.0769
10.22	1.279	-0.0756
11.12	1.321	-0.0727
11.93	0.921	-0.1875
13.00	0.959	-0.1912
14.02	0.959	-0.1897
14.89	0.986	-0.1955
15.98	1.017	-0.2016
15.73	0.986	-0.1870
14.83	1.011	-0.1835
13.83	0.985	-0.1800
12.76	0.927	-0.1698
11.60	0.897	-0.1619
10.82	0.902	-0.1562
9.71	0.897	-0.1484
8.80	0.937	-0.1381
7.74	1.195	-0.0806
6.71	1.143	-0.0854
5.73	1.091	-0.0898
4.87	1.035	-0.0945
3.66	0.968	-0.0998
2.71	0.925	-0.1070
1.63	0.890	-0.1168
0.62	0.701	-0.1111
-0.45	0.466	-0.0967
-1.43	0.364	-0.0876
-2.28	0.306	-0.0891
-3.38	0.225	-0.0905
-4.45	0.146	-0.0947
-5.55	0.058	-0.0989
-6.32	-0.008	-0.1022
-7.61	-0.107	-0.1055
-8.55	-0.177	-0.1089
-9.51	-0.246	-0.1119

Run: 07207sn
Re = 199954.6

α	C_l	C_m
-10.42	-0.252	-0.1361
-9.32	-0.195	-0.1314
-8.21	-0.129	-0.1257
-7.34	-0.068	-0.1222
-6.24	0.008	-0.1182
-5.20	0.084	-0.1143
-4.13	0.170	-0.1122
-3.10	0.279	-0.1128
-2.08	0.386	-0.1136
-0.97	0.511	-0.1159
-0.11	0.699	-0.1274
0.96	0.865	-0.1274
1.96	0.857	-0.1136
3.06	0.896	-0.1039
3.93	0.946	-0.0988
5.16	1.029	-0.0932
6.07	1.101	-0.0907
7.17	1.187	-0.0877
8.07	1.257	-0.0857

9.24	1.339	-0.0824
10.23	1.416	-0.0804
11.12	1.467	-0.0777
12.20	1.513	-0.0755
13.14	1.523	-0.0803
14.10	1.457	-0.0963
15.11	1.399	-0.1067
15.86	1.025	-0.1927
16.85	1.065	-0.2043
16.68	1.021	-0.1910
15.60	1.037	-0.1872
14.64	1.016	-0.1818
13.81	1.023	-0.1815
12.66	0.976	-0.1748
11.74	0.972	-0.1695
11.06	1.456	-0.0706
9.84	1.386	-0.0746
8.80	1.303	-0.0767
7.88	1.243	-0.0789
6.75	1.157	-0.0820
5.73	1.077	-0.0848
4.69	1.006	-0.0889
3.75	0.937	-0.0929
2.78	0.886	-0.0990
1.83	0.867	-0.1095
0.80	0.871	-0.1228
-0.41	0.644	-0.1180
-1.44	0.463	-0.1082
-2.42	0.350	-0.1067
-3.40	0.250	-0.1069
-4.56	0.146	-0.1090
-5.52	0.065	-0.1106
-6.34	0.010	-0.1151
-7.57	-0.078	-0.1190
-8.49	-0.135	-0.1230
-9.58	-0.201	-0.1285

Run: 07205sn
Re = 400027.7

α	C_l	C_m
-10.38	-0.189	-0.1415
-9.36	-0.125	-0.1404
-8.27	-0.062	-0.1345
-7.13	0.019	-0.1308
-6.24	0.086	-0.1281
-5.27	0.171	-0.1262
-4.17	0.269	-0.1249
-3.10	0.379	-0.1255
-2.15	0.544	-0.1353
-1.08	0.766	-0.1457
0.00	0.823	-0.1321
1.04	0.851	-0.1236
1.91	0.893	-0.1162
2.97	0.938	-0.1087
4.09	1.007	-0.1026
5.15	1.082	-0.0979
6.16	1.163	-0.0935
7.05	1.234	-0.0906
8.07	1.307	-0.0855
9.27	1.409	-0.0828
10.20	1.490	-0.0797
11.29	1.574	-0.0775
12.31	1.607	-0.0746
13.13	1.496	-0.0987
14.14	1.445	-0.1081
15.06	1.400	-0.1148
14.90	1.401	-0.1128
13.94	1.466	-0.1053
12.95	1.525	-0.0892
11.87	1.597	-0.0746
10.95	1.548	-0.0765
9.83	1.461	-0.0796
8.85	1.383	-0.0822
7.92	1.307	-0.0851
6.78	1.215	-0.0894
5.77	1.133	-0.0932
4.74	1.060	-0.0979
3.75	0.992	-0.1028
2.67	0.918	-0.1081
1.78	0.885	-0.1155
0.73	0.842	-0.1243
-0.35	0.814	-0.1337
-1.32	0.732	-0.1430
-2.39	0.504	-0.1308
-3.43	0.336	-0.1222
-4.49	0.240	-0.1233
-5.34	0.160	-0.1246
-6.54	0.069	-0.1276
-7.54	-0.007	-0.1312
-8.55	-0.071	-0.1359
-9.63	-0.126	-0.1401

W1015 (30%) **fp20**

Fig. 6.233

Run: 07210sn
Re = 100015.9

α	C_l	C_m
-10.21	-0.291	-0.1232
-9.24	-0.203	-0.1247
-8.20	-0.110	-0.1280
-7.30	-0.026	-0.1254
-6.28	0.061	-0.1230
-5.11	0.156	-0.1180
-4.19	0.235	-0.1150
-3.09	0.328	-0.1150
-2.19	0.409	-0.1123
-1.04	0.506	-0.1193
0.02	0.726	-0.1395
0.90	0.853	-0.1410
1.99	0.902	-0.1278
2.94	0.947	-0.1213
4.10	1.021	-0.1167
5.12	1.091	-0.1133
6.19	1.163	-0.1101
7.19	1.221	-0.1052
8.06	1.273	-0.1026
9.18	1.350	-0.1000
10.13	1.399	-0.0969
11.18	1.443	-0.0942
11.94	1.046	-0.2118
12.91	1.007	-0.2114
13.95	1.047	-0.2223
14.87	1.069	-0.2260
16.02	1.090	-0.2353
15.55	1.065	-0.2166
14.62	1.090	-0.2142
13.75	1.053	-0.2028
12.73	1.059	-0.2006
11.64	0.979	-0.1876
10.81	0.995	-0.1867
9.69	0.995	-0.1759
8.66	0.986	-0.1638
7.85	1.287	-0.0942
6.79	1.213	-0.0968
5.71	1.154	-0.1018
4.80	1.090	-0.1043
3.76	1.016	-0.1071
2.69	0.942	-0.1107
1.72	0.914	-0.1196
0.64	0.833	-0.1272
-0.28	0.660	-0.1200
-1.43	0.494	-0.1038
-2.38	0.423	-0.1026
-3.42	0.321	-0.1019
-4.39	0.239	-0.1028
-5.41	0.157	-0.1092
-6.33	0.079	-0.1163
-7.50	-0.022	-0.1204
-8.48	-0.111	-0.1213
-9.57	-0.215	-0.1206

Run: 07211sn
Re = 200109.2

α	C_l	C_m
-10.35	-0.238	-0.1378
-9.19	-0.141	-0.1373
-8.33	-0.072	-0.1363

-7.16	0.026	-0.1359
-6.17	0.115	-0.1355
-5.24	0.206	-0.1358
-4.09	0.317	-0.1347
-3.20	0.405	-0.1346
-2.02	0.519	-0.1335
-0.97	0.641	-0.1369
0.03	0.791	-0.1426
1.03	0.814	-0.1294
2.08	0.866	-0.1209
2.95	0.934	-0.1174
4.01	1.014	-0.1140
5.02	1.100	-0.1126
6.13	1.199	-0.1106
7.07	1.270	-0.1079
8.19	1.361	-0.1058
9.18	1.450	-0.1049
10.20	1.525	-0.1034
11.20	1.583	-0.1008
12.23	1.613	-0.1001
13.19	1.530	-0.1158
14.15	1.497	-0.1220
14.83	1.094	-0.2227
15.92	1.126	-0.2332
15.71	1.109	-0.2208
14.68	1.103	-0.2155
13.72	1.101	-0.2164
12.66	1.058	-0.2049
11.65	1.021	-0.1969
10.79	1.048	-0.1934
9.98	1.503	-0.0978
8.82	1.418	-0.0994
7.81	1.329	-0.1001
6.79	1.248	-0.1018
5.84	1.170	-0.1044
4.82	1.076	-0.1046
3.72	0.998	-0.1088
2.68	0.911	-0.1117
1.69	0.844	-0.1168
0.64	0.819	-0.1290
-0.45	0.726	-0.1333
-1.39	0.586	-0.1270
-2.38	0.491	-0.1281
-3.29	0.394	-0.1286
-4.36	0.294	-0.1297
-5.55	0.179	-0.1308
-6.45	0.093	-0.1308
-7.53	-0.005	-0.1301
-8.52	-0.088	-0.1326
-9.50	-0.165	-0.1339

Run: 07213sn

Re = 400260.7

α	C_l	C_m
-10.33	-0.220	-0.1456
-9.35	-0.127	-0.1465
-8.24	-0.007	-0.1470
-7.37	0.090	-0.1499
-6.22	0.200	-0.1497
-5.36	0.281	-0.1492
-4.22	0.393	-0.1492
-3.07	0.510	-0.1503
-2.09	0.654	-0.1588
-1.08	0.826	-0.1669
-0.10	0.802	-0.1486
0.99	0.845	-0.1370
2.01	0.925	-0.1315
3.06	1.021	-0.1284
4.07	1.100	-0.1237
5.10	1.184	-0.1202
6.13	1.272	-0.1172
7.22	1.357	-0.1132
8.13	1.429	-0.1099
9.22	1.519	-0.1065
10.15	1.591	-0.1033
11.16	1.657	-0.1012
12.20	1.662	-0.1029
13.08	1.533	-0.1295
14.03	1.474	-0.1341
15.08	1.446	-0.1391
14.84	1.470	-0.1382
13.90	1.487	-0.1289
12.82	1.566	-0.1228
11.87	1.692	-0.0974
10.94	1.652	-0.1000
9.84	1.570	-0.1027
8.90	1.499	-0.1056
7.85	1.410	-0.1083
6.79	1.328	-0.1130
5.79	1.250	-0.1160
4.72	1.161	-0.1196
3.80	1.084	-0.1231
2.65	0.976	-0.1261
1.72	0.897	-0.1299
0.70	0.835	-0.1376
-0.38	0.824	-0.1519
-1.30	0.829	-0.1683
-2.27	0.618	-0.1532
-3.44	0.472	-0.1475
-4.36	0.385	-0.1479
-5.44	0.275	-0.1477
-6.47	0.177	-0.1479
-7.54	0.073	-0.1469
-8.45	-0.036	-0.1454
-9.51	-0.144	-0.1429

W1015 (30%) **fp25**

Fig. 6.236

Run: 07219sn

Re = 100102.9

α	C_l	C_m
-10.31	-0.149	-0.1445
-9.19	-0.038	-0.1507
-8.32	0.047	-0.1556
-7.32	0.133	-0.1535
-6.12	0.229	-0.1447
-5.07	0.313	-0.1409
-4.23	0.410	-0.1376
-3.01	0.542	-0.1423
-2.19	0.631	-0.1457
-0.99	0.691	-0.1445
-0.10	0.835	-0.1516
1.08	0.941	-0.1442
2.08	0.985	-0.1348
3.13	1.069	-0.1333
4.10	1.132	-0.1287
5.07	1.200	-0.1265
6.11	1.275	-0.1241
7.15	1.341	-0.1205
8.19	1.414	-0.1190
9.23	1.476	-0.1166
10.24	1.527	-0.1146
11.21	1.562	-0.1130
11.88	1.130	-0.2331
12.99	1.159	-0.2417
13.92	1.202	-0.2510
15.01	1.204	-0.2539
14.73	1.199	-0.2366
13.74	1.164	-0.2276
12.79	1.144	-0.2206
11.75	1.139	-0.2161
10.78	1.100	-0.2063
9.64	1.099	-0.1979
8.80	1.092	-0.1874
7.77	1.191	-0.1745
6.89	1.378	-0.1127
5.83	1.307	-0.1158
4.92	1.246	-0.1184
3.67	1.160	-0.1218
2.83	1.091	-0.1235
1.82	1.017	-0.1279
0.68	0.963	-0.1364
-0.38	0.821	-0.1350
-1.42	0.689	-0.1259
-2.41	0.631	-0.1253

-3.26	0.542	-0.1226
-4.51	0.409	-0.1190
-5.37	0.325	-0.1190
-6.49	0.245	-0.1281
-7.54	0.158	-0.1350
-8.41	0.071	-0.1393
-9.59	-0.053	-0.1327

Run: 07217sn
Re = 199993.6

α	C_l	C_m
-10.23	-0.069	-0.1651
-9.20	0.029	-0.1660
-8.29	0.110	-0.1675
-7.17	0.215	-0.1669
-6.25	0.303	-0.1664
-5.26	0.409	-0.1673
-4.06	0.525	-0.1667
-3.05	0.614	-0.1645
-2.04	0.706	-0.1642
-1.00	0.756	-0.1537
0.01	0.855	-0.1524
0.98	0.903	-0.1442
2.11	1.000	-0.1416
3.09	1.081	-0.1395
4.13	1.155	-0.1343
5.13	1.225	-0.1316
6.12	1.301	-0.1281
7.06	1.376	-0.1260
8.12	1.453	-0.1239
9.23	1.538	-0.1218
10.14	1.610	-0.1216
11.12	1.669	-0.1199
12.24	1.625	-0.1268
13.06	1.574	-0.1375
13.74	1.170	-0.2443
14.89	1.176	-0.2505
15.99	1.207	-0.2599
15.66	1.186	-0.2484
14.62	1.166	-0.2412
13.76	1.184	-0.2382
12.67	1.151	-0.2301
11.63	1.149	-0.2271
10.75	1.119	-0.2177
9.66	1.172	-0.2098
8.98	1.522	-0.1158
7.81	1.432	-0.1177
6.92	1.371	-0.1196
5.77	1.280	-0.1232
4.84	1.208	-0.1257
3.74	1.125	-0.1289
2.69	1.054	-0.1338
1.68	0.976	-0.1366
0.65	0.898	-0.1408
-0.28	0.847	-0.1481
-1.42	0.730	-0.1486
-2.46	0.672	-0.1568
-3.42	0.580	-0.1583
-4.47	0.486	-0.1587
-5.41	0.396	-0.1601
-6.46	0.293	-0.1607
-7.53	0.186	-0.1609
-8.56	0.094	-0.1619
-9.52	-0.005	-0.1590

Run: 07215sn
Re = 400162.1

α	C_l	C_m
-10.41	-0.080	-0.1679
-9.21	0.018	-0.1668
-8.25	0.111	-0.1671
-7.21	0.209	-0.1686
-6.21	0.303	-0.1680
-5.23	0.410	-0.1694
-4.10	0.512	-0.1685
-3.11	0.597	-0.1647
-2.21	0.739	-0.1740
-1.19	0.815	-0.1679
-0.11	0.863	-0.1559
0.93	0.940	-0.1518
1.97	1.023	-0.1462
2.92	1.102	-0.1436
4.12	1.192	-0.1376
5.09	1.276	-0.1349
6.15	1.361	-0.1313
7.19	1.456	-0.1290
8.07	1.538	-0.1280
9.12	1.626	-0.1263
10.25	1.720	-0.1236
11.17	1.764	-0.1193
12.20	1.614	-0.1368
13.07	1.556	-0.1475
14.10	1.529	-0.1553
15.16	1.477	-0.1626
14.88	1.485	-0.1586
13.91	1.518	-0.1523
12.95	1.565	-0.1459
11.88	1.663	-0.1282
10.86	1.750	-0.1184
9.86	1.685	-0.1223
8.84	1.614	-0.1256
7.85	1.519	-0.1262
6.89	1.441	-0.1286
5.76	1.334	-0.1301
4.75	1.248	-0.1337
3.76	1.169	-0.1381
2.70	1.080	-0.1424
1.67	0.998	-0.1460
0.70	0.922	-0.1502
-0.29	0.850	-0.1559
-1.28	0.811	-0.1665
-2.32	0.716	-0.1704
-3.30	0.580	-0.1650
-4.53	0.479	-0.1680
-5.52	0.377	-0.1671
-6.35	0.300	-0.1674
-7.51	0.186	-0.1673
-8.54	0.083	-0.1644
-9.59	-0.008	-0.1652

W1015 (30%) **fp30**

Fig. 6.239

Run: 07220sn
Re = 100001.2

α	C_l	C_m
-10.35	-0.058	-0.1521
-9.20	0.117	-0.1753
-8.16	0.157	-0.1641
-7.10	0.188	-0.1429
-6.11	0.289	-0.1440
-5.25	0.390	-0.1516
-4.13	0.535	-0.1624
-3.18	0.625	-0.1656
-2.14	0.733	-0.1709
-1.04	0.812	-0.1715
0.04	0.926	-0.1634
0.95	0.973	-0.1547
1.92	1.052	-0.1517
3.14	1.137	-0.1505
3.96	1.209	-0.1482
5.16	1.276	-0.1405
6.16	1.346	-0.1379
7.08	1.400	-0.1358
8.24	1.482	-0.1337
9.12	1.532	-0.1317
10.13	1.578	-0.1297
10.97	1.125	-0.2505
11.80	1.182	-0.2626
12.86	1.194	-0.2619
13.98	1.228	-0.2722
13.69	1.236	-0.2561
12.76	1.202	-0.2459
11.74	1.154	-0.2364
10.71	1.154	-0.2295
9.69	1.133	-0.2261
8.65	1.135	-0.2144
7.77	1.123	-0.1996

6.82	1.418	-0.1307
5.92	1.358	-0.1317
4.87	1.279	-0.1333
3.79	1.219	-0.1379
2.78	1.125	-0.1375
1.83	1.051	-0.1394
0.73	0.988	-0.1453
-0.20	0.913	-0.1479
-1.36	0.821	-0.1453
-2.20	0.741	-0.1442
-3.28	0.636	-0.1382
-4.46	0.500	-0.1294
-5.37	0.382	-0.1209
-6.44	0.265	-0.1147
-7.36	0.186	-0.1184
-8.35	0.159	-0.1391
-9.54	-0.014	-0.1154

Run: 07221sn
Re = 199986.9

α	C_l	C_m
-10.20	0.111	-0.1928
-9.22	0.197	-0.1943
-8.27	0.277	-0.1947
-7.14	0.362	-0.1930
-6.11	0.456	-0.1926
-5.15	0.554	-0.1911
-4.02	0.655	-0.1883
-3.04	0.750	-0.1873
-2.14	0.826	-0.1832
-0.96	0.889	-0.1715
-0.09	0.952	-0.1659
1.09	1.042	-0.1632
2.09	1.111	-0.1582
2.93	1.183	-0.1576
4.13	1.281	-0.1549
5.14	1.349	-0.1516
6.18	1.439	-0.1505
7.22	1.504	-0.1445
8.24	1.578	-0.1432
9.15	1.640	-0.1413
10.22	1.699	-0.1378
11.25	1.732	-0.1350
12.22	1.627	-0.1473
13.11	1.577	-0.1560
13.81	1.210	-0.2648
14.95	1.235	-0.2730
15.98	1.272	-0.2815
15.63	1.276	-0.2763
14.77	1.252	-0.2688
13.71	1.216	-0.2592
12.71	1.209	-0.2520
11.62	1.199	-0.2447
10.78	1.171	-0.2391
9.73	1.175	-0.2288
8.85	1.611	-0.1330
7.96	1.560	-0.1372
6.93	1.474	-0.1374
5.85	1.404	-0.1429
4.74	1.319	-0.1452
3.70	1.239	-0.1473
2.69	1.174	-0.1515
1.70	1.099	-0.1547
0.71	1.012	-0.1557
-0.36	0.944	-0.1620
-1.32	0.875	-0.1686
-2.27	0.821	-0.1779
-3.31	0.733	-0.1817
-4.45	0.630	-0.1840
-5.38	0.538	-0.1846
-6.37	0.455	-0.1872
-7.53	0.340	-0.1869
-8.40	0.273	-0.1879
-9.47	0.185	-0.1874

Run: 07222sn
Re = 399860.5

α	C_l	C_m
-10.26	0.117	-0.1957
-9.29	0.195	-0.1940
-8.33	0.275	-0.1931
-7.17	0.380	-0.1928
-6.24	0.470	-0.1928
-5.31	0.552	-0.1907
-4.18	0.641	-0.1869
-3.25	0.726	-0.1848
-2.08	0.826	-0.1814
-1.00	0.907	-0.1761
-0.09	0.979	-0.1728
0.95	1.063	-0.1692
2.01	1.152	-0.1652
3.05	1.227	-0.1602
4.05	1.320	-0.1588
4.99	1.382	-0.1530
6.09	1.484	-0.1505
7.18	1.562	-0.1453
8.06	1.653	-0.1448
9.12	1.739	-0.1430
10.21	1.813	-0.1391
11.23	1.745	-0.1401
12.13	1.632	-0.1589
12.99	1.606	-0.1646
14.04	1.542	-0.1713
13.92	1.538	-0.1684
12.91	1.583	-0.1637
11.84	1.660	-0.1531
10.96	1.846	-0.1348
9.85	1.794	-0.1390
9.02	1.728	-0.1402
7.84	1.647	-0.1447
6.90	1.558	-0.1454
5.82	1.457	-0.1487
4.92	1.385	-0.1522
3.86	1.301	-0.1561
2.78	1.216	-0.1600
1.69	1.133	-0.1652
0.69	1.041	-0.1672
-0.25	0.971	-0.1725
-1.31	0.882	-0.1744
-2.34	0.818	-0.1827
-3.42	0.710	-0.1841
-4.41	0.629	-0.1869
-5.47	0.536	-0.1898
-6.55	0.440	-0.1901
-7.44	0.356	-0.1908
-8.49	0.260	-0.1919
-9.58	0.165	-0.1925

W1015 (30%) **fp35**

Fig. 6.241

Run: 07225sn
Re = 100036.1

α	C_l	C_m
-10.12	-0.026	-0.1253
-9.13	0.063	-0.1355
-8.11	0.209	-0.1479
-7.10	0.297	-0.1458
-6.11	0.435	-0.1582
-5.04	0.559	-0.1706
-4.04	0.664	-0.1754
-2.99	0.757	-0.1819
-2.12	0.851	-0.1872
-1.08	0.923	-0.1861
0.04	1.020	-0.1785
0.97	1.075	-0.1784
2.07	1.146	-0.1711
3.14	1.233	-0.1702
4.17	1.301	-0.1634
5.15	1.356	-0.1575
6.14	1.437	-0.1552
7.06	1.504	-0.1544
8.10	1.575	-0.1517
9.12	1.619	-0.1462
10.21	1.657	-0.1442
10.98	1.185	-0.2717
12.01	1.195	-0.2758
12.96	1.231	-0.2814

13.93	1.290	-0.2948
13.62	1.258	-0.2725
12.78	1.272	-0.2688
11.64	1.206	-0.2531
10.61	1.178	-0.2442
9.73	1.181	-0.2401
8.78	1.159	-0.2310
7.67	1.162	-0.2159
6.87	1.527	-0.1453
5.90	1.456	-0.1453
4.96	1.392	-0.1484
3.73	1.316	-0.1529
2.73	1.242	-0.1553
1.73	1.167	-0.1569
0.69	1.081	-0.1576
-0.19	1.037	-0.1604
-1.35	0.933	-0.1608
-2.36	0.841	-0.1567
-3.33	0.748	-0.1512
-4.31	0.656	-0.1457
-5.41	0.538	-0.1384
-6.41	0.406	-0.1279
-7.43	0.299	-0.1232
-8.29	0.224	-0.1280
-9.53	0.095	-0.1194

Run: 07224sn
Re = 200044.8

α	C_l	C_m
-10.29	0.240	-0.2121
-9.23	0.337	-0.2126
-8.13	0.426	-0.2112
-7.06	0.528	-0.2119
-6.10	0.611	-0.2099
-5.10	0.705	-0.2082
-4.16	0.777	-0.2057
-3.11	0.868	-0.2023
-2.03	0.938	-0.1959
-0.97	1.003	-0.1863
-0.02	1.089	-0.1851
1.06	1.171	-0.1831
2.01	1.247	-0.1803
2.98	1.306	-0.1756
4.16	1.399	-0.1727
5.11	1.464	-0.1689
6.21	1.543	-0.1649
7.20	1.603	-0.1605
8.14	1.664	-0.1574
9.20	1.736	-0.1561
10.23	1.781	-0.1499
11.26	1.742	-0.1513
12.19	1.643	-0.1625
13.13	1.624	-0.1738
13.85	1.307	-0.2875
14.98	1.343	-0.2976
14.72	1.330	-0.2873
13.63	1.306	-0.2774
12.68	1.275	-0.2707
11.61	1.296	-0.2664
10.74	1.282	-0.2595
9.73	1.275	-0.2532
9.13	1.730	-0.1493
7.87	1.652	-0.1526
6.85	1.579	-0.1543
5.82	1.520	-0.1588
4.85	1.468	-0.1647
3.78	1.378	-0.1658
2.84	1.321	-0.1723
1.71	1.224	-0.1726
0.82	1.150	-0.1744
-0.35	1.058	-0.1772
-1.35	1.006	-0.1874
-2.37	0.934	-0.1918
-3.44	0.840	-0.1953
-4.34	0.769	-0.1984
-5.33	0.682	-0.2005
-6.36	0.596	-0.2027
-7.46	0.497	-0.2042
-8.53	0.398	-0.2054
-9.46	0.312	-0.2052

Run: 07223sn
Re = 399656.0

α	C_l	C_m
-10.22	0.244	-0.2131
-9.32	0.329	-0.2140
-8.24	0.414	-0.2115
-7.26	0.503	-0.2103
-6.23	0.583	-0.2065
-5.09	0.691	-0.2063
-4.17	0.768	-0.2045
-3.15	0.850	-0.1993
-2.00	0.921	-0.1915
-1.10	0.995	-0.1886
0.03	1.097	-0.1869
0.90	1.152	-0.1813
2.03	1.252	-0.1779
3.03	1.337	-0.1759
3.97	1.413	-0.1723
5.15	1.509	-0.1686
6.23	1.591	-0.1641
7.14	1.674	-0.1617
8.25	1.765	-0.1580
9.28	1.851	-0.1575
10.11	1.883	-0.1520
11.11	1.702	-0.1608
12.16	1.655	-0.1740
13.10	1.617	-0.1795
14.01	1.581	-0.1898
13.78	1.589	-0.1855
12.88	1.626	-0.1772
11.85	1.674	-0.1674
10.86	1.900	-0.1483
9.90	1.881	-0.1525
8.89	1.820	-0.1562
7.95	1.750	-0.1593
6.88	1.661	-0.1610
5.74	1.566	-0.1648
4.81	1.483	-0.1668
3.74	1.408	-0.1732
2.65	1.307	-0.1749
1.65	1.224	-0.1783
0.65	1.144	-0.1817
-0.42	1.055	-0.1840
-1.47	0.968	-0.1883
-2.41	0.903	-0.1922
-3.33	0.842	-0.2007
-4.47	0.745	-0.2026
-5.39	0.661	-0.2022
-6.42	0.575	-0.2058
-7.47	0.481	-0.2063
-8.49	0.394	-0.2085
-9.52	0.317	-0.2112

W1015 (**30**%) **fp40**

Fig. 6.243

Run: 07226sn
Re = 100103.7

α	C_l	C_m
-10.10	0.058	-0.1347
-9.09	0.182	-0.1486
-8.11	0.280	-0.1546
-7.06	0.380	-0.1615
-6.09	0.506	-0.1756
-5.27	0.583	-0.1843
-4.05	0.701	-0.1873
-3.00	0.798	-0.1935
-2.03	0.900	-0.1966
-0.90	0.996	-0.1964
-0.12	1.062	-0.1940
0.97	1.139	-0.1903
1.94	1.217	-0.1912
3.13	1.305	-0.1868
4.05	1.375	-0.1840
5.11	1.439	-0.1760
6.16	1.521	-0.1728
7.17	1.588	-0.1702

8.20	1.648	-0.1654
9.10	1.687	-0.1615
9.91	1.184	-0.2782
10.89	1.240	-0.2862
11.84	1.219	-0.2887
12.98	1.269	-0.3023
12.57	1.263	-0.2817
11.73	1.287	-0.2800
10.75	1.219	-0.2664
9.65	1.182	-0.2569
8.65	1.143	-0.2471
7.65	1.173	-0.2367
6.87	1.572	-0.1581
5.92	1.521	-0.1600
4.84	1.457	-0.1650
3.91	1.385	-0.1670
2.73	1.293	-0.1676
1.83	1.214	-0.1697
0.69	1.144	-0.1751
-0.25	1.076	-0.1769
-1.38	0.981	-0.1790
-2.25	0.894	-0.1750
-3.34	0.783	-0.1701
-4.42	0.677	-0.1640
-5.42	0.596	-0.1604
-6.36	0.484	-0.1520
-7.49	0.356	-0.1399
-8.31	0.277	-0.1349
-9.37	0.165	-0.1235

Run: 07227sn
Re = 200123.9

α	C_l	C_m
-10.14	0.387	-0.2300
-9.30	0.453	-0.2284
-8.25	0.555	-0.2306
-7.08	0.657	-0.2288
-6.19	0.730	-0.2264
-5.07	0.823	-0.2223
-4.17	0.883	-0.2162
-3.06	0.970	-0.2110
-2.00	1.060	-0.2082
-0.91	1.126	-0.2005
-0.06	1.196	-0.1991
1.09	1.277	-0.1956
2.08	1.342	-0.1901
3.10	1.429	-0.1903
4.13	1.510	-0.1879
5.11	1.569	-0.1832
6.23	1.646	-0.1807
7.13	1.700	-0.1765
8.12	1.763	-0.1725
9.27	1.829	-0.1697

10.28	1.884	-0.1681
11.14	1.753	-0.1640
12.18	1.698	-0.1773
12.81	1.364	-0.2996
13.81	1.363	-0.3020
13.77	1.371	-0.2978
12.69	1.351	-0.2908
11.64	1.331	-0.2791
10.66	1.328	-0.2728
9.64	1.304	-0.2641
9.12	1.833	-0.1660
7.88	1.740	-0.1643
6.86	1.682	-0.1694
5.77	1.615	-0.1731
4.86	1.552	-0.1768
3.77	1.482	-0.1808
2.75	1.417	-0.1862
1.73	1.340	-0.1889
0.81	1.280	-0.1927
-0.30	1.196	-0.1956
-1.31	1.093	-0.1940
-2.21	1.039	-0.2021
-3.29	0.946	-0.2047
-4.29	0.885	-0.2112
-5.35	0.807	-0.2163
-6.29	0.722	-0.2183
-7.51	0.627	-0.2222
-8.49	0.531	-0.2216
-9.46	0.450	-0.2224

Run: 07228sn
Re = 399792.6

α	C_l	C_m
-10.18	0.368	-0.2263
-9.14	0.461	-0.2281
-8.24	0.533	-0.2252
-7.19	0.622	-0.2243
-6.07	0.716	-0.2221
-5.14	0.805	-0.2222
-4.06	0.897	-0.2196
-3.05	0.973	-0.2141
-2.15	1.023	-0.2080
-1.02	1.130	-0.2082
0.02	1.215	-0.2043
1.02	1.302	-0.2020
2.06	1.374	-0.1962
2.98	1.449	-0.1933
4.06	1.526	-0.1873
5.12	1.613	-0.1843
6.23	1.703	-0.1802
7.16	1.771	-0.1759
8.23	1.863	-0.1746
9.36	1.921	-0.1682

10.15	1.968	-0.1657
11.14	1.716	-0.1759
12.02	1.677	-0.1837
13.05	1.631	-0.1935
14.10	1.620	-0.2089
13.85	1.621	-0.2031
12.97	1.663	-0.1920
11.94	1.711	-0.1842
10.97	1.721	-0.1718
9.97	1.964	-0.1641
8.88	1.910	-0.1704
7.86	1.838	-0.1727
6.91	1.758	-0.1759
5.82	1.674	-0.1802
4.89	1.607	-0.1854
3.83	1.513	-0.1867
2.69	1.436	-0.1943
1.83	1.359	-0.1956
0.80	1.287	-0.2008
-0.25	1.197	-0.2028
-1.33	1.106	-0.2061
-2.28	1.023	-0.2072
-3.33	0.954	-0.2149
-4.38	0.878	-0.2196
-5.48	0.781	-0.2210
-6.38	0.701	-0.2217
-7.46	0.602	-0.2223
-8.49	0.515	-0.2246
-9.56	0.425	-0.2259

W1015 (30%) **fp45**

Fig. 6.245

Run: 07231sn
Re = 99961.2

α	C_l	C_m
-10.13	0.143	-0.1454
-9.18	0.250	-0.1538
-8.26	0.363	-0.1642
-7.08	0.492	-0.1738
-6.24	0.607	-0.1884
-5.02	0.737	-0.1938
-4.00	0.839	-0.1980
-3.04	0.927	-0.2017
-2.06	1.031	-0.2052
-0.94	1.156	-0.2093
-0.09	1.200	-0.2057
1.11	1.285	-0.1994
2.10	1.363	-0.1988
3.15	1.439	-0.1968
4.19	1.523	-0.1934
5.10	1.561	-0.1888

6.08	1.625	-0.1865
7.10	1.689	-0.1835
8.26	1.742	-0.1783
9.24	1.777	-0.1735
9.98	1.280	-0.2841
11.02	1.297	-0.2953
11.96	1.353	-0.3046
12.99	1.373	-0.3101
12.79	1.381	-0.2922
11.79	1.391	-0.2863
10.64	1.349	-0.2739
9.67	1.325	-0.2636
8.72	1.302	-0.2561
7.70	1.286	-0.2474
6.84	1.696	-0.1674
5.89	1.648	-0.1699
4.76	1.579	-0.1721
3.84	1.513	-0.1731
2.90	1.457	-0.1757
1.75	1.376	-0.1799
0.75	1.321	-0.1847
-0.29	1.235	-0.1844
-1.36	1.150	-0.1877
-2.36	1.019	-0.1800
-3.33	0.945	-0.1823
-4.27	0.851	-0.1763
-5.29	0.750	-0.1721
-6.42	0.644	-0.1666
-7.47	0.502	-0.1552
-8.33	0.400	-0.1474
-9.38	0.276	-0.1352

Run: 07230sn
Re = 199992.2

α	C_l	C_m
-10.14	0.482	-0.2392
-9.18	0.563	-0.2384
-8.12	0.635	-0.2354
-7.23	0.709	-0.2328
-6.14	0.770	-0.2237
-5.01	0.850	-0.2169
-4.08	0.927	-0.2156
-3.00	1.033	-0.2156
-2.01	1.115	-0.2138
-1.07	1.173	-0.2083
0.10	1.260	-0.2051
1.00	1.329	-0.2030
2.06	1.394	-0.1986
3.08	1.479	-0.1987
4.19	1.560	-0.1968
5.13	1.625	-0.1925
6.21	1.704	-0.1912
7.10	1.746	-0.1843

8.12	1.803	-0.1817
9.25	1.869	-0.1799
10.17	1.907	-0.1785
11.23	1.722	-0.1754
11.76	1.372	-0.2972
12.96	1.386	-0.3052
13.84	1.408	-0.3134
13.63	1.407	-0.3053
12.76	1.399	-0.2999
11.57	1.365	-0.2888
10.75	1.353	-0.2804
9.67	1.335	-0.2692
8.78	1.348	-0.2649
8.02	1.817	-0.1777
7.01	1.757	-0.1824
5.95	1.688	-0.1840
4.82	1.606	-0.1858
3.77	1.535	-0.1893
2.80	1.474	-0.1926
1.84	1.390	-0.1927
0.72	1.323	-0.1982
-0.36	1.240	-0.1987
-1.29	1.169	-0.2021
-2.28	1.093	-0.2059
-3.27	0.998	-0.2056
-4.42	0.920	-0.2122
-5.31	0.851	-0.2140
-6.42	0.774	-0.2222
-7.43	0.706	-0.2294
-8.45	0.622	-0.2312
-9.53	0.533	-0.2311

Run: 07229sn
Re = 399695.9

α	C_l	C_m
-10.39	0.498	-0.2470
-9.11	0.597	-0.2463
-8.32	0.665	-0.2447
-7.19	0.766	-0.2438
-6.15	0.847	-0.2411
-5.19	0.927	-0.2385
-4.15	1.001	-0.2340
-3.11	1.066	-0.2246
-1.97	1.143	-0.2204
-1.13	1.218	-0.2194
-0.13	1.297	-0.2142
0.95	1.385	-0.2126
1.93	1.459	-0.2091
3.01	1.544	-0.2041
4.00	1.606	-0.1981
5.07	1.694	-0.1952
6.09	1.764	-0.1896
7.21	1.848	-0.1849

8.20	1.925	-0.1841
9.28	1.983	-0.1801
10.18	2.029	-0.1762
11.20	1.721	-0.1865
12.20	1.673	-0.1953
13.03	1.675	-0.2066
14.14	1.660	-0.2248
13.93	1.662	-0.2181
12.81	1.689	-0.2034
11.95	1.713	-0.1922
10.95	1.753	-0.1817
9.91	2.021	-0.1711
8.95	1.984	-0.1764
7.83	1.898	-0.1785
6.87	1.837	-0.1848
5.98	1.771	-0.1880
4.87	1.694	-0.1935
3.77	1.603	-0.1969
2.69	1.526	-0.2030
1.73	1.459	-0.2069
0.70	1.370	-0.2101
-0.26	1.293	-0.2138
-1.35	1.205	-0.2171
-2.41	1.113	-0.2181
-3.42	1.060	-0.2277
-4.45	0.985	-0.2343
-5.48	0.903	-0.2360
-6.53	0.812	-0.2366
-7.57	0.728	-0.2408
-8.54	0.637	-0.2411
-9.60	0.546	-0.2417

W1015 (30%) **fp50**

Fig. 6.247

Run: 07232sn
Re = 100001.4

α	C_l	C_m
-10.27	0.247	-0.1511
-9.11	0.405	-0.1703
-8.11	0.520	-0.1825
-7.03	0.647	-0.1934
-6.08	0.746	-0.1983
-5.03	0.845	-0.2012
-4.02	0.927	-0.2025
-2.94	1.030	-0.2072
-1.97	1.127	-0.2123
-0.98	1.218	-0.2140
0.11	1.300	-0.2118
1.00	1.366	-0.2105
2.18	1.464	-0.2044
3.04	1.506	-0.1987

4.10	1.579	-0.1966
5.09	1.637	-0.1931
6.21	1.702	-0.1880
7.25	1.757	-0.1848
8.18	1.804	-0.1811
9.04	1.334	-0.2866
10.03	1.366	-0.2958
11.05	1.376	-0.2990
12.02	1.421	-0.3128
11.62	1.394	-0.2874
10.81	1.403	-0.2823
9.72	1.356	-0.2701
8.72	1.363	-0.2643
7.65	1.369	-0.2563
6.74	1.306	-0.2378
5.90	1.713	-0.1771
4.79	1.657	-0.1788
3.75	1.582	-0.1785
2.87	1.542	-0.1831
1.73	1.474	-0.1870
0.76	1.392	-0.1872
-0.20	1.327	-0.1899
-1.32	1.251	-0.1937
-2.33	1.119	-0.1862
-3.32	1.036	-0.1851
-4.40	0.927	-0.1802
-5.28	0.862	-0.1794
-6.46	0.763	-0.1747
-7.36	0.659	-0.1676
-8.37	0.502	-0.1554
-9.46	0.373	-0.1405

Run: 07233sn
Re = 199925.1

α	C_l	C_m
-10.22	0.569	-0.2460
-9.27	0.628	-0.2414
-8.10	0.677	-0.2241
-7.09	0.753	-0.2204
-6.07	0.824	-0.2160
-5.20	0.900	-0.2147
-4.02	0.997	-0.2129
-3.01	1.075	-0.2132
-2.05	1.171	-0.2152
-1.03	1.239	-0.2108
0.08	1.330	-0.2104
1.14	1.401	-0.2072
2.01	1.467	-0.2061
3.07	1.531	-0.2011
4.19	1.605	-0.1975
5.03	1.665	-0.1958
6.20	1.746	-0.1924
7.20	1.805	-0.1894

8.17	1.872	-0.1888
9.23	1.916	-0.1838
10.26	1.930	-0.1794
11.10	1.727	-0.1794
11.73	1.390	-0.2999
12.83	1.419	-0.3100
13.95	1.462	-0.3267
13.62	1.431	-0.3096
12.64	1.407	-0.3009
11.65	1.399	-0.2942
10.68	1.374	-0.2852
9.65	1.397	-0.2786
8.77	1.413	-0.2663
7.89	1.863	-0.1845
6.88	1.807	-0.1862
5.86	1.732	-0.1870
4.95	1.662	-0.1880
3.86	1.603	-0.1933
2.73	1.522	-0.1957
1.75	1.458	-0.1996
0.71	1.391	-0.2033
-0.25	1.303	-0.2016
-1.24	1.241	-0.2065
-2.19	1.172	-0.2095
-3.35	1.066	-0.2097
-4.37	0.970	-0.2063
-5.37	0.890	-0.2080
-6.32	0.824	-0.2128
-7.32	0.754	-0.2172
-8.34	0.668	-0.2180
-9.43	0.635	-0.2378

Run: 07234sn
Re = 400073.8

α	C_l	C_m
-10.18	0.599	-0.2521
-9.18	0.692	-0.2533
-8.13	0.776	-0.2522
-7.21	0.841	-0.2478
-6.11	0.935	-0.2469
-5.14	1.017	-0.2445
-4.05	1.105	-0.2402
-3.00	1.156	-0.2320
-2.06	1.232	-0.2293
-1.10	1.288	-0.2215
0.01	1.386	-0.2193
0.96	1.445	-0.2138
2.07	1.534	-0.2094
2.97	1.603	-0.2072
4.02	1.679	-0.2016
5.04	1.746	-0.1965
6.16	1.844	-0.1944
7.17	1.926	-0.1921

8.16	1.987	-0.1879
9.30	2.046	-0.1826
10.17	1.785	-0.1797
11.12	1.754	-0.1911
12.08	1.706	-0.2005
13.02	1.707	-0.2141
12.92	1.687	-0.2079
11.90	1.720	-0.1946
10.94	1.740	-0.1856
10.05	2.077	-0.1770
9.05	2.038	-0.1815
7.89	1.979	-0.1880
7.07	1.924	-0.1891
6.00	1.839	-0.1928
4.93	1.759	-0.1978
3.84	1.676	-0.2011
2.79	1.585	-0.2035
1.74	1.518	-0.2094
0.80	1.444	-0.2133
-0.27	1.364	-0.2175
-1.28	1.289	-0.2218
-2.32	1.208	-0.2267
-3.37	1.135	-0.2307
-4.44	1.077	-0.2400
-5.42	0.998	-0.2427
-6.50	0.909	-0.2444
-7.51	0.826	-0.2467
-8.41	0.745	-0.2468
-9.43	0.667	-0.2492

W1015 (30%) **fp55**

Fig. 6.249

Run: 07237sn
Re = 100084.2

α	C_l	C_m
-10.21	0.348	-0.1661
-9.08	0.482	-0.1787
-8.24	0.579	-0.1907
-7.05	0.699	-0.1947
-6.07	0.786	-0.1978
-5.21	0.871	-0.1998
-3.94	0.975	-0.2032
-2.92	1.076	-0.2061
-2.01	1.181	-0.2162
-0.90	1.287	-0.2177
-0.01	1.330	-0.2122
1.01	1.411	-0.2097
2.02	1.438	-0.1995
2.99	1.533	-0.2020
4.11	1.598	-0.1966
5.20	1.657	-0.1922

6.25	1.727	-0.1894
7.24	1.762	-0.1828
8.24	1.811	-0.1802
9.00	1.341	-0.2879
10.02	1.360	-0.2990
10.92	1.372	-0.3045
11.99	1.410	-0.3152
11.60	1.407	-0.2953
10.68	1.422	-0.2898
9.68	1.341	-0.2742
8.78	1.362	-0.2683
7.66	1.296	-0.2542
6.56	1.289	-0.2432
5.93	1.732	-0.1781
4.86	1.671	-0.1797
3.90	1.608	-0.1818
2.77	1.552	-0.1850
1.90	1.491	-0.1861
0.92	1.429	-0.1902
-0.36	1.349	-0.1935
-1.32	1.285	-0.1974
-2.35	1.156	-0.1901
-3.26	1.065	-0.1856
-4.27	0.996	-0.1877
-5.30	0.893	-0.1807
-6.37	0.788	-0.1743
-7.34	0.688	-0.1687
-8.48	0.590	-0.1648
-9.48	0.479	-0.1544

Run: 07236sn
Re = 200038.7

α	C_l	C_m
-10.16	0.492	-0.1954
-9.23	0.585	-0.2034
-8.07	0.701	-0.2106
-7.04	0.813	-0.2176
-6.08	0.886	-0.2159
-5.00	0.972	-0.2167
-4.10	1.042	-0.2153
-3.12	1.137	-0.2182
-2.05	1.230	-0.2186
-1.01	1.301	-0.2123
0.04	1.383	-0.2116
0.98	1.471	-0.2137
2.17	1.538	-0.2077
3.04	1.602	-0.2056
4.05	1.663	-0.2024
5.23	1.733	-0.1976
6.21	1.784	-0.1921
7.28	1.843	-0.1883
8.23	1.902	-0.1874
9.25	1.953	-0.1838

10.29	1.837	-0.1712
11.20	1.724	-0.1833
11.96	1.425	-0.3054
12.99	1.463	-0.3144
13.90	1.496	-0.3203
13.64	1.491	-0.3164
12.64	1.441	-0.3019
11.78	1.429	-0.2968
10.72	1.433	-0.2925
9.63	1.428	-0.2829
8.66	1.411	-0.2715
7.87	1.906	-0.1822
6.85	1.839	-0.1837
5.96	1.792	-0.1867
4.86	1.723	-0.1916
3.83	1.647	-0.1920
2.89	1.588	-0.1968
1.89	1.503	-0.1958
0.85	1.445	-0.2018
-0.17	1.351	-0.1985
-1.32	1.282	-0.2051
-2.22	1.217	-0.2070
-3.25	1.128	-0.2057
-4.24	1.045	-0.2071
-5.26	0.940	-0.2015
-6.24	0.870	-0.2051
-7.44	0.780	-0.2069
-8.47	0.680	-0.2024
-9.43	0.565	-0.1927

Run: 07235sn
Re = 400027.1

α	C_l	C_m
-10.15	0.703	-0.2593
-9.22	0.772	-0.2579
-8.12	0.860	-0.2559
-7.14	0.931	-0.2526
-6.05	1.023	-0.2527
-5.12	1.101	-0.2501
-4.05	1.174	-0.2428
-3.05	1.224	-0.2362
-2.14	1.286	-0.2306
-0.96	1.364	-0.2245
-0.08	1.430	-0.2211
1.00	1.511	-0.2182
2.05	1.593	-0.2130
3.01	1.649	-0.2079
4.00	1.722	-0.2034
5.03	1.798	-0.2000
6.08	1.871	-0.1944
7.25	1.977	-0.1920
8.18	2.038	-0.1885
9.31	2.082	-0.1819

10.11	1.779	-0.1833
11.15	1.726	-0.1899
12.12	1.702	-0.2026
13.08	1.681	-0.2165
12.85	1.695	-0.2115
11.85	1.727	-0.1982
10.85	1.758	-0.1860
10.05	2.117	-0.1771
9.13	2.078	-0.1809
7.99	2.024	-0.1866
7.01	1.964	-0.1910
5.85	1.868	-0.1938
4.83	1.780	-0.1958
3.79	1.707	-0.2013
2.74	1.623	-0.2023
1.82	1.565	-0.2091
0.73	1.493	-0.2156
-0.25	1.425	-0.2217
-1.36	1.343	-0.2243
-2.27	1.269	-0.2271
-3.22	1.216	-0.2347
-4.44	1.145	-0.2414
-5.41	1.075	-0.2468
-6.46	0.999	-0.2494
-7.41	0.915	-0.2505
-8.37	0.840	-0.2527
-9.55	0.741	-0.2537

W1015 (30%) fp60
Fig. 6.251

Run: 07238sn
Re = 99918.8

α	C_l	C_m
-10.16	0.446	-0.1695
-9.03	0.583	-0.1812
-8.21	0.673	-0.1885
-7.02	0.778	-0.1960
-6.04	0.867	-0.2004
-5.00	0.955	-0.2043
-4.09	1.040	-0.2068
-2.95	1.137	-0.2131
-1.96	1.227	-0.2133
-1.04	1.315	-0.2167
0.04	1.370	-0.2084
1.03	1.433	-0.2027
2.04	1.504	-0.2029
3.01	1.563	-0.1989
4.05	1.624	-0.1931
5.25	1.699	-0.1894
6.13	1.746	-0.1860
7.11	1.795	-0.1789

8.28	1.842	-0.1760
8.99	1.334	-0.2789
9.91	1.372	-0.2896
10.96	1.390	-0.2966
11.96	1.420	-0.3084
11.64	1.421	-0.2944
10.79	1.413	-0.2876
9.79	1.355	-0.2734
8.83	1.346	-0.2658
7.66	1.344	-0.2583
6.81	1.324	-0.2480
5.69	1.314	-0.2312
5.00	1.705	-0.1778
3.81	1.633	-0.1791
2.83	1.579	-0.1813
1.74	1.512	-0.1855
0.86	1.447	-0.1871
-0.24	1.385	-0.1900
-1.14	1.342	-0.1947
-2.16	1.246	-0.1944
-3.21	1.132	-0.1866
-4.40	1.043	-0.1849
-5.28	0.969	-0.1836
-6.27	0.883	-0.1793
-7.30	0.787	-0.1734
-8.45	0.678	-0.1668
-9.47	0.558	-0.1581

Run: 07239sn
Re = 199859.3

α	C_l	C_m
-10.22	0.543	-0.1911
-9.07	0.683	-0.2070
-8.07	0.764	-0.2086
-7.08	0.861	-0.2133
-6.18	0.939	-0.2142
-5.07	1.025	-0.2130
-3.98	1.107	-0.2114
-2.97	1.213	-0.2179
-1.97	1.289	-0.2168
-1.03	1.362	-0.2171
0.12	1.435	-0.2102
1.13	1.498	-0.2079
2.16	1.567	-0.2054
3.02	1.621	-0.2018
4.06	1.679	-0.1972
5.20	1.744	-0.1921
6.17	1.811	-0.1897
7.25	1.877	-0.1873
8.13	1.928	-0.1849
9.22	1.973	-0.1803
10.27	1.827	-0.1716
10.81	1.427	-0.2996

11.93	1.446	-0.3078
12.96	1.453	-0.3129
13.95	1.510	-0.3285
13.76	1.494	-0.3161
12.74	1.477	-0.3086
11.63	1.456	-0.3003
10.68	1.442	-0.2914
9.70	1.417	-0.2825
8.60	1.399	-0.2697
8.01	1.931	-0.1768
6.88	1.863	-0.1803
5.86	1.807	-0.1833
4.92	1.747	-0.1885
3.82	1.670	-0.1912
2.78	1.622	-0.1966
1.90	1.569	-0.2024
0.86	1.498	-0.2046
-0.18	1.419	-0.2041
-1.14	1.347	-0.2049
-2.30	1.262	-0.2074
-3.17	1.195	-0.2096
-4.33	1.075	-0.2023
-5.28	1.017	-0.2077
-6.26	0.926	-0.2051
-7.39	0.839	-0.2047
-8.35	0.736	-0.1970
-9.38	0.640	-0.1927

Run: 07240sn
Re = 400006.4

α	C_l	C_m
-10.15	0.760	-0.2580
-9.26	0.834	-0.2584
-8.10	0.920	-0.2551
-7.10	0.991	-0.2525
-6.15	1.071	-0.2516
-5.09	1.148	-0.2470
-4.10	1.222	-0.2448
-3.01	1.274	-0.2357
-2.07	1.344	-0.2319
-1.07	1.410	-0.2256
0.09	1.473	-0.2166
1.02	1.545	-0.2140
1.99	1.613	-0.2101
2.98	1.670	-0.2023
4.01	1.742	-0.1985
5.22	1.817	-0.1920
6.15	1.896	-0.1912
7.28	1.974	-0.1866
8.17	2.035	-0.1820
9.24	2.095	-0.1784
10.14	1.768	-0.1801
11.17	1.726	-0.1912

12.09	1.716	-0.2047
11.84	1.724	-0.1988
10.99	1.744	-0.1871
10.05	2.122	-0.1749
8.94	2.082	-0.1783
7.94	2.024	-0.1833
6.91	1.954	-0.1863
5.90	1.894	-0.1922
4.93	1.819	-0.1938
3.83	1.742	-0.2000
2.81	1.666	-0.2041
1.90	1.598	-0.2060
0.82	1.527	-0.2111
-0.23	1.455	-0.2160
-1.25	1.385	-0.2211
-2.36	1.318	-0.2280
-3.36	1.259	-0.2367
-4.37	1.203	-0.2423
-5.42	1.131	-0.2482
-6.38	1.060	-0.2499
-7.30	0.981	-0.2514
-8.49	0.890	-0.2534
-9.47	0.821	-0.2570

W1015 (30%) fp65

Fig. 6.253

Run: 07243sn
Re = 100040.5

α	C_l	C_m
-10.09	0.463	-0.1715
-9.16	0.558	-0.1785
-8.17	0.673	-0.1937
-7.06	0.775	-0.1956
-6.02	0.883	-0.2023
-5.19	0.960	-0.2050
-4.01	1.076	-0.2089
-3.09	1.153	-0.2105
-1.94	1.275	-0.2200
-0.86	1.364	-0.2178
-0.05	1.427	-0.2182
1.06	1.473	-0.2078
2.04	1.537	-0.2022
3.18	1.614	-0.2024
4.21	1.679	-0.1980
5.13	1.724	-0.1950
6.28	1.769	-0.1879
7.20	1.813	-0.1841
8.00	1.338	-0.2744
9.05	1.378	-0.2866
9.89	1.342	-0.2926
10.99	1.368	-0.2987

12.00	1.397	-0.3084
11.58	1.409	-0.2916
10.65	1.363	-0.2787
9.68	1.318	-0.2664
8.59	1.329	-0.2578
7.67	1.338	-0.2519
6.67	1.334	-0.2439
5.61	1.345	-0.2333
4.88	1.735	-0.1793
3.93	1.675	-0.1793
2.77	1.609	-0.1809
1.94	1.541	-0.1802
0.78	1.494	-0.1868
-0.23	1.416	-0.1870
-1.31	1.345	-0.1910
-2.31	1.233	-0.1888
-3.27	1.153	-0.1864
-4.31	1.072	-0.1845
-5.23	0.983	-0.1815
-6.29	0.883	-0.1794
-7.36	0.778	-0.1748
-8.41	0.677	-0.1689
-9.33	0.583	-0.1625

Run: 07242sn
Re = 200107.8

α	C_l	C_m
-10.10	0.614	-0.1937
-9.07	0.703	-0.1959
-8.09	0.799	-0.2040
-7.03	0.881	-0.2031
-6.02	0.951	-0.2024
-5.04	1.032	-0.2039
-4.02	1.111	-0.2048
-3.07	1.212	-0.2107
-2.01	1.298	-0.2076
-1.04	1.370	-0.2077
0.01	1.437	-0.2028
1.12	1.519	-0.2015
2.10	1.576	-0.1958
3.08	1.629	-0.1948
4.17	1.707	-0.1927
5.08	1.758	-0.1890
6.21	1.817	-0.1830
7.30	1.882	-0.1808
8.25	1.918	-0.1786
9.32	1.948	-0.1722
10.26	1.783	-0.1679
10.77	1.406	-0.2906
11.90	1.432	-0.3020
12.84	1.522	-0.3214
12.68	1.494	-0.3095
11.81	1.419	-0.2922
10.70	1.401	-0.2844
9.77	1.417	-0.2811
8.77	1.401	-0.2691
8.10	1.913	-0.1705
6.89	1.854	-0.1734
5.79	1.798	-0.1779
4.84	1.734	-0.1803
3.85	1.670	-0.1836
2.92	1.621	-0.1870
1.76	1.550	-0.1890
0.73	1.486	-0.1941
-0.17	1.418	-0.1952
-1.21	1.352	-0.1977
-2.16	1.282	-0.1984
-3.33	1.183	-0.1997
-4.35	1.085	-0.1951
-5.37	0.995	-0.1949
-6.38	0.927	-0.1961
-7.41	0.837	-0.1907
-8.41	0.746	-0.1874
-9.43	0.658	-0.1835

Run: 07241sn
Re = 399963.0

α	C_l	C_m
-10.20	0.802	-0.2524
-9.18	0.892	-0.2556
-8.12	0.961	-0.2508
-7.19	1.025	-0.2467
-6.20	1.098	-0.2453
-5.06	1.174	-0.2397
-4.00	1.268	-0.2405
-3.00	1.312	-0.2305
-1.95	1.358	-0.2204
-1.05	1.412	-0.2139
0.05	1.494	-0.2115
1.04	1.558	-0.2073
2.08	1.615	-0.1990
3.13	1.685	-0.1943
4.01	1.744	-0.1923
5.18	1.819	-0.1860
6.18	1.878	-0.1815
7.15	1.956	-0.1818
8.21	2.007	-0.1750
9.20	2.058	-0.1713
10.21	1.773	-0.1736
11.15	1.719	-0.1851
12.07	1.679	-0.1975
12.09	1.513	-0.3088
12.34	1.531	-0.3112
11.69	1.516	-0.3042
11.58	1.695	-0.1892
9.97	1.783	-0.1703
8.96	2.072	-0.1742
7.94	2.020	-0.1789
6.98	1.957	-0.1815
5.98	1.894	-0.1846
4.81	1.816	-0.1891
3.91	1.754	-0.1935
2.90	1.700	-0.1989
1.91	1.625	-0.2006
0.77	1.557	-0.2093
-0.11	1.501	-0.2129
-1.27	1.424	-0.2191
-2.30	1.376	-0.2286
-3.21	1.310	-0.2318
-4.40	1.246	-0.2410
-5.40	1.163	-0.2417
-6.24	1.105	-0.2446
-7.46	1.015	-0.2463
-8.42	0.949	-0.2495
-9.44	0.869	-0.2496

Appendix D

MATLAB Code and Microsoft Excel Input File

Appendix D contains all of the MATLAB codes written to run XFOIL in a batch mode. The code is broken into two different programs. The first program is called “Main Program” and can be seen in Section D.1. This program opens a Microsoft Excel file to gather inputs, runs the program called “Polar Input Program” (see Section D.2) to generate the XFOIL input, and runs XFOIL to gather polar data. The second program, called “Polar Input Program,” creates the necessary inputs to execute XFOIL given inputs from a Microsoft Excel file. A screen grab of the Microsoft Excel input file can be seen in Section D.3 along with brief descriptions of the required inputs and an example. For completeness, it should be noted that the two MATLAB programs, Microsoft Excel input file, XFOIL executable, and required coordinate files need to be located in the same working directory (same folder). The outputs of these programs are polar data files for each Reynolds number and polar plots similar to the XFOIL example seen in Fig. 5.4. More information on the outputs can be found in the example presented in Section D.3.

D.1 Main Program

```
% Clear out Memory, Plots, and Display
clc; close all; clear all;

% Start Timer
tic

%% INPUT

% Define file name to read from
file_read = 'Runs.xlsx';

%% IMPORT DATA

% Import General Information from Excel File
[num_temp,str_temp] = xlsread(file_read,'Input','f2:f9');
re_run = num_temp(1);
num_airfoil = num_temp(2);
cl_run = num_temp(3);
row_start = num_temp(4);
```

```
cl_start = num_temp(5);
delta_cl = num_temp(6);
polar_col = str_temp{1};
cf_col = str_temp{2};

% Import Airfoil Info
airfoil_start = sprintf('a%s',num2str(row_start));
airfoil_end = sprintf('a%s',num2str((row_start+(re_run*num_airfoil))-1));
range = sprintf('%s:%s',airfoil_start,airfoil_end);
[~,airfoil] = xlsread(file_read,'Input',range);

% Import Reynolds Number Info
re_start = sprintf('b%s',num2str(row_start));
re_end = sprintf('b%s',num2str((row_start+(re_run*num_airfoil))-1));
range = sprintf('%s:%s',re_start,re_end);
re_info = xlsread(file_read,'Input',range);

% Import Polar Info
polar_start = sprintf('%s%s',polar_col,num2str(row_start));
polar_end = sprintf('%s%s',char(double(polar_col)+1),...
num2str((row_start+(re_run*num_airfoil))-1));
range = sprintf('%s:%s',polar_start,polar_end);
polar_info = xlsread(file_read,'Input',range);

% Import Cf Info
cf_start = sprintf('%s%s',cf_col,num2str(row_start));
cf_end = sprintf('%s%s',char(double(cf_col)+cl_run),...
num2str((row_start+(re_run*num_airfoil))-1));
range = sprintf('%s:%s',cf_start,cf_end);
cf_info = xlsread(file_read,'Input',range);


%% Organize Data for Input into XFOIL

% Polar Info
num_polar = length(airfoil)/re_run;
count1 = 1;
count2 = 1;
for ii = 1:num_polar
    polar_input{ii,1} = airfoil{count1};
    for jj = 1:re_run
        polar_input{ii,jj+1} = num2str(re_info(count2));
        count2 = count2 + 1;
    end
    count1 = count1 + re_run;
end

count = 1;
for ii = 1:num_polar
    aoa_start_info(ii) = polar_info(count,1);
    aoa_end_info(ii) = polar_info(count,2);
    count = count + re_run;
end
```

```
%% EXECUTE XFOIL

% Polars from XFOIL
delete plot.ps
delete polar_input_data_2.dat
for ii=1:num_polar
    re = polar_input(ii,2:end);
    airfoil_in = polar_input{ii,1};
    aoa_start = aoa_start_info(ii);
    aoa_end = aoa_end_info(ii);

    % Create Run File for XFOIL
    polar_input_data_2(airfoil_in,re,aoa_start,aoa_end,re_run)

    % Run XFOIL
    dos('xfoil.exe < polar_input_data_2.dat' );

    % Moving and Deleting Data
    delete polar_input_data_2.dat
    output_name = sprintf('%s_Polar.ps',airfoil_in);
    copyfile('plot.ps',output_name)
    delete plot.ps
end

% End Timer
toc
```

D.2 Polar Input Program

```
function polar_input_data_2(airfoil_in,re,aoa_start,aoa_end,re_run)
fid = fopen ('polar_input_data_2.dat', 'w+t');
fprintf(fid, 'PLOP \n');
fprintf(fid, 'G \n');
fprintf(fid, '\n\n\n');
fprintf(fid, 'LOAD %s.dat \n\n', airfoil_in);
fprintf(fid, 'PPAR \n');
fprintf(fid, 'N 240 \n');
fprintf(fid, '\n');
fprintf(fid, '\n\n');
fprintf(fid, 'OPER \n');
fprintf(fid, 'VPAR \n');
fprintf(fid, 'N 9 \n');
fprintf(fid, '\n');
fprintf(fid, 'ITER 75 \n');
fprintf(fid, 'v %s \n',re{1});
fprintf(fid, 'a 0 \n');
for ii = 1:re_run
    if ii~=1
```

```
    fprintf(fid, 'init \n');
        fprintf(fid, 'r %s \n',re{ii});
    end
fprintf(fid, 'aseq 0 %12.4g %12.4g \n',aoa_start,1);
    fprintf(fid, 'PACC \n');
    filename = sprintf('%s_%s_Polar.dat',airfoil_in,re{ii});
    fprintf(fid, '%s \n',filename);
    fprintf(fid, '\n');
    fprintf(fid, 'aseq %12.4g %12.4g %12.4g \n',aoa_start,aoa_end,0.25);
    fprintf(fid, 'PACC \n');
end
fprintf(fid, 'PPAX \n');
fprintf(fid, '-10 30 10');
fprintf(fid, '\n');
fprintf(fid, '-0.5 2.0 0.5');
fprintf(fid, '\n');
fprintf(fid, '0 0.05 0.01');
fprintf(fid, '\n');
fprintf(fid, '-0.2 0 0.1');
fprintf(fid, '\n');
fprintf(fid, 'PPLO \n');
fprintf(fid, 'HARD');
fprintf(fid, '\n\n\n');
fprintf(fid, 'QUIT \n');
fclose(fid);
```

D.3 Microsoft Excel Input File

The inputs for the MATLAB programs that run XFOIL are provided by a Microsoft Excel file. A screen grab of that file can be seen in Fig. D.1. This file is used by several programs that the author created. Therefore, some of the inputs will not be used by this program. In the next few paragraphs, a brief description of each input is provided. The last paragraph presents an example to aid in the understanding of the Microsoft Excel file and MATLAB codes.

The top portion of the input file (rows 2–9) contains information that controls how the airfoil information (starts row 14) is used. The first input (row 2) defines the number of Reynolds numbers that will be analyzed for each airfoil. This input groups a number of runs together to create a polar plot with multiple Reynolds numbers as seen in Chapter 5. The second input (row 3) defines the number of airfoils to be analyzed. The third input (row 4) is not used by this program. The fourth input (row 5) sets the row that the MATLAB program starts taking inputs. The next four inputs (rows 6–9) are not used by this program.

The structure of the airfoil inputs (starts row 14) can be seen in the lower portion of the screen grab seen in Fig. D.1. The name of the airfoil coordinates is listed in the first column (column A). The name should match the coordinate file exactly (case sensitive). The program assumes that the extension of the coordinate file is ".dat" to make inputs easier. The second column (column B) defines the Reynolds number that the airfoil will be analyzed. If multiple Reynolds numbers need to be analyzed, multiple rows need to be created as seen in Fig. D.1. The next two columns (columns C–D) define the starting and ending angles of attack respectively for the polar analysis. The step size between the starting and ending angles of attack is hard coded in the "Polar Input Program" to be 0.25 deg. The rest of the columns (columns E and above) are not used by this program.

In order to clarify any confusing aspects of the Microsoft Excel input file, an example is presented using information seen in Fig. D.1. For this example, the E472 airfoil will be analyzed at five Reynolds numbers of 100,000, 200,000, 300,000, 400,000, and 500,000. For each Reynolds number, the starting and ending angles of attack will be -5 and 18 deg respectively. Thus, the first input (row 2) should be set to "5," and the second input (row 3) to "1." The fourth input (row 5) should be set to "14." The other inputs in the top portion of the input file are not used and can remain the same. The name "e472" should be entered in the first column (column A) from row 14–18. The Reynolds numbers previously listed should be entered in the order that they should be analyzed in the second column (column B) using the same row range (rows 14–18) as the first column. In this case, the Reynolds numbers are entered in ascending order. The starting angles of attack are entered in third column (column C), and the ending angles of attack are entered in fourth column (column D) using the same row range (rows 14–18) as the first column. These inputs will create five polar data files for each Reynolds number and one plot with all five Reynolds number results coplotted similar to the XFOIL example plot seen in Fig. 5.4. The polar data files are preset by the MATLAB programs to have the form "airfoil name"_"Reynolds number"_Polar.dat.

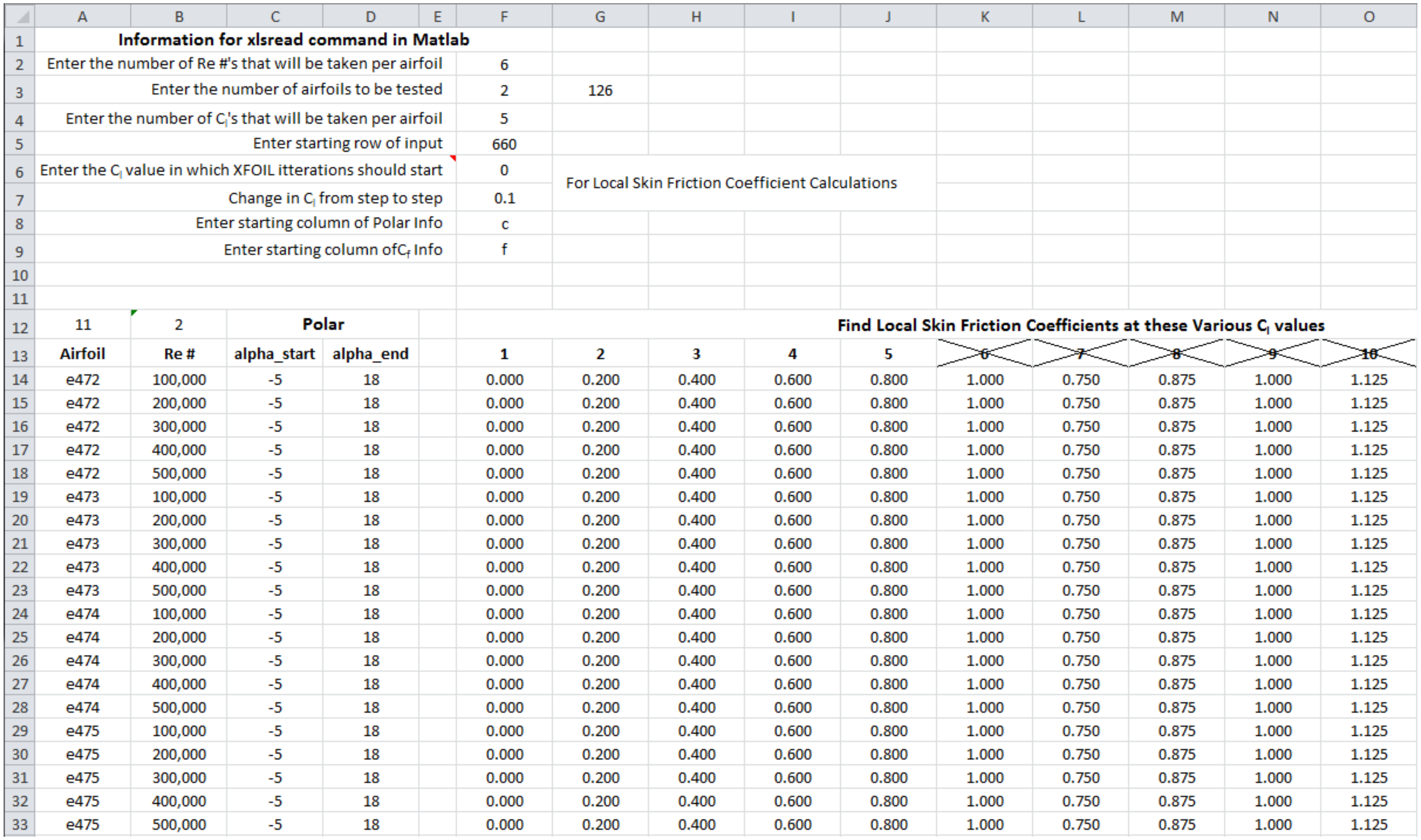

	A	B	C	D	E	F	G	H	I	J	K	L	M	N	O
1	**Information for xlsread command in Matlab**														
2	Enter the number of Re #'s that will be taken per airfoil					6									
3	Enter the number of airfoils to be tested					2	126								
4	Enter the number of C_l's that will be taken per airfoil					5									
5	Enter starting row of input					660									
6	Enter the C_l value in which XFOIL itterations should start					0	For Local Skin Friction Coefficient Calculations								
7	Change in C_l from step to step					0.1									
8	Enter starting column of Polar Info					c									
9	Enter starting column ofC_f Info					f									
10															
11															
12	11	2	**Polar**			**Find Local Skin Friction Coefficients at these Various C_l values**									
13	**Airfoil**	**Re #**	**alpha_start**	**alpha_end**		**1**	**2**	**3**	**4**	**5**	~~**6**~~	~~**7**~~	~~**8**~~	~~**9**~~	~~**10**~~
14	e472	100,000	-5	18		0.000	0.200	0.400	0.600	0.800	1.000	0.750	0.875	1.000	1.125
15	e472	200,000	-5	18		0.000	0.200	0.400	0.600	0.800	1.000	0.750	0.875	1.000	1.125
16	e472	300,000	-5	18		0.000	0.200	0.400	0.600	0.800	1.000	0.750	0.875	1.000	1.125
17	e472	400,000	-5	18		0.000	0.200	0.400	0.600	0.800	1.000	0.750	0.875	1.000	1.125
18	e472	500,000	-5	18		0.000	0.200	0.400	0.600	0.800	1.000	0.750	0.875	1.000	1.125
19	e473	100,000	-5	18		0.000	0.200	0.400	0.600	0.800	1.000	0.750	0.875	1.000	1.125
20	e473	200,000	-5	18		0.000	0.200	0.400	0.600	0.800	1.000	0.750	0.875	1.000	1.125
21	e473	300,000	-5	18		0.000	0.200	0.400	0.600	0.800	1.000	0.750	0.875	1.000	1.125
22	e473	400,000	-5	18		0.000	0.200	0.400	0.600	0.800	1.000	0.750	0.875	1.000	1.125
23	e473	500,000	-5	18		0.000	0.200	0.400	0.600	0.800	1.000	0.750	0.875	1.000	1.125
24	e474	100,000	-5	18		0.000	0.200	0.400	0.600	0.800	1.000	0.750	0.875	1.000	1.125
25	e474	200,000	-5	18		0.000	0.200	0.400	0.600	0.800	1.000	0.750	0.875	1.000	1.125
26	e474	300,000	-5	18		0.000	0.200	0.400	0.600	0.800	1.000	0.750	0.875	1.000	1.125
27	e474	400,000	-5	18		0.000	0.200	0.400	0.600	0.800	1.000	0.750	0.875	1.000	1.125
28	e474	500,000	-5	18		0.000	0.200	0.400	0.600	0.800	1.000	0.750	0.875	1.000	1.125
29	e475	100,000	-5	18		0.000	0.200	0.400	0.600	0.800	1.000	0.750	0.875	1.000	1.125
30	e475	200,000	-5	18		0.000	0.200	0.400	0.600	0.800	1.000	0.750	0.875	1.000	1.125
31	e475	300,000	-5	18		0.000	0.200	0.400	0.600	0.800	1.000	0.750	0.875	1.000	1.125
32	e475	400,000	-5	18		0.000	0.200	0.400	0.600	0.800	1.000	0.750	0.875	1.000	1.125
33	e475	500,000	-5	18		0.000	0.200	0.400	0.600	0.800	1.000	0.750	0.875	1.000	1.125

Figure D.1: Screen grab of the Microsoft Excel input file used by the MATLAB code to create the inputs for XFOIL.

References

[1] Selig, M. S., Guglielmo, J. J., Broeren, A. P., and Giguere, P., "Experiments on airfoils at low Reynolds numbers," *34th AIAA Aerospace Sciences Meeting and Exhibit*, 1996, AIAA 96-0062.

[2] Gopalarathnam, A. and Selig, M. S., "Design of Low Reynolds Number Airfoils with Trips," *Journal of Aircraft*, Vol. 40, No. 4, July–August 2003, pp. 768–775.

[3] Selig, M. S. and Guglielmo, J. J., "High-Lift Low Reynolds Number Airfoil Design," *Journal of Aircraft*, Vol. 34, No. 1, January–February 1997, pp. 72–78.

[4] Selig, Donovan, and Fraser, *Airfoils at Low Speeds*, SoarTech 8, SoarTech Publications, Virginia Beach, VA, 1989.

[5] Selig, M. S., Guglielmo, J. J., Broeren, A. P., and Giguère, P., *Summary of Low-Speed Airfoil Data - Vol. 1*, SoarTech Publications, Virginia Beach, VA, 1995.

[6] Selig, M. S., Lyon, C. A., Giguère, P., Ninham, C. P., and Guglielmo, J. J., *Summary of Low-Speed Airfoil Data - Vol. 2*, SoarTech Publications, Virginia Beach, VA, 1996.

[7] Lyon, C. A., Broeren, A. P., Giguère, P., Gopalarathnam, A., and Selig, M. S., *Summary of Low-Speed Airfoil Data - Vol. 3*, SoarTech Publications, Virginia Beach, VA, 1997.

[8] Selig, M. S. and McGranahan, B. D., "Wind Tunnel Aerodynamic Tests of Six Airfoils for Use of Small Wind Turbines," National Renewable Energy Laboratory, NREL/SR-500-34515, Golden, CO, 2004.

[9] Williamson, G. A., McGranahan, B. D., Broughton, B. A., Deters, R. W., Brandt, J. B., and Selig, M. S., "Summary of Low-Speed Airfoil Data - Vol. 5," `http://www.ae.illinois.edu/m-selig/uiuc_lsat.html`, Accessed April 2012.

[10] Eppler, R., *Airfoil Design and Data*, Springer, New York, NY, 1990.

[11] Ylilammi, N., *Experimental and Computational Study of Two Flapped Airfoils at Low Reynolds Numbers*, Master's thesis, Helsinki University of Technology, Helsinki, Finland, 2009.

[12] Anonymous, "Charles River Radio Controllers - Mark Drela's AG and HT Airfoils," `http://www.charlesriverrc.org/articles/drela-airfoilshop/markdrela-ag-ht-airfoils.htm`, Accessed February 2012.

[13] Selig, M. S. and Maughmer, M. D., "A Multi-Point Inverse Airfoil Design Method Based on Conformal Mapping," *AIAA Journal*, Vol. 30, No. 5, May 1992, pp. 1162–1170.

[14] Selig, M. S. and Maughmer, M. D., "Generalized Multipoint Inverse Airfoil Design and Analysis of Low-Speed Airfoils," *AIAA Journal*, Vol. 30, No. 11, November 1992, pp. 2618–2625.

[15] Gopalarathnam, A. and Selig, M. S., "Low-Speed Natural-Laminar-Flow Airfoils: Case Study in Inverse Design," *Journal of Aircraft*, Vol. 38, No. 1, 2001, pp. 57–63.

[16] Rot, N., "Note on the History of the Reynolds Number," *Annual Review of Fluid Mechanics*, Vol. 22, 1990, pp. 1–11.

[17] White, F. M., *Viscous Fluid Flow*, McGraw-Hill, New York, NY, 3rd ed., 2005.

[18] Carmichael, B. H., "Low Reynolds Number Airfoil Survey - Volume 1," NASA-CR-165803, 1981.

[19] Arena, A. V. and Mueller, T. J., "Laminar Separation, Transition, and Turbulent Reattachment near the Leading Edge of Airfoils," *Journal of Aircraft*, Vol. 18, No. 7, July 1980, pp. 747–753.

[20] Selig, M. S., "Low Re Number Airfoil Design Lecture Notes," VKI Lecture Series, von Karman Institute for Fluid Dynamics, Sint-Genesius-Rode, Belgium, 2003.

[21] Mueller, T. J. and DeLaurier, J. D., "Aerodynamics of Small Vehicles," *Annual Review of Fluid Mechanics*, Vol. 35, July 2003, pp. 89–111.

[22] Mueller, T. J. and Batill, S., "Experimental Studies of the Laminar Separation Bubble on a Two-Dimensional Airfoil at Low Reynolds Number," *13th AIAA Fluid and Plasma Dynamics Conference*, 1980, AIAA 80-1440.

[23] Lissaman, P. B. S., "Low-Reynolds-Number Airfoils," *Annual Review of Fluid Mechanics*, Vol. 15, 1983, pp. 223–239.

[24] Mueller, T. J., "Low Reynolds Number Vehicles," AGARDograph No. 288, 1985.

[25] Ricci, R., Montelpare, S., and Silvi, E., "Study of Acoustic Disturbances Effect on Laminar Separation Bubble by IR Thermography," *Experimental Thermal and Fluid Science*, Vol. 31, No. 4, 2007, pp. 349–359.

[26] Santhanakrishnan, A., Pern, N. J., Ramakumar, K., Simpson, A., and Jacob, J. D., "Enabling Flow Control Technology for Low Speed UAVs," *AIAA Infotech Aerospace in Washington, DC*, 2005, AIAA 2005-6960.

[27] Lin, J. C. and Pauley, L. L., "Low-Reynolds-Number Separation on an Airfoil," *AIAA Journal*, Vol. 34, No. 8, August 1996, pp. 1570–1577.

[28] Lyon, C., Selig, M., and Broeren, A., "Boundary Layer Trips on Airfoils at Low Reynolds Numbers," AIAA 97-0511, 1997.

[29] Selig, M. S., *Multi-Point Inverse Design of Isolated Airfoils and Airfoils in Cascade in Incompressible Flow*, Ph.D. thesis, The Pennsylvania State University, College Park, Pennsylvania, May 1992.

[30] Roskam, J., *Airplane Design*, DARcorporation, Lawrence, KS, 2nd ed., 2003.

[31] Selig, M. S., Deters, R. W., and Williamson, G. A., "Wind Tunnel Testing Airfoils at Low Reynolds Numbers," *49th AIAA Aerospace Sciences Meeting*, 2011, AIAA 2011-875.

[32] Khodadoust, A., *An Experimental Study of the Flowfield on a Semispan Rectangular Wing with a Simulated Glaze Ice Accretion*, Ph.D. thesis, University of Illinois at Urbana-Champaign, Urbana, Illinois, 1993.

[33] Selig, M. S. and McGranahan, B. D., "Wind Tunnel Aerodynamic Tests of Six Airfoils for Use on Small Wind Turbines," *Journal of Solar Energy Engineering*, Vol. 126, November 2004, pp. 986–1001.

[34] Selig, M. S., "UIUC APA - LSATs," `http://www.ae.illinois.edu/m-selig/uiuc_lsat.html`, Accessed February 2012.

[35] Drela, M., personal communication, 2003, 2011–2012.

[36] Anonymous, "Realize,® Inc. Rapid Prototyping, Rapid Prototypes, Stereolithography," `http://www.realizeinc.com/`, Accessed February 2012.

[37] Barlow, J. B., Rae, W. H., and Pope, A., *Low-Speed Wind Tunnel Testing*, Wiley-Interscience, New York, NY, 3rd ed., 1999.

[38] Jones, B., "The Measurement of Profile Drag by the Pitot Traverse Method," Aeronautical Research Council, R&M 1688, 1936.

[39] Anonymous, "MSK Instruments - 220DD Baratron® Differential Capacitance Manometer," `http://www.mksinst.com/product/product.aspx?ProductID=158`, Accessed February 2012.

[40] Guglielmo, J. J. and Selig, M. S., "Spanwise Variations in Profile Drag for Airfoils at Low Reynold Numbers," *Journal of Aircraft*, Vol. 33, No. 4, July–August 1996, pp. 699–707.

[41] Guglielmo, J. J., *Spanwise Variations in Profile Drag for Airfoils at Low Reynolds Numbers*, Master's thesis, University of Illinois at Urbana-Champaign, Urbana, Illinois, 1995.

[42] Anonymous, "MSK Instruments - 221B Baratron® Differential Capacitance Manometer," `http://www.mksinst.com/product/product.aspx?ProductID=160`, Accessed February 2012.

[43] Giguère, P. and Selig, M. S., "Freestream Velocity Corrections for Two-Dimensional Testing with Splitter Plates," *AIAA Journal*, Vol. 35, No. 7, July 1997, pp. 1195–1200.

[44] Evangelista, R., McGhee, R., and Walker, B., *Correlation of Theory to Wind-Tunnel Data at Reynolds Numbers below 500,000*, Vol. 54 of *Low Reynolds Number Aerodynamics*, Springer-Verlag, New York, NY, June 1989, pp. 131–145, Edited by T. J. Mueller.

[45] McGhee, R., Walker, B., and Millard, B., "Experimental Results for the Eppler 387 Airfoil at Low Reynolds Numbers in the Langley Low-Turbulence Pressure Tunnel," NASA TM-4062, October 1988.

[46] McGranahan, B. D. and Selig, M. S., "Surface Oil Flow Measurements on Several Airfoils at Low Reynolds Numbers," *21st AIAA Applied Aerodynamics Conference*, 2003, AIAA 2003-4067.

[47] Drela, M., *XFOIL: An Analysis and Design System for Low Reynolds Number Airfoils*, Vol. 54 of *Low Reynolds Number Aerodynamics*, Springer-Verlag, New York, NY, June 1989, pp. 1–12, Edited by T. J. Mueller.

[48] Drela, M., "XFOIL Subsonic Airfoil Development System," `http://web.mit.edu/drela/Public/web/xfoil/`, Accessed March 2012.

[49] Gopalarathnam, A., "MFOIL User's Manual v2.0," MFOIL documentation, March 1998.

[50] Hoerner, S. F., *Fluid-Dynamic Lift*, Hoerner Fluid Dynamics, Vancouver, WA, 2nd ed., 1985.